NOS Strategic Petroleum Reserve Support Project: Final Report

Volume One—Oceanography on the Louisiana Inner Continental Shelf

October 1981

U.S. DEPARTMENT OF COMMERCE
National Oceanic and Atmospheric Administration
National Ocean Survey

F
GC
130
M4N6
V.1

NOS Strategic Petroleum Reserve Support Project: Final Report

Volume One—Oceanography on the Louisiana Inner Continental Shelf

Henry R. Frey, Michael W. Szabados, and
Leonard E. Hickman

For those who turn to the sea for answers.
Hank Frey

Submitted by:
Wesley V. Hull
Associate Director
Office of Oceanography
National Ocean Survey

Submitted to:
Fredric A. Godshall
Program Manager
NOAA Brine Disposal Analysis Program
Environmental Data and Information Service

Supported by:
Interagency Agreement EL-78-1-01-7146
between
National Oceanic and Atmospheric Administration
and
Strategic Petroleum Reserve Office
U.S. Department of Energy
and cooperatively by
NOAA National Ocean Survey

October 1981

U.S.DEPARTMENT OF COMMERCE
Malcolm Baldrige, Secretary
National Oceanic and Atmospheric Administration
John Byrne, Administrator

National Ocean Survey
R. Adm. H.R. Lippold, Jr., Director

82 OC643

GEORGETOWN
CENTER
MAR 10 1982
N.O.A.A.
U. S. Dept. of Commerce

We dedicate this work to R. L. ("Bob") Charnell and N. P. ("Pat") Laird, NOAA oceanographers of the Pacific Marine Environmental Laboratory, who were lost at sea off Hawaii during December 1978.

Mention of a commercial company or product does not constitute an endorsement by the National Oceanic and Atmospheric Administration, the National Ocean Survey, or other agencies. Use for publicity or advertising purposes of information from this publication concerning proprietary products or the tests of such products is not authorized.

CONTENTS

Page

ACKNOWLEDGMENTS ix
LIST OF FIGURES xi
LIST OF TABLES. xxvii
ABBREVIATIONS xxix
CONCLUSIONS AND SUMMARY 1
INTRODUCTION. 22
1. Background. 23
1.1. Strategic Petroleum Reserve. 23
1.2. NOS SPR Support Project. 23
1.3. Geographical Setting 24
1.4. Experimental Design. 26
2. Regional Climatology and Oceanography 33
2.1. Climatology. 33
2.1.1. Polar Fronts. 33
2.1.2. Cyclones. 35
2.1.3. Land and Sea Breezes. 36
2.1.4. Temperature and Precipitation 36
2.2. Oceanography 41
2.3. River Runoff 45
3. Data Analysis 47
3.1. Data Quality Assurance 47
3.2. Dissolved Oxygen 49
3.3. Salinity, Temperature, and Density 49
3.4. Meteorology. 50
3.4.1. Spectral Analysis 50
3.4.2. Statistical Analysis. 50
3.5. Surface Waves. 50
3.5.1. Zero-Crossing Analysis. 51
3.5.2. Spectral Analysis 51

Page

3.6. Water Levels 53
3.6.1. Nonharmonic Analysis. 53
3.6.2. Harmonic Analysis 54
3.6.3. Spectral Analysis 55
3.7. Currents 55
3.7.1. Harmonic Analysis 55
3.7.2. Spectral Analysis 56
3.7.3. Statistical Analysis. 57
CHARACTERIZATION OF THE PROPOSED WEST HACKBERRY BRINE DISPOSAL SITE 60
4. Dissolved Oxygen. 61
4.1. Areal Averages and Ranges. 61
4.2. Spatial Distributions. 64
4.2.1. Summer 1978 64
4.2.2. Fall 1978 69
4.2.3. Winter 1979 69
4.2.4. Spring 1979 70
5. Salinity, Temperature, and Density. 73
5.1. Summer 1978. 76
5.2. Fall 1978. 82
5.3. Winter 1979. 87
5.4. Spring 1979. 94
6. Local Meteorology 101
6.1. Air Temperature. 101
6.2. Wind Speed and Direction 102
6.3. Spectral Characteristics 103
7. Surface Waves 111
7.1. Summer 1978. 111
7.2. Fall 1978. 114
7.3. Winter 1979. 116
7.4. Spring 1979. 118

Page

8. Water Levels. 119
9. Currents. 133
9.1. Temporal Characteristics 133
9.1.1. Current Speed 133
9.1.2. Relative Volume Transport 136
9.1.3. Tidal Currents. 140
9.2. Spatial Characteristics. 149
9.3. Spectral Characteristics 166
CHARACTERIZATION OF THE PROPOSED WEEKS ISLAND BRINE DISPOSAL SITE 176
10. Dissolved Oxygen. 177
10.1. Areal Averages and Ranges 177
10.2. Spatial Distributions 180
11. Salinity, Temperature, and Density. 187
11.1. Summer 1978 191
11.2. Fall 1978 197
11.3. Winter 1979 200
11.4. Spring 1979 203
12. Local Meteorology 207
12.1. Air Temperature 207
12.2. Wind Speed and Direction. 207
12.3. Spectral Characteristics. 215
13. Surface Waves 221
13.1. Summer 1978 221
13.2. Fall 1978 224
13.3. Winter 1979 226
13.4. Spring 1979 227
14. Water Levels. 229
15. Currents. 235
15.1. Temporal Characteristics. 235
15.1.1. Current Speed 235
15.1.2. Relative Volume Transport 238

Page

15.1.3. Tidal Currents. 242
15.2. Spatial Characteristics 249
15.3. Spectral Characteristics. 267
CHARACTERIZATION OF TRACKLINE STATIONS. 278
16. Dissolved Oxygen. 279
16.1. Ranges. 279
16.2. Spatial Distribution. 279
16.2.1. Summer 1978 279
16.2.2. Fall 1978 281
16.2.3. Winter 1979 281
16.2.4. Spring 1979 282
17. Salinity, Temperature, and Density. 283
17.1. Summer 1978 286
17.2. Fall 1978 286
17.3. Winter 1979 287
17.4. Spring 1979 287
EXTREME EVENTS. 290
18. Tropical Storm DEBRA. 291
18.1. Origin and Track of DEBRA 292
18.2. Meteorological Observations 297
18.3. Oceanographic Observations. 300
19. Extratropical Cyclone and Northers. 305
19.1. Meteorological Observations 305
19.2. Oceanographic Observations 312
20. Spring Storm. 319
20.1. Measurement System. 319
20.2. Observations. 320
REFERENCES CITED. 337
APPENDIX A. Equations used for calculation of conductivity, salinity, and sigma-t A-1
APPENDIX B. Water level theory B-1
APPENDIX C. Vertical profiles of temperature, salinity, and sigma-t at the West Hackberry site. C-1

Page

APPENDIX D. Time series plots of current speed and direction for observations 3 m above the bottom at the West Hackberry site. D-1

APPENDIX E. Transport and current vector diagrams for the West Hackberry site. E-1

APPENDIX F. Vertical profiles of temperature, salinity, and sigma-t at the Weeks Island site. F-1

APPENDIX G. Time series plots of current speed and direction for observations 3 m above the bottom at the Weeks Island site. G-1

APPENDIX H. Transport and current vector diagrams for the Weeks Island site. H-1

APPENDIX I. Vertical profiles of temperature, salinity, and sigma-t at the trackline stations. I-1

ACKNOWLEDGMENTS

Rear Admiral Richard Houlder and Captain Wesley Hull, the responsible NOS officials, were especially supportive of the NOS Project Manager and team members. Captain Charles Burroughs, NOAA Brine Disposal Analysis Program Manager, and Mr. Hal Delaplane, DOE Technical Project Officer, provided management support and encouragement throughout the project.

Engineering support for the project, provided by individuals of the NOS Office of Marine Technology (now part of NOAA's Office of Technology and Engineering Services), was enthusiastic and extremely helpful. Their active participation in the project was quite broad in scope and is documented in volume two of this report. Those who contributed to the technical and operational progress of the project are too numerous to mention here, but special thanks go to Messrs. Gerald Appell, Thomas Mero, David Crump, Bobby Taylor, Charles Kearse, Michael Basileo, Algis Kalvaitis, and Drs. Lloyd Huff and Joel Solomon.

Very special thanks are expressed to the officers and crew of the NOAA Ship FERREL for carrying out the field work with dedication to duty, particularly Commanders John Callahan and Dale North, Lieutenant Commander Michael Meyer, Lieutenants Robert King, Daniel Herlihy, and Robert Maxsom, Chief Boatswain David Brannan, Boatswain Group Leader G.T. Cooke, and Seaman Surveyor Gordon Pringle. The NOAA Research Vessel VIRGINIA KEY carried out the field work during December 1978 and January 1979; thanks are offered to the Master, Mr. Birnham Neil, and crew and to those who volunteered to serve with the NOS Project Manager in the field parties; Lieutenants (JG) Michael Sagalow and Timothy Roulon, Seaman Surveyor James Grant, Able Bodied Seaman Steven Bingham, James Bruce, and David R. Crump. Lieutenant Thomas Bergner was the pilot of the airplane from which evidence of Langmuir circulaton was observed and photographed.

Mr. Bruce Parker of the NOS Circulatory Surveys Branch (CSB) wrote the computer software for processing Grundy current meter and CTD data, and Aanderaa meteorological station and water level gage data. Mr. Richard Patchen of the CSB was consulted on the adaptation of analysis software for the project. Messrs. Parker and Patchen acted as reviewers for the authors; their criticism is especially appreciated. Mr. Charles Muirhead, Chief CSB, accommodated the NOS SPR Support Project Manager in various ways on numerous occasions. Messrs. Bernard Gotholm and Michael Connolly, CSB, were particularly helpful in the processing and analysis of data. Mrs. Su Lin Cheng and Ms. Cheryl Hughes, Optimum Systems, Inc., provided invaluable assistance in software development and data processing.

Dr. Robert Williams, NOAA Environmental Data and Information Service, acted as a reviewer for both the NOS Project Manager and the NOAA Program Manager. Dr. Joel Solomon, Director, Engineering Support Office also reviewed the draft manuscript and provided helpful suggestions.

Ms. Janet Springsteen coordinated word processing and performed technical editing with skill and professionalism. Mr. Thomas Allen coordinated the layout and production of the final graphic artwork from original graphs and sketches. Draft sections were typed by Mmes. Sondra Burman, Carol Goldstein, Ms. Tiyo Fonte, and Ms. Darice Ginn. Mrs. Elsa Bennett prepared the final copy.

LIST OF FIGURES

Figure		Page
1-1.	Proposed West Hackberry and Weeks Island brine disposal sites and the FERREL's trackline stations	25
1-2.	Measurement configuration	28
1-3.	Platform/mooring system	30
1-4.	GASP Experiment configuration	32
2-1.	Air temperature departure from 30-year mean for summer 1978	37
2-2.	Total and percentage of normal precipitation for summer 1978	38
2-3.	Air temperature departure from 30-year mean for fall 1978	39
2-4.	Total and percentage of normal precipitation for fall 1978	40
2-5.	Air temperature departure from 30-year mean for winter 1979	41
2-6.	Total and percentage of normal precipitation for winter 1979	42
2-7.	Air temperature departure from 30-year mean for spring 1979	43
2-8.	Total and percentage of normal precipitation for spring 1979	44
2-9.	Monthly mean discharges for the Mississippi and Atchafalaya Rivers, and the sum of the mean discharges from all rivers west of the Atchafalaya to the Rio Grande	46
3-1.	Comparison of spectral and zero-crossing methods for determining significant wave height	52
4-1.	DO areal averages and ranges at West Hackberry site, 1 m below sea surface	61
4-2.	DO areal averages and ranges at West Hackberry site, midwater	62
4-3.	DO areal averages and ranges at West Hackberry site, 1 m above sea floor	62
4-4.	DO spatial distributions at West Hackberry site, June and July 1978	65
4-5.	DO spatial distributions at West Hackberry site, October 1978 to January 1979	66
4-6.	DO spatial distributions at West Hackberry site, January to March 1979	67

Figure		Page
4-7.	DO spatial distributions at West Hackberry site, April to June 1979.	68
5-1.	Temperature vs. salinity (T-S) diagrams for CTD casts made at West Hackberry stations 11 through 14	74
5-2.	Temperature vs. salinity (T-S) diagrams for CTD casts made at West Hackberry stations 15 through 17	75
5-3.	Monthly mean temperature for station 11 at 1 m and 3 m above bottom from June 1978 through May 1979.	77
5-4.	Instantaneous values of (a) near-surface temperature (b) salinity at station 11 from June 3, 1978, June 2, 1979	78
5-5.	Monthly mean fresh water discharge for the Mississippi River at Baton Rouge, La..	79
5-6.	Fresh water discharge for the Atchafalaya River at (a) Sims Port, La. (mean) and (b) Morgan City, La. (daily discharge)	80
5-7.	Monthly mean fresh water discharges for Sabine and Calcasieu Lakes	81
5-8.	Salinity contours at West Hackberry for June 27, 1978	83
5-9.	Sigma-t contours at West Hackberry for June 27, 1978.	84
5-10.	Salinity contours at West Hackberry for July 26-27, 1979.	85
5-11.	Sigma-t contours at West Hackberry for July 26-27, 1978	86
5-12.	Salinity contours at West Hackberry for October 3, 1978	88
5-13.	Sigma-t contours at West Hackberry for October 3, 1978.	89
5-14.	Salinity contours at West Hackberry for October 31, 1978.	90
5-15.	Sigma-t contours at West Hackberry for October 31, 1978	91
5-16.	Salinity contours at West Hackberry for November 14, 1978	92
5-17.	Sigma-t contours at West Hackberry for November 14, 1978.	93
5-18.	Salinity contours at West Hackberry for January 9-10, 1979. . . .	95
5-19.	Sigma-t contours at West Hackberry for January 9-10, 1979	96
5-20.	Salinity contours at West Hackberry for June 2, 1979.	98
5-21.	Sigma-t contours at West Hackberry for June 2, 1979	99

Figure		Page
6-1.	Mean monthly air temperature at Lake Charles Airport.	101
6-2.	Time histories of meteorological data at station 18 for July 27 to September 3, 1978 and January 31 to February 21, 1979. . . .104,105	
6-3.	Time histories of meteorological data at station 18 for April 26 to June 1, 1979 106,107	
6-4.	Spectral density of wind at station 18 from (a) August 3-26, 1978, (b) January 31 to February 20, 1979	108
6-5.	Spectral density of wind at station 18 from May 9 to June 1, 1979	109
8-1.	Areal extent of tide types from Hicks (1977).	120
8-2.	Time series plots of West Hackberry water level fluctuations. . .	120
8-3.	Cotidal lines for M_2 based on Harris (1904)	125
8-4.	Time series plots of observations, predictions, and residuals for summer (June-July).	126
8-5.	Time series plots of observations, predictions, and residuals for winter (January-March).	127
8-6.	Spectral analysis of residuals from summer period	128
8-7.	Spectral analysis of residuals from winter period	128
8-8.	Frequency distribution of residuals during summer (June-July) . .	130
8-9.	Frequency distribution of residuals during winter (January-February)	130
8-10.	An example of a winter storm's effect on water level, January 1979	131
9-1.	Summary of relative volume transport in the alongshore and transhore quadrants at stations 11 and 13 through 15 at 1 m above the bottom.	137
9-2.	Summary of relative volume transport in the alongshore and transhore quadrants at stations 11 and 13 through 15 at 3 m above the bottom.	138
9-3.	Calculated tidal currents at station 11, 1 m above bottom (a) August 3-18, 1978, and (b) May 9-24, 1979	141
9-4.	Calculated tidal currents at station 11, 1 m above bottom (a) October 3 to November 1, 1978, and (b) February 1 to March 1, 1979	142

Figure		Page
9-5.	Tidal current ellipses for current series starting June 2, 1978, (a) 3 m above bottom and (b) 1 m above bottom for the M_2 constituents; (c) 3 m above bottom and (d) 1 m above bottom for the K_1 constituents.	143
9-6.	Tidal current ellipses for current series starting January 31, 1979, (a) 3 m above bottom and (b) 1 m above bottom for the M_2 constituents; (c) 3 m above bottom and (d) 1 m above bottom for the K_1 constituents	144
9-7.	Tidal current ellipticity and major axis orientation for the (a) M_2 and (b) K_1 constituents at the station 11 1-m level. . . .	146
9-8.	Tidal current ellipticity and major axis orientation for the (a) M_2 and (b) K_1 constituents at the station 11 3-m level. . . .	147
9-9.	Vertical profiles of currents at West Hackberry station 11, April 6, 1979	150
9-10.	Vertical profiles of currents at West Hackberry station 11, April 7, 1979	151
9-11.	Vertical profiles of currents at West Hackberry station 11, April 8, 1979	152
9-12.	Vertical profiles of currents at West Hackberry station 11, April 9, 1979	153
9-13.	Vertical profiles of currents at West Hackberry station 11, April 16, 1979.	154
9-14.	Vertical profiles of currents at West Hackberry station 11, April 26, 1979.	155
9-15.	Vertical profiles of currents at West Hackberry station 11, April 27, 1979.	165
9-16.	Current energy spectrum at West Hackberry site (a) station 15 3-m June 2-27, 1978, and (b) station 15 3-m August 3-26, 1978	167
9-17.	(a) Cross-spectra and (b) squared coherence of winds at station 18 and 1-m level currents at station 11, August 3-26, 1978	169
9-18.	Current energy spectrum at West Hackberry site (a) station 11 3-m October 3 to November 14, 1978, and (b) station 11 1-m January 31 to February 20, 1979.	171
9-19.	(a) Cross-spectra and (b) squared coherence of winds at West Hackberry station 18 and 1-m level currents at station 11, January 31 to February 20, 1979	172

Figure		Page
9-20.	Current energy spectrum at West Hackberry site (a) station 14 3-m February 23 to March 13, 1979, and (b) station 11 3-m May 9 to June 1, 1979.	173
9-21.	(a) Cross-spectra and (b) squared coherence of winds at West Hackberry site station 18 and 3-m level currents at station 11, May 9 to June 1, 1979	175
10-1.	DO areal averages and ranges at Weeks Island site, 1 m below sea surface	178
10-2.	DO areal averages and ranges at Weeks Island site, midwater . . .	178
10-3.	DO areal averages and ranges at Weeks Island site, 1 m above sea floor	179
10-4.	Spatial distributions for DO at Weeks Island site, June through July, 1978.	181
10-5.	Spatial distributions for DO at Weeks Island site, September through November, 1978.	182
10-6.	Spatial distributions for DO at Weeks Island site, January through February, 1979.	183
10-7.	Spatial distributions for DO at Weeks Island site, March through May, 1979	184
10-8.	Spatial distributions for DO at Weeks Island site, June 1979. . .	185
11-1.	Temperature vs. salinity (T-S) diagrams for CTD casts made at Weeks Island stations 21 through 24	188
11-2.	Temperature vs. salinity (T-S) diagrams for CTD casts made at Weeks Island stations 25 through 27	189
11-3.	Monthly mean temperature for station 21 at 1 and 3 m above bottom from July 1978 through May 1979	190
11-4.	Instantaneous values of (a) near-surface temperature and (b) salinity at station 21 from June 3, 1978, to June 2, 1979, 1 m below the surface	192
11-5.	Salinity (ppt) contours at Weeks Island for July 1, 1978.	193
11-6.	Sigma-t (g/cm^3) contours at Weeks Island for July 1, 1978	194
11-7.	Salinity (ppt) contours at Weeks Island for July 21, 1978	195
11-8.	Sigma-t (g/cm^3) contours at Weeks Island for July 21, 1978. . . .	196

Figure		Page
11-9.	Salinity (ppt) contours at Weeks Island for October 2 and 3, 1978	198
11-10.	Sigma-t (g/cm^3) contours at Weeks Island for October 2 and 3, 1978	199
11-11.	Salinity (ppt) contours at Weeks Island for January 6, 1979 . . .	201
11-12.	Sigma-t (g/cm^3) contours at Weeks Island for January 6, 1979. . .	202
11-13.	Salinity (ppt) contours at Weeks Island for June 2, 1979.	204
11-14.	Sigma-t (g/cm^3) contours at Weeks Island for June 2, 1979	205
12-1.	Time histories of meteorological data at station 28 for October 3 to November 11, and November 12 to December 10, 1978.	.208,209
12-2.	Time histories of meteorological data at station 28 for January 30 to February 22, and February 23 to March 12, 1979	.210,211
12-3.	Time histories of meteorological data at station 28 for March 29 to April 17, and May 22 to June 2, 1979	212
12-4.	Spectral density of wind at station 28 from (a) October 2 through 30, and (b) October 30 to December 12, 1978	216
12-5.	Spectral density of wind at station 28 from (a) January 29 to February 23, and (b) February 23 to March 12, 1979.	217
12-6.	Spectral density of wind at station 28 from (a) March 28 to April 17, and (b) May 21 to June 2, 1979.	218
14-1.	Areal extent of tide types from Hicks (1977).	229
14-2.	Time series plot of Weeks Island water level fluctuations	231
14-3.	Cotidal lines for M_2 based on Harris (1904)	232
14-4.	Frequency distribution of residuals at Weeks Island	234
15-1.	Summary of the percentage of relative volume transport in the alongshore and transhore quadrants at stations 21 and 23 through 25 at 1 m above the bottom.	239
15-2.	Summary of the percentage of relative volume transport in the alongshore and transhore quadrants at stations 21 and 23 through 25 at 3 m above the bottom.	240
15-3.	Calculated tidal currents at Weeks Island site, 1 m above bottom (a) station 23, June 2 through 30, 1978, and (b) station 21, October 31 to November 28, 1978	243

Figure		Page
15-4.	Calculated tidal currents at Weeks Island site, 1 m above bottom (a) station 21, February 11 to March 12, 1979, and (b) station 25, April 8 to May 7, 1979.	244
15-5.	Tidal current ellipses for current series starting June 29 for station 23, June 30 for station 25, and July 1, 1978, for stations 21, 22, and 24: (a) 3 m above bottom and (b) 1 m above bottom for the M_2 constituents (c) 3 m above bottom and (d) 1 m above bottom for the K_1 constituents	245
15-6.	Tidal current ellipses for current series starting February 20 for stations 21 and 23, and February 22, 1979, for station 24, (a) 3 m above bottom and (b) 1 m above bottom for the M_2 constituents; (c) 3 m above bottom and (d) 1 m above bottom for the K_1 constituents.	245
15-7.	Tidal current ellipticity and major axis orientation for the (a) M_2 and (b) K_1 constituents at station 21 1 m above the bottom. . . .	247
15-8.	Tidal current ellipticity and major axis orientation for the (a) M_2 and (b) K_1 constituents at station 21 3 m above the bottom. . . .	248
15-9.	Current vectors at 6-hour intervals, 1 m above bottom at Weeks Island site, July 6, 1978	250
15-10.	Current vectors at 6-hour intervals, 1 m above bottom at Weeks Island site, July 7, 1978	251
15-11.	Current vectors at 6-hour intervals, 1 m above bottom at Weeks Island site, February 25, 1979.	252
15-12.	Vertical profiles of currents at Weeks Island site station 21, February 25, 1979	253
15-13.	Current vectors at 6-hour intervals, 1 m above bottom at Weeks Island site, February 26, 1979.	254
15-14.	Vertical profiles of currents at Weeks Island site station 21, February 26, 1979	255
15-15.	Current vectors at 6-hour intervals, 1 m above bottom at Weeks Island February 27, 1979.	256
15-16.	Vertical profiles of currents at Weeks Island site station 21, February 27, 1979	257
15-17.	Current vectors at 6-hour intervals, 1 m above bottom at Weeks Island site, February 28, 1979.	258
15-18.	Vertical profiles of currents at Weeks Island site station 21, February 28, 1979	259

Figure		Page
15-19.	Current vectors at 6-hour intervals, 1 m above bottom at Weeks Island site, March 1, 1979.	260
15-20.	Vertical profiles of currents at Weeks Island site station 21, March 1, 1979	261
15-21.	Vertical profiles of currents at Weeks Island site station 21, March 11, 1979.	262
15-22.	Vertical profiles of currents at Weeks Island site station 21, March 12, 1979.	263
15-23.	Vertical profiles of currents at Weeks Island site station 21, March 13, 1979.	264
15-24.	Vertical profiles of currents at Weeks Island site station 21, March 14, 1979.	265
15-25.	Current energy spectral density at Weeks Island site (a) station 23 1 m above bottom July 1 to 28, 1978, and (b) station 21 1 m above bottom July 28 to August 8, 1978.	268
15-26.	Current energy spectral density at Weeks Island site (a) station 21 1 m above bottom October 2 to 30, 1978, and (b) station 21 1 m above bottom October 30 to December 10, 1978.	271
15-27.	(a) Cross-spectra and (b) squared coherence of winds at Weeks Island site station 28 and currents 1 m above bottom at station 21 from October 30 to December 10, 1978.	272
15-28.	Current energy spectral density at Weeks Island site (a) station 21 1 m above bottom January 6 to 21, 1979, and (b) station 21 1 m above bottom January 29 to February 23, 1979.	273
15-29.	(a) Cross-spectra and (b) squared coherence of winds at Weeks Island site station 28 and currents 1 m above bottom at station 21 from January 29 to February 23, 1979	275
15-30.	Current energy spectral density at Weeks Island site (a) station 21 1 m above bottom March 28 to April 17, 1979, and (b) station 21 1 m above bottom May 7 to 21, 1979.	276
15-31.	(a) Cross-spectra and (b) squared coherence of winds at Weeks Island site station 28 and currents 1 m above bottom at station 21 from March 28 to April 17, 1979	277
17-1.	Temperature vs. salinity (T-S) diagrams for CTD casts made at trackline stations 20 through 40.	284
18-1.	Daily surface weather map for August 27, 1978	291

Figure		Page
18-2.	Daily surface weather map for August 28, 1978	292
18-3.	Daily surface weather map for August 29, 1978	293
18-4.	GOES 2 satellite photograph of Tropical Storm DEBRA at 1931 GMT on August 28, with 0.93-km resolution	295
18-5.	National Hurricane Center's track line and the least-squares third-order fit for Tropical Storm DEBRA from August 26-29, 1978.	296
18-6.	Meteorological data obtained at station 18 August 27-29 during Tropical Storm DEBRA.	298
18-7.	Current meter data obtained at station 11 August 27-29, 1 m above bottom during Tropical Storm DEBRA.	299
18-8.	Current meter data obtained at station 11 August 27-29, 3 m above bottom during Tropical Storm DEBRA.	300
18-9.	Current meter data obtained at station 14 August 27-29, 1 m above bottom during Tropical Storm DEBRA.	301
18-10.	Maximum and significant wave heights obtained at station 11 August 27-29, during Tropical Storm DEBRA	302
19-1.	Meteorological time series at West Hackberry station 19, January 9-31, 1979.	306
19-2.	Meteorological time series at Lake Charles Airport, January 19-28, 1979.	307
19-3.	Surface weather map for January 12, 1979.	308
19-4.	Surface weather map for January 13, 1979.	309
19-5.	Surface weather map for January 21, 1979.	310
19-6.	Surface weather map for January 23, 1979.	311
19-7.	Currents 1 m above bottom at West Hackberry station 11, January 10-15, 1979	313
19-8.	Currents 1 m above bottom and waves at West Hackberry station 11, January 19-27, 1979	314
19-9.	Water levels at West Hackberry station 11, January 10 to March 11, 1979.	315
19-10.	Current vectors at 6-hour intervals, 1 m above bottom at West Hackberry site, February 25, 1979	316

Figure		Page
19-11.	Current vectors at 6-hour intervals, 3 m above bottom at West Hackberry site, February 25, 1979	317
20-1.	Surface weather map for April 10, 1979, at 1100 GMT	321
20-2.	Surface weather map for April 11, 1979, at 1100 GMT	322
20-3.	Surface weather map for April 12, 1979, at 1100 GMT	323
20-4.	Scatter diagrams of 1-hour vector-averaged speeds for instrument pairs at the 3-m level during 20 days of the GASP Experiment.	324
20-5.	Wind speed and direction (+15.8 m), oscillating current speed (+3 m), and wave height during the first 20 days of the GASP Experiment.	325
20-6.	Currents measured at 3-m level with a Grundy Model 9021 current meter during the GASP Experiment.	326
20-7.	Sixty consecutive 1-second velocity samples illustrate typical 1-hour burst-mode data obtained with NBIS (732) instrument at 3-m level	327
20-8.	Flow signal-to-noise (S/N) ratio for the first 20 days of the GASP Experiment.	328
20-9.	Progressive vector diagrams of currents during GASP Experiment.	329
20-10.	Current vectors at 6-hour intervals, 1 m above bottom at West Hackberry site, April 11, 1979.	330
20-11.	Current vectors at 6-hour intervals, 3 m above bottom at West Hackberry site, April 11, 1979.	331
20-12.	Current vectors at 6-hour intervals, 4 m above bottom at West Hackberry site, April 11, 1979.	332
20-13.	Current vectors at 6-hour intervals, 1 m above bottom at West Hackberry site, April 12, 1979.	333
20-14.	Current vectors at 6-hour intervals, 3 m above bottom at West Hackberry site, April 12, 1979.	334
20-15.	Current vectors at 6-hour intervals, 4 m above bottom at West Hackberry site, April 12, 1979.	335
20-16.	Vertical profiles of currents at West Hackberry station 11, April 11-12, 1979	336
C-1.	Vertical profiles of temperature, salinity, and sigma-t for June 27, 1978, at stations 11 through 14.	C-2

Figure		Page
C-2.	Vertical profiles of temperature, salinity, and sigma-t for June 27, 1978, at stations 16 and 17.	C-3
C-3.	Vertical profiles of temperature, salinity, and sigma-t for July 26-27, 1978, at stations 11 through 14	C-4
C-4.	Vertical profiles of temperature, salinity, and sigma-t for July 26-27, 1978, at stations 15 and 17	C-5
C-5.	Vertical profiles of temperature, salinity, and sigma-t for October 3, 1978, at stations 11 through 13 and 16	C-6
C-6.	Vertical profiles of temperature, salinity, and sigma-t for October 3, 1978, at station 17.	C-7
C-7.	Vertical profiles of temperature, salinity, and sigma-t for October 31, 1978, at stations 11 through 14.	C-8
C-8.	Vertical profiles of temperature, salinity, and sigma-t for October 31, 1978, at stations 15 and 16	C-9
C-9.	Vertical profiles of temperature, salinity, and sigma-t for November 14, 1978, at stations 11, 12, 14, and 15	C-10
C-10.	Vertical profiles of temperature, salinity, and sigma-t for November 14, 1978, at stations 16 and 17.	C-11
C-11.	Vertical profiles of temperature, salinity, and sigma-t for January 10, 1979, at stations 11 through 14	C-12
C-12.	Vertical profiles of temperature, salinity, and sigma-t for January 9-10, 1979, at stations 15 and 16	C-13
C-13.	Vertical profiles of temperature, salinity, and sigma-t for June 2, 1979, at stations 11 through 13 and 15.	C-14
C-14.	Vertical profiles of temperature, salinity, and sigma-t for June 2, 1979, at stations 16 and 17	C-15
D-1.	Time series of current meter data at station 11, 3 m above bottom, for August 3 to August 29, 1978, and October 4 to October 31, 1978.	D-2
D-2.	Times series of current meter data at station 11, 3 m above bottom, for November 1 to November 14, 1978, and November 15 to December 7, 1978.	D-4,D-5
D-3.	Time series of current meter data at station 11, 3 m above bottom, for December 7, 1978, to January 7, 1979, and January 31 to February 19, 1979.	D-6,D-7

Figure — Page

D-4. Time series of current meter data at station 11, 3 m above bottom, for February 21 to March 18, 1979, and April 4 to April 28, 1979. . . . . D-8,D-9

D-5. Time series of current meter data at station 11, 3 m above bottom, for May 8 to May 31, 1979 . . . . . D-10,D-11

E-1. Relative volume transports at West Hackberry site for June 2 to August 2, 1978. . . . . E-2

E-2. Relative volume transports at West Hackberry site for August 3 to October 3, 1978 . . . . . E-3

E-3. Relative volume transports at West Hackberry site for October 3 to November 14, 1978. . . . . E-4

E-4. Relative volume transports at West Hackberry site for November 14, 1978 to January 9, 1979 . . . . . E-5

E-5. Relative volume transports at West Hackberry site for January 9 to February 21, 1979. . . . . E-6

E-6. Relative volume transports at West Hackberry site for February 21 to April 4, 1979. . . . . E-7

E-7. Relative volume transports at West Hackberry site for April 4 to June 1, 1979. . . . . E-8

E-8. Current vectors at 6-hour intervals, 1 m above bottom at West Hackberry site, June 5, 1978. . . . . E-9

E-9. Current vectors at 6-hour intervals, 1 m above bottom at West Hackberry site, June 6, 1978. . . . . E-10

E-10. Current vectors at 6-hour intervals, 1 m above bottom at West Hackberry site, June 9, 1978. . . . . E-11

E-11. Current vectors at 6-hour intervals, 3 m above bottom at West Hackberry site, June 9, 1978. . . . . E-12

E-12. Current vectors at 6-hour intervals, 1 m above bottom at West Hackberry site, June 10, 1978 . . . . . E-13

E-13. Current vectors at 6-hour intervals, 3 m above bottom at West Hackberry site, June 10, 1978 . . . . . E-14

E-14. Current vectors at 6-hour intervals, 3 m above bottom at West Hackberry site, June 18, 1978 . . . . . E-15

E-15. Current vectors at 6-hour intervals, 3 m above bottom at West Hackberry site, June 19, 1978 . . . . . E-16

Figure | Page

E-16. Current vectors at 6-hour intervals, 1 m above bottom at West Hackberry site, June 28, 1978 . . . . . E-17

E-17. Current vectors at 6-hour intervals, 1 m above bottom at West Hackberry site, June 29, 1978 . . . . . E-18

E-18. Current vectors at 6-hour intervals, 1 m above bottom at West Hackberry site, July 7, 1978. . . . . E-19

E-19. Current vectors at 6-hour intervals, 1 m above bottom at West Hackberry site, July 23, 1978 . . . . . E-20

E-20. Current vectors at 6-hour intervals, 1 m above bottom at West Hackberry site, July 24, 1978 . . . . . E-21

E-21. Current vectors at 6-hour intervals, 3 m above bottom at West Hackberry site, November 3, 1978. . . . . E-22

E-22. Current vectors 3 m above bottom at West Hackberry site, 0000 GMT, November 4, 1978. . . . . E-23

E-23. Current vectors at 6-hour intervals, 3 m above bottom at West Hackberry site, November 6, 1978. . . . . E-24

E-24. Current vectors at 6-hour intervals, 3 m above bottom at West Hackberry site, November 7, 1978. . . . . E-25

E-25. Current vectors at 6-hour intervals, 1 m above bottom at West Hackberry site, February 2, 1979. . . . . E-26

E-26. Current vectors at 6-hour intervals, 3 m above bottom at West Hackberry site, February 2, 1979. . . . . E-27

E-27. Current vectors at 6-hour intervals, 1 m above bottom at West Hackberry site, February 5, 1979. . . . . E-28

E-28. Current vectors at 6-hour intervals, 3 m above bottom at West Hackberry site, February 5, 1979. . . . . E-29

E-29. Current vectors at 6-hour intervals, 1 m above bottom at West Hackberry site, February 8, 1979. . . . . E-30

E-30. Current vectors at 6-hour intervals, 3 m above bottom at West Hackberry site, February 8, 1979. . . . . E-31

E-31. Current vectors at West Hackberry site, 1 m and 3 m above bottom at 0000 GMT, February 9, 1979 . . . . . E-32

E-32. Current vectors at 6-hour intervals, 1 m above bottom at West Hackberry site, February 15, 1979 . . . . . E-33

Figure

E-33. Current vectors at 6-hour intervals, 3 m above bottom at West Hackberry site, February 15, 1979 . . . . . E-34

E-34. Current vectors at 6-hour intervals, 1 m above bottom at West Hackberry site, February 23, 1979 . . . . . E-35

E-35. Current vectors at 6-hour intervals, 3 m above bottom at West Hackberry site, February 23, 1979 . . . . . E-36

E-36. Current vectors at 6-hour intervals, 1 m above bottom at West Hackberry site, March 2, 1979 . . . . . E-37

E-37. Current vectors at 6-hour intervals, 3 m above bottom at West Hackberry site, March 2, 1979 . . . . . E-38

E-38. Current vectors at 6-hour intervals, 1 m above bottom at West Hackberry site, March 7, 1979 . . . . . E-39

E-39. Current vectors at 6-hour intervals, 3 m above bottom at West Hackberry site, March 7, 1979 . . . . . E-40

E-40. Current vectors at 6-hour intervals, 1 m above bottom at West Hackberry site, April 7, 1979 . . . . . E-41

E-41. Current vectors at 6-hour intervals, 3 m above bottom at West Hackberry site, April 7, 1979 . . . . . E-42

E-42. Current vectors at 6-hour intervals, 4 m above bottom at West Hackberry site, April 7, 1979 . . . . . E-43

E-43. Current vectors at 6-hour intervals, 1 m above bottom at West Hackberry site, April 8, 1979 . . . . . E-44

E-44. Current vectors at 6-hour intervals, 3 m above bottom at West Hackberry site, April 8, 1979 . . . . . E-45

E-45. Current vectors at 6-hour intervals, 4 m above bottom at West Hackberry site, April 8, 1979 . . . . . E-46

E-46. Current vectors at 6-hour intervals, 1 m above bottom at West Hackberry site, April 25, 1979. . . . . E-47

E-47. Current vectors at 6-hour intervals, 3 m above bottom at West Hackberry site, April 25, 1979. . . . . E-48

E-48. Current vectors at 6-hour intervals, 4 m above bottom at West Hackberry site, April 25, 1979. . . . . E-49

E-49. Current vectors at 6-hour intervals, 1 m above bottom at West Hackberry site, April 26, 1979. . . . . E-50

Figure		Page
E-50.	Current vectors at 6-hour intervals, 3 m above bottom at West Hackberry site, April 26, 1979.	E-51
E-51.	Current vectors at 6-hour intervals, 4 m above bottom at West Hackberry site, April 26, 1979.	E-52
F-1.	Vertical profiles of temperature, salinity, and sigma-t for July 1, 1978, at stations 21 through 24	F-2
F-2.	Vertical profiles of temperature, salinity, and sigma-t for July 1, 1978, at stations 25 and 26	F-3
F-3.	Vertical profiles of temperature, salinity, and sigma-t for July 21, 1978, at stations 21, 23, 24, and 25	F-4
F-4.	Vertical profiles of temperature, salinity, and sigma-t for July 21, 1978, at station 26.	F-5
F-5.	Vertical profiles of temperature, salinity, and sigma-t for September 8, 1978, at stations 21 through 24.	F-6
F-6.	Vertical profiles of temperature, salinity, and sigma-t for September 8, 1978, at stations 25 and 26.	F-7
F-7.	Vertical profiles of temperature, salinity, and sigma-t for October 2-3, 1978, at stations 21 through 24.	F-8
F-8.	Vertical profiles of temperature, salinity, and sigma-t for October 2-3, 1978, at stations 25 and 27.	F-9
F-9.	Vertical profiles of temperature, salinity, and sigma-t for November 1, 1978, at stations 21 through 24	F-10
F-10.	Vertical profiles of temperature, salinity, and sigma-t for November 1, 1978, at stations 25 and 27	F-11
F-11.	Vertical profiles of temperature, salinity, and sigma-t for November 13-14, 1978, at stations 21 through 24	F-12
F-12.	Vertical profiles of temperature, salinity, and sigma-t for November 13, 1978, at stations 26 and 27.	F-13
F-13.	Vertical profiles of temperature, salinity, and sigma-t for December 12, 1978, at stations 21, 24, 25, and 26	F-14
F-14.	Vertical profiles of temperature, salinity, and sigma-t for December 12, 1978, at station 27.	F-15
F-15.	Vertical profiles of temperature, salinity, and sigma-t for January 6, 1979, at stations 21 through 24.	F-16

Figure — Page

F-16. Vertical profiles of temperature, salinity, and sigma-t for January 6, 1979, at stations 25 and 26. . . . . F-17

F-17. Vertical profiles of temperature, salinity, and sigma-t for June 2, 1979, at stations 21 through 24 . . . . . F-18

F-18. Vertical profiles of temperature, salinity, and sigma-t for June 2, 1979, at stations 25 and 27 . . . . . F-19

G-1. Time series of current meter data at station 21, 3 m above bottom, for July 1-21, and September 9-15, 1978 . . . . . G-2,G-3

G-2. Time series of current meter data at station 21, 3 m above bottom, for September 17 to October 2 and October 3-30, 1978. . . . . G-4,G-5

G-3. Time series of current meter data at station 21, 3 m above bottom, for October 31 to November 13, 1978, and January 7-21, 1979 . . . G-6

G-4. Time series of current meter data at station 21, 3 m above bottom, for February 21 to March 10 and March 13-26, 1979 . . . . . G-7

G-5. Time series of current meter data at station 21, 3 m above bottom, for April 17 to May 2 and May 22 to June 1979 . . . . . G-8

H-1. Relative volume transports at Weeks Island site for June 1 to July 28, 1978 . . . . . H-2

H-2. Relative volume transports at Weeks Island site for July 28 to September 15, 1978. . . . . H-3

H-3. Relative volume transports at Weeks Island site for September 16 to October 30, 1978. . . . . H-4

H-4. Relative volume transports at Weeks Island site for October 30 to December 11, 1978 . . . . . H-5

H-5. Relative volume transports at Weeks Island site for December 10, 1978, to January 21, 1979 . . . . . H-6

H-6. Relative volume transports at Weeks Island site for January 29 to March 14, 1979. . . . . H-7

H-7. Relative volume transports at Weeks Island site for March 12 to April 17, 1979. . . . . H-8

H-8. Relative volume transports at Weeks Island site for April 17 to May 21, 1979. . . . . H-9

H-9. Relative volume transports at Weeks Island site for May 21 to June 3, 1979. . . . . H-10

Figure		Page
I-1.	Vertical profiles of temperature, salinity, and sigma-t for June 26 and July 27, 1978, at stations 30 and 40.	I-2
I-2.	Vertical profiles of temperature, salinity, and sigma-t for October 1978 at stations 20 through 40.	I-3
I-3.	Vertical profiles of temperature, salinity, and sigma-t for October 31 through November 1, 1978, at stations 20 through 30. .	I-4
I-4.	Vertical profiles of temperature, salinity, and sigma-t for November 14, 1978, at stations 20 through 40.	I-5
I-5.	Vertical profiles of temperature, salinity, and sigma-t for June 2, 1979, at stations 20 through 40	I-6

LIST OF TABLES

Table		Page
1-1.	Measurement station positions	29
2-1.	Approximate monthly frequency of frontal passages across the Louisiana shelf from 1965 to 1972	35
3-1.	Summary of total measurement uncertainties (TMU)	48
6-1.	Air temperature differential between station 18 and Lake Charles Airport	102
7-1.	Statistical summary of significant wave heights at the West Hackberry site	112
7-2.	Statistical summary of the periods of peak energy at the West Hackberry site	113
8-1.	Monthly means of water levels and ranges at the West Hackberry site	121
8-2.	Six-month mean of water levels and ranges at the West Hackberry site and historical values for Calcasieu Pass	121
8-3.	Results of 29-day harmonic analysis of water levels at the West Hackberry site	122
8-4.	Means of principal harmonic constants at the West Hackberry site and accepted values for Calcasieu Pass (1933-34)	124
8-5.	Monthly Greenwich intervals from 29-day harmonic analysis for the West Hackberry site	124
8-6.	Means of Greenwich intervals for the West Hackberry site and accepted values for Calcasieu and Galveston, Texas	125
8-7.	Results of 29-day harmonic analysis of West Hackberry residuals	131
9-1.	Mean speed and standard deviation of currents at the West Hackberry site	134
9-2.	Mean speed and standard deviation of currents at the West Hackberry site	135
9-3.	Coherency squared for currents and water levels at the diurnal and semidiurnal frequencies at the West Hackberry site	168
12-1.	Air temperature at station 28	213
13-1.	Statistical summary of significant wave heights at the Weeks Island site	222

Table		Page
14-1.	Mean water levels and ranges Weeks Island, Rabbit Island, and Eugene Island.	230
14-2.	Results of 29-day and 15-day harmonic analysis of Weeks Island and accepted values for Rabbit Island and Eugene Island	230
14-3.	Greenwich intervals for Weeks Island, Rabbit Island, and Eugene Island.	232
14-4.	Results of 29-day harmonic analysis of Weeks Island residuals	233
15-1.	Mean speed and standard deviation (cm/s) for currents at the Weeks Island site, 1 m above bottom	236
15-2.	Mean speed and standard deviation (cm/s) for currents at the Weeks Island site, 3 m above bottom	237
15-3.	Coherency squared for currents and water levels at the diurnal and semidiurnal frequencies	269
16-1.	Near-surface and near-bottom values of DO at trackline stations	280
17-1.	Near-surface and near-bottom values of salinity at trackline stations.	285
20-1.	Total Measurement Uncertainties for GASP Experiment current meters (at 16 cm/s).	320

ABBREVIATIONS USED

ASCII	American standard code for information interchange
AMI	Applied Microsystems, Incorporated
BCD	Binary coded decimal
BPI	Bits per inch (magnetic tape packing density)
CCIW	Canada Center for Inland Waters
CEAS	Center for Environmental Assessment Services (NOAA)*
Cl	Chlorinity
CL	Confidence level
CM	Current meter
cm/s	Centimeters per second
cP	Continental polar (air)
CPD	Cycles per day
CTD	Conductivity - temperature - depth
DHQ	Diurnal high water inequality
DLQ	Diurnal low water inequality
DO	Dissolved oxygen
DOE	Department of Energy
DQA	Data quality assurance
DT-NSRDC	David Taylor - Naval Ship Research and Development Center
ECU	Estimated calibration uncertainty
EDIS	Environmental Data and Information Service
EDL	Engineering Development Laboratory (NOS)*
EST	Eastern Standard Time
FFT	Fast Fourier Transformation
FM	Frequency modulation
FSR	Full scale reading
GASP	Gulf At-Sea Performance (Experiment)
GCLW	Gulf Coast Low Water
GMT	Greenwich Mean Time
Gt	Greater diurnal range

---

* NOAA organizations as of March 1, 1980

HP	Hewlett - Packard
I&A	Inspection and acceptance
IAPSO	International Association of Physical Sciences of the Ocean
IC	Integrated circuit
ID	Identification
I/O	Input/output
LED	Light emitting diode
LSD	Least significant digit
m/s	Meters per second
MHHW	Mean Higher High Water
MHW	Mean High Water
ml/l	Milliliters per liter
MLLW	Mean Lower Low Water
MLW	Mean Low Water
MMI	Marsh - McBirney, Incorporated
Mn	Mean range
MSD	Most significant digit
mT	Maritime tropical (air)
N/A	Not applicable
NAVOCEANO	U.S. Naval Oceanographic Office
NBIS	Neil Brown Instrument Systems, (Incorporated)
NBS	National Bureau of Standards
NMFS	National Marine Fisheries Service (NOAA)*
NOAA	National Oceanic and Atmospheric Administration
NODC	National Oceanographic Data Center (NOAA)*
NOS	National Ocean Survey (NOAA)*
NSTL	National Space Technology Laboratories
NSWC	U.S. Naval Surface Weapons Center
OMT	Office of Marine Technology (NOS)*
OOE	Office of Ocean Engineering (NOAA)*
OSI	Optimum Systems, Incorporated
PMEL	Pacific Marine Environmental Laboratory (NOAA)*

---

* NOAA organizations as of March 1, 1980

ppm	Parts per million
ppt	Parts per thousand
PVC	Polyvinyl chloride
RL	Rejection level
RMS	Root-mean-square
ROM	Read only memory
RSE	Residual standard error
SMU	Sensor measurement uncertainty
SN	Serial number
S/N	Signal to noise
SPR	Strategic Petroleum Reserve
T S	Temperature versus salinity
T&EL	Test and Evaluation Laboratory (NOAA)*
TMU	Total measurement uncertainty
TSU	Total systematic uncertainty
UNESCO	United Nations Educational, Scientific, and Cultural Organization
VPMM	Vertical planar motion mechanism
YSI	Yellow Springs Instruments Company

---

* NOAA organizations as of March 1, 1980

CONCLUSIONS AND SUMMARY

The National Ocean Survey (NOS) Strategic Petroleum Reserve (SPR) Support Project was a cooperative, reimbursable project carried out in collaboration with the NOAA Environmental Data and Information Service (EDIS) in response to Department of Energy (DOE) requirements. DOE is implementing the Strategic Petroleum Reserve by storing crude oil in underground salt domes beneath Texas and Louisiana near the Gulf of Mexico coast. Since the present capacity of existing caverns in the salt domes is insufficient for large volumes of oil, additional salt must be dissolved and the resulting brine solution discharged by pipeline into the Gulf of Mexico. The Environmental Protection Agency has issued a permit to DOE, under the National Pollutant Discharge Elimination System, to discharge brine from the West Hackberry SPR storage site into the Gulf of Mexico.

NOS collected oceanographic and related meteorological data from June 1978 to June 1979 to characterize the physical features of two proposed brine disposal sites on the Louisiana inner continental shelf. The National Marine Fisheries Service (NMFS) completed a companion study during the same period to characterize the chemical and biological features of the two sites. EDIS is synthesizing the physical, chemical, and biological data collected by NOS and NMFS into environmental assessments of the potential impact of brine disposal.

Measurements

The brine disposal sites, known as West Hackberry and Weeks Island after the inland locations of the salt domes (figure 1-1), are about 185 km apart. The proposed locations for the pipeline diffusers are 29°40.0' N, 93°28.0' W for the West Hackberry site, and 29°05.7' N, 91°47.6' W for the Weeks Island site. The sites are on the Louisiana inner continental shelf, which is generally broad with a gradually sloping bottom.

Oceanographic and meteorological conditions were observed during a 12-month period by the NOAA Ship FERREL and the NOAA Research Vessel VIRGINIA KEY. Time series recording instruments were deployed in diamond-shaped configurations at the two sites (shown in figure 1-2 and listed in table 1-1), and meteorological

instruments were mounted on existing oil production platforms with the special cooperation of the platform operators. Current meters were mounted on subsurface instrument platforms, rather than on compliant moorings, to minimize the contamination of current meter data by waves and swell. The current meters recorded speed and direction, water temperature, and conductivity. Water level and wave data were obtained at the center of each site with pressure-type instruments. In addition to the time series measurements, conductivity, temperature, depth, and dissolved oxygen (CTD/DO) data were collected approximately every month at seven stations within each site and at three trackline stations between the sites. The DO measurements at the sites were made 1 m below the surface, midwater, and 1 m above the bottom. Special experiments were conducted to observe the vertical shear of currents in the 4-m layer above the sea floor. A combined engineering-oceanographic experiment that provided both data quality assurance and oceanographic information was conducted at the West Hackberry site during April.

Background

The mixing of brine discharges on the Louisiana inner shelf is governed principally by water salinity and temperature (density structure) and by circulation, including mean and time varying flows, vertical and horizontal velocity shears, and turbulent processes. The density structure and circulation at the two sites are determined mainly by river runoff, wind stresses, tidal forces, and varying degrees of coupling, mostly weak, with the general circulation of the western Gulf of Mexico. These forces may act essentially alone at times and in combination at other times.

The regional climatic conditions that influence sea surface wind stresses, and thus affect the circulation on the Louisiana inner shelf, are principally polar frontal passages and tropical cyclones. The frontal incursions that move generally south-southeastward into the Gulf of Mexico contribute in a major way to the climate; winds following the incursions influence the circulation significantly. The frontal passages are accompanied by dramatic events such as gale force winds, squall lines, torrential rains, large temperature fluctuations, extreme humidity fluctuations, and sea fog. The most intense weather events that affect the Louisiana coastal waters are tropical cyclones.

Data Quality Assurance

All measurements obtained during the NOS SPR Support Project can be traced to laboratory standards. Total measurement uncertainties (TMU's) were developed to bound errors for 95 percent of the typical field measurements (table 3-1). The project data have been validated, processed, and archived at EDIS. Analysis of the data set is documented in section 3 of this report, and data acquisition and processing are described in NOS Strategic Petroleum Reserve Support Project: Final Report -- Volume Two, Measurements and Data Quality Assurance. Documentation of the data set obtained by NOS should enable those interested in the oceanography of the Louisiana shelf to perform additional analyses knowing the quality of the data. Although this report is in response to DOE's requirement to characterize the physical oceanography at the West Hackberry and Weeks Island sites, further analyses of the NOS data set may provide additional knowledge about water circulation. Indeed, further use of the data is encouraged.

Conclusions

The physical oceanography of both the West Hackberry and Weeks Island brine disposal sites is governed principally by meteorological forcing, river runoff, and, to a lesser extent, tidal influences. These mechanisms operate essentially alone at times, and in combination at other times, and their relative importance varies both seasonally and within seasons. We found little evidence of coupling between the inner shelf circulation at the sites and the general circulation of the western Gulf of Mexico; the broad and shallow Louisiana shelf apparently is not conducive to the lateral transfer of momentum required for strong coupling of inner shelf and general circulations.

Stratification of the water column at both sites is influenced more by salinity than by temperature, although both are important during early summer when a thermocline develops. At the West Hackberry site, a marked difference in the near-bottom salinity distributions from the beginning of June 1978 and June 1979, indicated an interyear variability of 5.32 ppt. The interyear variability at the Weeks Island site was less, 1.6 ppt, at the beginning of June 1978 and June 1979.

Anoxic bottom water was found at the West Hackberry site during June 1978, and hypoxic bottom water was found at the Weeks Island site during July 1978. The stable density stratification of June 1978 was accompanied by anoxic bottom water at the West Hackberry site, but anoxic conditions were not found there during June 1979. The lowest value of DO observed 1 m above the bottom at the Weeks Island site on June 3, 1978 was 3.29 ml/l; increasing stratification resulted in an areal average of DO of 1.48 ml/l at 1 m above the bottom during July 21, with a range from 0.80 ml/l to 3.05 ml/l, the lowest values of the 12-month study. DO distributions showed maximum spatial gradients, both vertical and horizontal, during the summer when density stratification was also strongest. DO gradients diminished with increasing mixing of the water column caused by wind stresses. The tendency toward DO homogeneity began with Tropical Storm DEBRA and continued through the spring of 1979, with the 12-month maximum of 8.75 ml/l occurring at the West Hackberry site during February, and the 12-month maximum of 6.98 ml/l occurring at the Weeks Island site during January. Moderate stratification was observed during mid-March at both sites when runoff from the Mississippi and Atchafalaya Rivers was near maximum; the stratification was more pronounced at the West Hackberry site. Intrayear and spacial variability of DO was thus greater at the West Hackberry site than it was at the Weeks Island site.

The discharge of brine during the summer at both sites, particularly at the West Hackberry site, could lead to increased stratification stability producing an even stronger barrier to keep surface and bottom waters from mixing. Enhanced stratification would tend to reduce DO concentrations in the bottom waters further, and impede the transfer of momentum from the sea surface to the near-bottom waters. It is therefore recommended that monitoring of brine discharges be given special attention and that discharges be controlled carefully whenever stratification is evident.

The intrayear variability in water temperature at both sites was approximately 20 Celsius degrees, from about 30°C in August to about 10°C during late January and early February. The intrayear variability in surface water salinity was approximately 25 ppt at the West Hackberry site, from 7.18 ppt during early June 1978 to 32.21 ppt during early October; it was 14 ppt at the Weeks Island site, from 18.2 ppt during July 1978 to 31.8 ppt during September; these extreme

ranges are similar to ranges observed in estuaries. Despite the 20 Celsius degree intrayear variability in temperature, the density structure during any given cruise was observed to be governed mainly by spatial salinity variations. The strong pycnocline separating the low salinity surface water from the slightly cooler, higher salinity bottom water during 1978 summer months was destabilized by the wind stresses of Tropical Storm DEBRA, and a pycnocline of comparable strength was not found again during our study.

The water column remained well mixed through the winter, although weak gradients were observed at both sites during October. A water temperature inversion due to seasonal cooling at the sea surface was observed at both sites during December 1978 and January 1979, but the inversion did not destabilize the water column because higher salinity in the bottom water offset the temperature effect. The southward spreading of river runoff was at its peak during May and June at the West Hackberry site with weak vertical gradients inshore and stronger vertical gradients 7.4 km further offshore. During May 9, 1979, the inshore (station 12) surface water value was 12.0 ppt while the offshore (station 13) value was 13.0 ppt; bottom water salinities were 12.5 ppt and 16.8 ppt, respectively. During June 2, 1979, surface water salinity was 12.5 ppt inshore and 13.5 ppt offshore, while bottom water salinity was 12.5 ppt inshore and 13.5 offshore. The southward spreading of river runoff observed at the Weeks Island site was at its peak during May 7 and 8, but the effect was much weaker than that observed at the West Hackberry site; the Weeks Island site is further off shore. The inshore (station 22) surface water salinity was 22.4 ppt during the early-May 1978 cruise, while the offshore (station 23) value was 23.0 ppt; bottom water salinities were 22.5 ppt and 23.0 ppt, respectively.

The inner shelf circulation responds rapidly (within hours) to winds and intrusions of river discharge to form a coastal boundary current. Tidal circulation appears to dominate only when the coastal boundary current dissipates. The development of the coastal boundary current occurs from the sea surface downward and from inshore to offshore, and its dissipation occurs in the opposite direction. Evidence of the coastal boundary current exists both in the NOS current meter and CTD data, and can be seen in our graphical presentations both of current vectors in plan view and in elevation views of salinity and density contours.

Inertial currents do not appear to persist as far inshore on the Louisiana inner shelf as the West Hackberry disposal site, although there appear to be infrequent cases when diurnal clockwise rotation of some measured currents lasted for several days following polar frontal passages. However, persistent alongshore drifts are far more common after frontal passages. The same behavior of currents appears to occur at the Weeks Island site. Bottom friction inhibits the local generation of inertial currents and causes strong dissipation of distantly generated inertial currents, especially when the water column is shallow and vertically homogeneous. Near vertical homogeneity of the water column was found to occur from norther-induced Langmuir circulation as described below. The period of rotation of inertial currents is one-half a pendulum day and is thus dependent on latitude. At the latitudes of the West Hackberry and Weeks Island sites, the period of inertial currents is nearly equal to the period of the diurnal tidal current, and the two different types of currents are exceedingly difficult to separate from one another.

Ekman transport, which results from frictional coupling and Coriolis accelerations, does not appear to be important at the shallow inner shelf site, although it may play an increasingly important role farther offshore on the gradually sloping Louisiana shelf. Ekman transport is evidenced by clockwise turning of currents with increasing depth (in the Northern Hemisphere) within the so-called depth of frictional influence. The turning effect decreases in part with decreasing water depths, and becomes negligible when the ratio of the water depth to the depth of frictional influence becomes less than about 0.1. Within the TMU of the current direction measurements, we do not see conclusive evidence of Ekman transport. The current vector plots in appendix E and section 15 show numerous instances during which currents turn toward the left with depth, opposite to Ekman transport.

Evidence of large-scale Langmuir circulation was observed visually during overflights at both sites during an October norther, and was recorded by aerial reconnaissance photography at the West Hackberry site. This type of circulation induces energetic vertical mixing of the water column, and we postulate that it has a dominant role in the oceanography of the Louisiana inner continental shelf during late fall, winter, and early spring, when northers contribute significantly to the regional climate. Langmuir circulation can be expected to occur

during storm events and we hypothesize that Langmuir circulation dominates whenever surface winds exceed about 7 m/s.

Langmuir circulation is a wind-induced hydrodynamic instability composed of solenoidal cells with their axes alined in the direction of the wind. The diameter of each cell is approximately equal to the water depth for the large-scale type of Langmuir circulation observed at the site, and adjacent cells rotate oppositely to one another. The opposite rotation of adjacent cells results in lines of both convergence and divergence at the sea surface. Lines of convergence are evidenced by parallel bands of entrapped air from white caps; these are separated by wider bands of sediment carried to the sea surface by upward motion of the rotating cells. When northers are infrequent, however, there is a tendency toward stratification of the water column, particularly from late winter to early summer when river runoff dilutes salt in the surface waters.

Summary of Measurements at the West Hackberry Site

Dissolved Oxygen:

Dissolved oxygen was measured 1 m beneath the surface, midwater, and 1 m above the bottom. Anoxic conditions existed in the bottom water during June 1978 when the water column was stably stratified. The stratification was enhanced by low salinity water, from 7.18 to 17.52 ppt, resulting from dilution of the inner shelf water by river runoff. DO values increased by late July 1978 in the bottom water, but remained below 3.50 ml/l. The DO observations made during summer 1978 show large gradients, both vertical and horizontal, with near-surface values ranging from a minimum of 4.89 ml/l at station 14 to a maximum of 8.37 ml/l at station 13.

In response to vertical mixing that was induced by wind stresses, gradients of DO decreased sharply during fall 1978. By mid-November, the gradients were negligible, and vertical homogeneity in DO continued through February 1979. DO values increased with decreasing water temperature, which is consistent with the physical chemistry of DO, and were accompanied by variations presumably caused by biological demand. The largest value for the 12-month survey was found to be 8.37 ml/l in late February. During mid-March, near bottom DO was sharply

reduced to a minimum of 2.21 ml/l in response to moderate stratification caused by salinity and temperature differences, apparently from river runoff. Midwater and near-surface values ranged from 5.88 to 6.58 ml/l during mid-March.

A storm during mid-April mixed the water column, thus producing a nearly homogeneous distribution of DO, with a nominal value of 5 ml/l. Data from our May cruise show near homogeneity in DO, except at the deepest station (farthest offshore) where the bottom value was 3.73 ml/l and the surface value was 6.64 ml/l. Data collected during the last cruise of the study did not replicate the DO data collected 12 months earlier. The early June 1979 data revealed no anoxic conditions as had been seen during June 1978. While there was evidence of stratification at stations to the south and east of the site center, the DO gradient at the site center was negligible compared to the estimated TMU of $\pm$0.03 ml/l. The minimum DO value observed during early June 1979 was 3.71 ml/l in the bottom water at offshore station 13. The average DO value at the site center was 4.13 ml/l.

Salinity, Temperature, and Density:

Conductivity and temperature measurements at the West Hackberry site, and the resulting computation of salinity and density, exhibit large variations which are similar to those of estuarine environments. The variability of density at any given time is dominated more by salinity than by temperature; it is controlled by runoff from the Mississippi and Atchafalaya Rivers and, to a much lesser extent, Calcasieu and Sabine Lakes.

Water temperature was found to vary about 20 Celsius degrees during the 12-month study, from a maximum of about 30°C in early August to a minimum of about 10°C during late January and early February (figures 5-3 and 5-4). Near-surface salinity was found to vary by about 25 ppt from a minimum of 7.18 ppt during early June 1978 to a maximum of 32.21 ppt during early October. Salinity remained high until mid-January (30.51 ppt), when it began to decrease because it was diluted by river water; the decrease continued to the end of the study on June 2, 1979, when it reached 12.50 ppt. Thus, the difference in values between June 1978 and June 1979 was 5.32 ppt, from 7.18 ppt to 12.50 ppt.

Stable stratification, which impedes vertical mixing, occurred during June and July 1978 with two very distinct layers separated by a pycnocline; additional layers were also found at some stations, but these were not as pronounced. Vertical temperature gradients were greatest during June 1978, but were far less 12 months later (see figures in appendix C). The vertical temperature gradient was weaker during late July than during June 1978. Thermal stratification is significant during the summer, but tends to be weak during the other seasons.

After Tropical Storm DEBRA passed directly over the West Hackberry site on August 28, 1978, the water column was well mixed and, in response to wind stresses, remained well mixed through the fall and early winter months. Weak gradients induced by salinity were observed during October 3; temperature was nearly uniform, but mean salinities at the surface and bottom were 27.5 ppt and 31.6 ppt, respectively.

Although CTD profile data were not obtained during the December 1978 cruise for operational reasons, mean temperatures measured 1 m and 3 m above bottom by sensors on the current meters were 19.5°C and 16.0°C, respectively, a negative gradient of about 1.8 Celsius degrees/m. This temperature inversion was caused by seasonal cooling at the sea surface.

CTD data obtained during early January 1979 indicate an isothermal layer in the uppermost 5 m of the water column, overlying a slightly warmer, but more saline, bottom layer. The water column at all stations during early January was nearly neutral in stratification, tending toward weakly stable, by the offsetting effects of temperature and salinity on the density.

Water sample data during the late February cruise indicate strong vertical mixing in response to wind stresses, with lower salinities toward shore. Salinity throughout the water column at the site center was 24.6 ppt. At 3.7 km further inshore, the surface value was 23.9 ppt, 0.7 ppt less than the offshore value, while the bottom salinity was 24.5 ppt. This salinity distribution indicates the development of an oceanic front.

Water samples from the mid-March cruise showed mean salinities to be 26.7 ppt at the surface and 28.8 ppt at the bottom, a mean difference of 2.1 ppt through the water column. The salinity difference was reinforced by a temperature difference to produce density stratification. Surface temperature was 15.7°C, while bottom temperature was 14.3°C.

Increasing river runoff was evident in the data obtained during the April cruise. The difference between the stations farthest offshore and inshore, separated by 7.4 km, was 6.9 ppt in the surface water; the value offshore was 24.7 ppt and the value inshore was 17.8 ppt. There was large variability in vertical salinity differences from station to station within the site, from 0.2 ppt to 5.6 ppt through the water column. Mean surface and bottom temperatures were 22.5°C and 22.2°C, respectively.

Data collected during the May cruise show southward spreading of river runoff to be at its peak at that time. The values of salinity at offshore station 13 were 13.0 ppt at the surface and 16.6 ppt at the bottom, while the values 7.4 km further inshore were 12.0 ppt at the surface and 12.4 ppt at the bottom. Data from the early June 1979 cruise show low salinity water continuing to dominate. The mean surface salinity was 12.8 ppt while the mean bottom salinity was 15.6 ppt. Higher salinity shelf water was found underlying the low salinity water at the offshore station 13; bottom salinity there was 23.1 ppt, and there was a strong pycnocline 1 to 2 m above the bottom. Mean surface and bottom temperatures were 25.5°C and 24.8°C, respectively.

Winds:

Time series meteorological data obtained at station 18 are shown in figures 6-2 and 6-3. Except during Tropical Storm DEBRA, winds during summer 1978 were predominantly southerly with a mean speed of about 5 m/s. Winds averaged over 5-minute intervals during DEBRA reached 18 m/s. Winter wind speeds, influenced by polar frontal passages, averaged about 50 percent higher than those of summer. Winds during late spring were generally southerly with a mean speed of about 6 m/s. The spectral characteristics of the summer winds show definite evidence of a land/sea breeze system with a period of 24 hours (figure 6-4a), while

winter winds show more energy at low frequencies, reflecting the polar frontal passages (figure 6-4b).

Surface Waves:

Statistical summaries of significant wave heights and periods of peak energy for measurements made at station 11 are shown in tables 7-1 and 7-2. Minimum, mean, and maximum values of significant wave heights for deployment periods indicated are shown in table 1.

Table 1: Significant wave heights at West Hackberry site.

Deployment period		Significant wave heights (cm)		
From	To	Minimum	Mean	Maximum
8/03/78	9/03/78	14	45	262*
9/05/78	10/03/78	7	51	116
11/01/78	11/14/78	9	44	124
11/14/78	12/07/78	22	56	177
12/08/78	12/17/78	10	35	96
1/09/79	1/31/79	5	64	190**
2/02/79	2/21/79	7	48	154
3/13/79	4/04/79	7	73	139
4/05/79	5/08/79	17	60	180

* Observed during Tropical Storm DEBRA.

** Observed during a norther.

The maximum value of significant wave height for the 12-month study was observed during Tropical Storm DEBRA at 2.62 m. A significant wave height of 1.45 m was associated with a January extratropical cyclone, while a January norther produced a significant wave height of 1.90 m.

Significant wave heights observed during summer periods were less than 50 cm more than 75 percent of the time, and less than 70 cm more than 90 percent of the time. Periods of peak energy during the summer were equal to or less

than 6 seconds for more than 90 percent of the time. Measurements made from September 5 to October 3 showed the most frequent occurrence of negligible wave heights during the entire 12-month study. During this period, more than 90 percent of the significant wave heights observed were less than 1 m, and more than 90 percent of the periods of peak energy were 6 seconds or less.

During November and the first half of December, significant wave heights remained less than 1 m more than 90 percent of the time. The minimum significant wave height during this period was 22 cm; no near quiescent observations were made. During the first 2 weeks of November, periods of peak energy remained 6 seconds or less for 87 percent of the time; during the following 3 weeks, they remained 6 seconds or less for 72 percent of the time, with fewer observations at 5 seconds and a shift toward longer periods. The second week of December was relatively quiescent with significant wave heights less than 70 cm for more than 90 percent of the time, and less than 30 cm for more than 60 percent of the time; periods of peak energy were 6 seconds or less for more than 90 percent of the time, and 4 seconds or less for 75 percent of the time. The 22-day wave record obtained during January 1979 indicates that significant wave heights were less than 1.2 m for 90 percent of the time, and that a maximum of 1.9 m was observed. Our 19-day record during February showed a decline in heights compared to the January data; significant wave heights were less than 1 m for more than 90 percent of the time.

A 22-day record beginning mid-March showed a shift toward greater wave heights compared to the previous record; significant wave heights were between 0.5 and 1.1 m for 53 percent of the time. During this period, periods of peak energy were 6 seconds or less for 87 percent of the time. Data obtained during April and May indicate that more than 90 percent of the observed wave heights were less than 1 m; 85 percent were between 20 and 80 cm.

Water Levels:

Water level data measured at station 11 provided six valid 29-day records for analysis. Water level fluctuations at the West Hackberry site are mixed, mainly semidiurnal. During the period of the largest inequality, the daily low

water inequality is larger than the daily high water inequality by a factor of two to three. The mean monthly range of from 71 to 90 cm included meteorological effects. Analysis of data obtained at the West Hackberry site produced results which are consistent with NOS historical tide data for Calcasieu Pass. Although the results of our harmonic and nonharmonic analyses are consistent with historical NOS data, "apparent" seasonal variations are shown in results of both types of analyses. Some of the effects are attributed to differences in the seasonal meteorological conditions. This can be seen primarily at the diurnal frequency, because of the limitations of the 29-day harmonic analysis program to resolve this constituent. The land/sea breeze effect, which results in set up or set down of water levels, will appear in our analysis as part of the S_1 constituent. However, the S_1 constituent cannot be separated from the K_1 constituent in a series less than 365 days long. Also, the P_1 constituent cannot be separated from the K_1 constituent in a series less than 180 days long. Both of these constituents are important in the Gulf of Mexico and contribute to the "apparent" variability.

Currents:

During the summer of 1978, currents at the West Hackberry site were generally weak; the range of mean scalar speeds observed from June 2 to August 29 was 6.8 to 12.7 cm/s. Currents reaching speeds of 79 cm/s were observed during Tropical Storm DEBRA, whose track passed over the site on August 28. The highest speed observed during the study was 84 cm/s during a spring storm described in section 12. During June 1978, the circulation was dominated either by river runoff or the tide, or a combination of the two forcing effects. The large variability observed in current directions during June, caused by the competing river runoff and tidal influences, was not observed during July 1978. A more persistent, generally eastward alongshore flow occurred during July. Westward alongshore currents tended to dominate the circulation during August.

The tidal components of the observed currents were found to average only about 2 cm/s over the 12-month study period. Tidal currents at the West Hackberry site are of the mixed type, generally semidiurnal-dominant in the fall and winter and diurnal-dominant in the spring and summer.

Wind stresses became a major influence on the circulation by the end of the summer. Westward alongshore circulation became persistent in September and continued well into the winter. Current speeds during fall did not increase significantly over summer values, but increased sharply during winter with generally increasing wind speeds. The response of the currents to the winds at the relatively shallow West Hackberry site is rapid, within several hours.

The range of mean scalar speeds for deployment periods during the winter months was from 8.3 to 21.0 cm/s; the highest speed was about 60 cm/s. During the winter, the spectral distribution of energy contained in the currents showed a concentration of energy toward the low frequencies. This is due to the strong meteorological forcing caused by winter storms.

Although the persistence of westward currents continued through most of winter, currents in late February and early March became variable and appeared to be tidally driven. During spring, the circulation at the West Hackberry site was similar to that of fall and early winter, with strong westward currents.

The current speeds tend to be slightly higher during spring than winter because of the dominant direction of the wind rather than wind speeds alone. Winter and spring winds were especially energetic, with wind speeds slightly higher in the winter. The winds in spring, however, were characteristically more southerly than those of winter, which were mostly northeasterly and southeasterly. Consequently, southerly spring winds were accompanied by a longer fetch for an enhanced transfer of momentum to the coastal circulation system, and thus generated stronger, wind-driven currents. The range of mean current speeds for deployment periods during the spring was from 11.0 to 25.3 cm/s; the highest speed was 60 cm/s.

By late spring, from May 9 to June 1, 1979, the circulation at the site exhibited variability in direction similiar to that observed nearly 12 months earlier.

Summary of Measurements at the Weeks Island Site

Dissolved Oxygen:

Dissolved oxygen was measured 1 m beneath the surface, midwater, and 1 m above the bottom. The lowest value of DO observed on June 3 at 1 m above the bottom was 3.29 ml/l at station 25, farthest toward the west-northwest; midwater and near-surface values were nominally 4.6 ml/l. Although stratification increased by July 1, DO in the bottom water was 4.22 ml/l, averaged over all stations, with a range from 3.44 ml/l to 4.82 ml/l; DO at midwater was nominally 5.1 ml/l. Stratification continued to increase and, during July 21, the areal average of DO values from samples obtained 1 m above the bottom was 1.48 ml/l, with a range from 0.80 ml/l to 3.05 ml/l; six of seven bottom samples indicated DO less than 2 ml/l. These were the lowest values observed during the 12-month study. DO in the surface water averaged 5.35 ml/l during July 21.

The horizontal DO gradients observed during June and July indicate generally decreasing DO with increasing depth which is consistent with gradients expected when density stratification is stable.

Mixing of the water column by wind stresses and the annual period of low river runoff accounts for the negligible gradients observed during September, October, and November. During these fall months, the ensemble average of all DO observations is 4.44 ml/l, 5.24 ml/l, and 5.09 ml/l, respectively.

No DO data were obtained during December. Water samples obtained during two January cruises indicate lower values at most stations in the near-bottom layer, while the surface and midwater layers appeared well mixed with each other. Negligible gradients observed during February 20 and 21 are attributed to mixing by winds of 8 to 14 m/s that prevailed for 4 days prior to the cruise.

The second largest DO gradients found during the 12-month study were observed during March 12 and 13; these gradients are attributed to the increased stratification of the water column induced by increased runoff from the Mississippi and Atchafalaya Rivers, and to reduced wind energy prior to and

during the cruise. Winds from polar front passages produced negligible gradients of DO during mid-April, when the ensemble average was 4.99 ml/l for all depths and the range was 4.91 ml/l to 5.10 ml/l. Small vertical gradients developed at two of the seven stations by May 7 and 8, with DO averaged over all stations and depths at 5.80 ml/l, ranging from 5.07 to 6.11 ml/l. Except at the station farthest offshore (station 23), water samples obtained on June 2 indicate negligible vertical gradients; the ensemble average is 4.98 ml/l, with a range from 4.41 ml/l to 5.50 ml/l.

Salinity, Temperature, and Density:

Water temperature was found to vary about 20 Celsius degrees during the 12-month study, from a maximum of about 30° C in July and August to a minimum of about 10° C during January and February (figures 11-3 and 11-4). Near-surface salinity was found to vary about 14 ppt, from a minimum of 18.2 ppt during July 1978 to a maximum of 31.8 ppt during September. Salinity remained high through early January (28.6 ppt), when it began to decrease by dilution with river water; the decrease continued to the end of the study on June 2, 1979, when it reached 23.9 ppt. The difference between the June 1978 and June 1979 minimum salinity values was 1.6 ppt, from 22.3 ppt to 23.9 ppt.

Stable stratification occurred during June and July 1978 with two very distinct layers separated by a pynocline. Stratification was stronger in late July than June and early July. Thermal stratification is significant with a developing summer thermocline, but tends to be weak during the other seasons.

Although CTD profile data were not obtained during August 1978, the intense meteorological conditions that occurred during the month of August suggest substantial mixing. After Tropical Storm DEBRA approached the coast of Louisiana on August 28, 1978, the water column was well mixed and, in response to wind stresses and a low rate of river discharge, remain mixed through most of fall and into winter.

During the winter months, fresh water discharge increased in volume from that observed during summer and fall, with a substantial increase during March.

Mixing of the water column by wind stress on the sea surface, however, apparently inhibited stratification at the Weeks Island site. During the January 29 and 30 cruise, thermohaline conditions were more favorable for stratification. Water samples taken at the Weeks Island site had a mean surface salinity of 23.1 ppt and a mean bottom salinity of 28.8 ppt. In contrast, water samples taken 3 weeks later indicate a well-mixed environment with only a 0.4 ppt salinity differential between the surface and bottom.

The hydrographic conditions in early to mid-spring were influenced by the strong winds that occurred during early spring and the higher volume of river discharge that peaked during the months of April and May. Although the discharge was sufficient to dilute the shelf water in the site area, the intense mixing that occurred inhibited strong vertical stratification. During May 7 and 8 there was a 0.2 ppt salinity differential between the mean surface salinity of 22.8 ppt and the mean bottom salinity of 23.0 ppt. The water column appeared to remain weakly stratified to the end of the study on June 2, 1979. The salinity differential between the mean surface salinity, 24.5 ppt, and the mean bottom salinity, 25.0 ppt, was 0.5 ppt.

Winds:

Winds during summer 1978 were predominantly southerly and weak, except during Tropical Storm DEBRA. Winds averaged 5.8 m/s during fall 1978 and prevailed from the northern quadrant, northeasterly to northwesterly; the increased wind speed and northerly direction is attributed to increased polar front passages. The average wind speed during winter and early spring was 7.1 m/s; average speed decreased to 5.1 m/s by mid-spring 1979, remaining at that value to summer.

Meteorological observations made by NOS at station 28, from October 1978 to March 1979, together with an analysis of daily weather maps for that period, shows that the number of frontal passages compared well with averages obtained from 1965 to 1972 by DiMego et al. (1976), except during January and February. We obtained no January data to compare with the 8-year average. During February, we found six frontal passages, while the 8-year average was nine and a

half passages. We found evidence of land/sea breeze from records for October and April. Spectra computed from wind records obtained from late fall to mid-spring show a concentration of energy at low frequencies, which is consistent with the domination of the local weather by frontal passages and by occasional cyclones.

Surface Waves:

Statistical summaries of significant wave heights and periods of peak energy for measurements made at station 21 are shown in tables 13-1 and 13-2. Minimum, mean, and maximum values of significant wave heights for deployment periods are shown below.

Table 2. Significant wave heights at Weeks Island site.

Deployment period		Significant wave heights (cm)		
From	To	Minimum	Mean	Maximum
7/01/78	7/27/78	7	32	105
7/28/78	8/22/78	15	33	93
9/02/78	9/13/78	7	48	120
9/16/78	9/21/78	20	43	68
10/02/78	10/30/78	8	32	121*
10/30/78	11/13/78	11	44	133**
11/13/78	12/11/78	16	64	190*
12/12/78	1/06/79	13	55	178*
1/06/79	1/29/79	1	66	175*
2/21/79	3/12/79	11	64	181*
3/27/79	4/04/79	26	74	106
4/18/79	4/27/79	37	67	120
5/08/79	5/14/79	20	47	88
5/21/79	6/02/79	8	45	101

*Observed during a norther following a polar frontal passage.

**Observed during an extratropical cyclone.

During July 1978, 88 percent of the wave observations showed significant wave heights to be less than 50 cm, and 83 percent of the observations showed periods of peak energy to be 5 seconds or less. During late July and the first 3 weeks of August, significant wave heights were less than 50 cm for 89 percent of the observations, while periods of peak energy were 6 seconds or less for 93 percent of the observations. The wave climate at the Weeks Island site was relatively quiescent during summer 1978, except during Tropical Storm DEBRA (section 18).

The increasing frequency of frontal passages during fall 1978 is evident in the wave data. During the first half of November, 93 percent of the observations indicate significant wave heights between 11 and 80 cm, while 85 percent indicate periods of peak energy of 6 seconds or less.

The longest period of peak energy observed at the Weeks Island site was 13 seconds on January 4; corresponding significant and maximum wave heights were 21 cm and 40 cm, respectively. During the last 3 weeks of January, significant wave heights were between 30 cm and 90 cm for 70 percent of the observations, and 94 percent of the significant wave heights were less than 110 cm. A 20-day record beginning February 21 shows the continuing effects of polar frontal passages, but an apparent decrease in the effects of distant storms is indicated by a shift to shorter periods of peak energy.

Wave data obtained during spring 1979 indicate a significant shift toward longer periods of peak energy; the shift in spectral composition is attributed to the longer fetch of predominately southerly spring winds (compared with the shorter fetch of winds associated with polar frontal passages). Wave data obtained during spring 1979 also indicate steadily decreasing significant wave heights. During the final week of the 12-month study, 87 percent of the observations indicate significant wave heights between 10 and 70 cm; 97 percent of the observed spectra peaked at 6 seconds or less.

Water Levels:

Validated water level data obtained at Weeks Island station 21 provided one 15-day and one 29-day record for analysis. The water level fluctuations at the

site are mixed, mainly diurnal. The diurnal inequality is predominately in the low waters. The mean monthly range was found to be 52 cm.

Analysis of data obtained at the Weeks Island site produced results that are consistent with NOS historical data for Rabbit Island and Eugene Island. Since seasonal data were not obtained, we cannot relate seasonal variations in water levels with those found at the West Hackberry site. We observed residual effects at the diurnal frequency that were similar to those observed at the West Hackberry site; these results are due to the limitations of the 29-day harmonic analysis program and the effects of the constituents P_1 and S_1.

Currents:

Currents at the Weeks Island site were generally weak during summer 1978; the range of mean scalar speed observed from June 1 to September 15, 1978, was 8.2 to 19.7 cm/s. Later in the summer, in August, current speed increased significantly during summer storms to as high as 68 cm/s. The highest speed observed during the study was 92 cm/s during a winter storm. During June and through the third week of July 1978, the circulation was affected alternately by river runoff and the tide. The variability observed in current direction during early-summer, caused by the competing river runoff and tidal influence, decreased when the circulation became more alongshore in late July and August. This increase of circulation alongshore was caused by the influence of wind stress during several summer storms.

The tidal components of the observed currents were found to average about 4 cm/s over the 12-month study period. Tidal currents at the Weeks Island site are of the mixed type, generally varying between semidiurnal-dominant and diurnal-dominant during the year, except in fall when the tidal currents were consistently mixed diurnal-dominant.

Wind stresses became a major influence on the circulation by the end of the summer. Although alongshore west-northwest circulation persisted in September and continued through most of fall, currents in the first half of November became variable and appeared to be tidally driven. Current speeds during fall

did not increase significantly over summer values, but increased sharply during winter with generally increasing wind speeds. The response of the currents to the winds at the relatively shallow Weeks Island site is rapid, within several hours.

The range of mean scalar speeds for deployments during the winter months was from 8.1 to 24.2 cm/s. During the winter, the spectral distribution of energy contained in the currents showed a concentration of energy toward the low frequency end of the spectrum. This was due to the strong meteorological forcing caused by winter storms.

Although circulation varied from strong alongshore to transhore currents in January through early-March, circulation in late winter through most of spring, mid-March to late-May, persisted alongshore with strong west-northwest flow. The high current speeds in winter continued in spring due to the energetic spring winds. The range of mean current speeds for deployments in spring was from 10.0 to 19.7 cm/s.

Circulation at the site by late spring, May 21 to June 3, exhibited variability with currents in the transhore and alongshore directions, although currents alongshore in the east-southeast direction were negligible.

INTRODUCTION

This volume presents oceanographic characterizations of the West Hackberry and Weeks Island brine disposal sites for the Strategic Petroleum Reserve (SPR). The introductory sections describe background information about the SPR and the NOAA Brine Disposal Analysis Program, the regional climatology and oceanography, and methods of data analysis. For further detail about measurement systems, data quality control and assurance, data processing, and the availability of the NOS data from the National Oceanographic Data Center archives, refer to volume two of this final report.

1. BACKGROUND

This volume of the final report on the National Ocean Survey (NOS) Strategic Petroleum Reserve (SPR) Support Project presents the analysis and interpretation of the oceanographic and related meteorological conditions observed during a 12-month period beginning June 2, 1978. The results do not purport to represent baseline conditions of the area, but rather to characterize the important physical oceanographic features that will affect brine discharges. Measurement systems, quality control procedures, Gulf At-Sea Performance (GASP) Experiment, measurement data quality assurance, and data processing and validation are described in NOS Strategic Petroleum Reserve Support Project: Final Report--Volume Two, Measurements and Data Quality Assurance.

1.1. Strategic Petroleum Reserve

The Department of Energy (DOE) is implementing the Strategic Petroleum Reserve by storing crude oil in underground salt domes beneath Texas and Louisiana near the Gulf Coast. Since the present capacity of existing caverns in the salt domes is insufficient for large volumes of oil, additional salt must be dissolved and the resulting brine solution discharged through a pipeline into the Gulf of Mexico. The diffusion of the brine solution into the receiving waters of the inner continental shelf may pose a hazard to the area's shrimp and demersal fish populations. The National Environmental Policy Act of 1969, and subsequent Federal legislation, require that the likelihood of environmental damage be assessed, and that the extent of possible damage be documented before the planned action is permitted. DOE is directing the Strategic Petroleum Reserve under the National Energy Policy and Conservation Act of 1975.

1.2. NOS SPR Support Project

As part of the Brine Disposal Analysis Program conducted for DOE and managed by the NOAA Environmental Data and Information Service (EDIS), NOS

collected oceanographic and related meteorological data to characterize the two proposed brine disposal sites off Louisiana from June 1978 to June 1979. To determine instrument performance and to develop total measurement uncertainties, NOS designed a strategy for assuring data quality.

The NOS SPR Support Project was a cooperative, reimbursable project carried out in collaboration with EDIS under an interagency agreement with DOE. In response to requests from EDIS and DOE, preliminary planning for the NOS SPR Support Project began in August 1977, and the project itself began on November 15, 1977, by an amendment to the agreement between NOAA and DOE. Although the NOS Office of Marine Surveys and Maps was responsible for the project initially, responsibility was transferred to the NOS Office of Oceanography during a reorganization of NOS in January 1979. The NOS Office of Marine Technology (OMT) provided engineering and technological support through the OMT Test and Evaluation Laboratory (T&EL) and Engineering Development Laboratory (EDL). As an adjunct cooperative task, the Office of Marine Surveys and Maps provided hydrographic surveys of the two proposed disposal sites; these were conducted by the NOAA Ship MT. MITCHELL. The Circulatory Surveys Branch of the Marine Environmental Services Division within NOS processed and analyzed most of the oceanographic and meteorological data. Since the number of NOS personnel available for the project were limited, NOS contracted Optimum Systems, Inc., (OSI) of Rockville, Md., to assist in developing additional software for special purpose processing of the data.

The Southeast Fisheries Center at Galveston, Tex., a component of the NOAA National Marine Fisheries Service (NMFS), has completed a companion study to characterize the chemical and biological features of the two sites. EDIS is synthesizing the physical, chemical, and biological data collected by NOS and NMFS into environmental assessments of brine disposal.

1.3. Geographical Setting

The Louisiana coastline between 91° and 94° W longitude is arcuate with an approximate west-northwest/east-southeast trend. Topography adjacent to the coast is composed of very gradual elevations. The region is bathymetrically

simple, with a relatively wide continental shelf. The shelf width is about 200 km at the West Hackberry site and 175 km at the Weeks Island site.

The proposed brine disposal sites, known as West Hackberry and Weeks Island after the inland locations of the salt domes (figure 1-1), are about 185 km apart. The proposed locations for the pipeline diffusers are 29°40.0' N, 93°28.0' W for the West Hackberry site and 29°05.7' N, 91°47.6' W for the Weeks Island site. The West Hackberry site is approximately 11 km south of Holly Beach, La., between the Sabine Pass and the Calcasieu Pass. The continental shelf in this region has a gradual slope of about 50 cm/km, and the 100-m isobath is 196 km seaward of the site. The Weeks Island site is about 42 km due south of Marsh Island and 93 km southwest of Berwick, La., the staging point for the NOS field study. The shelf in this region has a slope of about 70 cm/km, and the 100-m isobath is approximately 140 km seaward of the site.

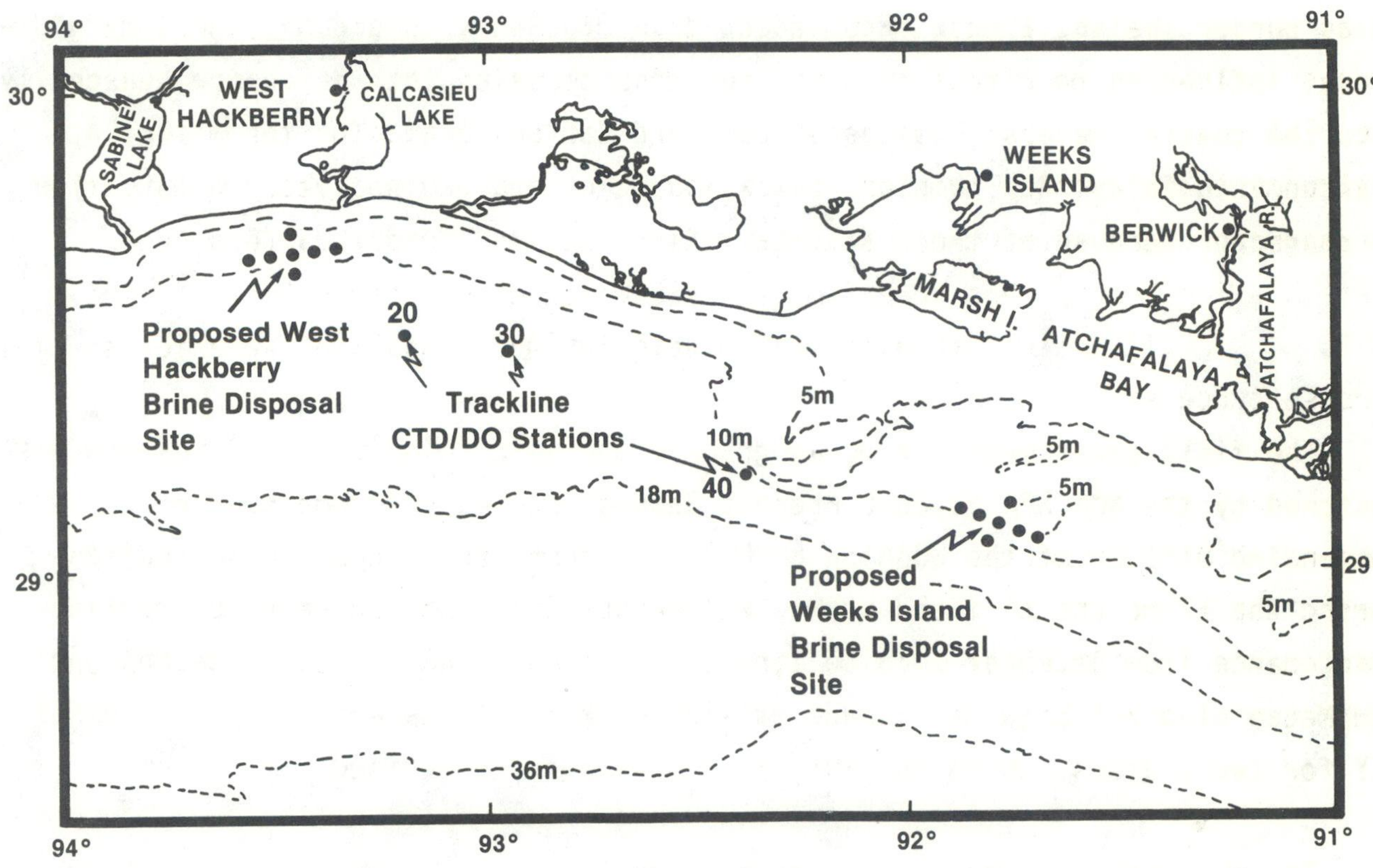

Figure 1-1. Proposed West Hackberry and Weeks Island brine disposal sites and the FERREL's trackline stations.

The two sites differ significantly in bottom type: sediments at the West Hackberry site consist of silt and clay with less than 40 percent sand, while the sediments at the Weeks Island site consist of more than 70 percent sand (Hausknecht, 1980). The center of the West Hackberry site is 9.1 m deep at Gulf Coast Low Water (GCLW), and the center of the Weeks Island site is 7.6 m deep at GCLW. GCLW Datum (Hicks, 1977) is defined as the mean lower low water when the type of tide is mixed and mean low water when the type of tide is diurnal.

The Atchafalaya River drains into Atchafalaya Bay, onshore of the proposed Weeks Island disposal site. Vermilion Bay and Cote Blanche Bay are relatively shallow and are northwest of Atchafalaya Bay. The Mississippi River has a dominant influence on the circulation of Louisiana's inner continental shelf waters. Satellite imagery also suggests a significant intrusion of Atchafalaya River water into the coastal system. This tends to reinforce the effect of the Mississippi River, and the combined effect has been seen all the way to the Texas border (Walsh, 1969). From about 92.5° to 94° W longitude, the only additional influences on circulation are two coastal lakes that discharge seasonally into the coastal waters: Calcasieu Lake and Sabine Lake. The Vermilion/Cote Blanche/Atchafalaya Bay complex, Calcasieu Lake, and Sabine Lake are estuarine in character because of their salinity distributions (Murray, 1976).

1.4. Experimental Design

The field experiment for oceanographic and meteorological observations was designed by the NOS SPR Support Project Manager and carried out by the Commanding Officer of the NOAA Ship FERREL. The FERREL conducted 18 cruises during the 12 months of field work. While the FERREL was in port for routine maintenance from December 1978 to January 1979, the NOAA Atlantic Oceanographic and Meteorological Laboratory made available the NOAA Research Vessel VIRGINIA KEY for two cruises, which the NOS Project Manager supervised.

The experimental design was based on preliminary information indicating that (1) meteorological data at each site were needed to analyze and interpret the oceanographic data; (2) over the same relative distance, alongshore events

in the currents would be more coherent than events occurring in the transhore* directions; (3) velocity shears, both vertical and horizontal, would enhance mixing; (4) current meter data might be significantly contaminated by waves and swell on the shallow Louisiana shelf; (5) locations of the diffuser sites might be subject to change; and (6) in situ equipment would be particularly subject to damage or loss because of commercial fishing, crew boat and supply ship traffic, other vessel activities, and storms.

The instrument configurations at the two sites were nearly identical except for the relative positions of the meteorological instruments, which were mounted on existing oil production platforms. These configurations are shown in figure 1-2, and the station positions are listed in table 1-1. An alongshore section, parallel to the local isobaths, extended 9.3 km to each side of the center station, while a transhore section extended both 3.7 km shoreward and 3.7 km offshore of the center station.

The NOAA Ship MT. MITCHELL conducted hydrographic surveys at the Weeks Island and West Hackberry brine disposal sites between August 9 and October 2, 1978. NOS performed these surveys on a cooperative basis in response to a request by DOE. The West Hackberry survey is registered as H-9785; the Weeks Island survey as H-9789. The main scheme hydrography was conducted with 200-m line spacing.

Subsurface instrument platforms were situated at the center of the site and at the extreme alongshore and transhore stations (figure 1-3). The subsurface platforms were equipped with two Grundy model 9021 current meters positioned 1 m and 3 m above the bottom. The current meters had sensors that recorded temperature and conductivity as well as current speed and direction.

Each center subsurface platform (stations 11 and 21) was equipped also with an Aanderaa Model WLR-5 water level gage and an Applied Microsystems, Inc.,

---

*Transhore is defined for this report as "normal to the shore."

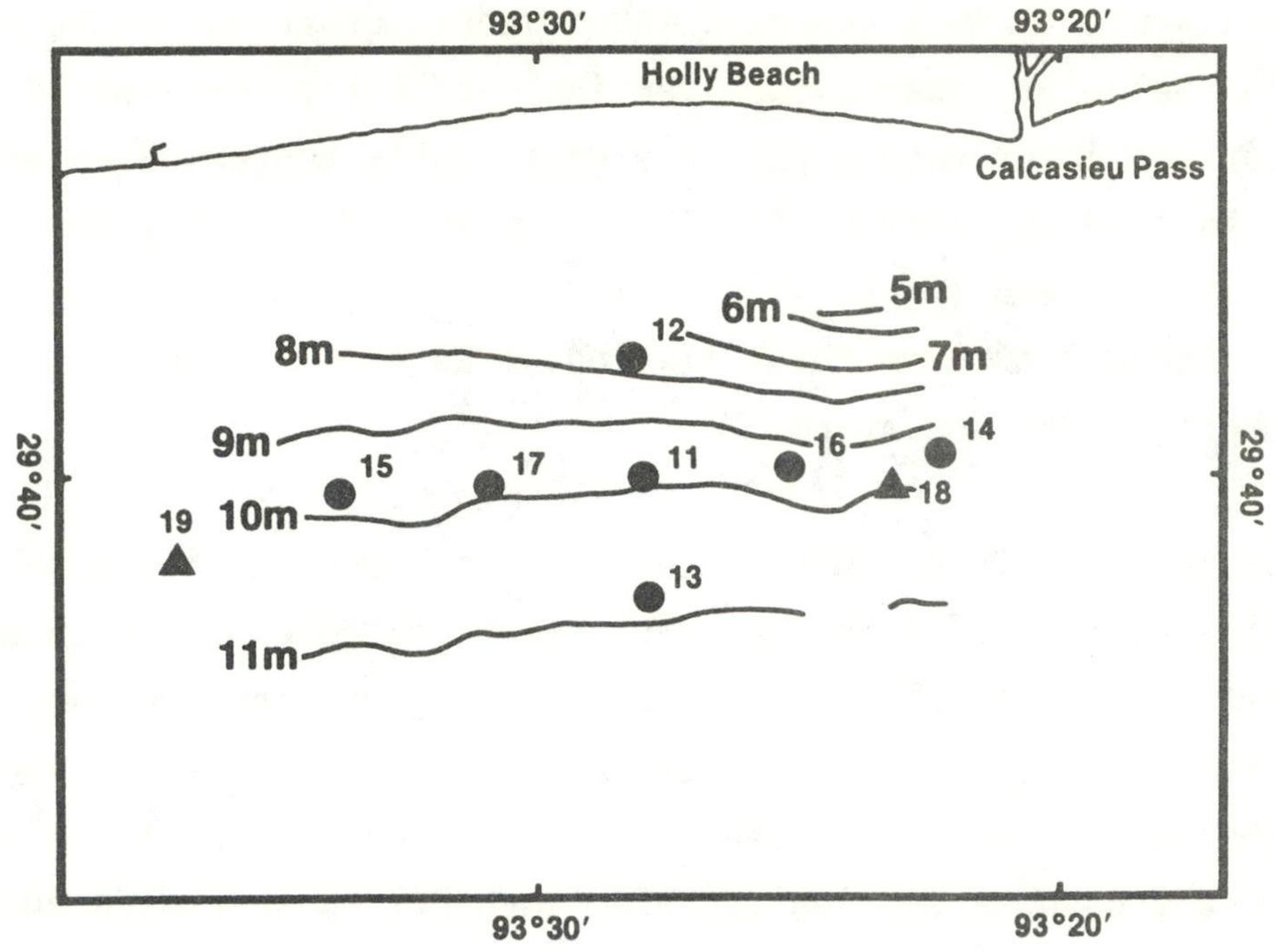

Figure 1-2. Measurement configuration. Depth contours (m) are shown at GCLW. Smaller face numbers indicate NOS measurement stations.

Table 1-1. Measurement station positions

Station	Relative position	North latitude	West longitude	Depth at GCLW (m)
		West Hackberry station positions		
11	Center	29°40.00'	93°28.00'	9.8
12	North	29°41.99'	93°28.14'	7.9
13	South	29°38.00'	93°27.86'	11.0
14	East	29°40.33'	93°22.29'	9.4
15	West	29°39.65'	93°33.70'	9.8
16	E. intermediate	29°40.18'	93°25.19'	9.4
17	W. intermediate	29°39.79'	93°30.99'	9.8
18	E. meteorological	29°39.79'	93°23.20'	-19.5*
19	W. meteorological	29°38.62'	93°36.74'	-15.8*
		Weeks Island station positions		
21	Center	29°05.70'	91°47.60'	7.9
22	North	29°07.49'	91°46.55'	5.8
23	South	29°03.94'	91°48.63'	11.0
24	East	29°03.43'	91°42.56'	7.0
25	West	29°07.95'	91°52.61'	8.2
26	E. intermediate	29°04.56'	91°45.06'	7.0
27	W. intermediate	29°06.82'	91°50.12'	8.2
28	E. meteorological	29°05.26'	91°41.43'	-14.0*
		Trackline station positions		
20		29°30.00'	93°11.70'	11.9
30		29°26.40'	92°56.26'	14.6
40		29°12.20'	92°22.93'	11.0

*Height above sea surface at GCLW.

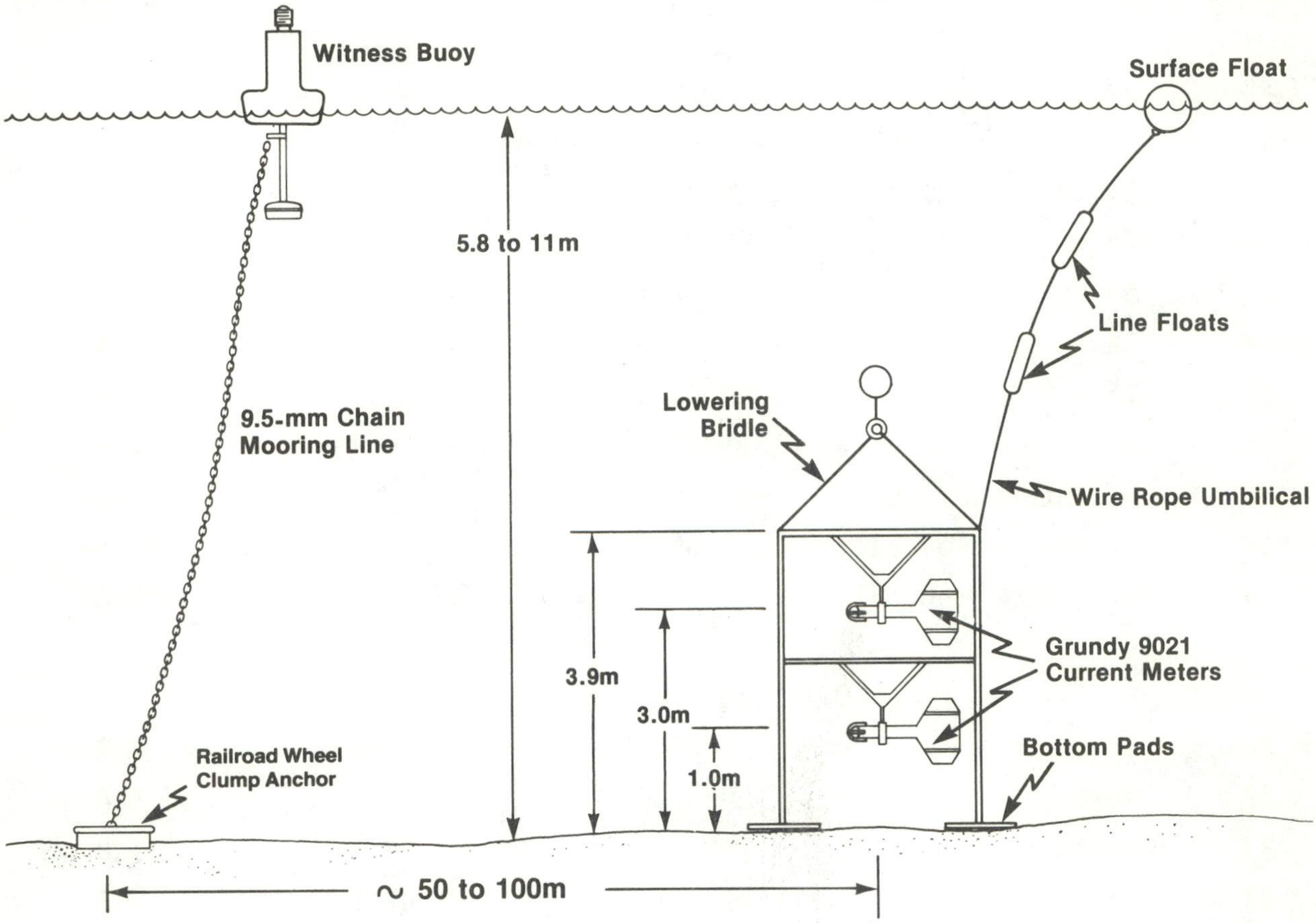

Figure 1-3. Platform/mooring system.

Model 750A wave gage. Aanderaa meteorological instruments, which recorded wind speed and direction, barometric pressure, and air temperature, were mounted on oil production platforms (designated in figure 1-2 by the symbol △) that were within 5.2 km of the extreme alongshore stations.

In addition to the data collected from the in situ time-series recording instruments, conductivity-temperature-depth/dissolved oxygen (CTD/DO) data were collected approximately once a month at the locations of the five subsurface platforms and at two stations midway between the center and the extreme alongshore stations (figure 1-2). CTD data were obtained with a Grundy model 9400 profiling instrument and, during December 1978 and January 1979, with a

Beckman RS-5 in situ salinometer. DO data, obtained from water samples collected with 1.7-l Niskin bottles 1 m below the surface, at midwater, and 1 m above the bottom, were analyzed by the micro-Winkler method. The water samples were also analyzed for salinity with a Guildline Autosal onboard the FERREL, and the results were compared with those from the CTD instrument. In addition to the data collected within each site for DOE, the FERREL collected data at three stations along the trackline between the two sites in cooperation with NMFS. Monthly CTD profiles were obtained at the trackline stations in conjunction with DO samples collected 1 m below the surface and 1 m above the bottom.

Additional current measurements were made at 2 m and 4 m above the bottom in February at the Weeks Island site and in April at the West Hackberry site to obtain time series of vertical profiles of the currents. This was accomplished by placing a second subsurface platform within about 15 m of the center station platform.

A 32-day experiment, the Gulf At-Sea Performance (GASP) Experiment, was conducted at the West Hackberry site beginning April 6, 1979. Although the main objective of the experiment was related to data quality assurance (DQA), oceanographic information was obtained that contributed significantly to understanding the physical characteristics of the West Hackberry site. The GASP Experiment is described at length in section 8, volume two of this report. The instruments and data that added oceanographic information about the West Hackberry site during a spring storm are discussed in section 20 of this volume.

The GASP Experiment configuration is shown in figure 1-4. The instruments labeled 832 and 132 were Neil Brown Instrument Systems (NBIS) acoustic current meters in the vector-averaging mode. An NBIS current meter in the burst-sampling mode was labeled 732. Data obtained from the Grundy Model 9021 current meters labeled 511, 321, 431, and 341 were validated for analysis and are discussed later in this report.

Data translation and processing, instrument transfer functions, and availability of the project data from the National Oceanographic Data Center are described in section 10, volume two of this report.

GASP EXPERIMENT ARRAY

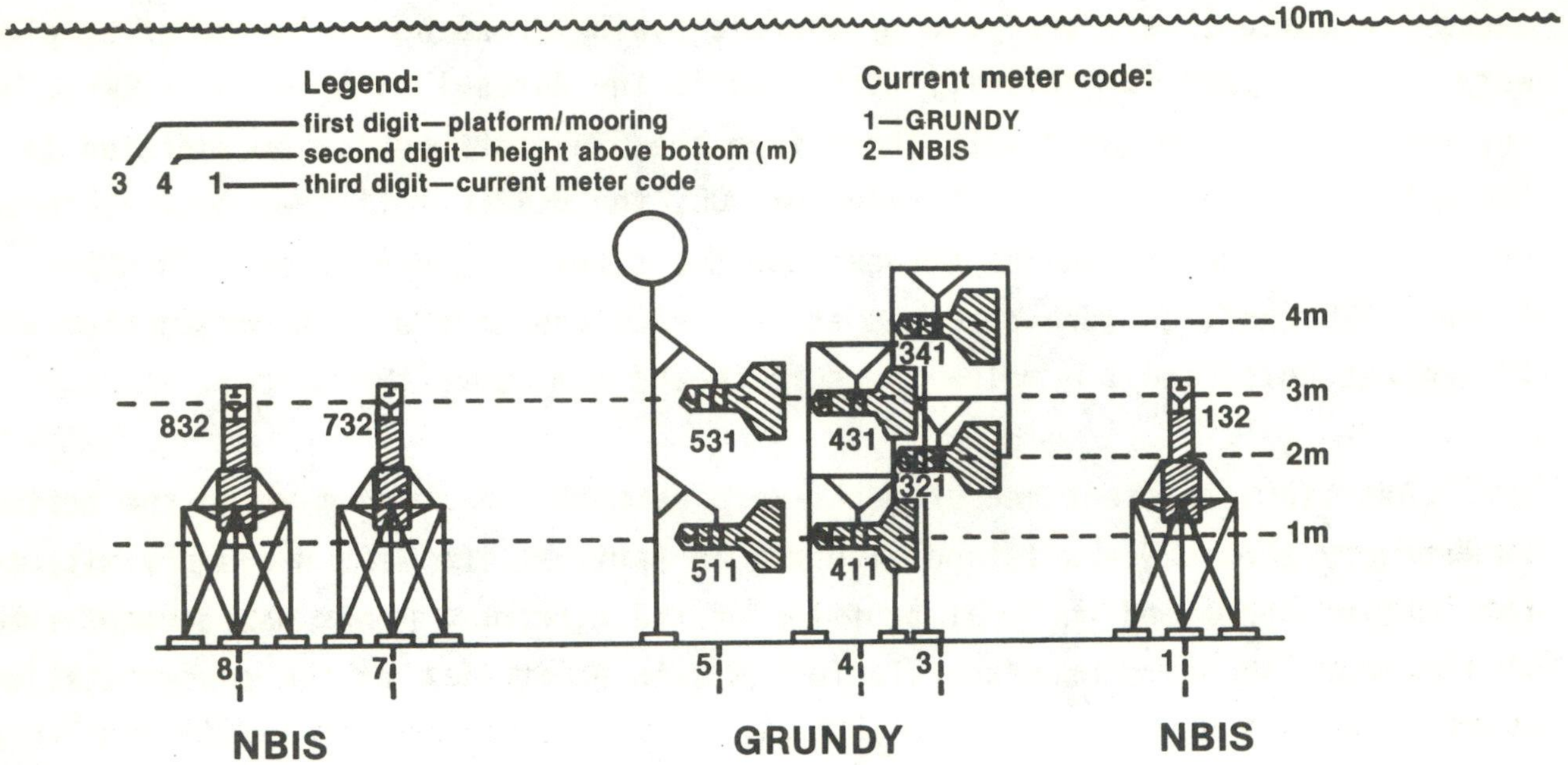

Figure 1-4. GASP Experiment configuration. Pressure-type wave gage on platform 4 not shown. See section 8, volume two for complete description of GASP Experiment.

2. REGIONAL CLIMATOLOGY AND OCEANOGRAPHY

Since we are concerned in this report with the physical characteristics that govern the mixing of brine into shelf waters, this section will describe factors that might be expected to affect those characteristics directly. The advection and dispersion of brine will be governed principally by salinity and temperature distributions (density structure) and by circulation, including mean and fluctuating currents, velocity shears, and turbulent processes. The density structure and circulation at the two sites are determined mainly by wind stresses, river runoff, and tidal forces. These mechanisms may act essentially alone at times and in combination at other times. As will be seen in later sections, the coastal boundary current appears dominantly tidal only when runoff is low and wind stresses are relatively weak. The current systems respond quickly, within several hours, to high runoff or strong wind stresses.

2.1. Climatology

The regional climatic conditions that significantly affect the circulation on the Louisiana inner shelf are polar fronts and cyclones, both tropical and extratropical. Seasonal wind reversals, caused by monsoon-like seasonal land/sea temperature differences, and daily land/sea breezes affect the circulation less strongly. Freshwater influx onto the Louisiana shelf, governed by precipitation over both local areas and the Mississippi River watershed, significantly affects circulation during periods of high discharge.

2.1.1. Polar Fronts

A polar (mid-latitude/tropical) cold front is a baroclinic zone separating a cold mass of relatively dry continental polar (cP) air from a warm mass of relatively moist maritime tropical (mT) air (Trewartha, 1954). These fronts, which move generally south-southeastward across Louisiana and into the Gulf of

Mexico, contribute in a major way to the climate; attendant winds influence the circulation significantly on the Louisiana inner continental shelf. The frontal passages are accompanied by dramatic weather events such as gale-force winds, squall lines, torrential rains, large temperature fluctuations, extreme humidity fluctuations, and sea fog.

The maritime tropical atmosphere may respond to cold fronts as much as 48 hours before their passage. During this period, surface air pressure falls, the dew point rises, and temperature increases. About 36 to 48 hours are needed after the passage of cold fronts for the air of polar origin to reach a new equilibrium with the warmer, moister, tropical atmosphere.

DiMego et al. (1976) analyzed the 6-hourly northern hemisphere surface weather maps produced by the National Weather Service from 1965 to 1972 for frequency and duration of fronts in the Gulf of Mexico and Caribbean Sea. They combined data for warm, cold, stationary, and occluded fronts for each 2.5-degree square. Analysis of the 8-year data base shows a trend of increasing frontal frequency in the northwestern Gulf of Mexico, along the Texas and Louisiana coasts. This trend is consistent with the source of cold, relatively dry cP air and principal areas of frontogenesis being situated to the north and northwest.

The mean monthly occurrences of frontal systems taken from the 8-year data base show that activity is at a maximum in winter and at a minimum in summer (table 2-1). When the frontal activity is at its maximum, the westerlies, which determine the dividing line between the warm, moist mT air and the cold, drier cP air, are at their southernmost extent. When frontal activity is at a minimum, the band of maximum westerlies is at its northernmost position. Fronts seldom penetrate south of 25° N during June, July, and August. The temperate westerlies are in southern Canada at this time, together with the cyclones required for frontogenesis.

The leeward side of the Rocky Mountains is a region of cyclogenesis. The flow of air around a developing cyclone can result in large meridional transport of cold air masses that lie to the north and west. Together with the topographic

Table 2-1. Approximate monthly frequency of frontal passages across the Louisiana shelf from 1965 to 1972

Passages/month		Passages/month	
January	9	July	2
February	9 1/2	August	2
March	8	September	3
April	6 1/2	October	6
May	4 1/2	November	7
June	2	December	9

Interpreted from DiMego et al. (1976).

steering effect of the Rocky Mountains, cyclonic air flow and associated transport provide ideal conditions for cold front passages across the Louisiana shelf.

2.1.2. Cyclones

Although the northers that follow frontal passages occur often enough to compose a significant part of the climatology, the most energetic and potentially destructive storms that affect the Louisiana coast are tropical cyclones. The tropical cyclone season extends from June to October; however, storms are most frequent in August and September (NOAA, 1975). During the 12-month study reported here, Tropical Storm DEBRA passed directly over the West Hackberry brine disposal site. (See section 18.)

Another type of storm observed on the Louisiana shelf is the extratropical cyclone, such as one observed in January 1979. (See section 19.) These tend to be much larger disturbances spatially and, through conservation of angular momentum, less severe than tropical cyclones.

The climate along the Louisiana coast, governed in large part by frontal passages, suggests a 4-month summer (June through September) and a 4-month

winter (December through March) with rapid transitions occurring during a 2-month spring (April and May) and a 2-month fall (October and November). Although this would be a reasonable way to group the four seasons, we use the more traditional grouping of four 3-month seasons.

2.1.3. Land and Sea Breezes

Hsu (1969) reported clearly defined land/sea breezes on the Gulf Coast near Ft. Walton Beach, Fla. Observations were made on May 20 and 21, 1969, when the synoptic influence on surface winds was at a minimum. The land-breeze front became apparent about 7 hours 20 minutes after sunset with a temperature decrease of about 2.2 Celsius degrees, measured both at 50 cm and 5 m above a sandy beach about 30 m onshore from the mean shoreline. Hsu estimated the accuracy of the temperature measurement to be $\pm$0.6°C. Wind speed and direction were measured at 10 m. The wind veered from southerly to northerly (clockwise) with the onset of the land breeze. The land breeze blew continuously until the onset of the sea breeze, about 5 hours after sunrise. The wind veered from north to south, while the air temperature decreased at both levels by approximately 3.3 Celsius degrees. The sea breeze blew continuously until 3 hours 20 minutes after sunset. The diurnal rotation of the observed land/sea breeze system is consistent with other observations on the Gulf Coast reported by Hsu (1969). This diurnal rotation results from the Coriolis effect, caused by the earth's rotation, which produces clockwise rotation in the Northern Hemisphere and counterclockwise rotation in the Southern Hemisphere. This sense of rotation applies to inertial currents as well as to land/sea breezes. Spectral analysis of data collected at NOS station 18 revealed a land/sea breeze effect, also. It is unlikely, however, that wind stresses from this system are of sufficient magnitude to alter the water circulation significantly.

2.1.4. Temperature and Precipitation

Surface air temperatures during summer 1978 were approximately 1 Celsius degree higher than the 30-year mean along the entire Louisiana coast, while precipitation was about normal (figure 2-1). Approximately 50 cm of precipitation fell on the western Louisiana shelf area during summer 1978, including that from

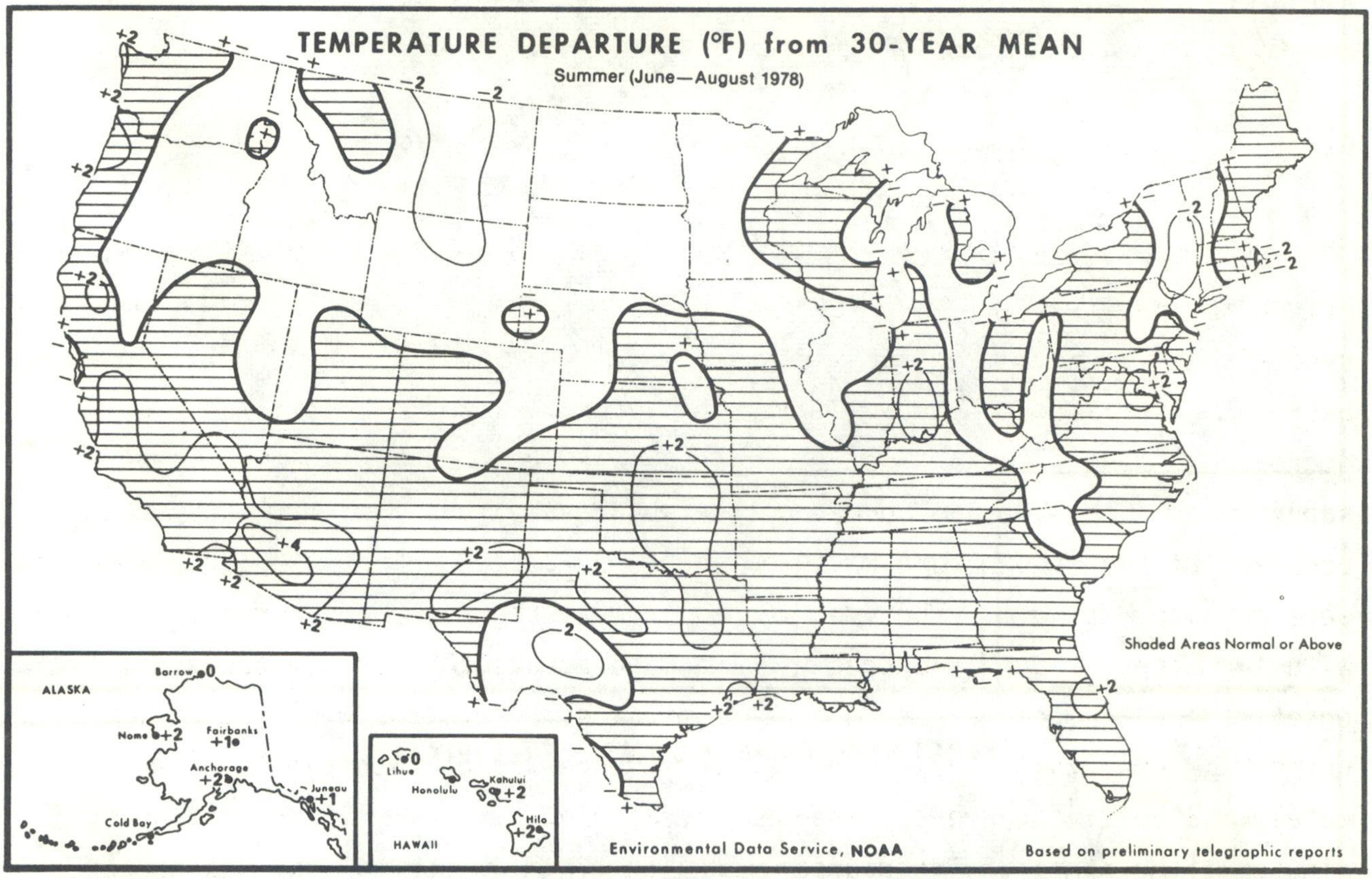

Figure 2-1. Air temperature departure from 30-year mean for summer 1978.

Tropical Storm DEBRA (figure 2-2). The much greater than normal precipitation over central Texas was caused by Tropical Storm AMELIA.

Comparison of air temperatures during fall 1978 against the 30-year mean is similar to the summer 1978 season; air temperatures were about 1 Celsius degree higher than normal (figure 2-3). Precipitation along the western Louisiana shelf area was only about 75 percent of normal during fall of 1978; total precipitation was about 20 cm during the fall (figure 2-4). However, during this season, precipitation in the Mississippi River watershed tended to be higher than normal.

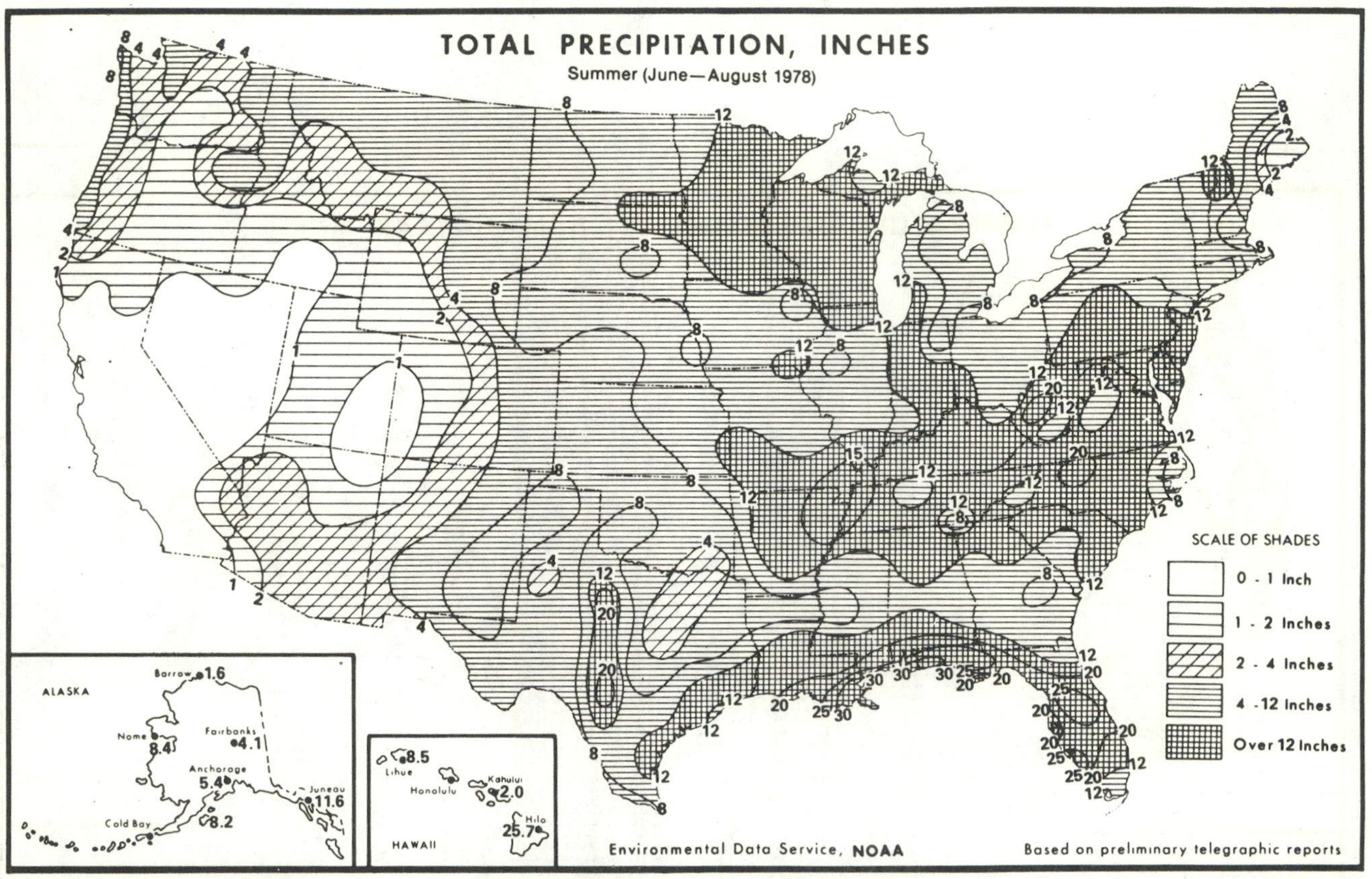

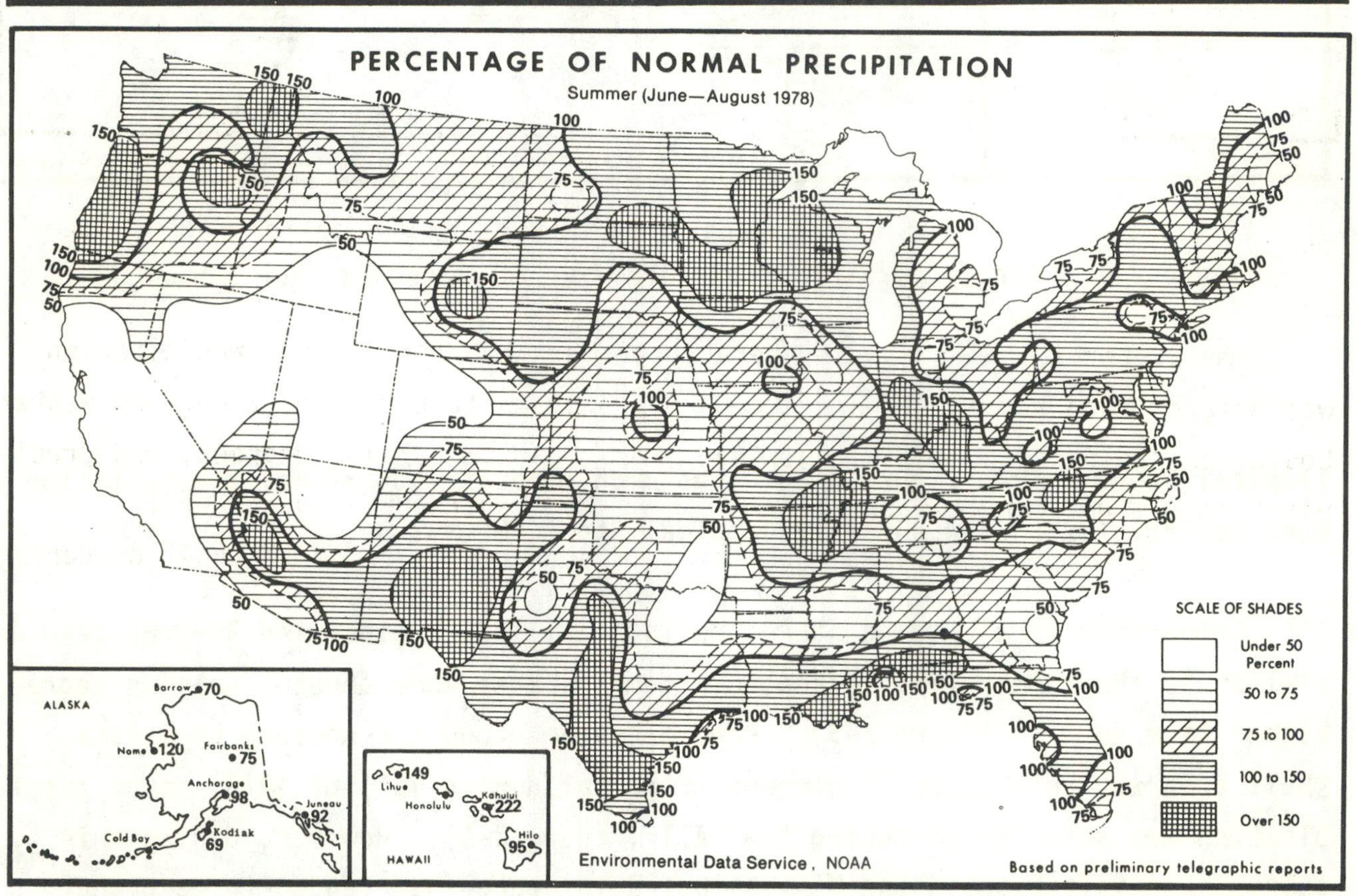

Figure 2-2. Total and percentage of normal precipitation for summer 1978.

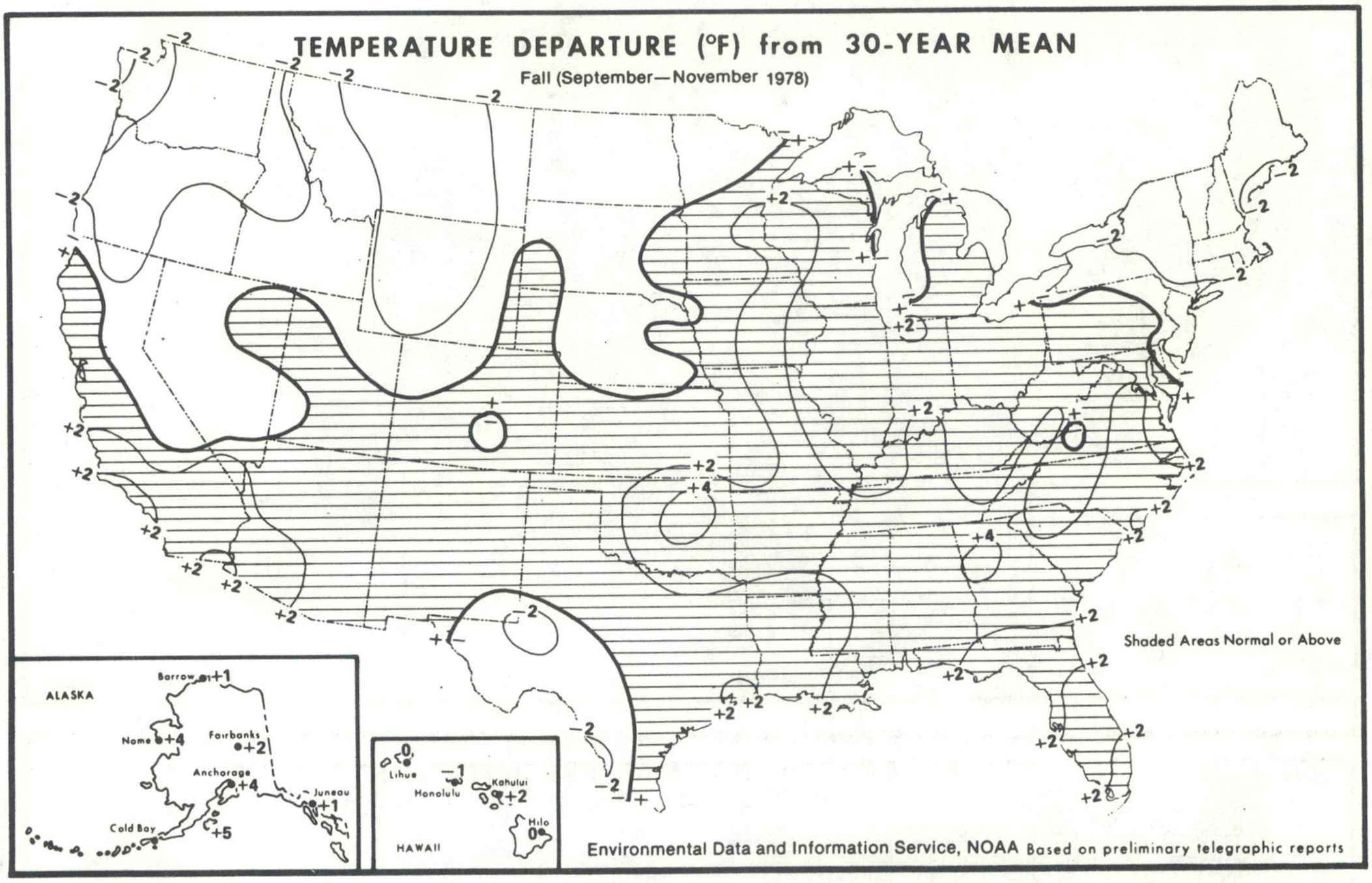

Figure 2-3. Air temperature departure from 30-year mean for fall 1978.

The winter of 1979 was considerably colder than normal and precipitation was greater than normal (figure 2-5). Surface air temperatures along the western Louisiana shelf region were lower than normal by 2.2 Celsius degrees, and precipitation was greater than normal by as much as 50 percent (figure 2-6). Precipitation along the western Louisiana shelf area was from 30 to 45 cm during the winter months.

The spring of 1979 was comparable in temperature to the 30-year mean, but precipitation was greater than normal along the Louisiana coast by as much as 50 percent (figures 2-7 and 2-8). Total precipitation over the west and central Louisiana coast was approximately 50 cm during the spring months; this, combined with above-normal winter and spring precipitation over most of the Mississippi watershed, resulted in local flooding during spring 1979.

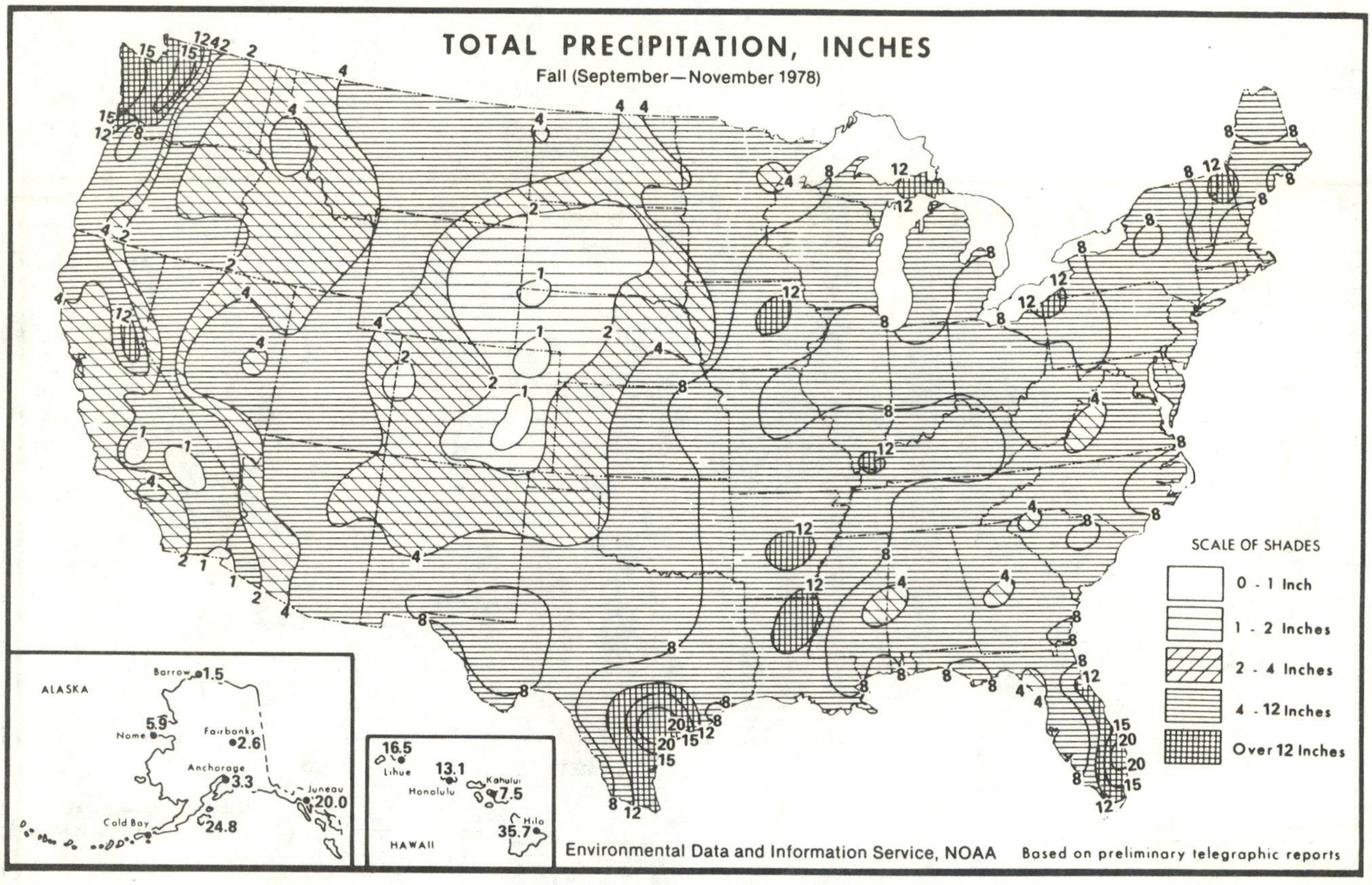

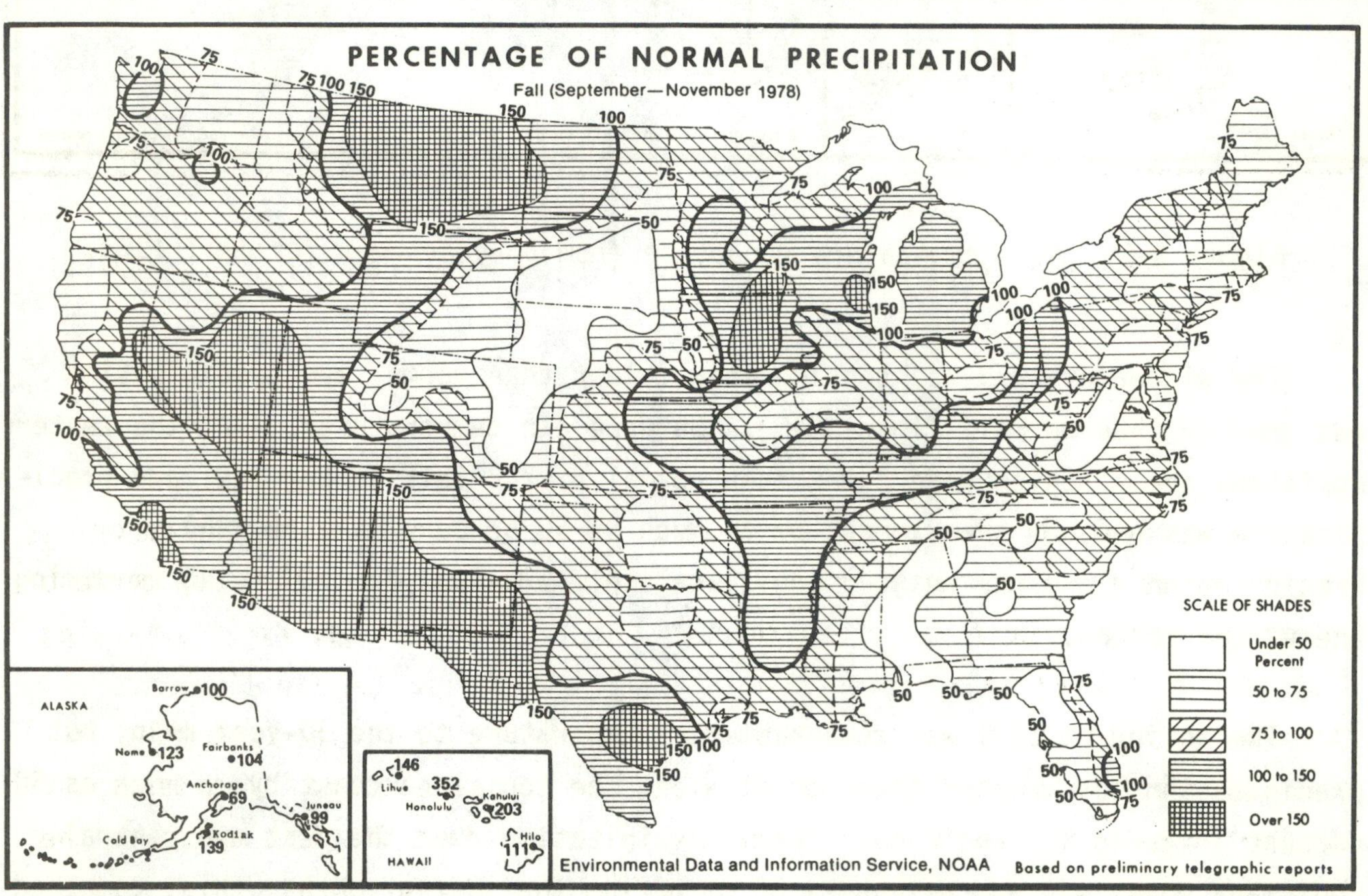

Figure 2-4. Total and percentage of normal precipitation for fall 1978.

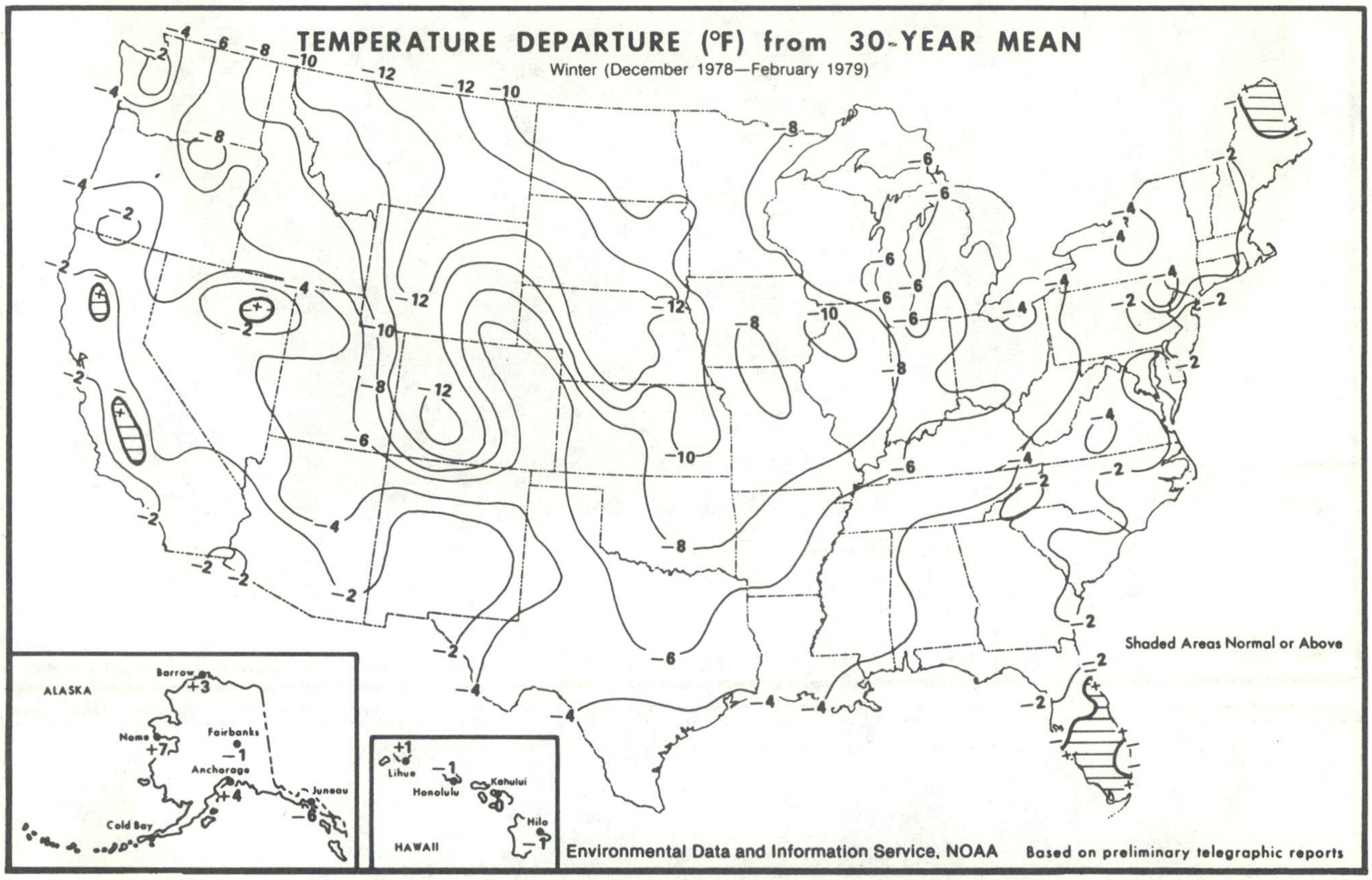

Figure 2-5. Air temperature departure from 30-year mean for winter 1979.

2.2. Oceanography

The general circulation of the Gulf of Mexico is governed by two major current systems: the loop current and an anticyclonic gyre. The loop current enters the eastern Gulf of Mexico through the Yucatan Straits, extends varying distances northward in an anticyclonic (clockwise) loop, and finally exits through the Straits of Florida. Speeds in the loop current reach 50 to 200 cm/s, generally transporting more than 25 x 10^6 m^3/s of water. This transport is about one-third of the Gulf Stream transport and is sufficient to flush the Gulf of Mexico basin in 30 months (Leipper, 1970). Behringer et al. (1977) suggest that the penetration of the loop current into the Gulf of Mexico reaches

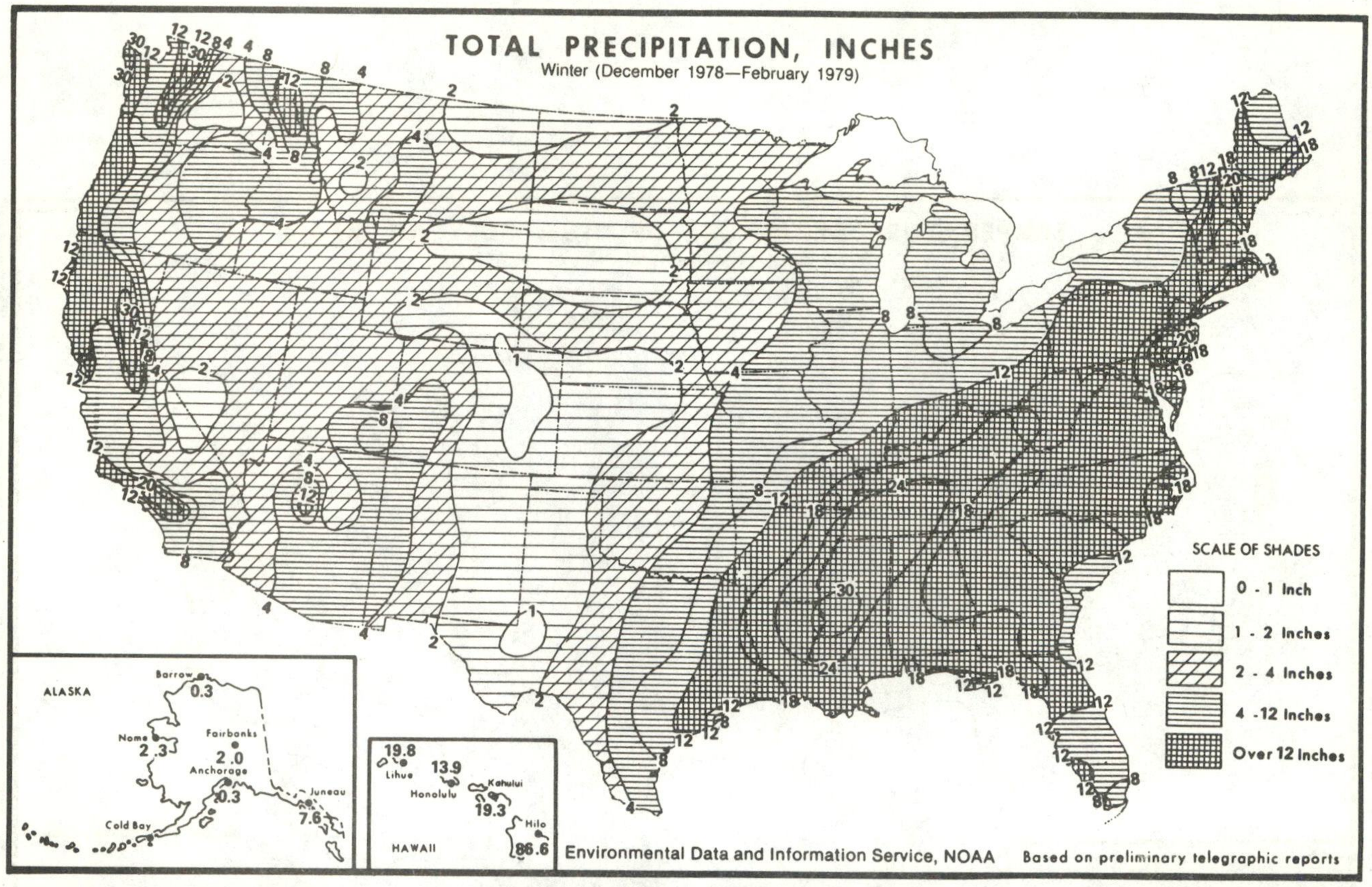

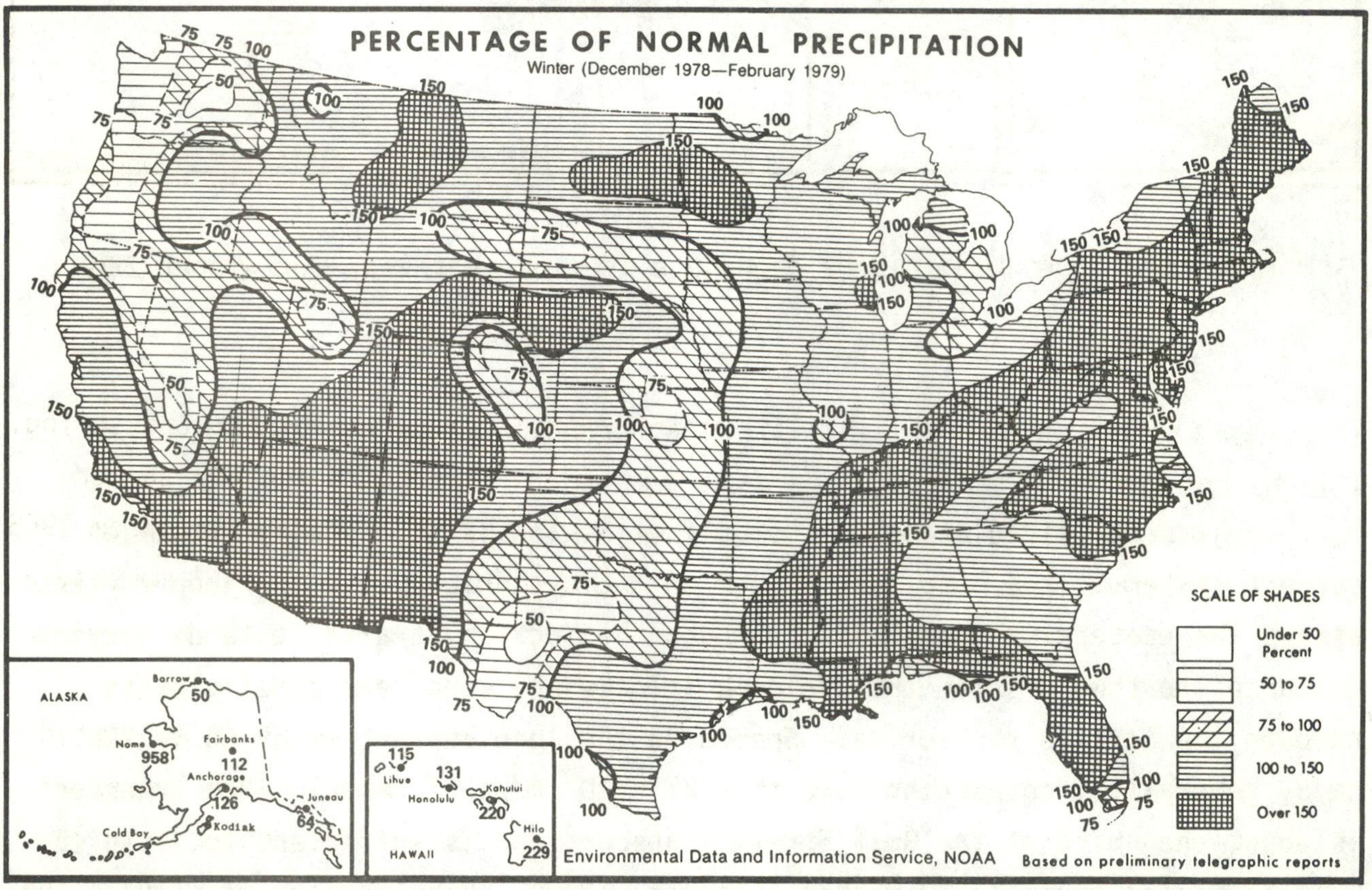

Figure 2-6. Total and percentage of normal precipitation for winter 1979.

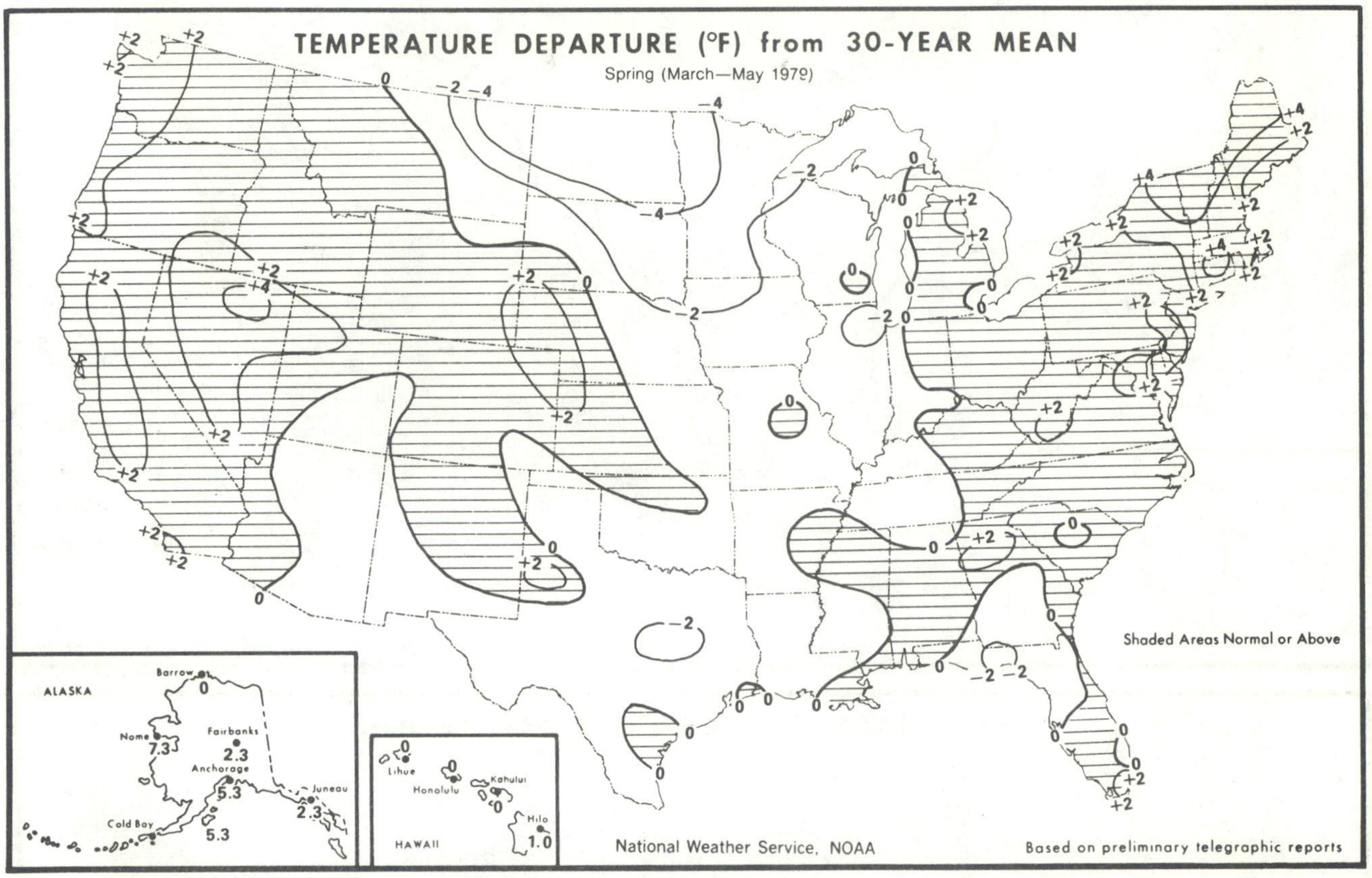

Figure 2-7. Air temperature departure from 30-year mean for spring 1979.

a maximum during the early summer after increasing during the winter and spring. A large anticyclonic eddy probably separates from the loop during the summer maximum penetration. The period between eddy separations is variable; from 1965 to 1977 the minimum period was 8 months and the maximum period was 17 months, a factor of approximately two.

Circulation in the central western Gulf in winter appears to be dominated by an anticyclonic gyre (Nowlin, 1972). There are two competing hypotheses about the genesis of the gyre. Nowlin and Hubertz (1972) and Cochrane (1972) postulate that the gyre was generated initially by an eddy which drifted to the west after being separated from the loop current. Sturges and Blaha (1976)

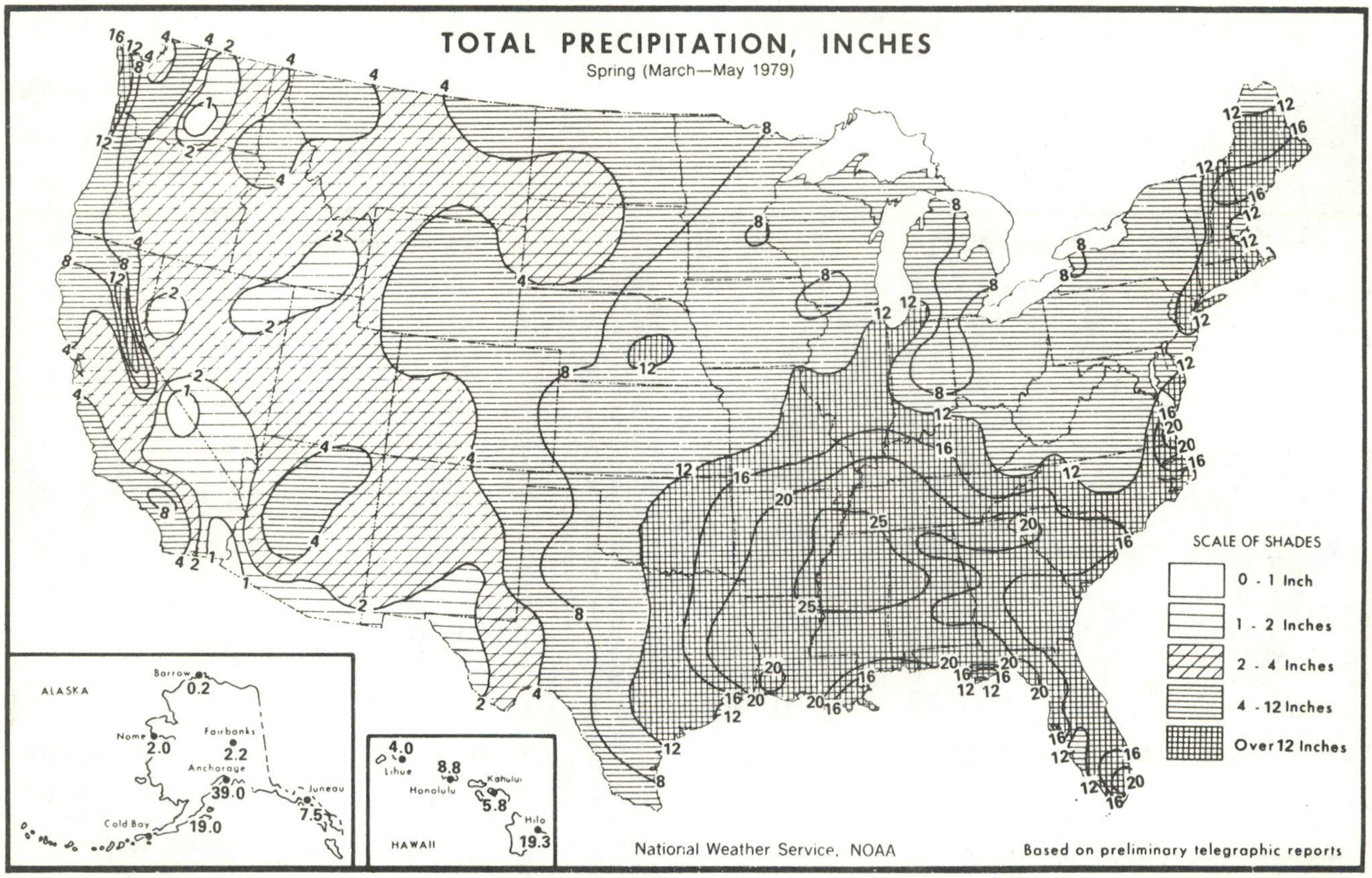

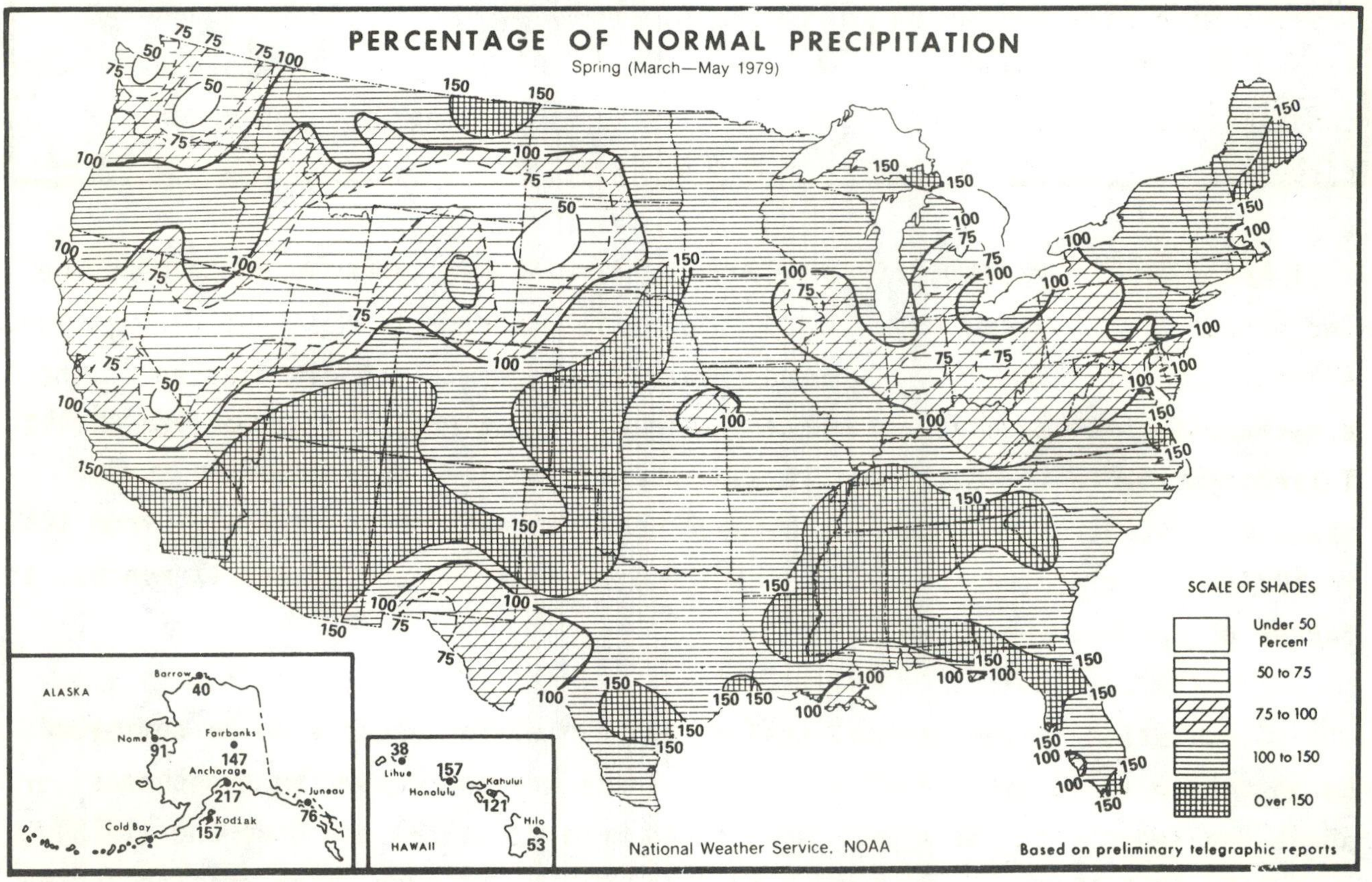

Figure 2-8. Total and percentage of normal precipitation for spring 1979.

believe that circulation in the eastern Gulf is governed by the curl of the wind stress, in direct analogy to the major oceanic gyres. Elliott (1979) argues that the primary energy source for the anticyclonic gyres observed in the western Gulf is the loop current; the mechanism is the westward translation of rings that separate from the loop current.

Both budgetary and operational constraints precluded NOS from obtaining CTD and current meter data further offshore to examine directly the coupling of the inner shelf circulation with the general circulation of the Gulf of Mexico. Our preliminary evaluation of the circulation at the two sites indicated that only weak or infrequent coupling existed between the general and inner shelf circulations, except during July and August when the net eastward flow is consistent with the findings of Behringer et al. (1977). River runoff and local wind stresses are the most important mechanisms. The relatively wide Louisiana shelf with a gradual shelf break is not conducive to lateral momentum transfer from the general circulation onto the shelf, as has been observed on narrow shelves with more pronounced shelf breaks (Allen and Kundu, 1978; Muench and Schumacher, 1979). Additional analysis of the NOS data set, together with other observations, may provide further insights into coupling with the general circulation, but will not be attempted here.

Prior to the NOS SPR Support Project, current measurements at or near the two proposed sites were too limited in spatial coverage to describe circulation. Although Murray (1976) reviewed and summarized currents and circulation in the coastal waters of Louisiana, emphasis was on the eastern shelf area from Terrebonne Bay to the Southwest Pass.

2.3. River Runoff

The circulation on the inner Louisiana shelf is largely affected by river runoff, particularly from the Mississippi and Atchafalaya Rivers. Iseri and Langbein (1974) report that the freshwater discharge from the Mississippi River is 1.28×10^4 m^3/s on the average, and the maximum discharge is 2.70×10^4 m^3/s during April. Ichiye (1960) showed that mixing of the Mississippi River freshwater discharge is confined to the shelf water landward of the shelf break.

Rouse and Coleman (1976) report that the configuration of the Mississippi River plume depends both on the volume of fresh water runoff and the speed and direction of surface winds. Their analysis of LANDSAT images indicate that plumes of suspended sediment extend greater than 75 km seaward when wind conditions are favorable. Low salinity water observed nearshore and west of the Mississippi and Atchafalaya Rivers result from the general westward spreading of their freshwater discharges (Nowlin, 1972).

The 20-year monthly mean river discharge from the Mississippi River, Atchafalaya River, and the total discharge from all other rivers west of the Atchafalaya River to the Rio Grande River are shown in figure 2-9. The Mississippi and Atchafalaya Rivers show similar seasonal variations, with maximum discharge in April and minimum discharge in September. The sum of the discharges of the other tributaries shows a maximum during May and a weak minimum during August.

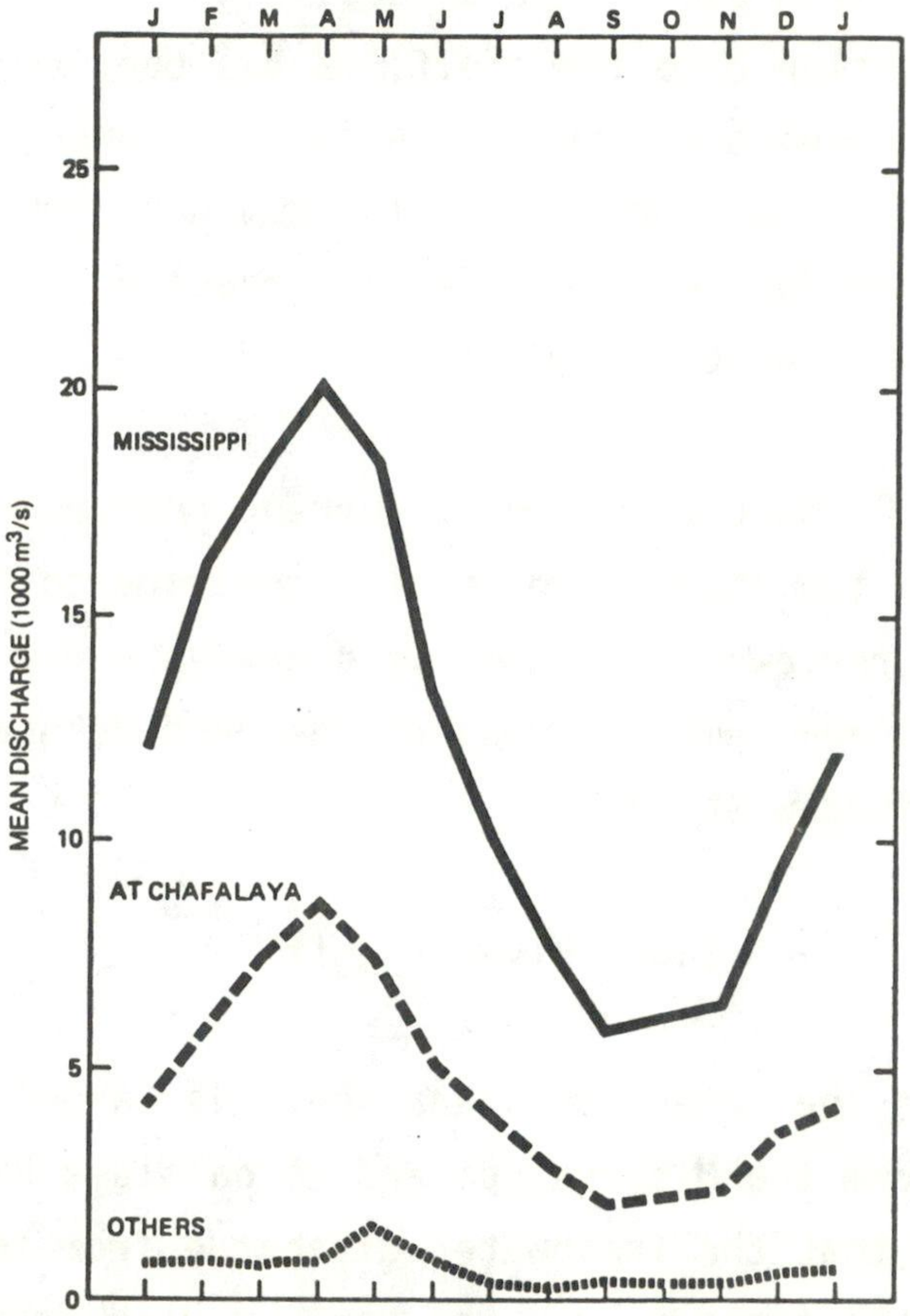

Figure 2-9. Monthly mean discharges for the Mississippi and Atchafalaya Rivers, and the sum of the mean discharges from all rivers west of the Atchafalaya to the Rio Grande. (Source: U.S. Geological Survey reports of surface water supplies of the United States, 1950-1970)

3. DATA ANALYSIS

Volume two of this report contains a complete description of the measurement systems, calibrations and sensor transfer functions, data processing and validating methods, and the availability of the project data from the National Oceanographic Data Center (NODC). Numerical measures of the quality of the NOS SPR Support Project data are documented in volume two of this report.

3.1. Data Quality Assurance

All measurements can be traced to laboratory standards. Error sources were identified and analyzed to develop uncertainty statements. A total measurement uncertainty (TMU) was computed for each measurand. The TMU includes an estimated calibration uncertainty, sensor measurement uncertainty, and environmental error sources. The TMU for each measurement is intended to bound errors for 95 percent of the "typical" field measurements. A summary of representative TMU's is given in table 3-1; it is necessary to apply the qualifications described in section 7, volume two of this report prior to using these TMU's.

Special emphasis was placed on developing current measurement uncertainties (table 3-1). Sources of current measurement errors include the uncertainties in the calibration process, sensor drift during the project, and environmentally induced effects, such as flow blockage by platforms and structural members, fouling of rotors, misalinement of current meters with the flow direction, and dynamic (principally wave) effects. A discussion and description of the current measurement uncertainties is presented in section 9 and appendices C and D in volume two of this report. Application of the current speed and direction TMU's to the project data should be done only after consulting volume two.

Table 3-1. Summary of total measurement uncertainties (TMU)*

Instrument/Parameter		TMU
Grundy Model 9021 Current Meter		
Speed TMU	at 5 cm/s:	+2.1, -3.0 cm/s
	at 40 cm/s:	+0.7, -6.3 cm/s
Speed TMU	at 5 cm/s:	+2.0. -3.3 cm/s
(during fouling season)	at 40 cm/s:	+0.0, -8.3 cm/s
Direction TMU	at 5 cm/s:	+13.9 degrees
	at 10-40 cm/s:	±10.9 degrees
Temperature		± 0.28°C
Conductivity		± 0.24 mS/cm
Time base		± 66 s/month
Aanderaa Meteorological Station		
Wind speed at 5 m/s		+ 1.1, -1.6 m/s
Wind direction		± 16 degrees
Air temperature		+ 0.83, -0.43°C
Air pressure		+ 0.5, -8.2 mbar
Applied Microsystems Model 750A Wave Gage		
Pressure		± 0.029 dbar
Aanderaa Model WLR-5 Water Level Gage		
Pressure (SN 360)		+ 0.083, -0.048 dbar
Differential water level (SN 360)		+ 0.13, -0.14 m
Grundy Model 9400 CTD System		
Temperature (1/78-12/78)		+ 0.20, -0.04°C
Conductivity		+ 0.06, -0.36 mS/cm
Pressure		+ 1.10, -0.85 dbar
Guildline Model 8400 Autosal		
Salinity		+ 0.023, -0.005 ppt
Micro-Winkler Titration Apparatus		
Dissolved oxygen		± 0.03 ml/l
Beckman RS-5 Salinometer		
Temperature		± 0.83°C
Conductivity		∓ 0.90 mS/cm
Salinity		∓ 1.56 ppt

* The uncertainty values in table 3-1 have been summarized from section 7, volume two of the final report. The TMUs do not apply to all instruments of a given model or to the entire duration of the field experiment. The values shown in table 3-1 should not be used without reviewing section 7, volume two.

3.2. Dissolved Oxygen

DO values were determined by micro-Winkler analyses of seawater samples obtained at three levels: 1 m below the sea surface, midwater, and 1 m above the sea floor. The modified Winkler technique used is described both by Carpenter (1965) and the USN Oceanographic Office (1968).

3.3. Salinity, Temperature, and Density

A Grundy model 9400 CTD system was used to record conductivity and temperature profiles except during December 1978 and January 1979, when a Beckman RS-5 instrument was used. No validated CTD profiles were obtained from February to May 1979 because the system malfunctioned. During this period, water samples collected 1 m below the surface, midwater, and 1 m above the bottom were used to determine salinity gradients. Profile data obtained by NMFS during 1979 with an instrument calibrated by NOS are included in our analysis; these data are summarized by Parker and Crowe (1980). Salinity was calculated from conductivity and temperature using a modified UNESCO equation (1971). Sigma-t = (density -1) x 10^3 gm-cm^{-3} was calculated from salinity and temperature using the equation of Fofonoff (1958).

The equations used for the calculation of conductivity, salinity, and sigma-t are presented in appendix A. The conductivity at 35 ppt, conductivity ratio, and salinity were calculated using the in situ temperature values recorded at each site. Sigma-t was calculated using the computed salinity and the temperature measured in situ. The equation used for the calculation of sigma-t is also shown in appendix A.

CTD data were interpreted by graphically displaying the various parameters and reviewing the plots. The data were plotted as profiles of salinity, temperature, and sigma-t vs. depth using a program labelled X-Y PLOT. This program produces a magnetic tape that is read by an Information International, Inc., FR80 microfilm recorder. Images displayed on a CRT were then reproduced directly onto 35-mm microfilm. The plots were analyzed to detect effects of waves, swell, and ship motion on the depth readings. Contours of temperature,

salinity, and sigma-t were plotted both for the alongshore and transhore sections.

3.4. Meteorology

Aanderaa Automatic Weather stations recorded the meteorological data: (1) wind speed and direction, (2) barometric pressure, and (3) air temperature. Wind data were analyzed at the anemometer height (table 3-1) and were not corrected to the standard 10-m height. The data were analyzed using both spectral and statistical techniques.

3.4.1. Spectral Analysis

The analysis of the meteorological data was incorporated into the analysis of the current meter data. The spectral analysis technique used on these data is based on the maximum entropy method discussed in section 3.7. An autospectrum of the wind and cross-spectra between wind and current were calculated. The program also calculated the phase lag and the coherency squared between the current and the wind data. This knowledge is fundamental to the understanding of the energy exchange at the air/sea interface.

3.4.2. Statistical Analysis

The statistical analysis performed on all meteorological data included the calculation of mean speed, standard deviation, and joint frequency. The joint frequency displays the percentage of wind observations found in both a specific direction sector and a specific speed sector. The speed sector ranges from 0 to 50 m/s in 2-m/s intervals. Direction is separated into 16 sectors of 22.5 degrees each using the convention for wind direction. (The wind direction represents the direction from which the wind is blowing, while current direction represents the direction towards which the current is flowing.)

3.5. Surface Waves

Applied Microsystems, Inc., model 750A wave gages with pressure transducers provided the wave data at stations 11 and 21. Differential pressures

corresponding to wave heights were computed by subtracting the mean pressure from each of the samples in the wave measuring interval. Wave data were analyzed both by zero-crossing and spectral methods.

3.5.1. Zero-Crossing Analysis

The zero-crossing analysis method estimates wave periods from distances on the time axis between two adjacent up zero-crossing points. Using the linear wave theory for shallow water (U.S. Army Coastal Engineering Research Center, 1975), the period, maximum wave height, and significant wave height were computed. Wave heights were adjusted by the hydrodynamic attenuation factor. The results of the zero-crossing analysis are used in this volume to describe maximum wave heights during storms, because this method provides better estimates than the spectral method.

3.5.2. Spectral Analysis

Each 4-hourly sample has 966 data values. The length of the data series must be some power of two to use the Fast Fourier Transform (FFT). For maximum frequency resolution, each record was padded with zeros at each end to extend the series length to 1,024 data values. In each frequency band, each point energy (raw estimate) was adjusted by the square of the corresponding hydrodynamic attenuation factor. The total energy of the selected bands was computed by integrating the point energy values over each bandwidth. The number of degrees of freedom depends on the number of point energies integrated per band.

The frequency bands with periods lower than 4 seconds as well as those greater than 20 seconds were neglected because of the limitation of the equipment (sample rate and total data storage) and the depth of the wave gage. Although the 0.5-second sampling rate of the pressure type wave gage should, in theory, allow detection of 1-second period waves without aliasing, the minimum wave period that could be detected with confidence was 4 seconds. This difficulty in detecting the short period waves is associated with the increasing attenuation factor correction required for pressure type wave gages at the higher frequencies. Band widths of approximately 1 second were used to compute the wave spectra. Therefore, if the period of peak energy was less than

5 seconds, it could not be detected except to say that it must be equal to or less than 4 seconds.

The significant wave heights were calculated from the spectra by multiplying the square root of the total energy by four, assuming a Raleigh distribution of wave energy (U.S. Army Coastal Engineering Research Center, 1975). Whenever the energy reached a maximum between 4 and 20 seconds, the period of peak energy was listed. Spectral densities were displayed whenever the significant wave height exceeded 1 m.

The calculated significant wave heights were recorded in NODC format and forwarded to EDIS for archiving. The summary tables of significant wave heights (tables 7-1 and 13-1) were derived from the spectral analysis, as were the summary tables of periods of peak energy (tables 7-2 and 13-2). The significant wave heights computed both by the zero-crossing method and by the spectral method are shown in figure 3-1 for comparison.

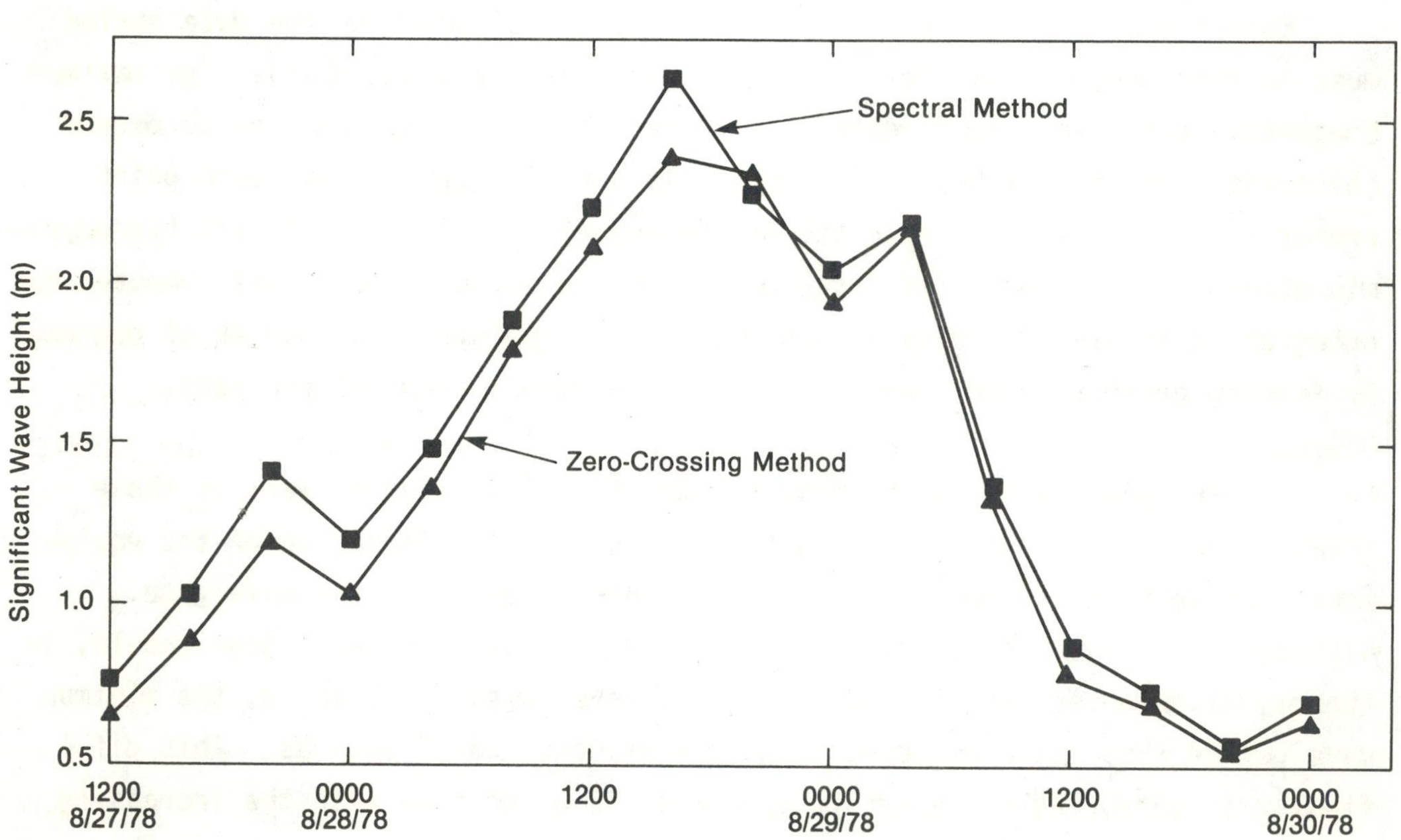

Figure 3-1. Comparison of spectral and zero-crossing methods for determining significant wave height.

3.6. Water Levels

Water level data were recorded as pressure using Aanderaa model WLR-5 water level recorders mounted on the instrument platforms at stations 11 and 21. The pressure records were converted to depths. The data were not corrected for water density or air pressure fluctuations. The equation for converting pressure to depth used monthly mean values for temperature. The resulting pressure uncertainty was calculated to be in the interval from +0.005 to -0.015 dbar (1 dbar is approximately equal to 1 m of water depth). The water level data were then analyzed using nonharmonic, harmonic, and spectral techniques.

The water level data were reduced to the Gulf Coast Low Water Datum (Hicks, 1977). This datum corresponds to mean lower low water (MLLW) for a station with mixed-type tides and to mean low water (MLW) for a station with diurnal-type tides. A diurnal tide is one in which only one high and one low water occur during a tidal day (24.84 hours). Quantitatively, a diurnal tide is classified as having a ratio greater than 1.50.

Qualitatively, a mixed tide is defined as a tide having a large diurnal inequality in the two daily high waters, the two daily low waters, or both (Schureman, 1958). The tides can also be characterized quantitatively by the ratio F of the amplitudes of the major diurnal constituents, K_1 and O_1, to the major semidiurnal constituents, M_2 and S_2 [$F = (K_1 + O_1)/(M_2 + S_2)$]. If the value of F is from 0.25 to 1.50, the tide is classified as mixed. Some authors have suggested that mixed tides should be classified further as mixed, mainly semidiurnal, $0.25 < F \leq 1.50$, and mixed, mainly diurnal, $1.50 < F \leq 3.00$ (Defant, 1961; Marmer, 1954).

3.6.1. Nonharmonic Analysis

Nonharmonic analysis procedures were used to calculate the various mean water levels, i.e., mean high and higher high water and mean low and lower low water. These mean water levels are used to calculate mean ranges. For a mixed tide station, a mean range and a greater diurnal range were calculated. For diurnal tide stations, only a mean range was calculated.

To determine the mean water levels, the tide curve was examined for the daily high and low water extremes. This was done using a program obtained from the Tidal Analysis Branch of the NOS Tides and Water Levels Division, which was modified to accept the 5- or 10-minute interval data that were recorded during this study. The values of the times and heights of the water level extremes obtained with this program were then verified using the time series plot of the raw data.

The values of the daily high and low water extremes were tabulated to determine the daily higher high and lower low water values. The arithmetic mean of the high waters (MHW), the higher high waters (MHHW), the low waters (MLW), and the lower low waters (MLLW) were calculated for each month of data. These mean values were then used to calculate the mean range (Mn = MHW - MLW) and the greater diurnal range (Gt = MHHW - MLLW). The diurnal high water inequality (DHQ) is obtained by subtracting MHW from MHHW. The diurnal low water inequality (DLQ) is obtained by subtracting MLLW from MLW (Marmer, 1951). The mean values obtained for the various ranges and inequalities were compared with NOS historical data for this region.

3.6.2. Harmonic Analysis

The data were analyzed using a modified version of a 29-day harmonic analysis program developed by Dennis and Long (1971). From the 29-day analysis program, we obtain the amplitudes and phases of the five major constituents K_1, O_1, M_2, S_2, and N_2, some higher harmonics (M_4, M_6, etc.) and a few other minor constituents. Additional information on water level theory is in appendix B.

The program also calculates the Greenwich high and low water intervals and the tropic intervals. The Greenwich high water interval is the time interval between the transit of the moon over the meridian of Greenwich and the occurrence of the following high water at the measurement location. Similarly, the low water lunitidal interval is the elapsed time between the transit of the moon and the following low water. The tropic higher high water and lower low water intervals are the lunitidal intervals pertaining to the higher high and lower low waters, respectively, at the time of the Tropic Tides. The Tropic

Tide refers to those tides that occur during the period of maximum declination of the moon. The times of the tide at a secondary station can be referenced to those of a primary control station by subtracting their respective lunitidal intervals.

Using the prediction formula from Schureman (1958), discussed in appendix B, a predicted series for a given time period can be generated. Subtracting this predicted series from the observed series for corresponding time periods, produces what we define as the residual series. However, before forming the residual series the observed series were averaged to form hourly data. The residual series was then analyzed by both harmonic and spectral techniques.

3.6.3. Spectral Analysis

The observed and residual (observed minus predicted) water level time series for each monthly period was analyzed using the maximum entropy method developed by Burg (1968), discussed in section 3.7.2. An autospectrum of the original and residual were calculated and plotted on 35-mm microfilm (discussed in section 3.3). These results, together with the results of the harmonic analysis, were used to determine the characteristics of the astronomical tide at each site.

3.7. Currents

Current data were collected using Grundy model 9021 current meters. The data were analyzed by three different methods: (1) harmonic analysis, (2) spectral analysis, and (3) statistical analysis. Any data record with a time discrepancy or with irreparable data errors was not used for spectral or harmonic analysis. When used for statistical or descriptive purposes, however, the amount of time discrepency was noted.

3.7.1. Harmonic Analysis

Current data records were analyzed using either the 29-day harmonic analysis program, discussed in section 3.6.2., or a modified version of the 29-day

program, a 15-day analysis program. The 15-day harmonic analysis requires the constituent N_2 to be inferred since a series of at least 27.555 days is needed in order to separate N_2 from M_2. Before each record was analyzed it was resolved into major and minor components, with the major component being alined along the local isobath. The major axis at West Hackberry was alined along 86 degrees True, and at Weeks Island it was along 118 degrees True.

The calculated harmonic constituents were used to predict the associated tidal current for a specified period, which was then subtracted from the original time series to obtain a residual series. The residual series is composed predominantly of nontidal currents. The original, predicted, and residual current series were graphically displayed for additional analysis.

Tidal current ellipses for the calculated harmonic constituents were determined from formulas in Doodson and Warburg (1941), and graphically displayed by a computer graphics program. The following parameters were determined from each ellipse: (1) orientation of the major axis of the ellipse, (2) speed values for the major and minor axes, (3) phase lag, and (4) rotation of the constituent flow.

The phase lag is the epoch for the constituent's cycle relative to Greenwich Mean Time (GMT, the reference time meridian for this project). The small dots on the ellipse, if vectors are drawn to them from the center of the ellipse, represent the direction of flow for each hour of the constituent cycle (with zero hour referenced to the time of the maximum astronomic force over Greenwich).

The direction of maximum constituent flow is a valuable result of the analysis. The ellipses for the primary semidiurnal constituent M_2 and the primary diurnal constituent K_1 were transferred to a chartlet of each site. These figures represent the tidal current characteristics at each location.

3.7.2. Spectral Analysis

The spectral analytic technique is based on the maximum entropy method (Burg, 1968). This technique provides autospectra, cross-spectra, phase lag,

and coherency squared with an improvement in frequency resolution over the Blackman-Tukey method (Radoski et al., 1975). Program BURG's spectral results are given in terms of two polarized rotating components, one clockwise (+) and the other counterclockwise (-).

The analysis of a vector series in terms of two components rotating in opposite directions can be useful in studying the coupling of the wind field and currents (Gonella, 1972). Since inertial currents are always clockwise in the Northern Hemisphere, such a method also allows clearer distinction of inertial effects.

The maximum entropy method allows one a choice in the number of filter weights used to calculate the error filters. However, care must be taken in choosing the number of terms for the filter used because too few will give poor resolution, while too many will result in instabilities (Chen and Stegen, 1974). A more detailed discussion of the maximum entropy method and the mathematical development of the minimum phase prediction error filter can be found in Chen and Stegan (1974) and Radoski et al. (1975).

To determine the optimum filter weights for this study, two steps were followed. First, several applications of the method were made on data from both sites using different filter weights. The spectral results were reviewed for instability, and a rough indication of the performance for each run was given by Akaike's FPE criterion (Strand, 1977). Second, a known time series was used as a control when making parallel runs using the Burg method and the Cooley-Tukey method (Cooley and Tukey, 1965). The Burg method provided superior results over the Cooley-Tukey method at 75 to 100 filter weights while maintaining stability.

3.7.3. Statistical Analysis

The analysis performed on all current meter records included the calculation of mean speed, standard deviation, mean current vector, and joint frequency in speed and direction. The joint frequency results indicate the percentage of current observations jointly in a direction sector and a speed interval. The speed intervals range from 0 to 50 cm/s in 2-cm/s increments. Direction is

divided into 16 sectors of 22.5 degrees each, representing the cardinal, intercardinal, and combination points of the compass, e.g., N, NNE, NE, ENE, E, etc.

A relative volume transport, shown graphically in appendices E and H, is defined here to facilitate the graphical summary of the large current meter data set. It is the volume of sea water advected past the effective cross-sectional area at a current meter within a 22.5-degree azimuthal sector, divided by the total transport of all sectors. The transports are given for specified heights above the bottom and for the 16 azimuthal sectors of 22.5 degrees each that were chosen for computing joint frequencies. Our definition of relative volume transport at fixed heights above the bottom within azimuthal sectors differs from the more traditional concept of total mass transport. The integral expression for mass transport (Neumann and Pierson, 1966) provides the x- and y-components of a total mass transport vector across a vertical section of fixed width. Having made the distinction between relative volume transport at fixed heights above bottom in azimuthal sectors and total mass transport across vertical sections, we refer to the former simply as the transport.

The weighted scalar speed in each azimuthal sector is given by:

$$u_{\Theta} = \sum_{n,j=0}^{m,26} n_j u_j$$

where:

Θ identifies the 22.5-degree azimuthal sector (Θ = 1, 2, . . ., 16);

u_j are discrete values of scalar speeds from 0 to 50 cm/s, in 2-cm/s increments, observed at the end of each instrument averaging interval;

$j = 0,1,2,\ldots,25$;

n_j = number of observations of each discrete u_j.

The relative percent transport for each azimuthal sector during a deployment period is given by:

$$T_{\Theta} = \frac{u_{\Theta}}{\sum_{\Theta=1}^{16} u_{\Theta}} \times 100$$

Note that the effective cross-sectional area of the current meter over which the transport occurs cancels out in the computation of relative transport. The relative volume transport distribution was further categorized into four quadrants generally representing the transhore and alongshore directions. Although plots of relative transport data in quadrants provide a concise graphical summary and facilitate the display of trends, caution must be used in interpreting the meaning of the plots. The reference of direction for transport in the shoreward quadrant, for example, refers to the direction of the current vector in the shoreward quadrant, not the decomposed component of current along the shoreward axis.

At West Hackberry, the shoreward quadrant was from the northwest through northeast (315° to 45°); the alongshore eastern quadrant was from the northeast through southeast (45° to 135°); the seaward quadrant was from the southeast through southwest (135° to 225°); the alongshore western quadrant was from the southwest through northwest (225° to 315°).

At Weeks Island, the shoreward quadrant was from the north-northwest through east-northeast (337.5° to 67.5°), the alongshore eastern quadrant was from the east-northeast through south-southeast (67.5° to 157.5°); the seaward quadrant was from the south-southeast through west-southwest (157.5° to 247.5°); and the alongshore western quadrant was from the west-southwest through north-northwest (247.5° to 337.5°).

CHARACTERIZATION OF THE PROPOSED WEST HACKBERRY BRINE DISPOSAL SITE

Information described in this part characterizes the physical oceanography and local meteorology at the West Hackberry brine disposal site as observed from June 2, 1978 to June 2, 1979. The intrayear variabilities are described for the 12-month observation period. Reliable measures of interyear variabilities and determination of mean (baseline) conditions require analysis of multiyear time series data. Because the Louisiana inner continental shelf water responds relatively quickly to wind stresses and river runoff, estimates of interyear variability may be made by examining departures of winds and river discharges from the longer data sets available for these phenomena.

4. DISSOLVED OXYGEN

Seawater samples were obtained monthly, except for two extended intervals. The first was August 1978 when the FERREL was unable to steam to the West Hackberry site because of mechanical problems, and the second was December 1978 when the VIRGINIA KEY was unable to obtain samples at the West Hackberry site because of heavy seas and a priority to recover and redeploy current meters. Listings of the data are available as described in section 10, volume two of this report.

4.1. Areal Averages and Ranges

The 12-month time history is summarized in figures 4-1 to 4-3 as areal averages and ranges. At each sample level, data from all stations within the

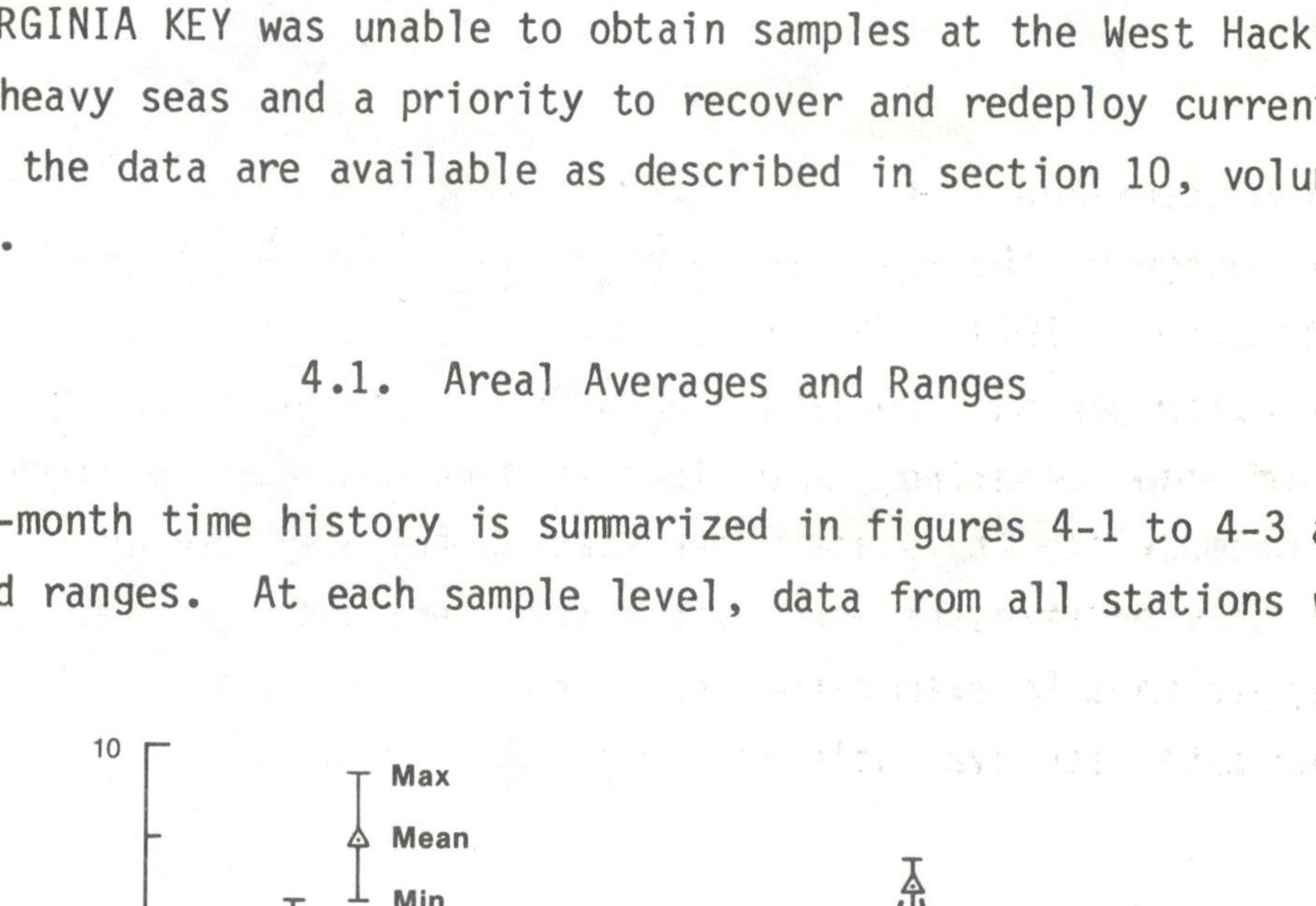

Figure 4-1. DO areal averages and ranges at West Hackberry site, 1 m below sea surface.

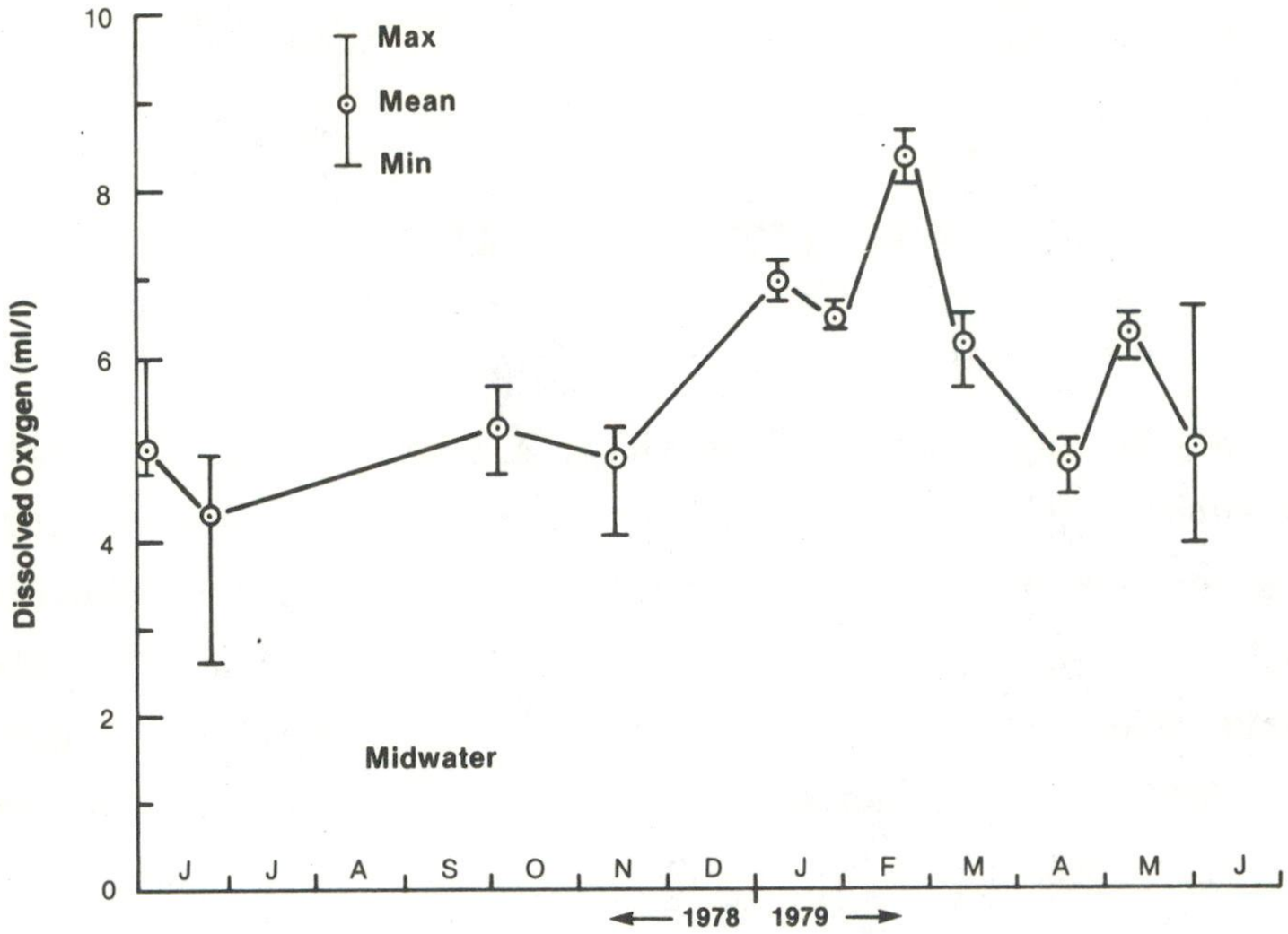

Figure 4-2. DO areal averages and ranges at West Hackberry site, midwater.

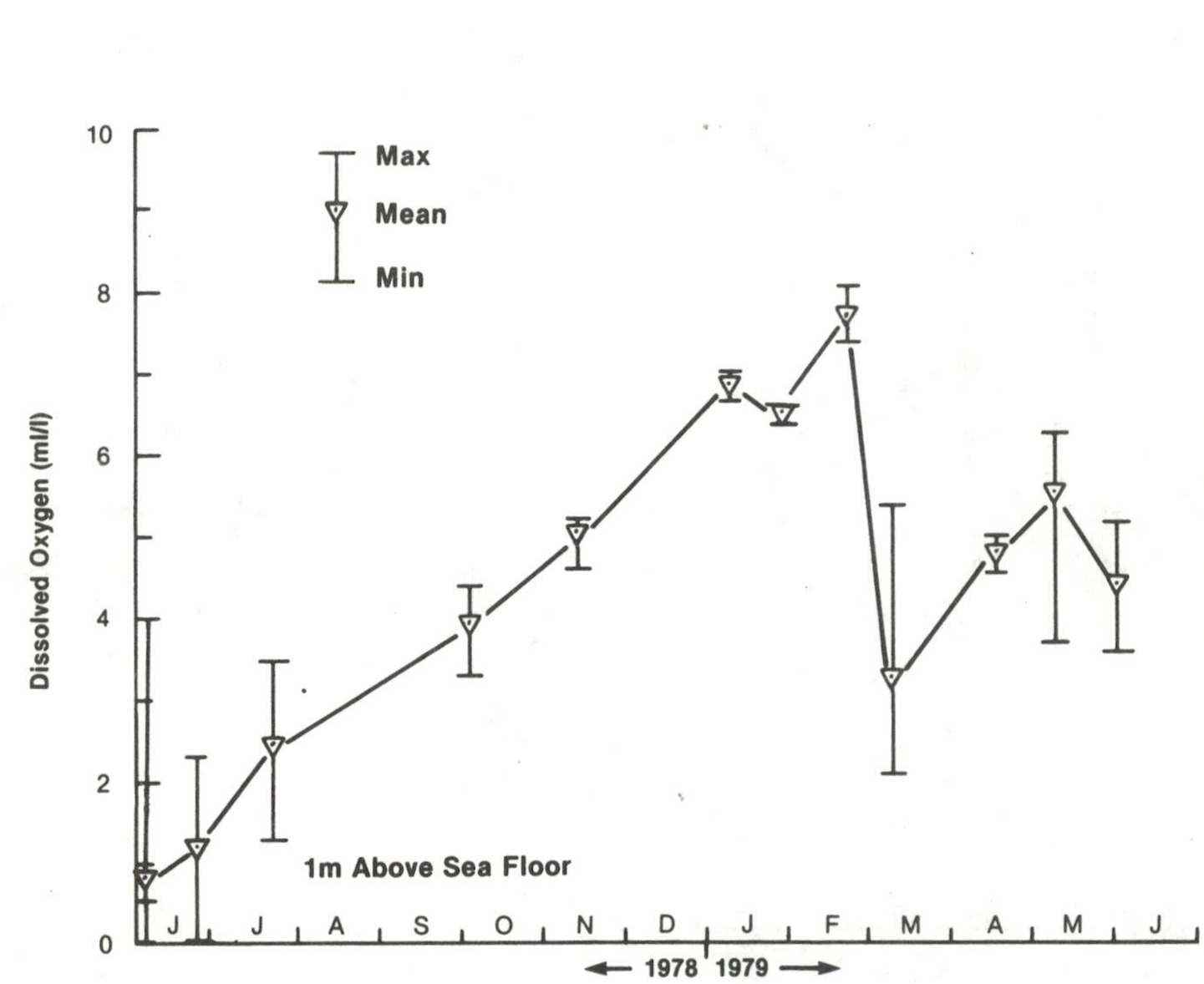

Figure 4-3. DO areal averages and ranges at West Hackberry site, 1 m above sea floor.

site are averaged and plotted as a point; bars around the points denote the ranges between the minimum and maximum values, and they provide a measure of horizontal DO gradients at the given level. The measure of horizontal DO gradients contains an unknown uncertainty, because the data were not obtained synoptically (simultaneously) at the different stations.

The largest DO gradients occurred during June 1978, when stratification of the density structure was highly stable. Both vertical and horizontal DO gradients were maximum during this period. Samples obtained 1 m above the bottom were anoxic (devoid of oxygen) within the TMU (± 0.03 ml/l) at four stations during June 2-3, 1978; the remaining three stations had DO values of 0.56, 0.86, and 3.99 ml/l at this time. During June 27, 1978, two stations were anoxic within the TMU, while three stations exhibited less than 1 ml/l, and the remaining two stations had DO values of 2.24 and 2.38 ml/l. The spatial distributions are discussed later in this section.

The smallest DO gradients were observed from November 1978 through January 1979, and again during April 1979. Vertical and horizontal DO gradients were at a minimum because of energetic mixing by winds. Average DO values were in excess of 5 ml/l during these periods.

The 12-month DO history obtained from June 1978 to June 1979 did not form a complete oscillation except at midwater. The near-bottom anoxic condition observed during the early summer of 1978 did not recur during the early summer of 1979. While the average DO during June 2-3, 1978, was 0.77 ml/l, it was 4.43 ml/l on June 2, 1979, a difference of 3.66 ml/l. The near-surface DO values on the same dates were 6.58 and 5.31 ml/l, respectively, a difference of 1.27 ml/l between the beginning and end of the 12-month period. The midwater average DO during June 2-3, 1978, was the same as the June 2, 1979, value of 5.17 ml/l.

Oxygen saturation values were computed for the level 1 m below the sea surface from the observed salinity and temperature data at the site and atmospheric pressure data obtained both at Lake Charles Airport and NOS station 18. Maximum saturation of 95 percent occurred during mid-July 1978 and mid-February 1979 in the near-surface waters, indicating minimal demand on the

DO. Depletion of O_2 in the near-bottom waters occurred during June 1978, but only a small vertical gradient was present during February 1979. The minimum saturation value found in the near-surface layer was 66 percent during April; values of 70 percent or less were observed during November 1978, January 1979, and June 1979.

4.2. Spatial Distributions

DO values at the three sample levels are plotted for the transhore and alongshore stations in figures 4-4 to 4-7. These plots represent the spatial distribution of DO for each sampling cruise.

4.2.1. Summer 1978

The June 1978 data indicate that the bottom layer was anoxic over most of the site area. The near-bottom transhore distribution at the beginning of the month displayed higher DO inshore than at the center and southernmost stations. This was due to greater mixing of the water column inshore, as suggested by the attendant decrease of DO in the near-surface layer. The alongshore distribution shows little variation over the 18.5-km section; the near-bottom layer was anoxic.

The DO in the near-surface layer at the beginning of June 1978 was 82-percent saturated; it was 75-percent saturated at the end of the month. River runoff was dominant in the surface layer on June 2-3, 1978; this is evident by the average salinity of 9.8 ppt with a range from 7.2 to 17.5 ppt. These salinity values are far more typical of estuarine waters than of coastal seas. The average salinity of the surface layer increased by June 27, 1980, to 23.1 ppt, with a range from 22.5 to 23.6 ppt.

The near-bottom values during July 26-27, 1978, were no longer anoxic, although they remained low. The near-surface values increased significantly over the 1-month period from June 27 to July 26, 1978. No midwater data were obtained during July 1978 because of temporary shortages of calibrated Ehrlenmeyer flasks. The trends in the July 1978 data indicate slightly higher values toward the east (station 14) than toward the west (station 15); the

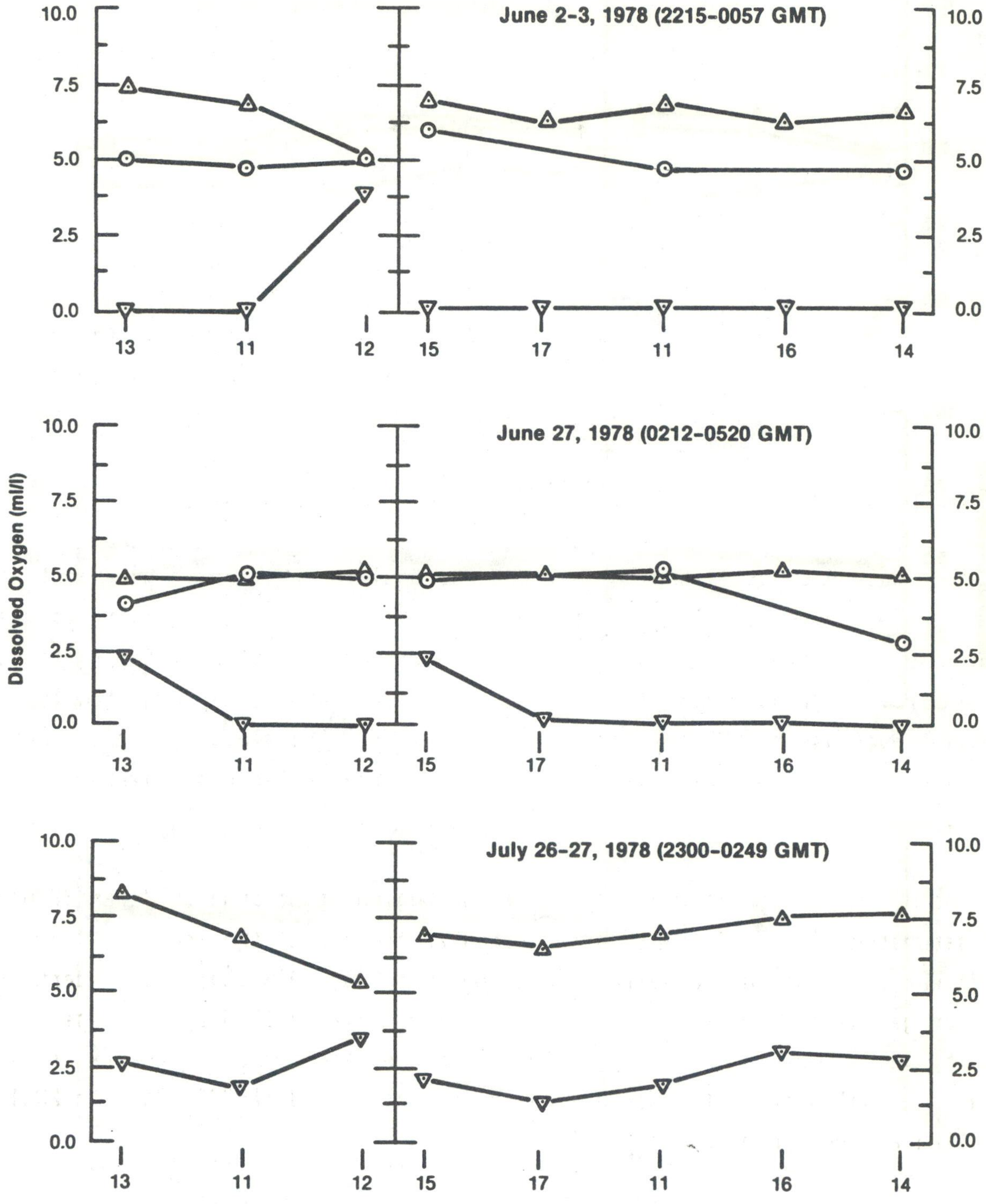

Figure 4-4. DO spatial distributions at West Hackberry site, June and July 1978.

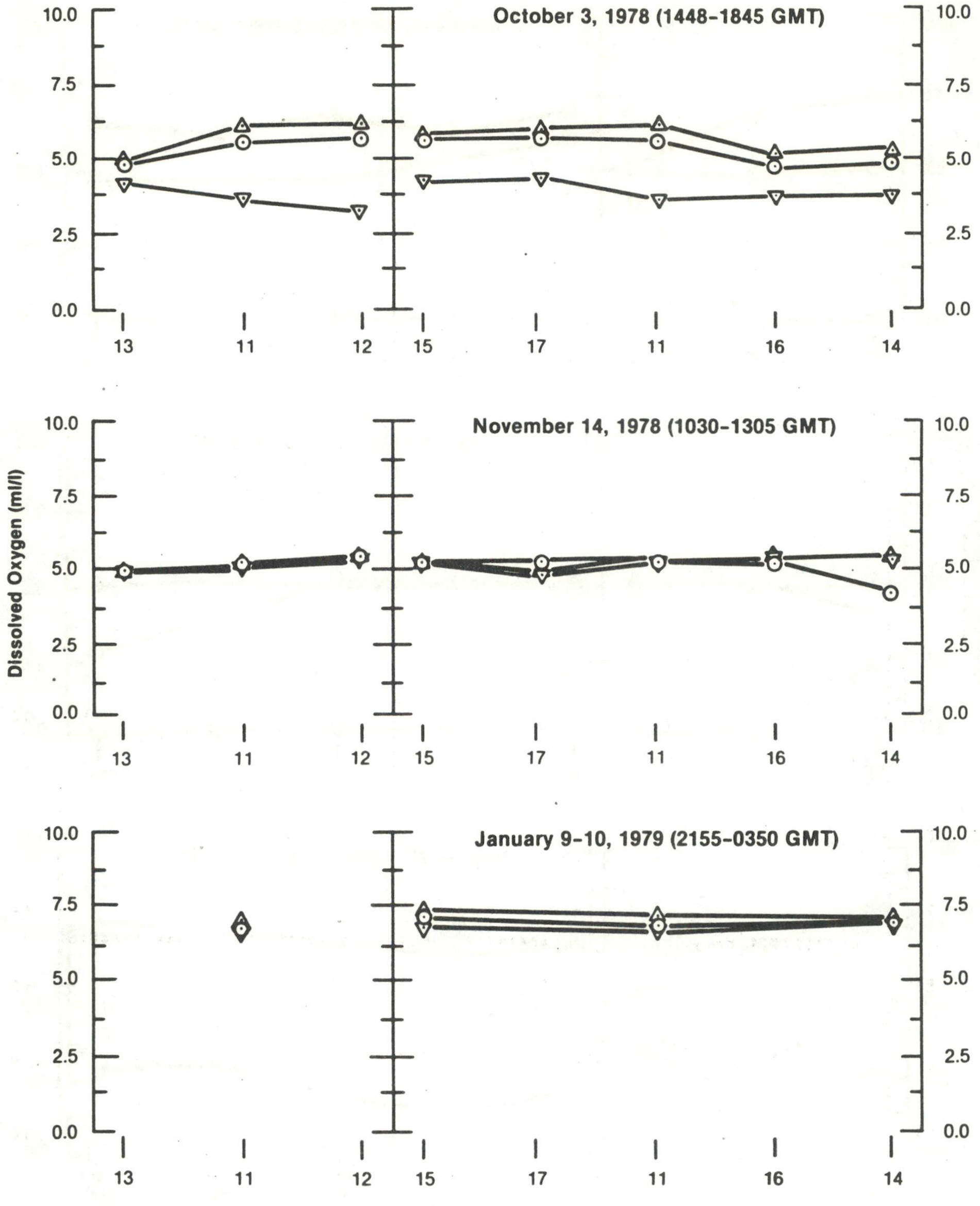

Figure 4-5. DO spatial distributions at West Hackberry site, October 1978 to January 1979.

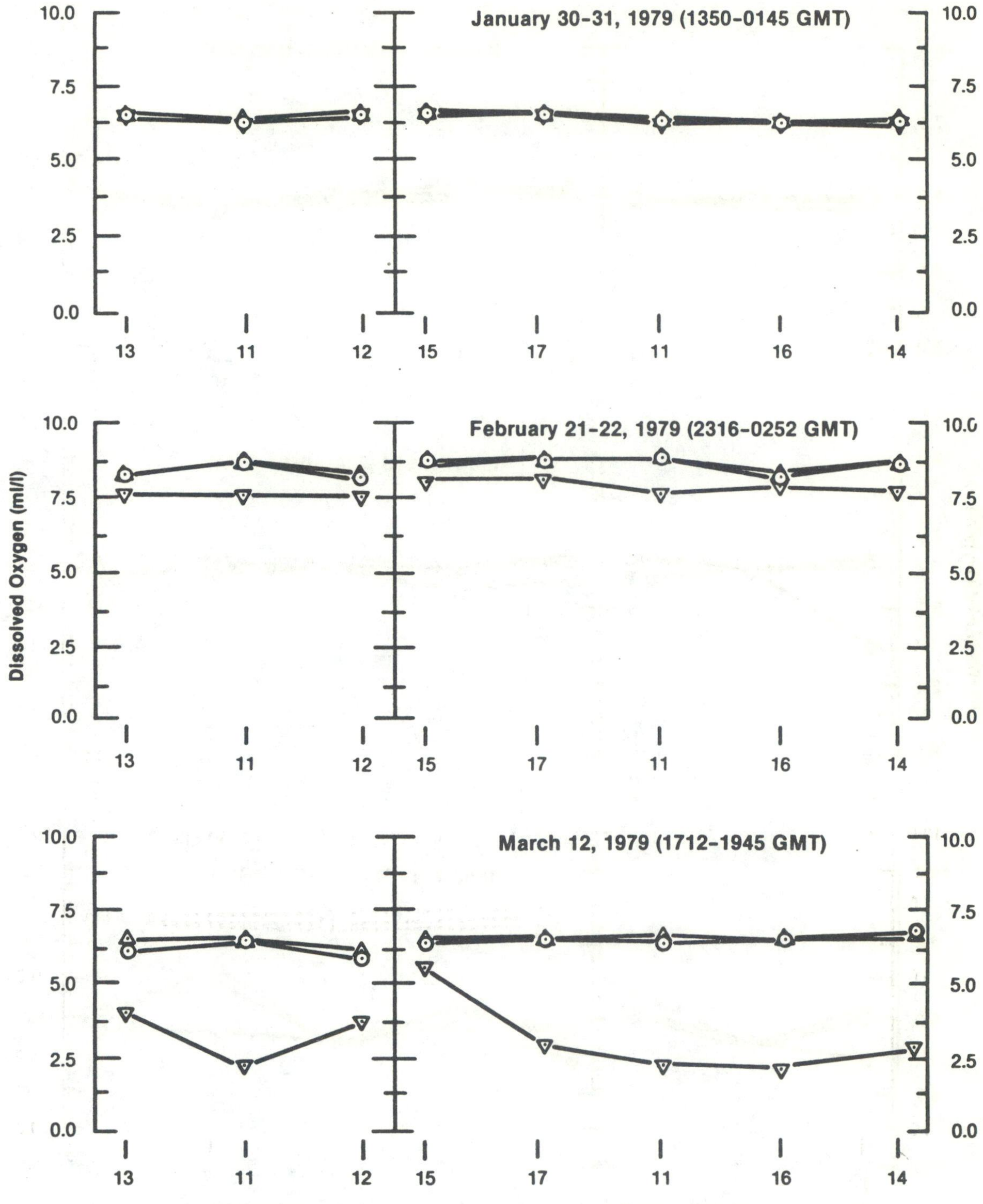

Figure 4-6. DO spatial distributions at West Hackberry site, January to March 1979.

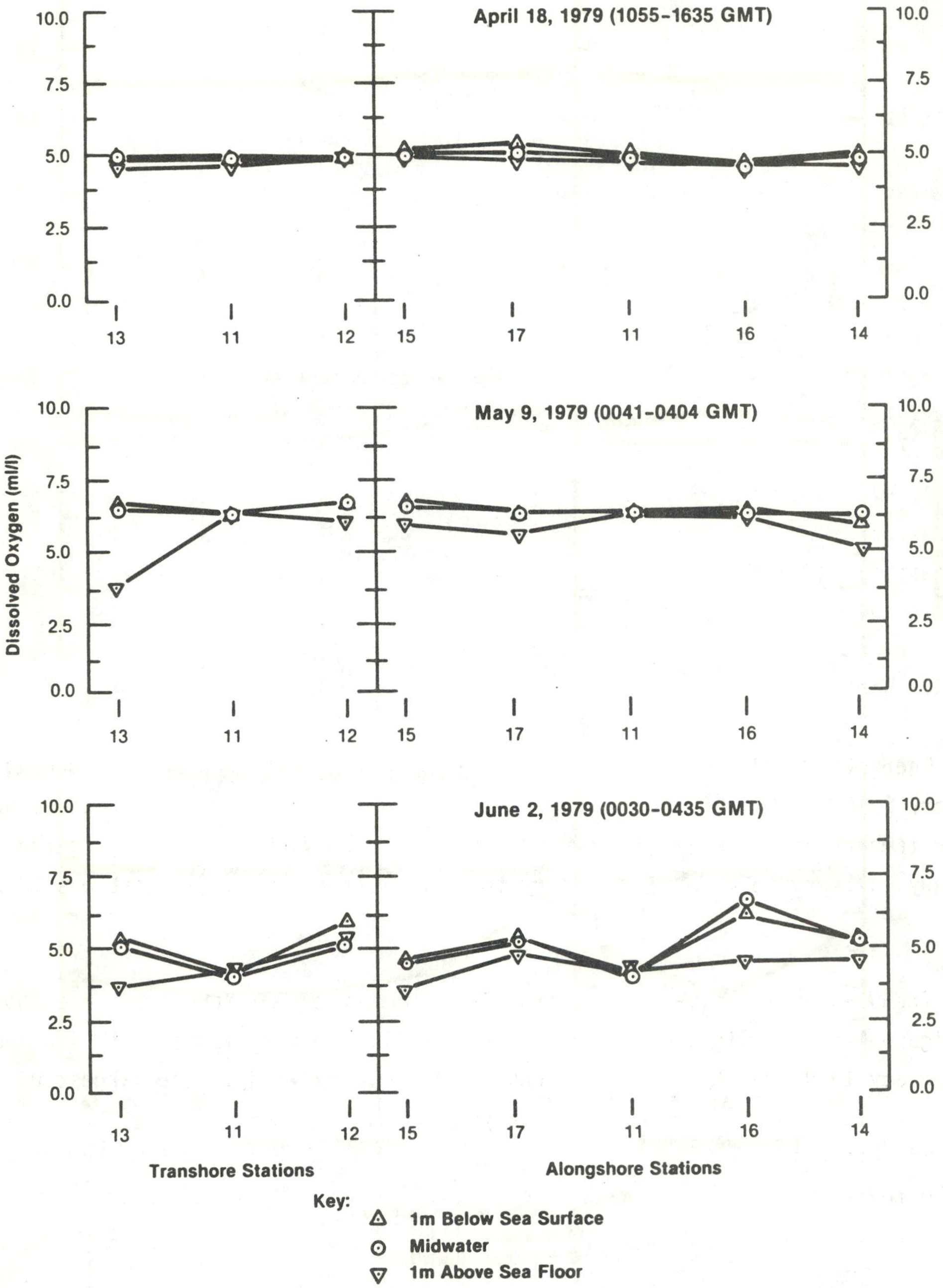

Figure 4-7. DO spatial distributions at West Hackberry site, April to June 1979.

alongshore minimum occurred at station 17. DO values along the transhore section show a minimum gradient farthest inshore. As with the data obtained during June 2-3, 1978, we believe that increased vertical mixing toward the shore was responsible for the nearly monotonic decrease in the near-surface DO.

4.2.2. Fall 1978

As mentioned earlier, there is a gap in the DO data during August and September 1978. Data obtained on October 3, 1978, are shown in figure 4-5. The near-surface layer is 85-percent saturated on the average. Vertical gradients have decreased markedly compared with the summertime gradients, mainly because of vertical mixing of the water column by winds.

By mid-November 1978, DO gradients became nearly nonexistent, except at the easternmost alongshore station (station 14). There was a very slight decrease in DO in the offshore direction. The fall plankton bloom apparently reduced the DO saturation to 68 percent.

4.2.3. Winter 1979

Energetic wind events were responsible for the small DO gradients during January 9-10, 1979, while the general DO increase is due in part to decreasing water temperature. Heavy weather encountered by the VIRGINIA KEY during the January 1979 cruise made it necessary to forego water samples at stations 12 and 13.

The DO spatial distributions from late January to mid-March 1979 are shown in figure 4-6. Negligible gradients, both vertical and horizontal, at the end of January 1979 are attributed to continued mixing by winds. The largest DO values of the 12-month study were observed during February 21-22, 1979. Stratification in the DO structure is apparent in figure 4-6, which shows mixing in the near-surface and midwater layers, and consistently lower values in the near-bottom layer. A saturation value of 95-percent is evidence of little demand on the DO during this period. The temperature in the near-surface layer indicated a slight warming trend since the late January 1979 cruise; the average

near-surface value was 10.9°C. The February 1979 near-surface average DO value was 8.46 ml/l, with an maximum value observed of 8.75 ml/l.

4.2.4. Spring 1979

Data obtained during mid-March 1979 (figure 4-6) indicate mixing between the near-surface and midwater layers with very small horizontal gradients. The lower DO values for the near-bottom water indicated the combined effect of increased oxygen demand and water column stratification. The most noticeable change since the February 1979 cruise is the very large increase in the vertical DO gradient, especially at the eastern half of the alongshore section. A pronounced change occurred between March 12 and April 18, when the gradient between the midwater and bottom layers disappeared. Also, the surface and midwater DO values decreased from about 7 to 5 ml/l.

The DO spatial distributions from mid-April to early June 1979 are shown in figure 4-7. The April 1979 data were obtained midway through the Gulf-At-Sea Performance (GASP) Experiment, during which the West Hackberry site was more heavily instrumented than usual. The mixing due to strong southerly winds account for the negligible DO gradients, both vertical and horizontal. The DO distribution during mid-April 1979 is very nearly the same as it was during mid-November 1978, with minimal gradients and a nominal value of 5 ml/l.

The May 1979 data indicate a tendency toward stratification in the near-bottom layer, while the near-surface and midwater layers appear to be mixed.

Data obtained on June 2, 1979, bear little resemblance to the data obtained exactly 12 months earlier, with the exception that the midwater averages are comparable. The June 1979 data show a weak tendency toward decreasing DO values toward the west but nearly complete mixing at the center of the site (station 11).

The DO spatial distributions from mid-April to early June 1979 are shown in figure 4-7. The April 1979 data were obtained midway through the Gulf-At-Sea Performance (GASP) Experiment, during which the West Hackberry site was more heavily instrumented than usual. Strong southerly winds account for the negligible DO gradients, both vertical and horizontal. The DO distribution during

mid-April 1979 is very nearly the same as it was during mid-November 1978, with minimal gradients and a nominal value of 5 ml/l.

The May 1979 data indicate a tendency toward stratification in the near-bottom layer, while the near-surface and midwater layers appear to be mixed.

Data obtained on June 2, 1979, bear little resemblance to the data obtained exactly 12 months earlier, with the exception that the midwater averages are comparable. The June 1979 data show a weak tendency toward decreasing DO values toward the west but with near perfect mixing at the center of the site (station 11).

5. SALINITY, TEMPERATURE, AND DENSITY

Temperature and conductivity observations and the resulting computations of salinity and density (sigma-t) at the West Hackberry site exhibit extreme variability. The variability is particularly sensitive to the discharge of fresh water from the Mississippi River, Atchafalaya River, Calcasieu Lake, and Sabine Lake. Variability at the site is also dependent on thermal heating and cooling due to weather changes, energetic mixing by wind stress on the sea surface, and changes in the characteristics of the coastal boundary layer.

Figures 5-1 and 5-2 show temperature vs. salinity (T-S) diagrams for CTD casts made during the 12-month period. Data obtained by NMFS on May 2, 1979, and summarized by Parker and Crowe (1980) are included in figures 5-1 and 5-2, because the CTD profiler used by NOS malfunctioned; the Hydrolab Surveyor used by NMFS was calibrated by T&EL. Each continuous curve shown in the T-S diagrams represents the temperature/salinity structure through the entire water column for each cruise. The length of the curves indicates whether the water column is stratified or well mixed; relatively long curves indicate stratification, shorter curves (approaching points) indicate a well-mixed water column. Warm, low-salinity surface water is associated with the highly stable thermohaline stratification during the summer. Colder, higher-salinity water occurred through the water column during the winter months, when wind stresses induced vertical mixing.

The water temperature reached a maximum of about 30°C during August 1978 and was at its minimum during January and February 1979, approximately 10°C at 1 m above the sea floor. The 12-month near-bottom temperature variation was thus 20 Celsius degrees. The time series of mean monthly temperatures obtained

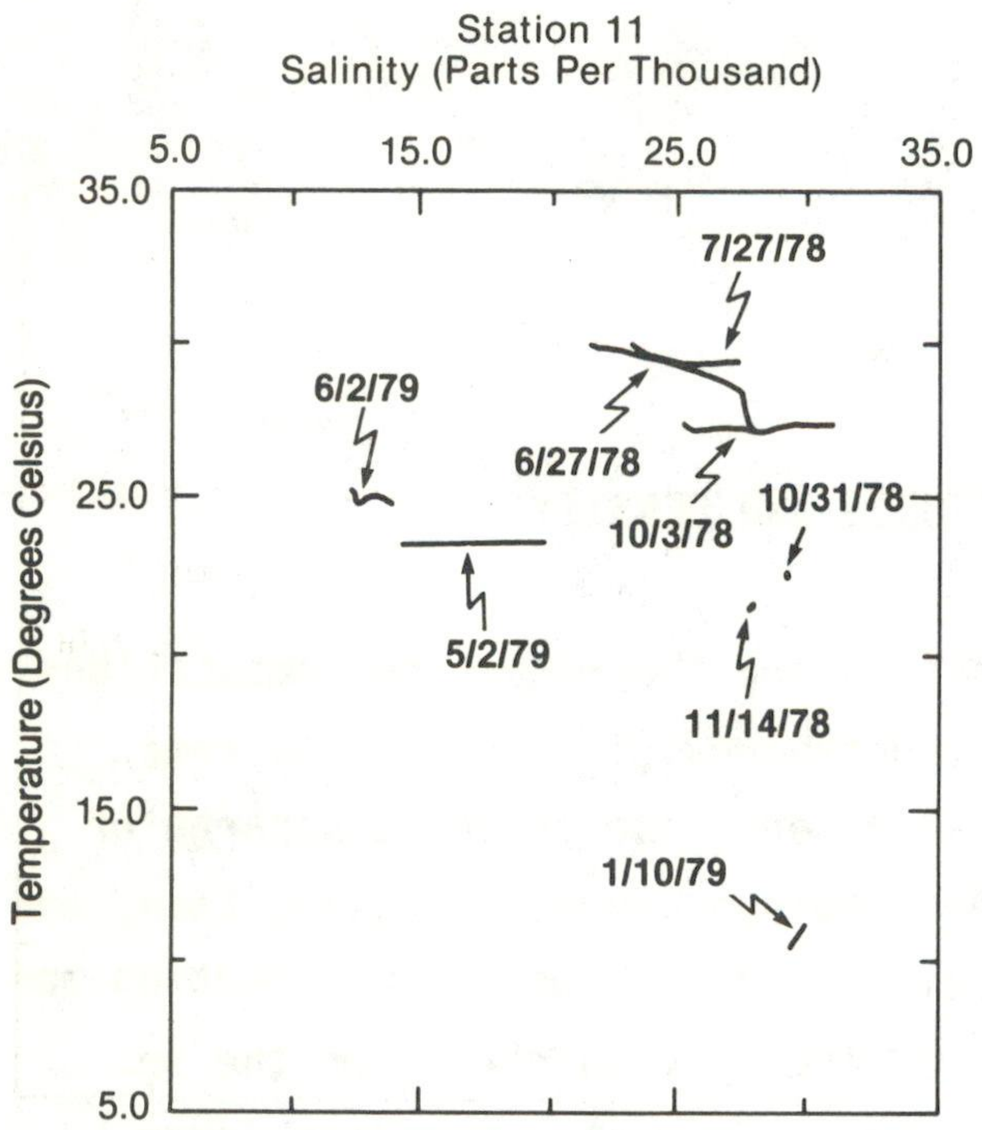

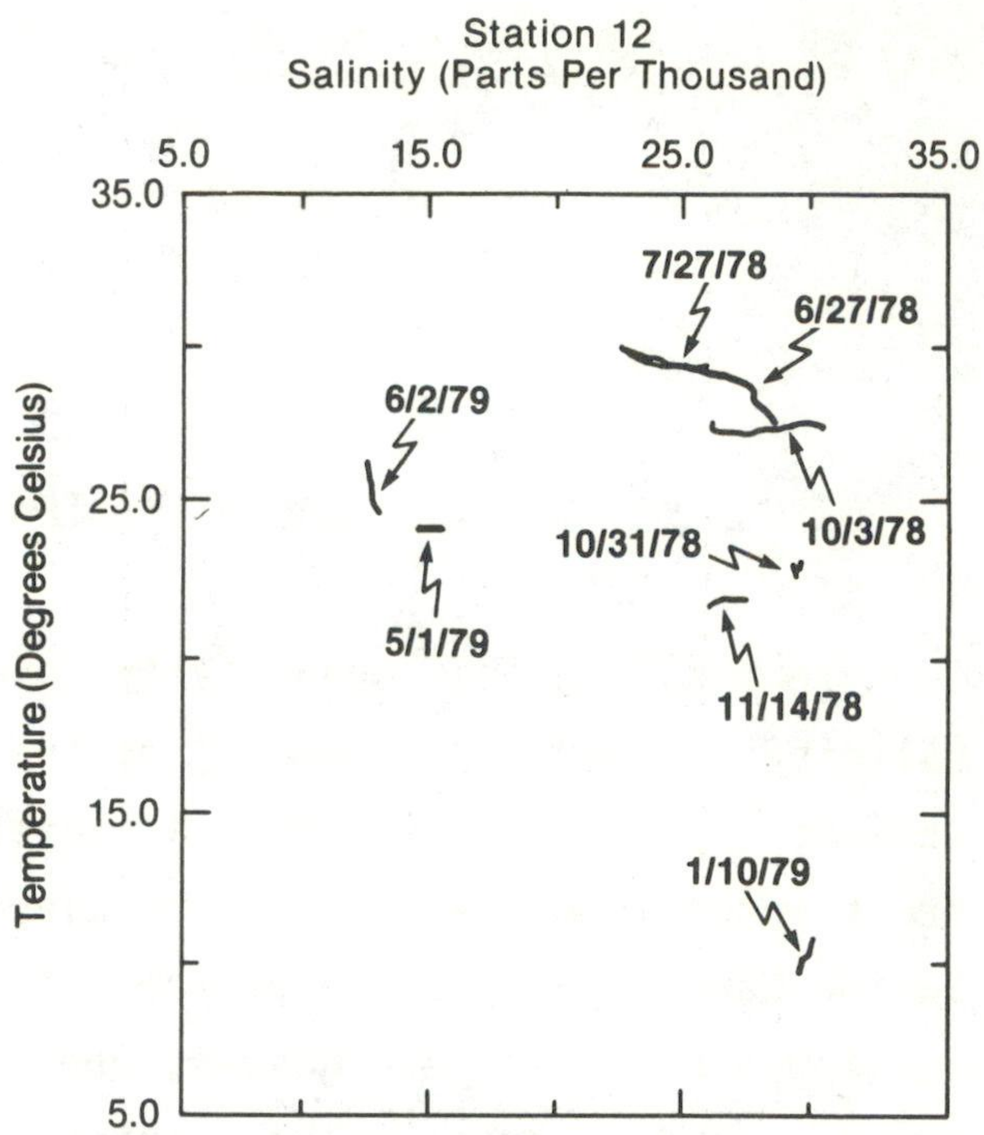

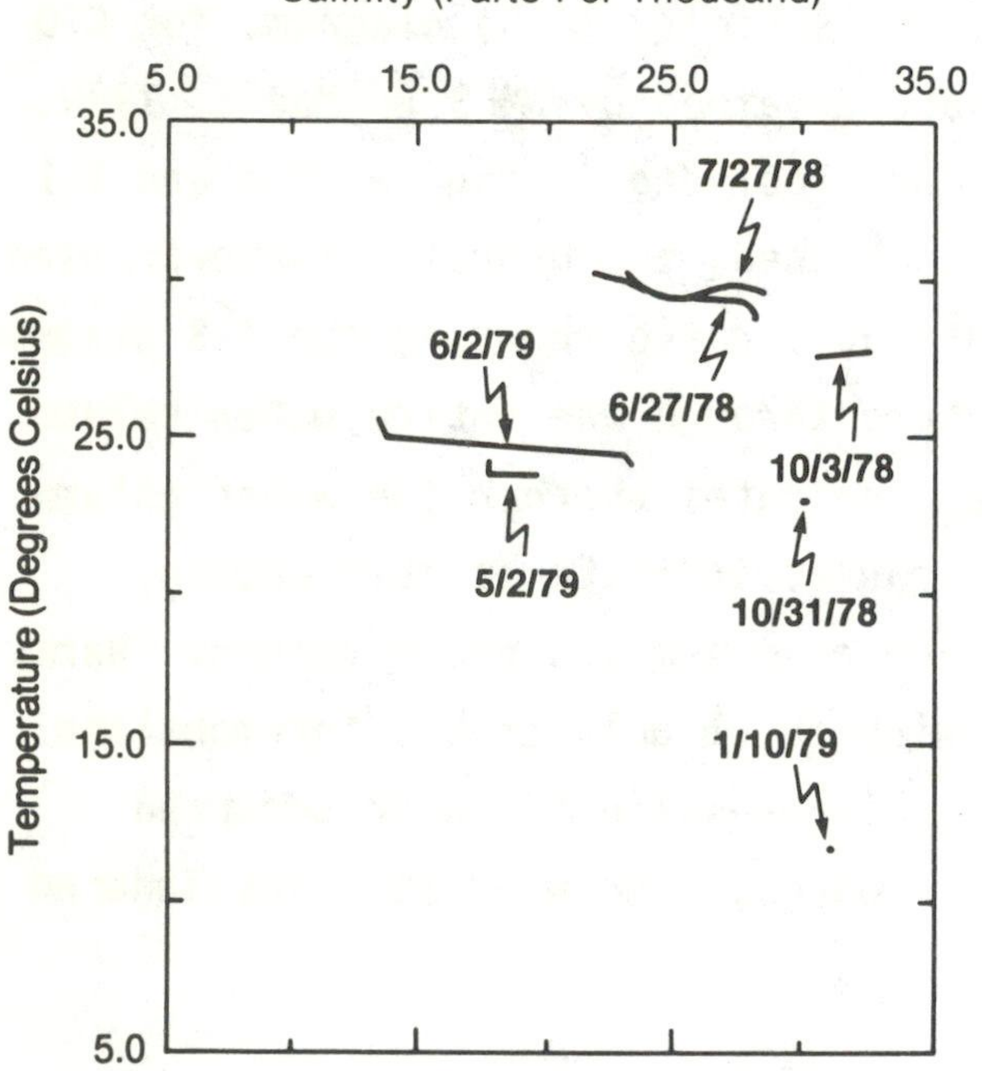

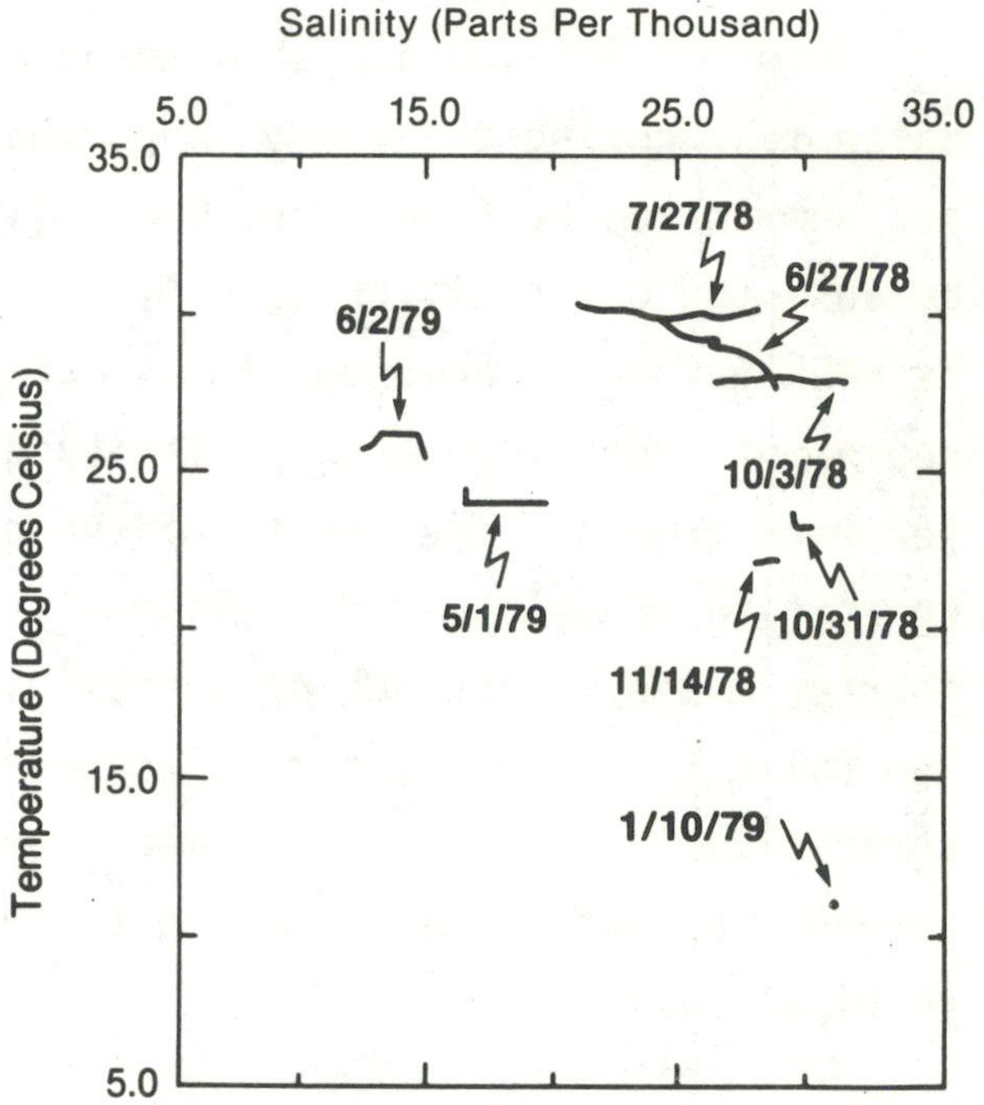

Figure 5-1. Temperature vs. salinity (T-S) diagrams for CTD casts made at West Hackberry stations 11 through 14.

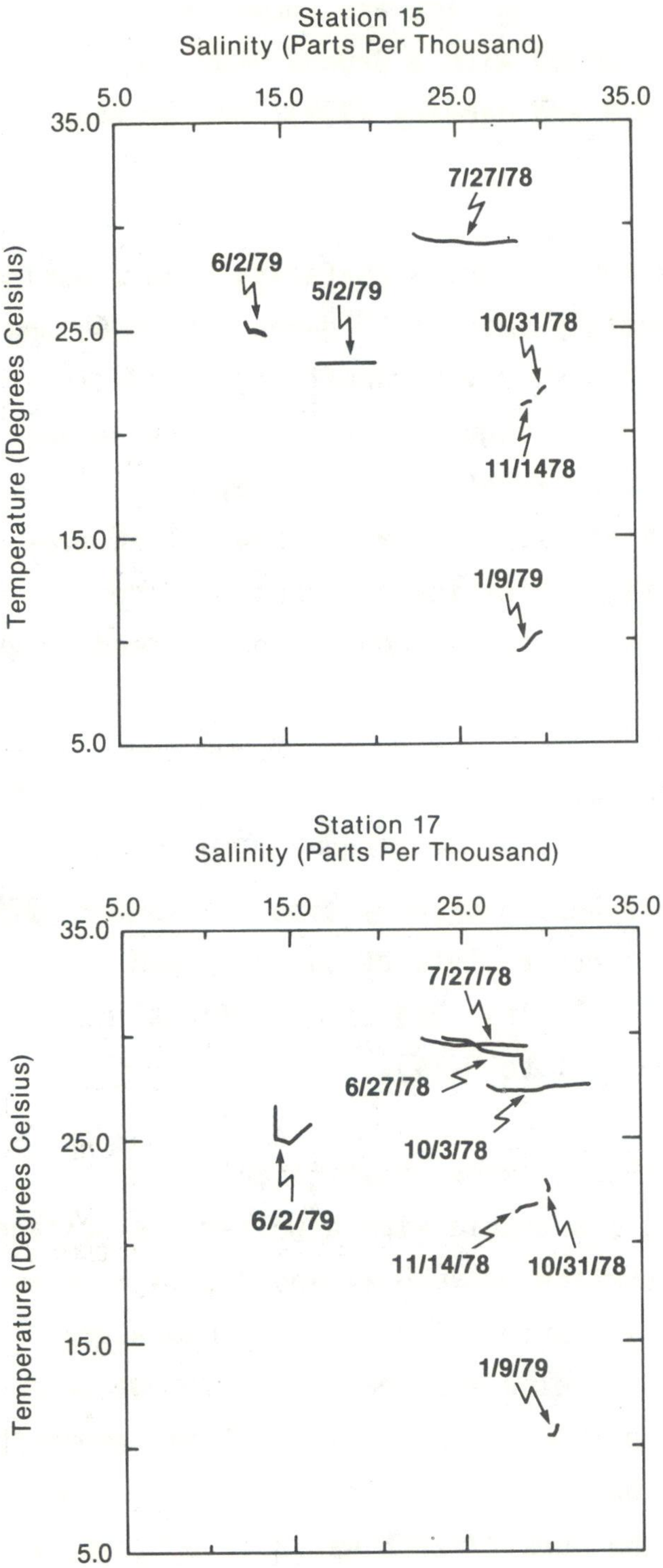

Figure 5-2. Temperature vs. salinity (T-S) diagrams for CTD casts made at West Hackberry stations 15 through 17.

with current meters 1 m and 3 m above the sea floor is shown in figure 5-3. Water temperature and salinity 1 m below the sea surface are shown in figure 5-4. The near-surface temperatures were obtained with a Grundy 9400 CTD, a Beckman RS-5 instrument (during December 1978 and January 1979), and by bucket thermometer measurements.

Freshwater discharges from the Mississippi River, Atchafalaya River, Sabine Lake, and Calcasieu Lake, are plotted as monthly means in figures 5-5, 5-6, and 5-7. As will be seen in this and later sections, river runoff significantly affects the hydrography and circulation. The average observed salinity values tended to be higher during periods of low river runoff. In a study of the hydrologic balance of the Gulf of Mexico, Franceschini (1961) showed that evaporation can exceed precipitation; therefore, salinities in excess of those found in the winter might be expected during the summer months and, indeed, have been observed (Nowlin, 1972).

5.1. Summer 1978

The hydrographic characteristics at the West Hackberry site for summer 1978 are summarized as alongshore and transhore contour plots of salinity and sigma-t. Vertical profiles of temperature, salinity, and sigma-t for all cruises are presented in appendix C (figures C-1 to C-14).

Vertical profiles for June 27 and July 26-27 show stratification during early and mid-summer 1978 to be significant and stable with a well-mixed surface layer and a pycnocline 5 to 6 m below the surface on June 27 and 3 to 4 m below the surface on July 26-27. The halocline at station 11 on June 27 had a gradient of 6.9 ppt/m, and was from 5.8 to 6.0 m below the sea surface. The well-defined halocline was accompanied by a sharp thermocline of 1.6 Celsius degrees/m, and the resulting pycnocline separated the nearly homogeneous layers. The mean salinity in the surface layer during the June 27 cast was 23.1 ppt, while the mean salinity in the bottom layer was 28.3 ppt.

The mid-summer 1978 hydrographic characteristics were similar to those observed during late June, except that a third layer appeared and the southernmost station exhibited more gradual gradients. Stratification during late July

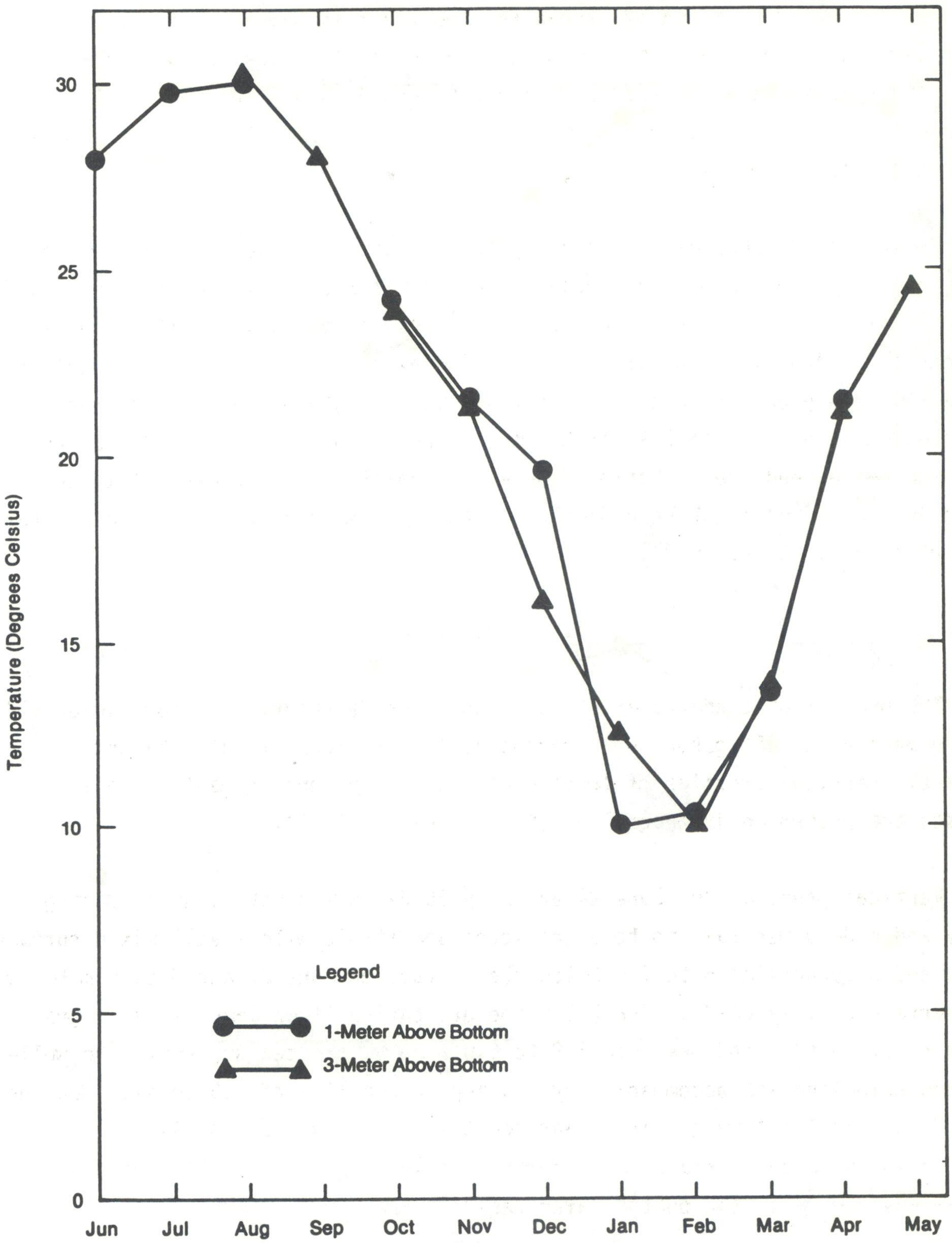

Figure 5-3. Monthly mean temperature for station 11 at 1 m and 3 m above bottom from June 1978 through May 1979.

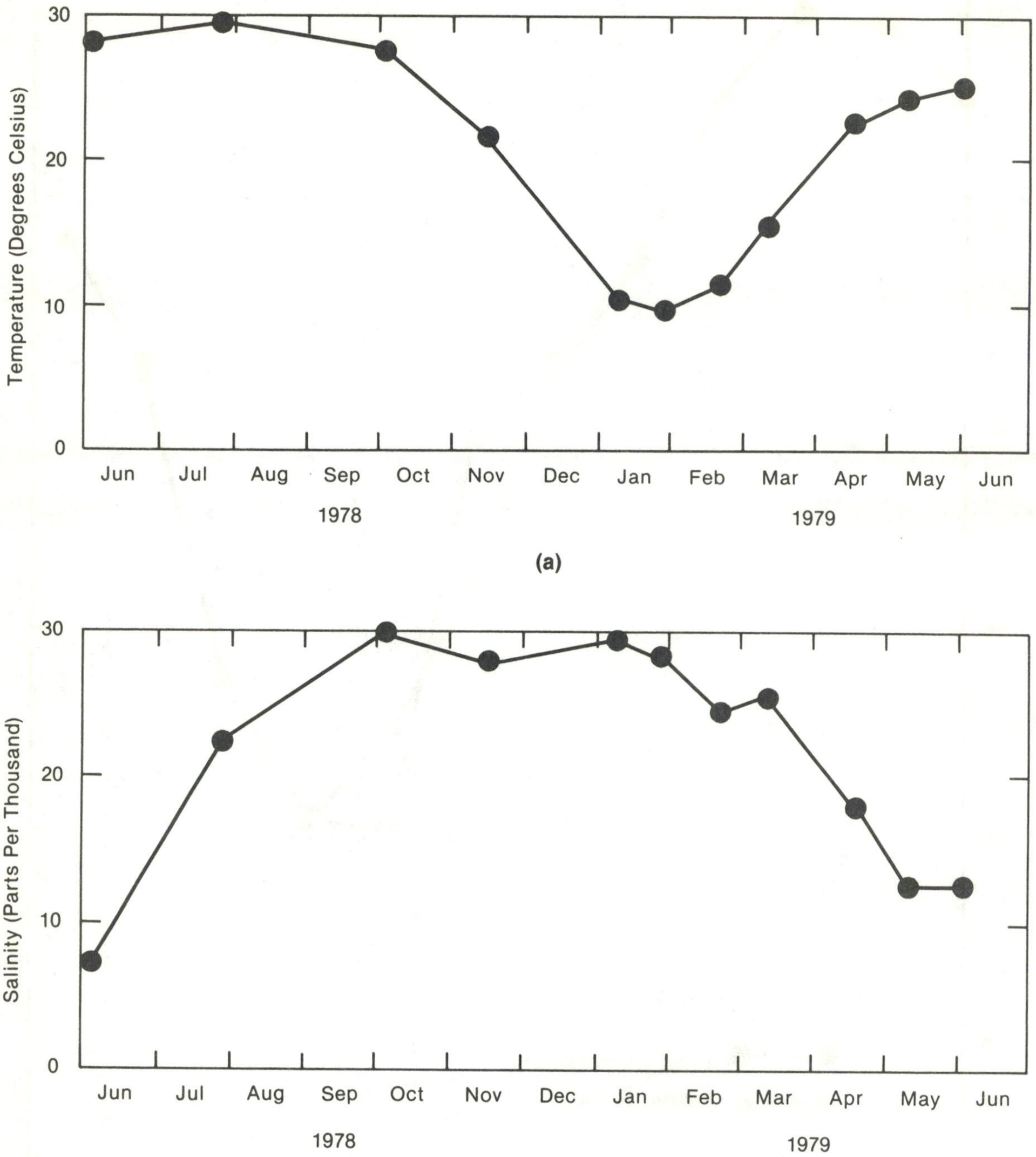

Figure 5-4. Instantaneous values of (a) near-surface temperature and (b) salinity at station 11 from June 3, 1978, to June 2, 1979.

1978 was not accompained by the strong temperature gradients of late June 1978; vertical temperature gradients were much weaker at this time. The mid-summer stratification was more dependent on a well-mixed, low salinity surface layer with a halocline beginning at 3 to 5 m below the surface, depending on the station location. A relatively well-mixed bottom layer was evident at stations 11, 14, 15, and 17. The vertical structure at station 12 (northernmost) consisted of two layers, with the uppermost 5.5 m being nearly homogeneous. The three-layer stratification at stations 14 and 15 was verified by NOS divers, who observed three distinct layers of visibility while servicing the instrument platforms. The mean near-surface and near-bottom salinity for the late July 1978 observations were 21.9 and 27.5 ppt, respectively.

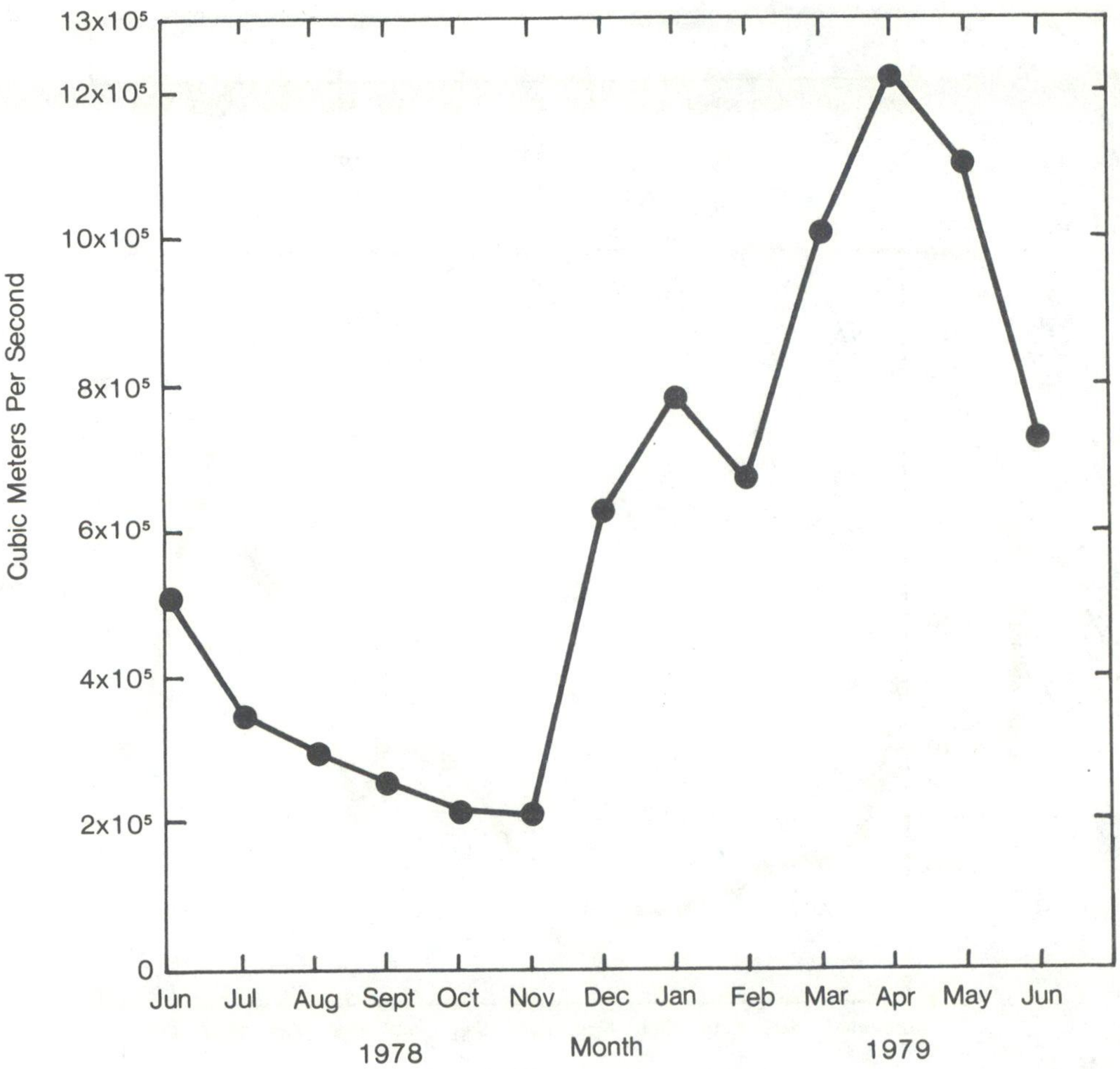

Figure 5-5. Monthly mean fresh water discharge for the Mississippi River at Baton Rouge, La.

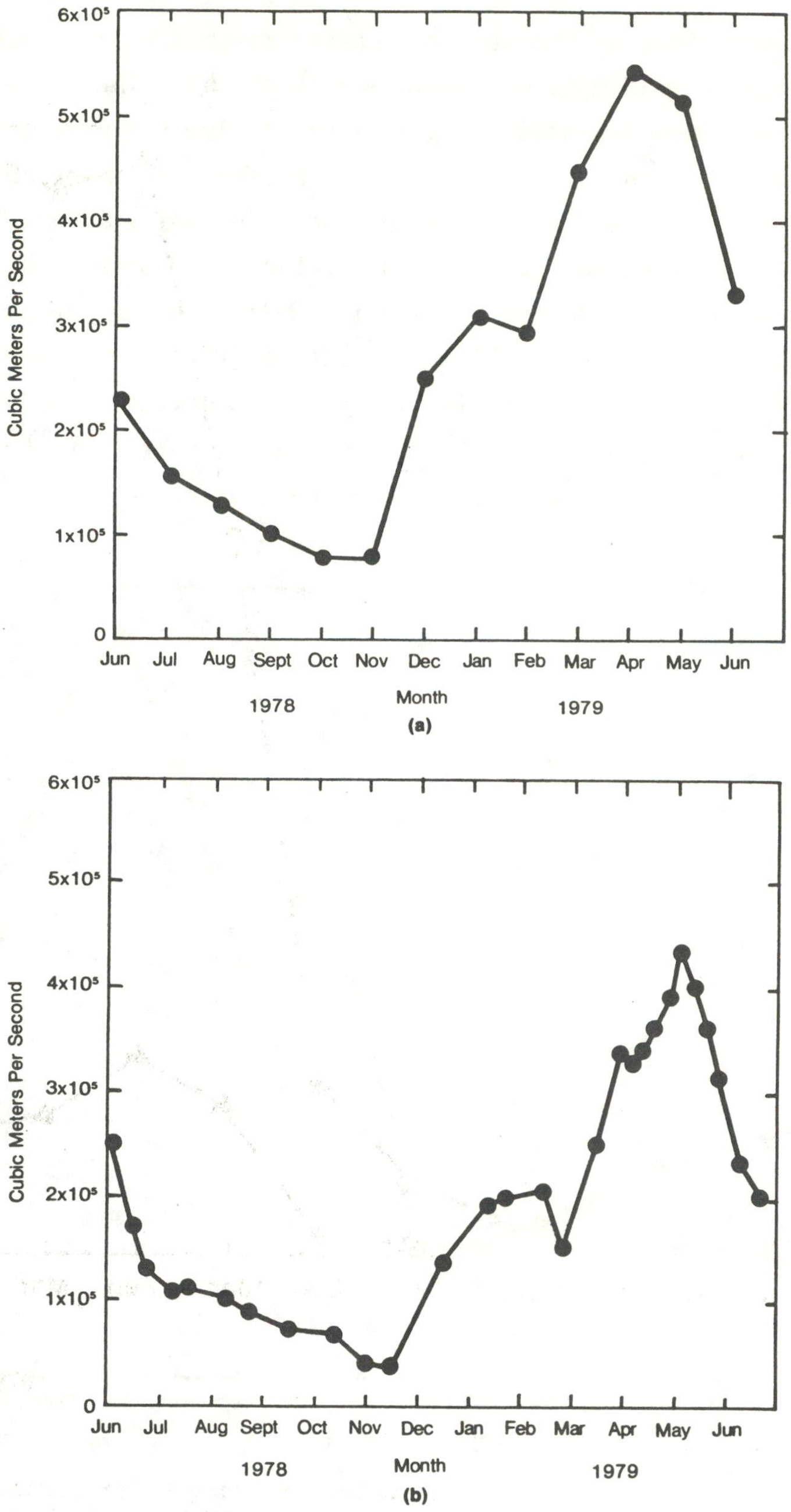

Figure 5-6. Fresh water discharge for the Atchafalaya River at (a) Sims Port, La. (monthly mean) and (b) Morgan City, La. (daily discharge). (Source: U.S. Geological Survey preliminary water resources data for Louisiana--water years 1978 and 1979)

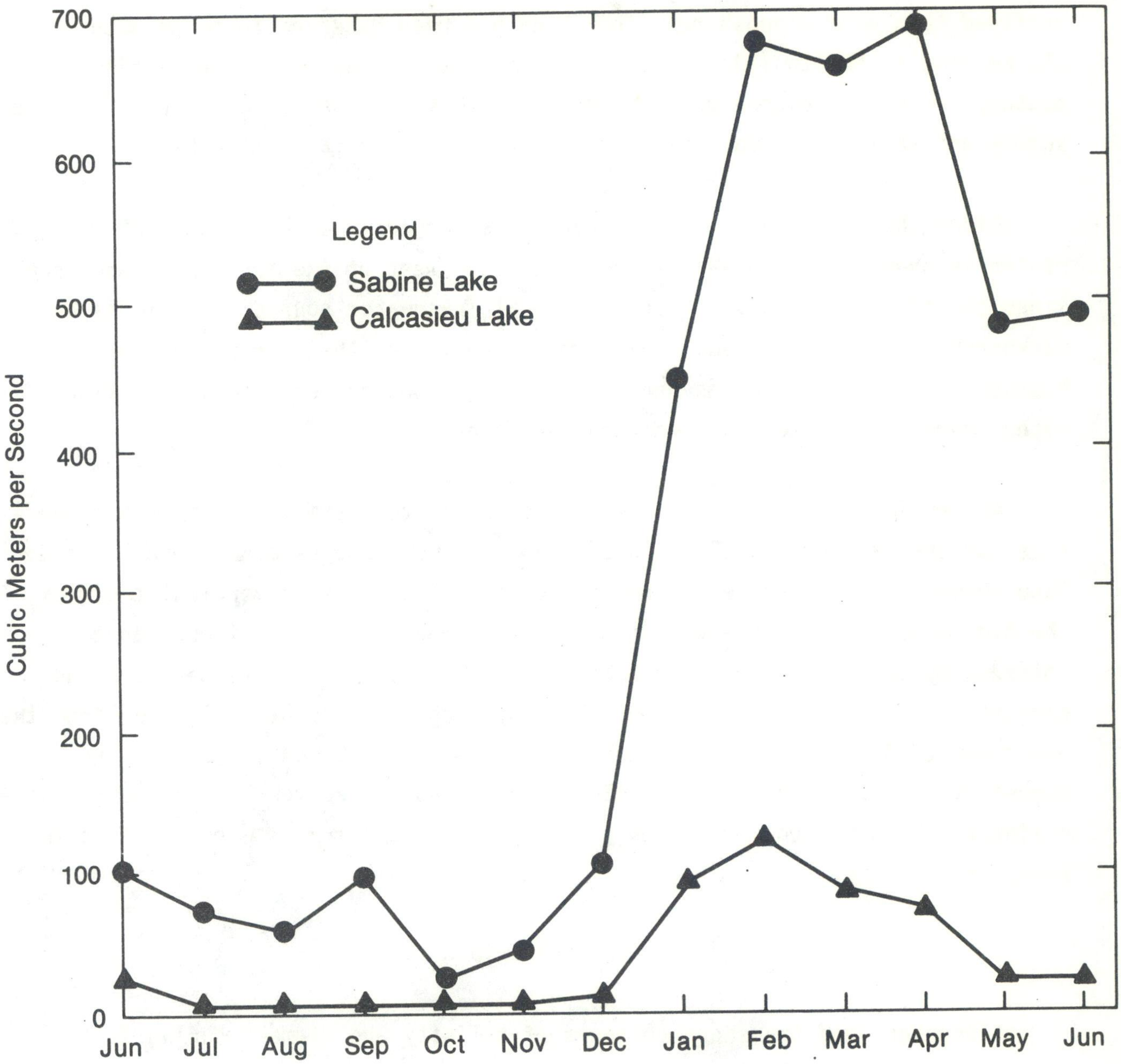

Figure 5-7. Monthly mean fresh water discharges for Sabine Lake and Calcasieu Lake. (Source: U.S. Geological Survey preliminary water resources data for Louisiana--water years 1978 and 1979)

Salinity as low as 21.7 ppt was observed at the southernmost station. Such water, resulting from the mixing of river discharge and shelf water, is confined to a band alongshore. This band has been observed to be as much as 110 km wide by Nowlin (1972). In sharp contrast to the winter and spring months, freshwater discharge from the Sabine Lake and Calcasieu Lake during the summer and fall months was lower by more than 80 percent (figure 5-7).

Since the low volume of fresh water discharged into the West Hackberry region is shown in the upward slope toward the west of the isopycnals and isohalines in figures 5-8 to 5-11, an additional freshwater source east of the West Hackberry site is indicated. It is most likely that the Atchafalaya and Mississippi River discharges were the principal sources of this less saline water, suggesting a general westward spreading.

As mentioned earlier, the FERREL was unable to steam to the West Hackberry site for the late August 1978 cruise; thus, no CTD cast data were available for late summer 1978. Despite the unavailability of continuous vertical profiles, the hydrographic structure within the first 3 m above the sea floor can be inferred by examining the current meter time series records (temperature and conductivity data). The bottommost 3-m layer appeared to be well mixed from the beginning of August to the approach of Tropical Storm DEBRA at 1800 GMT on August 27, 1978. Tropical Storm DEBRA, described in section 18, caused complete mixing of the water column not only at the West Hackberry site but also at the Weeks Island site.

5.2. Fall 1978

Alongshore and transhore contours of salinity and sigma-t during fall 1978 are shown in figures 5-12 to 5-17; vertical profiles of salinity, temperature, and sigma-t for the same period are shown in figures C-5 to C-10. No hydrographic data were obtained at the West Hackberry site during September 1978 because of operational problems.

The distinctive haloclines observed during the summer months were reduced by early fall to more gradual gradients of salinity. The vertical profiles for

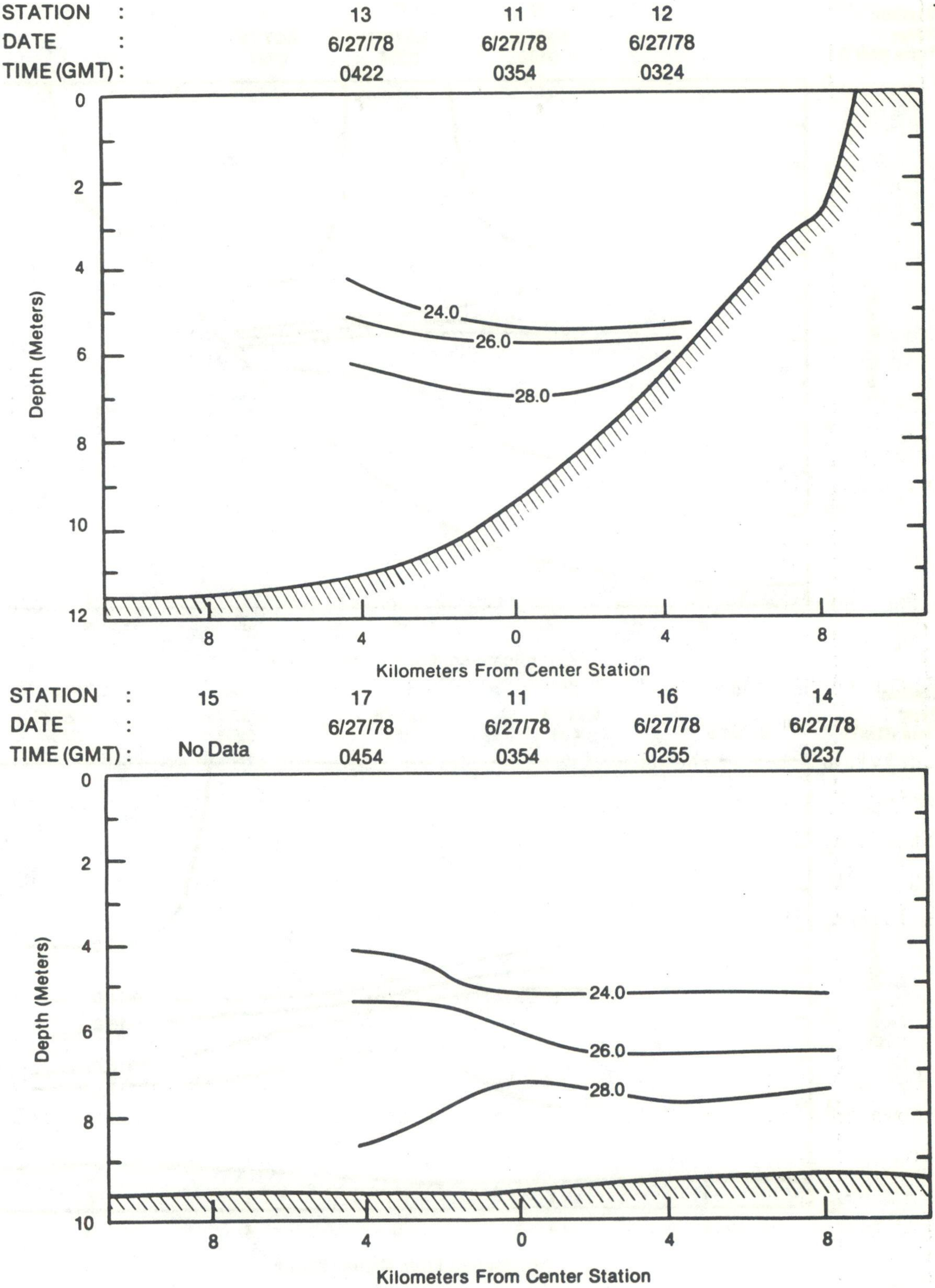

Figure 5-8. Salinity contours at West Hackberry for June 27, 1978. Vertical exaggeration 1200:1.

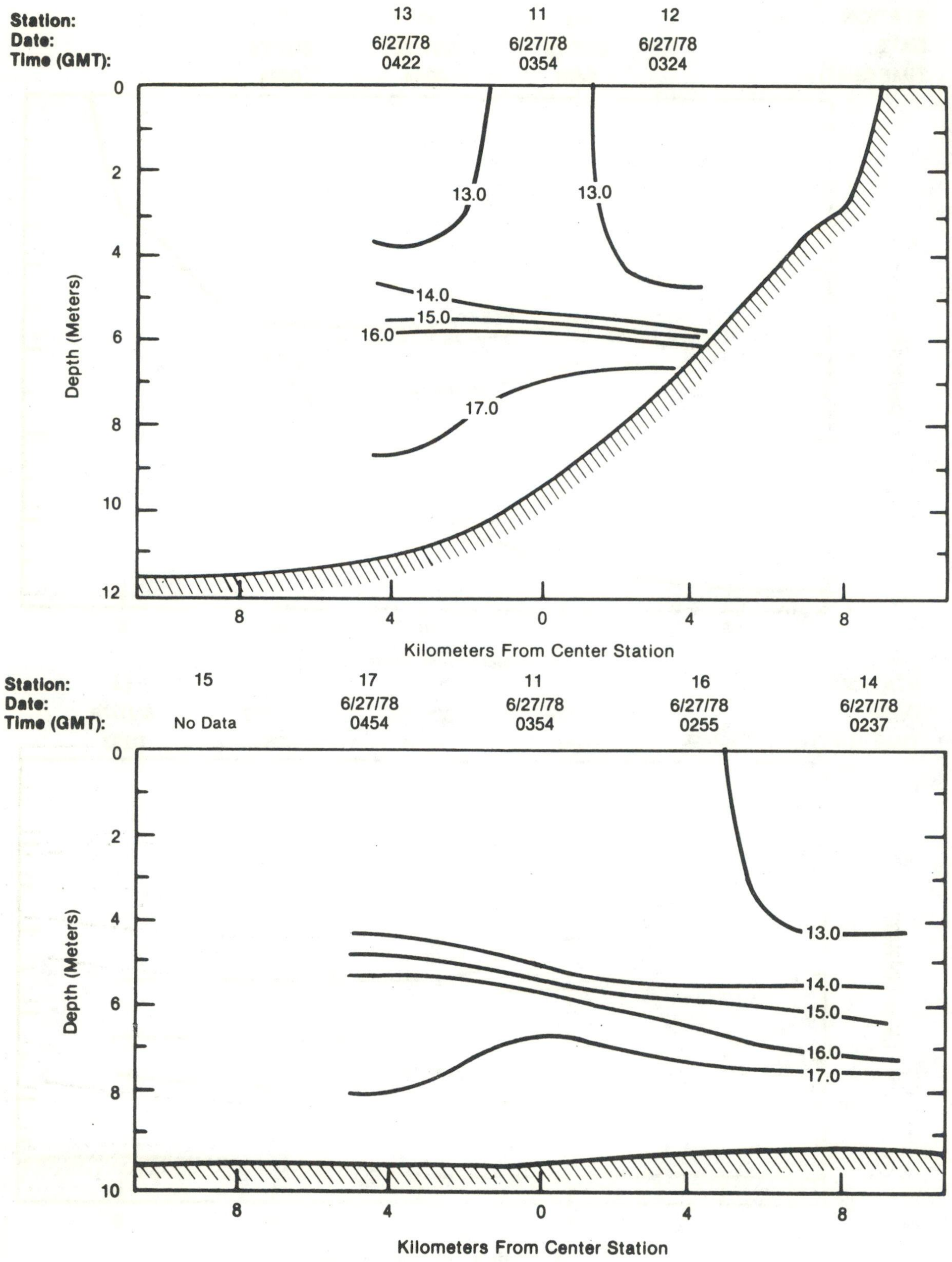

Figure 5-9. Sigma-t contours at West Hackberry for June 27, 1978. Vertical exaggeration 1200:1.

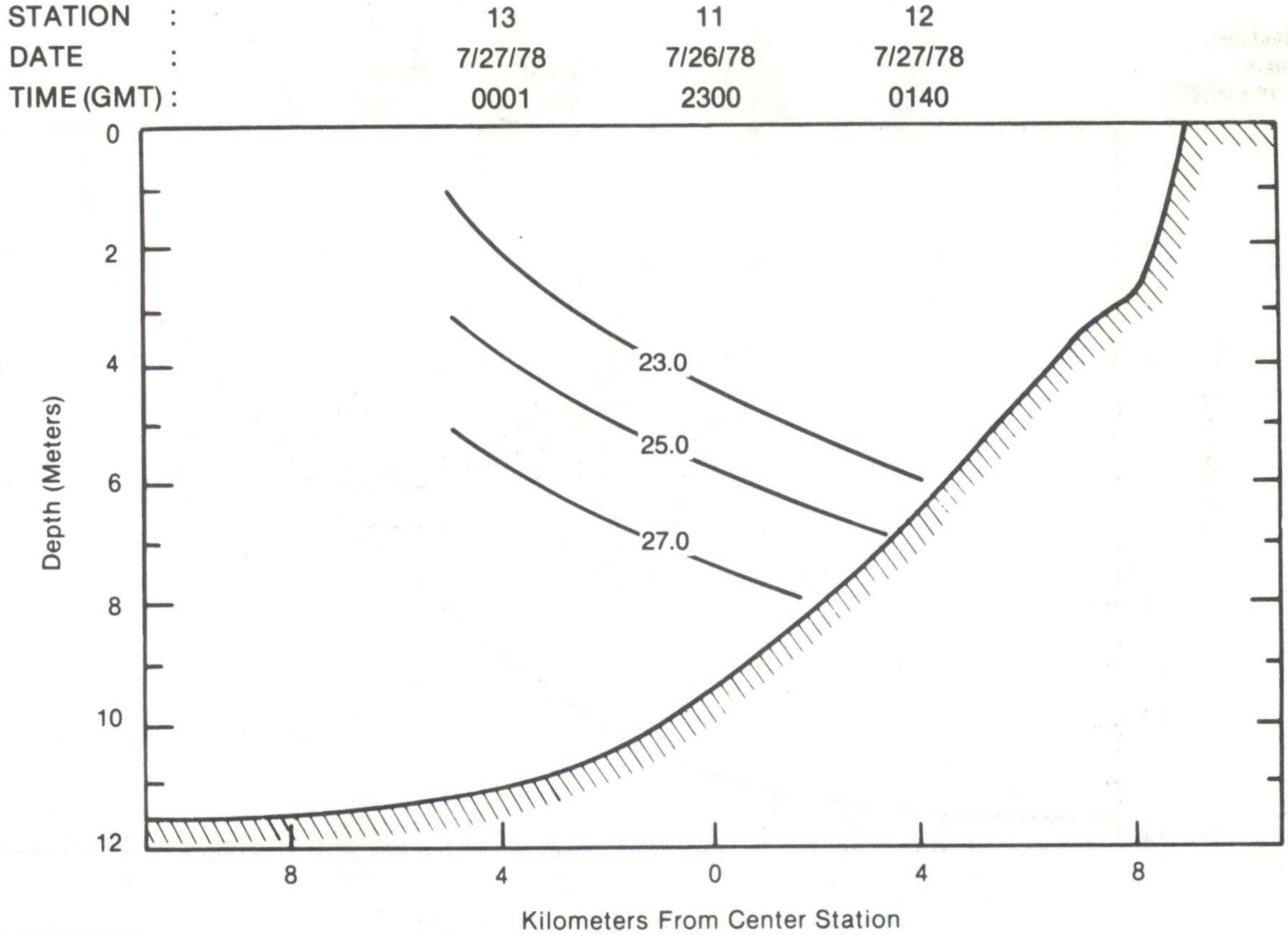

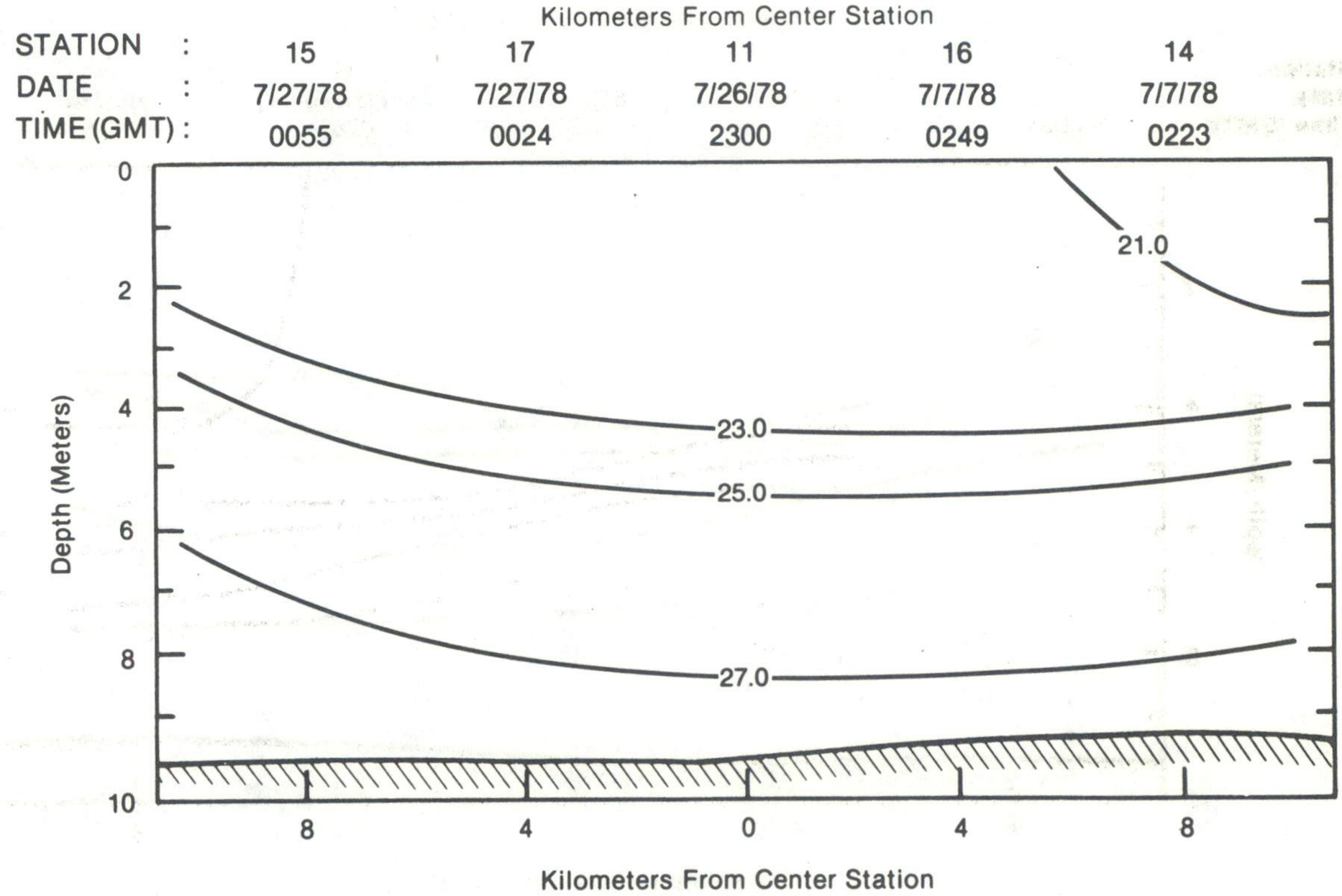

Figure 5-10. Salinity contours at West Hackberry for July 26-27, 1978. Vertical exaggeration 1200:1.

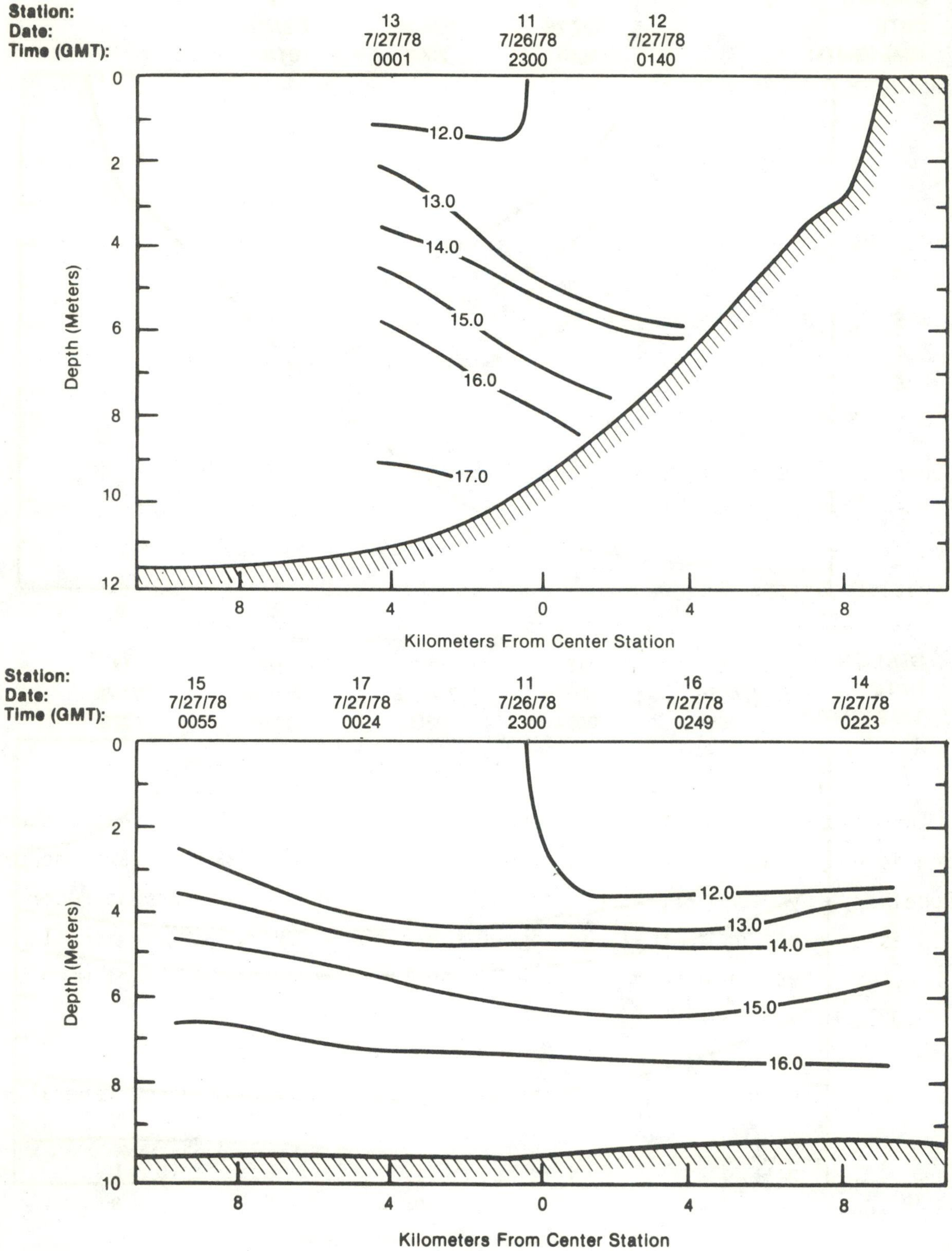

Figure 5-11. Sigma-t contours at West Hackberry for July 26-27, 1978. Vertical exaggeration 1200:1.

October 3 show weak salinity gradients at stations 13 and 16, an approximate three-layer structure at station 12, and a four-layer structure at stations 11 and 17. The salinity contours shown in figure 5-12 show a salinity front which slopes downward from the surface at station 13 to the bottom at station 12. The sigma-t contours reflect this downward slope (figure 5-13). Temperature was nearly uniform throughout the water column at all stations. Mean salinities ranged from 27.5 ppt at the surface to 31.6 ppt at the bottom.

Vertical distribution of temperature and salinity on October 31 and November 14 reflected a well-mixed environment. Figures 5-14 and 5-16 show nearly vertical homogeneity in salinity, while figures 5-15 and 5-17 show nearly vertical homogeneity in density at the site. Large-cell Langmuir circulation had been observed during mid-October by aircraft observations; this type of circulation enhances vertical mixing. Density increased gradually offshore as a result of the continued low volume freshwater discharge into the region and temperature cooling due to weather. Temperature and salinity both exhibited near-zero vertical gradients. The mean surface salinity on October 31 was slightly higher at 29.6 ppt than on November 14 at 27.7 ppt.

5.3. Winter 1979

The discharge from the Mississippi and Atchafalaya Rivers increased sharply during November, and the discharge from Sabine Lake and Calcasieu Lake increased in December. By December, a thermocline appeared between the current meter levels as a result of thermal cooling of the surface layer. At station 11, the mean temperatures for December at the 1-m and 3-m current meter level were 19.5° and 16.0°C, respectively.

Temperature and salinity vertical profiles in winter exhibited generally small gradients. Temperature profiles for January 9 and 10 indicate an isothermal layer in the upper 5 m, below which the temperature at stations 11, 12, and 15 increased with depth, but stability was maintained by an increase in salinity. At station 15, the temperature of the colder surface waters associated with lower salinities was 9.7°C, with a salinity of 28.2 ppt. The bottom water had a temperature of 10.6°C and a salinity of 29.3 ppt. Freshwater

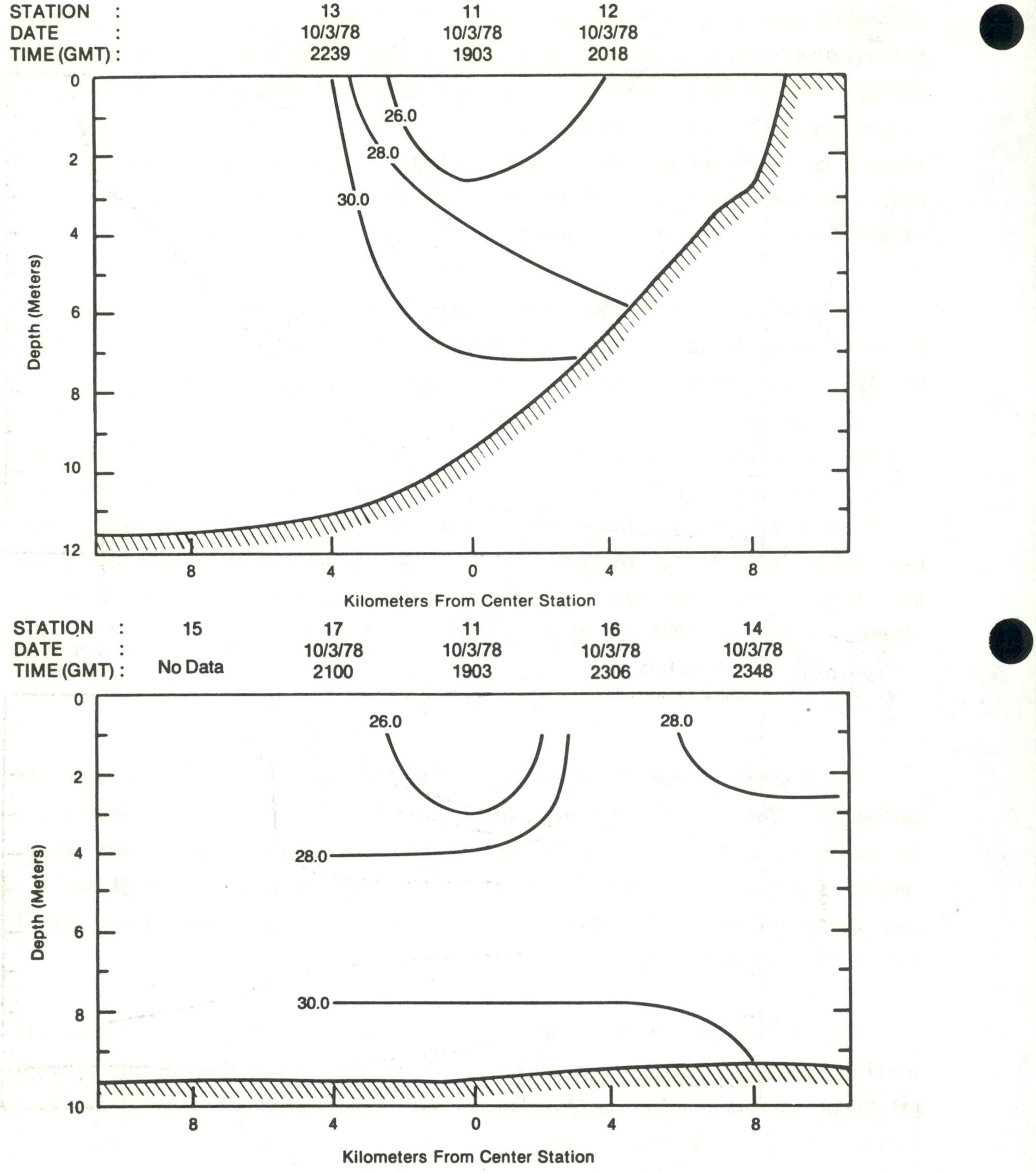

Figure 5-12. Salinity contours at West Hackberry for October 3, 1978. Vertical exaggeration 1200:1.

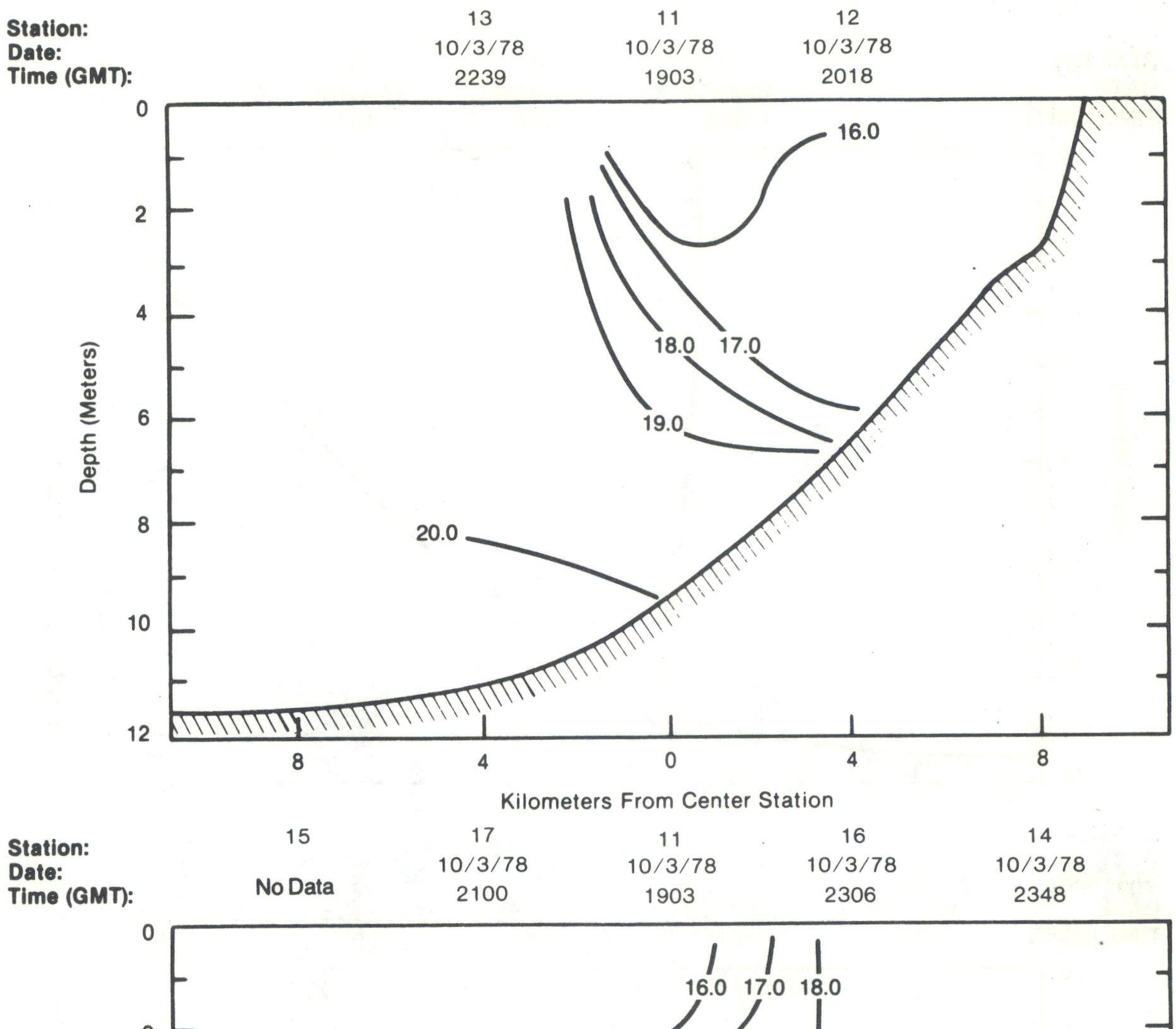

Figure 5-13. Sigma-t contours at West Hackberry for October 3, 1978. Vertical exaggeration 1200:1.

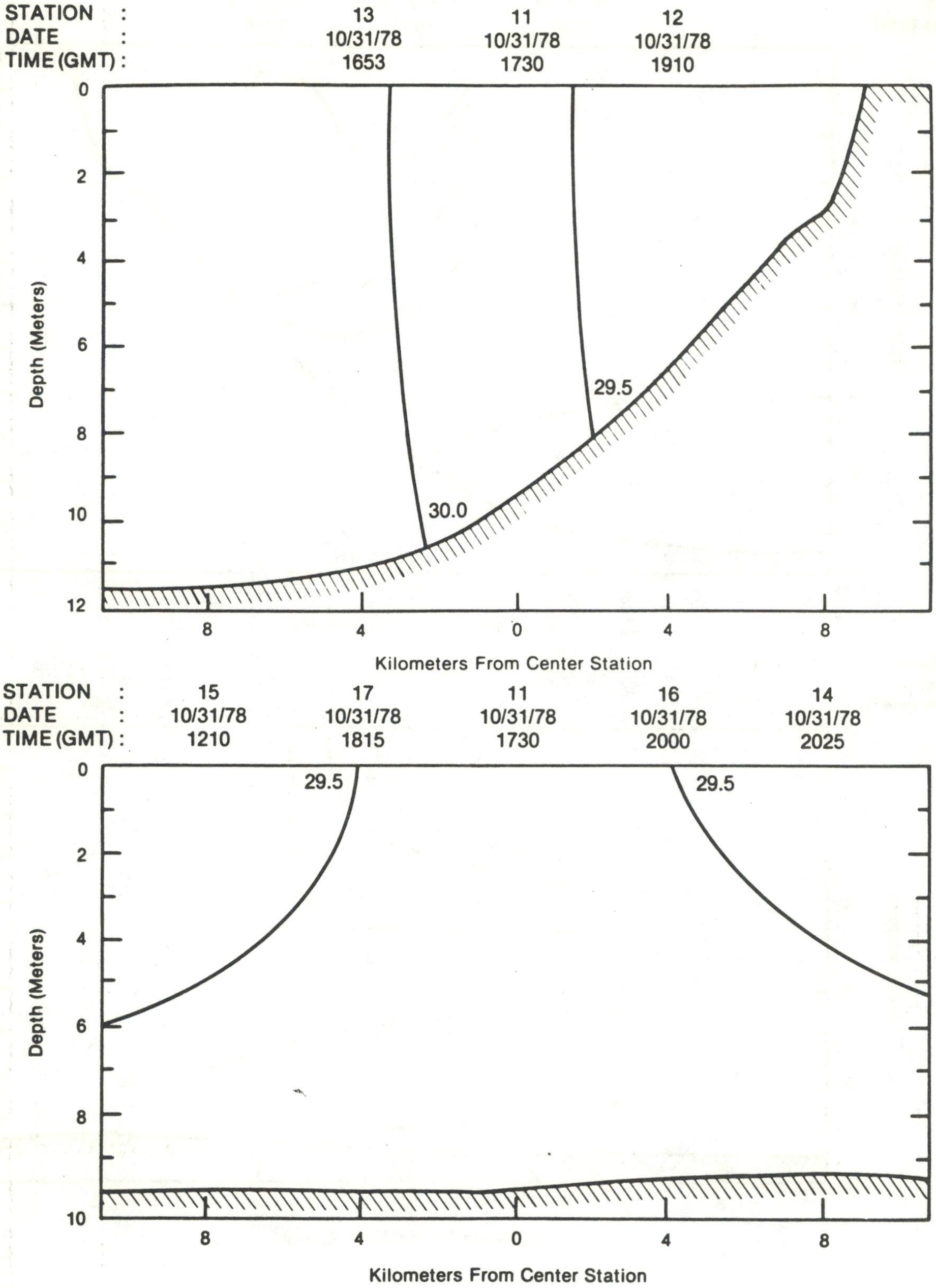

Figure 5-14. Salinity contours at West Hackberry for October 31, 1978. Vertical exaggeration 1200:1.

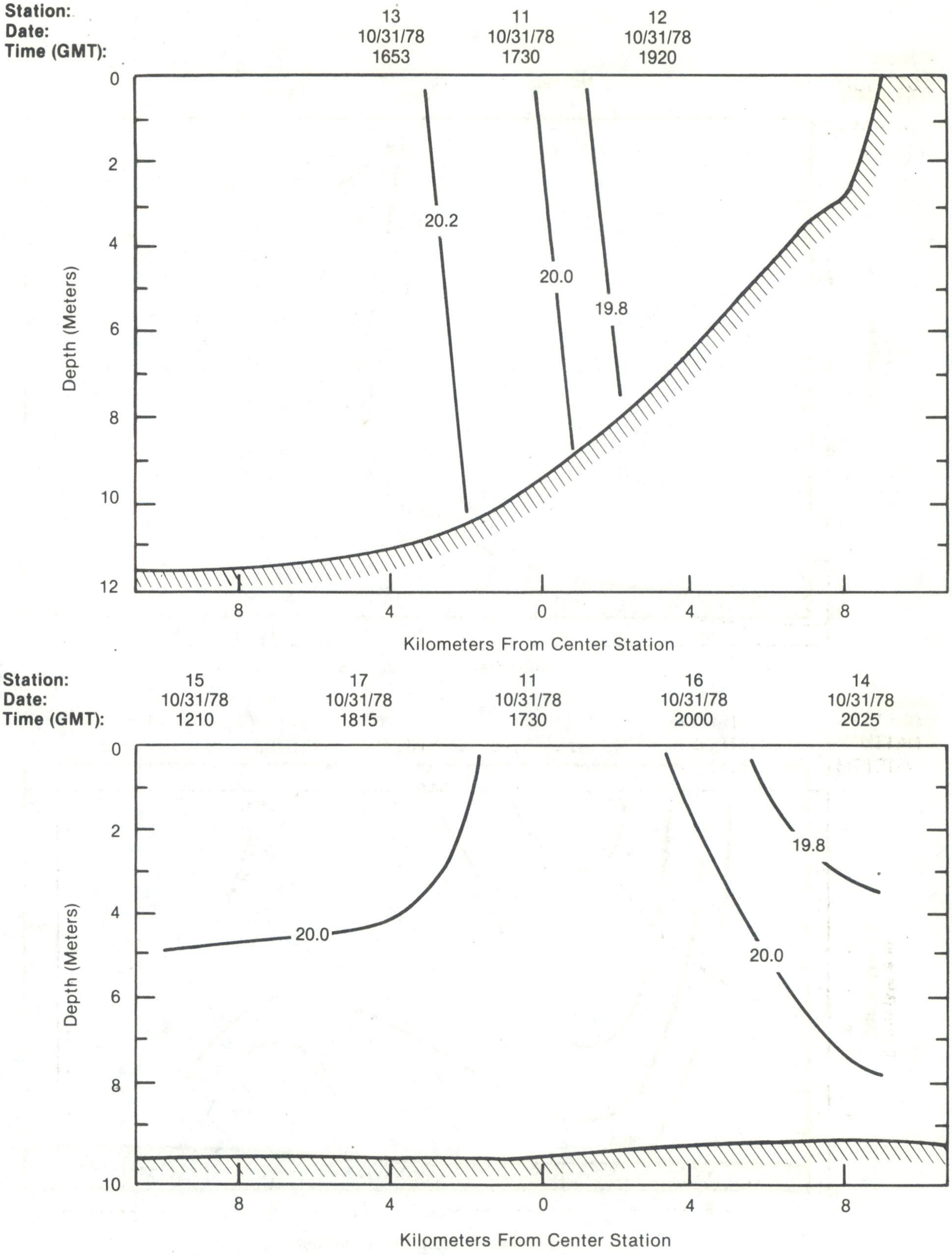

Figure 5-15. Sigma-t contours at West Hackberry for October 31, 1978. Vertical exaggeration 1200:1.

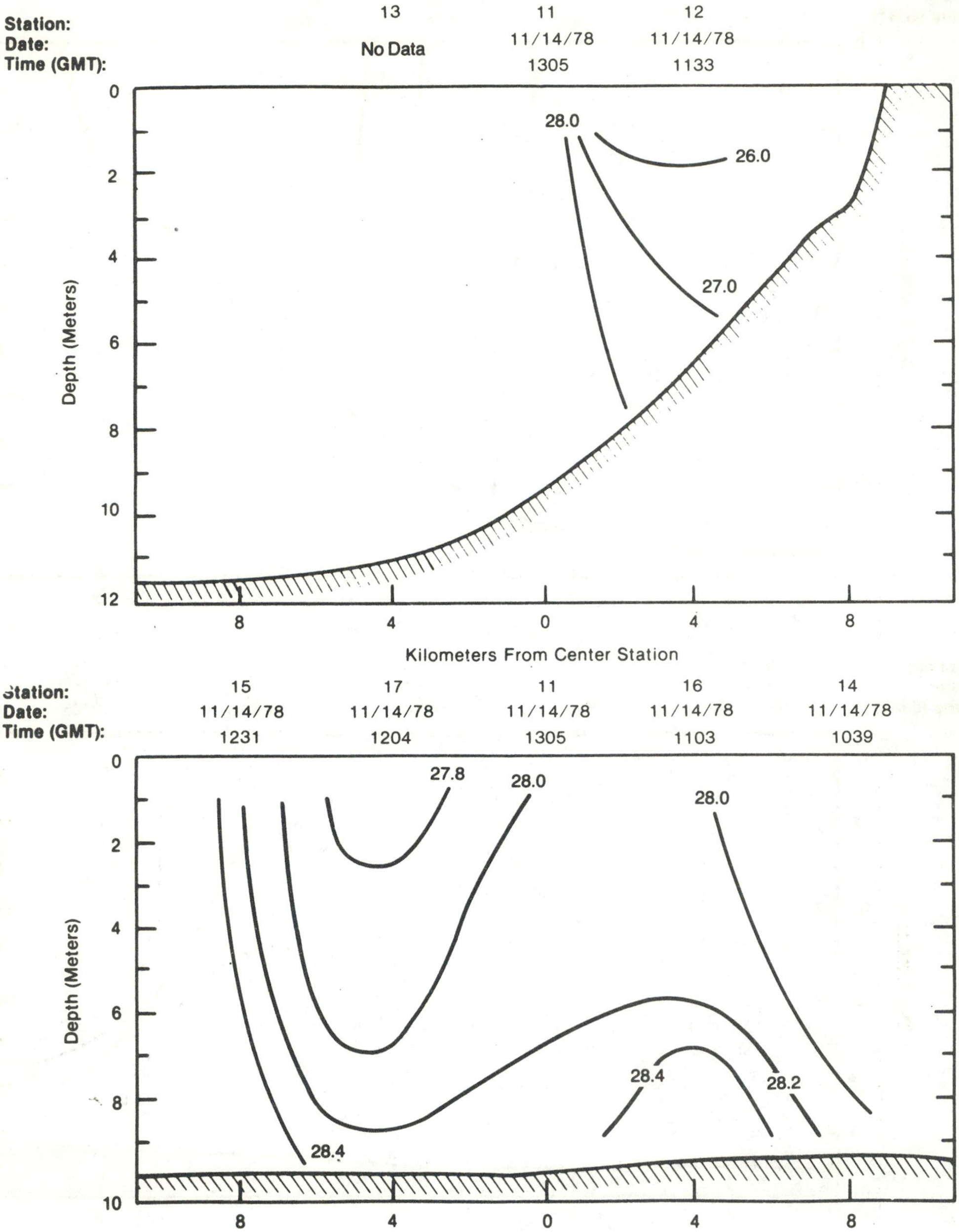

Figure 5-16. Salinity contours at West Hackberry for November 14, 1978. Vertical exaggeration 1200:1.

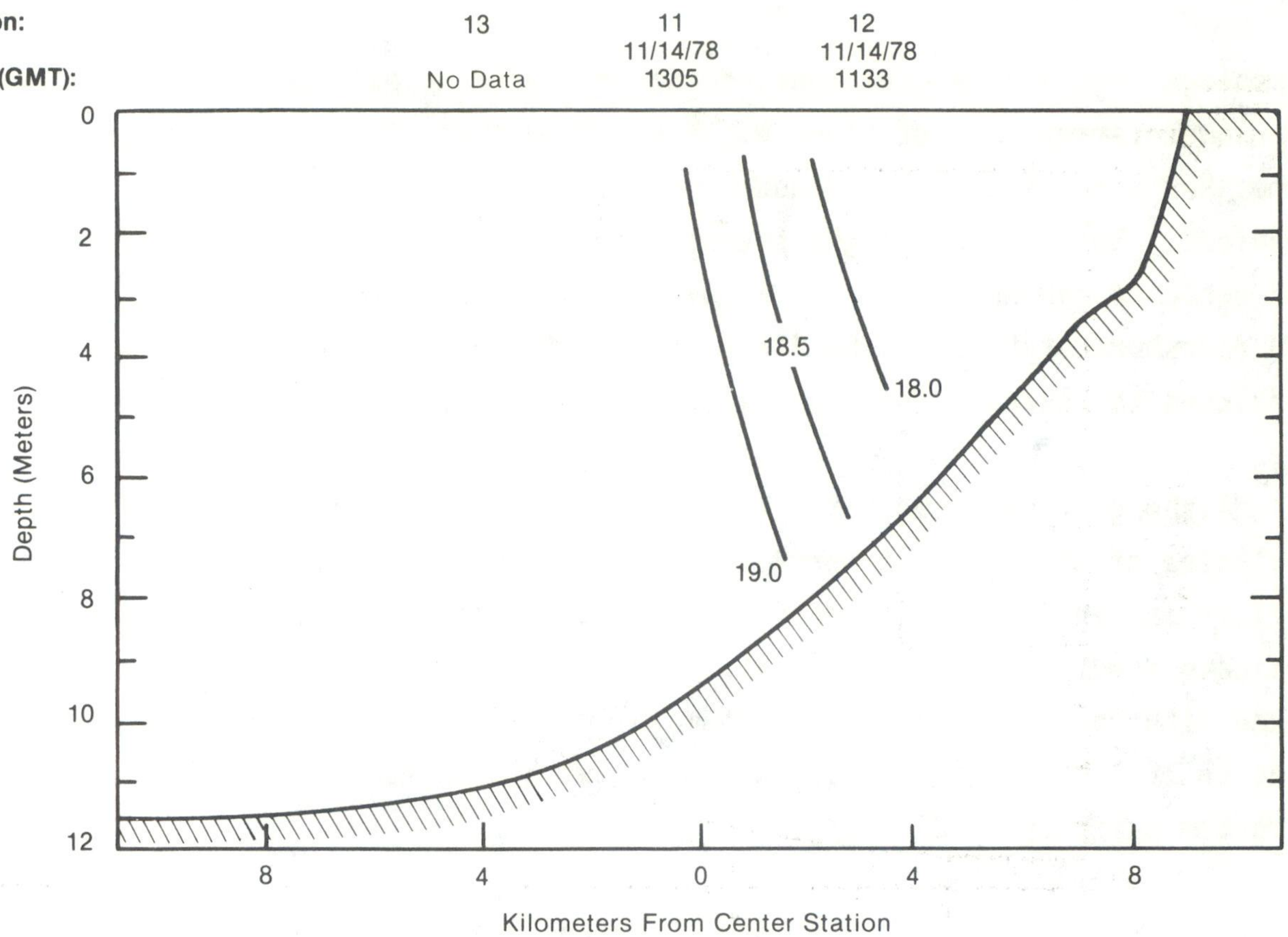

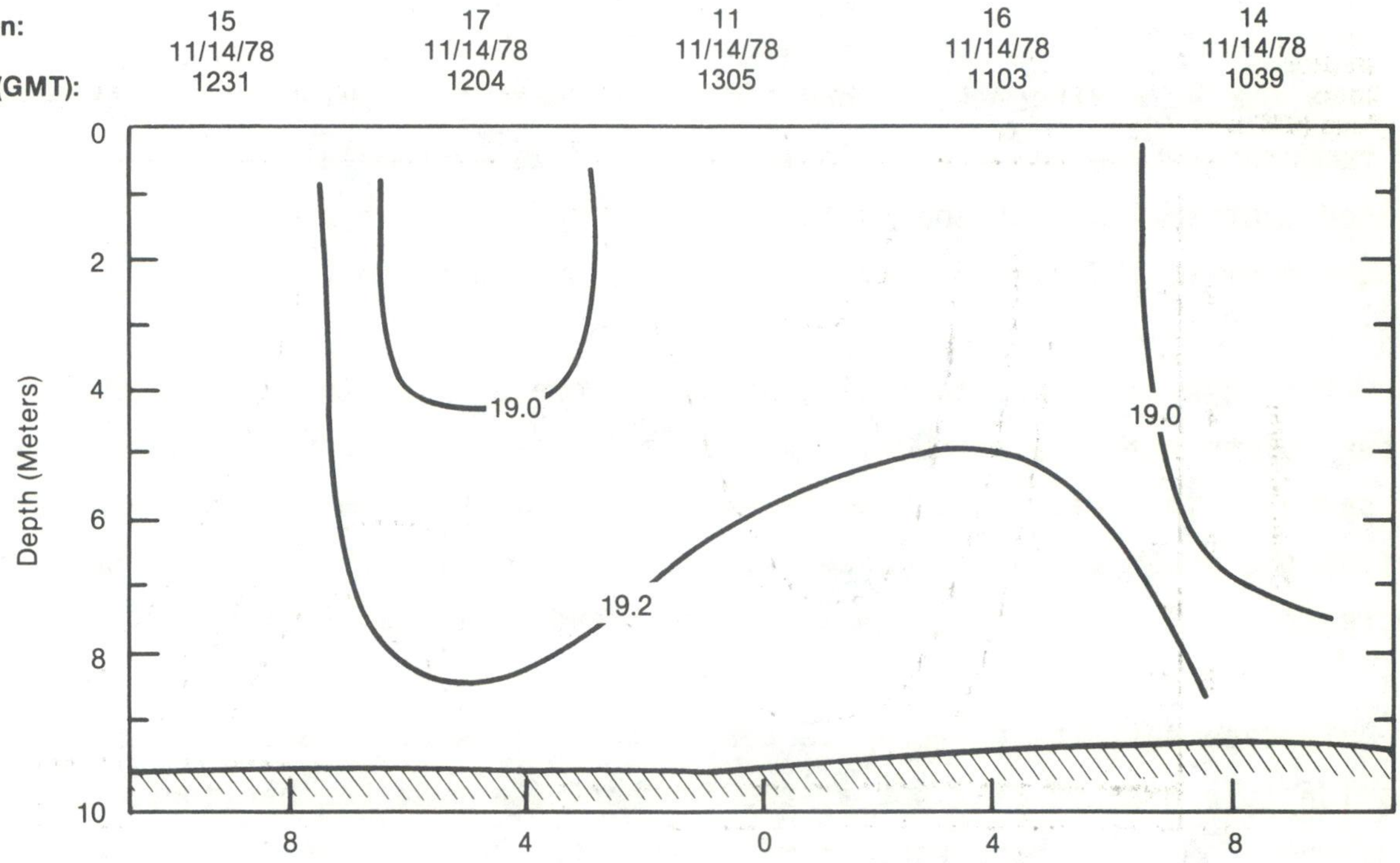

Figure 5-17. Sigma-t contours at West Hackberry for November 14, 1978. Vertical exaggeration 1200:1.

discharge from Sabine Lake appeared to be the principal cause of stratification. The lower temperature of river discharge from that of shelf water, together with atmospheric cooling during January, resulted in the inversion of the temperature gradient. Salinity and sigma-t contours in figures 5-18 and 5-19 reflect the influence of Sabine Lake. The isopycnal surfaces sloped away from the western and nearshore stations. The large volume of freshwater discharge in January continued to increase for the remainder of winter.

Although river runoff had affected significantly the physical characteristics of the West Hackberry site, mixing caused by wind stresses was influential in limiting stratification. Water samples obtained on February 22 indicate a well-mixed environment. At station 11, the water column was well mixed with both a surface and bottom salinity of 24.6 ppt. At the nearshore station 12, the stratification was weak, with a surface salinity of 23.9 ppt and a bottom salinity of 24.5 ppt.

5.4. Spring 1979

By March, environmental conditions were more favorable for stratification of temperature and salinity. In the March 12 water samples, the mean salinity ranged from 26.7 ppt at the surface to 28.8 ppt at the bottom. Temperature ranged from 15.7°C at the surface to 14.3°C at the bottom.

The physical characteristics in April were similar to those of March. The water column was stratified with warmer and less saline waters. The low value of salinity in April was caused by high river discharge which reached a maximum during the month of April. (See figures 5-5 to 5-7.) The water temperature increase was due to the seasonal warming trend in the Gulf of Mexico.

Surface salinity on April 18 ranged from a low of 17.8 ppt at the nearshore station to a high of 24.7 ppt at the farshore station; the horizontal gradient resulted from an inshore band of river runoff. Vertical gradients of salinity at the nearshore and farshore stations were relatively weak due to energetic mixing that resulted from the passage of a storm a week earlier. The salinity differential was only 0.2 to 0.3 ppt from surface to bottom; this is comparable

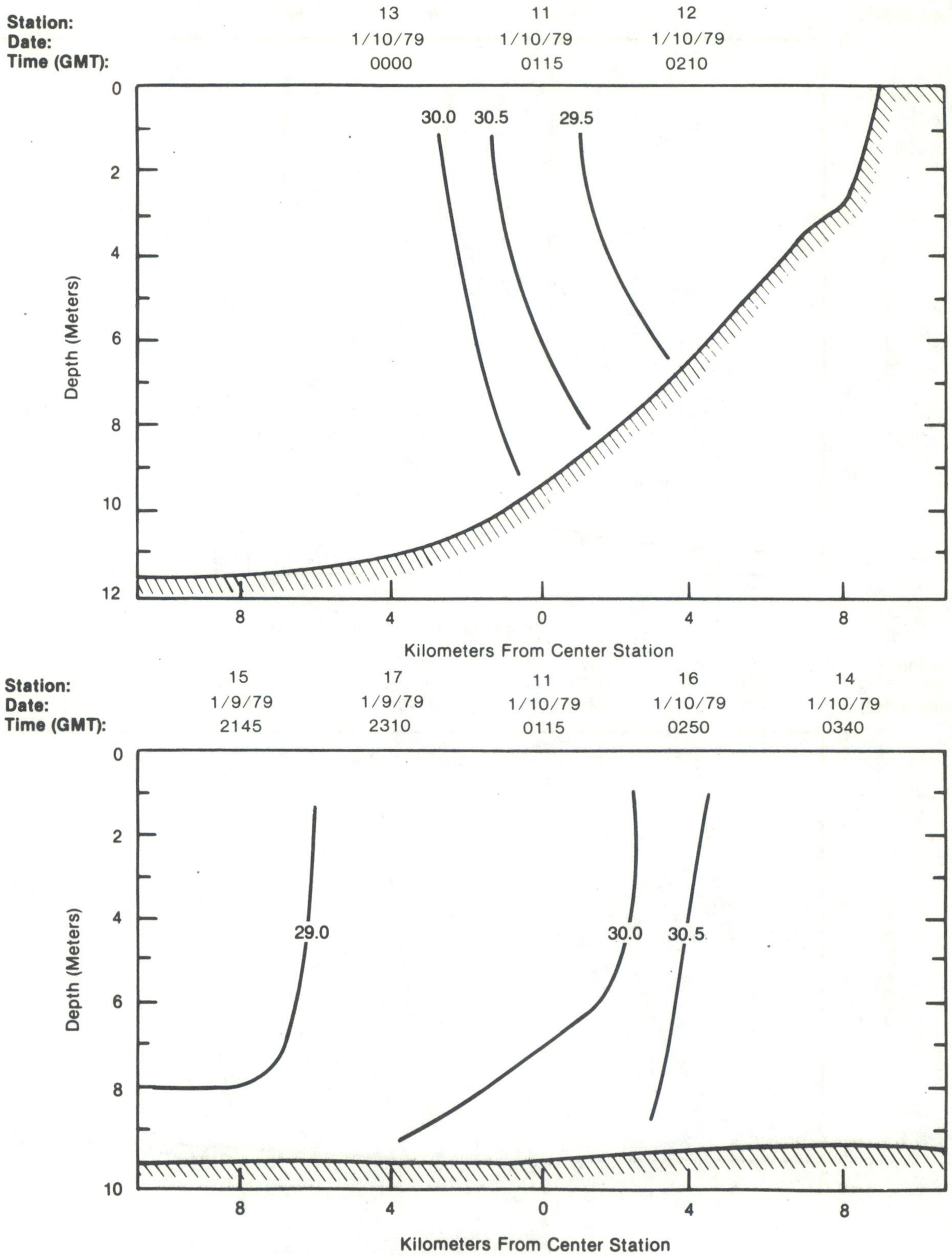

Figure 5-18. Salinity contours at West Hackberry for January 9-10, 1979. Vertical exaggeration 1200:1.

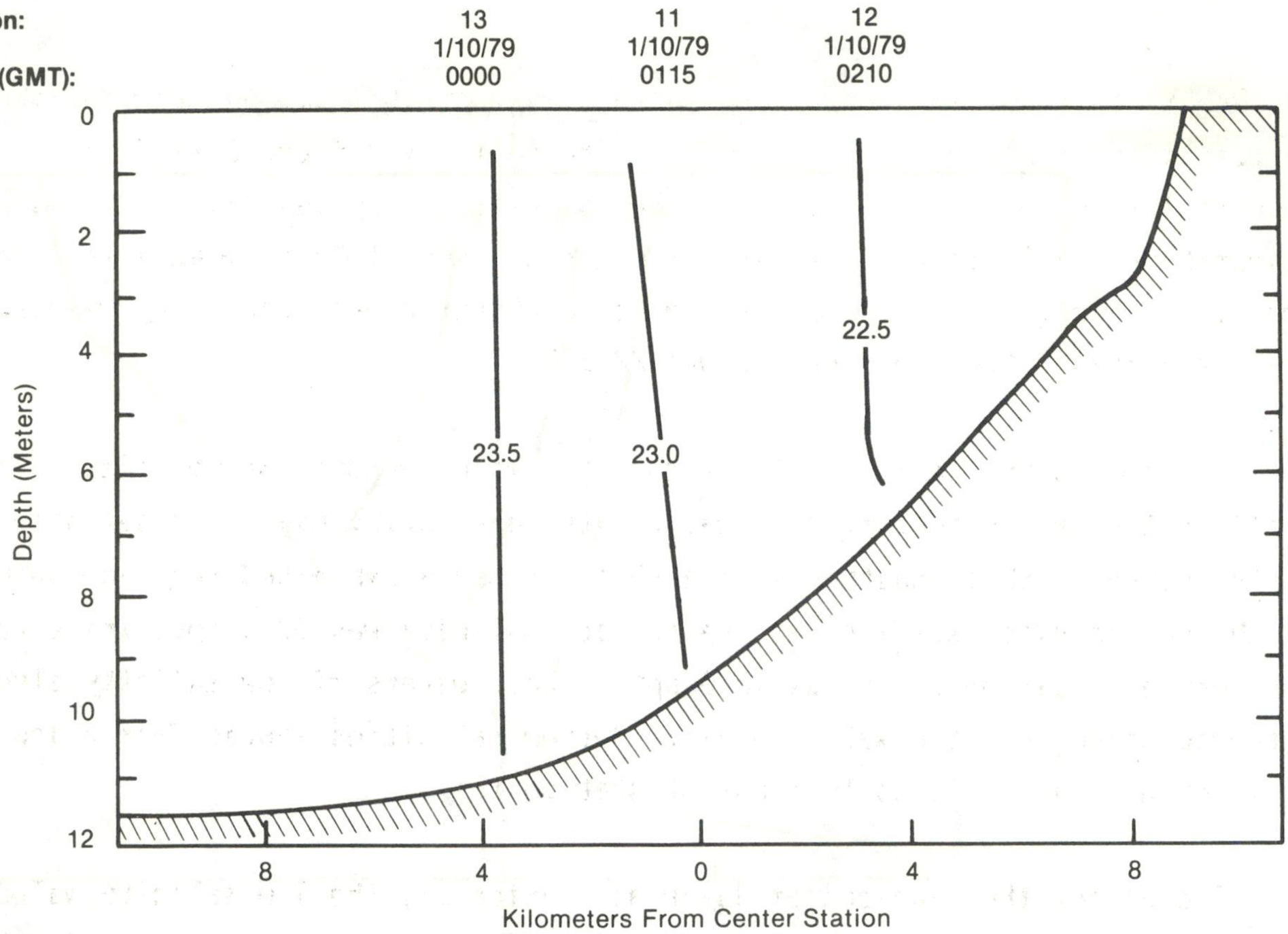

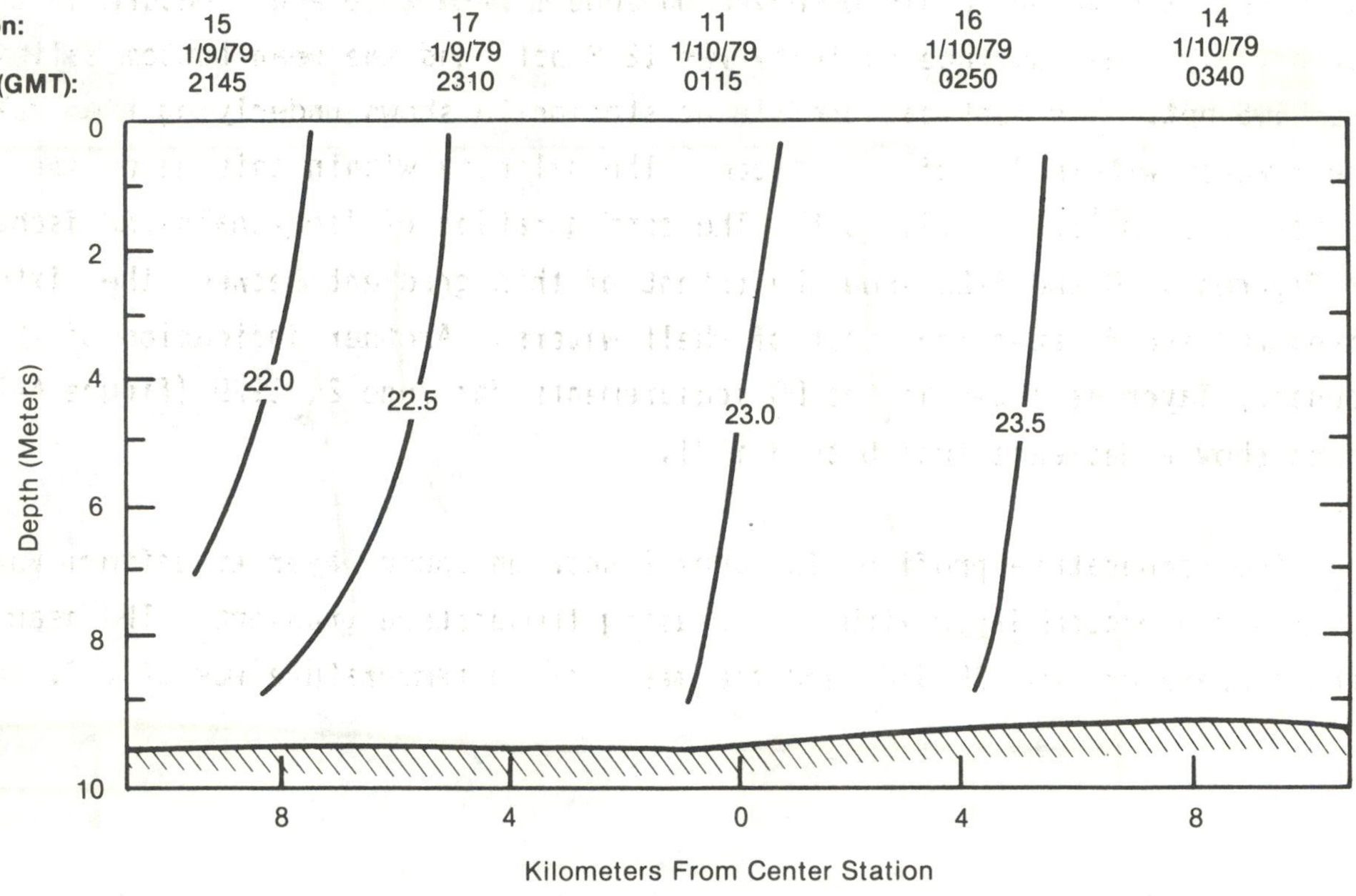

Figure 5-19. Sigma-t contours at West Hackberry for January 9-10, 1979. Vertical exaggeration 1200:1.

to the TMU of +0.1, -0.4 ppt. In contrast, the stratification was considerable between these stations and station 11. The salinity differential from the surface to the bottom was 5.6 ppt, and the bottom salinity was 23.6 ppt. Water temperatures in April were warmer; although in general their gradients were small. On April 18, the mean surface temperature at West Hackberry was 22.5°C, while the mean bottom temperature was 22.2°C.

The southward spreading of low salinity water across the Louisiana inner shelf at the West Hackberry site was at its peak during May. The salinity distribution north to south over the shelf on May 9 exhibited very low values. At the southernmost station 13, the surface salinity was 13.0 ppt, while at the northernmost station 12 it was 12.0 ppt. These waters of low salinity also extended throughout the water column. Bottom salinities ranged from a low of 12.4 ppt at station 12 to 16.6 ppt at station 13.

Except for the near-bottom layer at station 13, the low salinity values throughout the water column observed on June 2 were a general feature in this region. The mean surface salinity was 12.8 ppt, and the mean bottom salinity was 15.6 ppt. The vertical profile at station 13 shows underlying high salinity shelf water within 2 m of the bottom. The salinity within this halocline decreased from 23.1 to 14.4 ppt. The configuration of isopycnals and isohalines in figures 5-20 and 5-21 show the extent of this gradient between the mixture of river and shelf water from that of shelf waters. Another indication of this boundary layer is shown in the DO measurements for June 2, 1979 (figure 4-7), which show a decrease from 5 to 3 ml/l.

The temperature profiles for June 2 show an upper layer of uniform warmer water and a bottom layer with a decreasing temperature gradient. The mean surface temperature was 25.5°C, and the mean bottom temperature was 24.8°C.

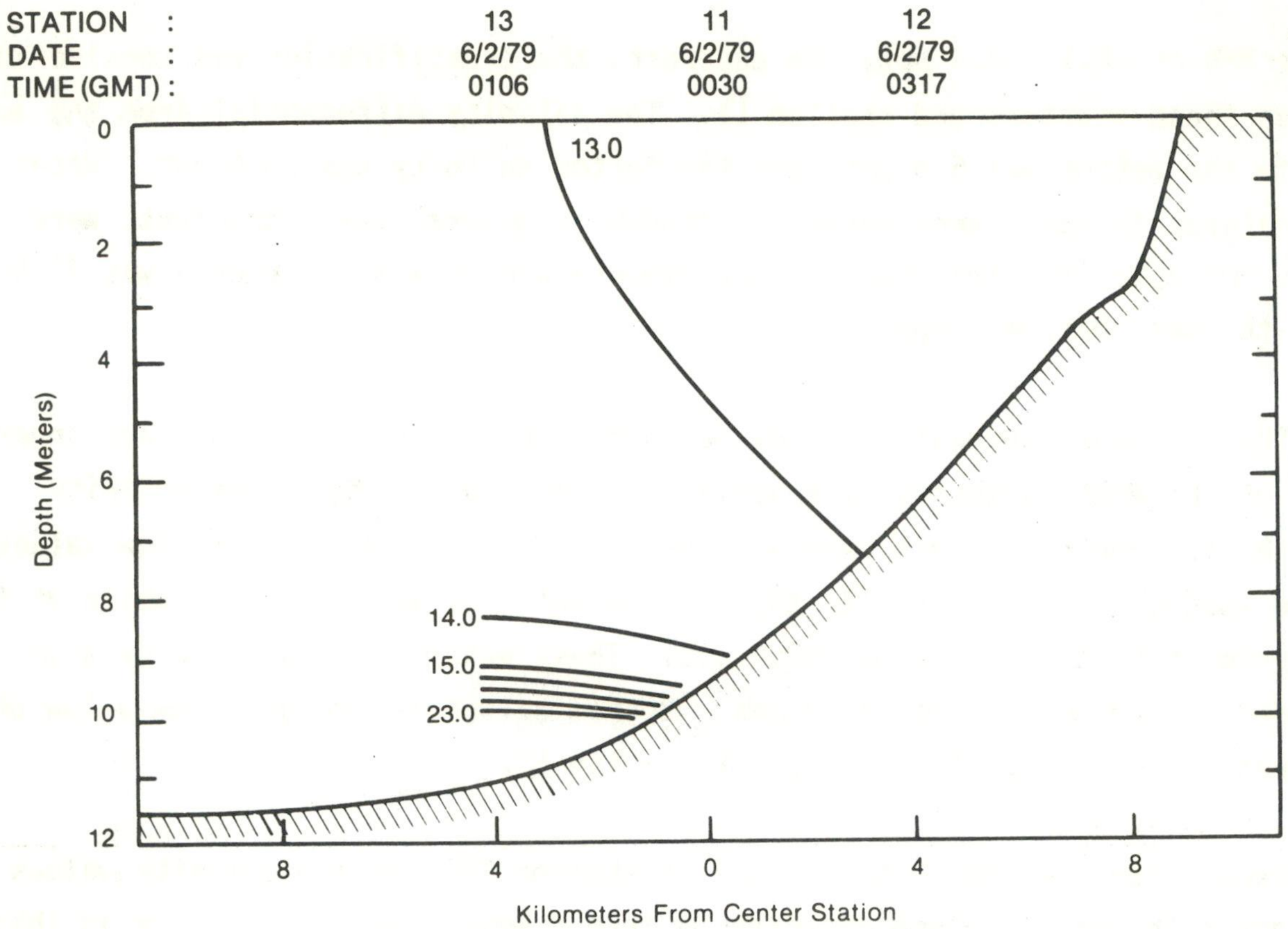

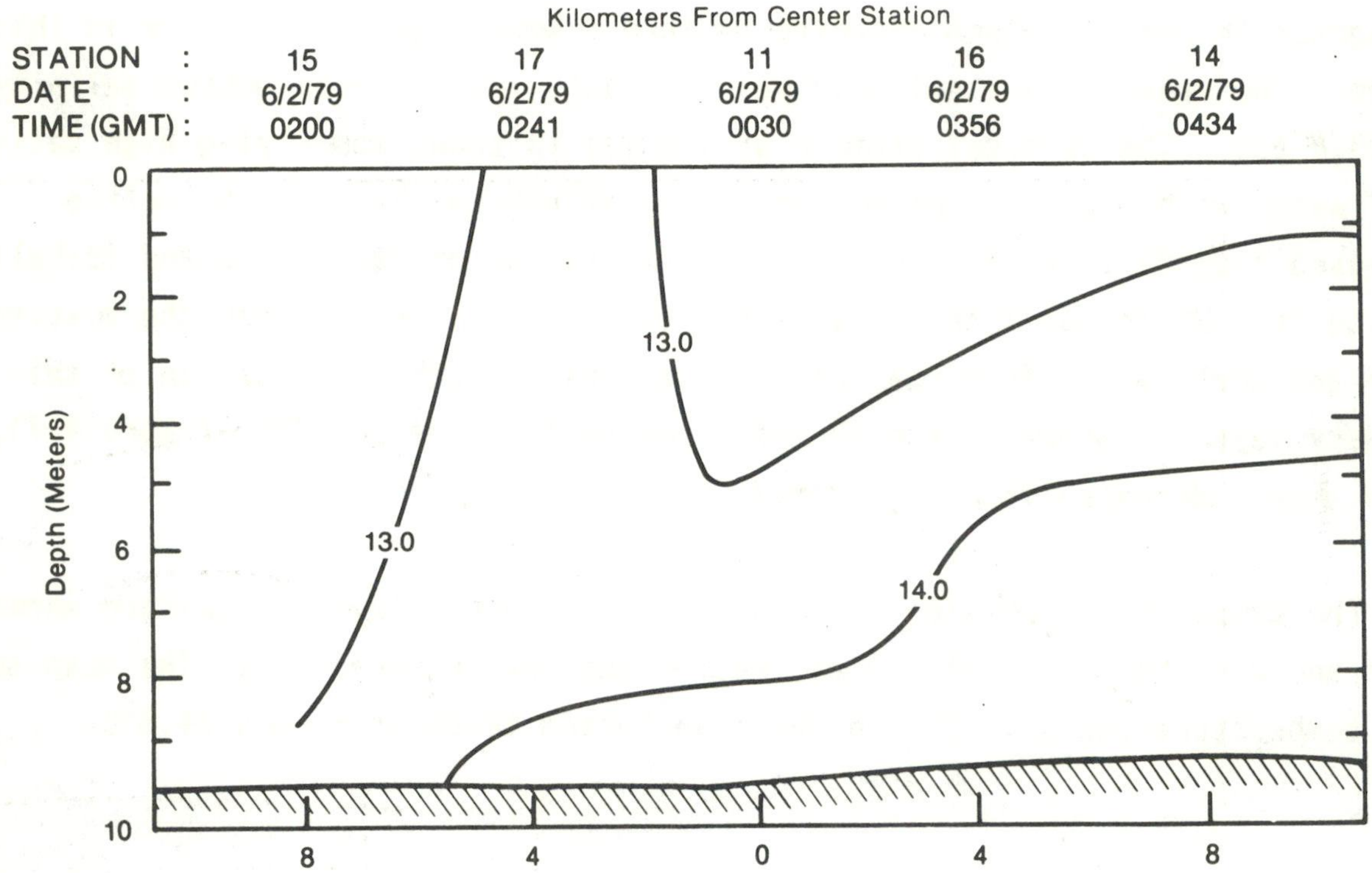

Figure 5-20. Salinity contours at West Hackberry for June 2, 1979. Vertical exaggeration 1200:1.

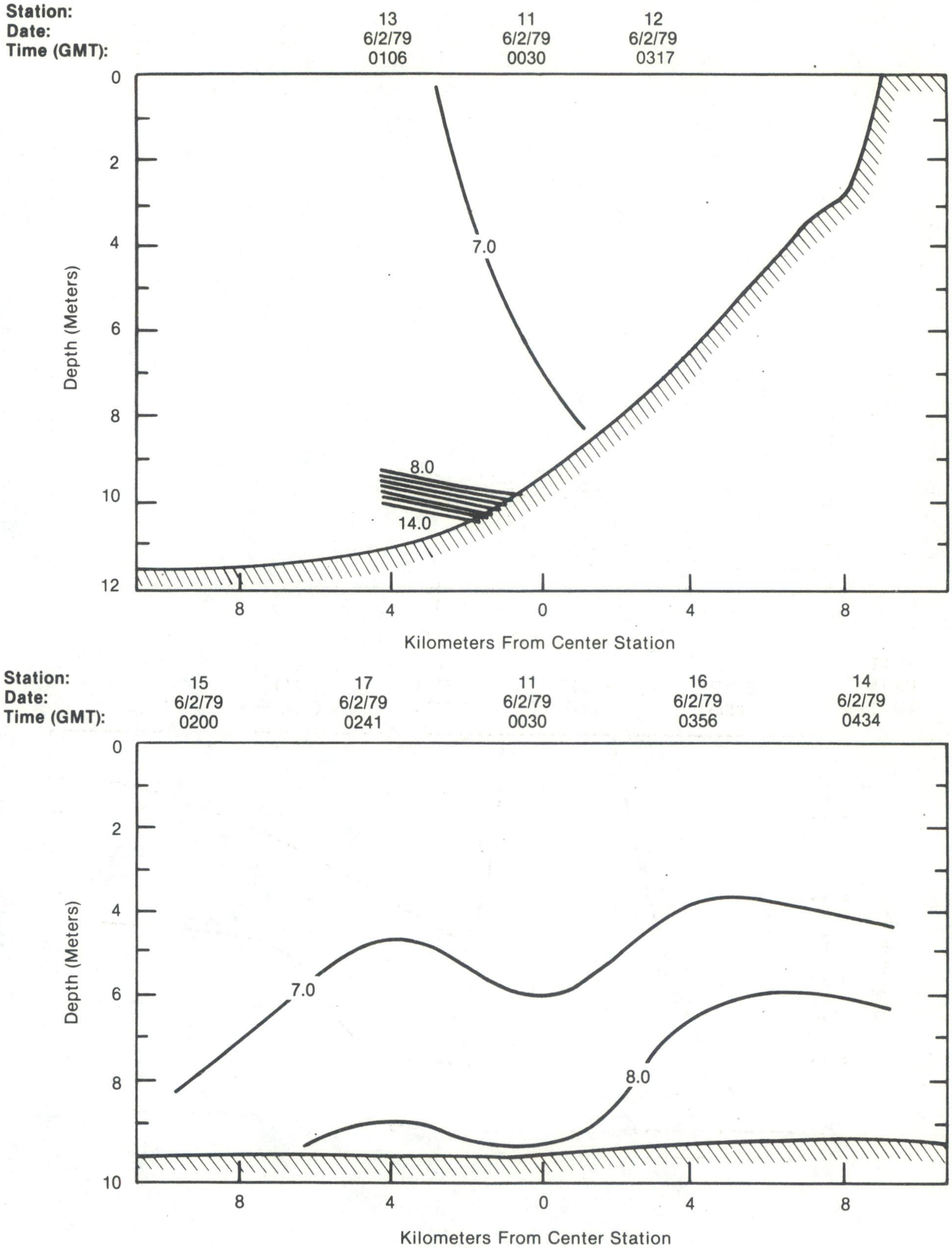

Figure 5-21. Sigma-t contours at West Hackberry for June 2, 1979. Vertical exaggeration 1200:1.

6. LOCAL METEOROLOGY

Meteorological conditions at the West Hackberry site are subject to large annual variations, which are dominated by the regional atmospheric and oceanographic conditions discussed in section 2. This section describes observation at NOS stations 18 and 19, and at Lake Charles Airport, 50 km inland from the site area. Storms are described further in sections 18 to 20.

6.1. Air Temperature

Mean monthly temperatures at the site may be inferred from temperatures measured at Lake Charles Airport (figure 6-1) for periods when data were not obtained at station 18. Table 6-1 summarizes temperature differentials observed

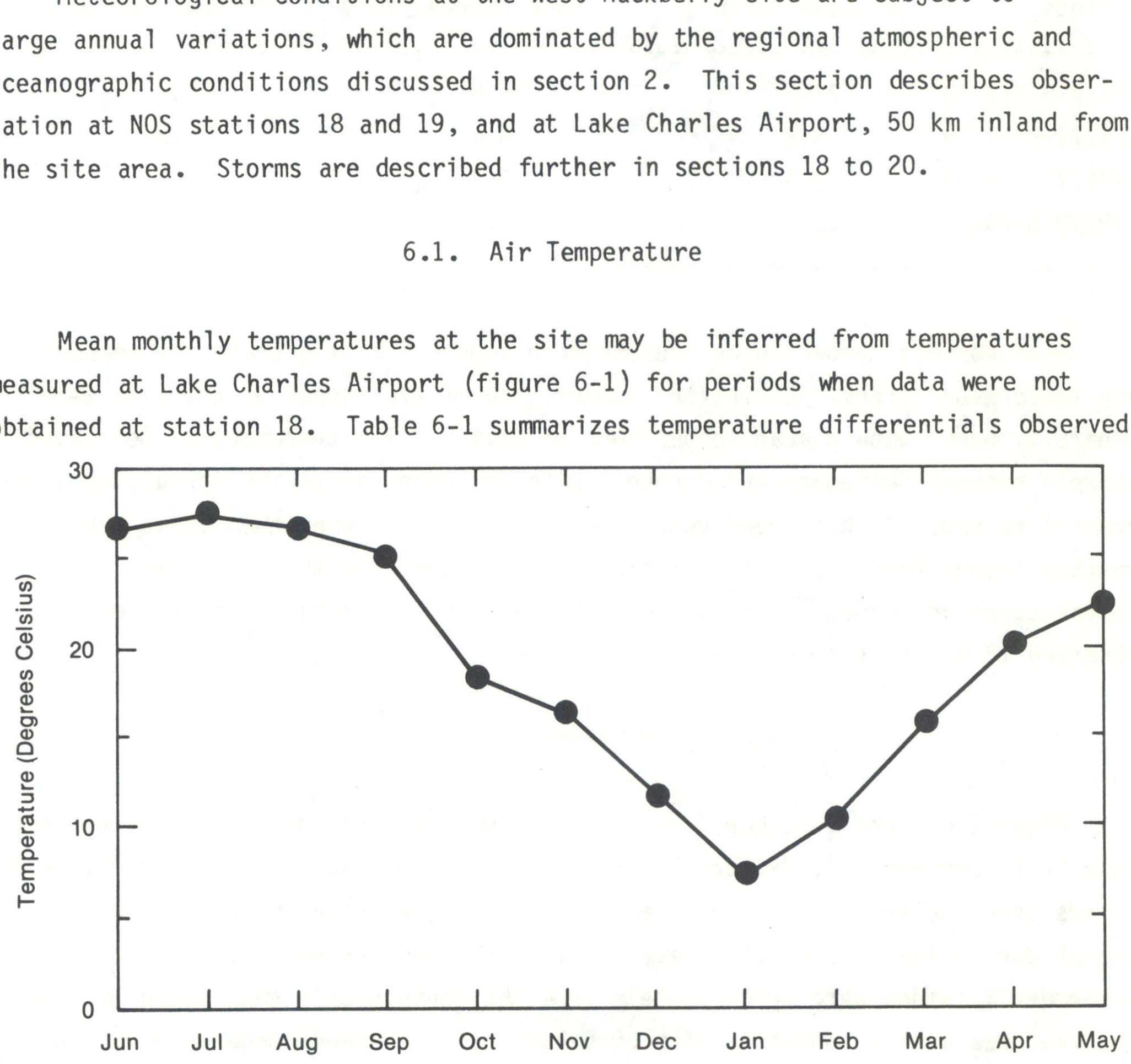

Figure 6-1. Mean monthly air temperature at Lake Charles Airport.

between the site area and Lake Charles. The mean values were found not to differ more than 1 Celsius degree over each observation period.

Table 6-1. Air temperature differential between station 18 and Lake Charles Airport

Periods	Mean air temperature station 18 (C°)	Mean air temperature Lake Charles (C°)	Mean Air temperature differential (C°)
7/27/78-9/2/78	27.7	26.8	0.9
2/4/79-2/21/79	8.8	8.6	0.2
4/26/79-5/7/79	21.4	20.4	1.0
5/9/79-5/30/79	23.5	22.5	1.0

Mean monthly temperatures presented in figure 6-1 illustrate the seasonal air temperature trend. During the summer, the mT air masses at the site were generally warm, with a mean temperature of 26.4°C. The temperatures decreased sharply between September and October, with increases in cP air intrusions after frontal passages. This trend continued until January, when the lowest mean monthly temperature was 7.1°C. The mean temperature for the winter was 11.0°C. Temperatures increased after January and, by June, had returned to values observed 12 months earlier.

6.2. Wind Speed and Direction

Figures 6-2 and 6-3 show time series of wind at station 18 for the periods July 27 to September 3, January 31 to February 21, and April 27 to May 31. Wind speeds over the West Hackberry site during the summer were generally weak, except during the passage of summer storms. For the period July 27 through September 3, winds were predominately from the south with a mean speed of 5 m/s. The wind was mostly southerly with 60 percent of the speeds under 6 m/s. On August 28 and 29 Tropical Storm DEBRA passed through the site with winds, averaged over 5-minute intervals, reaching 18 m/s. The drop in atmospheric pressure caused by DEBRA is apparent in figure 6-2.

Wind speeds during winter averaged 50 percent greater than those observed during summer. The wind speeds averaged 7.5 m/s and were predominately from the northeast. These stronger winter winds continued through the spring.

In May the winds at stations 18 and 19 were statistically similar to conditions observed the previous August. Winds were generally southerly with speeds of 6 m/s. A high correlation between stations 18 and 19 signifies a uniform wind field over the site area. In contrast, winds at station 18 and winds measured at Lake Charles exhibited low correlation throughout the year. Therefore, winds recorded at Lake Charles were not used to relate wind and currents at the site.

6.3. Spectral Characteristics

Power spectral plots of wind at station 18 for periods in summer, winter, and spring are presented in figures 6-4 and 6-5. The maximum entropy technique discussed in section 3 was used to determine the spectral density. Spectral plots are helpful in establishing the frequency composition of data, which demonstrates the relative importance of the various frequency components within the system.

Figure 6-4(a) shows the spectral density for winds observed from August 3 to 26. The distinctly sharp peaks of energy at the frequency of 1 CPD are evidence of the sea breeze/land breeze effect during this season. Energy peaks at 1 CPD show the energy associated with the clockwise and counterclockwise rotation to be about equal, with counterclockwise rotation slightly higher.

This phenomenon represents a component of wind that oscillates 1 CPD within a narrow elliptical path, which should be alined transhore. Narrow energy peaks were also observed at the low frequency of 0.4 CPD and the low frequency end of the spectrum, less than 0.09 CPD.

In contrast to the sharp spectral peaks in August, the spectral density for the period January 31 through February 20 in figure 6-4(b) was characterized by a wide band of higher energy at the low frequency. Most of the energy was contained within the frequencies less than 0.6 CPD.

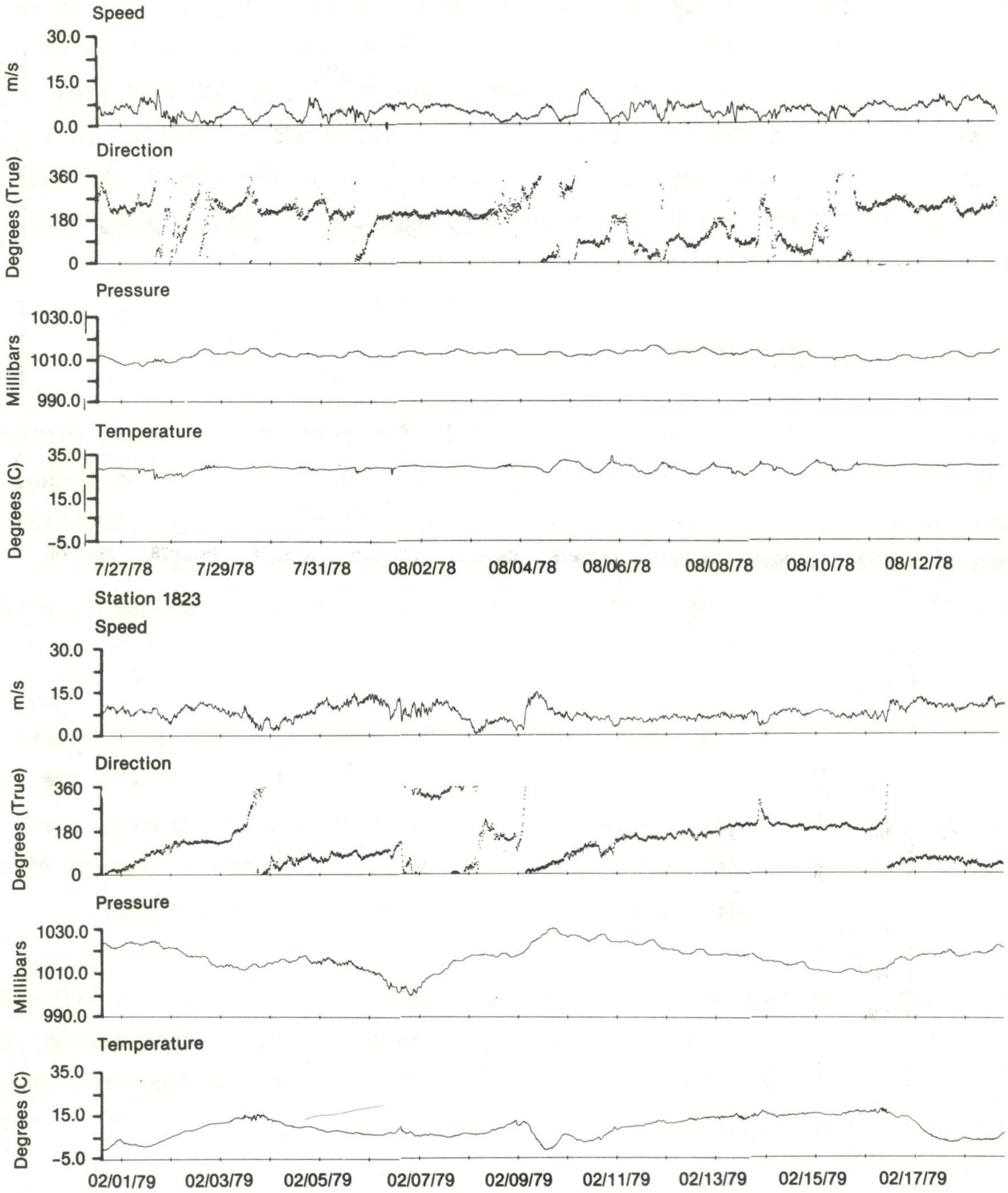

Figure 6-2. Time histories of meteorological data at station 18 for July 27 to September 3, 1978 and January 31 to February 21, 1979.

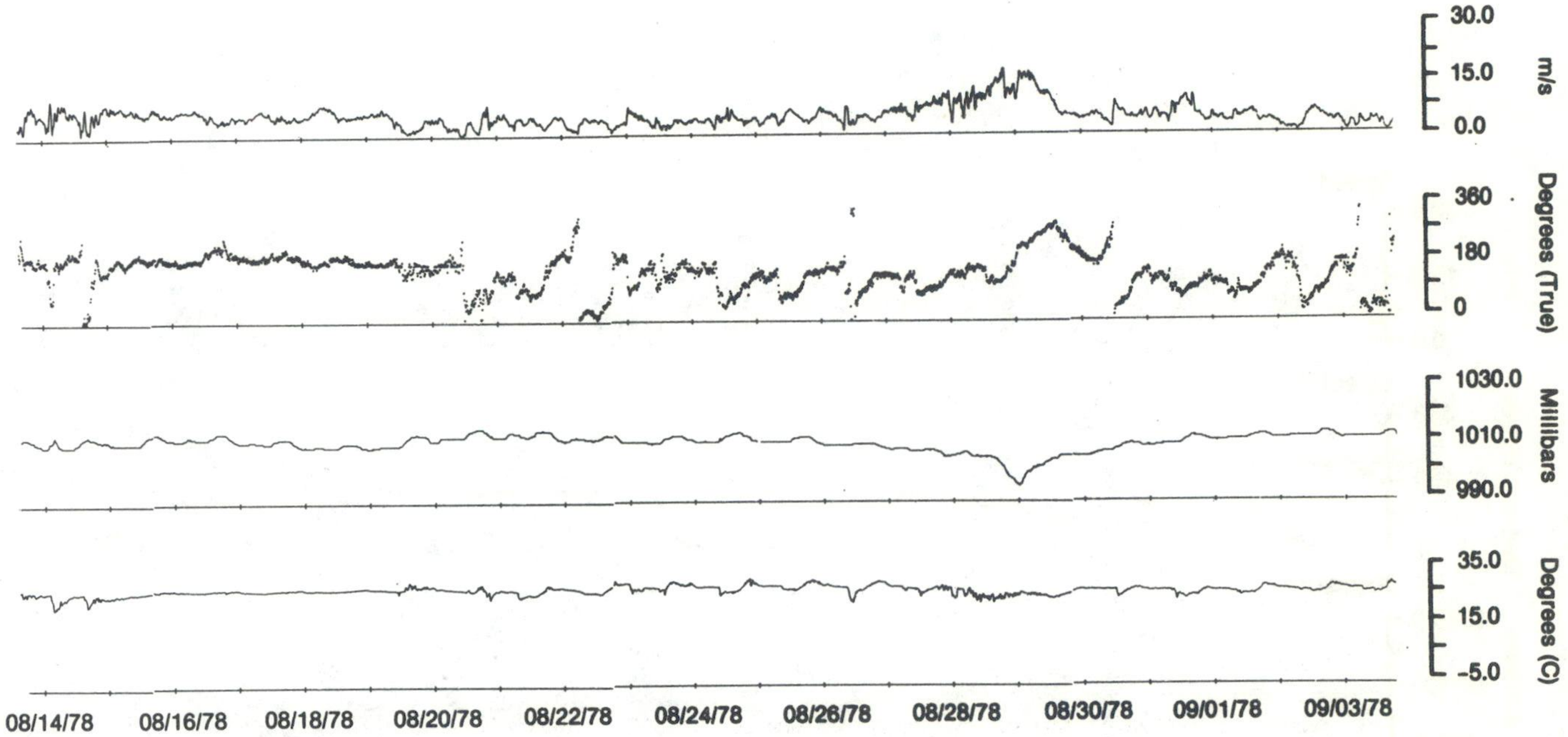

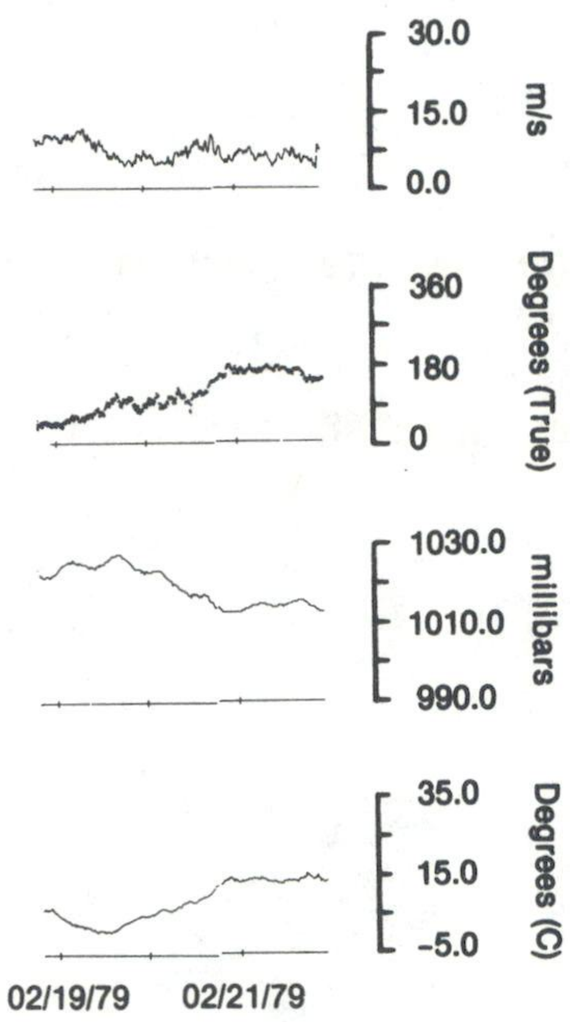

Figure 6-2. Time histories of meteorological data at station 18 for July 27 to September 3, 1978 and January 31 to February 21, 1979.

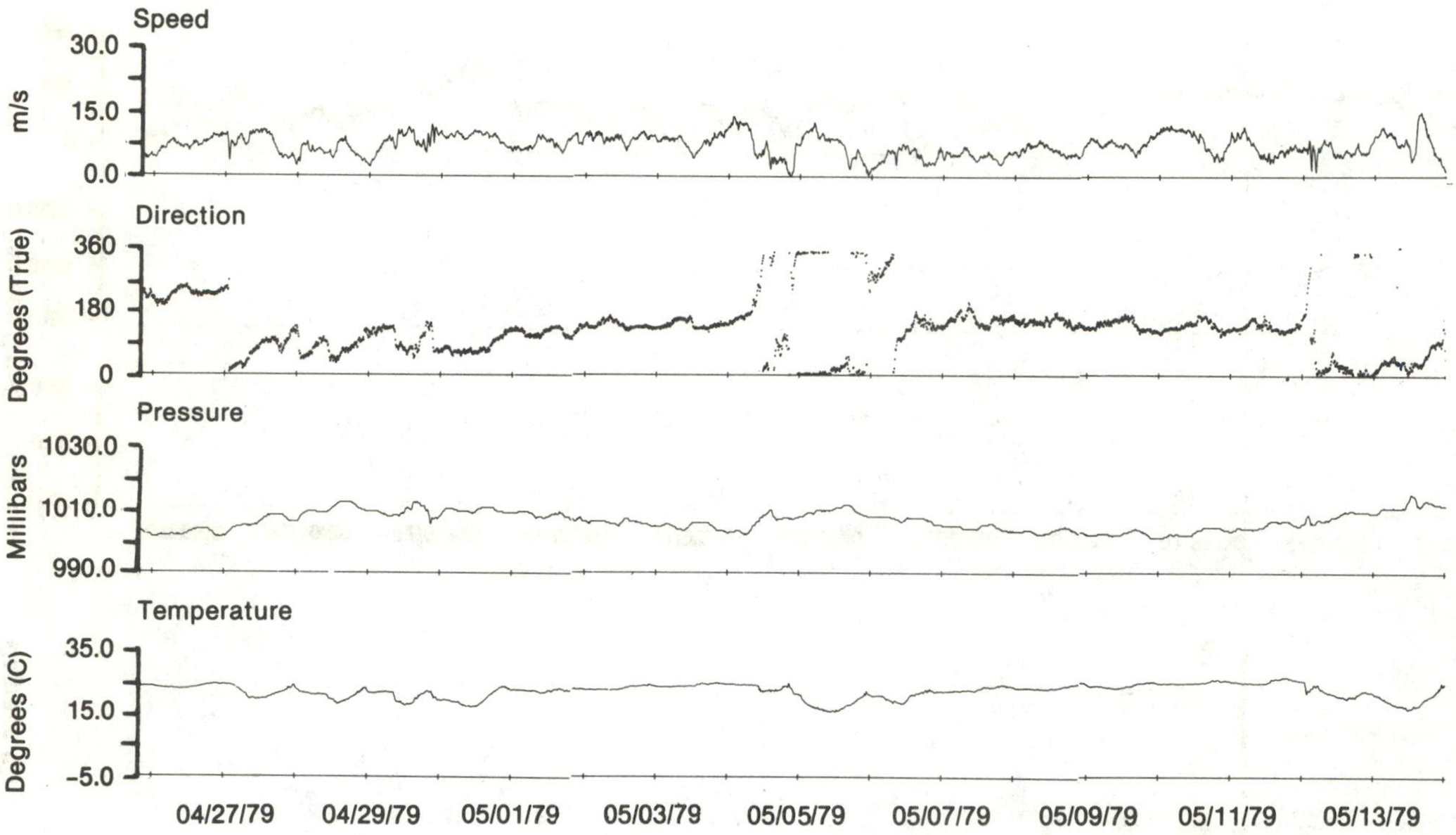

Figure 6-3. Time histories of meteorological data at station 18 for April 26 to June 1, 1979.

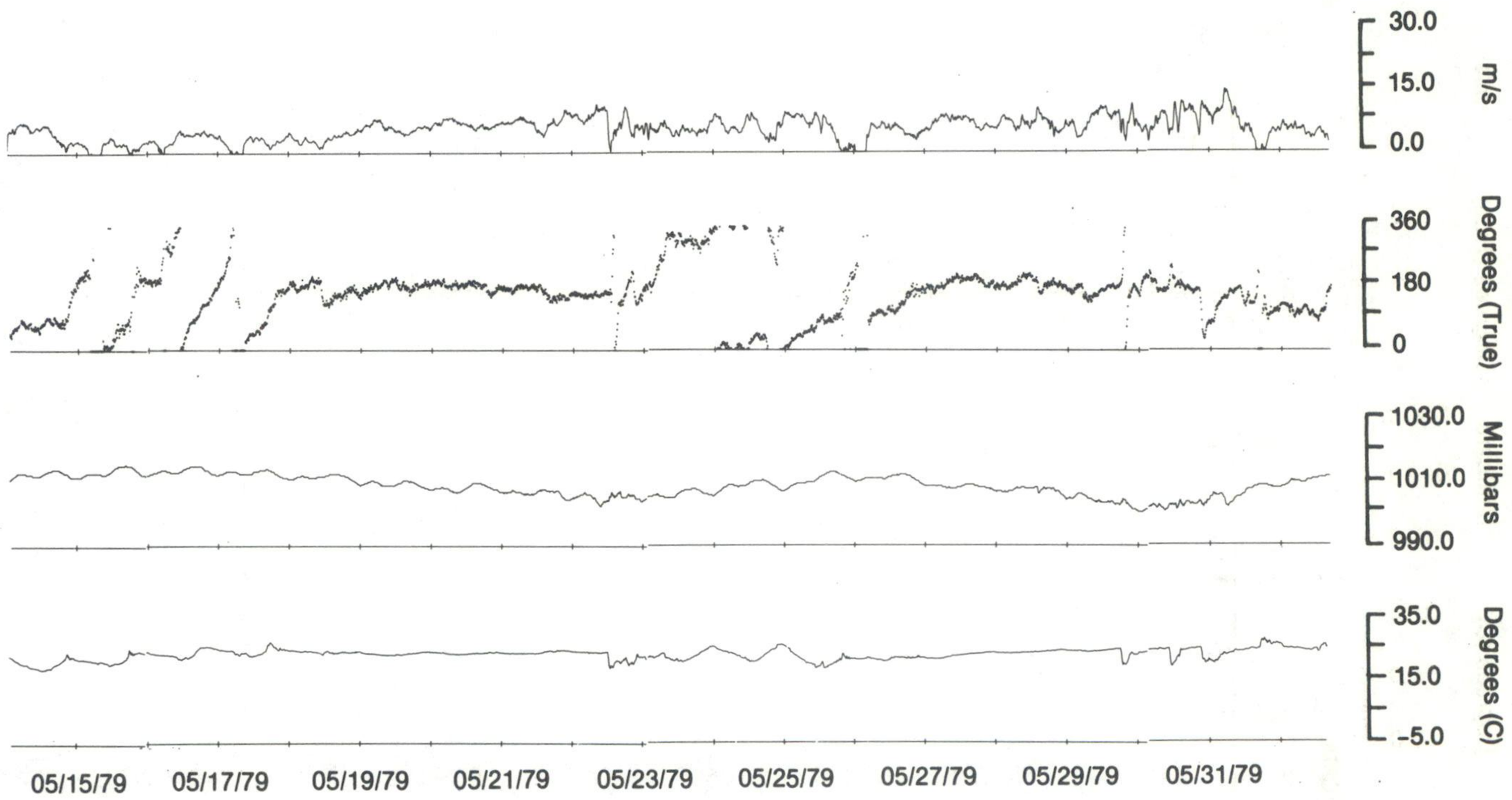

Figure 6-3. Time histories of meteorological data at station 18 for April 26 to June 1, 1979.

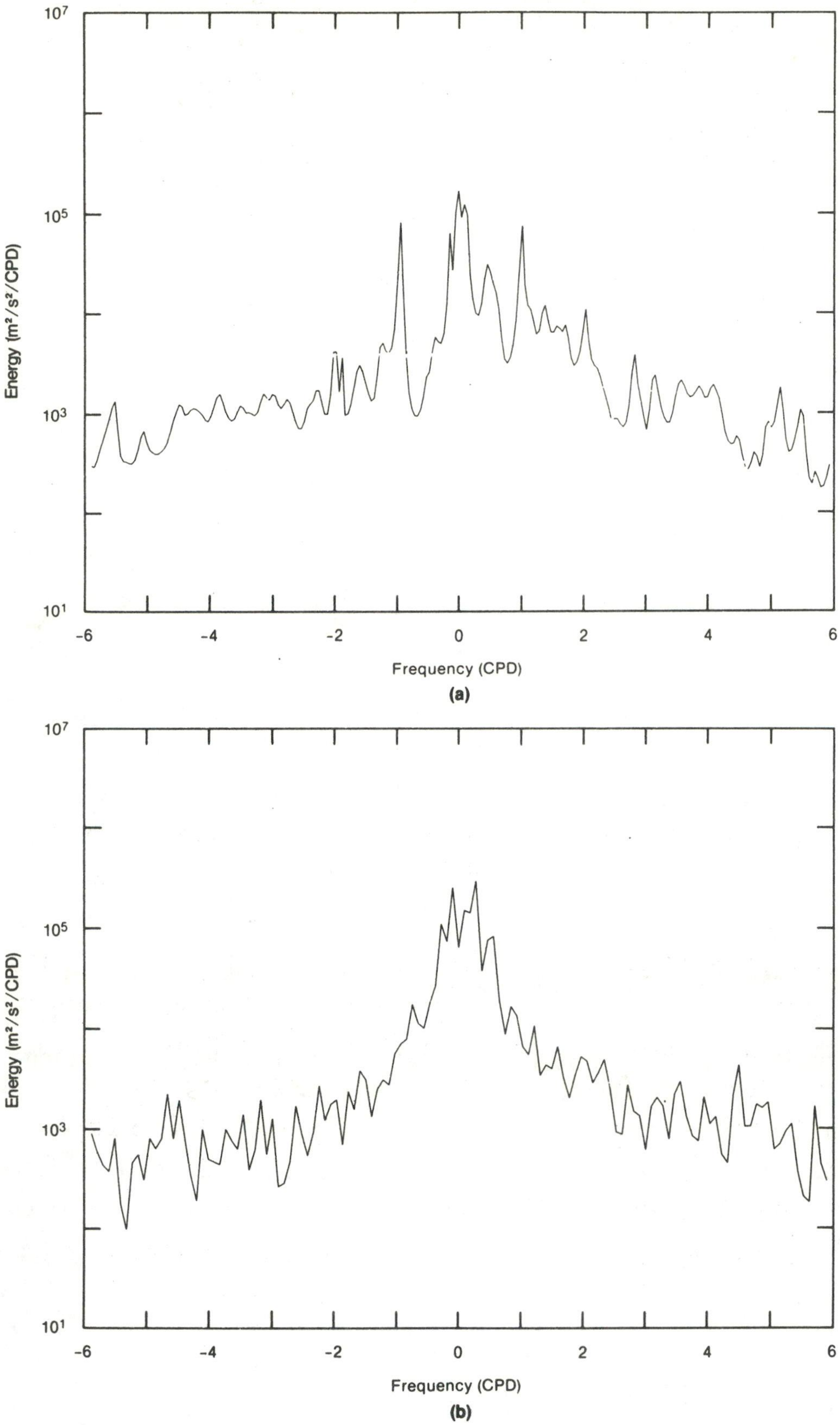

Figure 6-4. Spectral density of wind at station 18 from (a) August 3-26, 1978, (b) January 31 to February 20, 1979.

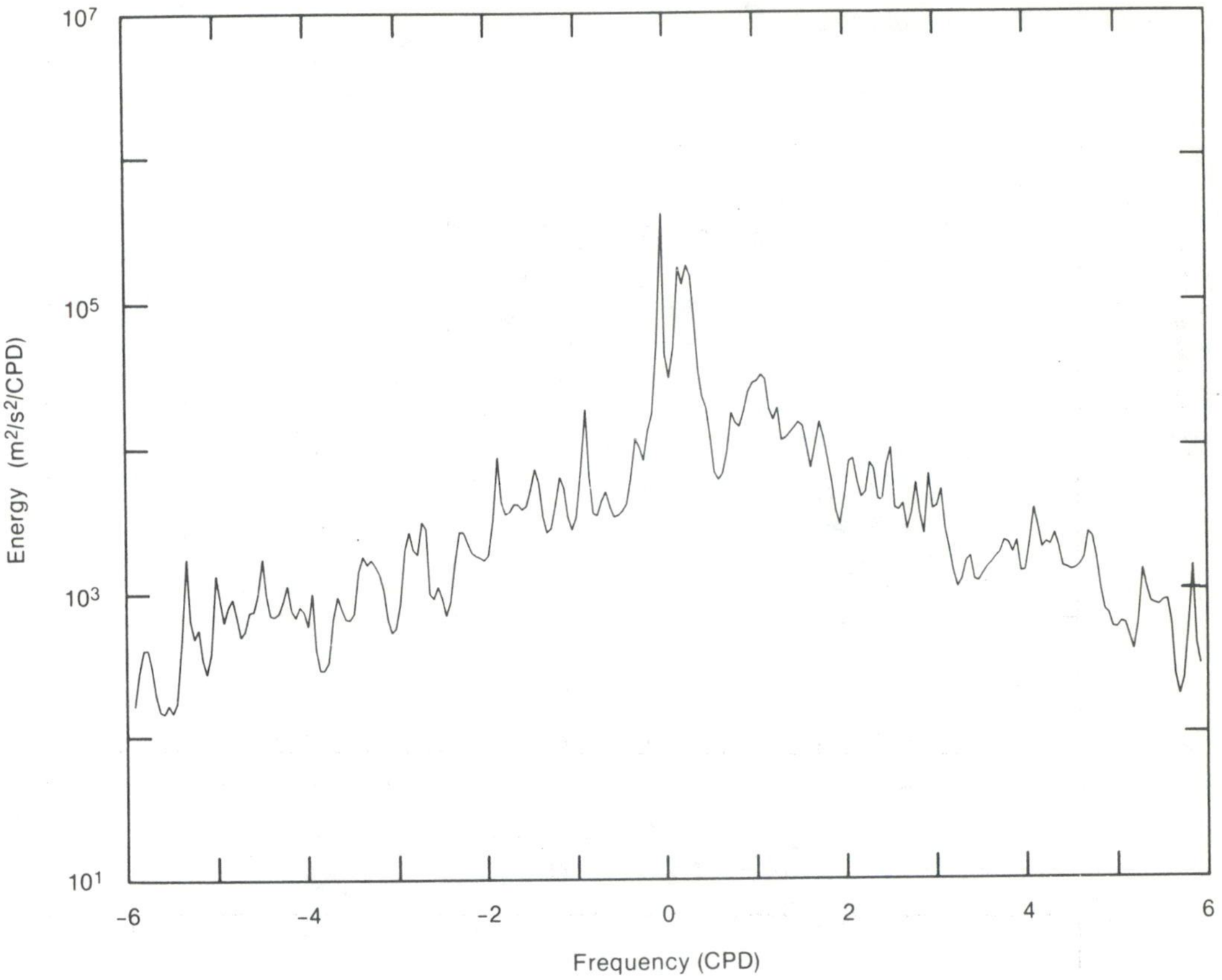

Figure 6-5. Spectral density of wind at station 18 from May 9 to June 1, 1979.

The spectral density in figure 6-5 for May 9 through June 1, 1979, was similar to that of August 1978 in that there was a relatively narrow band of energy at the low frequencies. The spectral density had distinct peaks of energy at the diurnal frequency, but these were not as significant as those observed in August. The sea/land breeze phenomenon appears to be weak during this period. The time series for the first 20 days of February indicates four instances of clockwise rotation of winds following decreasing air pressure and followed by decreasing air temperature. These were associated with polar frontal passages.

7. SURFACE WAVES

The wave climate as observed during the 12-month study is described in this section. The pressure-type wave gage that was deployed at station 11, availability of the wave data, and measurement uncertainty analysis are described in volume two of this report; processing and analysis of the wave data are described in section 3 of this volume. The wave climate at the West Hackberry site is summarized as seasonal statistics describing frequencies of significant wave height and periods of peak energy. Plots of 4-hour samples during storm events are presented in sections 18 to 20.

Consideration must be given to the unequal statistics when evaluating the summary data. Approximately 31 days of observations were obtained from August 3 to September 3, and about 65 days of observations were made from September 5 to December 7, 1978. During winter 1979, 49 days of wave observations were obtained on three records (December 8 to 17, January 9 to 31, and February 2 to 21). A nearly continuous 45-day time series was obtained during spring 1979 from March 13 to May 8. Thus, observations were obtained for about 50 percent of the time during summer 1978, 71 percent during fall, 54 percent during winter, and 49 percent during spring.

The data in tables 7-1 and 7-2 show the frequency of occurrence of significant wave heights and periods of peak energy separately; they do not indicate joint frequency of occurrences. Examples of joint frequency follow.

7.1. Summer 1978

The first valid wave record obtained at the West Hackberry site covered the period from August 3 to September 3. The maximum significant wave height

Table 7-1. Statistical summary of significant wave heights at the West Hackberry site (NOS station 11)*

From:	Day	8/3/78	9/5/78	11/1/78	11/14/78	12/8/78	1/9/79	2/2/79	3/13/79	4/5/79
	Hour (GMT)	1955	1959	0000	2030	2201	1801	1920	1700	1204
To:	Day	9/3/78	10/3/78	11/14/78	12/7/78	12/17/78	1/31/79	2/21/79	4/4/79	5/8/79
	Hour (GMT)	1155	1559	1600	1230	1001	1401	1520	1300	1204
No. of days		30.67	28.83	13.67	22.67	8.50	21.83	18.83	21.83	33.00
Significant height (m)**										
2.6 ≤ H < 2.7		0.54								
2.2 ≤ H < 2.3		1.08								
2.1 ≤ H < 2.2		0.54								
1.8 ≤ H < 1.9		0.54					0.76			0.50
1.7 ≤ H < 1.8					0.73					0.50
1.6 ≤ H < 1.7							1.53			0.50
1.5 ≤ H < 1.6					0.73		0.76	0.88		1.49
1.4 ≤ H < 1.5		0.54					3.05	0.88		0.99
1.3 ≤ H < 1.4		1.08			0.73		2.29	0.88	2.27	0.50
1.2 ≤ H < 1.3				1.30	2.19		2.29	2.63	5.30	0.99
1.1 ≤ H < 1.2		0.54	0.60	2.60	1.46		3.82	3.51	7.58	0.99
1.0 ≤ H < 1.1		0.54	5.36	1.30	2.92		6.87	1.75	8.33	2.97
0.9 ≤ H < 1.0			7.74	2.60	5.84	3.85	5.34	0.88	11.36	3.47
0.8 ≤ H < 0.9		1.62	6.55	3.90	5.11	1.92	7.63	2.63	9.09	6.93
0.7 ≤ H < 0.8		2.70	9.52	6.49	5.84	3.85	6.87	1.75	12.88	11.39
0.6 ≤ H < 0.7		2.16	6.55	10.39	10.95	7.69	6.87	11.40	10.61	10.40
0.5 ≤ H < 0.6		12.43	14.88	12.99	9.49	7.69	6.11	7.89	9.09	12.87
0.4 ≤ H < 0.5		15.14	9.52	6.49	14.60	5.77	10.69	11.40	0.76	14.36
0.3 ≤ H < 0.4		24.32	10.71	7.79	18.25	7.69	8.40	21.93	6.06	15.84
0.2 ≤ H < 0.3		21.62	10.12	23.38	21.17	26.92	10.69	13.16	8.33	13.86
0.1 ≤ H < 0.2		14.05	11.31	19.48		32.69	9.16	15.79	5.30	1.49
0.0 ≤ H < 0.1		0.0	7.14	1.30		1.92	6.87	2.63	3.03	
Maximum		2.62	1.16	1.24	1.77	0.96	1.90	1.54	1.39	1.80
Mean		0.45	0.51	0.44	0.56	0.35	0.64	0.48	0.73	0.60
Minimum		0.14	0.70	0.09	0.22	0.10	0.05	0.07	0.07	0.17

*Percentage of data in time period with significant wave height within indicated bands.
**There were no observations of significant wave heights between 2.3 and 2.6 m.

observed during the 12-month study, 262 cm, occurred during this period and was associated with Tropical Storm DEBRA. Time series plots of both significant wave height and maximum wave height during DEBRA are shown in section 18. Despite the bias from the passage of DEBRA, the significant wave heights were less than 70 cm for 90 percent of the time. For 75 percent of the time, the

Table 7-2. Statistical summary of the periods of peak energy at West Hackberry*

From:	Day	8/3/78	9/5/78	11/1/78	11/14/78	12/8/78	1/9/79	2/2/79	3/13/79	4/5/79
	Hour (GMT)	1955	1959	0000	2030	2201	1801	1920	1700	1204
To:	Day	9/3/78	0/3/78	11/14/78	12/7/78	12/17/78	1/31/79	2/21/79	4/4/79	5/8/79
	Hour (GMT)	1155	1559	1600	1230	1001	1401	1520	1300	1204
No. of days		30.67	28.83	13.67	22.67	8.50	21.83	18.83	21.83	33.00
Period of peak energy (seconds)										
≤ 4.05		56.2	45.8	27.3	27.7	75.0	46.6	55.3	44.7	42.6
5.02		22.7	28.0	35.0	19.0	13.5	21.4	9.6	26.5	15.8
5.99		12.4	18.5	24.7	25.6	3.8	13.0	24.6	15.9	14.4
7.02		3.8	6.5	11.7	20.4		11.4	9.6	9.1	11.9
8.03		2.2	0.6		4.4	7.7	3.0	0.9	3.0	7.9
9.08		2.2			2.9		2.3		0.8	4.4
10.10		0.5	0.6	1.3			2.3			3.0

*Percentage of data in time period with indicated period of peak energy.

significant wave heights were between 14 cm and 50 cm; no observations less than 14 cm were made.

The periods of peak energy during late summer 1978 were equal to or less than 6 seconds more than 90 percent of the time. Periods of peak energy of 7 seconds and greater were associated with DEBRA, except for 0755 and 1155 GMT on August 9 when the periods were 8 and 7 seconds, respectively. At that time, the significant wave heights were only 20 and 22 cm, respectively. The maximum period of peak energy was observed at 2355 GMT on August 27 at 10.1 seconds, with a corresponding significant wave height of 120 cm. The maximum significant wave height was observed some 16 hours later, at 1555 GMT on August 28 at 262 cm.

The effects of DEBRA on the period of peak energy could be seen until 0755 GMT on August 30, when the significant wave height was 47 cm and the period of peak energy was 7.02 seconds. After that, the periods remained at 6 seconds or less.

7.2. Fall 1978

From September 5 to October 3, significant wave heights remained less than 100 cm for more than 90 percent of the time. The minimum significant wave height observed during late summer 1978 was 7 cm; negligible wave heights were more frequent at the West Hackberry site during this period than for any other record obtained during the study, with significant wave heights between 7 and 10 cm occurring about 7 percent of the time.

Periods of peak energy from September 5 to October 3 remained at 6 seconds or less for more than 90 percent of the time. A 10-second peak period was observed only once, at 1159 GMT on September 20; the corresponding significant wave height was 53 cm.

Wave data were not obtained during October, except for the first 3 days. Although neither a validated wave record nor onsite meteorological data were obtained, visual observations made by an NOS photo mission group and examination of the Lake Charles Airport data suggest an energetic wave climate during October 1978.

Wind speeds observed during October 1978 at Lake Charles Airport were equal to or less than 3 m/s for 51.4 percent of the time, while they were between 4 and 9 m/s 48.6 percent of the time. Depending on the type of weather system and on the wind direction, wind speeds at the offshore site were greater than those observed at the airport by a factor of from 2 to 4. This is why, as mentioned in section 6, winds measured at Lakes Charles were not used to relate wind and currents at the offshore site. The October winds blew out of the north to east-northeast for 60 percent of the time (in response to frontal passages), out of the south for only 7 percent of the time, and were nearly evenly distributed in space for the remainder of the time.

Wind stresses at the sea surface can generate instabilities in the water column in addition to generating surface waves. Alternating narrow bands of foam and sediment were observed on the sea surface during the late morning of October 15 by the principal investigator during a reconnaissance flight. These observations indicate large cell Langmuir circulation in which wind stress at

the sea surface excites juxtaposed solenoidal (cellular) circulation and resulting near-perfect vertical mixing at the boundaries of the cells (Assaf et al., 1971). The bands of foam resulted from entrapped air from white caps being forced into narrow convergence lines, while the bands of sediment indicated divergence. Convergence occurs at the sea surface when two adjacent circulation cells rotate toward each other, and divergence occurs when the next two cells rotate away from each other.

Significant wave heights observed during the first half of November 1978 were less than 90 cm for more than 90 percent of the time, with a mean height of 44 cm. During the second half of November and the first week of December, significant wave heights were less than 1 m for more than 90 percent of the time, although the maximum height during this period was 177 cm. No quiescent observations were made; the minimum significant wave height observed was 22 cm.

The periods of peak energy during the first half of November 1978 were equal to or less than 6 seconds for 87 percent of the time. Compared with the August and September data, the distribution of energy shifted toward an increase in the 5- to 7-second bands and a sharp decrease in the bands at 4 seconds and less. A single observation of an 11-second period was made at 2000 GMT on November 3 with a corresponding significant wave height of 24 cm.

During the second half of November and the first week of December 1978, periods of peak energy were equal to or less than 7 seconds more than 90 percent of the time, but the distribution had shifted from the previous 2-week period. Periods of 4 seconds and less remained nearly the same as during the first 2 weeks of November, as did periods of 6 seconds. There was a sharp decrease in the 5-second energy band (from 35 to 19 percent of the observations), a marked increase in the 7-second band (from 11.7 to 20.4 percent), and an increase in the 8- and 9-second bands. No observations of periods of peak energy of 10 seconds or greater were made during the second half of November and first week of December 1978. The maximum periods of peak energy (9 seconds) were observed from 0830 to 1630 GMT on December 4 and at 0030 GMT on December 5; the significant wave heights associated with these observations ranged from 32 to 65 cm.

7.3. Winter 1979

The 8.5-day wave record obtained during mid-December indicated that significant wave heights were less than 70 cm for 90 percent of the time. The lowest values of mean and maximum significant wave heights observed during the 12-month study were obtained during this relatively brief period; the mean wave height was 35 cm, while the maximum significant wave height was 96 cm. Relative quiescence during this 8.5-day period is attributed to the absence of cold fronts (NOAA/NWS Daily Weather Maps from December 4 to 17, 1978). A high pressure area over Texas on December 9 affected coastal Louisiana until December 14, when an occluded front developed offshore.

The mid-December record of 8.5 days is biased by its short duration over a period of moderate weather. Periods of peak energy of 4 seconds or less occurred 75 percent of the time, and 5 seconds or less about 90 percent of the time. These frequencies of occurrence are in sharp contrast with the periods before and after. Three of the 7.5-minute wave records indicated an 8-second period of peak energy; these occurred at 2200 GMT on December 8, at 1400 GMT on December 11, and at 0200 and 0600 GMT on December 12. The corresponding significant wave heights were 42 cm on December 8, 19 cm on December 11, and 17 and 13 cm on December 12. The maximum significant wave height observed during the 8.5-day record was 96 cm at 1000 GMT on December 9, when the period of peak energy was equal to or less than 4 seconds.

The wave records obtained during midwinter and late winter 1979 indicated high levels of wave energy associated with the passage of polar fronts and an extratropical cyclone.

The 22-day January record displayed a maximum wave height of 190 cm, second only to that observed during Tropical Storm DEBRA, while heights between 5 and 10 cm prevailed for about 7 percent of the time between storm events. Significant wave heights remained below 120 cm for 90 percent of the time.

The longest periods of peak energy (9 and 10 seconds) were observed in connection with an extratropical cyclone, which is described in section 11. The long periods did not coincide with the maximum significant wave heights seen at

1400 GMT on January 11 (145 cm) and at 0200 GMT on January 14 (114 cm), associated with periods of 5 seconds and 4 seconds or less, respectively. Significant wave heights associated with the 10-second periods of peak energy did not exceed 43 cm from 1400 GMT on January 12 to 0600 GMT on January 13. A norther on January 20 increased the significant height to 190 cm and the maximum wave height to 223 cm, with a period of peak energy of 4 seconds or less. Another norther on January 23 caused significant wave heights to reach 157 cm, while the period of peak energy did not exceed 7 seconds. The relatively short fetch associated with the northers influences periods of peak energy. It is presumed that a distant storm on January 25th resulted in two consecutive 8-second peak energy observations with significant wave heights at 21 and 13 cm, respectively. Despite decaying signficant wave heights following a norther on January 25, the period of peak energy remained at 7 seconds (except for one 8-second observation) from 1000 GMT on January 26 to 2200 GMT on January 27; at the end of this time, the significant wave height was 19 cm, while at the beginning it was 1.17 cm.

The February 1979 record showed that significant wave heights were less than 100 cm for more than 90 percent of the time, while the maximum significant wave height observed was 154 cm; this indicated a decline compared with the January data. Significant wave heights of less than 50 cm were observed for 65 percent of the time during February, but only 46 percent of the time during January. While the maximum significant wave height observed during the late winter 1979 record was less than that observed during January and February, 75 percent of the wave energy was distributed at significant wave heights between 50 cm and 120 cm.

Data obtained during the 19-day period of February 1979 show a bimodal distribution of periods of peak energy with 55 percent of the observations at 4 seconds and less and 25 percent of the observations at 6 seconds. All observations of 6 to 8 seconds were made between February 5 and 10, 1979; they were 6 seconds or less at all other times. The single 8-second peak energy observation was made at 0720 on February 10 when the significant wave height was only 13 cm. The maximum significant height observed during February was 154 cm at 1920 hours on February 4, with a corresponding 5-second period of peak energy.

7.4. Spring 1979

A 22-day wave record obtained beginning 1700 GMT on March 13 indicated significant wave heights between 5 cm and 110 cm for 53 percent of the time. Zero-crossing analysis indicates that the greatest maximum wave height of 276 cm occurred at 0100 GMT on April 3; the corresponding significant wave height and period of peak energy were 56 cm and 4 seconds or less. The maximum significant wave height of 139 cm was observed at 0500 GMT on March 30, with a corresponding period of peak energy of 5 seconds. Peak energy periods were 6 seconds or less 87 percent of the time. The single 9-second observation for the March 13 to April 4 period occurred at 1300 GMT on March 25, when the significant wave height was only 8 cm. For 32 hours before and 36 hours after, the periods of peak energy were 4 seconds or less, and the significant wave heights did not exceed 60 cm; the shift in energy is associated with a distant storm.

Although the April-May 1979 wave data indicate a maximum significant wave height of 180 cm, more than 90 percent of the wave heights observed were less than 100 cm, and 85 percent were between 20 and 80 cm. The minimum significant wave height observed was 17 cm. The significant wave heights greater than 100 cm were associated with the southerly winds that accompanied a storm on April 11, 1979; the storm is described in section 20 of this volume and in section 8 of volume two.

About 73 percent of the observations during April and May indicate periods of peak energy of 6 seconds or less, about 12 percent were 7 seconds, while 15 percent were between 8 and 10 seconds. The number of observations with periods of peak energy between 8 and 10 seconds was about twice as frequent during this 33-day period than during the late fall and winter observations. The period of peak energy was 8 seconds or greater from 1604 GMT on April 23 to 0404 GMT on April 26, when significant wave heights ranged between 26 and 47 cm. The largest significant wave height of 180 cm occurred at 1604 GMT on April 11 when the period of peak energy was 7 seconds; this occurred during a storm described in section 20. Peak energies remained between 7 and 9 seconds until 1604 GMT on April 14, when the significant wave height decreased to 47 cm.

8. WATER LEVELS

Water level data at the West Hackberry site were analyzed for six time periods using the techniques discussed in section 3. As mentioned in section 3, the data were not corrected for water density or air pressure fluctuations. We determined that the water level fluctuations at West Hackberry were of the mixed tide type, which is consistent with NOS historical results (unpublished NOS data). The first source of data examined was historical NOS tidal records. Hicks (1977) summarized the results in figure 8-1. The second source of data was the nonharmonic analyses of the time series plots of the raw water level data. Figure 8-2 is a sample of a 1-week period of water levels at West Hackberry. These time series were also analyzed, using harmonic methods described in section 3, to produce the third set of information used in our determination of the characteristics of West Hackberry's water level data.

The tide curve in figure 8-2 shows a small high water inequality (DHQ), while the low water inequality (DLQ) is quite large. Table 8-1 presents the results of the nonharmonic analysis of the West Hackberry water level records. Here, the DLQ is more than twice the value of the DHQ. The means of the various datums were calculated and referenced to the sample MLLW so that the West Hackberry data could be compared to historical data for Calcasieu Pass. The results for West Hackberry are consistent with the historical data available for Calcasieu Pass (table 8-2).

Table 8-3 shows large monthly variability in the value of the ratio $F = (K_1+O_1)/(M_2+S_2)$. However, the mean of the six periods is 1.51, which is consistent with the mixed, mainly semidiurnal type of tide characterized by the time series plots of the raw data.

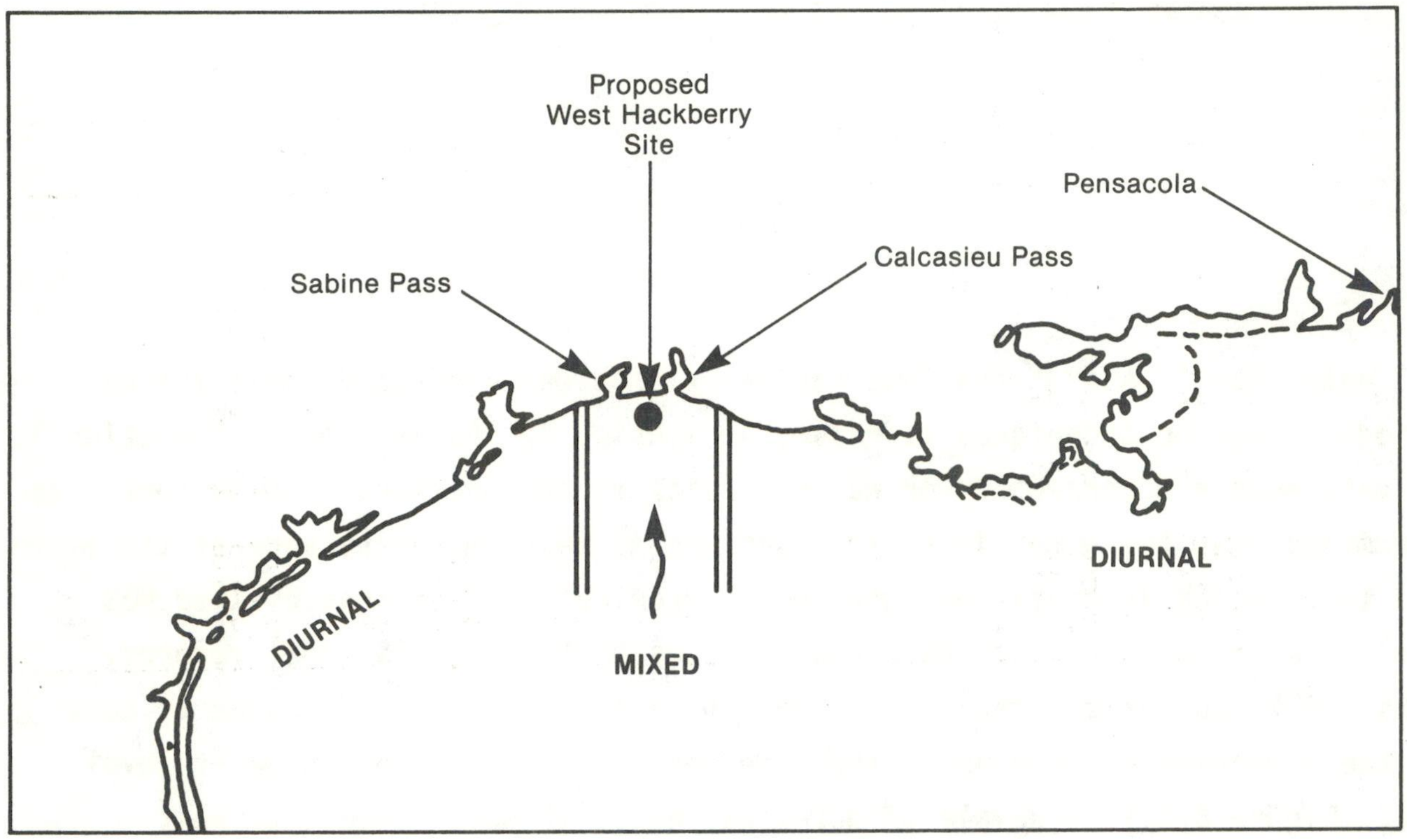

Figure 8-1. Areal extent of tide types from Hicks (1977).

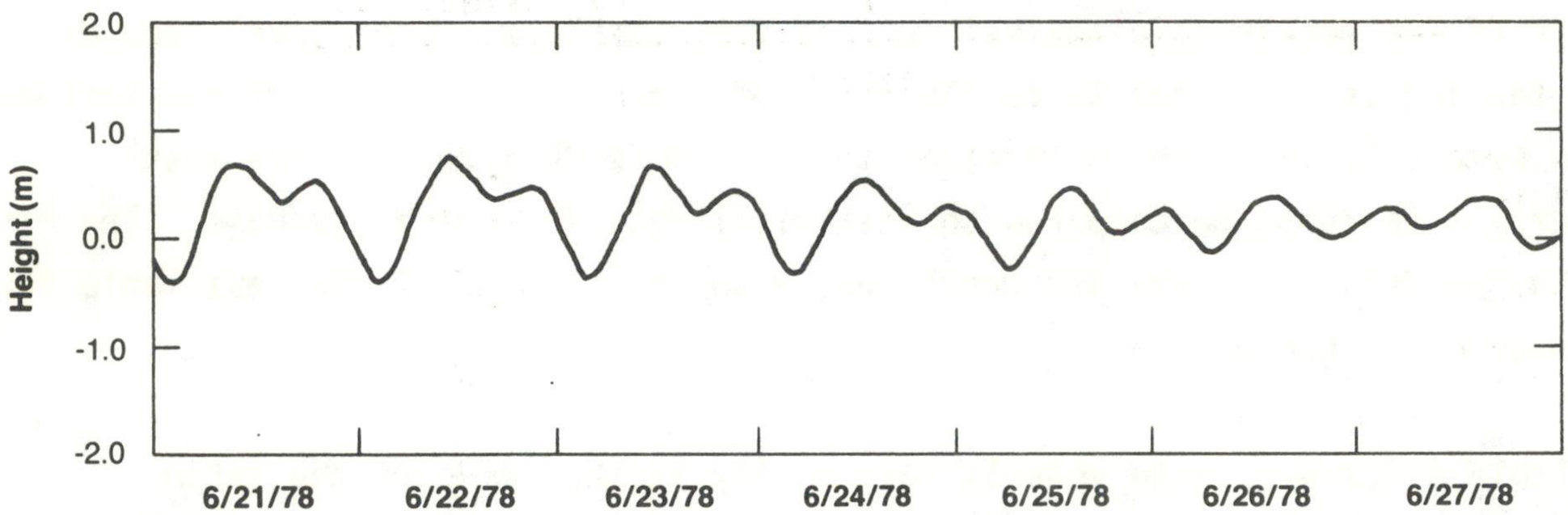

Figure 8-2. Time series plots of West Hackberry water level fluctuations.

Table 8-1. Monthly means of water levels and ranges for West Hackberry

	June	July	November	December	January	February
			--meters--			
MHHW	0.34	0.32	0.32	0.38	0.35	0.33
MHW	0.27	0.25	0.24	0.30	0.22	0.25
MLW	-0.23	-0.23	-0.24	-0.24	-0.31	-0.25
MLLW	-0.44	-0.45	-0.39	-0.46	-0.55	-0.43
Mn	0.50	0.48	0.48	0.54	0.53	0.50
DHQ	0.07	0.07	0.08	0.08	0.13	0.08
DLQ	0.21	0.22	0.15	0.22	0.24	0.18
Gt	0.78	0.77	0.71	0.84	0.90	0.76

Table 8-2. Six-month mean of water levels and ranges at West Hackberry and historical values for Calcasieu Pass

	West Hackberry	Calcasieu Pass
	--meters--	
MHHW	0.79	0.61
MHW	0.71	0.55
MLW	0.20	0.15
MLLW	0.00	0.00
Mn	0.51	0.40
DHQ	0.08	0.06
DLQ	0.20	0.15
Gt	0.79	0.61

Table 8-3. Results of 29-day harmonic analysis of water levels at West Hackberry

	June		July		November		December		January		February	
	Amp. (H)	Epoch (k)	Amp. (H)	Epoch (k)	Amp. (H)	Epoch (k)	Amp. (H)	Epoch (k)	Amp. (H)	Epoch (k)	Amp. (H)	Epoch (k)
	m	°	m	°	m	°	m	°	m	°	m	°
M_2	0.151	70.4	0.162	67.5	0.172	81.2	0.184	79.2	0.215	70.7	0.215	66.4
S_2	0.066	53.5	0.055	51.2	0.061	61.2	0.062	49.1	0.069	62.8	0.068	53.1
N_2	0.046	25.6	0.045	22.2	0.057	55.4	0.064	24.1	0.052	62.4	0.035	64.3
K_1	0.104	303.8	0.084	292.0	0.268	276.4	0.277	280.5	0.178	247.6	0.314	290.1
M_4	0.021	161.0	0.021	179.9	0.028	328.1	0.028	303.8	0.019	143.2	0.022	175.8
O_1	0.215	301.6	0.230	297.6	0.097	265.5	0.074	304.4	0.150	302.4	0.255	283.1
M_6	0.024	34.8	0.023	68.8	0.025	148.3	0.024	102.7	0.023	201.6	0.022	248.7
S_4	0.004	304.2	0.005	4.5	0.004	31.2	0.002	28.6	0.006	64.8	0.003	84.0
Nu_2*	0.009	31.6	0.009	28.2	0.011	58.8	0.012	31.5	0.010	63.5	0.007	64.6
S_6	0.004	213.1	0.001	64.0	0.002	111.4	0.004	36.8	0.004	65.5	0.001	11.3
$(2N_2)$*	0.006	340.9	0.006	336.8	0.008	29.6	0.008	329.1	0.007	54.2	0.005	62.2
$(OO)_1$*	0.009	306.1	0.010	286.4	0.004	287.3	0.003	256.5	0.006	192.8	0.011	297.2
$Lamda_2$*	0.001	62.2	0.001	59.9	0.001	71.9	0.001	65.2	0.002	67.0	0.002	60.2
M_1*	0.015	302.7	0.016	294.8	0.007	271.0	0.005	292.5	0.011	275.0	0.018	286.6
J_1*	0.017	304.9	0.018	289.2	0.008	281.9	0.006	268.5	0.012	220.2	0.020	293.6
Rho_1*	0.008	300.6	0.009	300.0	0.004	260.8	0.003	314.8	0.006	326.0	0.010	280.0
Q_1*	0.042	300.4	0.044	300.4	0.019	260.1	0.014	316.4	0.029	329.9	0.050	279.5
T_2*	0.004	53.5	0.003	51.2	0.004	61.2	0.004	49.1	0.004	62.8	0.004	53.1
R_2*	0.001	53.5	0.000	51.2	0.001	61.2	0.001	49.1	0.001	62.8	0.001	53.1
$(2Q)_1$*	0.006	299.3	0.006	303.2	0.002	254.6	0.002	328.4	0.004	357.3	0.007	276.0
P_1*	0.034	303.8	0.028	292.0	0.089	276.4	0.092	280.5	0.058	247.6	0.104	290.1
L_2*	0.004	115.2	0.004	112.8	0.005	107.0	0.005	134.2	0.006	78.9	0.006	68.5
K_2*	0.018	53.5	0.015	51.2	0.016	61.2	0.017	49.1	0.019	62.8	0.018	53.1
M_8	0.019	282.9	0.021	333.3	0.022	313.8	0.023	262.6	0.022	267.3	0.022	327.9
$F = \frac{K_1 + O_1}{M_2 + S_2}$	1.47		1.45		1.57		1.43		1.15		2.01	

* These values are inferred.

The phase relationship of the semidiurnal constituent M_2 to the diurnal constituents K_1 and O_1 can be used to determine if the diurnal inequality is in the high or low waters or both (Marmer, 1954). If the value of $M°_2 - (K°_1 + O°_1)$ is equal to zero, where ° denotes the phase in degrees of the constituent, the inequality is wholly in the high waters; if the difference is 90°, the inequality is exhibited in equal degrees in both high and low waters; if the difference is 180°, the inequality is wholly in the low waters. Using a mean value for the six periods the value of $M°_2 - (K°_1 + O°_1)$ is calculated to be 219°. This result confirms our earlier observation that the diurnal inequality was primarily in the low waters.

Figure 8-2 also shows the influence of the declination of the moon on diurnal inequalities. When the moon is at its farthest declination, north or south of the equator, the diurnal inequalities are the largest. The moon at maximum southern declination June 20 produced the observed large DLQ. When the moon is over the equator, the diurnal inequalities are at a minimum, as can be seen for June 26 and 27.

The means of the principal harmonic constituents M_2, S_2, N_2, K_1, O_1, and P_1 are presented in table 8-4 along with the values obtained from an NOS least squares analysis of 365 days of observations at Calcasieu Pass for 1933-34. The amplitudes and phases of the two sets are consistent; the largest amplitude difference is 6.3 cm in K_1 and the largest phase difference is 11.9° in S_2. It must be pointed out, however, that our data sample for West Hackberry is biased by a larger quantity of data for winter than for summer.

In table 8-3 we see apparent seasonal variations in the amplitudes of M_2, K_2, and O_1. The amplitude of M_2 is larger during the winter months than the summer months, while there is no significant variation in the phase of M_2 from winter to summer.

The dominant diurnal constituent during June and July is O_1 with an amplitude of approximately twice that of K_1. During the winter months, however, K_1 becomes the dominant diurnal constituent. The phases of K_1 and O_1 remain constant through both sampling periods.

Additional products of the harmonic analysis are the Greenwich intervals. The Greenwich intervals for each period analyzed are presented in table 8-5. In table 8-6, the mean values of the data from table 8-5 are compared with those for Calcasieu Pass and Galveston, the NOS control station for the region. Our results for the intervals at West Hackberry are consistent with the historical data on file for Calcasieu Pass.

Harris (1904) developed a cotidal chart for the Gulf of Mexico (figure 8-3). The values for the cotidal lines were obtained by dividing the epoch of the M_2 constituent by its speed. From figure 8-3, we should expect to obtain a

Table 8-4. Means of principal harmonic constants at West Hackberry and accepted values for Calcasieu Pass (1933-34)

	West Hackberry		Calcasieu Pass	
	Amplitude (H)	Phase (k)	Amplitude (H)	Phase (k)
	m	°	m	°
M_2	0.183	72.6	0.159	72.2
S_2	0.064	55.2	0.055	67.1
N_2	0.050	42.3	0.033	47.8
K_1	0.204	281.2	0.141	291.7
O_1	0.170	292.4	0.127	280.9
P_1	0.068	281.7	0.042	295.5

Table 8-5. Monthly Greenwich intervals from 29-day harmonic analysis for West Hackberry

	June	July	November	December	January	February
	--hours--					
HWI	9.123	8.701	8.957	9.820	8.773	9.269
LWI	1.728	1.191	2.065	2.046	2.561	2.773
TcHHWI	23.584	22.957	22.689	23.647	22.304	23.583
TcLLWI	14.413	13.859	13.876	14.383	14.446	14.638

Table 8-6. Means of Greenwich intervals for West Hackberry and accepted values for Calcasieu and Galveston, Texas

	West Hackberry	Calcasieu Pass	Galveston
	--hours--		
HWI	9.107	8.667	10.250
LWI	2.061	2.883	4.183
TcHHWI	23.127	22.670	24.903
TcLLWI	14.269	14.787	16.187

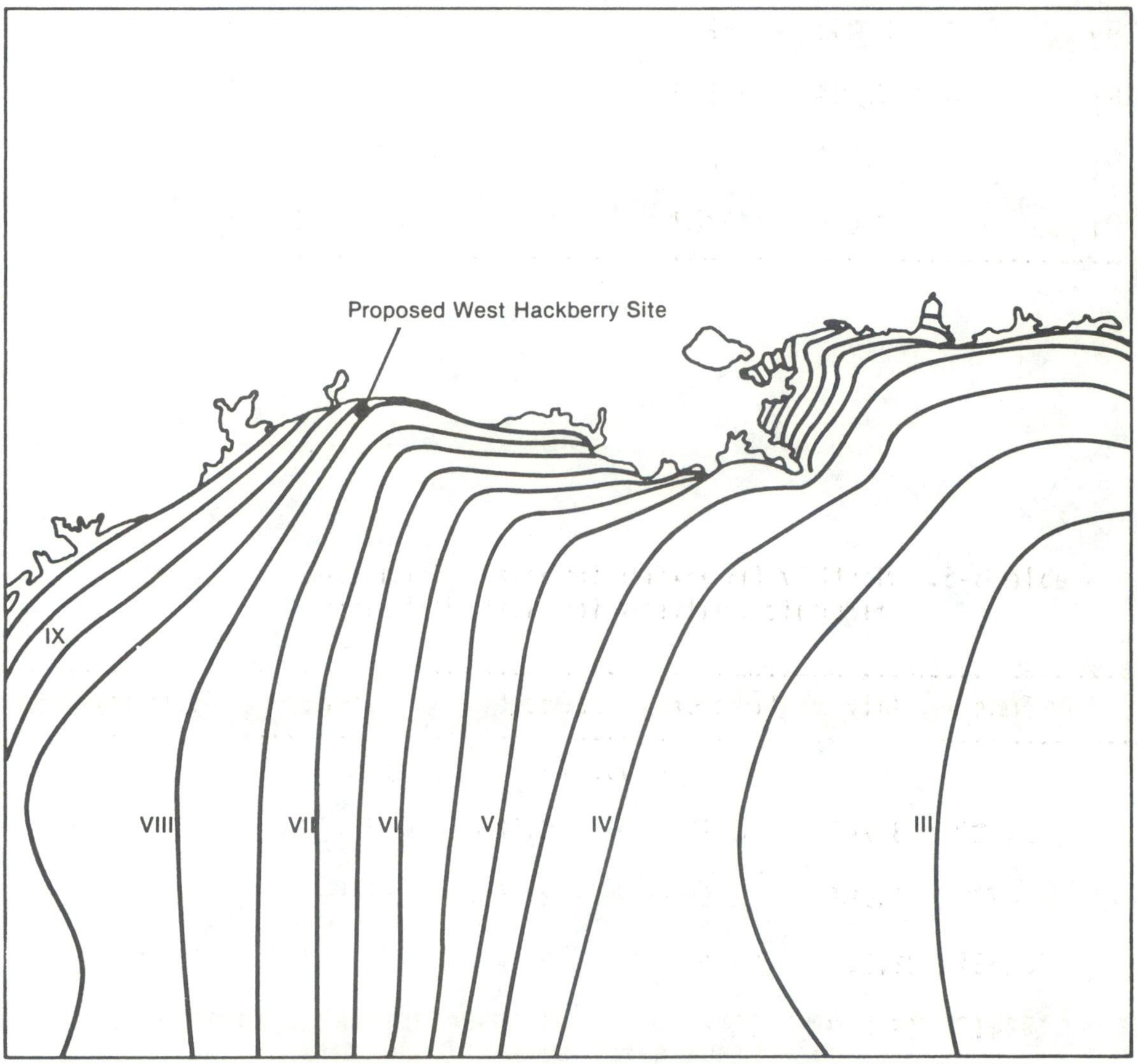

Figure 8-3. Cotidal lines for M_2 based on Harris (1904).

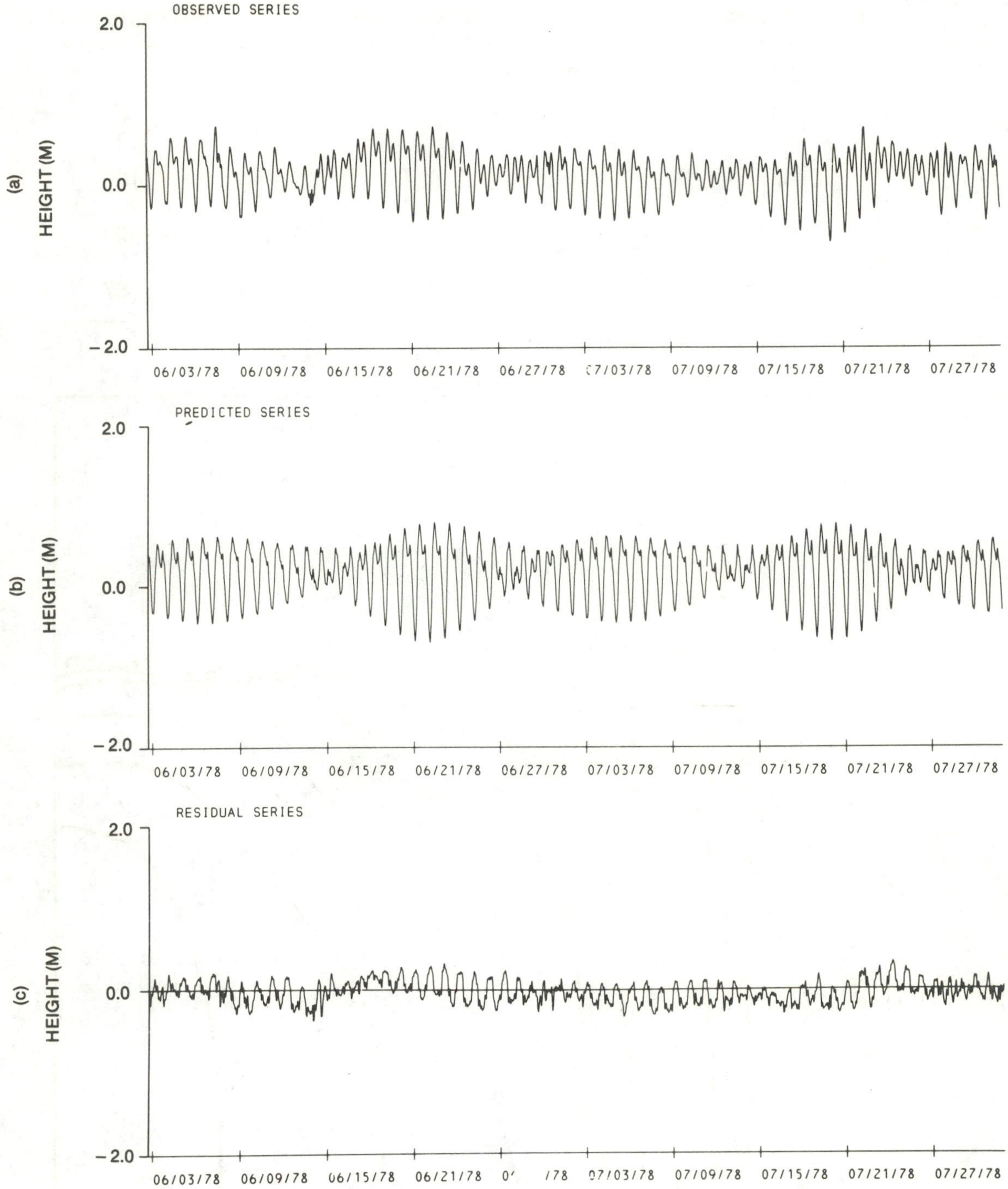

Figure 8-4. Time series plots of observations, predictions, and residuals for summer (June-July).

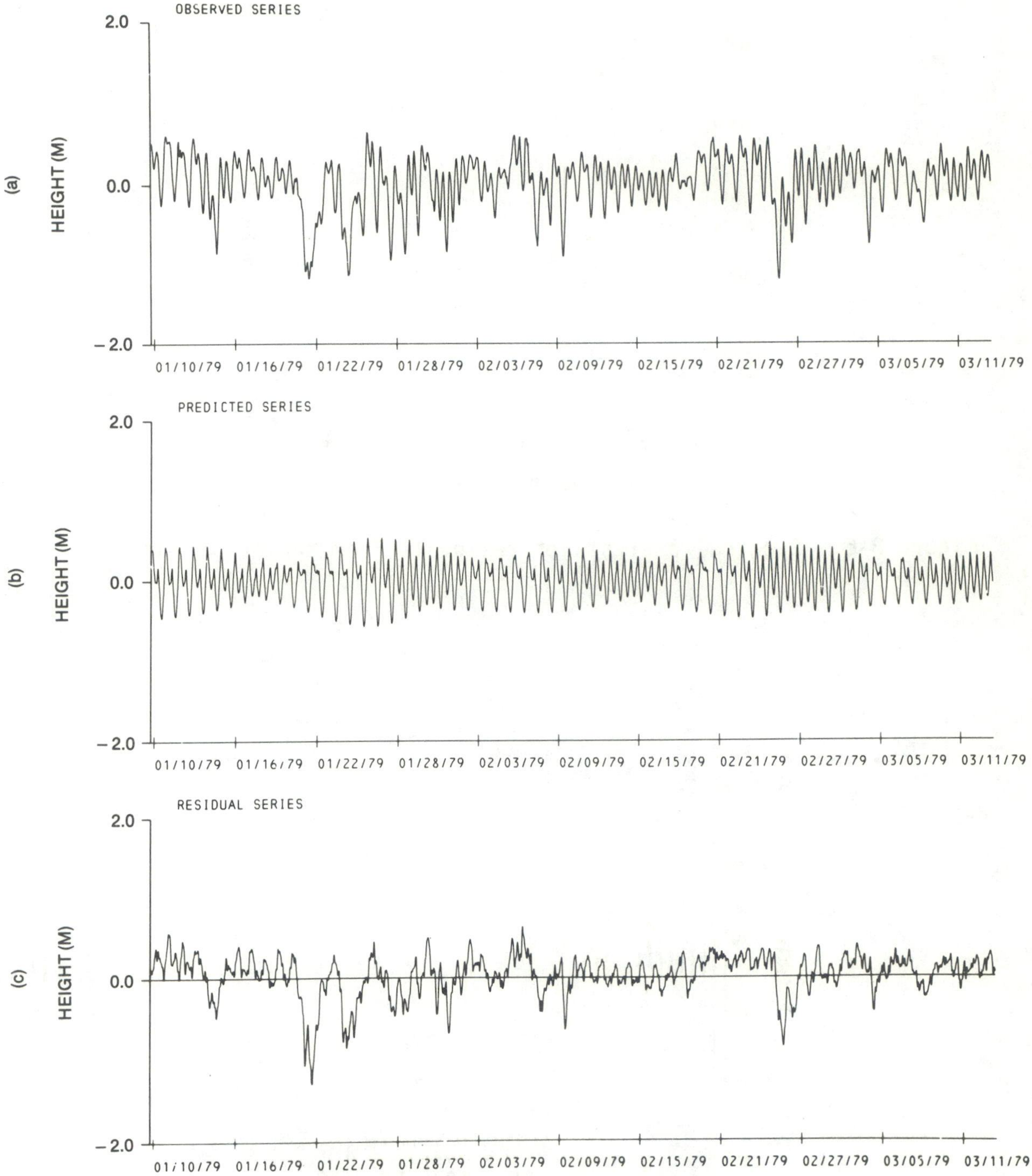

Figure 8-5. Time series plots of observations, predictions, and residuals for winter (January-March).

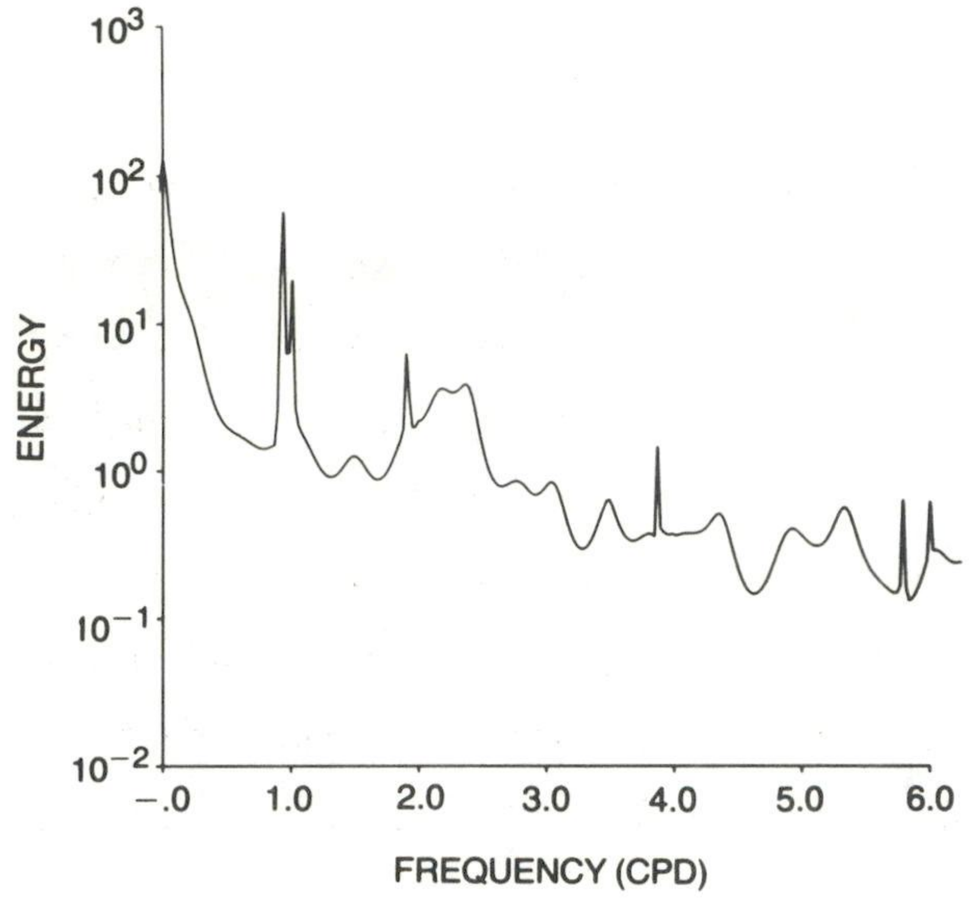

Figure 8-6. Spectral analysis of residuals from summer period.

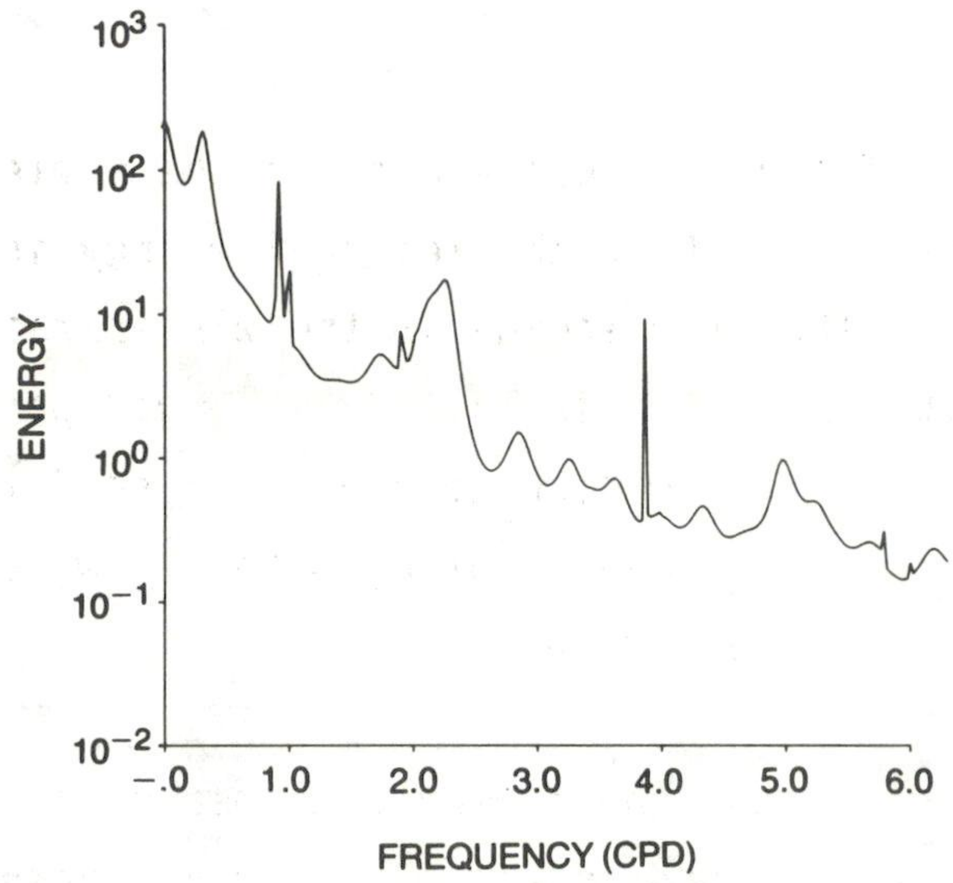

Figure 8-7. Spectral analysis of residuals from winter period.

cotidal value for M_2 between 8.0 and 9.0 at West Hackberry. Using a 6-month average of the epoch of M_2, obtained as a result of our harmonic analysis, we arrived at a value of 8.96. This value is in good agreement with the expected value, despite the age of the Harris tidal data.

The constituents developed by the harmonic analysis were used to predict a time series of water levels; the predicted series was subtracted from the observed water levels to produce a residual series. Figures 8-4 and 8-5 are time series plots of the predicted, observed, and residual water level data for two seasonally representative periods. Figure 8-4 is a summer series from June 2 to August 3, 1978. Figure 8-5 is a winter series from January 9 to March 13, 1979. These two periods were chosen to illustrate the extremes in meteorological conditions that are present. The residuals from each representative period were analyzed using the Burg spectral analytic technique and the harmonic analysis discussed in section 3.

By inspecting the plots of the observations (figures 8-4a and 8-5a) and the residuals (figure 8-4c and 8-5c), it is evident that stronger meteorological activities occur during the winter months. This observation is verified by the results of the spectral analysis of the residuals (figures 8-6 and 8-7). It is also seen in the frequency distribution plots of the residuals (figures 8-8 and 8-9).

Figure 8-6 is a plot of the residual energy in the summer series. When this plot is compared with the plot of the residual energy in the winter series (figure 8-7), it is obvious that the energy in the winter residuals is concentrated at less than 0.5 CPD. This is caused by longer periods of strong meteorological activity during the winter season. Figure 8-10 illustrates the effect of a winter storm on water levels, along with the water level fluctuations observed by the NOS tide gage at Galveston.

Figures 8-6 and 8-7 also show the presence of peaks in the residual energy at the diurnal (1 CPD) and the semidiurnal (2 CPD) frequencies. There are also smaller energy peaks at the higher frequencies, i.e., 4 and 6 CPD; however these occurrences are the result of hourly averaging of the observed data before the predictions were subtracted.

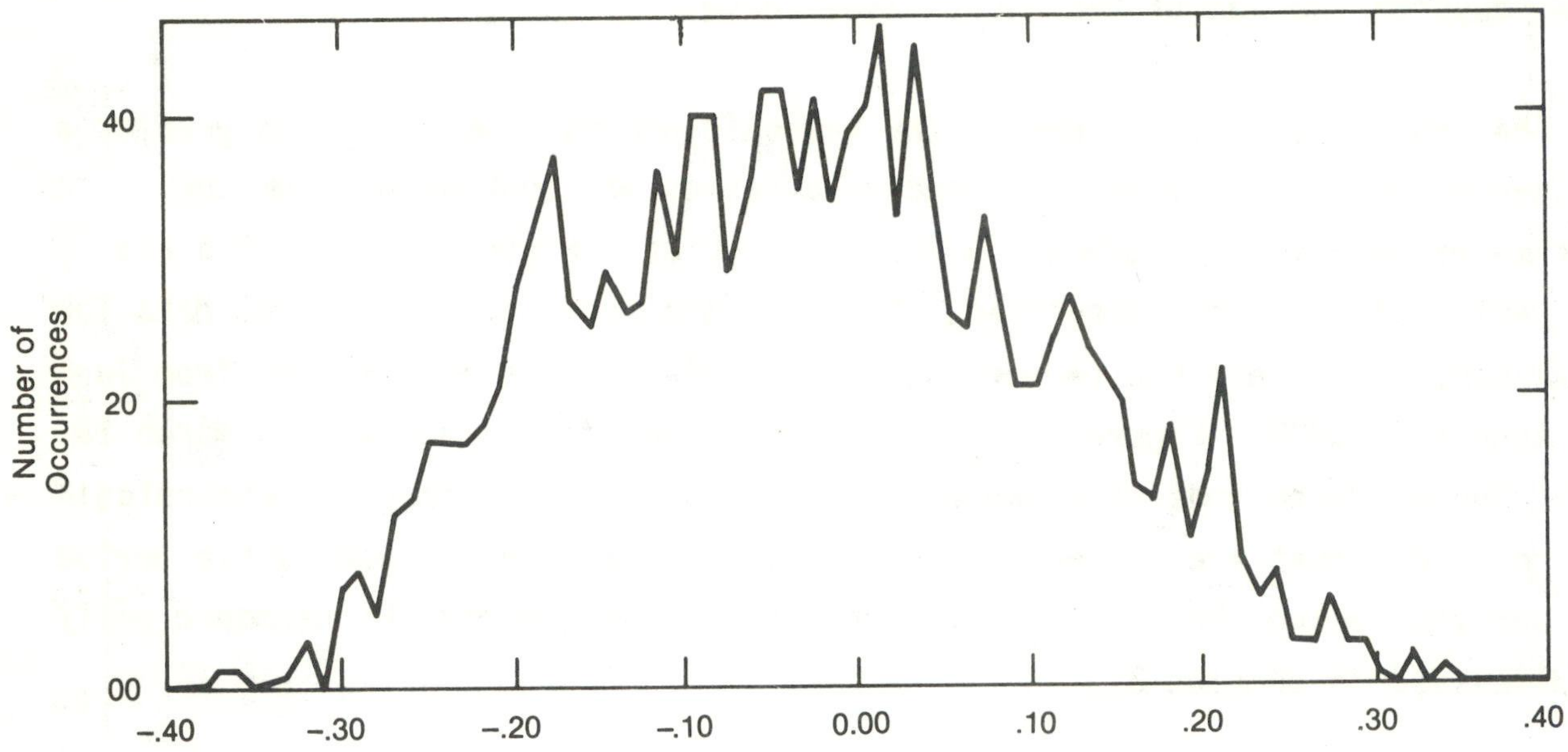

Figure 8-8. Frequency distribution of residuals during summer (June-July).

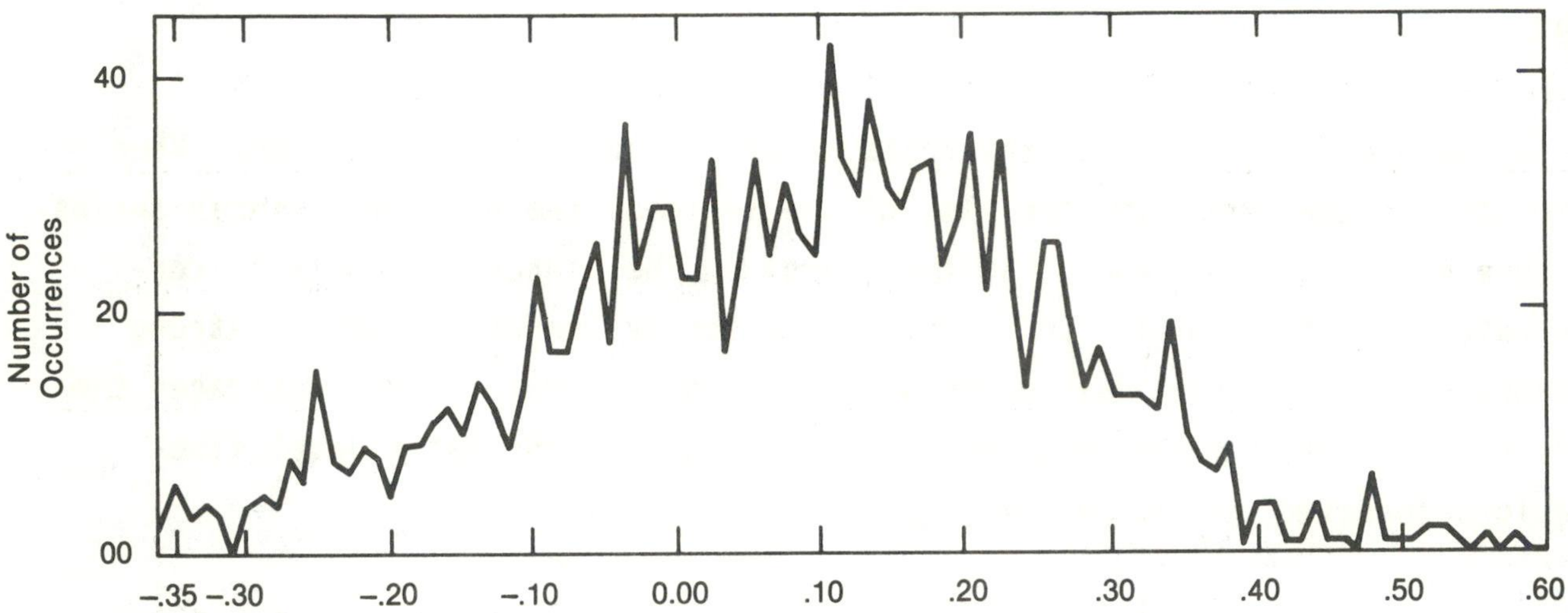

Figure 8-9. Frequency distribution of residuals during winter (January-February).

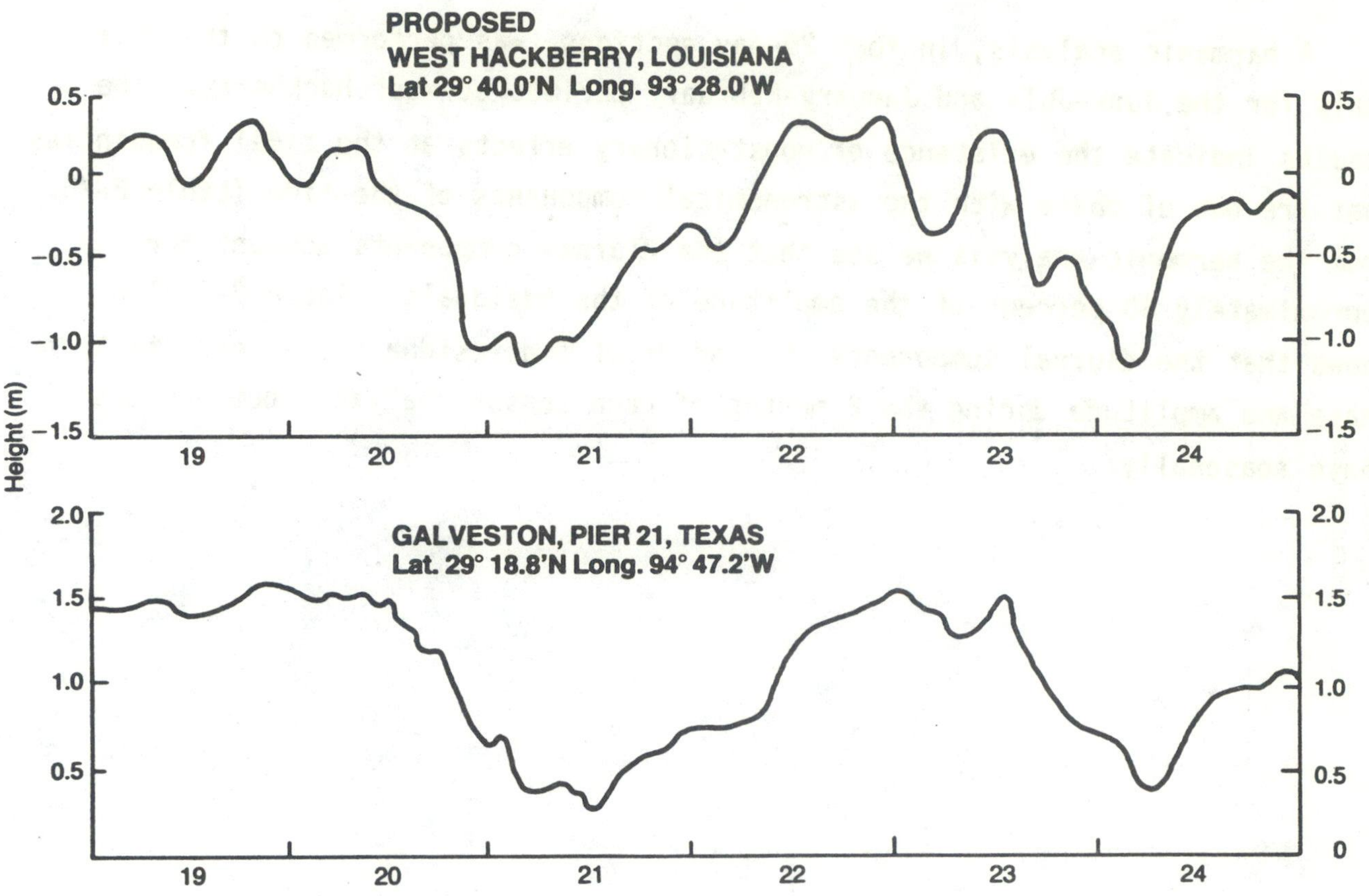

Figure 8-10. An example of a winter storm's effect on water level, January 1979.

Table 8-7. Results of 29-day harmonic analysis of West Hackberry residuals

	June		July		January		February	
	Amp. (H)	Phase (k)	Amp. (H)	Phase (k)	Amp. (H)	Phase (k)	Amp. (H)	Phase (k)
	m	°	m	°	m	°	m	°
M_2	0.027	188.9	0.019	168.6	0.028	255.1	0.035	292.4
S_2	0.001	288.3	0.016	246.4	0.005	230.3	0.012	329.6
N_2	0.011	243.6	0.015	258.1	0.010	295.4	0.010	295.2
K_1	0.098	138.4	0.098	138.3	0.107	004.2	0.109	352.2
O_1	0.085	050.4	0.087	050.8	0.073	225.0	0.082	216.8

A harmonic analysis, in four 29-day sections, was performed on the residuals for the June-July and January-February periods at West Hackberry. The results indicate the existence of nonstationary effects at the tidal frequencies that are out of phase with the astronomical components of the tide (table 8-7). From the harmonic analysis we see that the diurnal components account for approximately 80 percent of the amplitude of the residuals. Table 8-7 also shows that the diurnal components, K_1 and O_1 of the residuals are consistent in phase and amplitude during the 2 months of each season analyzed, but are out of phase seasonally.

9. CURRENTS

A major objective of the NOS SPR Support Project was to obtain long term, time series of currents at multiple stations and depths for analysis of the circulation at the West Hackberry site. During the 12-month survey, 47 meter-months of current meter data were recorded at the site. A listing of the current observations at the different stations and availability of the data are presented in section 10, volume two of this report. The circulation and its variability at the proposed West Hackberry site are described in this section through a discussion of temporal, spatial, and spectral characteristics of the currents.

9.1. Temporal Characteristics

Appendix D shows time series plots of current speed and direction for all observations obtained 3 m above the bottom at station 11. These plots illustrate the time variability of currents at the center of the West Hackberry site during the survey period. It is apparent that the current system fluctuates on a variety of time scales, from periods of several hours to several months. Variability of the currents is attributed to direct meteorological forcing, density gradients caused both by river discharge and the thermohaline properties of the shelf water, and astronomical forcing.

9.1.1. Current Speed

Mean current speeds during deployment periods are summarized for all stations in tables 9-1 and 9-2. To represent the variability, both the scalar speed values and their standard deviations are shown; 68.3 percent of the observed speeds around each mean speed are within one standard deviation.

Table 9-1. Mean speed and standard deviation (cm/s) of currents at the West Hackberry site, 1 m above bottom.

Deployment periods	Station 11	Station 12	Station 13	Station 14	Station 15
1978					
6/2-6/27		14.9 ± 8.2	8.6 ± 4.5	10.9 ± 8.3	
6/27-7/24					9.7 ± 5.0
6/27-7/26				7.6 ± 3.6	
6/27-8/2	7.1 ± 3.5				
7/26-8/29				7.7 ± 6.0	8.1 ± 6.3
8/3-8/28	8.6 ± 5.5				
10/3-10/31	7.2 ± 3.8				
10/31-11/14	7.6 ± 4.8				7.9 ± 4.0
11/14-12/7	7.2 ± 5.8				
1979					
1/9-1/31	11.3 ± 5.9				
1/31-2/21	9.3 ± 5.3		9.8 ± 5.6	10.7 ± 7.2	
2/1-2/21					10.8 ± 5.2
2/21-3/13	8.3 ± 5.0		10.5 ± 6.5		
2/22-3/13					8.8 ± 5.9
4/4-4/20					14.9 ± 8.5
4/4-5/4	12.9 ± 8.8				
4/4-5/8			11.0 ± 6.8		
5/9-6/1	11.2 ± 6.8				

Table 9-2. Mean speed and standard deviation (cm/s) of currents at West Hackberry site, 3 m above bottom.

Date	Station 11	Station 12	Station 13	Station 14	Station 15
1978					
6/2-6/27			12.7 ± 6.7	8.5 ± 4.3	8.6 ± 4.7
6/27-7/26			9.0 ± 4.4		6.8 ± 3.2
7/26-8/14				7.5 ± 5.1	
7/26-8/15			9.9 ± 5.0		
7/26-8/17		8.9 ± 5.7			
8/3-8/29	11.7 ± 8.7				
9/5-10/3	14.2 ± 8.4				
10/3-10/31	10.8 ± 6.3				
10/31-11/14	9.9 ± 6.1		9.0 ± 4.6		9.8 ± 4.8
11/14-12/7	11.8 ± 7.0				
12/7-1/9	14.3 ± 7.6				
1979					
1/9-1/31					16.1 ± 8.1
1/31-2/21	13.6 ± 7.9		13.1 ± 7.8	15.2 ± 9.8	12.4 ± 7.3
2/21-3/13	15.5 ± 8.8		15.9 ± 8.5	18.2 ± 9.7	
2/22-3/13					15.0 ± 8.2
3/13-4/4			12.8 ± 6.9		21.0 ± 10.6
4/4-4/20					25.3 ± 13.5
4/4-5/8			18.4 ± 9.3		
4/5-4/29	17.2 ± 11.7				
5/8-6/1			16.1 ± 9.1		
5/9-6/1	17.9 ± 9.9				

Mean current speeds at the West Hackberry site were found to be higher during winter and spring than during summer and fall. The range of mean speed at 3 m above the bottom during the winter and spring deployment periods was 12.4 to 25.3 cm/s. At 1 m above the bottom, the mean speed range was 8.3 to 14.9 cm/s. Speeds tended to be slightly higher during spring than winter because of the dominant direction of the wind rather than wind speed alone. Winter and spring winds were especially energetic, with wind speeds slightly higher in the winter. (See section 6.) The winds in spring were characteristically more southerly than those of winter, which blew mostly from the northeast and southeast. Consequently, southerly spring winds were accompanied by a longer fetch for enhanced transfer of momentum into the coastal circulation system, and thus generated stronger, wind-driven currents.

During summer and fall deployment periods, the range of mean speed 3 m above the bottom was 6.8 to 14.3 cm/s, while at the 1-m level the mean speed range was 7.1 to 9.7 cm/s. Slower currents during the summer and fall are attributed to the generally lower wind speeds and the lower volume of river runoff observed during those seasons. During storms, however, extremely fast currents can occur at any time. Such was the case during Tropical Storm DEBRA on August 28 and 29. Currents during DEBRA 3 m above the bottom reached 79 cm/s. During a spring storm, currents were observed as high as 84 cm/s. Storm events are discussed in sections 18, 19, and 20 of this report.

9.1.2. Relative Volume Transport

The diagrams shown in figures E-1 through E-7 (appendix E) show the relative volume transports at the West Hackberry stations during specified deployment periods. The computation of relative volume transports is described in section 3. Figures 9-1 and 9-2 summarize the relative transports in the alongshore and transhore quadrants.

Summer 1978

From June 2 to 27, the transport distribution at the West Hackberry current meter stations showed a diverse current system. The current patterns varied

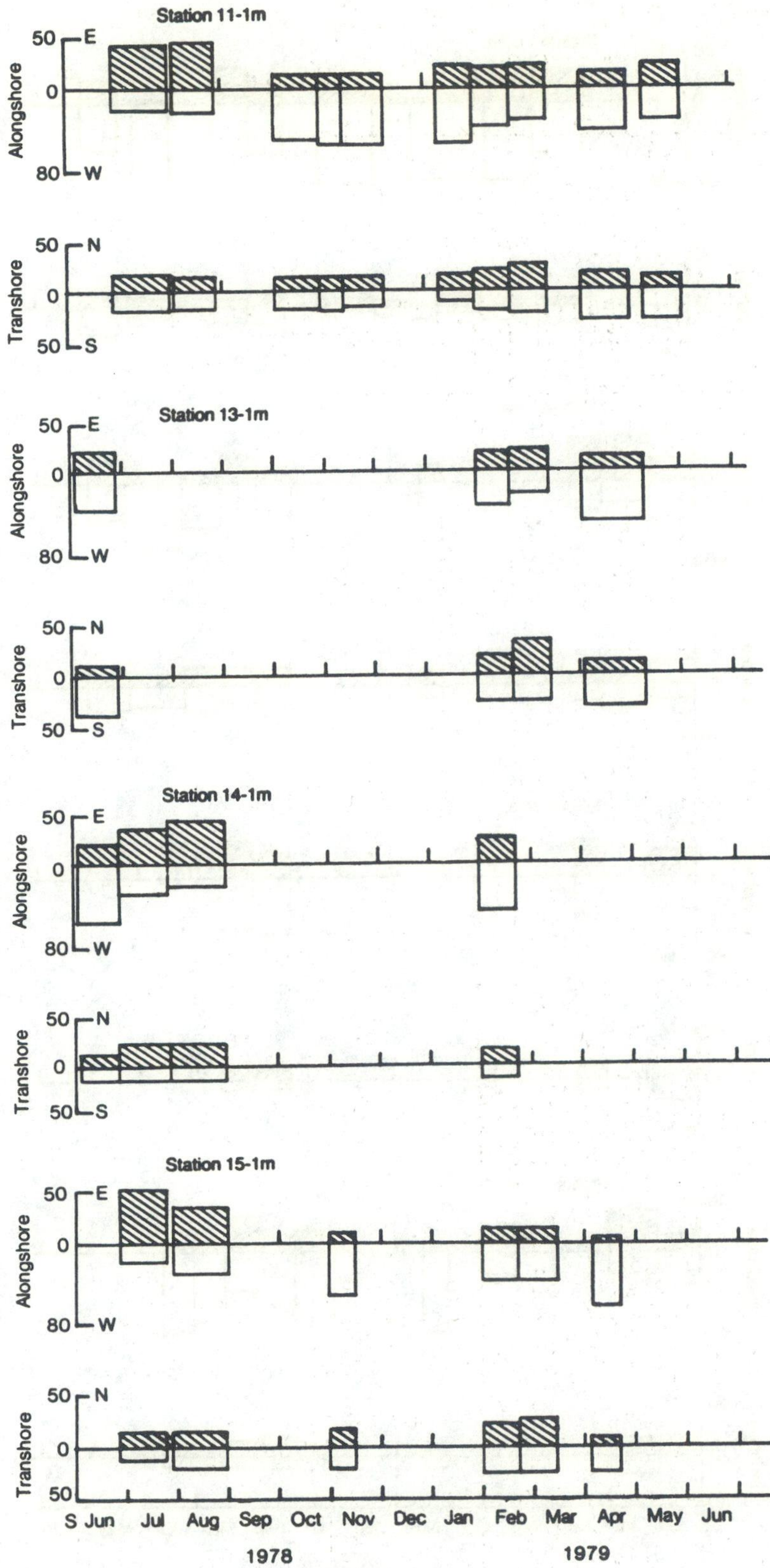

Figure 9-1. Summary of relative volume transport in the alongshore and transhore quadrants at stations 11 and 13 through 15 at 1 m above the bottom.

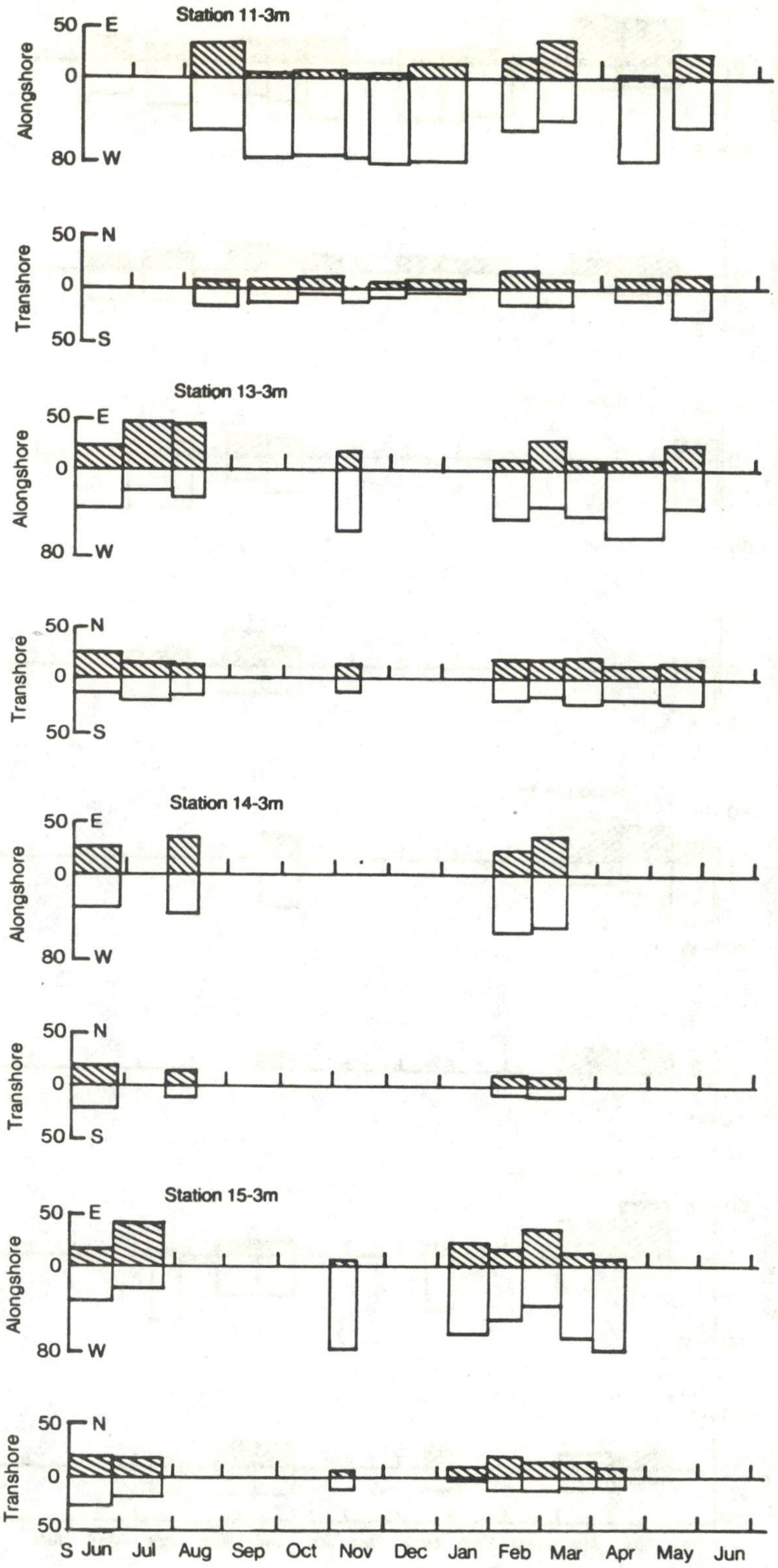

Figure 9-2. Summary of relative volume transport in the alongshore and transhore quadrants at stations 11 and 13 through 15 at 3 m above the bottom.

from the nearly uniform directional distribution of near-bottom transport at station 13 to an alongshore-dominated transport at the nearshore station 12. From June 27 to August 28, alongshore transport dominated in the eastern quadrant at all stations. The observed summer transport is thus characterized as principally alongshore in the eastern quadrant.

Fall 1978

Transport was predominantly alongshore in the western quadrant from September 5 to October 3. This persisted through the fall and was at a maximum during mid-November to early December, when 83 percent of the total transport at 3 m above the bottom was in the western quadrant.

Winter 1979

Transport patterns at the beginning of winter, which were mainly in the western quadrant, remained similar to those observed during fall. The transport distribution from January 9 to 31, however, was marked by a change. The percentage of alongshore transport in the eastern quadrant increased, but the onshore and offshore quadrant transports were still relatively low. From January 31 to February 21, mid-winter bottom transport tended to be more evenly distributed, although transport in the western quadrant continued to be high. From February 21 to March 13, the bottom layer showed a significant percentage of the total transport flowing diagonally to the 10-m contour. The 10-m contour at the West Hackberry site is approximately parallel to the shoreline at 86-266 degrees. The axis of this late winter flow was in the northeast-southwest sectors. This distribution resulted in a higher percentage of transport flowing in the onshore and offshore quadrants. The alongshore western quadrant had its lowest percentage of transport since August. At the 3-m level, the transport had a strong bimodal distribution alongshore.

Spring 1979

By spring (March 13 to April 4), transports displayed a distribution similar to those of fall and early winter, with a strong westward component. From

April 4 to May 8, the bottom transport was divided principally between the western and offshore quadrants.

From May 9 to June 1, the bottom transport distribution at station 13 returned very nearly to that observed in late spring 1978. From June 2 to 27, transport was almost evenly distributed. Station 11 showed that transport distribution dominated in the western and southern quadrants.

9.1.3. Tidal Currents

Tidal currents result from astronomical forces, and they may respond to these forces in either a barotropic or baroclinic mode. Barotropic tidal currents fluctuate in a consistent phase difference with tidal sea surface fluctuations. Baroclinic tidal currents are the internal motions along pycnoclines and generally vary in their phase relationship with the tidal sea surface fluctuations.

The amplitudes and phases of the tidal constituents are determined from harmonic analysis (section 3), and the harmonic constituents are combined into a composite tidal current. Plots of tidal currents 1 m above bottom at station 11 during four different periods within the 12-month study are shown in figures 9-3 and 9-4. These currents are separated into alongshore and transhore components. Tidal currents at the West Hackberry site are of the mixed type, generally semidiurnal-dominant in fall and winter and diurnal-dominant in spring and summer. Speeds of tidal currents were found to average only about 2 cm/s, with the tidal current peaking normally between 3 to 4 cm/s, although tidal current calculations were as high as 10 cm/s on occasion. The TMU for a current speed of 5 cm/s is +2.1, -3.0 cm/s when fouling was not significant, and +2.0, -3.3 cm/s when it was significant.

Tidal current ellipses for the harmonic constituents determine the orientation of the major and minor axes of the constituent flow, the speed values for the major and minor axes, the phase lag, and the rotation of the progression of each constituent. Figure 9-5 shows tidal current ellipses of the semidiurnal (M_2) and diurnal (K_1) constituents for current series at 1 m and 3 m above the bottom starting June 2, 1978. Figure 9-6 shows the same information for

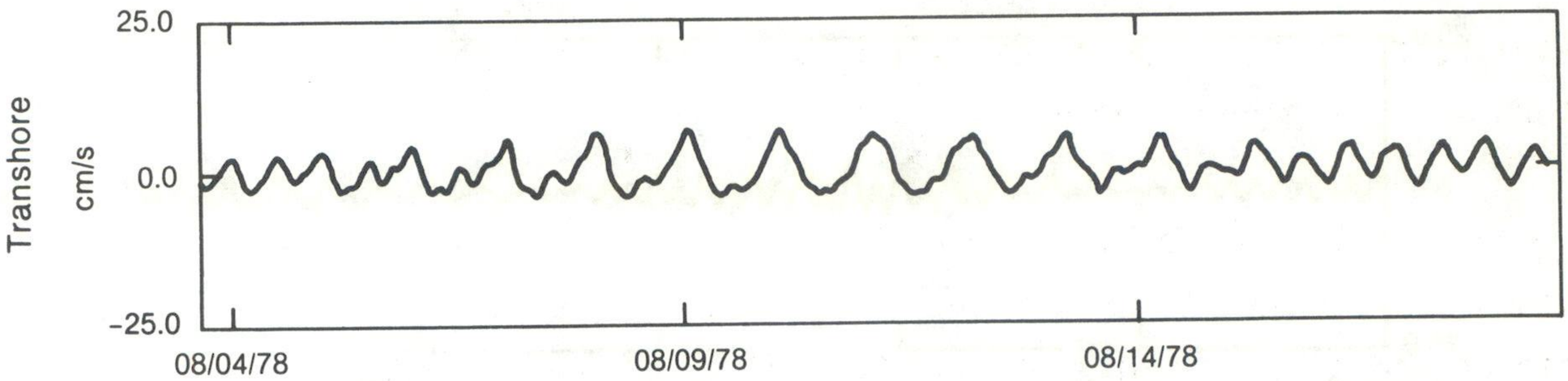

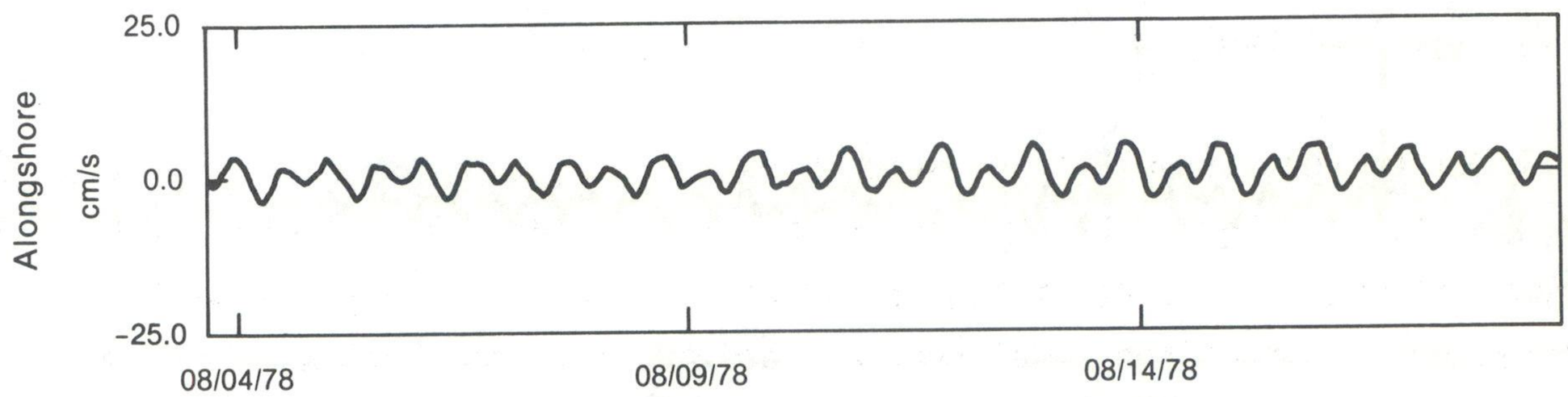

(a)

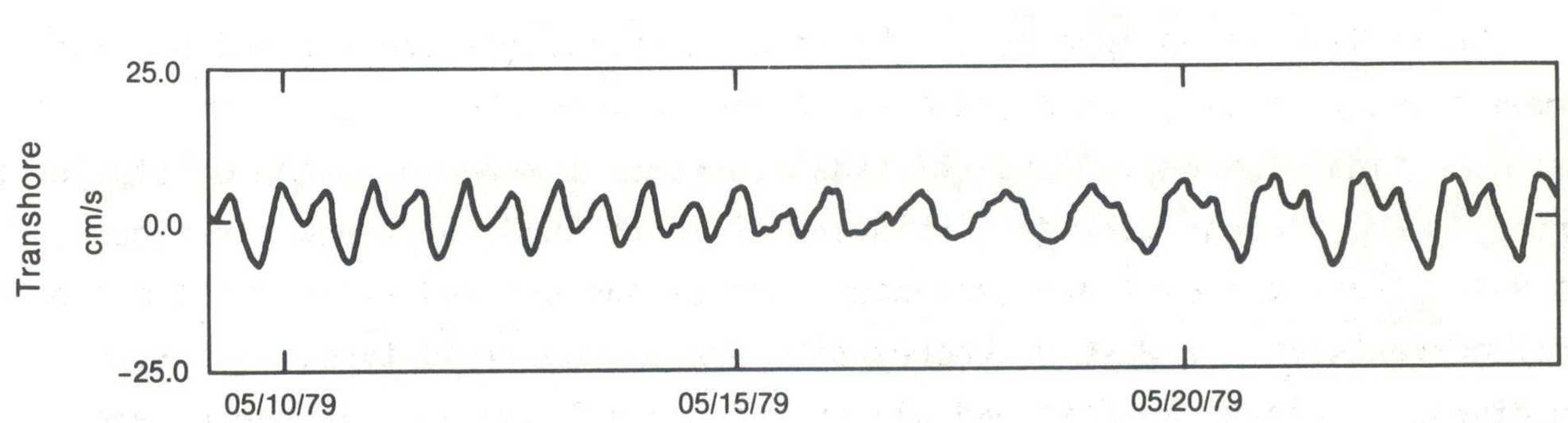

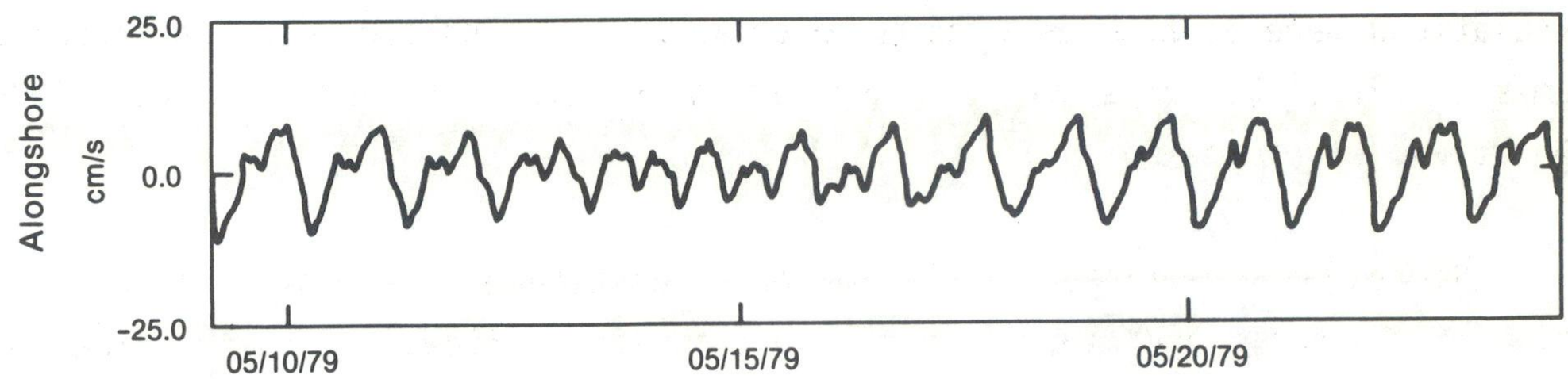

(b)

Figure 9-3. Calculated tidal currents at station 11, 1 m above bottom (a) August 3-18, 1978, and (b) May 9-24, 1979.

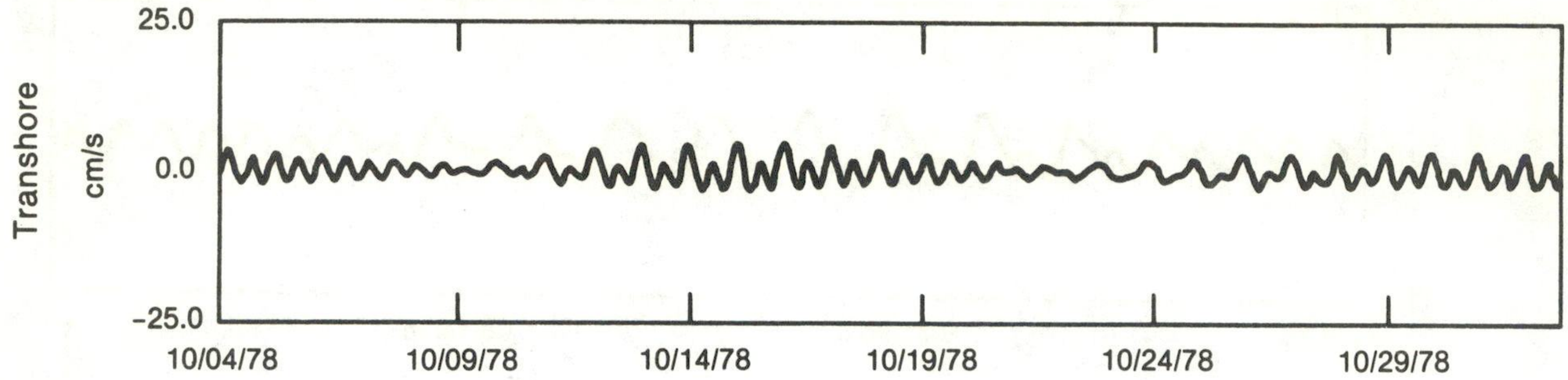

Figure 9-4. Calculated tidal currents at station 11, 1 m above bottom (a) October 3 to November 1, 1978, and (b) February 1 to March 1, 1979.

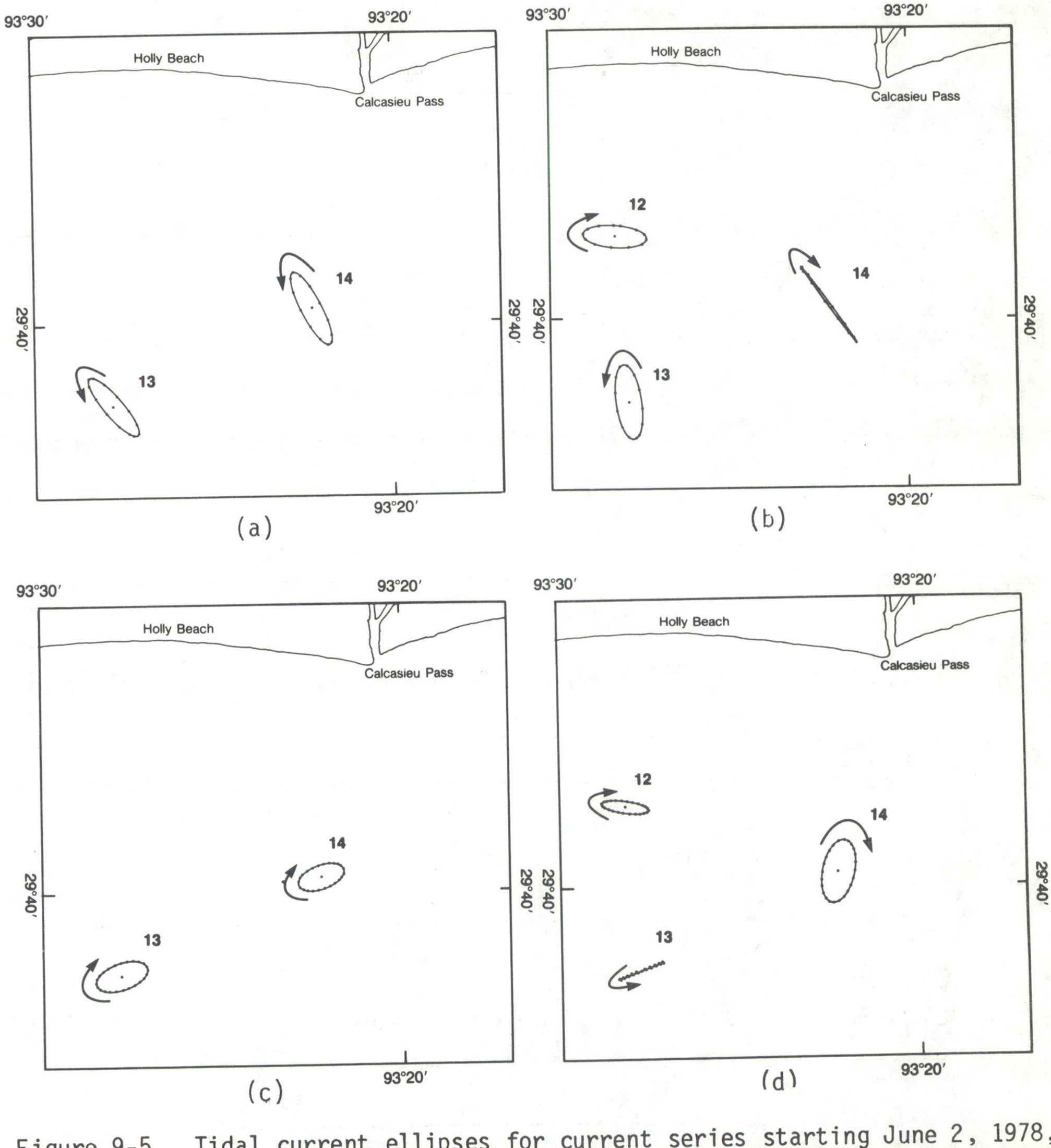

Figure 9-5. Tidal current ellipses for current series starting June 2, 1978, (a) 3 m above bottom and (b) 1 m above bottom for the M_2 constituents; (c) 3 m above bottom and (d) 1 m above bottom for the K_1 constituents.

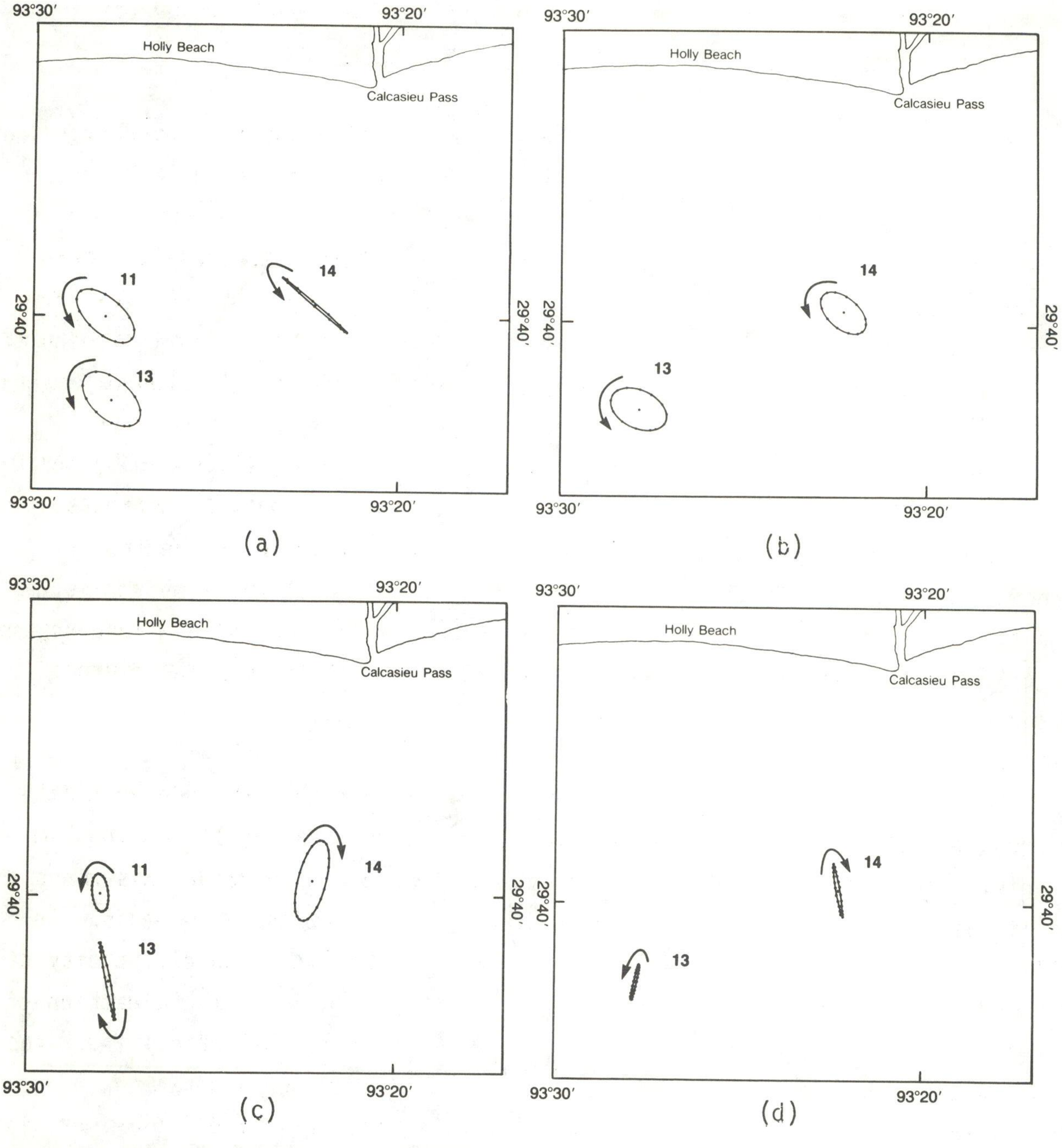

Figure 9-6. Tidal current ellipses for current series starting January 31, 1979, (a) 3 m above bottom and (b) 1 m above bottom for the M_2 constituents; (c) 3 m above bottom and (d) 1 m above bottom for the K_1 constituents.

January 31, 1979. These ellipses show how the tidal currents vary in both time and space. This variation is an accumulation of two factors:

- o The interaction of the tidal wave and bottom topography generates internal tides when the waters are stratified.

- o As the tidal wave propagates shoreward toward the coastal boundary, tidal current ellipses elongate in a direction parallel to shore.

Depending on the relative strengths of these two factors, the phase difference and amplitude ratio between barotropic and baroclinic components at tidal frequencies fluctuate at any given location (Torgrimson, 1979). This unlocking of the phase and amplitude causes incoherent variance in the tidal frequency bands.

The determination of the diurnal tidal constituents K_1 (1.0042 CPD) and O_1 (0.93023 CPD) are further complicated by the presence of inertial currents at the frequency of 0.9926 CPD for the latitude at the site and by the sea breeze/land breeze effect at 1.0 CPD. Since the length of the time series was insufficient to separate these nontidal effects, the diurnal tidal frequency may be biased during the occurrence of nontidal currents at or near the diurnal frequency.

Figures 9-7 and 9-8 show the M_2 and K_1 yearly variability for the tidal current ellipticity and major axis orientation at the station 11 1-m and 3-m levels. The ellipticity is defined as the amplitude of the major axis minus the amplitude of the minor axis, divided by the amplitude of the major axis. An ellipticity of 1.0 indicates a pure reversing current, while an ellipticity of 0.0 indicates a circular rotary current. When the flow is in the direction of the major axis orientation, the time is referenced to the GMT zone. The direction of the major axis corresponds to the first maximum epoch after the 0 hour GMT, which is the time of the maximum astronomic force over the 0 time meridian.

The ellipticity of the M_2 constituent in figures 9-7 and 9-8 for station 11 was found to have a yearly mean of 0.55. Variation from the mean value at the 1-m level was small with a variance of only 0.01. At the 3-m level, the variation from the mean value was also generally small, although significant

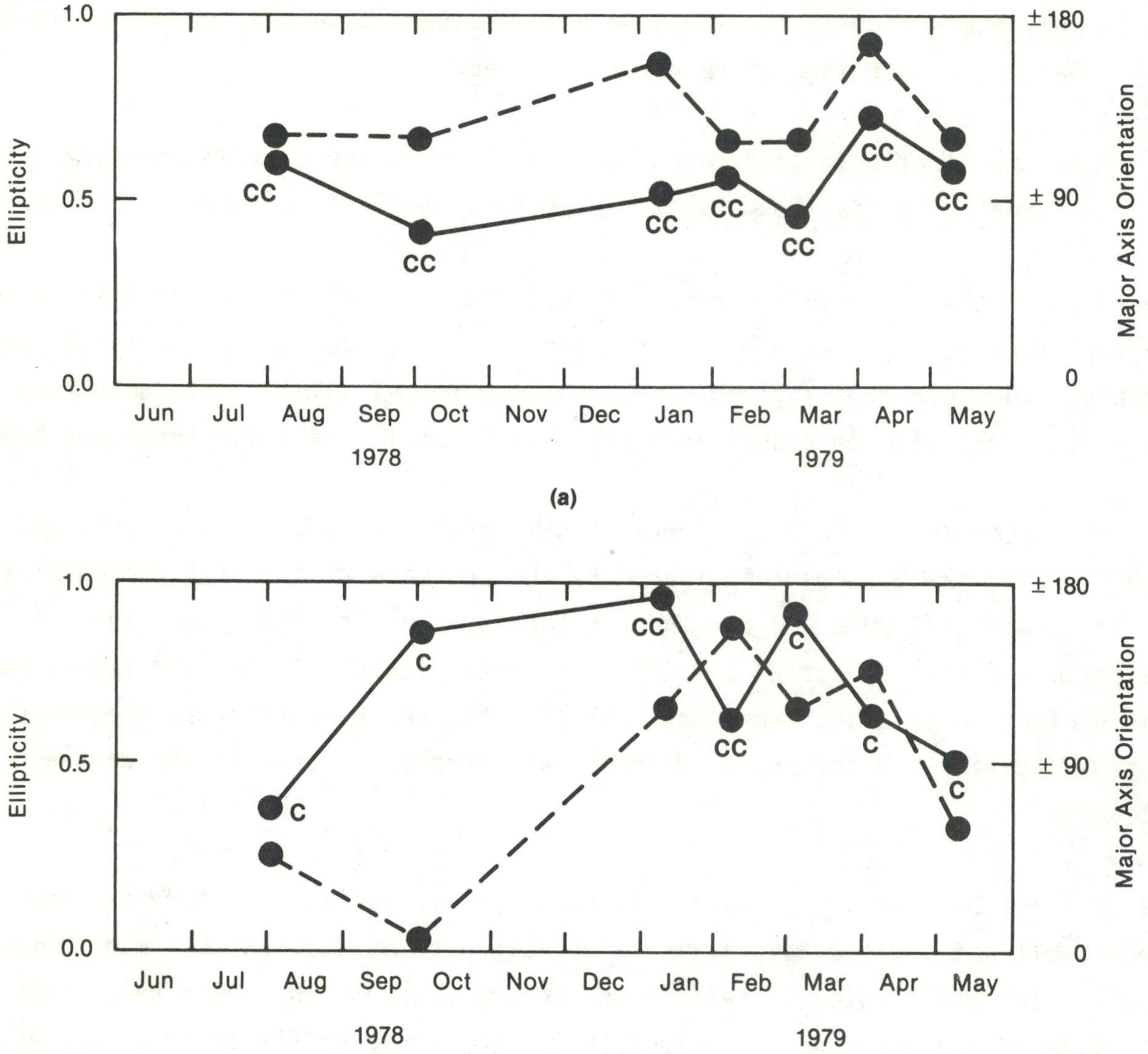

Figure 9-7. Tidal current ellipticity and major axis orientation for the (a) M_2 and (b) K_1 constituents at the station 11 1-m level.

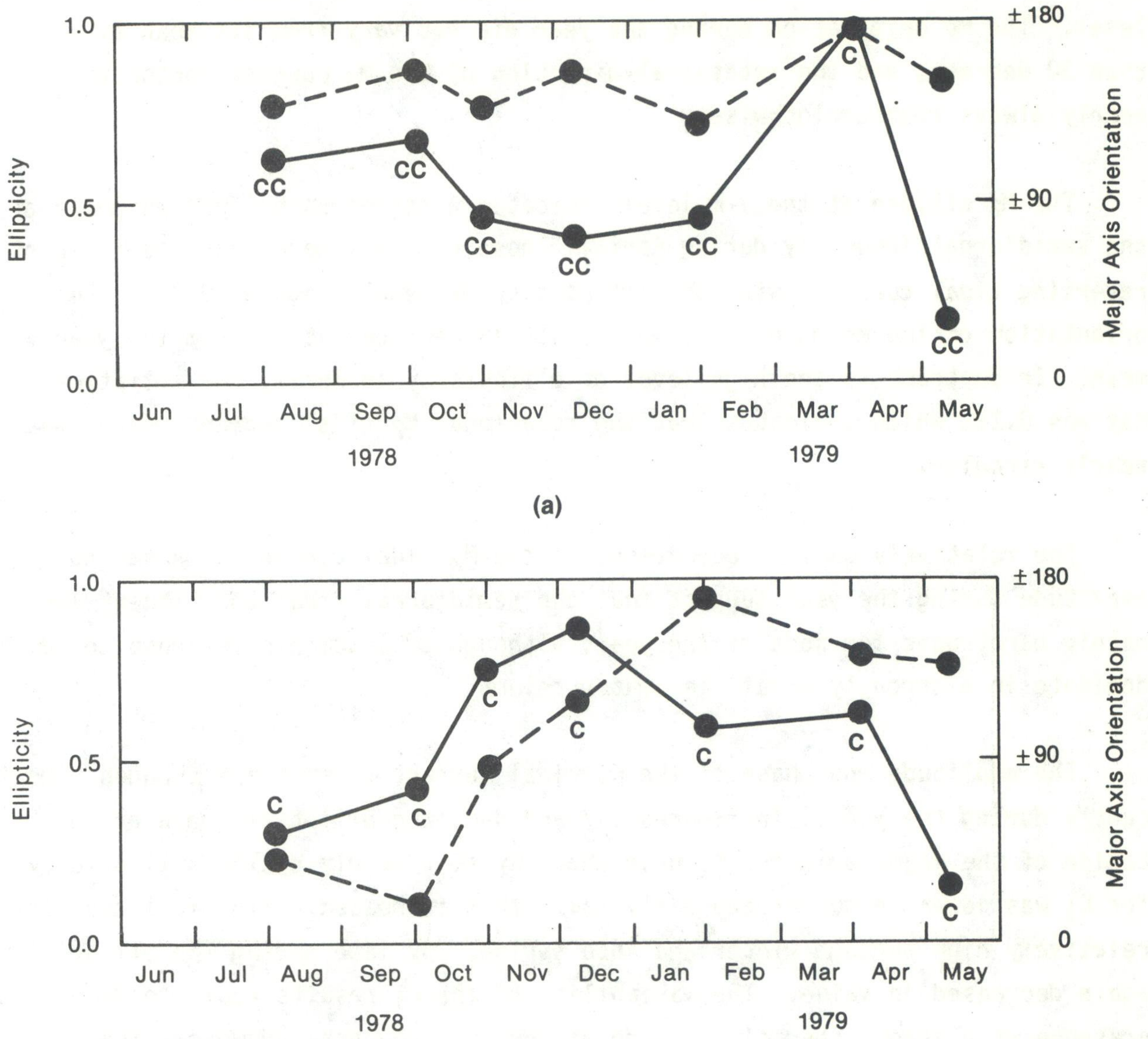

Figure 9-8. Tidal current ellipticity and major axis orientation for the (a) M_2 and (b) K_1 constituents at the station 11 3-m level.

variation occurred during April and May. The orientation of the M_2 major axis was found to average 134 degrees at the 1-m level and 148 degrees at the 3-m level. The M_2 orientation during the year did not vary from its mean by more than 30 degrees, and the rotational direction of the M_2 current vector was nearly always counterclockwise.

The M_2 ellipse at the 3-m level indicated a strong baroclinic response at the semidiurnal frequency during April. These ellipses were characteristic of a reversing tidal current, with the ellipticity extremely high at 0.99. The orientation of the M_2 major axis was at its largest deviation from the yearly mean. In contrast to the high level of ellipticity in April, the ellipticity in May was 0.18, which indicates that the rotational M_2 tidal current vector was nearly circular.

The relatively small fluctuations of the M_2 tidal current's phase and amplitude during the year suggest that the semidiurnal tidal constituent was mainly barotropic for most of the year, although a baroclinic response could dominate in a strongly stratified water column.

The amplitude and phase of the K_1 tidal current constituent changed significantly during the year. In figures 9-7 and 9-8, the ellipticity and orientation of the major axis for K_1 have what may be a yearly cycle. Ellipticity for K_1 was lower in summer and early fall, then increased during fall and stayed relatively high through winter and into spring. By late spring the ellipticity again decreased in value. The variability of the K_1 results could be due to the presence of a strong baroclinic mode at the K_1 frequency. However, the variation of phase and amplitude may also be attributed to land/sea breeze effects, which have a yearly cycle and would show maximum contribution to clockwise energy during the summer. Inertial effects may also contribute energy at the diurnal period. A possibility exists that some of the variation in K_1 is erroneous, and is due to the inability to determine P_1; half-year data is required to separate K_1 and P_1, and their combined effect has a half-yearly cycle.

9.2 Spatial Characteristics

For insights into the circulation at the West Hackberry site beyond those available from temporal and spectral considerations, a series of spatial examples that are vector-averaged over 1-hour intervals is presented. Dilution of salt brine discharge by mixing will be governed mainly by spatial gradients of the currents, both vertical and horizontal. Substances are advected away by mean currents and mixed into the surrounding waters by eddy diffusion processes that are governed by turbulence.

Figures E-8 to E-51 (appendix E) indicate the horizontal spatial variability of currents at the West Hackberry site when different forces dominate the system. Examples of the circulation show that the system was driven essentially by river runoff, wind stresses acting in different directions, and tidal influences. Examples are shown during the transition from one dominant force to another. Current vectors are plotted in the figures at 6-hour intervals; each figure shows current vectors at the same level above the bottom (1 m, 3 m, or 4 m). Current speed and direction for each vector were determined by computing 1-hour vector averages of 10-minute data samples. Vector averages were centered in time around the hours noted in the figures. Because some very low current speeds had to be plotted for the vector presentations, the tails of the vectors begin at the circumference of the circles shown at each station, not at the centers of the circles.

Vertical current profiles in the bottommost 4 m at station 11 during April 1979 (figures 9-9 to 9-14) were obtained during the GASP Experiment. Vertical profiles during a storm on April 11-12, 1979, are shown in section 20.

We referred to the time series current records in describing the current vectors. Time series plots of the currents observed at the station 11 3-m level are shown in appendix D. Time series plots for other stations and for the 1-m level at station 11 are not presented in this report because of their volume. The data are available through NODC as described in section 10, volume two of this report. The following is a discussion of field observations compiled in a log format to describe seasonal variations in circulation at the West Hackberry disposal site.

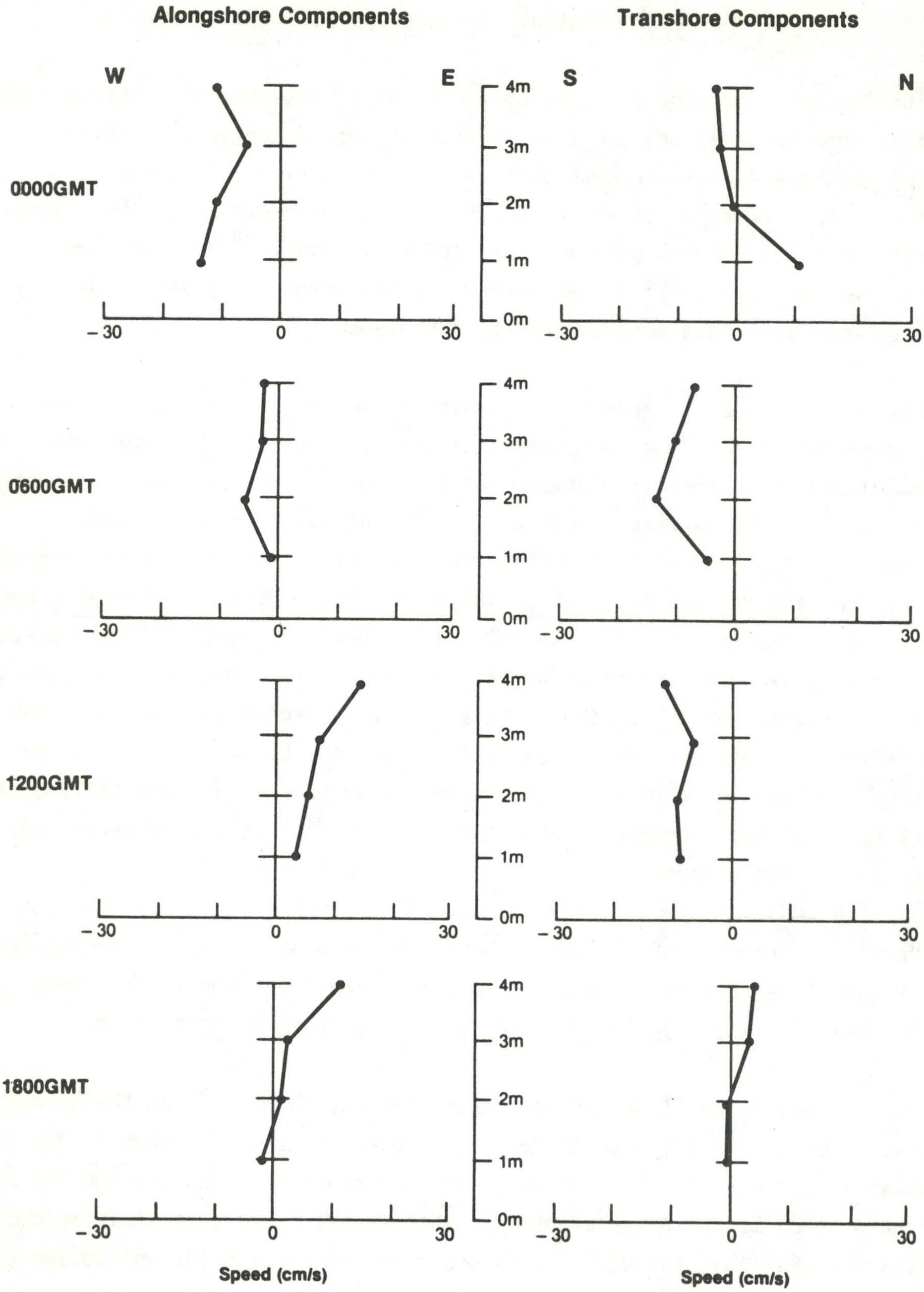

Figure 9-9. Vertical profiles of currents at West Hackberry station 11, April 6, 1979.

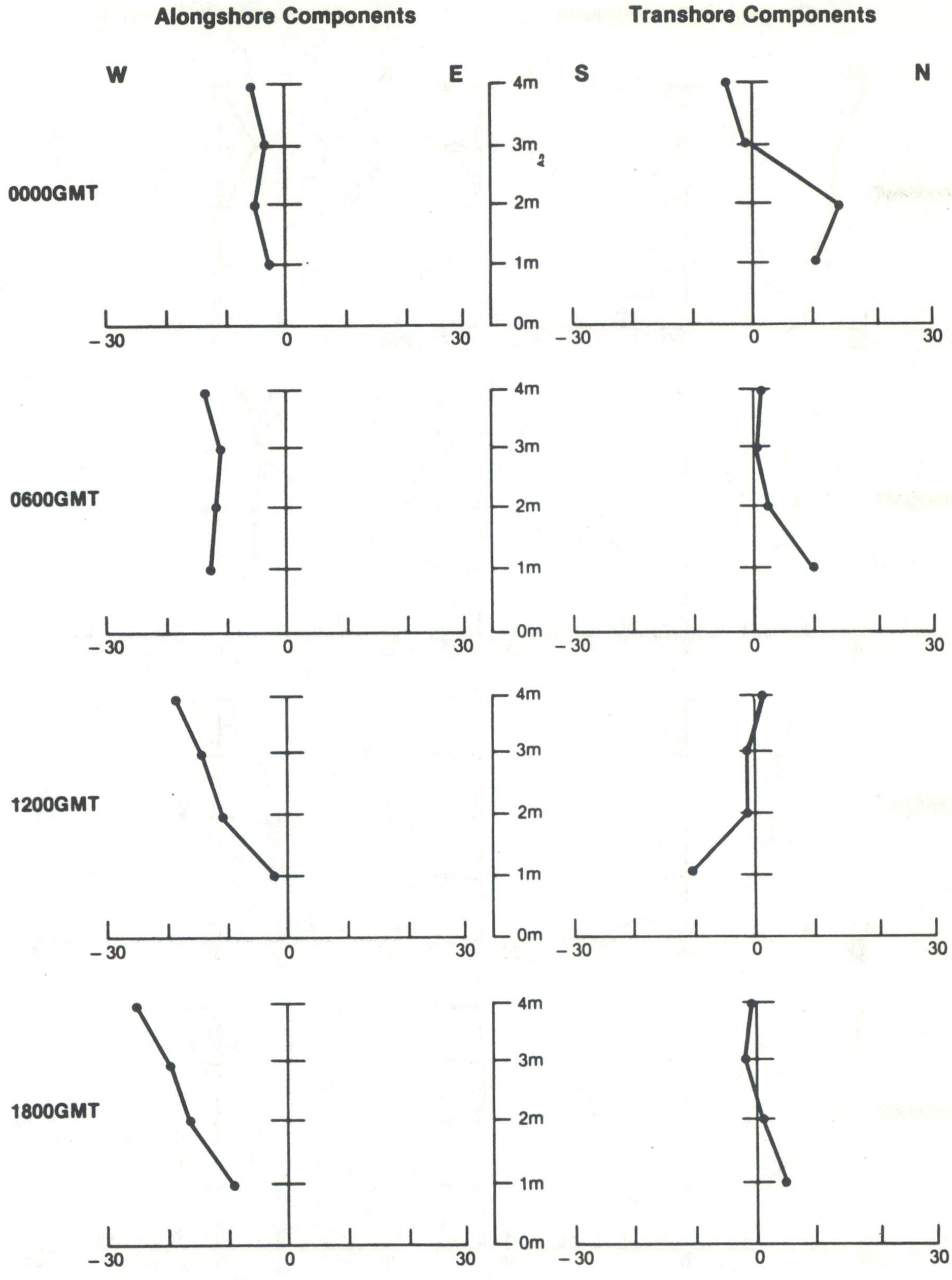

Figure 9-10. Vertical profiles of currents at West Hackberry station 11, April 7, 1979.

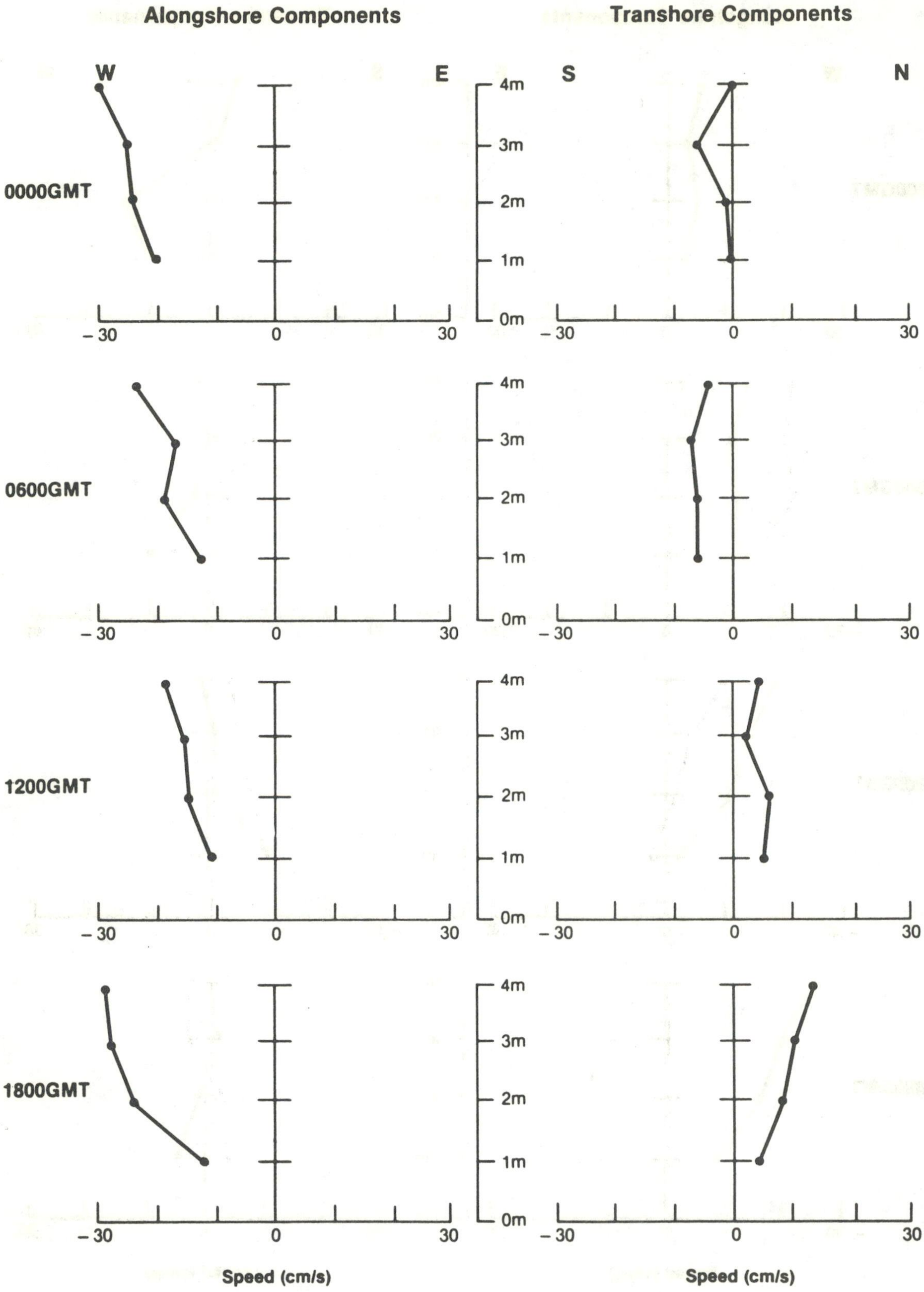

Figure 9-11. Vertical profiles of currents at West Hackberry station 11, April 8, 1979.

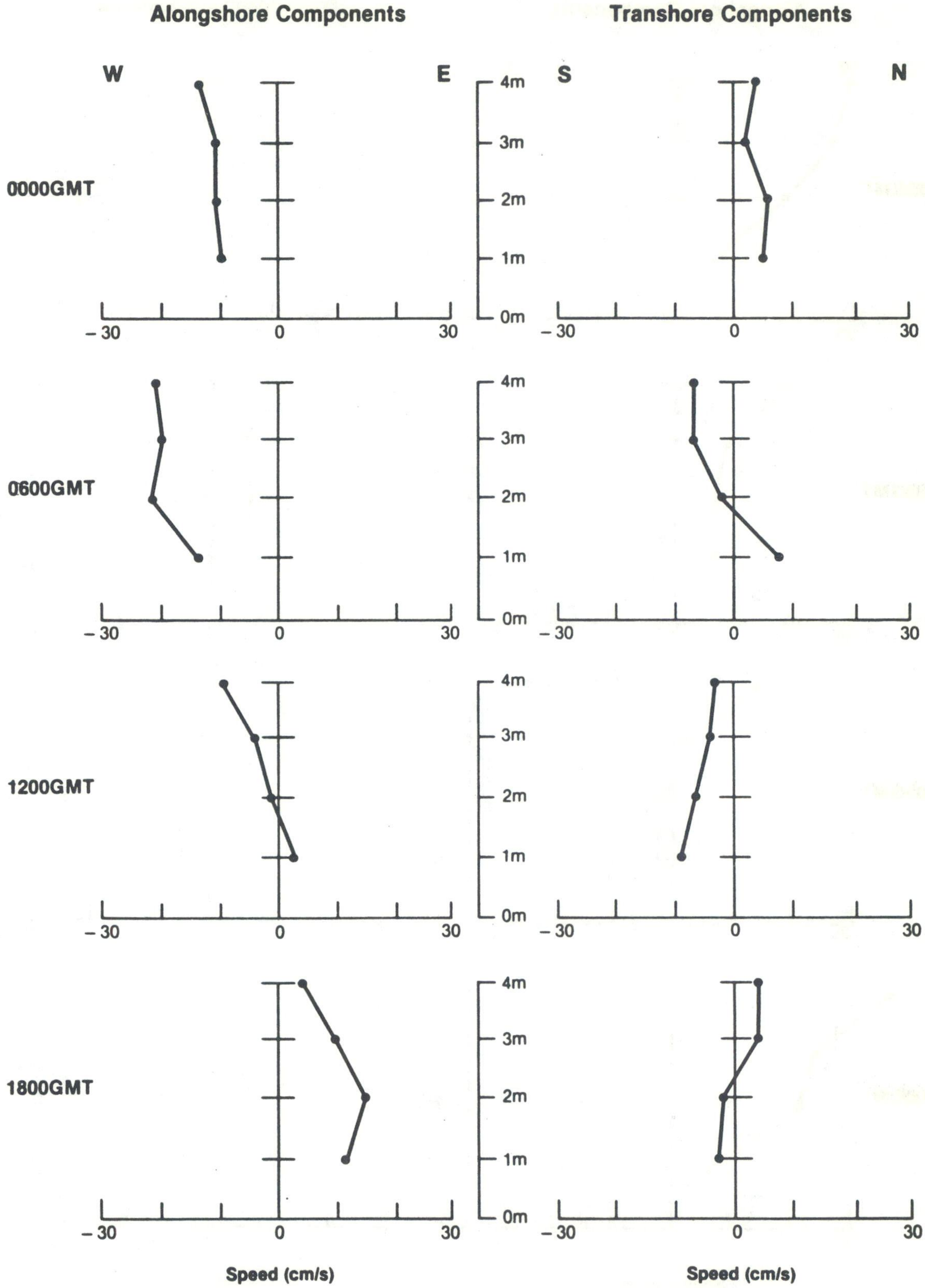

Figure 9-12. Vertical profiles of currents at West Hackberry station 11, April 9, 1979.

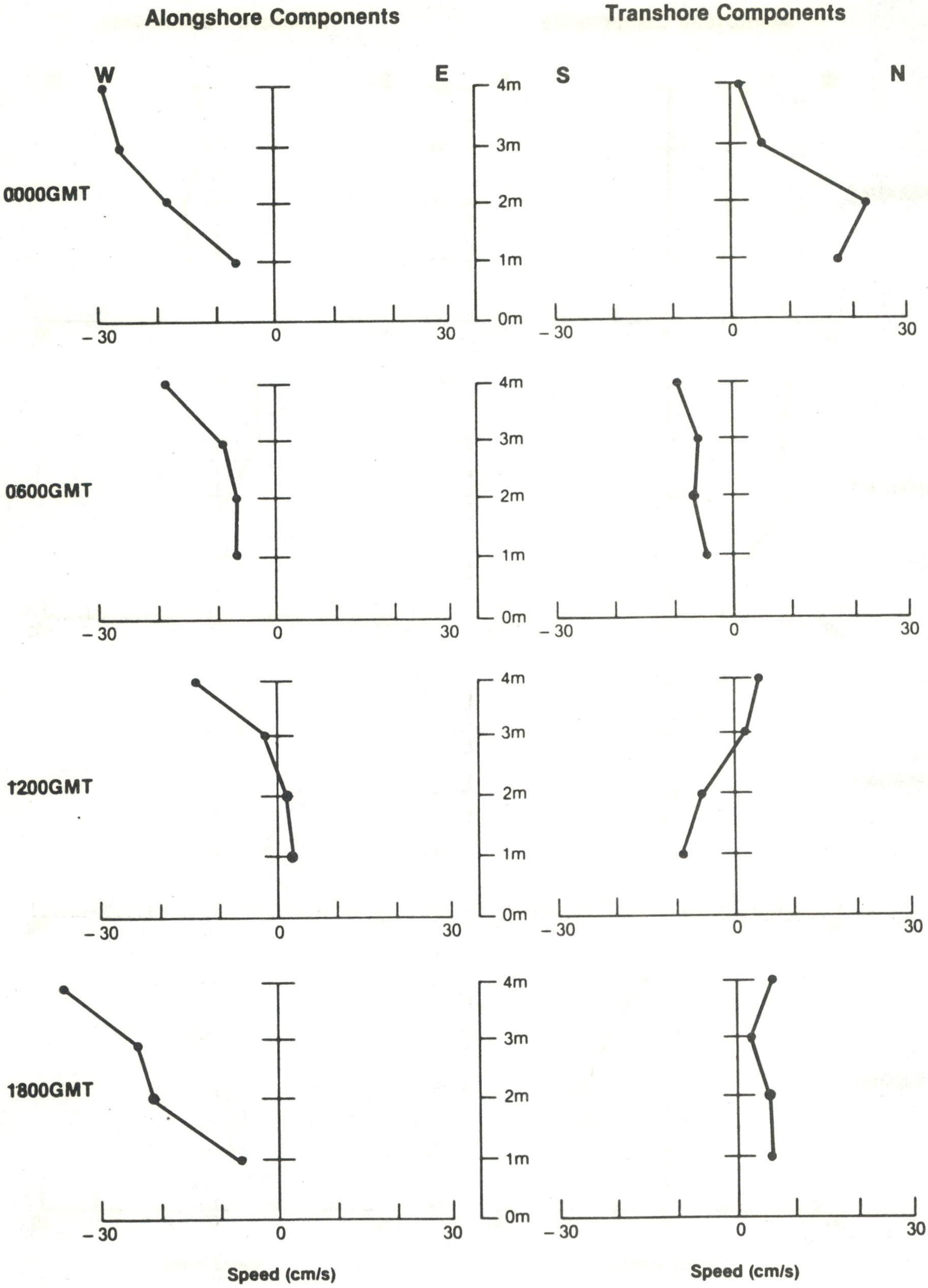

Figure 9-13. Vertical profiles of currents at West Hackberry station 11, April 16, 1979.

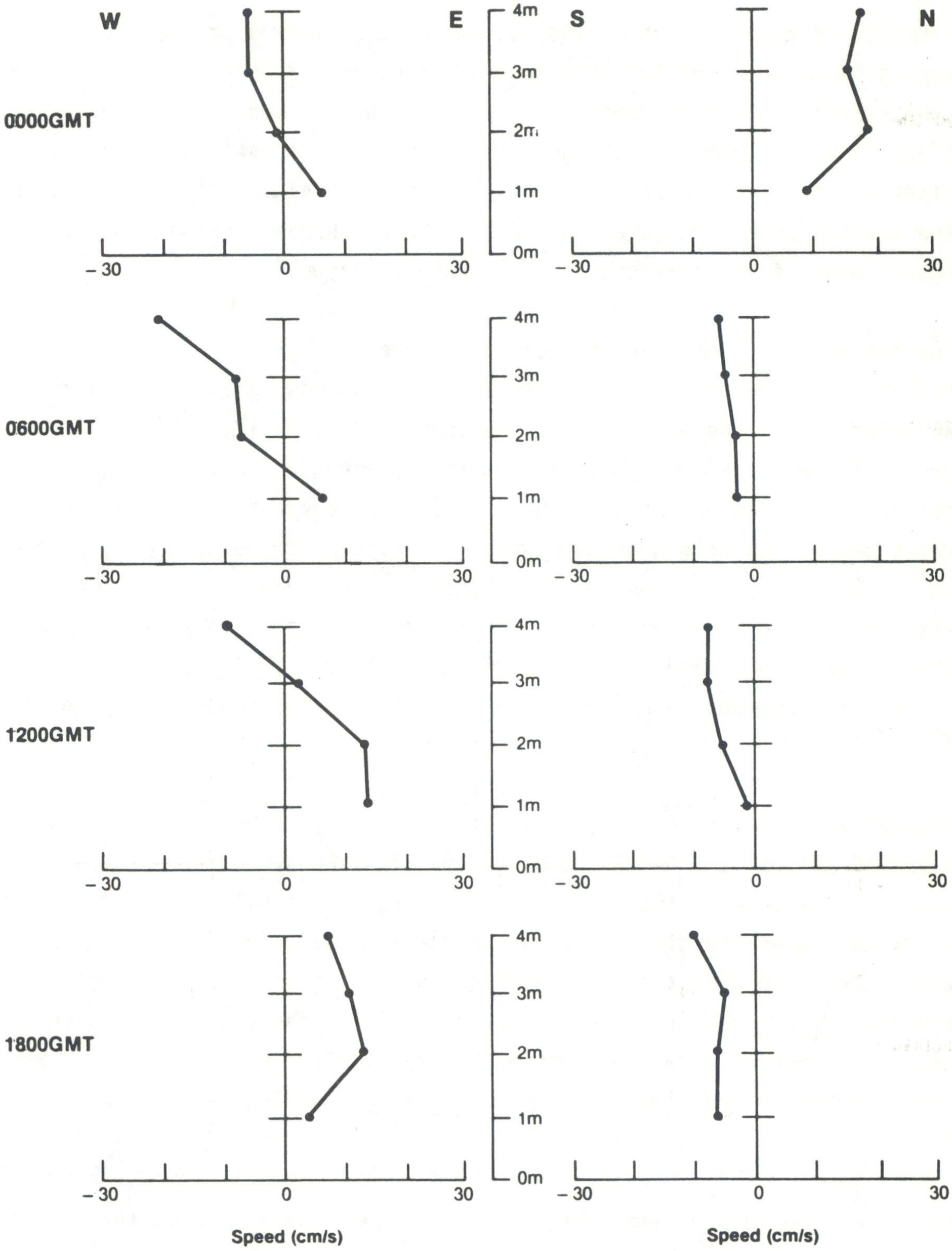

Figure 9-14. Vertical profiles of currents at West Hackberry station 11, April 26, 1979.

Summer 1978

Examples of current vectors indicating the circulation at the West Hackberry site during June 1978 are shown in figures E-8 to E-17. During June 1978, the circulation at the West Hackberry site was driven alternately by river runoff and tidal influence; although river discharge was waning, it was still sufficient to affect circulation. It is evident that mixing of brine discharges into the coastal receiving waters would have been enhanced by the significant horizontal shear of the currents for the examples shown.

Current vectors 1 m above the bottom on June 5 and 6 are shown in figures E-8 and E-9. The time series for the three stations shown indicate mainly diurnal currents on June 5, except at the inshore station 12, where a persistent westward drift began at 2000 GMT. Time series at station 12 shows that lower conductivity water was advected at 50 cm/s past the current meter when the westward drift began; the origin of this water is believed to be Calcasieu Lake, and station 12 appears to have been within the discharge plume. River discharge dominated the station 12 currents on June 6 with a decrease in speed and less persistent direction toward the end of the day. In contrast, currents at stations 13 and 14 remained weaker and more variable, influenced mainly by diurnal forces.

Figures E-10 through E-13 display current vectors at 6-hour intervals on June 9 and 10 at both the 1-m and 3-m levels. This 2-day example indicates large variability between the stations and strong horizontal and vertical shear of the currents when the circulation is primarily tidal. The large differences in current speed and direction from station to station and from level to level indicate that dispersion of brine discharges will be enhanced during these periods. The circulation at the West Hackberry site during June 9 and 10 was governed principally by tidal currents, with slight influence of winds or river runoff.

Early on June 10 the time series at the inshore station 12 at the 1-m level indicates a mixed tidal current with drift toward the south accompanied by warmer, lower conductivity water. The time series at the 1-m level for station 14 appears to be tidally mixed, accompanied by variations in the conductivity

data believed to correspond to fluctuations of river water. The apparent dominance of river runoff in the circulation on June 18 and 19 (figures E-14 and E-15) is supported by the time series of water temperature and conductivity as well as current speed and direction for this period.

The station 13 time series indicates advection of warmer, lower conductivity water following increasing, generally westward currents beginning early on June 17. The warmer, lower conductivity water was first observed at station 14 nearly 3 hours later than it was observed at station 13. This lag seems to be due to the widening southward development of the river plume during the westward drift. The warmer, lower conductivity water was seen at westernmost station 15 at about 1500 GMT on June 17 with relatively strong mixing occurring for an additional 21 hours. The current vectors on June 18 describe a circulation governed almost completely by river runoff. This dominance continues into June 19, with some undulation of the river plume evident in the circulation pattern.

Current vectors at the 1-m level on June 28 and 29 (figures E-16 and E-17) indicate a tidally dominant circulation, mainly diurnal. Rotation of the current vectors at stations 14 and 15 was clockwise during the 2-day period.

Current vectors at the 1-m level for July 7 (figure E-18), show a general eastward drift during the entire day. Beginning midday (GMT) on July 2, current directions were mainly eastward to northward. Temperature and conductivity time series indicate a gradual increase in temperature and conductivity beginning July 2 and continuing into July 11.

Current vectors at the 1-m level are shown in figures E-19 and E-20 for July 23 and 24. The time series at both stations 14 and 15 indicate a general westward drift during both days, with relatively large direction scatter during the first half of July 23. The water temperature and conductivity time series at station 14 indicate a cooling, lower conductivity trend beginning late during July 21 with complete mixing by about 0000 GMT on July 25. The time series record at station 15 indicates slight warming and lowering of conductivity, also beginning about midday on July 21 and continuing through July 24.

Fall 1978

Current vectors at the 3-m level for November 3 and 4 are shown in figures E-21 and E-22. The circulation was governed by mixed tidal currents with strong semidiurnal components. At midday on November 2, a 1-week general westward drift ceased at station 11, and counterclockwise rotation with an approximate one-half day period persisted until 0000 GMT on November 4. The time series at the stations 13 and 15 3-m levels resemble a mixed tidal current with a strong semidiurnal component, accompanied by no significant changes in water temperature or conductivity.

Current vectors at the 3-m level from 0000 GMT on November 6 to 0600 GMT on November 7 are shown in figures E-23 and E-24. The time series at station 11 indicates westward flow with increasing speed beginning at about 2000 GMT on November 5, and a sudden decrease in current speed to near zero at 1700 GMT on November 6. The time series at the station 13 3-m level showed similar characteristics, but much lower speeds compared to the station 11 data. The time series at station 15 also indicated a westward drift beginning at about 2200 GMT on November 5, with speeds similar to those observed at station 13, but lower than station 11. Despite the general westward drift, both the direction and the sense of rotation of the current vectors were variable.

Winter 1979

Vectors at both levels for February 2 (figures E-25 and E-26) show a westward drift resulting from wind stresses. The meteorological time series at station 18 indicated east-southeasterly winds averaging about 8 m/s at about 0600 on February 2. Winds remained east-southeasterly for the remainder of February 2 and became northerly by 2100 GMT on February 3. The surface weather map for February 2 (NOAA Daily Weather Maps, Weekly Series, January 29-February 4, 1979) shows a high pressure center over Indiana, Ohio, and Kentucky with southeasterly winds occurring at Lake Charles as a result of an anticyclonic flow of air. A front moved past the site at 2100 GMT on February 3 and stalled offshore, causing easterly to northeasterly winds through February 5.

The current time series for both levels at station 11 were similar on February 2, except that the 3-m level current became persistent later than the 1-m level current, a lag of about 7 hours. At both levels, the westward drift was accompanied by a very gradual increase both in water temperature and conductivity. The time series at station 13 resembled those at station 11, including the lag in attaining westward persistence at the lower level compared with the upper level and the gradual increase in water temperature and conductivity that began with the westward drift. At station 14, the lag in directions at the two levels was not apparent; the direction data were nearly identical. The time series at the two station 15 levels differed from those for the other stations. At the 3-m level, westward drift was attained at about 1800 GMT on February 1. At the 1-m level a westward drift was not attained until about 0900 GMT on February 2, a lag of 15 hours. Temperature and conductivity increased after the flow became persistent toward the west.

At 0000 GMT on February 2, the 3-m level currents were consistently faster and to the right of the 1-m level currents, except at station 14, where the direction was the same and the 1-m level current was only slightly faster. At 0600 GMT, directions and speeds at the two levels were nearly equal, except at station 15 where the near-bottom layer flowed south-southwestward, while the 3-m level flowed west-northwestward.

At 1200 GMT, the vectors at both levels were similar at stations 11, 13, and 14, but there was more shear at station 15, with an onshore component in the near-bottom layer and an offshore component in the 3-m level. At 1800 GMT, the directions were comparable (within the TMU's); speeds in the 3-m level were consistently higher, except at station 15 where they were nearly equal.

Current vectors at the 1-m and 3-m levels during February 5 are shown in figures E-27 and E-28. Meteorological time series at station 18 show east-northeasterly winds freshening during February 4, with speeds increasing into February 6, along with decreasing atmospheric pressure. Wind speeds during February 5 were from 8 to 15 m/s, resulting in a westward drift of the currents.

At 0000 GMT on February 5, time series at both levels of station 11 were similar, but with speeds consistently higher at the 3-m level. The currents at

both levels had been rotating counterclockwise for about 9 hours. At the 1-m level, the current was backing northward to westward, but was already west-northwestward at the 3-m level. The time series at station 13 was similar to that at station 11. The westward drift was achieved at the 3-m level before the 1-m level. Current speed at the 3-m level reached 35 cm/s on February 5 and continued building to 40 cm/s early on February 6. The time series at station 14 was similar to those at stations 11 and 13, including the lag in direction between the two levels and a trend toward warmer water with lower conductivity. The time series at station 15 was also similar to the other stations. The current vector at the station 15 3-m level displayed a westward drift at about 0500 GMT on February 5. The current at the 1-m level attained a westward drift at 0900 GMT, a 4-hour lag.

Thus, a westward drift began to develop early on February 5, and its development continued through the day. With this circulation, it is evident that brine discharges would be advected from the site, and dispersed by velocity gradients.

Current vectors on February 8 and 9 are shown in figures E-29 to E-31. (Note that both 1-m and 3-m levels are shown in figure E-31.) A decrease in wind speed and veering of wind direction from midday of February 7 reversed the westward current that developed on February 5 (figures E-27 and E-28).

The surface weather map (NOAA Daily Weather Maps, Weekly Series, February 5-11, 1979) for February 8 shows a high pressure center situated just offshore of the South Pass, Mississippi River. February 8 began with northerly winds at NOS station 18, veering to southerly winds by 1000 GMT, and remaining southerly to south-southeasterly for the remainder of the day.

The time series at both levels for February 8 suggest that the circulation was predominately, but not completely, tidally influenced. Records at both levels at station 13 indicate diurnal currents, with a significant semidiurnal component at the 1-m level. Stations 14 and 15 both show apparently stronger semidiurnal components than observed at station 13.

Current vectors at both levels for February 15 are shown in figures E-32 and E-33. Station 18 meteorological time series indicate a southerly wind beginning during February 11 and persisting into February 16 (except for a 7-hour period late on February 13 when the wind veered west-northwest and backed southerly again). A cold front passed over the site at about 1000 GMT on February 16 with a sudden veering of wind direction to east-northeasterly, an increase in speed to 11.5 m/s, and a decrease in air temperature from 15° to 3.5°C. Southerly winds averaging from 6 to 8 m/s prevailed during February 14 and 15 prior to the passing of the cold front.

The 1-m and 3-m level time series at station 11 are similar all day February 15, with a southeastward trend. Station 13 time series are similar to those at station 11, but with more variability in the direction data. The 1-m level direction was toward the southeast on the average, while the 3-m level data averaged toward south-southeast. The current direction was more variable at both levels at station 14, and both levels tended toward east-southeast. The station 15 data showed the least similarity to any other station during February 15; the 1-m level was northeastward, while the 3-m level current showed a tendency toward counterclockwise rotation from an eastward current at the beginning of the day to a north-northeastward current at the end. A strong tendency toward increasing water temperature can be seen at the 3-m level, and a lesser tendency toward warming occurred at the 1-m level.

Current vectors at the 1-m and 3-m level for February 23 are shown in figures E-34 and E-35. No meteorological data were obtained that day at station 18; the end of the previous record was February 21, indicating southerly winds all day averaging about 6 m/s. The surface weather map at 0700 EST on February 23 (NOAA Daily Weather Maps, Weekly Series, February 19-25, 1979) indicates south-southeasterly surface winds at both the West Hackberry and Weeks Island sites.

Time series records of currents at both levels and all stations show a fully developed southwestward drift all day on February 22, continuing throughout the day on February 23. Accompanying this southwestward drift was a gradual increase in water temperature and decrease in conductivity. The exception was

at station 13, where the current rotated counterclockwise initially, then clockwise.

The 3-m level current vectors were consistently to the right of the 1-m level vectors; drift in the 3-m level layer was essentially alongshore, while a substantial component toward offshore in the 1-m level layer can be seen.

Spring 1979

Current vectors at the 1-m and 3-m levels for March 2 are shown in figures E-36 and E-37. The surface weather map at 0700 EST on March 1 (NOAA Daily Weather Maps, Weekly Series, February 26 to March 4, 1979) indicates winds out of the northeast following the passage of a cold front; a warm front was progressing northward, just east of Mobile, Ala., at the same time. The warm front developed and passed Lake Charles on March 2, resulting in easterly winds that generated a westward drift. The current was slower and more variable in direction at the 1-m level compared with the 3-m level. During the second half of March 1 and the first half of March 2, currents at the 3-m level appeared to be nearly diurnal. The westward drift that began midday March 2 continued through the day on March 3. Horizontal and vertical shear of the currents are apparent in figures E-36 and E-37.

Currents at the 1-m and 3-m levels during March 7 are shown in figures E-38 and E-39. The winds (at both sites) were governed on March 7 by a high pressure center in the western Gulf of Mexico with attendant anticyclonic air flow causing west-southwesterly winds at the sites. The generally eastward drift in the 3-m level layer persisted, while currents at the 1-m level were considerably slower and flowed persistently onshore during the second half of the day.

The Gulf At-Sea Performance (GASP) Experiment was conducted at the West Hackberry site for 32 days beginning April 5, 1979. While the GASP Experiment was concerned with data quality assurance (section 8, volume 2 of this report), the oceanographic objectives included four levels of current meter observations to obtain vertical profiles at station 11 over a variety of conditions. An extreme meteorological event occurred during April 11 and 12, during which south-

southeasterly winds reached 15 m/s, and the current speed at the 4-m level reached 84 cm/s. (See section 20.)

Current vectors at three levels on April 7 and 8 are shown in figures E-40 to E-45. Time series records at all stations and levels during April 6 indicate that the circulation was principally tidal. This tidal influence continued into April 7, except at stations 13 and 15, where a wind drift current was developing. By 0600 GMT on April 7, a westward wind drift current that persisted through April 8 was established at station 11 at the 3-m and 4-m levels. South-southeasterly winds prevailed during April 7 and 8 with speeds from about 6 to 10 m/s, averaging 7.5 m/s. The surface weather map at 0700 EST on April 8 (NOAA Daily Weather Maps, Weekly Series, April 2-8, 1979) indicates that a low pressure area situated over northeast Mexico with attendant cyclonic airflow may have influenced the winds at both sites. Thus, the circulation shows a transition from tidal influence early on April 7 to a wind-driven near-surface system for the rest of the period, which was associated with meandering direction in the near-bottom layer, particularly at station 13 (figures E-40 to E-45).

Vertical profiles of the alongshore and transhore components of the currents at four levels are shown for April 6 and 7 in figure 9-9 and 9-10, and for April 8 and 9 in figures 9-11 and 9-12. The alongshore component is positive toward 86 degrees and negative toward 266 degrees, while the transhore component is positive toward 354 degrees and negative toward 176 degrees. The profiles were constructed from 1-hour vector average currents obtained at four levels at station 11.

The alongshore and transhore components of the current vectors for station 11 shown in figures E-40 to E-42 are plotted as vertical profiles in figure 9-10. The profiles shown in figures 9-11 and 9-12 suggest that dispersion together with advection would tend to dilute brine discharges in the alongshore direction.

The vertical profiles of currents at station 11 for April 16 are shown in figure 9-13. Southeasterly to easterly winds blew during April 16 from 5 to 10 m/s, increasing during the day. Wave heights also increased during the day

(section 20). Consistent with previous observations, the current direction at the 1-m level fluctuated more than at the higher levels. Currents at the 2-m, 3-m, and 4-m layers rotated clockwise until midday, when a westward drift became established.

The vertical profile of the transhore components at 0000 GMT indicates upwelling because of the onshore component at the 2-m level of about 22 cm/s. The daily weather maps for April 14 to 16 and unvalidated station 18 meteorological data (time off by 40 minutes) suggest that winds persistent from the northeast account for the high westward drift of about 30 cm at 4-m above bottom and for the upwelling, which is believed to compensate for offshore drift in the near-surface layers.

Current vectors for stations 11 and 13 for April 25 and 26 are shown in figures E-46 to E-51. Vertical profiles of the alongshore and transhore components at station 11 for April 26 and 27 are shown in figures 9-14 and 9-15, respectively. The meteorological time series obtained at station 18 shows winds from the southwest all day April 26 with speeds increasing from 4 to 9.5 m/s. The wind veered suddenly at 0030 GMT on April 27, decreased to 3.5 m/s, became easterly at midday and southeasterly by 0000 GMT on April 28, when it fluctuated from easterly to southeasterly. The wind speed average reached 10.5 m/s midday on April 27 and diminished to 3 m/s by 0000 GMT on April 28. The surface weather map for 0700 EST on April 26 (NOAA Daily Weather Map, Weekly Series, April 23-29, 1979) indicates winds out of the southeast prior to a front.

The 2-m, 3-m, and 4-m currents at station 11 and the 3-m current at station 13 appear from their time series to be mainly diurnal. As mentioned earlier, winds were predominantly from the southwest all day. The time series records at stations 11 and 13 for April 17 show that the influence of the wind decreased; the currents appeared mixed tidal, mainly diurnal.

Although we present no vector plots or profiles for May 1979, circulation during that month was influenced by tidal, wind-driven, and density currents. Decreases in conductivity were apparent but gradual when the currents at the 3-m level at station 11 were southward to westward, but much greater when the currents were southeastward to southwestward.

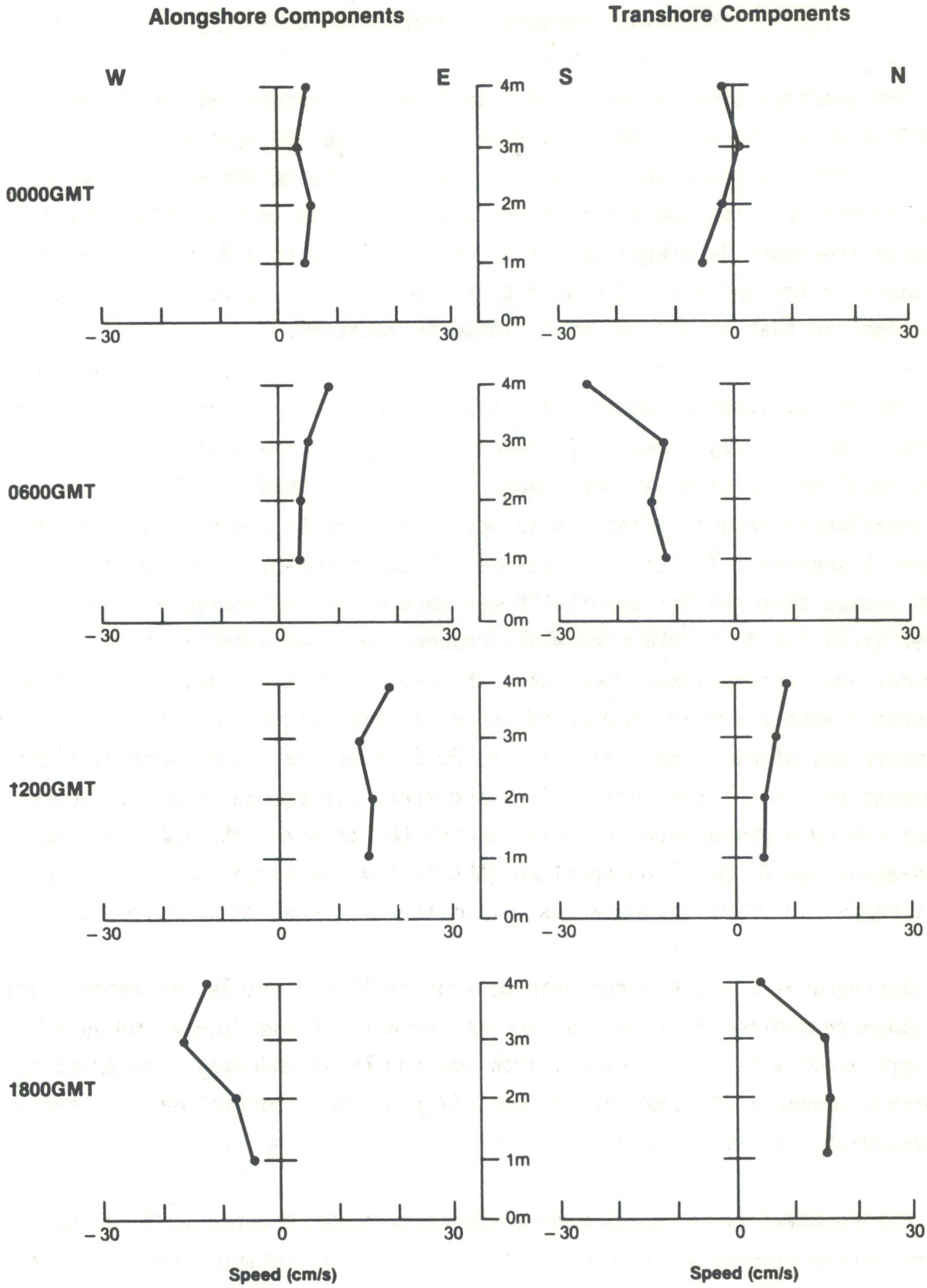

Figure 9-15. Vertical profiles of currents at West Hackberry station 11, April 27, 1979.

9.3. Spectral Characteristics

The spectral plots shown in this section are representative of the energy distribution at the West Hackberry site for each period specified. The maximum entropy technique discussed in section 3 was used to determine the spectral characteristics. The spectral results are defined in angular frequency. Although frequency is always positive, it is noted with a negative sign for that part of the spectra associated with counterclockwise rotation and a positive sign for that associated with clockwise rotation.

The energy spectral density for the 3-m level at station 15 during late spring (June 2 to 27) showed high peaks of energy at the semidiurnal, diurnal, and several narrow bands at low frequencies of less than 0.5 CPD (figure 9-16(a)). The semidiurnal frequency had a distinct sharp peak of energy in the counterclockwise spectra. This finding agrees well with the M_2 tidal ellipse analysis, which showed that the M_2 constituent was generally counterclockwise. This peak of energy at the M_2 counterclockwise frequency was consistently found in the spectral results throughout the year. Energy near the diurnal frequency was associated mostly with clockwise rotation. Energy around the clockwise diurnal frequency was within a band of frequencies from 0.7 to 1.5 CPD. A distinct peak of energy at 1.0 CPD can be seen. In contrast, the energy level at 1.0 CPD within the counterclockwise spectrum was almost an order of magnitude lower. There was a narrow band of energy at 0.5 CPD and a band at frequencies less than 0.35 CPD.

During June 2 to 27, coherency squared between currents and water levels are shown in table 9-3 to be high at the semidiurnal and diurnal frequencies (M_2,O_1,K_1). The O_1 and M_2 tidal constituent with a coherency squared of 0.96 and 0.99, respectively, had higher coherency in the counterclockwise portion of the spectrum.

The K_1 tidal constituent with a coherency squared value of 0.80 was higher in the clockwise spectrum. The rotational orientation for the main tidal constituents is in agreement with the results from the ellipse analysis.

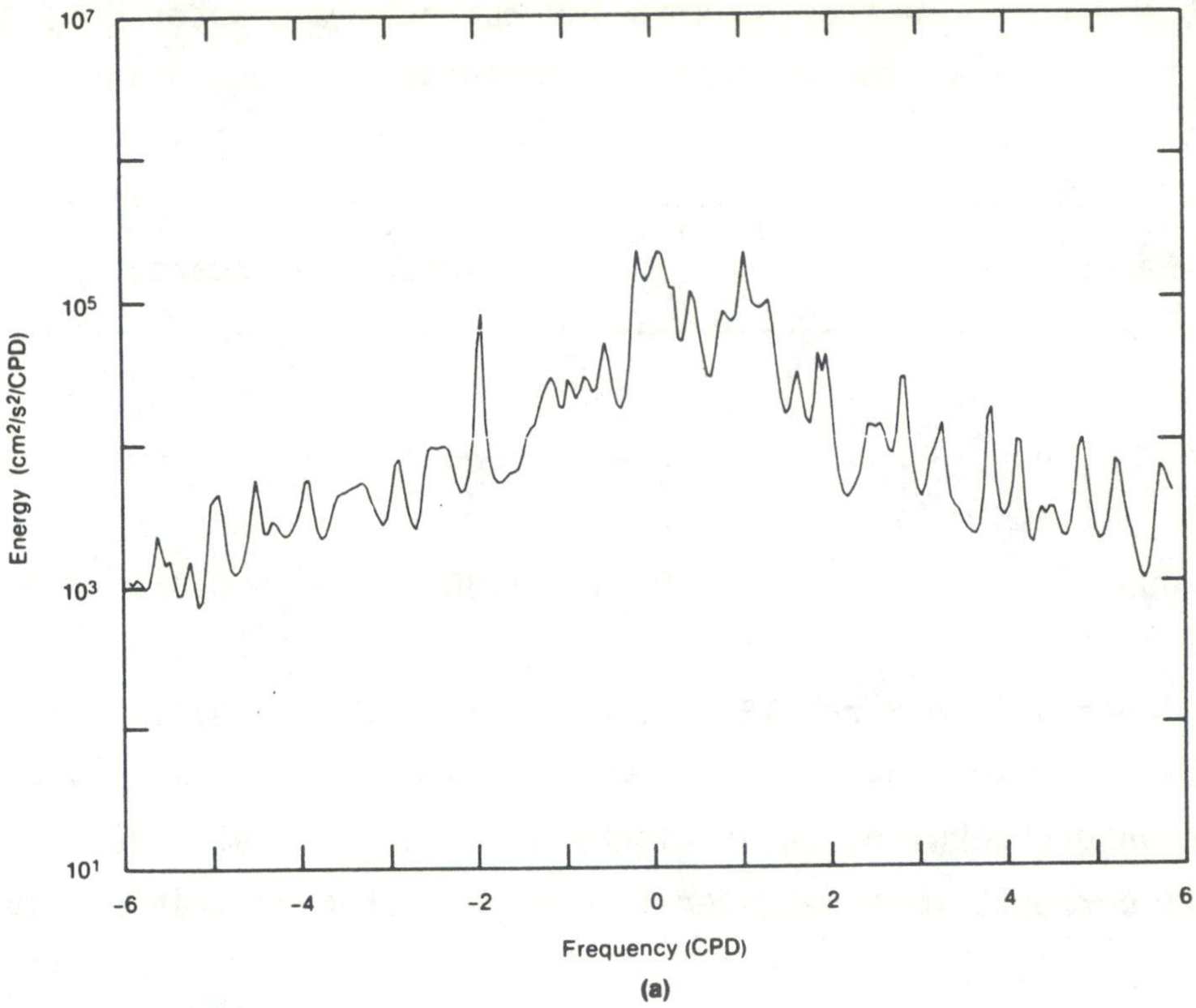

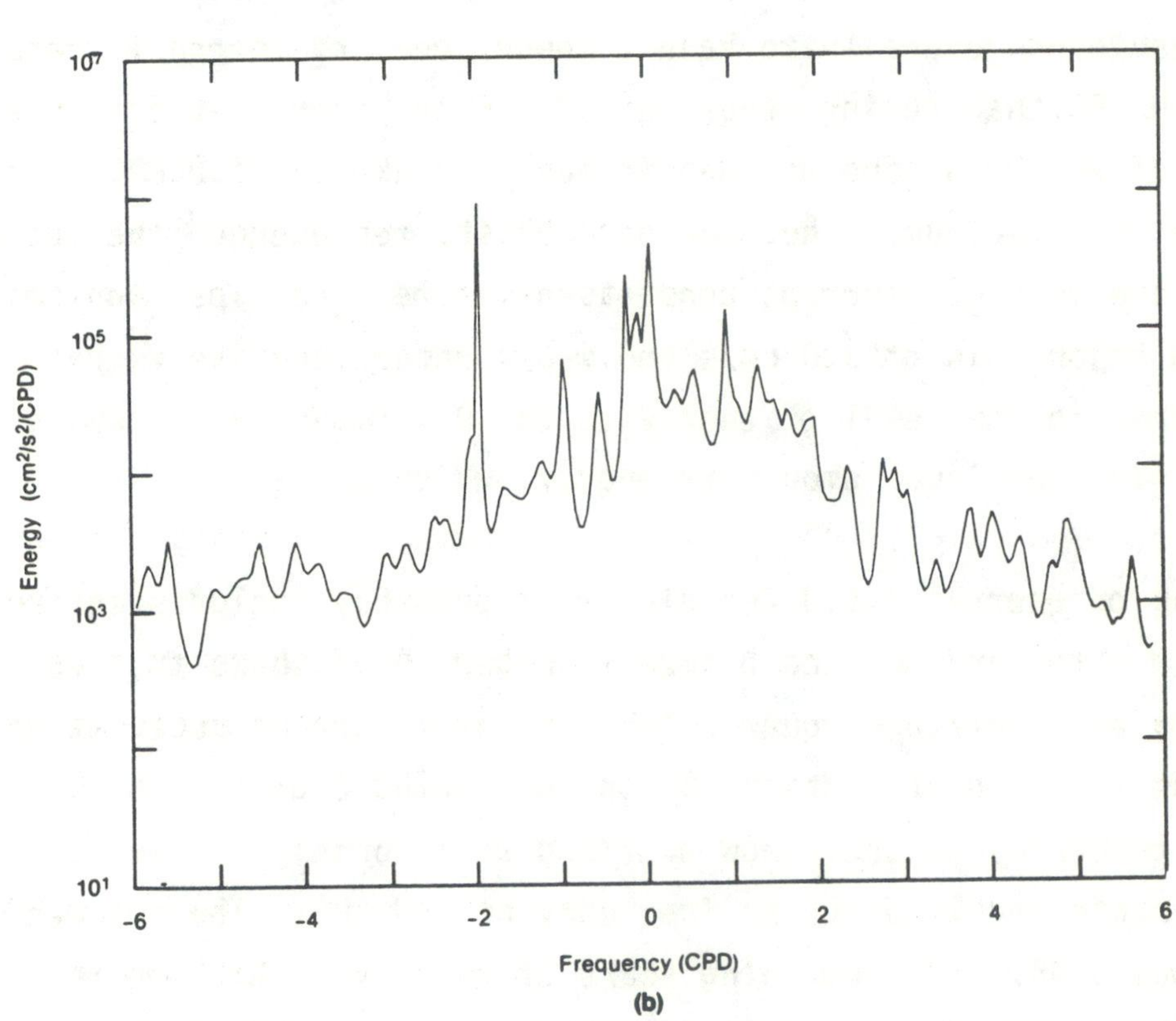

Figure 9-16. Current energy spectrum at West Hackberry site (a) station 15 3-m June 2-27, 1978, and (b) station 15 3-m August 3-26, 1978.

Table 9-3. Coherency squared for currents and water levels at the diurnal and semidiurnal frequencies.

Stations	Period	Coherency squared					
		K_1		O_1		M_2	
		CCW	CW	CCW	CW	CCW	CW
11WL/13(+1)	June 2 to 27	0.34	0.80	0.96	0.48	0.99	0.90
11WL/11(+1)	January 9 to March 13	0.88	0.41	0.34	0.01	0.98	0.43

ccw is counterclockwise, cw is clockwise. Water levels (WL) were measured at station 11; currents were measured 1 m above bottom at stations 11 and 13.

During midsummer, from August 3 to 26, the energy spectrum for West Hackberry was found generally to have a lower level of energy at frequencies less than 1.0 CPD than during other periods of the year. In figure 9-16(b) the narrow band of energy at the diurnal frequency peaked at 1.0 CPD in the clockwise part of the spectrum. The peak at 0.93 CPD represented the energy associated with the O_1 tidal current constituent. The O_1 ellipse for this time series had a major axis of 3.0 cm/s and was counterclockwise with an ellipticity of 0.8. Therefore the level of energy at the O_1 frequency clockwise would be expected to have the lower amount of energy, which was found.

The peak of energy of 1.0 CPD clockwise probably includes the wind-driven circulation due to land and sea breezes. Figure 9-17 shows the results of the cross-spectra and coherency squared for 1-m level current meter at station 11 and for winds recorded at station 18 for the period August 3 to 26. The cross-spectra and coherency squared show a strong relationship between the energy peaks of currents and wind at the frequency of 1.0 CPD. The coherency squared at 1.0 CPD was 0.85. The remaining peaks of relatively high energy for the current spectrum showed low levels of coherency with wind, except at about -0.3 CPD. This suggests that from August 3 to 26 the local winds, other than land breeze and sea breeze, transferred less energy to the sea than during other

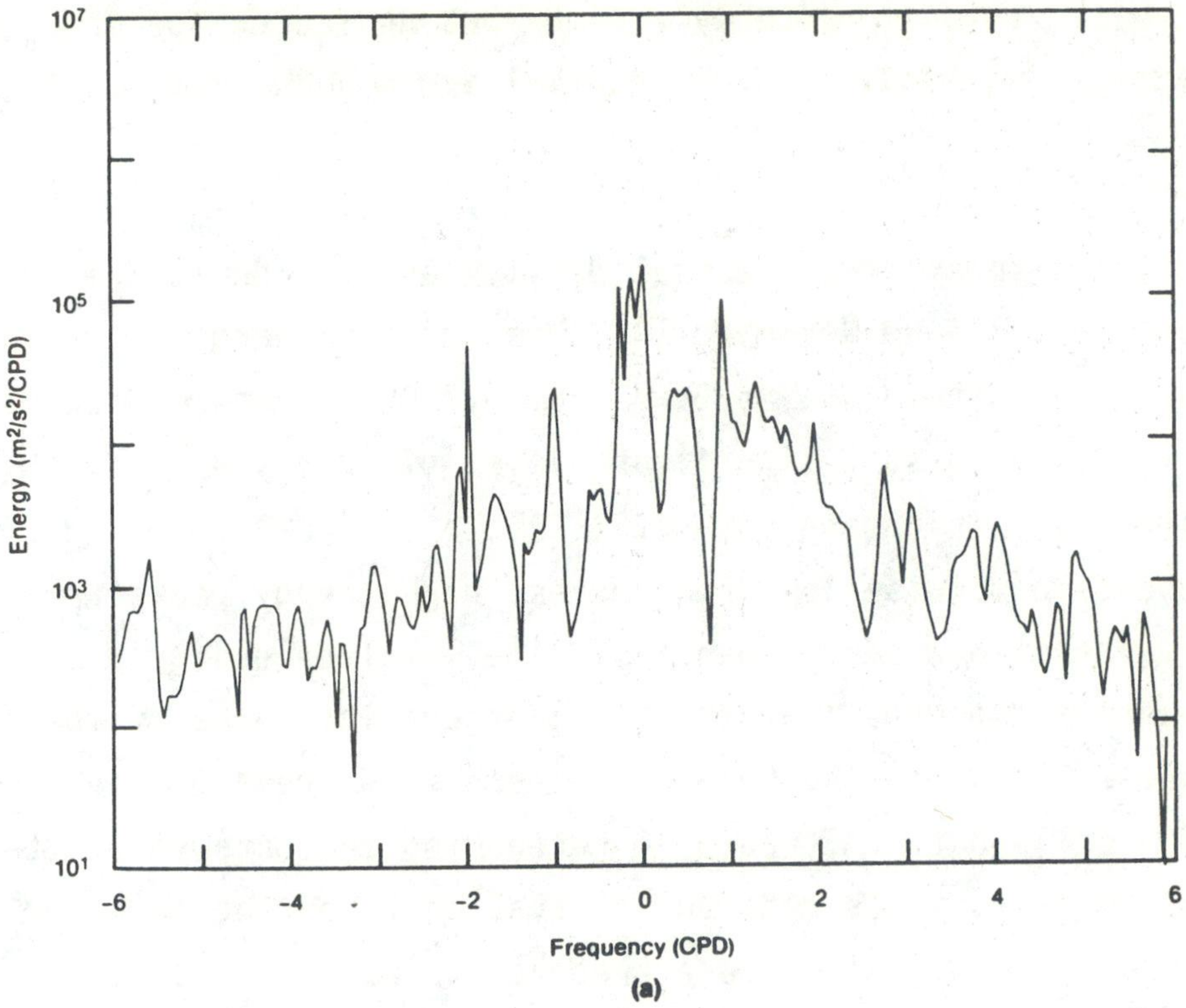

Figure 9-17. (a) Cross-spectra and (b) squared coherence of winds at station 18 and 1-m level currents at station 11, August 3-26, 1978.

periods of the year. This is probably a contributing factor for the low values of current speeds during August, until Tropical Storm DEBRA moved into the area on August 28.

Figure 9-18(a) displays the spectral density at station 11 3-m level during early fall, from October 3 to November 14. Most of the energy is concentrated at the low frequencies within a wide band from 0.7 CPD counterclockwise to 0.6 CPD clockwise. There is also a significant level of energy around 1.0 CPD clockwise contained within a band from 0.75 CPD to 1.25 CPD. In addition to the energy at the counterclockwise low frequencies, high energy peaks were found at the M_2 and O_1 counterclockwise frequencies. The level of energy distribution at the lower frequencies suggests that the dominant driving force of the currents was the wind stress, although the M_2 peak is nearly as great as the lower frequency meteorological input. Although no meteorological data were obtained at the site to confirm this, waves observed at station 11 during this period indicated that relatively strong winds were present at least part of the time. Wave data in table 7-1 indicate that significant wave heights were greater than 1 m for 5 percent of the observations from November 1 to 14.

The energy density during the winter, like that of fall, showed energy concentrated at the low frequency end of the spectrum. The energy at the station 11 1-m level from January 31 to February 20 was concentrated between 0.75 CPD counterclockwise and 1.0 CPD clockwise (figure 9-18(b)). The energy was at its highest peak at 0.28 CPD. Data presented in sections 18 and 19 indicate that this peak was due to cold front passages. Within this wide band of energy there were additional peaks of energy at 0.5 CPD and 0.65 CPD. Cross-spectra between currents at the station 11 1-m level and winds at station 18 (figure 9-19) show a strong relationship between winds and currents, the coherency squared at 0.28 CPD was 0.91. Within the clockwise spectrum from 0.25 CPD to 0.6 CPD, the coherency squared was 0.8 or greater. Within the counterclockwise spectrum from 0.25 CPD to 0.4 CPD, the coherency squared was 0.8 or greater.

From February 23 to March 13, the energy distribution (figure 9-20(a)) at the station 14 3-m level also had a wide band of energy at the low frequencies. A wide band of energy is apparent from 1.6 CPD counterclockwise to 2.5 CPD clockwise. There was also a sharp peak of energy at the frequency 0.2 CPD in

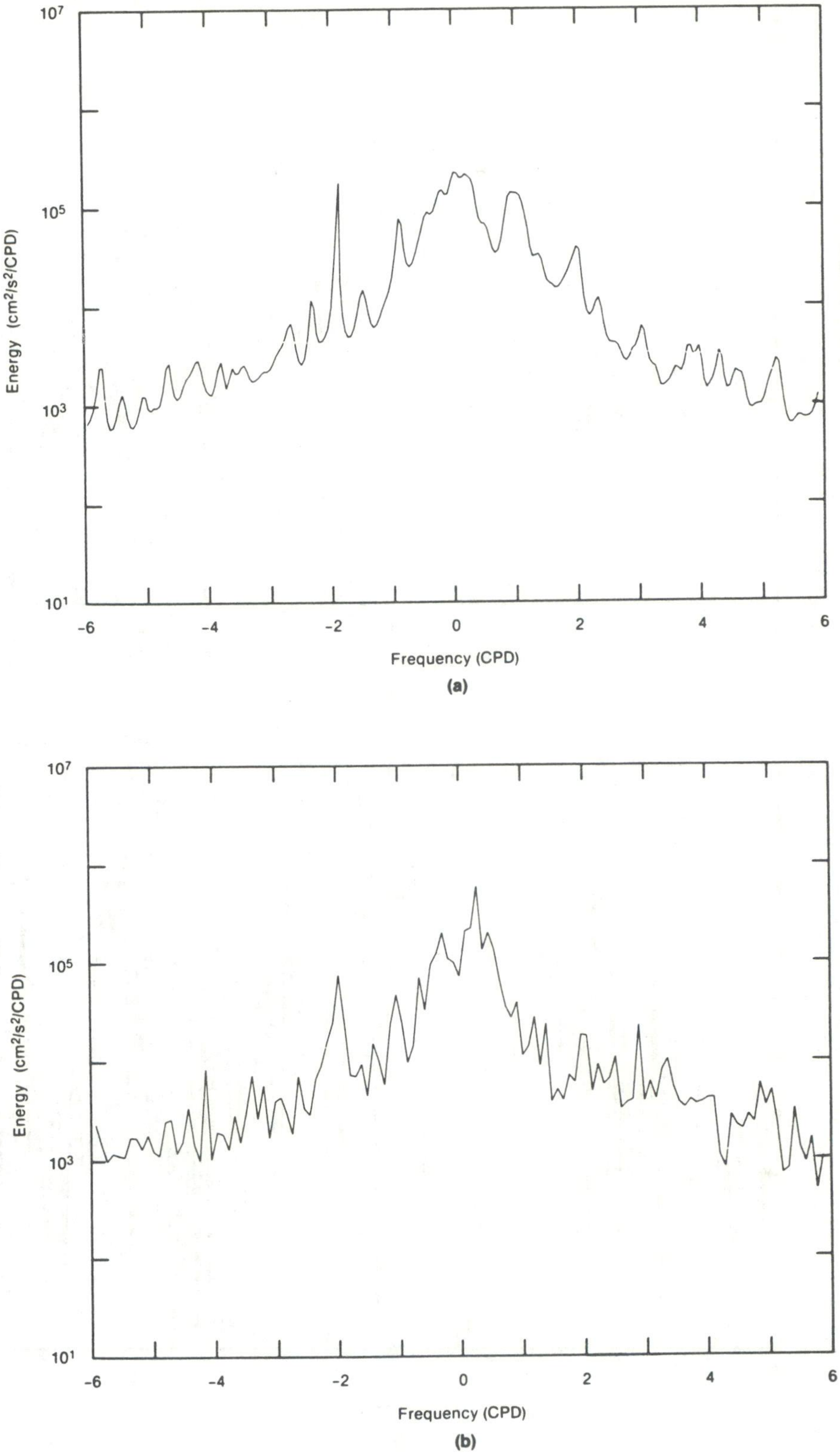

Figure 9-18. Current energy spectrum at West Hackberry site (a) station 11 3-m October 3 to November 14, 1978, and (b) station 11 1-m January 31 to February 20, 1979.

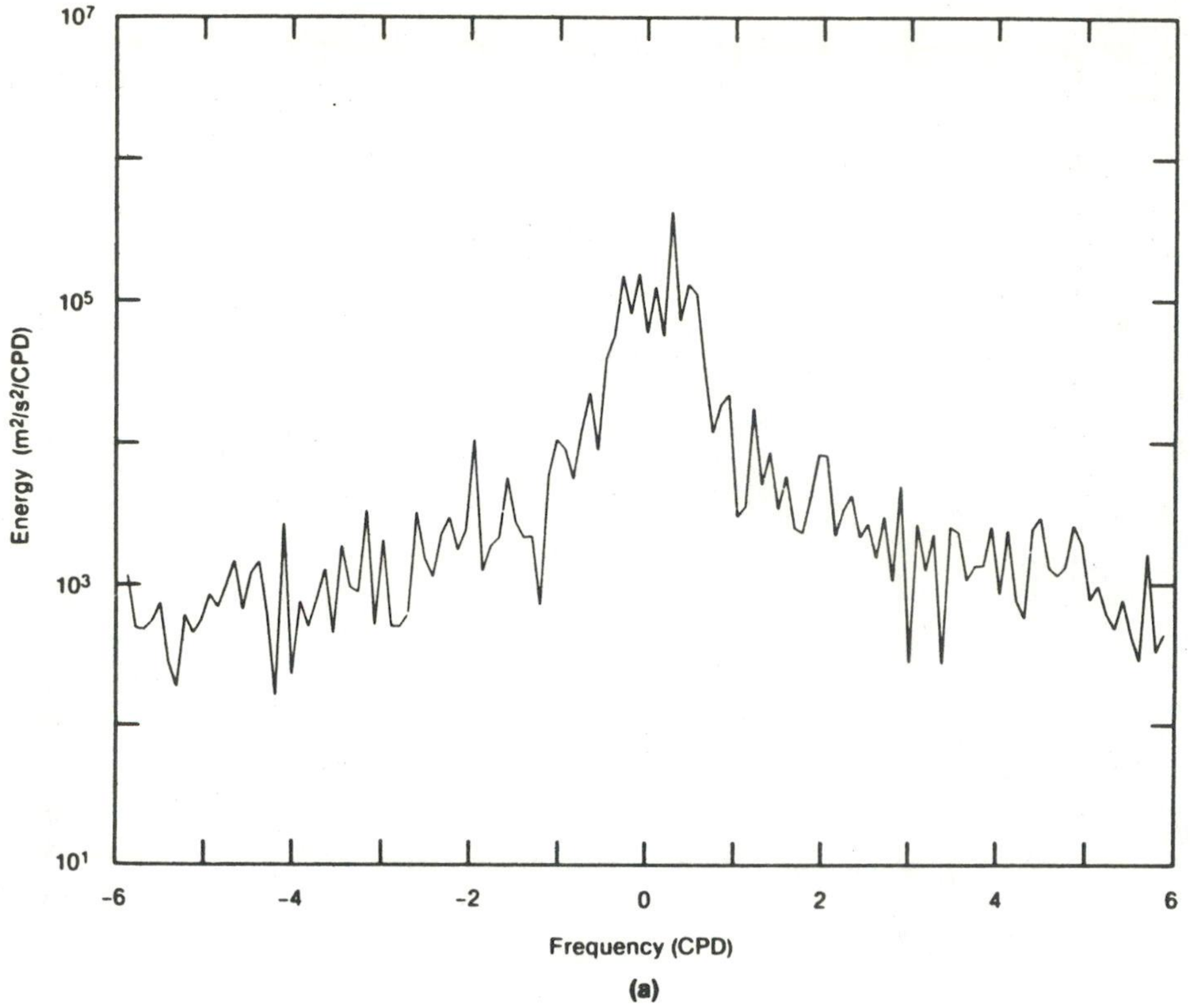

Figure 9-19. (a) Cross-spectra and (b) squared coherence of winds at West Hackberry station 18 and 1-m level currents at station 11, January 31 to February 20, 1979.

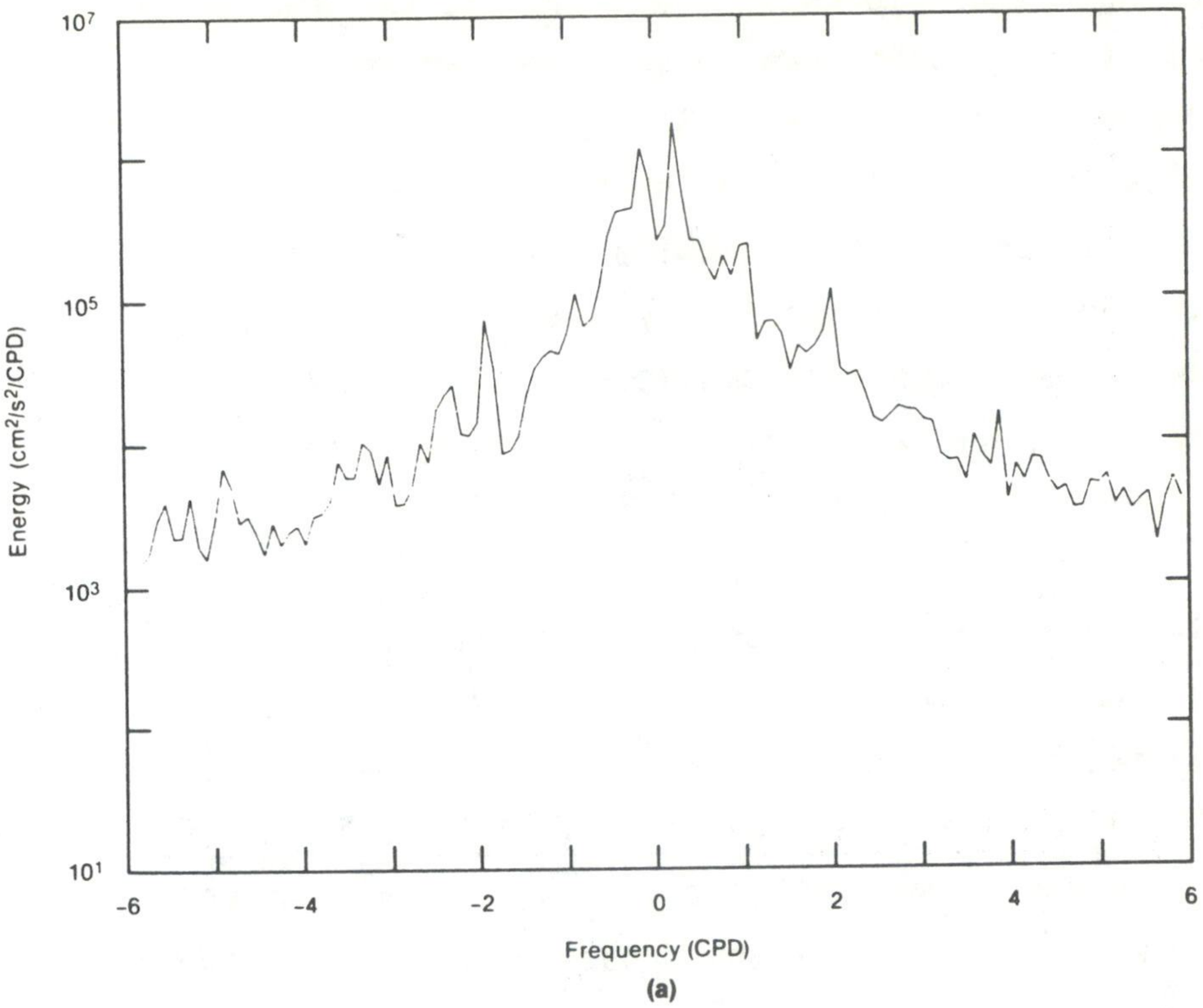

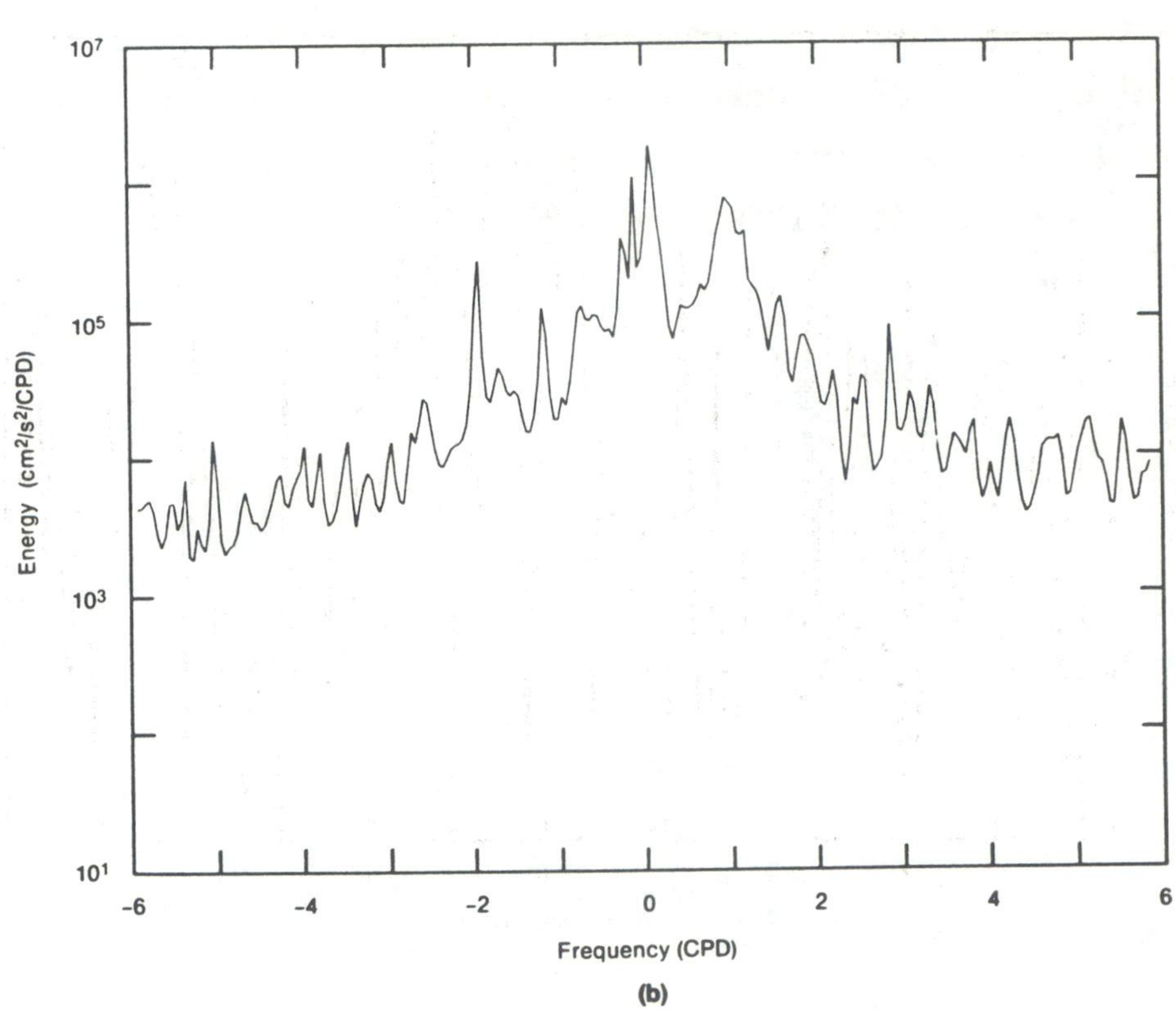

Figure 9-20. Current energy spectrum at West Hackberry site (a) station 14 3-m February 23 to March 13, 1979, and (b) station 11 3-m May 9 to June 1, 1979.

the clockwise and counterclockwise spectrum. At the diurnal frequency K_1 (1.004 CPD), a peak in the counterclockwise spectrum can be seen. This peak was also found in the spectra during January 31 to February 20. Coherency squared between currents and water levels at station 11 from January 9 to March 13 showed coherency in the counterclockwise spectrum to high at 0.98 and 0.88, for the frequencies M_2 and K_1, respectively. At the O_1 frequency, the coherency in both the clockwise and counterclockwise spectra was poor. The rotation orientation for the M_2 and K_1 frequencies was found in agreement with the results from the ellipse analysis in figures 9-9 and 9-10.

Figure 9-20(b) displays the spectral density at station 11 at the 3-m level during spring from May 9 to June 1. The energy distribution was similiar to that found in figure 9-16 from June 2 to 27, 1978. A band of energy can be seen around the clockwise diurnal frequencies, from 0.4 CPD to 1.5 CPD. The energy at the lower frequencies was within a narrow band that peaked at 0.1 CPD. Figure 9-21 shows the results of the cross-spectra and coherency squared for the 3-m level currents at station 11 and meterological station 18. The cross-spectra, like the spectra for current and wind had a wide band of energy from 0.7 CPD clockwise to 1.5 CPD clockwise and a sharp peak of energy at 0.1 CPD. The coherency squared indicated that there was strong coherency within narrow bands of low frequencies at 0.1 CPD and 0.85 CPD.

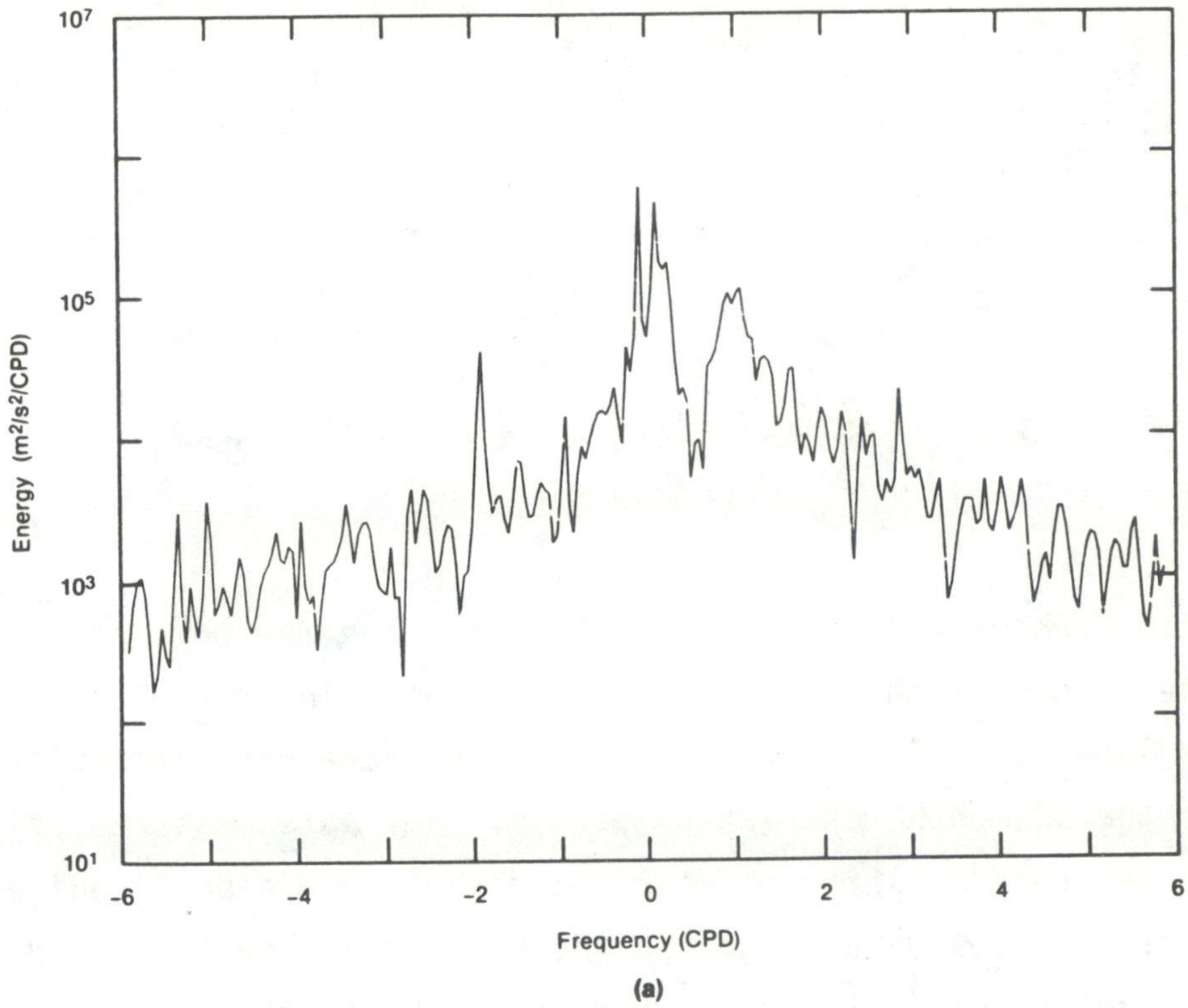

Figure 9-21. (a) Cross-spectra and (b) squared coherence of winds at West Hackberry site station 18 and 3-m level currents at station 11, May 9 to June 1, 1979.

CHARACTERIZATION OF THE PROPOSED WEEKS ISLAND BRINE DISPOSAL SITE

Information described in this part characterizes the physical oceanography and local meteorology at the proposed Weeks Island brine disposal site as observed from June 3, 1978 to June 2, 1979. The intrayear variabilities are described for the 12-month observation period. Reliable measures of interyear variabilities and determination of mean (baseline) conditions require analysis of multiyear time series data. Because the Louisiana inner continental shelf water responds relatively quickly to wind stresses and river runoff, estimates of interyear variability may be made by examining departures of winds and river discharges from the longer data sets available for these phenomena.

10. DISSOLVED OXYGEN

Seawater samples were obtained monthly except for two extended intervals. The first was August 1978 when the FERREL was unable to steam to the Weeks Island site because of mechanical problems, and the second was December 1978 when the VIRGINIA KEY was unable to obtain samples at the Weeks Island site because of heavy seas and a priority to recover and redeploy current meters. No midwater DO values were obtained for July 21 due to a temporary shortage of calibrated Ehrlenmeyer flasks. Listings of the data are available as described in section 10, volume two, of this final report.

10.1. Areal Averages and Ranges

The 12-month time history for DO is summarized in figures 10-1 to 10-3 as areal averages and ranges. At each sample level, data from all the stations within the site are averaged and plotted as a point; bars around the points denote the ranges between the minimum and maximum values, and provide a measure of horizontal DO gradients at the given level. The measure of horizontal DO gradients contains an unknown uncertainty because the data were not obtained synoptically (simultaneously) at the different stations.

The largest DO gradients were observed during the July 21 cruise of the FERREL, when stratification of the density structure was highly stable. Vertical gradients at all stations and horizontal gradients in the near-bottom layer were maximum during this period. A secondary maximum in vertical gradients was observed March 12 and 13. No anoxic ($\leq$ 0.03 ml/l) water samples were found at the Weeks Island site during the 12-month survey; the lowest value observed was 0.98 ml/l at 1 m above the sea floor on July 21. Spatial distributions are discussed later in this section.

The smallest DO gradients, both vertical and horizontal, began during August 1978 with energetic mixing caused by Tropical Storm DEBRA; minimal

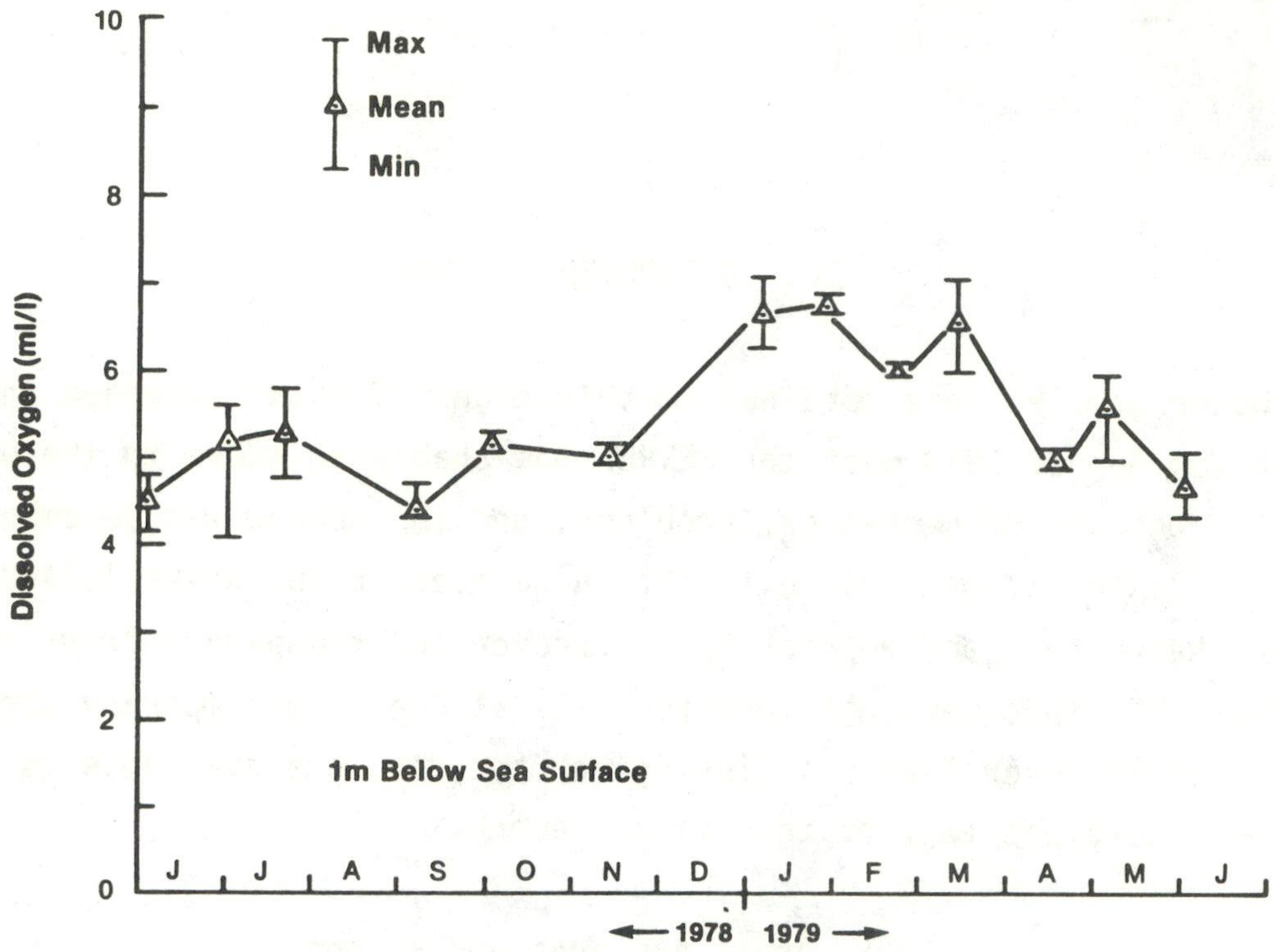

Figure 10-1. DO areal averages and ranges at Weeks Island site, 1 m below sea surface.

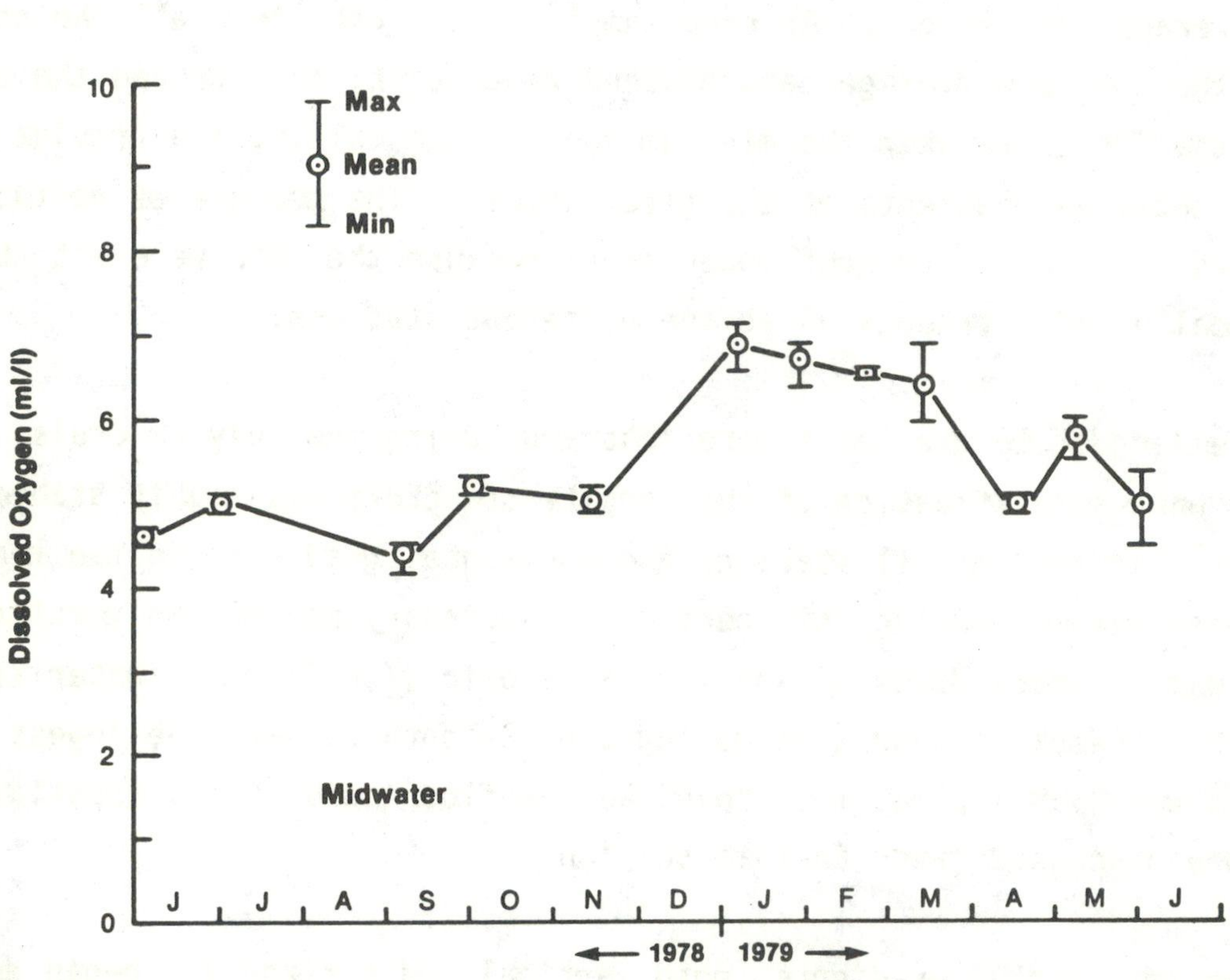

Figure 10-2. DO areal averages and ranges at Weeks Island site, midwater.

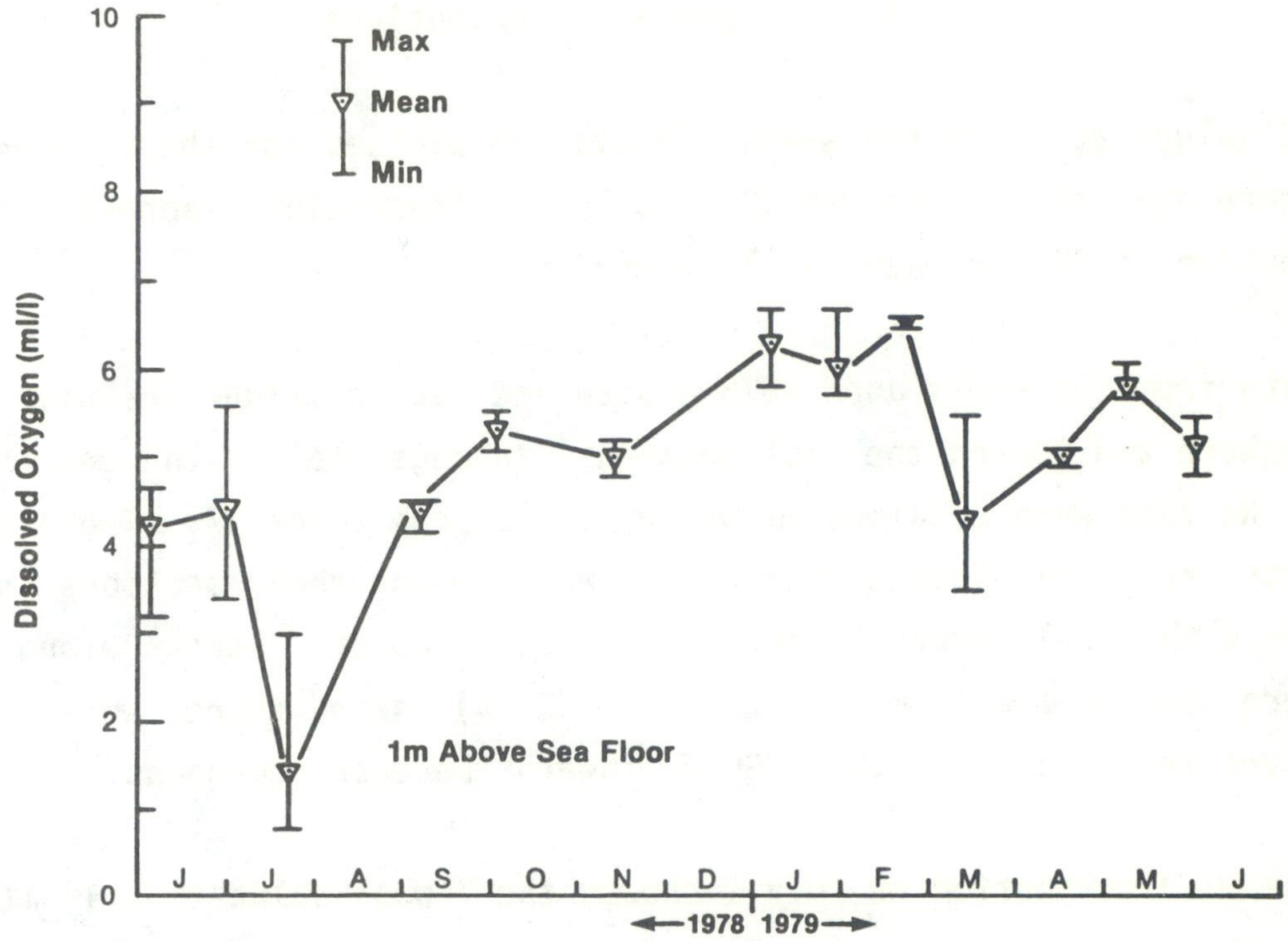

Figure 10-3. DO areal averages and ranges at Weeks Island site, 1 m above sea floor.

gradients continued into December 1978 because of continued mixing by winds and low volumes of river runoff. Relatively small gradients developed during January and February, but vanished before the February 20 and 21 cruise.

The 12-month DO history obtained from June 1978 to June 1979 did not form a complete oscillation of the average values at any of the three layers, but the ranges at 1 m below the sea surface and at midwater overlapped. The average DO value in the near-surface layer on June 3, 1978, was 4.57 ml/l; it was 5.13 ml/l on June 2, 1979, a difference of 0.56 ml/l. The average DO value at midwater on June 3, 1978, was 4.65 ml/l; it was 5.02 ml/l on June 2, 1979, a difference of 0.37 ml/l. These relatively minor differences in DO values and overlapping of ranges in the near-surface and midwater levels at the beginning and end of the 12-month survey suggest that a cyclical model may apply for those levels during the study period. The average DO value obtained on June 3, 1978, 1 m above the sea floor was 4.23 ml/l; on June 2, 1979, it was 4.80 ml/l, a difference of 0.57 ml/l. Despite the small (0.57 ml/l) difference, the ranges of values observed at the beginning and end of the survey did not overlap 1 m above the sea floor.

10.2. Spatial Distributions

DO values at the three sample levels are plotted for the transhore and alongshore stations in figures 10-4 to 10-8. These plots represent the spatial distribution of DO for each sampling cruise.

Data from the early June 1978 cruise indicate a slight positive DO gradient both onshore and toward the east-southeast (alongshore) in the near-bottom layer. No data were obtained midwater at stations 26 or 27. These positive DO gradients are attributed to decreasing depths along those sections in combination with two-layered thermohaline stratification. Depths along the transhore section are from 11.0 to 5.8 m (GCLW) toward shore, while alongshore depths are from 8.2 m to 7.0 m (GCLW) toward the east-southeast.

The DO distribution on July 1 showed the lowest value of 3.44 ml/l 1 m above bottom at station 23, the deepest station. A positive onshore DO gradient, similar to that observed on June 3, existed when a two-layered density structure was obvious. DO in the near-surface layer and in the midwater layer increased during the 1-month interval since the June 2 cruise. The average value of DO in the transhore stations 1-m below the surface was 5.26 ml/l.

As mentioned earlier, no midwater samples were obtained on July 21. The average value of all near-surface data on July 21 was 5.26 ml/l. Although the DO gradient from station 23 to 21 was slightly negative, the positive gradient onshore of the site center was much greater than that observed during the early June and July cruises. A positive DO gradient was also observed alongshore toward the east-southeast, consistent with early June and early July observations.

Meteorological data at station 28 were not obtained until October 2, and inland airport data for interpreting observations at the Weeks Island site are questionable. Wind data obtained by the NOAA National Weather Service at Mobil Platform 333 in the adjacent Eugene Island area show winds freshening to 25 m/s at 2250 GMT on August 27 with the approach of Tropical Storm DEBRA. Winds reached 22 m/s at 1700 GMT on August 28, and remained above 15 m/s more than 90 percent of the time until 0500 GMT on August 28. The winds of Tropical Storm

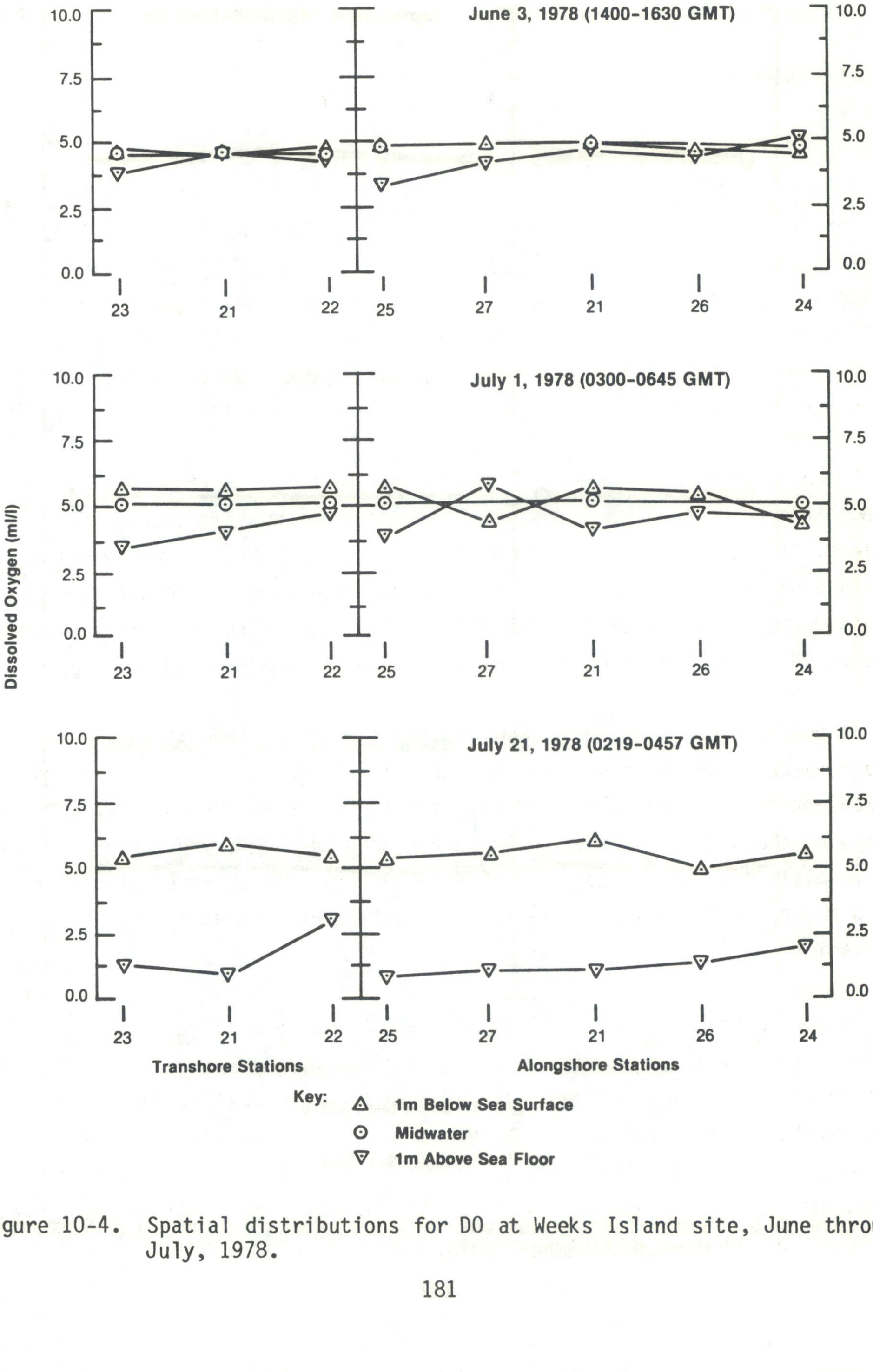

Figure 10-4. Spatial distributions for DO at Weeks Island site, June through July, 1978.

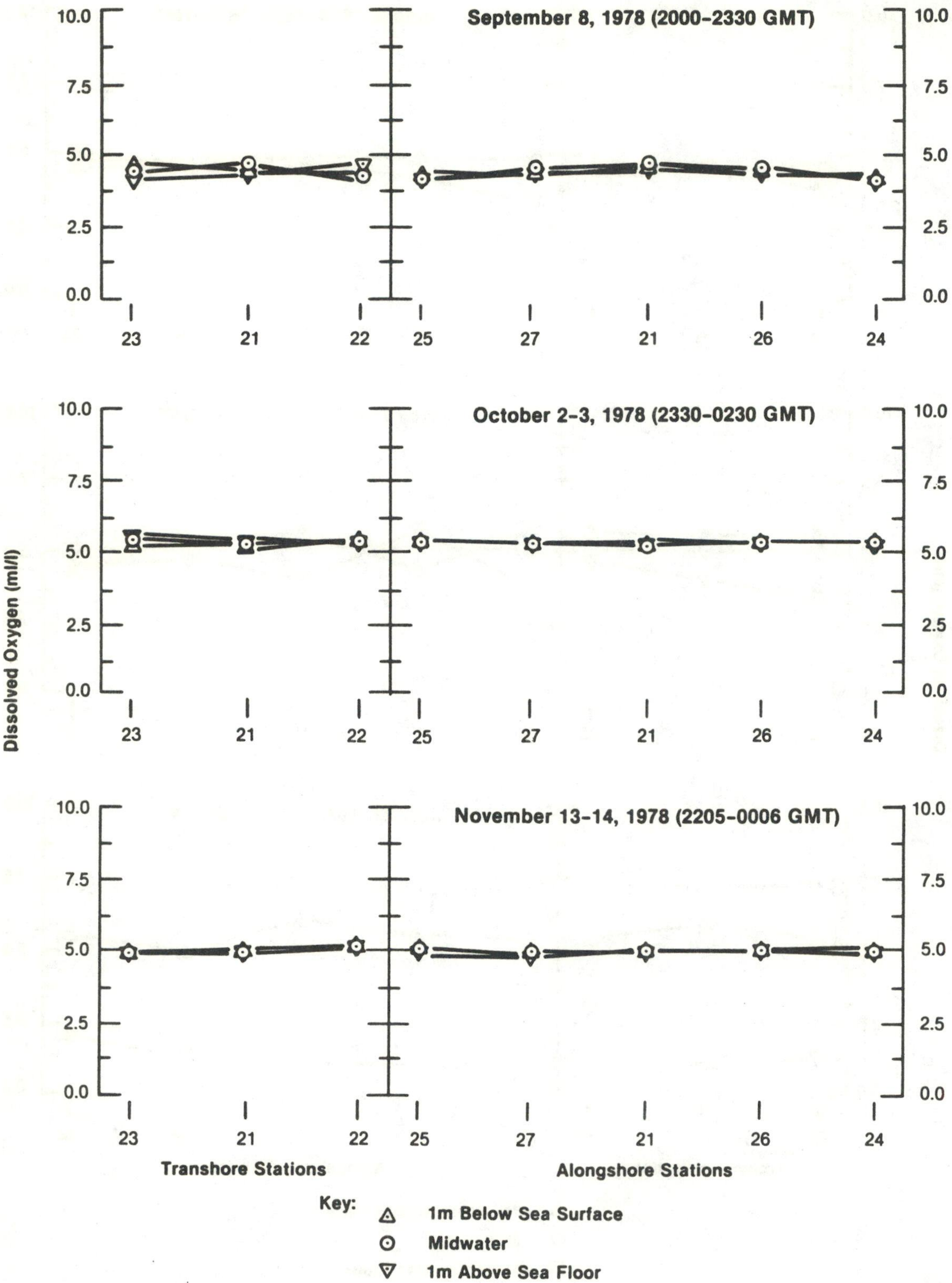

Figure 10-5. Spatial distributions for DO at Weeks Island site, September through November, 1978.

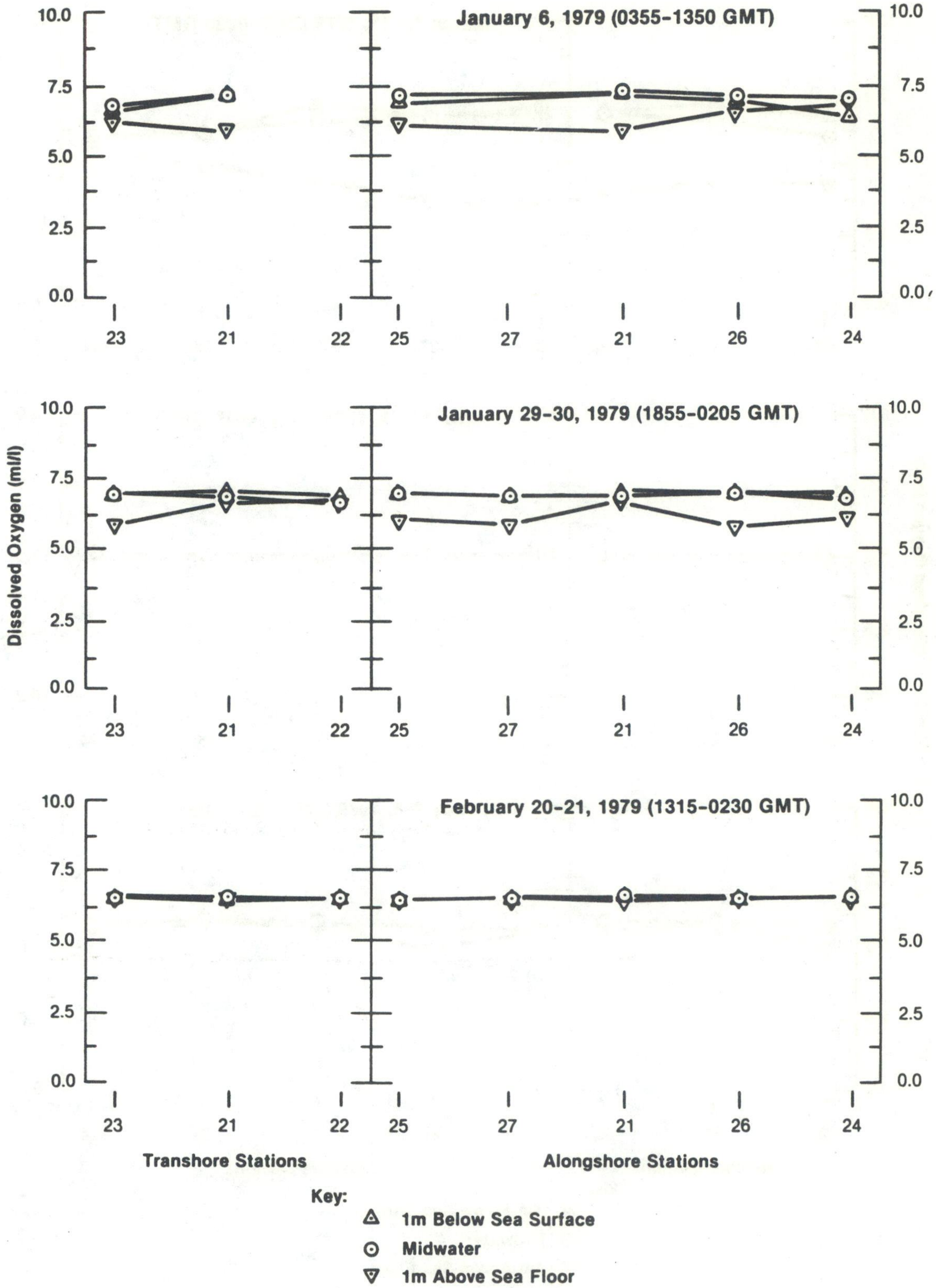

Figure 10-6. Spatial distributions for DO at Weeks Island site, January through February, 1979.

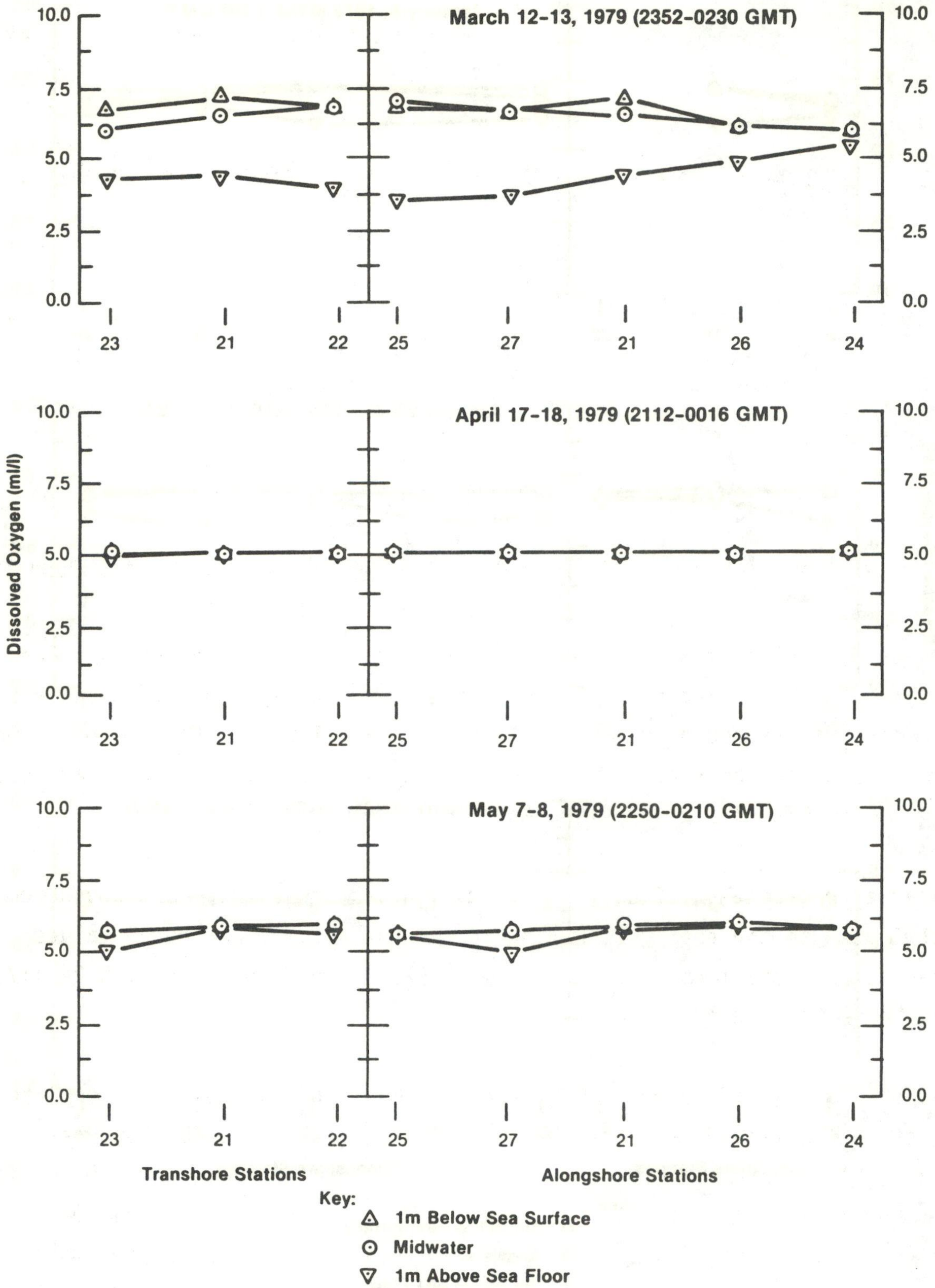

Figure 10-7. Spatial distributions for DO at Weeks Island site, March through May, 1979.

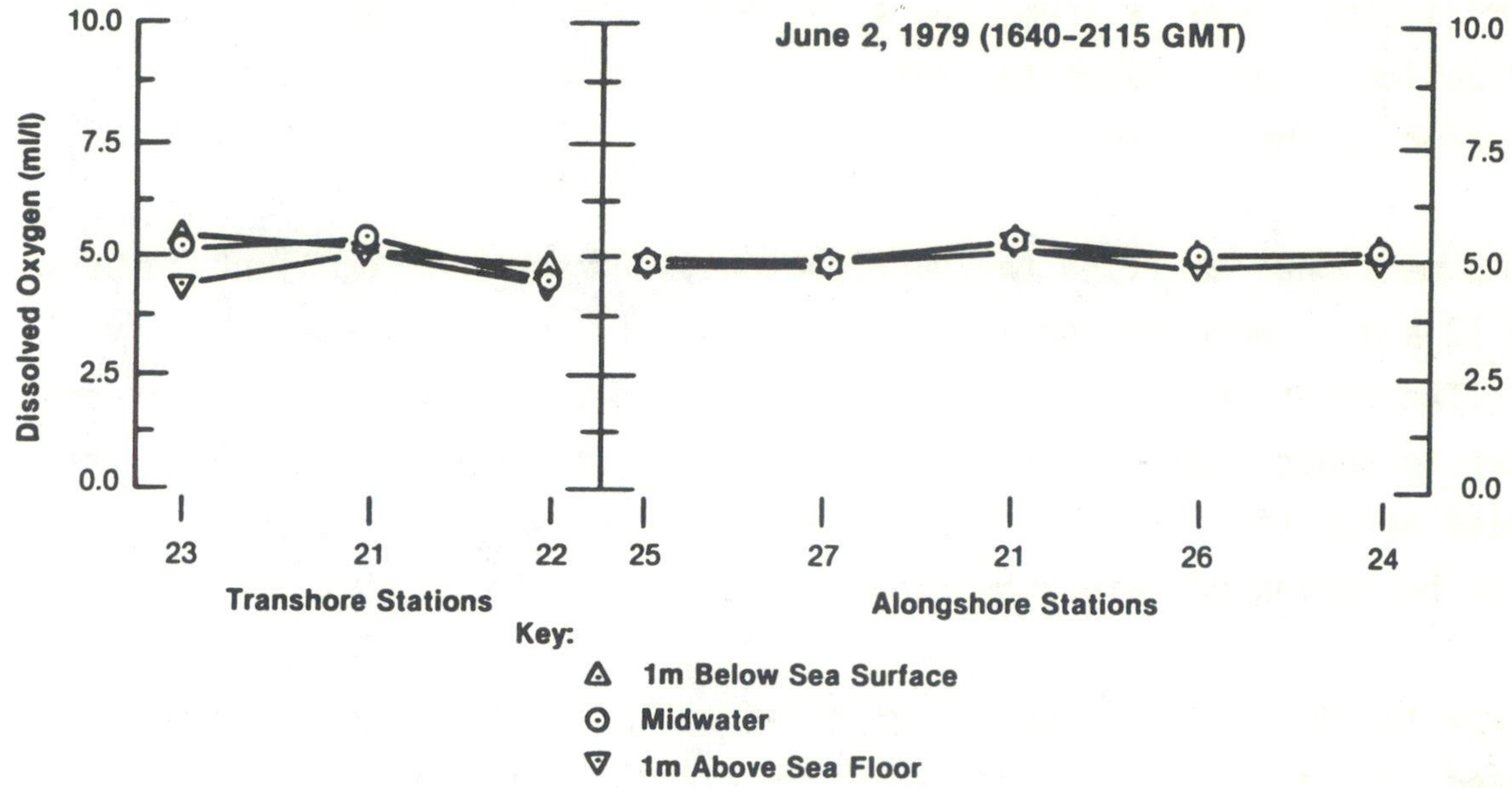

Figure 10-8. Spatial distributions for DO at Weeks Island site, June 1979.

DEBRA caused complete mixing of the water column at the shallow Weeks Island site. The FERREL steamed to the Weeks Island site on September 1 to recover instruments; divers found only about 40 cm of visibility at all stations. On September 8, winds observed by the FERREL gusted to 21 m/s and generated estimated wave heights of 1.2 m by 1500 GMT.

Near-zero gradients of DO observed during September, October, and November are attributed to the energetic mixing of the water column. The DO values averaged for all stations and depths are 4.44 ml/l for September 8, 5.24 ml/l for October 2 to 3, and 5.09 ml/l for November 13 to 14.

DO data obtained during the two January 1979 cruises show near complete mixing of the near-surface and midwater layers, with lower values at most stations in the near-bottom layer. CTD casts made with a Beckman RS-5 in situ salinometer on the VIRGINIA KEY show warmer, more saline water in the near-bottom compared to the midwater and near-surface levels. The warmer, more saline water moved northeastward from offshore, according to the near-bottom current meter at station 21. No CTD data were obtained during the FERREL's January 29-30 cruise.

The DO averaged over all stations and depths for February 20 and 21 is 6.56 ml/l; the range is from 6.51 to 6.61 ml/l. The nearly homogeneous DO distribution is attributed to mixing by winds that were about 8 to 14 m/s for 4 days prior to the cruise.

As mentioned earlier, the vertical and horizontal DO gradients observed on March 12 and 13 were second in magnitude only to those observed on July 21, 1978. The relatively low values of DO in the near-bottom layer are attributed in part to reduced wind energy and increased river runoff which tended to increase stratification; circulation appeared from current meter time series data to be dominated mainly by tidal influence.

Spatial DO gradients were negligible on April 17 and 18. The DO value averaged over all stations and depths is 4.99 ml/l for that cruise, while the range is from 4.91 to 5.10 ml/l. The nearly homogeneous DO distribution is attributed to mixing by strong, veering winds that accompanied frontal passages on April 9 and 14, as observed at station 28.

An overall increase in DO is observed for the May 7-8 cruise, with vertical gradients developing at stations 23 and 27.

On June 2, 1979, vertical mixing was nearly complete, except at station 23 where the near-bottom layer value was 4.47 ml/l, while the midwater and near-surface values were 5.24 and 5.50 ml/l, respectively. CTD profiles obtained then show warming and mixing in the midwater and near-surface layers, with stratification due mainly to cooler water in the near-bottom layer. The lower value of DO near-bottom at station 23 was due to a combination of stratification and depth.

11. SALINITY, TEMPERATURE, AND DENSITY

Temperature and conductivity observations and the resulting computations of salinity and density (sigma-t) at the Weeks Island site exhibit extreme variability. The variability is particularly sensitive to the discharge of fresh water from the Mississippi and Atchafalaya Rivers. Variability at the site also depends on thermal heating and cooling due to weather changes, energetic mixing by wind stress on the sea surface, and changes in the characteristics of the coastal boundary layer.

Figures 11-1 and 11-2 show temperature vs. salinity (T-S) diagrams for CTD casts made during the 12-month period. Data obtained by NMFS on April 30, 1979, and summarized by Parker and Crowe (1980) are included in figures 11-1 and 11-2 because the CTD profiler used by NOS malfunctioned; the Hydrolab Surveyor used by NMFS was calibrated by NOS. Each continuous curve shown in the T-S diagram represents the temperature/salinity structure through the entire water column for each cruise. The length of the curves indicates whether the water column is stratified or well mixed; relatively long curves indicate stratification, shorter curves (approaching points) indicate a well-mixed water column. Warm, low-salinity surface water was associated with highly stable thermohaline stratification during the summer. Colder, higher salinity water occurred through the water column during the winter months when wind stresses induced vertical mixing.

The water temperature reached a maximum of about 30°C during July and August 1978, and was at its minimum of about 10°C during January and February 1979. The time series of mean monthly temperatures obtained with current meters at 1 and 3 m above the sea floor is shown in figure 11-3. Temperatures 1 m above bottom were not obtained for August and December 1978. Water temperature and salinity 1 m below the sea surface are shown in figure 11-4. The near-surface temperatures were obtained with a Grundy 9400 CTD, a Beckman RS-5

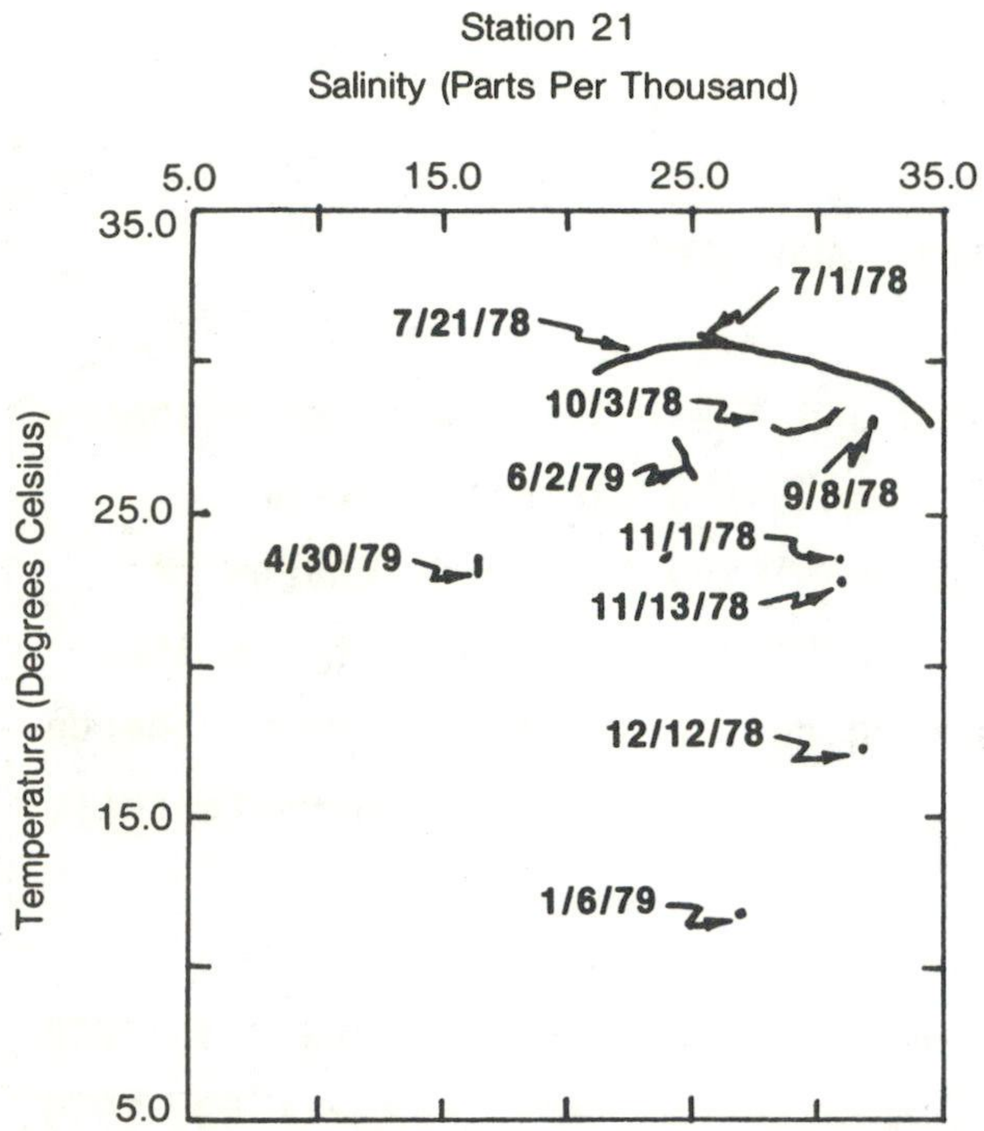

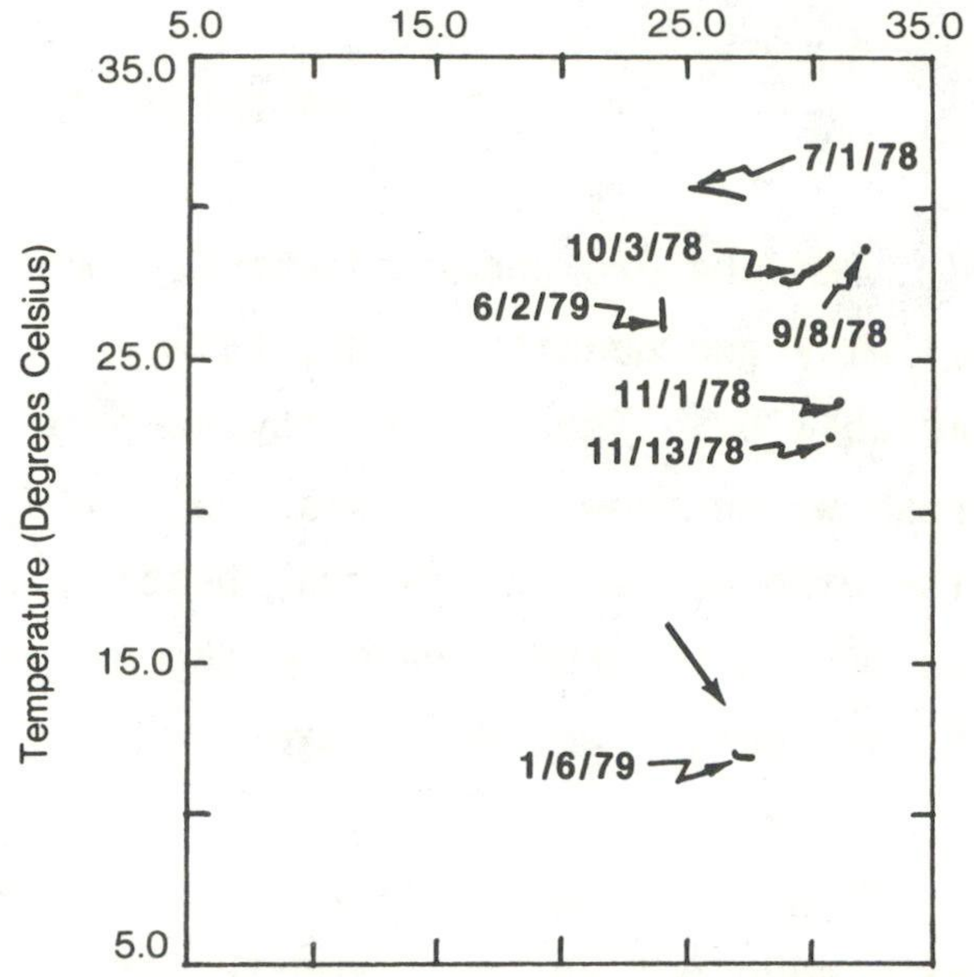

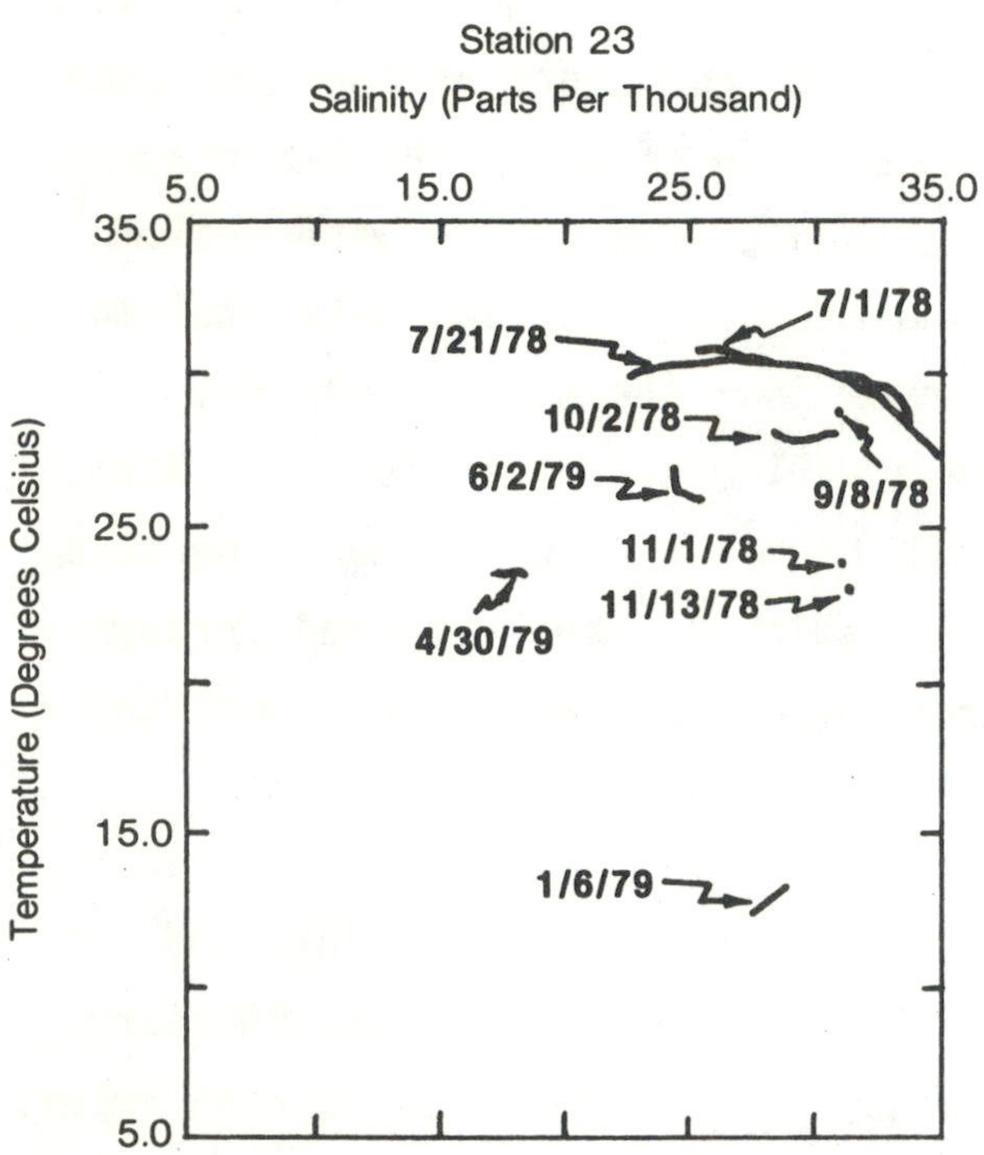

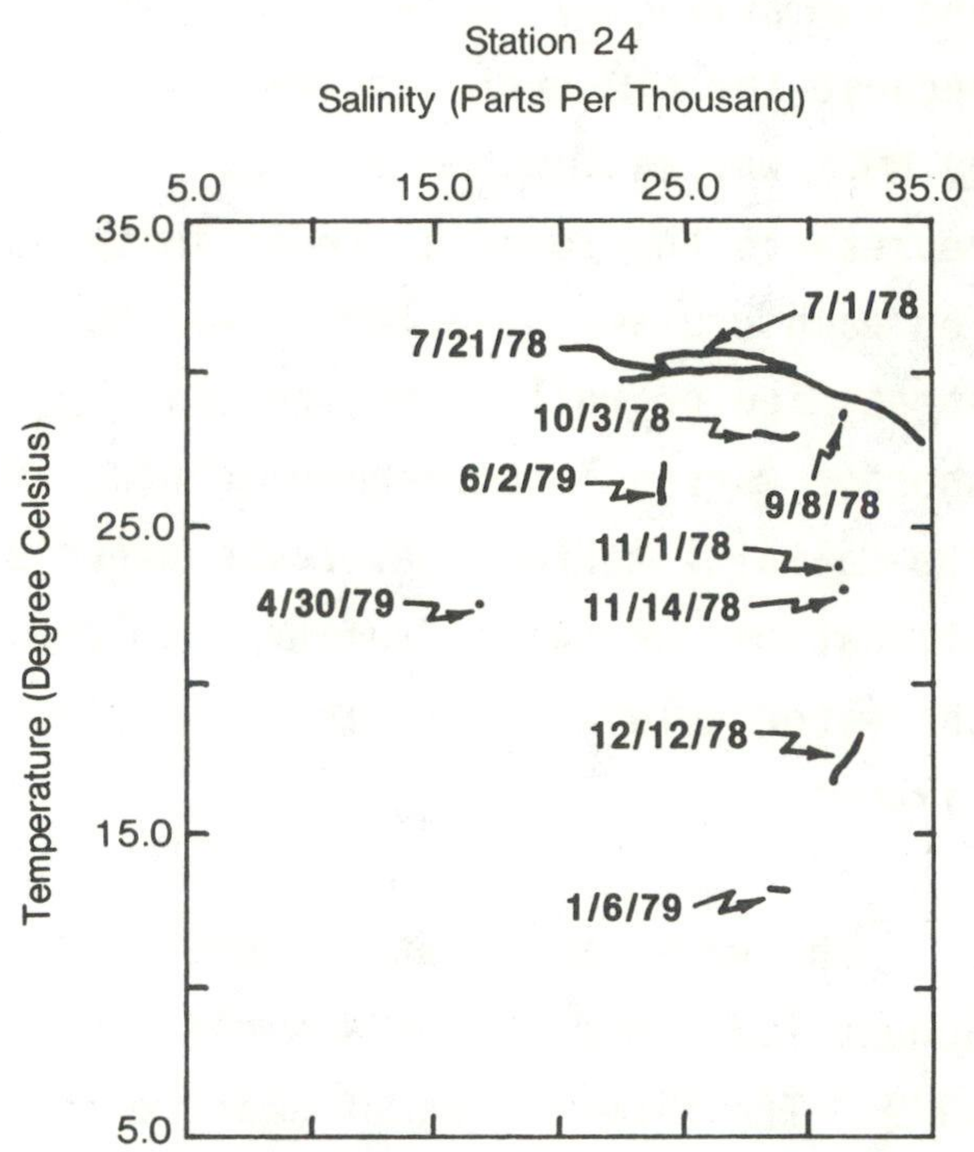

Figure 11-1. Temperature vs. salinity (T-S) diagrams for CTD casts made at Weeks Island stations 21 through 24.

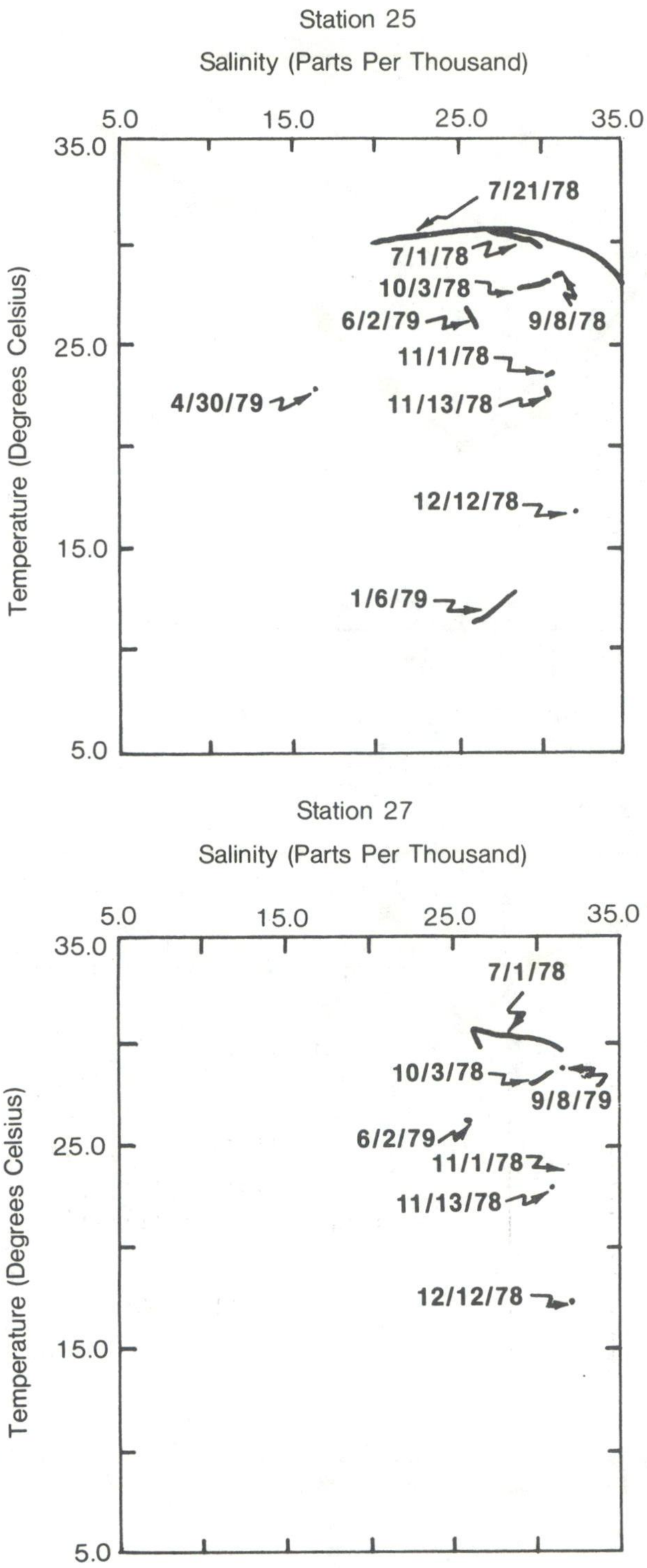

Figure 11-2. Temperature vs. salinity (T-S) diagrams for CTD casts made at Weeks Island stations 25 through 27.

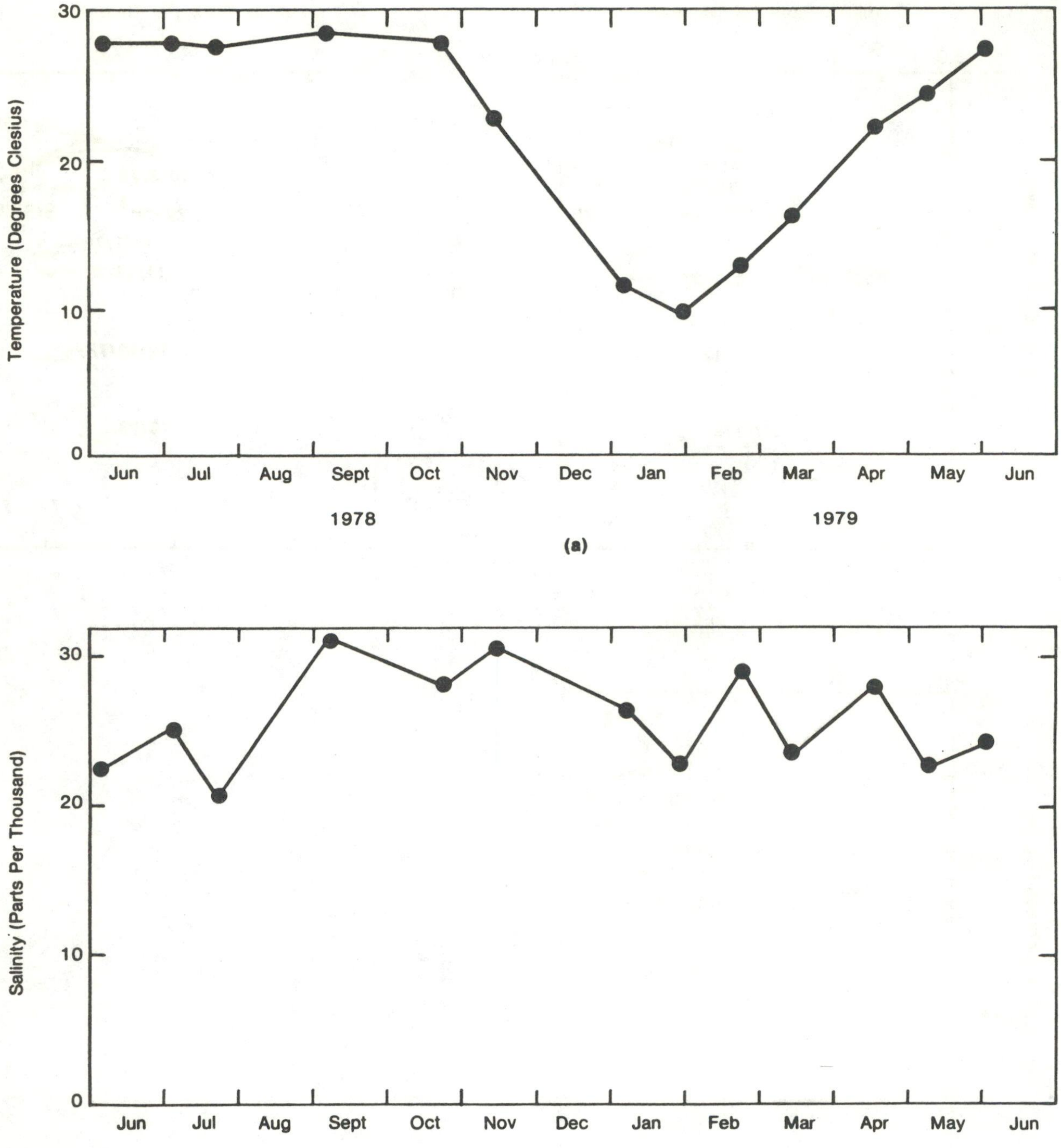

Figure 11-3. Monthly mean temperature for station 21 at 1 and 3 m above bottom from July 1978 through May 1979.

instrument (during December 1978 and January 1979), and by bucket thermometer measurements.

Fresh water discharges from the Mississippi and Atchafalaya Rivers are plotted as monthly means in figures 5-5 and 5-6. As was seen in this and previous sections, river runoff affects the hydrography and circulation significantly. The average observed salinity values tended to be higher during periods of low river runoff.

The hydrographic characteristics at the Weeks Island site are summarized as alongshore and transhore contour plots of salinity and sigma-t. Vertical profiles of temperature, salinity, and sigma-t for all cruises are presented in appendix F (figures F-1 to F-18).

11.1. Summer 1978

Stratification during the early summer 1978 was significant and stable with a well-mixed surface layer and strong gradients. The halocline at station 21 on July 1 had a gradient of 3.5 ppt/m and was from about 5.5 to 6.5 m below the sea surface. The well-defined halocline was accompanied by a thermocline of 0.6°C/m. The mean salinity observed in the surface layer during the July 1 cruise was 25.2 ppt, while the mean salinity in the bottom layer was 30.4 ppt.

Contours of the isohalines and isopycnals for July 1 (figures 11-5 and 11-6) slope upwards the west in the surface layer. The source of this less saline water was the runoff from the Atchafalaya River and the Mississippi River. Figures 5-6 and 5-7 show the discharge from the Mississippi River and Atchafalaya River decreasing in volume during early summer 1978. This trend continued through the summer months.

The contours of salinity and sigma-t (figures 11-7 and 11-8), which are based on data taken during the July 21 CTD cruise, show a higher level of stratification present at Weeks Island on July 21 than July 1. At the site, well-mixed surface and bottom layers were separated by gradients of both temperature and salinity. At station 21, a 7.0 ppt/m halocline 3.3 to 5.0 m below the surface was accompanied by a thermocline of 1.0 C°/m. There was a 13.5 ppt

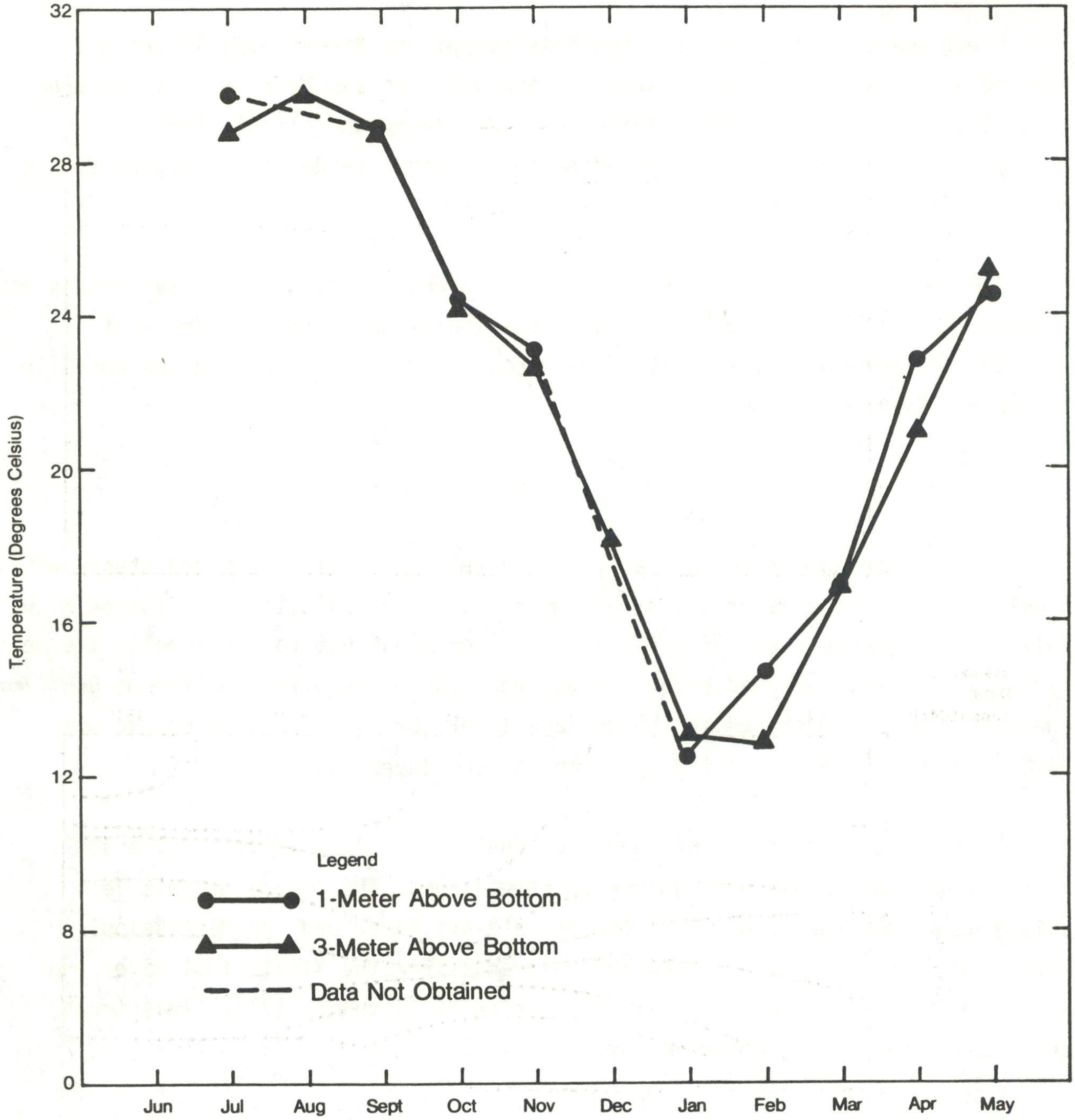

Figure 11-4. Instantaneous values of (a) near-surface temperature and (b) salinity at station 21 from June 3, 1978, to June 2, 1979, 1 m below the surface.

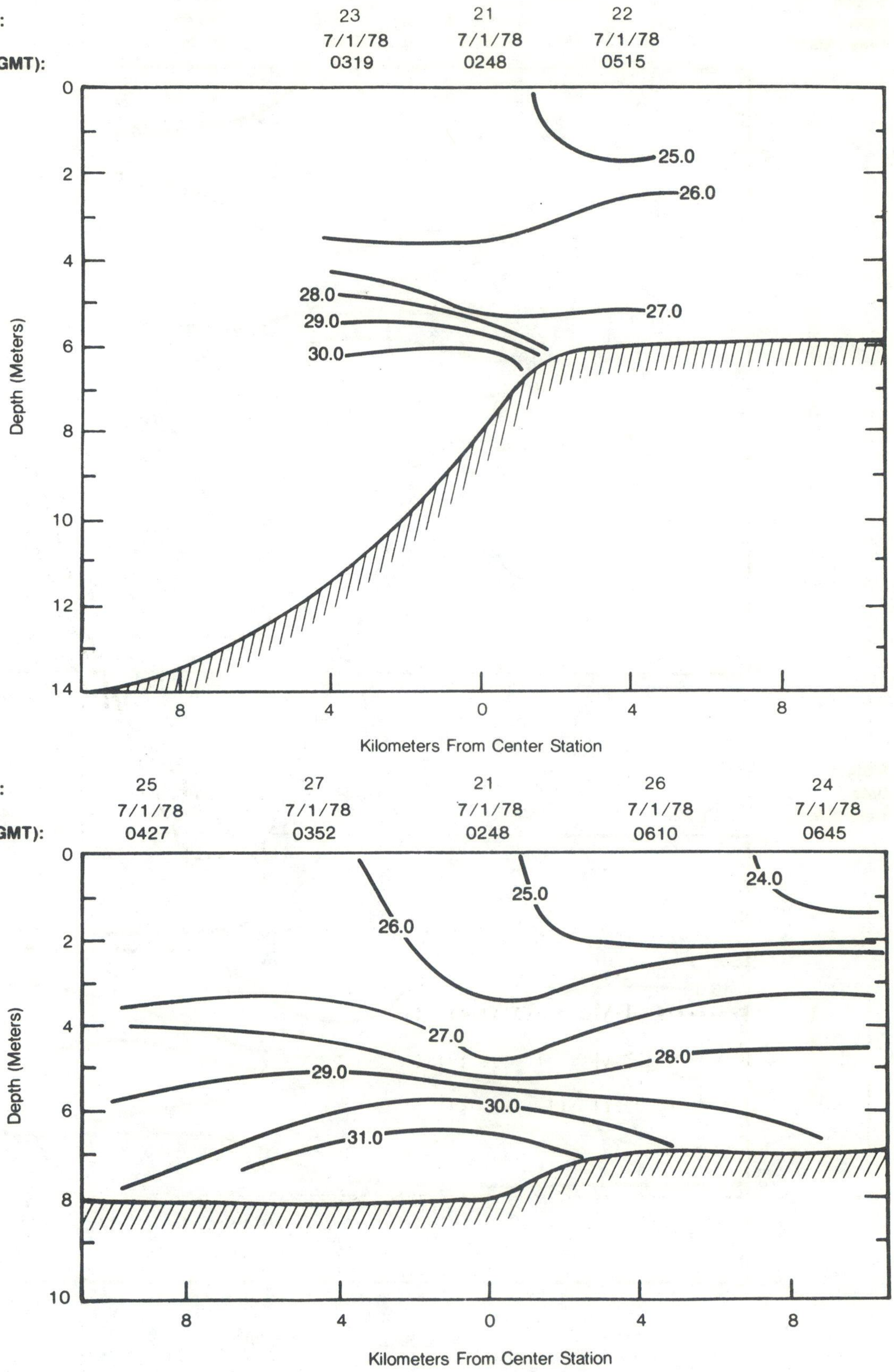

Figure 11-5. Salinity (ppt) contours at Weeks Island for July 1, 1978. Vertical exaggeration 1200:1.

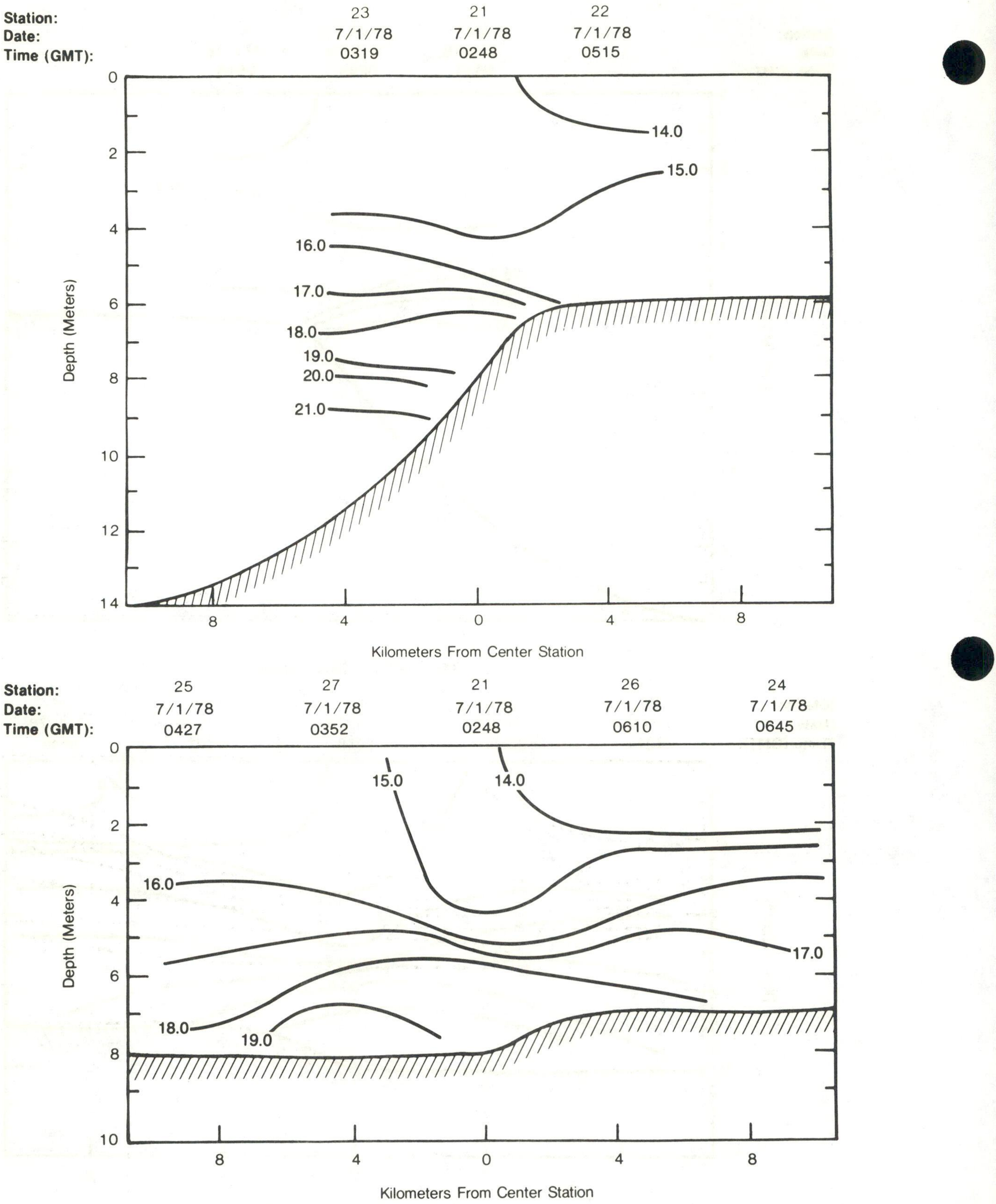

Figure 11-6. Sigma-t (g/cm^3) contours at Weeks Island for July 1, 1978. Vertical exaggeration 1200:1.

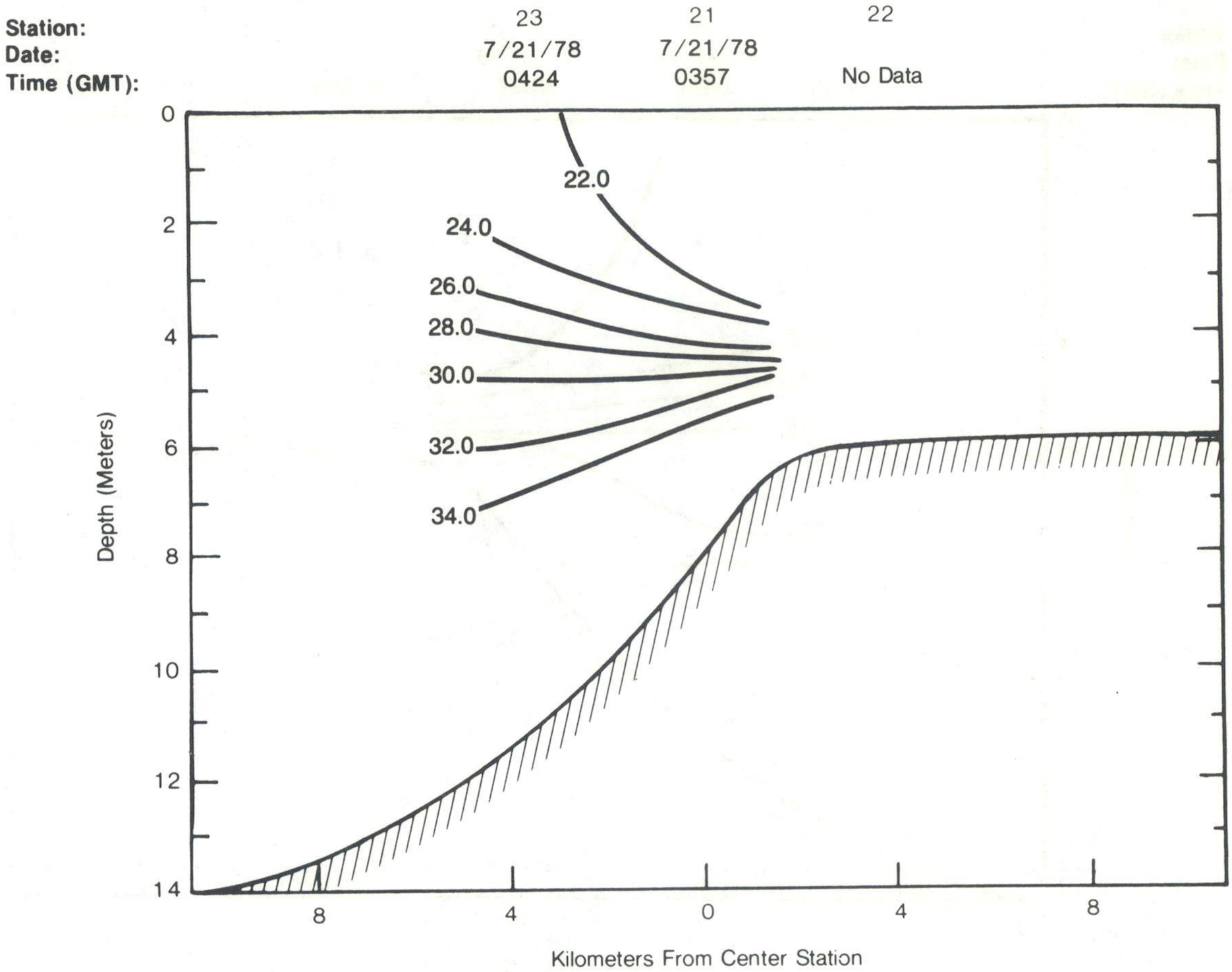

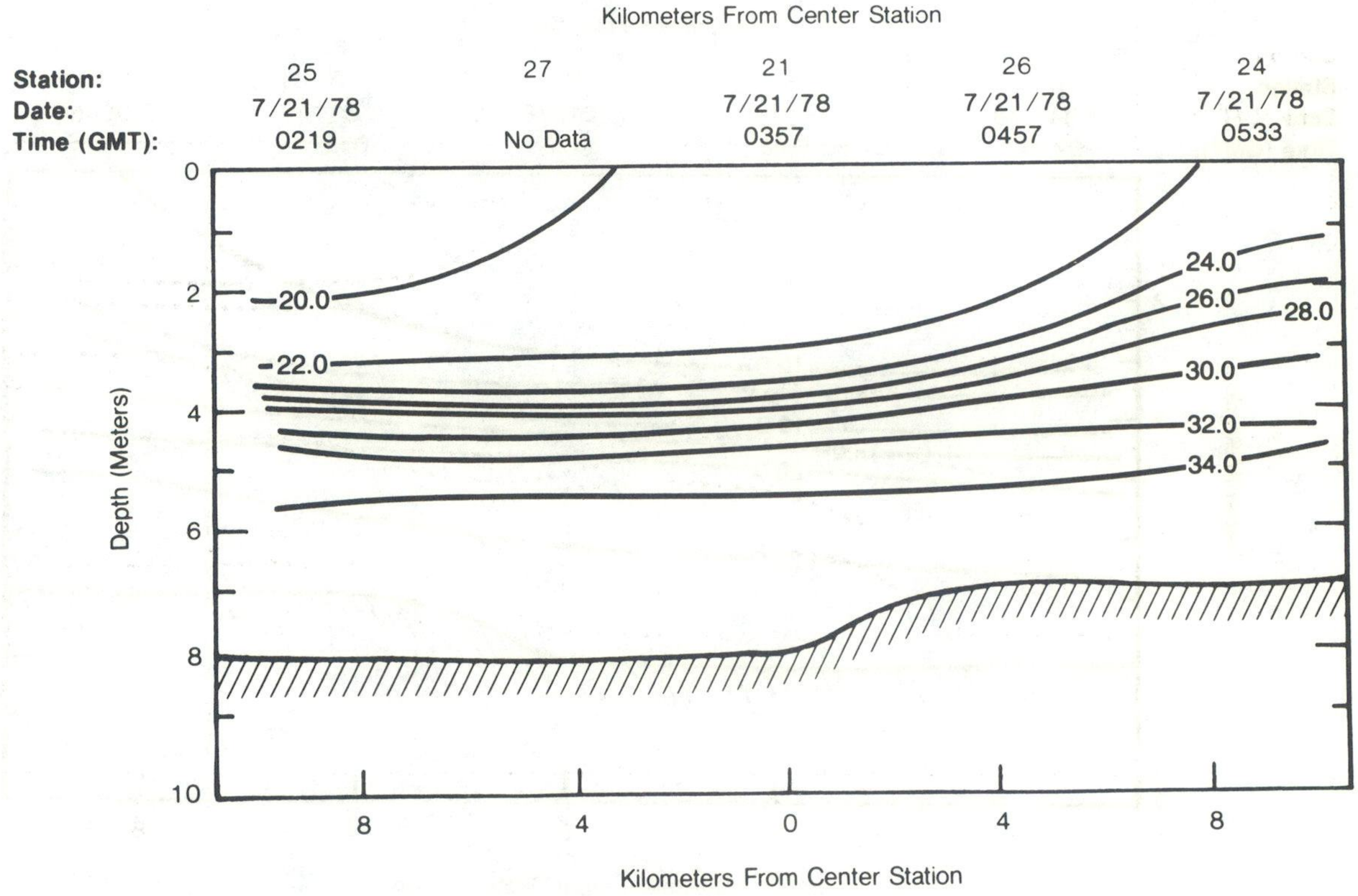

Figure 11-7. Salinity (ppt) contours at Weeks Island for July 21, 1978. Vertical exaggeration 1200:1.

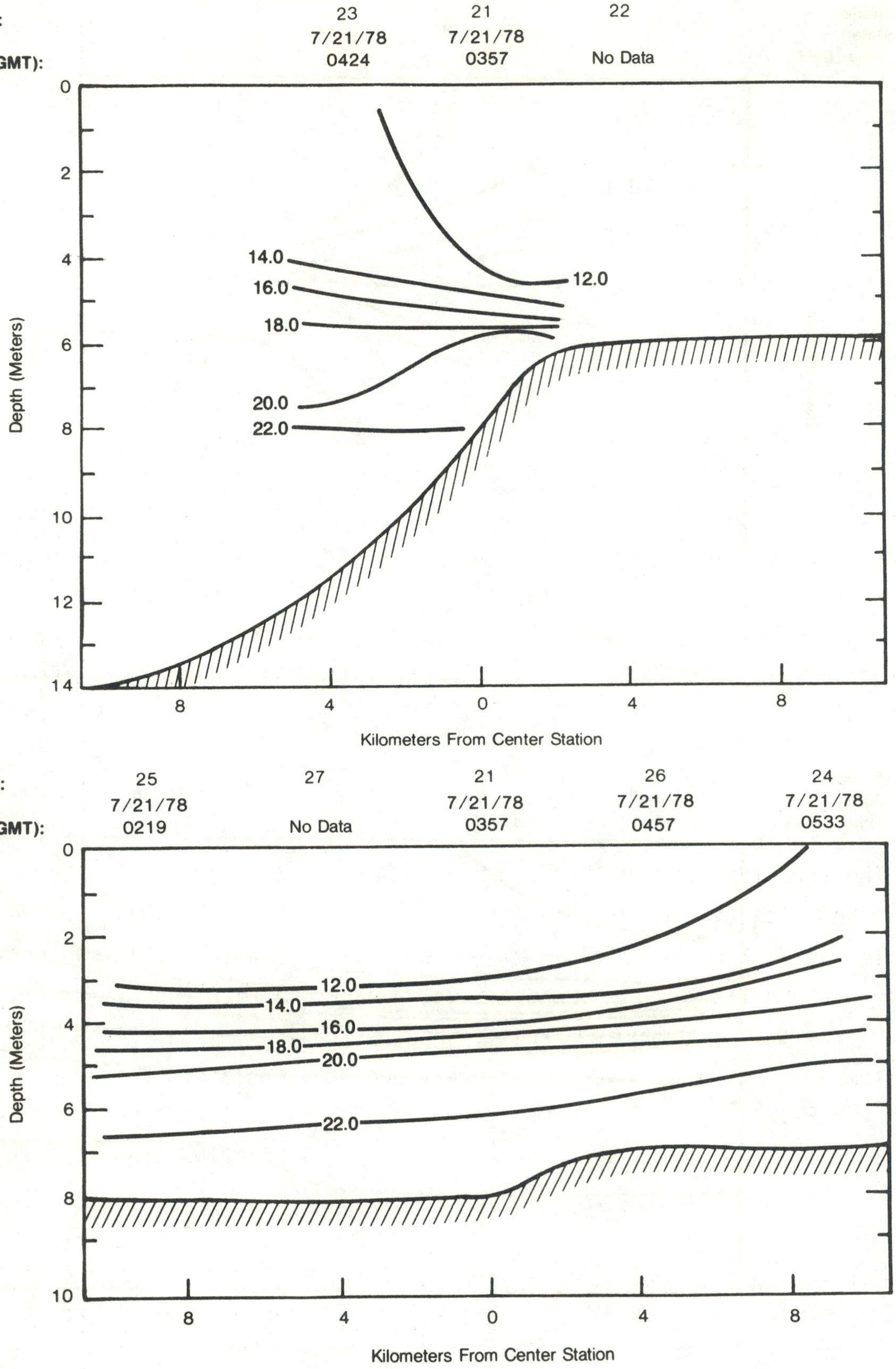

Figure 11-8. Sigma-t (g/cm^3) contours at Weeks Island for July 21, 1978. Vertical exaggeration 1200:1.

salinity differential between the mean near-surface salinity of 21.2 ppt and the mean near-bottom salinity of 34.7 ppt. Although river discharge continued to decrease in July, the stratification remained higher due to low wind stresses.

As mentioned earlier, the FERREL was unable to steam to the Weeks Island site for the August 1978 cruise; thus, no CTD cast data were available for August. The intense meteorological conditions that occurred during the month of August suggest substantial mixing. The sea state during August 8 to 11 was sufficiently severe to cause several of the current meters at Weeks Island to part from their platforms. Tropical Storm DEBRA, described in section 18, approached the western coast of Louisiana on August 27, causing complete mixing of the water column at both the Weeks Island and West Hackberry sites. The well-mixed water column at Weeks Island, as shown in figures F-5 and F-6 on September 8, indicates strong vertical mixing. The mean near-surface salinity of 31.2 ppt for September 8 was an increase in value of salinity from that of early summer. This was the result of the continued low volume of fresh water discharge into the region and the mixing of this discharge with shelf water throughout the water column.

11.2. Fall 1978

The stratification observed during October 2 and 3 was relatively weak in comparison with that observed in July (figures 11-9 and 11-10). The vertical profiles in figures F-7 and F-8 for October 2 and 3 show small gradients of temperature and salinity. The increase in temperature with depth, rather than a decrease as was observed previously, resulted from atmospheric cooling. The mean temperature in the surface layer at the Weeks Island site during October 2 and 3 was 27.9°C, while the mean temperature in the bottom layer was 28.2°C; the mean salinity in the surface layer was 28.4 ppt, while the mean salinity in the bottom layer was 30.2 ppt.

Vertical distribution of temperature and salinity during mid-fall (November 1 and 13-14) indicate a well-mixed environment (figures F-9 through F-12). Both temperature and salinity exhibit negligible gradients. The mean temperature observed on November 1 was 23.6°C, while the mean salinity was

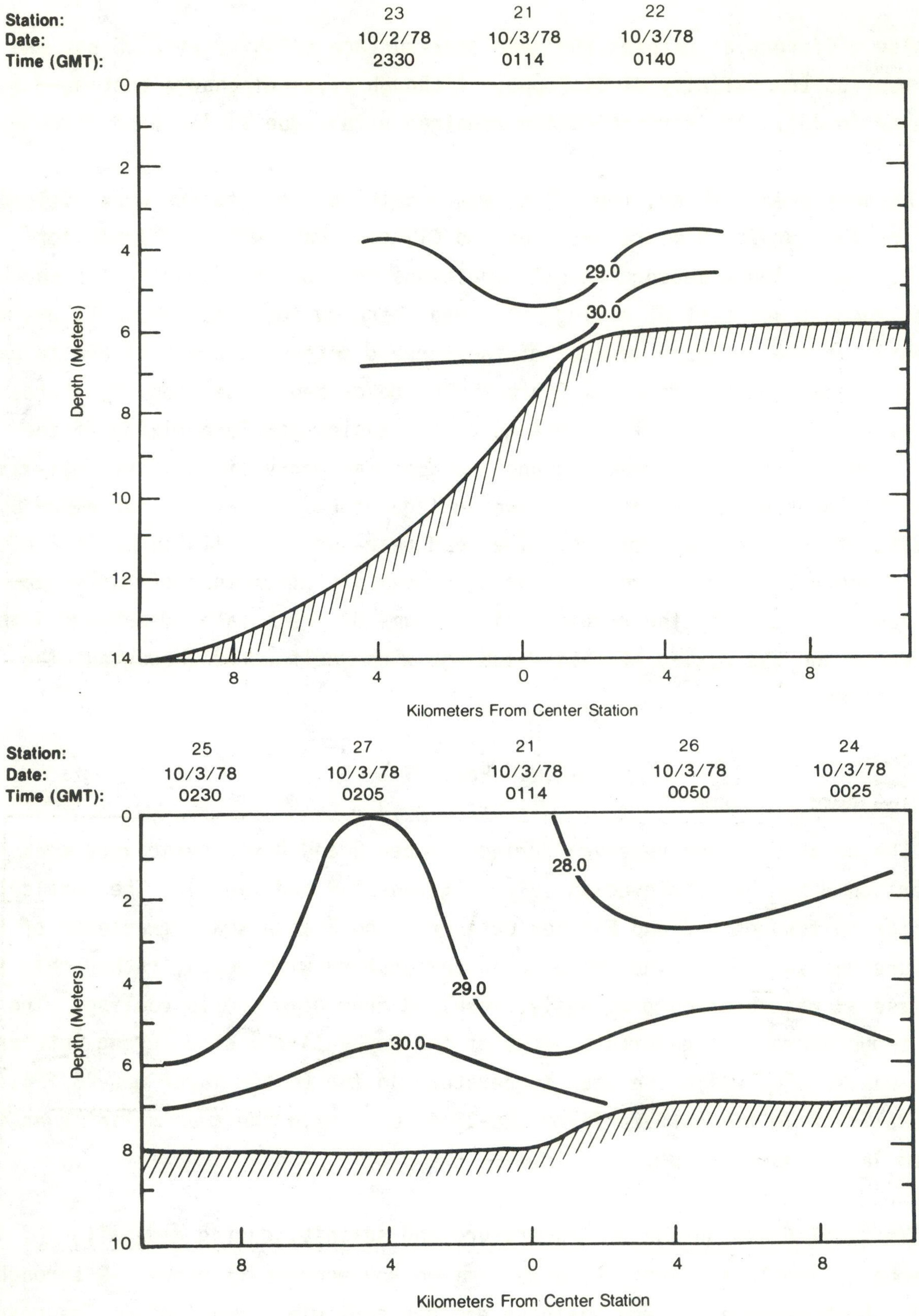

Figure 11-9. Salinity (ppt) contours at Weeks Island for October 2 and 3, 1978. Vertical exaggeration 1200:1.

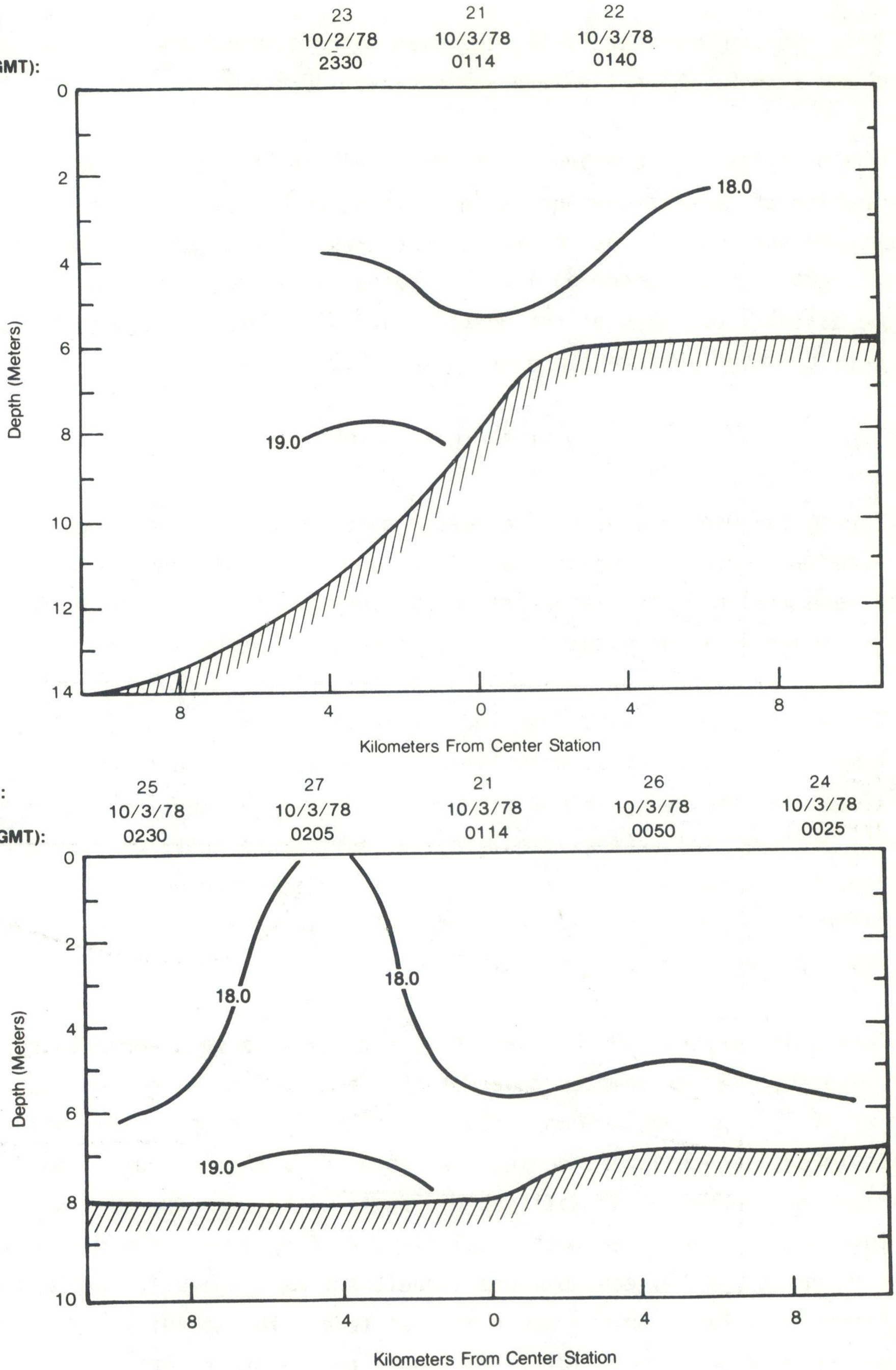

Figure 11-10. Sigma-t (g/cm^3) contours at Weeks Island for October 2 and 3, 1978. Vertical exaggeration 1200:1.

30.7 ppt. During November 13-14, the mean water temperature observed at Weeks Island was 22.8°C, while the mean salinity was 30.8 ppt.

The profiles for December 12 (figures F-13 and F-14) show the vertical distribution of temperature and salinity to be well mixed, with the exception of the eastern station 24. At station 24 the presence of a small temperature and salinity gradient was observed 4 to 5 m below the surface. The mean near-surface salinity observed at the Weeks Island site during December 12 was 31.6 ppt; the mean surface temperature was 17.0°C.

11.3. Winter 1979

During the winter months, freshwater discharge increased in volume from that observed during summer and fall, with a substantial increase during March. The extreme mixing of the water column by wind stress on the sea surface, however, apparently inhibited stratification at the Weeks Island site.

The contours of salinity and sigma-t in figures 11-11 and 11-12, based on data taken during January 6, show the waters at the site to be weakly stratified. At the Weeks Island site during January 6, there was only a 0.6 ppt salinity differential between the mean near-surface salinity of 27.4 ppt and the mean near-bottom salinity of 28.0 ppt. This was accompanied by a 0.5°C temperature differential between the mean near-surface temperature of 12.1°C and the mean near-bottom temperature of 12.6°C.

During January 29 and 30, thermohaline conditions were more favorable for stratification. Water samples taken at the Weeks Island site had a mean surface salinity of 23.1 ppt and a mean bottom salinity of 28.8 ppt. In contrast, water samples taken 3 weeks later, during the February 20 and 21 cruise indicate a well-mixed environment; the salinity differential between the mean surface salinity, 29.0 ppt, and the mean bottom salinity, 29.4 ppt, was only 0.4 ppt. During March 12 and 13, environmental conditions were again favorable for stratification. Based on the water samples taken, the salinity differential between the near-surface salinity, 25.9 ppt, and the near-bottom salinity, 31.5 ppt, was 5.6 ppt.

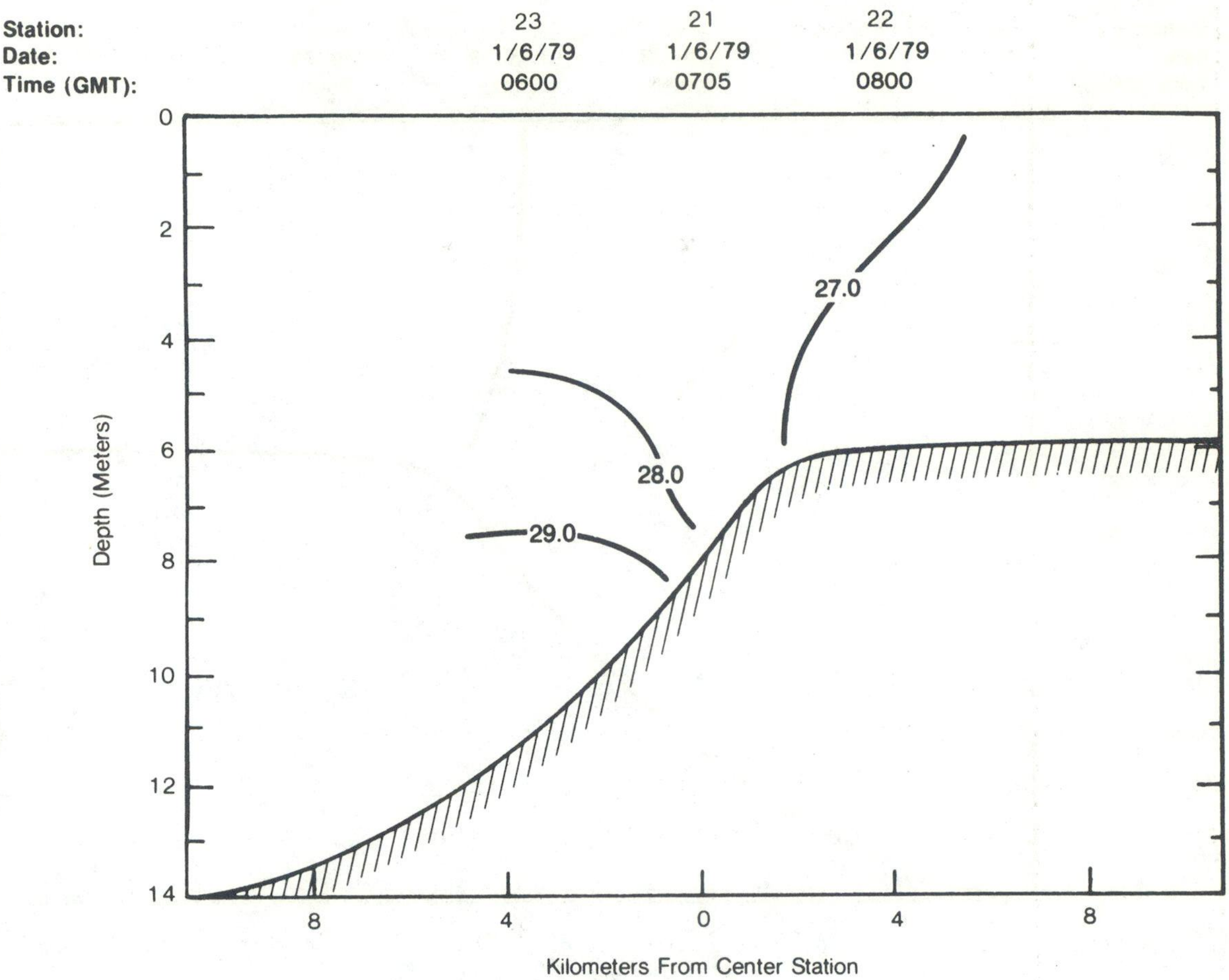

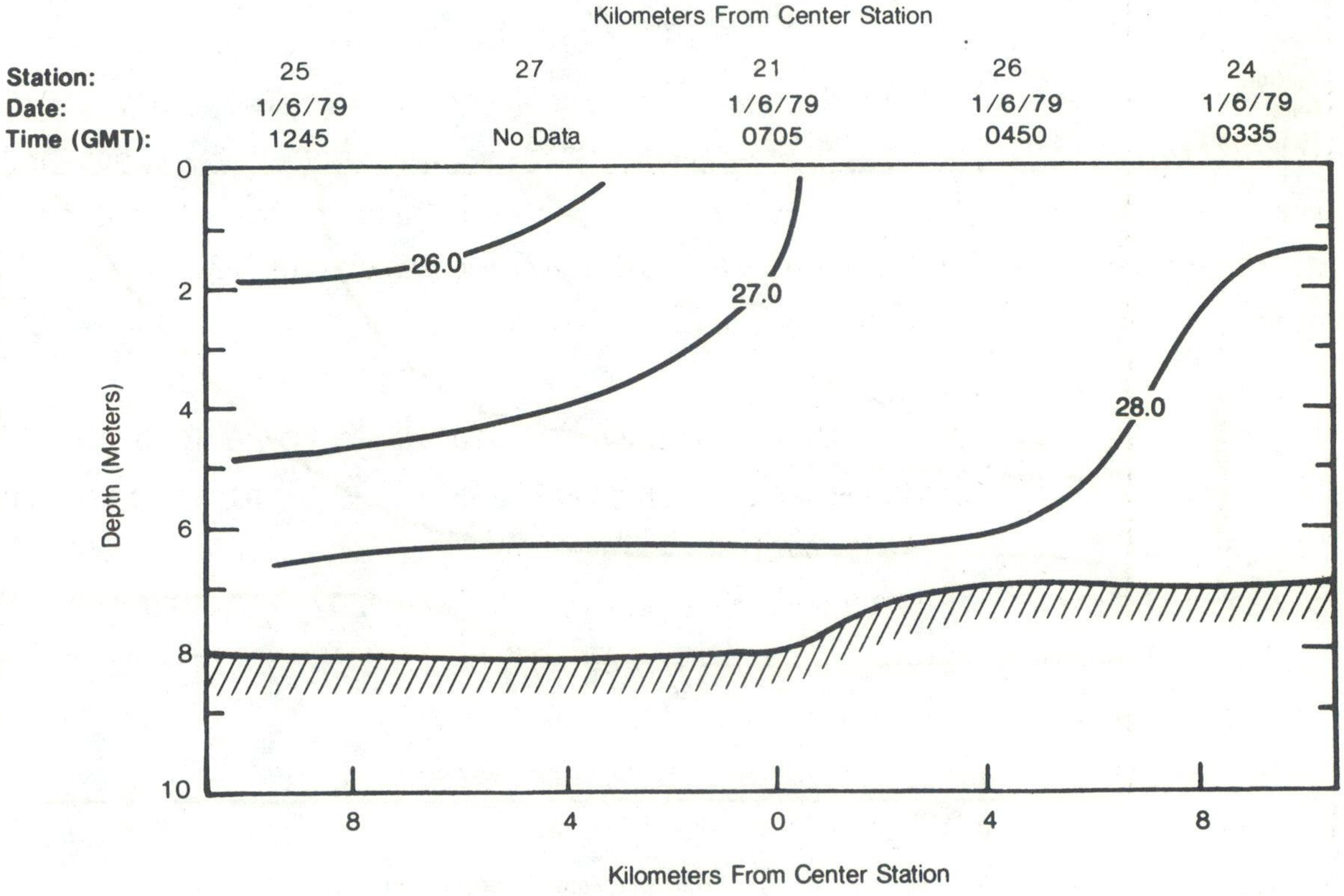

Figure 11-11. Salinity (ppt) contours at Weeks Island for January 6, 1979. Vertical exaggeration 1200:1.

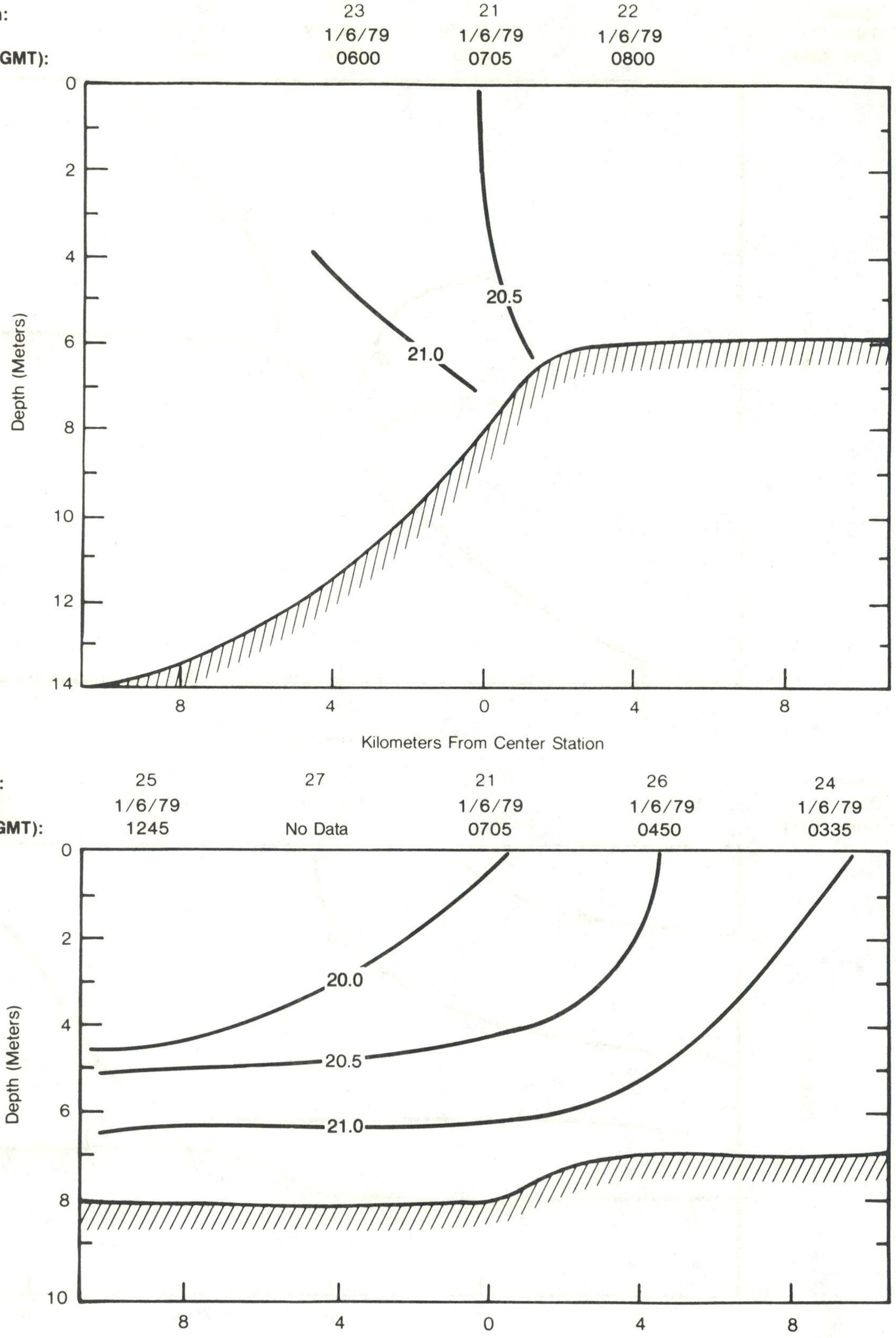

Figure 11-12. Sigma-t (g/cm^3) contours at Weeks Island for January 6, 1979. Vertical exaggeration 1200:1.

11.4. Spring 1979

The hydrographic conditions in early to mid-spring were influenced by the strong winds that occurred during early spring and the higher volume of river discharge that peaked during the months of April and May. Although the discharge was sufficient to dilute the shelf water in the site area, the intense mixing that occurred inhibited strong vertical stratification. At Weeks Island on April 17 and 18, the water column was well-mixed with both the near-surface and near-bottom layers having a salinity of 28.3 ppt. On May 7 and 8 the water column was again well-mixed, but was substantially lower in salinity with a mean surface salinity of 22.8 ppt and a mean bottom salinity of 23.0 ppt.

Figures F-17 and F-18 show vertical distribution of temperature, salinity, and sigma-t on June 2. These profiles and the contours of salinity and sigma-t (figures 11-13 and 11-14) show the water column to be weakly stratified with the salinity differential between the mean surface salinity, 24.5 ppt, and the mean bottom salinity, 25.0 ppt, to be 0.5 ppt. The mean surface temperature was found to be 26.9°C, while the mean bottom temperature was 26.0°C.

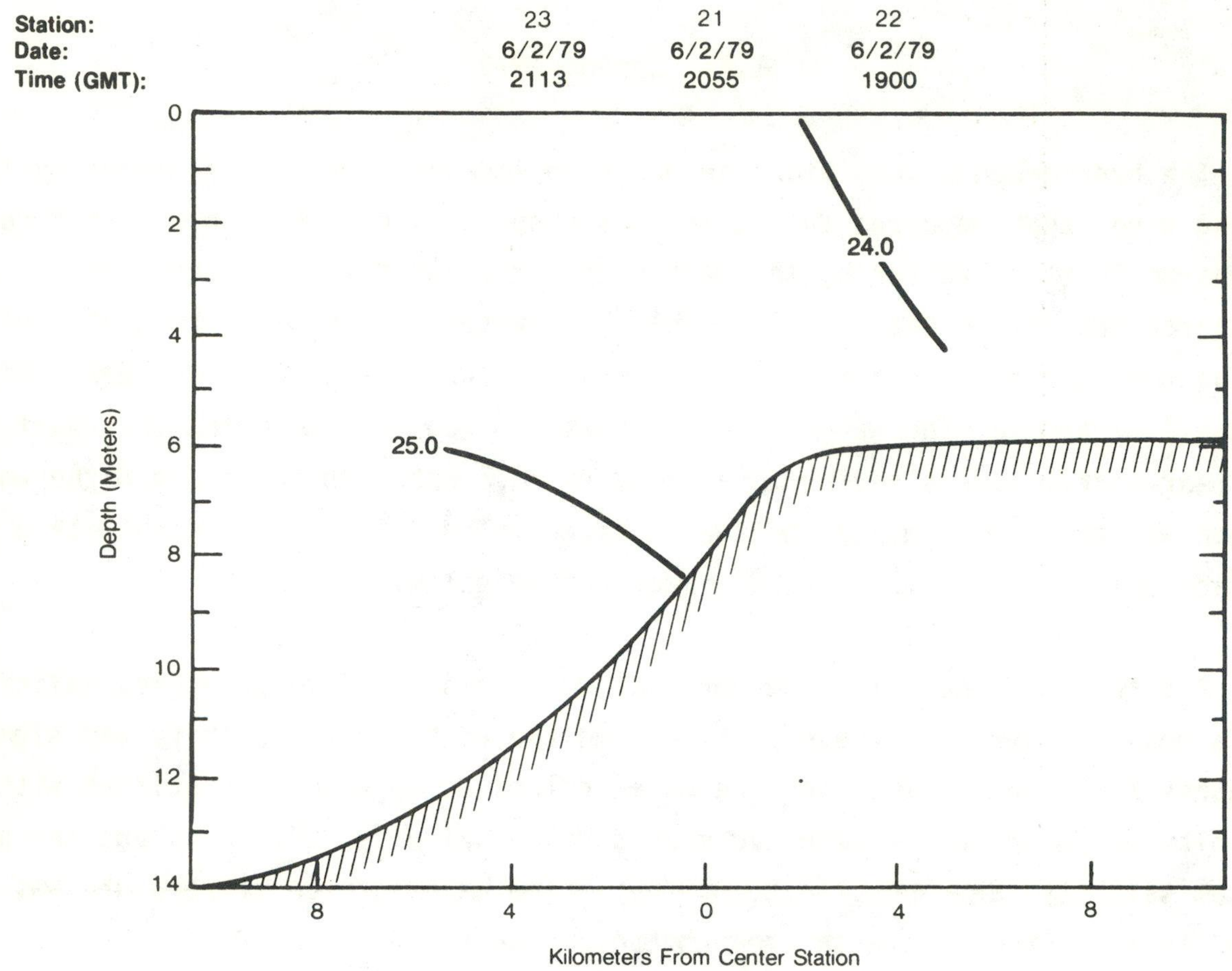

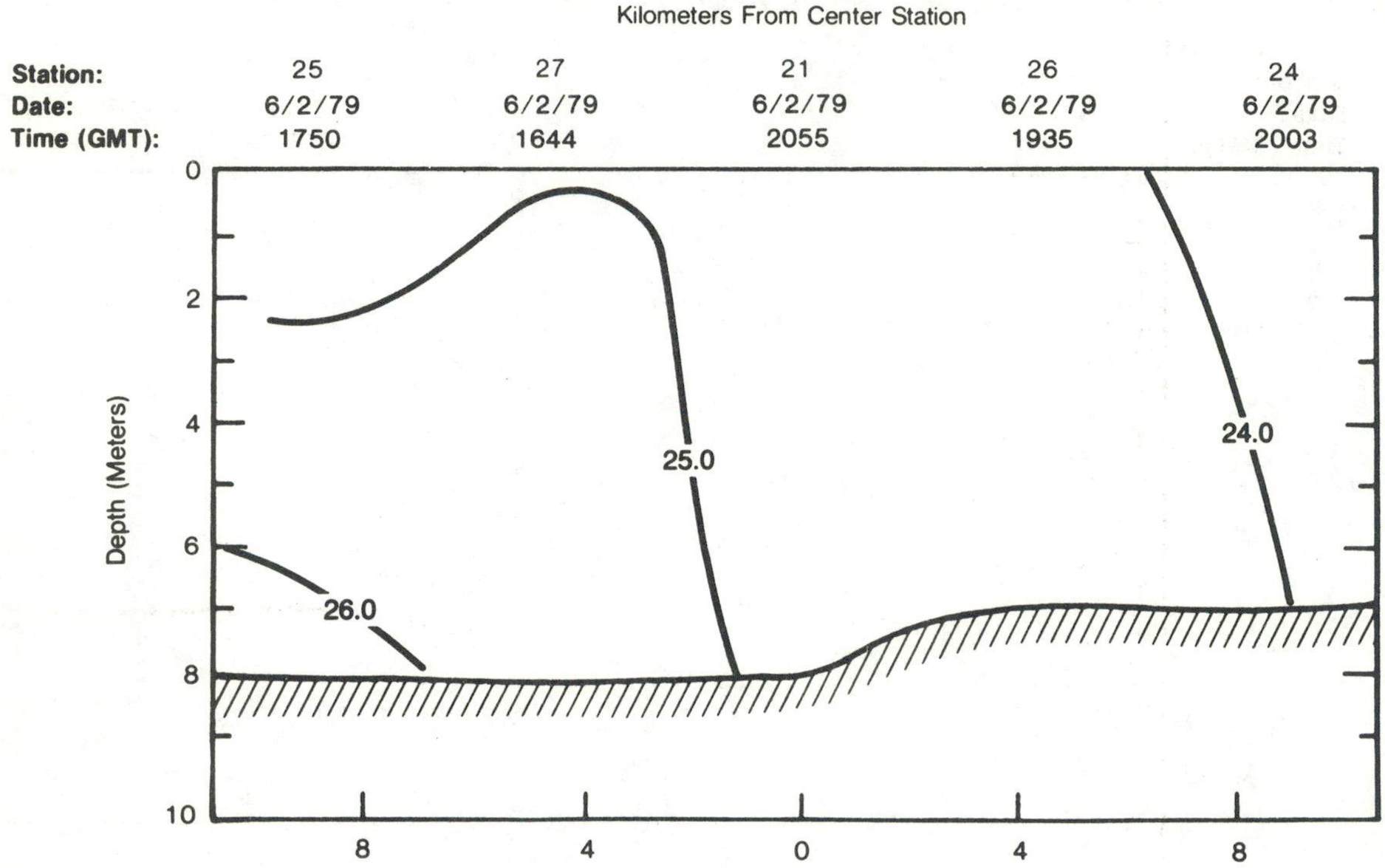

Figure 11-13. Salinity (ppt) contours at Weeks Island for June 2, 1979. Vertical exaggeration 1200:1.

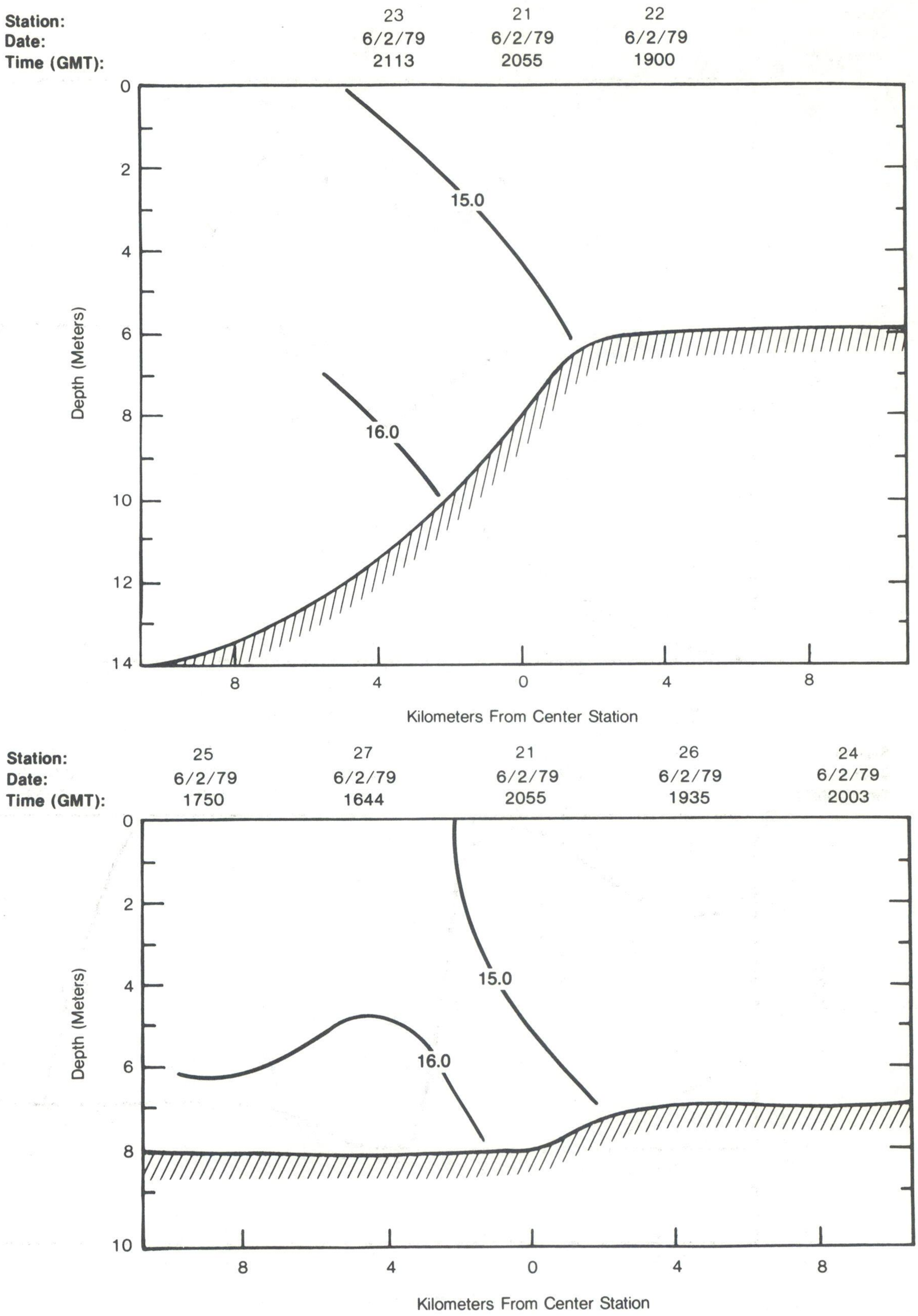

Figure 11-14. Sigma-t (g/cm^3) contours at Weeks Island for June 2, 1979. Vertical exaggeration 1200:1.

12. LOCAL METEOROLOGY

There are large annual variations in the meteorological conditions at the Weeks Island site, which are dominated by the regional atmospheric and oceanographic conditions discussed in section 2. In this section, we describe observations at NOS station 28. Surface weather observations recorded by the National Weather Service at Intracoastal City, La., located 90 km northwest of the site area, were used for a general weather synopsis when station 28 was inoperable. Storms are described further in sections 18 to 20.

12.1. Air Temperature

During the summer, the mT air mass at Intracoastal City was generally warm; daytime air temperature was predominately in the high 20's (°C). Air temperatures decreased sharply between September and October, with increases in cP air intrusions after frontal passages. This trend continued until January. During January and February, temperatures reached a low of about 3.0°C at station 28. Air temperature increased during the end of February and, by June, returned to values observed 12 months earlier. Table 12-1 summarizes the air temperature observed at station 28 for several data collection periods.

12.2. Wind Speed and Direction

During the summer, winds were predominantly from the south and generally weak, except during the passage of summer storms. The wind direction changed during September to a more predominant northeasterly direction, in response to increasing passages of polar fronts.

Figures 12-1 to 12-3 show time histories of meteorological data at station 28 for periods during fall, winter, and spring. Wind direction refers to the direction from which the wind is coming. Wind speeds during the fall averaged 5.8 m/s, and were predominantly from the northeast and northwest.

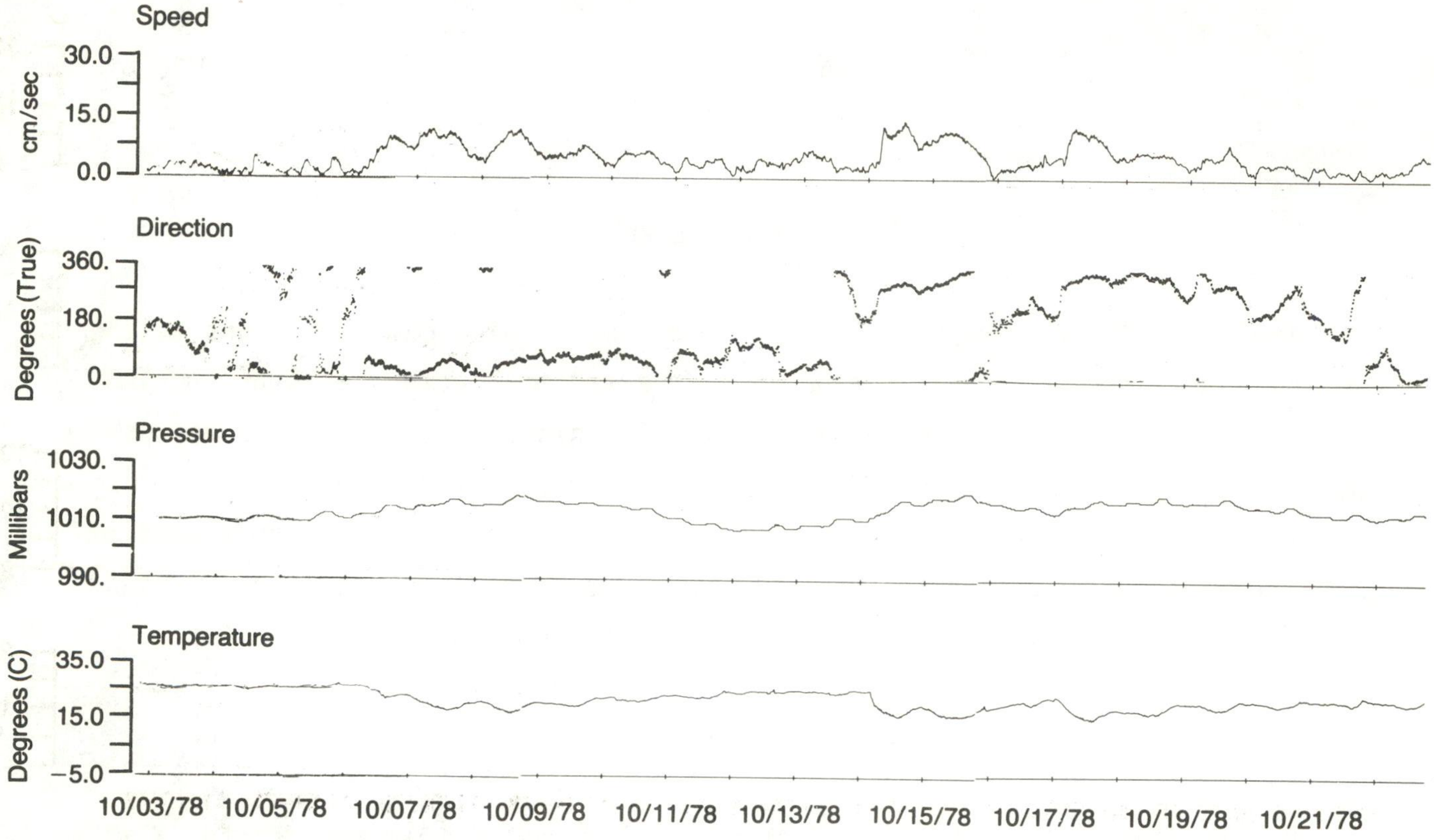

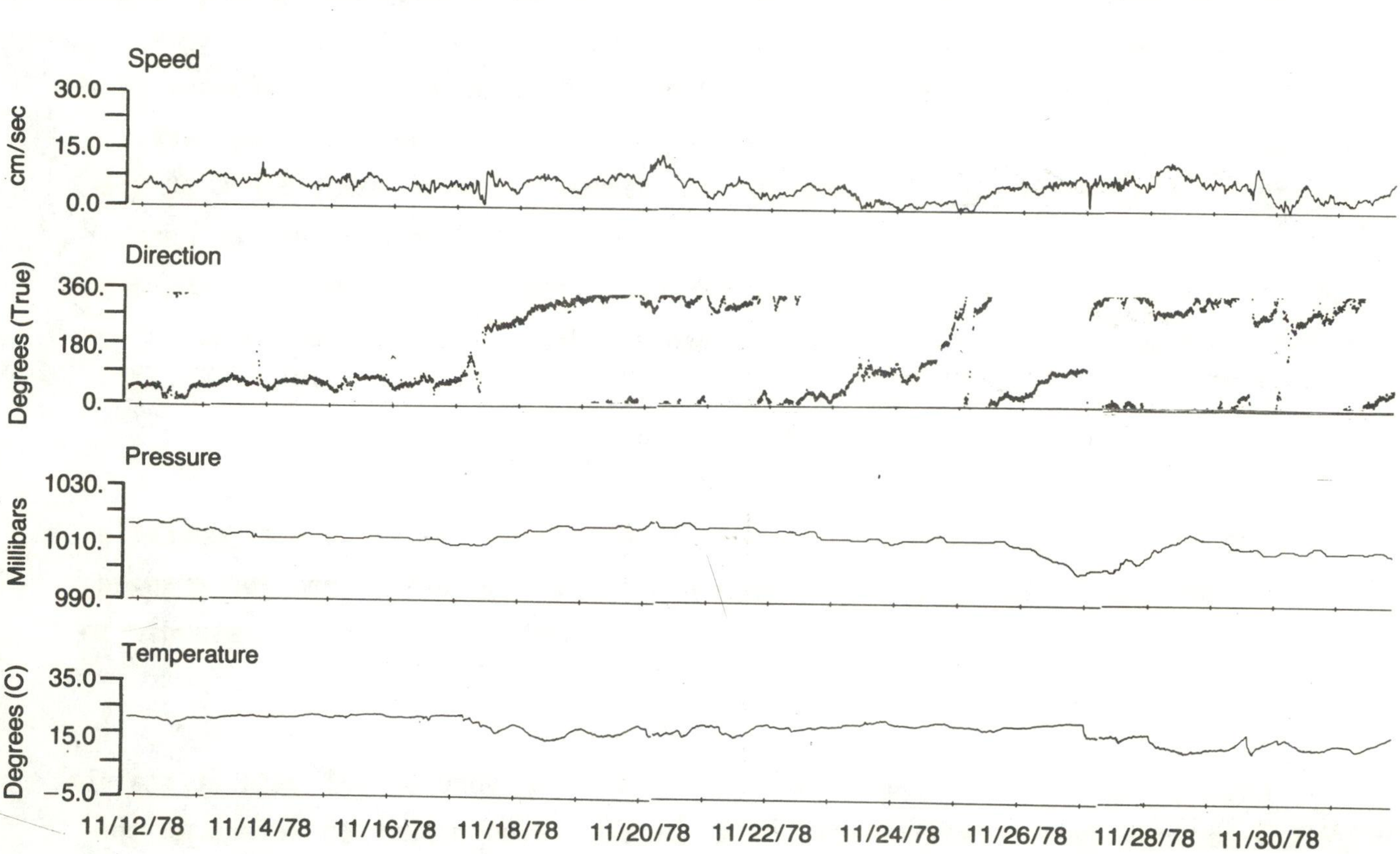

Figure 12-1. Time histories of meteorological data at station 28 for October 3 to November 11, and November 12 to December 10, 1978.

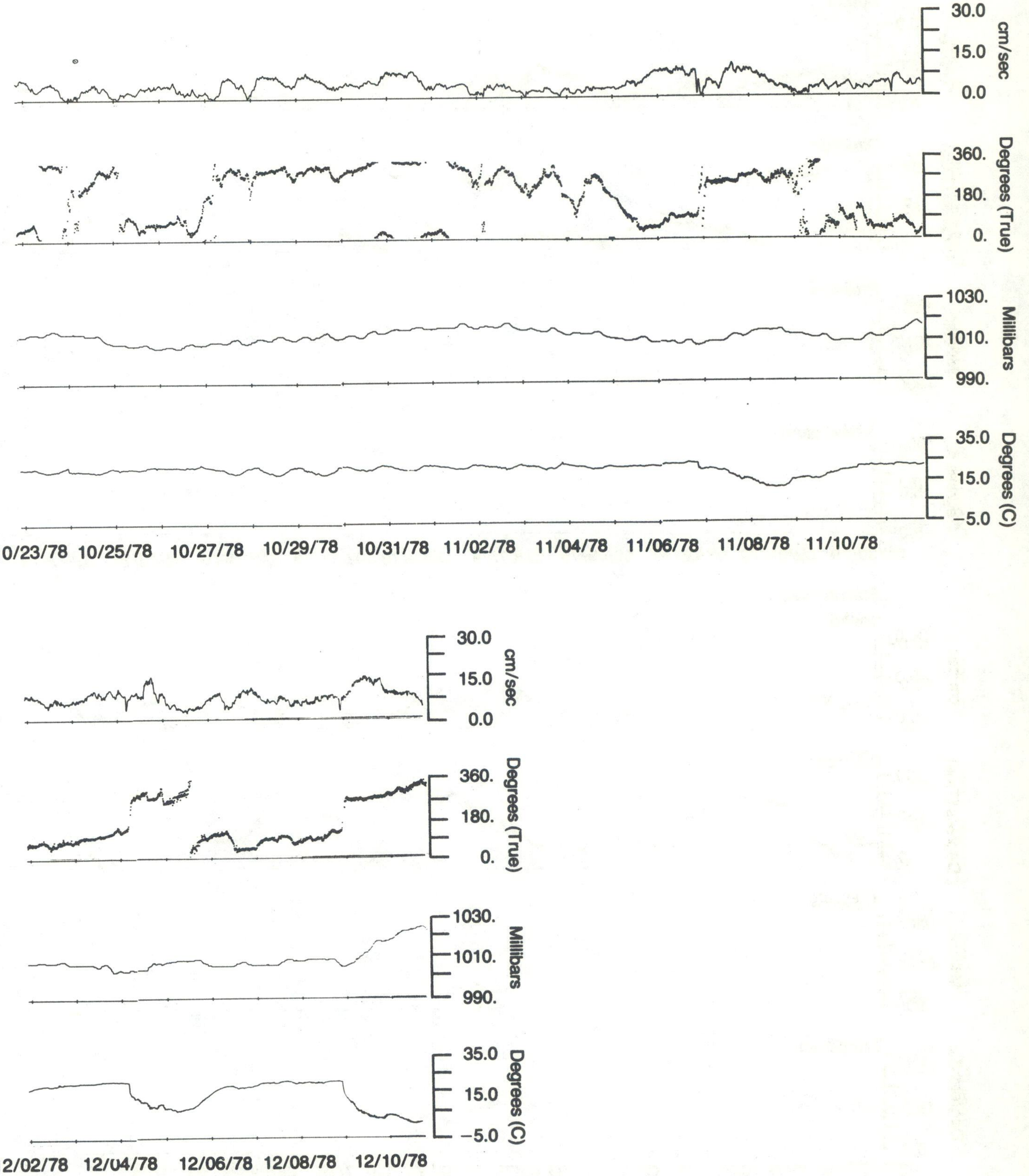

Figure 12-1. Time histories of meteorological data at station 28 for October 3 to November 11, and November 12 to December 10, 1978.

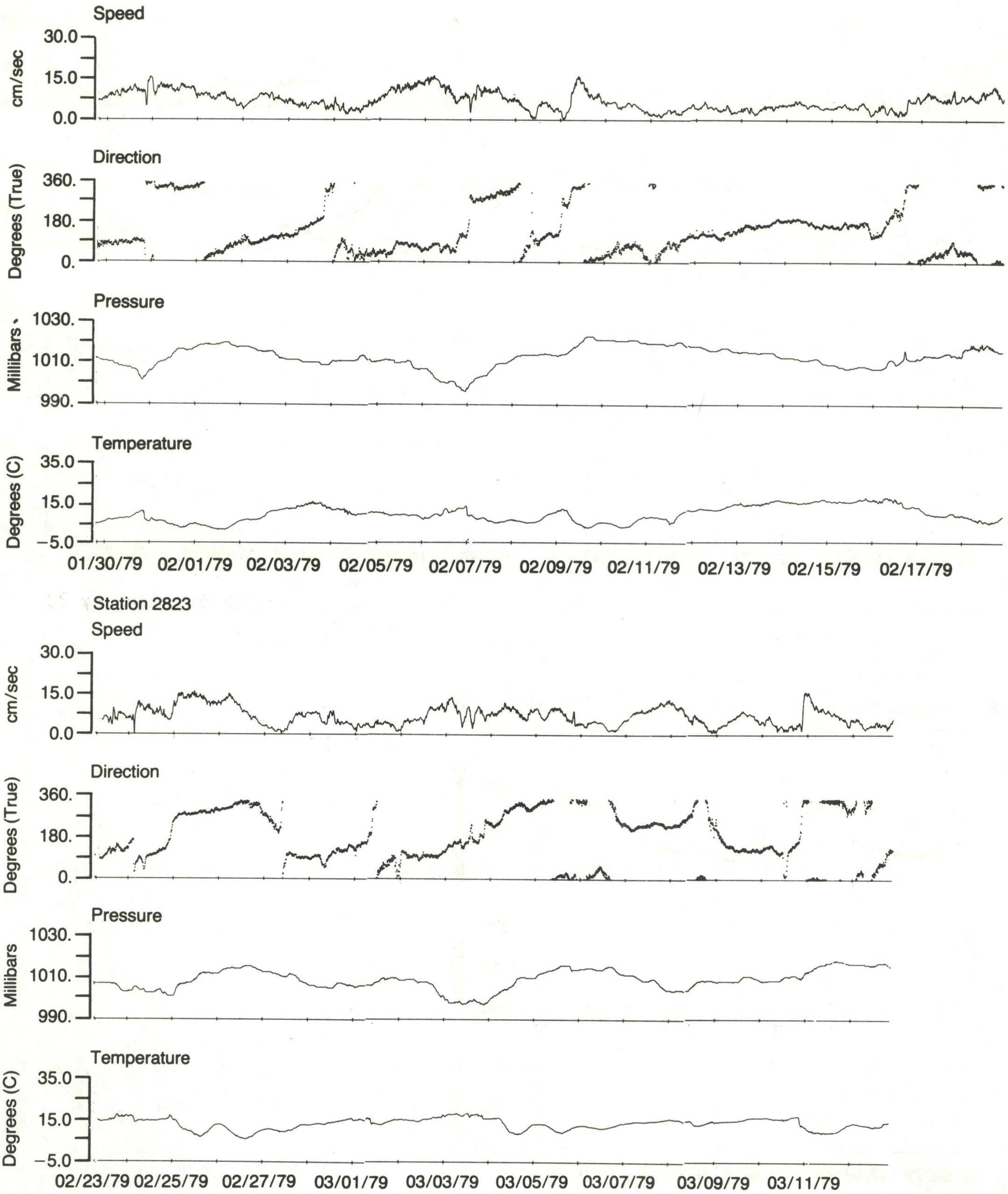

Figure 12-2. Time histories of meteorological data at station 28 for January 30 to February 22, and February 23 to March 12, 1979.

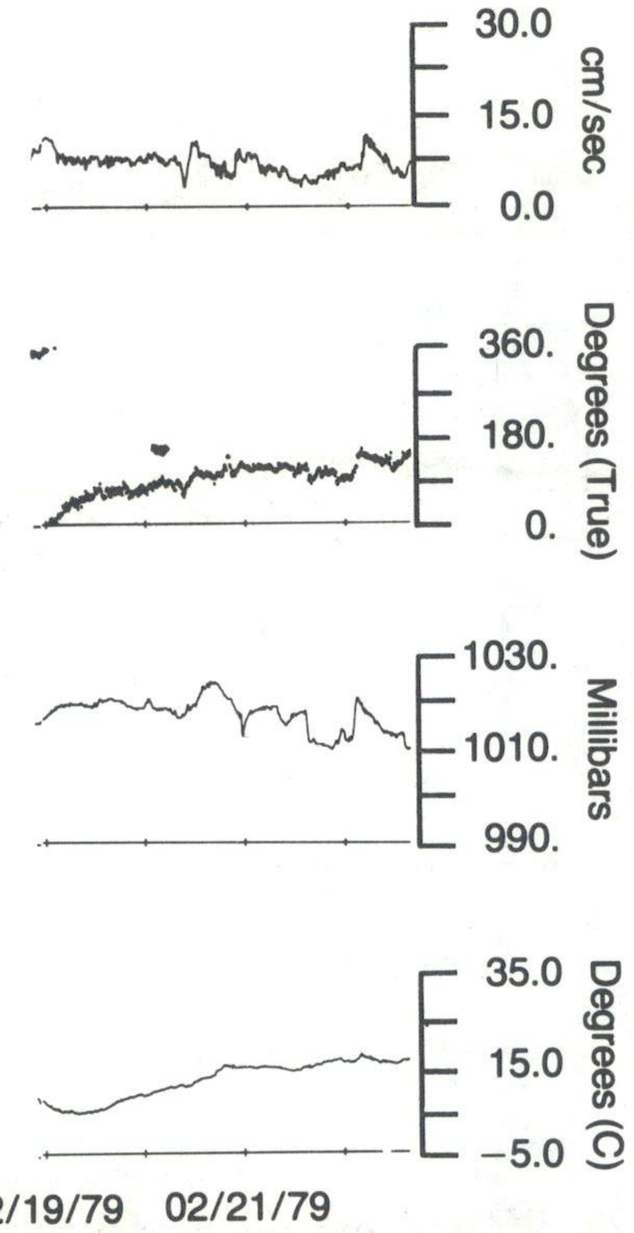

Figure 12-2. Time histories of meteorological data at station 28 for January 30 to February 22, and February 23 to March 12, 1979.

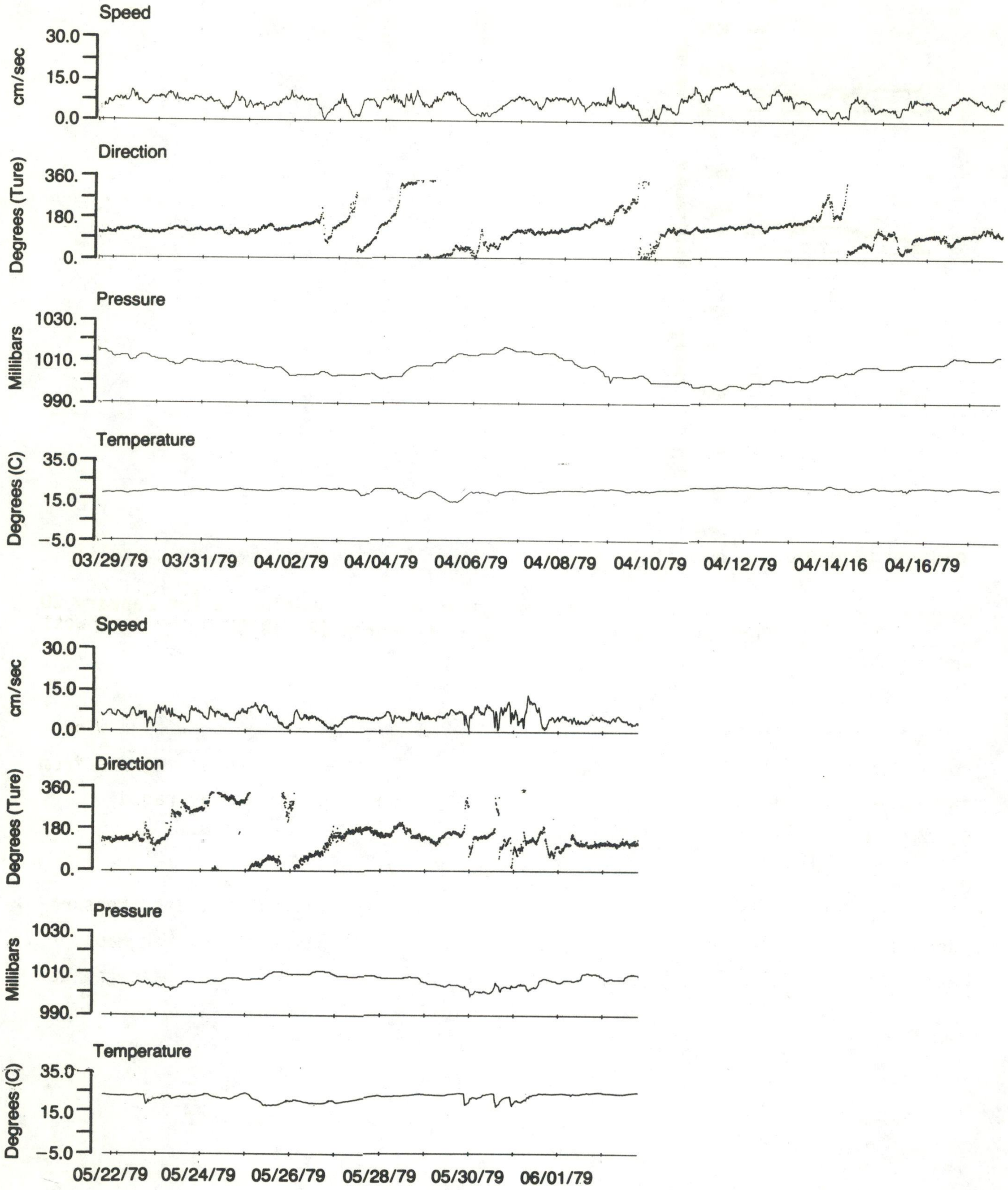

Figure 12-3. Time histories of meteorological data at station 28 for March 29 to April 17, and May 22 to June 2, 1979.

Table 12-1. Air temperature at station 28

Periods	Mean air temperature (°C)	Standard deviation (°C)
10/3/78 - 10/31/78	22.4	±2.2
11/1/78 - 11/30/78	20.9	±2.8
12/1/78 - 1/9/79	17.9	±5.7
2/1/79 - 2/28/79	10.4	±3.8
3/1/79 - 3/11/79	14.9	±2.1
4/1/79 - 4/16/79	20.9	±1.5
5/22/79 - 5/31/79	23.5	±1.2

Wind speeds during winter were stronger than those observed during fall; they averaged 7.1 m/s. The predominant wind direction for the first half of winter was from the northeast, and for the latter half it was from the northwest and southeast.

The strong winds during winter continued through early spring with a wind speed average of 7.1 m/s. The predominant wind direction during spring was from the southeast. By mid-spring the winds were somewhat weaker and averaged 5.1 m/s during the latter half of spring.

The time series of wind speed and direction, air temperature, and pressure shown in figure 12-1 and supporting information from NOAA Daily Weather Maps, Weekly Series from October 2 to December 10, 1978, indicate frontal passages at the Weeks Island site during the following days:

October 6, 14, 17, 22, 24, 26;
November 6, 17, 24, 25 (warm front), 27, 29 (warm front); and
December 1, 4, 8.

Table 2-1 indicates that the approximate monthly frequency of frontal passages across the Louisiana shelf from 1965 to 1972 was six for October and

seven for November; we observed six during October 1978 and six during November 1978. There were three polar frontal passages during the first 10 days of December, which compares well with the estimate of nine passages for the month (table 2-1).

An extratropical cyclone formed on November 4 when low pressures at the surface and at the 500-mb height came into alinement over north central Mexico (NOAA Daily Weather Maps, Weekly Series, October 30-November 5, 1978). The cyclone moved northeastward past the Weeks Island site on November 5 as a polar front approached from the northwest. A stalled front and line of frontogenesis extended offshore on November 20 from Texas to Florida, across the entire Louisiana shelf and northern Gulf of Mexico; this resulted in a freshening north-northeasterly wind.

The time series of wind speed and direction, air temperature, and pressure shown in figure 12-2 and supporting information from NOAA Daily Weather Maps, Weekly Series from January 29 to March 18, 1979, indicate frontal passages at the Weeks Island site during the following days:

January 30 (warm front);
February 3 (warm front), 6, 9, 16, 24, 27; and
March 1, 9 (warm front), 10.

The six frontal passages observed at station 28 during February 1979 were only two-thirds the approximate monthly frequency for February passages during the period 1965 to 1972 (table 2-1), whereas the number observed during March was comparable.

A similar analysis of the station 28 data during the first half of April 1978 (figure 12-3) indicates frontal passages on April 2, 9, and 13; this compares well with the estimate of six and one-half passages for April during the period 1965 to 1972.

A stalled front appeared to dominate on April 3 and 4; this was associated with the polar front passage on April 2, and is counted as only one passage. The spring storm during April 10 to 12, described in section 20, is evident in

the wind data shown in figure 12-3. Winds at 15 m/s were observed both at the West Hackberry site (station 18) and at station 28; wind direction was southeasterly at the Weeks Island site, while it was more south-southeasterly at the West Hackberry site.

12.3. Spectral Characteristics

Power spectral plots of wind at station 28 are presented in figures 12-4 through 12-6. The maximum entropy technique discussed in section 3 was used in determining the spectral density.

Figure 12-4 shows the spectral density for winds during the fall. The energy distribution from October 2 to 30, 1978, was concentrated in the low frequency band from 0.4 CPD counterclockwise to 0.6 CPD clockwise. There was a narrow band of energy at 1.0 CPD counterclockwise. At 1.0 CPD clockwise, the energy was distributed within a broader band from 0.8 CPD to 1.2 CPD. The air temperature and wind speed data shown in figure 12-1 suggest a land/sea breeze effect. During the period October 30 to December 10, 1978, the energy distribution for the spectral density continued to be characterized by a wide band of energy at the low frequency. The energy level at the diurnal frequencies was considerably lower than that observed earlier in the fall.

As in the fall, the energy during the winter months was concentrated at the low frequency end of the spectrum. From January 29 to February 23, 1979, figure 12-5(a) shows a wide band of energy between the frequencies 0.7 CPD counterclockwise and 0.7 CPD clockwise. The energy spectra for the period February 23 to March 12 [fig. 12-5(b)] shows the energy to be concentrated within three very narrow bands at the lower frequency. However, there was a wide frequency band at a lower level of energy from 1.2 CPD counterclockwise to 1.3 CPD clockwise.

The energy distribution during early spring continued to show high levels of energy at the low frequency. For March 28 to April 17, the energy at the low frequency was mostly between 0.3 CPD counterclockwise to 0.8 CPD clockwise [fig. 12-6(a)]. There was a strong peak of energy within a narrow frequency band around the clockwise diurnal frequency of 1.0 CPD. The energy spectral density from May 21 to June 2 show that although there are some high peaks of

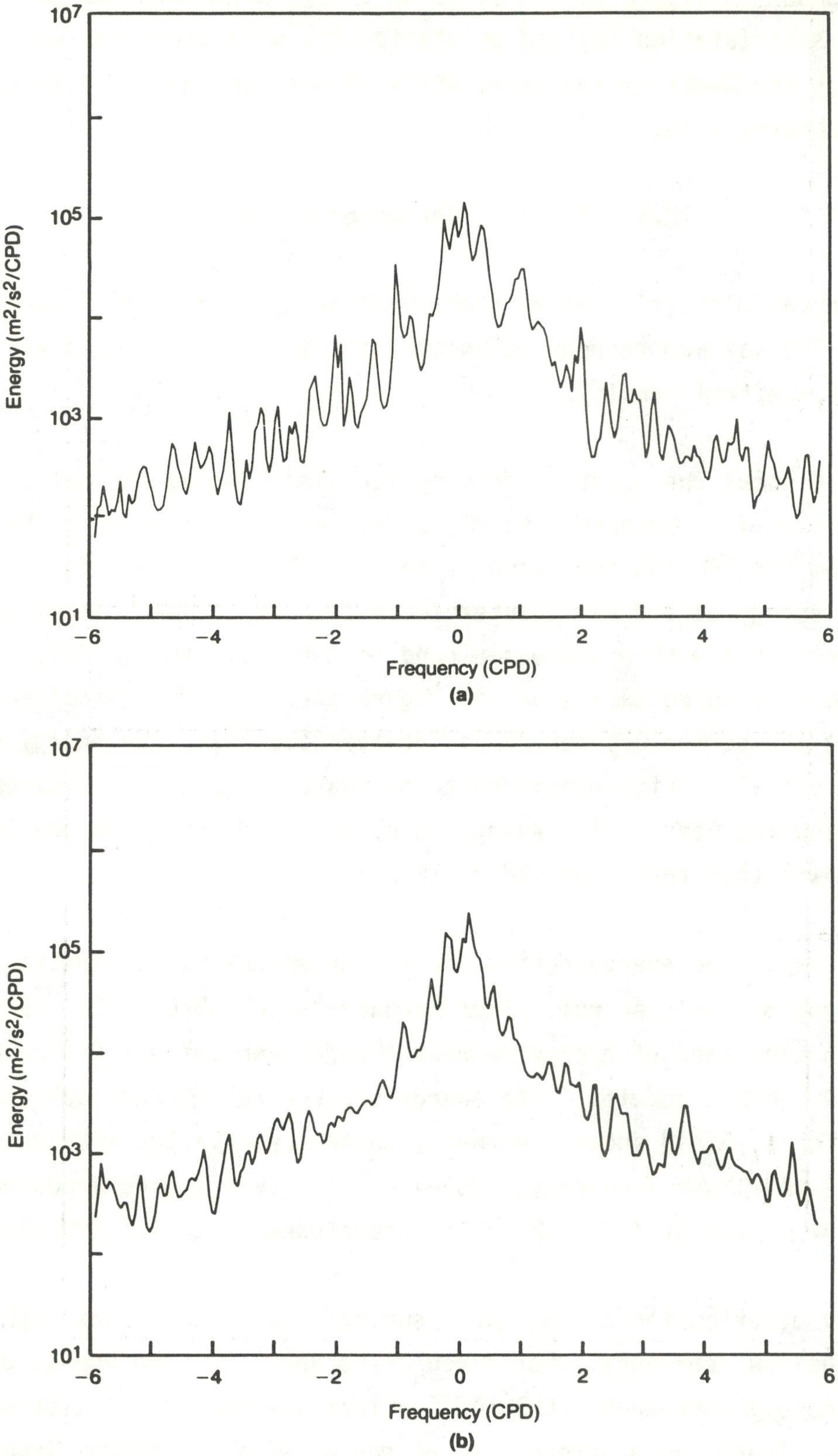

Figure 12-4. Spectral density of wind at station 28 from (a) October 2 through 30, and (b) October 30 to December 12, 1978.

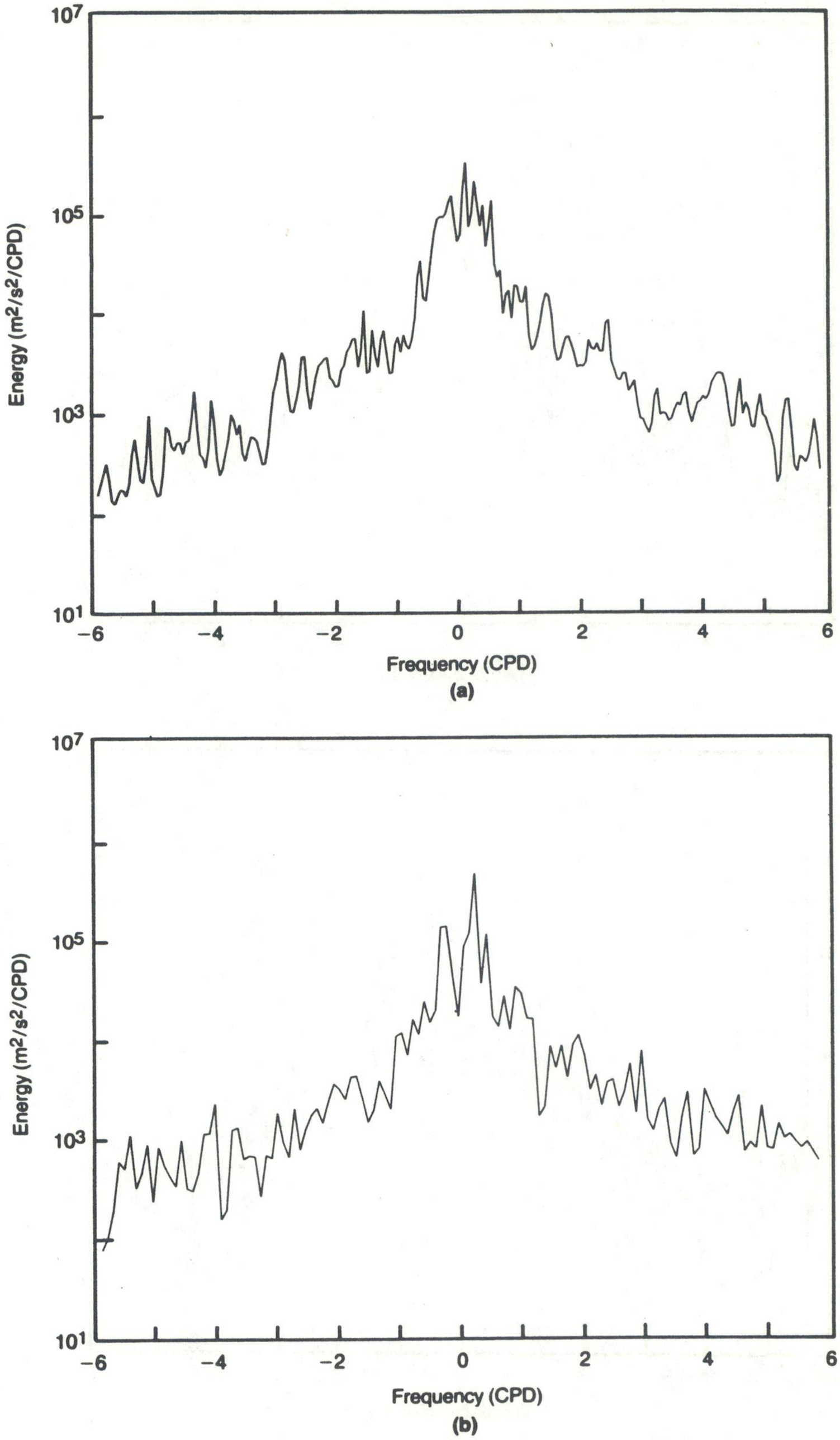

Figure 12-5. Spectral density of wind at station 28 from (a) January 29 to February 23, and (b) February 23 to March 12, 1979.

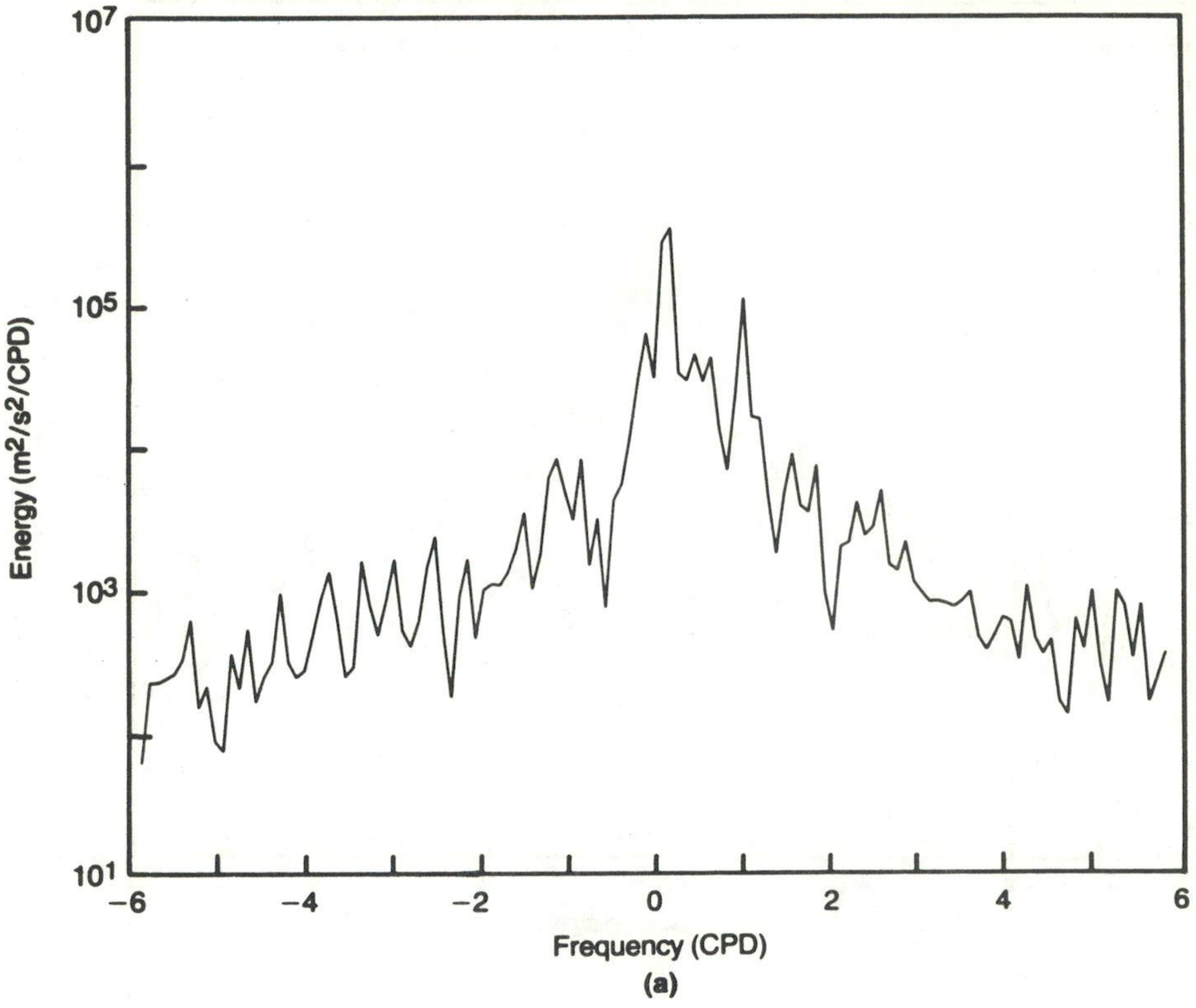

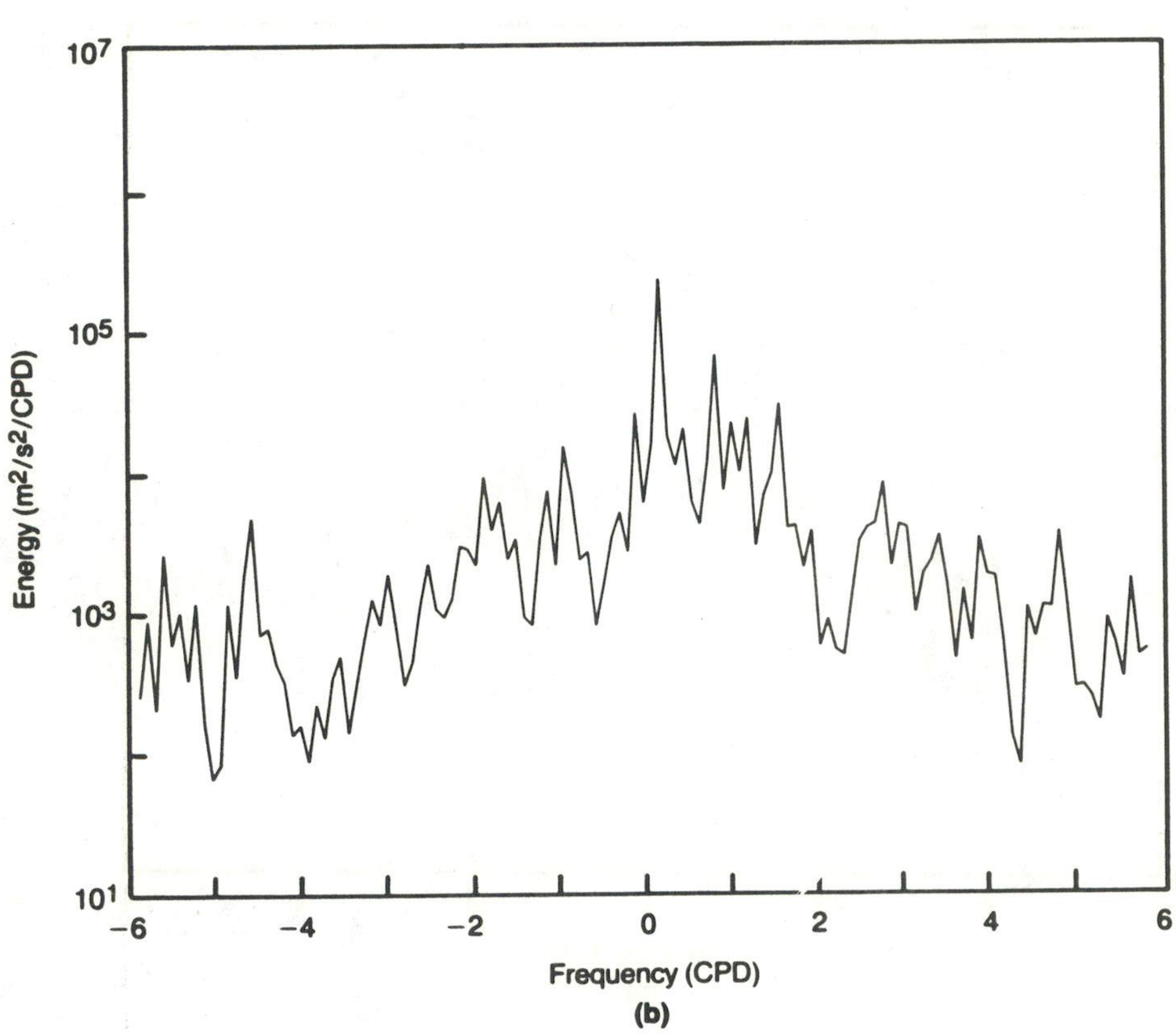

Figure 12-6. Spectral density of wind at station 28 from (a) March 28 to April 17, and (b) May 21 to June 2, 1979.

energy within narrow frequency bands, less than 1.0 CPD, the high levels of energy that had been concentrated at the low frequency since fall were no longer present [fig. 12-6(b)].

13. SURFACE WAVES

The wave climate at the Weeks Island site observed during the 12-month study is summarized in this section as seasonal statistics describing frequencies of significant wave heights and periods of peak energy. The pressure-type wave gage that was deployed at station 21, availability of the wave data, and measurement uncertainty analysis are described in volume two of this report; processing and analysis of the wave data are described in section 3 of this volume. Plots of 4-hourly samples during storm events are presented in sections 18 to 20.

Consideration must be given to the unequal statistics when evaluating the summary data. Approximately 51 days of observations were obtained during summer 1978, from July 1 to August 22. During fall 1978, 86 days of observations were made between September 2 and December 11. During winter 1979, 67 days of wave observations were obtained in the period from December 12 to March 12. Four relatively short records were obtained during spring 1979, totalling 35 days. Thus, observations were obtained for about 56 percent of the time during summer 1978, 94 percent of the time during fall 1978, 73 percent of the time during winter 1979, and 38 percent of the time during spring 1979.

The data in tables 13-1 and 13-2 show the frequency of occurrence of significant wave heights and periods of peak energy separately; they do not indicate joint frequency of occurrences. Examples of joint frequency follow.

13.1. Summer 1978

The wave statistics for July indicate that significant heights were less than 50 cm for 88 percent of the observations. Periods of peak energy during the same time were 5 seconds or less for 83 percent of the 160 observations.

Table 13-1. Statistical summary of significant wave heights at the Weeks Island site*

From:														
Day	7/1/78	7/28/78	9/2/78	9/16/78	10/2/78	10/30/78	11/13/78	12/12/78	1/6/79	2/21/79	3/27/79	4/18/79	5/8/79	5/21/79
Hour (GMT)	0400	1709	0047	1927	2105	2300	2200	0100	2359	0000	0000	1159	0502	1900
To:														
Day	7/27/78	8/22/78	9/13/78	9/21/78	10/30/78	11/13/78	12/11/78	1/6/79	1/29/79	3/12/79	4/4/79	4/27/79	5/14/79	6/2/79
Hour (GMT)	2000	0909	0447	2327	1705	1500	1400	2100	1959	1600	0400	0359	2102	1500
Number of days	26.67	24.67	11.17	5.17	27.83	12.67	28.67	24.83	22.83	19.67	8.17	8.67	6.67	11.83
Significant height (m)														
$1.8 \leq H < 1.9$							0.61			0.85				
$1.7 \leq H < 1.8$							1.23	1.94	1.55					
$1.6 \leq H < 1.7$							0.61		0.78	0.85				
$1.5 \leq H < 1.6$							1.84		0.78	0.85				
$1.4 \leq H < 1.5$								0.65	2.33	4.24				
$1.3 \leq H < 1.4$						1.20	2.45		2.33	3.39				
$1.2 \leq H < 1.3$			1.47		0.60	2.41	3.07	2.58	3.10	0.85				
$1.1 \leq H < 1.2$					0.60	1.20	4.29	4.52	1.55	2.54		1.89		
$1.0 \leq H < 1.1$	0.62		1.47		1.19	1.20	5.52	4.52	5.43	1.69	4.00	3.77		1.45
$0.9 \leq H < 1.0$	0.62	0.67	7.35		2.38		2.45	2.58	4.65	5.08	14.00	5.66		4.35
$0.8 \leq H < 0.9$	2.48		11.76		1.19	1.20	6.75	5.16	11.63	9.32	12.00	13.21	5.00	1.45
$0.7 \leq H < 0.8$	0.62		16.18		2.38	10.84	4.91	7.10	10.08	5.93	30.00	16.98	2.50	2.90
$0.6 \leq H < 0.7$	3.73	2.68	5.88	3.13	2.38	8.43	7.36	8.39	10.85	9.32	20.00	13.21	10.00	10.14
$0.5 \leq H < 0.6$	4.35	7.38	4.41	31.25	3.57	14.46	14.11	10.97	10.85	14.41	14.00	28.30	27.50	23.19
$0.4 \leq H < 0.5$	11.80	14.09	1.47	18.13	5.95	10.84	14.72	11.61	13.18	12.71	4.00	13.21	20.00	14.49
$0.3 \leq H < 0.4$	20.50	26.85	2.94	18.75	14.29	4.82	14.11	7.74	13.95	5.93		3.77	20.00	13.04
$0.2 \leq H < 0.3$	27.95	34.23	14.71	18.75	40.48	19.28	9.82	17.42	6.98	8.47	2.00		12.50	10.14
$0.1 \leq H < 0.2$	26.09	14.09	17.65		20.24	24.10	6.13	14.84	4.65	12.71			2.50	15.94
$0.0 \leq H < 0.1$	1.24		14.71		4.76				1.55					2.90
Maximum	1.05	0.93	1.20	0.68	1.21	1.33	1.90	1.78	1.75	1.81	1.06	1.20	0.88	1.01
Mean	0.32	0.33	0.48	0.43	0.32	0.44	0.64	0.55	0.66	0.64	0.74	0.67	0.47	0.45
Minimum	0.07	0.15	0.07	0.20	0.08	0.11	0.16	0.13	0.01	0.11	0.26	0.37	0.20	0.08

*Percentage of data in time period with significant wave height within indicated bands.

Table 13-2. Statistical summary of the periods of peak energy at Weeks Island site*

From:														
Day	7/1/78	7/28/78	9/2/78	9/16/78	10/2/78	10/30/78	11/13/78	12/12/78	1/6/79	2/21/79	3/27/79	4/18/79	5/8/79	5/21/79
Hour (GMT)	0400	1709	0047	1927	2105	2300	2200	0100	2359	0000	0000	1159	0502	1900
To:														
Day	7/27/78	8/22/78	9/13/78	9/21/78	10/30/78	11/13/78	12/11/78	1/6/79	1/29/79	3/12/79	4/4/79	4/27/79	5/14/79	6/2/79
Hour (GMT)	2000	0909	0447	2327	1705	1500	1400	2100	1959	1600	0400	0359	2102	1500
Number of days	26.67	24.67	11.17	5.17	27.83	12.67	28.67	24.83	22.83	19.67	8.17	8.67	6.67	11.83
Period of peak energy (seconds)														
≤ 4.05	58.4	40.9	38.2	40.6	57.1	30.1	30.1	58.7	44.2	25.6	10.0	35.8	37.5	42.0
5.02	24.2	26.9	11.8	28.1	16.1	24.1	21.5	15.5	15.5	17.9	18.0	13.2		21.7
5.99	13.1	24.8	38.2	6.3	13.1	31.3	17.8	13.5	19.4	24.8	24.0	5.7	22.5	31.9
7.02	2.5	6.7	7.4	6.3	7.1	14.5	20.8	3.9	13.2	21.4	18.0	7.5	22.5	4.4
8.03	1.2	0.7	4.4	9.4	6.6		8.6	3.9	3.9	9.4	20.0	3.8	12.5	
9.08	0.6			6.2				0.7	1.5	0.9	10.0	17.0	2.5	
10.10				3.1			0.6	1.9	2.3			17.0	2.5	
11.99							0.6	1.3						
13.03								0.6						

*Percentage of data in time period with peak energy at period indicated.

Four observations produced spectra that peaked at 7 seconds; with corresponding significant wave heights from 17 to 41 cm. Spectra peaked twice at 8 seconds and only once at 9 seconds; the corresponding significant wave heights were from 13 to 15 cm. The greatest value of maximum wave height was 1.6 m as determined by the zero-crossing method (see section 3); the corresponding period of peak energy was equal to or less than 4 seconds, as determined by the spectral method.

The 24.7-day record beginning July 28, 1978, indicates that significant wave heights were less than 50 cm for 89 percent of the observations, while periods of peak energy were 6 seconds or less for 93 percent of the observations. Ten of the 148 observations resulted in spectra that peaked at 7 seconds, and in corresponding significant wave heights from 18 to 69 cm. One observation produced an 8-second spectral peak and a 29-cm significant wave height. The greatest value of maximum wave height was 1.65 m (zero-crossing method) with a corresponding energy peak at 5 seconds (spectral method). The August record obtained at the Weeks Island site does not include the effects of Tropical Storm DEBRA. The wave statistics for summer 1978 thus indicate significant wave heights of less than 50 cm for 88 percent of the 4-hourly observations. Spectra peaked at 5 seconds or less for 75 percent of the observations, and at 6 seconds or less for 94 percent of the time. The wave climate was thus relatively quiescent during summer 1978, except during Tropical Storm DEBRA. (See sections 7 and 18.)

13.2. Fall 1978

The statistics shown for September 2 to December 11 in tables 13-1 and 13-2 are discussed in this subsection. Note that the 28.7-day record beginning November 13 extends 11 days into winter, according to the season convention used in this report.

The September statistics were derived from two relatively short records of 11.2 and 5.2 days. The record from September 2 to 13 shows a bimodal distribution of significant wave heights; 47 percent were from 7 to 30 cm, and 41 percent were from 60 to 100 cm. There was also a bimodal distribution of periods of peak energy; 38 percent were equal to or less than 4 seconds, and 38 percent were

at 6 seconds. The 60- to 100-cm waves occurred from September 8 to 13; spectra peaked at 6 seconds during 77 percent of the observations in this period. The greatest value of maximum wave height was 202 cm at 1247 GMT on September 12 when the spectrum peaked at 5 seconds. Southerly winds from 7.5 m/s to 10 m/s prevailed from September 9 to 14 at the Weeks Island site. The 5.2-day record beginning September 16 shows concentration of both heights and peak energies; 87 percent of the observations showed significant wave heights between 20 and 60 cm, while 70 percent of the spectra peaked at 5 seconds or less. The greatest value of maximum wave height observed during this 5.2-day period was 112 cm at 2327 GMT on September 21 with a corresponding period of peak energy equal to or less than 4 seconds.

The October statistics indicate that 75 percent of the observed significant wave heights were between 10 and 40 cm, and 73 percent of the spectra peaked at 5 seconds or less. The greatest value of maximum wave height was 275 cm at 0905 GMT on October 7 with a corresponding significant wave height of 75 cm and a peak energy equal to or less than 4 seconds. The wave data listings reflect the increasing frequency of frontal passages during October compared to the summer months.

Wave data obtained during the first half of November show increases both in significant wave height and period of peak energy compared to the summer and early fall, because more polar fronts passed over the site. The greatest value of maximum wave height was 231 cm at 1100 GMT on November 6, when the significant wave height was 118 cm and the period of peak energy was 6 seconds. The greatest value of significant wave height of 133 cm was observed 4 hours later at 1500 GMT, with a corresponding maximum wave height of 212 cm and a period of peak energy of 6 seconds. The surface weather maps (NOAA Daily Weather Maps, Weekly Series, October 30 to November 5, and November 12, 1978) for November 5 through 7 show an extratropical cyclone over northeast Mexico that migrated east-northeast, while a polar front approached and passed the site from the northwest. Wind speed measured at station 28 was 11 m/s as the front approached, and the wind direction veered from westerly to easterly at about midnight (GMT) on November 6. During the first half of November, 93 percent of the significant wave height observations were between 11 and 80 cm, and 85 percent of the periods of peak energy were 6 seconds or less.

The time series of meteorological data shows five passages of fronts from November 13 to December 11, with sustained high winds most of the time between passages. This accounts for the large increase in significant wave heights shown in table 13-1 and in increasing periods of peak energy shown in table 13-2. The maximum value of significant wave height was 190 cm at 0200 GMT on December 4; the corresponding maximum wave height and period of peak energy were 205 cm and 8 seconds, respectively. About 60 percent of the observations from November 13 to December 11 resulted in significant wave heights between 20 and 70 cm, while 90 percent of the observations fell between 16 and 120 cm. The values of significant wave height greater than 136 cm and periods of peak energy greater than 8 seconds occurred during the December portion of the wave record obtained from November 13 to December 11.

13.3. Winter 1979

The 25-day record beginning December 12 produced the longest period of peak energy observed during the study at either site; the maximum period of peak energy of 13 seconds was observed at 0100 GMT on January 4 concurrently with a significant wave height of 21 cm and a maximum wave height of 40 cm. The greatest values of both significant and maximum wave heights were observed at 0900 GMT on January 2 at 178 cm and 298 cm, respectively, with a concurrent period of peak energy equal to or less than 4 seconds. The surface weather map at 1100 GMT on January 2 (NOAA Daily Weather Maps, Weekly Series, January 1-7, 1979) shows a high pressure over south-central Texas reinforcing a norther that had passed the day before. During the first 6 days of January, maximum wave heights exceeded 150 cm during 47 percent of the observations.

The 23-day record beginning January 6 reflects an extratropical cyclone and the relatively high frequency of polar frontal passages during January. About 70 percent of the observations show significant wave heights approximately evenly distributed between 30 and 90 cm, with 94 percent of the significant wave height observations less than 110 cm. The extratropical cyclone described further in section 19 generated 10-second periods of peak energy from 1200 to 2000 GMT on January 12, with corresponding maximum wave heights of 207 cm, 154 cm, and 240 cm, respectively, and significant wave heights of 109 cm, 80 cm, and 71 cm, respectively. The maximum wave heights associated with northers

later in the month are 278 cm (0800 GMT on January 21), 239 cm (2000 GMT on January 23), 250 cm (0000 GMT on January 26), and 217 cm (0400 GMT on January 28); these heights correspond to 35, 30 32, and 27 percent of the depth at GCLW, respectively. The periods of peak energy observed during the January northers varied from 6 to 7 seconds.

The 20-day record beginning Feruary 21 shows the continuing efffects of polar front passages, but with an apparent decrease in the effects of distant storms as indicated by the shift to shorter periods of peak energy. The period from 0400 GMT on February 25 to 0800 GMT on February 26 was especially energetic, with significant and maximum wave heights ranging from 99 to 181 cm and 186 to 255 cm, with averages of 133 and 229 cm, respectively; periods of peak energy remained 7 seconds or less. Winds during this period veered from westerly to northerly at 12 m/s to 15 m/s. Another relatively prolonged energetic period occurred between 0400 GMT on March 3 and 1200 GMT on March 4, when significant and maximum wave heights ranged from 100 to 150 cm and from 180 to 243 cm, with averages of 135 and 200 cm, respectively; periods of peak energy during this time ranged from 6 to 9 seconds. The meteorological record at station 28 indicates a slowly moving polar front during this period.

Northerly winds throughout the day on March 5 and well into March 6 produced a maximum wave height of 201 cm at 1200 GMT on March 6 at station 28; the corresponding significant wave height was 56 cm and the spectrum peaked at less than 4 seconds; the northerly winds, associated with a high pressure center at the Texas coast, produced a fetch-limited spectrum at the Weeks Island site. Late in the day on March 6, barometric pressure decreased and the wind backed from northerly to west-southwesterly, and freshened to 13 m/s on March 7. This generated significant and maximum wave heights that ranged from 75 to 152 cm and from 165 to 256 cm, with averages of 115 and 208 cm, respectively. The periods of peak energy did not exceed 7 seconds.

13.4. Spring 1979

The four short records obtained from late March to early June, totalling 35 days, indicate a significant shift toward longer periods of peak energy. We believe that this shift in spectral composition is associated with the longer

fetch of the predominately southerly spring winds, which enhances spectral growth of waves. The four records also show a steadily decreasing distribution of significant wave heights.

The 8-day record beginning March 27 shows that 90 percent of the significant wave heights were between 50 and 100 cm, while 48 percent of the observed spectra peaked between 7 and 9 seconds. The 9-day record beginning April 18 shows that 85 percent of the significant wave heights were between 40 and 90 cm, while 45 percent of the observed spectra peaked between 7 and 10 seconds; 34 percent of the observed spectra peaked at 9 to 10 seconds, representing the most frequent occurrence of 9- and 10-second periods observed during the 12-month study. The 7-day record beginning May 8 shows that 90 percent of the significant wave heights were between 20 and 70 cm, while 58 percent of the spectra peaked between 6 and 8 seconds. The last record obtained during the study, beginning May 21, shows that 87 percent of the observed significant wave heights were between 10 and 70 cm, while 97 percent of the observed spectra peaked at 6 seconds or less.

As mentioned above, the record beginning April 18 produced more observations of 9- and 10-second periods of peak energy than were observed at any other time during the 12-month survey. From 1200 GMT on April 23 to 0800 GMT on April 26, periods of peak energy persisted at 9 to 10 seconds, while significant wave heights, averaging 65 cm, ranged from 41 to 80 cm. During the same period, maximum wave heights were from 47 to 194 cm. The greatest value of maximum wave height observed during the spring 1979 was 307 cm (39 percent of the depth at GCLW) at 0400 GMT on March 30, 1979. Maximum wave heights exceeded 200 cm on March 29 and 30, April 18 to 22, and April 26.

14. WATER LEVELS

One 15-day and one 29-day series were used at the Weeks Island site to determine the site characteristics. Using the technique discussed in sections 3 and 8, we characterized the Weeks Island site as having daily water level fluctuations that are of the mixed, mainly diurnal, type.

Figure 14-1 is a time series plot of a week of water level fluctuations at the Weeks Island site with no major meteorological disturbances. In contrast to the West Hackberry site, the Weeks Island site had more diurnal-dominant days during the month, i.e., only one high and one low water were observed during a tidal day. On May 15 the lower high and higher low water started to merge, showing the effect of the moon's declination on diurnal inequalities (fig. 14-1). At the Weeks Island site, the low water inequality (DLQ) is much larger than the high water inequality (DHQ), i.e., 0.10 m and 0.03 m, respectively (table 14-1). The phase relationship of M_2 to K_1 and O_1, determined from the 29-day harmonic analysis (section 8), indicates that the diurnal inequality should be primarily in the low waters. This was confirmed by investigating the time series plot (fig. 14-1) and the results of the 29-day harmonic analysis presented in table 14-1.

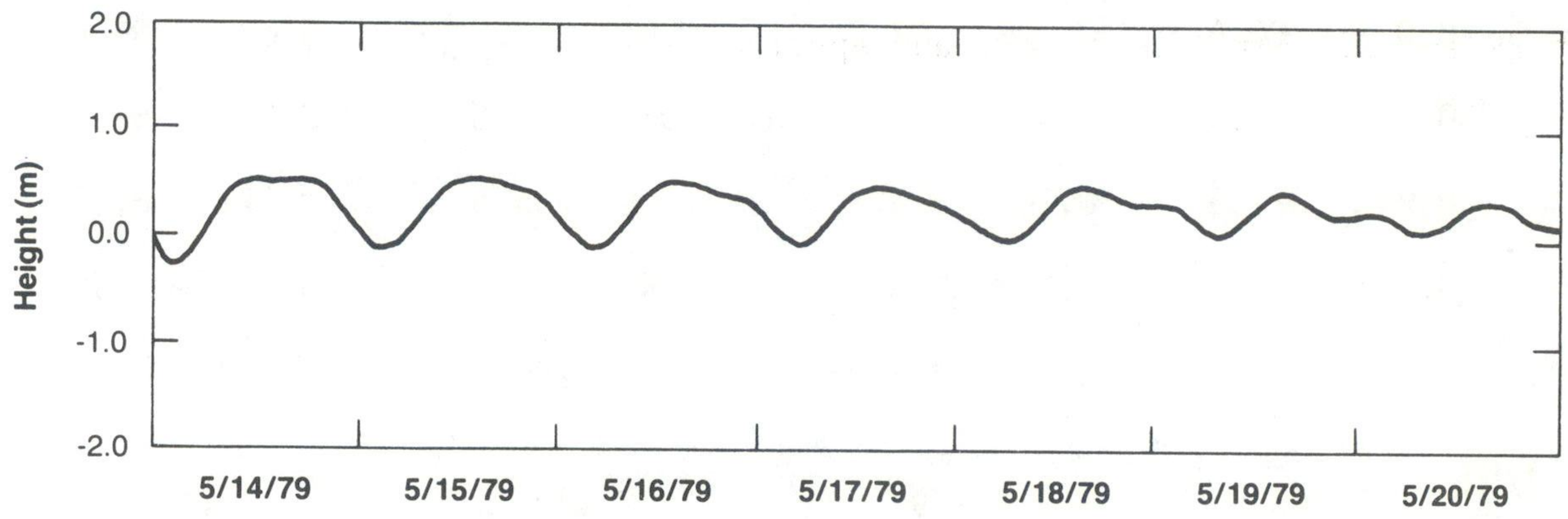

Figure 14-1. Areal extent of tide types from Hicks (1977).

Table 14-1. Mean water levels and ranges Weeks Island, Rabbit Island, and Eugene Island

	Weeks Island	Rabbit Island	Eugene Island
	--meters--		
MHHW	0.52	0.61	0.58
MHW	0.49	*	0.52
MLW	0.10	*	0.18
MLLW	0.00	0.00	0.00
Mn	0.39	*	0.34
DHQ	0.03	*	0.06
DLQ	0.10	*	0.18
Gt	0.52	0.61	0.58

Table 14-2. Results of 29-day and 15-day harmonic analysis of Weeks Island and accepted values for Rabbit Island and Eugene Island

	Weeks Island (15-day)		Weeks Island (29-day)		Rabbit Island		Eugene Island	
	Amp. (H)	Epoch (k)	Amp. (H)	Epoch (k)	Amp. (H)	Epoch (k)	Amp. (H)	Epoch (k)
M_2	0.115	41.6	0.114	54.8	0.105	65.1	0.093	70.6
S_2	0.033	20.6	0.029	33.2	0.036	57.9	0.035	69.6
N_2	0.022	52.9	0.030	1.7	0.033	45.8	0.027	52.1
K_1	0.245	321.3	0.101	325.2	0.158	295.5	0.171	301.8
O_1	0.161	268.3	0.182	258.0	0.144	292.1	0.139	297.2
P_1	0.081	321.3	0.033	325.2	0.052	290.0	0.057	287.2
$F = \frac{K_1 + O_1}{M_2 + S_2}$	2.743		1.979		2.142		2.422	

The results of our harmonic analysis of the two time periods, March 26 to April 17 and April 18 to May 18, 1979, are consistent with accepted historical analyses of nearby sites. Table 14-2 shows the values of the amplitude and phase of the five major diurnal and semidiurnal constituents for Weeks Island and two historical sites, Rabbit Island and Eugene Island. As was mentioned in section 3 the values of other constants are obtained by our analyses, but for comparison with the historical data it was only necessary to look at these five.

The ratio of the diurnal constituents $K_1 + O_1$ to the semidiurnal constituents $M_2 + S_2$ for Weeks Island is 1.979. This quantity was defined in section 8 as the ratio F and is used to define quantitatively the characteristic of the tide. The value 1.979 is in the range defined to be mixed, mainly diurnal which compares well with the values obtained for the two historical sites (Table 14-2). Table 14-3 shows that the Greenwich intervals that were obtained by our 29-day harmonic analysis of the Weeks Island data are similar to those obtained for Rabbit Island and Eugene Island. It also agrees with the tide type expected from Hicks (1977) (fig. 14-2).

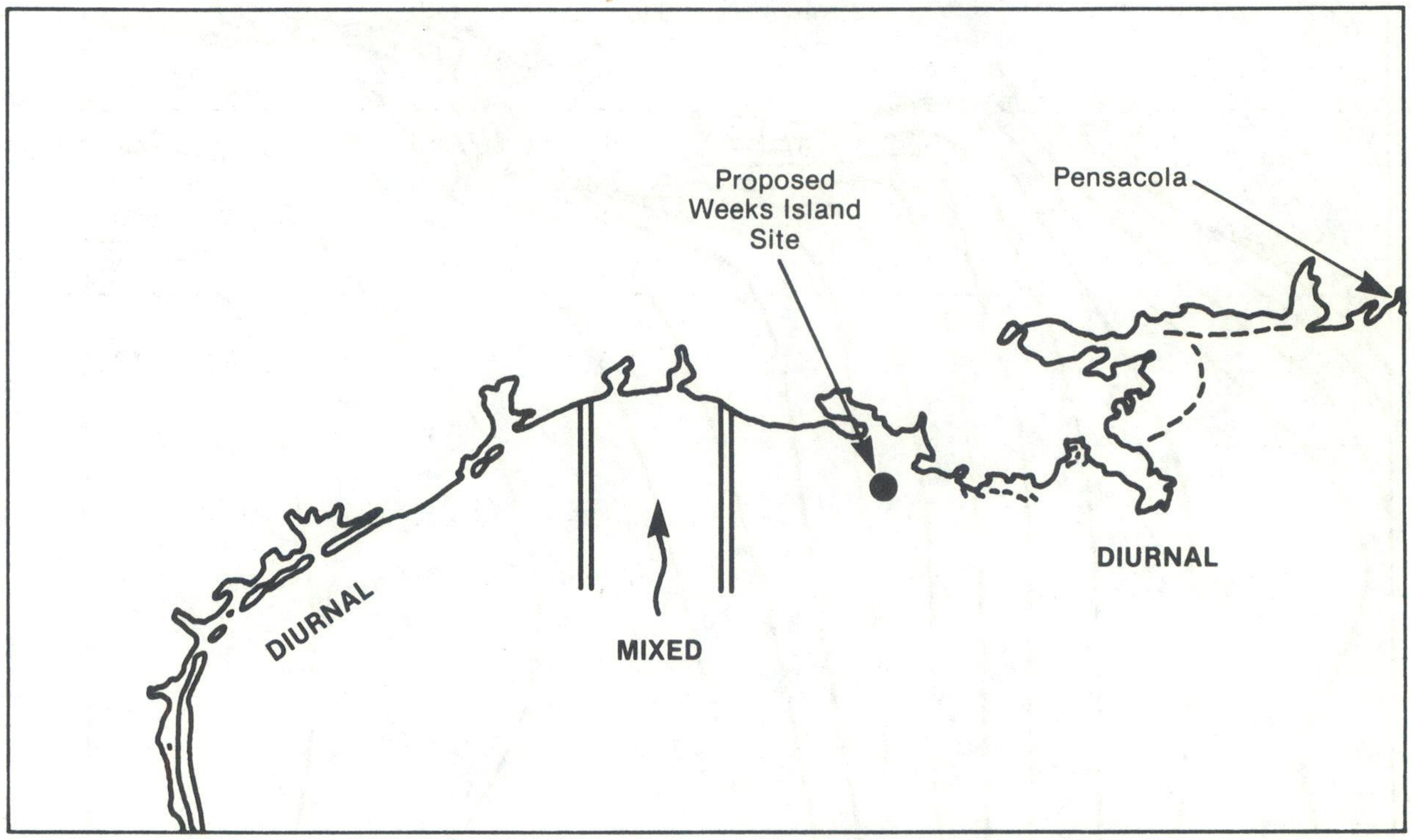

Figure 14-2. Time series plot of Weeks Island water level fluctuations.

Table 14-3. Greenwich intervals for Weeks Island, Rabbit Island, and Eugene Island

	Weeks Island	Rabbit Island	Eugene Island
	--hours--		
HWI	8.872	8.77	9.117
LWI	2.226	2.11	2.650
TcHHWI	23.371	23.71	23.650
TcLLWII	14.413	14.42	14.430

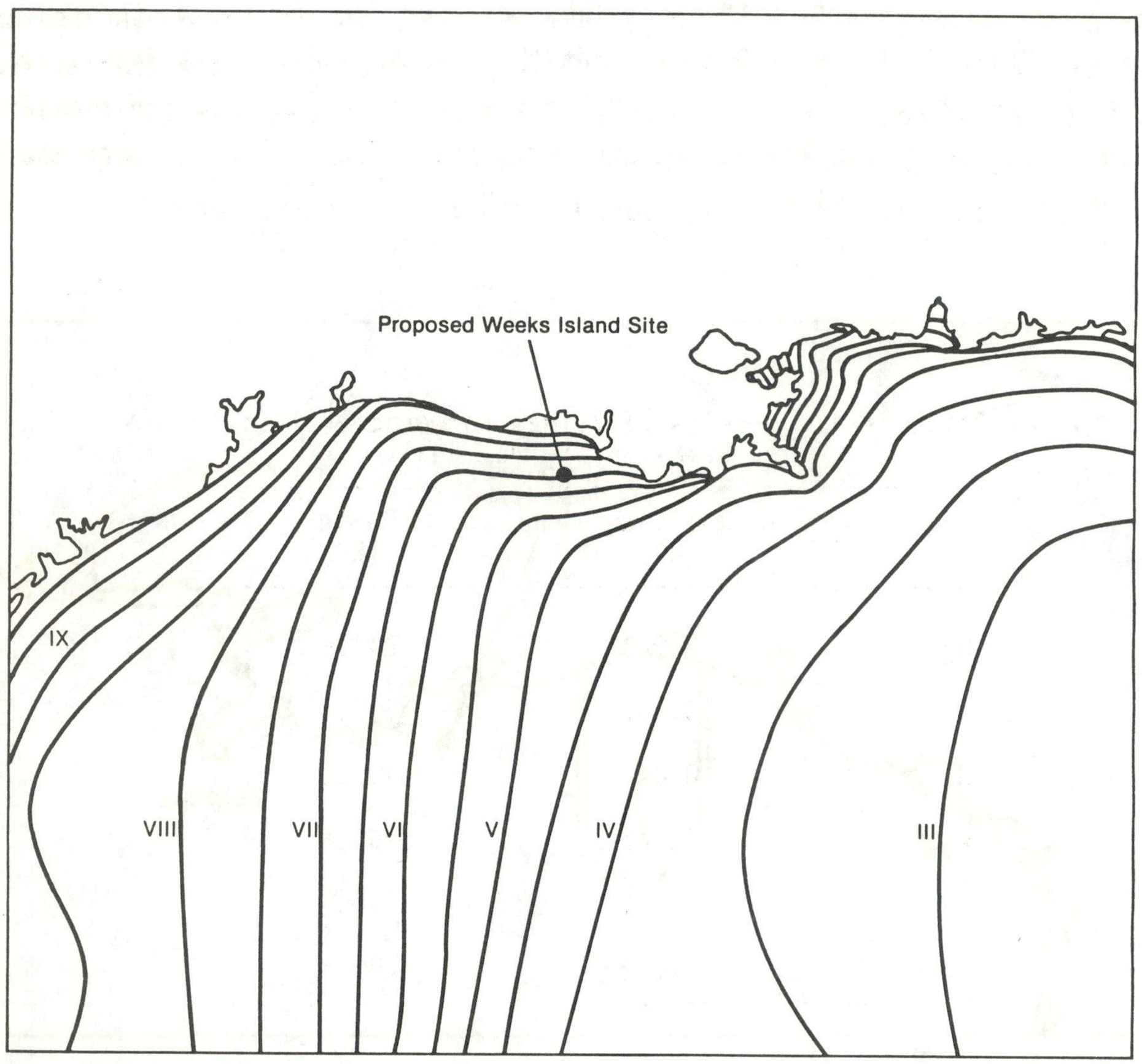

Figure 14-3. Cotidal lines for M_2 based on Harris (1904).

As input to Harris' M_2 cotidal chart (fig. 14-3) we use the phase of M_2, from our 29-day harmonic analysis, and the speed of M_2. This ratio is 8.24. From figure 14-3 we expected a value of approximately 8.00. Our value of 8.24 is in good agreement with that expected from the cotidal chart, considering the age of Harris' data.

We did not have seasonally variant data available for the Weeks Island site, as for the West Hackberry site. Because no major meteorological disturbances occurred during either of the two time periods, we could not make a comparison of the seasonal variability of the harmonic constants, as was done for the West Hackberry site.

We did, however, use the residual analysis technique discussed in sections 3 and 8 to see if there was any evidence of effects present at the diurnal frequency similar to those observed at West Hackberry. A Burg analysis of the residuals for the period April 18 to May 18 showed a peak at the diurnal frequency similar to that observed for June and July at West Hackberry.

Table 14-4. Results of 29-day harmonic analysis of Weeks Island residuals

	Amplitude (H)	Phase (k)
M_2	0.023	247.4
S_2	0.001	232.4
N_2	0.014	100.3
K_1	0.121	250.8
O_1	0.080	18.7
P_1	0.040	250.8

The results of a harmonic analysis of the residuals are presented in table 14-4. The amplitude of the K_1 constituent of the residuals is larger than the amplitude obtained for K_1 in the original analysis. The residual K_1 is, however, approximately 70 degrees out of phase with the K_1 from the original series. This result is a combination of not being able to separate P_1 from K_1 in a 29-day harmonic analysis, and the effect of S_1 the land/sea breeze. The amplitude of the original O_1 is twice as large as the residual O_1 and they are out of phase by about 240 degrees. The amplitude of the semidiurnal constituents were much smaller than those of the diurnal with the largest being the amplitude of M_2 of 0.023 m. The diurnal constituents accounted for 70.9 percent of the height of the residuals.

These results are similar to those obtained by our analysis of the West Hackberry residuals and therefore tend to confirm our earlier observations. The phases of the harmonic constants of the residuals at Weeks Island are, as we expected, out of phase with the harmonic constants of the West Hackberry residuals. Part of this difference is spatial and part, perhaps the most significant, is seasonal.

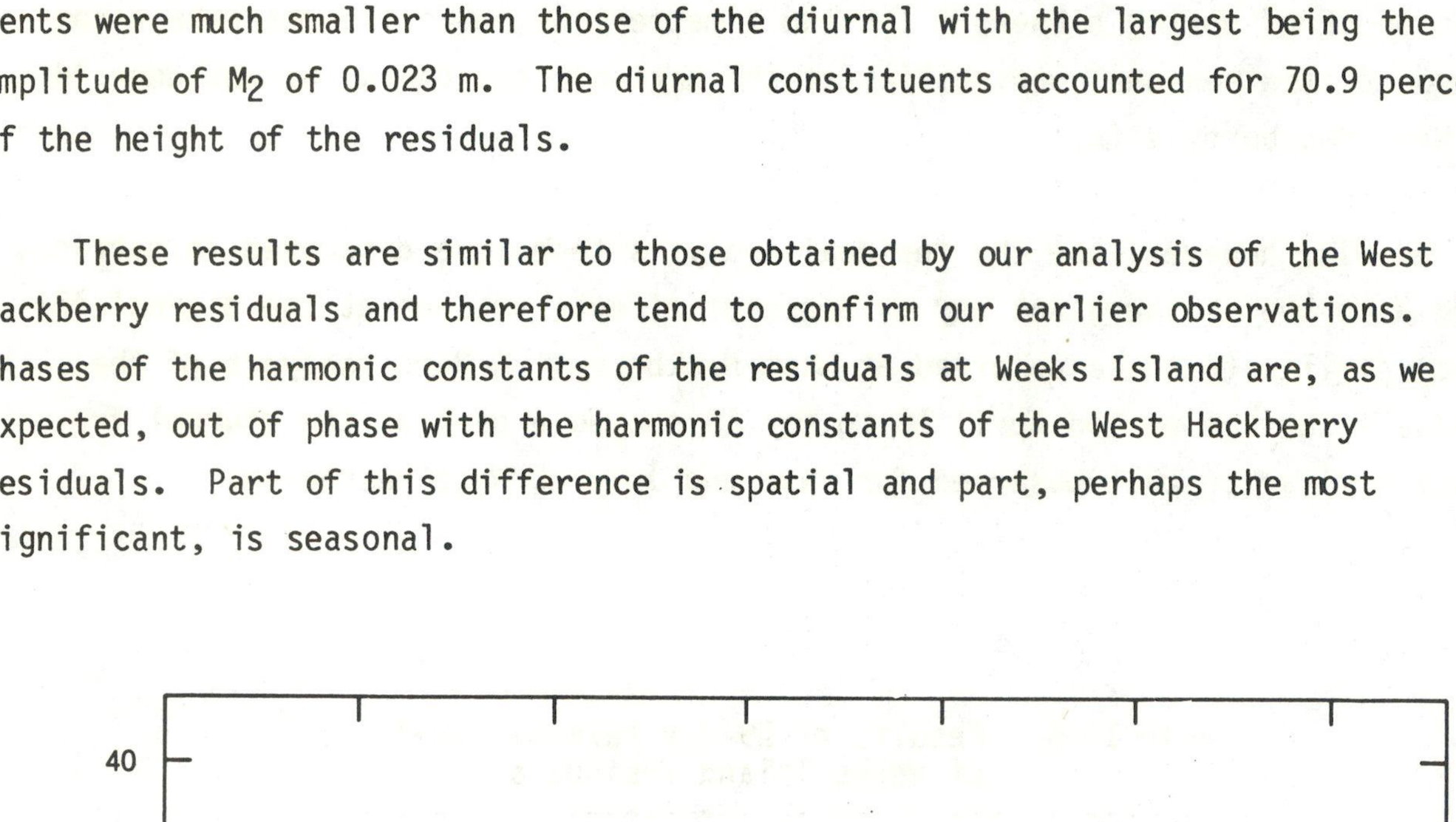

Figure 14-4. Frequency distribution of residuals at Weeks Island.

15. CURRENTS

A major objective of the NOS SPR Support Project was to obtain long-term current time series for analysis of the circulation at the Weeks Island site. During the 12-month survey, 43 meter-months of data were recorded at the site. A listing of the current observations at the different stations and the availability of the data are presented in section 10, volume two of this report. The circulation and its variability will be examined in this section through a discussion of temporal, spatial, and spectral characteristics of the currents.

15.1. Temporal Characteristics

Appendix G shows time-series plots of current speed and direction for all observations obtained 3 m above the bottom at station 21. These plots illustrate the time variability of currents at the center of the Weeks Island site during the survey period. It is apparent that the current system fluctuates on a variety of time scales, from periods of several hours to several months. Variability of the currents is attributed to direct meteorological forcing, density gradients caused by river discharge and thermohaline properties of the shelf water, and astronomical forcing.

15.1.1. Current Speed

Mean current speeds during deployment periods are summarized for all stations in tables 15-1 and 15-2. To illustrate the variability, both the scalar speed values and their standard deviations are shown.

Mean current speeds at the Weeks Island site, like those observed at the West Hackberry site, were found to be higher during the winter and spring months. The range of mean speed 3 m above the bottom during winter and spring deployment periods was 14.4 to 24.2 cm/s. At 1 m above the bottom, the mean

Table 15-1. Mean speed and standard deviation (cm/s) for currents at the Weeks Island site, 1 m above bottom.

Deployment periods	Station 21	Station 22	Station 23	Station 24	Station 25
1978					
6/1-6/30			8.2 ± 4.9		
6/30-7/28		12.1 ± 6.1	8.6 ± 4.4		9.2 ± 4.9
7/1-7/28	9.2 ± 5.0			9.7 ± 4.6	
7/28-8/8	17.2 ± 9.5				
7/28-8/11		8.9 ± 5.4			
7/29-8/8				12.6 ± 6.7	
9/1-9/15	11.5 ± 6.1				
9/16-10/2	9.4 ± 4.7				
10/2-10/30	7.2 ± 5.4				
10/30-11/13	11.0 ± 5.8		8.5 ± 4.8		10.1 ± 5.5
11/13-12/10			10.6 ± 5.7		11.2 ± 5.6
11/13-12/11	12.7 + 6.8				
12/10-1/6					
12/11-1/6	6.8 ± 4.5		12.0 ± 7.8		
1979					
1/6-1/21	15.1 ± 10.0		14.4 ± 10.2		15.2 ± 10.2
1/29-2/20	11.6 ± 7.3		11.9 ± 7.4		
2/1-2/21					8.1 ± 5.5
2/20-3/12	10.3 ± 8.7				
2/20-3/13				11.6 ± 10.5	
2/20-3/14			8.3 ± 7.2		
3/14-3/27			14.2 ± 7.6		14.0 ± 7.5
3/27-4/17			11.5 ± 6.7		12.4 ± 7.3
4/17-5/7					13.1 ± 6.8
5/7-5/21	12.1 ± 5.7		12.0 ± 7.3		12.7 ± 6.3
5/21-6/3			10.0 ± 5.5		11.9 ± 6.3

Table 15-2. Mean speed and standard deviation (cm/s) for currents at the Weeks Island site, 3 m above bottom.

Deployment periods	Station 21	Station 22	Station 23	Station 24	Station 25
1978					
6/30-7/28					16.0 ± 9.2
7/1-7/28	15.8 ± 8.6				
7/28-8/16			19.7 ± 11.4		
7/28-8/20				16.7 ± 11.1	
9/1-9/15	16.4 ± 15.1				
9/16-10/2	12.1 ± 7.3				
10/2-10/30	11.7 ± 7.5				
10/30-11/13	15.2 ± 7.0				14.2 ± 7.0
12/10-1/6			16.6 ± 10.1		
1979					
1/6-1/21	19.8 ± 13.2				21.2 ± 13.5
2/1-2/21					16.1 ± 9.4
2/20-3/12	18.6 ± 12.6				
2/20-3/14			14.4 ± 10.3		
2/22-3/12				24.2 ± 15.6	
3/12-3/26	19.1 ± 10.3				
3/14-3/27			19.7 ± 9.7		
3/14-3/27					20.1 ± 10.2
3/27-4/17					18.4 ± 9.0
4/18-5/5	19.7 ± 9.6				
5/7-5/21			19.5 ± 11.8		18.3 ± 9.6
5/21-6/2	19.6 ± 10.3				
5/21-6/3			16.0 ± 9.3		18.7 ± 11.3

speed range was 8.1 to 15.2 cm/s. The higher current speeds found during winter and early spring are attributed to the greater occurrence of higher wind speeds and thus stronger wind-driven currents during these seasons. The mean wind speed at station 28 for both winter (January 29 to March 12) and early spring (March 28 to April 17) was 7.1 m/s.

During summer and fall deployment periods, the range of mean speed 3 m above the bottom was 11.7 to 19.7 cm/s; at 1 m above the bottom, the mean speed range was 6.8 to 17.2 cm/s. Slower currents during the summer and fall are attributed to the generally lower wind speeds and the lower volume of river runoff observed during these seasons. The mean wind speed at station 28 for fall, from October 2 to December 10, 1978, was 5.8 m/s. Although wind speed was not recorded at Weeks Island during the summer of 1978 because of instrument malfunction, wind speeds within the western Louisiana coastal region, based on observations at the West Hackberry site and Intracoastal City, were found to be generally less than in the winter and early spring. In summer, high winds may occur under storm conditions, as was the case August 6-8 when current speeds (driven by the wind) reached 48.4 cm/s at station 21. These strong wind-driven currents increased the mean current speeds during the August deployments.

15.1.2. Relative Volume Transport

The diagrams shown in figures H-1 through H-9 (appendix H) show the relative volume transports at the Weeks Island site stations during specified deployment periods. The computation of relative volume transports is described in section 3. Figures 15-1 and 15-2 summarize the relative transports in the alongshore and transhore quadrants.

Summer 1978

At the Weeks Island site, from June 1 to July 28, the transport distribution was balanced fairly equally between the alongshore and transhore quadrants. During the period July 28 to August 8, the passage of a major summer storm resulted in strong wind-driven currents increasing the percentage of transport in the alongshore east-southeast quadrant. The transport remained high in both alongshore quadrants throughout the month until August 20, when the last

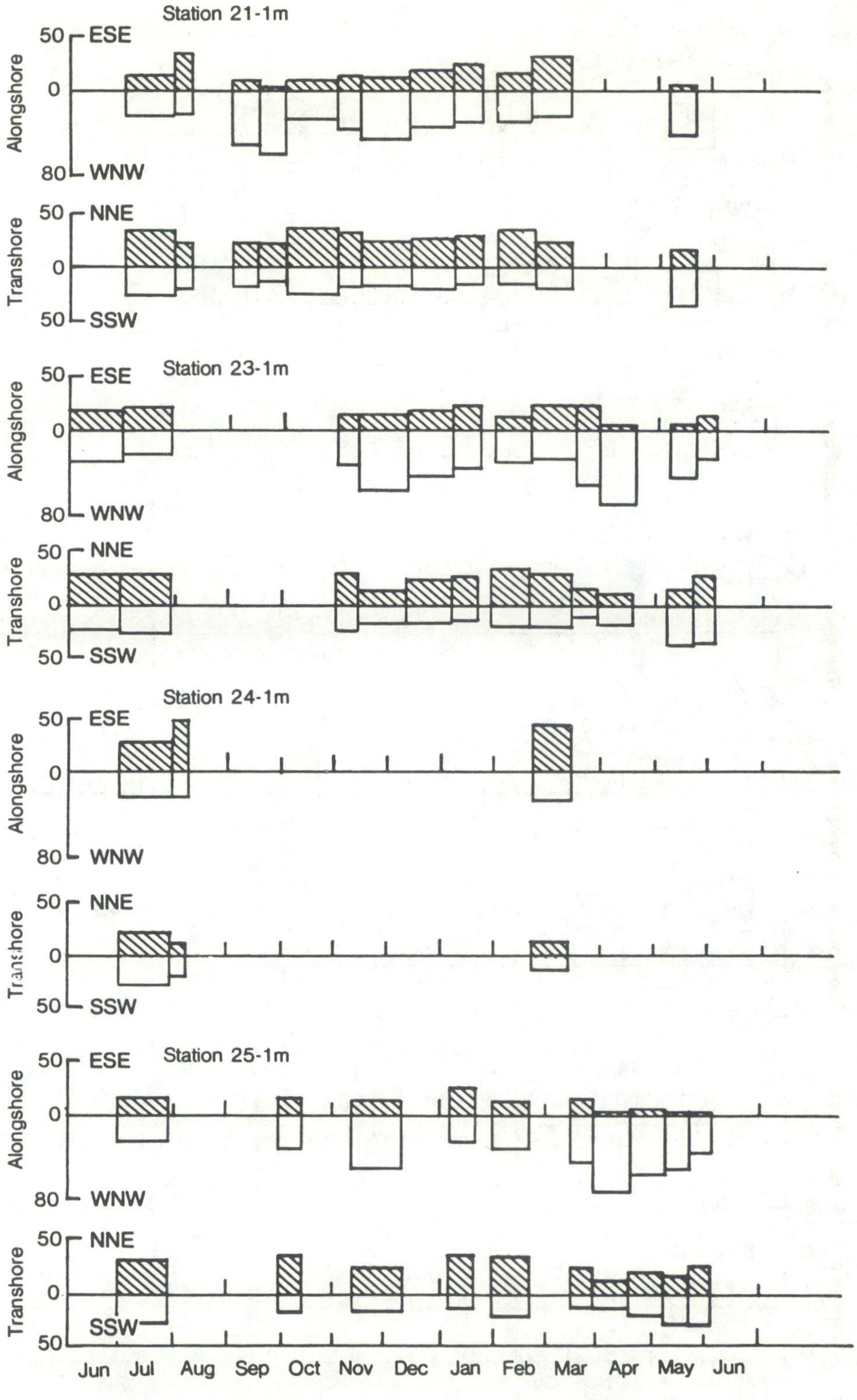

Figure 15-1. Summary of the percentage of relative volume transport in the alongshore and transhore quadrants at stations 21 and 23 through 25 at 1 m above the bottom. (Compass direction represents center of quadrant.)

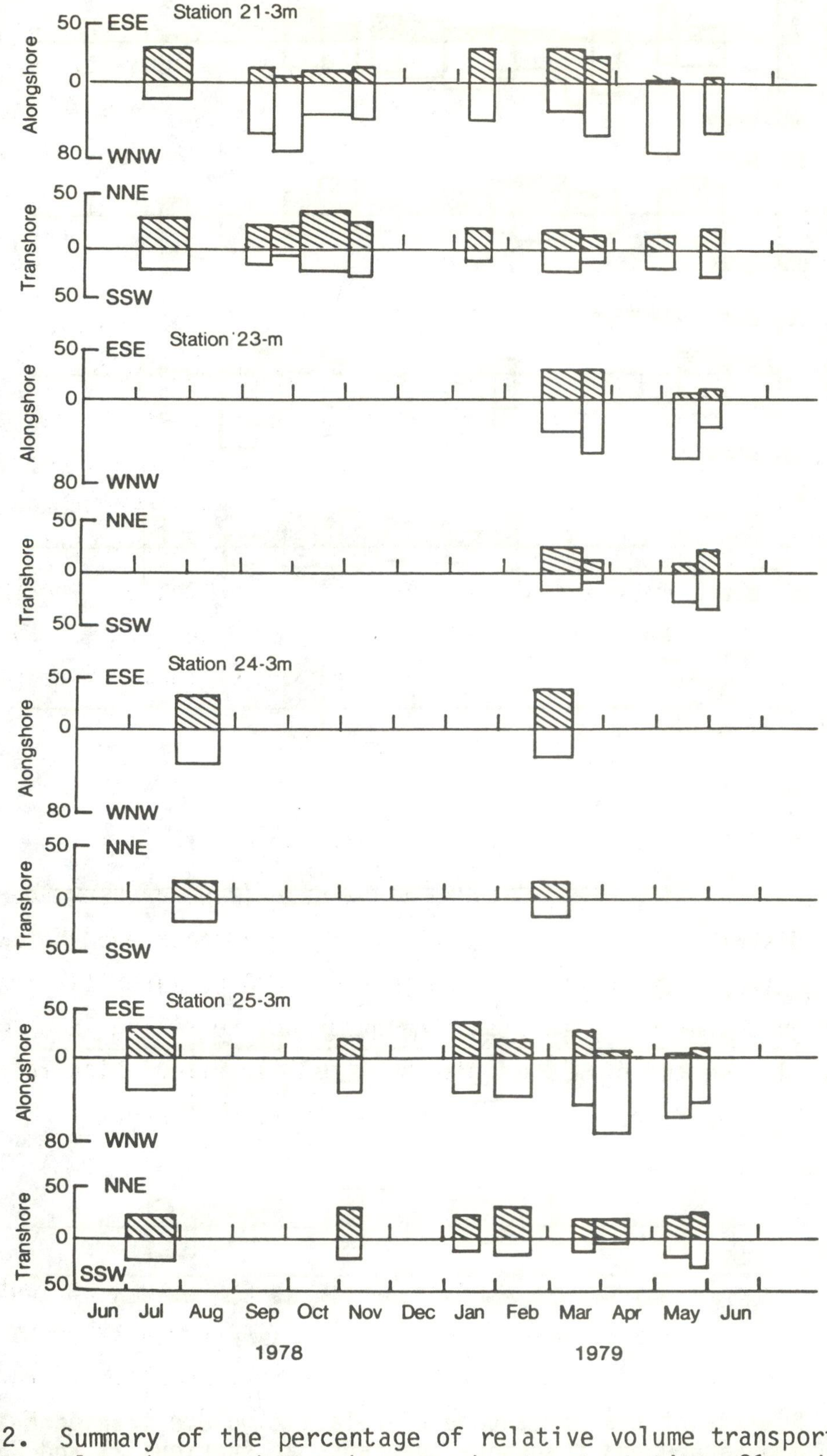

Figure 15-2. Summary of the percentage of relative volume transport in the alongshore and transhore quadrants at stations 21 and 23 through 25 at 3 m above the bottom. (Compass direction represents center of quadrant.)

operable current meter, station 24 3 m above the bottom, separated from its platform during severe sea conditions. By late summer (September 1 to 15) the transport distribution was found to be mainly alongshore in the west-northwest quadrant. At station 21 1 m above the bottom, 51 percent of the transport flowed through the west-northwest quadrant and at 3 m above the bottom, 53 percent.

Fall 1978

During fall, the relative volume transport at the Weeks Island site was concentrated alongshore in the west-northwest quadrant and transhore in the shoreward north-northeast quadrant. Although circulation became variable and appeared to be tidally driven during the first half of November, the percentage of transport through the west-northwest quadrant increased during the second half of November and into mid-December (November 13 to December 11). At station 23 1 m above the bottom, the percentage of transport in the west-northwest was 55 percent. By late fall and into early winter (December 11, 1978 to January 6, 1979), the transport distribution in the west-northwest quadrant decreased slightly.

Winter 1979

Transport at the site from early to mid-winter (January 6 to February 20) was primarily distributed between both alongshore quadrants and shoreward in the north-northeast transhore quadrant. From February 20 to March 14, transport increased in the south-southeast transhore quadrant, resulting in a more even distribution. By the end of winter (March 14 to 28), circulation returned to a more persistent alongshore flow in the west-northwest quadrant.

Spring 1979

During early spring the relative volume transports were distributed principally in the west-northwest alongshore quadrant. Although currents continued to persist west-northwest, the percentage of transport in this quadrant was offset slightly by a transhore increase during the period April 17 to May 7. From May 7 to 21, transport was primarily in the west-northwest quadrant and in the seaward south-southwest quadrant. The transport distribution from May 21 to

June 3 displayed a more uniform balance of circulation between all the quadrants except the east-northeast alongshore quadrant. The percentage of transport in the east-northeast quadrant during this period was negligible.

15.1.3. Tidal Currents

Tidal currents result from astronomical forces, and they may respond to these forces in either a barotropic mode or baroclinic mode. Barotropic tidal currents fluctuate in a consistent phase difference with tidal sea surface fluctuations. Baroclinic tidal currents are the internal motions along pycnoclines and generally vary in their phase relationship with the tidal sea surface fluctuations.

The amplitudes and phases of the tidal current constituents are determined from the harmonic analysis (section 3) and the harmonic constituents are then combined into a composite tidal current. Plots of tidal currents at the Weeks Island site during four different periods within the 12-month survey are shown in figures 15-3 and 15-4. These currents are separated into alongshore and transhore components. Tidal currents at the Weeks Island site are of the mixed type, varying between semidiurnal-dominant and diurnal-dominant throughout the survey period except during fall, when the tidal currents were consistently mixed diurnal-dominant. Speeds of tidal currents were found to average about 4 cm/s, with the tidal currents peaking normally between 8 to 12 cm/s, although tidal current calculations were as high as 16 cm/s on occasion.

Tidal current ellipses for the harmonic constituents determine the orientation of the major and minor axes of the constituent flow, the speed values for the major and minor axes, the phase lag, and the rotation of the progression of each constituent. Figure 15-5 shows tidal current ellipses of the semidiurnal (M_2) and diurnal (K_1) constituents for current series at 1 m and 3 m above the bottom starting in late June and early July 1978. Figure 15-6 shows the same information for late February 1979. These ellipses show how the tidal currents vary in both time and space. This variation is an accumulation of two factors:

- The interaction of the tidal wave and bottom topography generates internal tides when the waters are stratified.

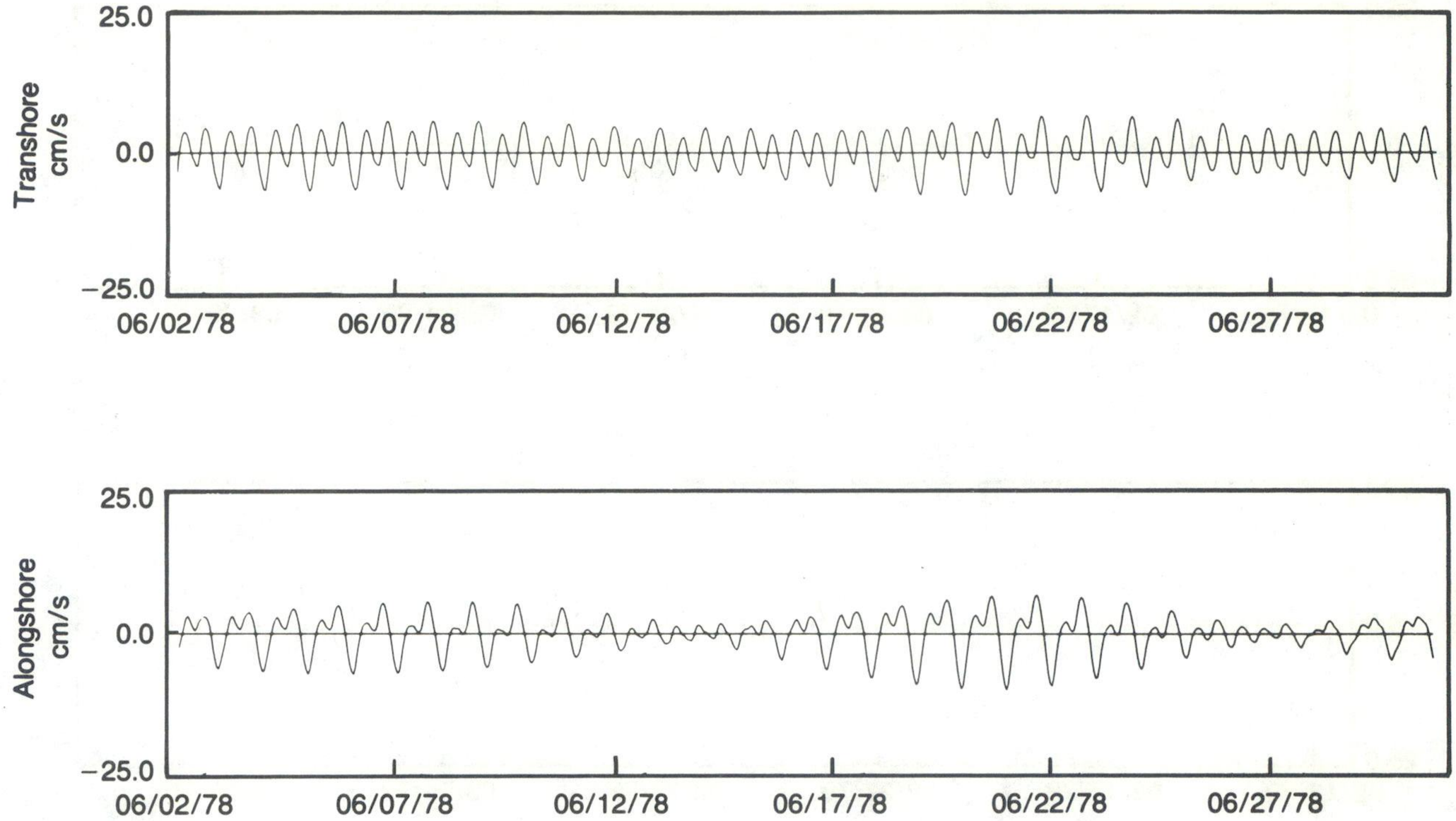

Figure 15-3. Calculated tidal currents at Weeks Island site, 1 m above bottom (a) station 23, June 2 through 30, 1978, and (b) station 21, October 31 to November 28, 1978.

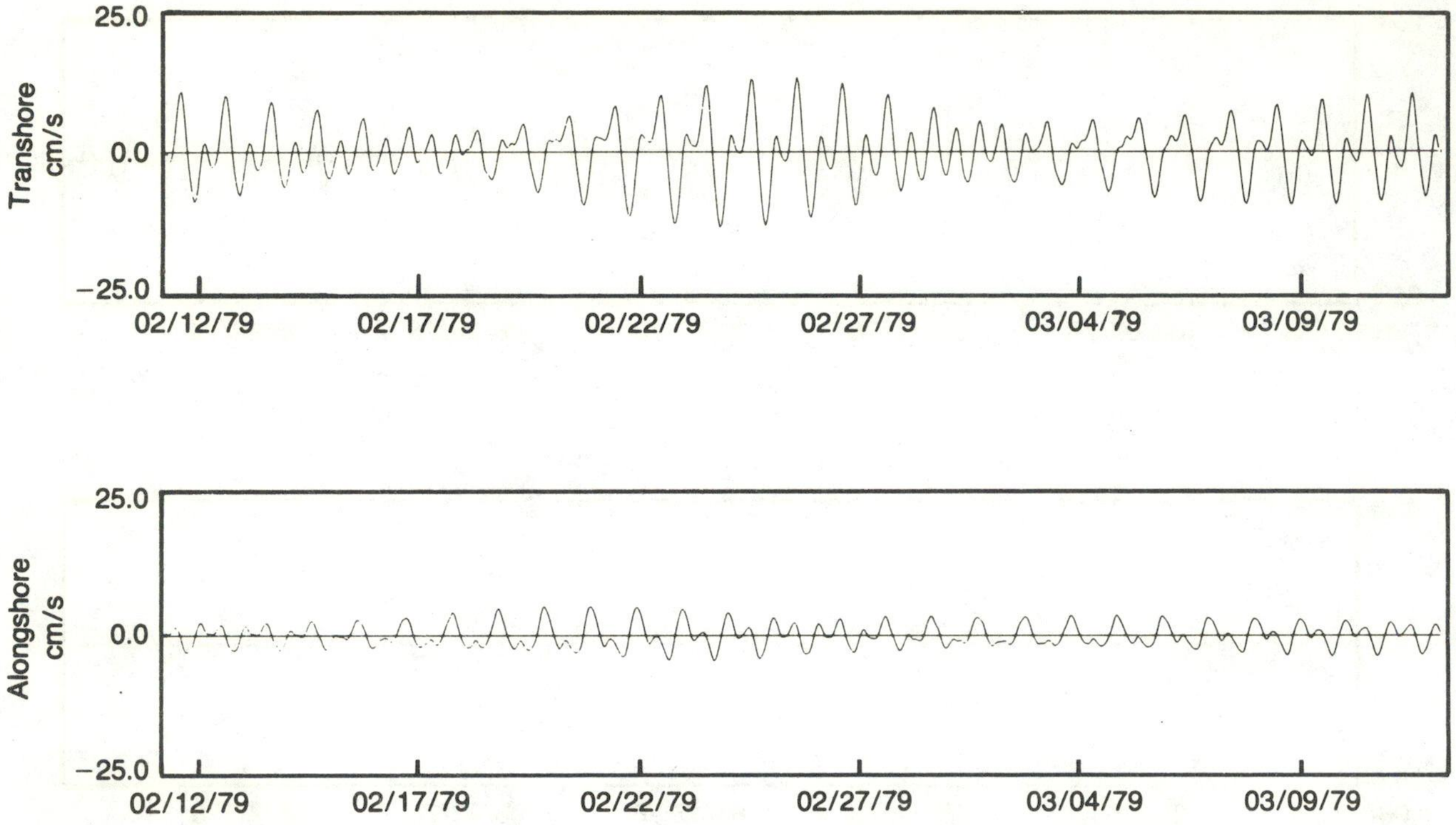

Figure 15-4. Calculated tidal currents at Weeks Island site, 1 m above bottom (a) station 21, February 11 to March 12, 1979, and (b) station 25, April 8 to May 7, 1979.

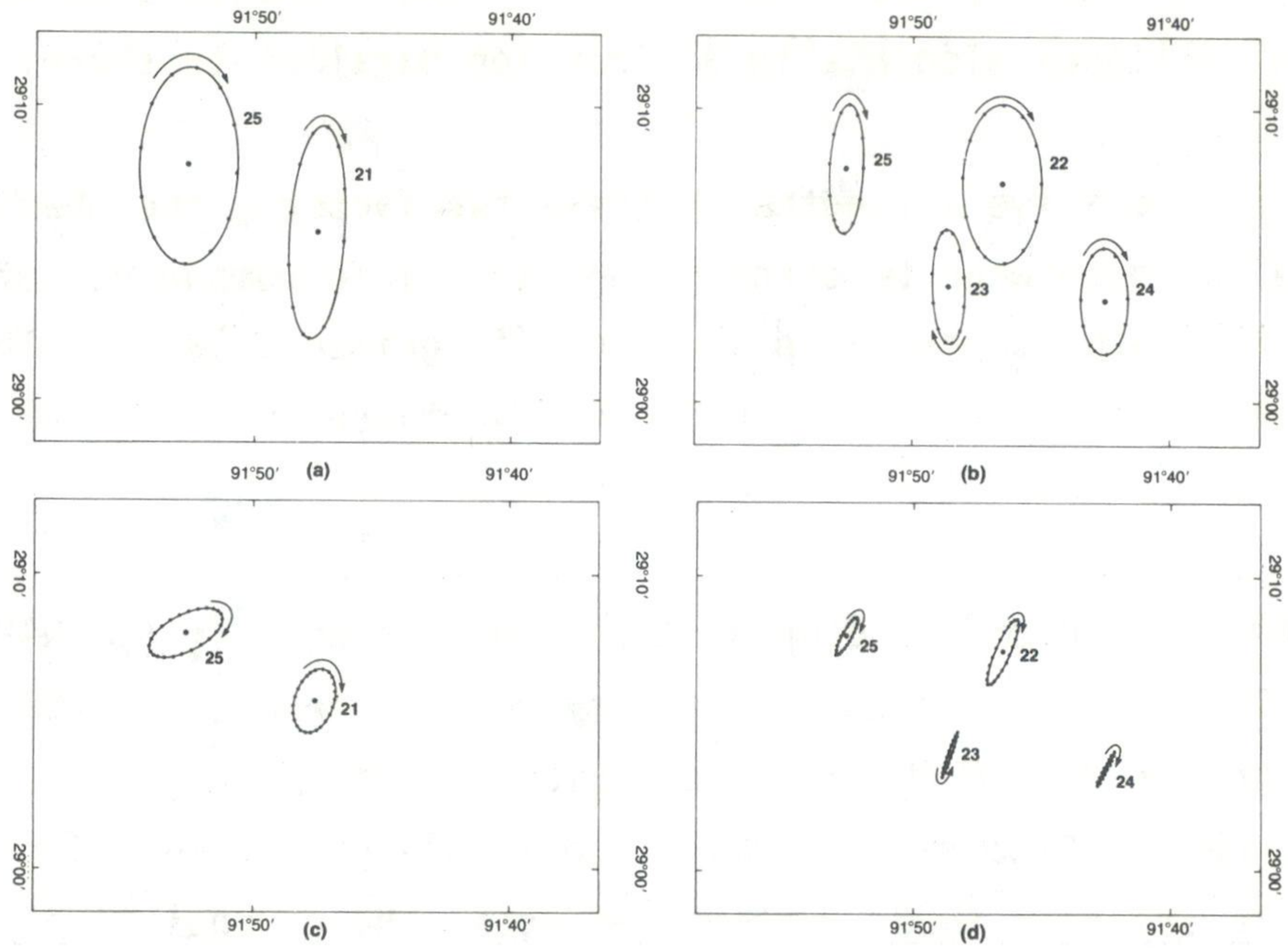

Figure 15-5. Tidal current ellipses for current series starting June 29 for station 23, June 30 for station 25, and July 1, 1978, for stations 21, 22, and 24: (a) 3 m above bottom and (b) 1 m above bottom for the M_2 constituents; (c) 3 m above bottom and (d) 1 m above bottom for the K_1 constituents.

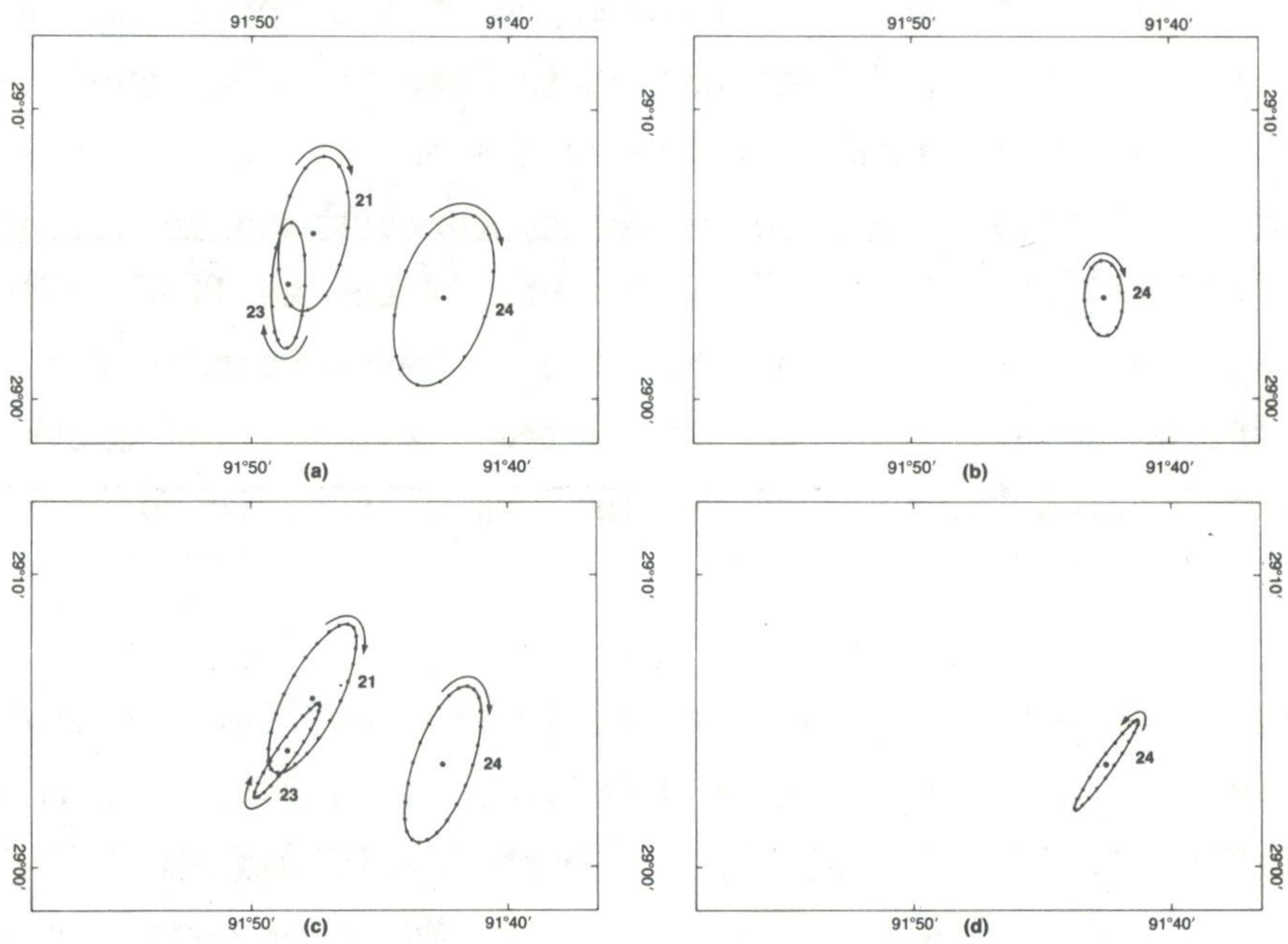

Figure 15-6. Tidal current ellipses for current series starting February 20 for stations 21 and 23, and February 22, 1979, for station 24, (a) 3 m above bottom and (b) 1 m above bottom for the M_2 constituents; (c) 3 m above bottom and (d) 1 m above bottom for the K_1 constituents.

- o As the tidal wave propagates shoreward toward the coastal boundary, tidal current ellipses elongate in a direction parallel to shore.

Depending on the relative strengths of these two factors, the phase difference and amplitude ratio between barotropic and baroclinic components at tidal frequencies fluctuate at any given location (Torgrimson, 1979). This unlocking of the phase and amplitude causes incoherent variance in the tidal frequency bands.

The determination of the diurnal tidal constituents K_1 (1.0042 CPD) and O_1 (0.93023 CPD) are further complicated by the presence of inertial currents at the frequency of 0.9926 CPD for the latitude at the site and by the sea breeze/land breeze effect at 1.0 CPD. Since the length of the time series was insufficient to separate these nontidal effects, the diurnal tidal frequency may be biased during the occurrence of nontidal currents at or near the diurnal frequency.

Figures 15-7 and 15-8 show the M_2 and K_1 yearly variability of the tidal current ellipticity and major axis orientation at station 21 1 m and 3 m above the bottom. The ellipticity is defined as the amplitude of the major axis minus the amplitude of the minor axis, divided by the amplitude of the major axis. An ellipticity of 1.0 indicates a pure reversing current and an ellipticity of 0.0 indicates a perfectly circular rotary current. When the flow is in the direction of the major axis orientation, the time is referenced to the GMT zone. The direction of the major axis corresponds to the first maximum epoch after the 0 hour (with 0 hour being the time of the maximum astronomic force over the 0 time meridian).

The ellipticity of the M_2 constituent in figures 15-7 and 15-8 for station 21 was found to have a yearly mean of 0.68 at 1 m and 0.59 at 3 m above the bottom. Variation from the mean value at both levels was small, with a standard deviation of only 0.07. The orientation of the M_2 major axis was found to average 21 degrees at 1 m and 18 degrees at 3 m above the bottom. The M_2 orientation during the year did not vary from its mean by more than 6 degrees, and the rotational direction of the M_2 current vector was nearly always clockwise. The relatively small fluctuations of the M_2 tidal currents phase and

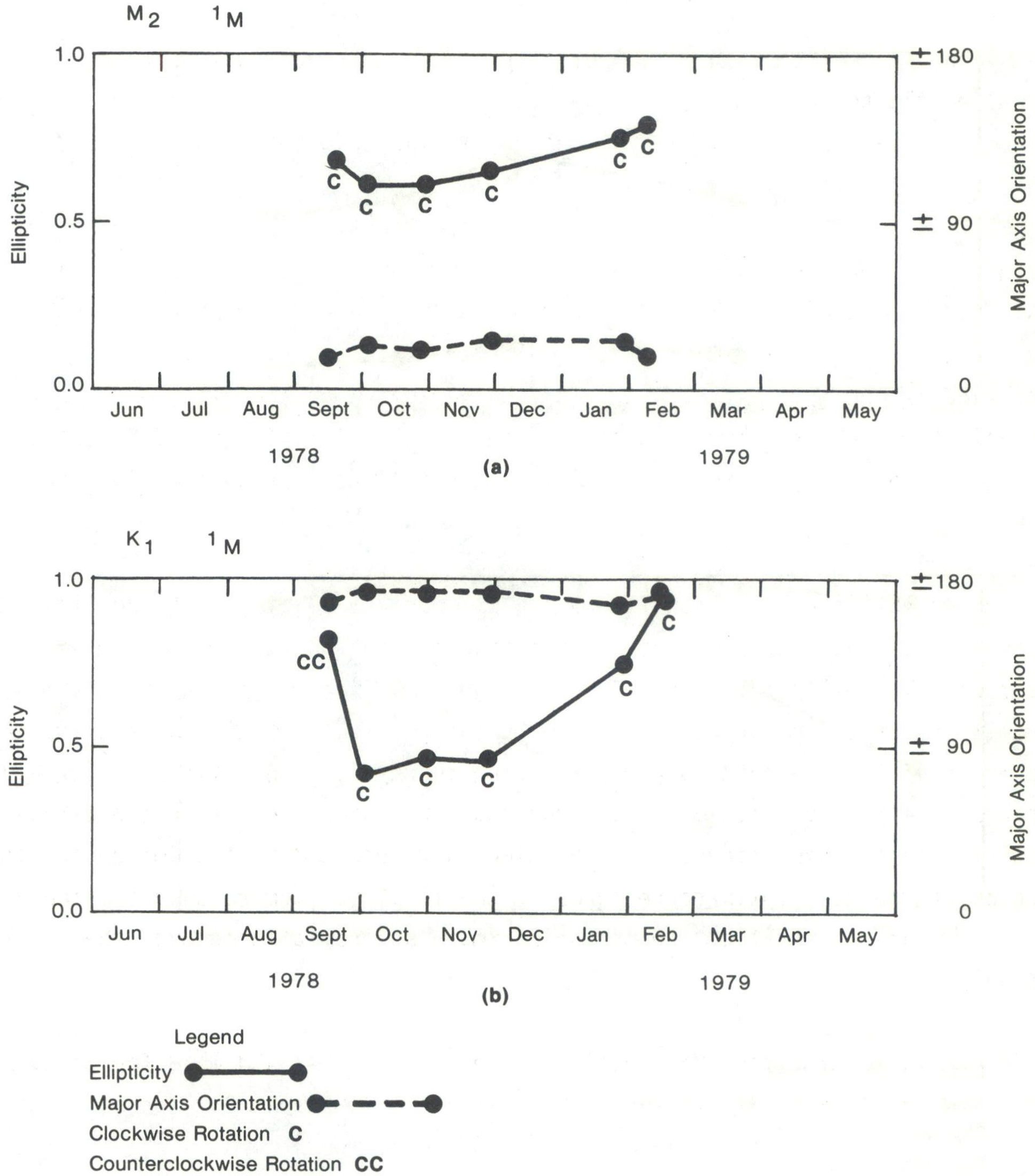

Figure 15-7. Tidal current ellipticity and major axis orientation for the (a) M_2 and (b) K_1 constituents at station 21 1 m above the bottom.

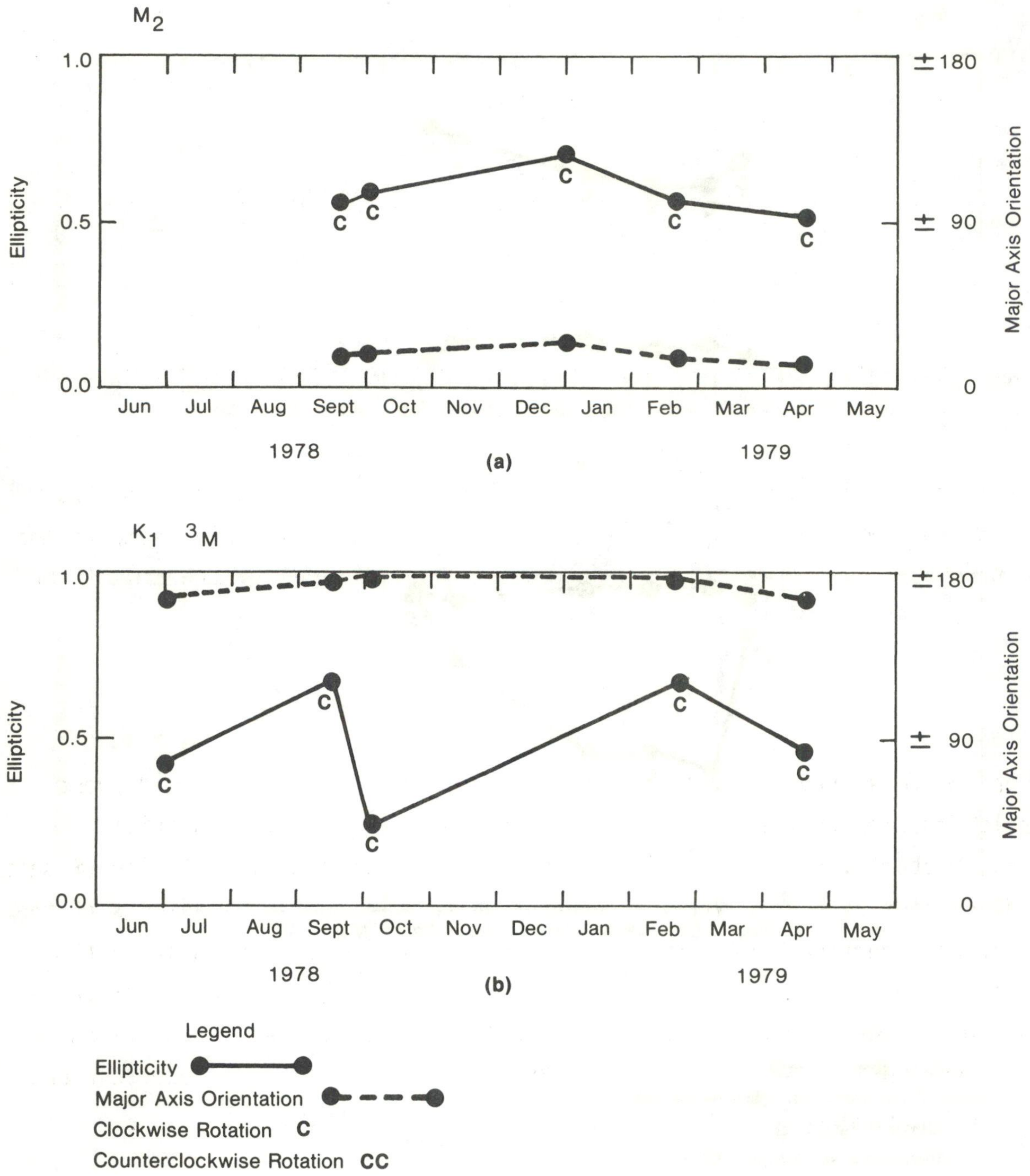

Figure 15-8. Tidal current ellipticity and major axis orientation for the (a) M_2 and (b) K_1 constituents at station 21 3 m above the bottom.

amplitude during the year suggests the semidiurnal tidal constituent had a strong barotropic mode for most of the year, although a baroclinic response could dominate in a strongly stratified water column.

The ellipticity of the K_1 tidal current ellipses varied significantly during the year, while the orientation of the major axis remained fairly consistent. At station 21, the ellipticity of the K_1 constituent was found to have a mean of 0.64 at 1 m and 0.49 at 3 m above the bottom. Variation from the mean values was large at both levels, with a standard deviation of 0.22. The orientation of the K_1 major axis was found to average 170° at 1 m and 174 degrees at 3 m above the bottom. The K_1 orientation during the year did not vary from its mean by more than 6 degrees, and the rotational direction of the K_1 current vector was nearly always clockwise.

The variability of the K_1 ellipticity suggests the presence of a dominant baroclinic mode at the diurnal frequency. As discussed previously, some of the unlocking of the amplitude may be attributed to the nontidal components of the current that can be generated at the diurnal frequency.

15.2. Spatial Characteristics

For insights into the circulation at the Weeks Island site beyond those available from temporal and spectral considerations, a series of spatial examples, vector-averaged over 1-hour intervals, is presented. Dilution of salt brine discharges by mixing will be governed in part by spatial gradients of the currents, both vertical and horizontal. Substances are advected away by the currents, and are mixed into the surrounding waters by eddy diffusion processes that are governed by turbulence. In figures 15-9 to 15-24, we show horizontal current distributions at stations 21 to 25 and the vertical profile of currents at station 21, when different forces dominate the circulation.

Current vectors indicating the circulation at 1 m above the bottom at the Weeks Island site during July 6 and 7 are shown in figures 15-9 and 15-10. The time series and autospectra of currents for July indicate that the circulation was influenced mainly by the tide on July 6 and 7, and that there was an added influence of a land/sea breeze system during the month.

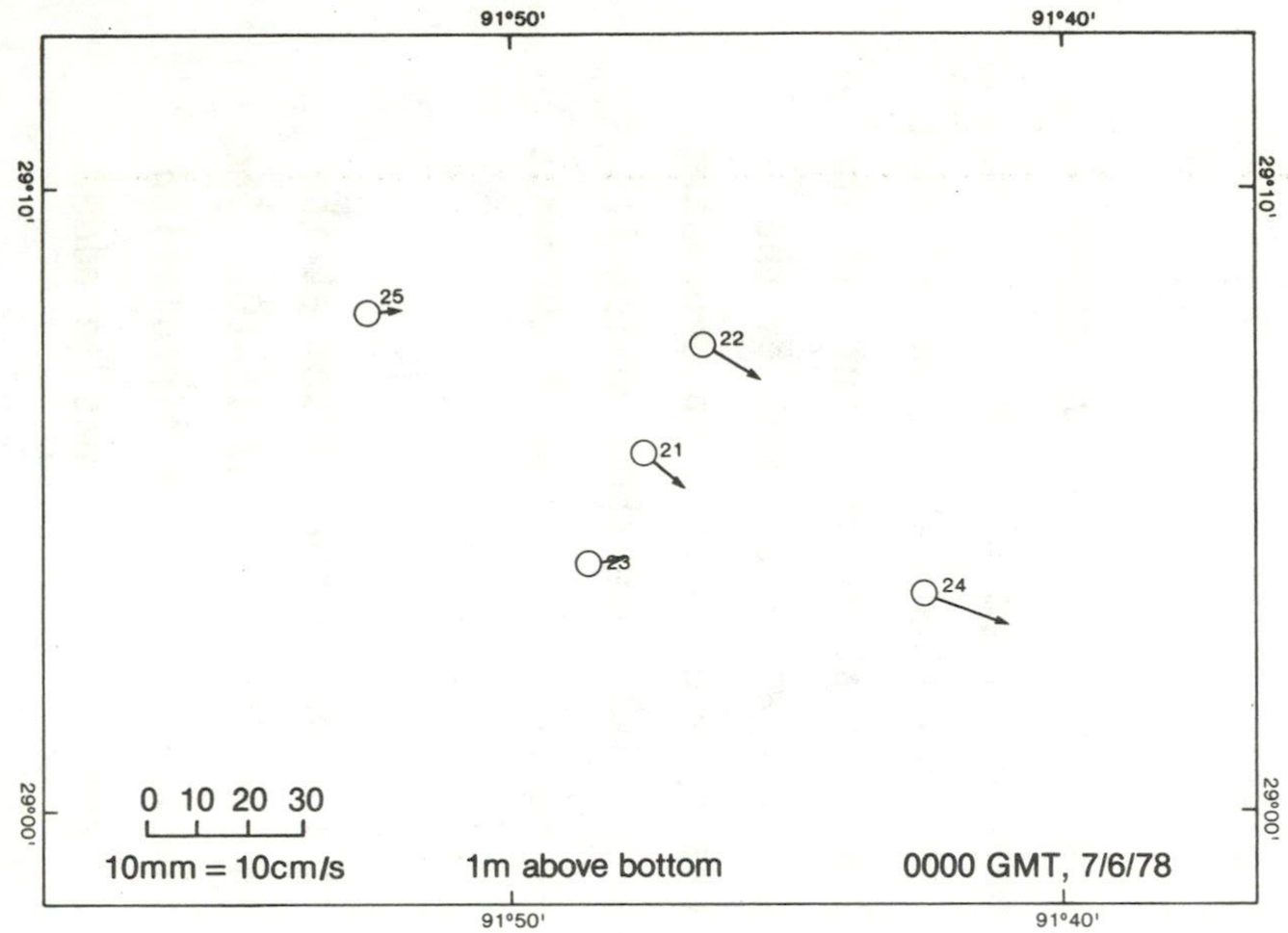

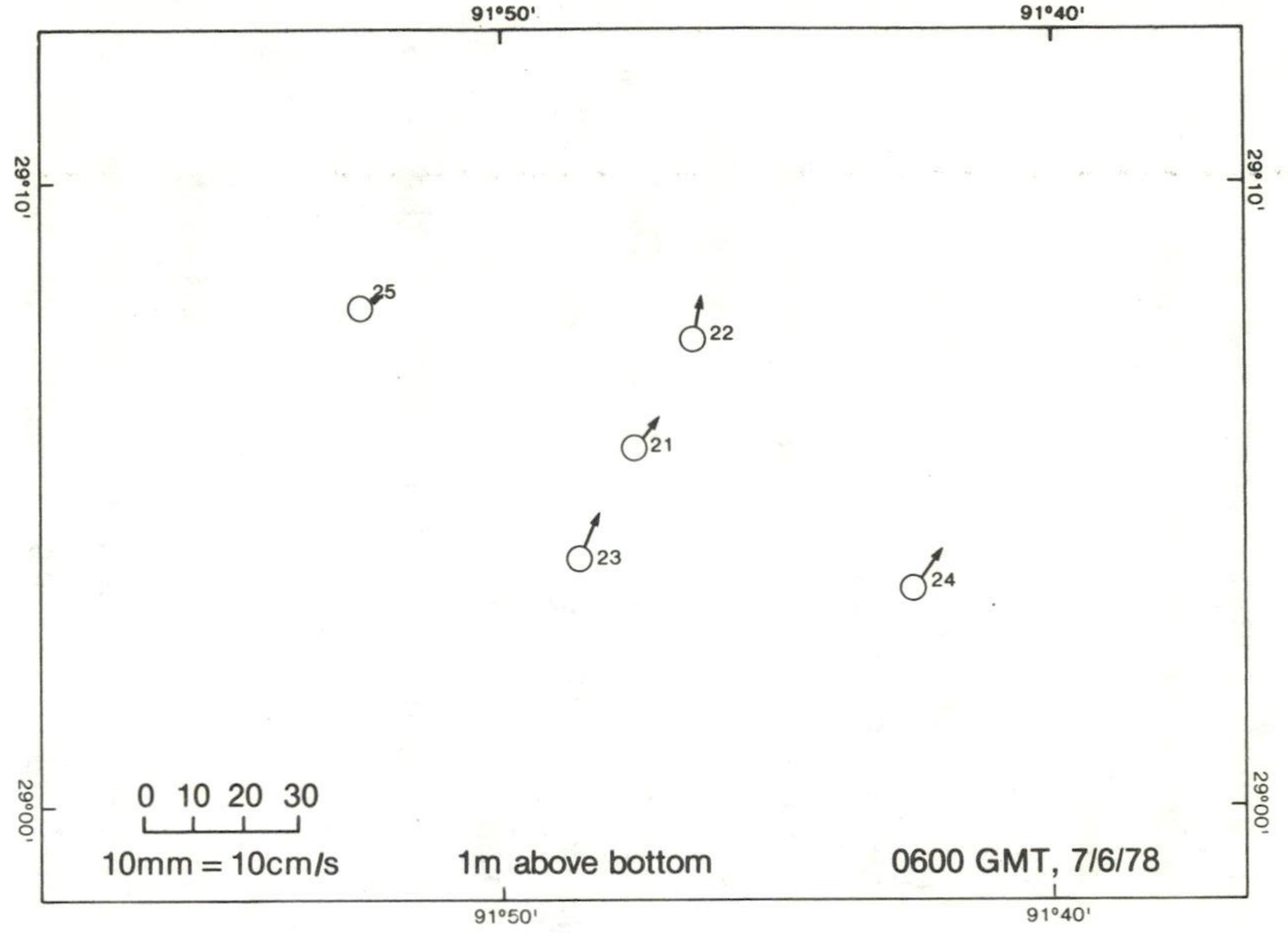

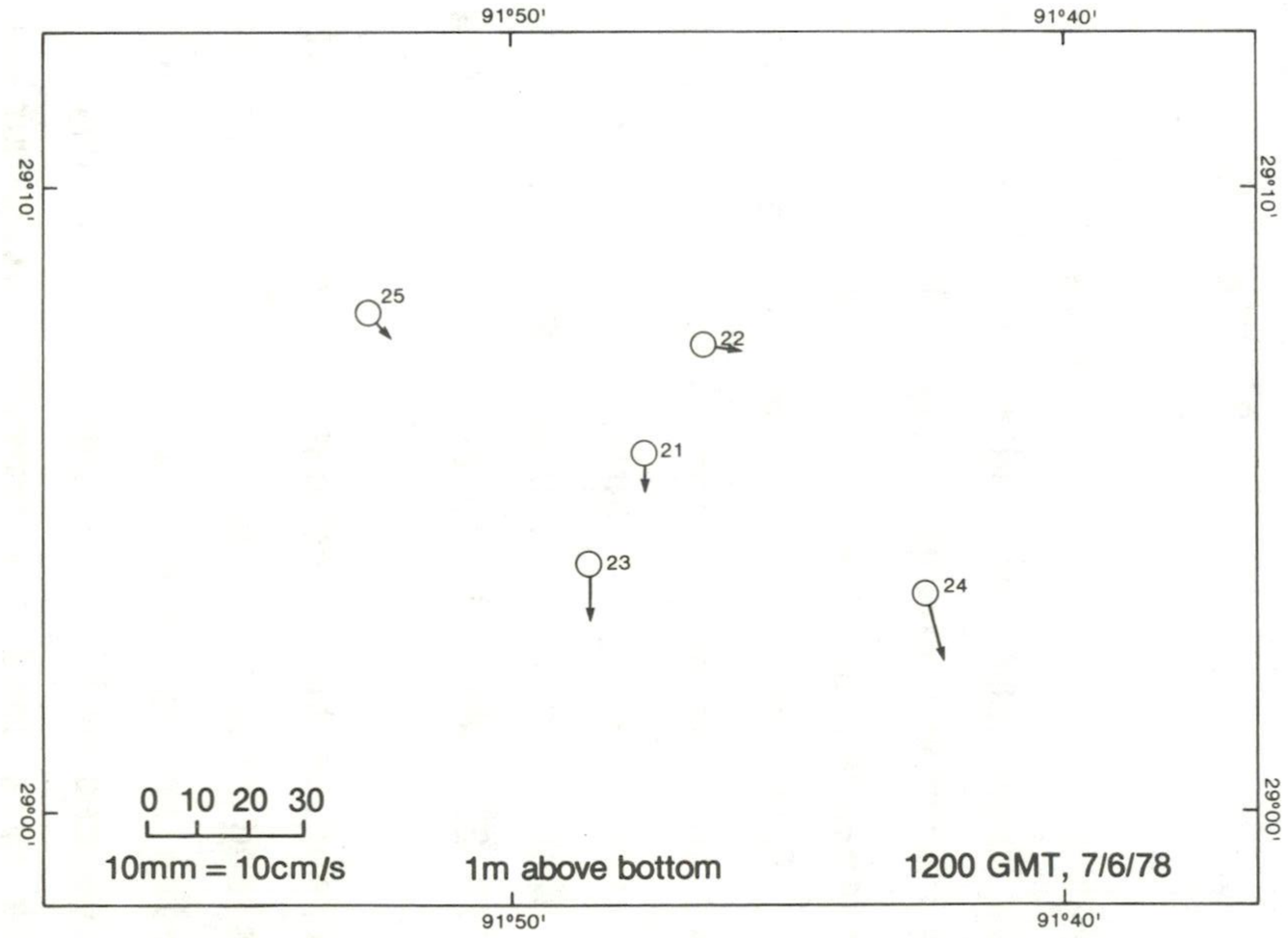

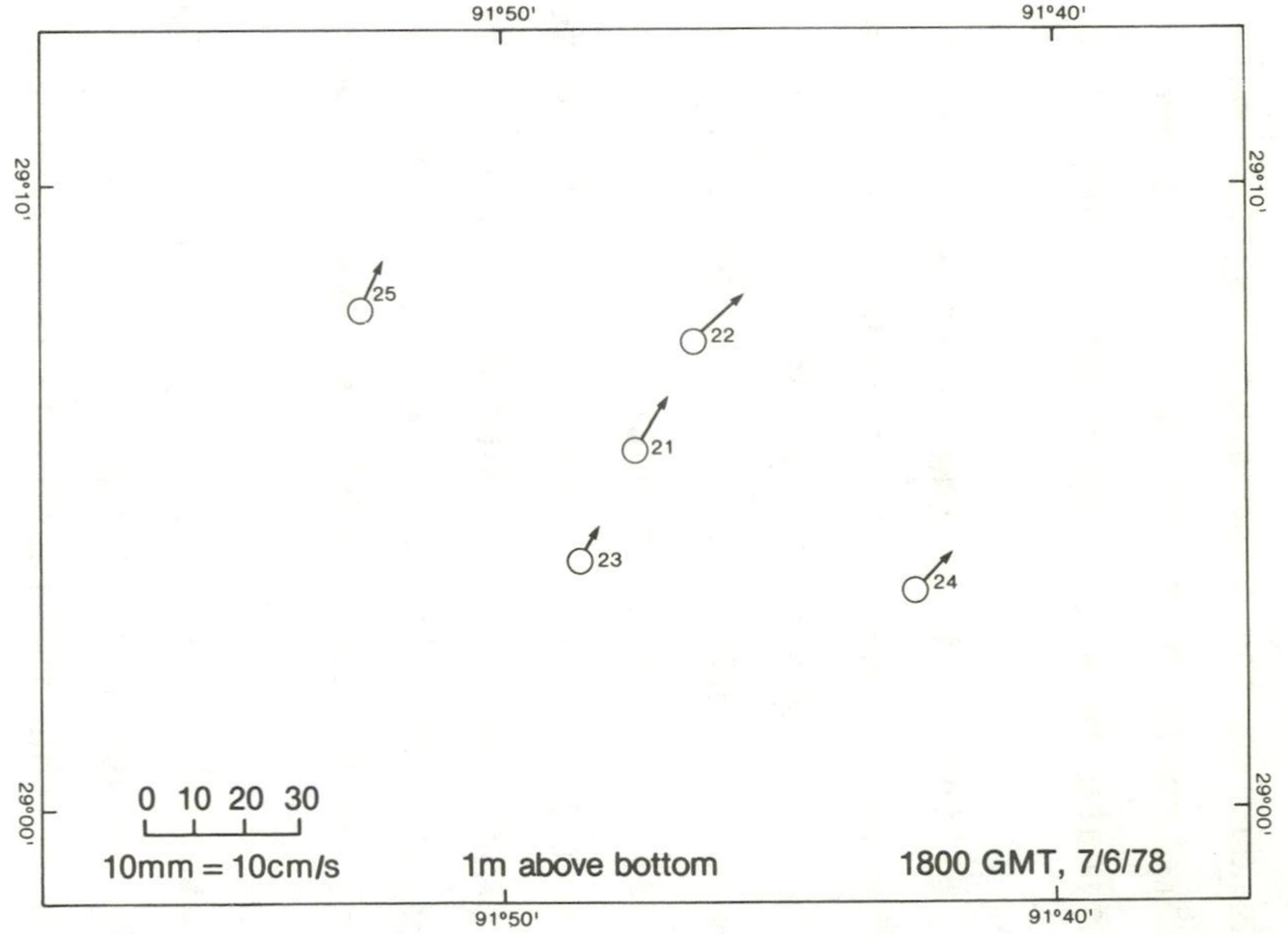

Figure 15-9. Current vectors at 6-hour intervals, 1 m above bottom at Weeks Island site, July 6, 1978.

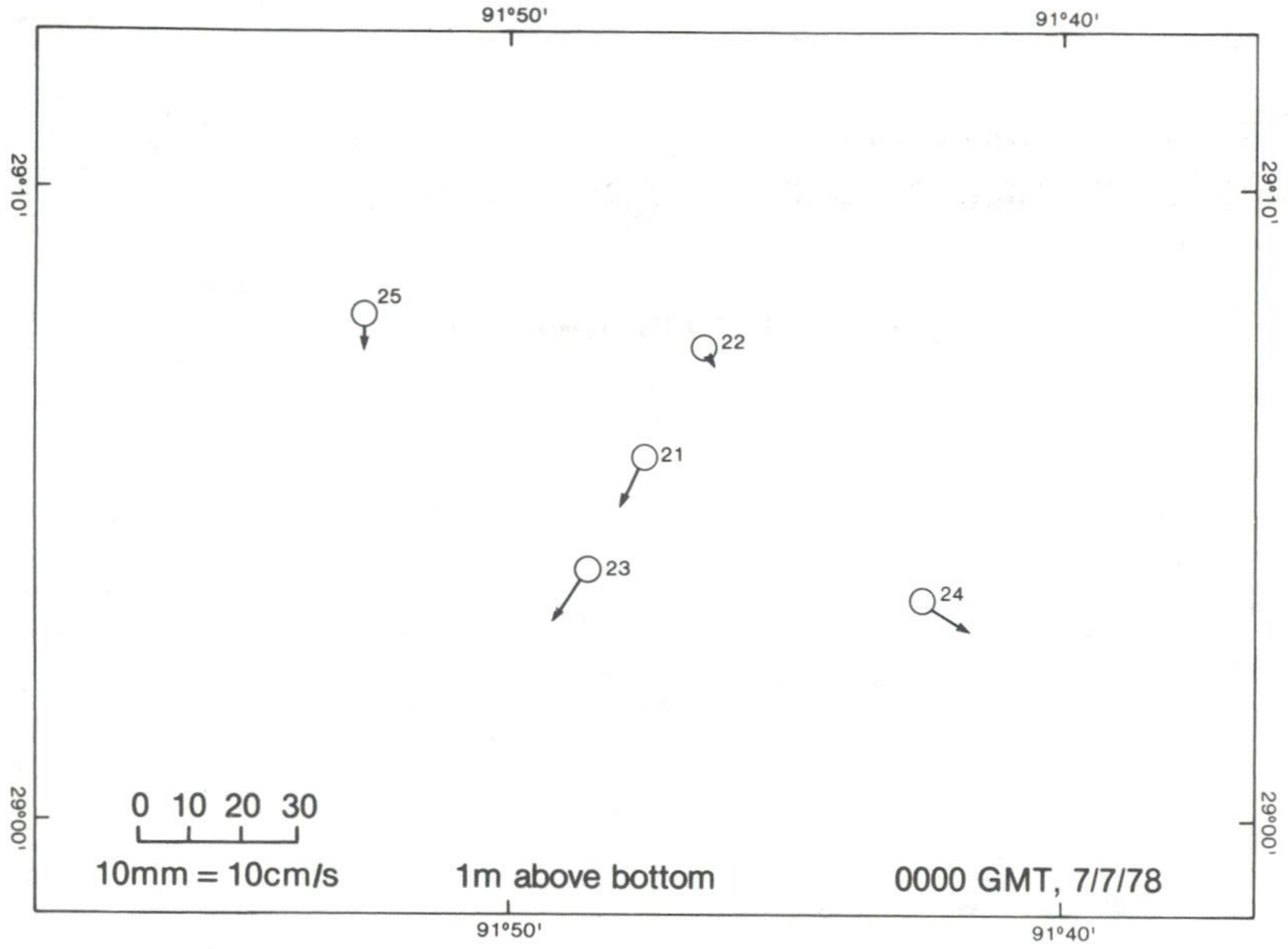

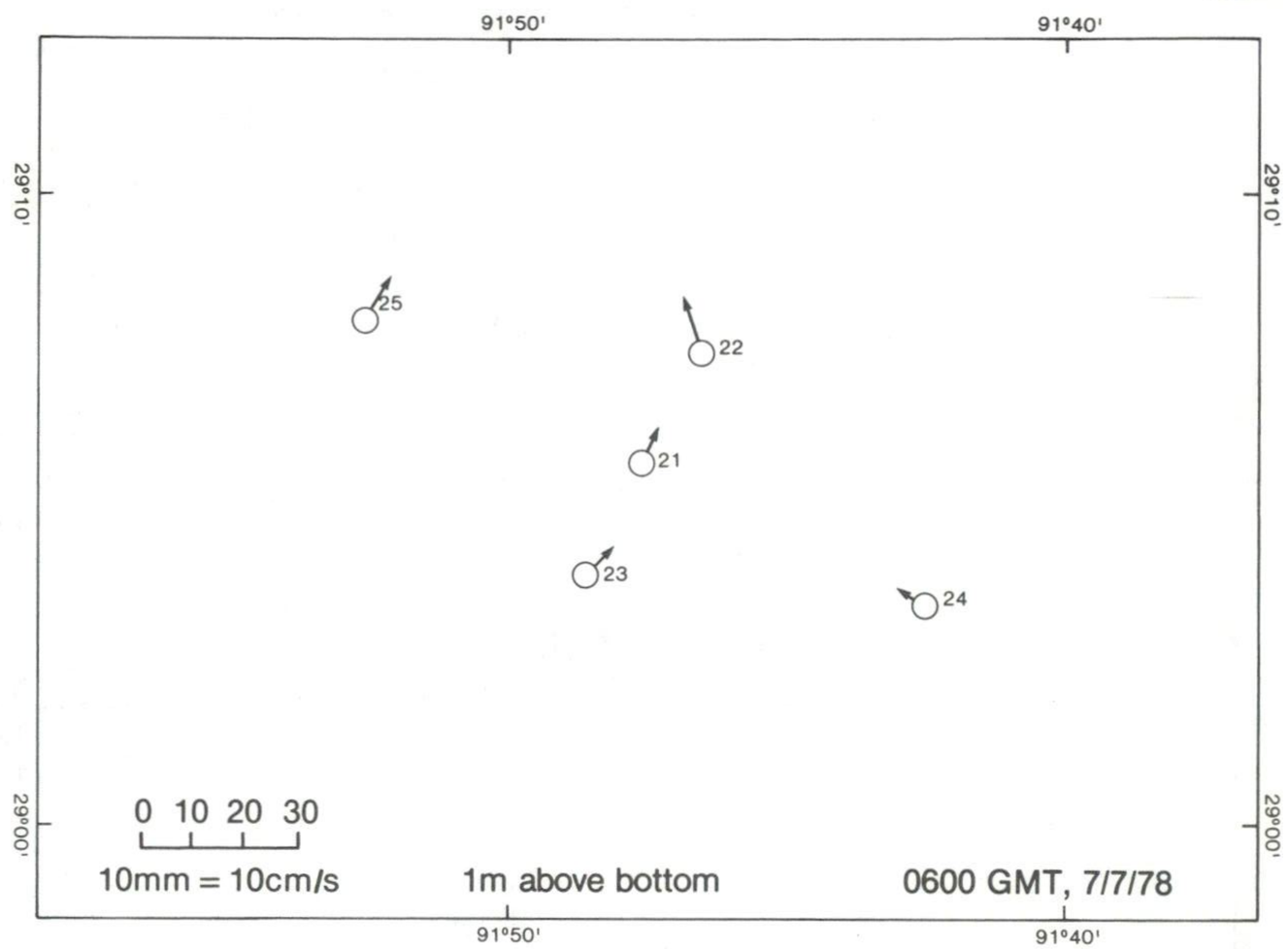

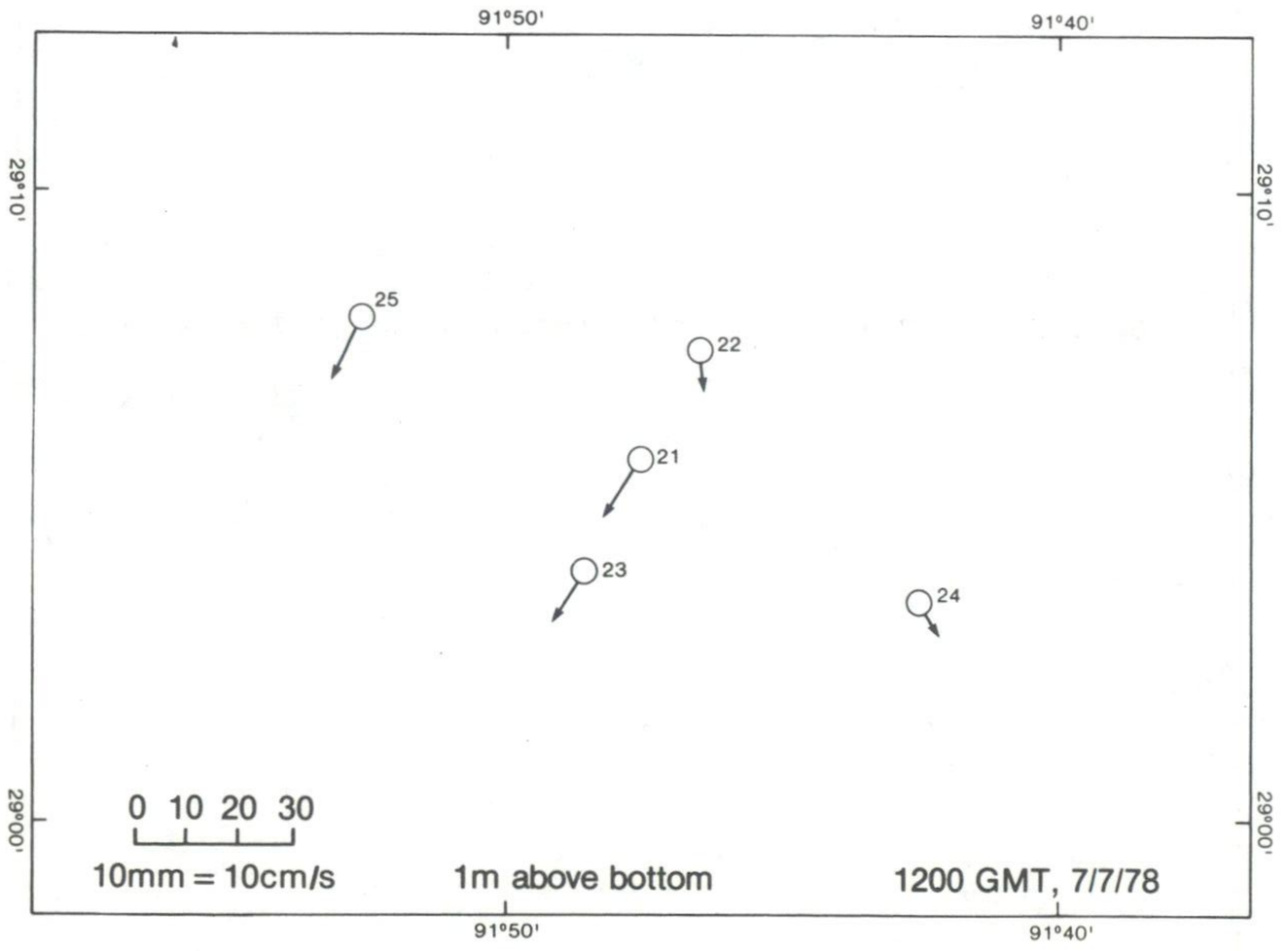

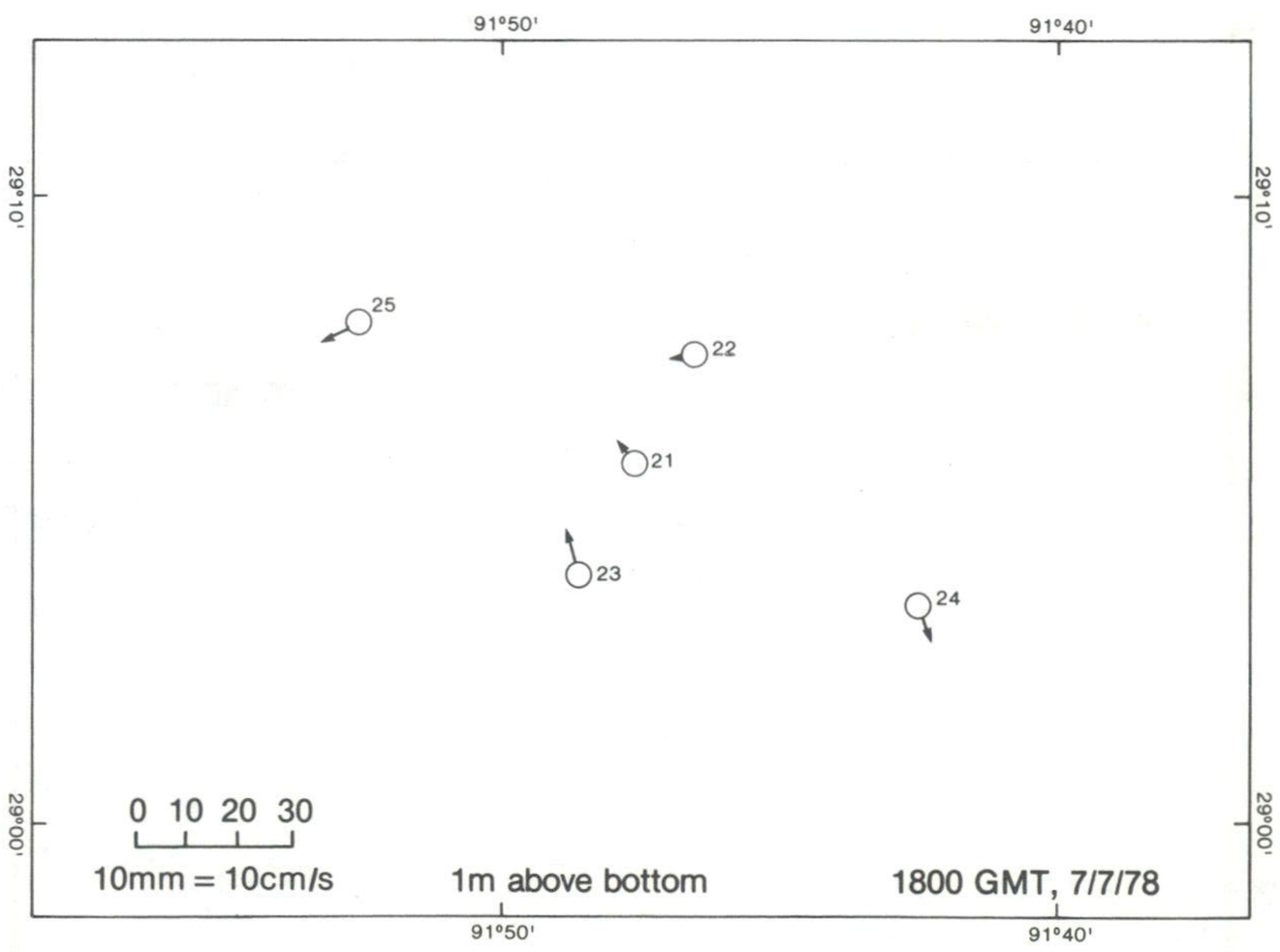

Figure 15-10. Current vectors at 6-hour intervals, 1 m above bottom at Weeks Island site, July 7, 1978.

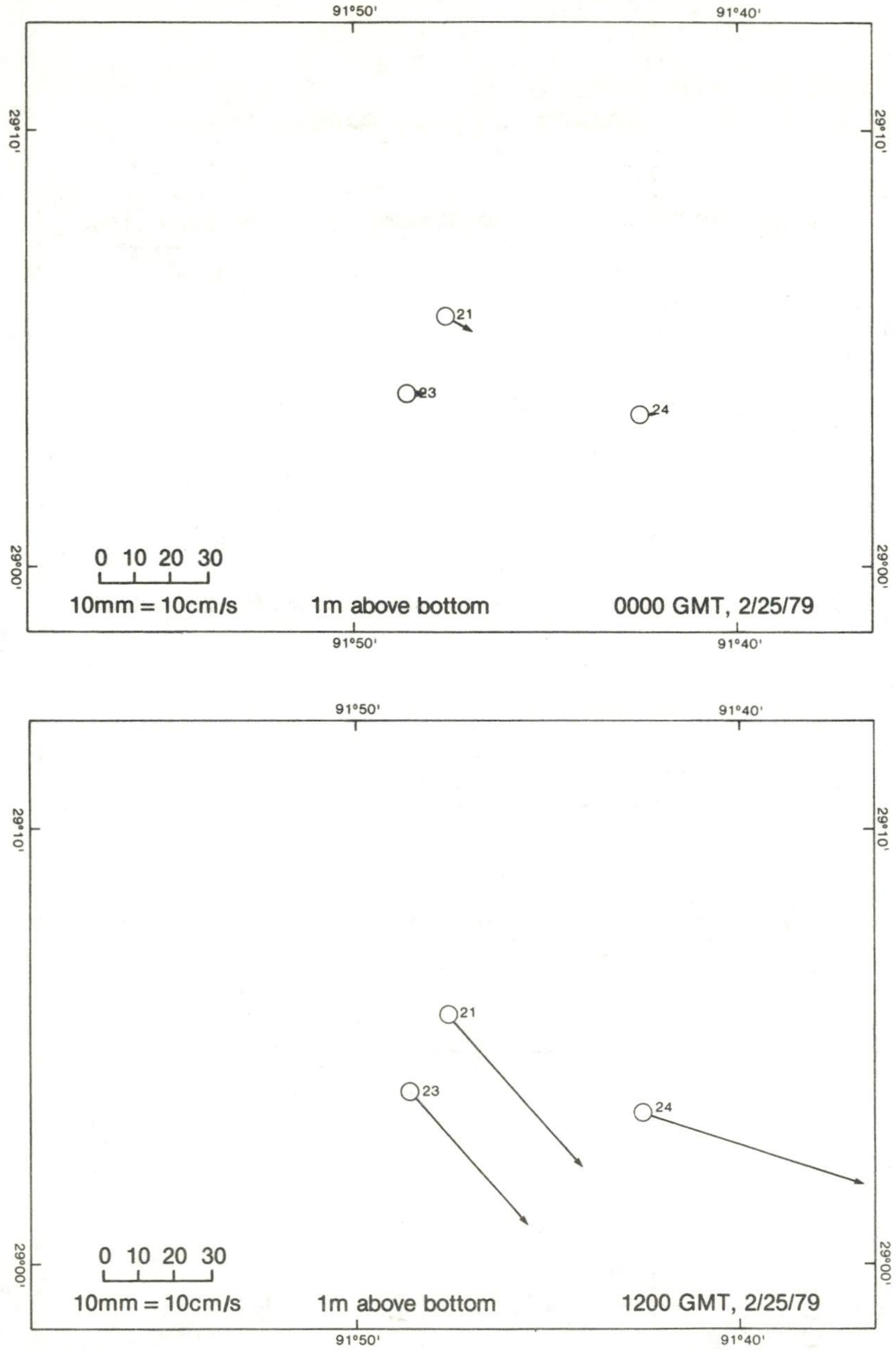

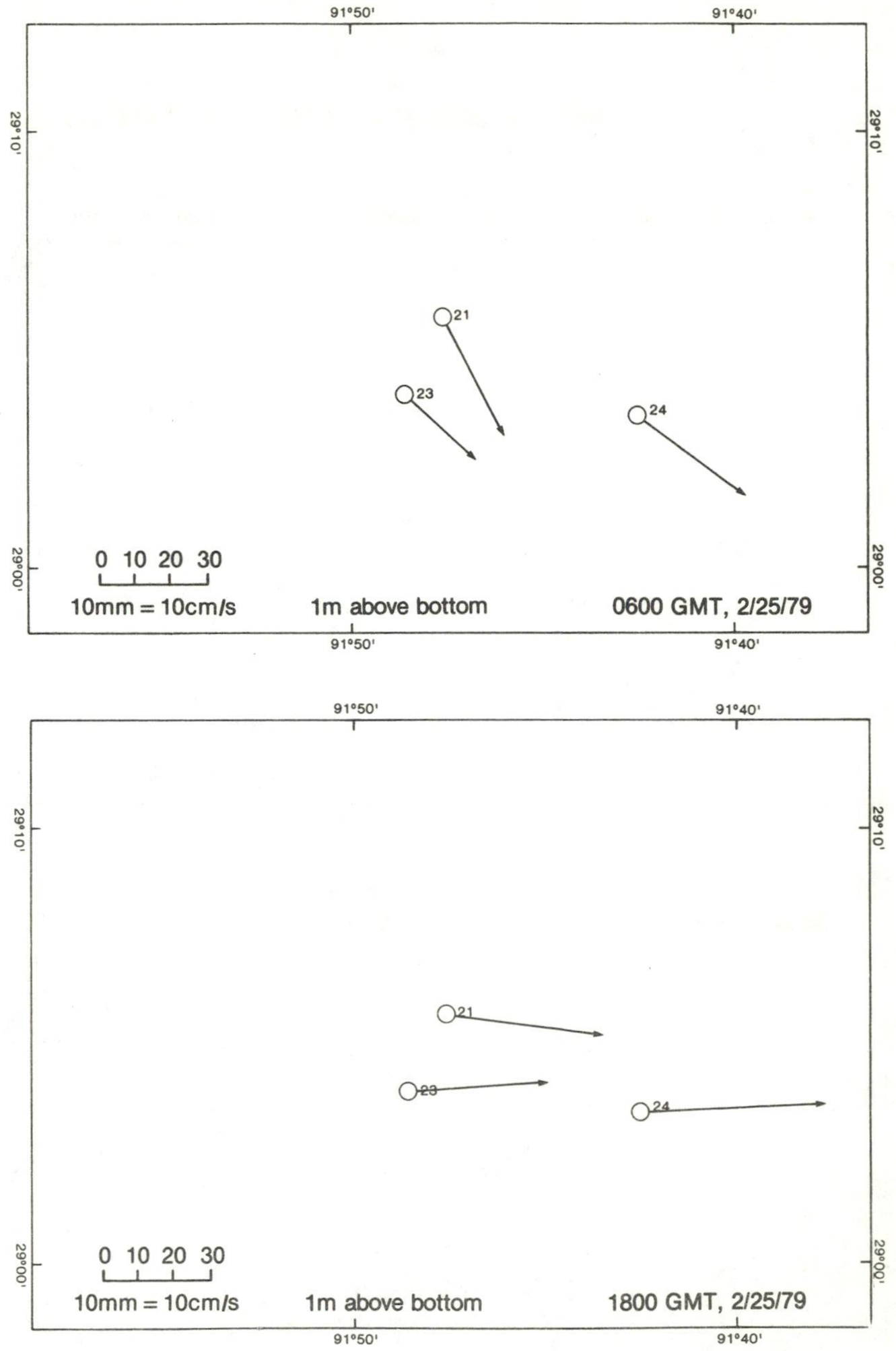

Figure 15-11. Current vectors at 6-hour intervals, 1 m above bottom at Weeks Island site, February 25, 1979.

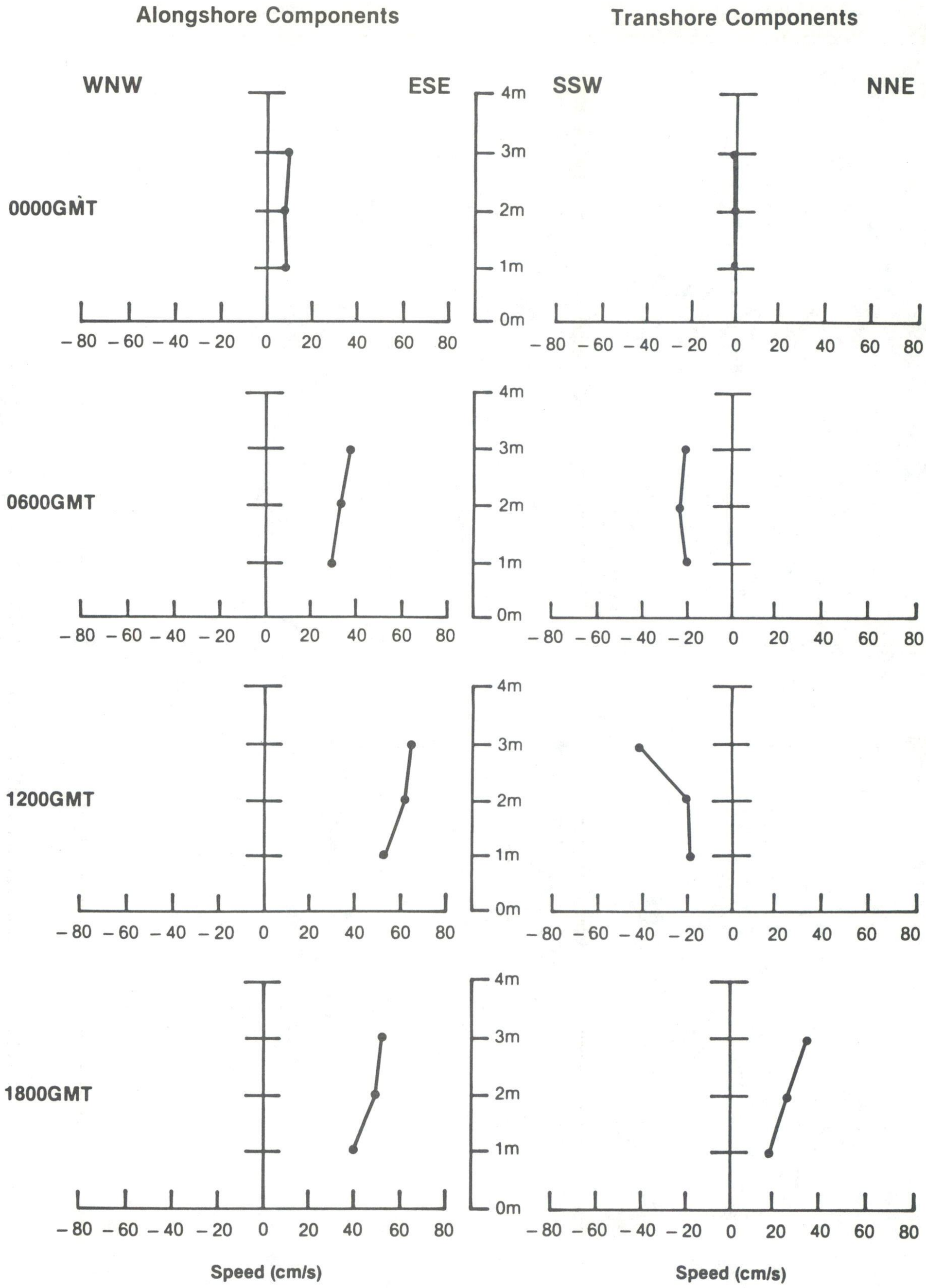

Figure 15-12. Vertical profiles of currents at Weeks Island site station 21, February 25, 1979.

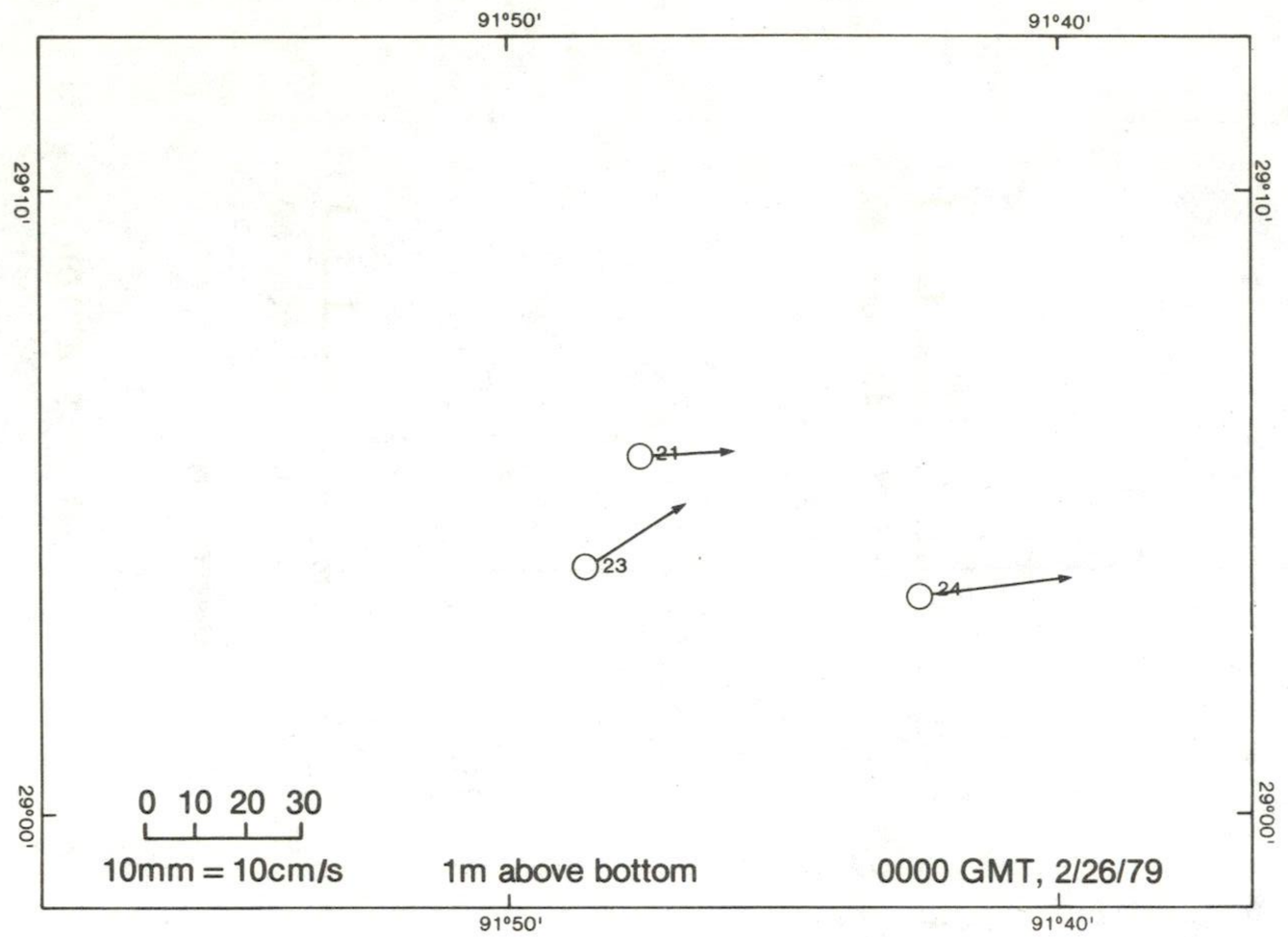

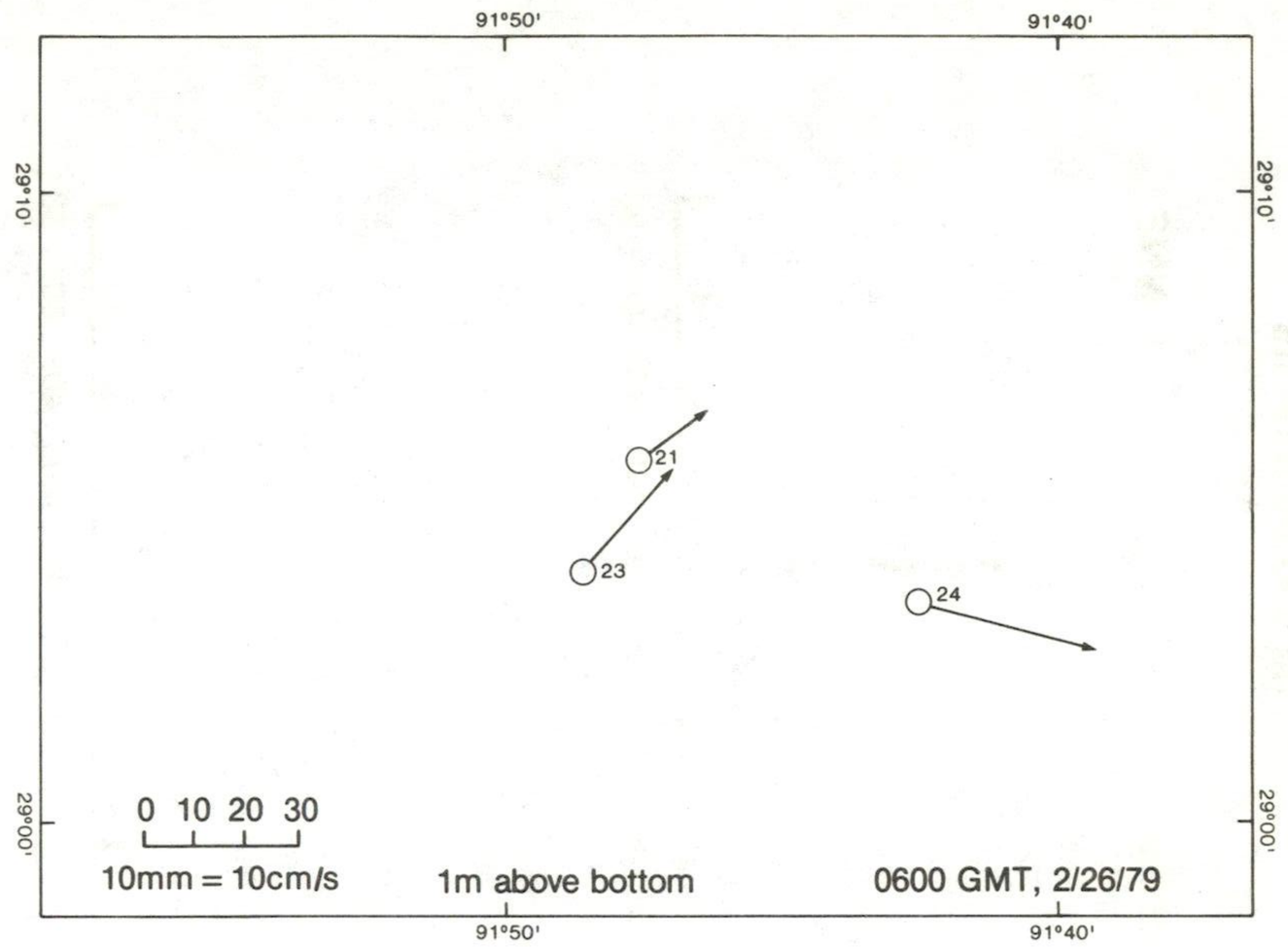

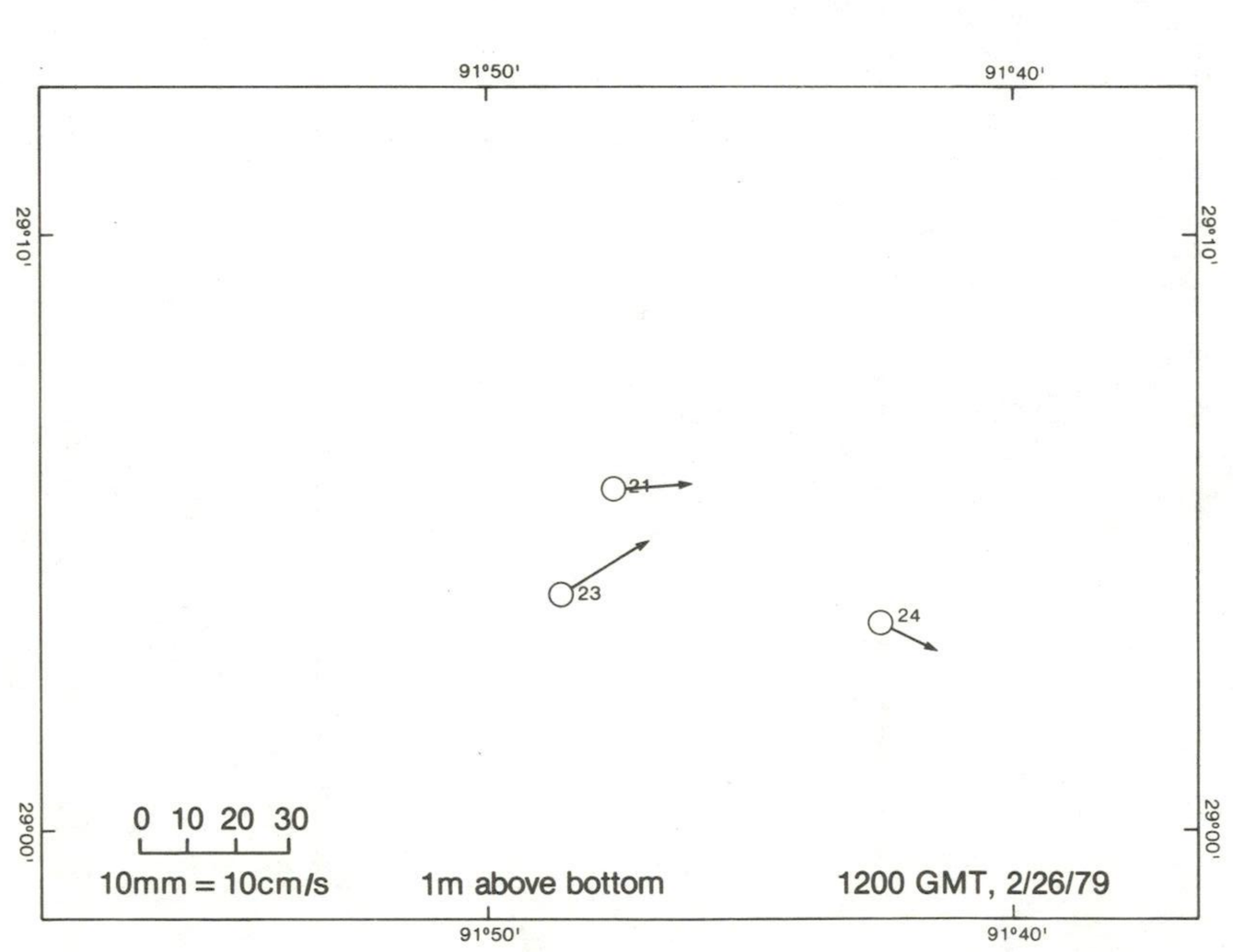

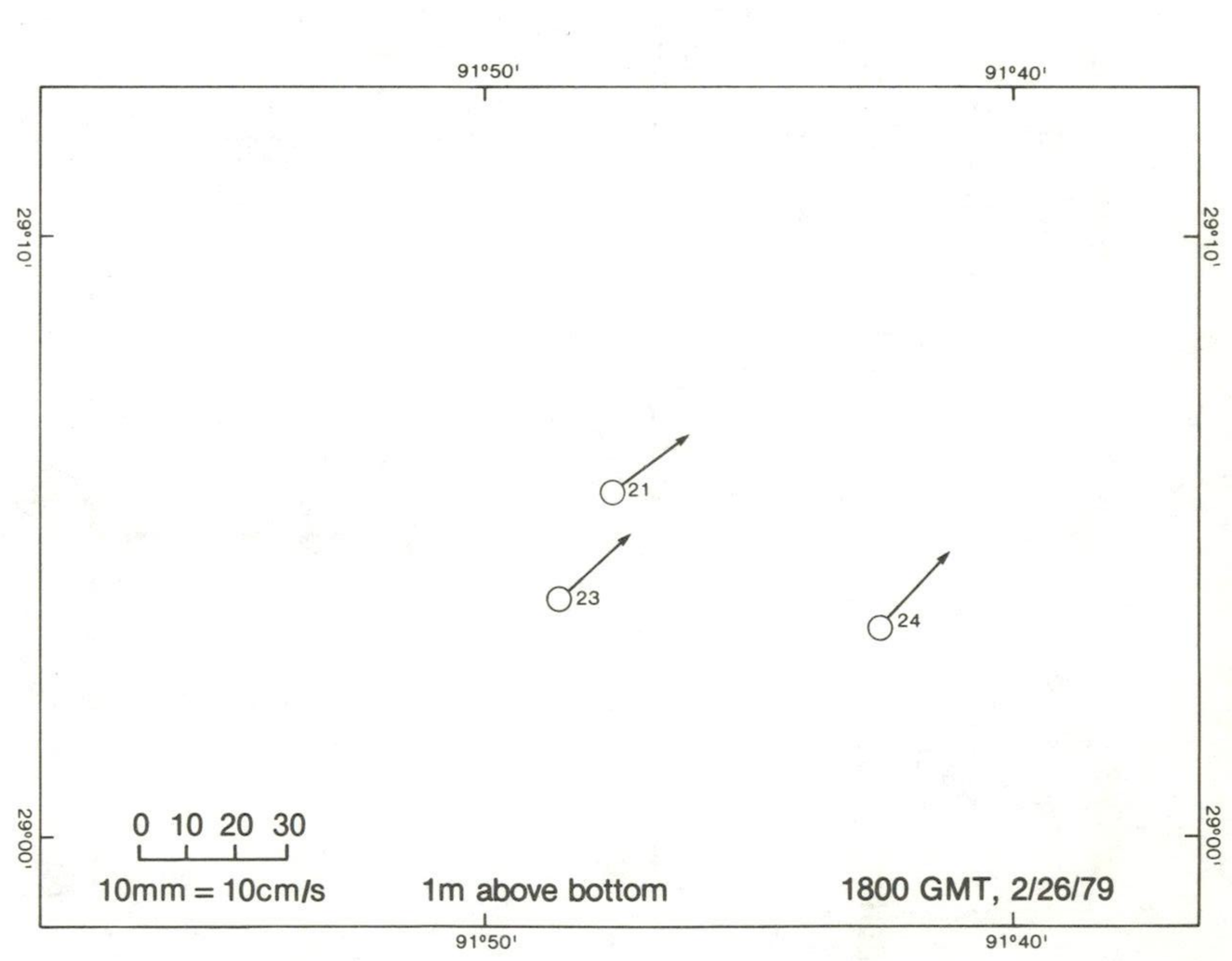

Figure 15-13. Current vectors at 6-hour intervals, 1 m above bottom at Weeks Island site, February 26, 1979.

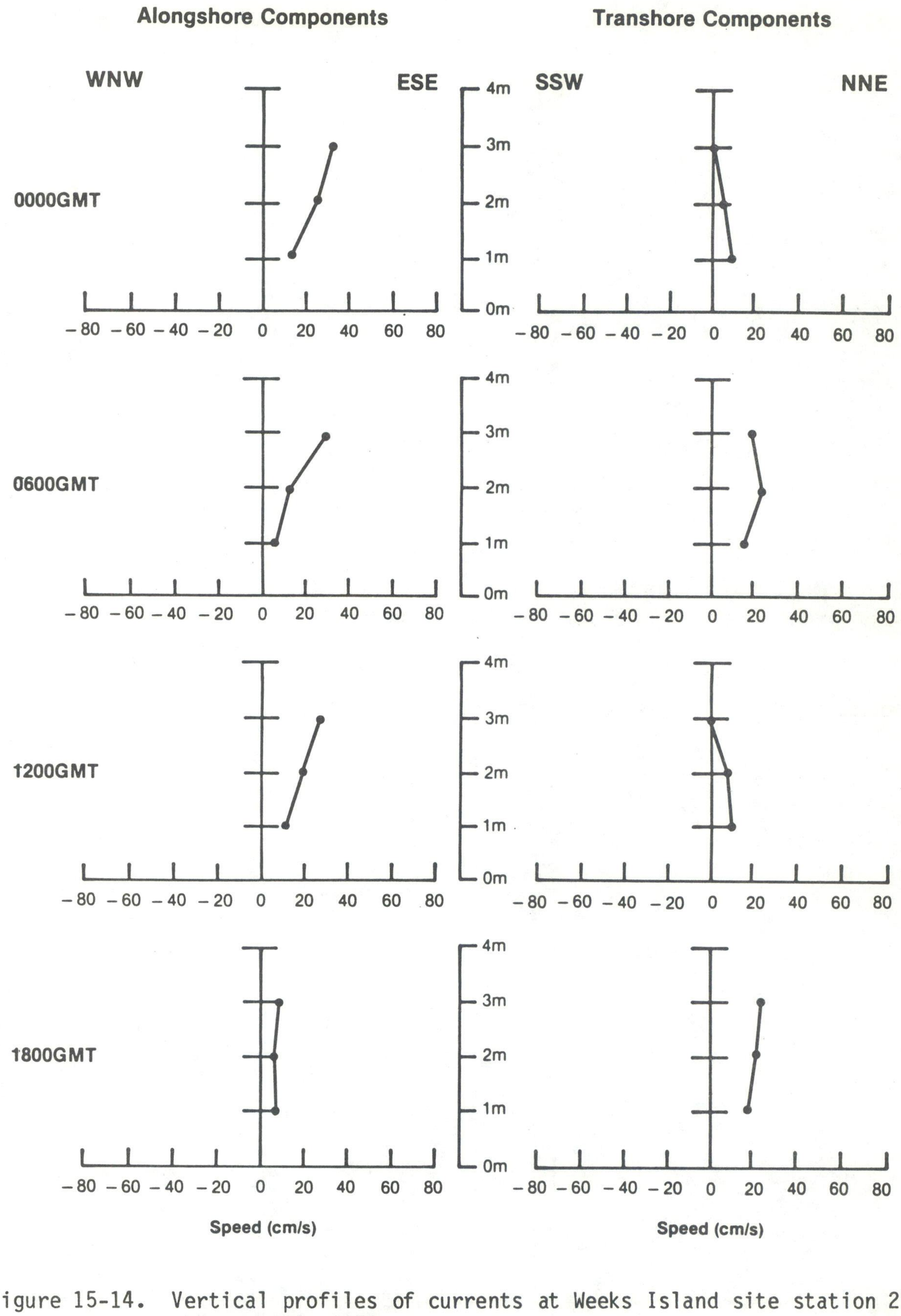

Figure 15-14. Vertical profiles of currents at Weeks Island site station 21, February 26, 1979.

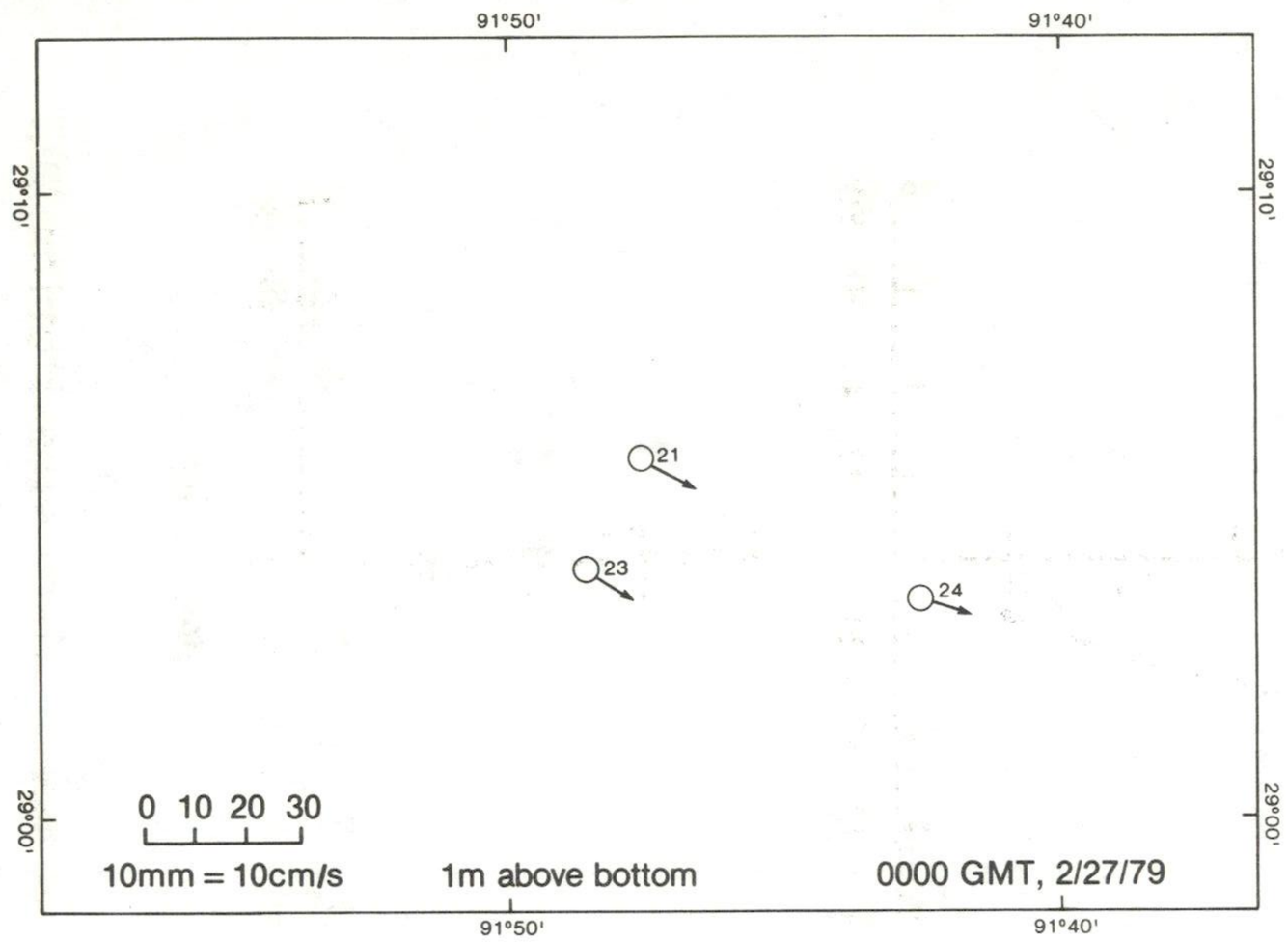

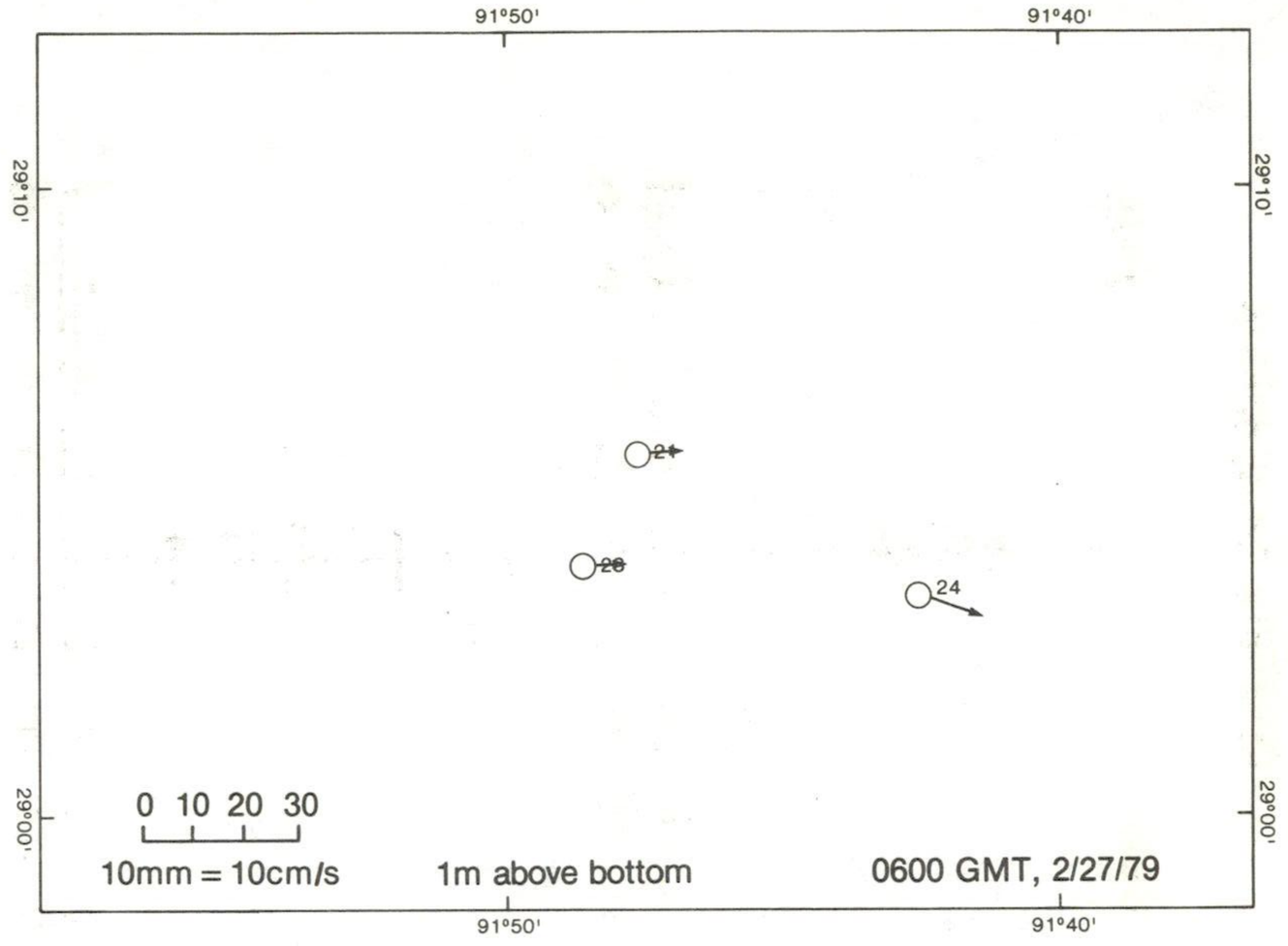

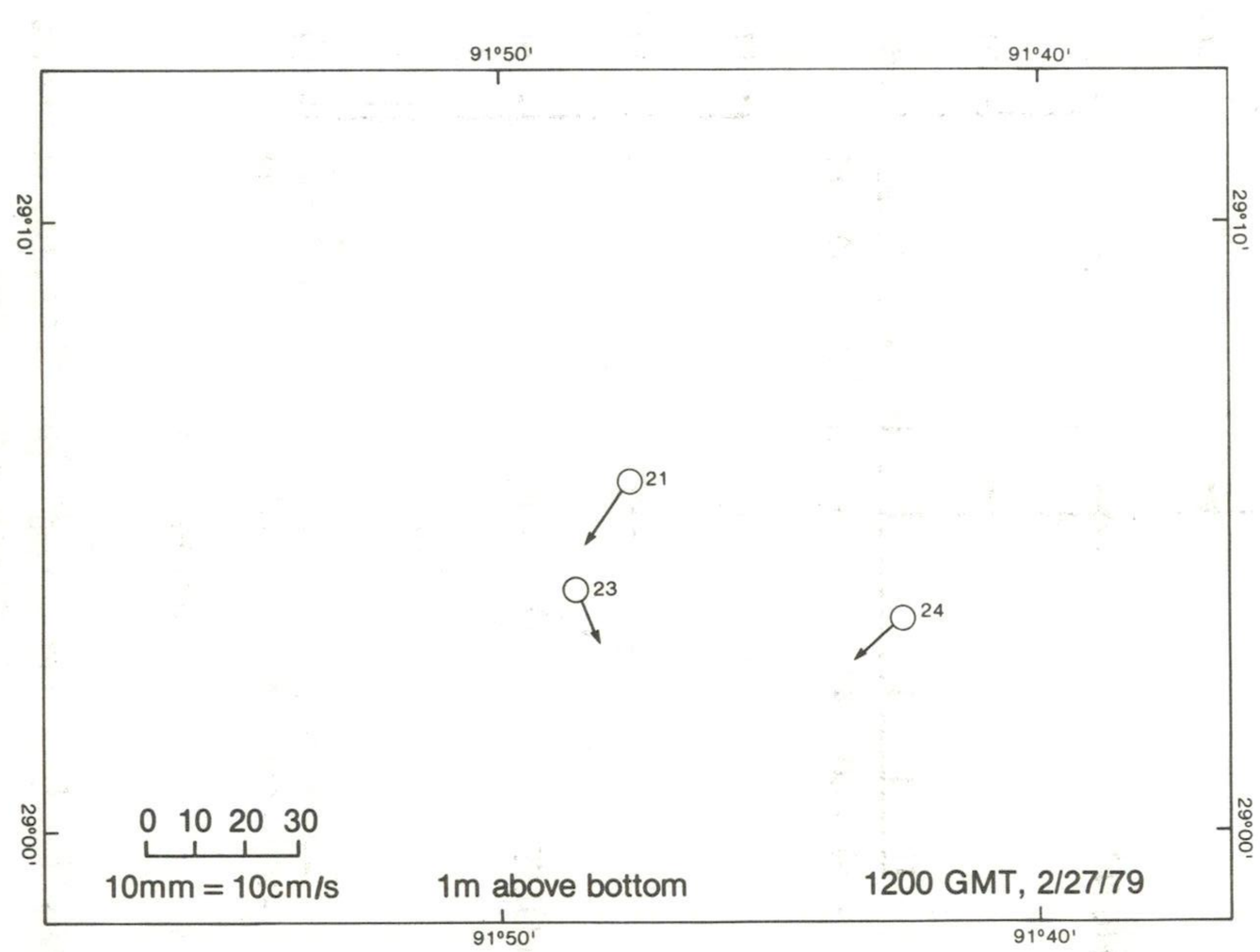

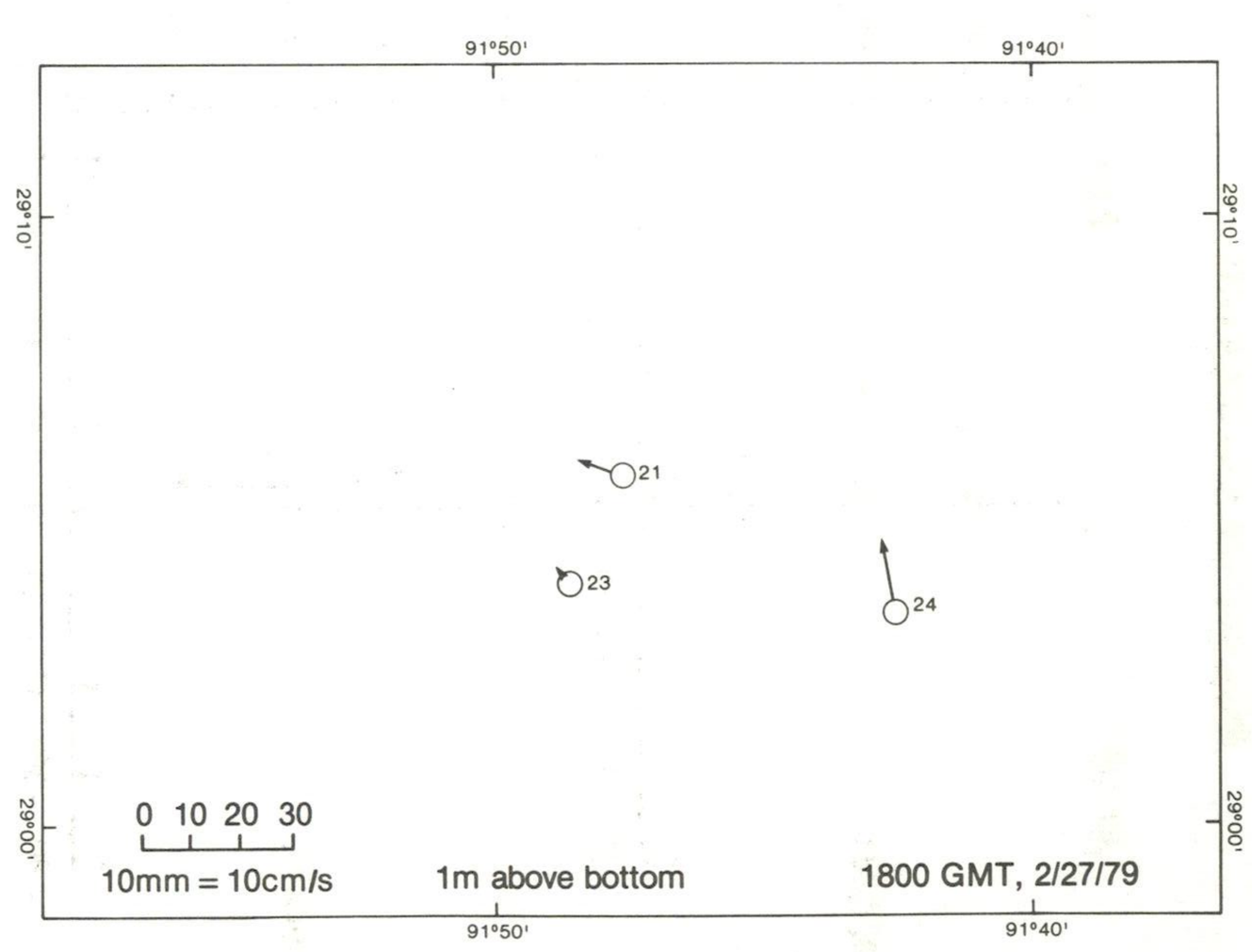

Figure 15-15. Current vectors at 6-hour intervals, 1 m above bottom at Weeks Island site, February 27, 1979.

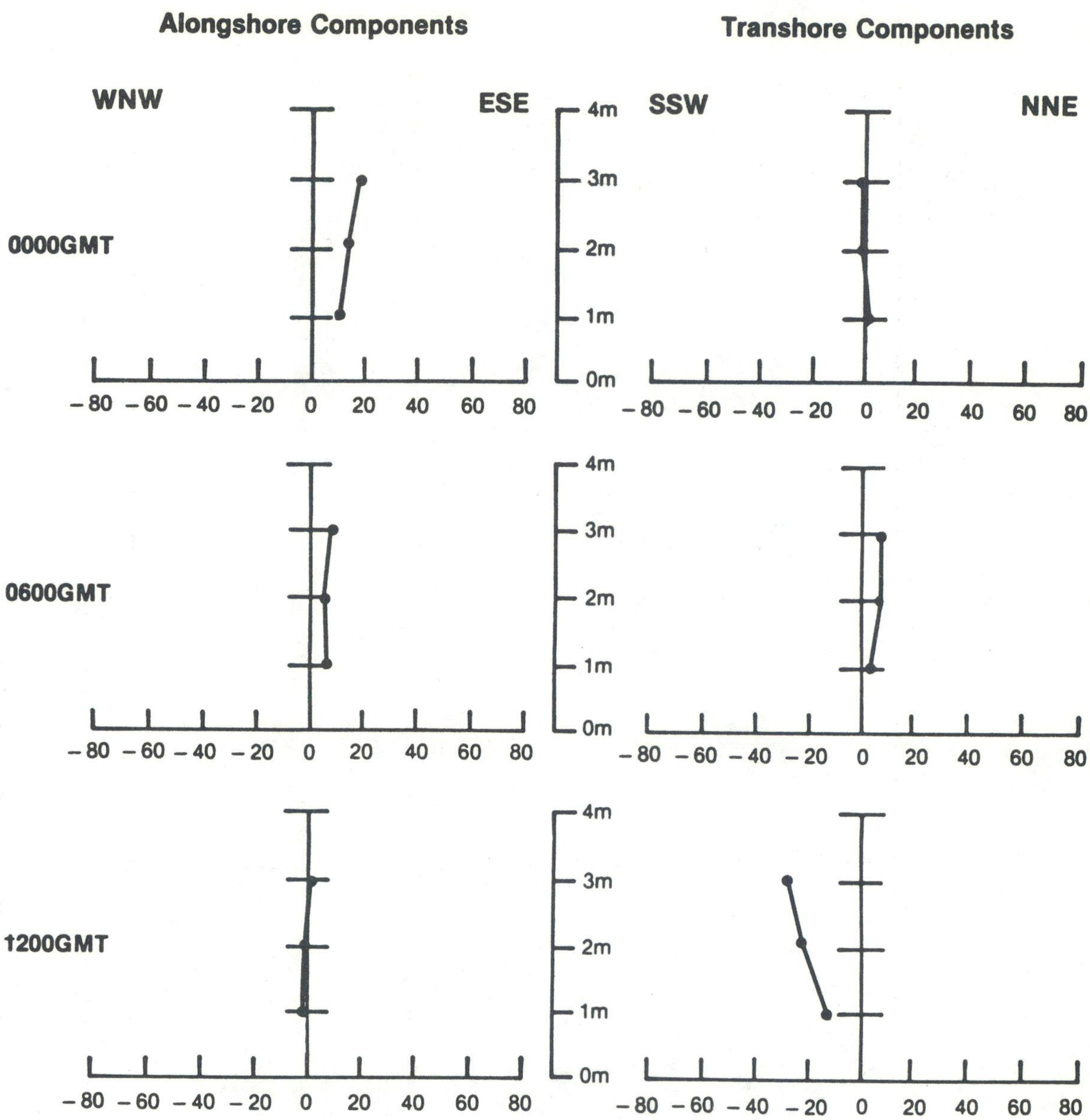

Figure 15-16. Vertical profiles of currents at Weeks Island site station 21, February 27, 1979.

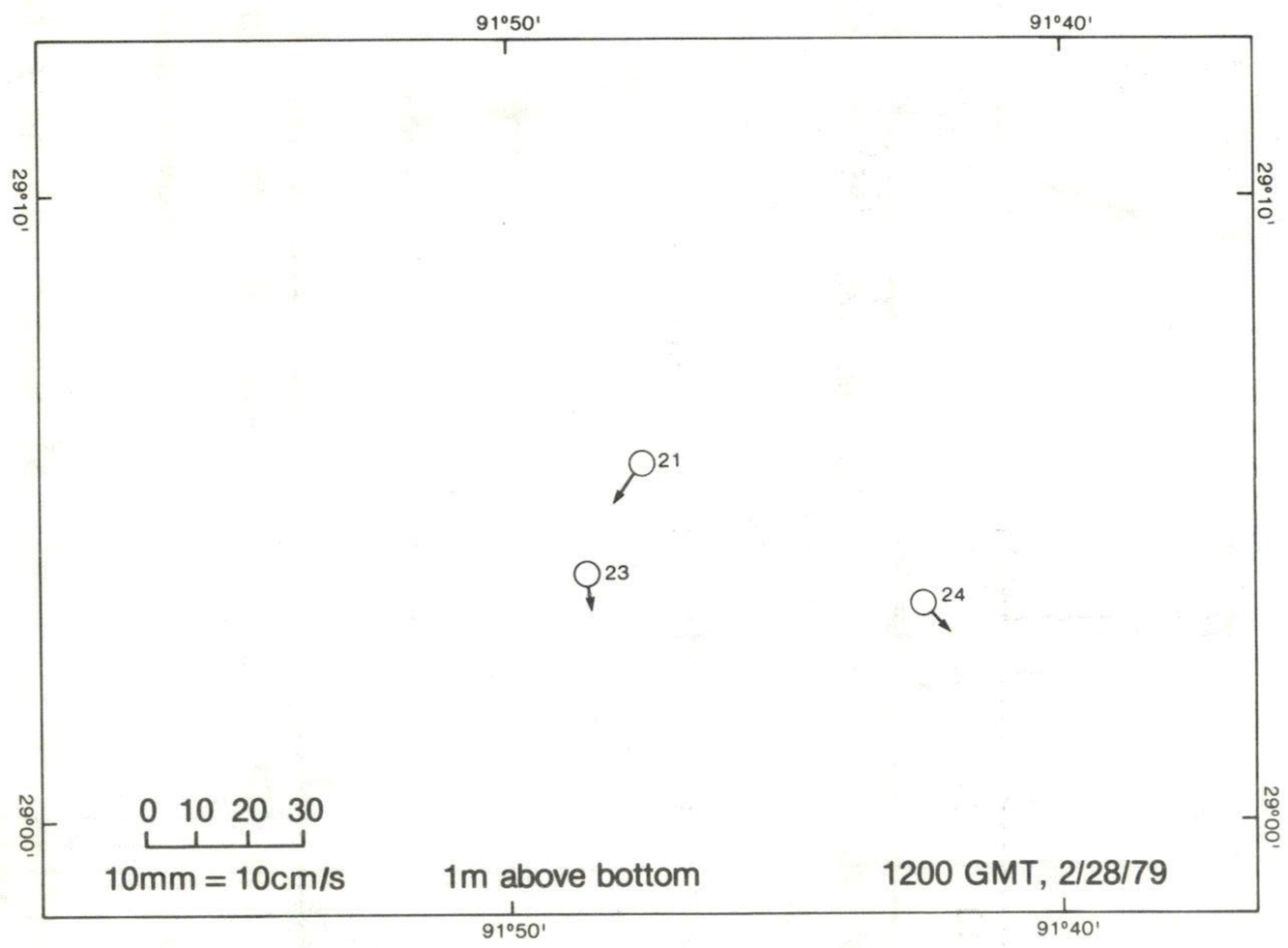

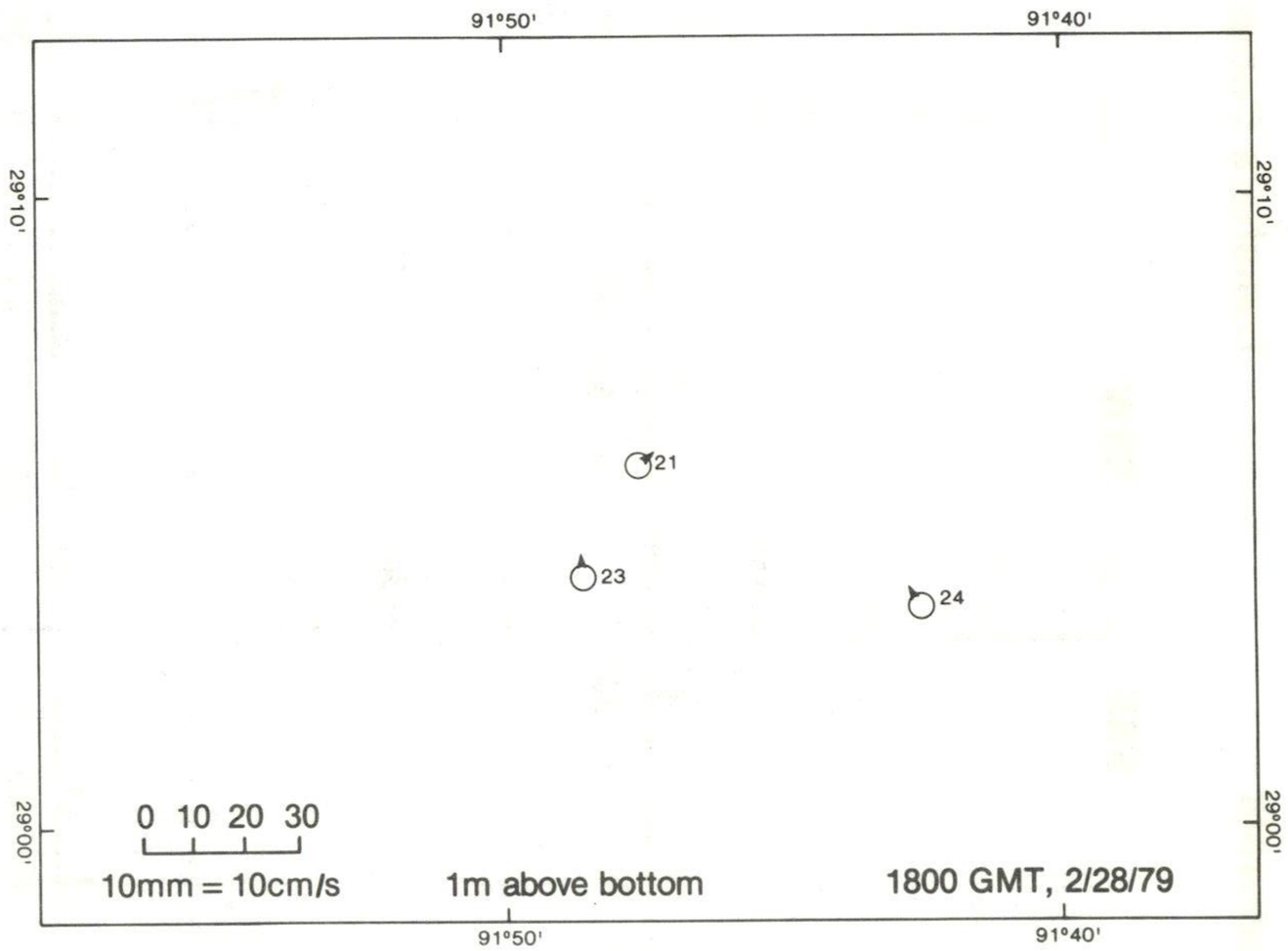

Figure 15-17. Current vectors at 6-hour intervals, 1 m above bottom at Weeks Island site, February 28, 1979.

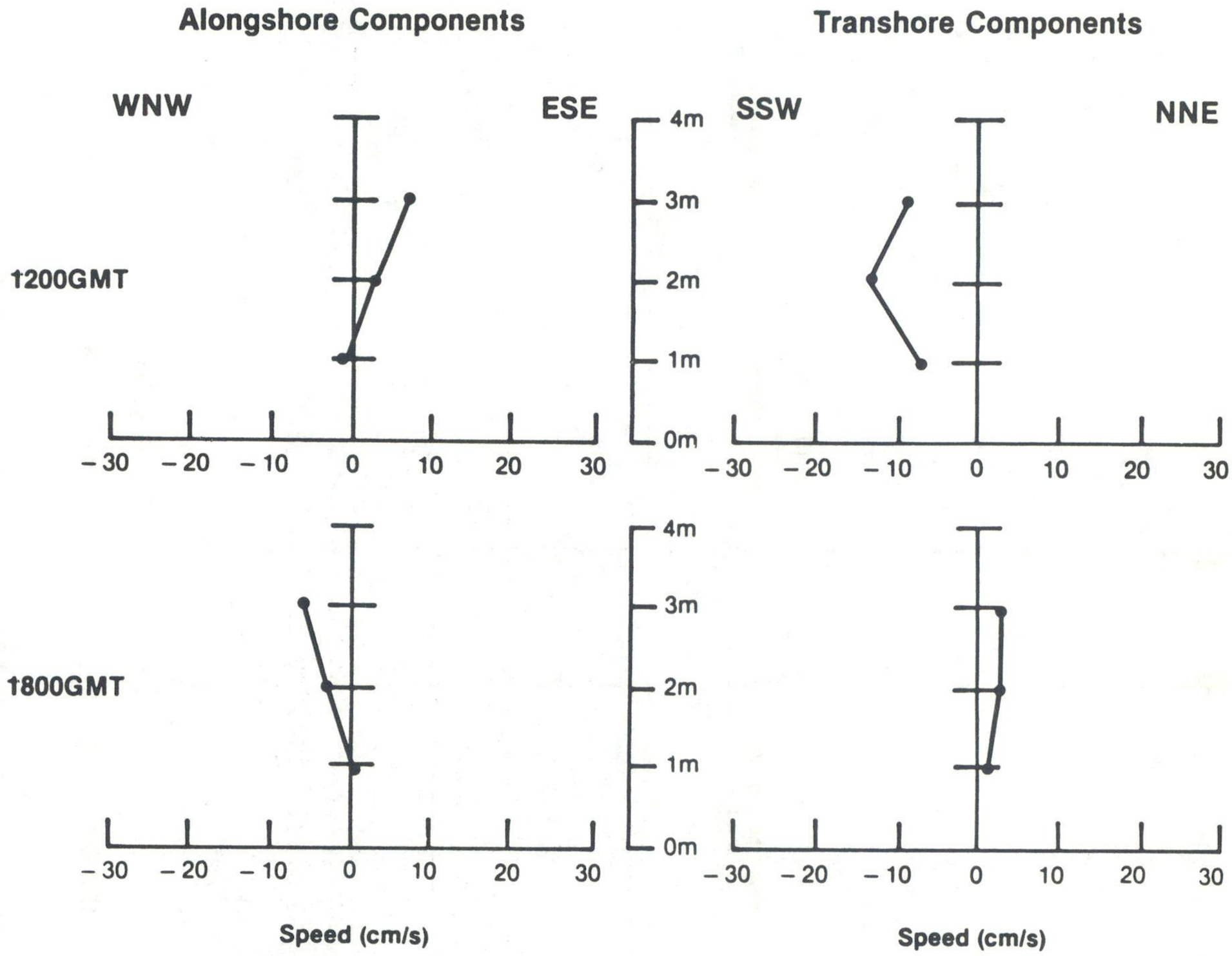

Figure 15-18. Vertical profiles of currents at Weeks Island site station 21, February 28, 1979.

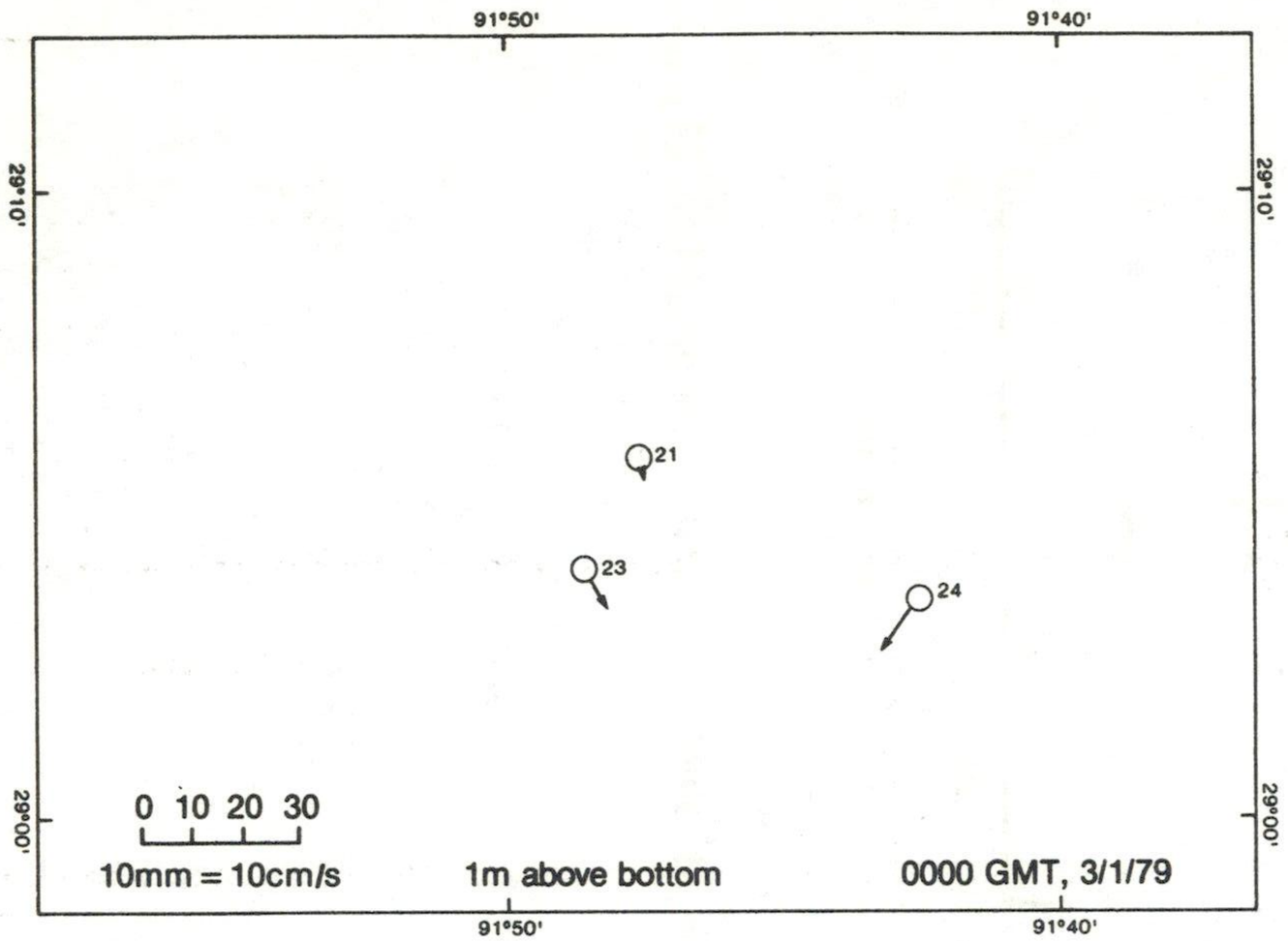

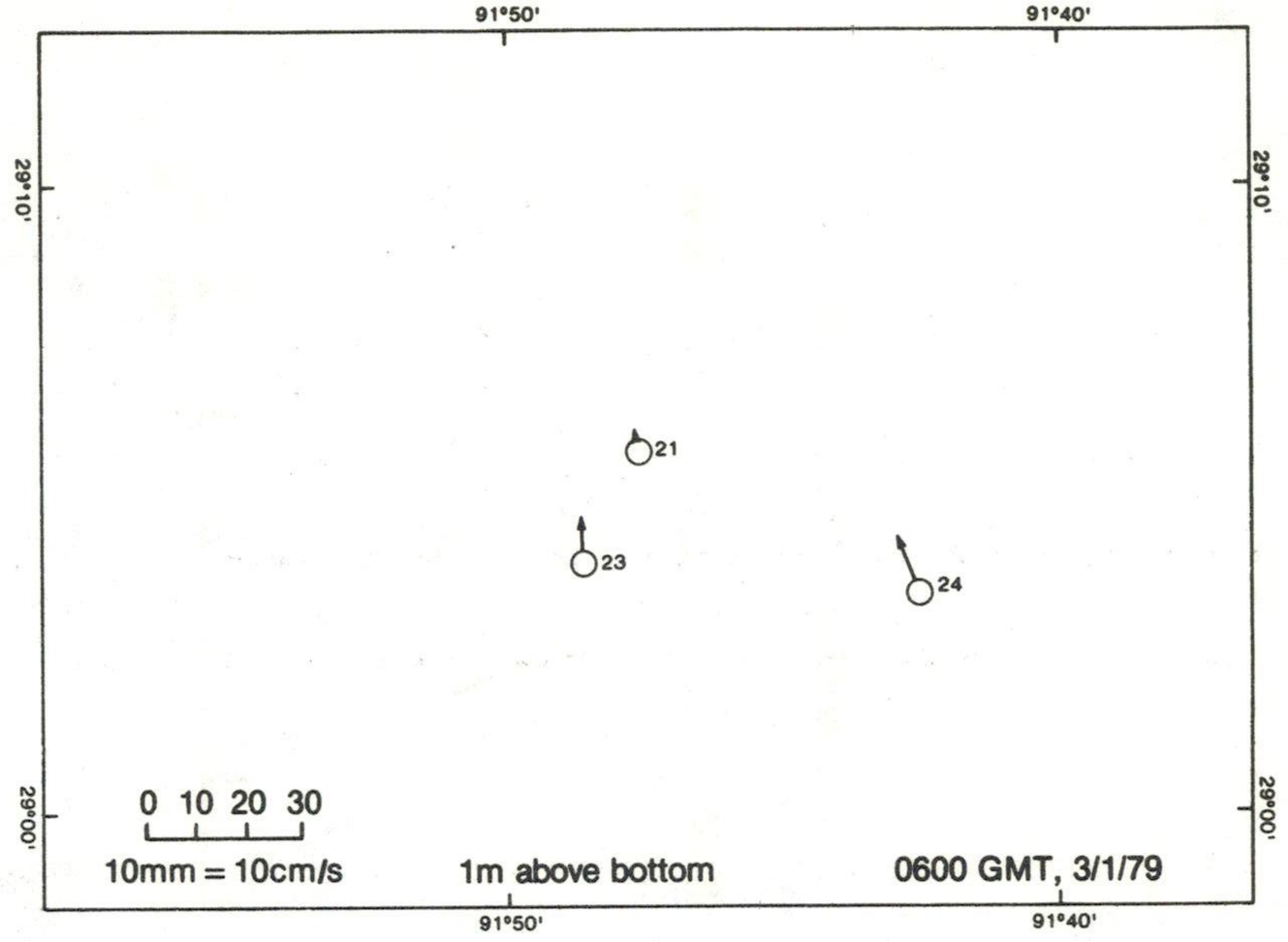

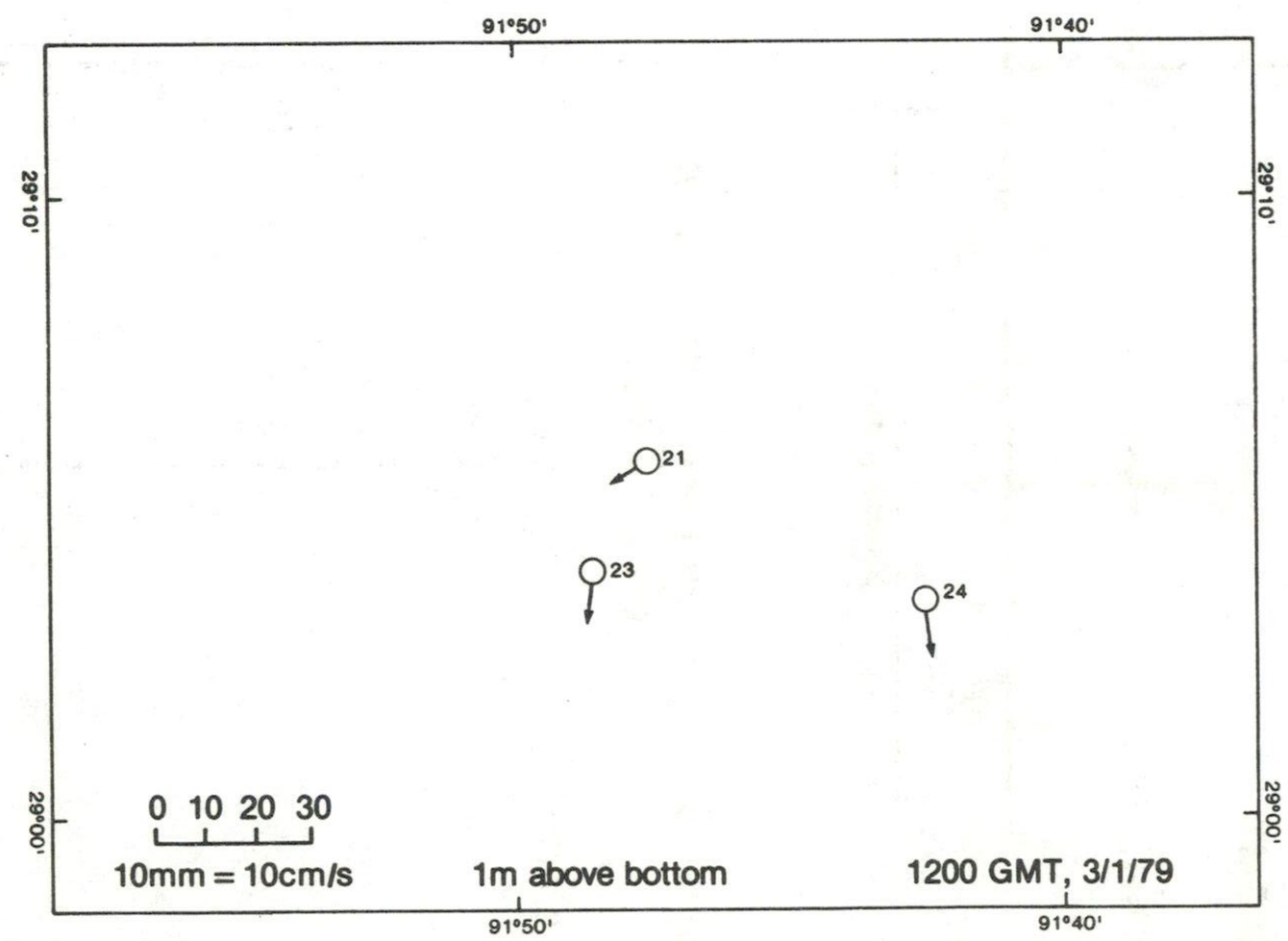

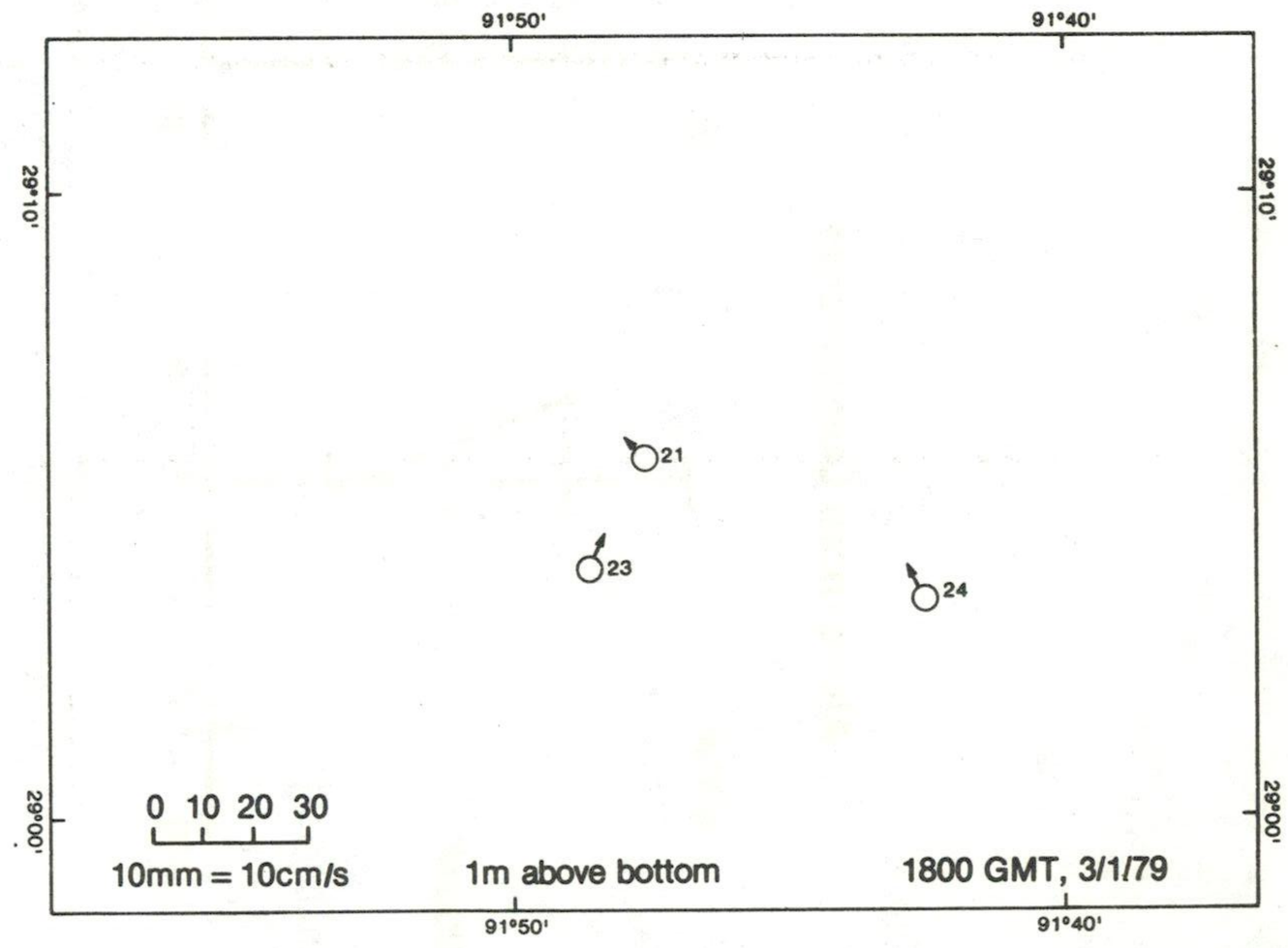

Figure 15-19. Current vectors at 6-hour intervals, 1 m above bottom at Weeks Island site, March 1, 1979.

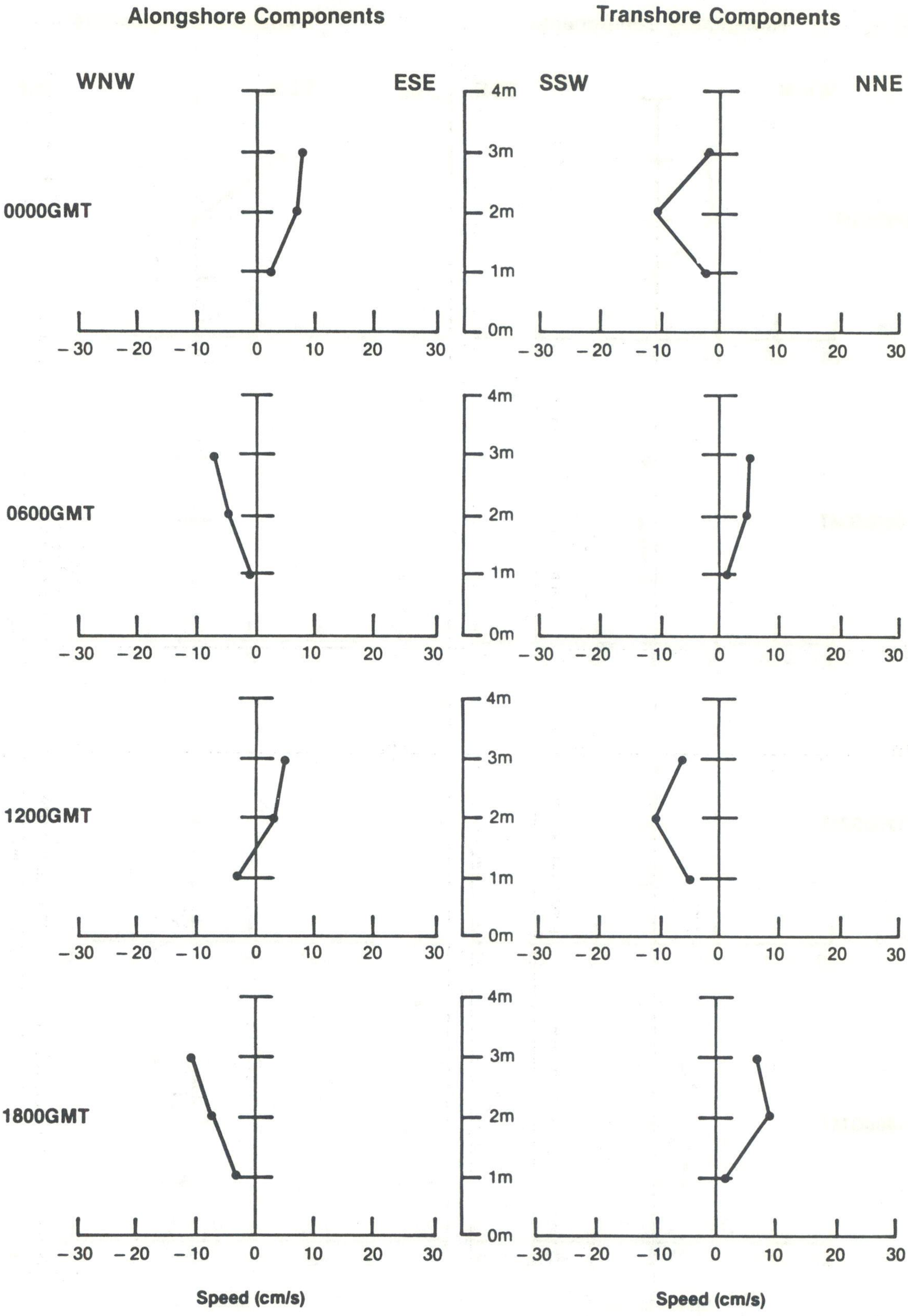

Figure 15-20. Vertical profiles of currents at Weeks Island site station 21, March 1, 1979.

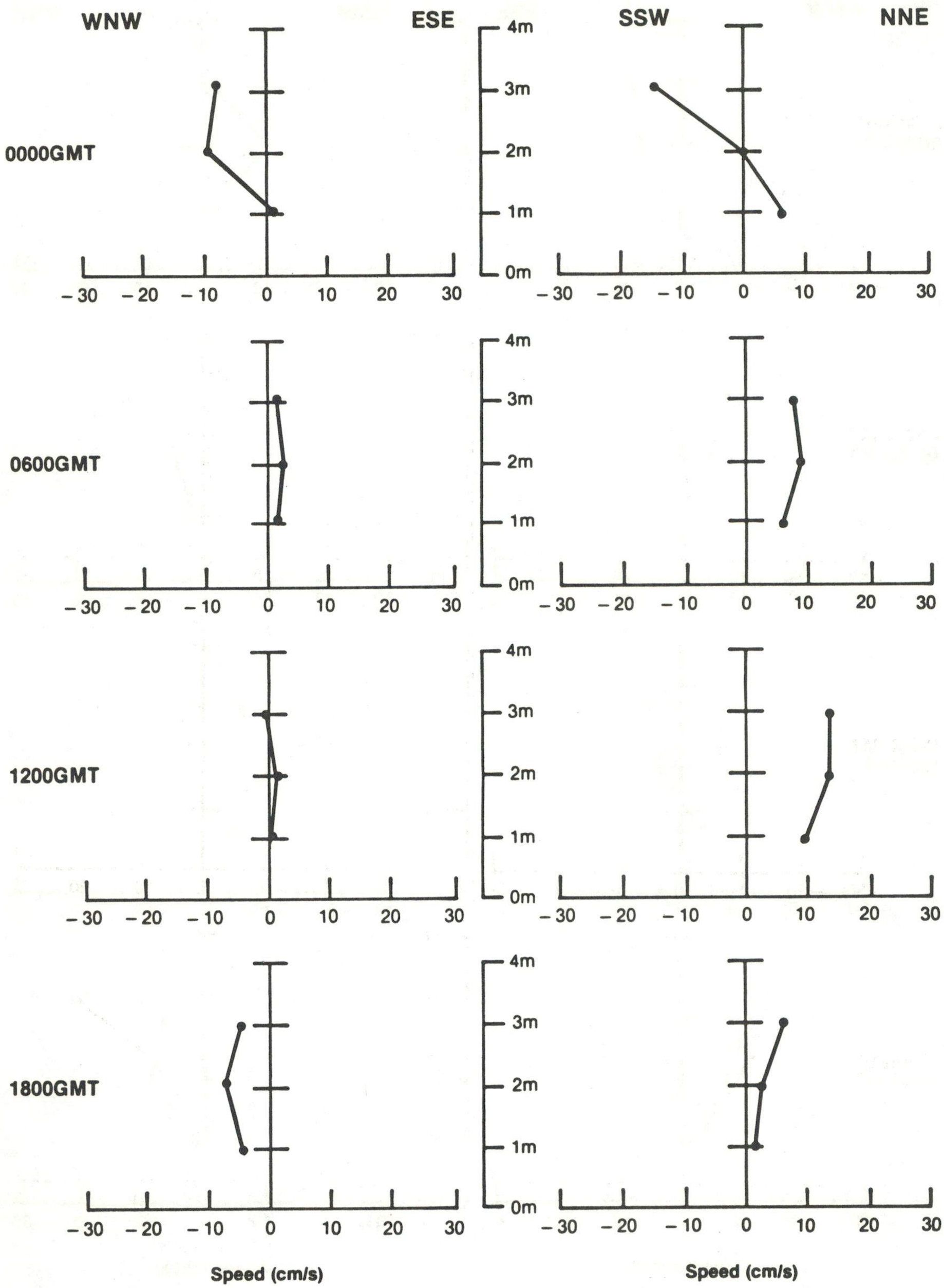

Figure 15-21. Vertical profiles of currents at Weeks Island site station 21, March 11, 1979.

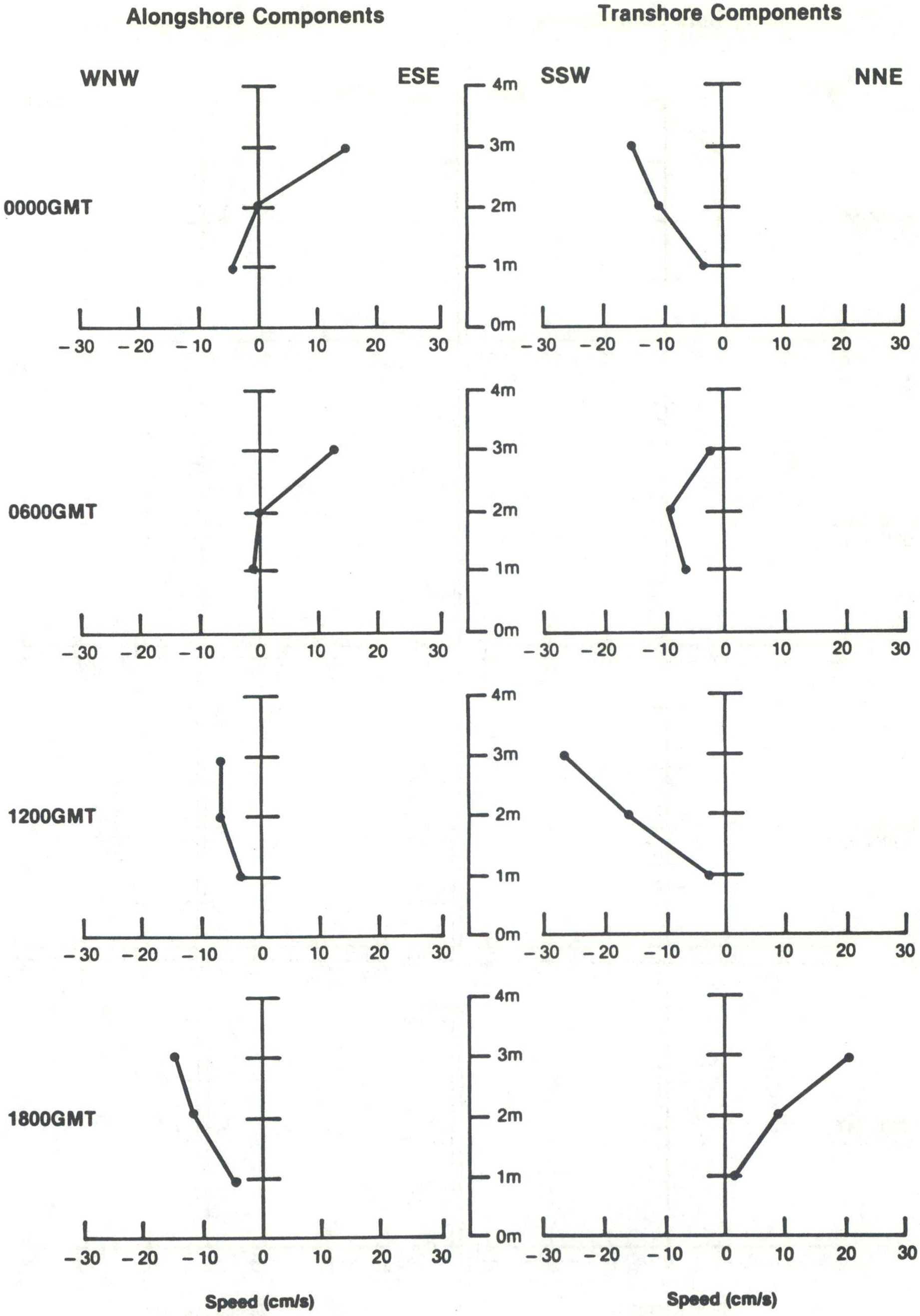

Figure 15-22. Vertical profiles of currents at Weeks Island site station 21, March 12, 1979.

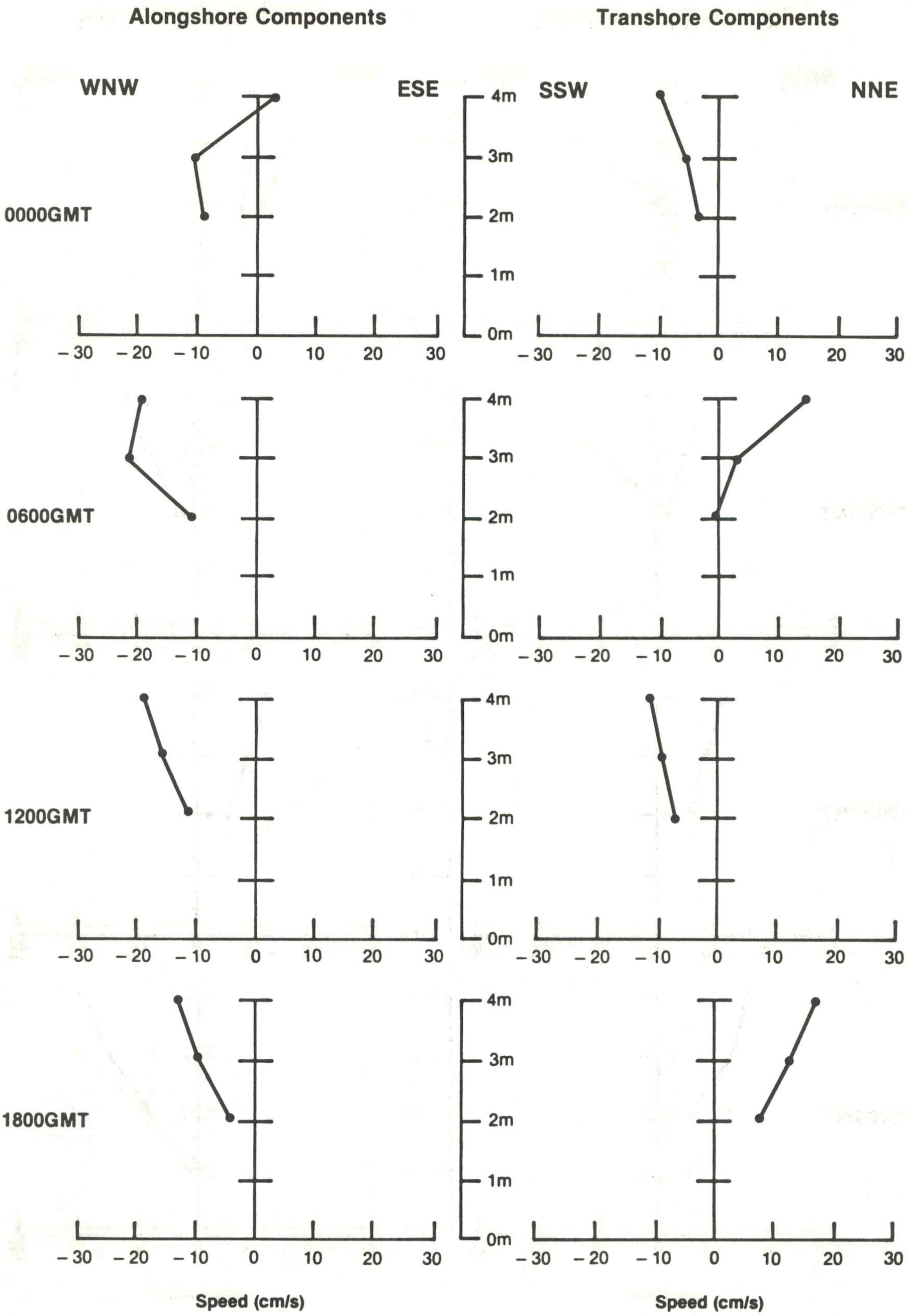

Figure 15-23. Vertical profiles of currents at Weeks Island site station 21, March 13, 1979.

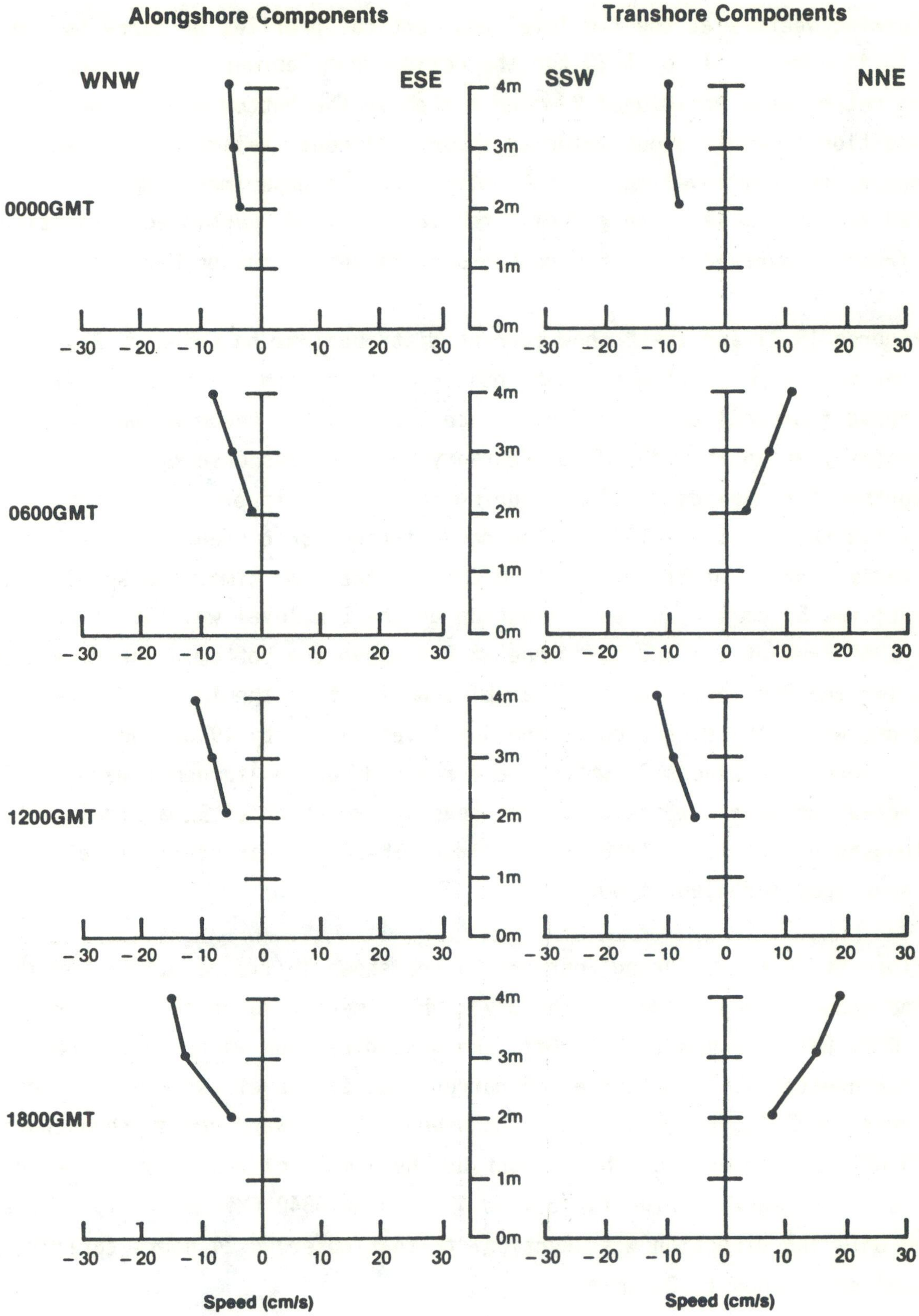

Figure 15-24. Vertical profiles of currents at Weeks Island site station 21, March 14, 1979.

Current vectors at the 1-m level and vertical profiles of currents are shown in figures 15-11 to 15-20 for the period from February 25 to March 1. Current meters were positioned 2 m and 4 m above the bottom at station 21 to gain additional detail about velocity shear. Although validated data were obtained at the 2-m level during the entire special experiment, data were obtained at the 4-m level only from March 12 to 26. As mentioned in section 12, polar fronts traversed the sites on February 24 and 27 and on March 1.

Figures 15-11 and 15-12 show current distributions on February 25. According to the meteorological data obtained at station 28 (figure 12-2), the wind veered from southeasterly during late February 24, becoming west-northwesterly at about 0230 GMT on February 25. The response of the currents to west-northwesterly winds of 14 m/s during the first half of February 25 is evident in figures 15-11 and 15-12. The data listing for currents at the 3-m level shows maximum speed of 81 cm/s at 1130 GMT; at the same time, the speed at the 1-m level was 57 cm/s. Current direction at the 1-m level was 156° True, while it was 135° True at 1 m and 137° True at 2 m above the bottom. The directions at the 1-m and 2-m levels were comparable, well within the TMU for current direction, while the direction at the 3-m level varied by 19 degrees. This was one of numerous instances in which the current direction turned toward the left with increasing depth, opposite to the sense of rotation of Ekman transport. The alongshore profile at 1200 GMT in figure 15-12 is characteristic of nearly fully developed turbulent flow.

Plots of currents during February 26 are shown in figures 15-13 and 15-14. The wind speed decreased during the day, approximately monotonically, from 15 m/s at 0510 GMT to 3 m/s at 2210 GMT; the wind direction was predominately north-northwesterly. Time series of currents at all levels show a distinct semidiurnal oscillation of direction between northeastward and southeastward. At 0000 GMT on February 26, the current at the 3-m level was 35 cm/s toward 124° True. It peaked during the day to 51 cm/s at 0840 GMT toward 137° True. At 2400 GMT, the direction was identical to that observed 24 hours earlier, but the speed diminished to 20 cm/s.

Plots of currents during February 27 are shown in figures 15-15 and 15-16. Winds measured at station 28 did not exceed 4 m/s until 1310 GMT; after that, it

did not exceed 8 m/s for the remainder of the day. The peak current speed at the 3-m level was 38 cm/s at 1000 GMT; a secondary peak of 35 cm/s occurred at 1710 GMT. Figure 15-4 indicates that the maximum calculated tidal current at the 1-m level during February 27 was 12 cm/s; the observed maximum current at the same level was 21 cm/s at 0950 GMT. Approximately half of the kinetic energy was tidal.

Figures 15-17 and 15-18 depict a principally tidal current at 1200 GMT and at 1800 GMT on February 28. Wind speeds at station 28 varied from 2 to 9 m/s during the day, averaging about 5 m/s. The time series plot of currents at the 3-m level at station 21 indicates a dominance of the semidiurnal component.

The meteorological data in figure 12-2 show a polar front traversing station 28 on March 1. The wind veered from south-southwesterly, becoming northerly at 1130 GMT, and east-southeasterly by the end of the day. Wind speed did not exceed 5 m/s during the day; the average speed was 3.5 m/s. Figures 15-19 and 15-20 depict predominantly semidiurnal tidal currents.

Vertical profiles of currents at station 21 for March 11 through 14 are shown in figures 15-21 to 15-24.

15.3. Spectral Characteristics

The spectral plots shown in this section are representative of the energy distribution at the Weeks Island site for each time period specified. The maximum entropy technique discussed in section 3 was used to determine the spectral characteristics. The spectral results are defined in angular frequency. Although frequency is always positive, it is noted with a negative sign for that part of the spectra associated with counterclockwise rotation and a positive sign for that associated with clockwise rotation.

The energy spectral density for 1 m above the bottom at station 23 from July 1 to 28, [figure 15-25(a)], shows high peaks of energy at the semidiurnal, diurnal, and at a narrow band at the low frequency of 0.16 CPD. The semidiurnal frequency had distinct sharp peaks of energy in the clockwise and counterclockwise spectrum. The level of energy associated with the clockwise semidiurnal

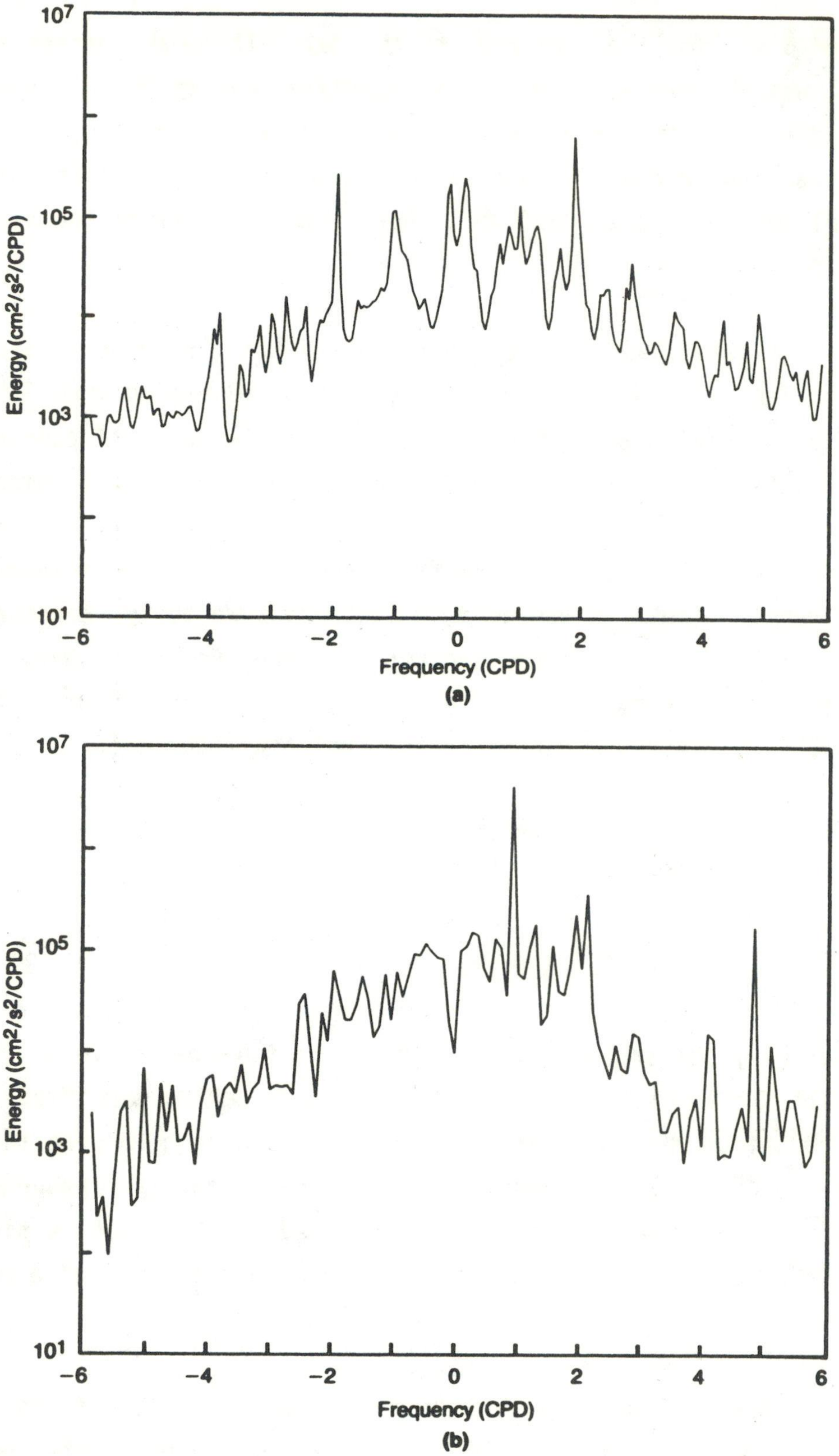

Figure 15-25. Current energy spectral density at Weeks Island site (a) station 23 1 m above bottom July 1 to 28, 1978, and (b) station 21 1 m above bottom July 28 to August 8, 1978.

frequency was higher than that at the counterclockwise frequency. This finding agrees well with the M_2 tidal ellipse analysis, which showed that the M_2 constituent was generally clockwise. This peak of energy at the M_2 clockwise frequency was generally found in the spectral results throughout the year. Energy near the diurnal frequency was also associated mostly with clockwise rotation. Energy around the clockwise diurnal frequency was within a band of frequencies from 0.6 to 1.4 CPD. The narrow band of energy around the diurnal counterclockwise frequencies was from 0.8 to 1.1 CPD.

The results of the coherency squared between currents and water levels at the tidal constituents K_1, O_1, and M_2 are presented in table 15-3, for the deployment periods September 1-15, October 30-November 13, March 27-April 17, and April 18-May 5. The coherency squared at the diurnal and semidiurnal constituents was generally very high. The M_2 tidal constituent had high coherency in both the clockwise and counterclockwise spectrum, while the diurnal constituents, K_1 and O_1 had, at times, low coherency in the counterclockwise end of the spectrum.

Table 15-3. Coherency squared for currents and water levels at the diurnal and semidiurnal frequencies.

Stations	Period	Coherency squared					
		K_1		O_1		M_2	
		ccw	cw	ccw	cw	ccw	cw
21WL/21(+1)	September 1 to 15	0.21	0.98	0.97	0.99	0.98	0.95
21WL/21(+1)	October 30 to November 13	0.74	0.78	0.76	0.99	0.94	0.99
21WL/23(+1)	March 27 to April 17	0.31	0.60	0.53	0.96	0.88	0.99
21WL/21(+3)	April 18 to May 5	0.80	0.76	0.92	0.94	0.91	0.99

ccw is counterclockwise, cw is clockwise.
Water levels (WL) were measured at station 21; currents were measured at stations 21 and 23.
(+1) indicates 1 m above bottom.
(+3) indicates 3 m above bottom.

From July 28 to August 8, the energy spectrum for Weeks Island was found to have high levels of energy distributed between the bands of frequencies less than 2.5 CPD. At station 21 1 m above the bottom [figure 15-25(b)] the energy was principally distributed between the frequency bands from 0.1 to 1.4 CPD (clockwise), 1.8 to 2.3 CPD (clockwise), and 0.1 to 0.8 CPD (counterclockwise). There was a distinct energy peak at the clockwise O_1 frequency.

During the fall (figure 15-26) the energy was concentrated mainly at the low end of the spectrum. At station 21 1 m above the bottom, from October 2-30, the energy was concentrated between 0.5 CPD counterclockwise and 0.3 CPD clockwise. There were high peaks of energy at the diurnal tidal frequency clockwise and at the semidiurnal tidal frequency both clockwise and counterclockwise. By late fall, from October 30 to December 10, the level of energy at the lower frequencies increased. At station 21 1 m above the bottom, there was a wide band of energy between the 0.7 CPD counterclockwise and 0.5 CPD clockwise frequencies. There were distinct high peaks of energy at 0.2 CPD in the clockwise and counterclockwise end of the spectrum. The diurnal and semidiurnal frequencies continued to have the high level of energy previously observed.

Figure 15-27 shows the results of the cross spectra and coherency squared between currents at station 21 and winds recorded at station 28 for the period October 30 to December 10. In the cross spectra, high energy levels are found principally at the low frequency. The coherency squared was found to have a maximum value of 0.8 at the 0.2 CPD clockwise frequency and 0.75 at the 0.2 CPD counterclockwise frequency.

Energy during the winter months, like that during fall, was concentrated at the low end of the spectrum, like that of fall. Figure 15-28 shows the energy at station 21 1 m above the bottom from January 6 to 21 concentrated between the frequencies 1.2 CPD counterclockwise and 1.4 CPD clockwise. The highest peaks of energy were at 0.2 CPD. In contrast to fall and summer, energy peaks at the diurnal and semidiurnal tidal frequencies were considerably less than the energy peaks at the low frequency.

Throughout the winter months, the energy continued to be concentrated at the low end of the spectrum. At station 21 1 m above the bottom, from

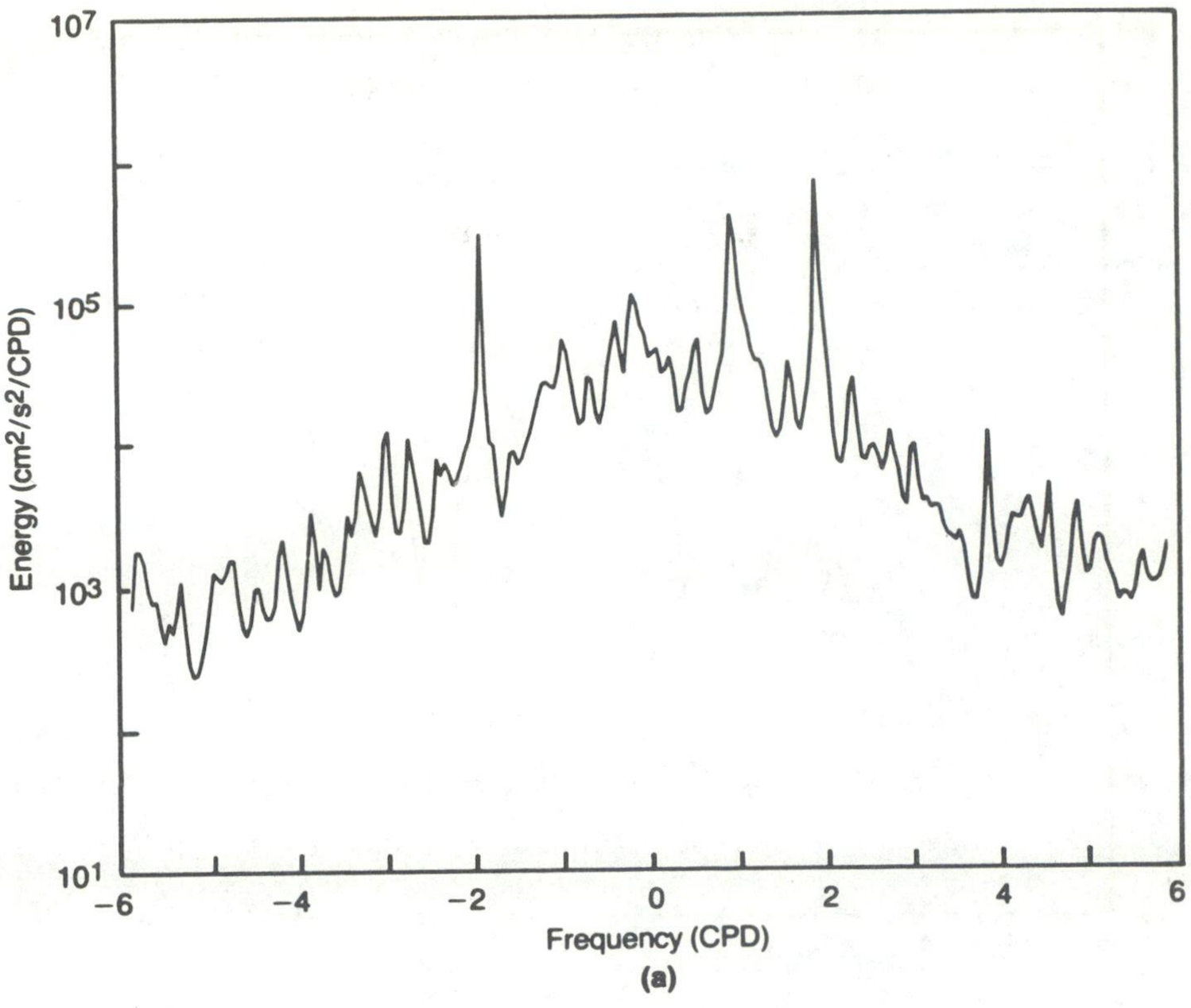

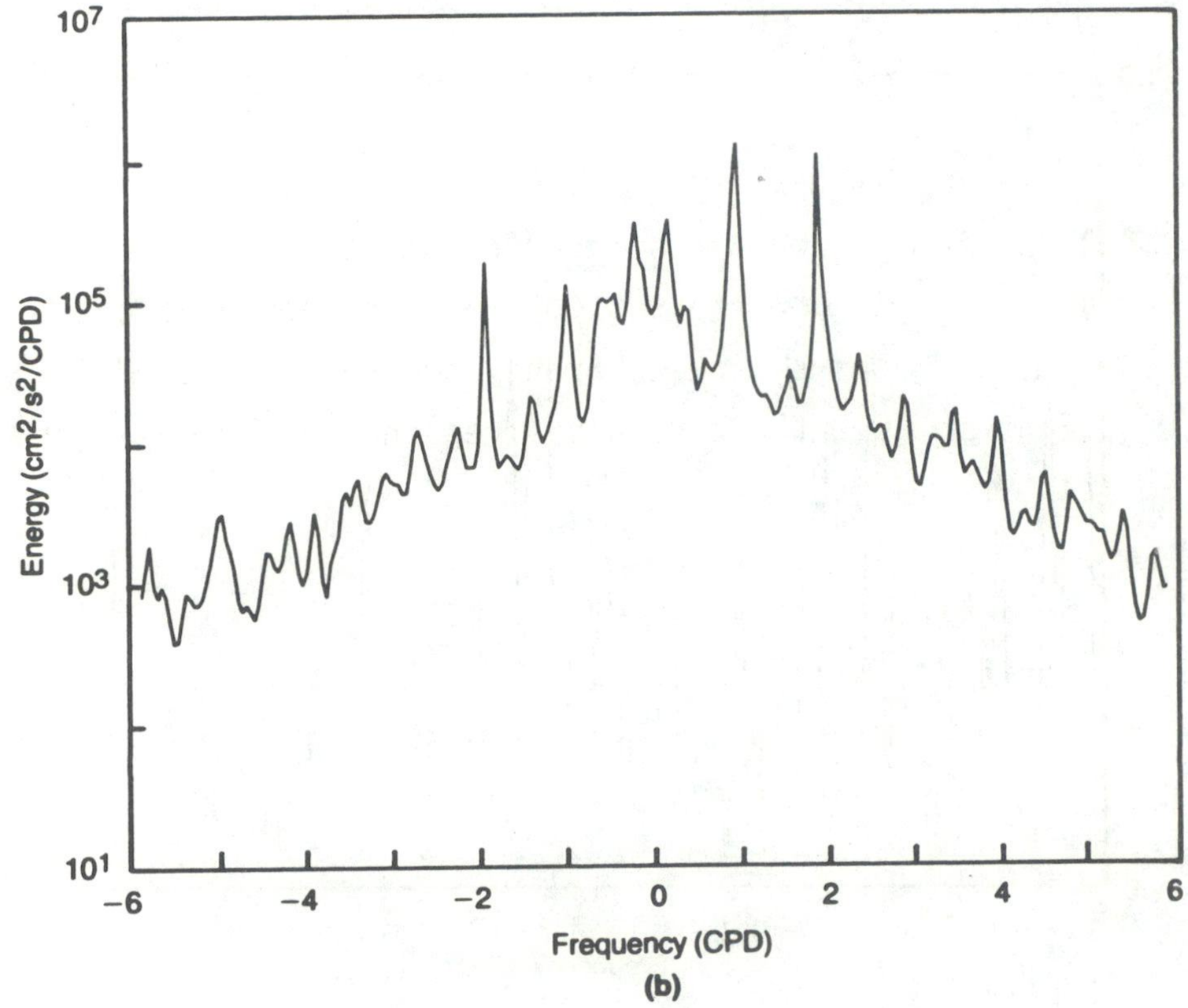

Figure 15-26. Current energy spectral density at Weeks Island site (a) station 21 1 m above bottom October 2 to 30, 1978, and (b) station 21 1 m above bottom October 30 to December 10, 1978.

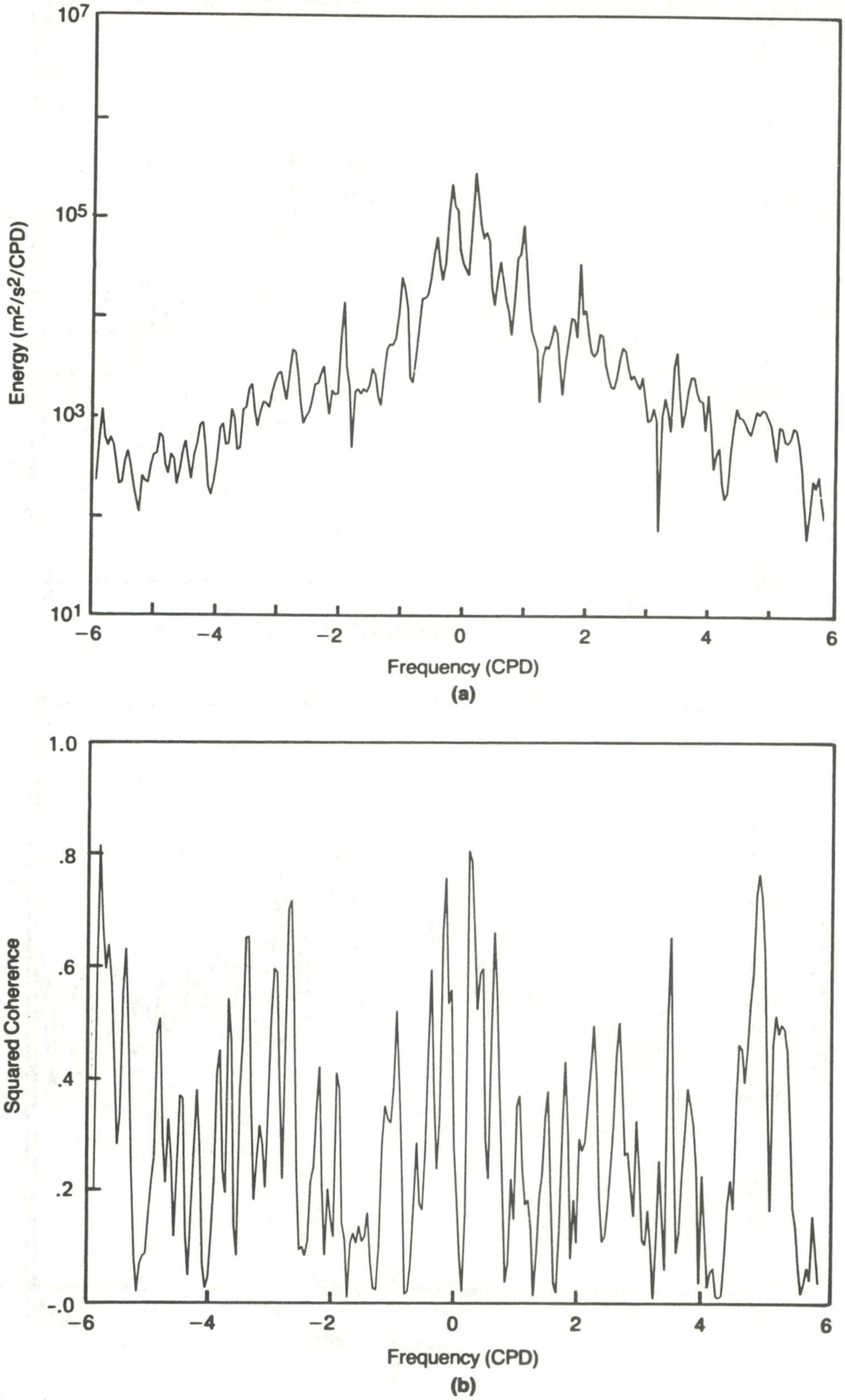

Figure 15-27. (a) Cross-spectra and (b) squared coherence of winds at Weeks Island site station 28 and currents 1 m above bottom at station 21 from October 30 to December 10, 1978.

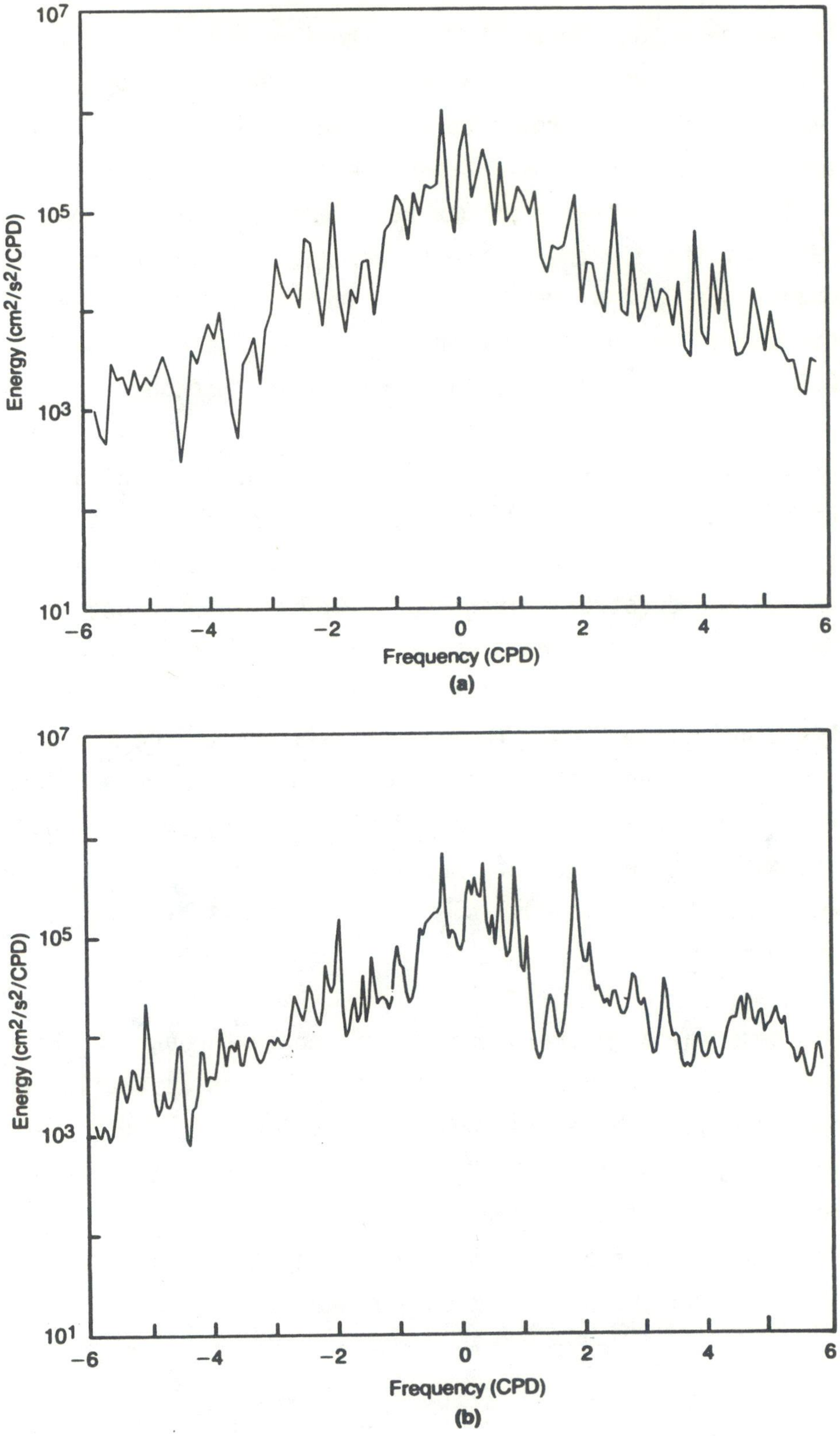

Figure 15-28. Current energy spectral density at Weeks Island site (a) station 21 1 m above bottom January 6 to 21, 1979, and (b) station 21 1 m above bottom January 29 to February 23, 1979.

January 29 to February 23, figure 15-28(b) shows a wide band of energy between the frequencies 0.7 CPD counterclockwise and 1.2 CPD clockwise. In addition, there was a narrow band of energy around the semidiurnal (M_2) tidal frequency in the clockwise end of the spectrum. Cross spectra between currents at station 21 and winds at station 28, shows a strong relationship between winds and currents (figure 15-29). At the low end of the spectrum, from 0.2 CPD to 0.7 CPD, the coherency squared was 0.72 or greater. At the 0.41 CPD frequency (clockwise) the coherency squared was 0.93. Within the counterclockwise spectrum from 0.3 CPD to 0.5 CPD, the coherency squared was 0.7 or greater.

Figure 15-30(a) displays the spectral density at station 23 1 m above the bottom during spring from March 28 to April 17. The energy distribution in early spring, like that of fall and winter, had a high concentration of energy at the low end of the spectrum. There was a wide band of energy between 0.4 CPD counterclockwise and 1.3 CPD clockwise. Within this frequency band, there were several peaks of energy, in particular 1.0 CPD clockwise and 0.2 CPD clockwise. The level of energy at the tidal frequencies relative to the energy levels at the low frequency was higher than that observed during the winter months. Cross spectra between currents at station 23 and winds at station 28 shows a continued strong relationship between currents and winds (figure 15-31). The coherency squared between the frequencies 0.1 CPD counterclockwise to 0.52 CPD clockwise was 0.7 or greater.

Although there was a general increase of energy throughout the current spectrum later in spring, May 7 to 21, the distribution at the low end of the spectrum remained high. The energy peaks at the low end of the spectrum were within the frequency bands from 0.1 CPD to 1.1 CPD (clockwise), and 0.1 CPD to 0.4 (counterclockwise). There was a substantial level of energy at the semi-diurnal and diurnal tidal frequencies. The energy level was greater at the clockwise than the counterclockwise tidal frequencies.

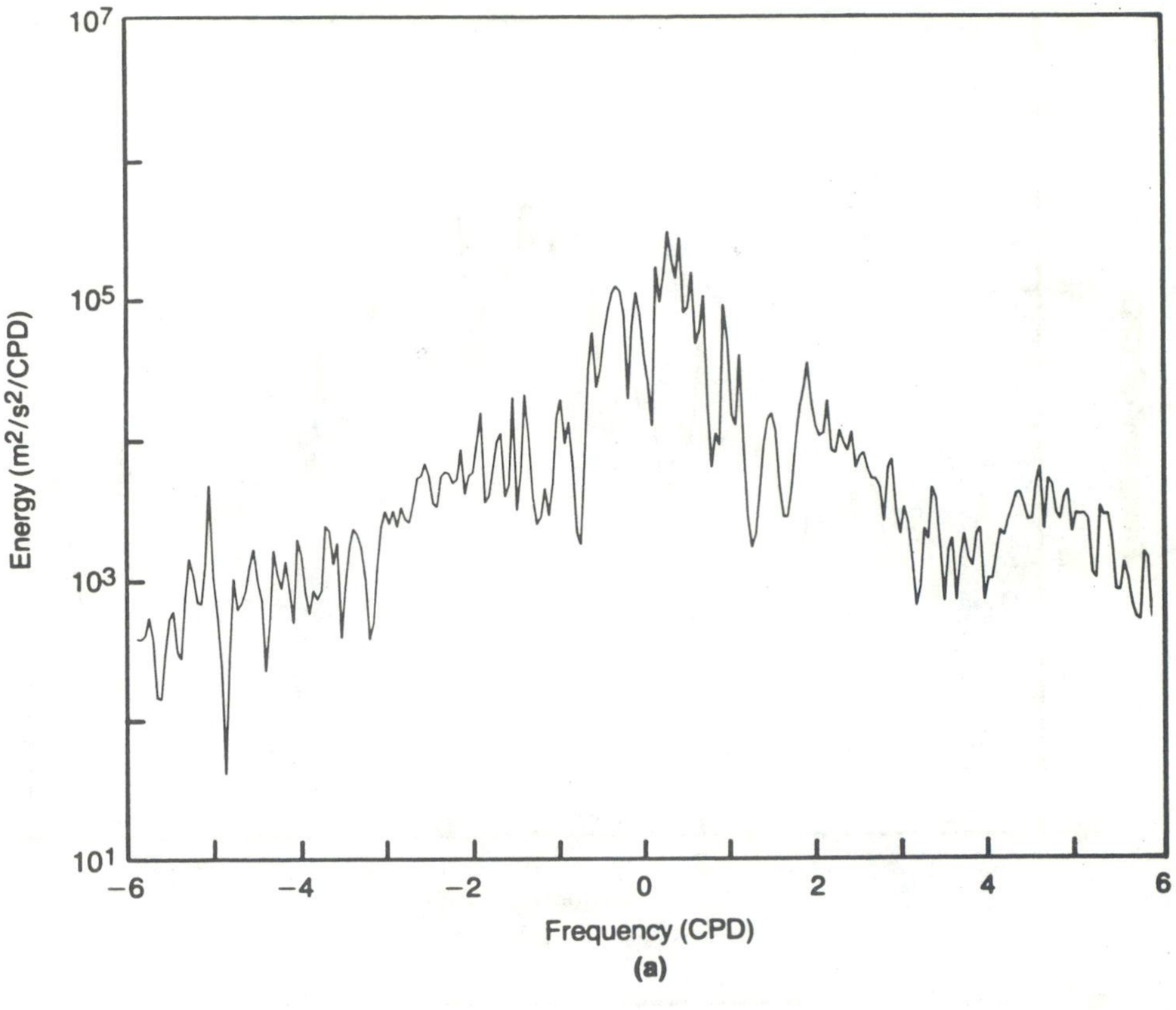

Figure 15-29. (a) Cross-spectra and (b) squared coherence of winds at Weeks Island site station 28 and currents 1 m above bottom at station 21 from January 29 to February 23, 1979.

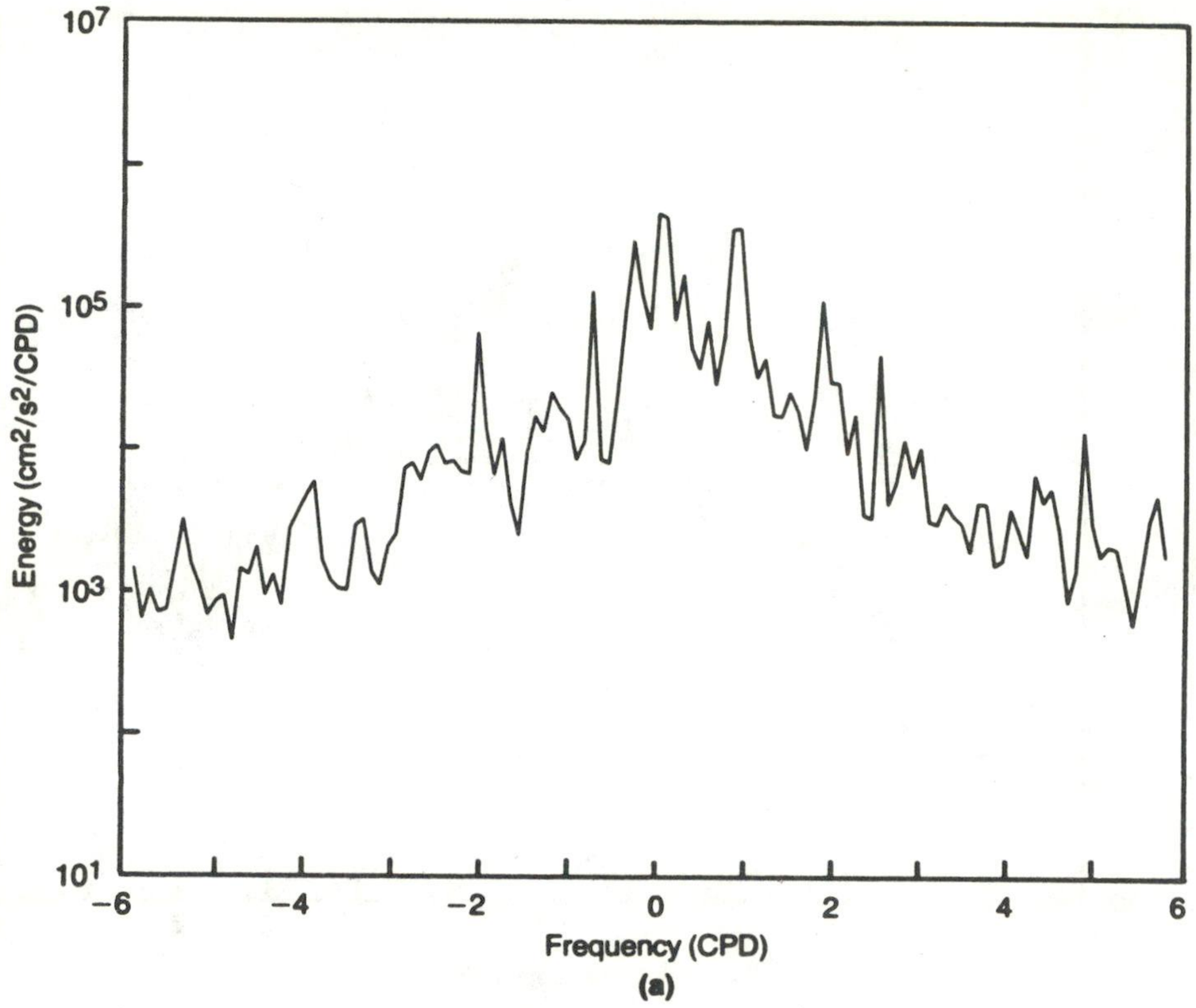

Figure 15-30. Current energy spectral density at Weeks Island site (a) station 21 1 m above bottom March 28 to April 17, 1979, and (b) station 21 1 m above bottom May 7 to 21, 1979.

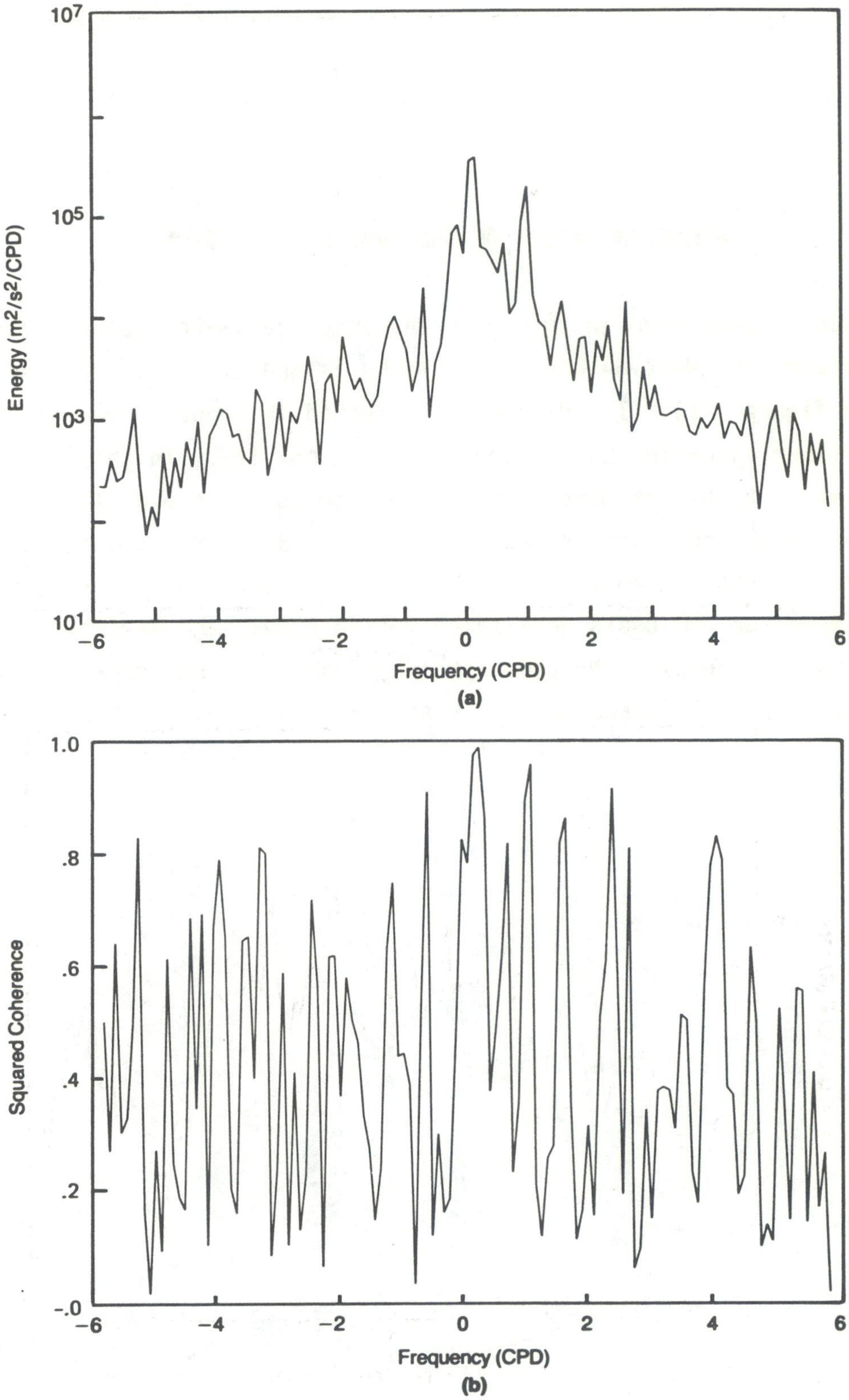

Figure 15-31. (a) Cross-spectra and (b) squared coherence of winds at Weeks Island site station 28 and currents 1 m above bottom at station 21 from March 28 to April 17, 1979.

CHARACTERIZATION OF THE TRACKLINE STATIONS

Information described in this part characterizes water column measurements obtained between the West Hackberry and Weeks Island sites at stations 20, 30, and 40 (see figure 1-1). The data were collected in cooperation with the NMFS Southeast Fisheries Center Laboratory at Galveston, Tex.; in this regard, the FERREL served as a ship of opportunity. Seawater samples and CTD casts were taken at the trackline stations monthly from June 3, 1978, to June 2, 1979, with the exception of station 20 where sampling did not begin until October 4, 1978. No water samples or CTD casts were taken during August and December 1978 due to weather and ship schedule. No CTD casts were taken at the trackline stations from January to May 1979 because of a system malfunction.

16. DISSOLVED OXYGEN

Dissolved oxygen (DO) values were obtained from the seawater samples using the modified Winkler technique that was described in section 3.2. Samples were taken with 1.7-l Niskin bottles 1 m below the surface and 1 m above the bottom at the trackline stations. The depths at stations 20, 30, and 40 at GCLW are 11.9 m, 14.6 m, and 11.0 m, respectively.

16.1. Ranges

The values of DO measured at the trackline stations are summarized in table 16-1. DO at the stations ranged from 0.33 to 8.64 ml/l during the period June 3, 1978, to June 2, 1979. The highest values of DO occurred during the months of January, February, and March 1979. The highest value of DO (8.64 ml/l) observed at the trackline stations was found at station 30 on February 22. The lower DO values were observed during late spring and summer. The near-bottom water was nearly anoxic (0.33 ml/l) at station 30 on July 26, 1978, and at stations 20 (0.44 ml/l) and 30 (0.78 ml/l) on June 2, 1979.

16.2. Spatial Distributions

DO values in table 16-1 indicate the distribution of DO along the trackline for each sampling cruise. The DO spatial distribution, like that at the proposed disposal sites, was found to vary seasonally.

16.2.1. Summer 1978

The June 3, 1978, data indicates there was a relatively small DO gradient at stations 30 and 40. The DO in the near-surface layer at station 30 was 4.14 ml/l, while it was 3.79 ml/l in the near-bottom layer, a difference of 0.35 ml/l through the water column. At station 40, the DO in the near-surface

Table 16-1. Near-surface and near-bottom values of DO at trackline stations

Date	Sample depth (m)	Dissolved oxygen (ml/l)		
		Station 20	Station 30	Station 40
1978				
6/3	-1		4.14	4.61
	+1		3.79	4.26
7/3	-1		5.47	5.38
	+1		1.43	3.50
7/26	-1		6.53	4.67
	+1		0.33	4.26
10/4	-1	5.48	4.74	4.59
	+1	5.06	4.48	4.89
11/14	-1	5.30	4.91	4.75
	+1	5.26	4.93	4.75
1979				
1/30	-1		6.36	6.86
	+1	6.46	6.34	6.40
2/22	-1	8.38	8.64	7.64
	+1	5.65	6.17	6.79
3/13	-1	6.45	6.41	7.00
	+1	3.78	4.36	5.49
4/18	-1	5.01	4.99	5.02
	+1	5.00	4.89	4.96
5/8	-1	5.69	5.61	6.47
	+1	3.40	4.57	5.48
6/2	-1	6.04	5.17	4.61
	+1	0.44	0.78	4.56
Station depth at GCLW (m)		Station 20 11.9	Station 30 14.6	Station 40 11.0

- indicates distance beneath surface
+ indicates distance above bottom

layer was 4.61 ml/l, while it was 4.26 ml/l in the near-bottom layer, also a difference of 0.35 ml/l through the water column.

Strong DO gradients were found at the trackline stations during the beginning of July 1978. At station 30, DO in the near-surface layer was 5.47 ml/l and 1.43 ml/l in the near-bottom layer. At station 40, the DO in the near-surface layer was 5.38 ml/l, while it was 3.50 ml/l in the near-bottom layer.

The near-bottom layer at station 30 on July 26, 1978, approached being anoxic, with a value of 0.33 ml/l. In contrast, DO in the near-bottom layer at station 40 was significantly higher, at 4.25 ml/l. At station 30, the vertical gradient was quite large, with a 6.20 ml/l difference between the near-surface and near-bottom layer.

16.2.2. Fall 1978

As mentioned earlier, there is a gap in the DO data during August and September 1978. The DO data obtained in October and November 1978 show that the DO vertical gradient at the trackline station was fairly low during fall 1978. Along the trackline stations, there was a trend toward higher levels of DO west of station 40. At station 40 on October 4, the DO in the surface layer was 4.59 ml/l. In the near-surface layers, at stations 30 and 20, the DO increased westward, with values of 4.74 and 5.48 ml/l, respectively. This trend of increasing DO levels westward along the trackline was present again in the November 14 seawater samples.

16.2.3. Winter 1979

The DO listings in table 16-1 from late January to mid-March 1979 show that high levels of DO occurred at the trackline station. Although there were no large DO gradients observed during winter, the small vertical gradient that was observed at the end of January increased by the end of February and mid-March.

The largest values of DO along the trackline during the 12-month study were observed on February 22, 1979. The maximum DO in the near-surface layer was

8.64 ml/l at station 30; DO in the near-bottom layer was 6.17 ml/l. Although DO was slightly less at the other trackline stations, the vertical gradients were similar.

16.2.4. Spring 1979

Data obtained on March 13 indicate a decreasing DO trend that continued into spring. Although the horizontal gradient was small on March 13, there was a significant vertical gradient at all stations. The areal average for the near-surface layer at the trackline stations was 6.62 ml/l. In the near-bottom layer, the areal average was 4.54 ml/l.

Data obtained during mid-April 1979 indicate mixing between the near-surface and near-bottom layers with very small vertical gradients. During the month of April, storm conditions occurred which enhanced mixing along the western Louisiana coast. These conditions are discussed in section 20. Data taken from the April 18 cruise show that relatively small horizontal and vertical gradients were present. The DO level of 5.02 ml/l in the surface layer at station 40 during the cruise was slightly higher than that observed at the other trackline stations. In the near-bottom layer at station 40, the level of DO was measured at 4.96 ml/l.

The DO spatial distributions from early May to June 1979 show a tendency towards increasing vertical gradients, with the exception of station 40. The DO in the near-surface layers at stations 20 and 30 on June 2 was 6.04 and 5.17 ml/l, respectively; DO in the near-bottom layers was nearly anoxic, at 0.44 and 0.78 ml/l. In contrast, the DO gradient was weak at station 40. The difference between the near-surface and near-bottom layers was 0.05 ml/l. DO in the near-surface layer was measured at 4.61 ml/l. These conditions observed at the trackline stations during early June 1979 were very similar to those observed in late July 1978.

17. SALINITY, TEMPERATURE, AND DENSITY

Temperature and conductivity observations and the resulting computations of salinity and density (sigma-t) at the trackline stations exhibit large variability. The variability is particularly sensitive to the discharge of fresh water from the Mississippi River and the Atchafalaya River. Variability at the stations is also dependent on seasonal heating and cooling, mixing by wind stress on the sea surface, and changes in the characteristics of the coastal boundary layer.

Figure 17-1 shows temperature versus salinity (T-S) diagrams for CTD casts made during the 12-month period. Each continuous curve shown in the T-S diagrams represents the temperature/salinity structure through the entire water column for each cruise. The surface water temperature reached a maximum of about 32°C as observed during the July 1978 CTD cast, and was at its minimum during January and February 1979, at approximately 10° C, as observed with a bucket thermometer.

Freshwater discharges from the Mississippi River and Atchafalaya River are plotted as monthly means in figures 5-5 and 5-6. As was seen in the previous sections, river runoff significantly affects the hydrography and circulation on the Louisiana inner shelf. The observed salinity values tended to be higher during periods of low river runoff. Salinity at the trackline stations taken from seawater samples 1 m below the surface and 1 m above the bottom are summarized in table 17-1. Vertical profiles of temperature, salinity, and sigma-t for all CTD casts at the trackline station are presented in appendix I (figures I-1 to I-5).

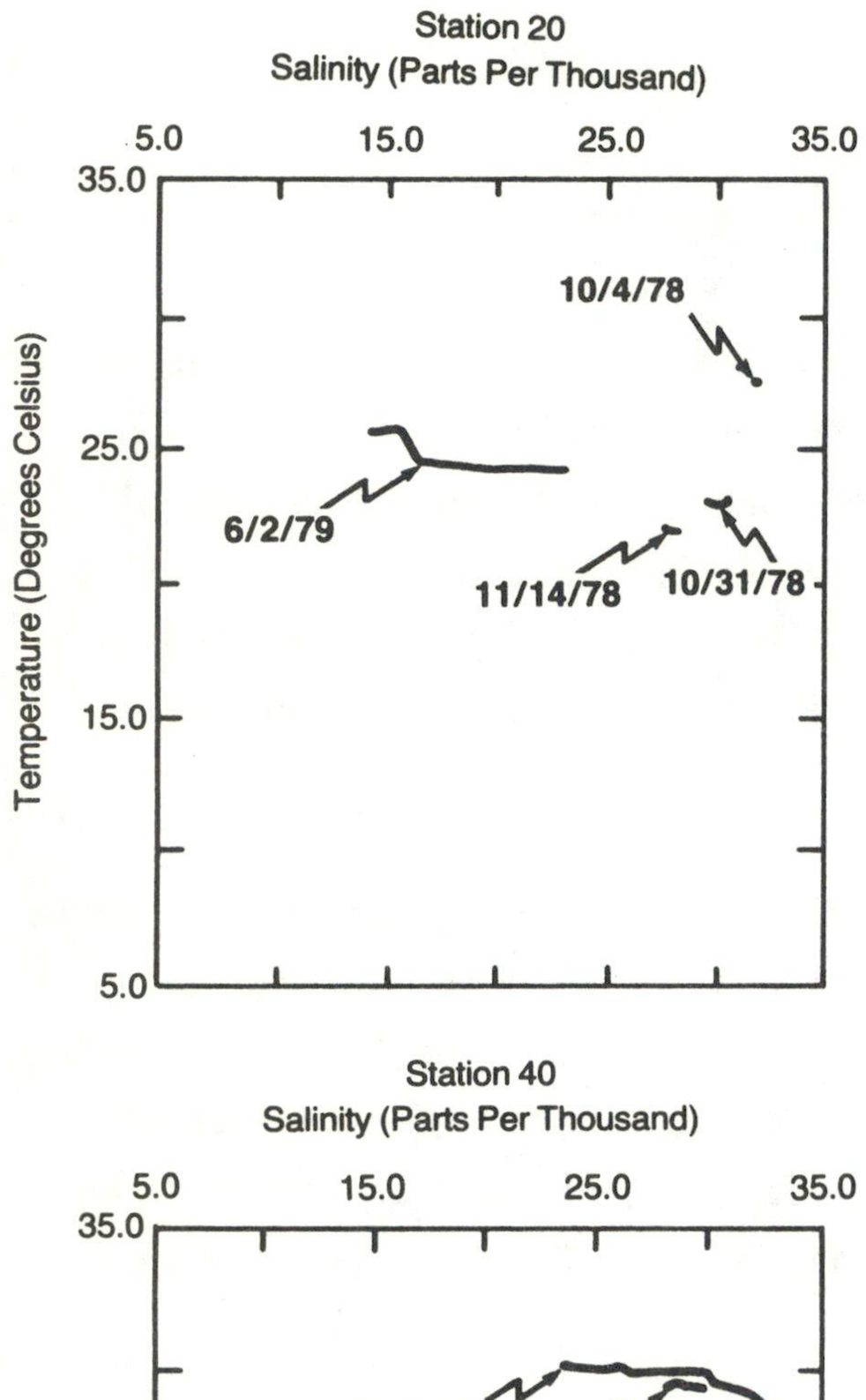

Figure 17-1. Temperature vs. salinity (T-S) diagrams for CTD casts made at trackline stations 20 through 40.

Table 17-1. Near-surface and near-bottom values of salinity at trackline stations.

Date	Sample depth (m)	Salinity (parts per thousand) Station 20	Station 30	Station 40
1978				
6/3	-1		29.403	26.987
	+1		31.966	29.412
7/3	-1		20.501	22.843
	+1		33.122	30.071
7/26	-1		28.466	27.968
	+1		33.272	29.373
10/4	-1	32.270	30.938	31.603
	+1	32.266	31.906	31.386
11/14	-1	28.239	32.062	31.606
	+1	28.285	32.131	31.639
1979				
1/30	-1		31.493	25.172
	+1	30.566	31.524	28.142
2/22	-1	23.249	21.871	26.480
	+1	29.088	28.970	28.910
3/13	-1	25.939	26.604	25.421
	+1	31.914	33.772	31.188
4/18	-1	30.475	31.198	28.447
	+1	30.501	31.450	29.291
5/8	-1	19.309	16.030	22.697
	+1	24.347	20.988	25.831
6/2	-1	15.940	17.279	28.343
	+1	23.227	30.622	28.399

Station depth at CLW m	Station 20 11.9	Station 30 14.6	Station 40 11.0

- indicates distance beneath surface
+ indicates distance above bottom

17.1. Summer 1978

Vertical profiles for June 26 show strong stratification during early-summer 1978. There was a stable well-mixed surface layer at station 30 with a mean salinity value of 20.4 ppt and a pycnocline 3 to 10 m below the surface. Below this pycnocline the bottom layer was moderately mixed with a mean salinity value of 33.1 ppt. The difference of 4.9°C between the surface temperature of 31.0°C and the bottom temperature 26.1°C reinforced the stability of the water column. Although the water column at station 40 was stratified, a well-mixed surface layer as observed at station 30 was not found.

The stratification at the trackline stations continued into July. On July 26 the well-mixed upper layer at station 30 extended approximately 10 m below the surface with a mean salinity of 28.4 ppt and a temperature of 29.2°C; there was a strong pycnocline between 10.5 and 11.0 m. The halocline had a gradient of 6.2 ppt/m. The well-defined halocline was accompanied by a sharp thermocline of 2.8°C/m. The resulting pycnocline separated the bottom layer, which was further separated into a second and third layer by a small pycnocline. At station 40, the water column was weakly stratified. The difference between the surface salinity, 27.9 ppt, and the bottom salinity, 29.8 ppt, was only 1.9 ppt. The temperature differential was less than 0.1 Celsius degrees. The GCLW depth at station 30 exceeded the depth at station 40 by 3.6 m. At station 30, the greater water depth permitted colder more saline Gulf water to intrude further north along the bottom.

As mentioned earlier, the FERREL was unable to steam to the trackline stations for the August and September 1978 cruise; thus, no water samples or CTD cast data were available for that period.

17.2. Fall 1978

Salinities determined from the water sample analysis and profiles of temperature, salinity, and sigma-t obtained from profile data taken in October and November 1978 show that the vertical density structure at the trackline stations was fairly uniform during fall 1978. The volume of freshwater discharge

along the western Louisiana coast continued to decrease during most of fall, and values of salinity observed were correspondingly higher than those in summer. The mean salinity on October 4 at the trackline stations 20, 30, and 40 was calculated at 31.6 ppt in the near-surface layer and 31.8 ppt in the near-bottom layer. On November 14, the salinity at stations 30 and 40 averaged 31.8 ppt in the near-surface layer and 31.9 ppt in the near-bottom layer. At station 20 the salinity was lower with a near-surface salinity of 28.2 ppt and a near-bottom salinity of 28.3 ppt.

17.3. Winter 1979

The discharge from the Mississippi and Atchafalaya Rivers increased sharply near the end of fall 1978 and continued to flow at a higher rate in winter 1979. This increase in discharge resulted in a decrease in salinity from fall to winter. Intense vertical mixing caused by wind stresses limited the stratification. The greatest stratification observed during the winter cruises was on February 22 at station 30. At station 30, the differential between the near-surface salinity of 21.9 ppt and the near-bottom salinity of 29.0 ppt was 7.1 ppt. At the trackline stations during the months of January, February, and March, salinities were observed to vary between 21.9 and 31.5 ppt in the near-surface layer and 28.1 to 33.8 ppt in the near-bottom layer.

17.4. Spring 1979

The discharges from the Mississippi and Atchafalaya Rivers peaked during April and May. The stratification of the waters at the trackline stations were generally stable during spring; although during the passage of spring storms they could become well-mixed. Vertical gradients of salinity on April 18 at the trackline stations were relatively weak; mixing resulted from the passage of a storm a week earlier. The salinity differential at station 20 was only 0.03 ppt from near-surface to near-bottom. The near-surface salinity value of 30.5 ppt at station 20 suggest a flow of high salinity Gulf water shoreward on April 18.

The southward spreading of low salinity water across the Louisiana inner shelf at the trackline stations was at its peak during May. At station 30 a

salinity value of 21.0 ppt was observed in the near-bottom layer during the May 8 cruise. The salinity differential at station 30 was 5.0 ppt from the near surface to the near-bottom. The salinity distributions from early May to June 1979 show a tendency towards increasing vertical gradients. The salinity differential between the near-surface salinity, 17.3 ppt, and the near-bottom salinity, 30.6, was 13.3 ppt at station 30 on June 2.

EXTREME EVENTS

Information in this part of the report describes four different types of storms that occurred during the 12-month observation period. The descriptions include a tropical storm (DEBRA), an extratropical cyclone, northers following polar frontal passages, and a spring storm. Although storms are termed as extreme events, northers are frequent enough to be considered part of the regional climatology.

18. TROPICAL STORM DEBRA

During the Atlantic hurricane season of 1978, 11 weather systems were named as tropical storms; 5 of these became hurricanes. Six of the storms formed from tropical waves which moved off the Atlantic Coast, and the others began as baroclinic developments, such as cold fronts and upper level cold lows. Lawrence (1979) reported that the duration of hurricane force winds during 1978 was far below normal, although there were more individual storms than normal. Three

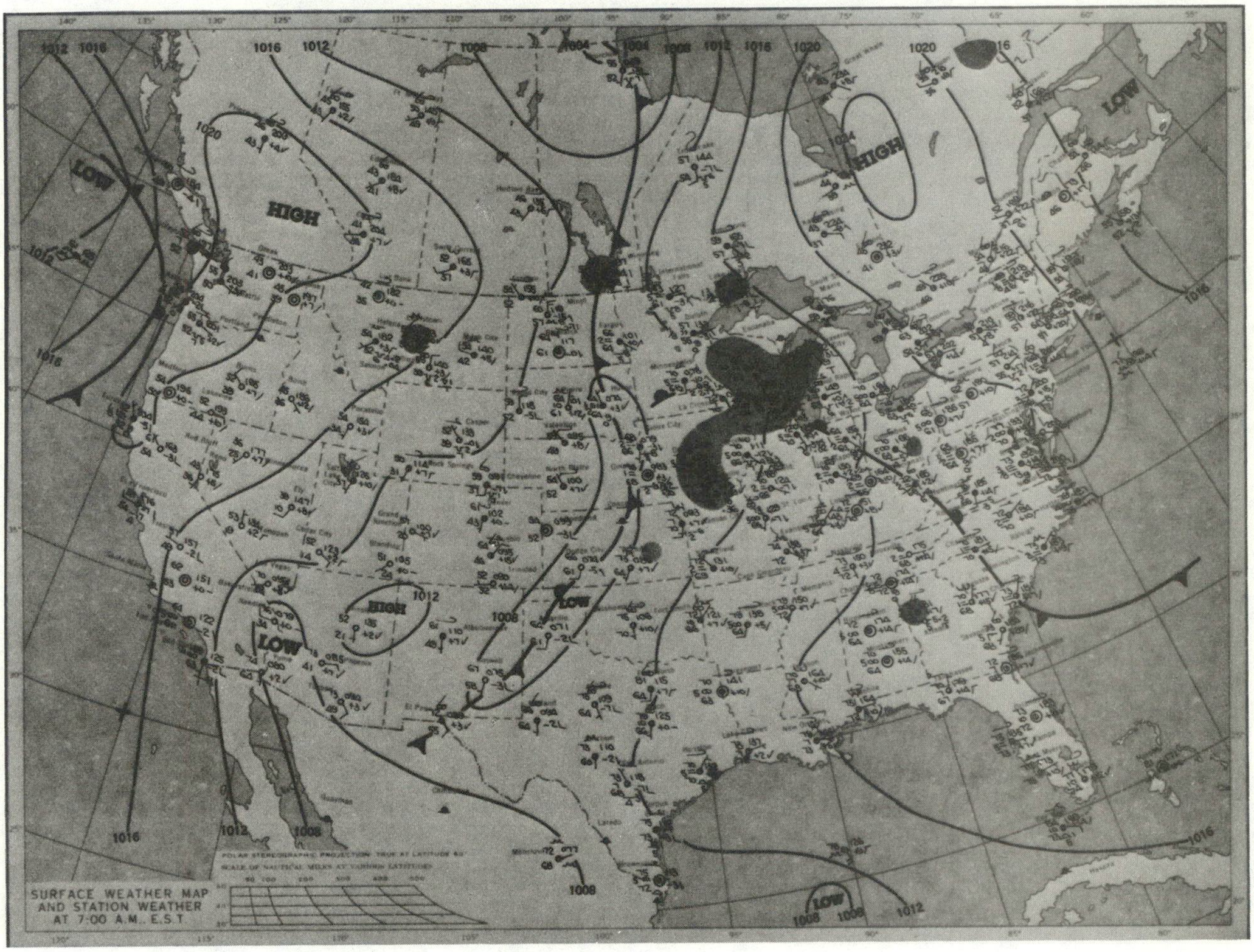

Figure 18-1. Daily surface weather map for August 27, 1978. (Source: U.S. Department of Commerce daily weather maps, weekly series, August 21 to August 27, 1978).

tropical storms made landfall in the western Gulf of Mexico: AMELIA made landfall south of Corpus Christi late on July 30; BESS made landfall near Nautala, Mexico, about 350 nautical miles south of Brownsville early on August 8; DEBRA's storm track crossed the West Hackberry site on August 28.

18.1. Origin and Track of DEBRA

Daily surface weather maps shown in figures 18-1 to 18-3 indicate the progress of DEBRA from August 27 to 29. DEBRA developed initially with an upper tropospheric cold low which formed over southwest Florida at about 0000 GMT on

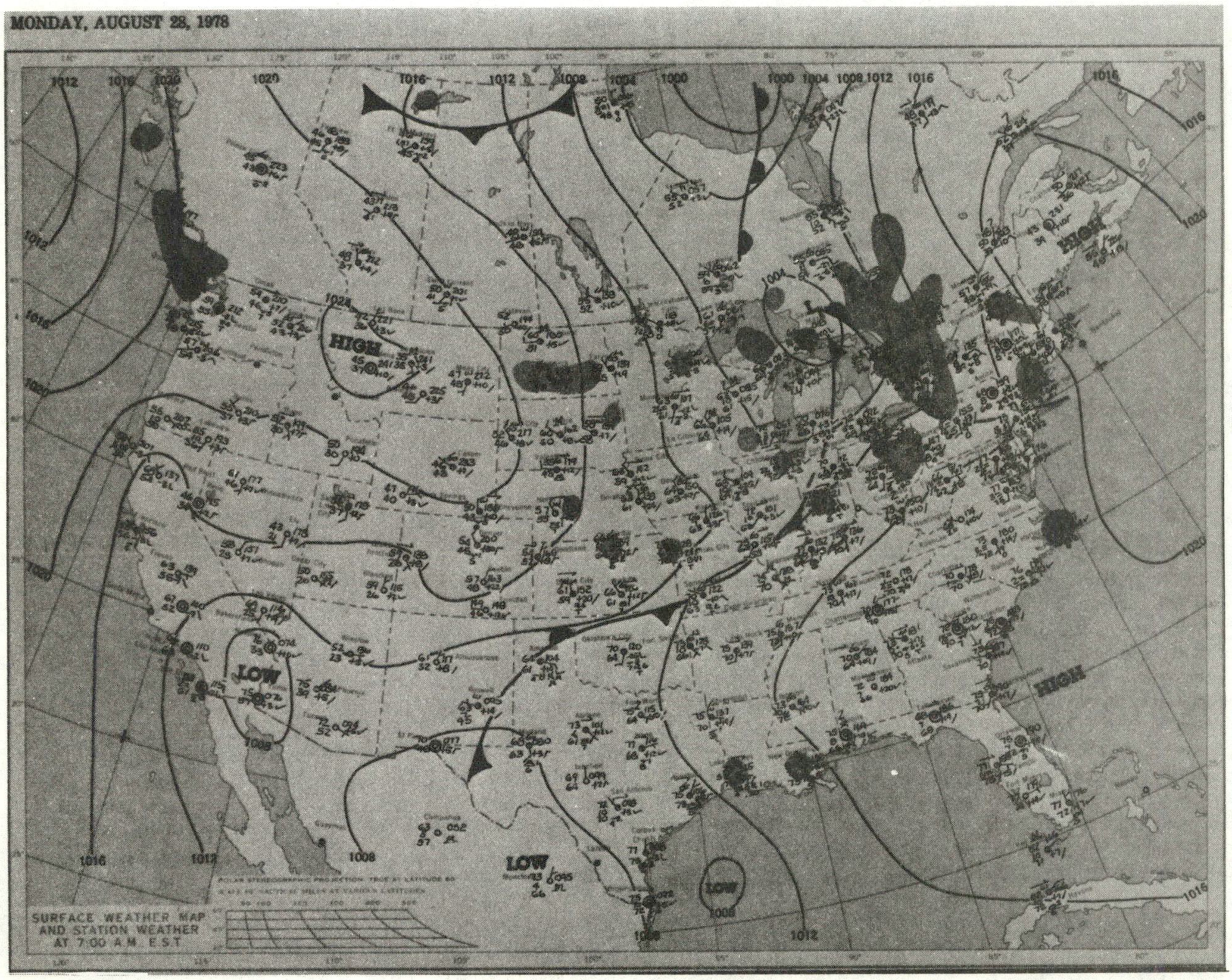

Figure 18-2. Daily surface weather map for August 28, 1978. (Source: U.S. Department of Commerce daily weather maps, weekly series, August 28 to September 3, 1978).

August 25. During the next 36 hours, the low drifted southwestward to a position north of the Yucatan Peninsula, while the cold low penetrated downward into the lower atmospheric levels (National Hurricane Center, 1978). Meanwhile, a tropical wave moved westward through the western Caribbean and into Yucatan. At 1200 GMT August 25, the wave and low level vorticity center generated by the cold low came into alinement. The wave enhanced the low level inflow and a tropical depression formed at about 1200 GMT August 26.

The depression tracked initially westward under the influence of the surface ridge to the north, but as the western extension of the ridge eroded, the

Figure 18-3. Daily surface weather map for August 29, 1978. (Source: U.S. Department of Commerce daily weather maps, weekly series, August 28 to September 3, 1978).

depression gradually turned toward the north. Meanwhile, the depression strengthened slowly and was upgraded to a tropical storm when 40-knot (20.6 m/s) surface winds and 1002-mbar air pressure were reported. DEBRA became the third storm of 1978 to develop in the Gulf of Mexico west of 93 degrees west longitude.

Since DEBRA was an immediate threat to the coast, the first tropical storm advisory, which was issued at 1800 GMT August 28, posted gale warnings from Galveston, Tex., to Grand Isle, La. In a short time, 3,000 persons were evacuated from lower Cameron Parrish, La., and an undetermined number were evacuated from neighboring Vermilion Parish.

Figure 18-4 shows a GOES 2 satellite picture, with 0.93-km resolution, of Tropical Storm DEBRA at 1931 GMT on August 28. The satellite picture shows that DEBRA was not a particulary well-defined cloud system; it was not a well-organized storm. Furthermore, the National Hurricane Center's preliminary report apparently had an eastward bias caused by the large, poorly defined storm center. Powell (1979) analyzed data from aircraft, surface radars, and high frequency (HF) sky wave radar. Maresca and Carlson (1978) found the sky wave radar measurements during Tropical Storm DEBRA to have significant deviations between surface wave radar position estimates and estimates obtained from the NOAA reconnaissance aircraft, ground based microwave Doppler radar, and GOES satellite images. Sky wave radar observations, aircraft radar observations, and Doppler radar observations were in much closer agreement than any one of the three was with the satellite observations. At 2100 GMT August 28, the aircraft and sky wave estimates differed by 10 km; the Doppler radar and sky wave radar estimates differed by 13 km. The sky wave radar and satellite estimates differed by 53 km. The large deviation of the satellite estimate was the result of a poorly defined storm center. Powell (1979) used a least-squares third-order regression fit of all data to estimate the track. The least-squares third-order fit, along with the track shown in the preliminary National Hurricane Center (NHC) Report, is shown in figure 18-5. The two tracks agree well after 1800 GMT August 28, but the eastward bias of the NHC track is obvious in the figure. Powell (1979) estimates landfall just west of Holly Beach at 0130 GMT August 29. The storm track made landfall 23.2 km west of the Calcasieu Pass--21.5 km, 299

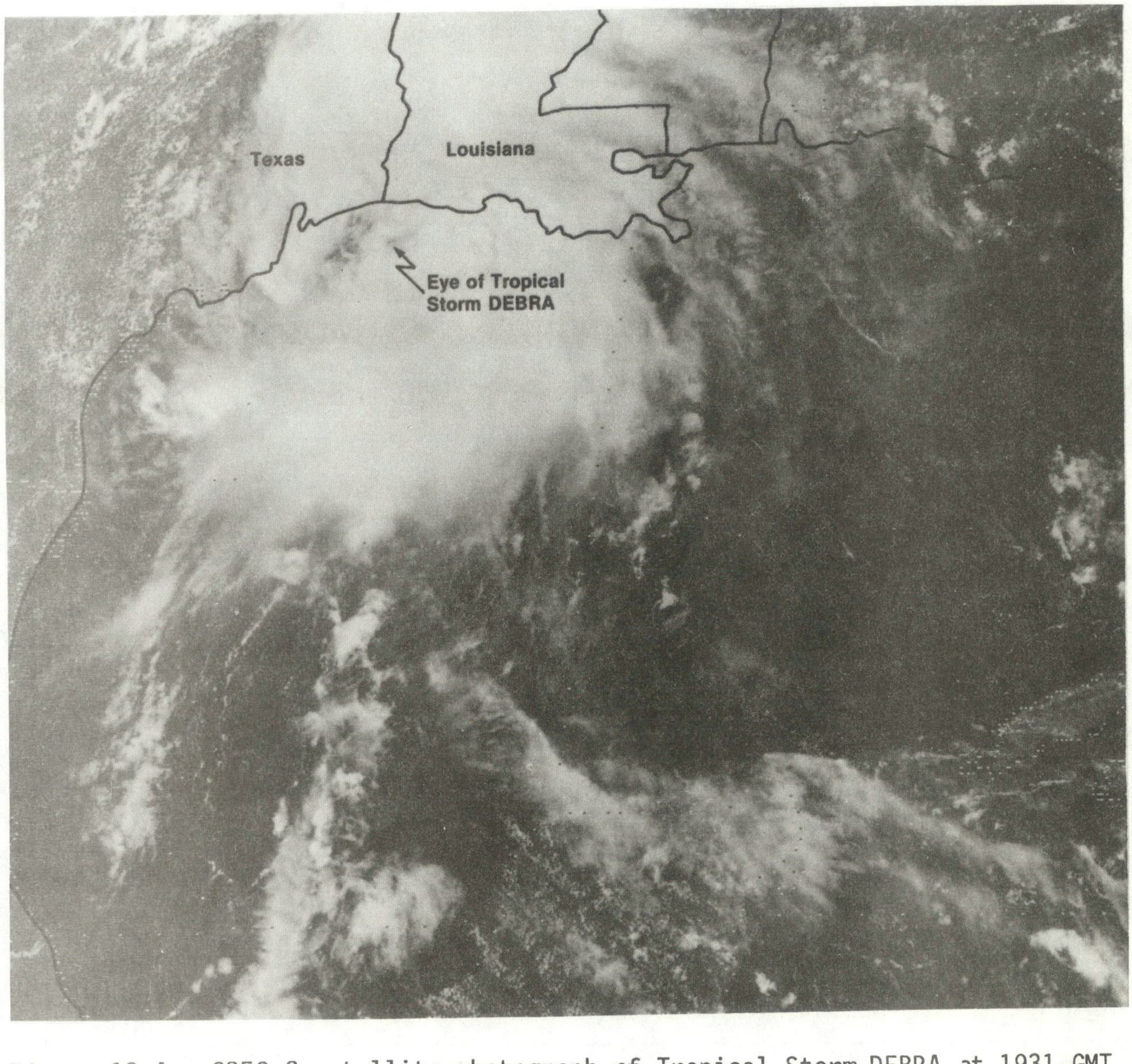

Figure 18-4. GOES 2 satellite photograph of Tropical Storm DEBRA at 1931 GMT on August 28, with 0.93-km resolution.

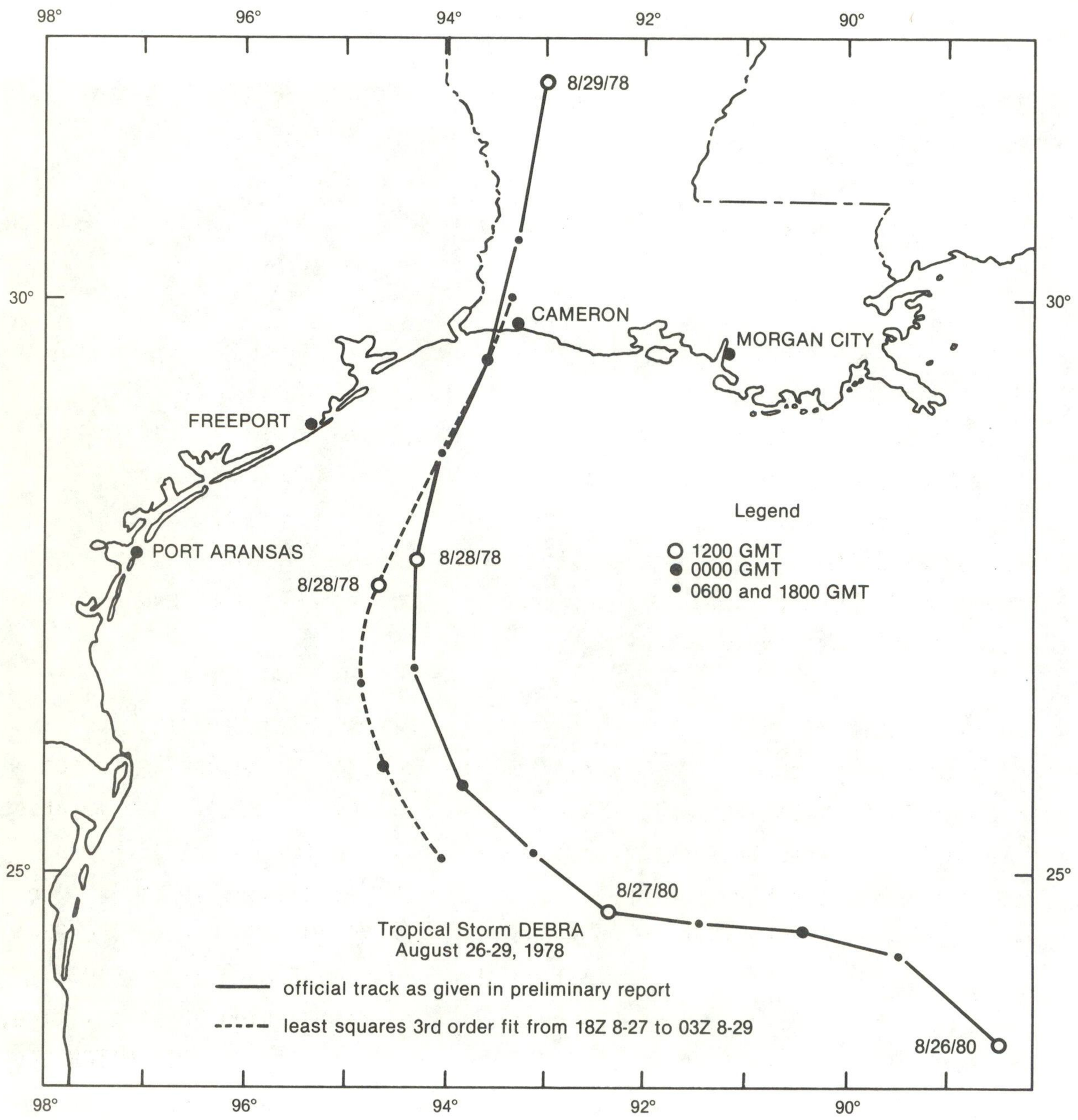

Figure 18-5. National Hurricane Center's track line and the least-squares third-order fit for Tropical Storm DEBRA from August 26-29, 1978.

degrees True from NOS station 18. This estimate is in excellent agreement with the NOS station 18 data.

18.2. Meteorological Observations

Meteorological data were obtained at NOS station 18 and Lake Charles Airport, and by NOAA aircraft 43RF and the NOAA Ship MT. MITCHELL. SEASAT made an overpass during the storm, but no attempt is made here to include that data. The meteorological data set obtained during Tropical Storm DEBRA is rich indeed.

A NOAA WP-3D aircraft made observations from 1756 GMT on August 28 to 0321 GMT August 29. The aircraft was hit by lightning at about 2100 GMT, parting an antenna. The aircraft landed at Houston, cut away the remaining antenna cable, and returned to the storm at about 2300 GMT. The maximum sustained flight level wind speed was 120 km/hr, about 30 km southeast of the Rockefeller Wildlife Refuge; this results in a 10-m level computed sustained wind speed of 85 km/hr, which is in agreement with automatic stations on oil production platforms some distance away.

The NOAA Ship MT. MITCHELL, in the area to perform a cooperative hydrographic survey, observed heavy rain beginning 0636 GMT August 28, which continued until 0718 GMT August 29 (National Ocean Survey, 1978). The greatest total rainfall reported by the National Weather Service for August 1978 was 27.5 cm at Fresh Water Bay Lock, La. Local rainfall amounts of 15 cm or more occurred in southwest Louisiana. On August 28, the MT. MITCHELL observed 23-m/s winds from 140 degrees True at 1500 GMT in the vicinity of 29° 37.1' N, 93° 28.8' W. The ship, about 9.3 km, 235 degrees True from station 18 at the time, was in that vicinity from 0900 to 1700 GMT August 28. While the MT. MITCHELL was approaching 29° 29' N, 93° 18' W, the minimum barometric pressure of 1001.0 mbar was observed at 0000 GMT August 29. At 2000 GMT, the ship observed a 1.2-m swell from 150 degrees True and estimated 1.5-m waves (approximately the same as significant wave height). From 0300 to 1200 GMT August 29, the ship estimated 2.4-m waves with no apparent swell. The NOAA research aircraft measured a minimum pressure of 1000 mbar at 0000 GMT on August 29 (National Ocean Survey, 1978).

Meteorological data obtained 19.5 m above the sea surface at station 18 are shown in figure 18-6. Wind speeds were averaged over 10-minute intervals, while wind direction and pressure were instantaneous readings. Maximum winds of 17 m/s were observed from 1930 to 2300 GMT August 28 and again at 0150 GMT August 29. The direction data show backing (counterclockwise rotation) of the winds, consistent during the passage of a cyclone. As will be seen in the next subsection, the currents responded rapidly to the winds. A minimum air pressure

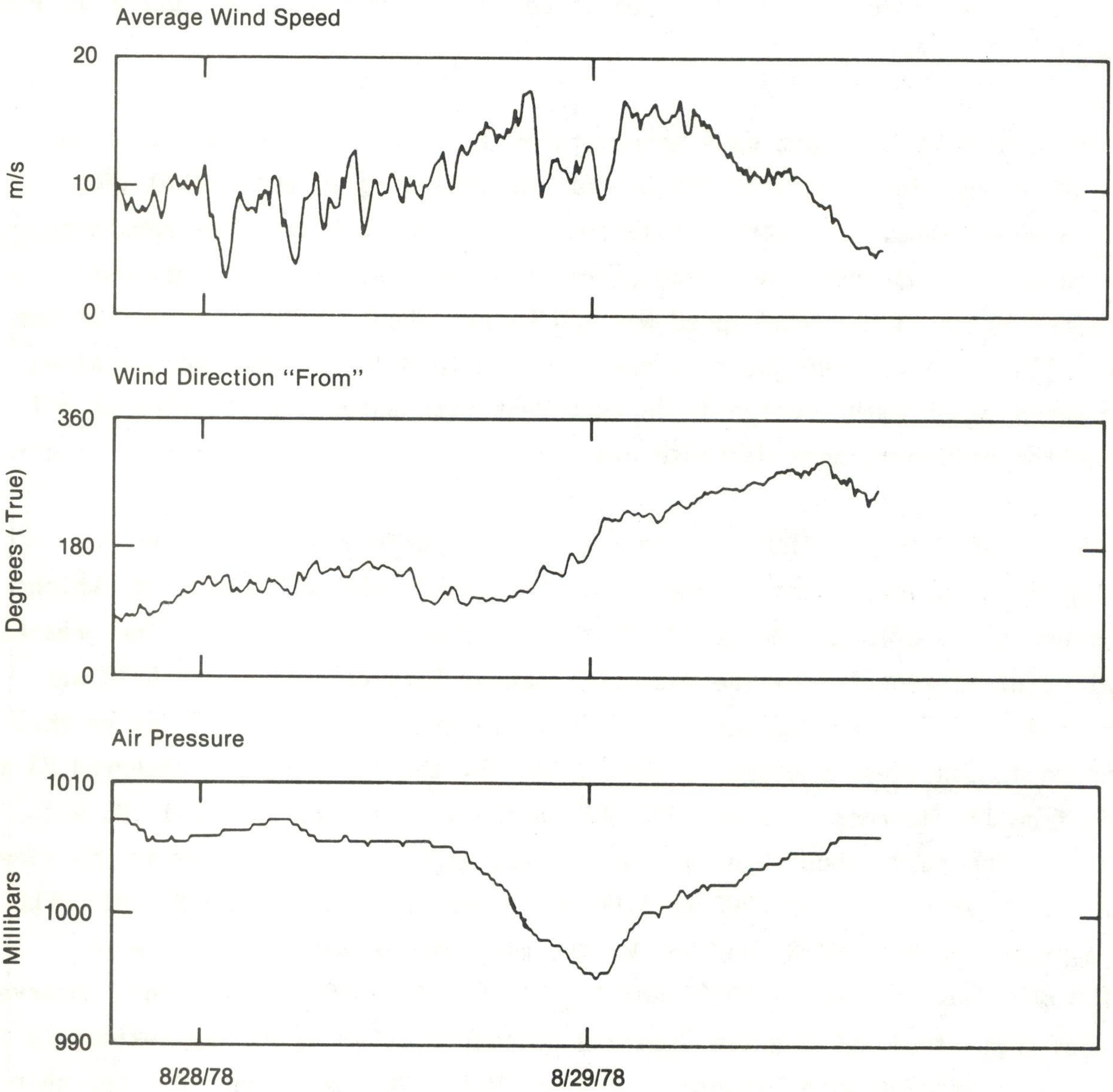

Figure 18-6. Meteorological data obtained at station 18 August 27-29 during Tropical Storm DEBRA (data obtained at 19.5 m, uncorrected to 10 m).

of 997.96 mbar was observed at station 18 from 0140 to 0150 GMT August 29; this was the lowest observation from all of the various sources. The TMU for the NOS air pressure measurements is +0.5, -8.2 mbar (section 7.4.7, volume two of this report). No meteorological data were obtained at the Weeks Island site, but the effects of the whole gale winds observed by an automatic recording instrument on an oil production platform in the Eugene Island area were obvious; five NOS subsurface instrument platforms at the Weeks Island site toppled and were scoured about 1 m into the sand bottom.

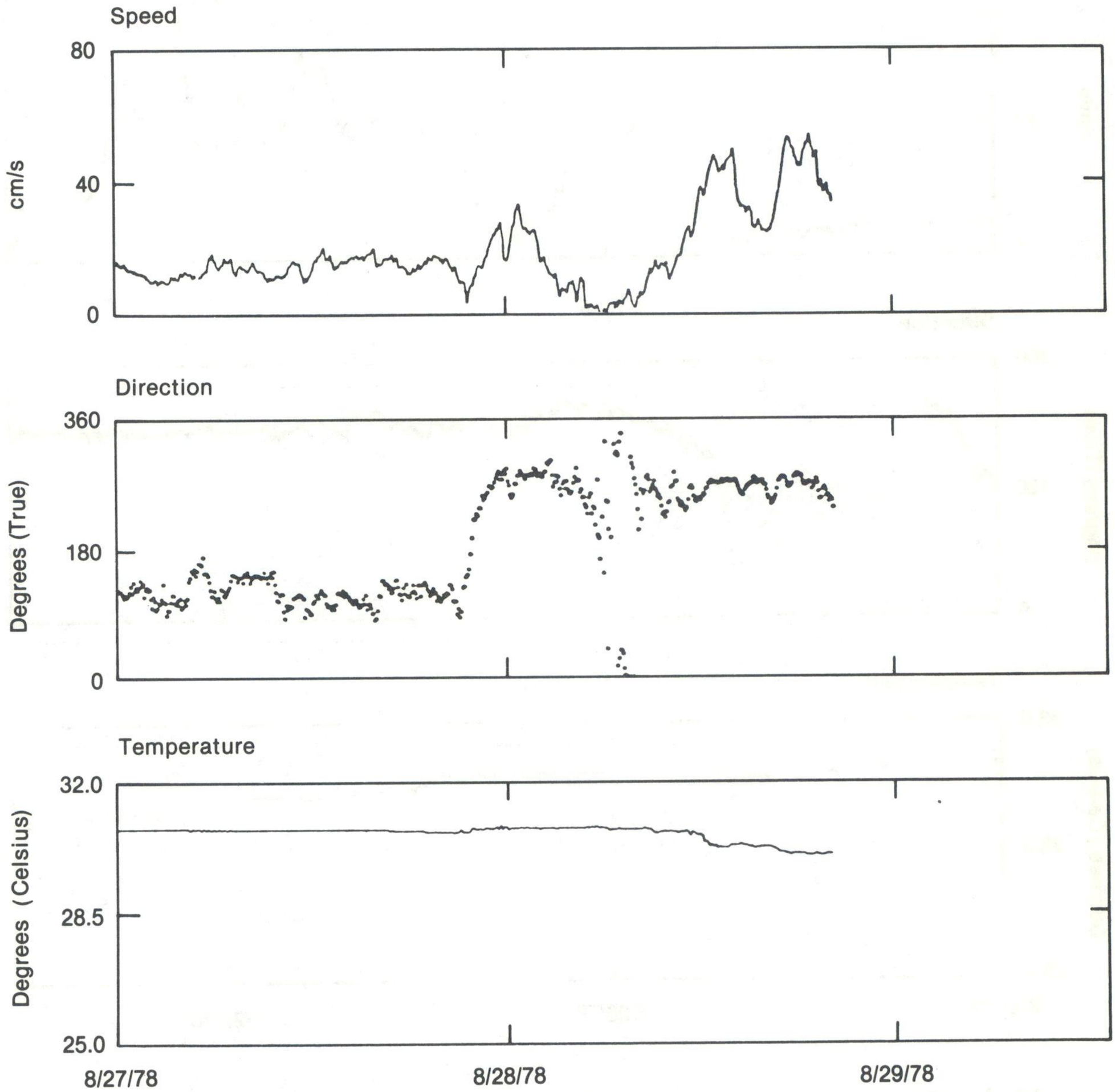

Figure 18-7. Current meter data obtained at station 11 August 27-29, 1 m above bottom during Tropical Storm DEBRA.

18.3. Oceanographic Observations

Current meter data obtained at stations 11 and 14, and wave data obtained at station 11, are shown in figures 18-7 to 18-10. Metal fatigue caused the current meter at the 1-m level of station 11 to part from the platform and become imbedded halfway into the bottom sediments, nose down; thus, the shorter record.

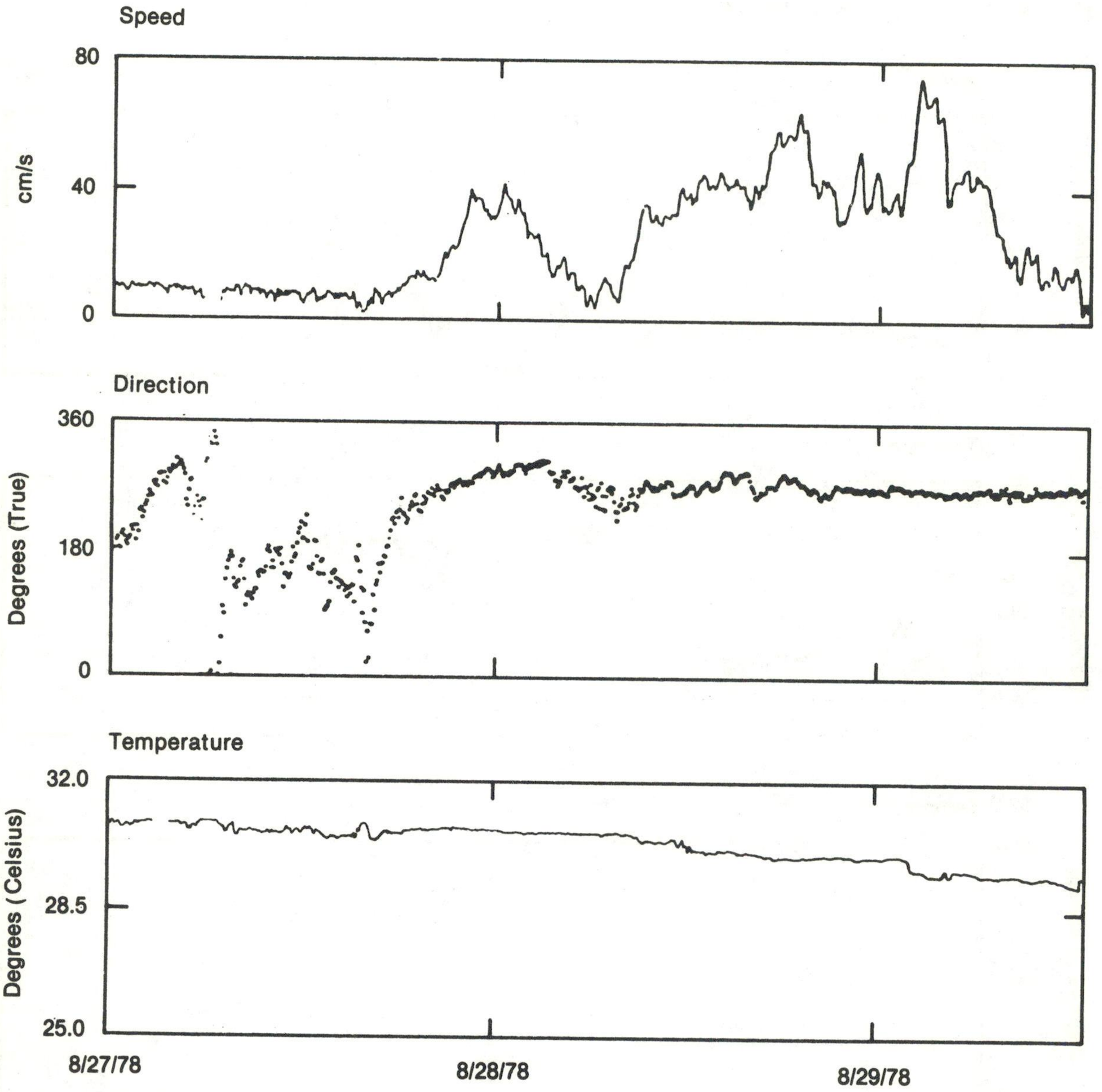

Figure 18-8. Current meter data obtained at station 11 August 27-29, 3 m above bottom during Tropical Storm DEBRA.

The south-southeasterly winds at 12 m/s that preceded the eye of the storm set up the westward current drift on August 27. The response to the changing wind direction and increasing wind speed is clear in the current meter records.

The speed at the 3-m level at station 11 began to increase at 1800 GMT on August 27 and reached 41 cm/s at 2225 GMT August 27. The speed reached 43 cm/s at 0030 GMT August 28. The maximum current speed at the 3-m level associated

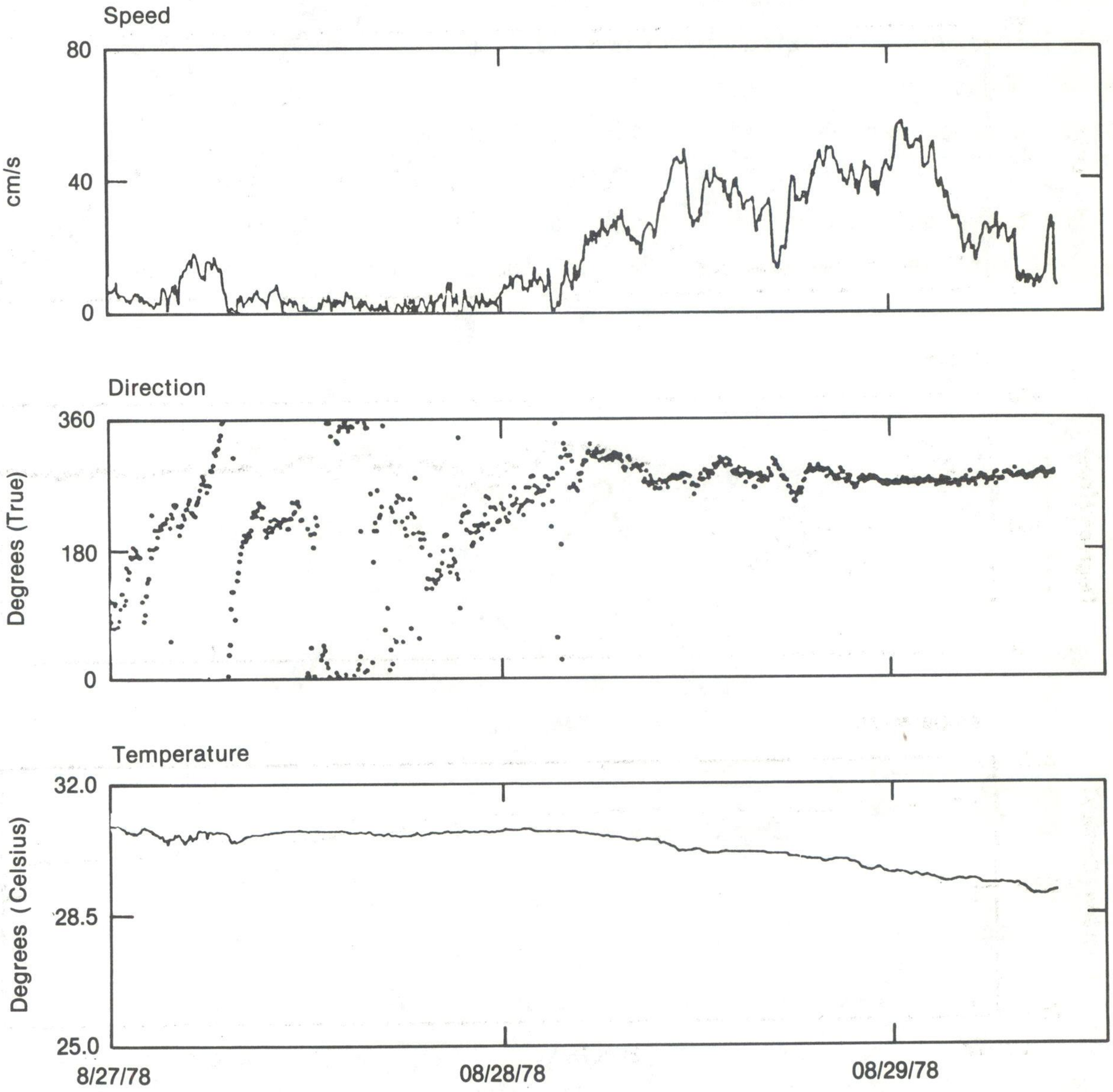

Figure 18-9. Current meter data obtained at station 14 August 27-29, 1 m above bottom during Tropical Storm DEBRA.

with the leading edge of DEBRA was 67 cm/s nearly due westward at 1855 GMT; the speed associated with the trailing edge was 77 cm/s at 0215 GMT.

In comparison with DEBRA, Smith (1978) found alongshore currents during Hurricane ANITA 21.5 km off the central Texas Gulf Coast, reaching speeds of

At the 1-m level at NOS station 11, speed began to increase at 2150 GMT August 27, reached a relative maximum of 28 cm/s at 2345 GMT, and peaked again at 0050 GMT at 33 cm/s. The speed values and times associated with the leading and trailing radii of maximum winds were 57 cm/s at 1850 GMT and 56 cm/s at 0035 GMT August 29, respectively. The peak speed observed late August 28 was 48 cm/s; this speed was observed from 2010 to 2030 GMT.

The speed at the 3-m level at station 11 began to increase at 1800 GMT on August 27 and reached 41 cm/s at 2225 GMT August 27. The speed reached 43 cm/s

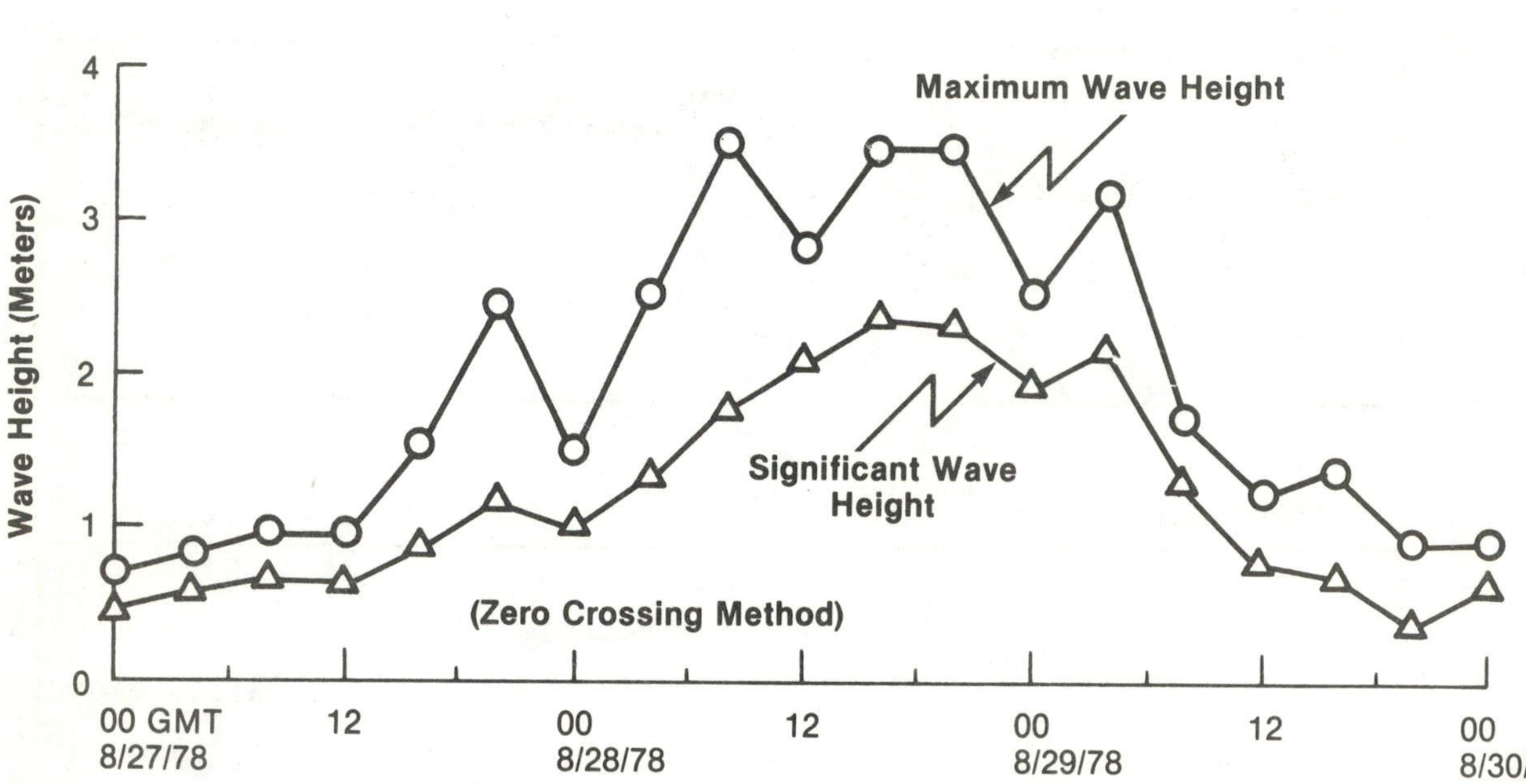

Figure 18-10. Maximum and significant wave heights obtained at station 11 August 27-29, during Tropical Storm DEBRA.

at 0030 GMT August 28. The maximum current speed at the 3-m level associated with the leading edge of DEBRA was 67 cm/s nearly due westward at 1855 GMT; the speed associated with the trailing edge was 77 cm/s at 0215 GMT.

In comparison with DEBRA, Smith (1978) found alongshore currents during Hurricane ANITA 21.5 km off the central Texas Gulf Coast, reaching speeds of

The station 14, 1-m level temperature data show a gradual decrease during the westward drift from 30.5°C at 0500 August 27 to 29.1°C until 1000 GMT, when it increased 0.1°C.

Wave data obtained at station 11 during Tropical Storm DEBRA are presented in figure 18-10 both as maximum and significant wave heights. The values shown were computed from the pressure data by the zero crossing method. (See section 3). Apparent variability in the maximum wave heights may be due to the relatively short (7.5-minute) records obtained over the relatively long intervals (4 hours) necessary to obtain wave gage records of length comparable to those of the current meter records.

The maximum wave height associated with the late August 27 wind was 2.49 m at 1955 GMT. The significant wave height data indicate increasing values to 1555 GMT August 28; the maximum total energy also occurred at 1555 GMT with a period of peak energy at 9 seconds. The maximum wave height at 1555 GMT August 28 was 3.47 m.

The wave height data shown in figure 18-10 are consistent with the meteorological data shown in figure 18-6. They reflect the minimum winds as the eye of the storm passed, a tendency toward increased wave height as the trailing radius of maximum winds approached, and a decrease in wave heights as the winds veered almost exactly through 180 degrees. The decay of wave energy is attributed in part to the fetch; momentum transfer from the atmosphere to the Gulf of Mexico waters was not limited by fetch when the winds were southeasterly and occurred over the entire scale of the storm, but the fetch was limited by land when the winds were northwesterly. In addition, transfer of momentum opposed the developed seas.

Forristall et al. (1977) reported currents, winds, waves, and barometric pressure measured during Tropical Storm DELIA (September 1973) at an oil production platform located 50 km south of Galveston, Tex., where the water depth was 20 m. DELIA was similar to DEBRA in that it made landfall with an ill-defined center and was a relatively weak storm. Despite this, DELIA produced a minimum pressure of 987 mbar and a peak wind gust of 32 m/s. The maximum wave heights observed during DELIA were 7 to 8 m. DELIA began as a weak, cyclonic circulation that strengthened on November 2, 1973, and followed a northwestward course toward Galveston, Tex. Waves were measured with a wave-staff transducer. Currents greater than 2 m/s toward the west-southwest (approximately parallel to the local isobaths) were observed 17 m above the sea floor. Peak currents at 3 m above the bottom had speeds that were 75 percent of those at the upper level. Currents during part of the storm were swift enough so that the total particle velocities, including wave motion, did not reverse direction. This finding was consistent with the NOS observations found in the GASP Experiment, during which the steady currents were greater in magnitude than the orbital velocities of the highest waves most of the time.

19. EXTRATROPICAL CYCLONE AND NORTHERS

The effects of winter storms during January and February 1979 on currents, water levels, and waves at the West Hackberry site are discussed in this section. The storm activity consists of an extratropical cyclone and four northers that followed frontal passages.

19.1. Meteorological Observations

Meteorological data were obtained at NOS station 19, except during a February norther, and at the Lake Charles Airport. The station 19 data were collected at a height of 15.8 m above GCLW during the January storms, and are uncorrected to the standard 10-m anemometer level. Because of a time discrepancy of 40 minutes in the station 19 data, the data were not validated for archiving at NODC. The data are statistically valid, however, and provide approximate times for major storm events.

Time series plots of the meteorological data at station 19 for January 9 to 31 are shown in figure 19-1. Wind speeds were averaged over 10-minute intervals, while wind direction and air pressure readings were instantaneous. Data collected at Lake Charles Airport for January 19 to 28 are shown in figure 19-2. As mentioned in section 6, the relationship between winds measured at the Lake Charles Airport and those measured over water at the site is poor; we make no attempt to interpret oceanographic observations using inland airport data. Winds at Lake Charles are shown so that readers can examine the differences, and to show air pressure fluctuations caused by the polar frontal passages.

The effects of an extratropical cyclone were greatest at the West Hackberry site on January 12 to 14. The development of the extratropical cyclone over New Mexico on January 10 is evident in the 500-mbar height contours for that day

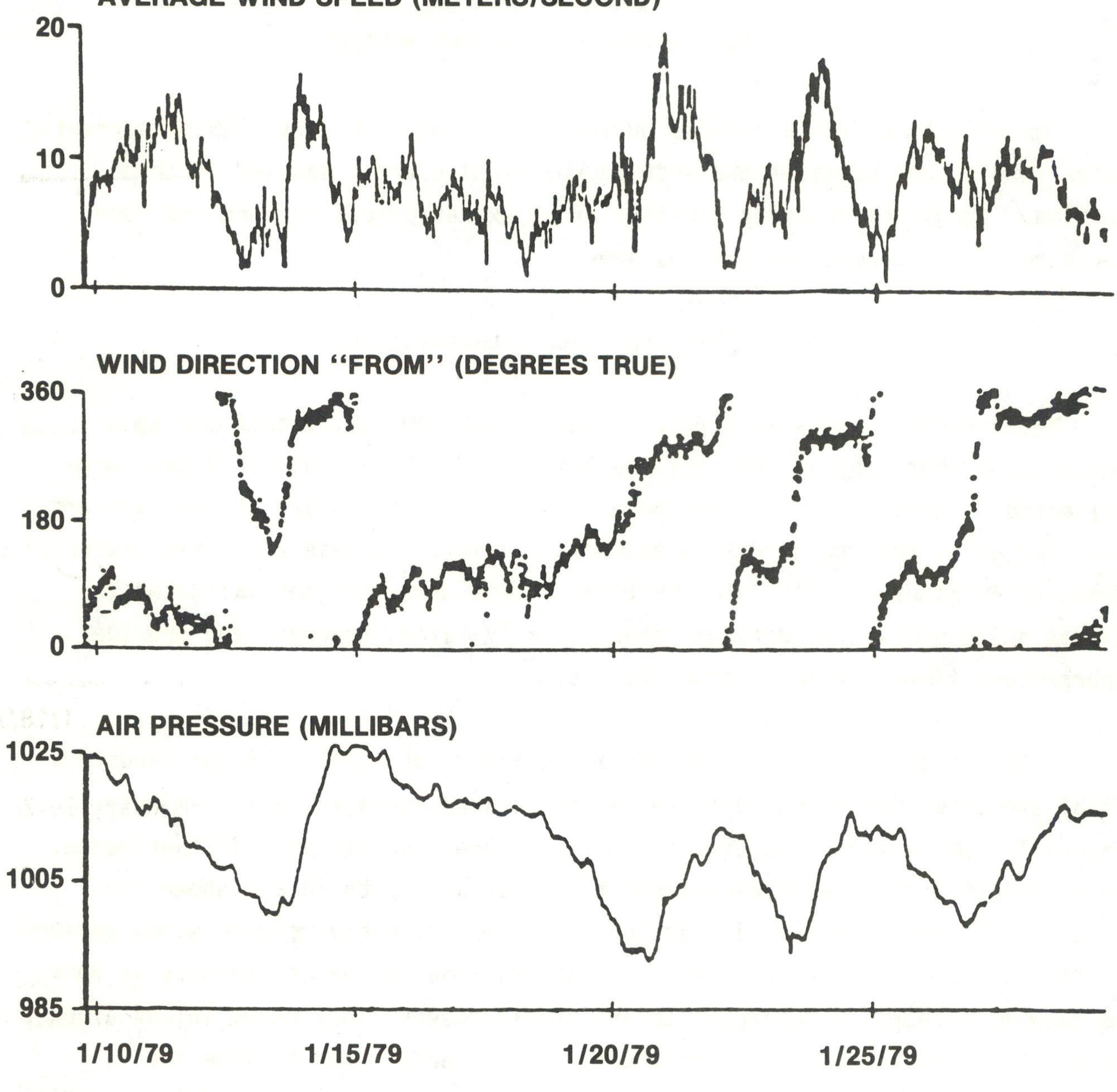

Figure 19-1. Meteorological time series at West Hackberry station 19, January 9-31, 1979.

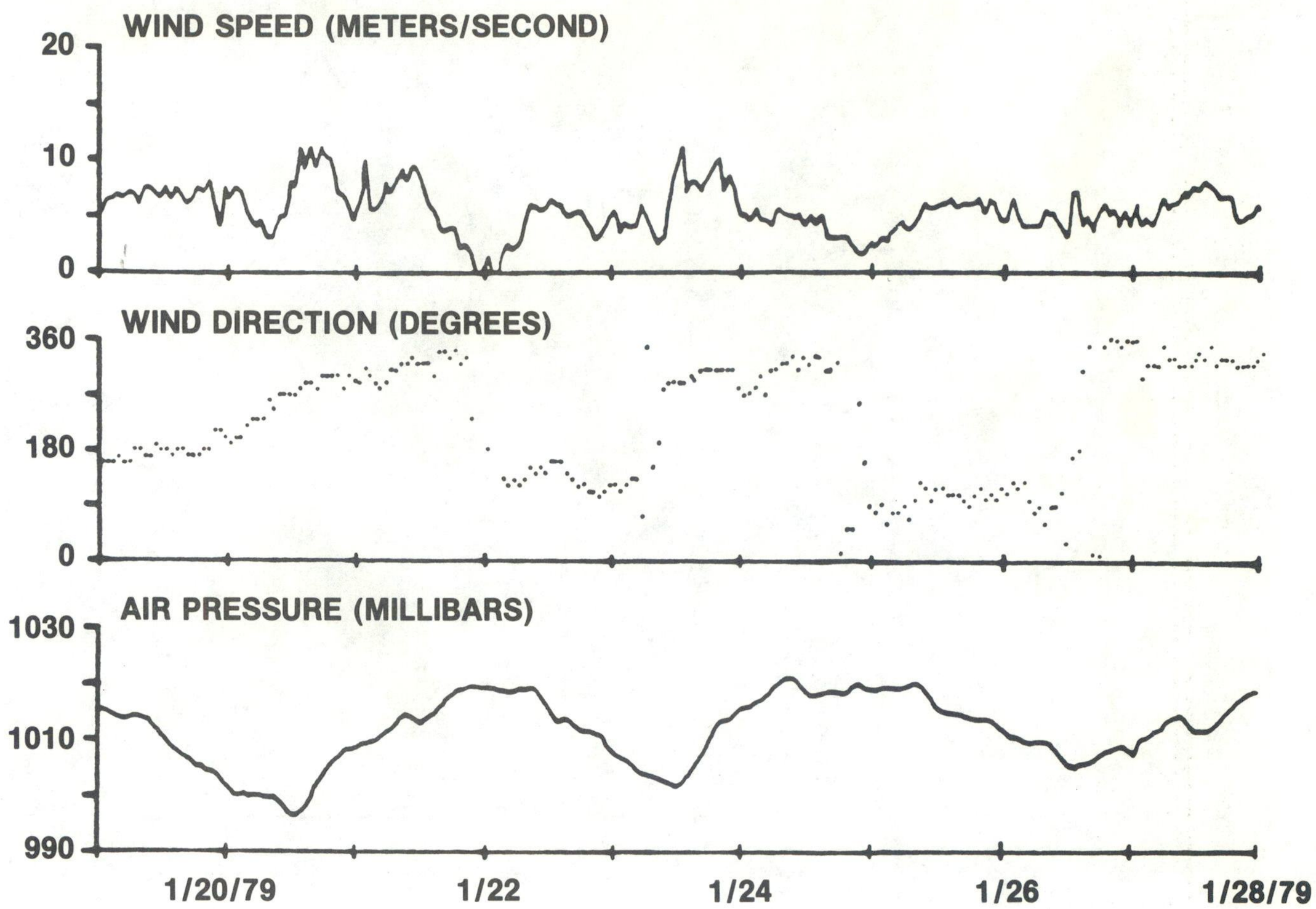

Figure 19-2. Meteorological time series at Lake Charles Airport, January 19-28, 1979.

(NOAA Daily Weather Maps, Weekly Series, January 8-14, 1979), as well as in the surface weather map. The cyclone moved off the Texas coast by midday (GMT) on January 11, became well developed at the 500-mbar height, and continued its eastward progression across the northern Gulf of Mexico and into the Atlantic Ocean. Surface weather maps for January 12 and 13 are shown in figures 19-3 and 19-4.

Figure 19-3. Surface weather map for January 12, 1979.

Data obtained at station 19 (figure 19-1) show counterclockwise rotation (backing) of the winds, consistent with the passage of a cyclone, which began January 10 and continued until 1200 GMT on January 13. Air pressure dropped continuously from 1024.41 mbar on January 10 to 999.62 mbar at 0700 GMT on January 13, a decrease of 24.79 mbar. Following the passage of the cyclone center, the wind speed increased sharply to a maximum of 16.5 m/s from 320° True at 2300 GMT on January 13. Air temperature decreased 20.3 Celsius degrees from 15.7°C at 1500 GMT on January 13 to -4.6°C, the lowest temperature of the month, at 1100 GMT on January 14.

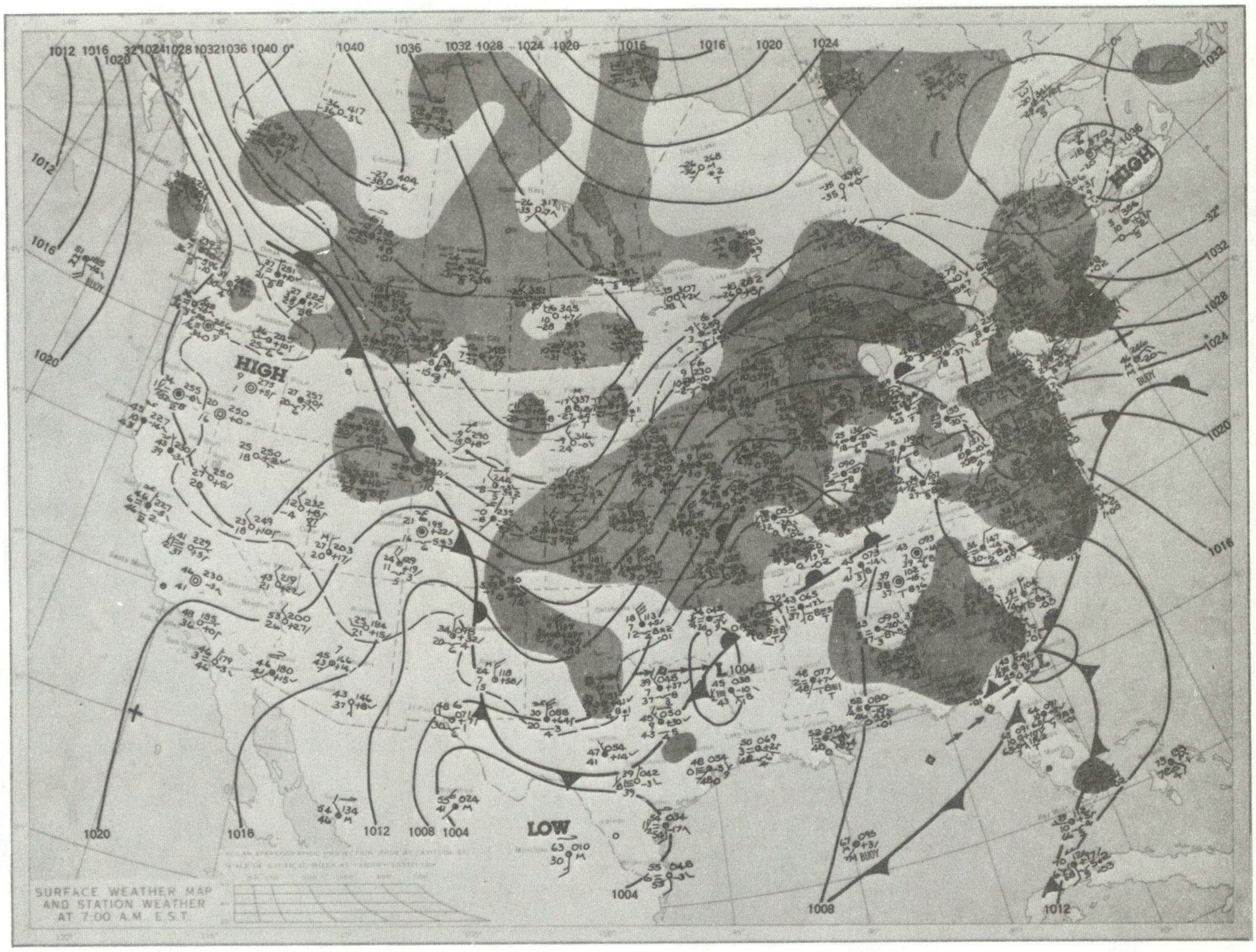

Figure 19-4. Surface weather map for January 13, 1979.

Beginning on January 20 (figure 19-1), the effects of the passage of three successive polar fronts through the West Hackberry site can be seen. The minimum pressures observed were 992.97 mbar at 1700 GMT on January 20, 995.0 mbar at 1100 GMT on January 23, and 997.96 mbar at 1900 GMT on January 26. Minimum temperatures were 6.0° C at 1200 GMT on January 21, 1.0° C at 1200 GMT on January 24, and 6.3° C at 0500 GMT on January 27.

The maximum wind speeds observed were 19.7 m/s at 2300 GMT on January 20, 17.7 m/s on January 23, and 11.8 m/s on January 26. On January 20 and 23, the maximum winds were from the west-northwest, from 280° to 300° True, while on January 26 the maximum wind was southerly.

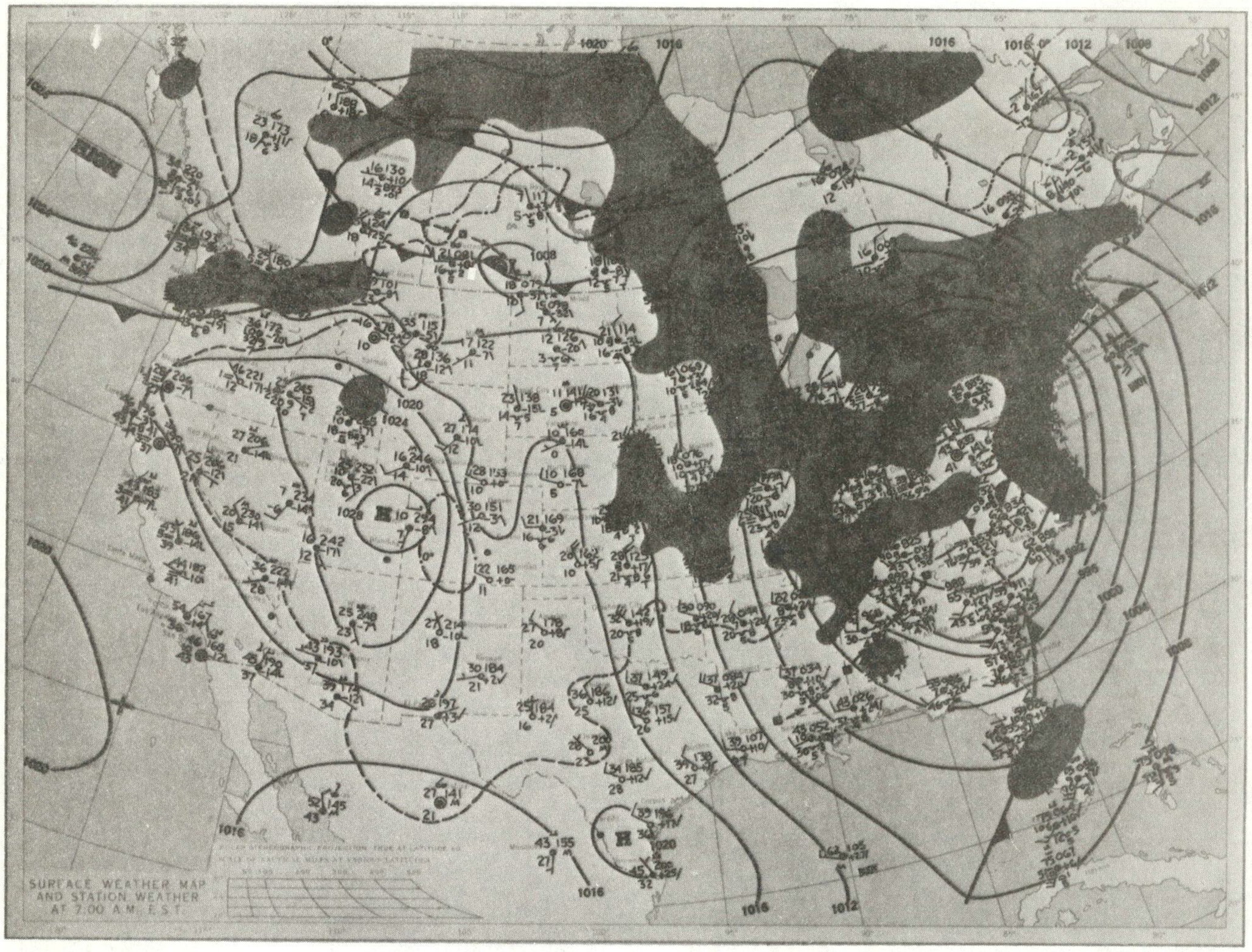

Figure 19-5. Surface weather map for January 21, 1979.

The surface weather map for January 20 (NOAA Daily Weather Maps, Weekly Series, January 15-21, 1979) shows a polar front over Louisiana. By January 21, the front had moved over the mid-Atlantic states (figure 19-5), and westerly winds were observed at the site. The weather map for January 23 (figure 19-6) shows a low pressure area moving through Oklahoma, while the polar front extended south over central Texas. On January 24, the polar front had moved through Louisiana and was over the eastern United States. The weather maps of January 26 and 27 show a polar front which had moved along the Gulf Coast from eastern Mexico through Louisiana (NOAA Daily Weather Maps, Weekly Series, January 22-28, 1979).

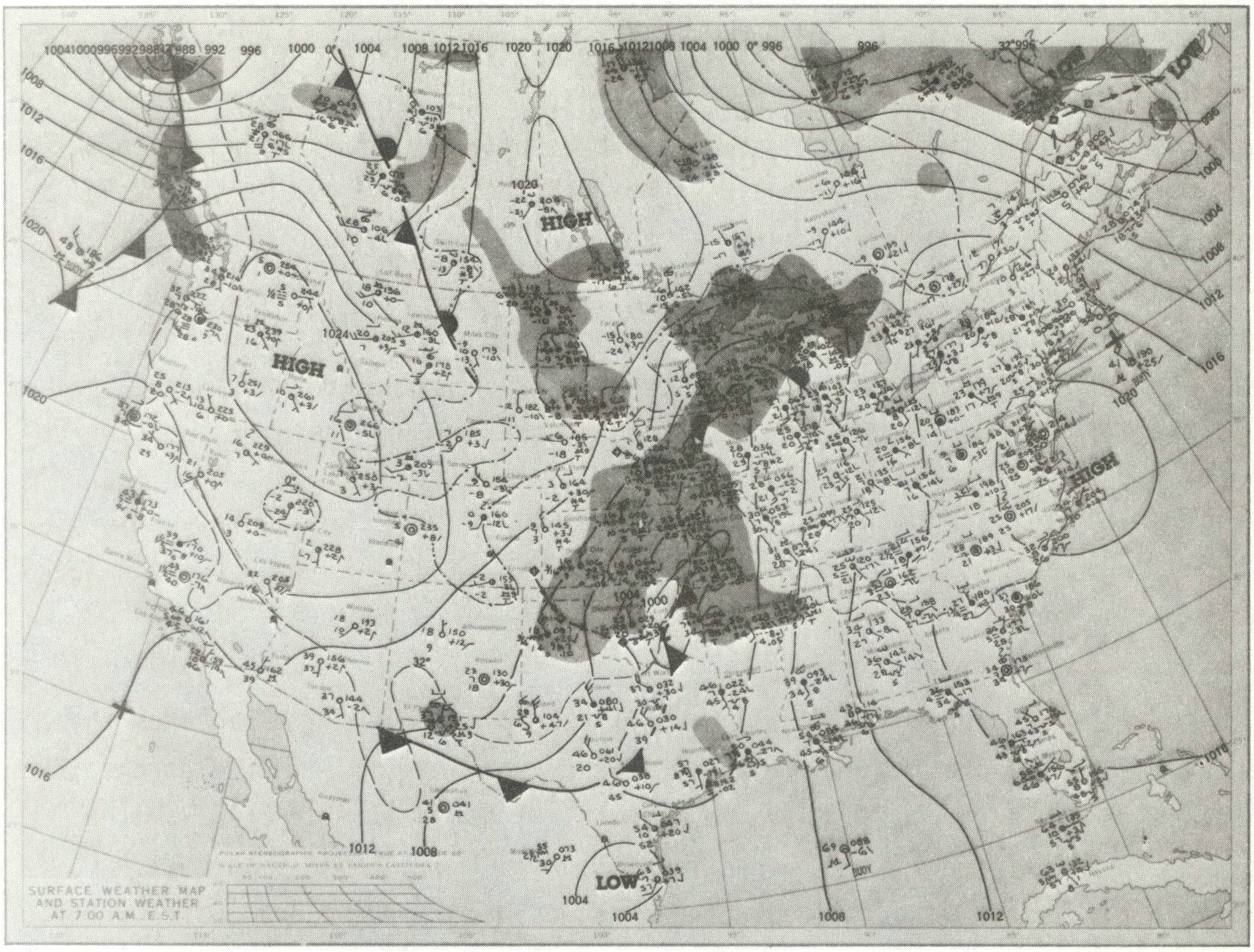

Figure 19-6. Surface weather map for January 23, 1979.

The surface weather maps for February 24 and 25 (NOAA Daily Weather Maps, Weekly Series, February 19-25, 1979) show a polar front, preceded by a squall line, that had swept over the Louisiana shelf. This front was followed by west-northwesterly winds offshore.

19.2. Oceanographic Observations

Currents measured 1 m above the bottom at station 11 from January 10 to 15, 1979, are shown in figure 19-7; this record includes the extratropical cyclone. Currents 1 m above the bottom, maximum wave heights (determined by the zero-crossing method), and significant wave heights (determined by the spectral method) for the period from January 19 to 27, 1979, are shown in figure 19-8. Water levels at station 11 are shown in figure 19-9 for the period from January 10 to March 11, 1979. The predicted series, using results of a 29-day harmonic analysis, was subtracted from the observed series to obtain the residual series. The depression, or set-down, of the sea surface corresponding to the extratropical cyclone and subsequent polar frontal passages can be seen. The rise in air pressure on January 14 was accompanied by strong northerly winds which produced the lower than normal low water and the higher current speeds by midday.

The high winds associated with the extratropical cyclone began from the south, gradually rotating clockwise until they were coming from the north. The response of the currents began on January 12, with a gradual decline in the current speed (figure 19-7). Directional changes began about 1500 GMT on January 12. The current rotated north-northwestward and, by 2300 GMT, current speeds were less than 5 cm/s and east-northeastward. The current direction continued to be variable until 1600 GMT January 15, when the current resumed its predominately westward flow.

Figures 19-10 and 19-11 illustrate the spatial effects on currents of a polar front passing the West Hackberry site on February 24. Prior to the frontal passage, the currents had been persistently westward for at least 3 days. Clockwise rotation of the currents was in response to the changing direction of wind stress. The maximum current speed observed was 60 cm/s at 1300 GMT on February 25 at 3 m above the bottom.

Wind speeds were greater and directions were more persistent during the northers of January 20 to 26 than during the earlier cyclone. The effect of the increased wind speed and directional persistence can be seen in the time series plot of currents 1 m above the bottom (figure 19-8). Strong westerly winds

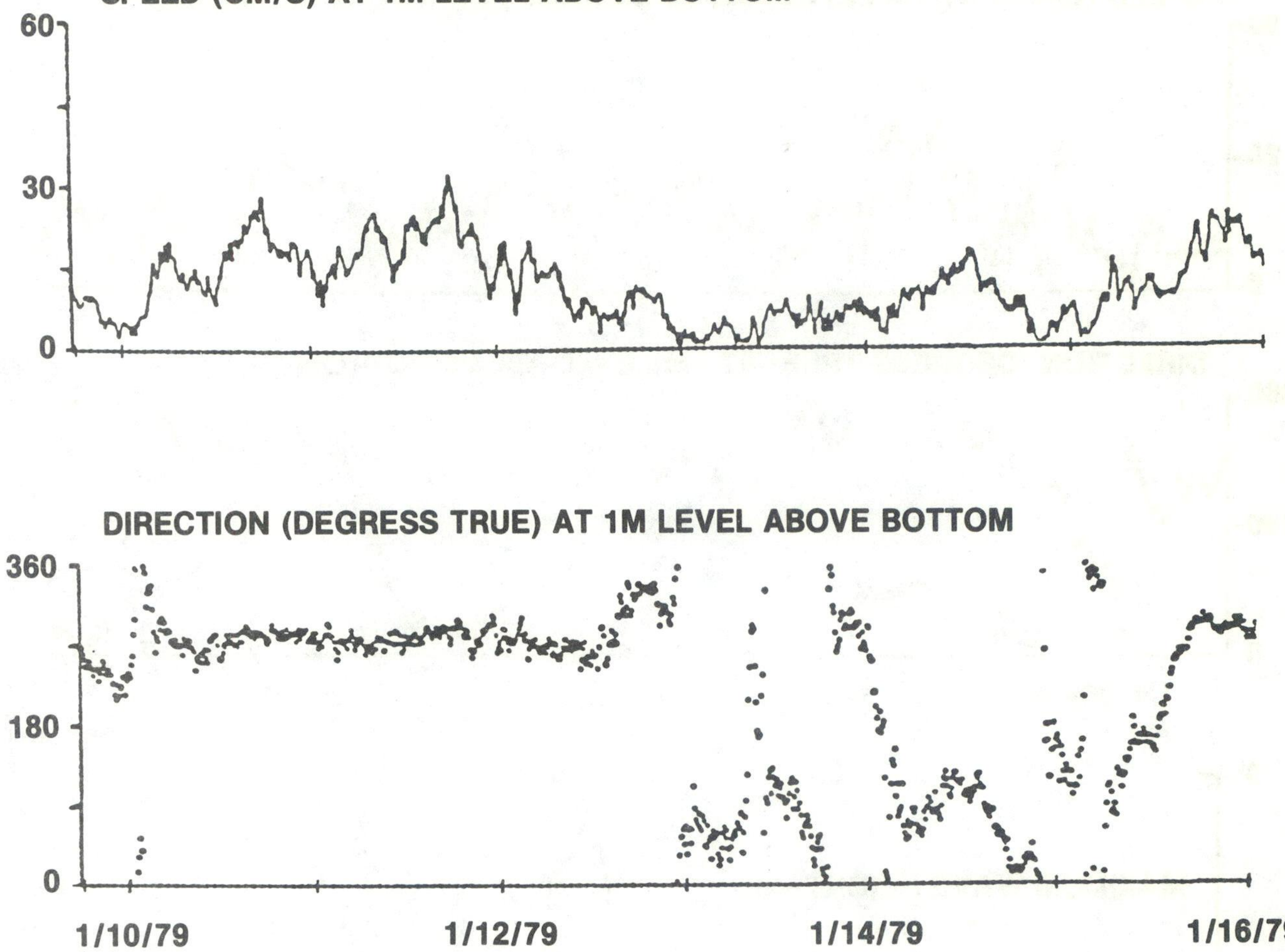

Figure 19-7. Currents 1 m above bottom at West Hackberry station 11, January 10-15, 1979.

caused reversals in the direction of current flow from westward to eastward. The highest current speeds of the month were also observed during this storm period. The highest average speed, 17 cm/s, was eastward. The highest current speed observed was 43 cm/s towards 100° True at 0810 GMT on January 21, in response to west-northwesterly winds; the second highest current speed was 38 cm/s at 0840 GMT January 24 with a direction of 83° True, also in response to west-northwesterly winds. Persistent westward currents during January 23 and 26 can be seen in figure 19-8; the westward flow was in response to the generally east-southeasterly winds that accompanied the approaching fronts.

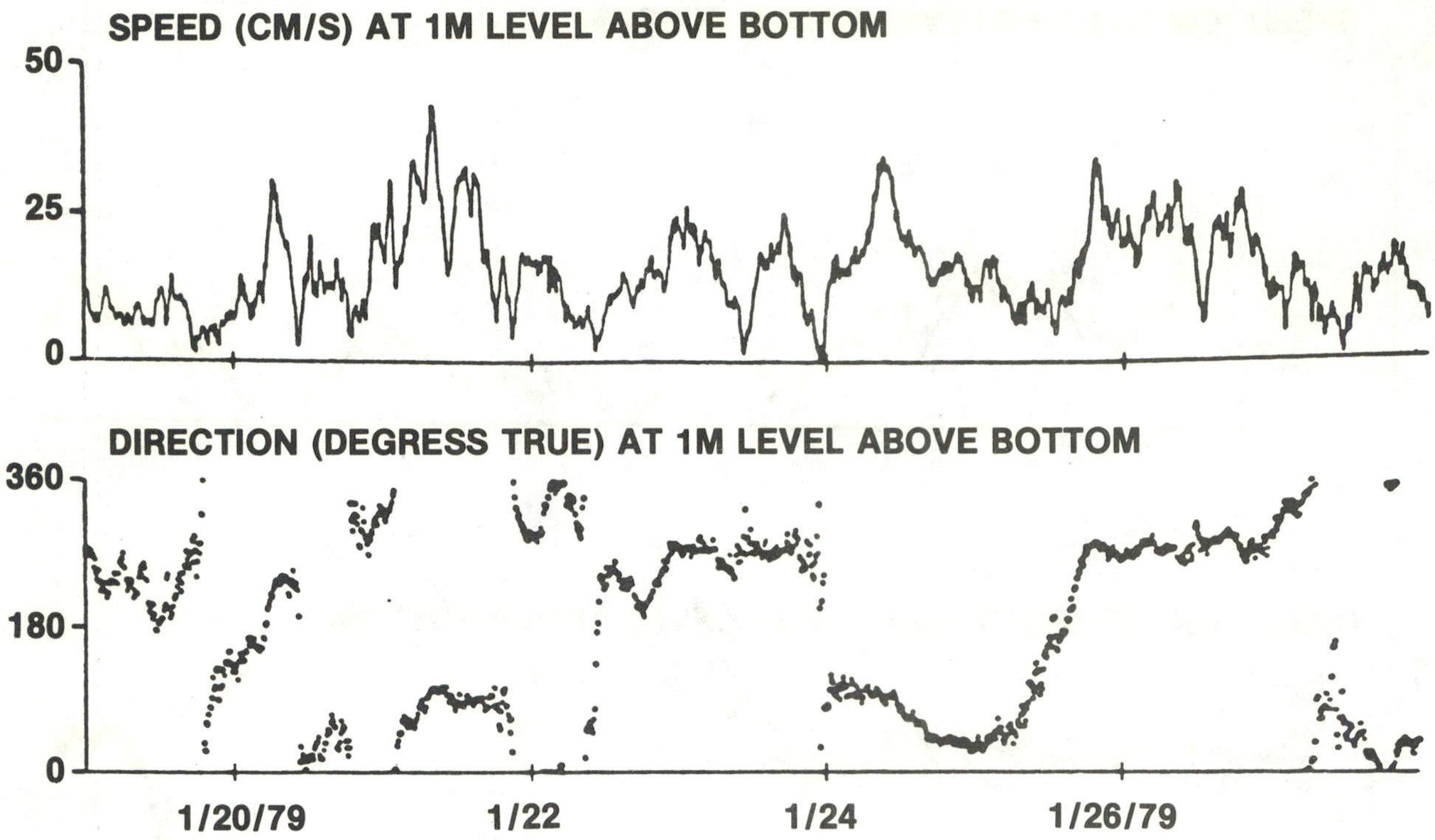

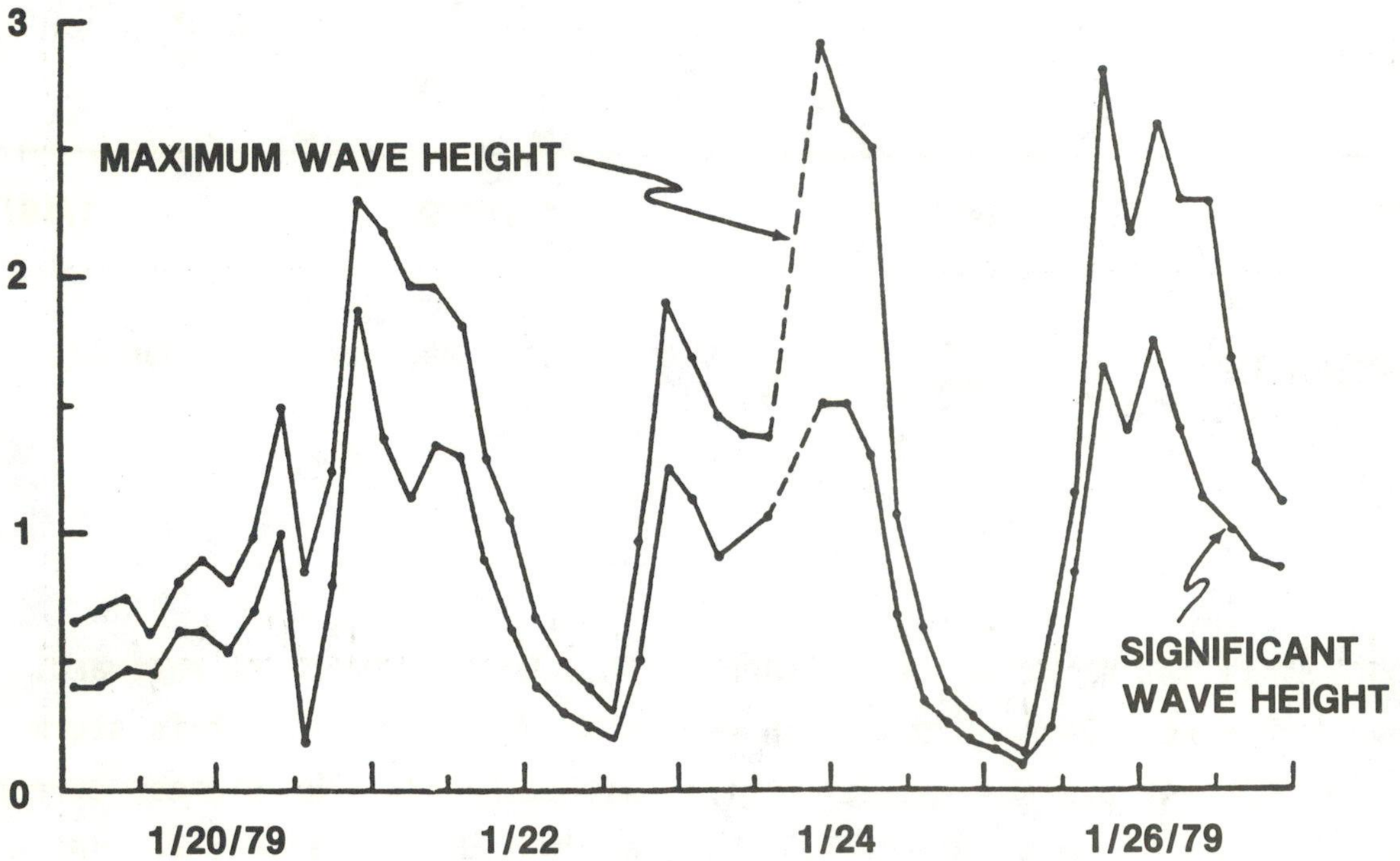

Figure 19-8. Currents 1 m above bottom and waves at West Hackberry station 11, January 19-27, 1979.

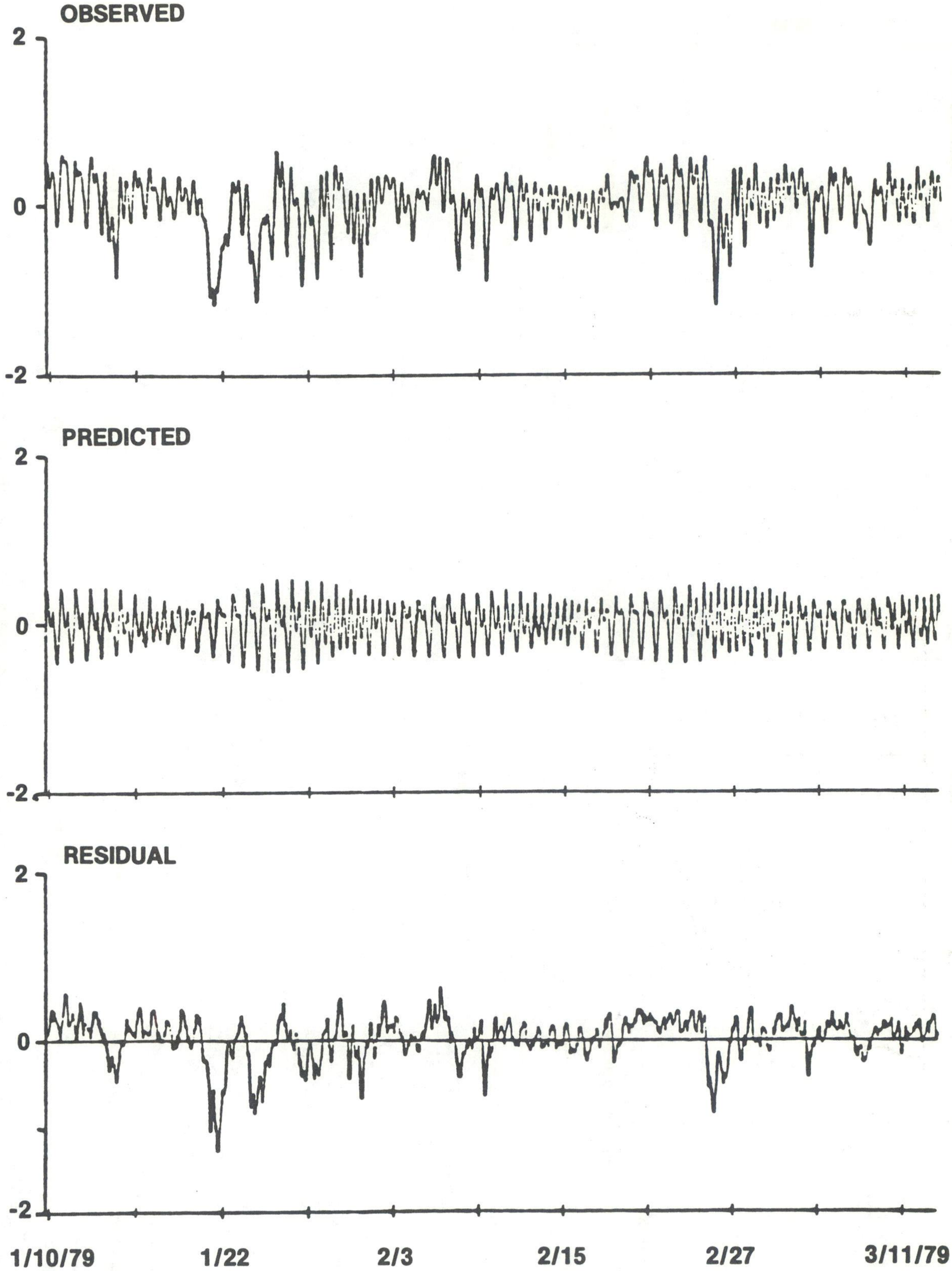

Figure 19-9. Water levels at West Hackberry station 11, January 10 to March 11, 1979.

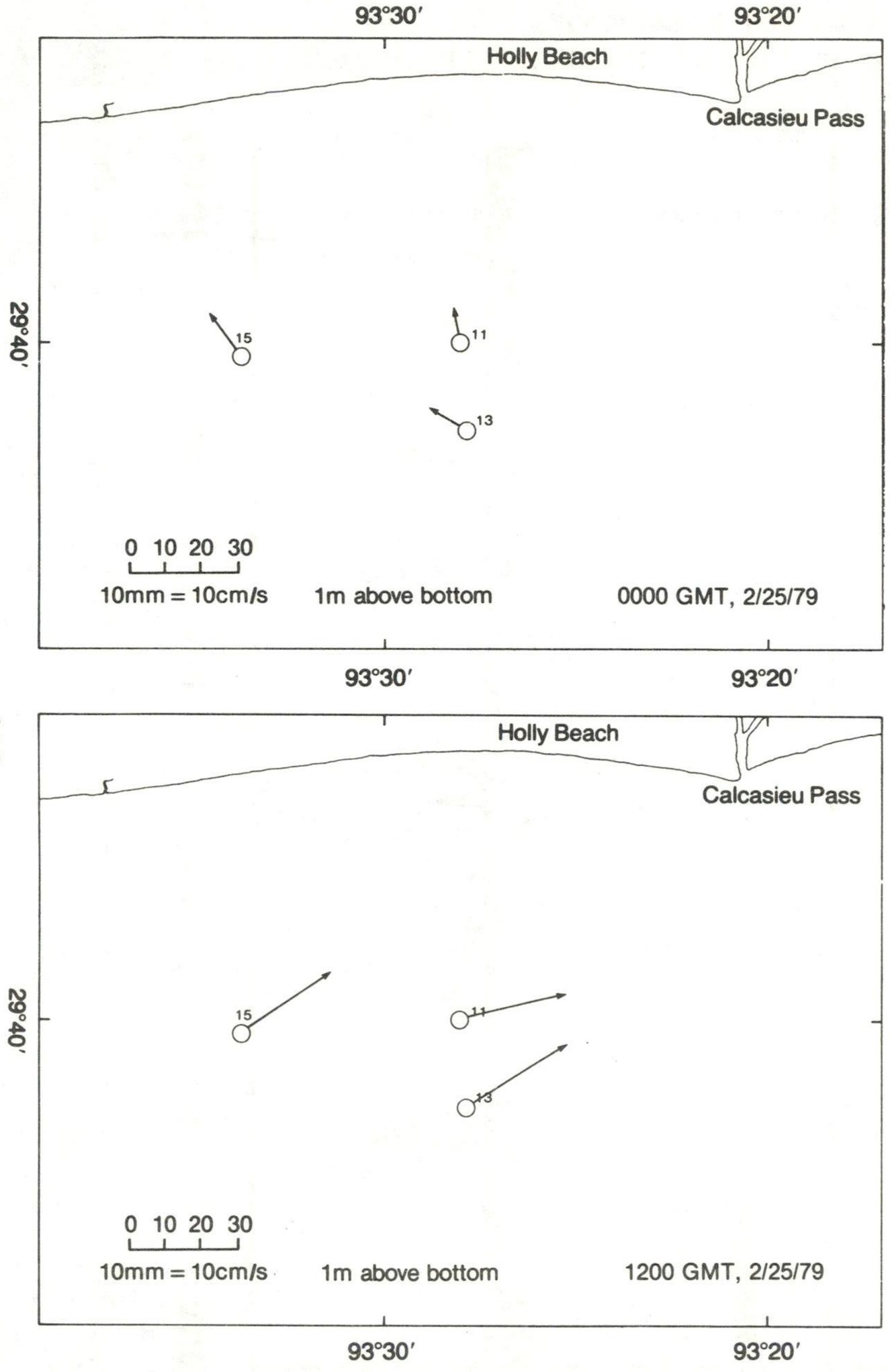

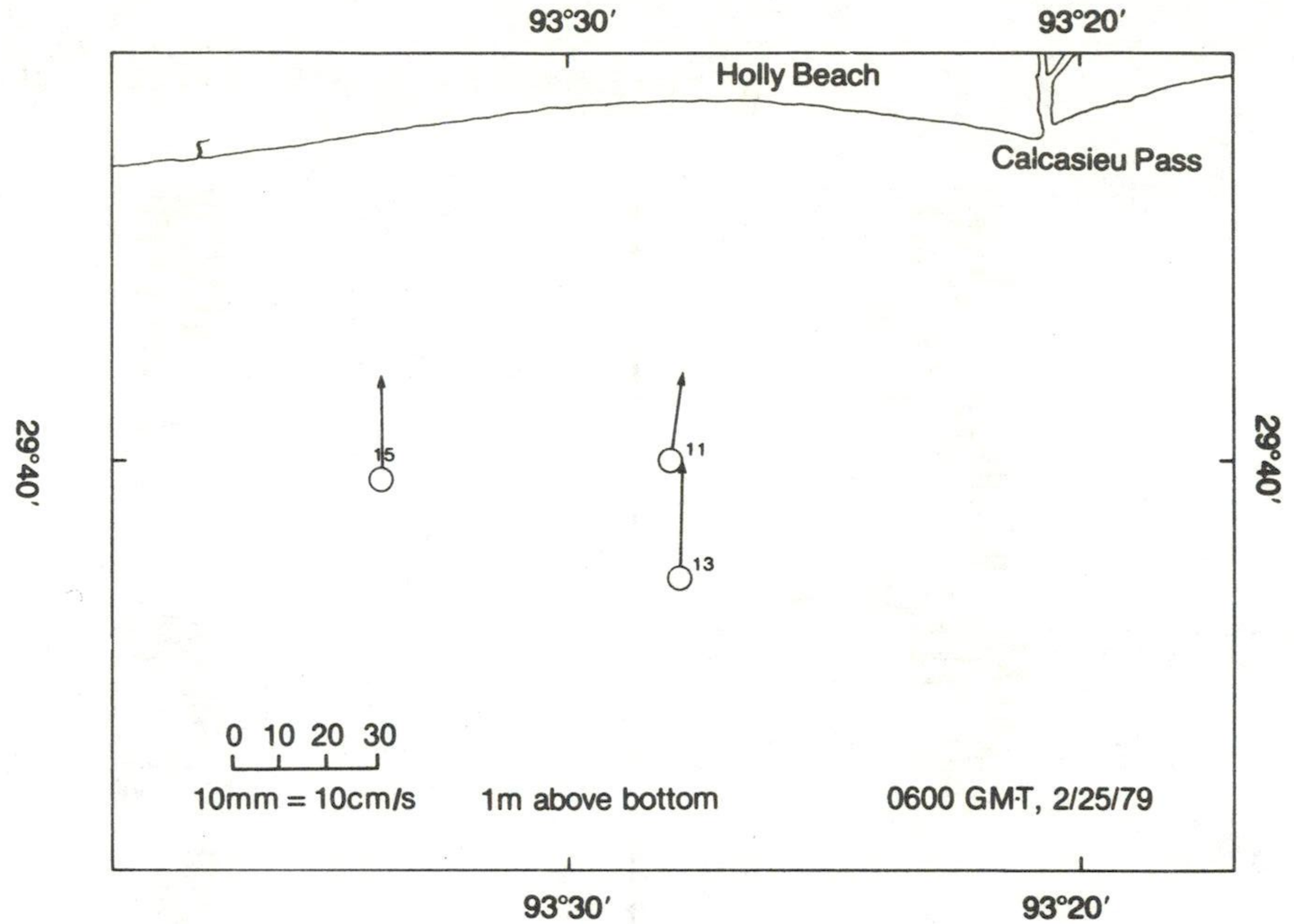

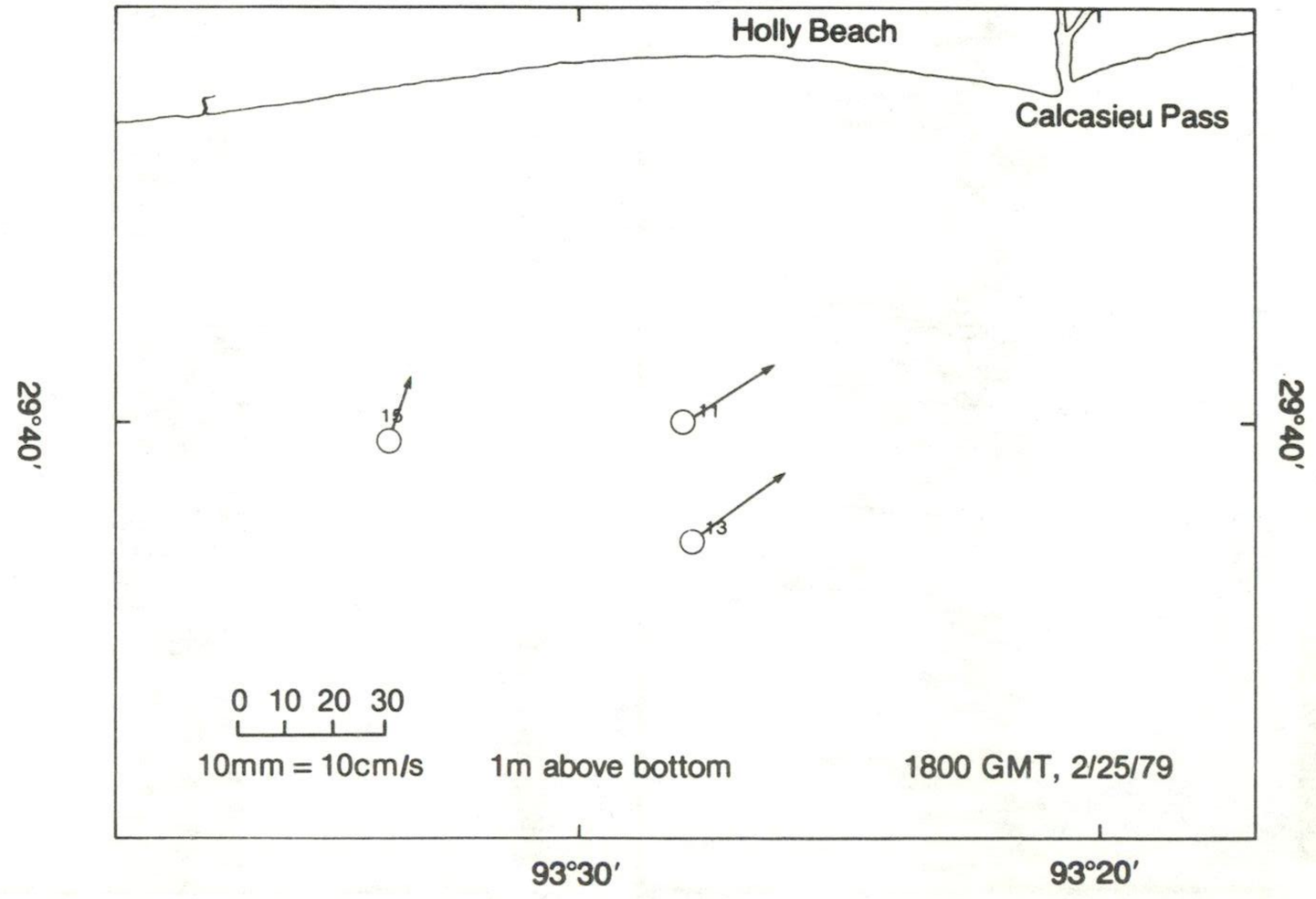

Figure 19-10. Current vectors at 6-hour intervals, 1 m above bottom at West Hackberry site, February 25, 1979.

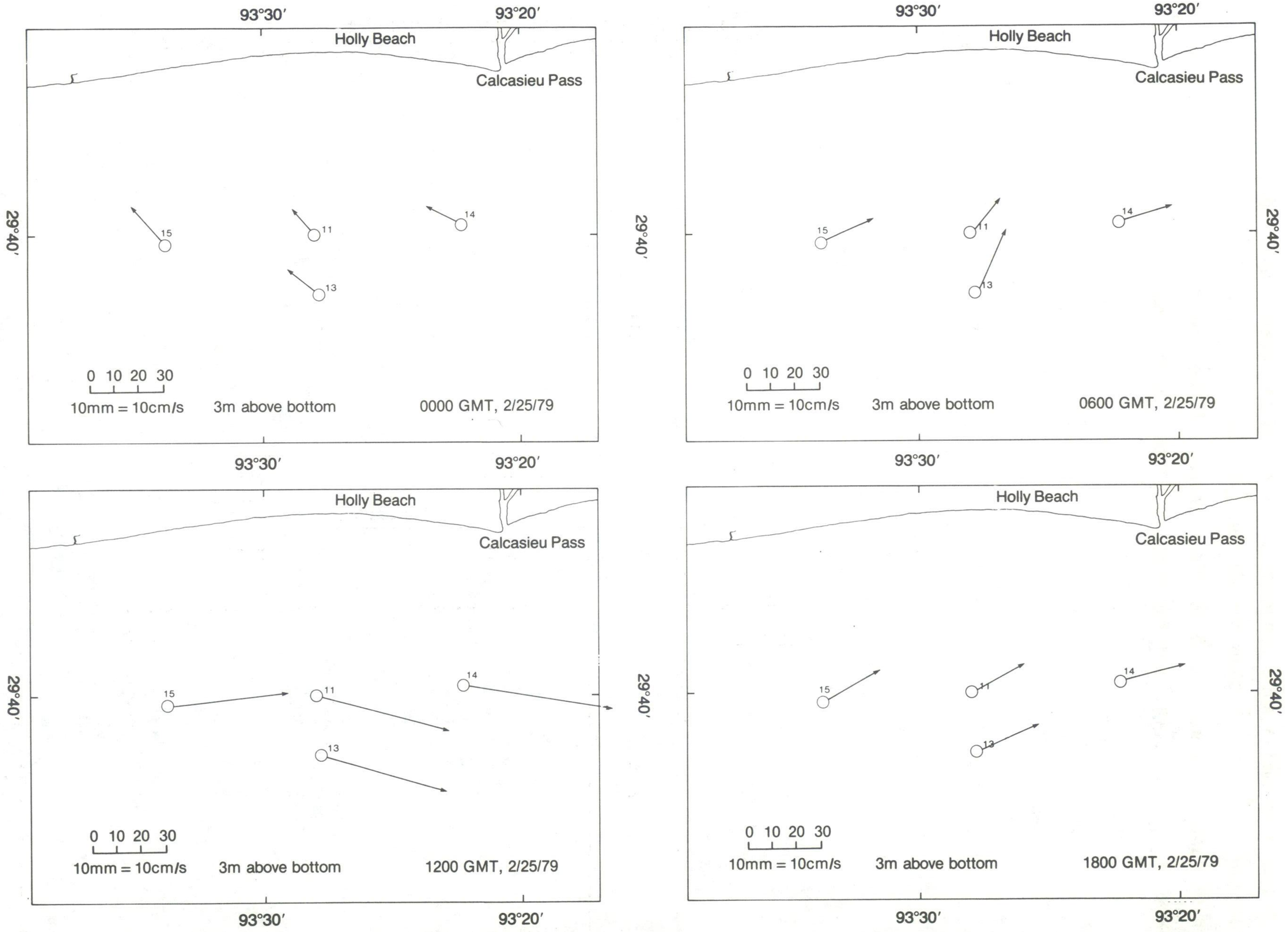

Figure 19-11. Current vectors at 6-hour intervals, 3 m above bottom at West Hackberry site, February 25, 1979.

Winds also had a more pronounced effect on the water level during the period January 20 to 26 than during the cyclone of January 13. The lowest low water of January 14 was -0.86 m. For January 21 the lowest low was -1.17 m, for January 24 it was -1.14, and for January 27 the lowest low was -0.95.

20. SPRING STORM

The Gulf At-Sea Performance (GASP) Experiment was conducted at the West Hackberry site for 32 days beginning April 5, 1979. The physical oceanographic results of the experiment, especially measurements obtained during a spring storm, are described in this section; objectives and results related to data quality assurance are described in volume two of this report.

20.1. Measurement System

The GASP Experiment instrument configuration shown in figure 1-4 includes only the current meters whose data are discussed in this section. The array of instruments was deployed in a single straight line at station 11, parallel to the local isobaths along the principal axis of the flow. Grundy current meters were positioned at 1 m, 2 m, 3 m, and 4 m above the bottom to observe vertical shear of the horizontal current. Horizontal shear was monitored at the 3-m level with Neil Brown Instrument Systems (NBIS) vector-averaging acoustic current meters at each end of the array. Wave-induced current fluctuations were measured with an NBIS burst-sampling acoustic current meter at the 3-m level; an AMI wave gage was mounted on the platform supporting the burst-sampling current meter. The two NBIS vector averaging current meters (132 and 832) recorded data every 10 minutes. The burst-sampling current meter was set to sample at a 1-second rate for 1 minute each hour.

Quality control of GASP Experiment data made possible the estimation of measurement uncertainties for each current meter (table 20-1) and provided the basis for determining how closely measurements among instruments could be compared. The instruments were calibrated before deployment and after recovery from the GASP Experiment, except for the Grundy current meters that could not be withdrawn from the 12-month study to obtain individual calibrations. The measurement uncertainty of the Grundy current meters is based on the ensemble of

Table 20-1. Total Measurement Uncertainties for GASP Experiment current meters (at 16 cm/s)

Manufacturer	GASP number	Speed uncertainty (cm/s)	Direction uncertainty (degrees)
NBIS	132	-3.5, +3.1	-1.8, +7.3
NBIS	732	-4.1, +3.8	-2.0, +7.5
NBIS	832	-3.1, +2.8	-1.6, +7.1
Grundy	(A11)	-4.0, +1.8	-10.9, +10.9

36 instrument uncertainties developed in section 9, volume two, of the final report. The TMU's for the wave and water level gages and for the meteorological sensors are listed in table 3-1. The platforms used with the NBIS current meters had no structural members upstream and were designed to minimize data contamination.

The TMU's listed here indicate the 95-percent level of estimated uncertainty associated with each speed measurement and were calculated for a speed of 16 cm/s. Additional environmental uncertainties for the NBIS meters were negligible.

20.2. Observations

A wide range of meteorological and oceanographic conditions existed during the 32-day GASP Experiment period. Prefrontal southerly storm winds of 15 m/s drove 3-m level currents to over 80 cm/s; on the other hand, there were occasions when currents were within a few centimeters/second of zero. Before the GASP Experiment, the maximum observed current speed was 79 cm/s, observed during Tropical Storm DEBRA on August 28, 1979; thus, the full range of current speeds observed during the entire 12-month field effort was encountered during the GASP Experiment.

The weather system that dominated the Louisiana shelf from April 10 to 12, 1979, is shown in figures 20-1 to 20-3. The surface weather map for 1100 GMT on

April 10 (figure 20-1) shows a stalled front over the shelf with southeasterly winds (also see figure 20-5 for wind data at the West Hackberry disposal site). The system was influenced by a low pressure center situated over Wyoming, just east of the Rocky Mountains. The low migrated southward to New Mexico by 1100 GMT on April 11, while frontal activity consisted of a warm front moving north-northeastward away from the site and a cold front approaching from the west-northwest; surface winds were southeasterly at approximately 15 m/s at the West Hackberry site (figure 20-2), they were less than the wind speeds of Tropical Storm DEBRA, but with a much greater fetch. Weather over the Louisiana shelf on April 12 was dominated by a stalled front that was accompanied by continuing southeasterly winds (figure 20-3). The persistent southeasterly winds that blew over the site from midday (GMT) on April 10 to midday on April 12 produced a strong westward drift current, the strongest observed during our study.

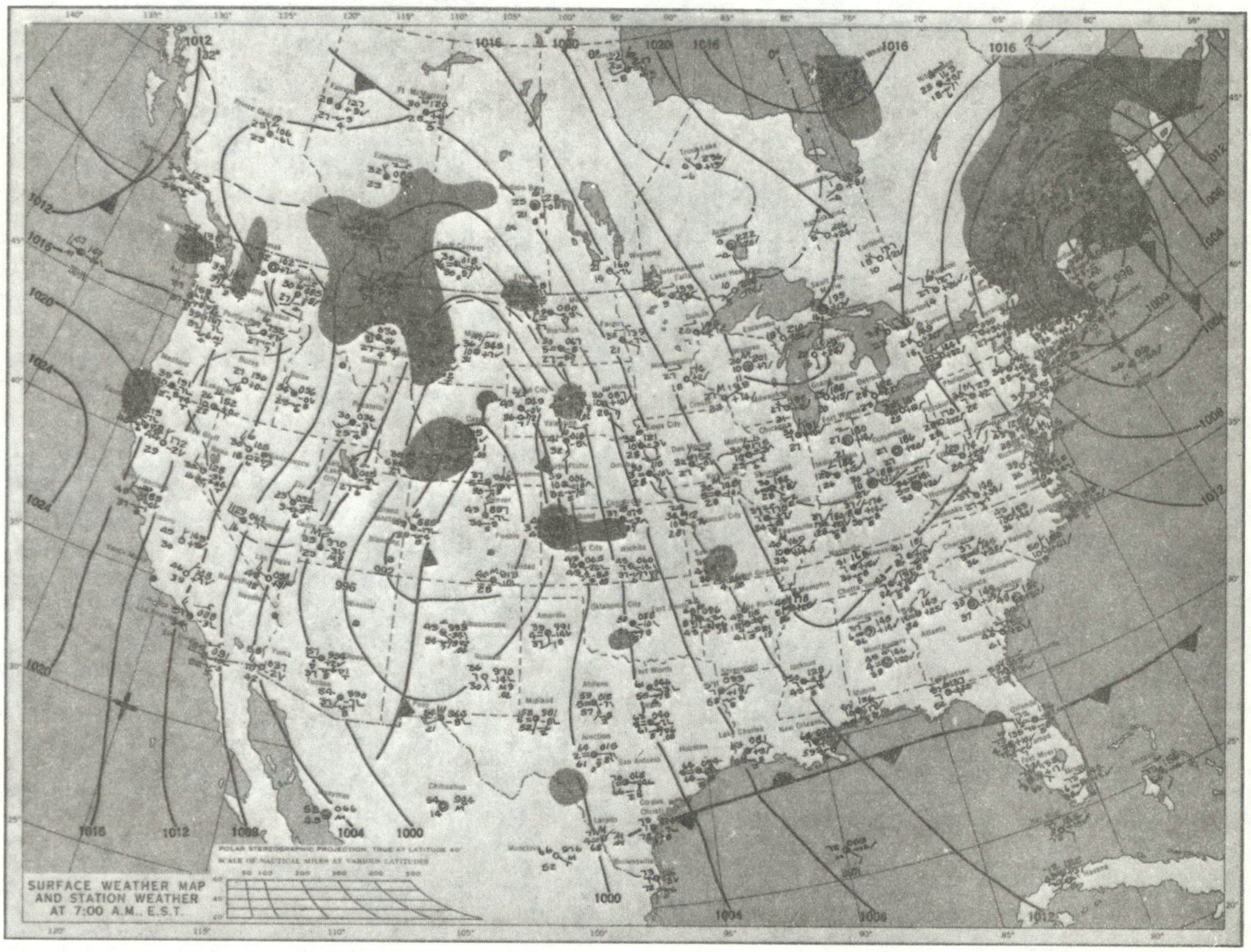

Figure 20-1. Surface weather map for April 10, 1979, at 1100 GMT.

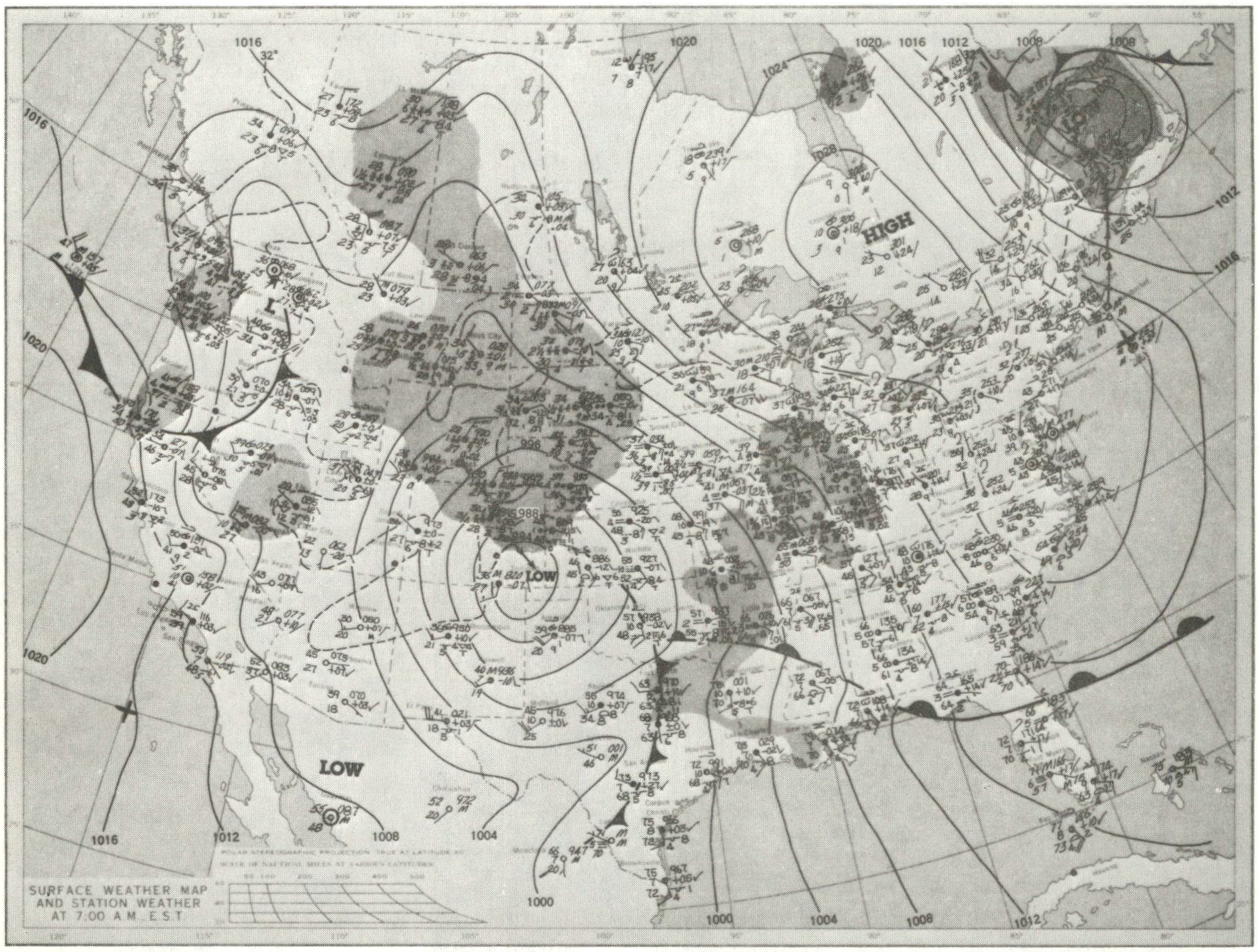

Figure 20-2. Surface weather map for April 11, 1979, at 1100 GMT.

Figure 20-4 shows the scatter diagrams from the 3-m level for the 1-hour vector-averaged speeds during the first 20 days of the experiment. Each frame shows the hour-by-hour comparison of the instrument pair. A 45-degree diagonal line representing perfect correlation has been added to each frame for reference. Note that the smallest scatter exists over the largest horizontal separation, suggesting that larger scatter is caused by instrument, depth, or sampling effects. Because the observed currents along the 3-m level were nearly

Figure 20-3. Surface weather map for April 12, 1979, at 1100 GMT.

identical across the array axis (figure 20-4), the distance between the NBIS current meters (132 and 832) was apparently less than the scale of any oceanographic event. The NBIS current meters were separated by approximately 90 m; therefore, an upper bound for the combined ocean and instrument mean horizontal shear is approximately 8×10^{-5} s^{-1}. The vertical shear of the horizontal currents, computed from 20 days of vector-averaged data, is approximately 5×10^{-2} s^{-1}, or about 10^3 times larger than the horizontal shear. Thus, separation in the vertical of 10 cm was as important as 100 m of horizontal separation. One prominent feature in this presentation is the relatively low bias at all speeds for the Grundy (431) instrument; possible mechanisms include flow blockage by the platform rods, calibration uncertainties, instrument tilt, and cosine errors. The actual cause is not apparent from study of the field data, but the offset is contained in the TMU.

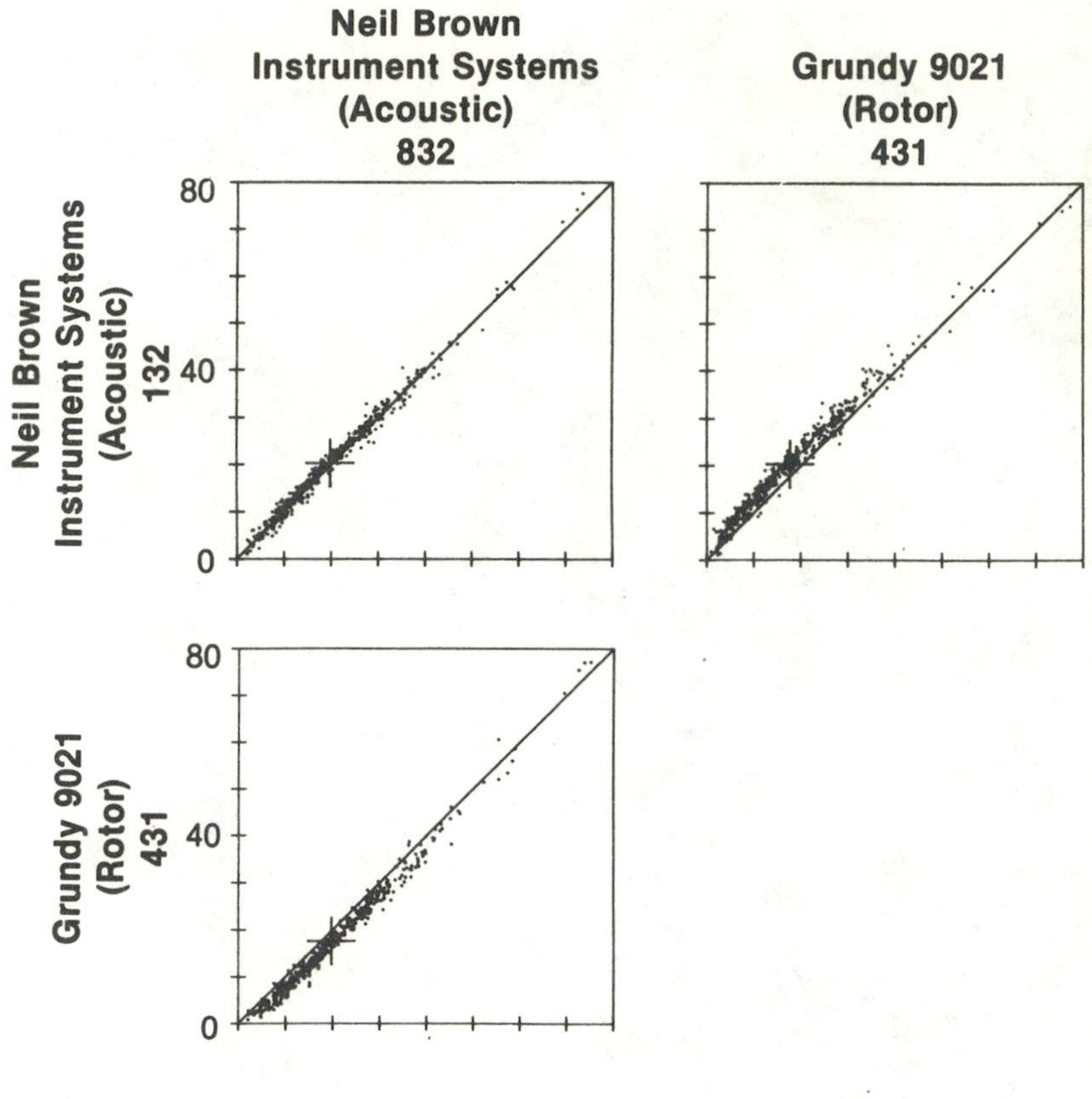

Figure 20-4. Scatter diagrams of 1-hour vector-averaged speeds for instrument pairs at the 3-m level during 20 days of the GASP Experiment.

Figure 20-5 shows wind speed and direction at 15.8 m above the sea surface, wave-induced speed fluctuations at the 3-m level, and maximum and significant surface wave heights. Figure 20-6 shows current speed and direction at the 3-m level and a storm occurring on April 11, 1979. The mean currents exhibited a westward drift during most of the 32-day experiment.

Figure 20-7 shows a typical 1-minute sample of 60 consecutive 1-second velocity measurements made each hour by the NBIS (732) acoustic meter. The scatter illustrates wave-induced flow; the large arrow is the mean for the burst. The flow signal-to-noise (S/N) ratio is defined here as the ratio of the mean flow to the standard deviation of the fluctuations in each 1-minute burst. When the S/N is high, the mean flow is large compared with the fluctuations; when the ratio is below about 1.4, the fluctuations exceed the mean, and the

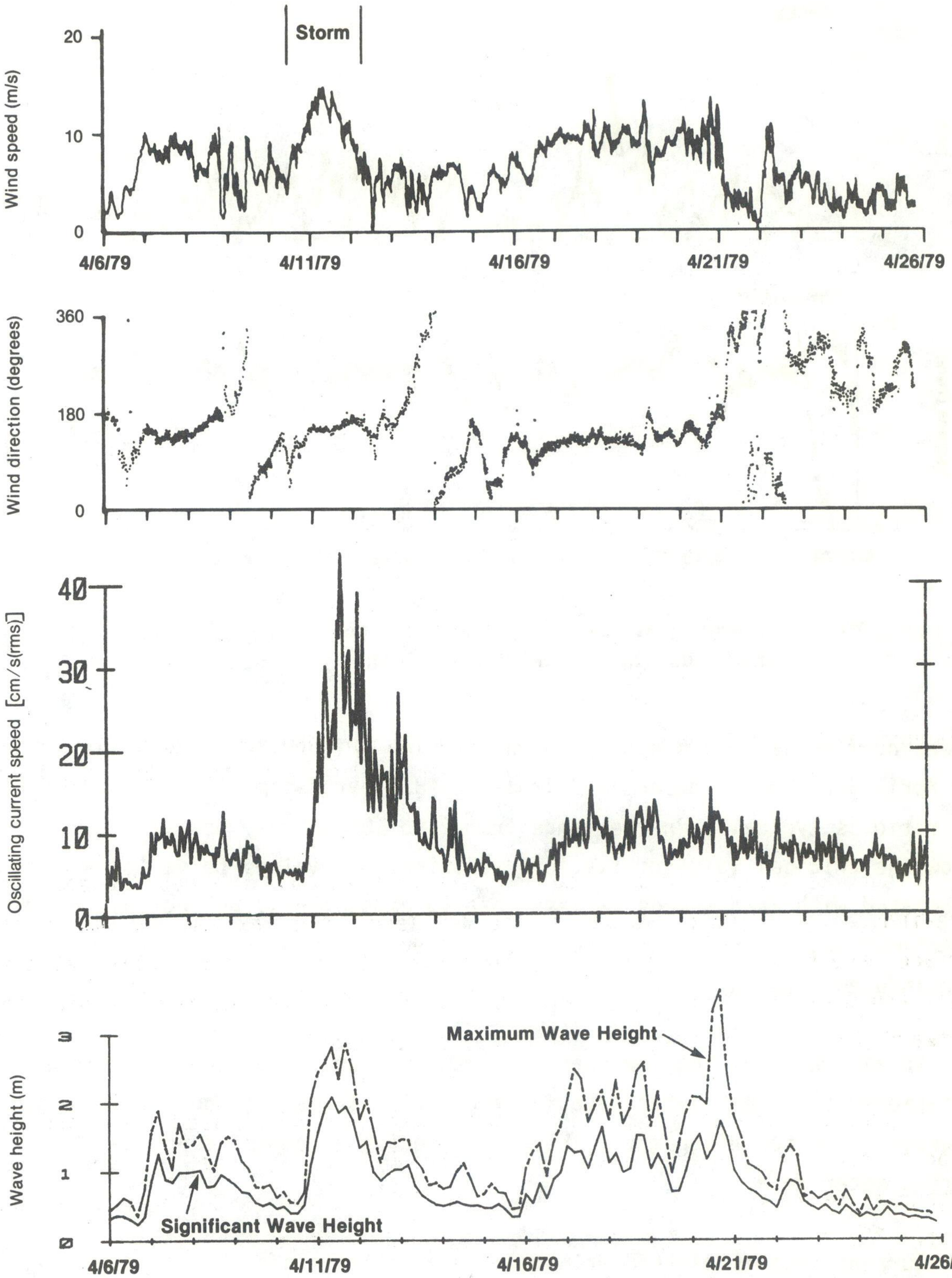

Figure 20-5. Wind speed and direction (+15.8 m), oscillating current speed (+3 m), and wave height during the first 20 days of the GASP Experiment.

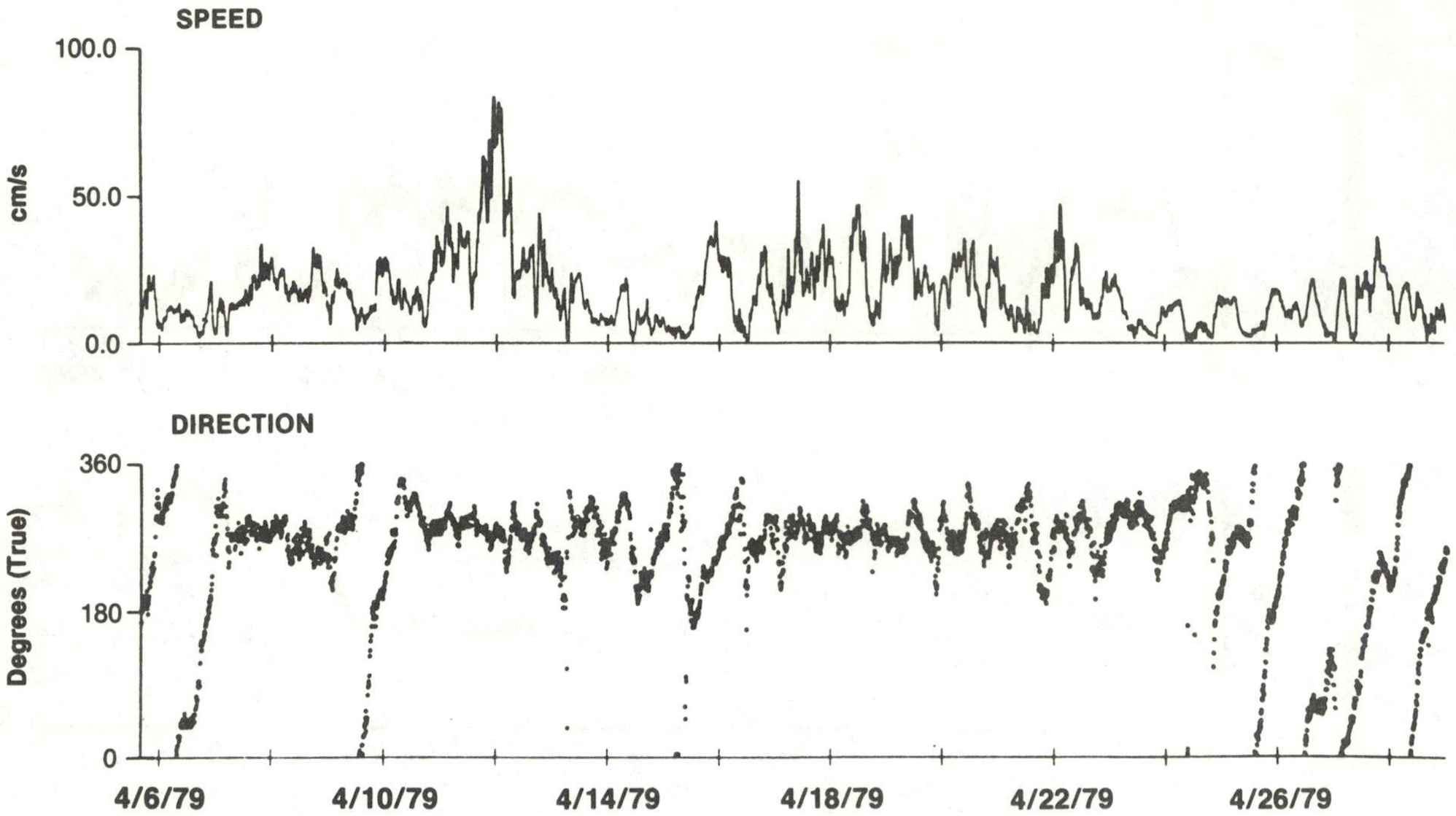

Figure 20-6. Currents measured at 3-m level with a Grundy Model 9021 current meter during the GASP Experiment.

reversing flow is possible in each wave cycle. Figure 20-8 shows the S/N values for April 6 to 26, as determined from the NBIS burst-sampling instrument (732). The ratio is typically in the range from 2 to 10 and only occasionally falls below the critical value of 1.4. In addition, all values below 1.4 are associated with mean speeds of less than 10 cm/s. Thus, during most of the experiment and during all of the energetic events, mean speeds exceeded the wave-induced fluctuations.

In figure 20-9, the low-frequency response and long-term directional variations of current meter data for the entire 32-day period are displayed as progressive vector diagrams. The plots provide a compact overview of all the current meter data.

Current vectors plotted at 6-hour intervals are shown in figures 20-10 to 20-15. The vectors were determined by vector averaging the data over 1-hour periods that were centered around the times shown in the figures. The plots include vectors at the 1-m, 3-m, and 4-m levels above the bottom.

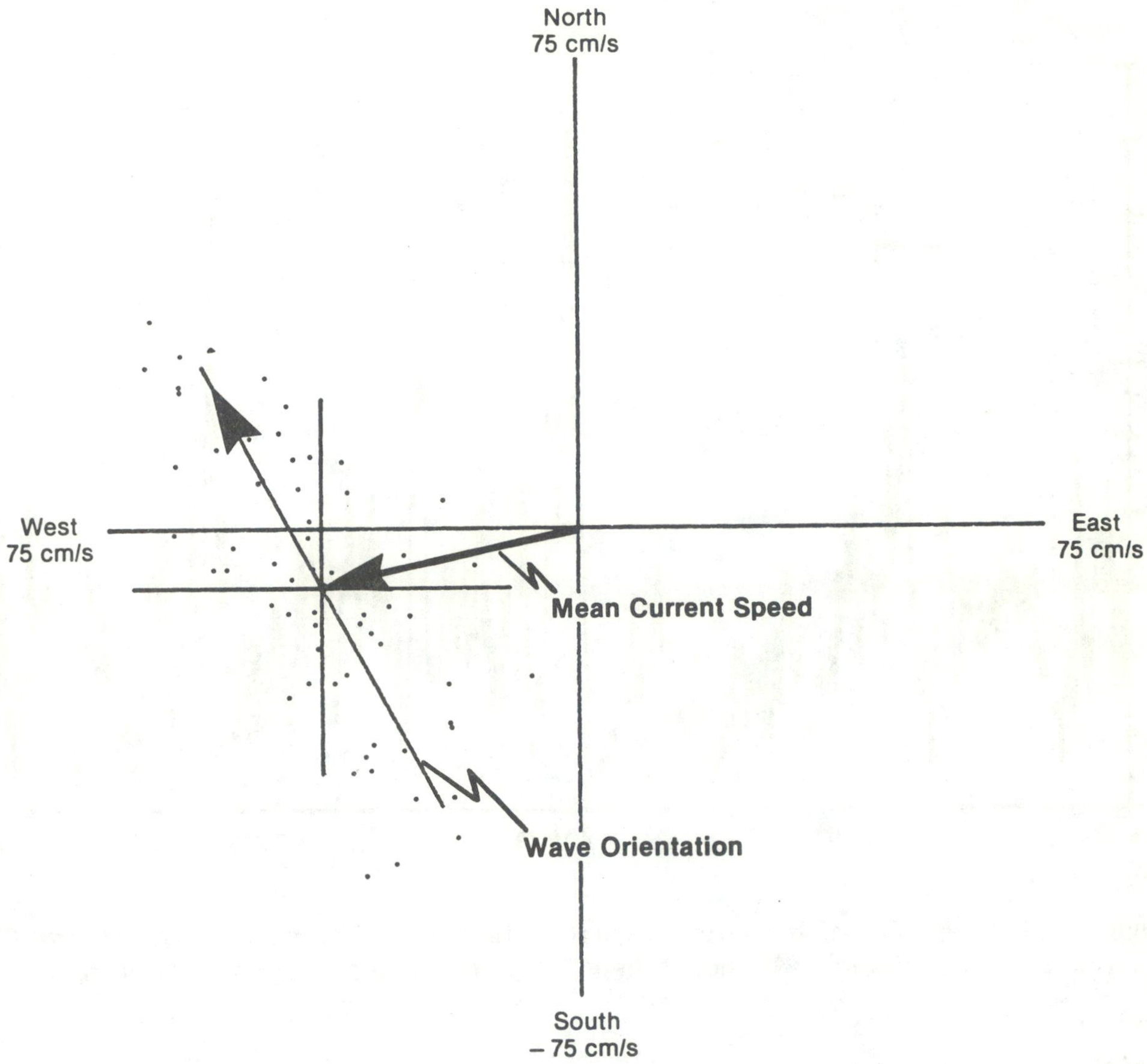

Figure 20-7. Sixty consecutive 1-second velocity samples illustrate typical 1-hour burst-mode data obtained with NBIS (732) instrument at 3-m level. Scatter points represent the heads of instantaneous vectors (April 11, 1979, 2000 GMT, S/N = 1.6).

The vector plots for April 11 indicate that the wind-induced coastal boundary current developed downward in the water column and from inshore to offshore, consistent with the theory of coastal boundary currents (Csanady, 1981). The vector plots for April 12 indicate a boundary current diminishing upward in the water column and from offshore to inshore as a result of diminishing winds (figure 20-5). By noon (GMT) on April 12, the near-bottom remained persistently westward; the frictional slowing of the currents had not affected the 4-m level yet.

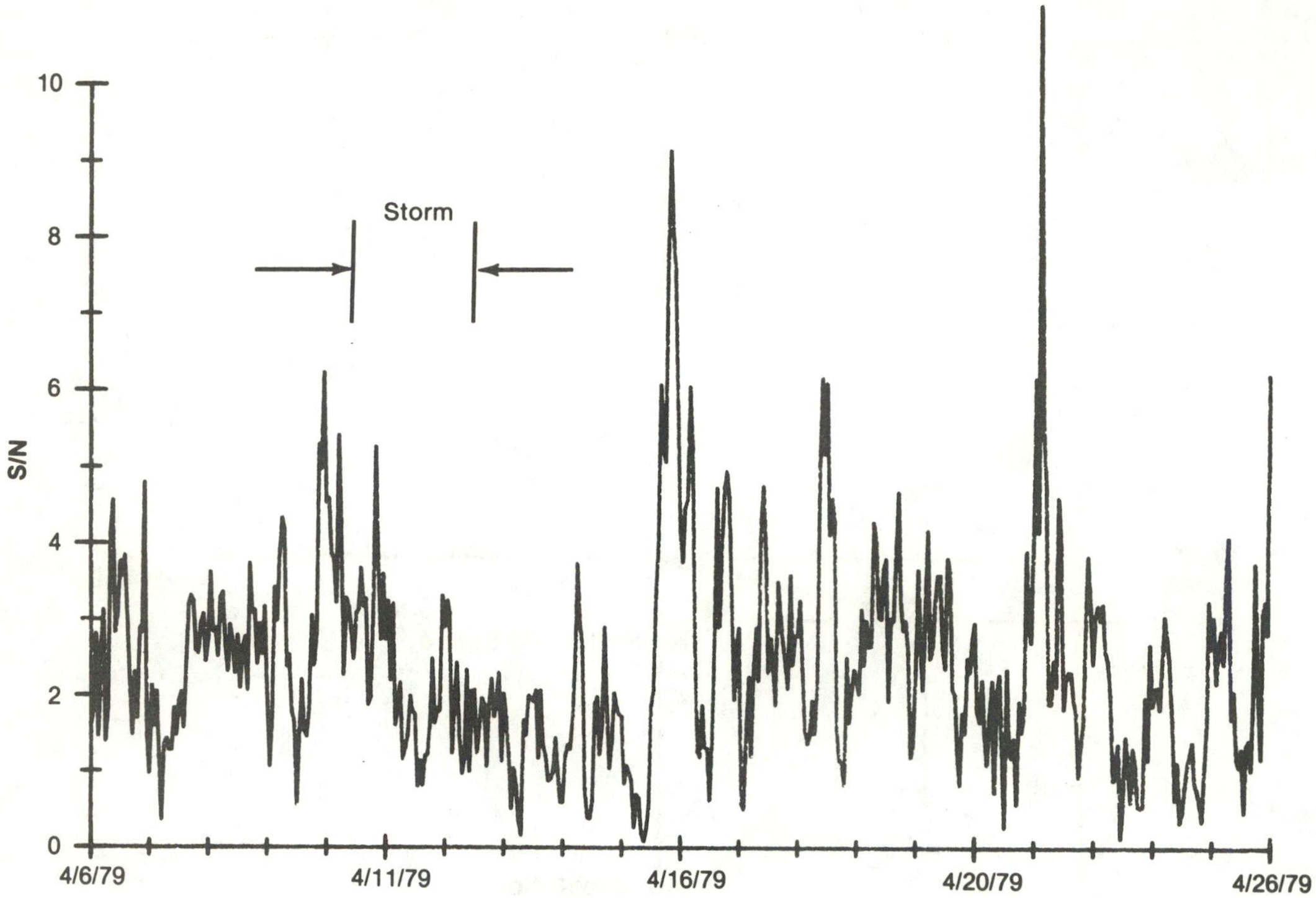

Figure 20-8. Flow signal-to-noise (S/N) ratio for the first 20 days of the GASP Experiment. Values shown for S/N < 1 occur at mean speeds < 10 cm/s.

The vertical shear of the alongshore and transhore components of currents at station 11 is shown in figure 20-16. The current profile was still developing at 1800 GMT on April 11 when winds began to subside. The profile shown for 0000 GMT on April 12 resembles that of fully developed turbulence with strong shear occurring in the bottom boundary layer. The vertical profile tends toward being linear later in the day as the storm-induced current subsides. Note the offshore components of currents at all measurement levels at 1800 GMT on April 11 and at 0000 GMT on April 12. The very significant offshore flow measured from 1-m to 4-m above the bottom suggests that a compensating onshore flow must have occurred in the upper layers; this would be consistent with stresses at the sea surface caused by southerly winds over the relatively shallow inner shelf.

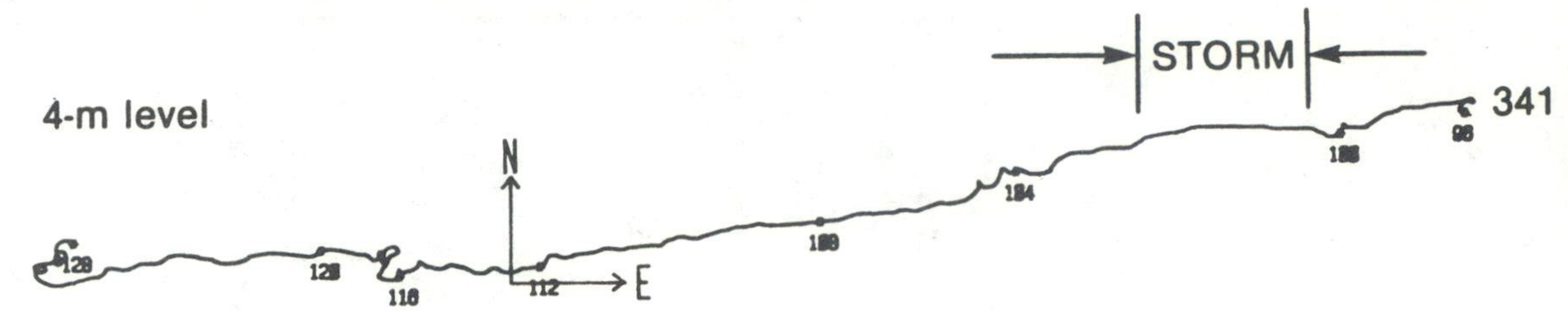

Figure 20-9. Progressive vector diagrams of currents during GASP Experiment.

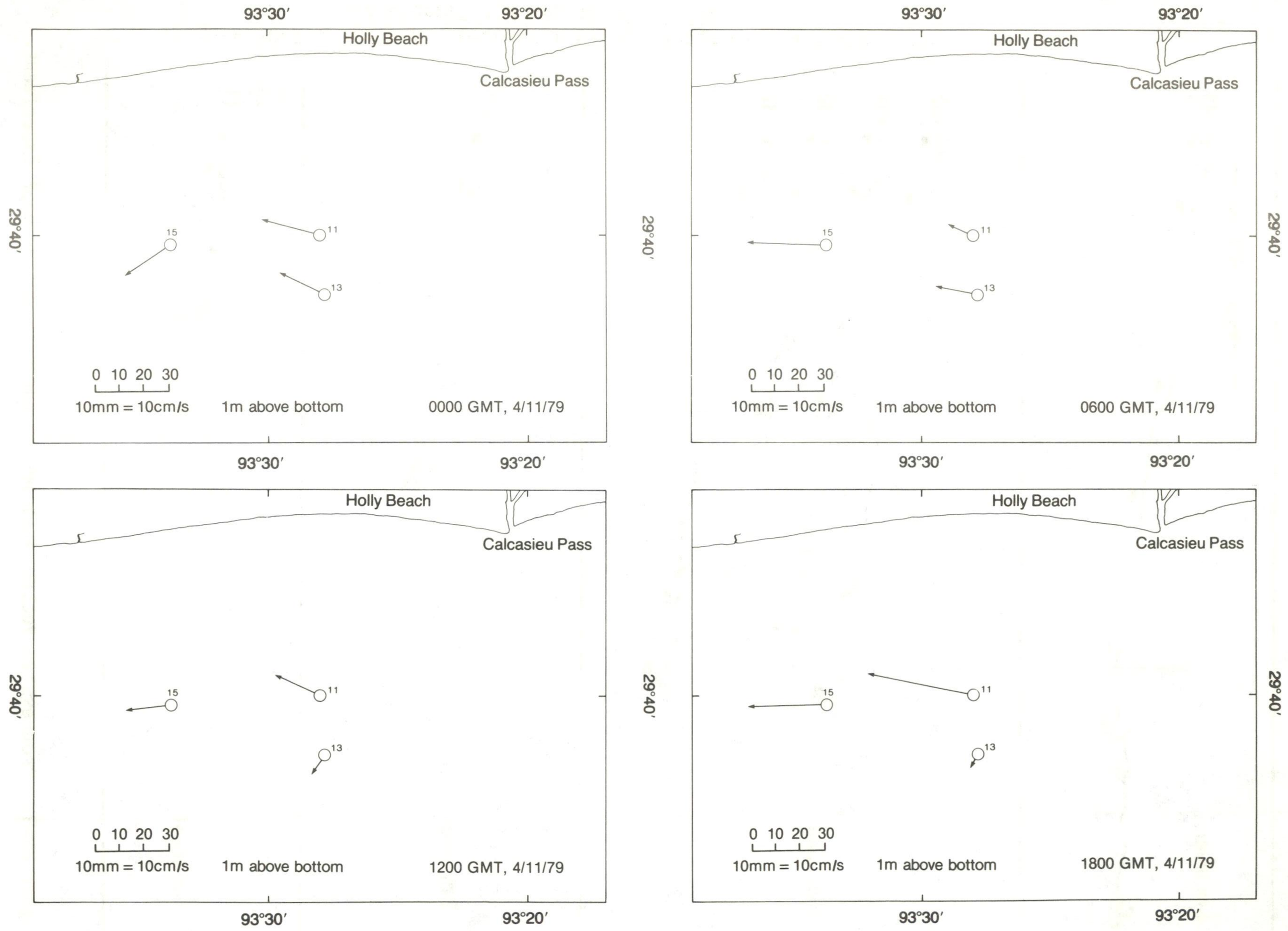

Figure 20-10. Current vectors at 6-hour intervals, 1 m above bottom at West Hackberry site, April 11, 1979.

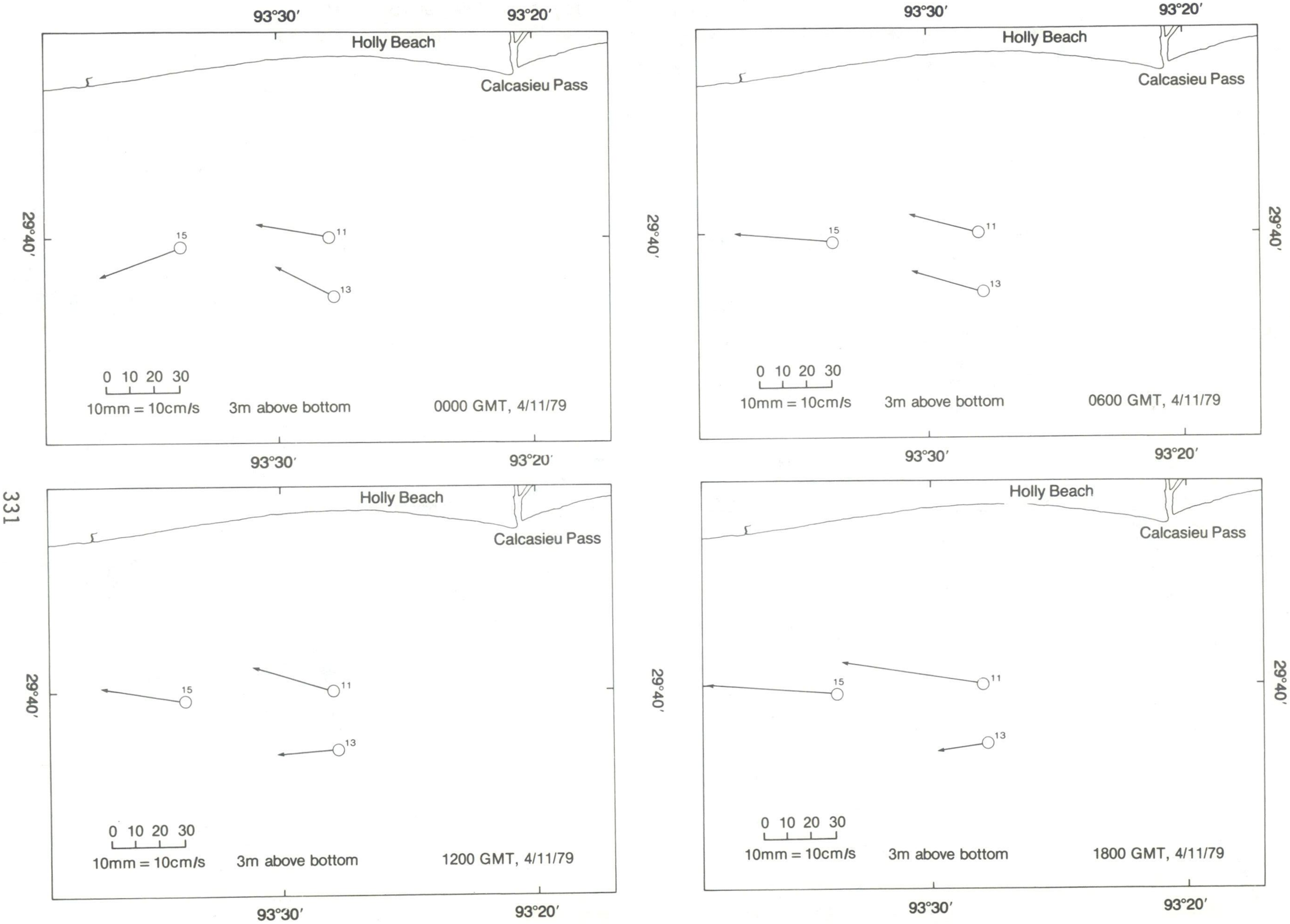

Figure 20-11. Current vectors at 6-hour intervals, 3 m above bottom at West Hackberry site, April 11, 1979.

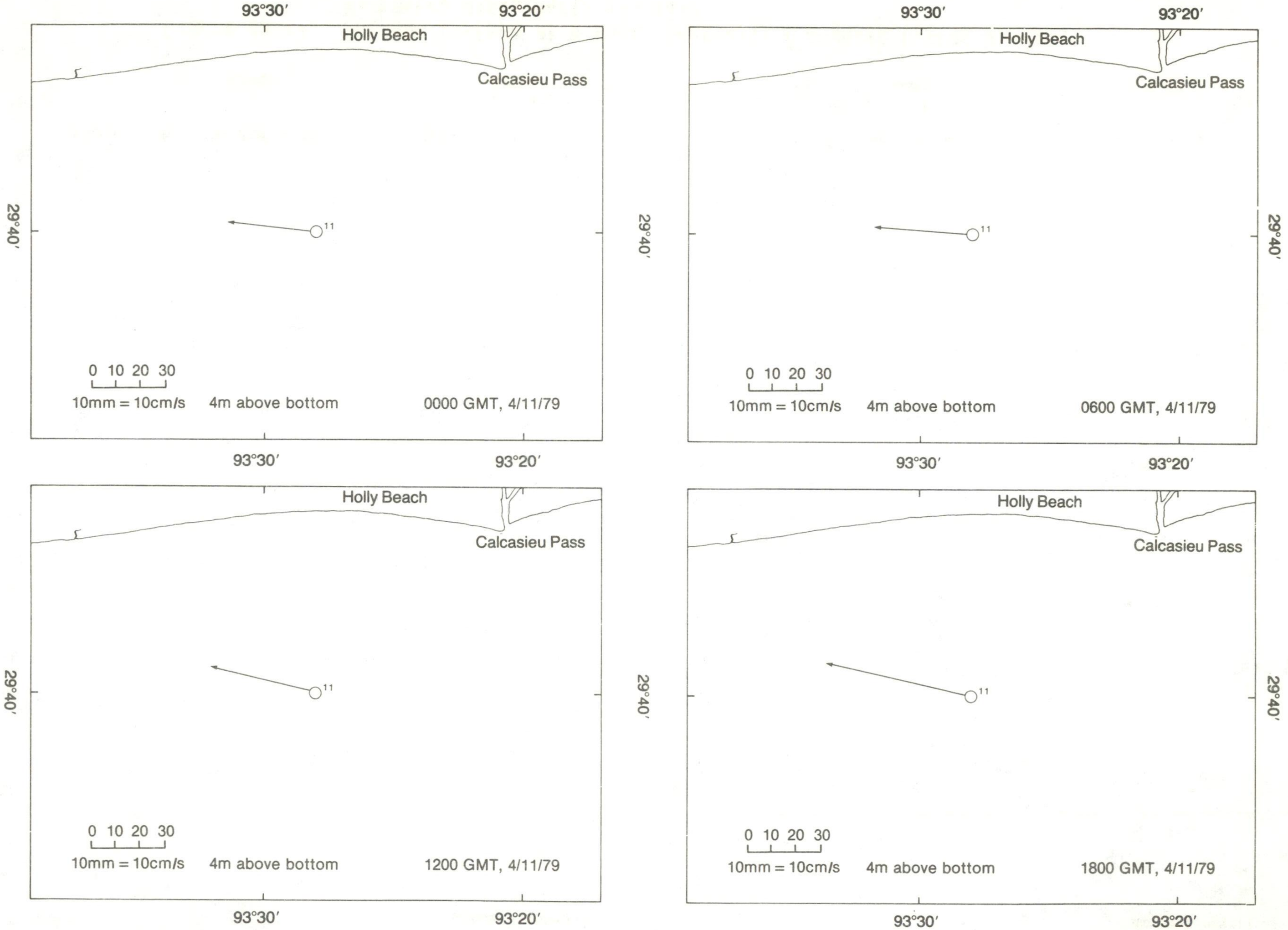

Figure 20-12. Current vectors at 6-hour intervals, 4 m above bottom at West Hackberry site, April 11, 1979.

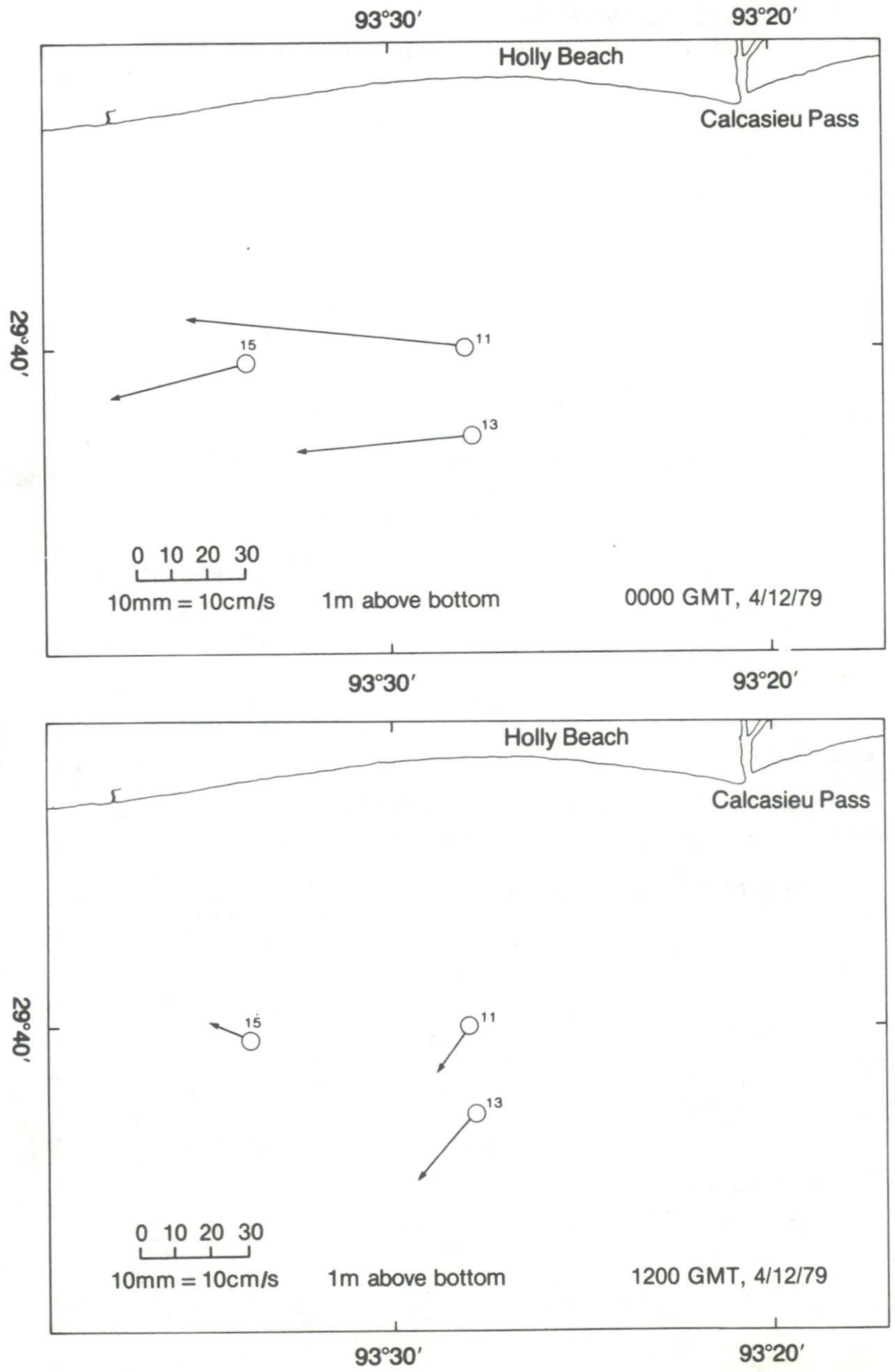

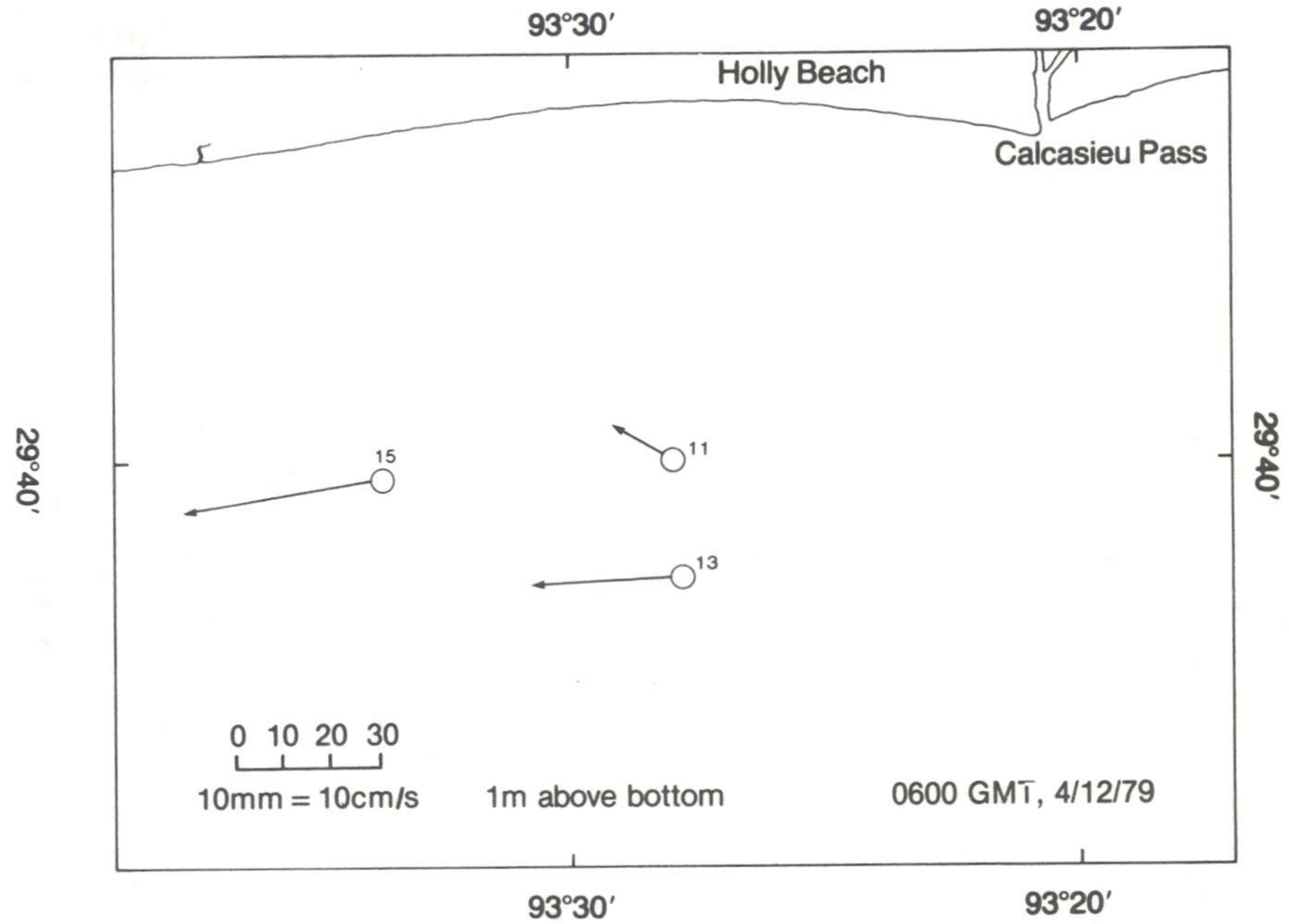

Figure 20-13. Current vectors at 6-hour intervals, 1 m above bottom at West Hackberry site, April 12, 1979.

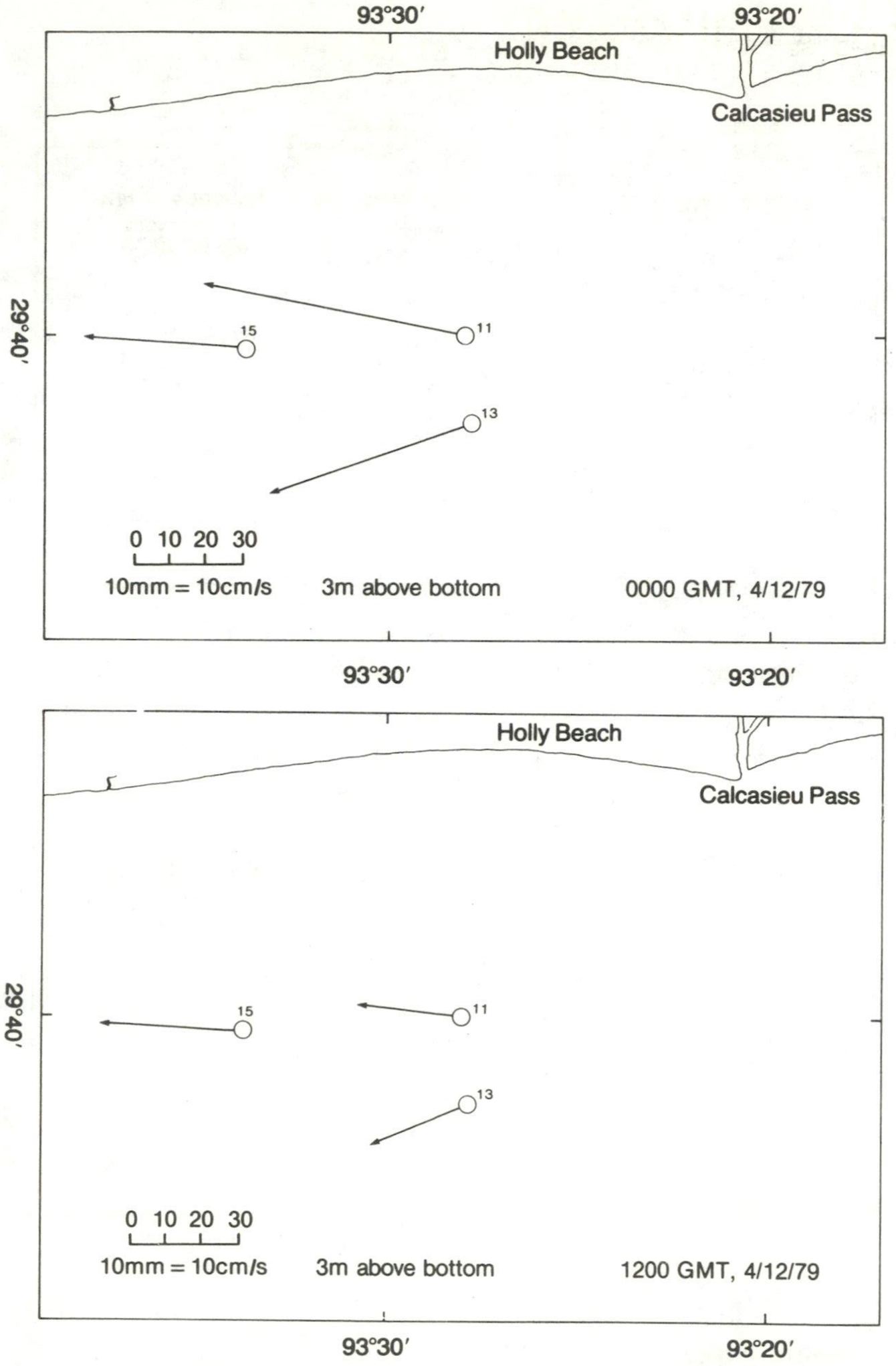

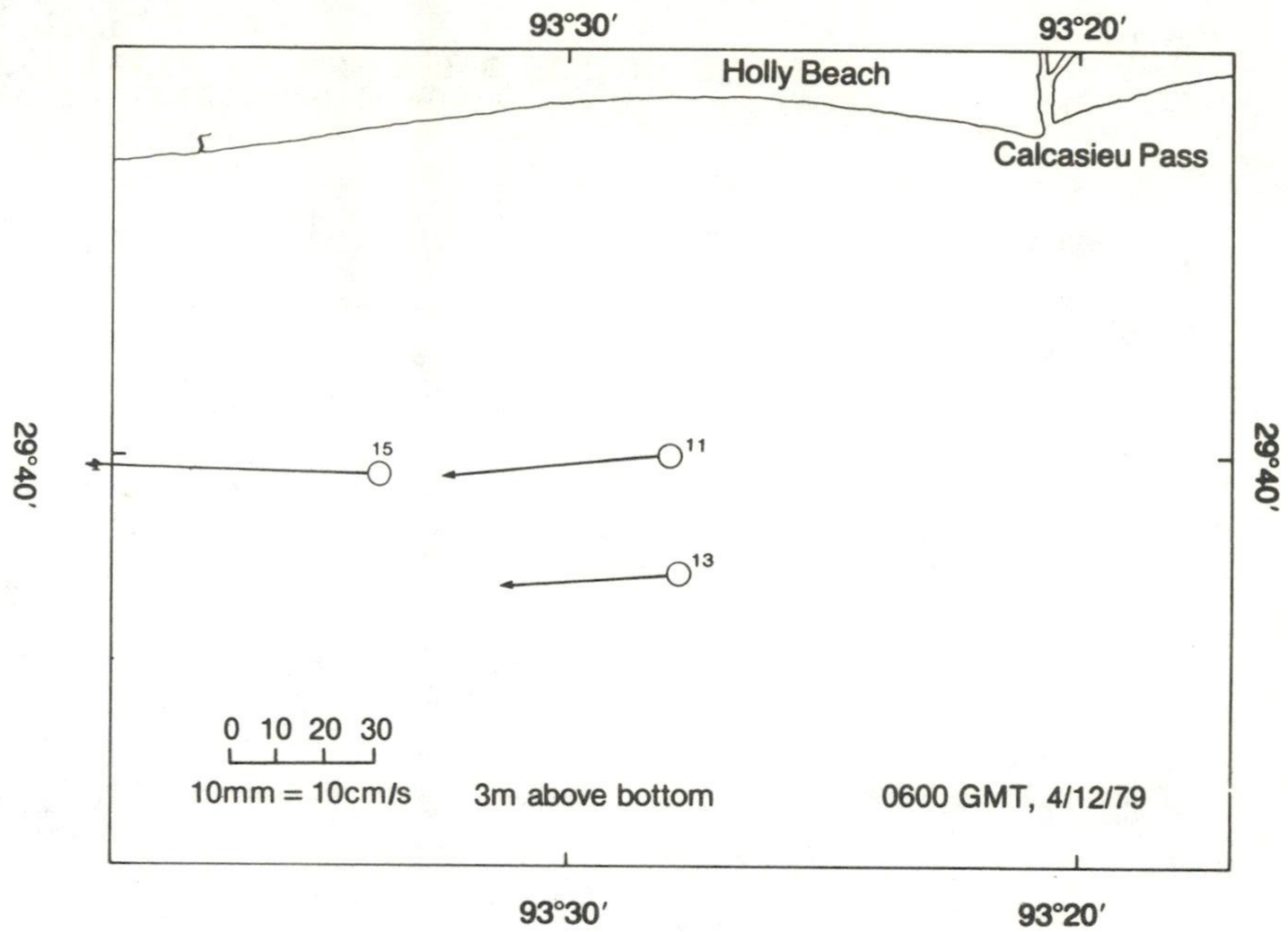

Figure 20-14. Current vectors at 6-hour intervals, 3 m above bottom at West Hackberry site, April 12, 1979.

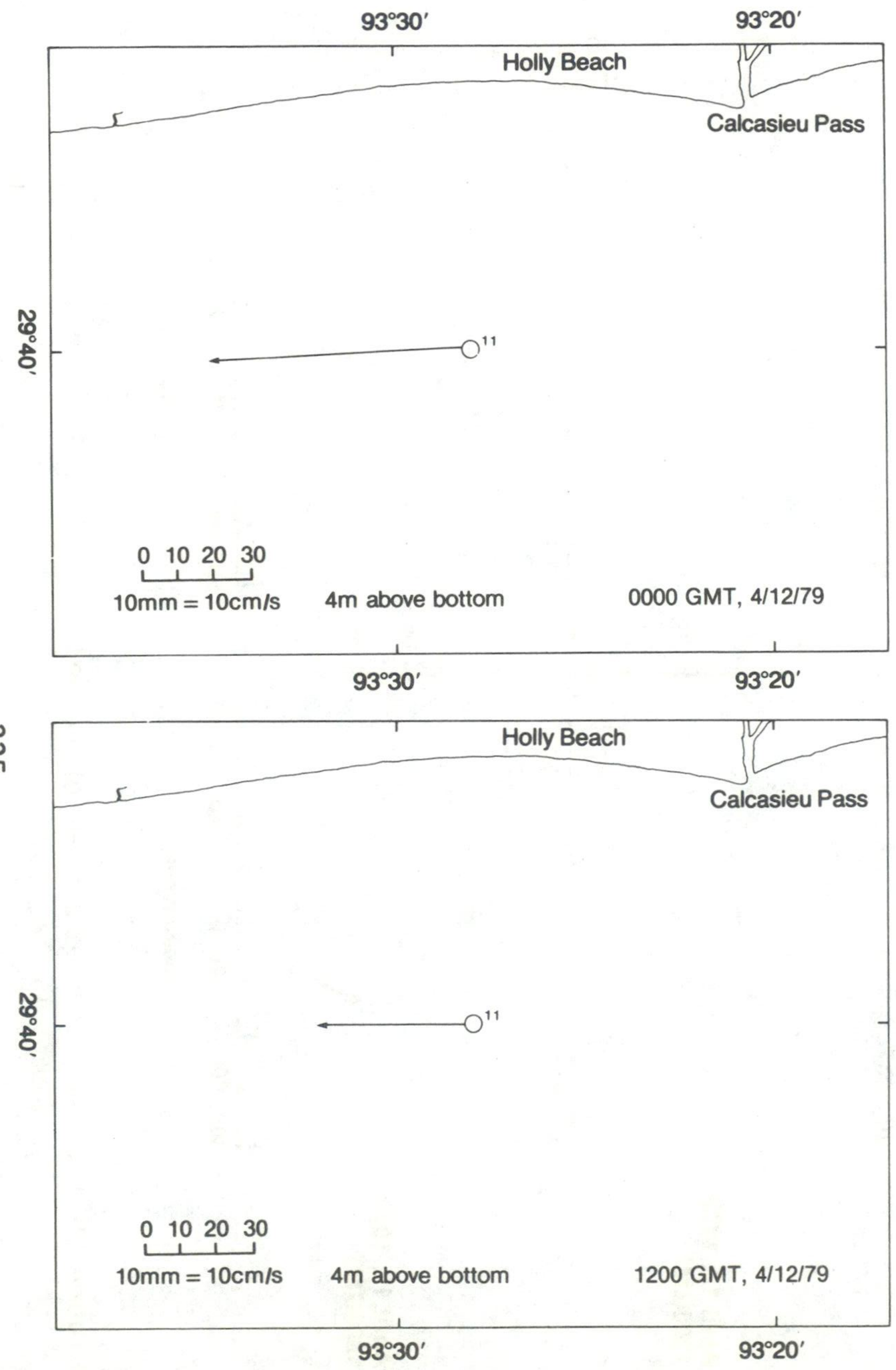

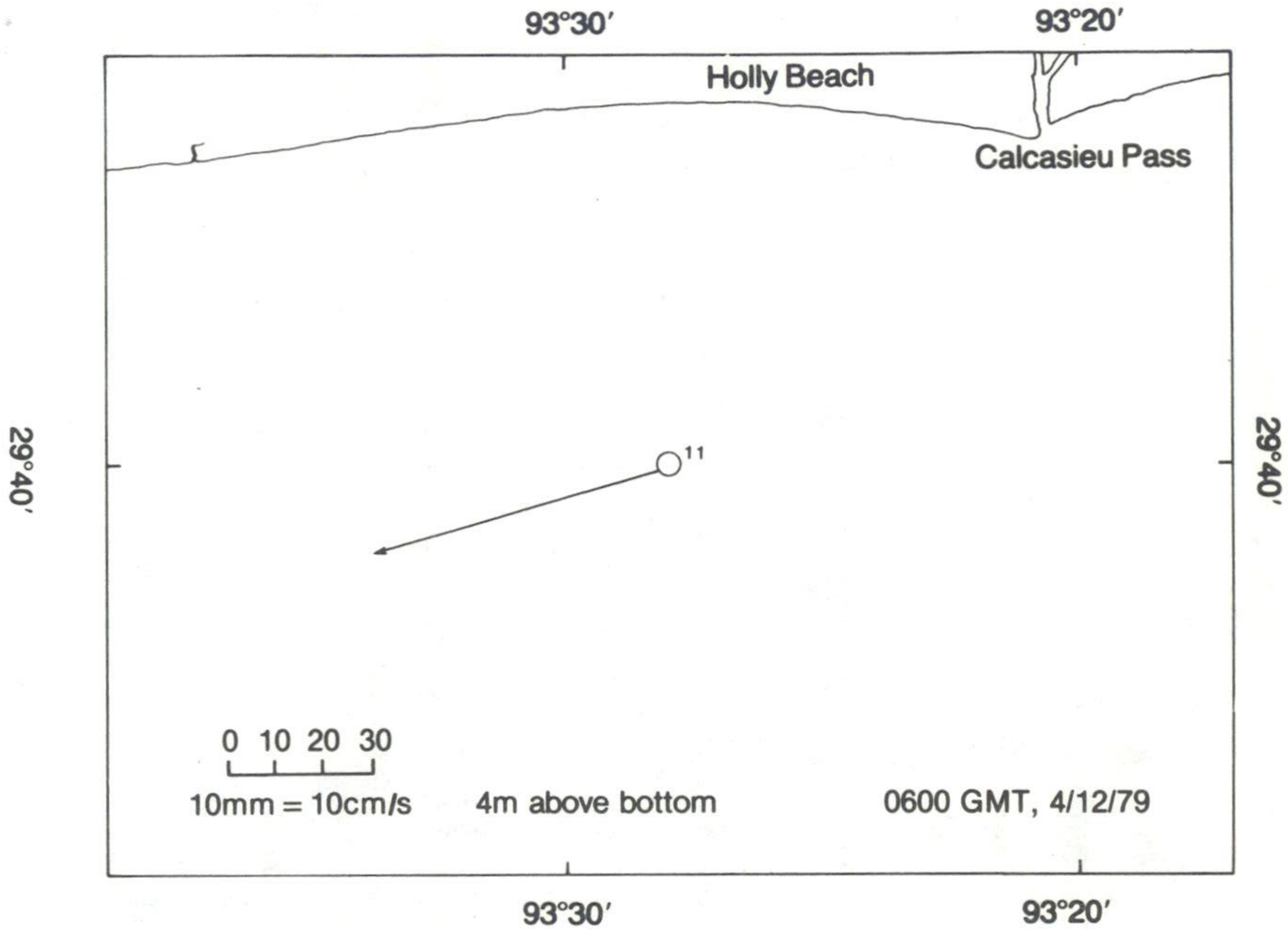

Figure 20-15. Current vectors at 6-hour intervals, 4 m above bottom at West Hackberry site, April 12, 1979.

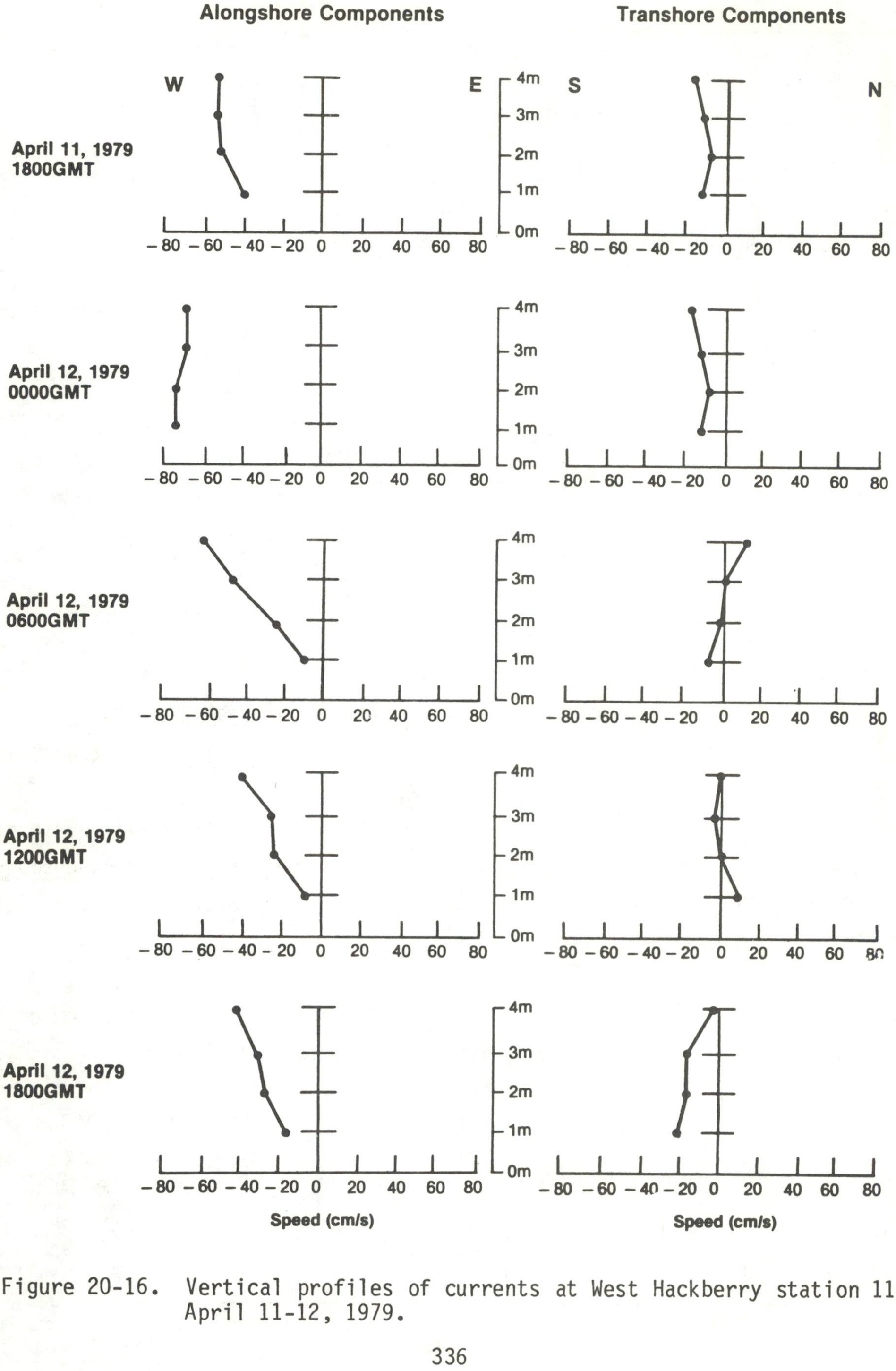

Figure 20-16. Vertical profiles of currents at West Hackberry station 11, April 11-12, 1979.

REFERENCES CITED

Allen, J. S., and P. K. Kundu, 1978: On the momentum, vorticity, and mass balance off the Oregon coast. Journal of Physical Oceanography, 8:13-37.

Behringer, D. W., R. L. Molinari, and J. F. Festa, 1977: The variability of anticyclonic current patterns in the Gulf of Mexico. Journal of Geophysical Research, 82(34):5469-5476.

Brown, N. L., and B. Allentoft, 1966: Salinity, conductivity, and temperature relationships of seawater over the range of 0 to 50 ppt (curve fit to data from). Manual, Bissett-Berman Corp.

Burg, J.P., 1968: A new analysis technique for time series data. Paper presented at the Advanced Study Institute on Signal Processing with Emphasis on Underwater Acoustics, NATO, Enschede, Netherlands, Aug. 1968.

Carpenter, J. H., 1965: The Chesapeake Bay Institute technique for the Winkler dissolved oxygen method. Limnology and Oceanography, 10(1):141-143.

Chen, W. Y., and G. R. Stegen, 1974: Experiments with maximum entropy power spectra of sinusoids. Journal of Geophysical Research, (20):3019-3022.

Cochrane, J. D., 1972: Separation of an anticyclone and subsequent developments in the Loop Current (1969). In Contributions on the Physical Oceanography of the Gulf of Mexico, Texas A&M University Oceanography Studies, vol. 2, Gulf Publishing, Houston, Tex., 228 pp.

Cooley, J.W., and J. W. Tukey, 1965: An algorithm for the machine calculation of complex Fourier series. Mathematics of Computation, XIX(90).

Csanady, G.T., 1981: Circulation in the coastal ocean. EOS, Transactions, American Geophysical Union, 62 (2, 5, 8):9-11, 41-43, 73-75.

Defant, A., 1961: Physical Oceanography. Vol. II., MacMillan Co., New York, N.Y., 598 pp.

Dennis, R. E., and E. E. Long, 1971: A user's guide to a computer program for harmonic analysis of data at tidal frequencies. NOAA Technical Report NOS 41, Washington, D.C., 31 pp.

DiMego, G. J., L. F. Bosart, and G. W. Endersen, 1976: An examination of the frequency and mean conditions surrounding frontal incursions into the Gulf of Mexico and Caribbean Sea. Monthly Weather Review, 104:709-718.

Doodson, A. T., and H. D. Warburg, 1941: Admiralty Manual of Tides. Hydrographic Dep., Admiralty, London, pp. 176-182.

Elliott, B. A., 1979: Anticyclonic rings and the energetics of the circulation of the Gulf of Mexico. Ph. D. dissertation, Graduate College of Texas A&M University.

Fofonoff, N. P., 1958: Interpretation of oceanographic measurements --thermodynamics. In Physical and Chemical Properties of Sea Water, National Academy of Sciences/National Research Council Publication 600, pp. 38-66.

Forristall, G. Z., R. C. Hamilton, and V. J. Cardone, 1977: Continental shelf currents in Tropical Storm DELIA: Observations and theory. Journal of Physical Oceanography, 7:532-546.

Franceschini, G. A., 1961: Hydrologic balance of the Gulf of Mexico. Unpublished doctoral dissertation. Department of Meteorology, The A&M College of Texas.

Gonella, J., 1972: A rotary-component method for analyzing meteorological and oceanographic vector time series. Deep-Sea Research, 19:833-846.

Harris, R. A., 1904: Manual of Tides. Part IV B, Cotidal Lines of the World, Government Printing Office, Washington, D.C., Appendix V, pp. 313-400.

Hausknecht, K. A., 1980: Sediments. Vol. V. In: W. B. Jackson and G. M. Faw (editors), Biological/chemical survey of Texoma and Capline sector salt dome brine disposal sites off Louisiana, 1978-1979. NOAA/NMFS Final Report to DOE, project number DOE-CG-13-70040-00, 56 pp.

Hicks, S., 1977: Gulf Coast Low Water Datum. National Ocean Survey, NOAA, Washington, D.C., 70 pp.

Hsu, Shih-Ang, 1969: Land- and sea-breeze fronts near 50 cm on the Gulf Coast. Bulletin of the American Meteorological Society, 50(11):880-882.

Hsu, Shih-Ang, 1967: Mesoscale surface temperature characteristics of the Texas coast sea breeze. Atmospheric Science Group Technical Report No. 6, The University of Texas at Austin, 74 pp.

Ichiye, T., 1960: On the hydrology of the Mississippi Delta. Oceanographical Magazine, Japan Meteorological Agency, 11:65-78.

Iseri, K. T., and W. B. Langbein, 1974: Large rivers of the United States. U.S. Geological Survey Circular No. 686.

Lawrence, M. B., 1979: Atlantic hurricane season of 1978. Monthly Weather Review, 107:447-488.

Leipper, D. F., 1970: A sequence of current patterns in the Gulf of Mexico. Journal of Geophysical Research, 75(3):637-657.

Maresca, J. W., Jr., and C. T. Carlson, 1978: Tracking and monitoring hurricanes by H. F. sky wave radar over the Gulf of Mexico. Final Report, contract F49620-76-C0023, SRI International, Menlo Park, Calif., 70 pp.

Marmer, H. A., 1951: Tidal datum planes. Special Publication No. 135, U.S. Coast and Geodetic Survey, Washington, D.C., 142 pp.

Marmer, H. A., 1954: Tides and sea level in the Gulf of Mexico. Fishery Bulletin, Fish and Wildlife Service, Washington, D.C., pp. 101-118.

Muench, R. D., and J. D. Schumacher, 1979: Some observations of physical oceanographic conditions on the northeast Gulf of Alaska continental shelf. NOAA TM ERL PMEL-17, Pacific Marine Environmental Laboratory, Seattle, Wash., 84 pp.

Murray, S. P., 1976: Currents and circulation in the coastal waters of Louisiana. Sea Grant Publication No. LSU-T76-003, 33 pp.

National Hurricane Center, 1978: Preliminary Report, Tropical Storm DEBRA. National Weather Service, NOAA, Miami, Fla.

National Ocean Survey, 1978: Deck log, weather observation sheet for NOAA Ship MT. MITCHELL S-222, Monday, August 28 and Tuesday, August 29, 1978.

National Oceanic and Atmospheric Administration, 1976: Physical oceanography. Vol. II. In: Environmental Studies of the South Texas Outer Continental Shelf, 1975. NOAA Final Report to BLM, interagency agreement number 08550-1A5-19.

Neumann, G., and W. J. Pierson, Jr., 1966: Principles of Physical Oceanography, Prentice-Hall, Inc.

Nowlin, W. D., Jr., 1972: Winter circulation patterns and property distributions. In Contributions on the Physical Oceanography of the Gulf of Mexico, Texas A&M University Oceanography Studies, vol. 2, Gulf Publishing, Houston, Tex., pp. 3-51.

Nowlin, W. D., Jr., and J. M. Hubertz, 1972: Contrasting circulation patterns for the eastern gulf. In Contributions on the Physical Oceanography of the Gulf of Mexico, Texas A&M University Oceanography Studies, vol. 2, Gulf Publishing, Houston, Tex., pp. 191-138.

Parker, R. H., and A. L. Crowe, 1980: Describe living and dead benthic (macro- and meio-) communities. Vol. I. In: W. B. Jackson and G. M. Faw (editors), Biological/chemical survey of Texoma and Capline sector salt dome brine disposal sites off Louisiana, 1978-1979. NOAA Technical Memorandum NMFS-SEFC-25, 103 pp.

Powell, M. D. (National Hurricane and Experimental Meteorological Laboratory, ERL, NOAA, Coral Gables, Fla.), 1979: Personal communication, November 29.

Radoski, H. R., P. F. Fougere, and E. J. Zawalick, 1975: A comparison of power spectral estimates and applications of the maximum entropy method. Journal of Geophysical Research, 80(4):619-625.

Rouse, L. J., and J. M. Coleman, 1976: Circulation observations in the Louisiana Bight using LANDSAT imagery. Remote Sensing of the Environment, 5:55-66.

Schureman, P., 1958: Manual of harmonic analysis and prediction of tides. Special Publication 98, U.S. Coast and Geodetic Survey, U.S. Department of Commerce, Washington, D.C., 317 pp.

Smith, N. P., 1978: Longshore currents on the fringe of Hurricane Anita. Journal of Geophysical Research, 83(C-12):6047-6051.

Sprenke, 1977: Precision Conductivity Measurement, 4th STD/Oceans Conference (Plessey).

Strand, O. N., 1977: Proceedings of the 1977 IEEE Conference on Acoustics, Speech, and Signal Processing. Institute of Electrical and Electronics Engineers.

Sturges, W., and J. P. Blaha, 1976: A western boundary current in the Gulf of Mexico. Science, 192(4237):367.

Torgrimson, G. M. and B. M. Hickey, 1979: Barotropic and baroclinic tides over the continental slope and shelf off Oregon. Journal of Physical Oceanography, 9:945-961.

Trewartha, G. T., 1954: An Introduction to Climate. McGraw-Hill Book Co., New York, N.Y., third edition, 402 pp.

U.S. Army Coastal Engineering Research Center, 1975: Shore Protection Manual, vol. 1, second edition, Department of the Army Corps of Engineers, Fort Belvoir, Va., 504 pp.

U.S. Coast and Geodetic Survey, 1952: Manual of harmonic constant reductions. Special Publication No. 260, Washington, D.C., 74 pp.

U.S. Coast and Geodetic Survey, 1965: Manual of tide observations. Publication 30-1, U.S. Government Printing Office, 72 pp.

U.S. Navy Oceanographic Office, 1968: Instruction manual for obtaining hydrographic data. Publication 607, pp. J-1 to J-12.

UNESCO, 1971: International oceanographic tables. Vol. 1, National Institutes of Oceanography of Great Britain and UNESCO.

Winant, C. D., 1979: Coastal current observations. Reviews of Geophysics and Space Physics, 17(1):89-98.

Wunsch, C., 1975: Internal tides in the ocean. Reviews of Geophysics and Space Physics, 13(1):167-182.

Zetler, B. D., and D. V. Hansen, 1972: Tides in the Gulf of Mexico. In Contributions on the Physical Oceanography of the Gulf of Mexico, Texas A&M University Oceanography Studies, vol. 2, Gulf Publishing, Houston, Tex., pp. 265-275.

APPENDIX A.

EQUATIONS USED FOR CALCULATION OF CONDUCTIVITY, SALINITY, AND SIGMA-T.

APPENDIX A

EQUATIONS FOR CALCULATING CONDUCTIVITY, SALINITY, AND SIGMA-t

1. Compute conductivity at 35 ppt at in situ temperature (T)

$$C(35,T) = \frac{C(35,\ T)}{C(35,15)} \times C(35,15)$$

$$= [0.676641 + 2.0058 \times 10^{-2}\ T + 1.0952 \times 10^{-4}\ T^2$$

$$-6.417 \times 10^{-7}\ T^3] \quad 42.896$$

(See Sprenke, 1977)

2. Compute conductivity ratio R_T

$$R_T = \frac{C(S,T)}{C(35,T)} \text{ where } C(S,T) = \text{measured conductivity}$$

3. Correct R_T to R_{15}

$R_{15} = R_T + A\ (T,\ R_T)$

For T = 10° --→ 30°

$$R_{15} = R_T + (T-15)\ [\ 62.0\ \ (R_T-1) + 64.6\ \ (R_T-1)^2$$

$$+ 39.9\ \ (R_T-1)^3 + 37.3\ (R_T-1)^4] \times 10^{-5}$$

$$- (T-15)^2\ [0.84\ R_T-1) + 1.26\ (R_T-1)^2 + 0.63\ (R_T-1)^3$$

$$+ 0.21\ (R_T-1)^4] \times 10^{-5}$$

(See UNESCO, 1971)

For T < 10°C

$$R_{15} = R_T + (T-15)\ [64.58\ (R_T-1) + 72.55\ (R_T-1)^2$$

$$+ 38.72\ (R_T-1)^3 + 30.02\ (R_T-1)^4] \times 10^{-5}$$

$$- (T-15)^2\ [1.481\ (R_T-1) - 1.611\ (R_T-1)^2$$

$$-6.450\ (R_T-1)^3 - 3.427\ (R_T-1)^4] \times 10^{-5}$$

(See Brown and Allentoft, 1966)

4. Compute salinity

$$S(ppt) = -0.8996 + 28.2972 \cdot R_{15} + 12.80832 \cdot R_{15}^2 - 10.67869 \cdot R_{15}^3 + 5.98624 \cdot R_{15}^4 - 1.32311 \cdot R_{15}^5$$

(See Sprenke, 1977)

5. Compute density (sigma-t)

At atmospheric pressure and at temperature of 0°C the density is a function of the salinity only, and is computed as:

$$\sigma 0(S) \quad \sum_{j=0}^{3} b_j S^j$$

$b_0 = -9.344586324 \times 10^{-2}$ $\quad b_2 = -4.824961403 \times 10^{-4}$

$b_1 = +8.14876576925 \times 10^{-1}$ $\quad b_3 = +6.767861356 \times 10^{6}$

σ_t is computed for a specific temperature T as:

$$\sigma_t(T,\sigma_0) = \sum_{i=1}^{4} (a_i T^i) / (T + a_0) + \sum_{i=0}^{3} (b_i T^i) \sigma_0 + \sum_{i=0}^{3} (C_i T^i) \sigma_0^2$$

$a^0 = +67.26$

$a_1 = +4.531684262$

$a_2 = -0.5459391107$

$a_3 = -1.9824839871 \times 10^{-3}$

$a_4 = -1.438030609 \times 10^{-7}$

$b_0 = +1.0$

$b_1 = -4.7867 \times 10^{-3}$

$b_2 = +9.8185 \times 10^{-5}$

$b_3 = -1.0843 \times 10^{-6}$

$c_0 = 0$

$c_1 = +1.803 \times 10^{-5}$

$c_2 = -8.164 \times 10^{-7}$

$c_3 = +1.667 \times 10^{-8}$

(See Fofonoff, 1958)

APPENDIX B.

WATER LEVEL THEORY

APPENDIX B
WATER LEVEL THEORY

With a series of observations 29 days in length, it is not possible to separate two harmonic constituents with frequencies less than approximately 4 x 10^{-7} cycles/s apart (or, equivalently, with constituent speeds less than approximately 9 x 10^{-3} °/hour apart). For example, one cannot separate the effects of S_2 and K_2, K_1 and P_1, or N_2 and V_2, with only 29 days of data. Since S_2, K_1, and N_2 are major constituents, generally much larger than their respective nearby constituents, the 29-day harmonic analysis can calculate them approximately, with an error due to the unknown effect of each nearby minor constituent. The minor constituents cannot, however, be calculated at all.

The above program attempts to overcome this problem using equilibrium tidal theory; that is, assuming the water responds instantaneously to the astronomic tide-producing forces. It assumes that harmonic constituent amplitudes should have relative magnitudes the same as the constituent tide-producing forces. It also assumes that the differences between harmonic constituent phases should be the same as the differences between constituent speeds (or frequencies). With these two assumptions, all minor constituents are inferred from the major constituents (M_2, S_2, N_2, O_1, and K_1), which were already determined by Fourier series methods, and an elimination procedure is used to adjust the major constituent results for the effect of the minor constituents. Specific procedures and formulas are given in Schureman (1958).

Another way of expressing the effect of length of series on frequency resolution is with synodic periods. The synodic period is the length of a time series needed to separate two harmonic constituents of known frequencies. It is calculated by dividing 360° by the difference in the two constituent speeds, the result being given in hours. Thus, to separate K_1 (speed = 15.0410686°/hour) and P_1 (speed = 14.9589314°/hour) one needs 4,382 hours, or 182 days, of data. Schureman gives a table of synodic periods for all important constituent pair combinations.

Equilibrium tidal theory does not describe the real tide well, especially in semi-enclosed basins and coastal areas. However, as long as the minor constituents are much smaller than the major ones, this method provides reasonable corrections to the Fourier series results. In some areas, however, P_1 can be fairly large, and in such cases, K_1 and P_1 results from this program may not be of sufficient accuracy. The principal reason for performing a harmonic analysis is the determination of the amplitudes and phases of the various harmonic constituents. The harmonic constituents obtained from the analysis can be used to make tide predictions using the formula:

$$h = H_o - fH \cos [at + (v_o + u) - k]$$

in which

h = height of tide at any time

H_o = mean height of water level above datum used for prediction

H = mean amplitude of any constituent A

f = node factor for reducing mean amplitude H to year of prediction (accounting for the 18.6 year cycle of the angle of the moon's orbital plane with the celestial equator)

a = speed of constituent A

t = time reckoned from some initial epoch such as beginning of year of prediction

$(v_o + u)$ = value of equilibrium argument of constituent A when $t = 0$

k = epoch of constituent A

H and k are derived from the harmonic analysis of the observations. The values of f, a, and $(v_o + u)$ can either be obtained from tables (i.e., Schureman, 1958) or calculated directly using the various astronomical constants based on the position of the earth, moon, and sun.

APPENDIX C.

VERTICAL PROFILES OF TEMPERATURE, SALINITY, AND SIGMA-T.

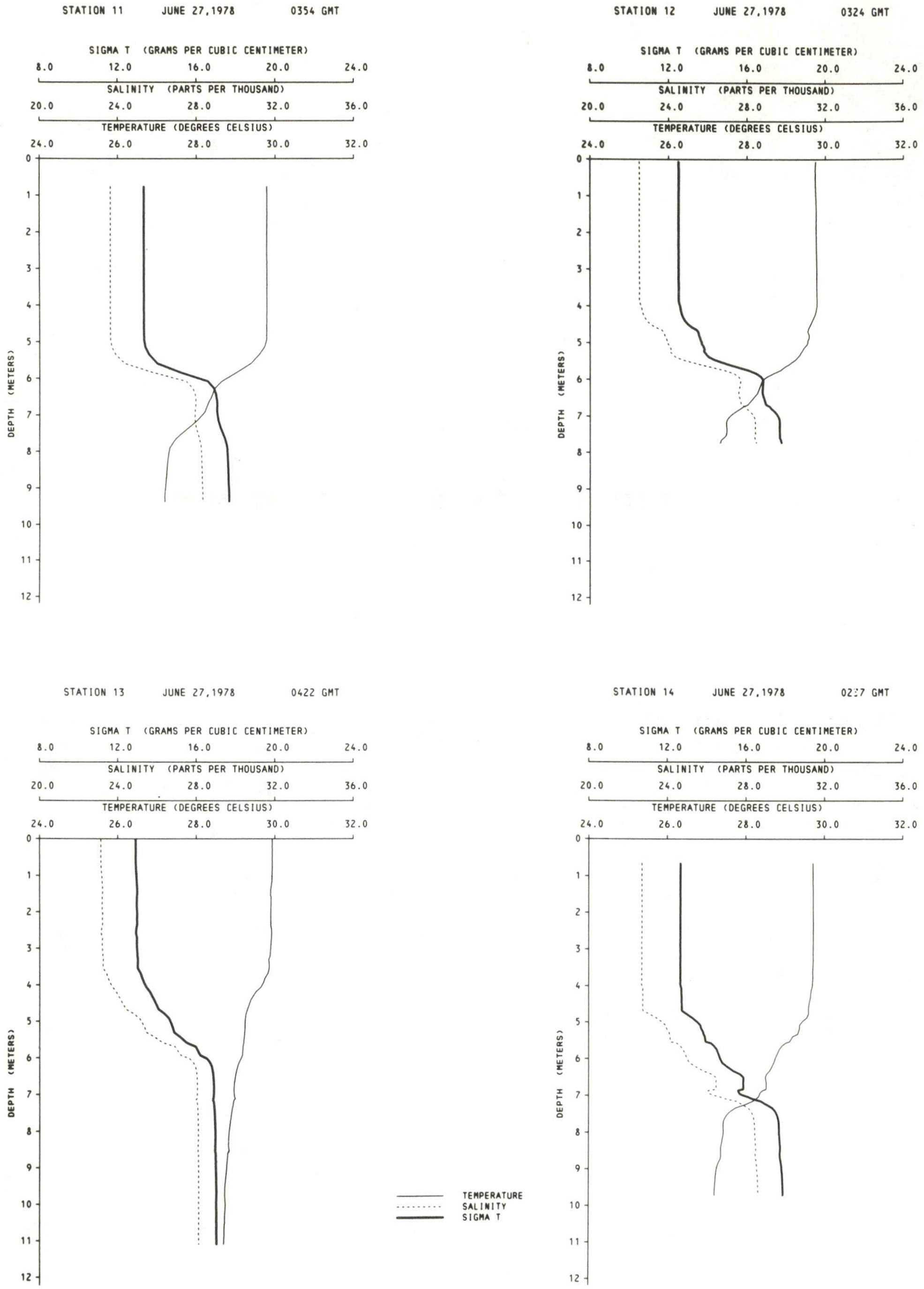

Figure C-1. Vertical profiles of temperature, salinity, and sigma-t for June 27, 1978, at stations 11 through 14.

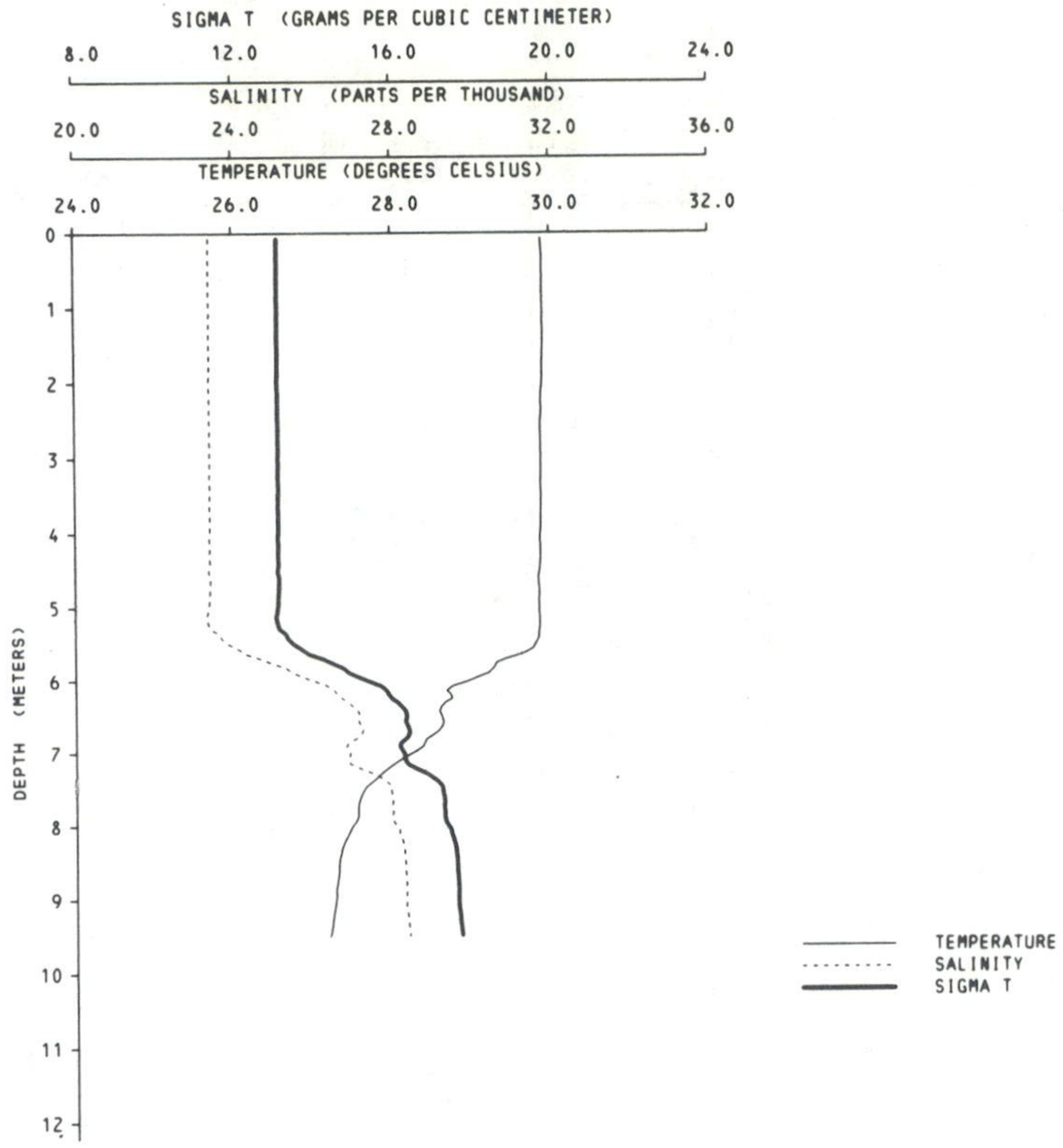

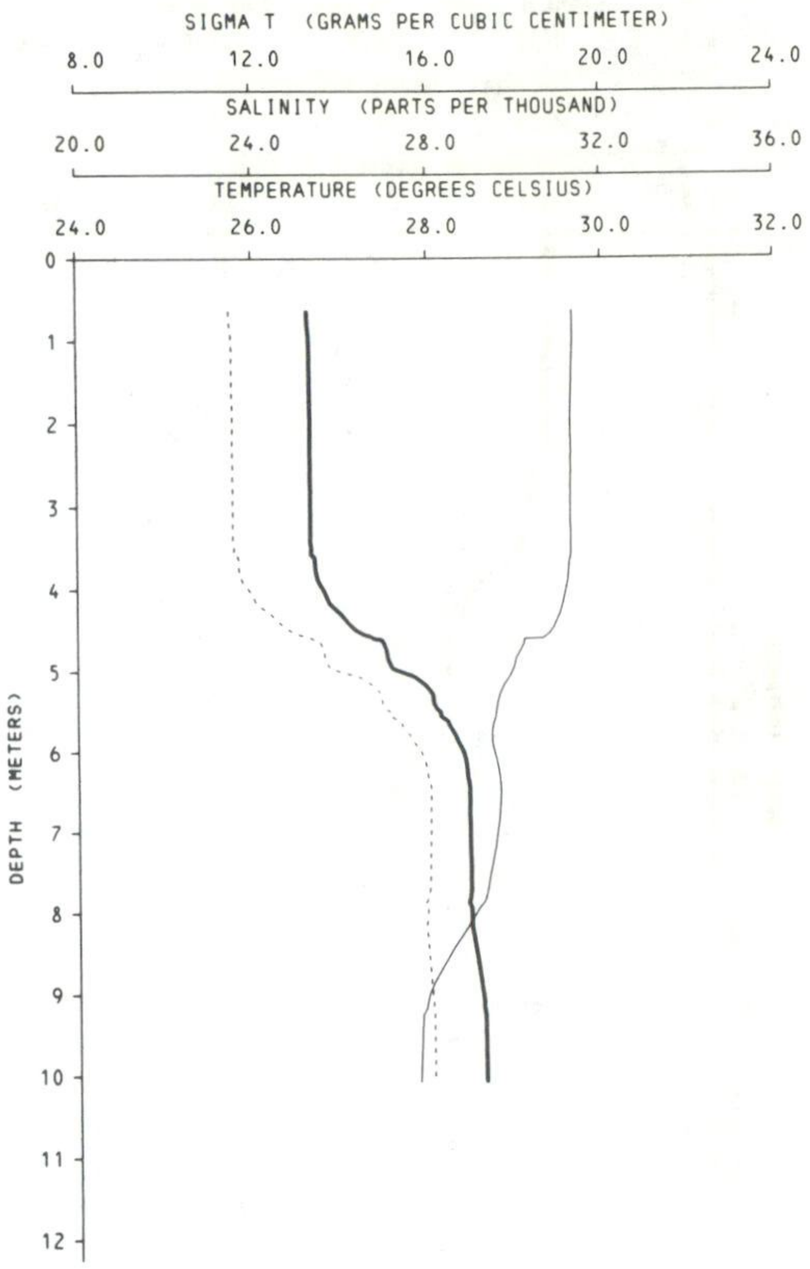

Figure C-2. Vertical profiles of temperature, salinity, and sigma-t for June 27, 1978, at stations 16 and 17.

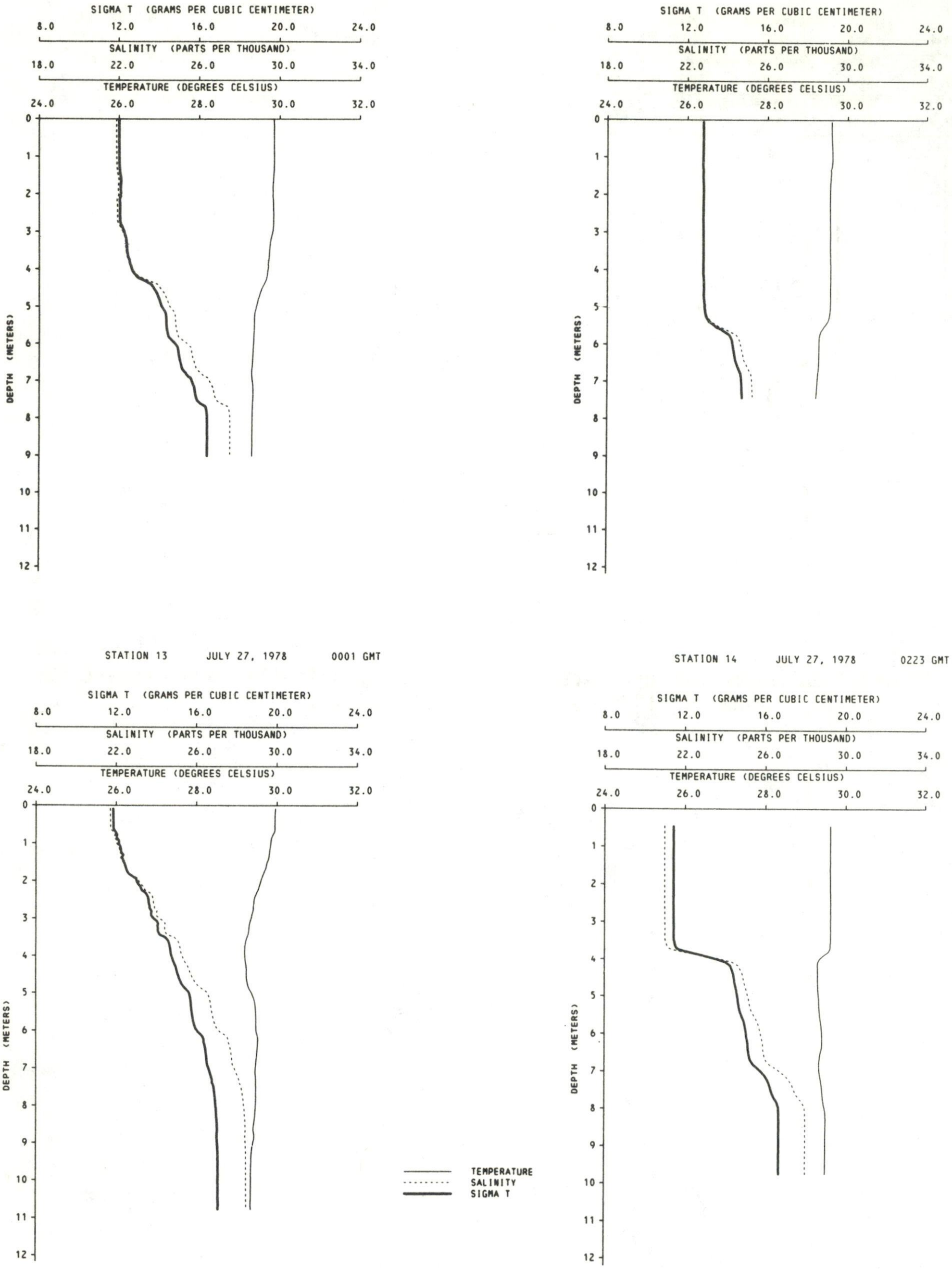

Figure C-3. Vertical profiles of temperature, salinity, and sigma-t for July 26-27, 1978, at stations 11 through 14.

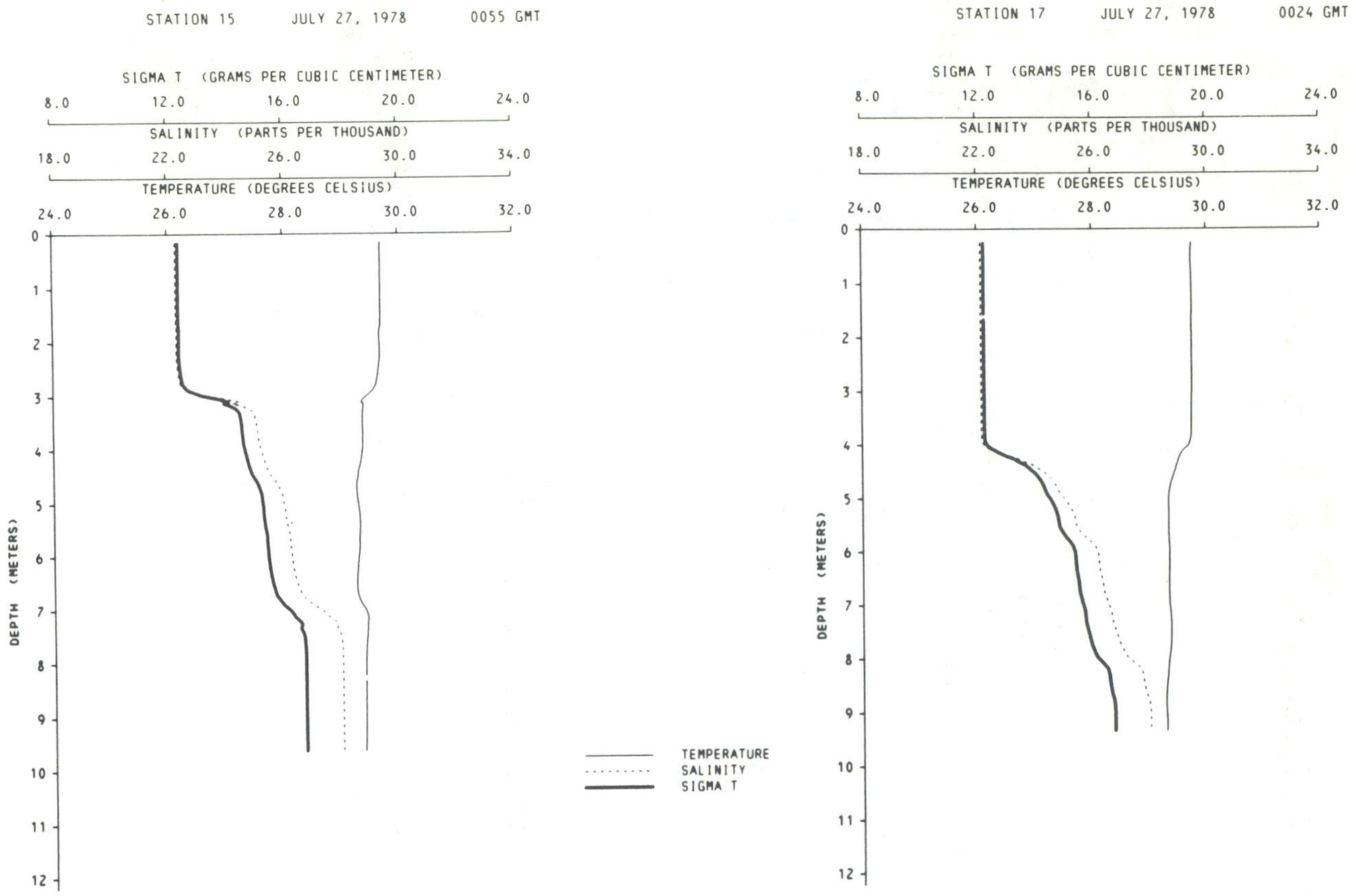

Figure C-4. Vertical profiles of temperature, salinity, and sigma-t for July 26-27, 1978, at stations 15 and 17.

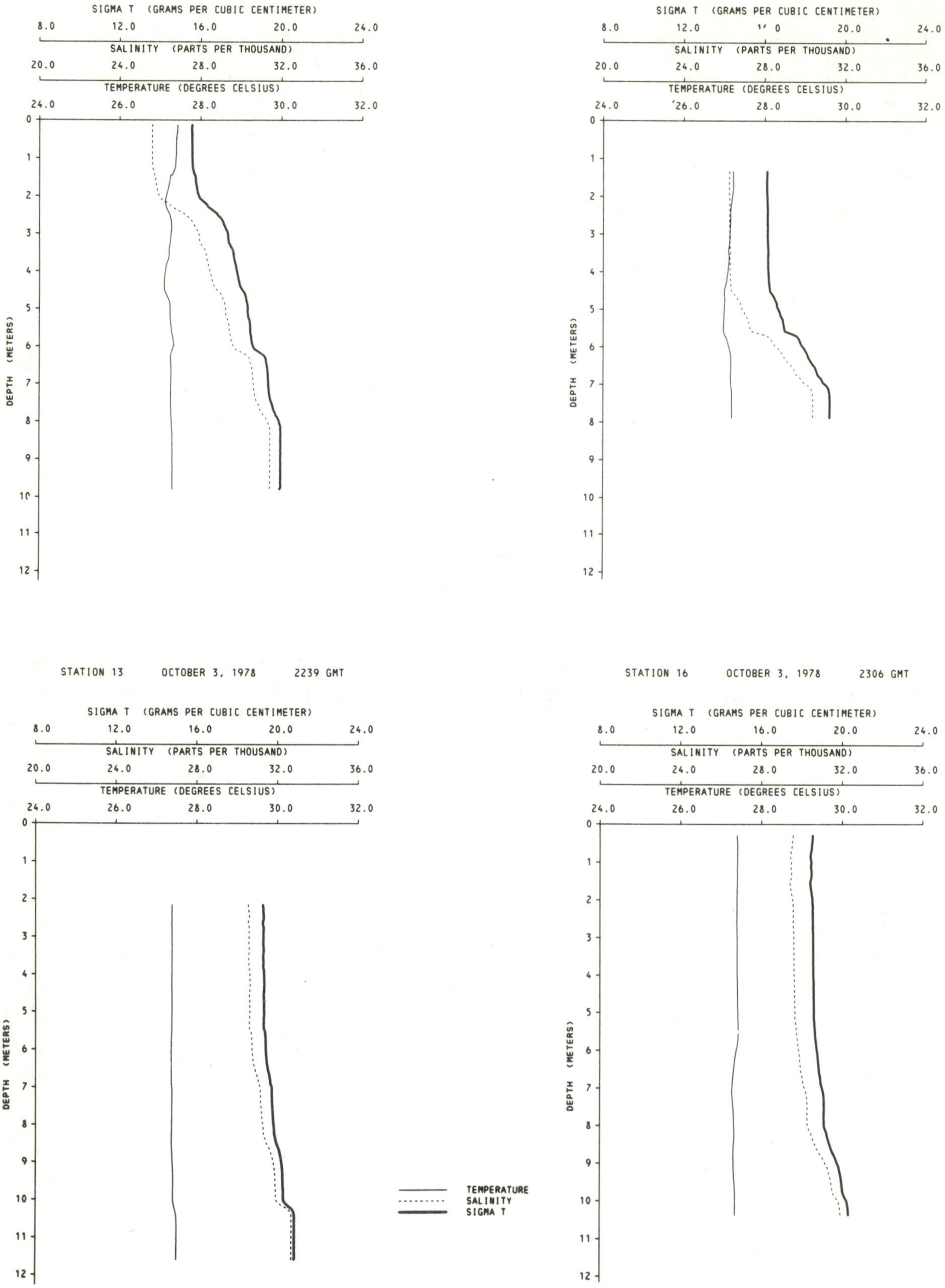

Figure C-5. Vertical profiles of temperature, salinity, and sigma-t for October 3, 1978, at stations 11 through 13 and 16.

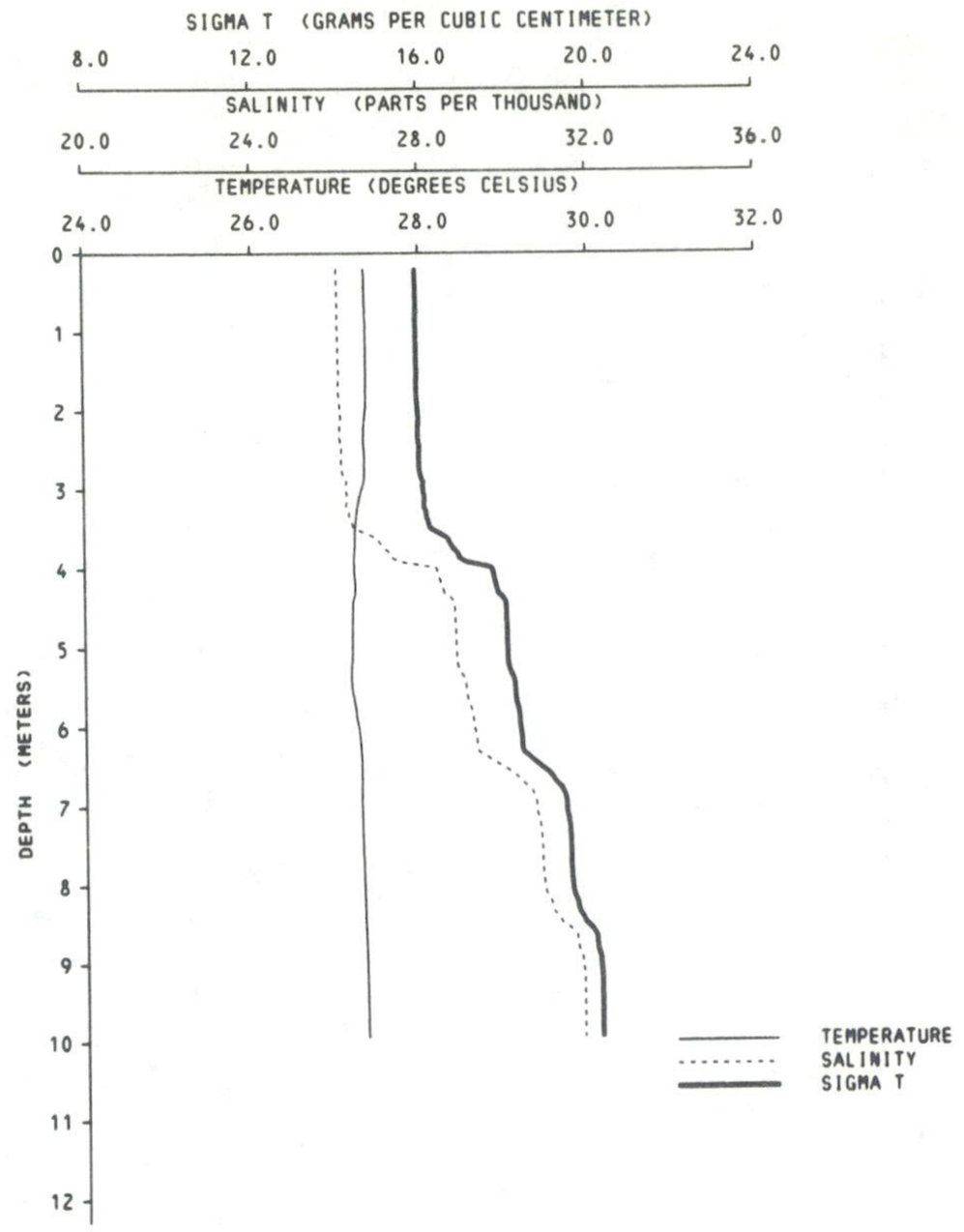

Figure C-6. Vertical profiles of temperature, salinity, and sigma-t for October 3, 1978, at station 17.

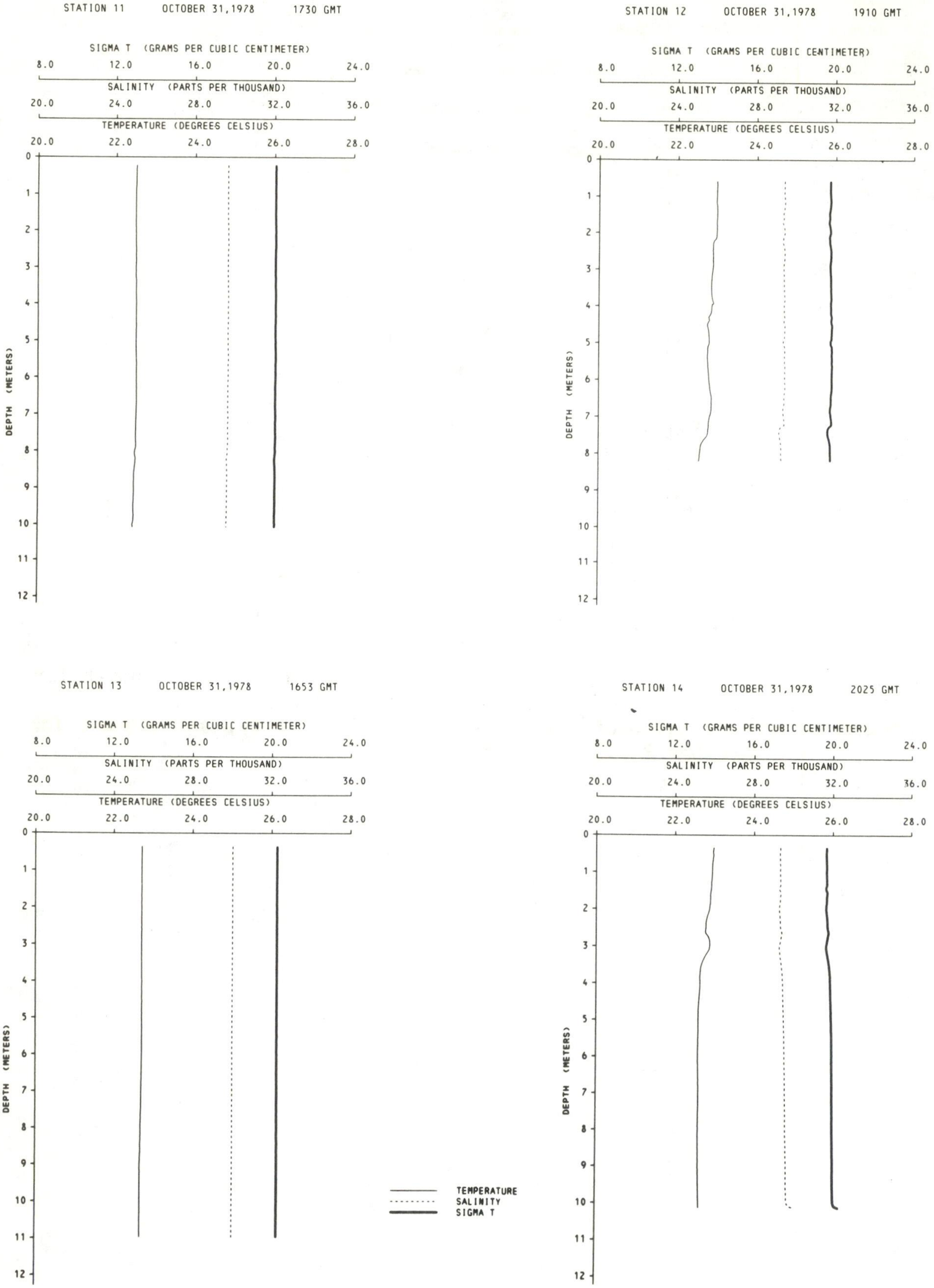

Figure C-7. Vertical profiles of temperature, salinity, and sigma-t for October 31, 1978, at stations 11 through 14.

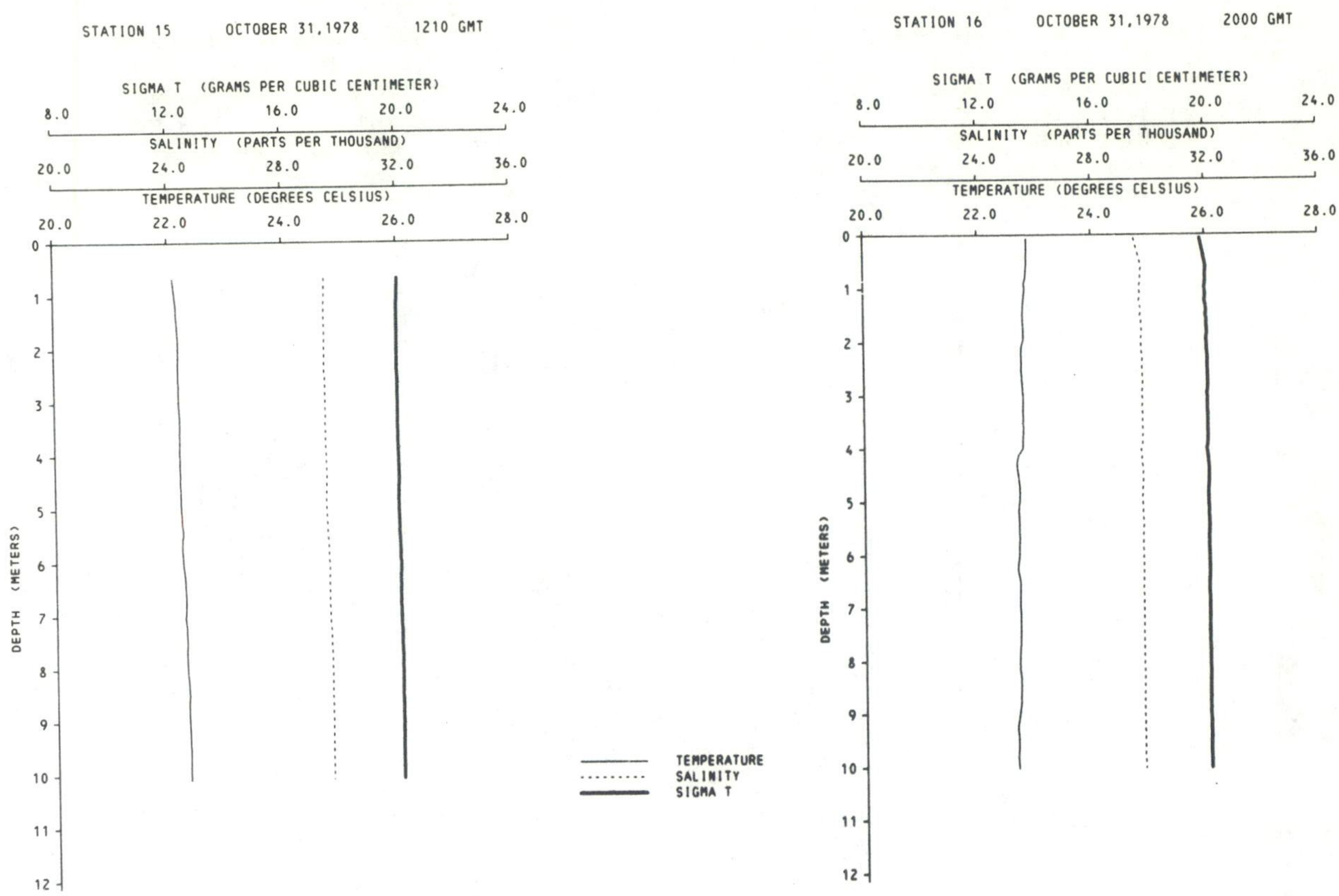

Figure C-8. Vertical profiles of temperature, salinity, and sigma-t for October 31, 1978, at stations 15 and 16.

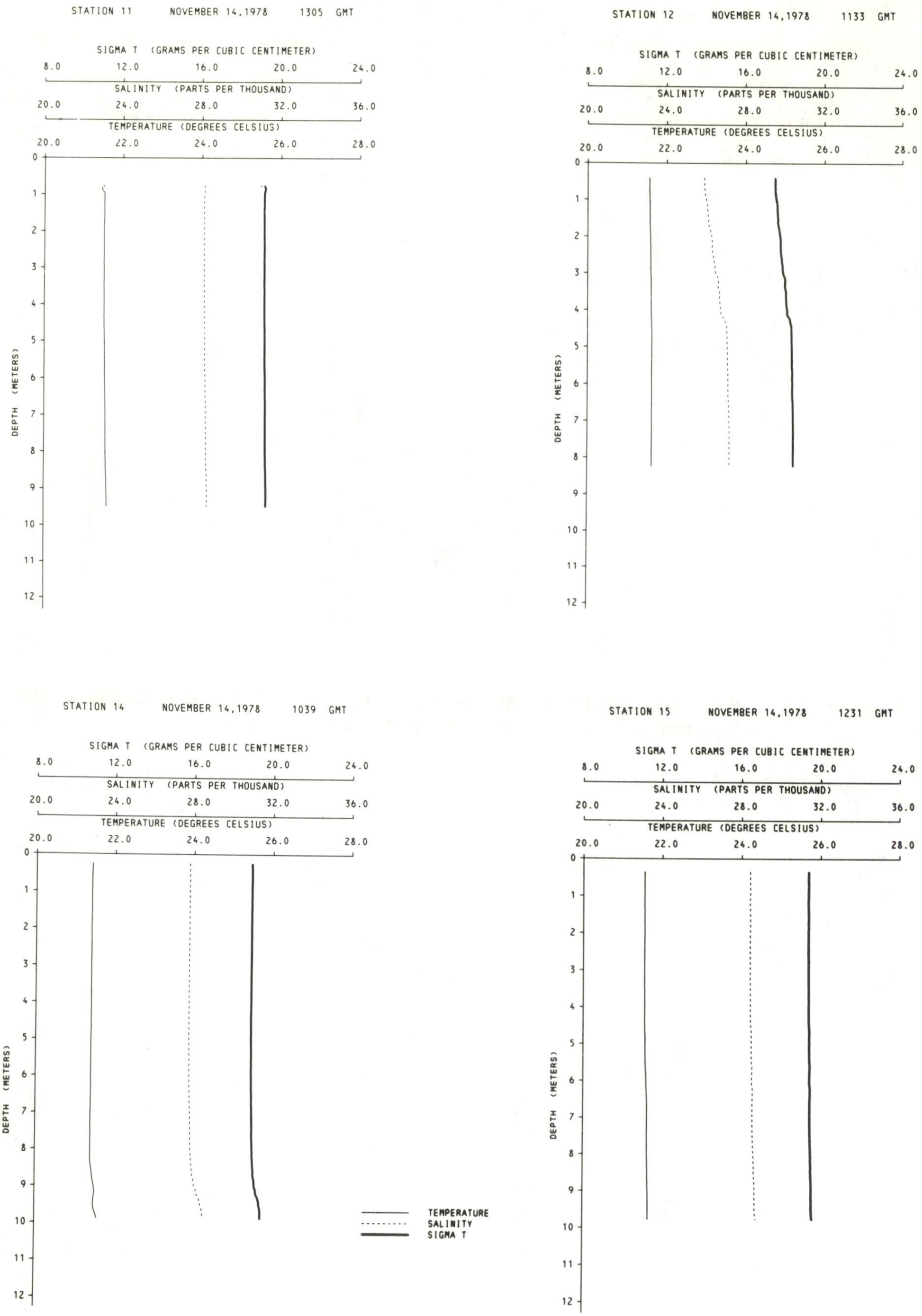

Figure C-9. Vertical profiles of temperature, salinity, and sigma-t for November 14, 1978, at stations 11, 12, 14, and 15.

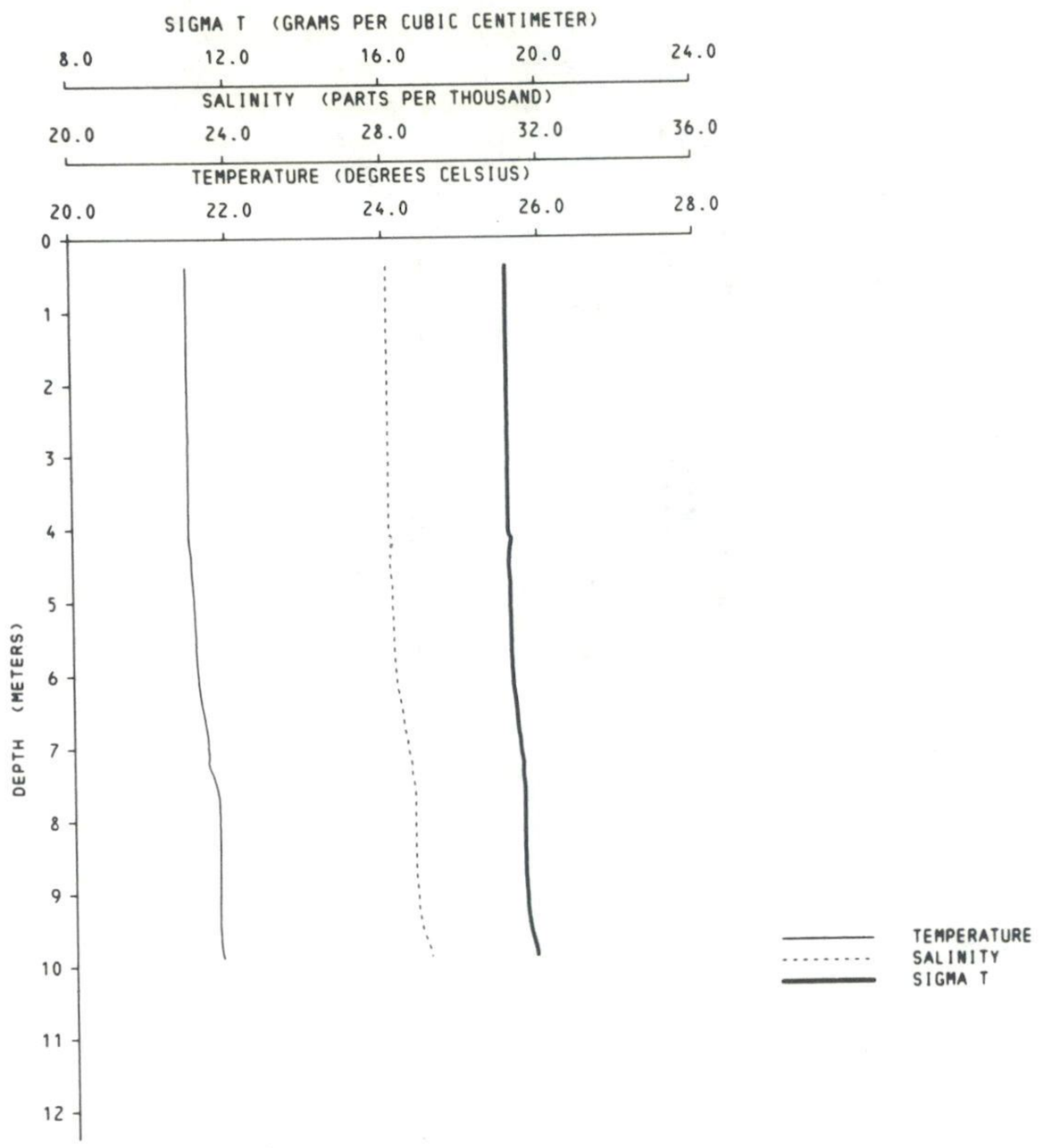

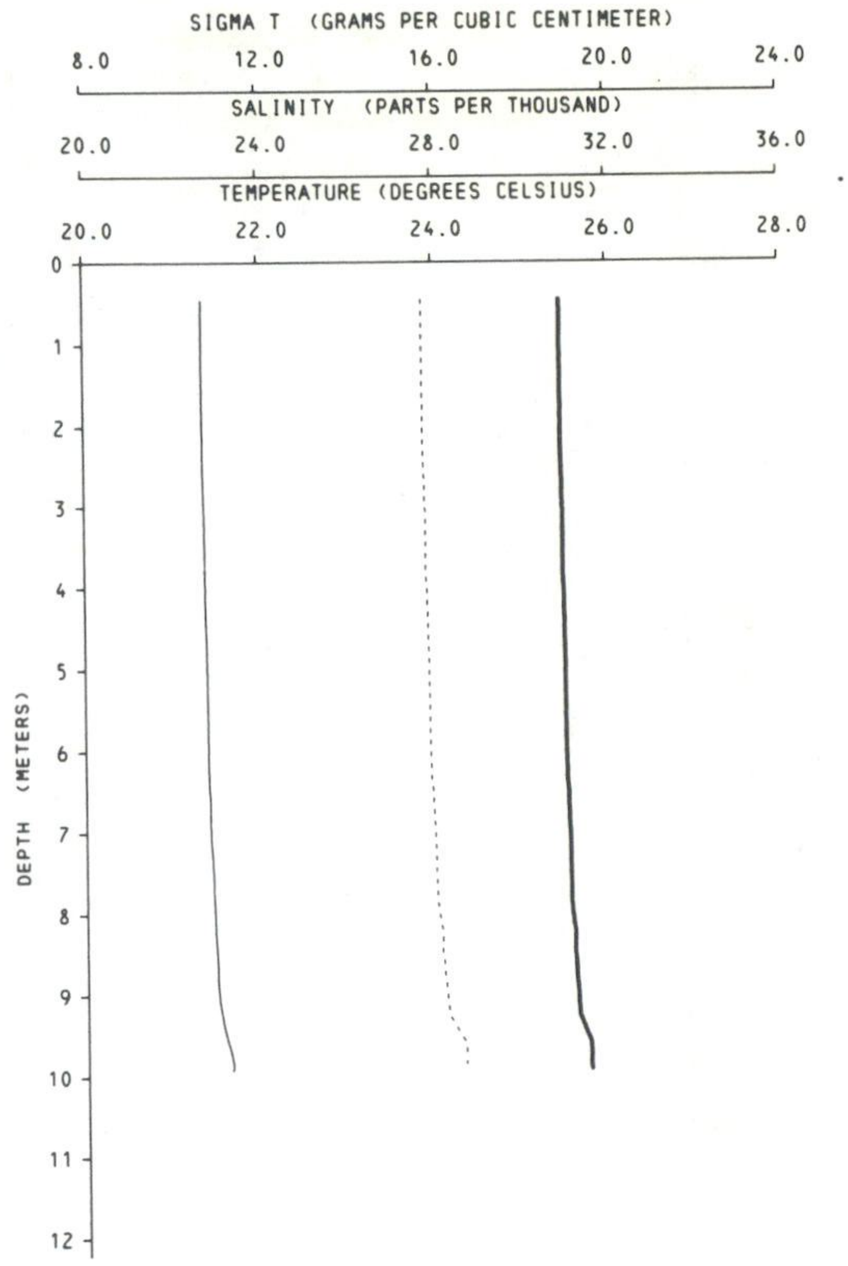

Figure C-10. Vertical profiles of temperature, salinity, and sigma-t for November 14, 1978, at stations 16 and 17.

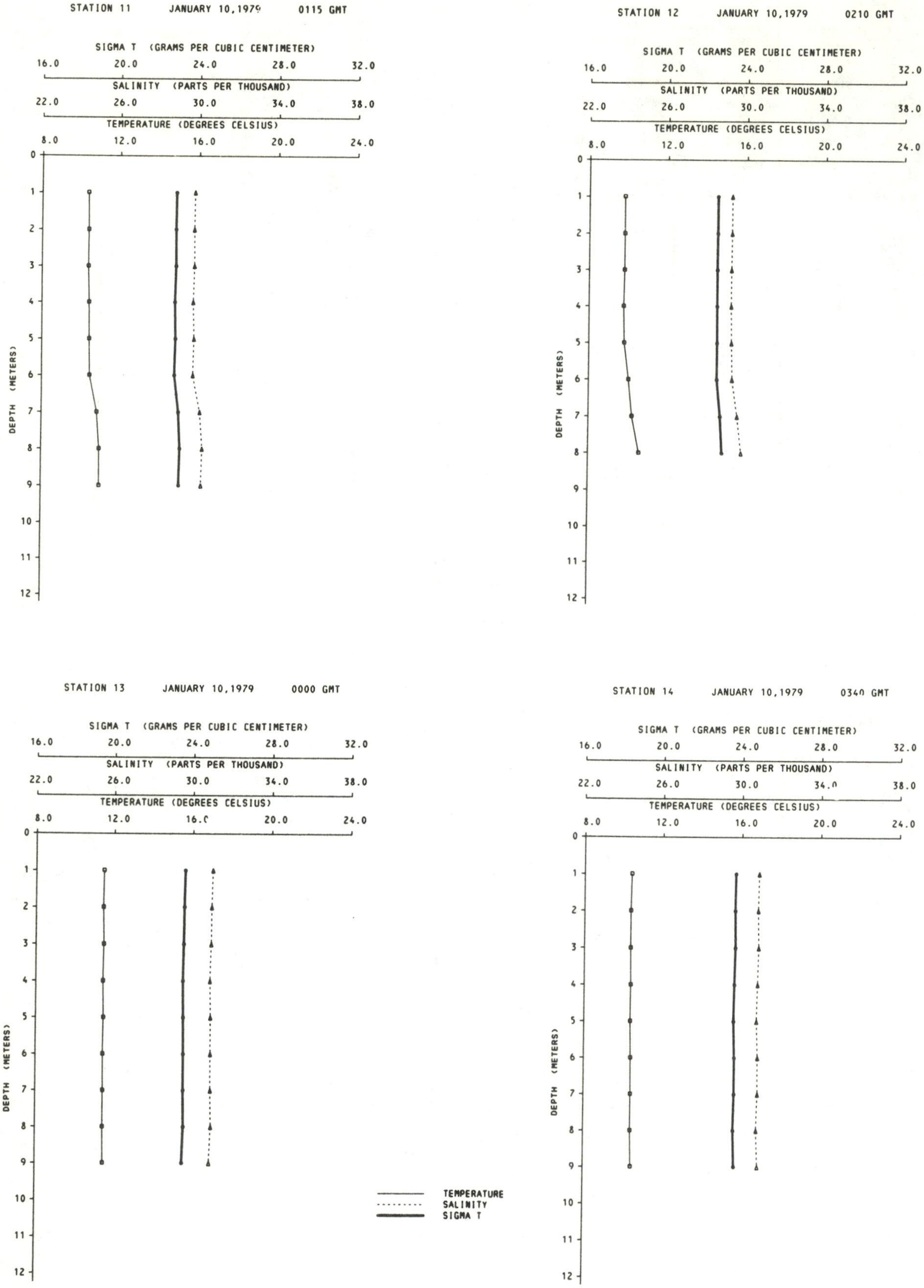

Figure C-11. Vertical profiles of temperature, salinity, and sigma-t for January 10, 1979, at stations 11 through 14.

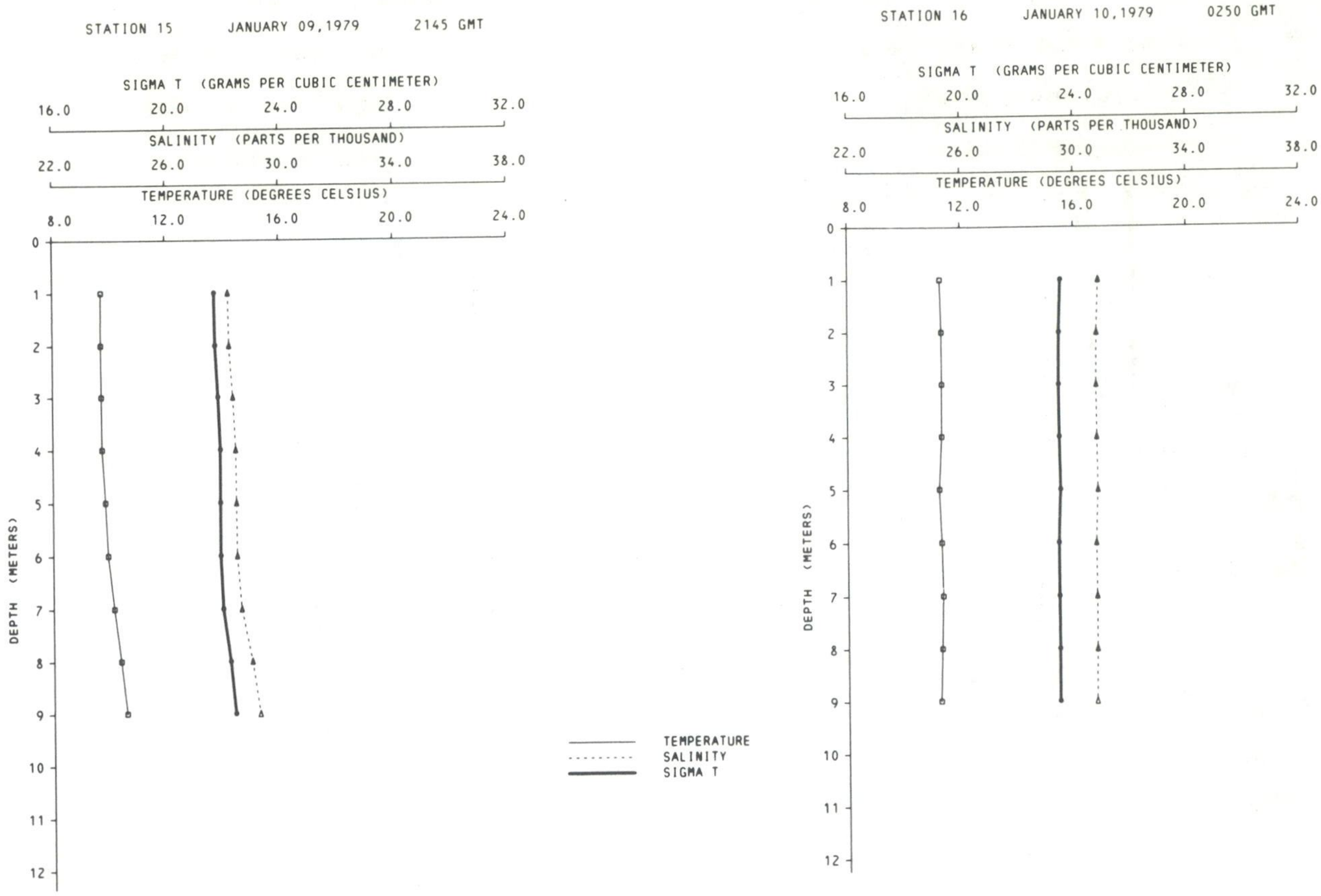

Figure C-12. Vertical profiles of temperature, salinity, and sigma-t for January 9-10, 1979, at stations 15 and 16.

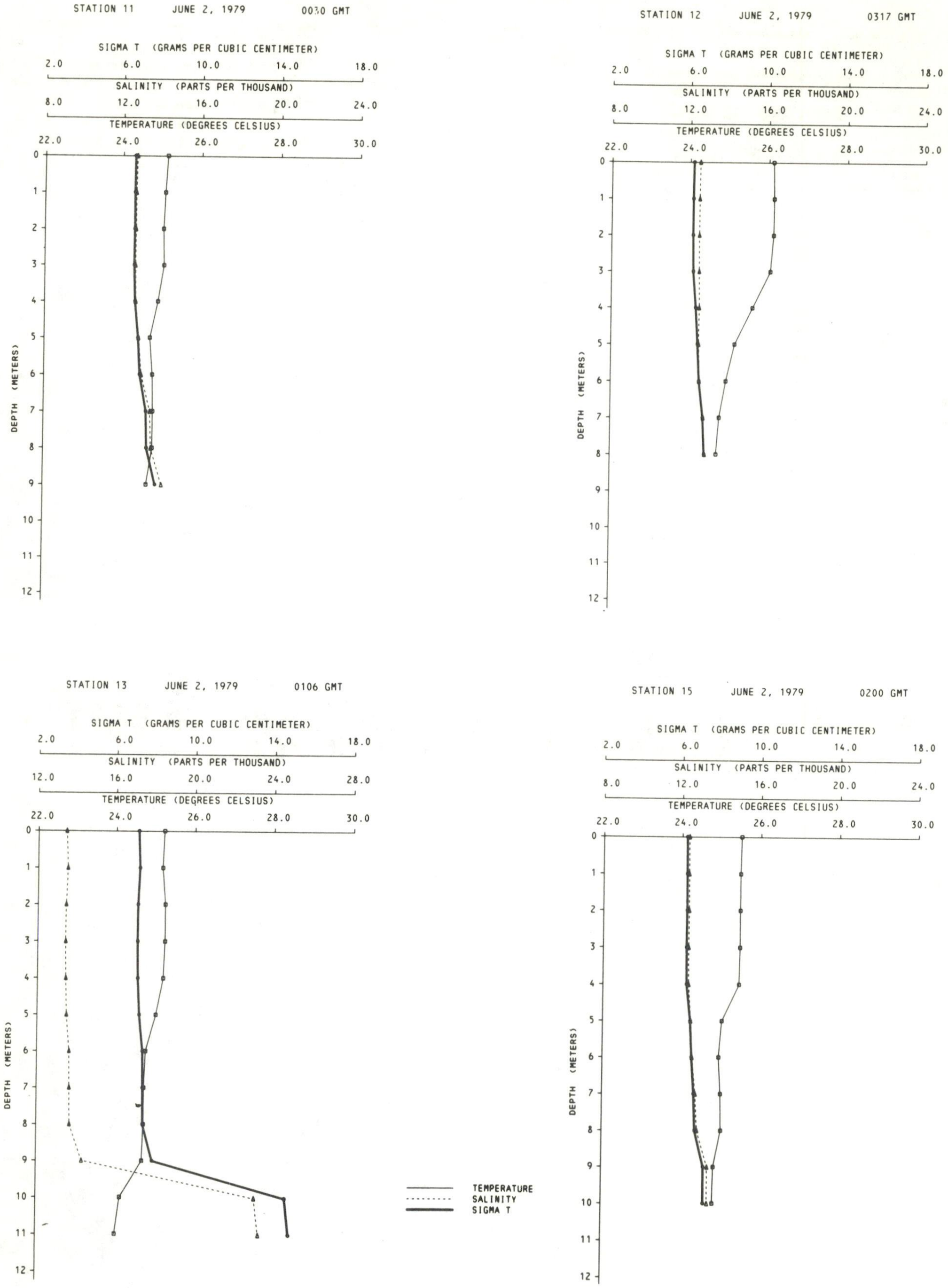

Figure C-13. Vertical profiles of temperature, salinity, and sigma-t for June 2, 1979, at stations 11 through 13 and 15.

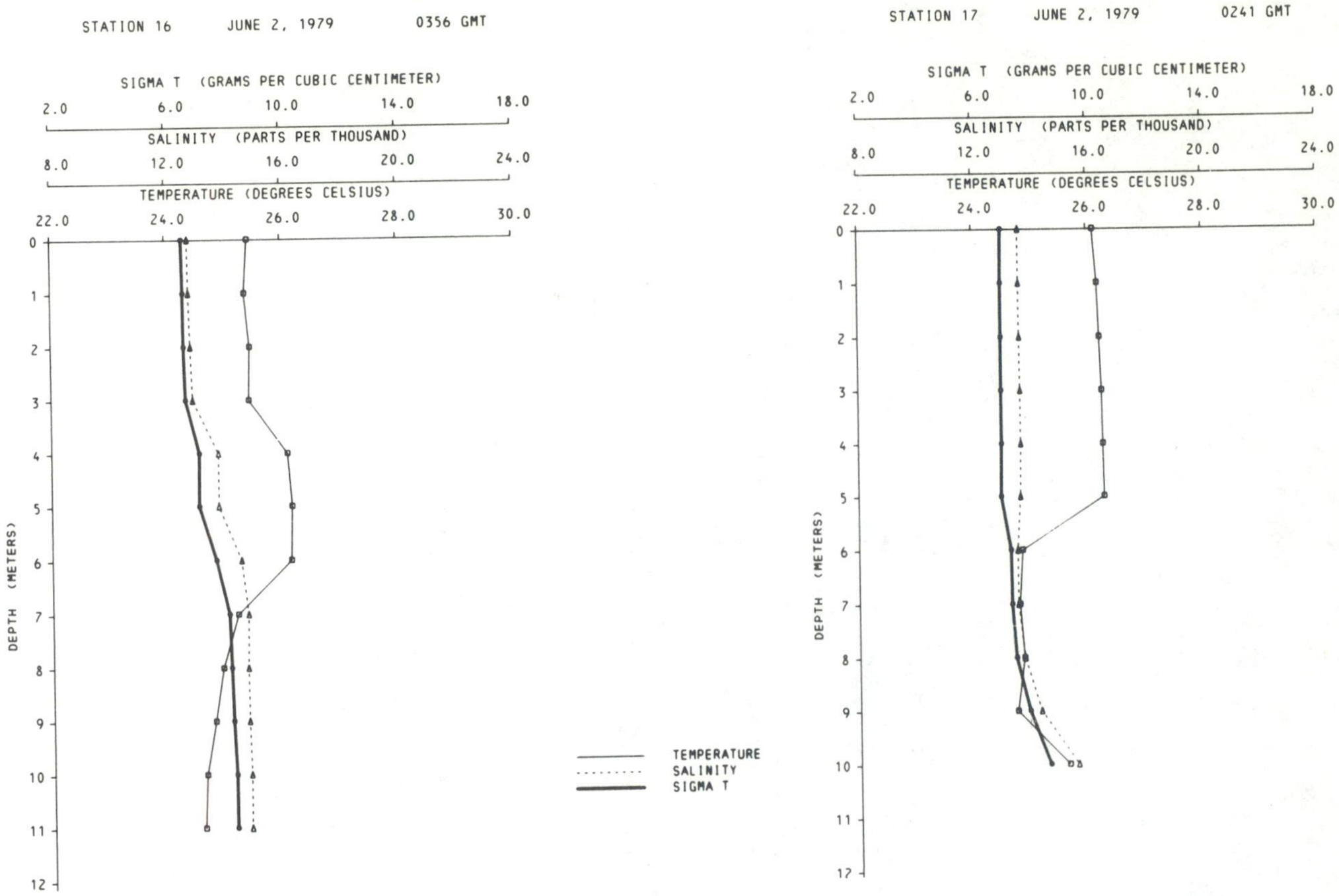

Figure C-14. Vertical profiles of temperature, salinity, and sigma-t for June 2, 1979, at stations 16 and 17.

APPENDIX D.

TIME SERIES PLOTS OF CURRENT SPEED AND DIRECTION FOR OBSERVATIONS 3 m ABOVE THE BOTTOM AT STATION 11.

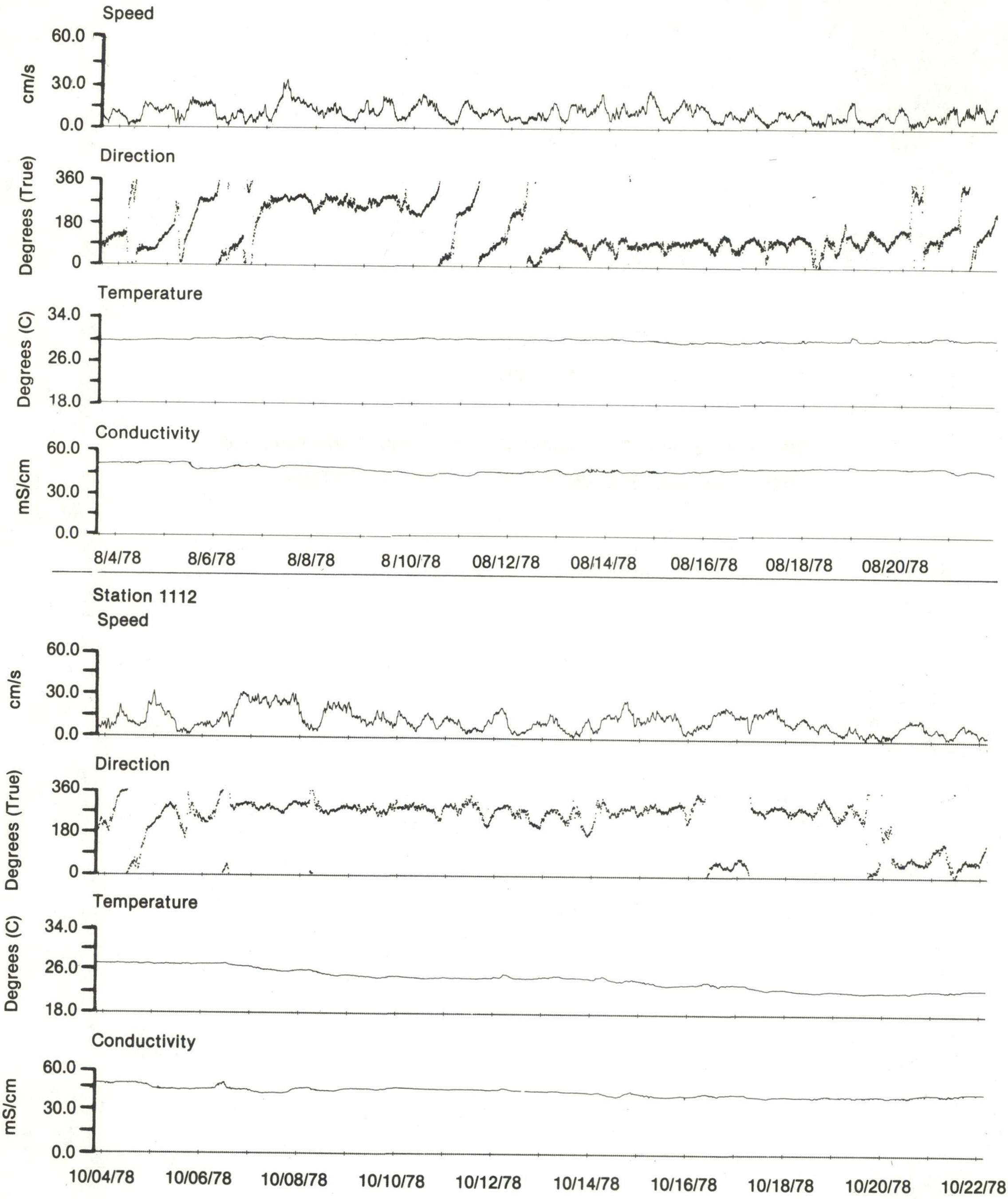

Figure D-1. Time series of current meter data at station 11, 3 m above bottom, for August 3 to August 29, 1978, and October 4 to October 31, 1978.

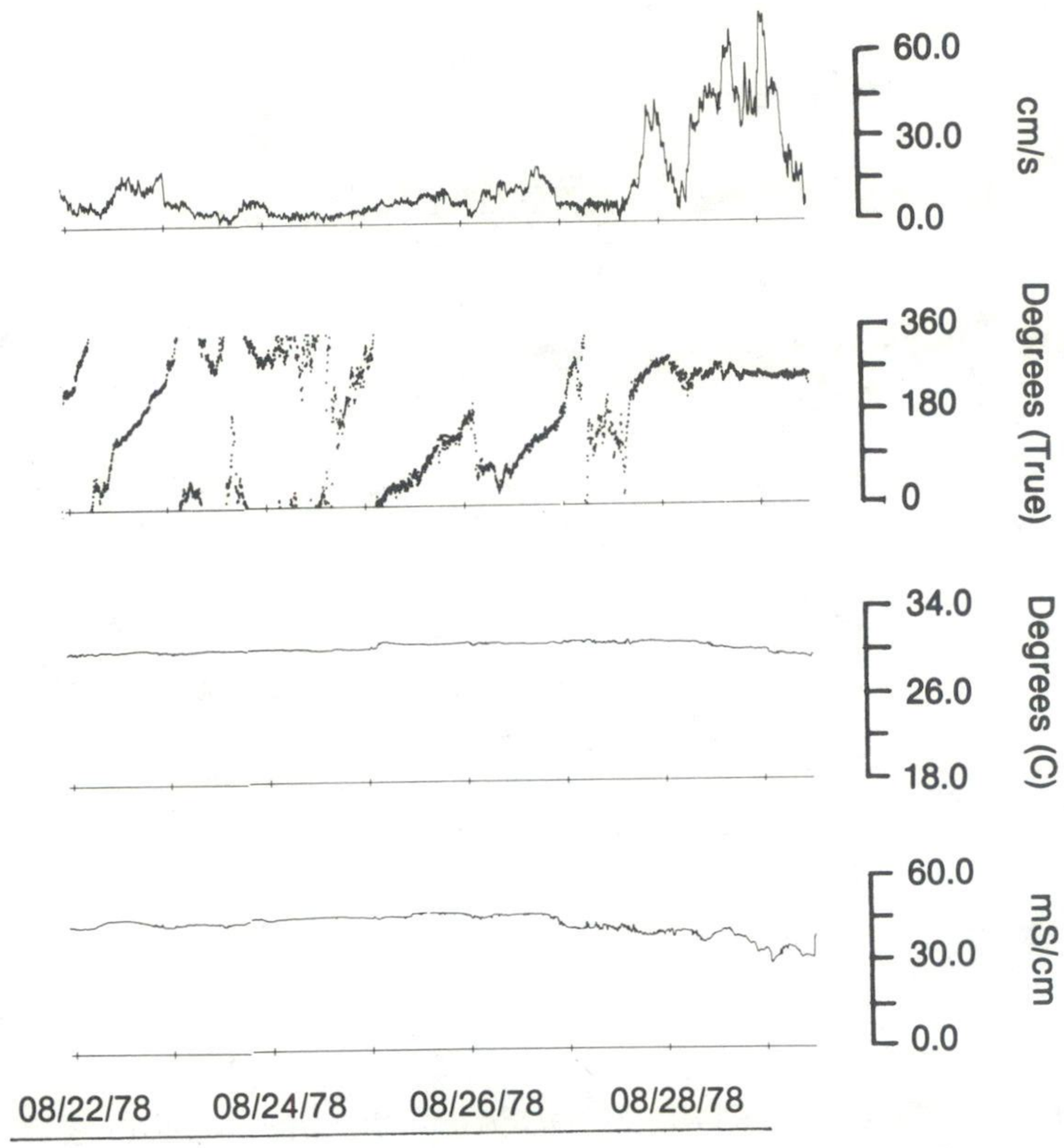

Figure D-1. Time series of current meter data at station 11, 3 m above bottom, for August 3 to August 29, 1978, and October 4 to October 31, 1978.

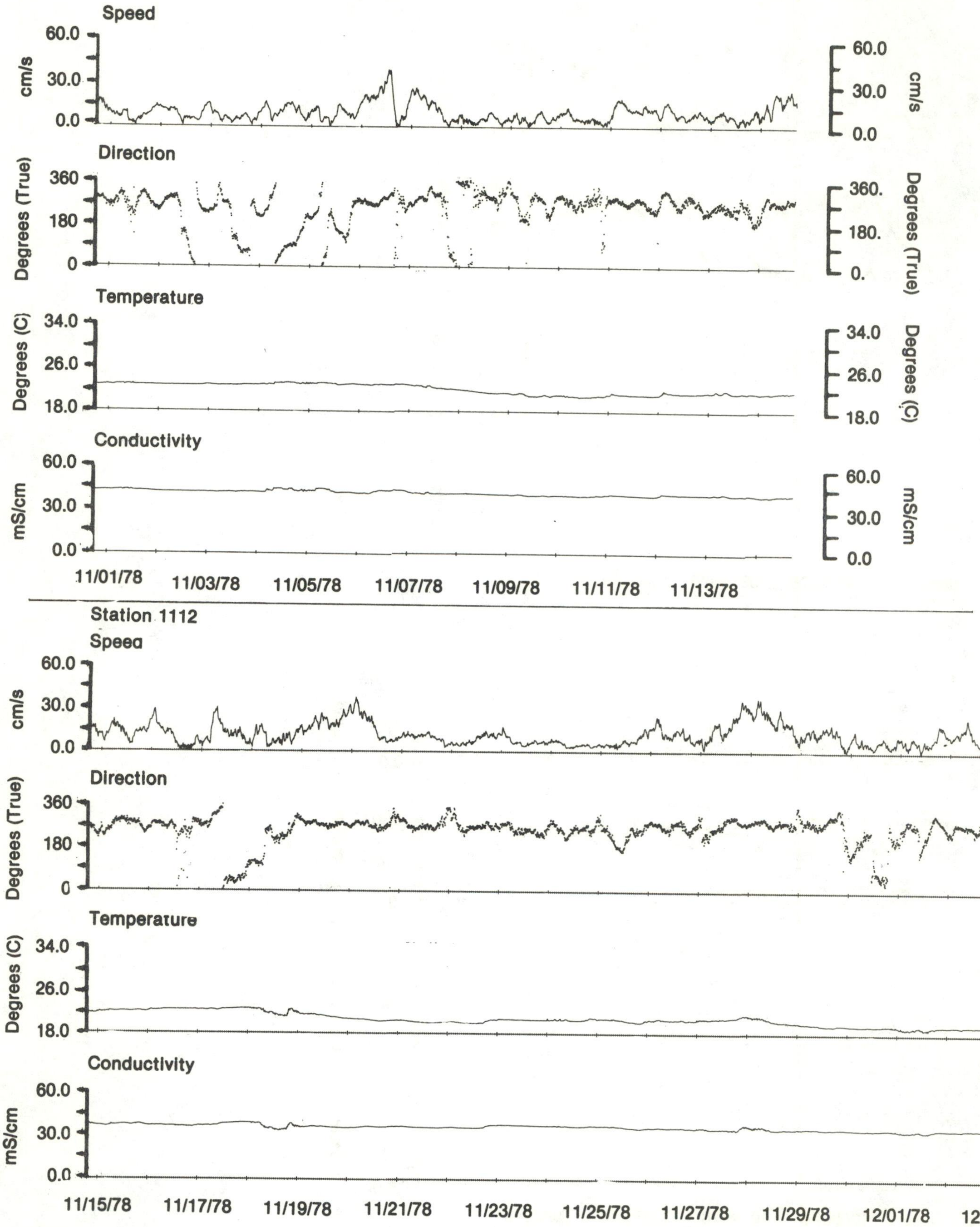

Figure D-2. Times series of current meter data at station 11, 3 m above bottom, for November 1 to November 14, 1978, and November 15 to December 7, 1978.

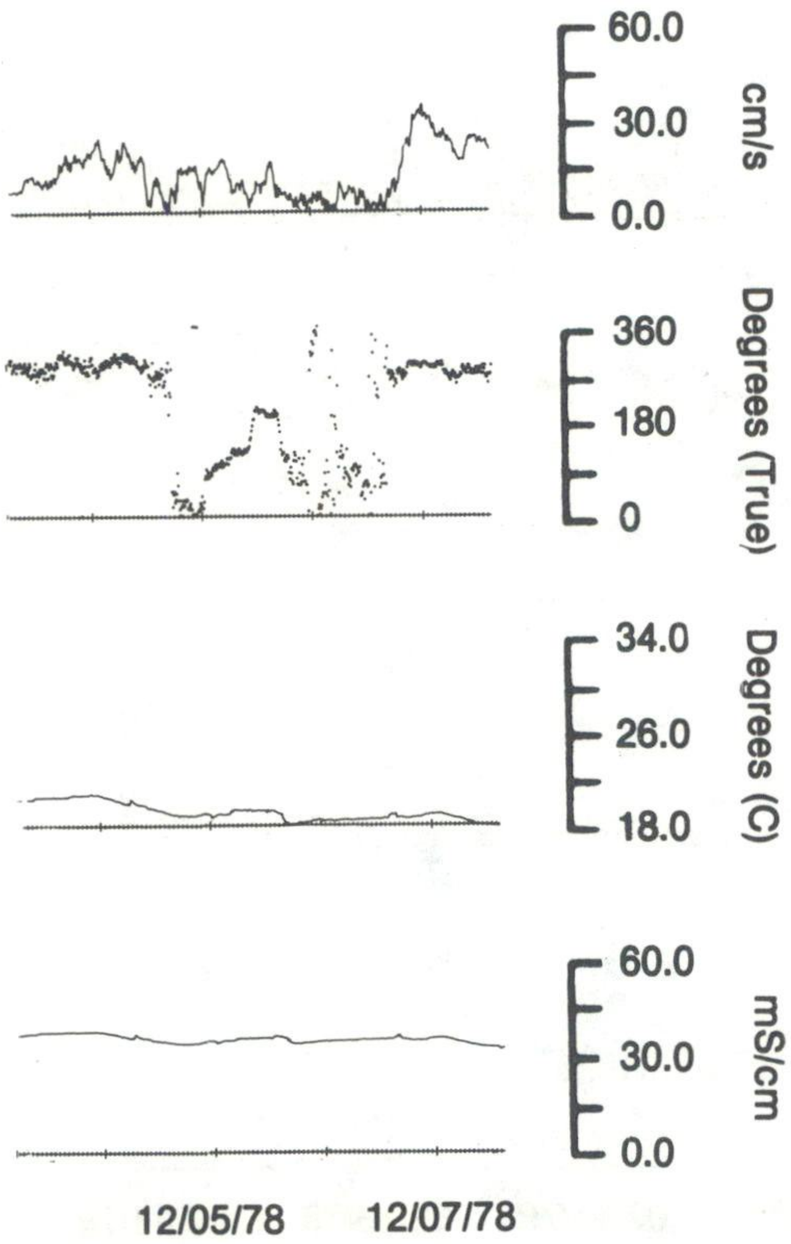

Figure D-2. Times series of current meter data at station 11, 3 m above bottom, for November 1 to November 14, 1978, and November 15 to December 7, 1978.

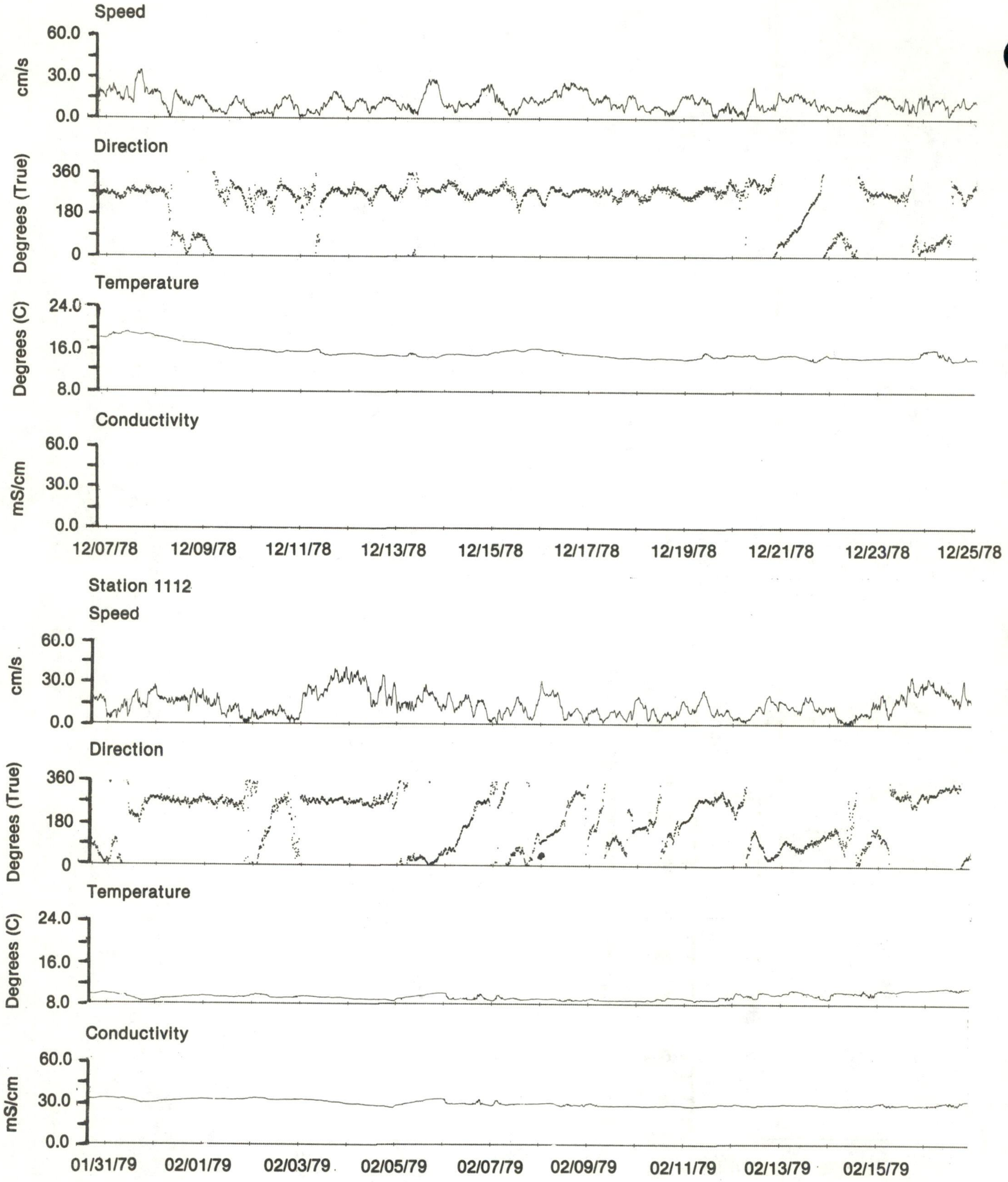

Figure D-3. Time series of current meter data at station 11, 3 m above bottom, for December 7, 1978, to January 7, 1979, and January 31 to February 19, 1979.

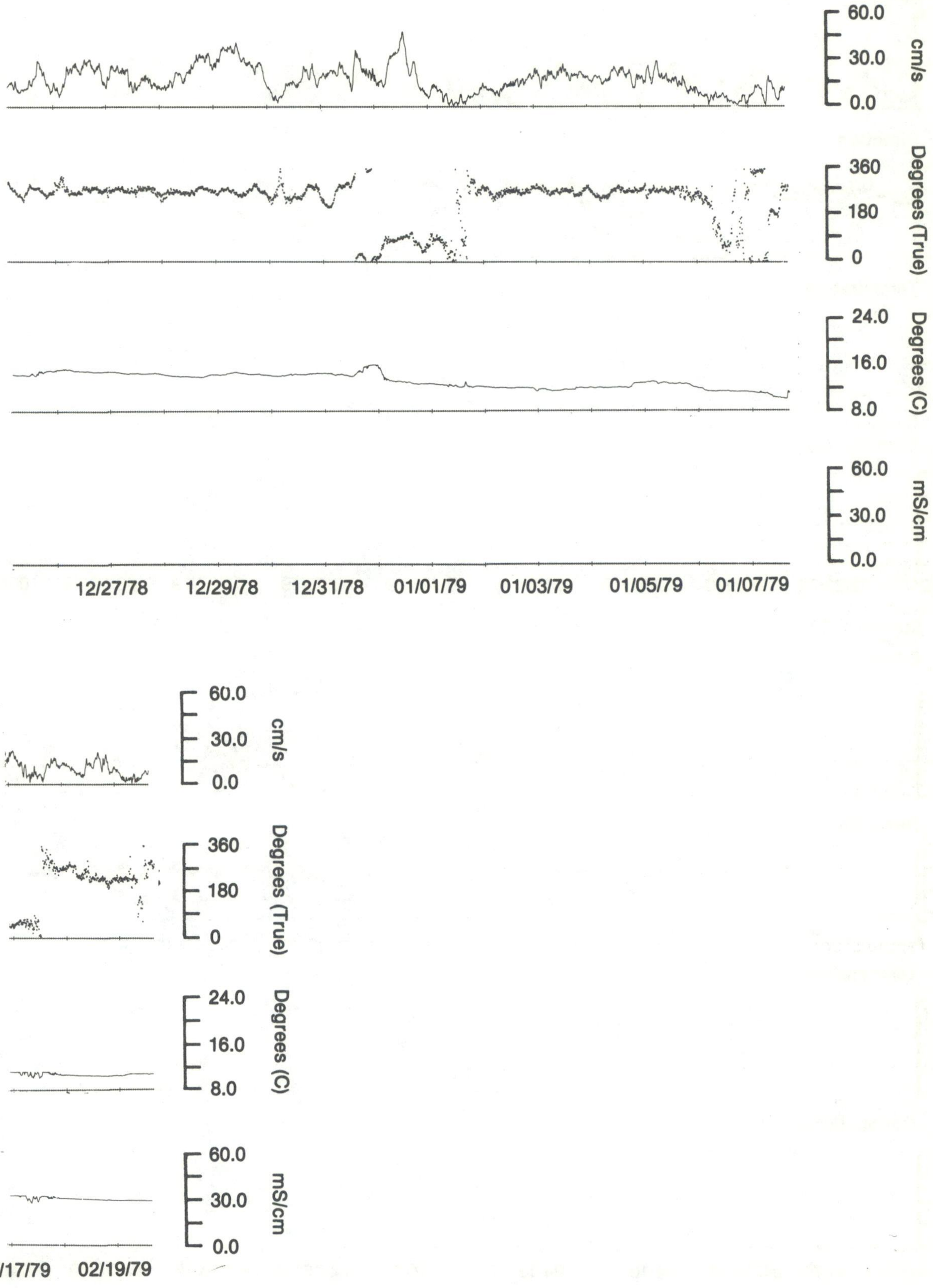

Figure D-3. Time series of current meter data at station 11, 3 m above bottom, for December 7, 1978, to January 7, 1979, and January 31 to February 19, 1979.

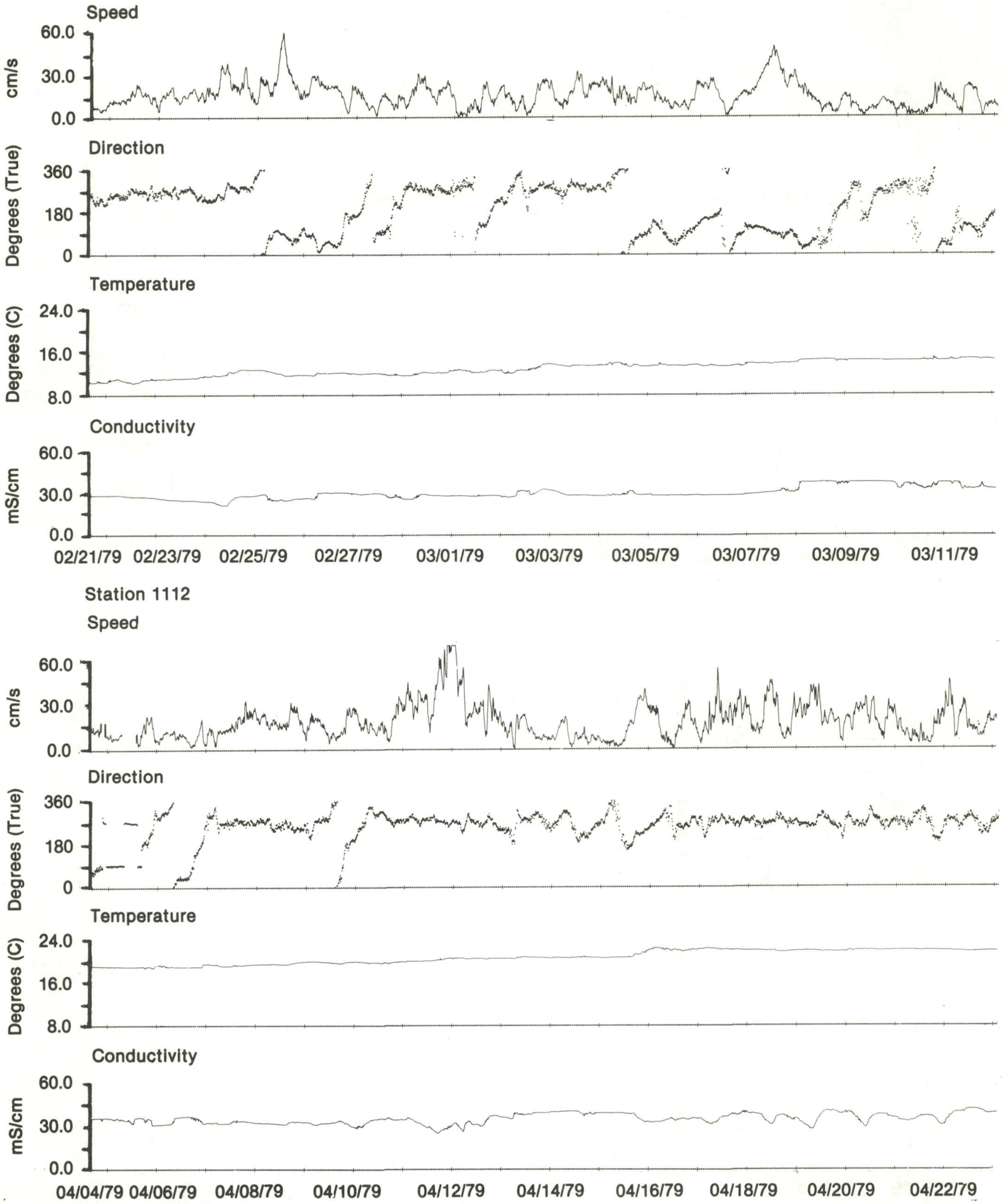

Figure D-4. Time series of current meter data at station 11, 3 m above bottom, for February 21 to March 18, 1979, and April 4 to April 28, 1979.

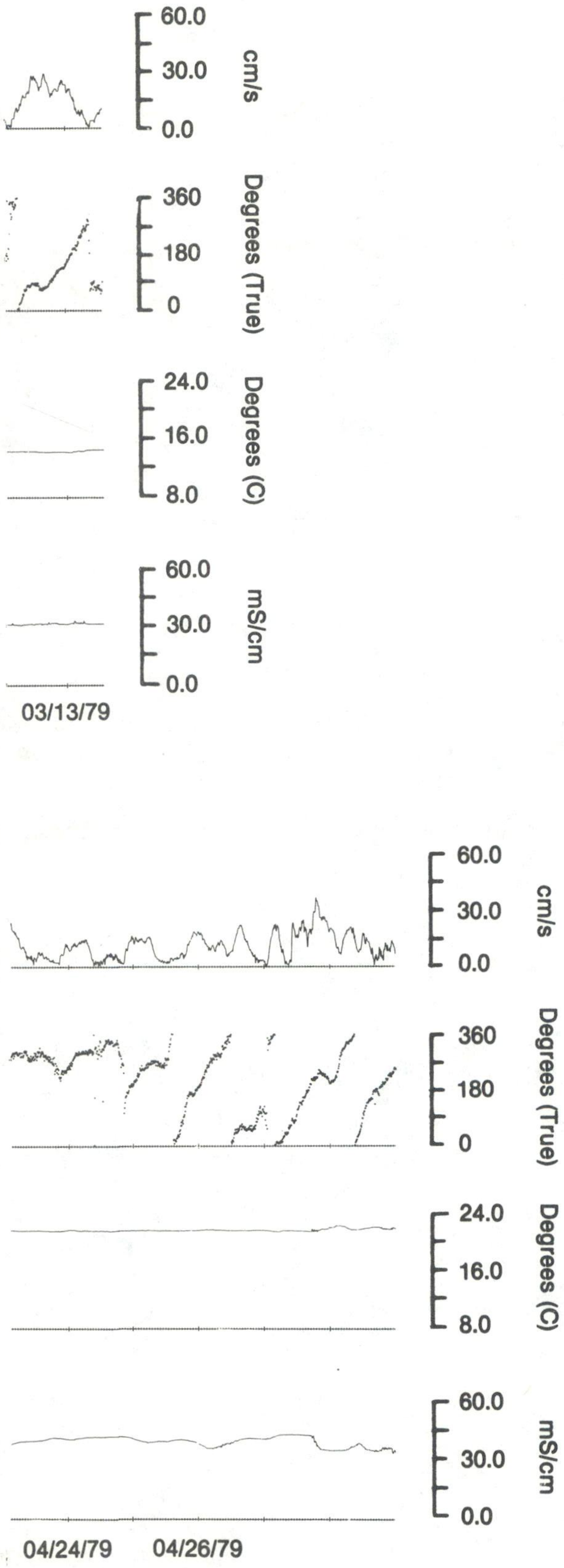

Figure D-4. Time series of current meter data at station 11, 3 m above bottom, for February 21 to March 18, 1979, and April 4 to April 28, 1979.

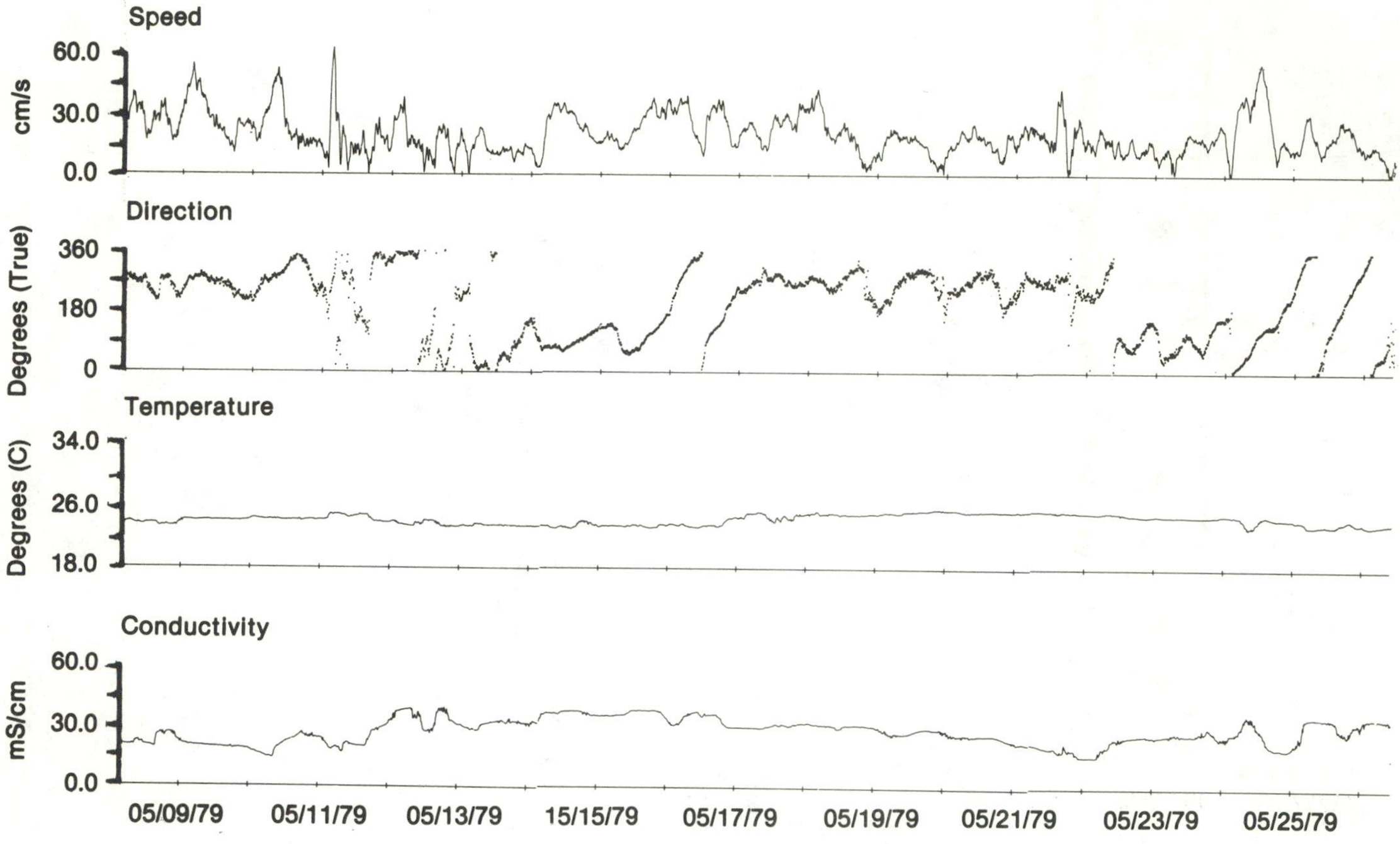

Figure D-5. Time series of current meter data at station 11, 3 m above bottom, for May 8 to May 31, 1979.

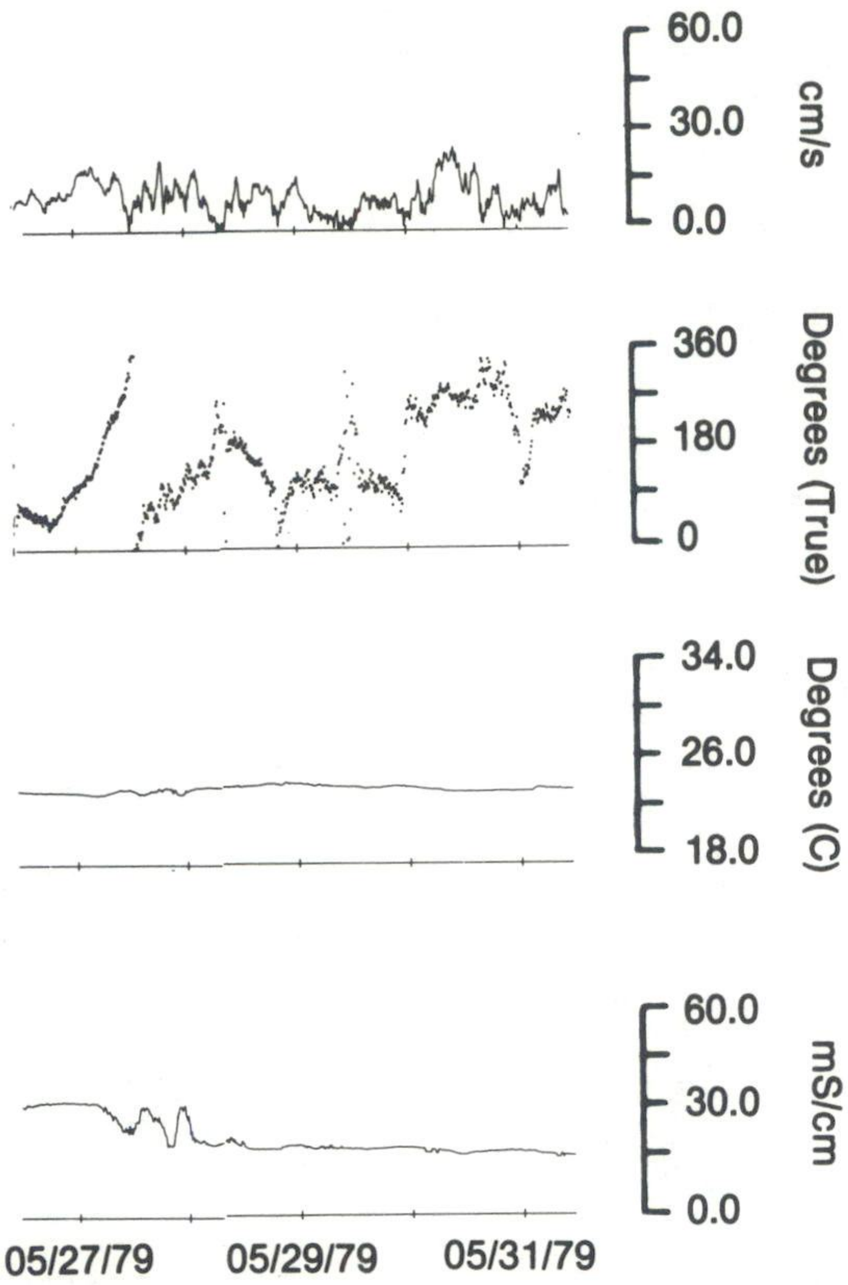

Figure D-5. Time series of current meter data at station 11, 3 m above bottom, for May 8 to May 31, 1979.

APPENDIX E.

TRANSPORTS AND CURRENT VECTOR DIAGRAMS.

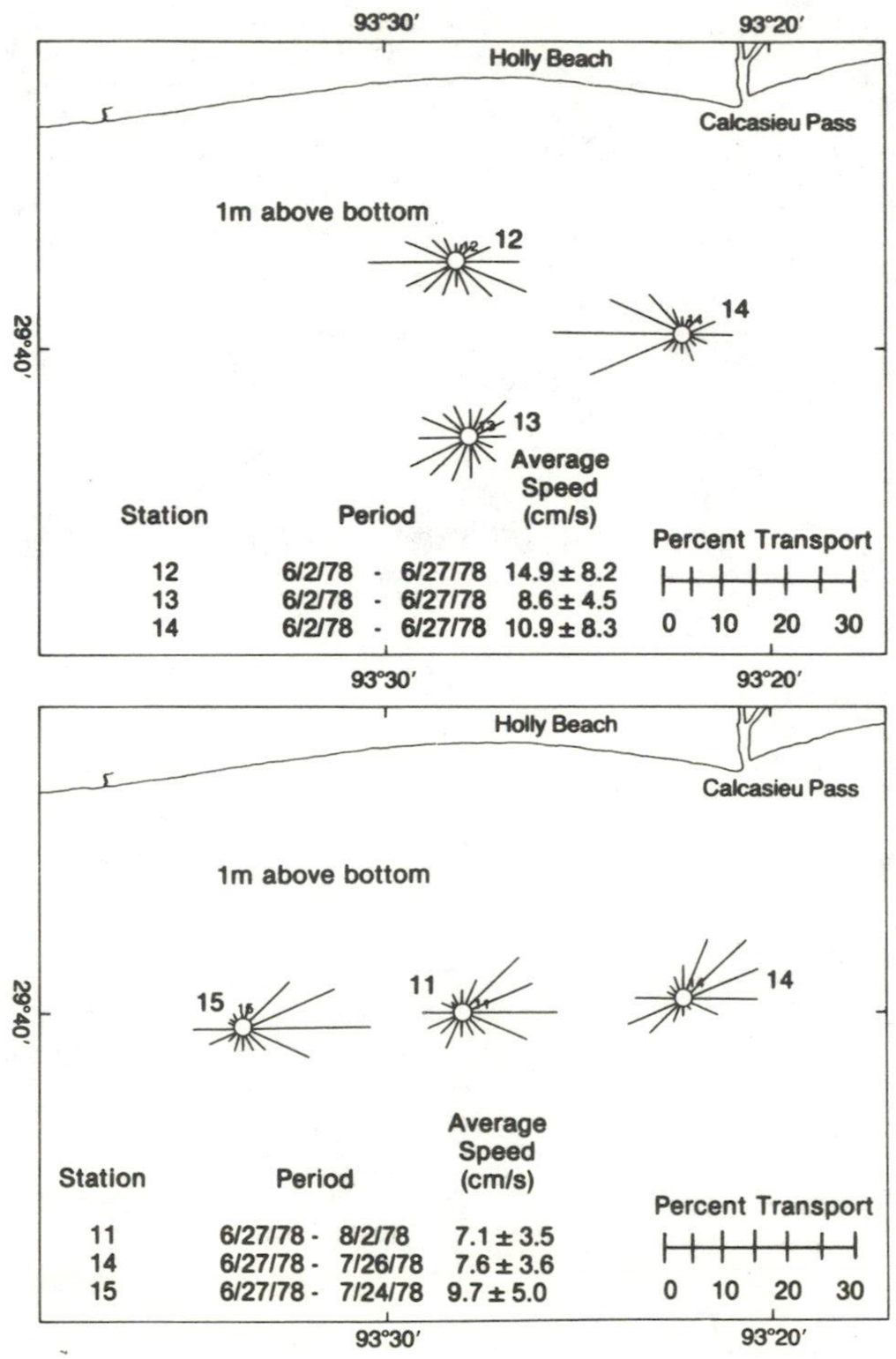

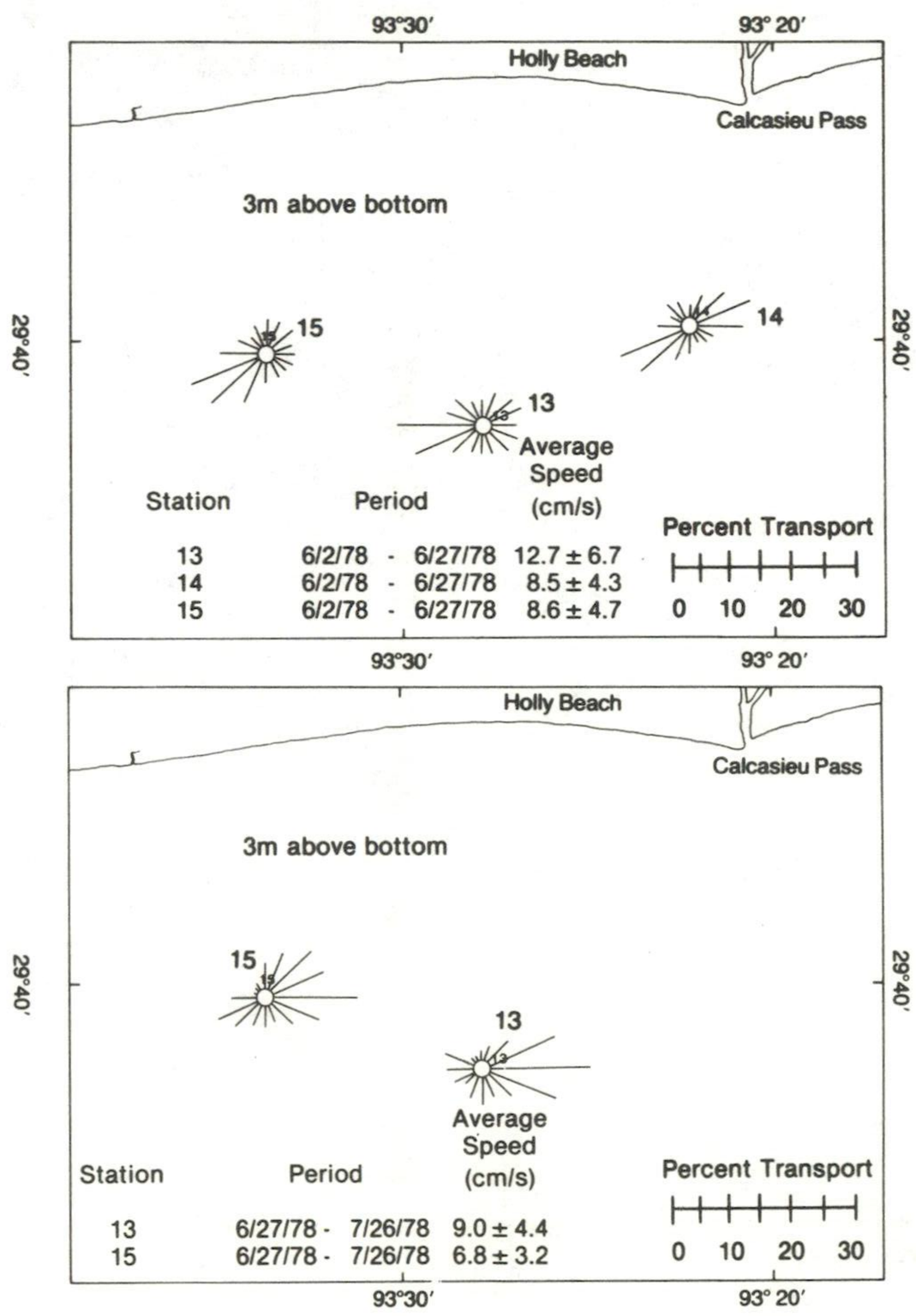

Figure E-1. Relative volume transports at West Hackberry site for June 2 to August 2, 1978.

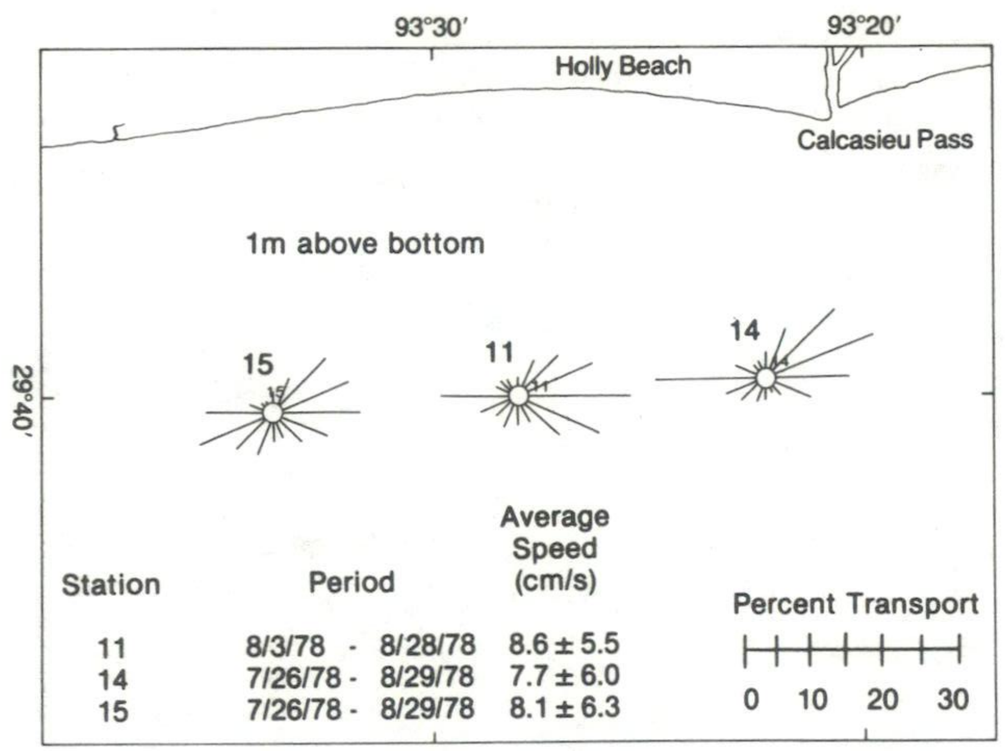

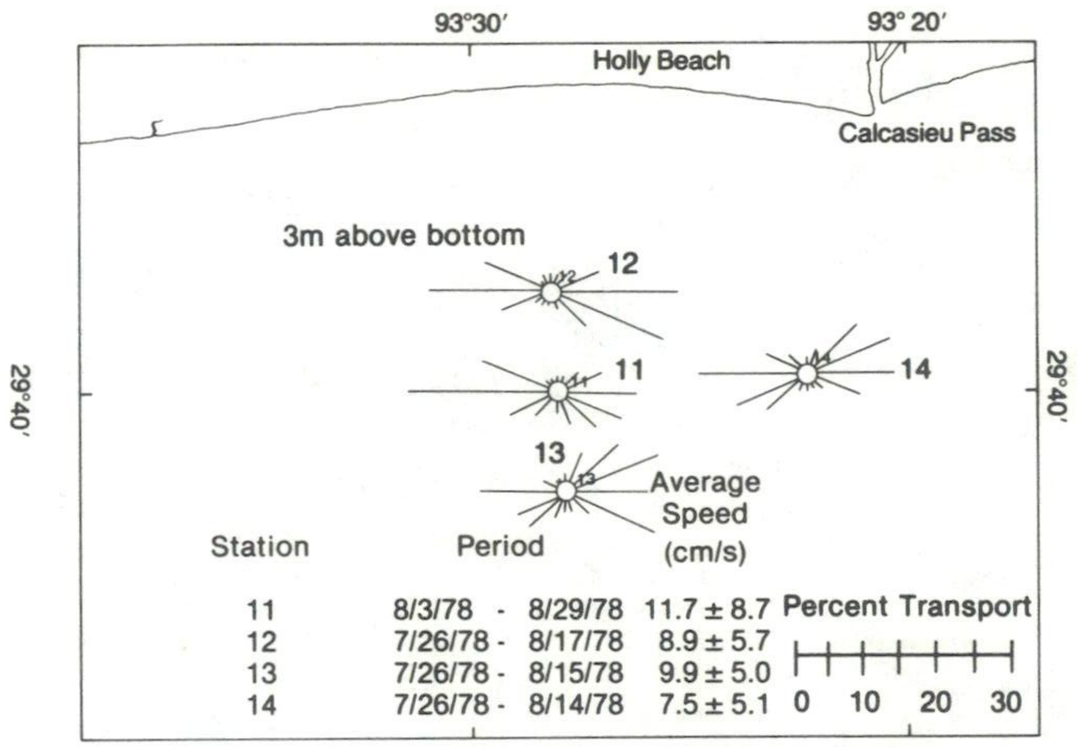

No 1-m level data obtained from September 5, 1978 to October 3, 1978.

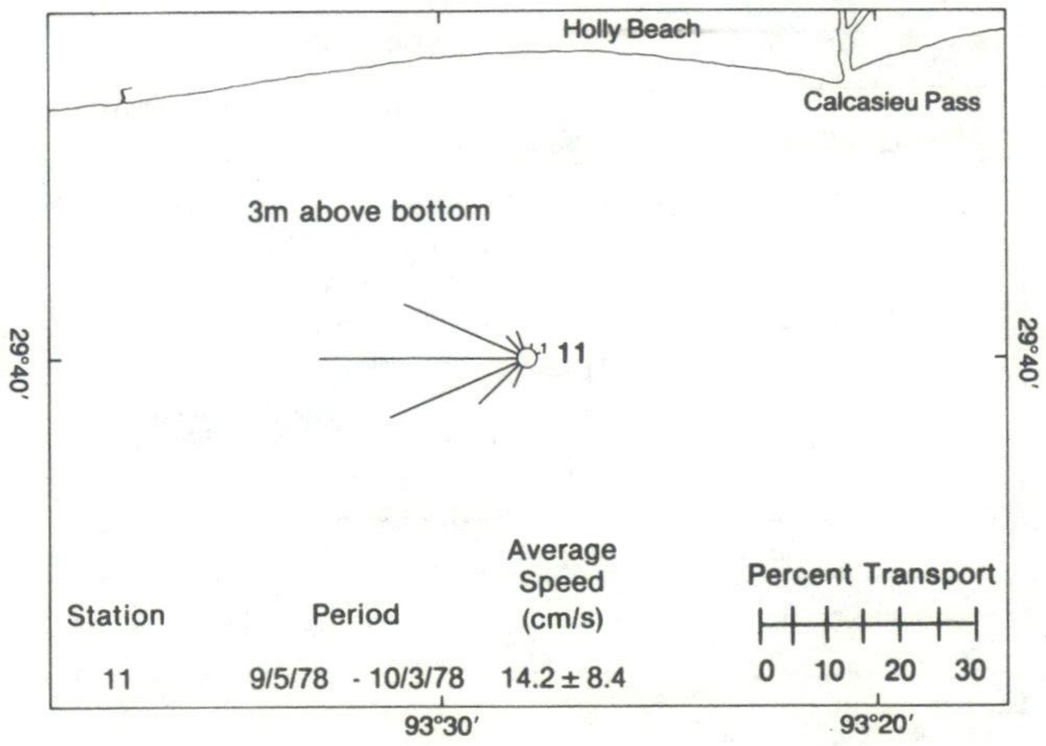

Figure E-2. Relative volume transports at West Hackberry site for August 3 to October 3, 1978.

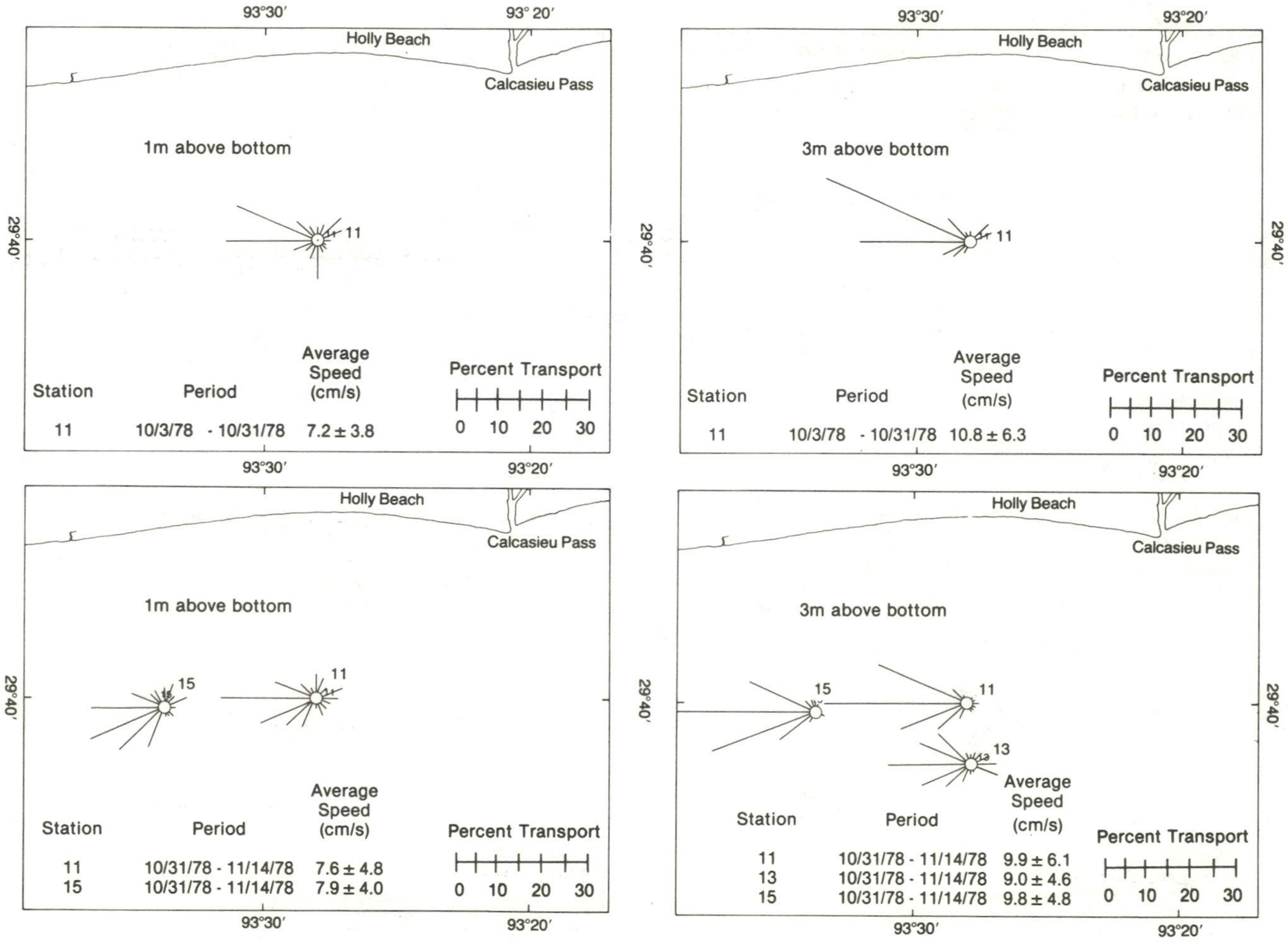

Figure E-3. Relative volume transports at West Hackberry site for October 3 to November 14, 1978.

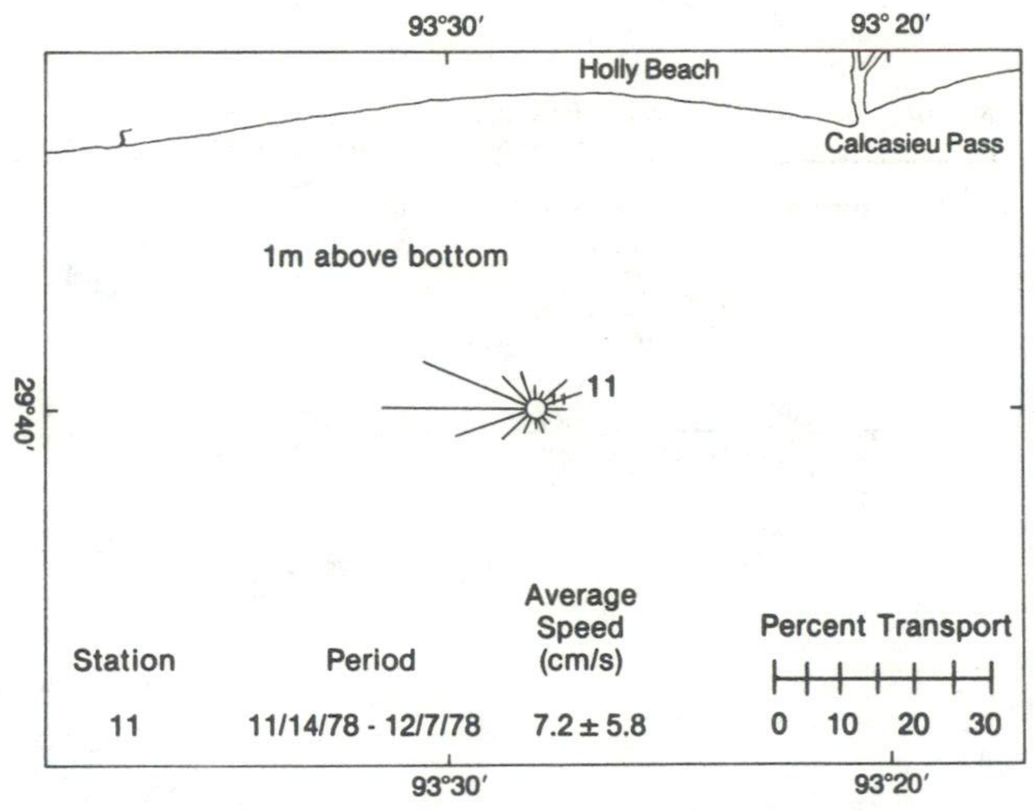

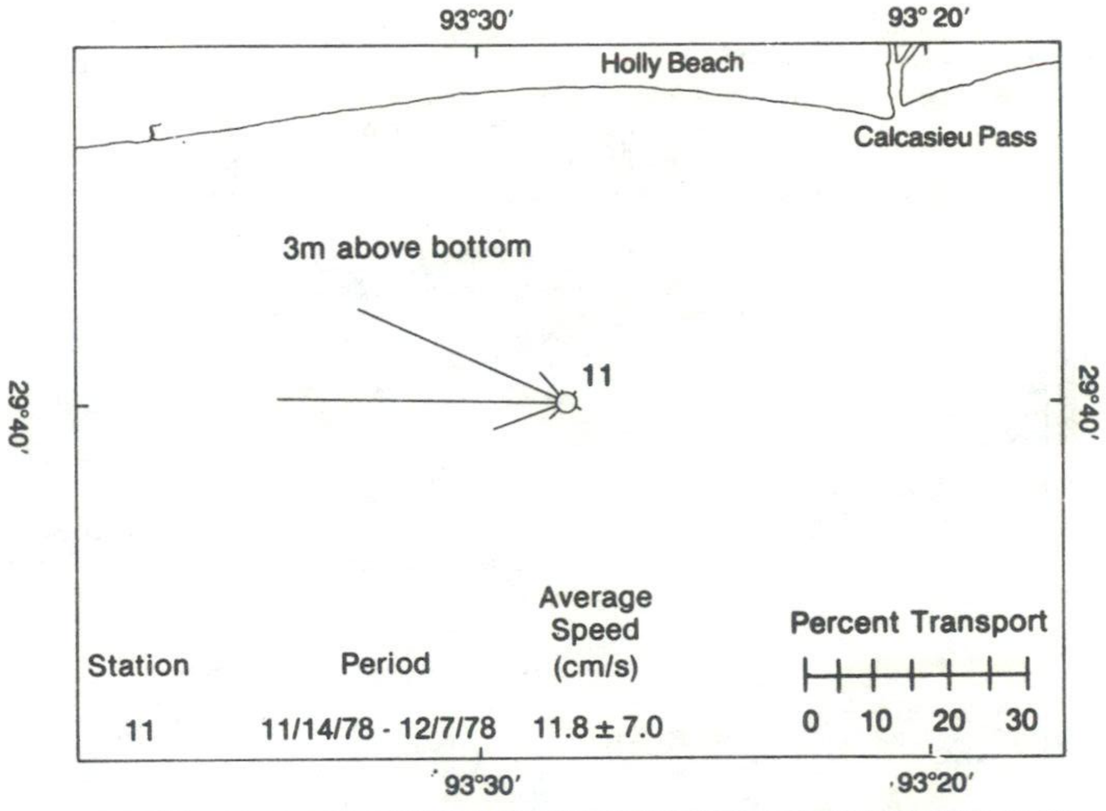

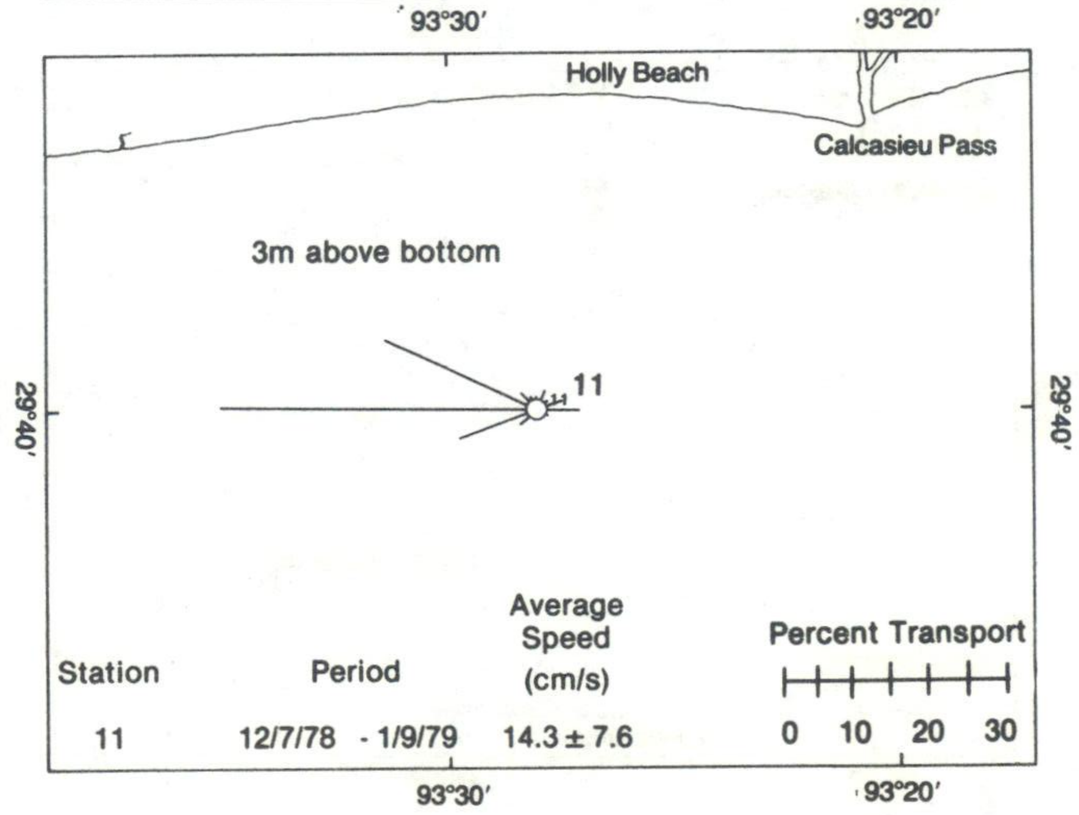

No 1-m level data obtained from December 7, 1978 to January 9, 1979.

Figure E-4. Relative volume transports at West Hackberry site for November 14, 1978 to January 9, 1979.

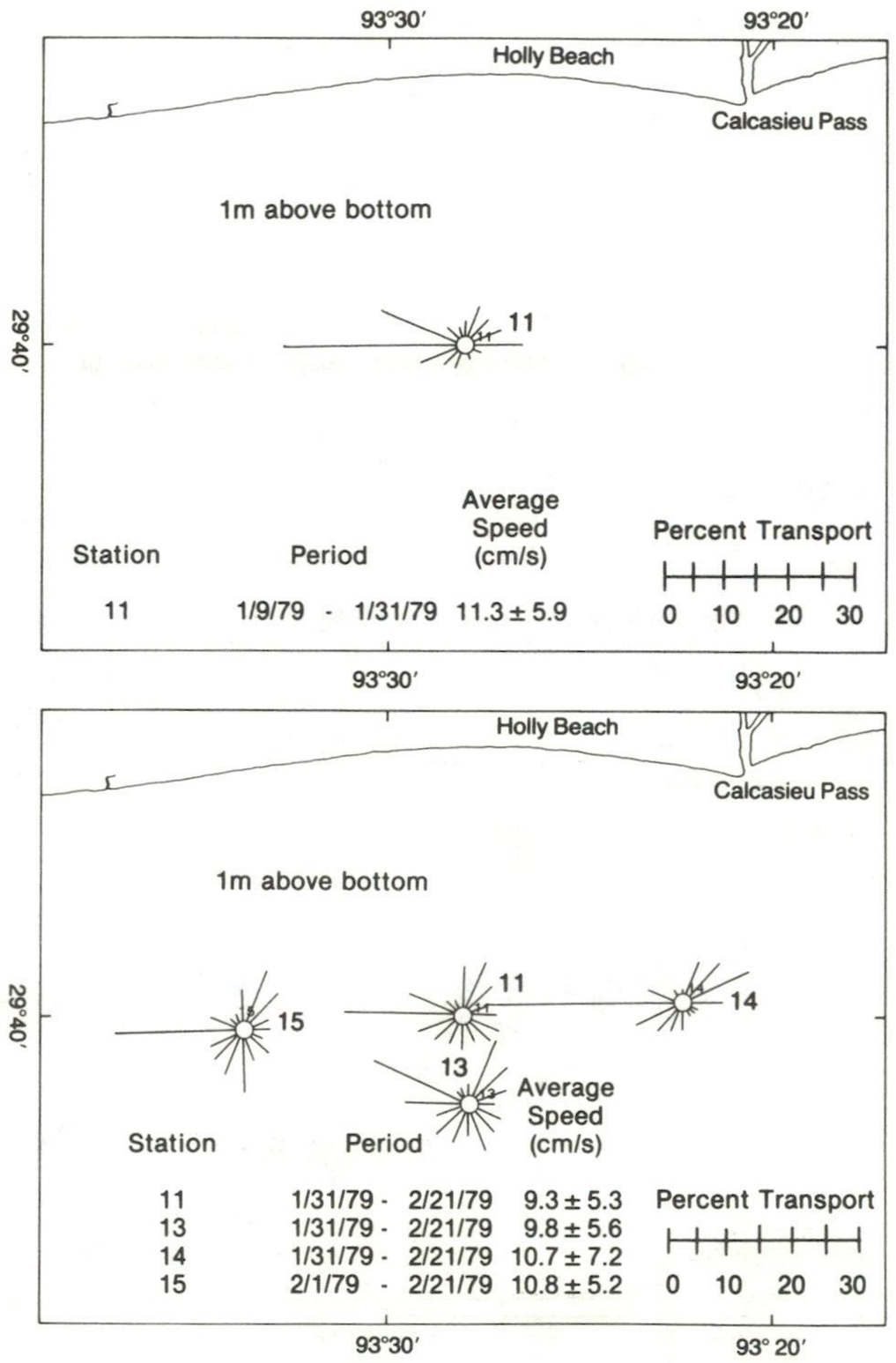

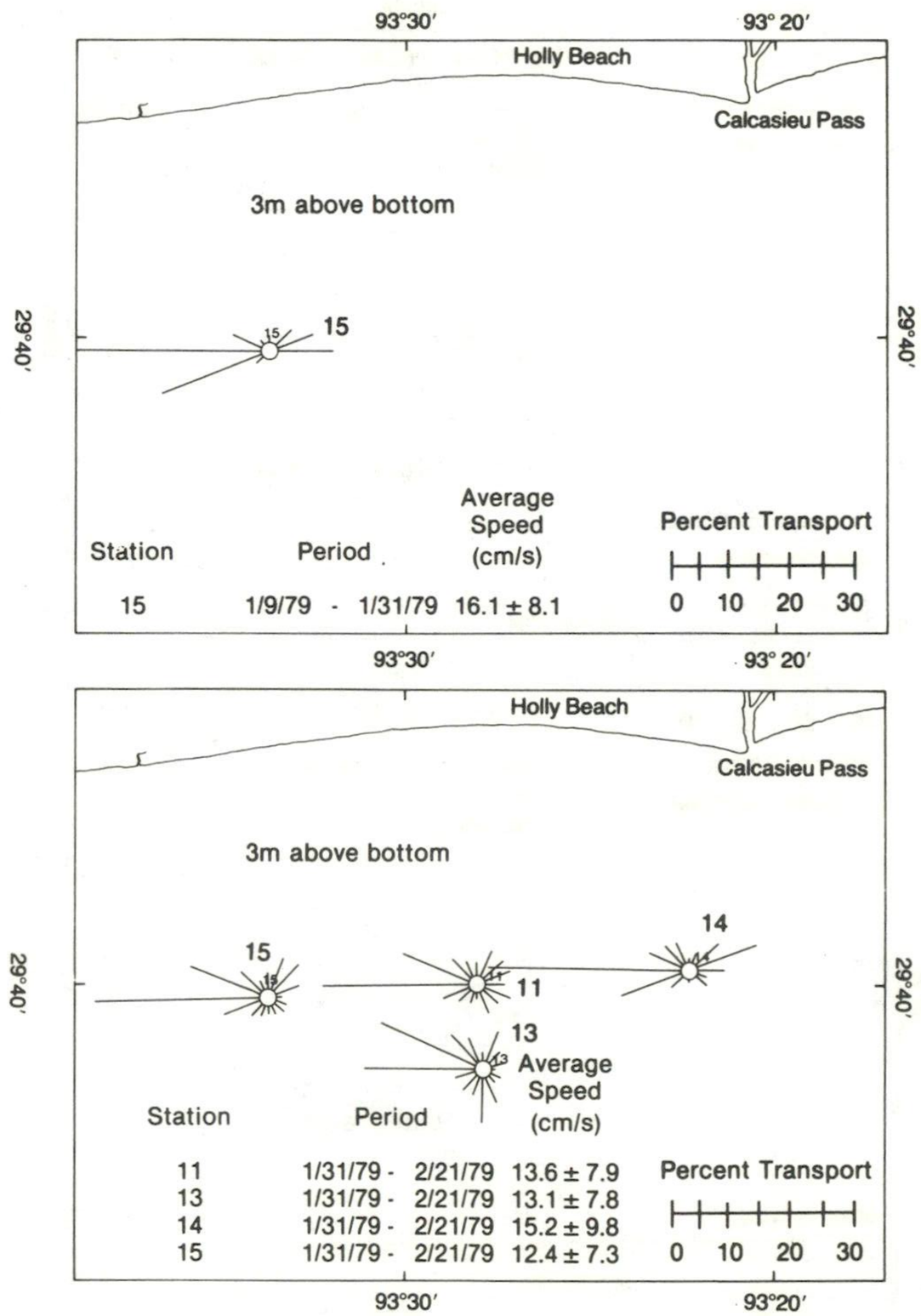

Figure E-5. Relative volume transports at West Hackberry site for January 9 to February 21, 1979.

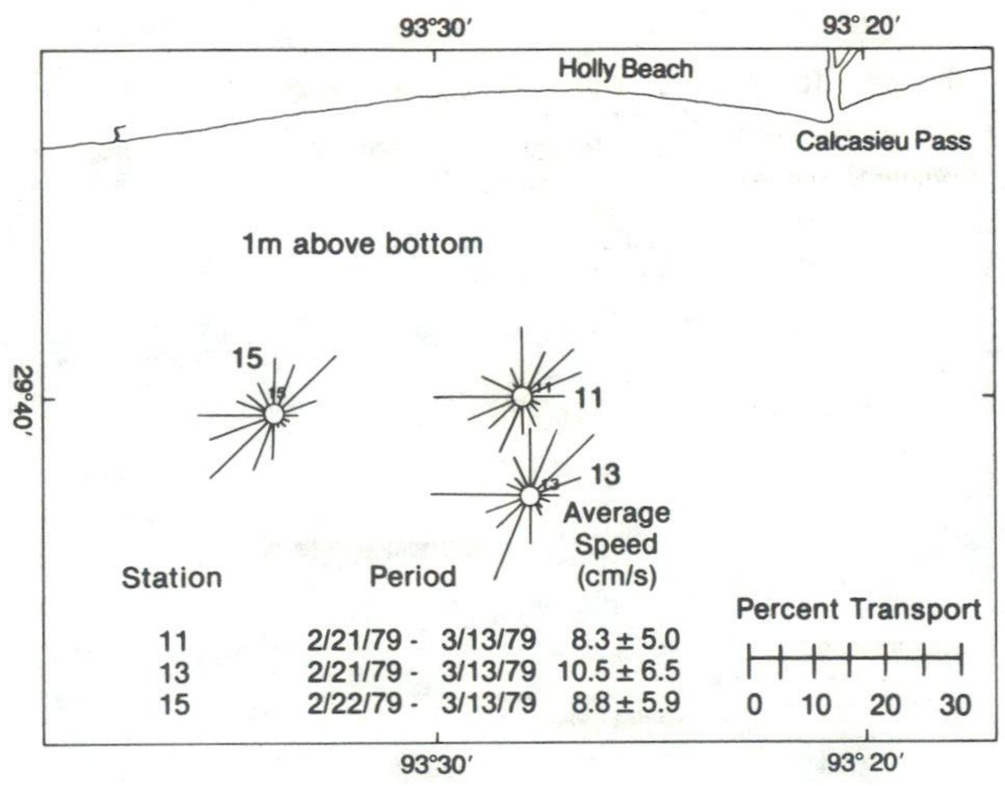

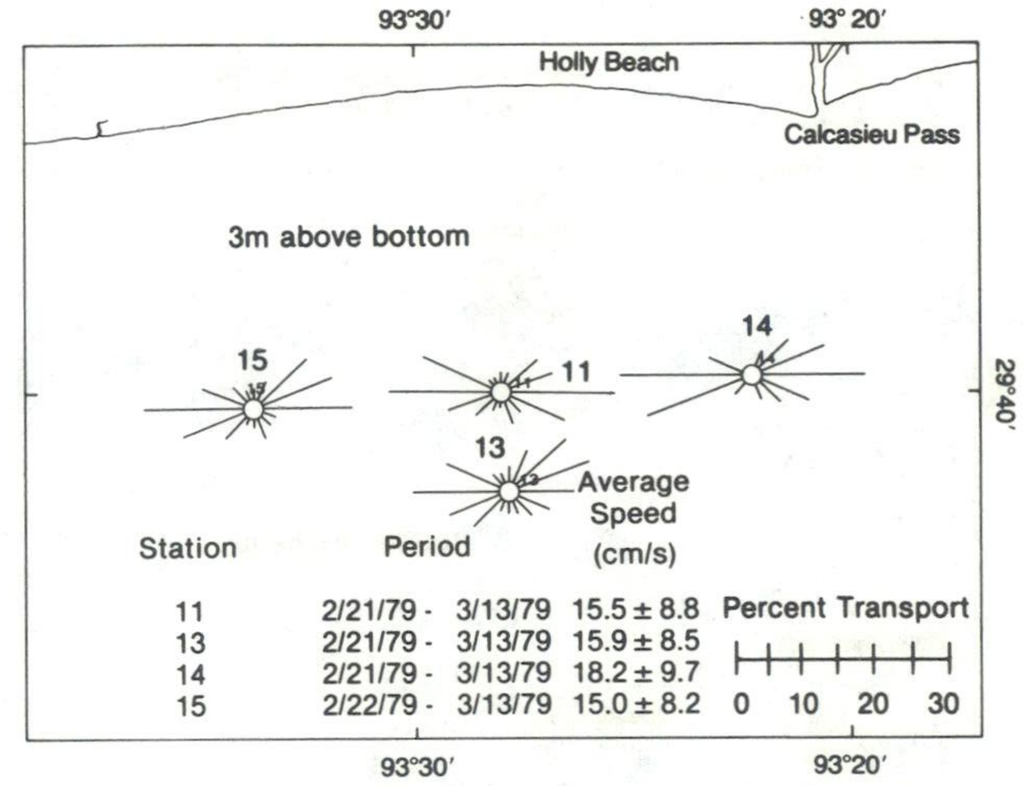

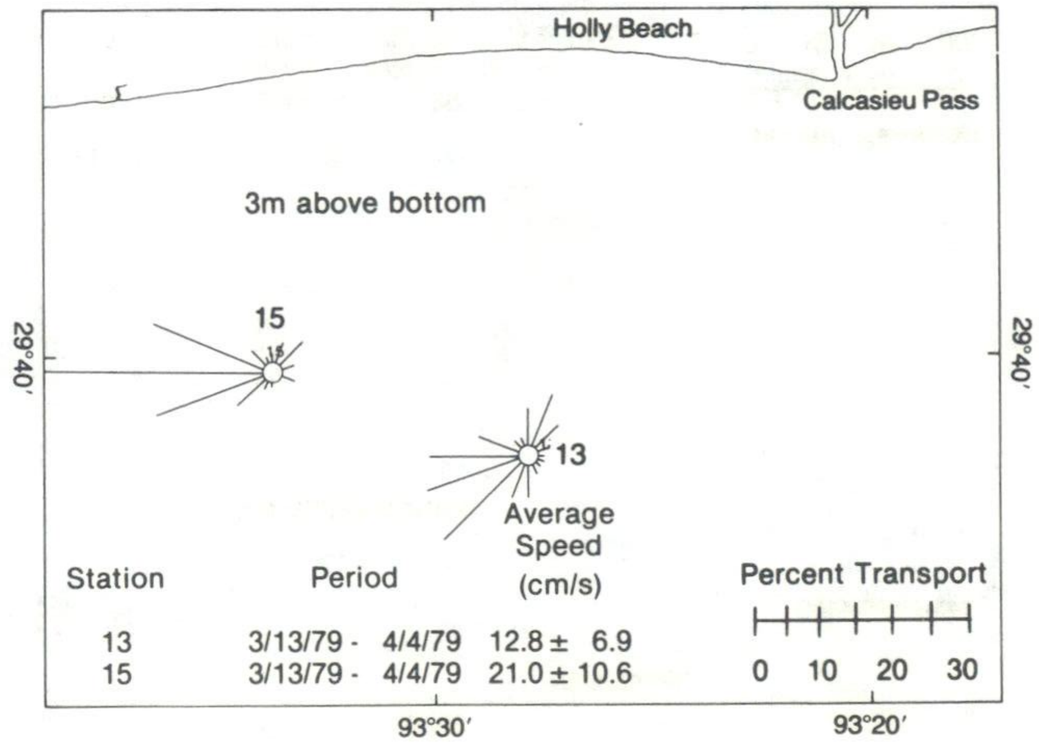

No 1-m level data obtained from March 13, 1979 to April 4, 1979.

Figure E-6. Relative volume transports at West Hackberry site for February 21 to April 4, 1979.

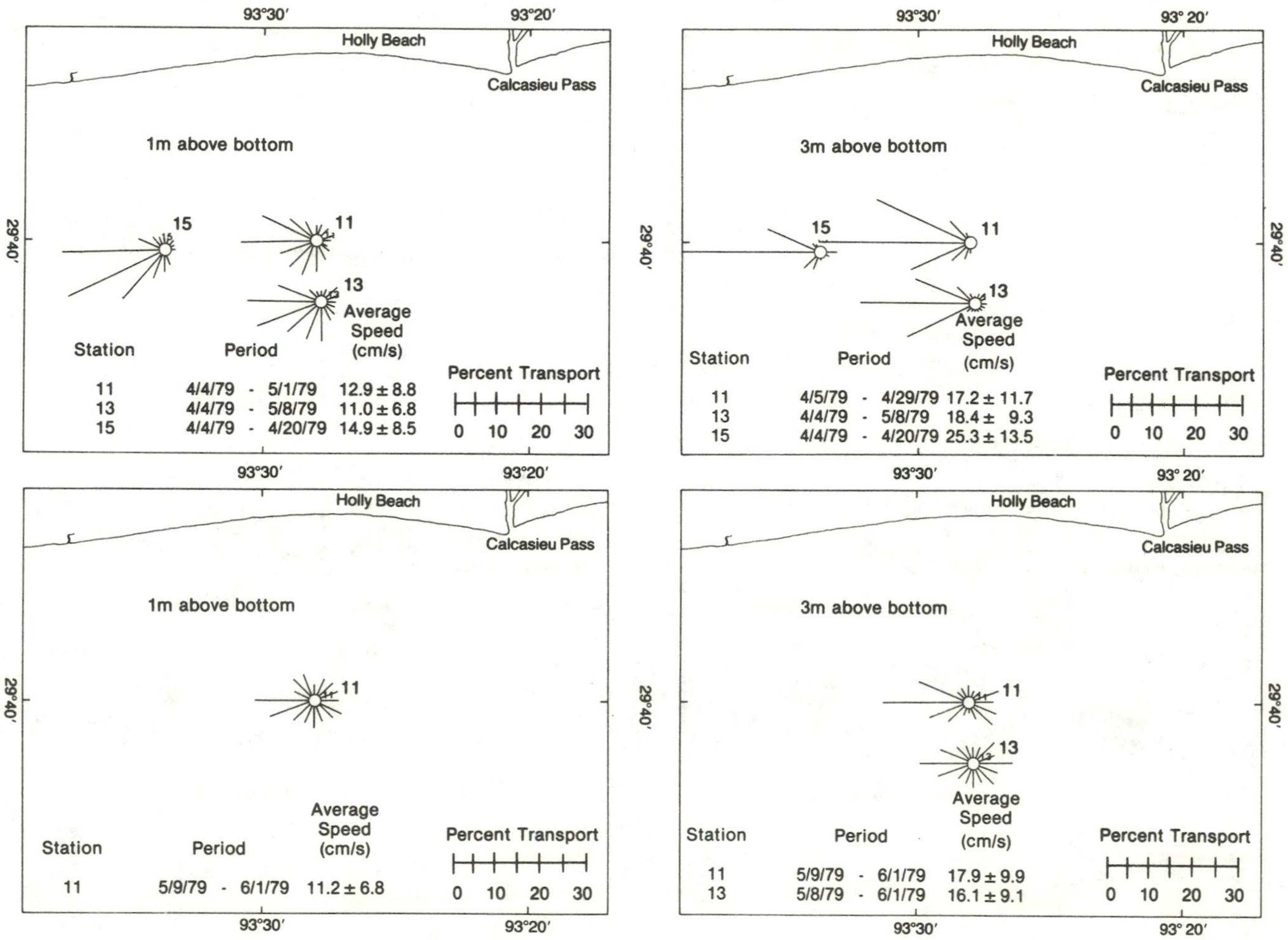

Figure E-7. Relative volume transports at West Hackberry site for April 4 to June 1, 1979.

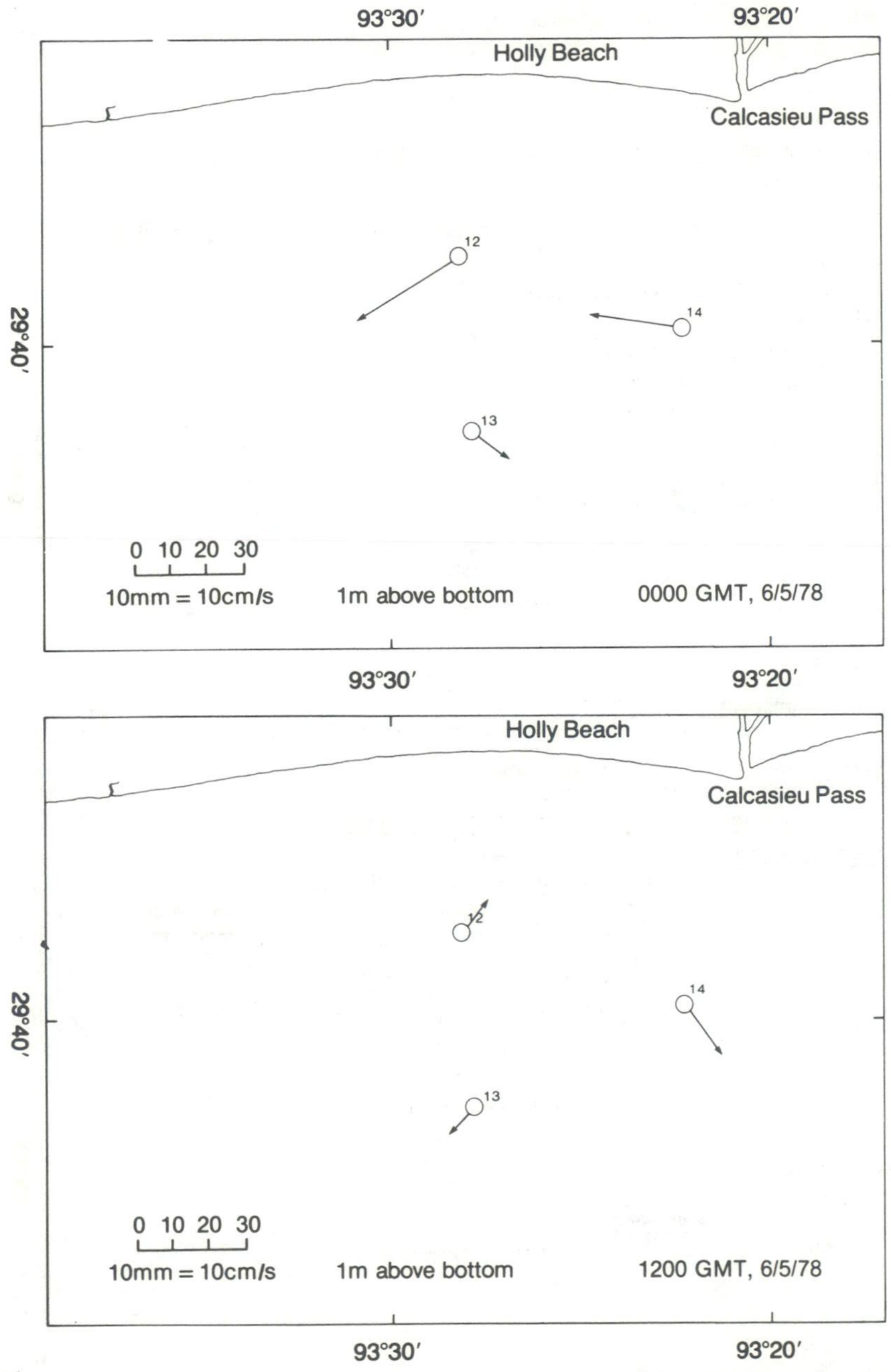

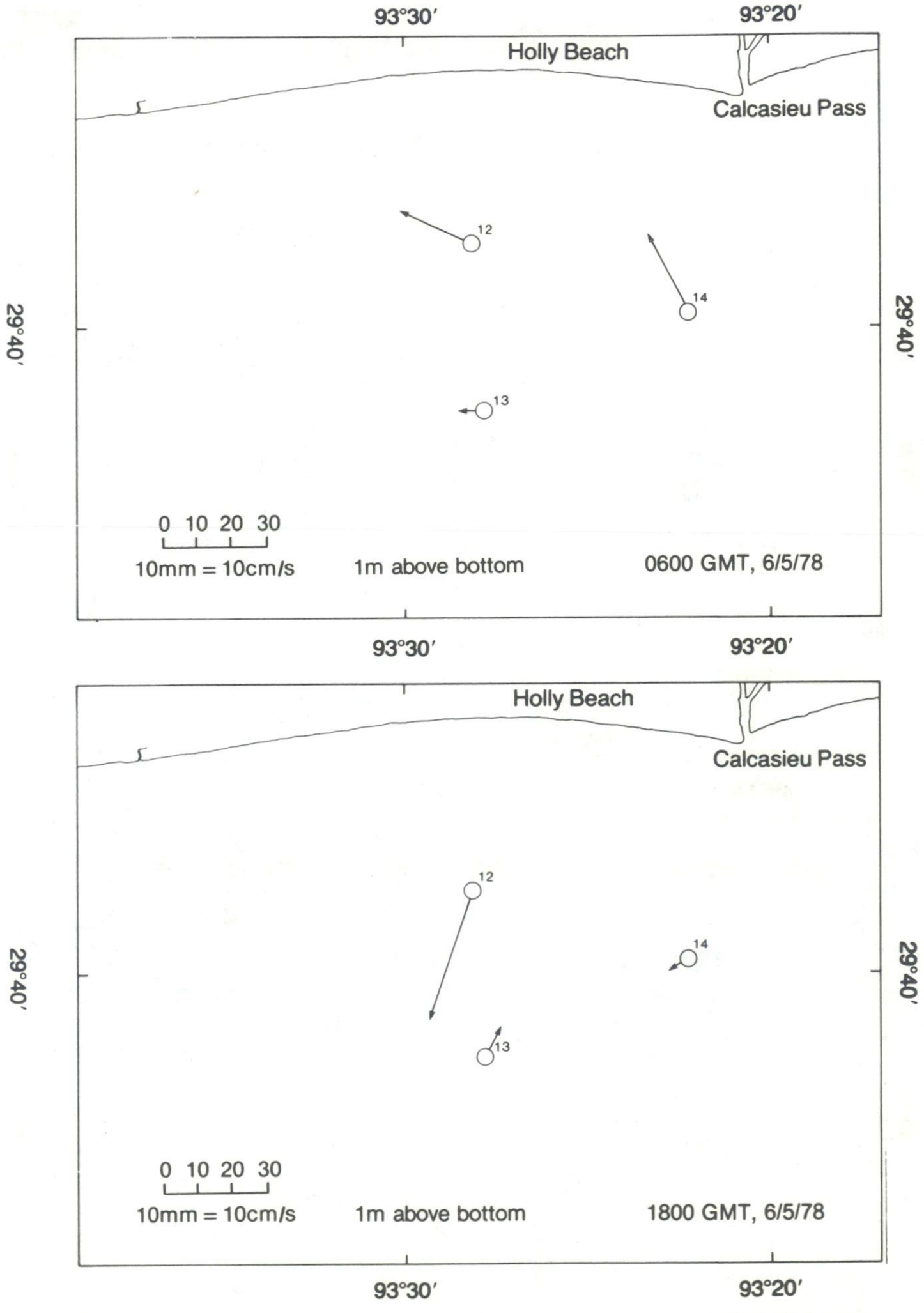

Figure E-8. Current vectors at 6-hour intervals, 1 m above bottom at West Hackberry site, June 5, 1978.

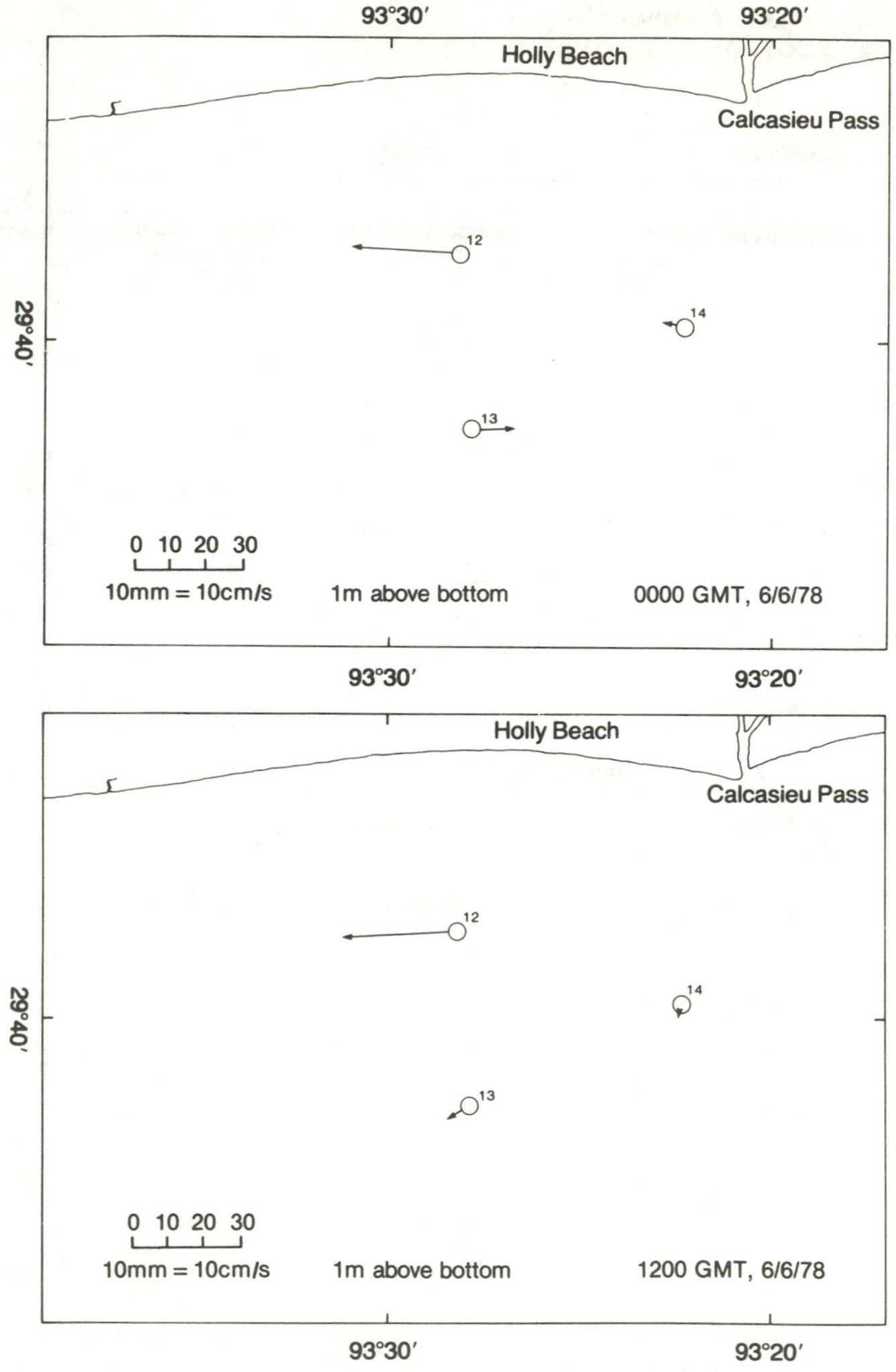

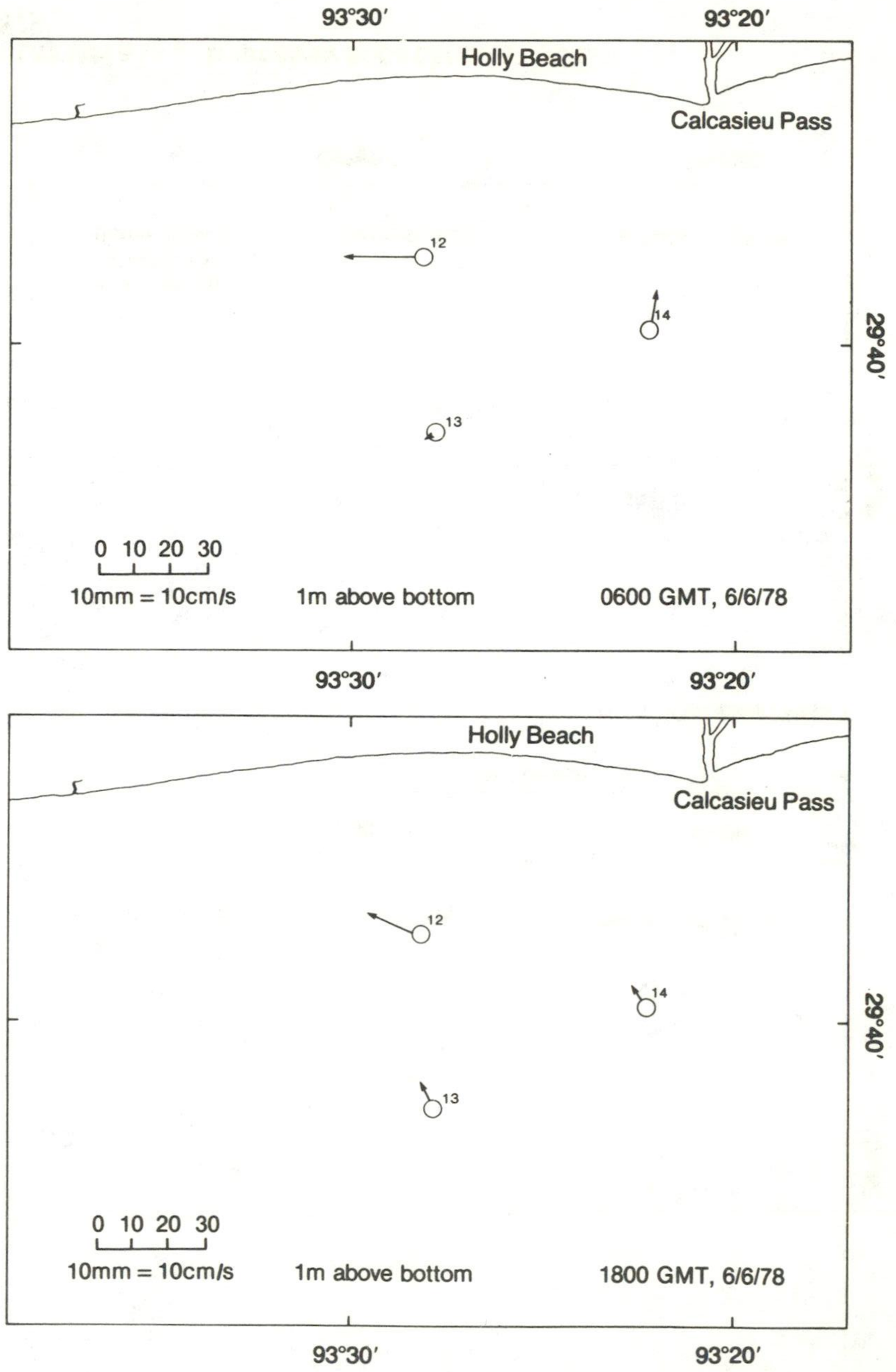

Figure E-9. Current vectors at 6-hour intervals, 1 m above bottom at West Hackberry site, June 6, 1978.

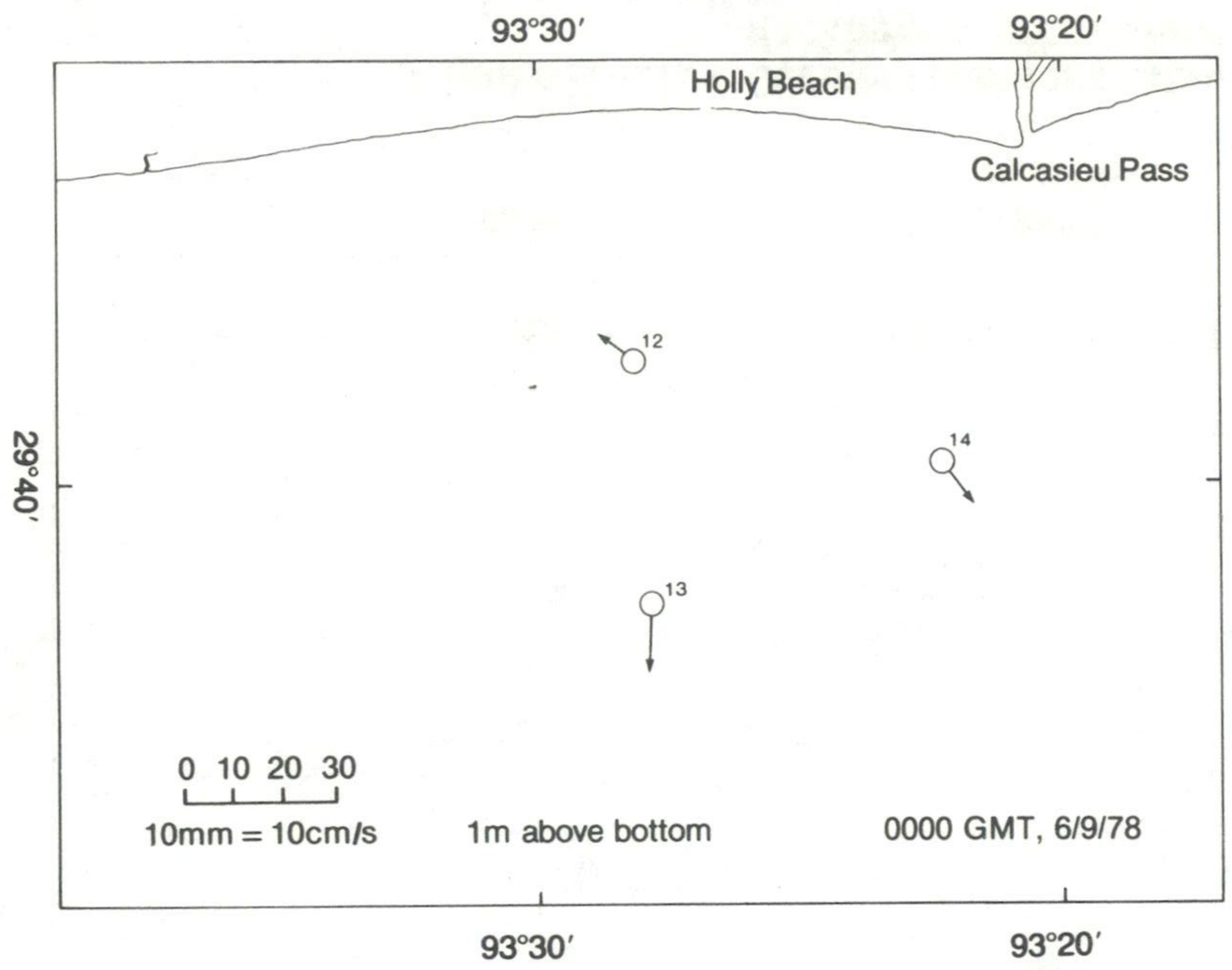

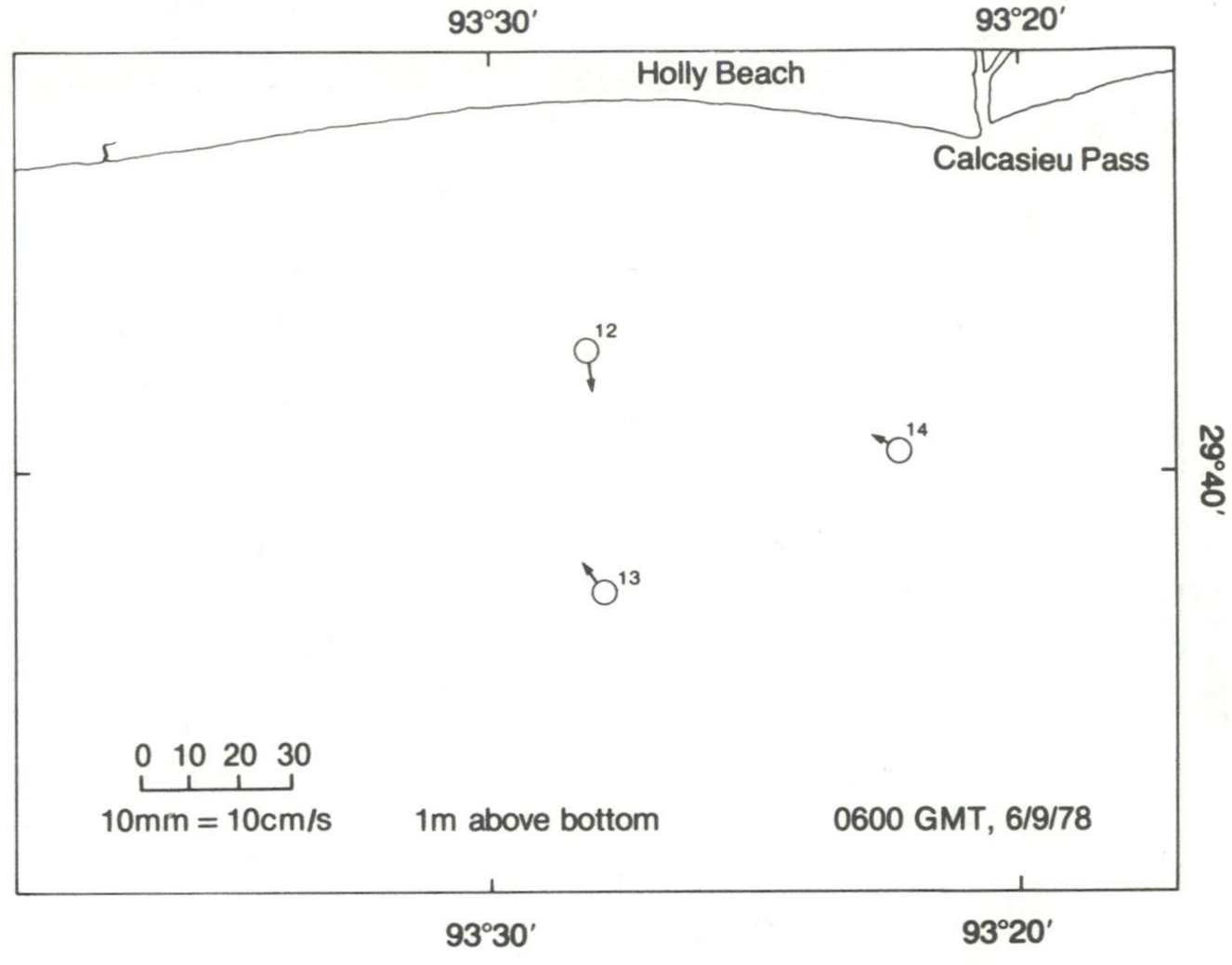

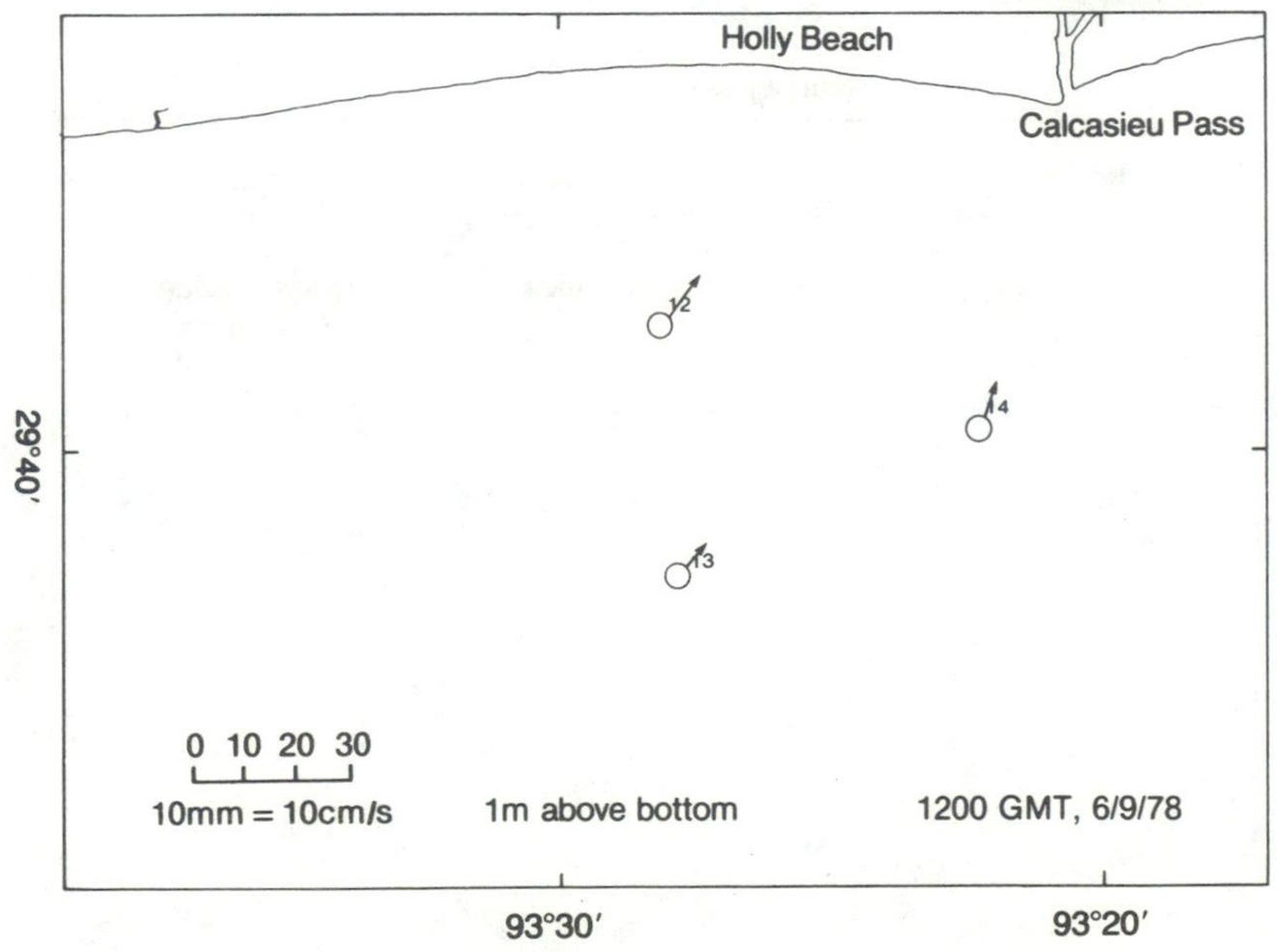

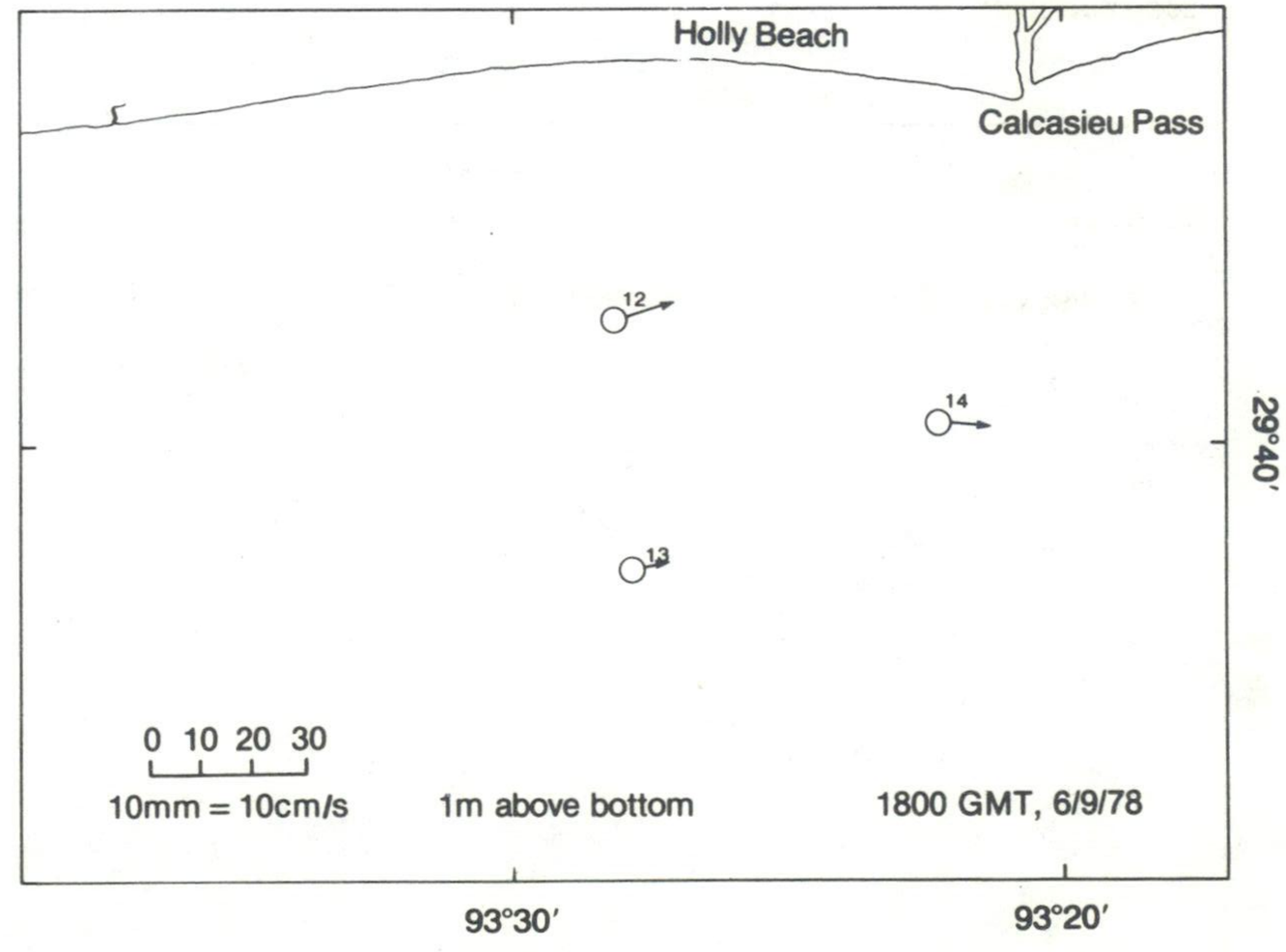

Figure E-10. Current vectors at 6-hour intervals, 1 m above bottom at West Hackberry site, June 9, 1978.

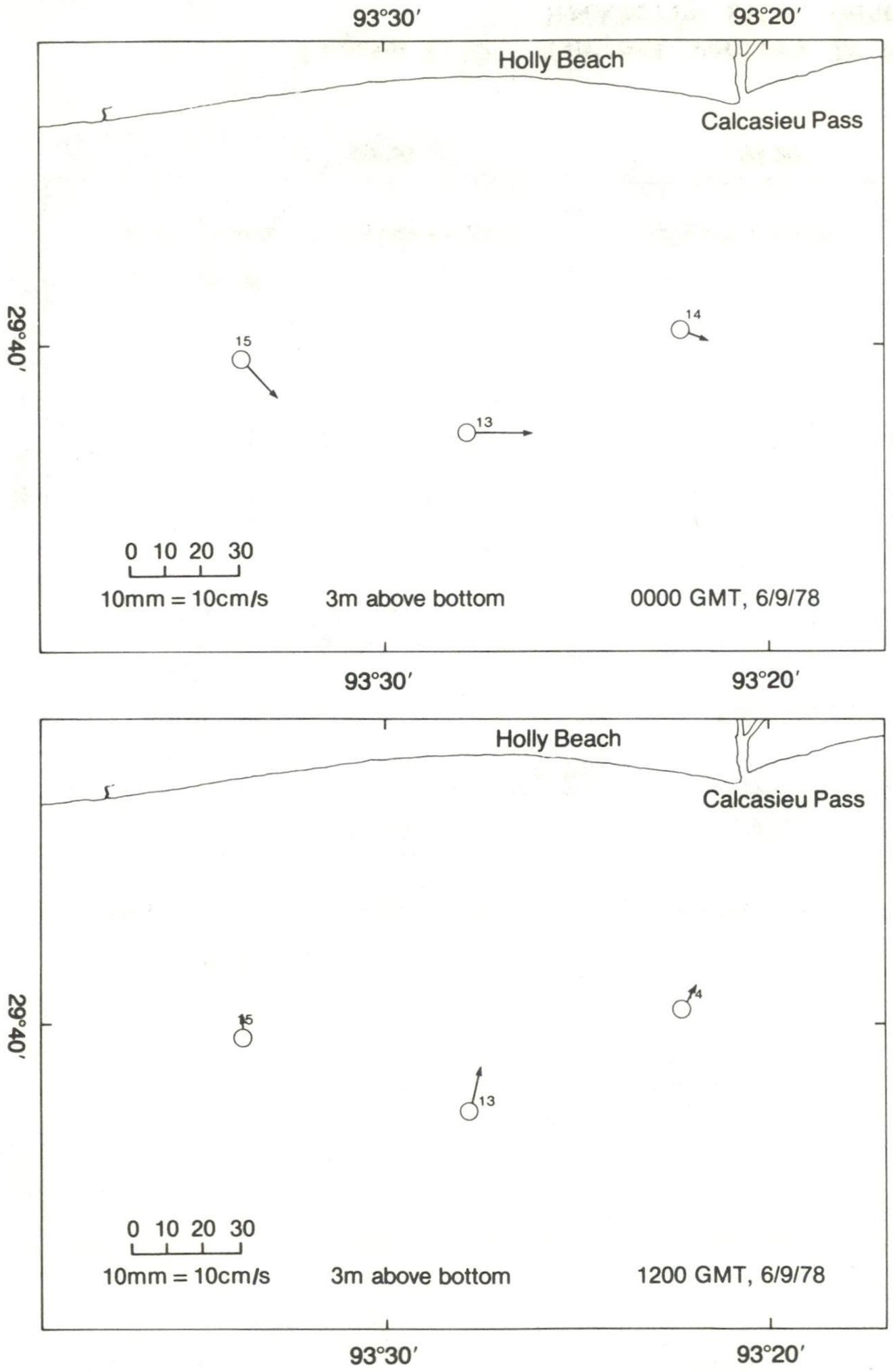

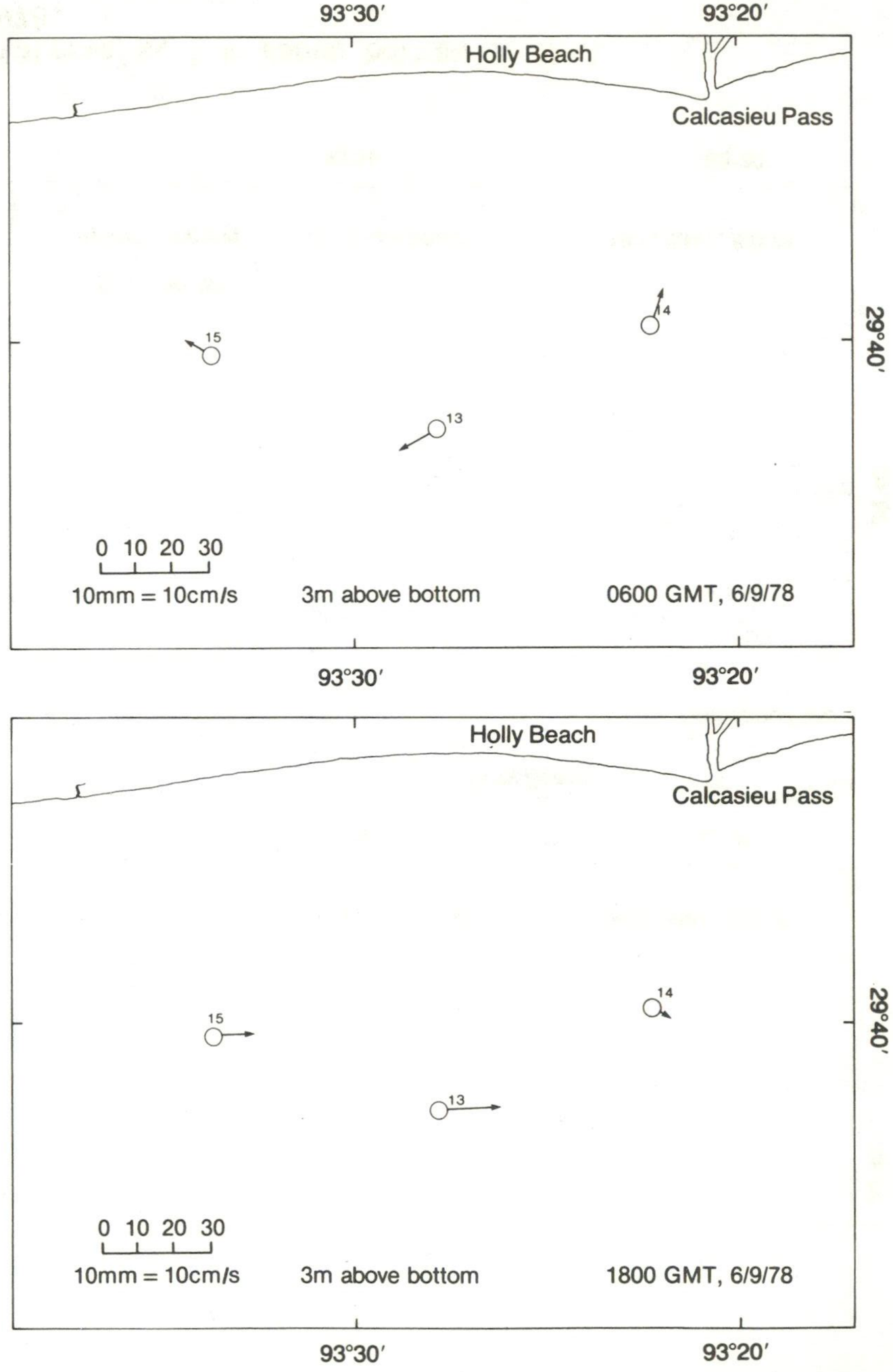

Figure E-11. Current vectors at 6-hour intervals, 3 m above bottom at West Hackberry site, June 9, 1978.

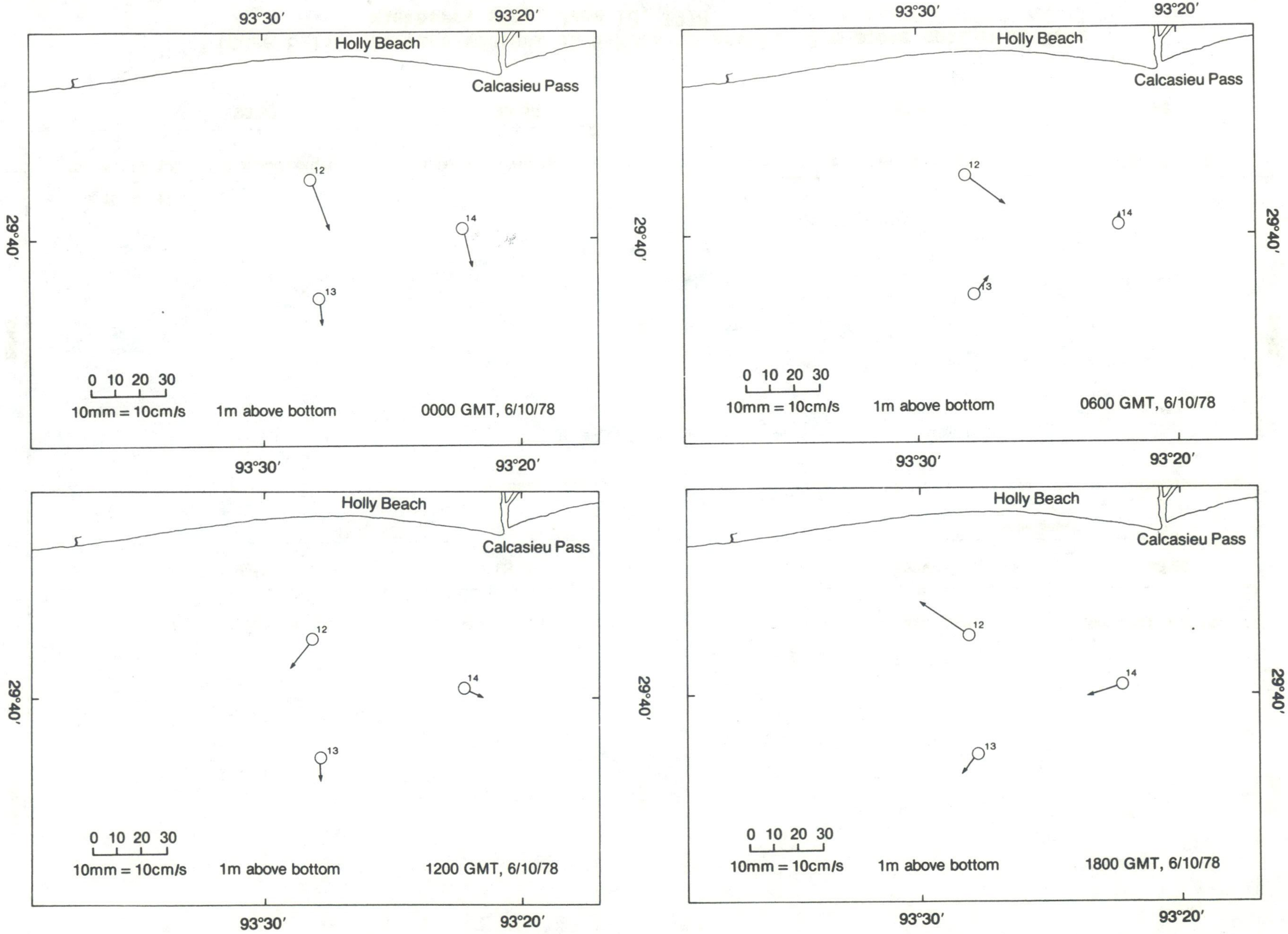

Figure E-12. Current vectors at 6-hour intervals, 1 m above bottom at West Hackberry site, June 10, 1978.

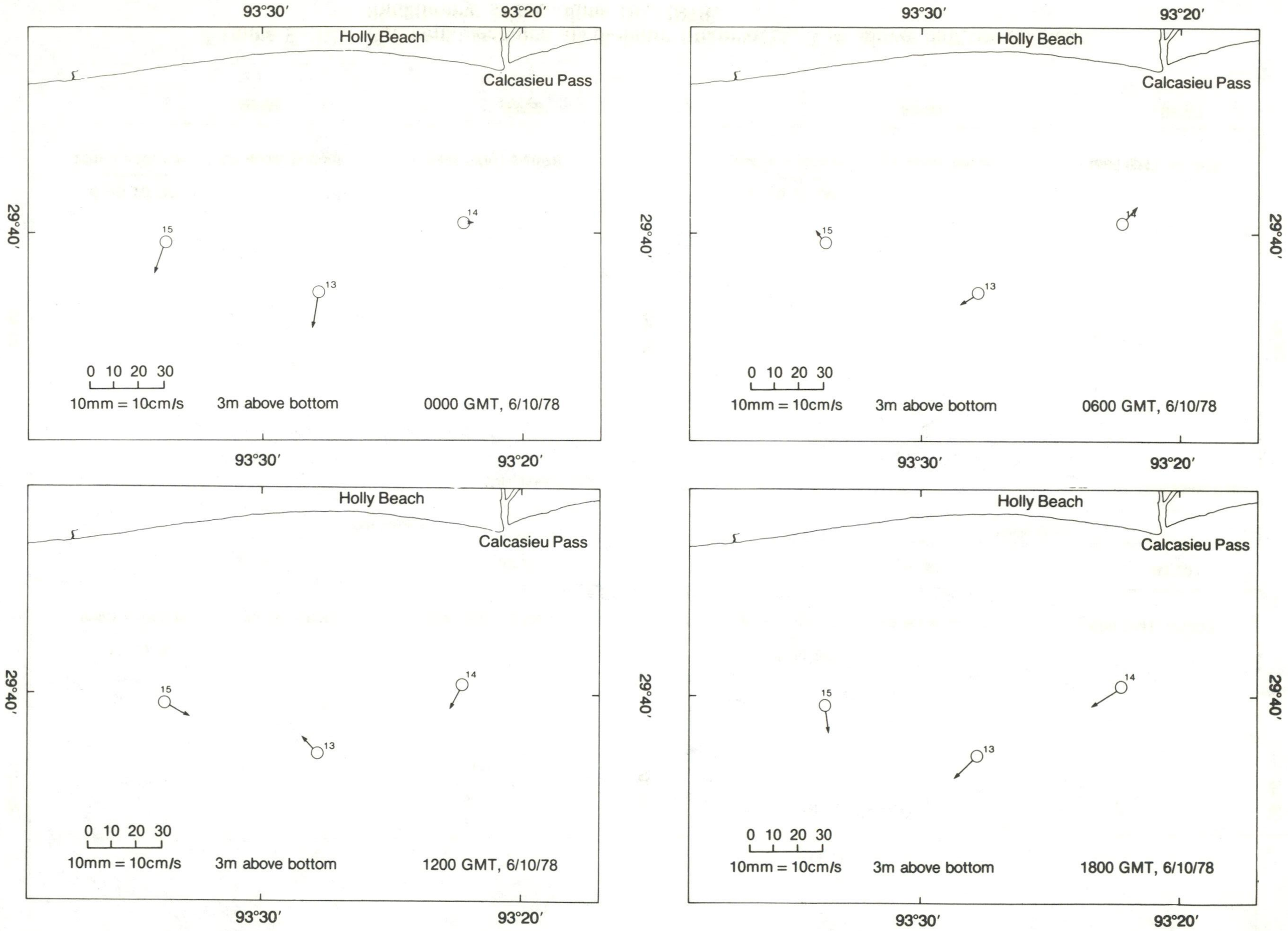

Figure E-13. Current vectors at 6-hour intervals, 3 m above bottom at West Hackberry site, June 10, 1978.

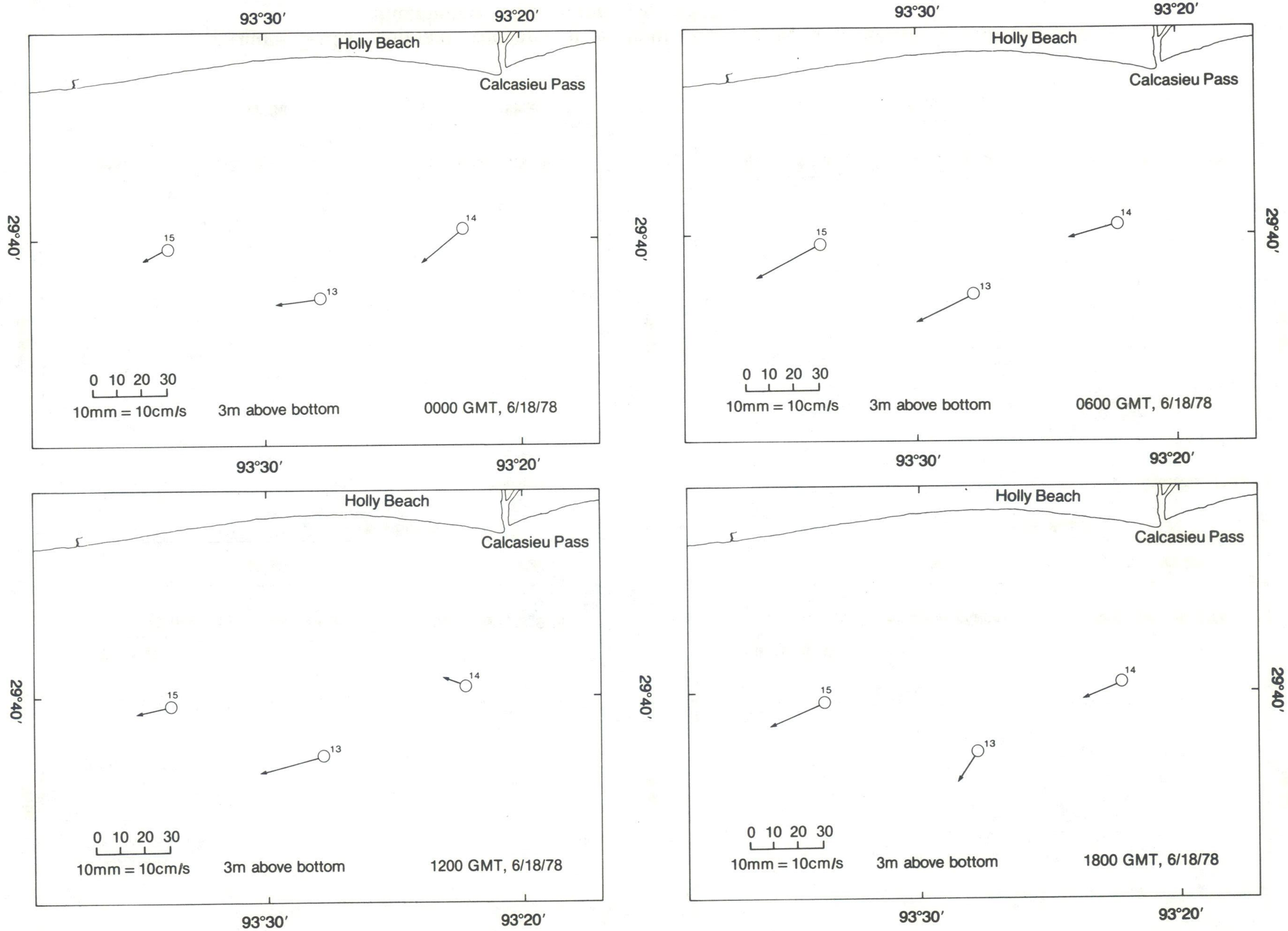

Figure E-14. Current vectors at 6-hour intervals, 3 m above bottom at West Hackberry site, June 18, 1978.

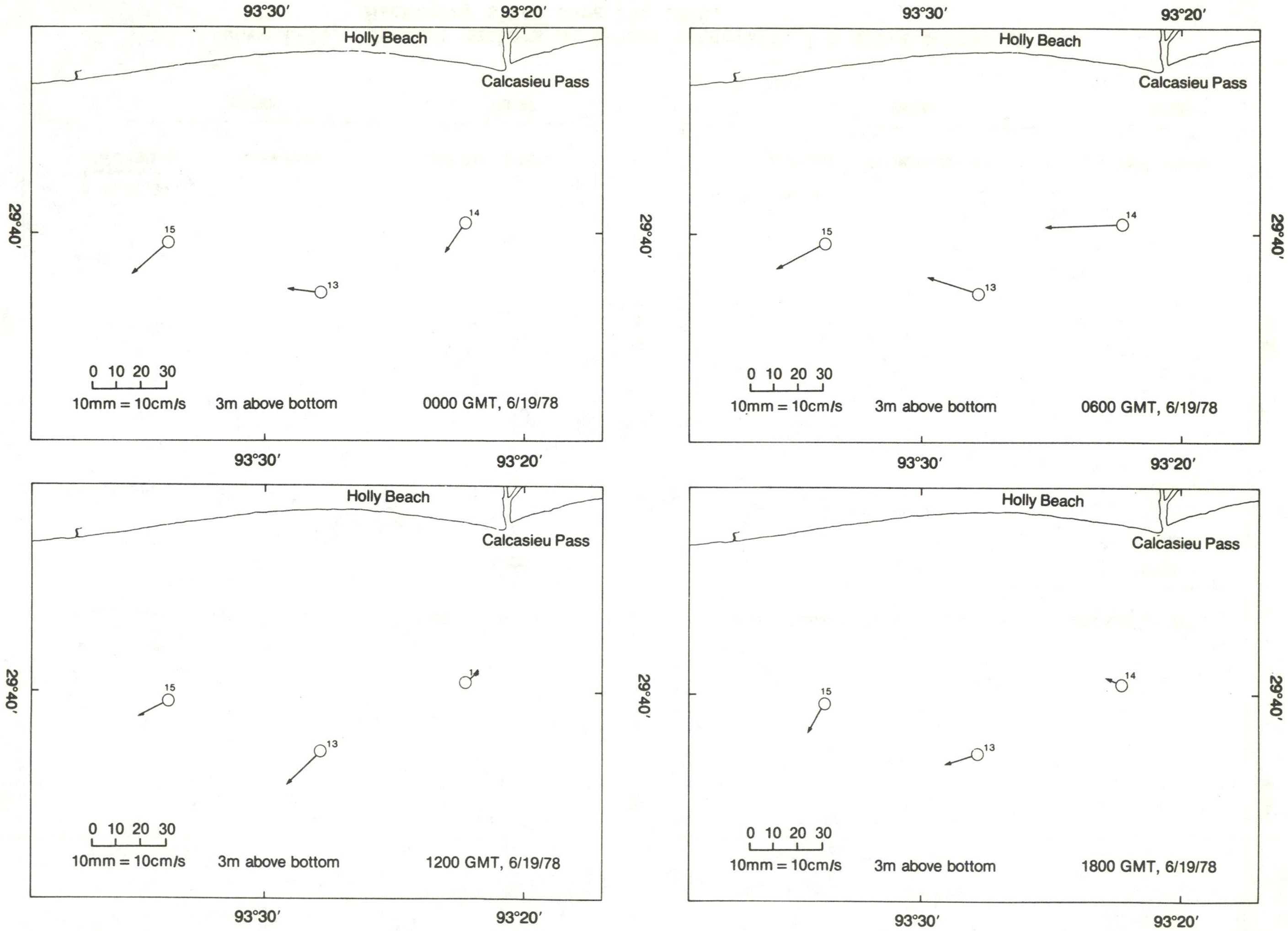

Figure E-15. Current vectors at 6-hour intervals, 3 m above bottom at West Hackberry site, June 19, 1978.

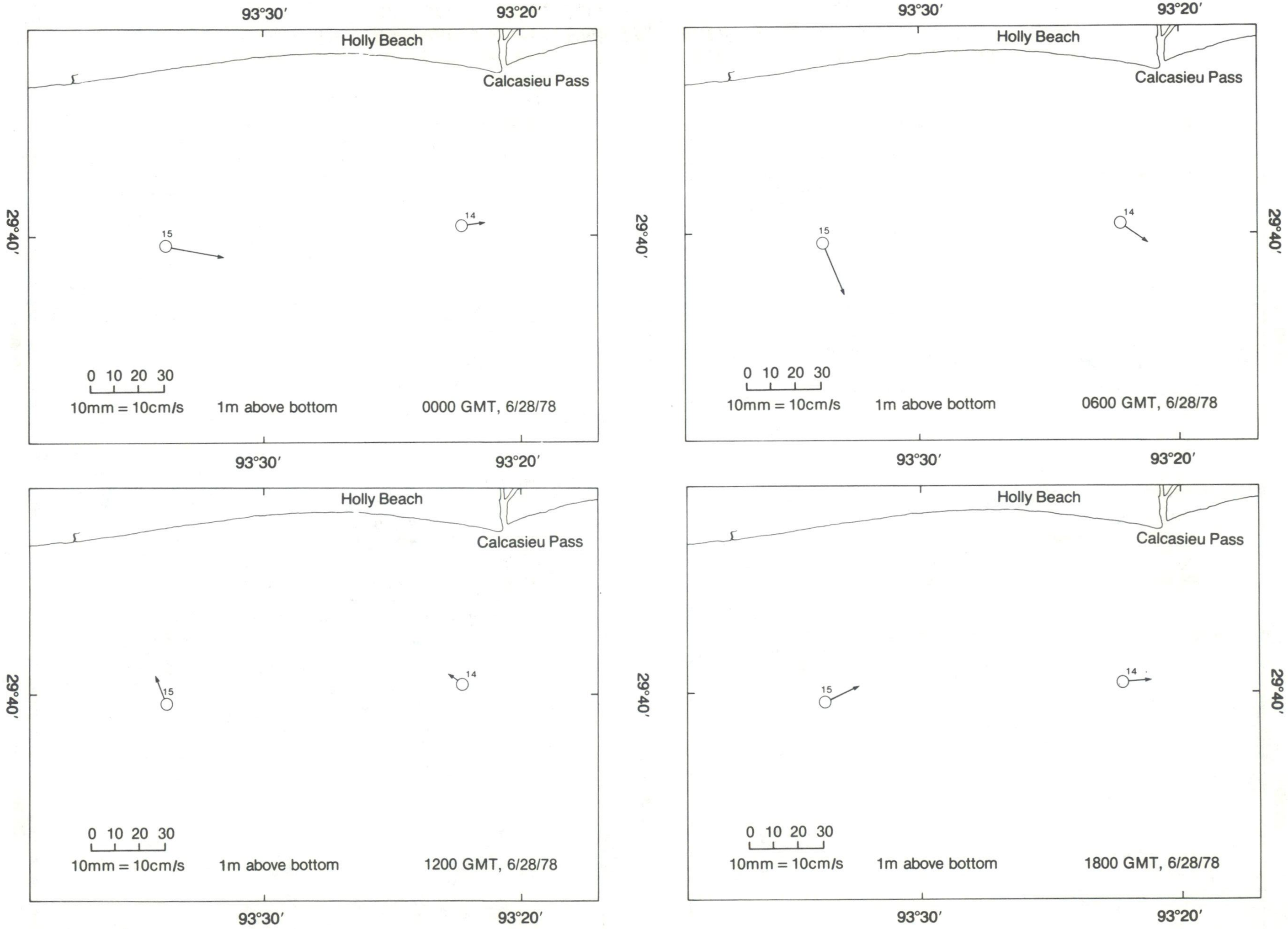

Figure E-16. Current vectors at 6-hour intervals, 1 m above bottom at West Hackberry site, June 28, 1978.

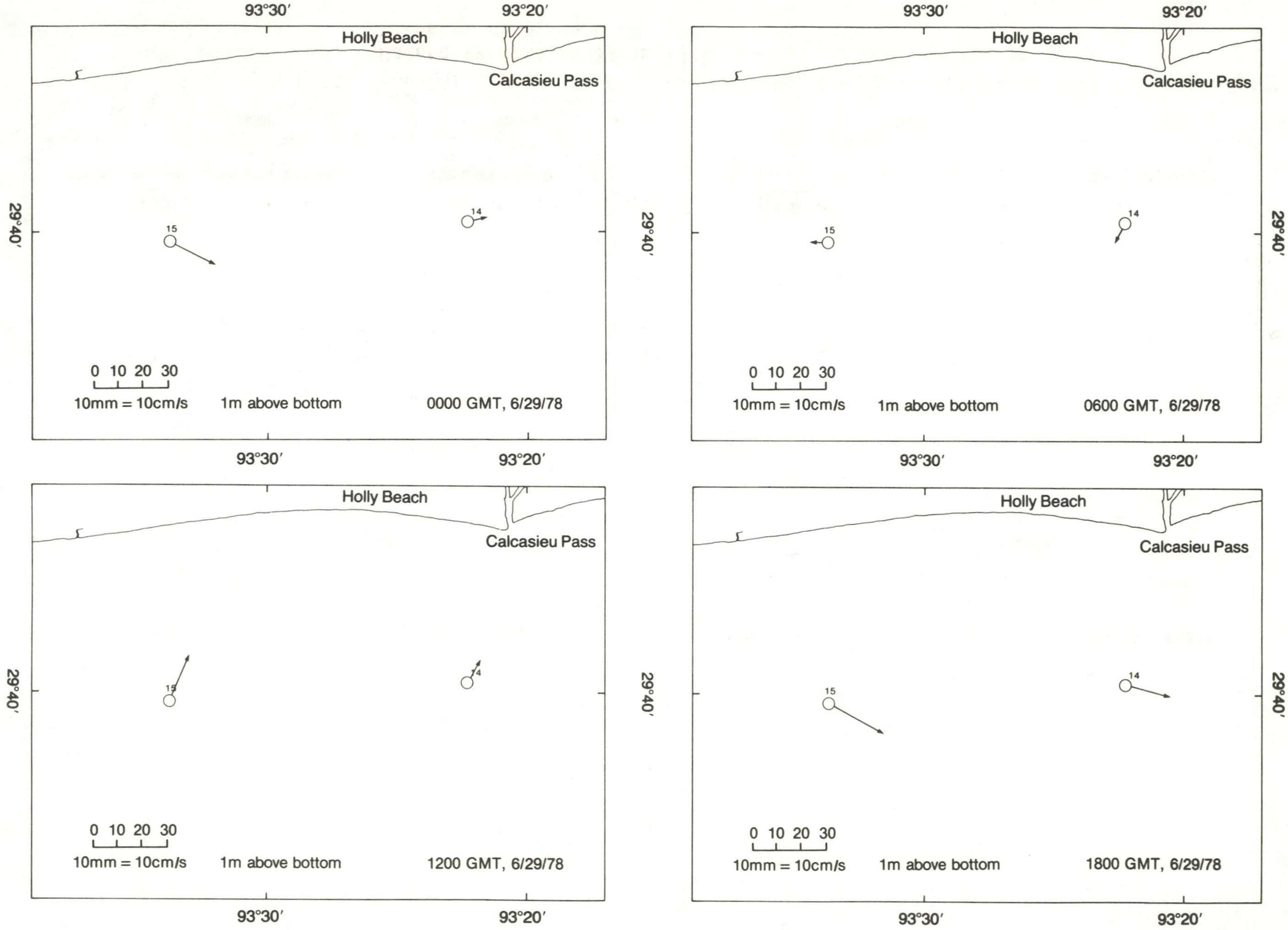

Figure E-17. Current vectors at 6-hour intervals, 1 m above bottom at West Hackberry site, June 29, 1978.

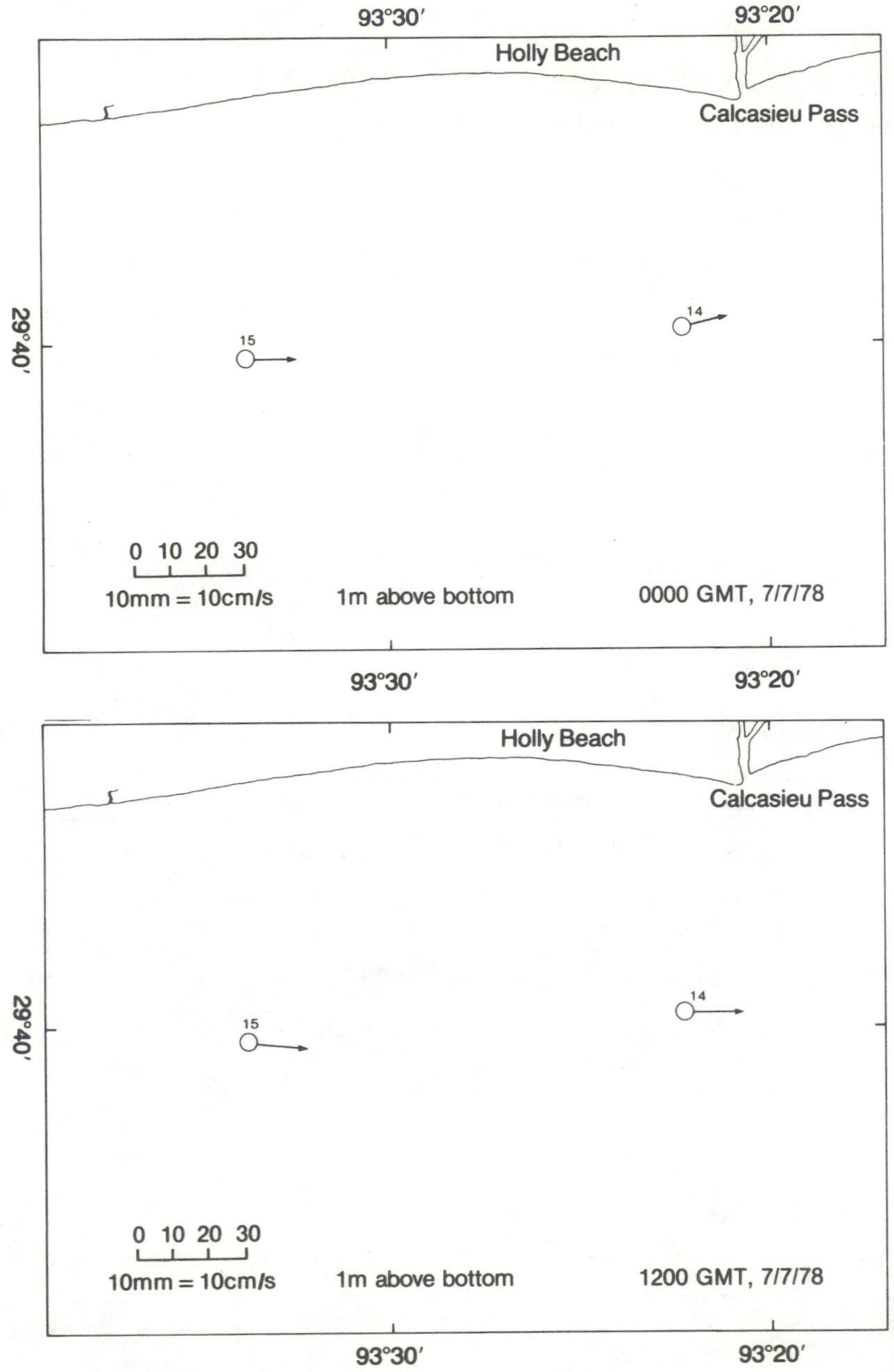

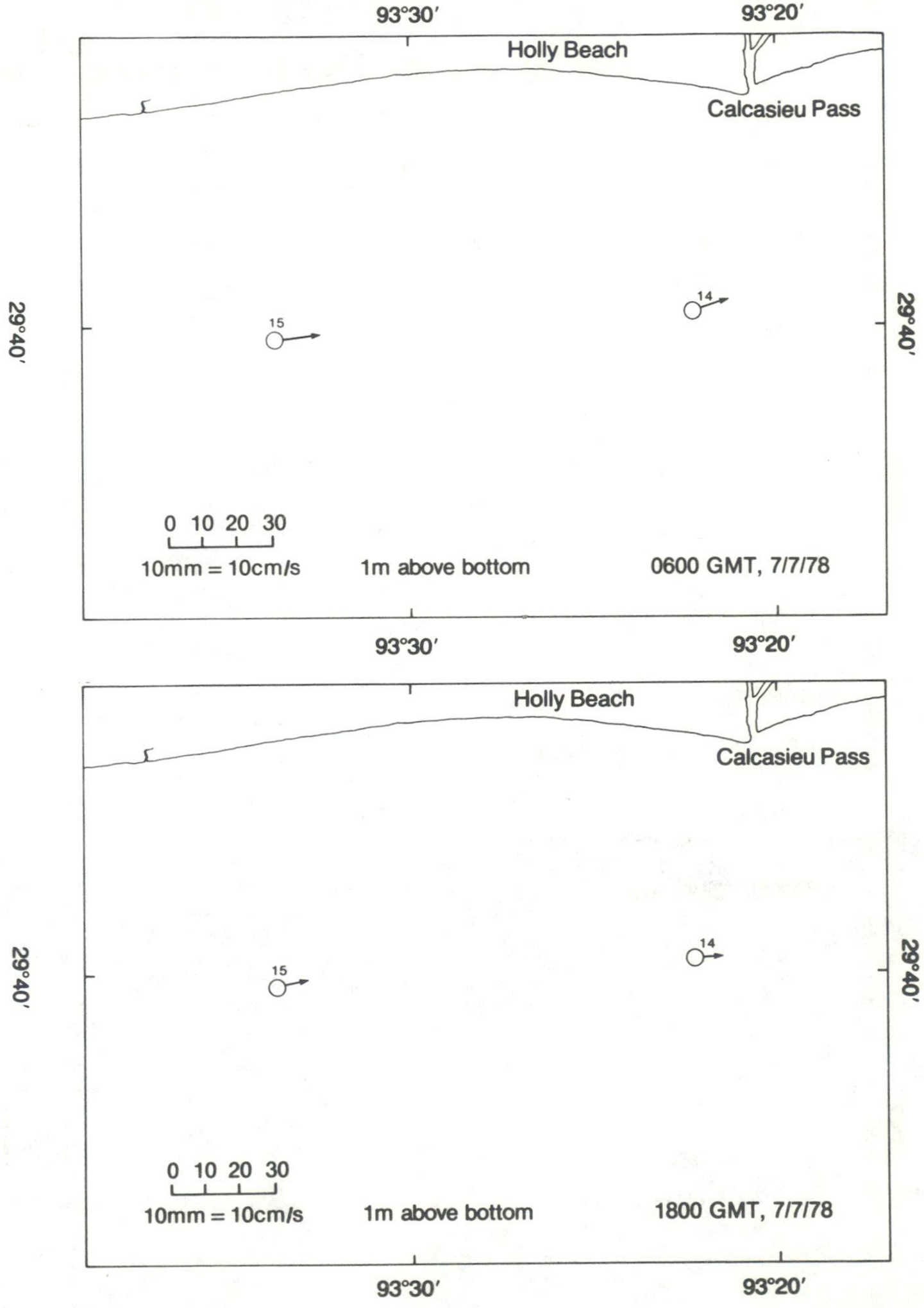

Figure E-18. Current vectors at 6-hour intervals, 1 m above bottom at West Hackberry site, July 7, 1978.

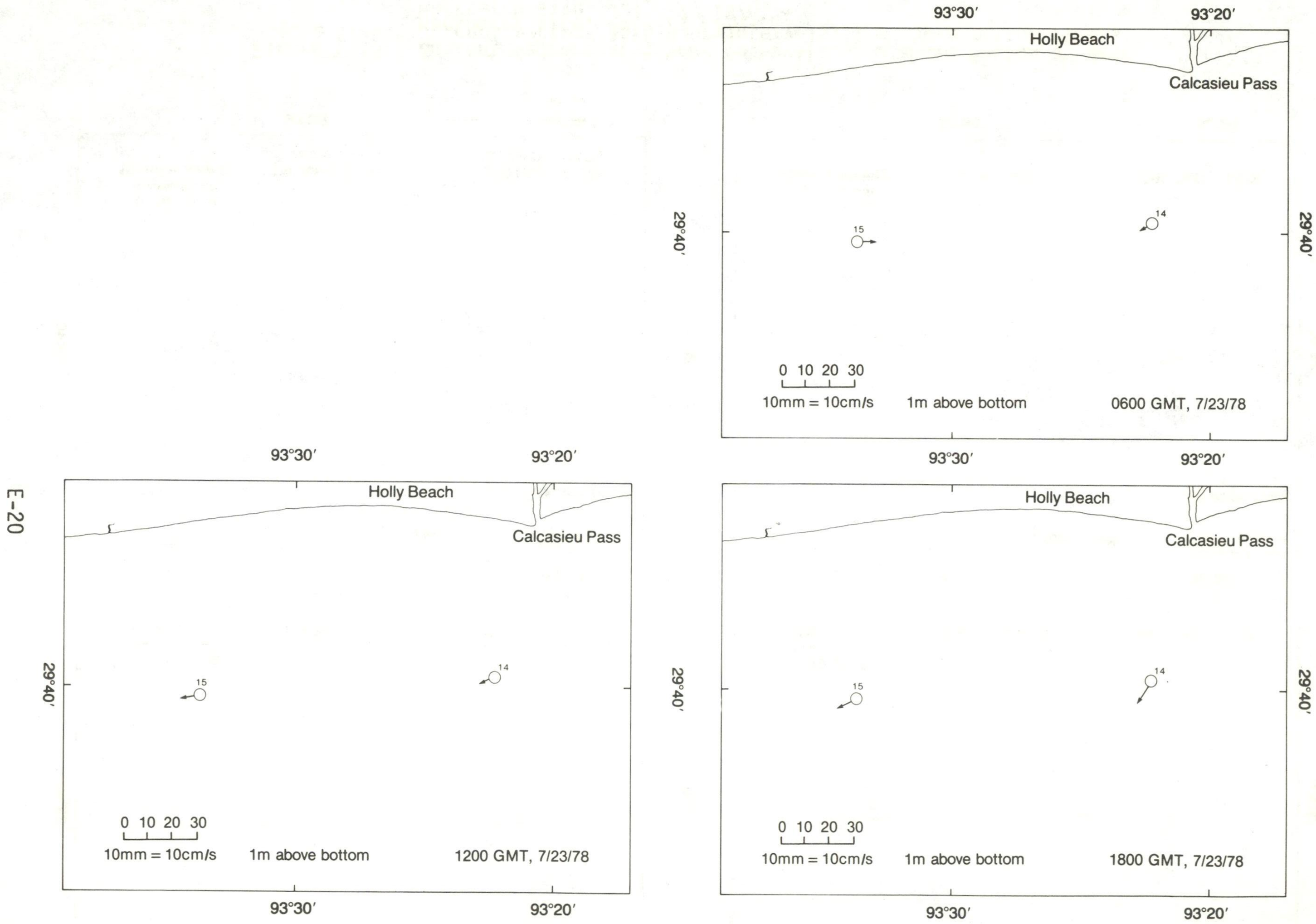

Figure E-19. Current vectors at 6-hour intervals, 1 m above bottom at West Hackberry site, July 23, 1978.

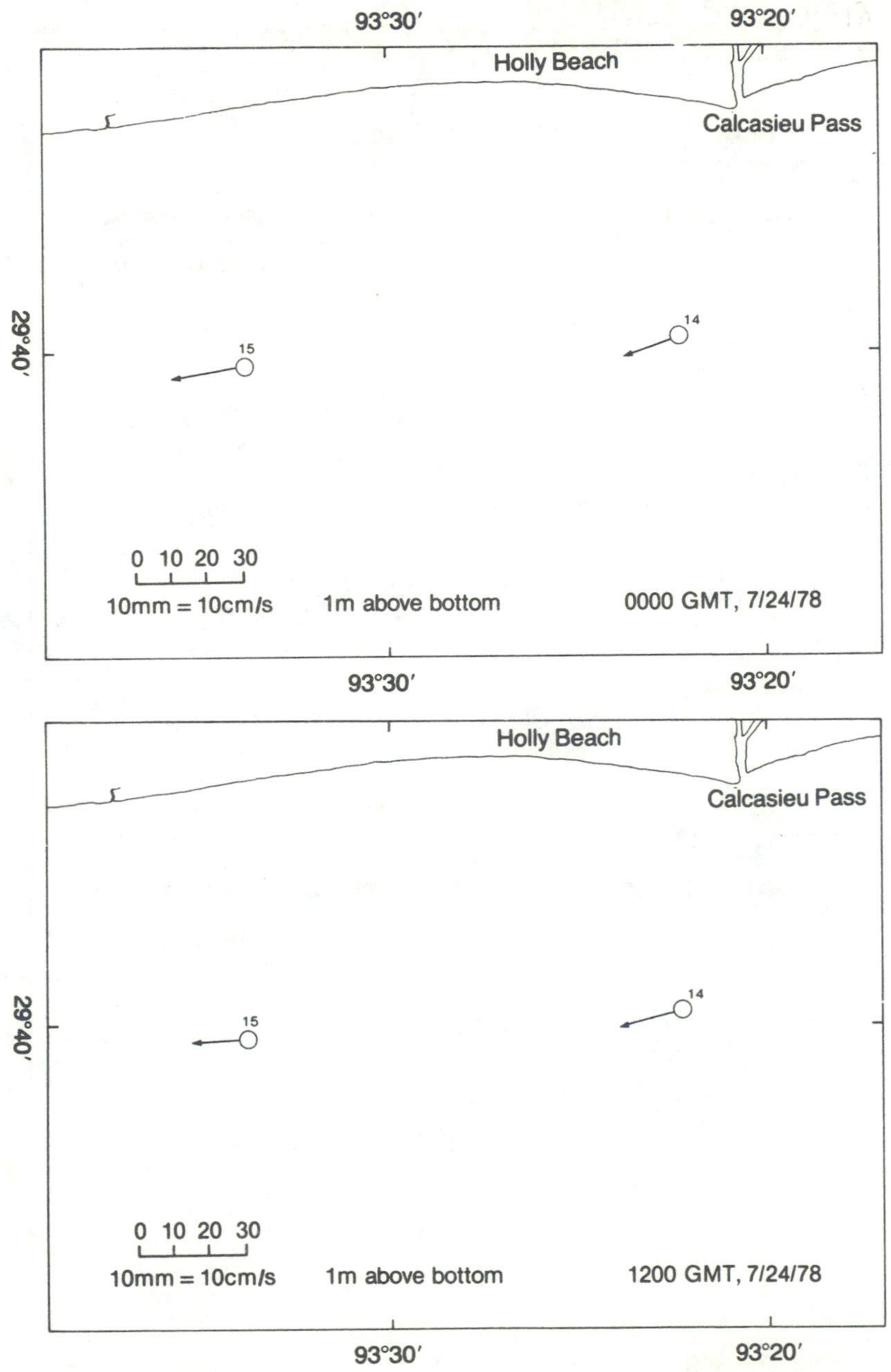

Figure E-20. Current vectors at 6-hour intervals, 1 m above bottom at West Hackberry site, July 24, 1978.

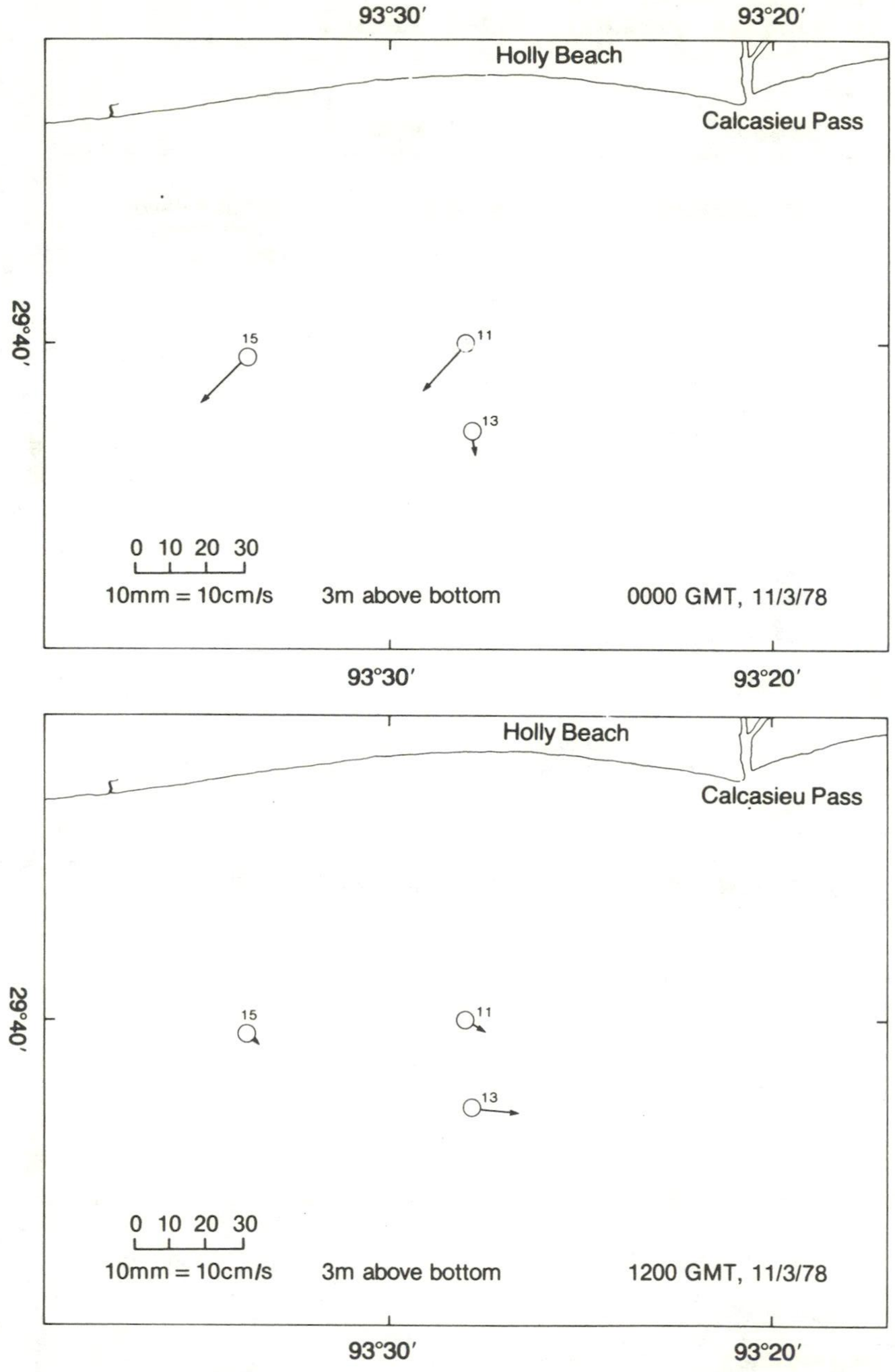

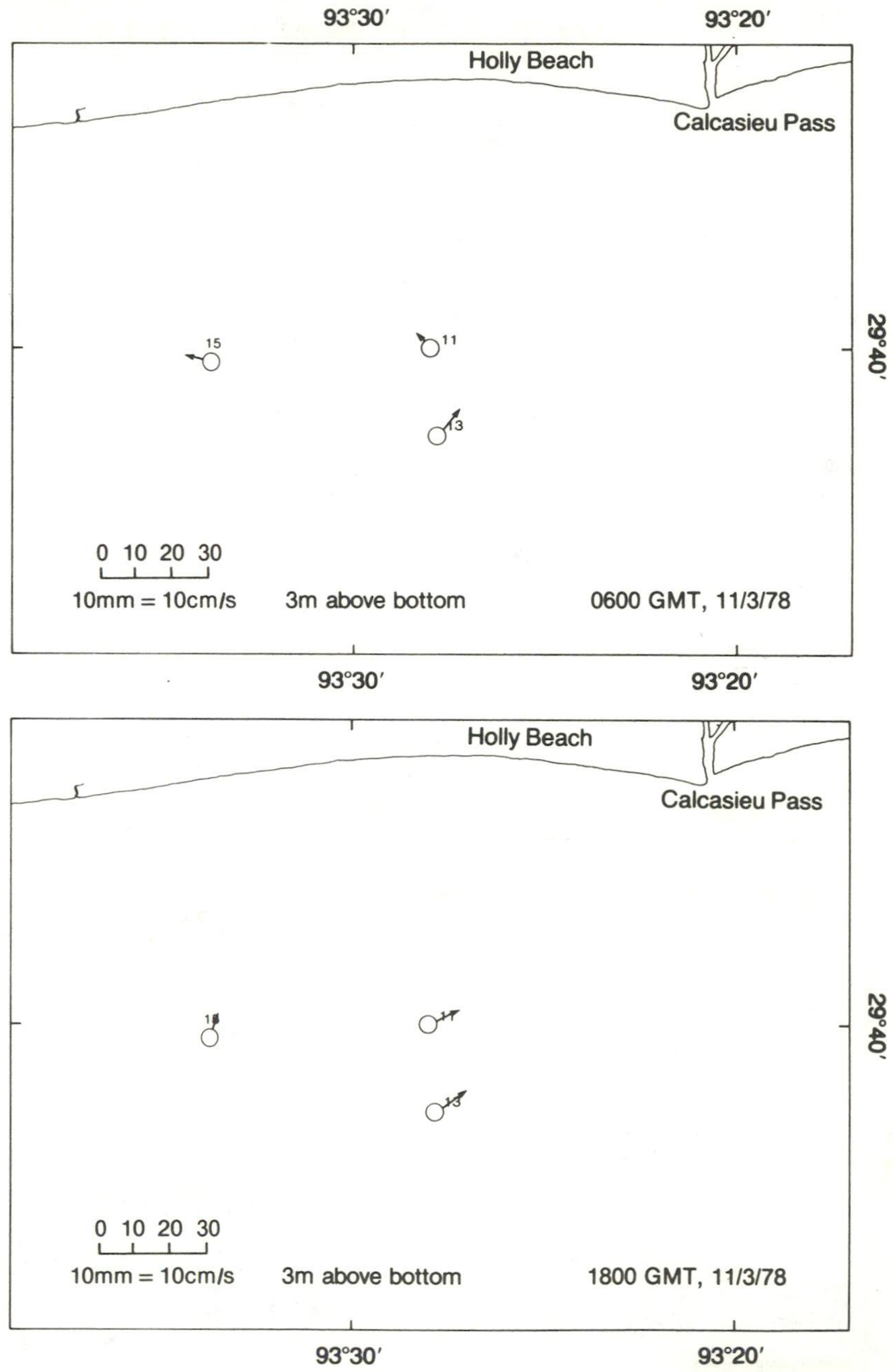

Figure E-21. Current vectors at 6-hour intervals, 3 m above bottom at West Hackberry site, November 3, 1978.

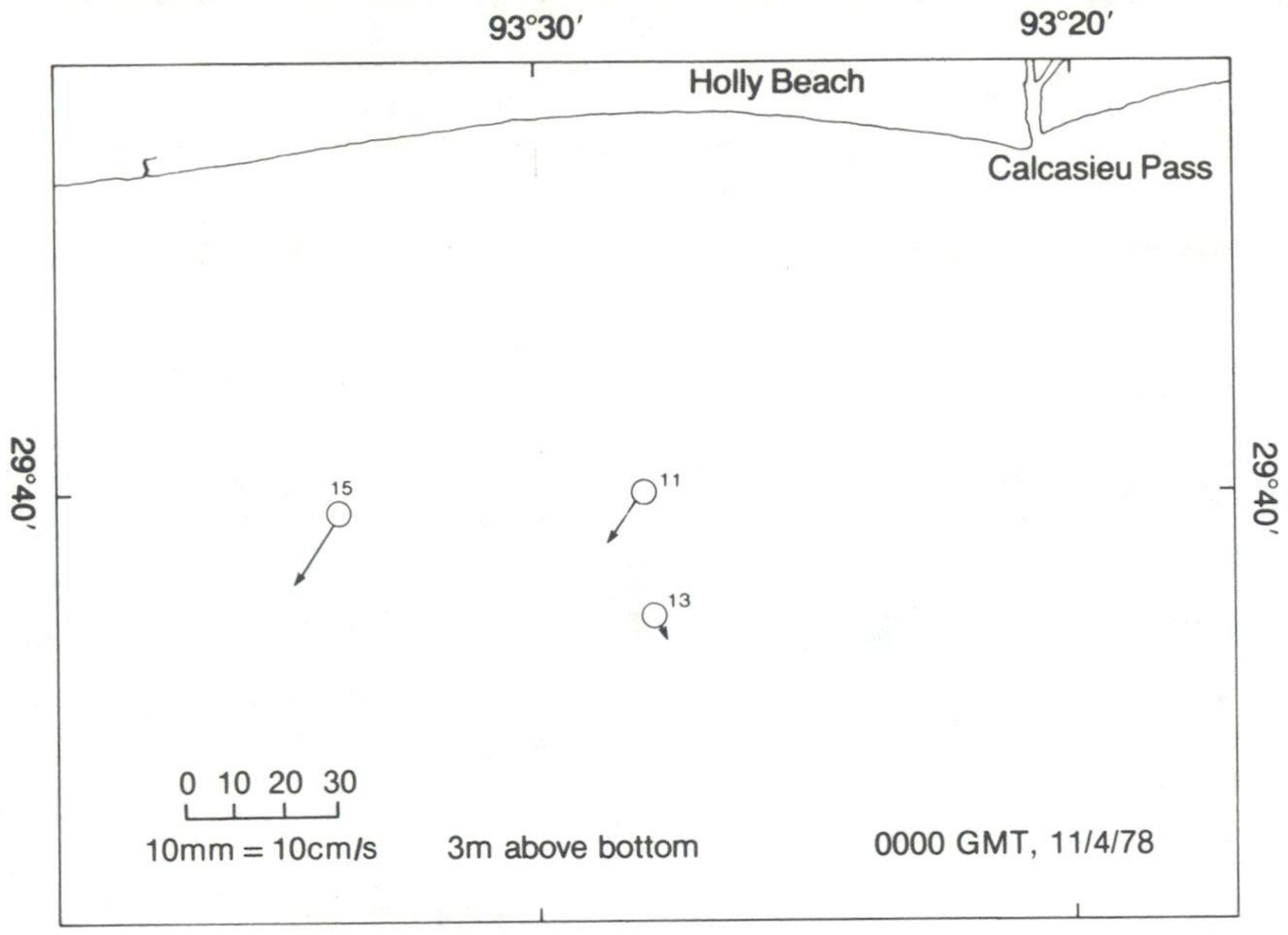

Figure E-22. Current vectors 3 m above bottom at West Hackberry site, 0000 GMT, November 4, 1978.

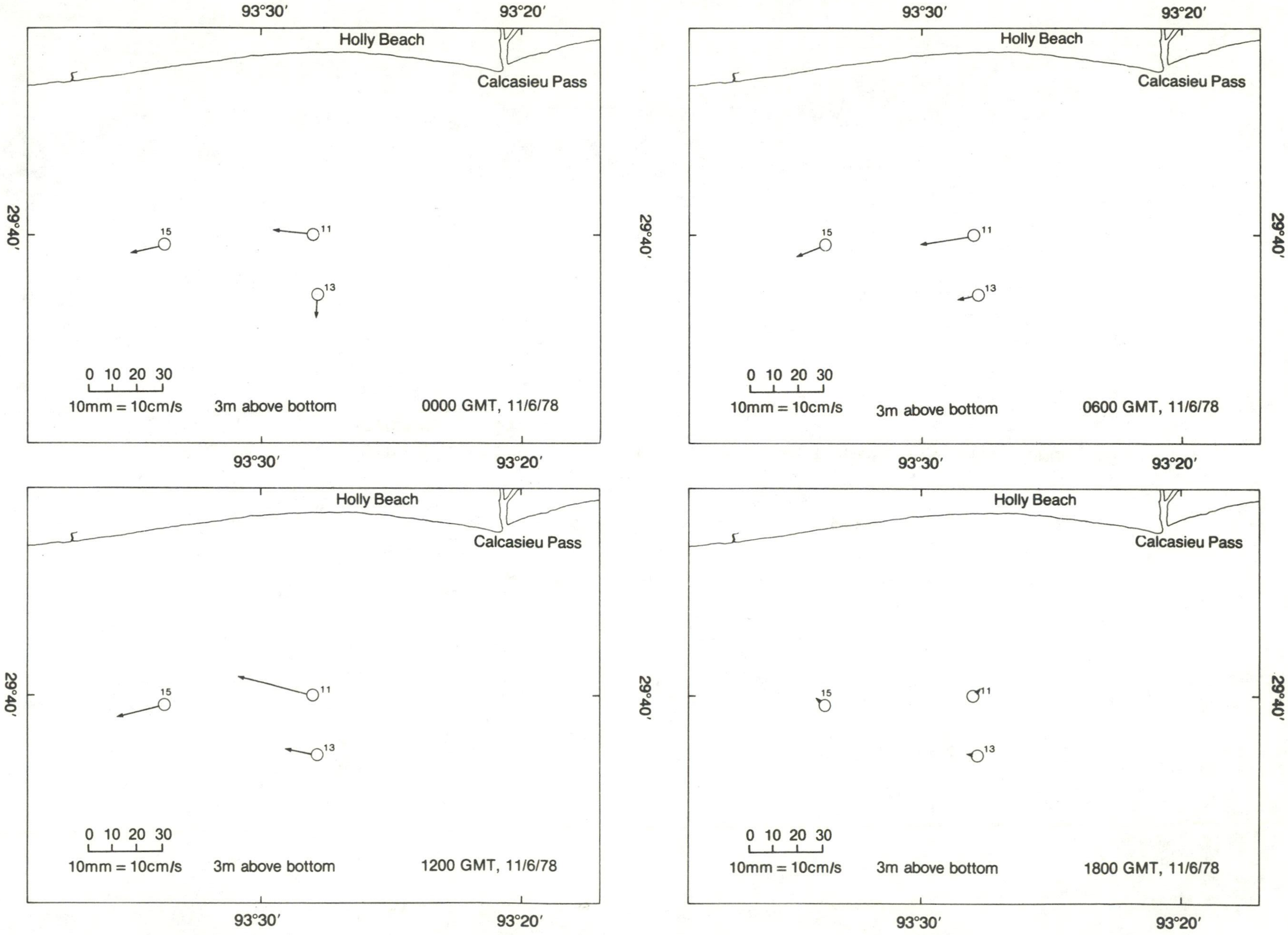

Figure E-23. Current vectors at 6-hour intervals, 3 m above bottom at West Hackberry site, November 6, 1978.

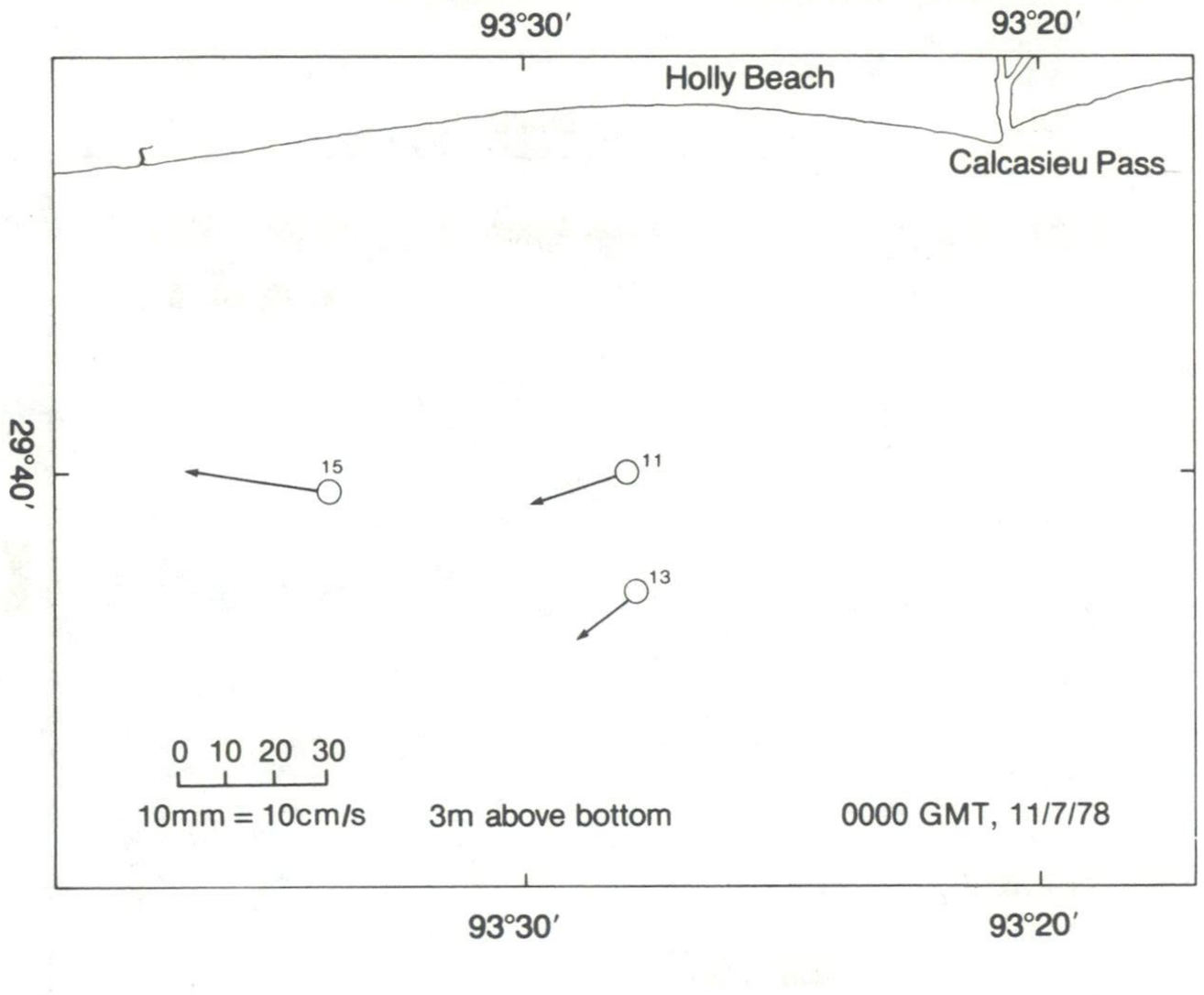

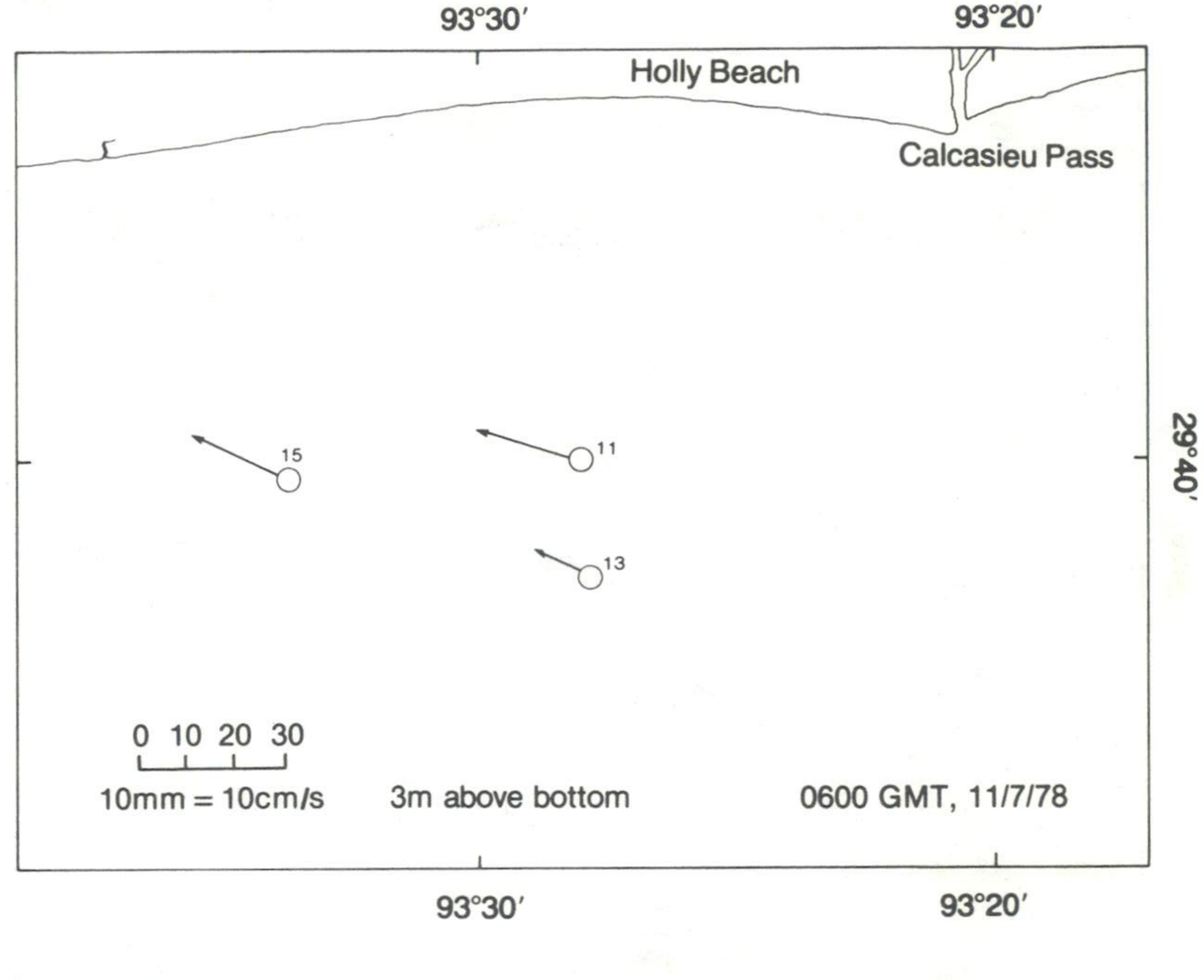

Figure E-24. Current vectors at 6-hour intervals, 3 m above bottom at West Hackberry site, November 7, 1978.

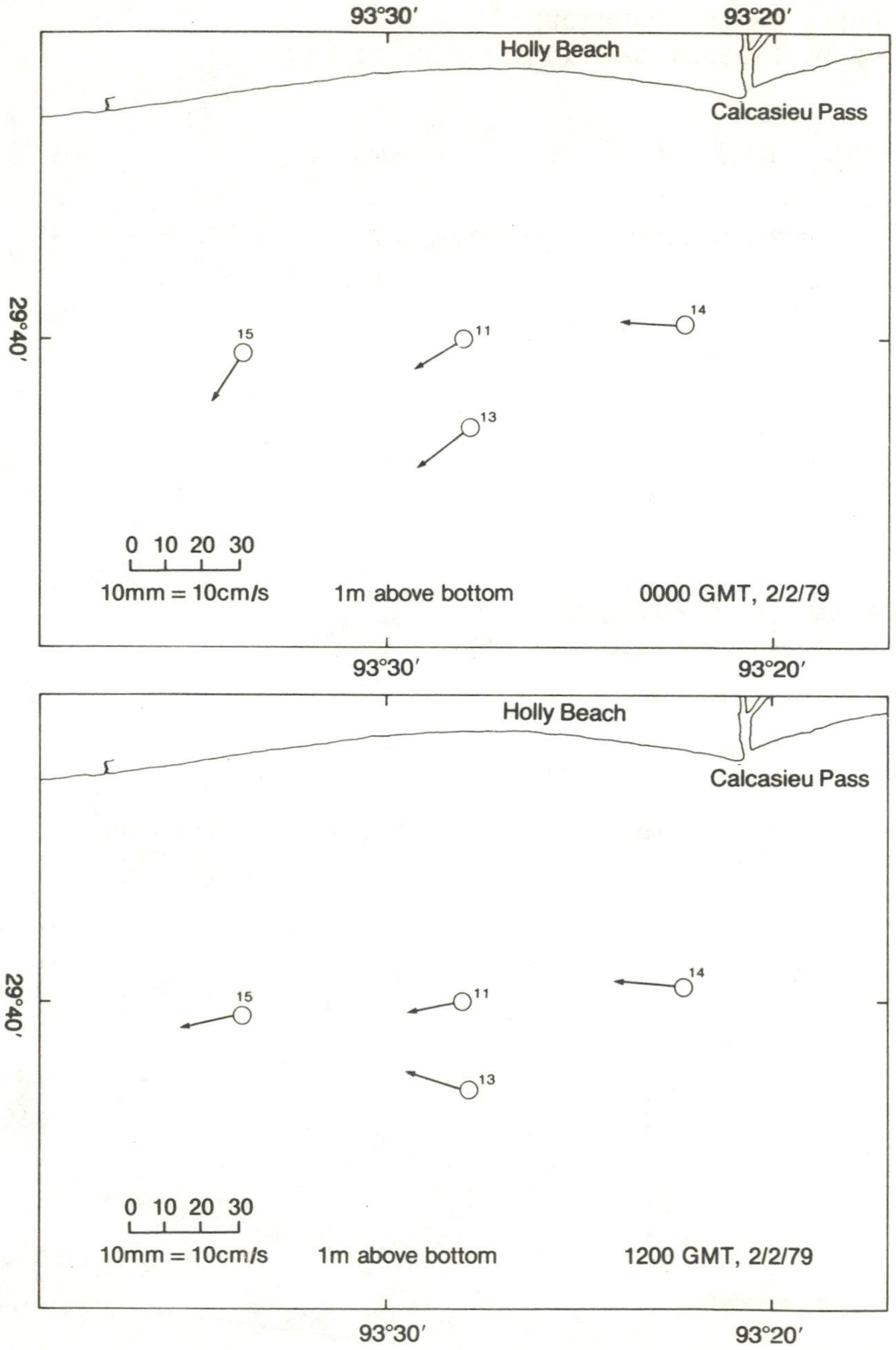

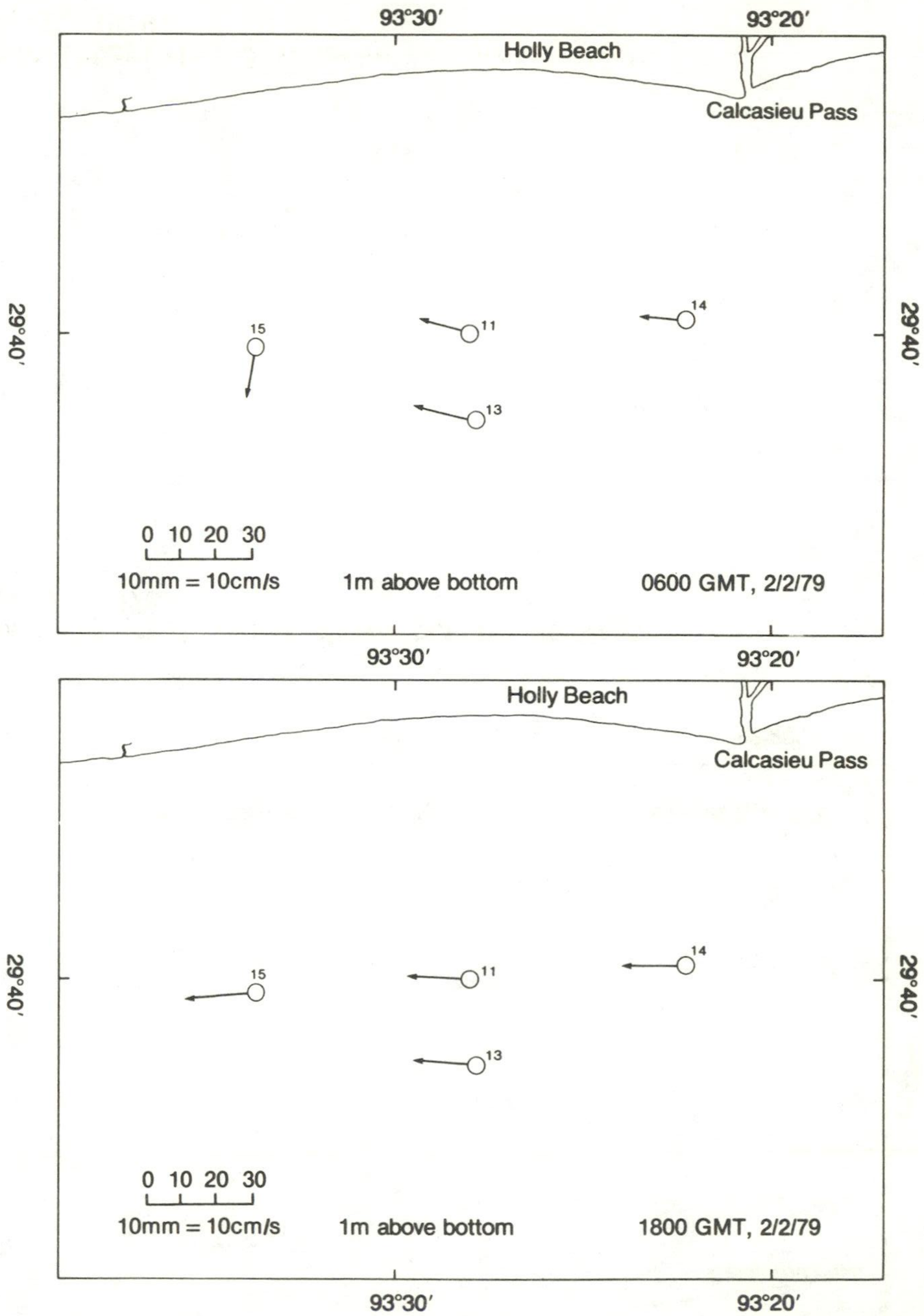

Figure E-25. Current vectors at 6-hour intervals, 1 m above bottom at West Hackberry site, February 2, 1979.

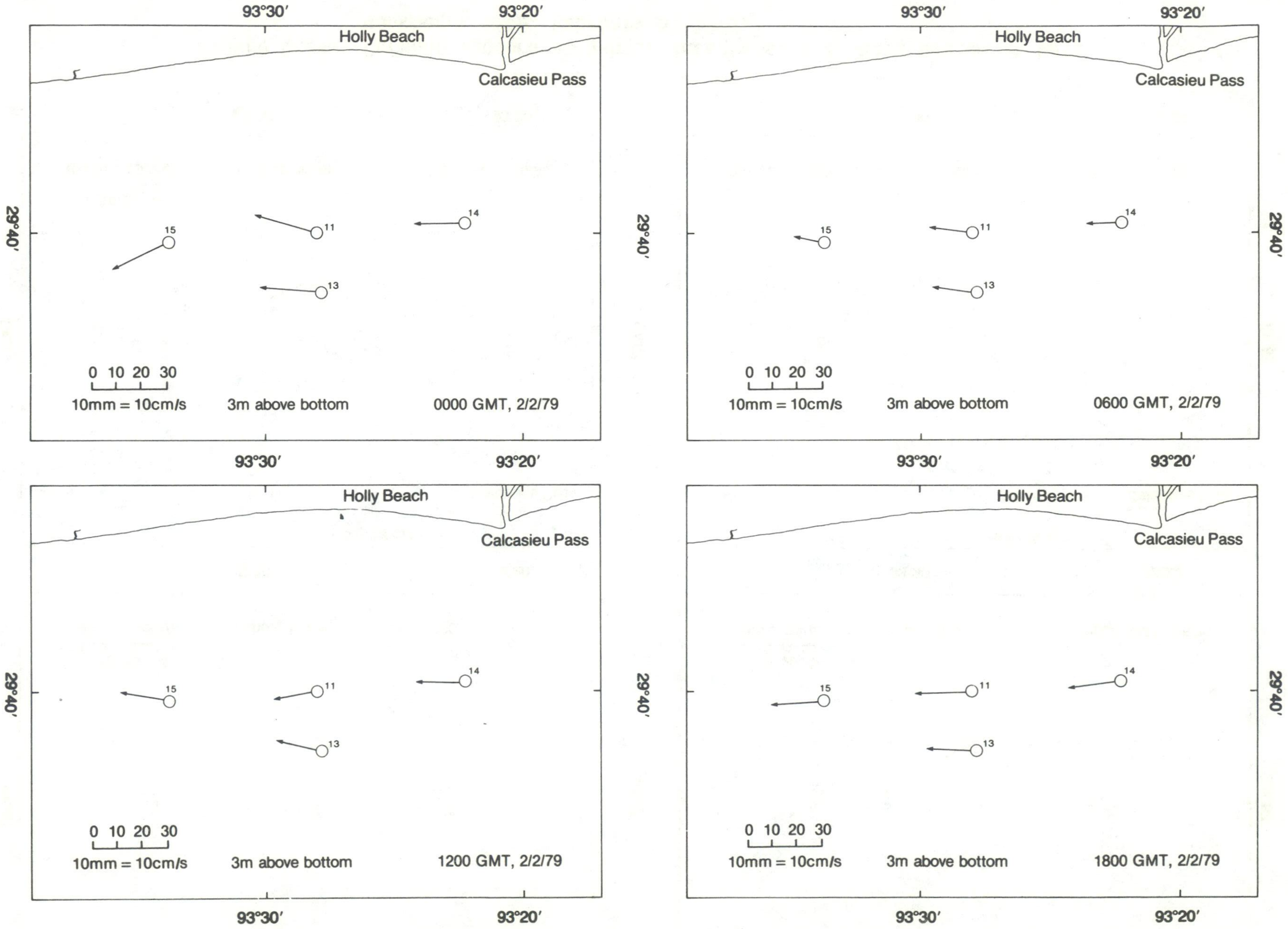

Figure E-26. Current vectors at 6-hour intervals, 3 m above bottom at West Hackberry site, February 2, 1979.

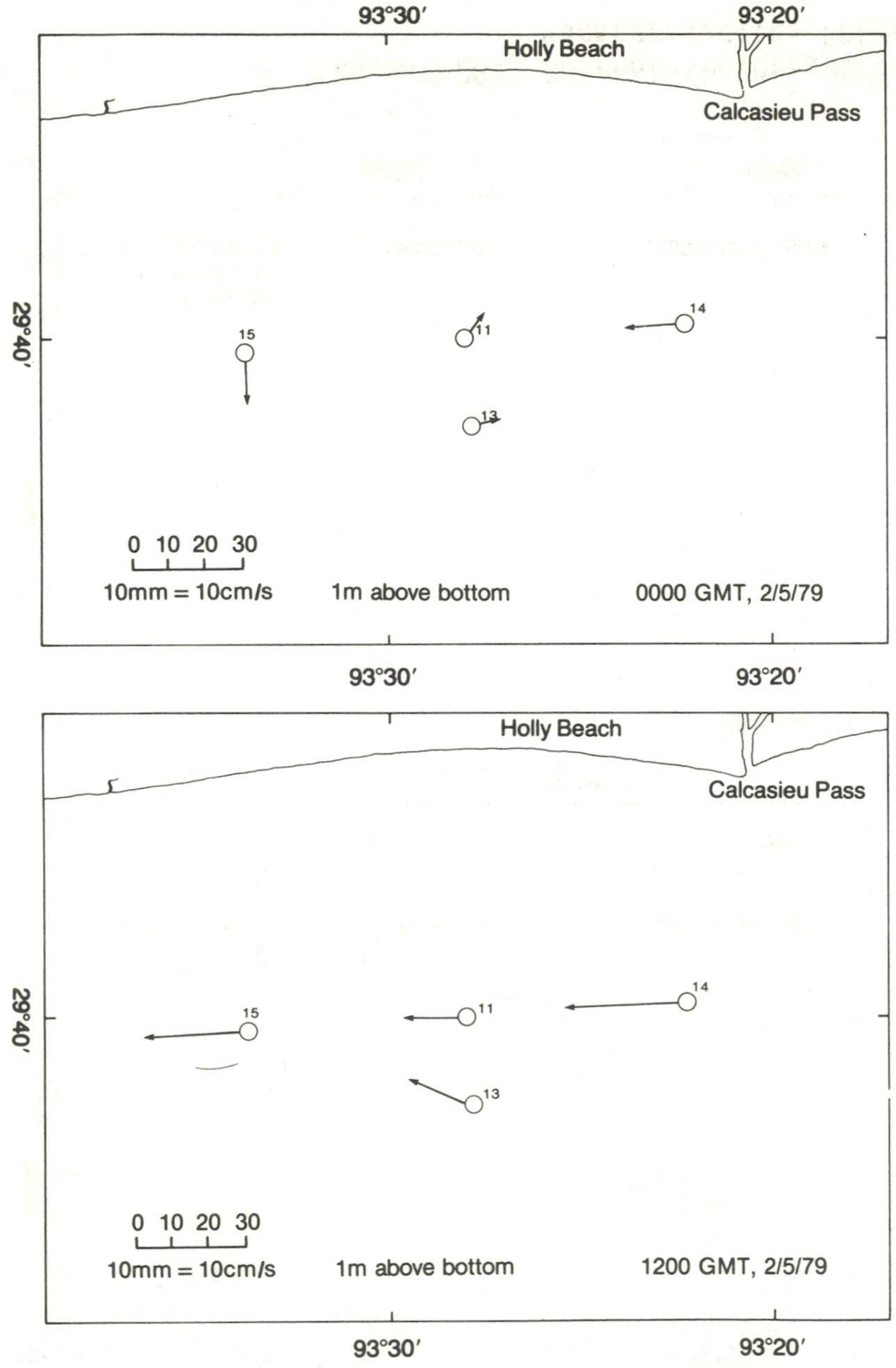

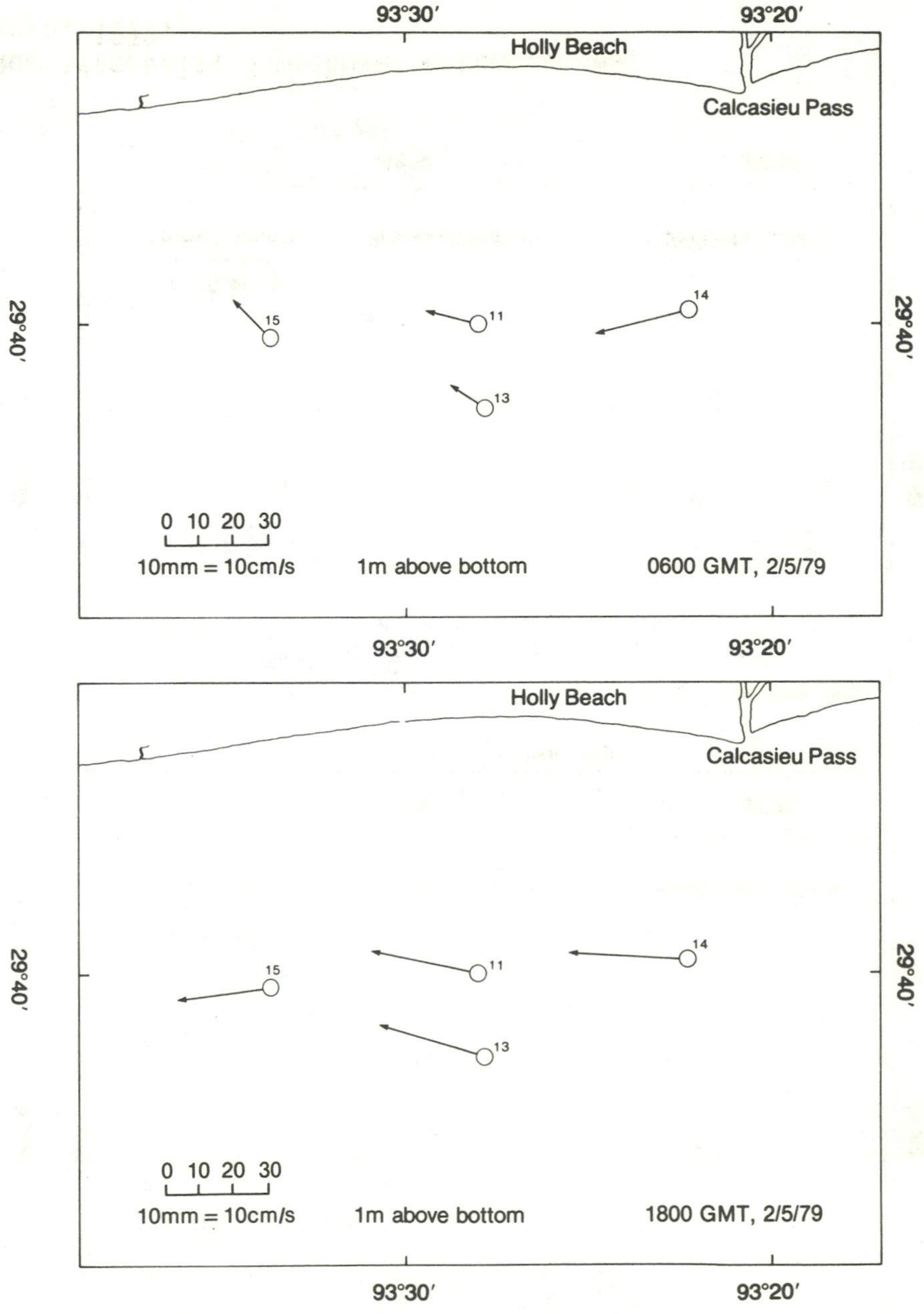

Figure E-27. Current vectors at 6-hour intervals, 1 m above bottom at West Hackberry site, February 5, 1979.

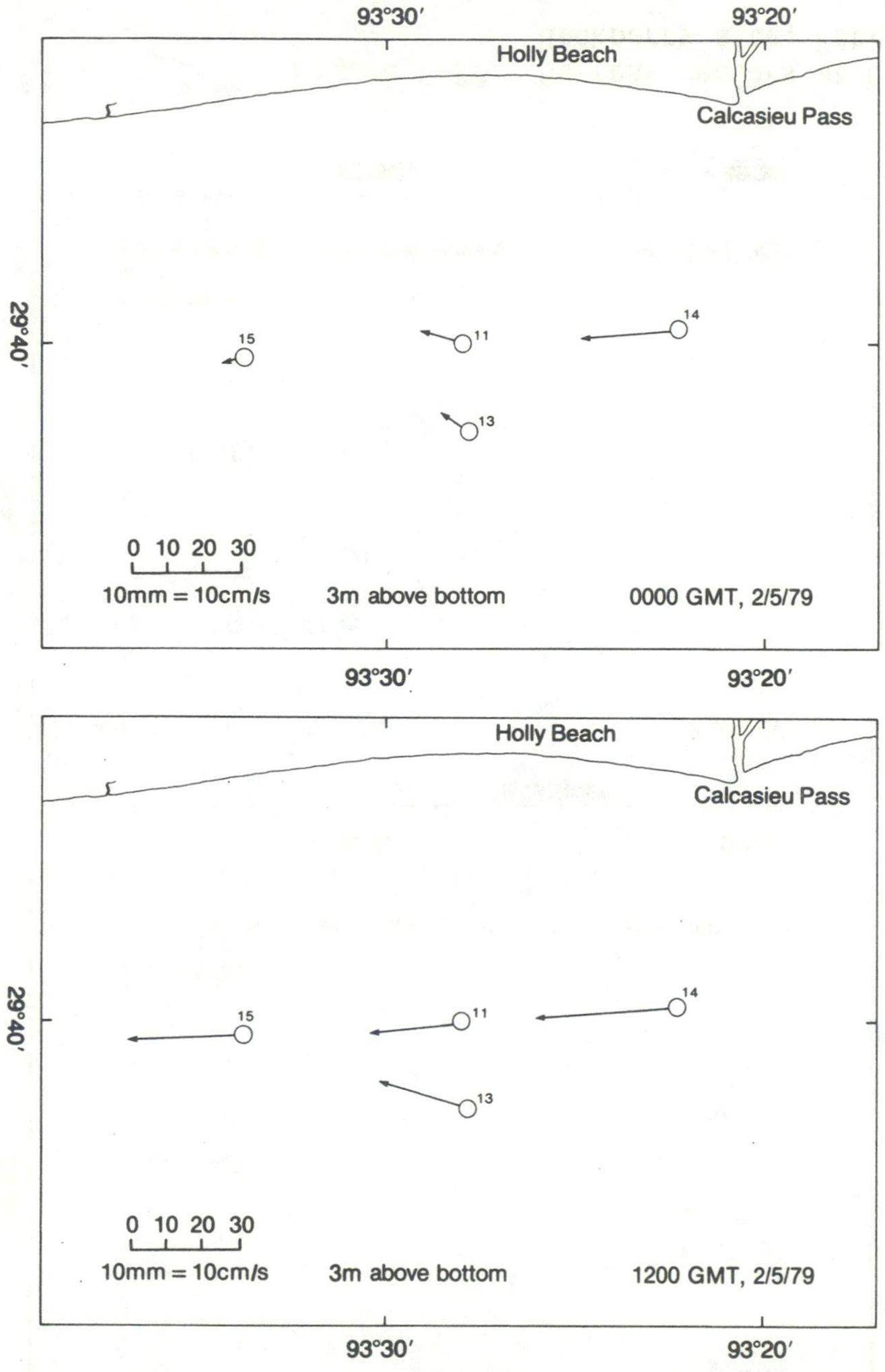

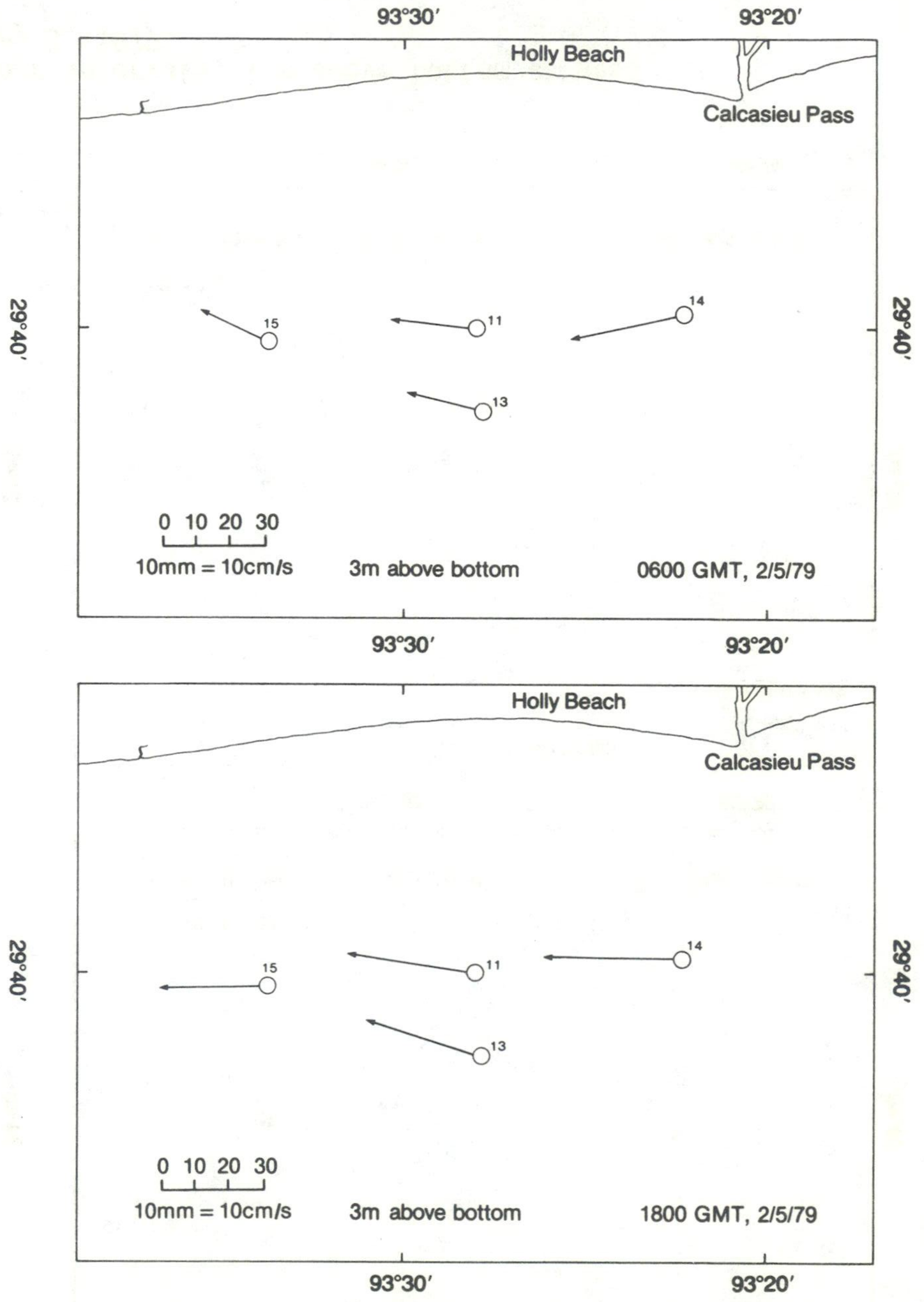

Figure E-28. Current vectors at 6-hour intervals, 3 m above bottom at West Hackberry site, February 5, 1979.

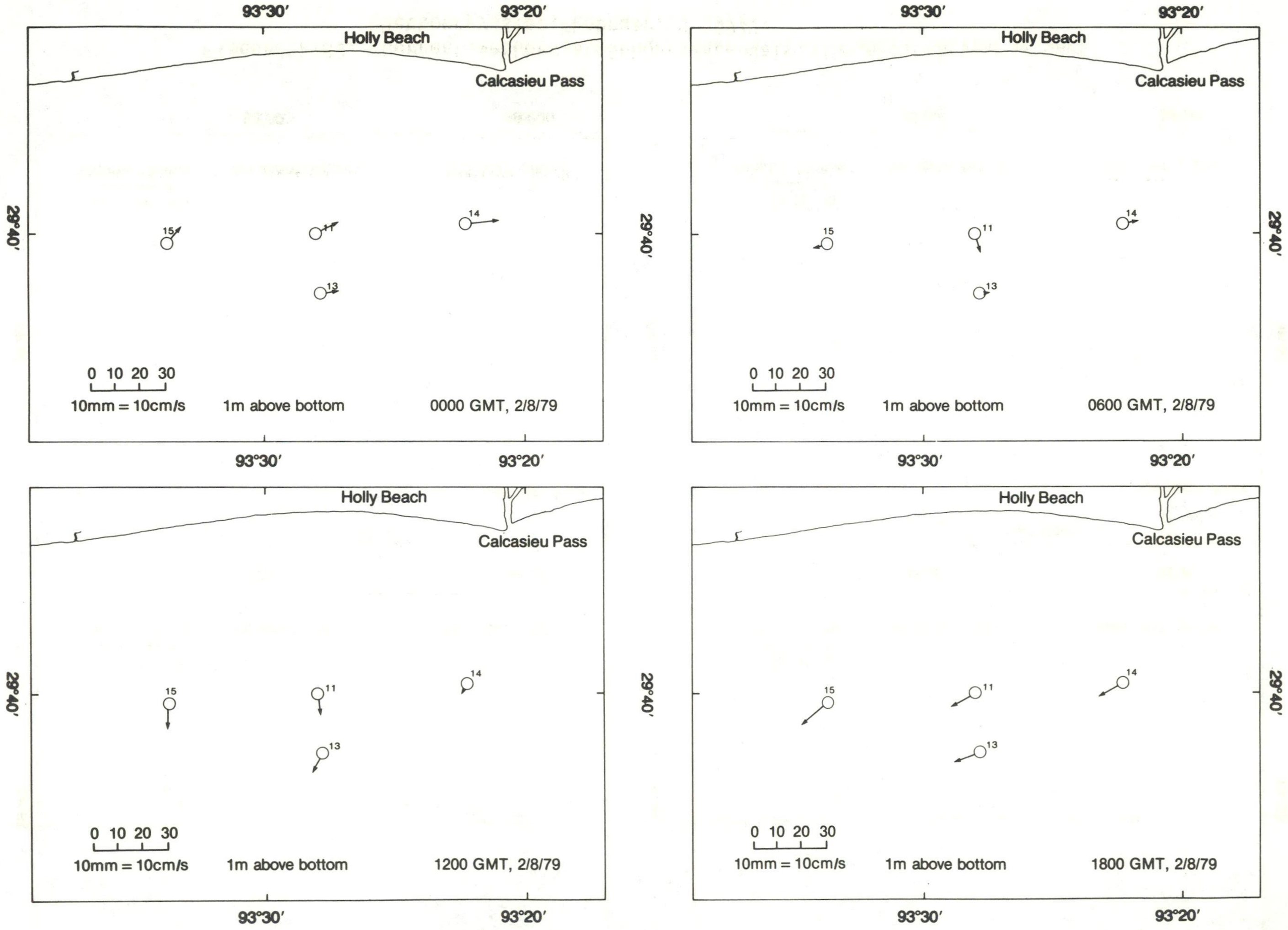

Figure E-29. Current vectors at 6-hour intervals, 1 m above bottom at West Hackberry site, February 8, 1979.

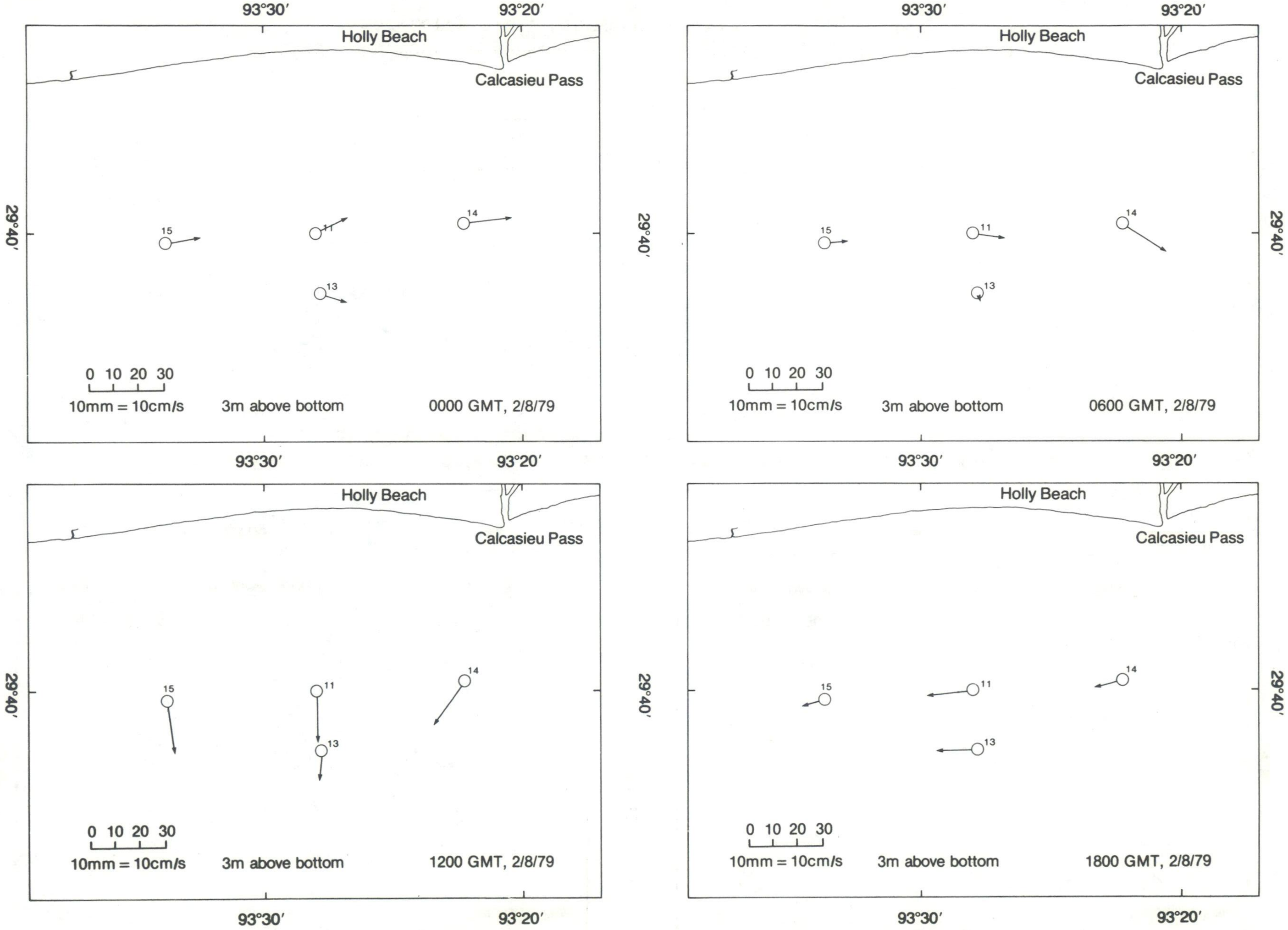

Figure E-30. Current vectors at 6-hour intervals, 3 m above bottom at West Hackberry site, February 8, 1979.

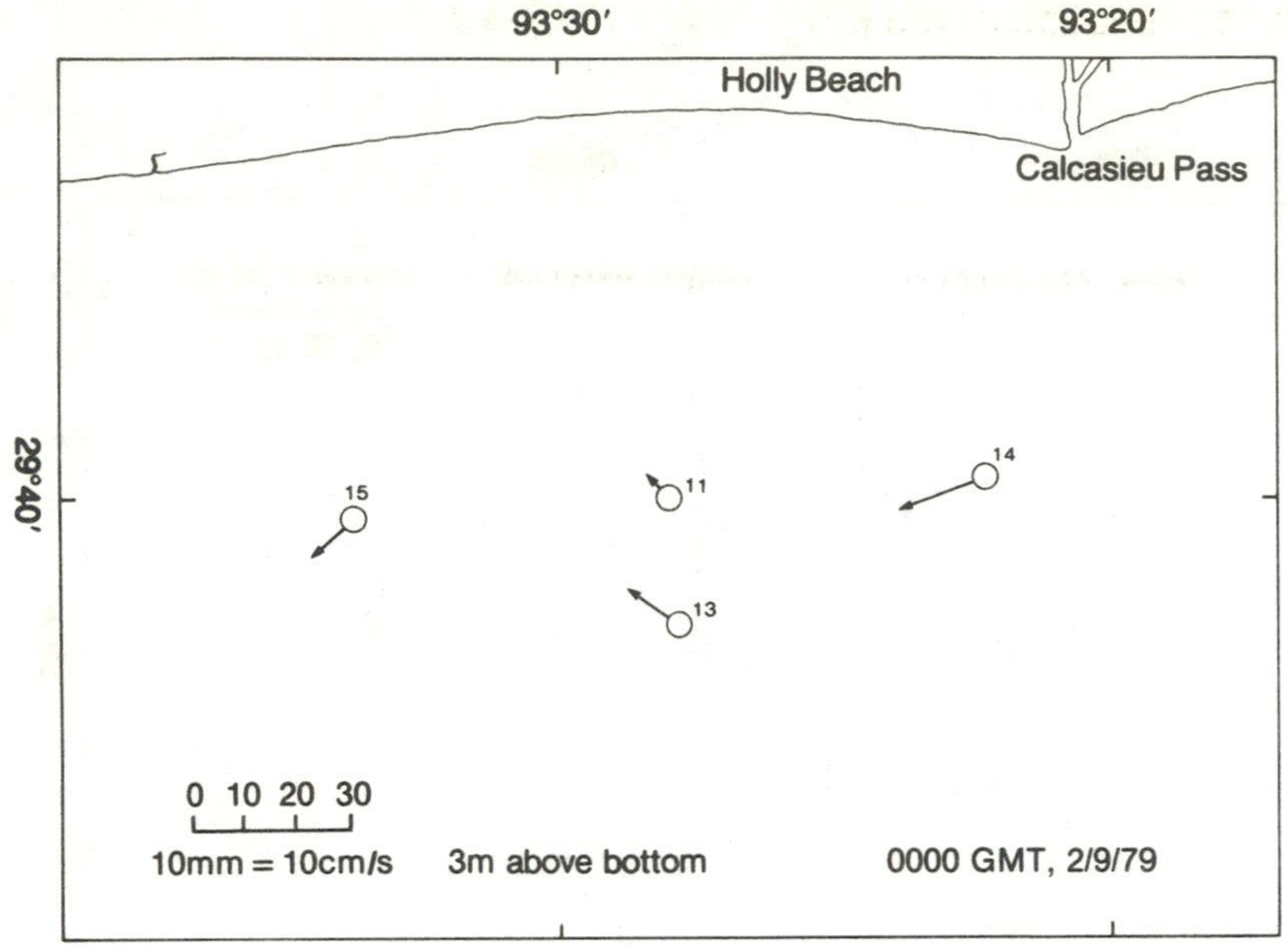

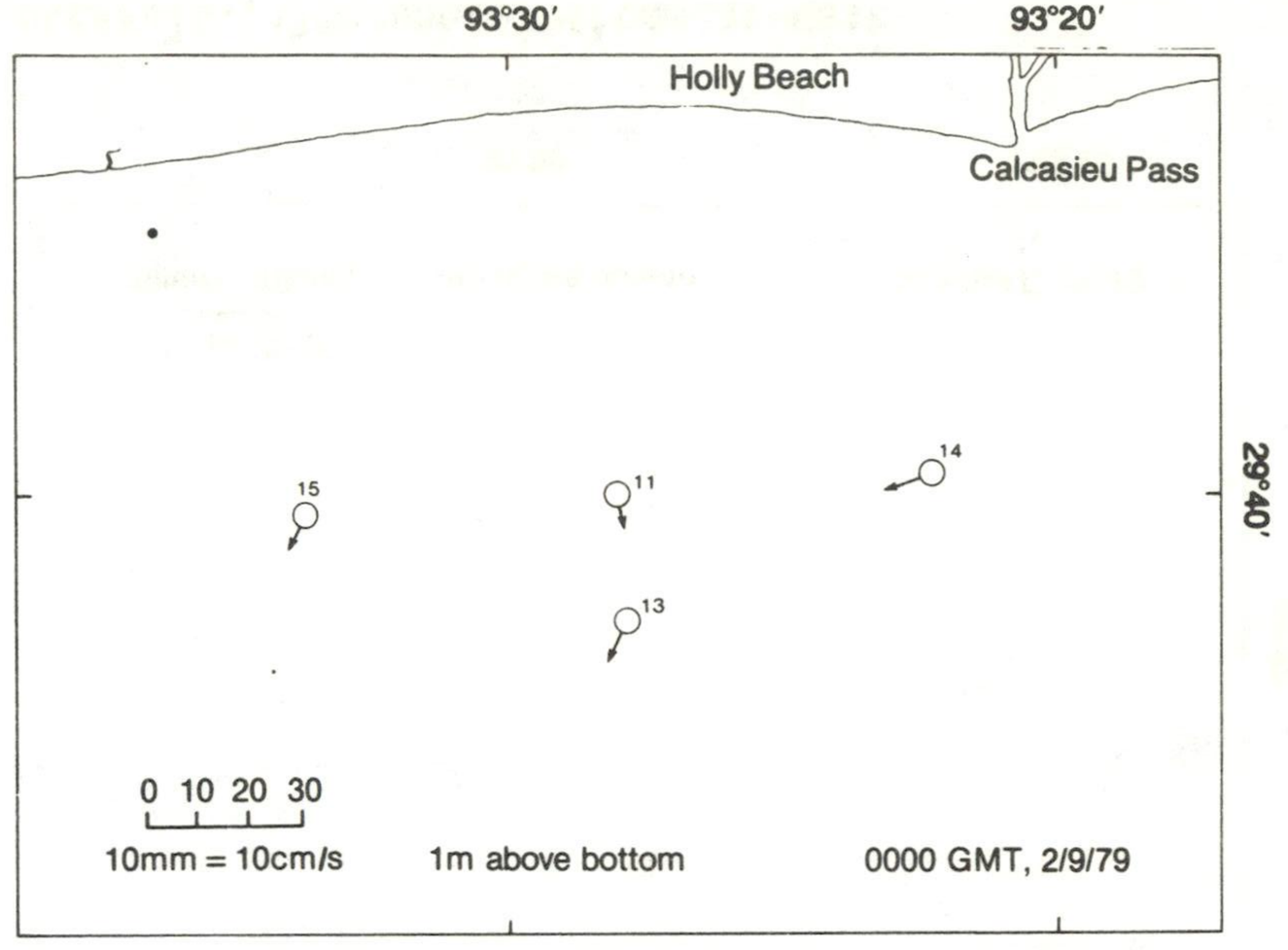

Figure E-31. Current vectors at West Hackberry site, 1 m and 3 m above bottom at 0000 GMT, February 9, 1979.

Figure E-32. Current vectors at 6-hour intervals, 1 m above bottom at West Hackberry site, February 15, 1979.

Figure E-33. Current vectors at 6-hour intervals, 3 m above bottom at West Hackberry site, February 15, 1979.

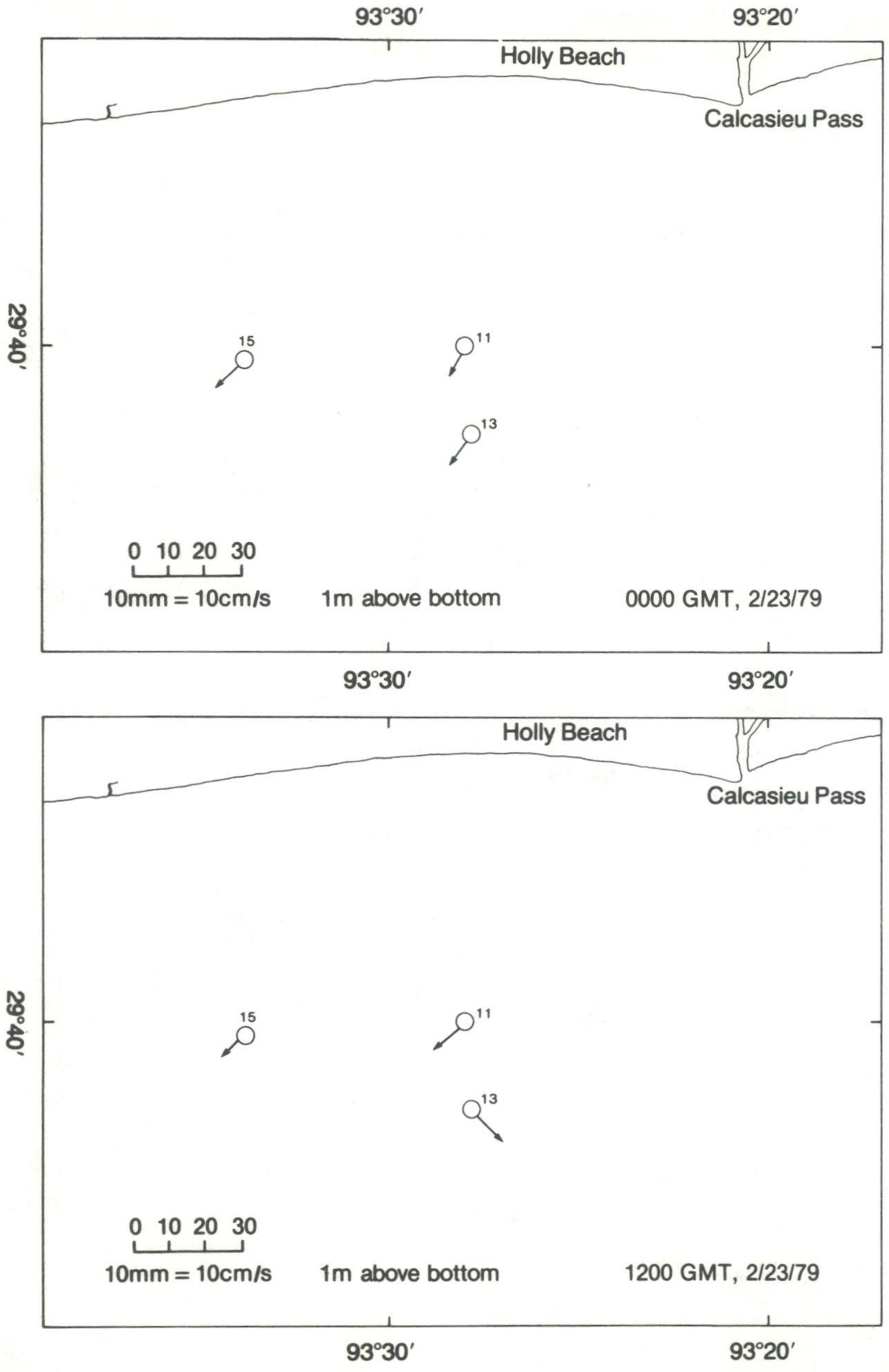

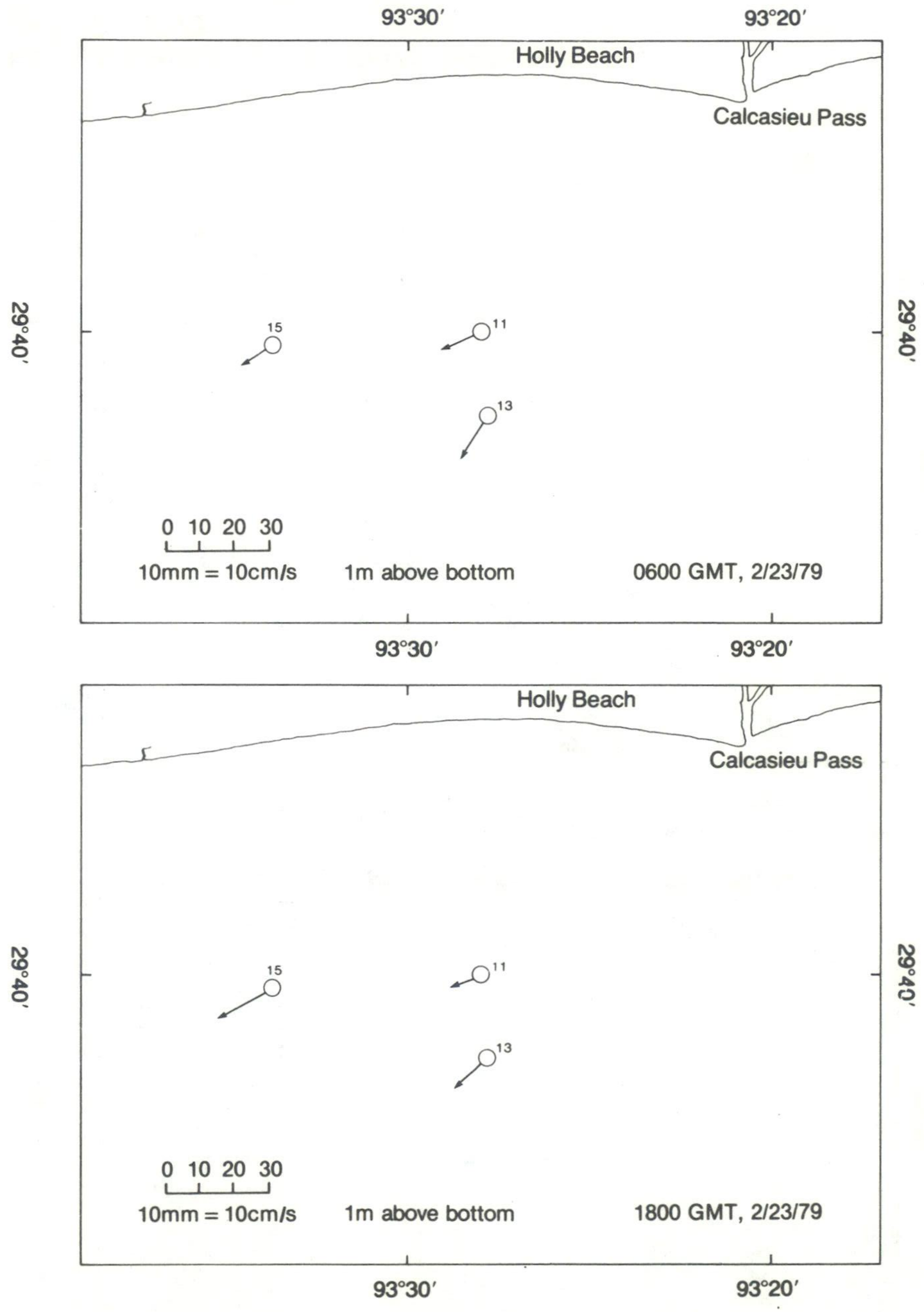

Figure E-34. Current vectors at 6-hour intervals, 1 m above bottom at West Hackberry site, February 23, 1979.

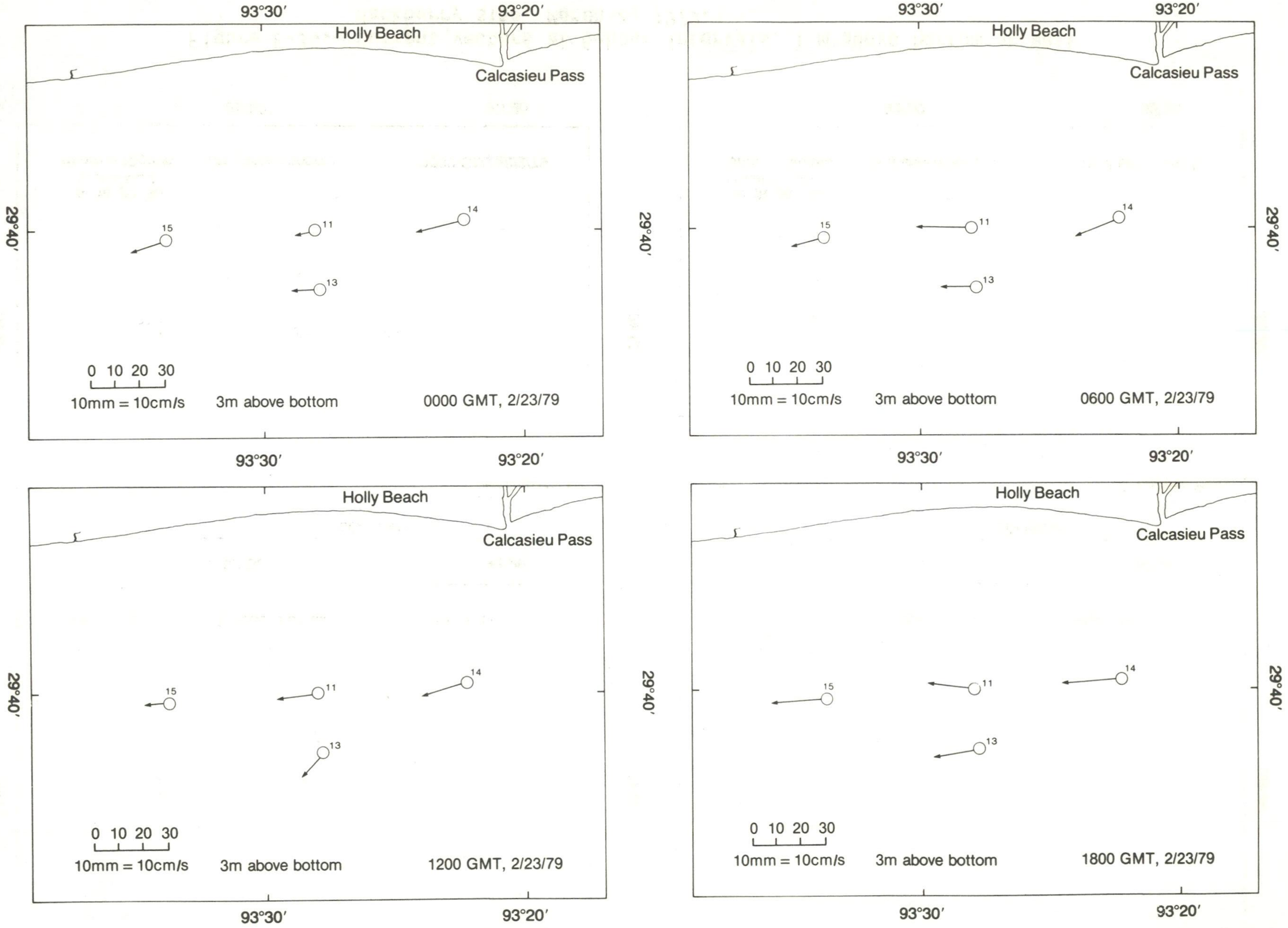

Figure E-35. Current vectors at 6-hour intervals, 3 m above bottom at West Hackberry site, February 23, 1979.

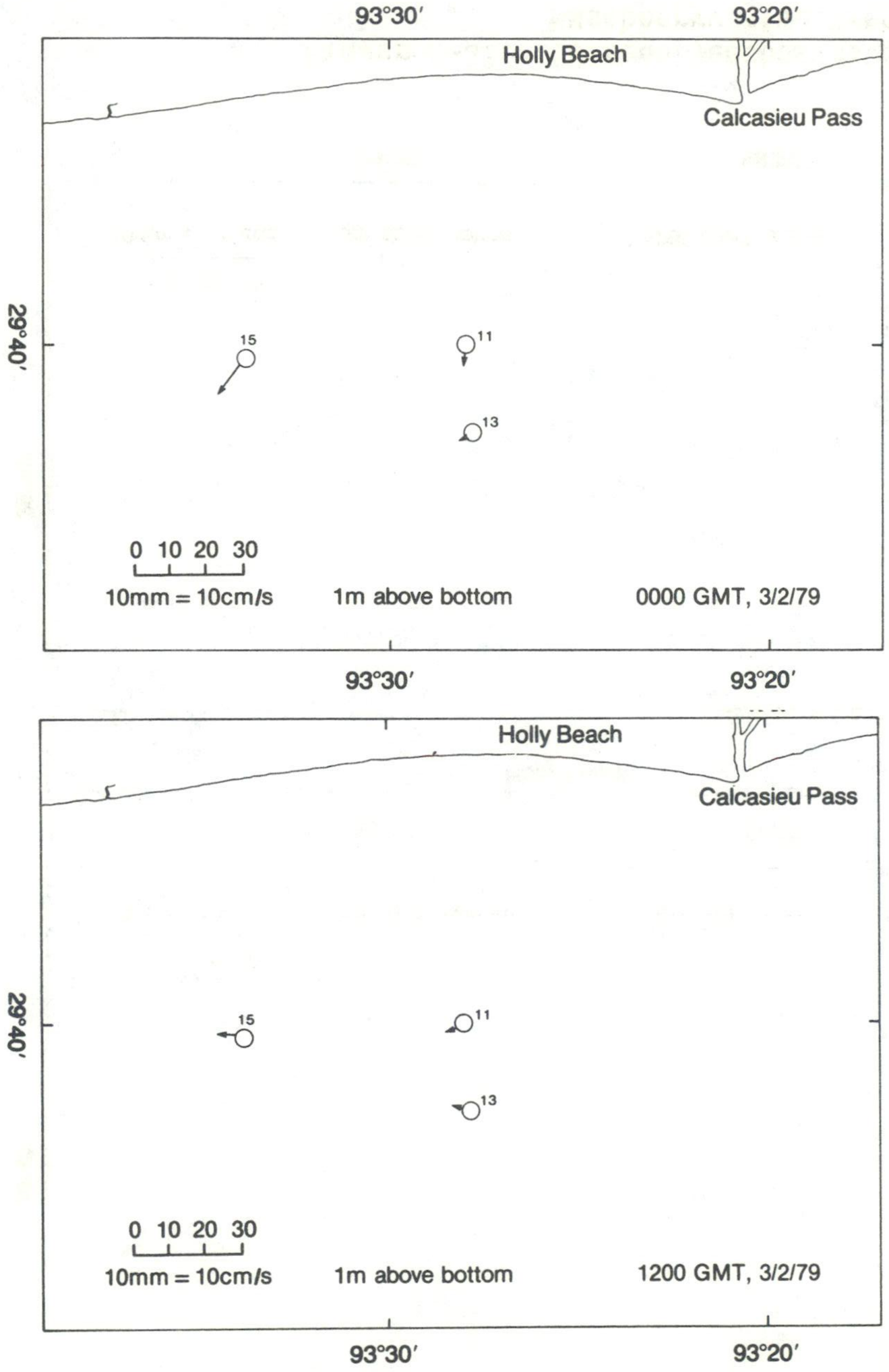

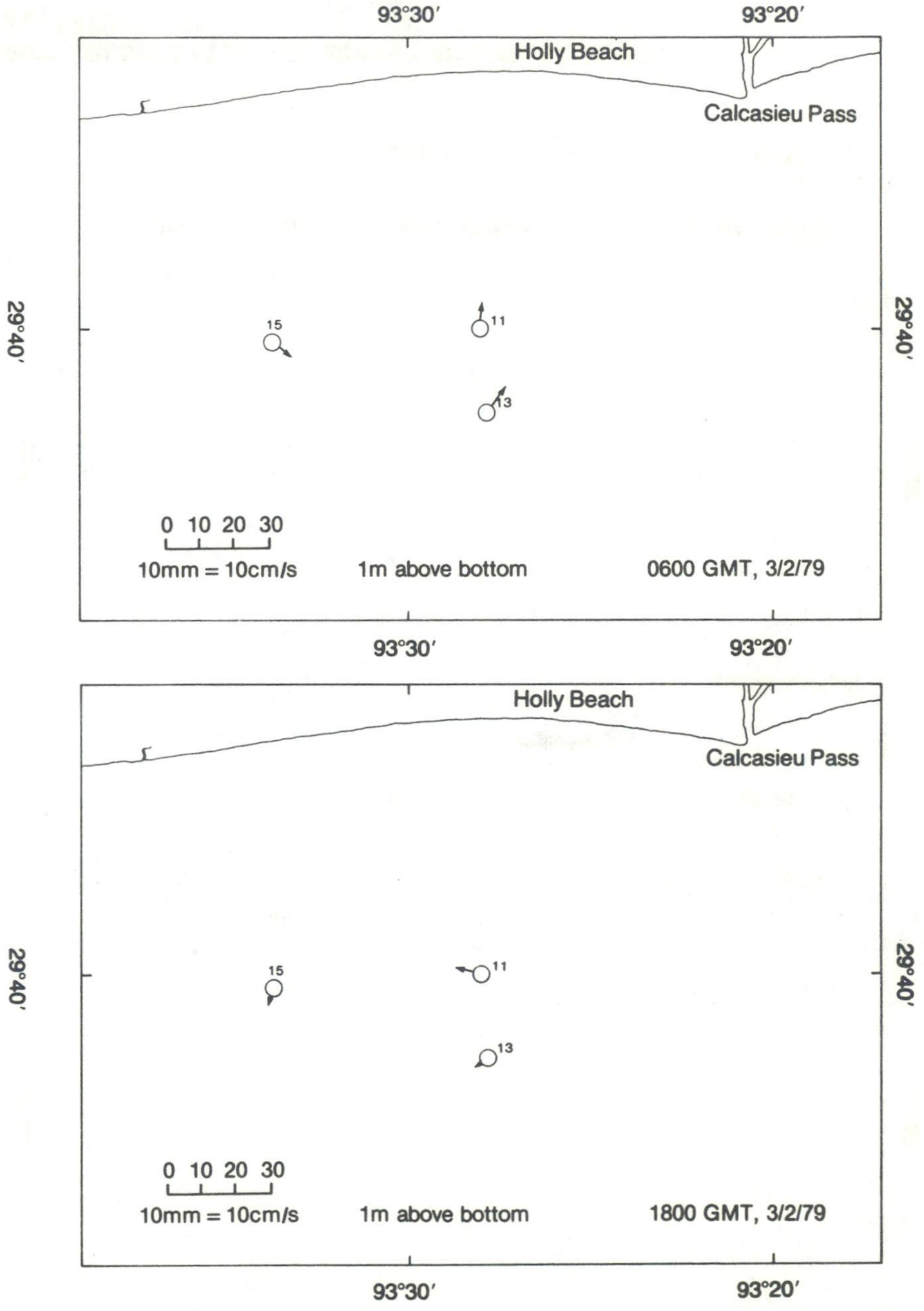

Figure E-36. Current vectors at 6-hour intervals, 1 m above bottom at West Hackberry site, March 2, 1979.

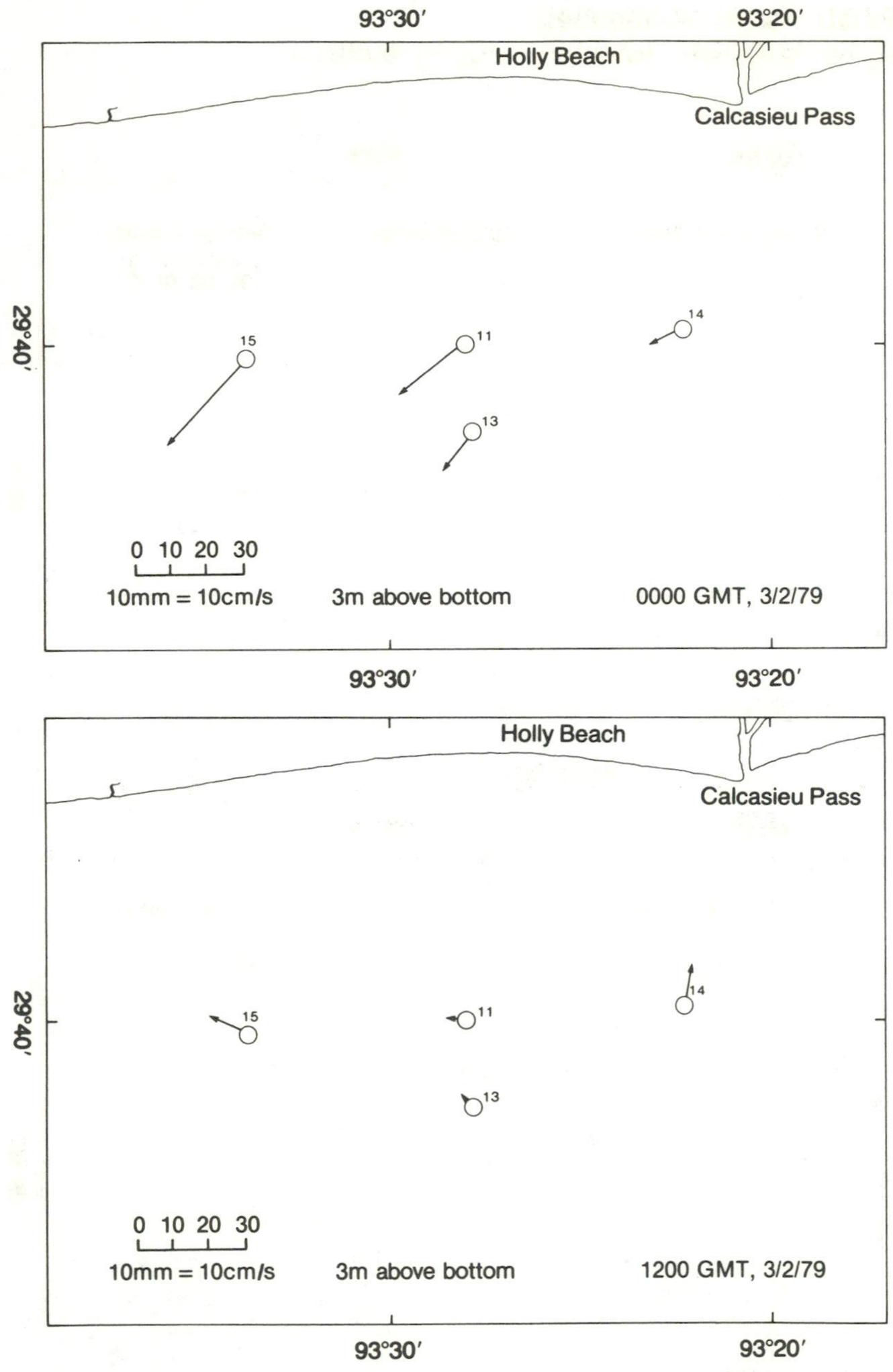

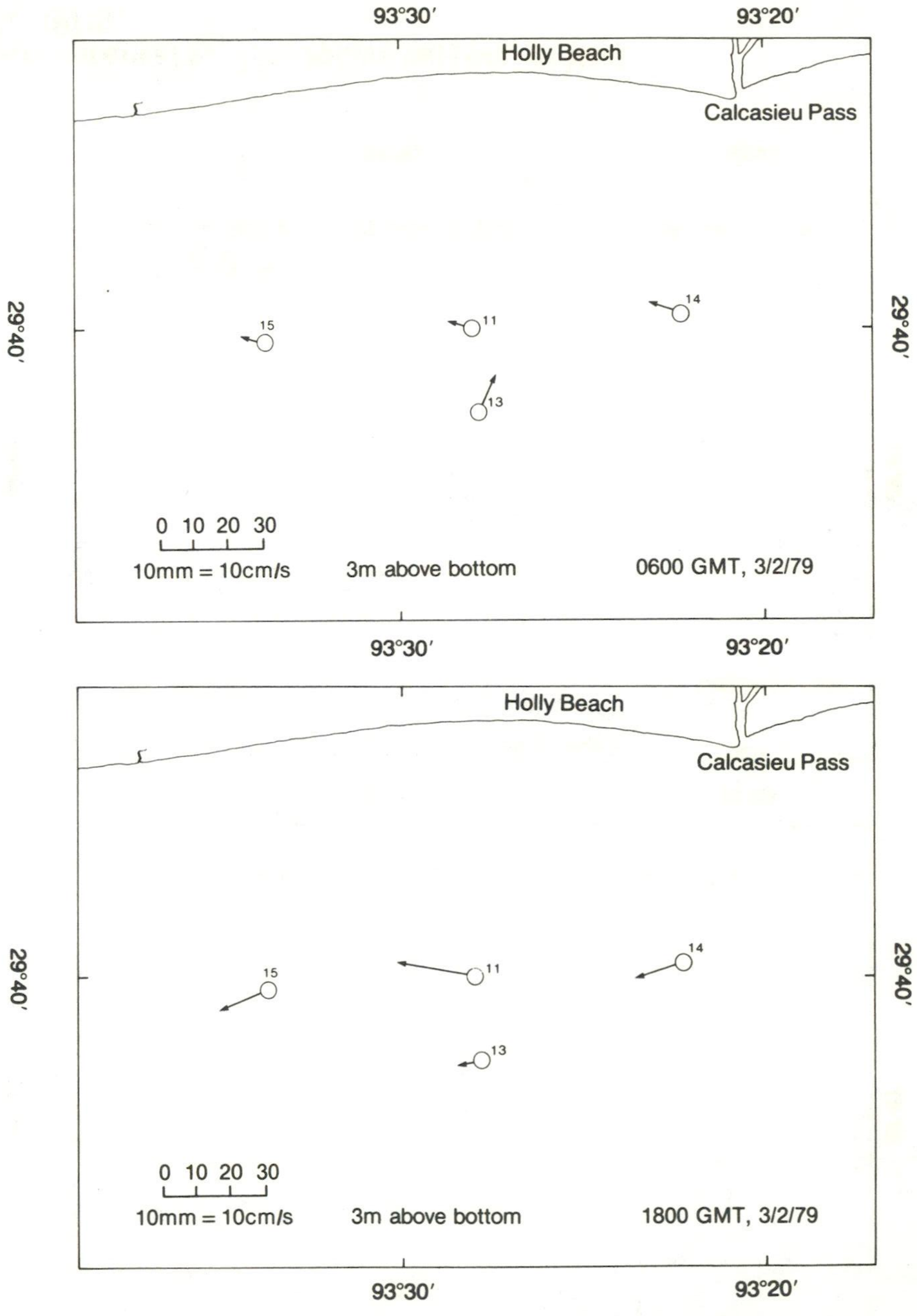

Figure E-37. Current vectors at 6-hour intervals, 3 m above bottom at West Hackberry site, March 2, 1979.

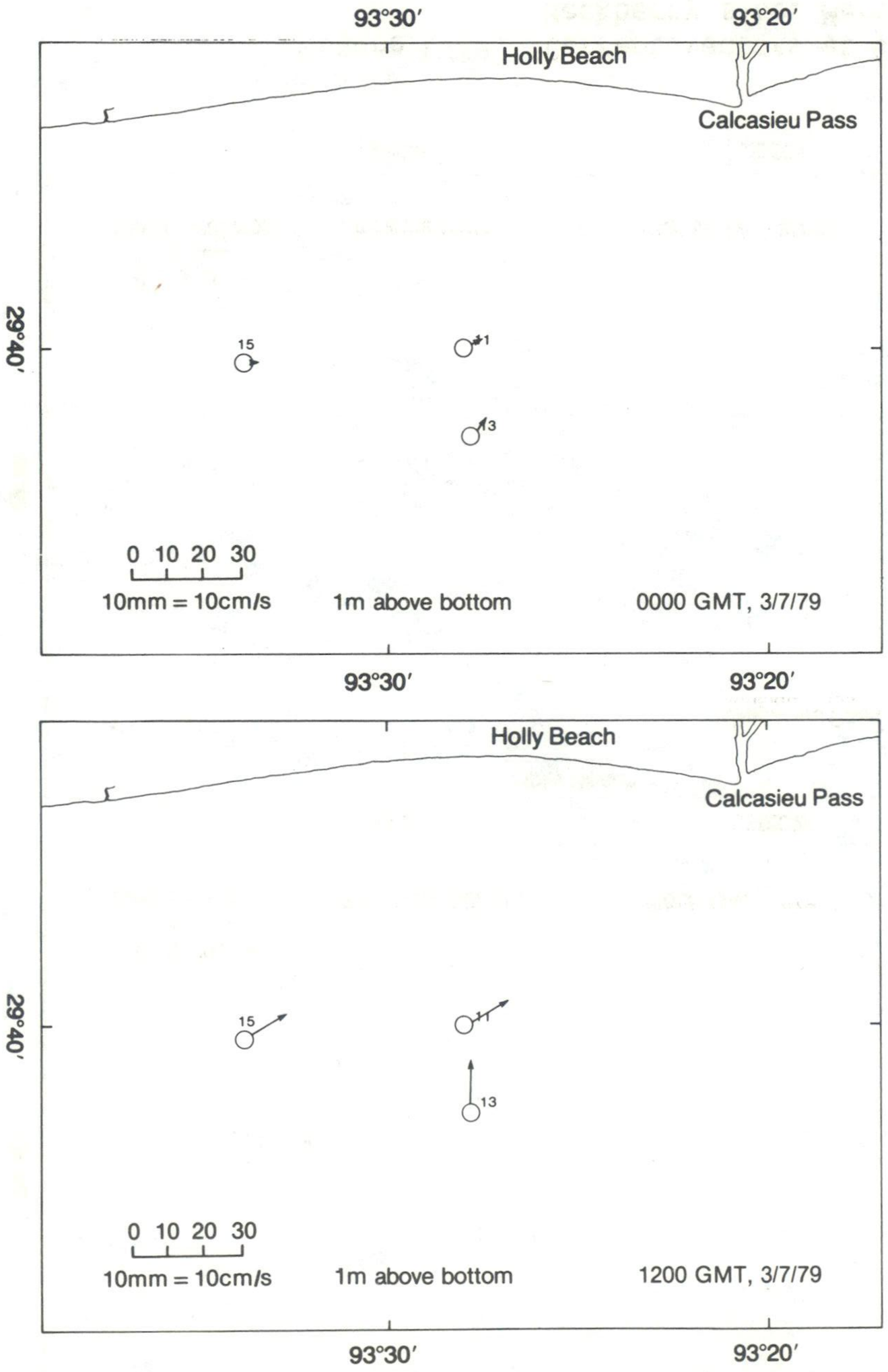

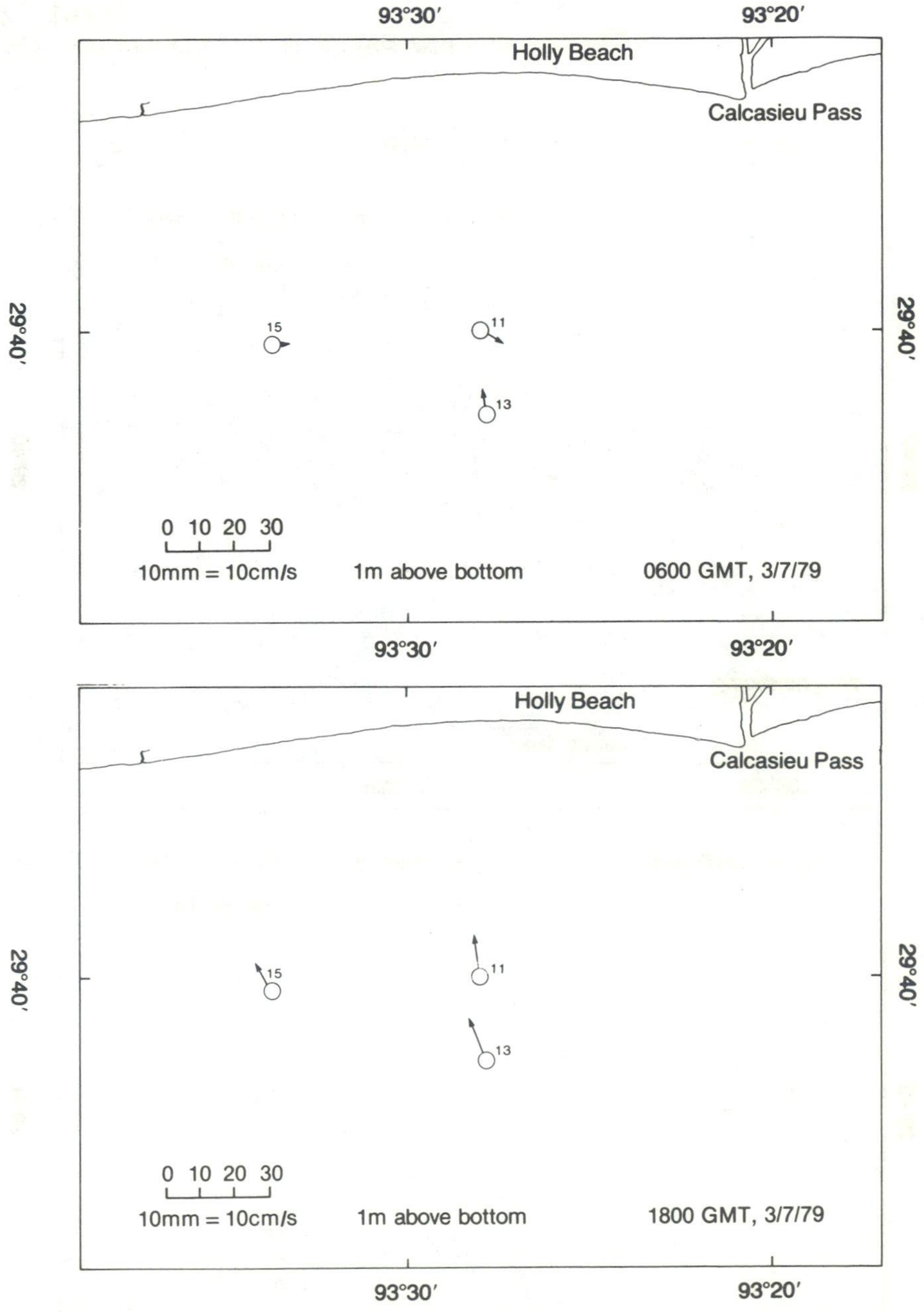

Figure E-38. Current vectors at 6-hour intervals, 1 m above bottom at West Hackberry site, March 7, 1979.

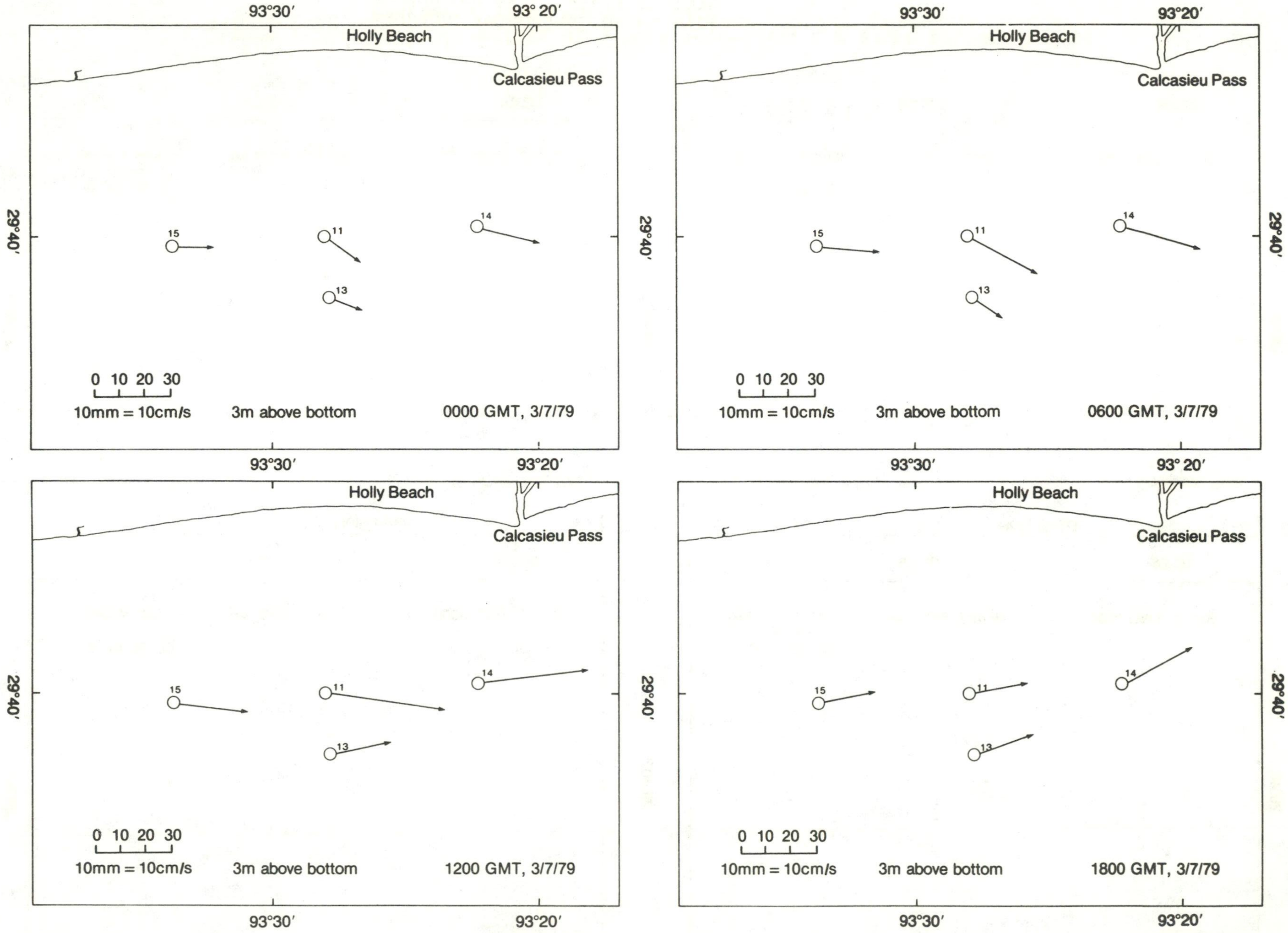

Figure E-39. Current vectors at 6-hour intervals, 3 m above bottom at West Hackberry site, March 7, 1979.

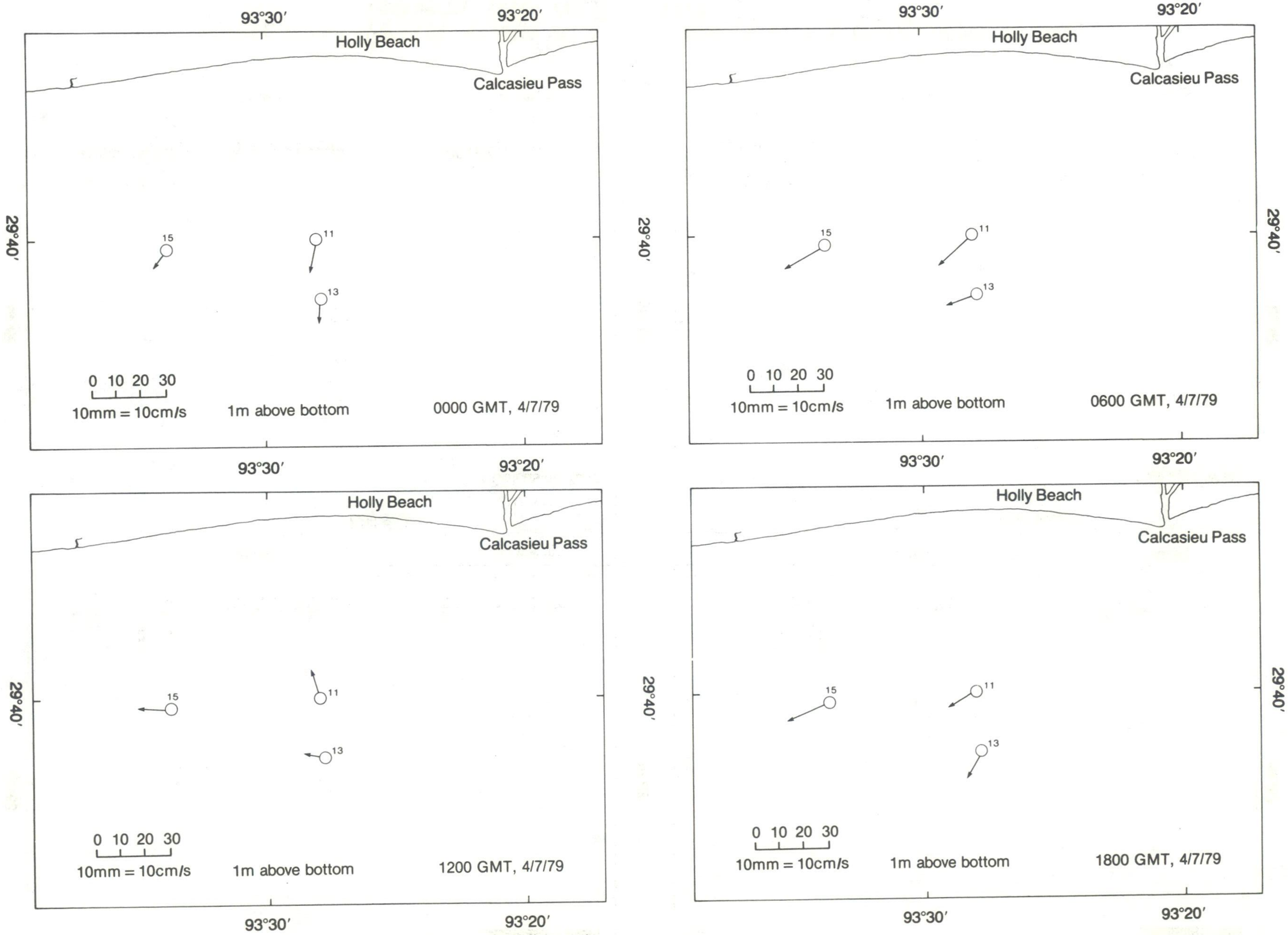

Figure E-40. Current vectors at 6-hour intervals, 1 m above bottom at West Hackberry site, April 7, 1979.

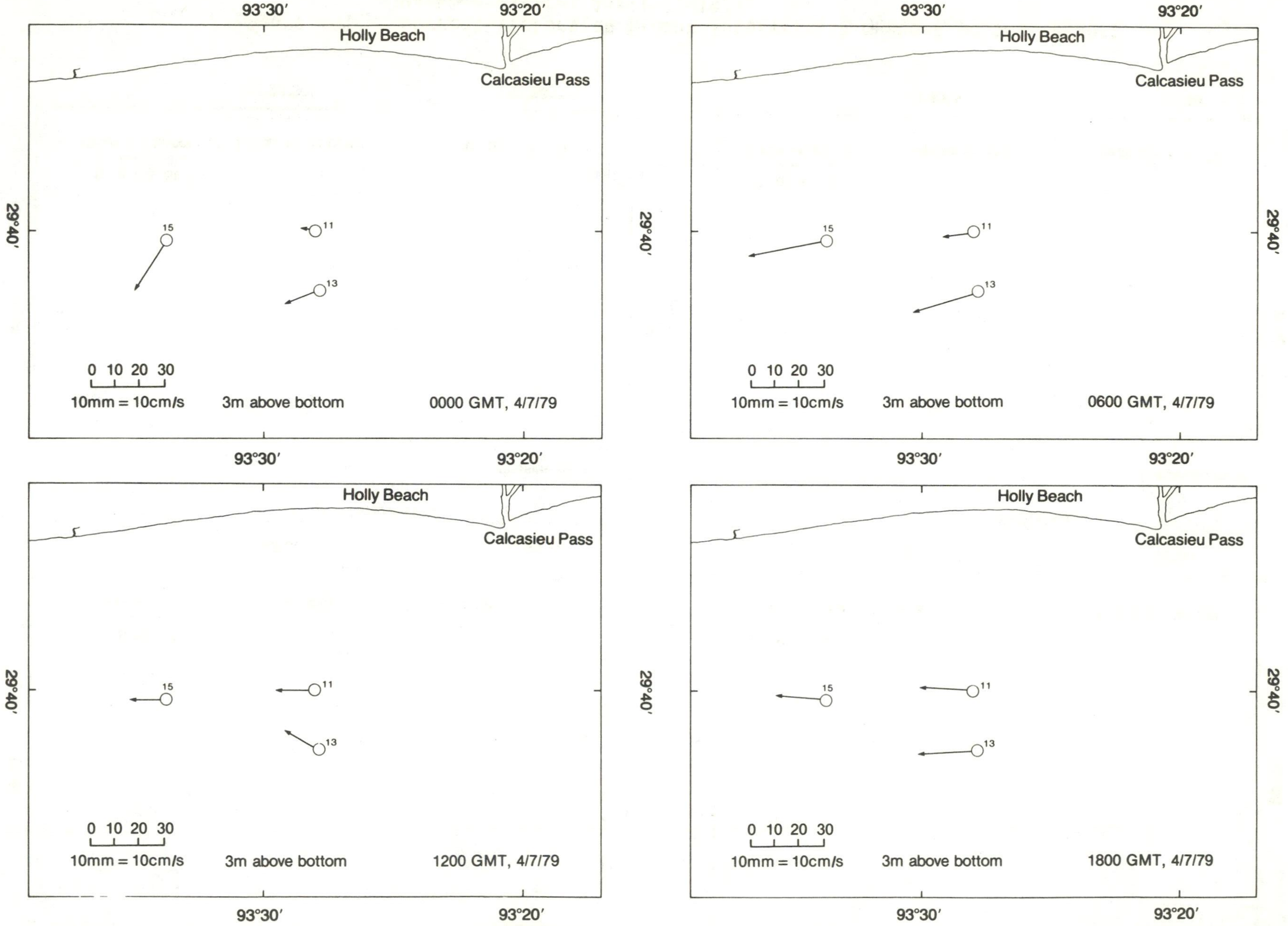

Figure E-41. Current vectors at 6-hour intervals, 3 m above bottom at West Hackberry site, April 7, 1979.

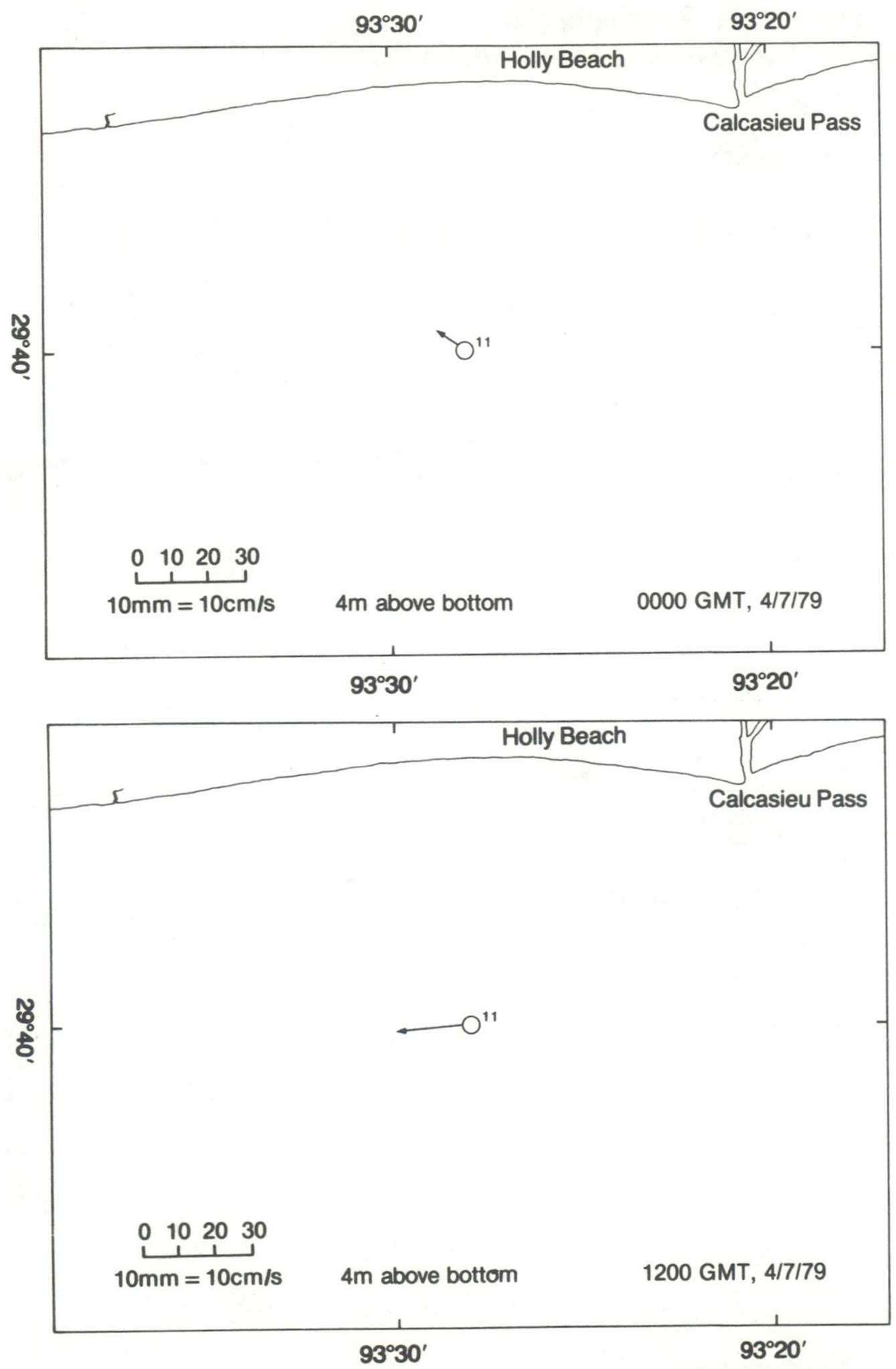

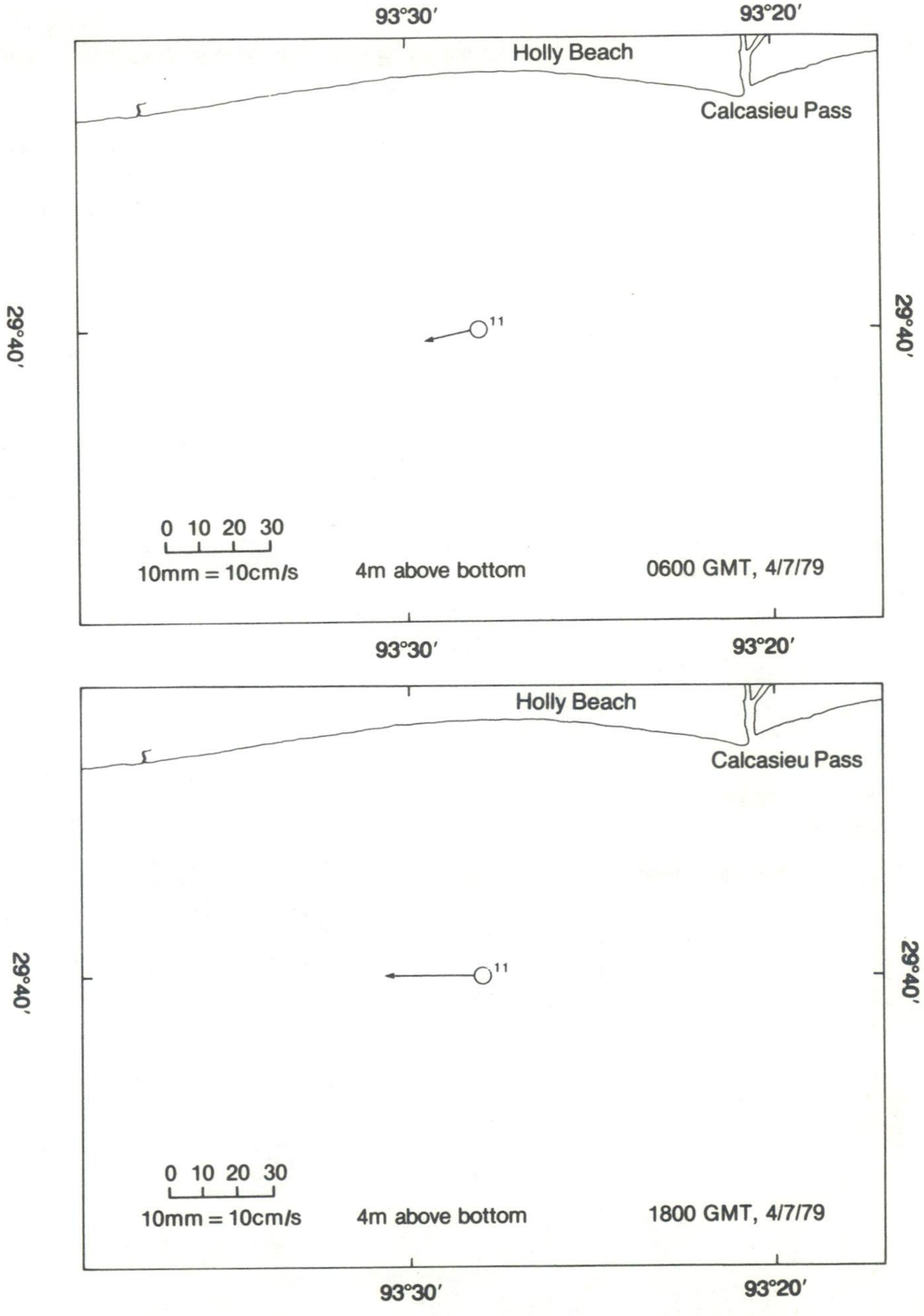

Figure E-42. Current vectors at 6-hour intervals, 4 m above bottom at West Hackberry site, April 7, 1979.

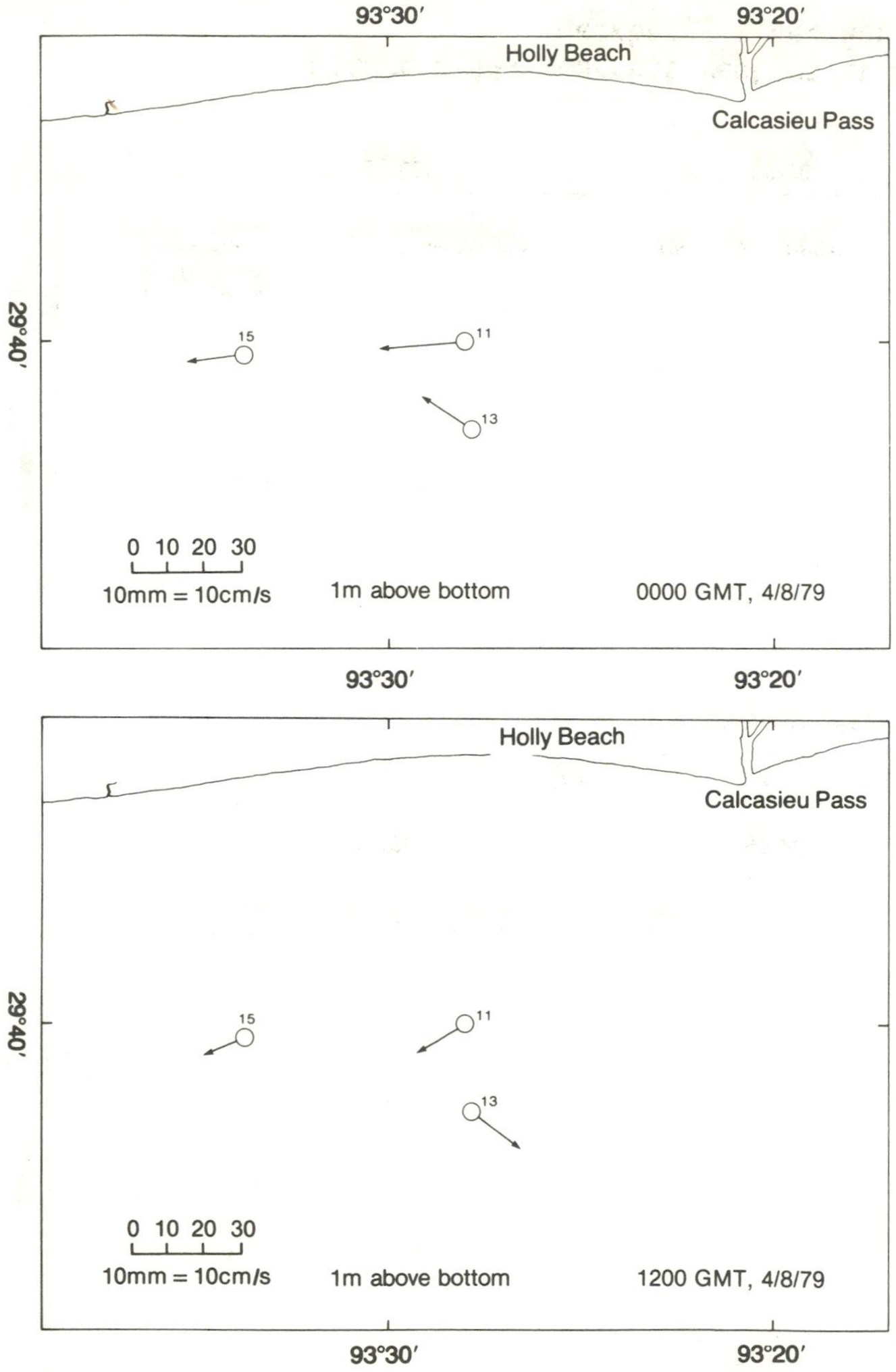

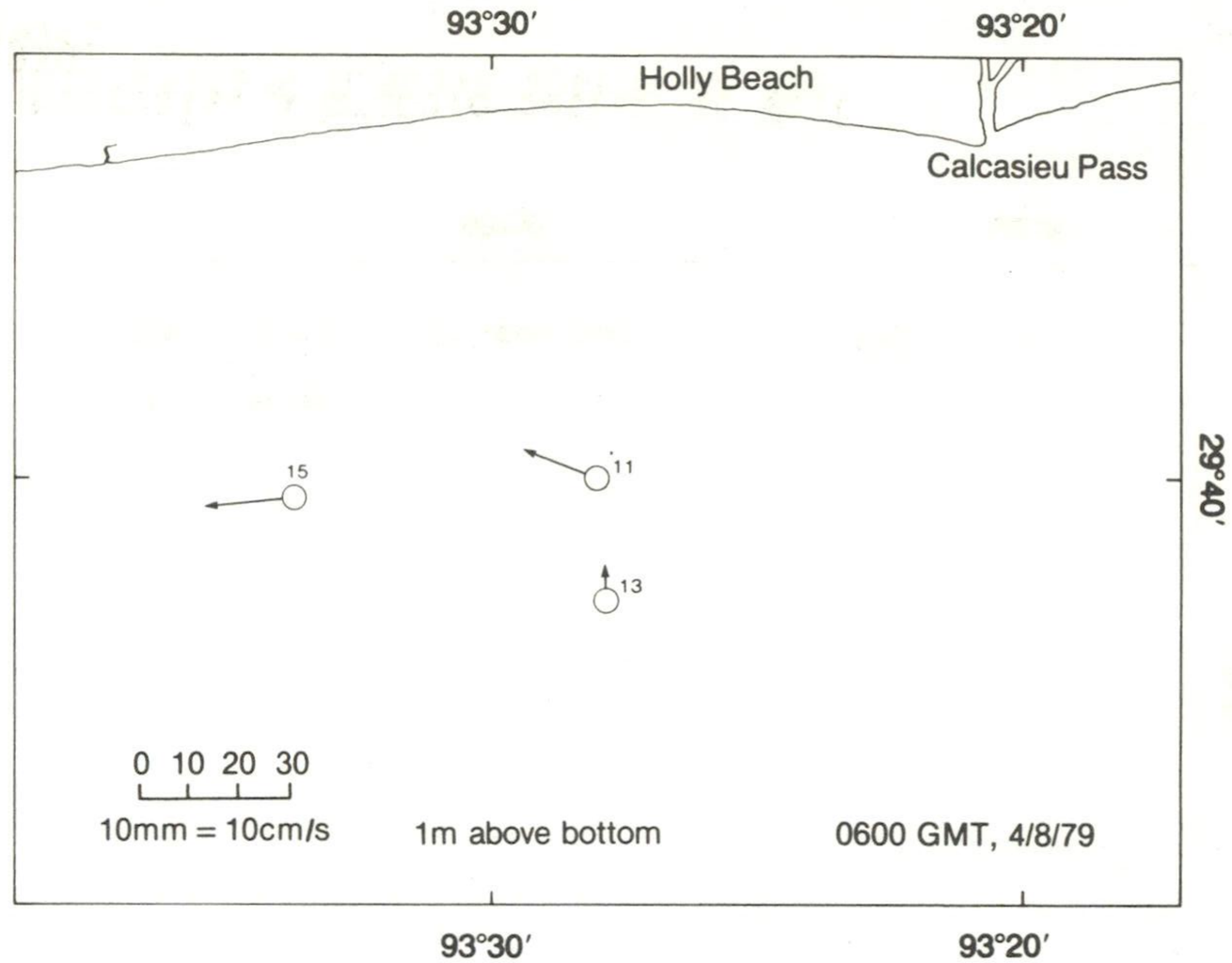

Figure E-43. Current vectors at 6-hour intervals, 1 m above bottom at West Hackberry site, April 8, 1979.

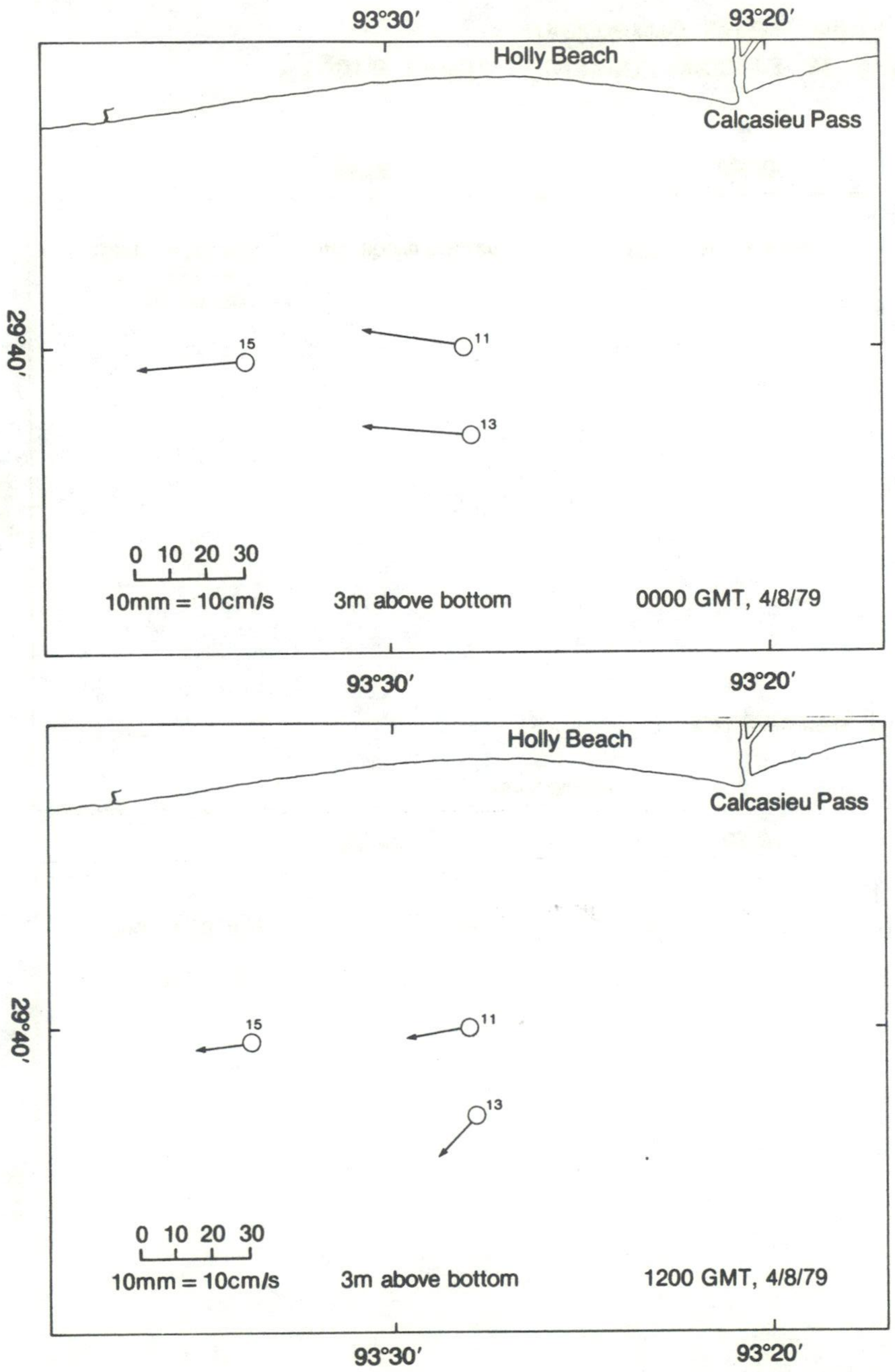

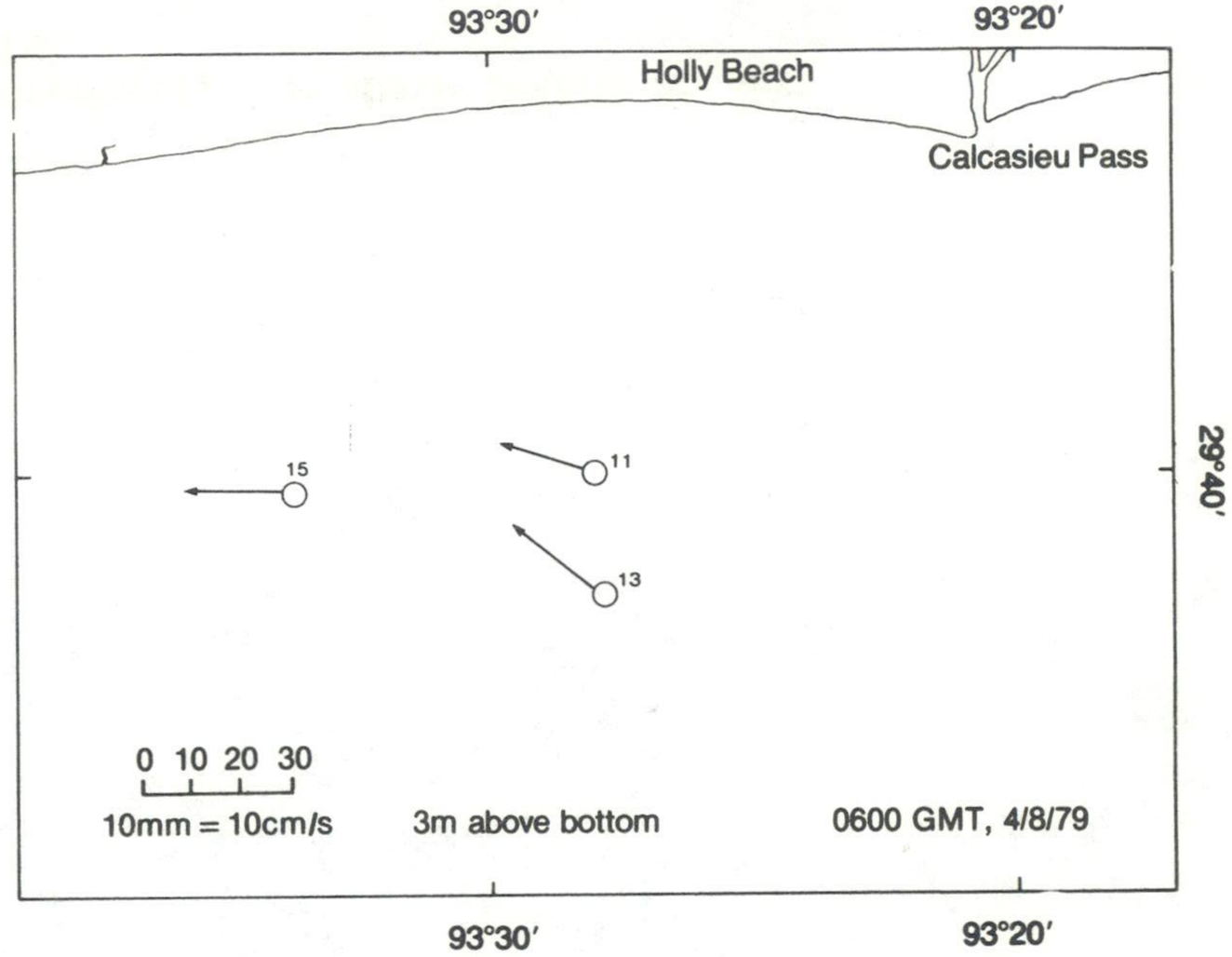

Figure E-44. Current vectors at 6-hour intervals, 3 m above bottom at West Hackberry site, April 8, 1979.

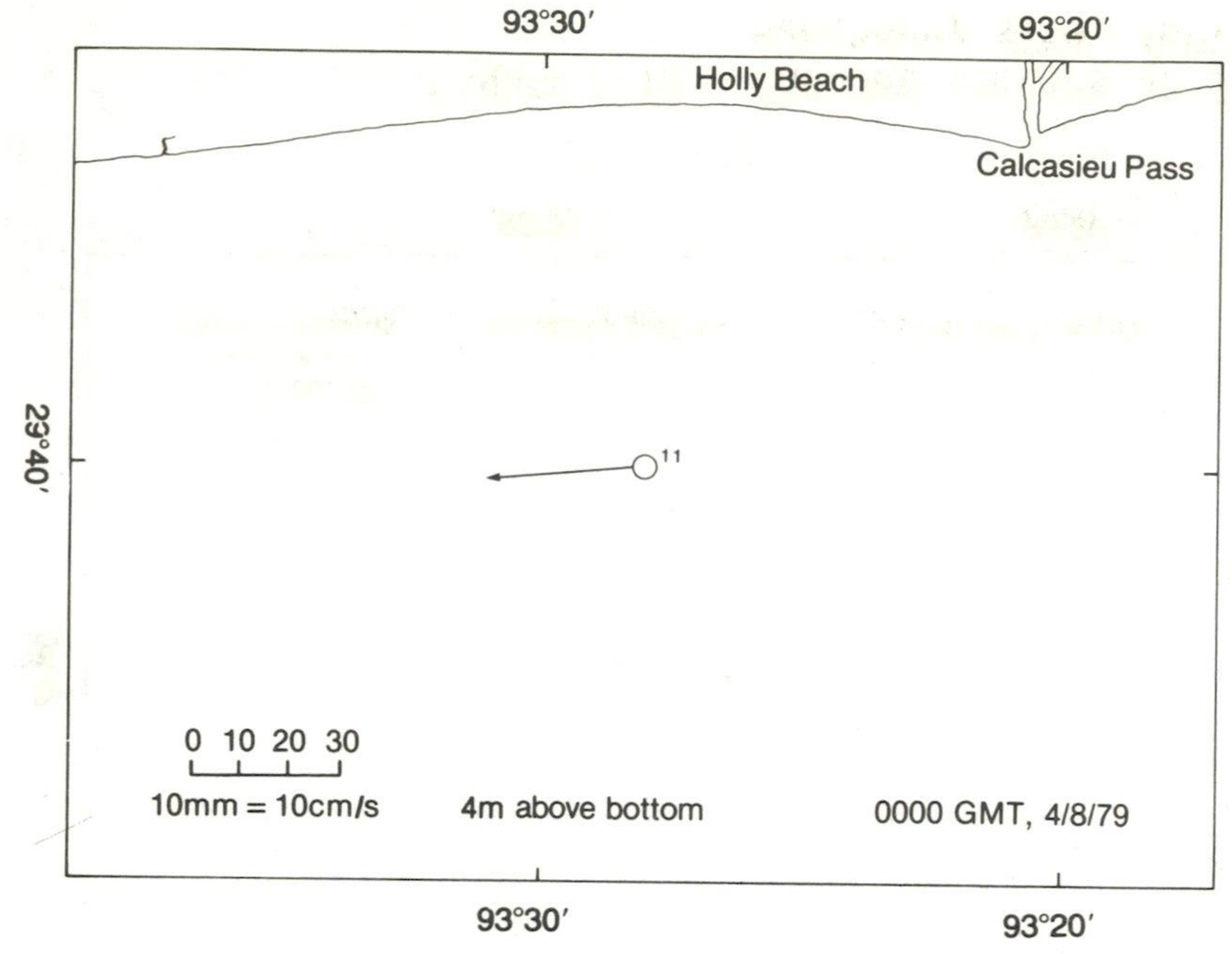

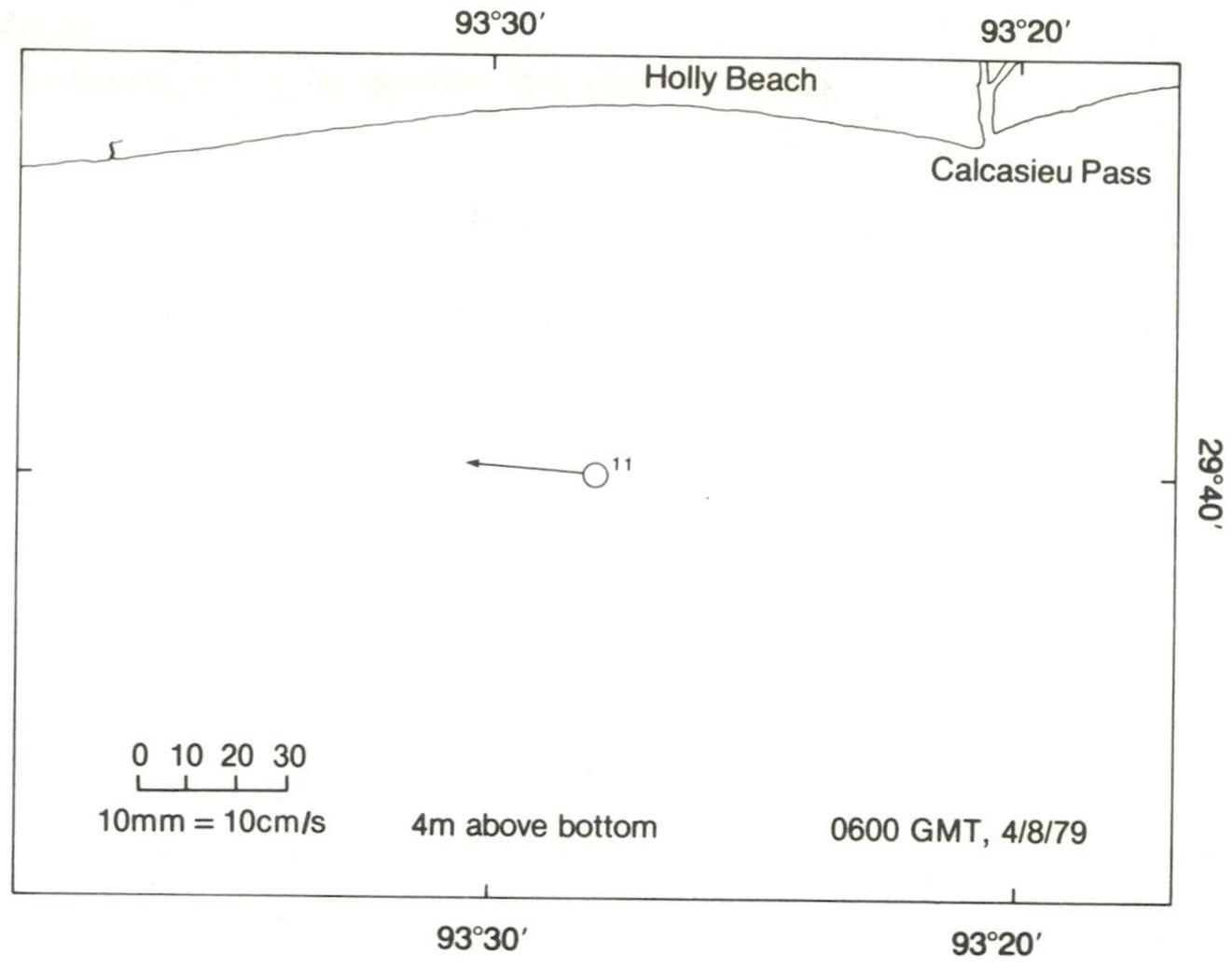

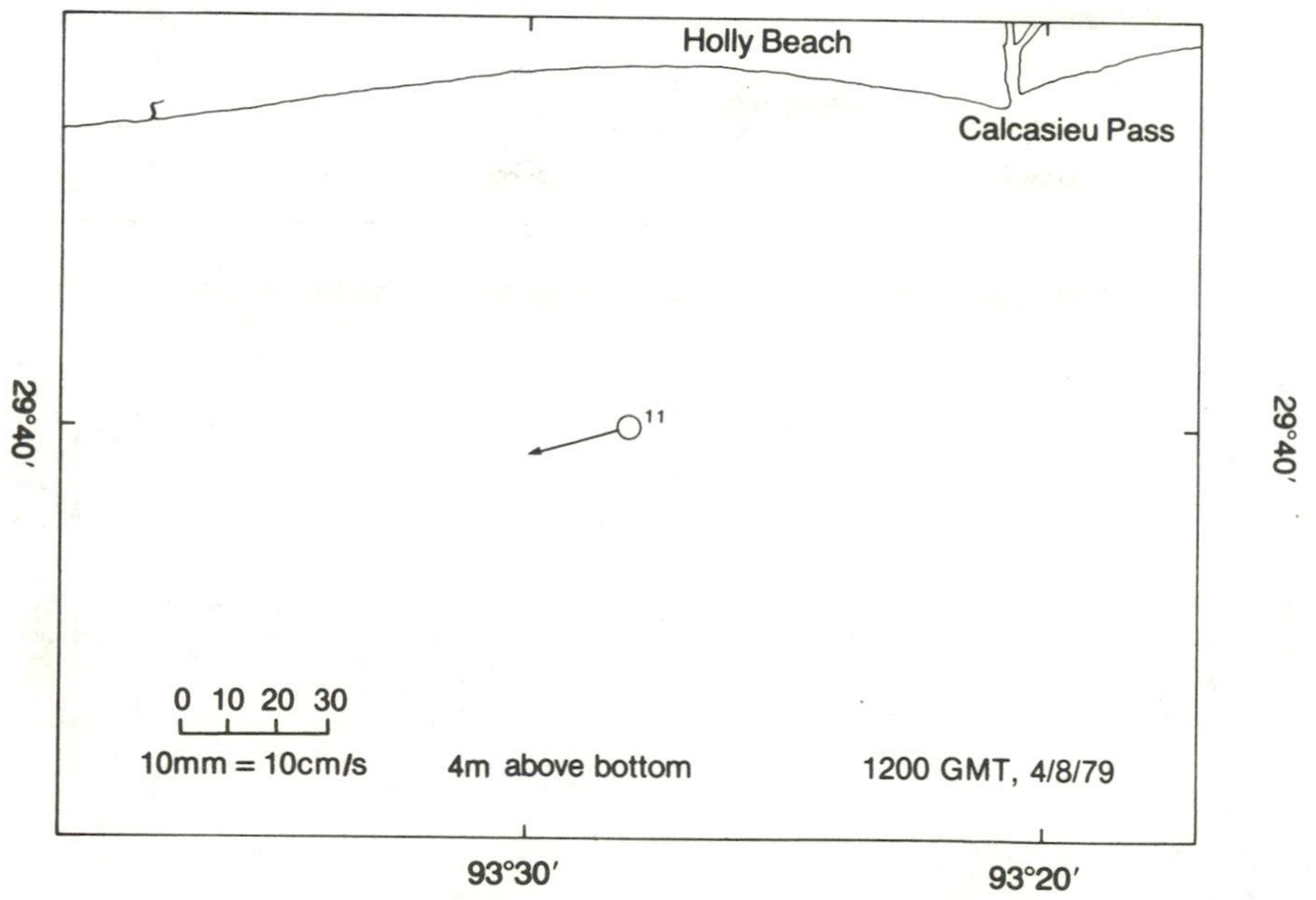

Figure E-45. Current vectors at 6-hour intervals, 4 m above bottom at West Hackberry site, April 8, 1979.

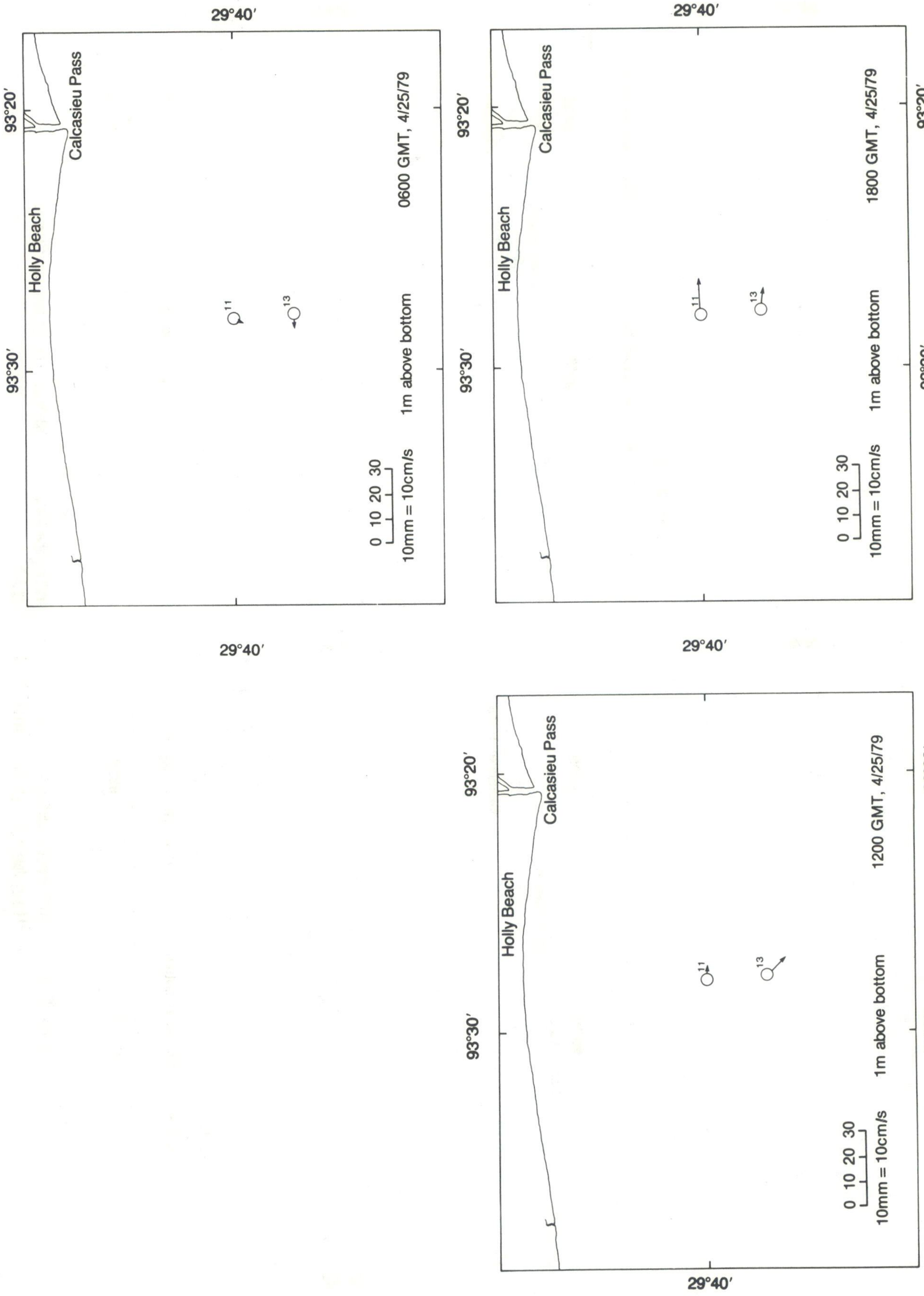

Figure E-46. Current vectors at 6-hour intervals, 1 m above bottom at Hackberry site, April 25, 1979.

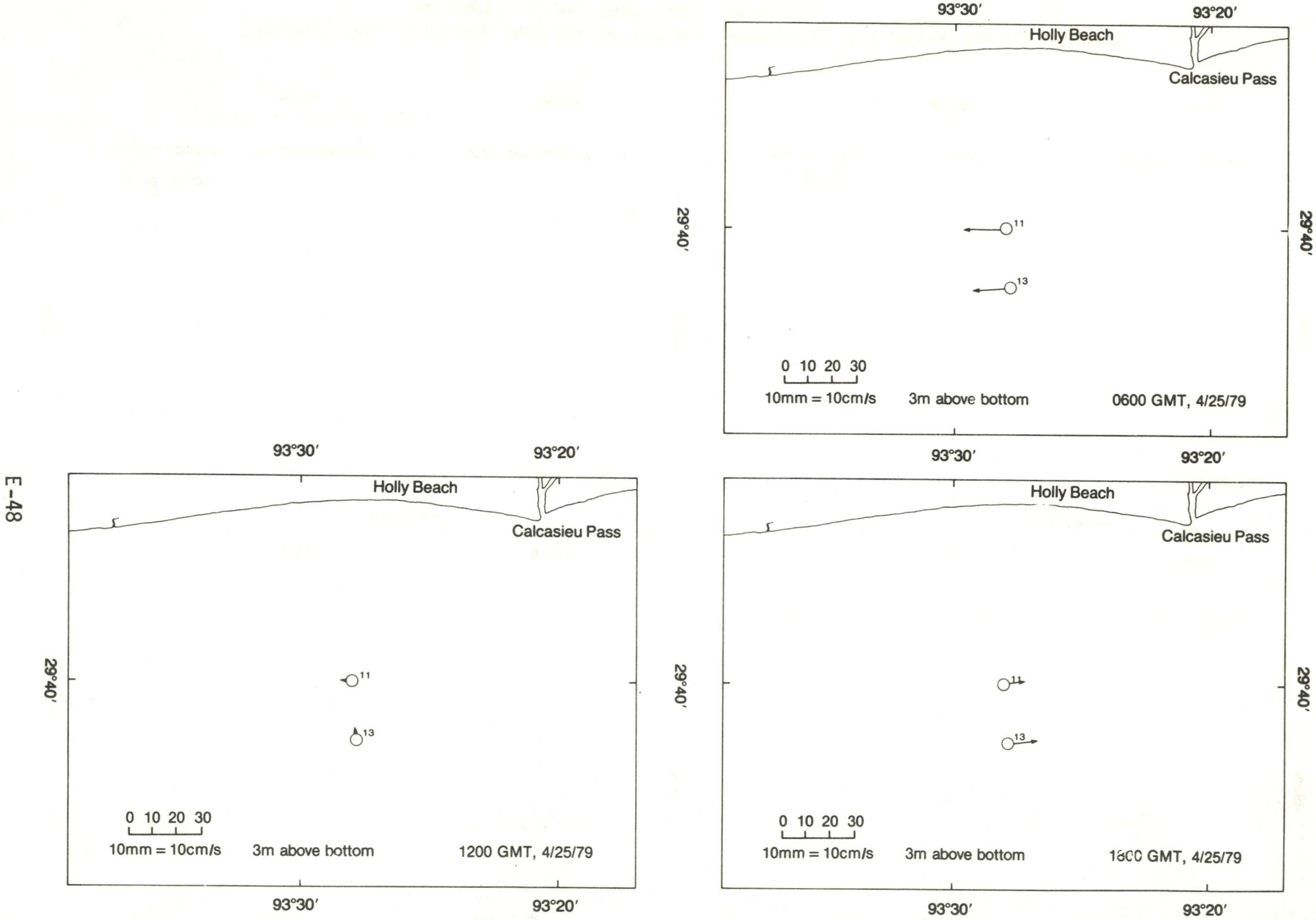

Figure E-47. Current vectors at 6-hour intervals, 3 m above bottom at West Hackberry site, April 25, 1979.

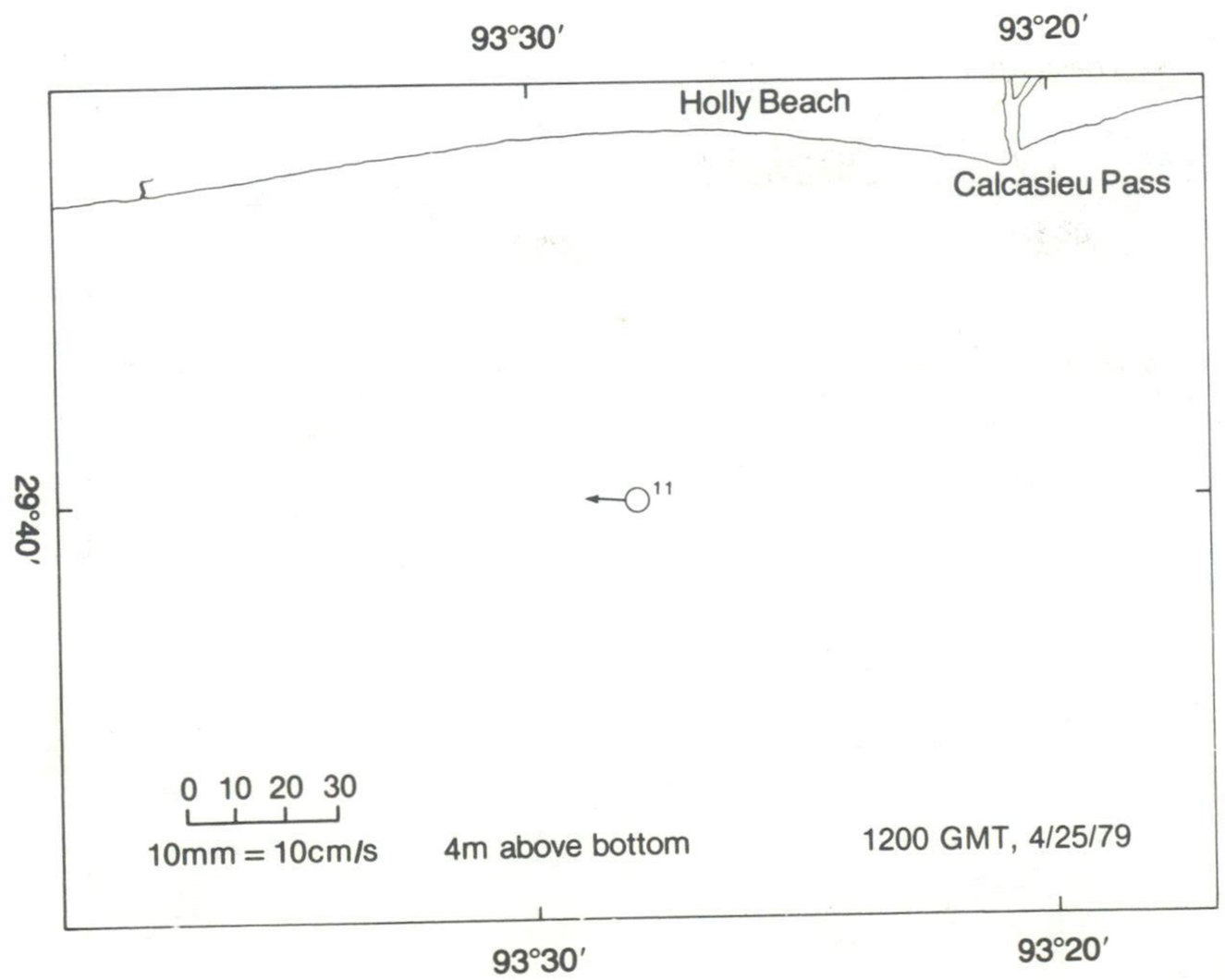

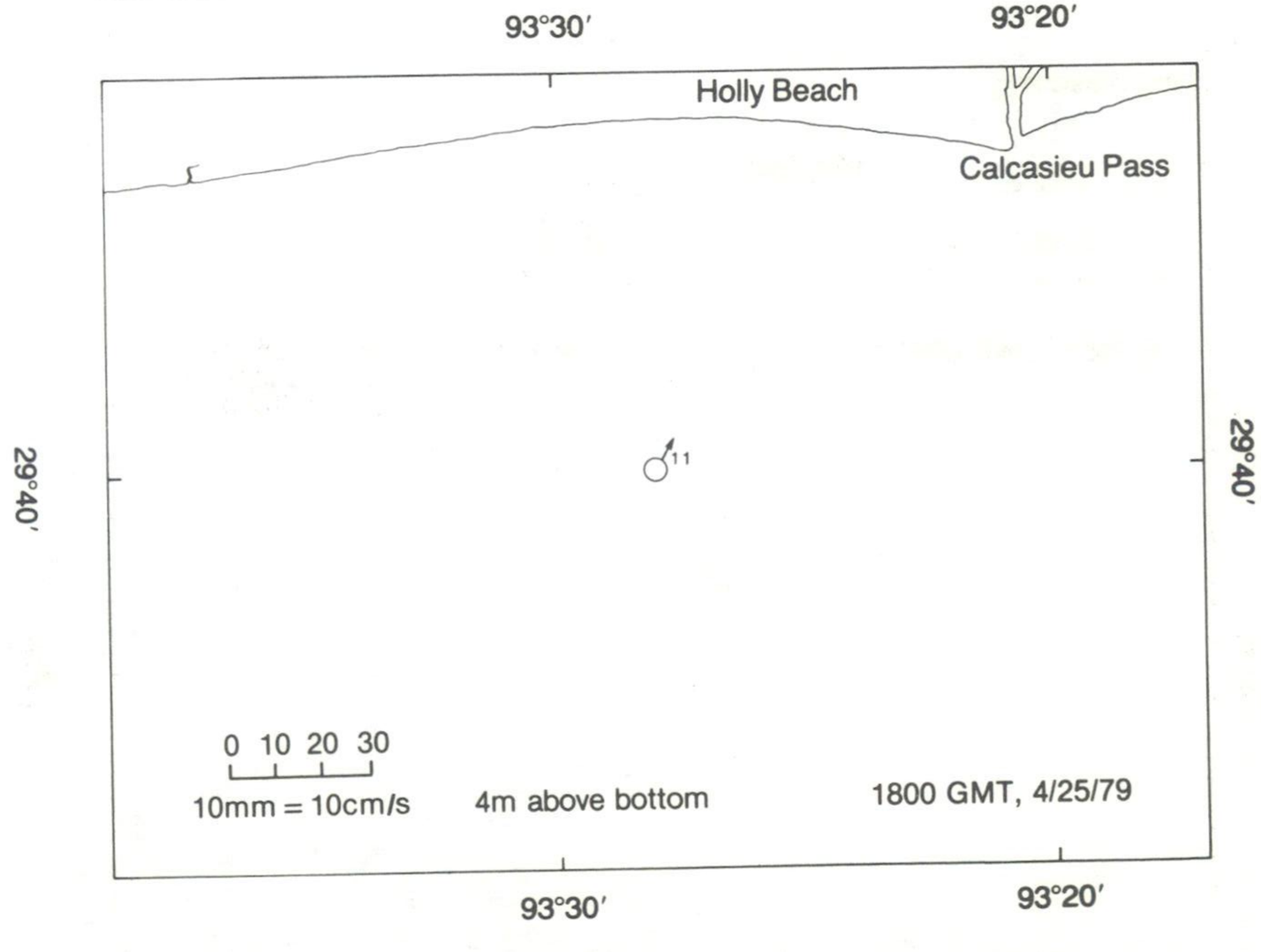

Figure E-48. Current vectors at 6-hour intervals, 4 m above bottom at West Hackberry site, April 25, 1979.

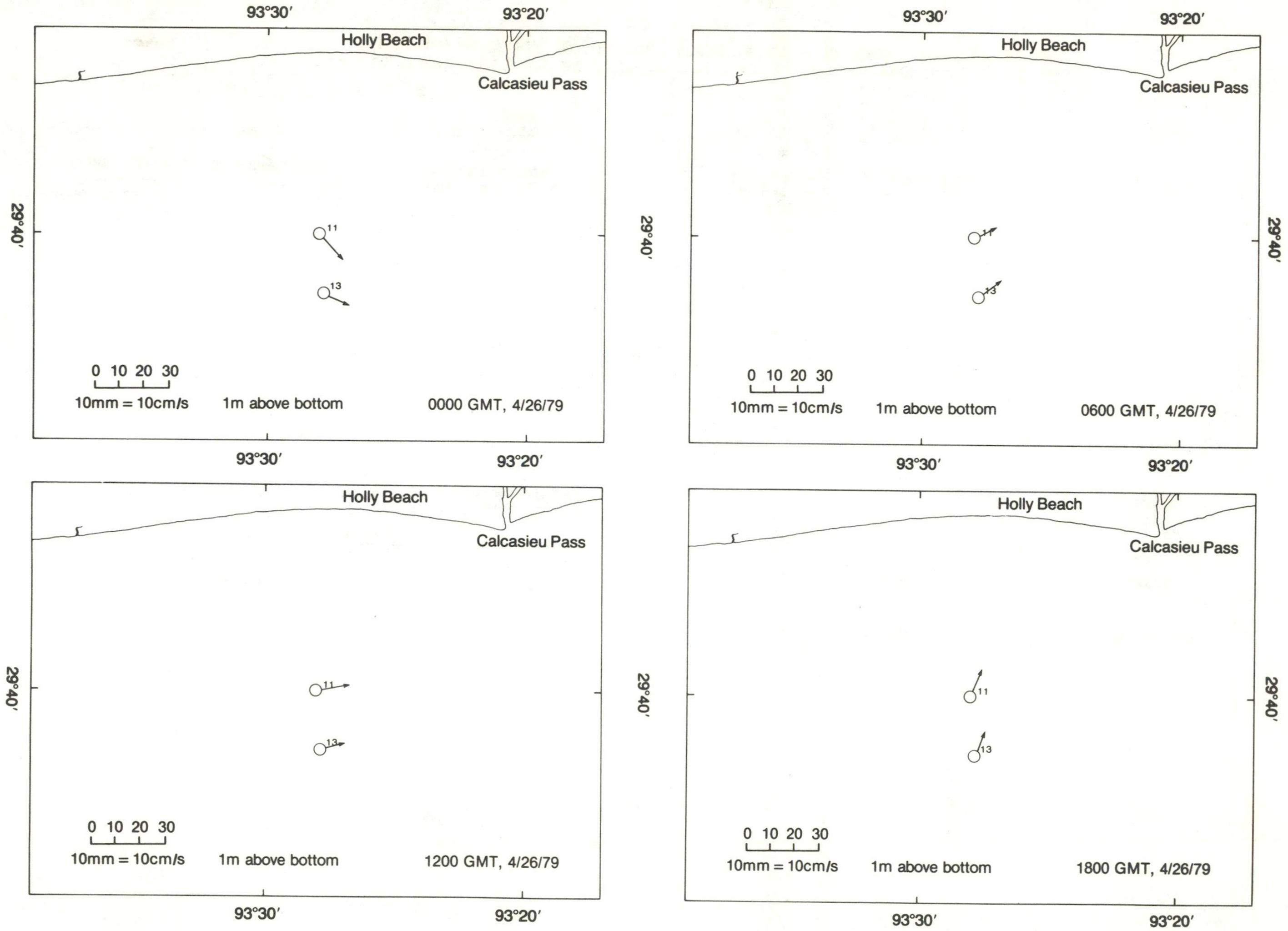

Figure E-49. Current vectors at 6-hour intervals, 1 m above bottom at West Hackberry site, April 26, 1979.

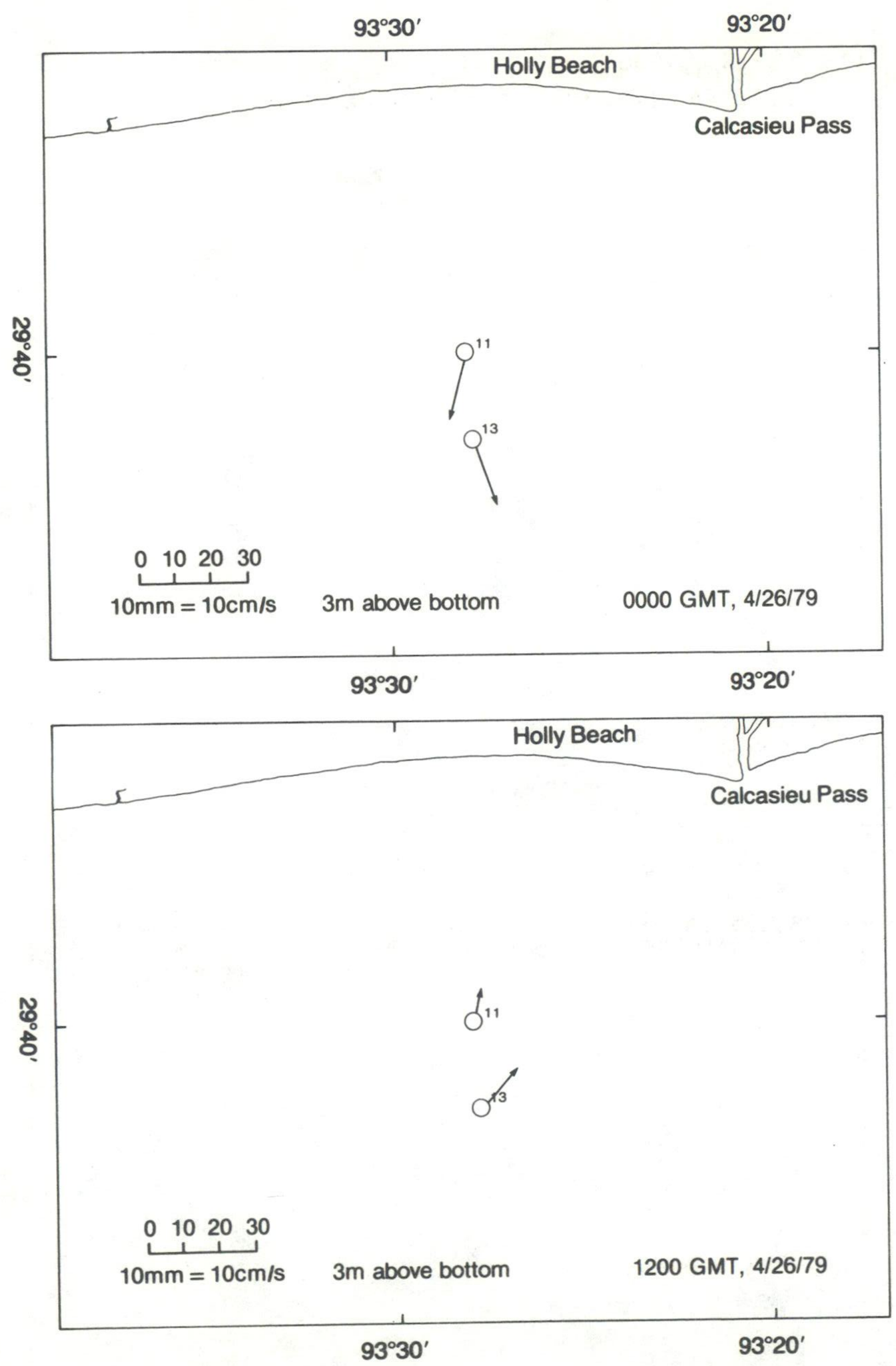

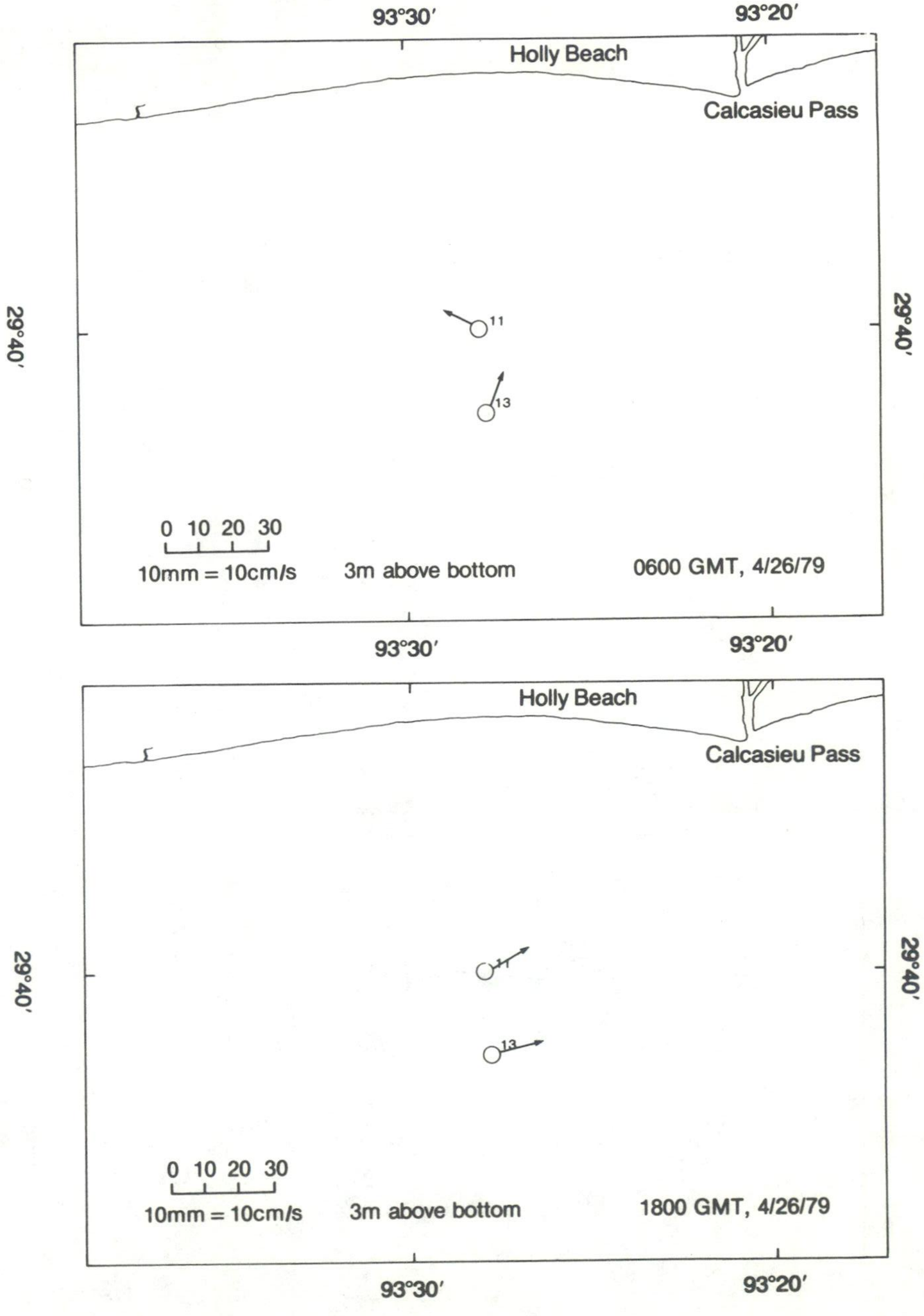

Figure E-50. Current vectors at 6-hour intervals, 3 m above bottom at West Hackberry site, April 26, 1979.

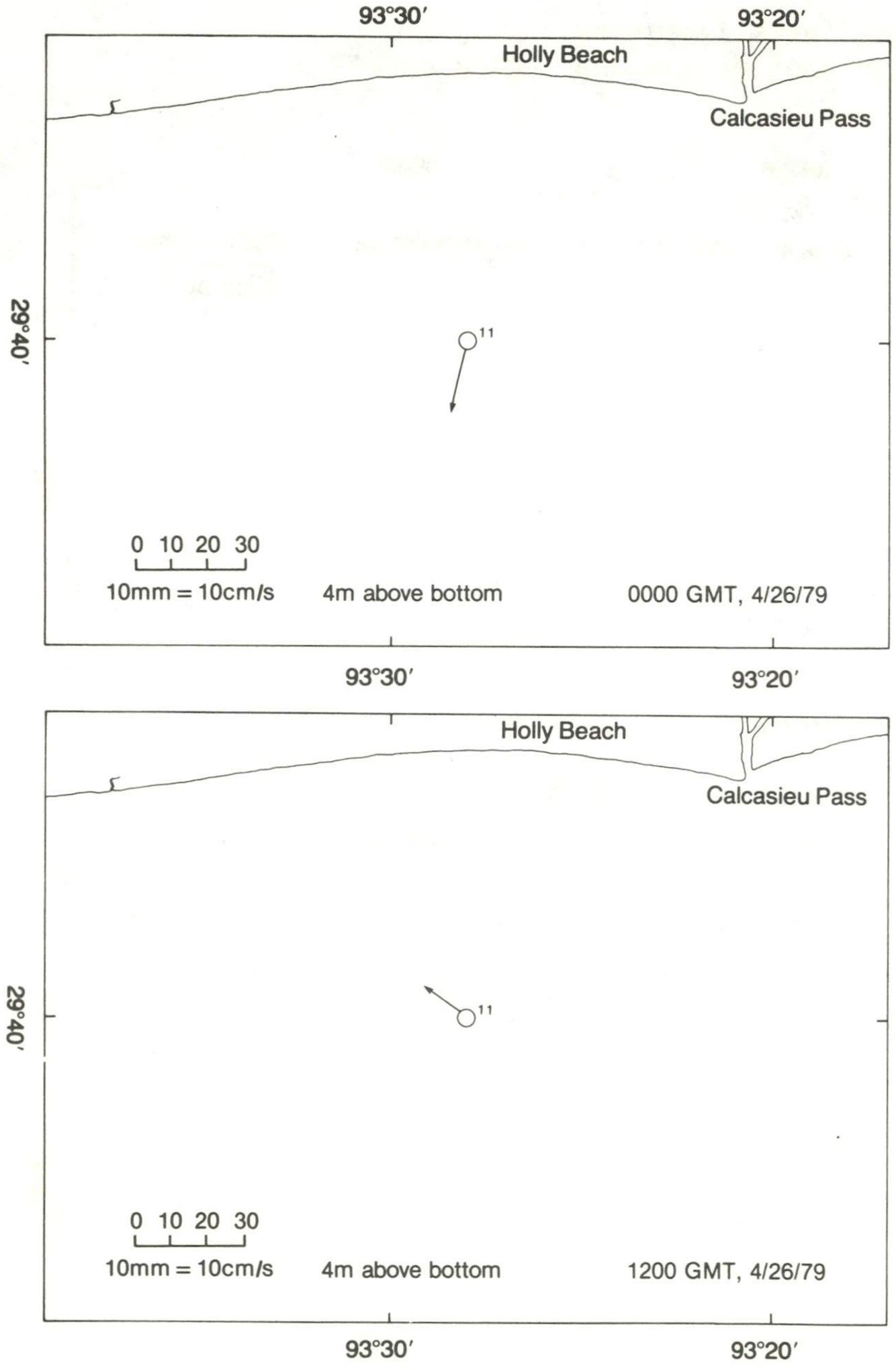

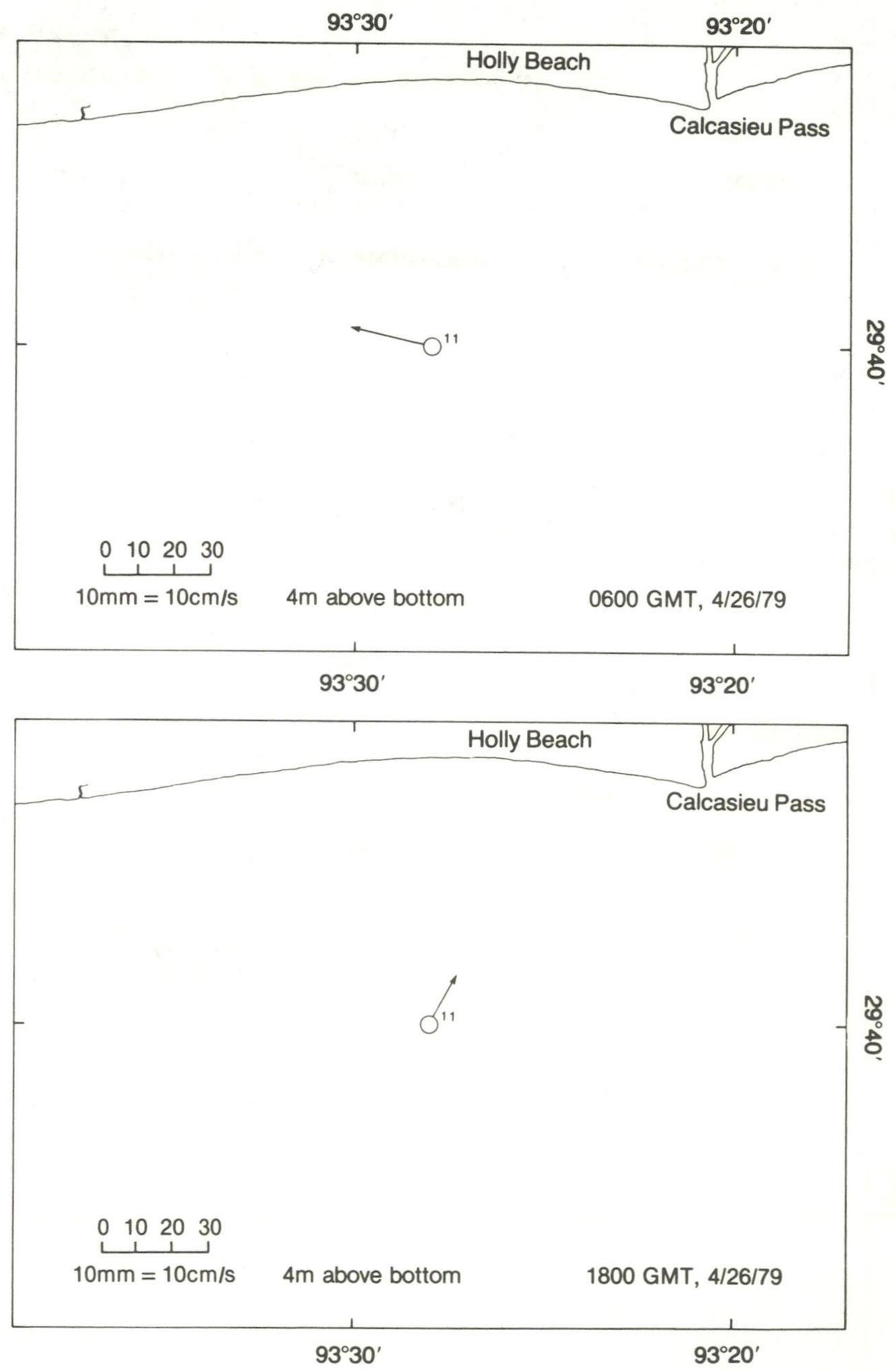

Figure E-51. Current vectors at 6-hour intervals, 4 m above bottom at West Hackberry site, April 26, 1979.

APPENDIX F.

VERTICAL PROFILES OF TEMPERATURE, SALINITY, AND SIGMA-T AT THE WEEKS ISLAND SITE.

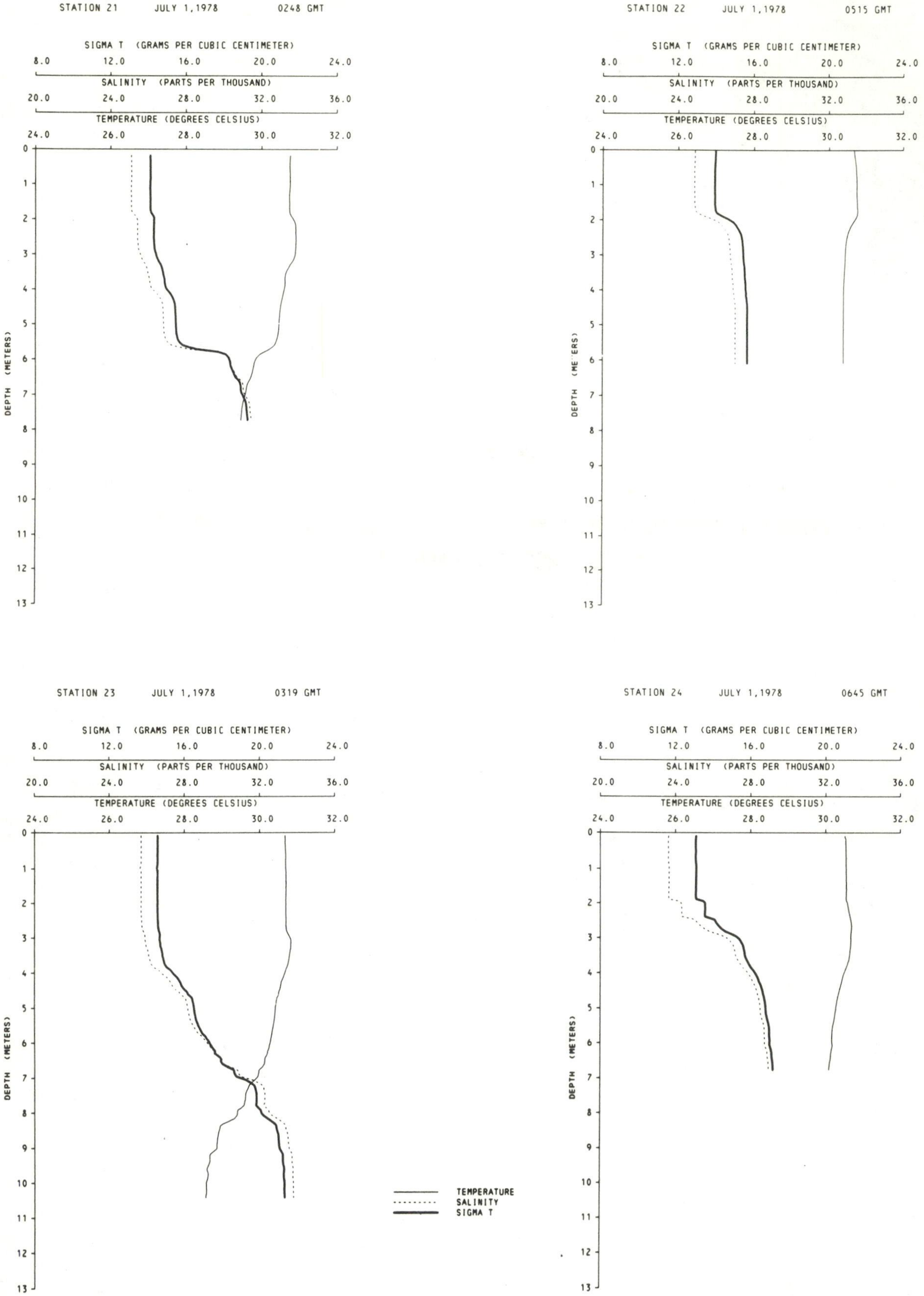

Figure F-1. Vertical profiles of temperature, salinity, and sigma-t for July 1, 1978, at stations 21 through 24.

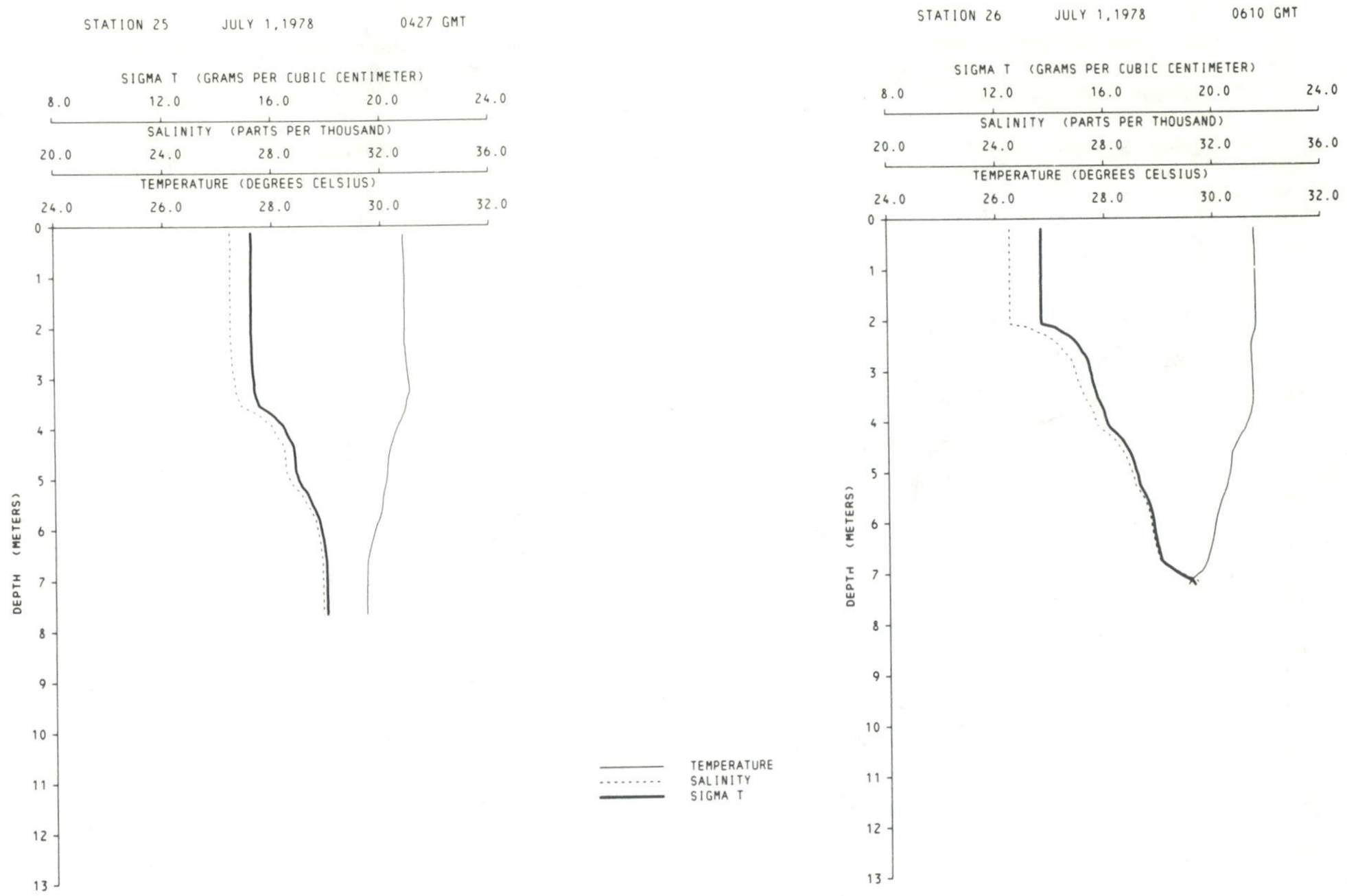

Figure F-2. Vertical profiles of temperature, salinity, and sigma-t for July 1, 1978, at stations 25 and 26.

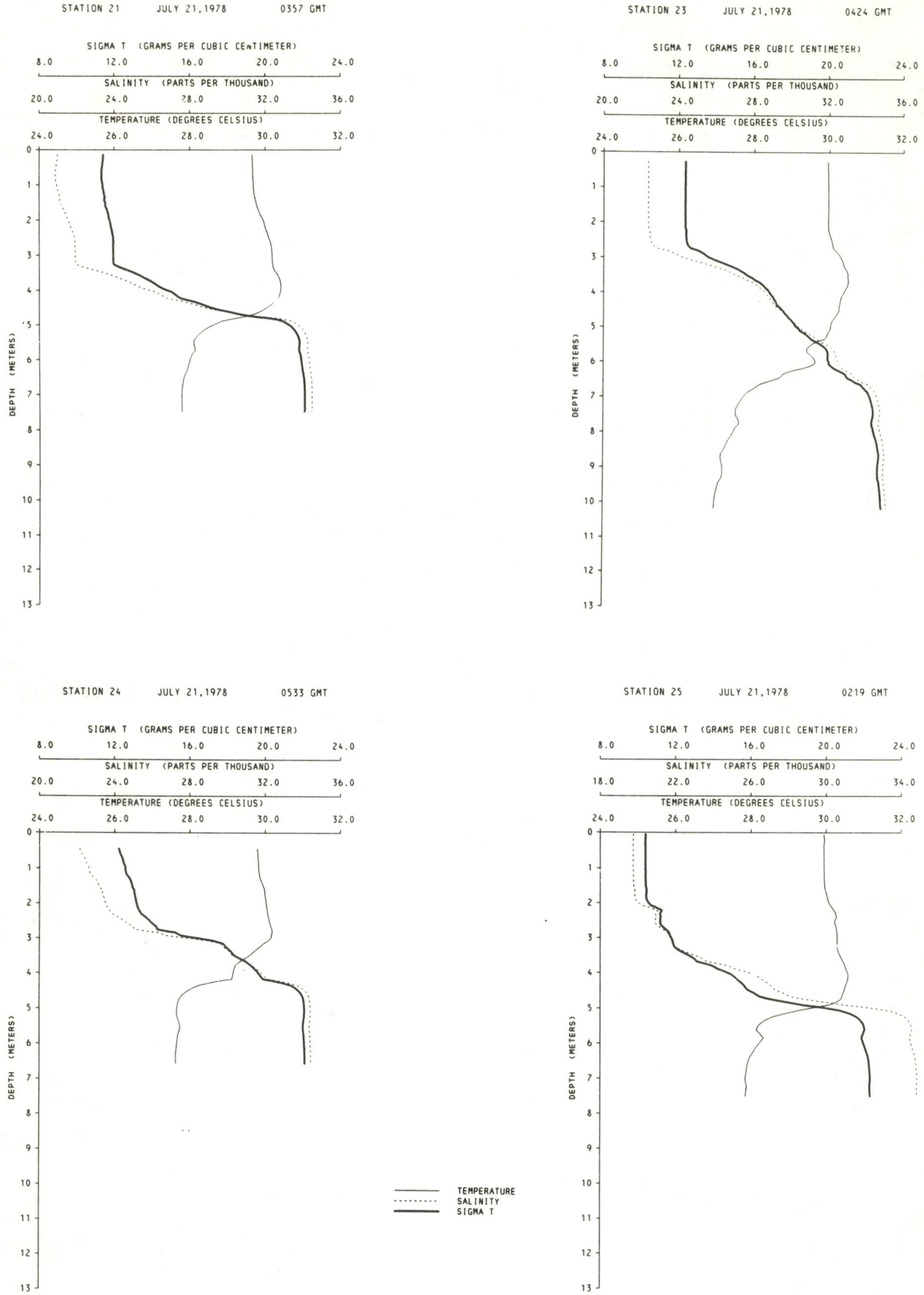

Figure F-3. Vertical profiles of temperature, salinity, and sigma-t for July 21, 1978, at stations 21, 23, 24, and 25.

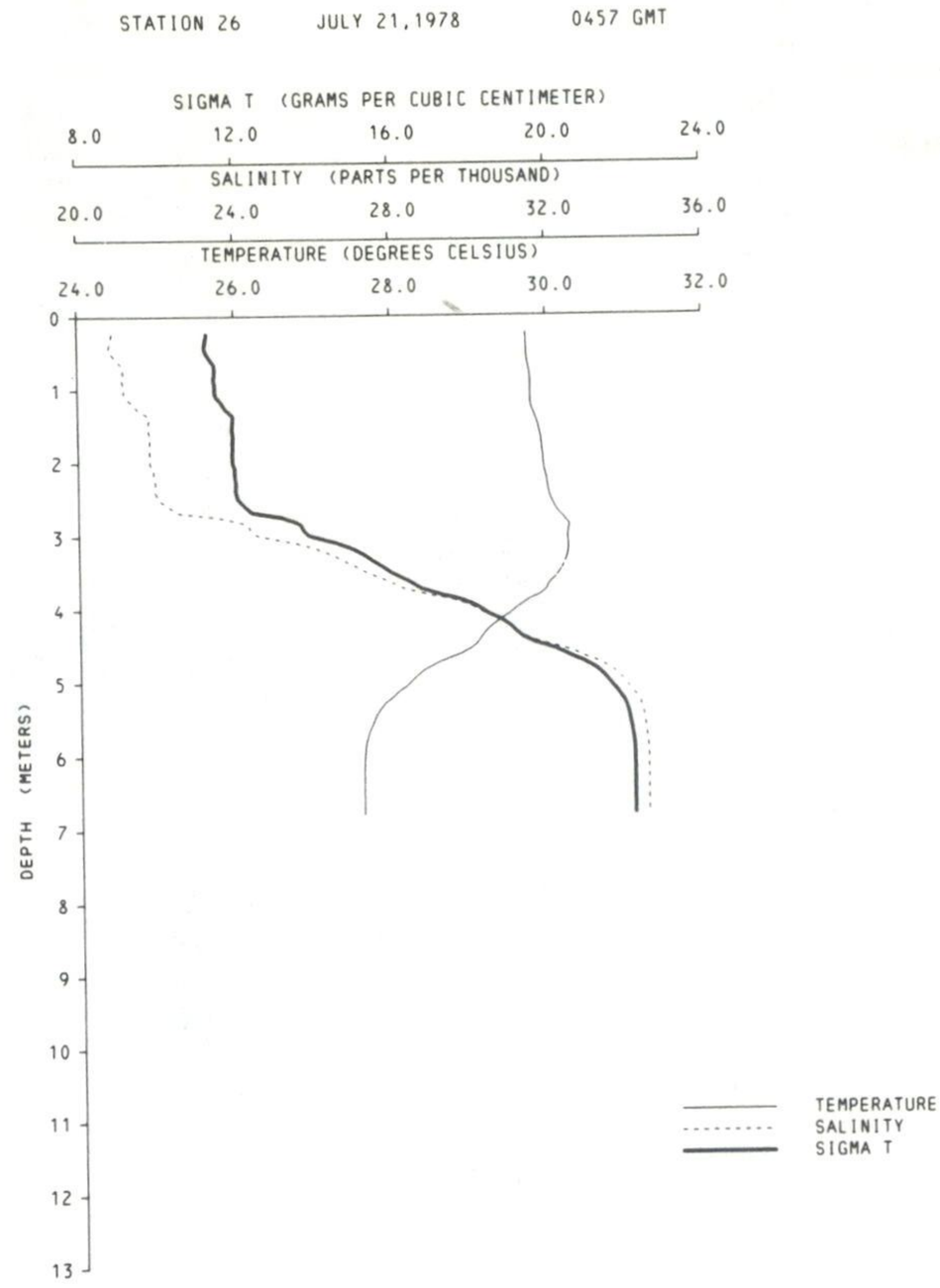

Figure F-4. Vertical profiles of temperature, salinity, and sigma-t for July 21, 1978, at station 26.

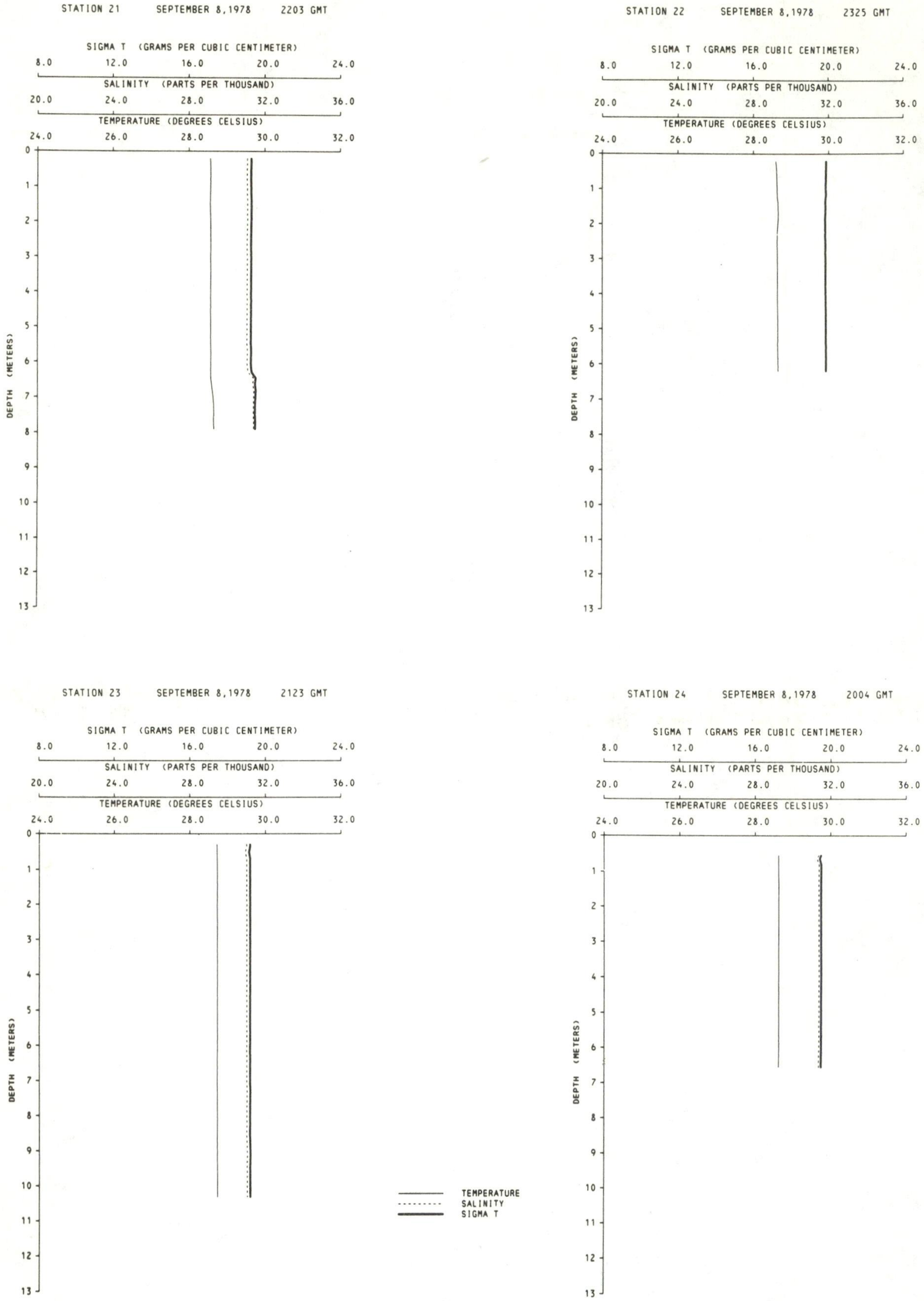

Figure F-5. Vertical profiles of temperature, salinity, and sigma-t for September 8, 1978, at stations 21 through 24.

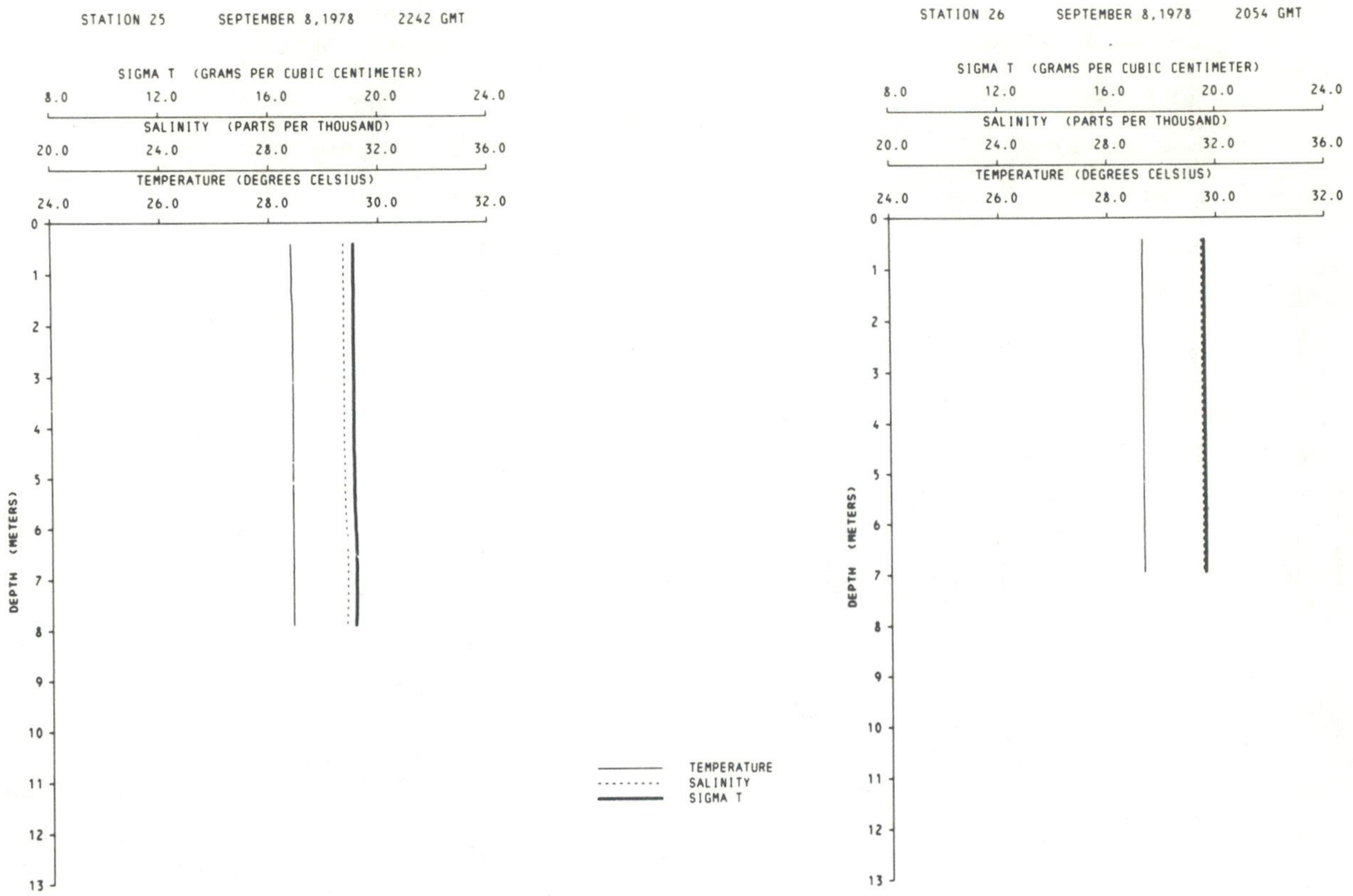

Figure F-6. Vertical profiles of temperature, salinity, and sigma-t for September 8, 1978, at stations 25 and 26.

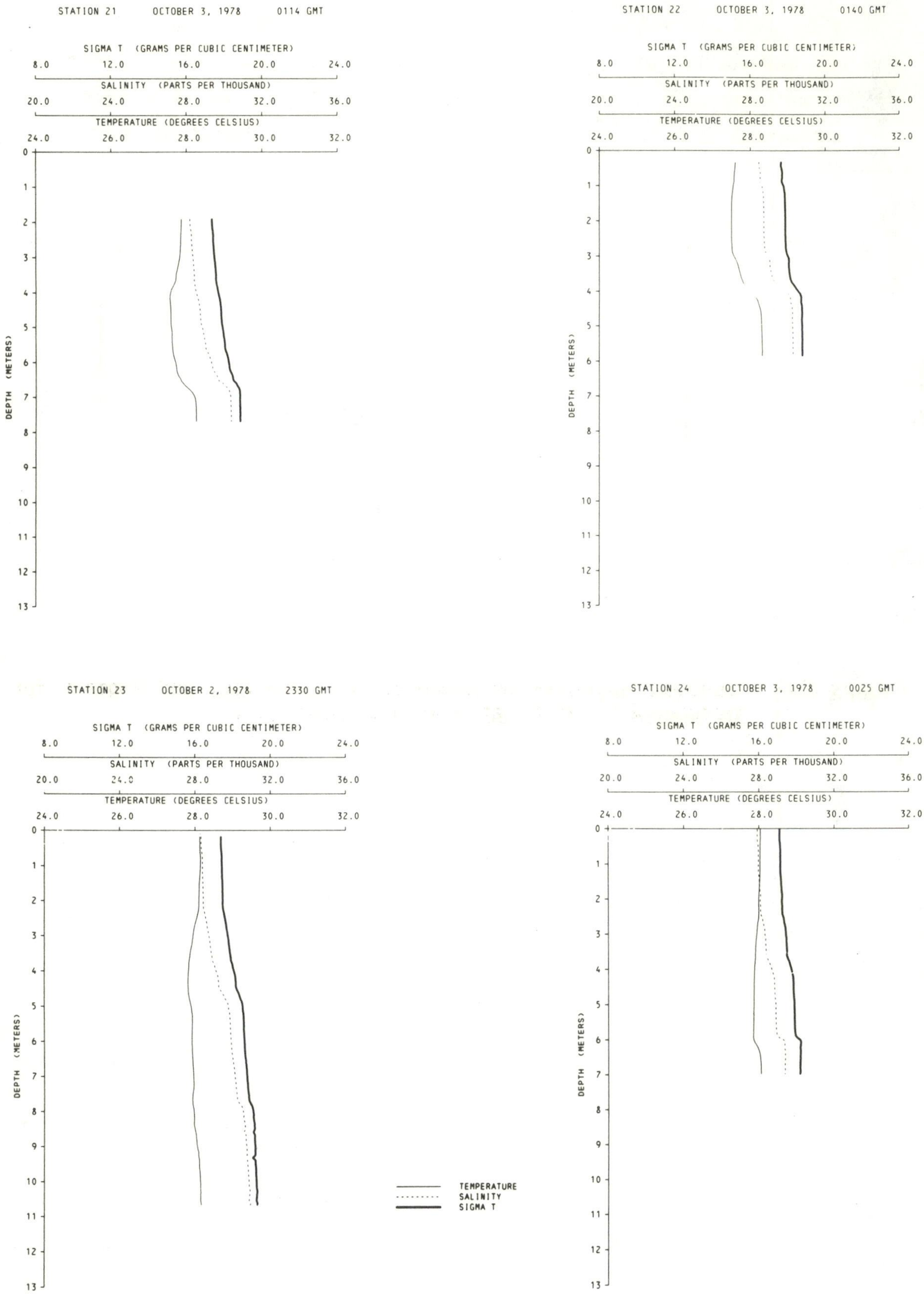

Figure F-7. Vertical profiles of temperature, salinity, and sigma-t for October 2-3, 1978, at stations 21 through 24.

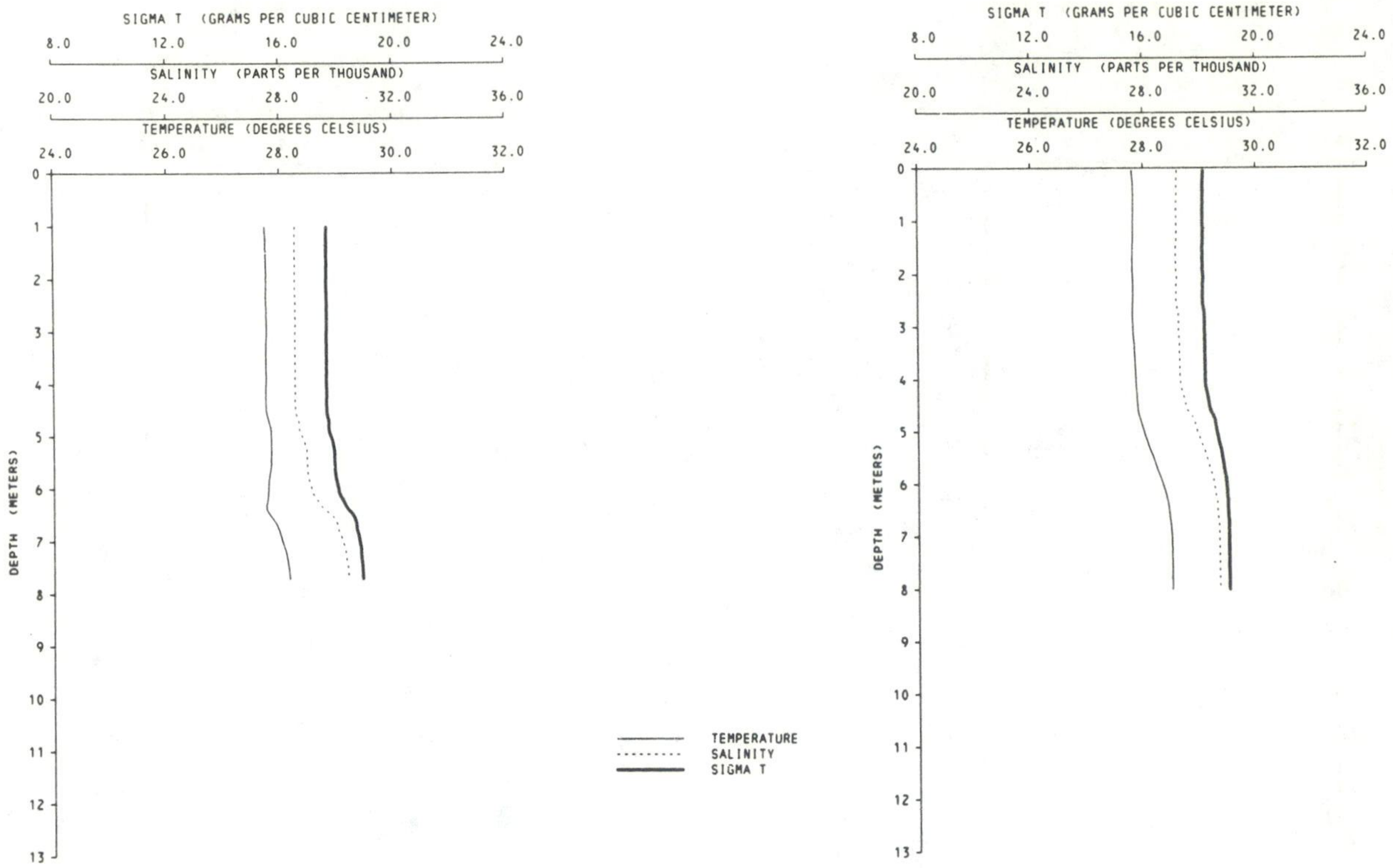

Figure F-8. Vertical profiles of temperature, salinity, and sigma-t for October 2-3, 1978, at stations 25 and 27.

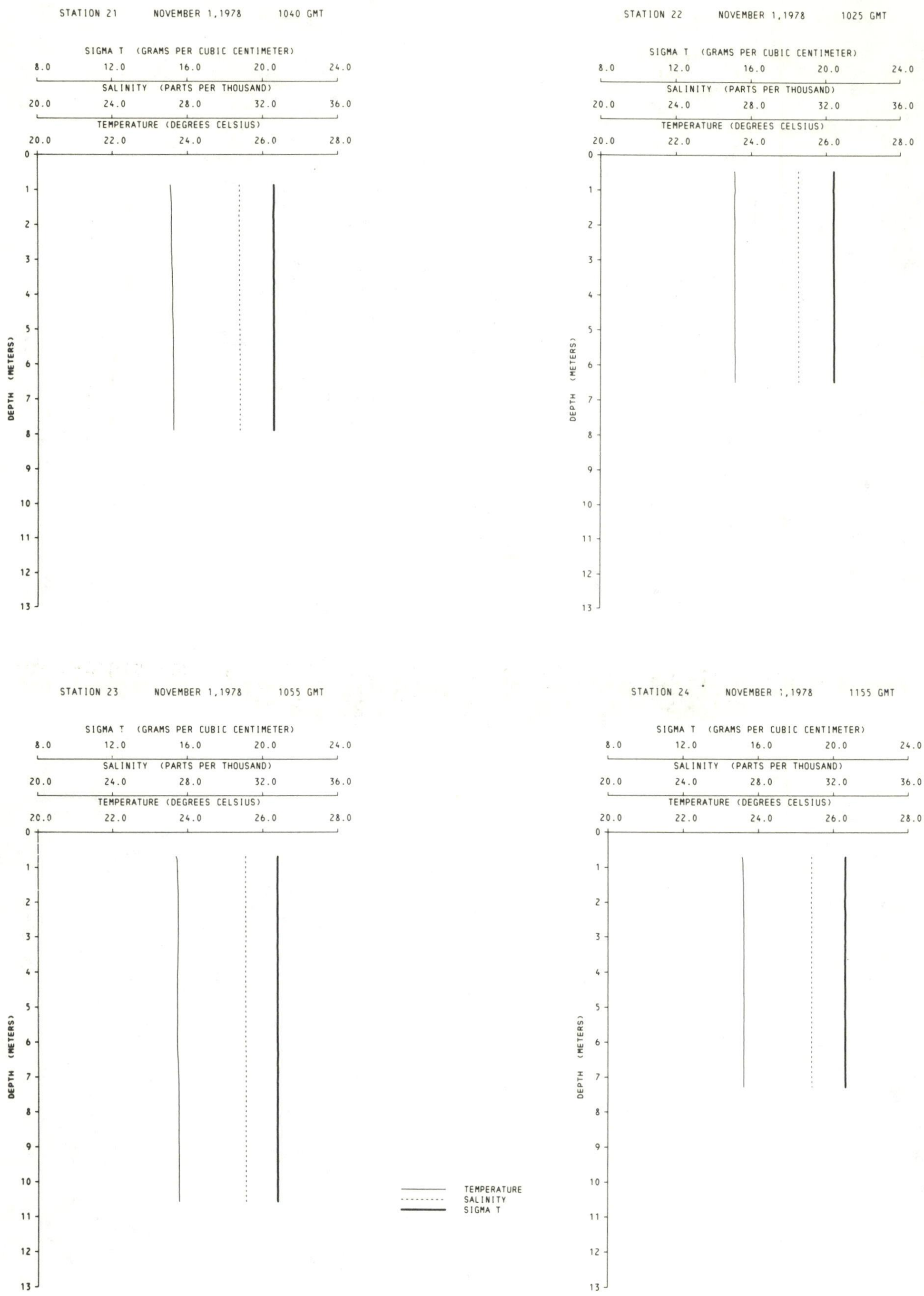

Figure F-9. Vertical profiles of temperature, salinity, and sigma-t for November 1, 1978, at stations 21 through 24.

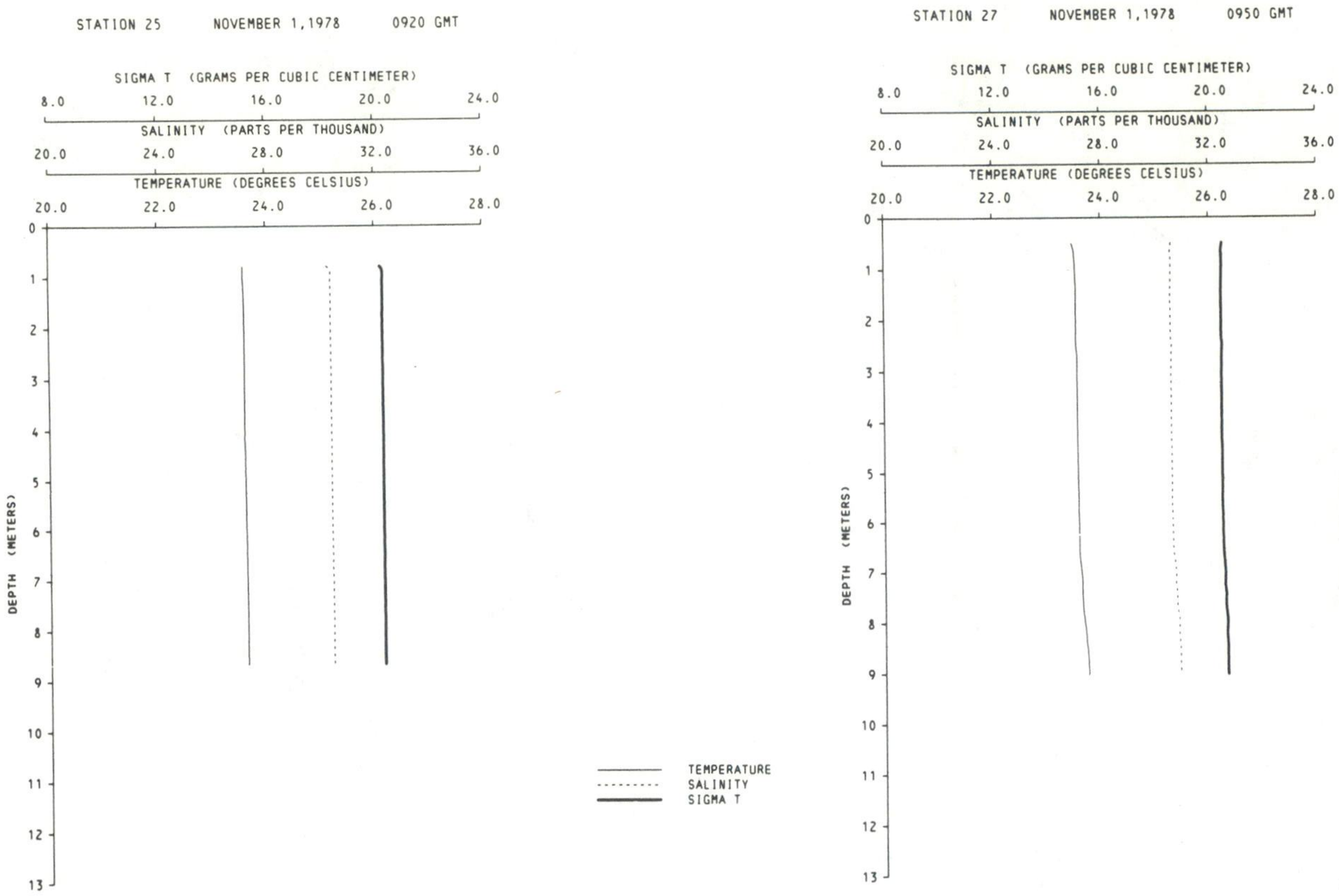

Figure F-10. Vertical profiles of temperature, salinity, and sigma-t for November 1, 1978, at stations 25 and 27.

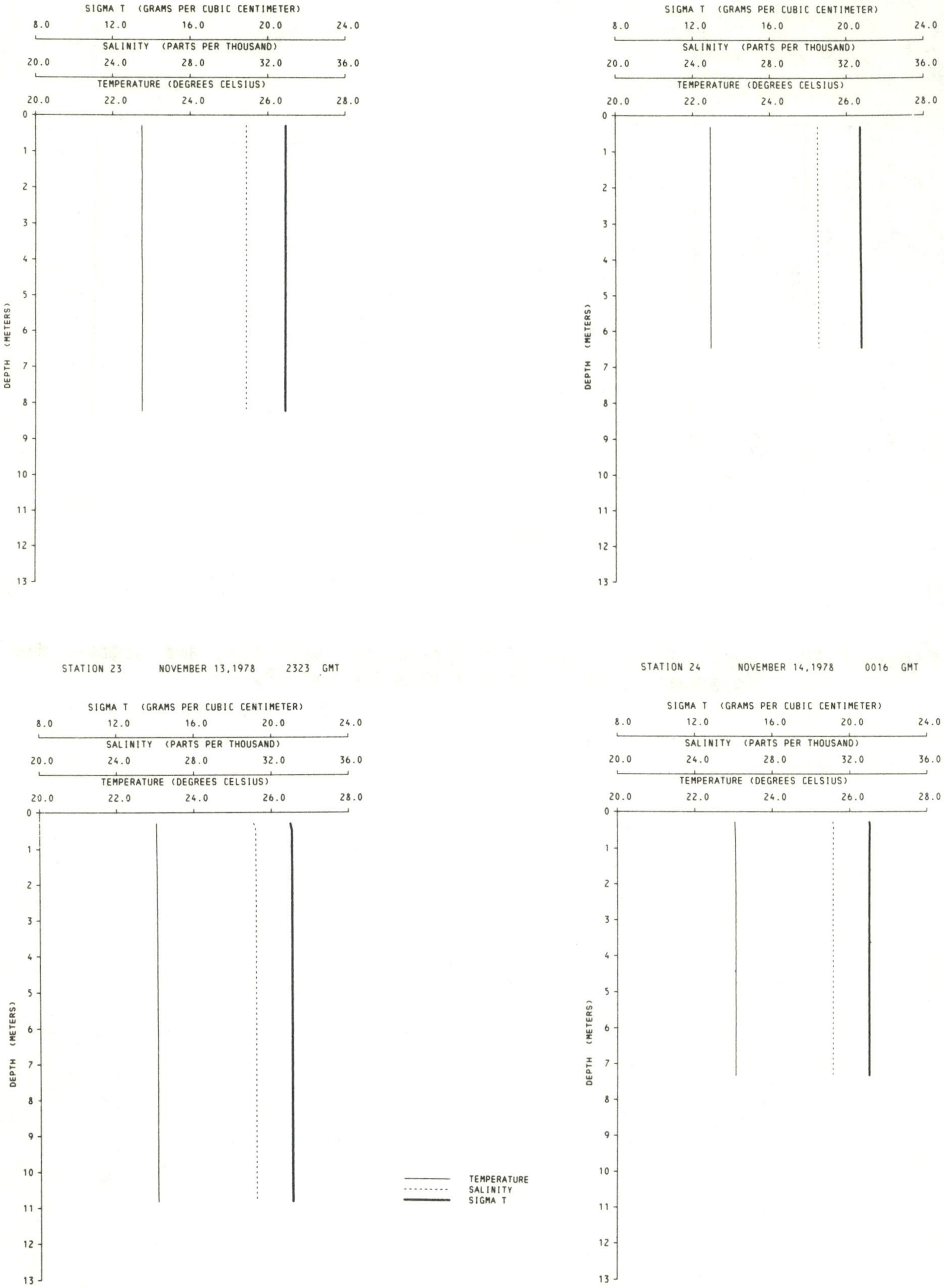

Figure F-11. Vertical profiles of temperature, salinity, and sigma-t for November 13-14, 1978, at stations 21 through 24.

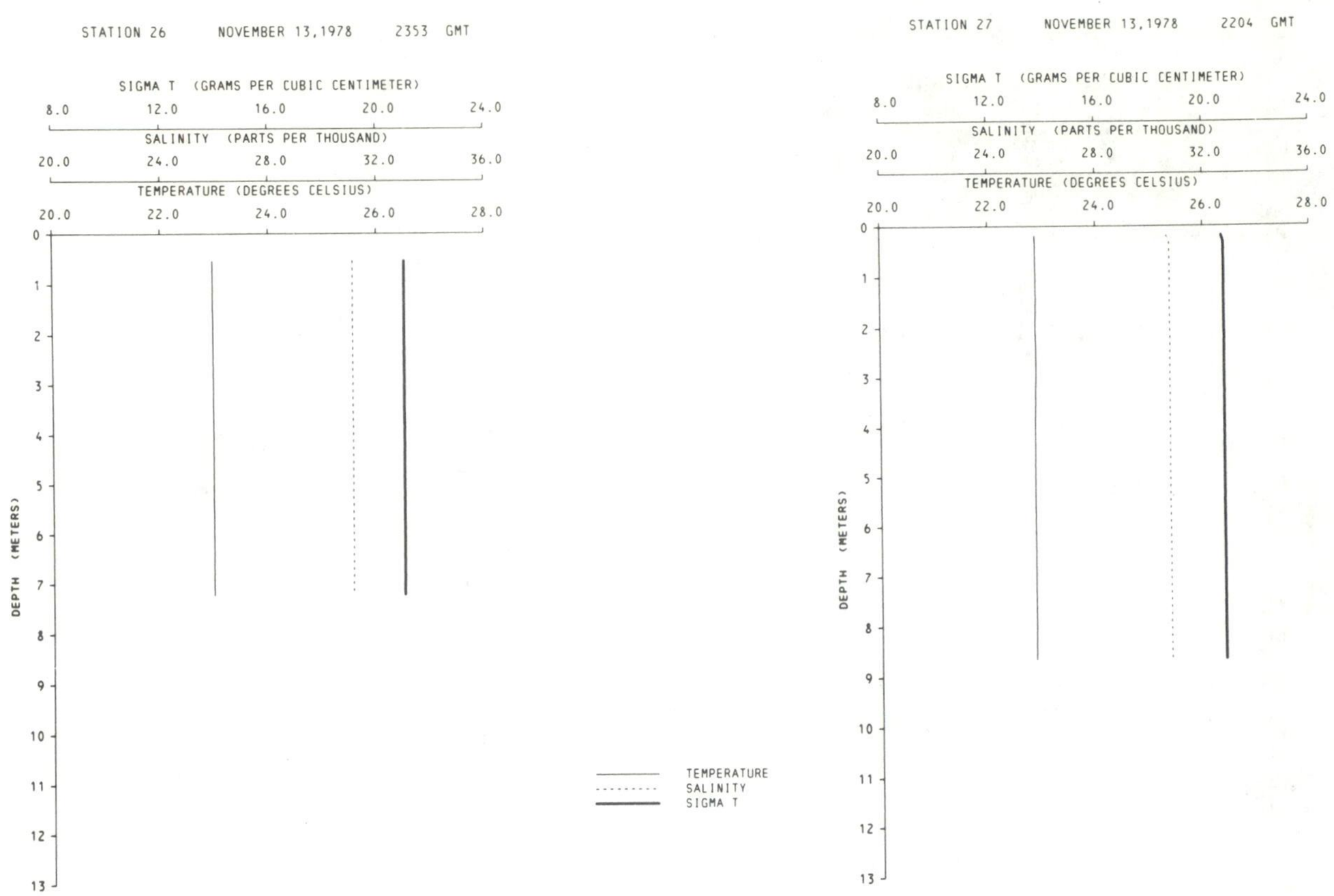

Figure F-12. Vertical profiles of temperature, salinity, and sigma-t for November 13, 1978, at stations 26 and 27.

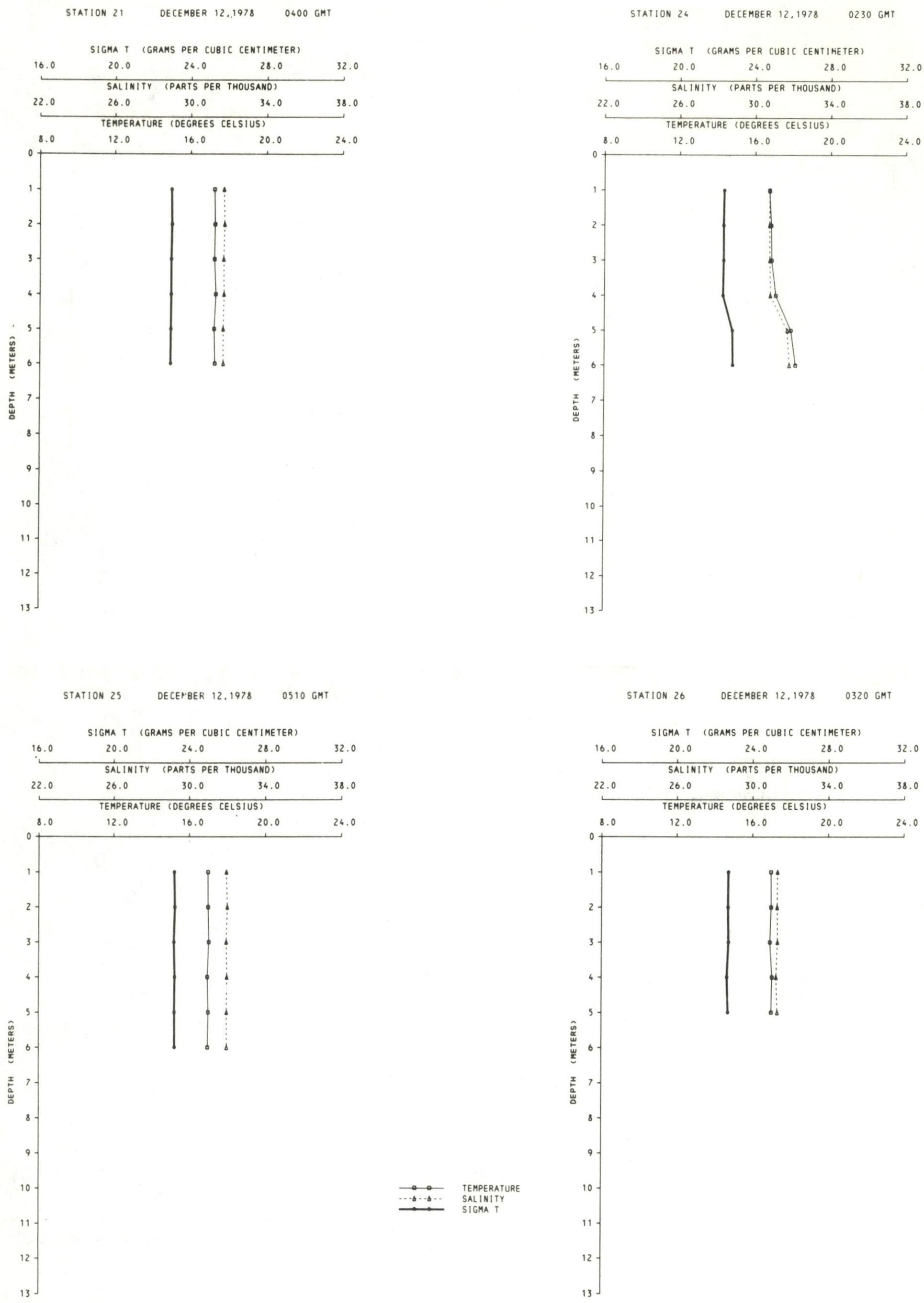

Figure F-13. Vertical profiles of temperature, salinity, and sigma-t for December 12, 1978, at stations 21, 24, 25, and 26.

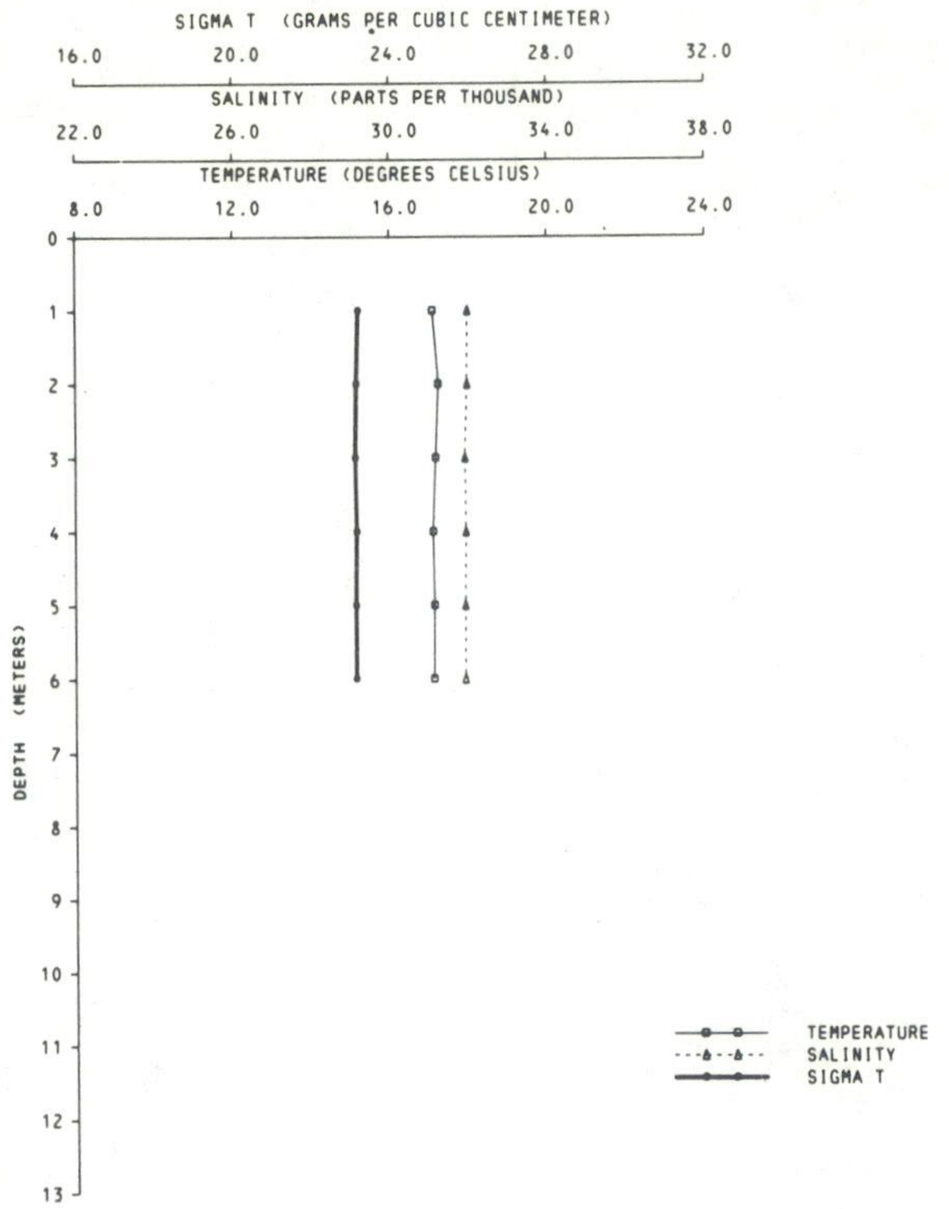

Figure F-14. Vertical profiles of temperature, salinity, and sigma-t for December 12, 1978, at station 27.

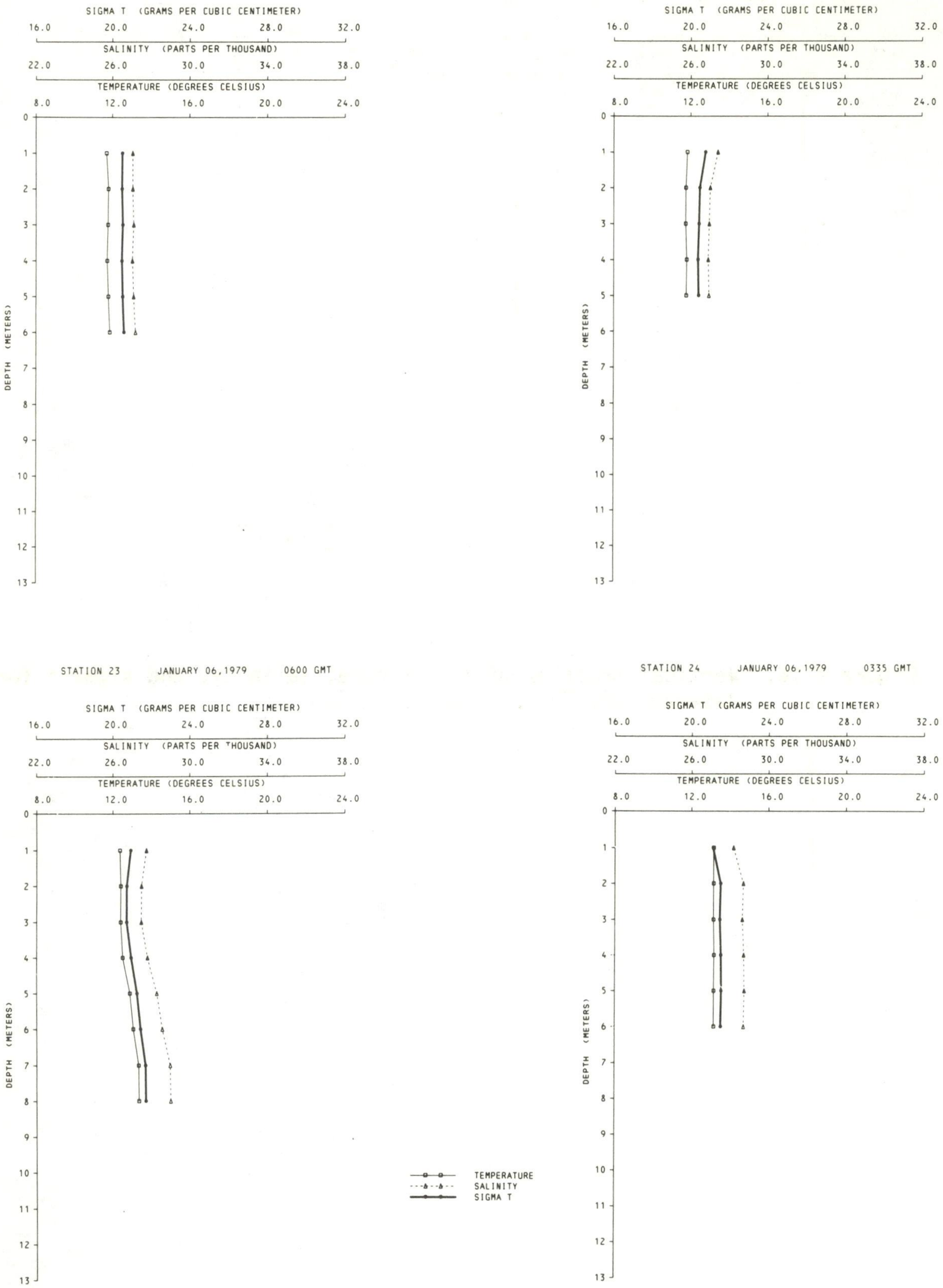

Figure F-15. Vertical profiles of temperature, salinity, and sigma-t for January 6, 1979, at stations 21 through 24.

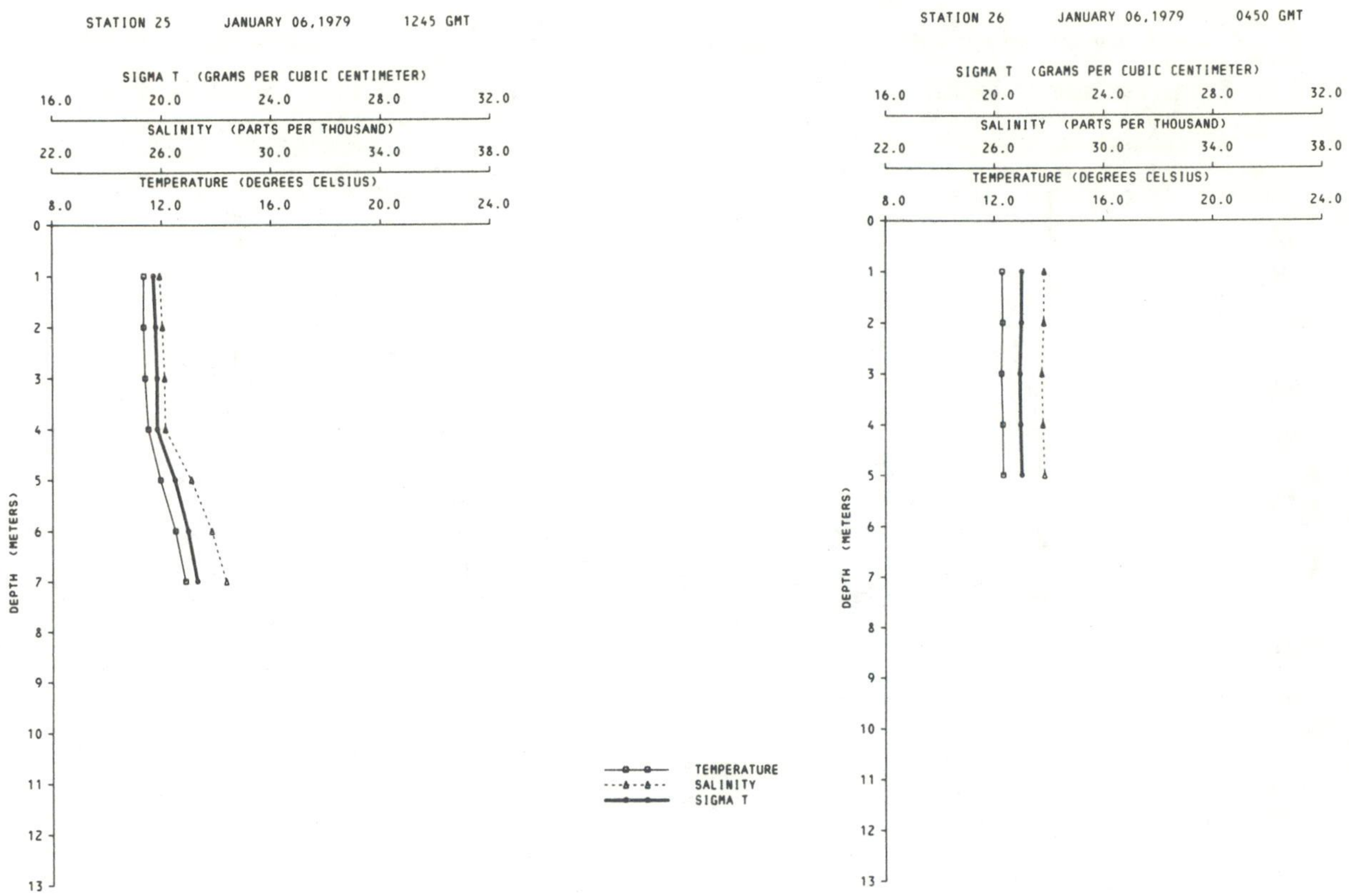

Figure F-16. Vertical profiles of temperature, salinity, and sigma-t for January 6, 1979, at stations 25 and 26.

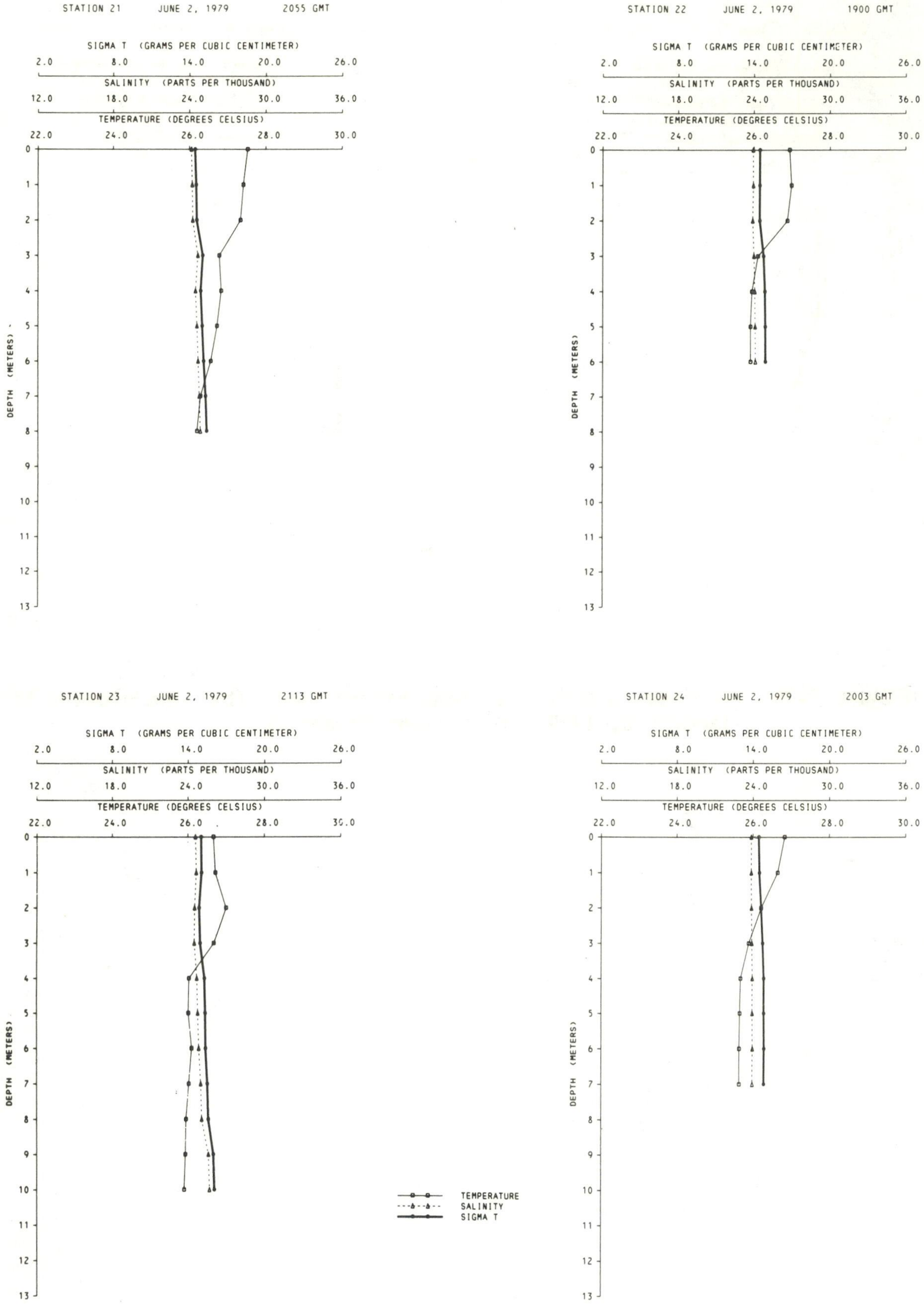

Figure F-17. Vertical profiles of temperature, salinity, and sigma-t for June 2, 1979, at stations 21 through 24.

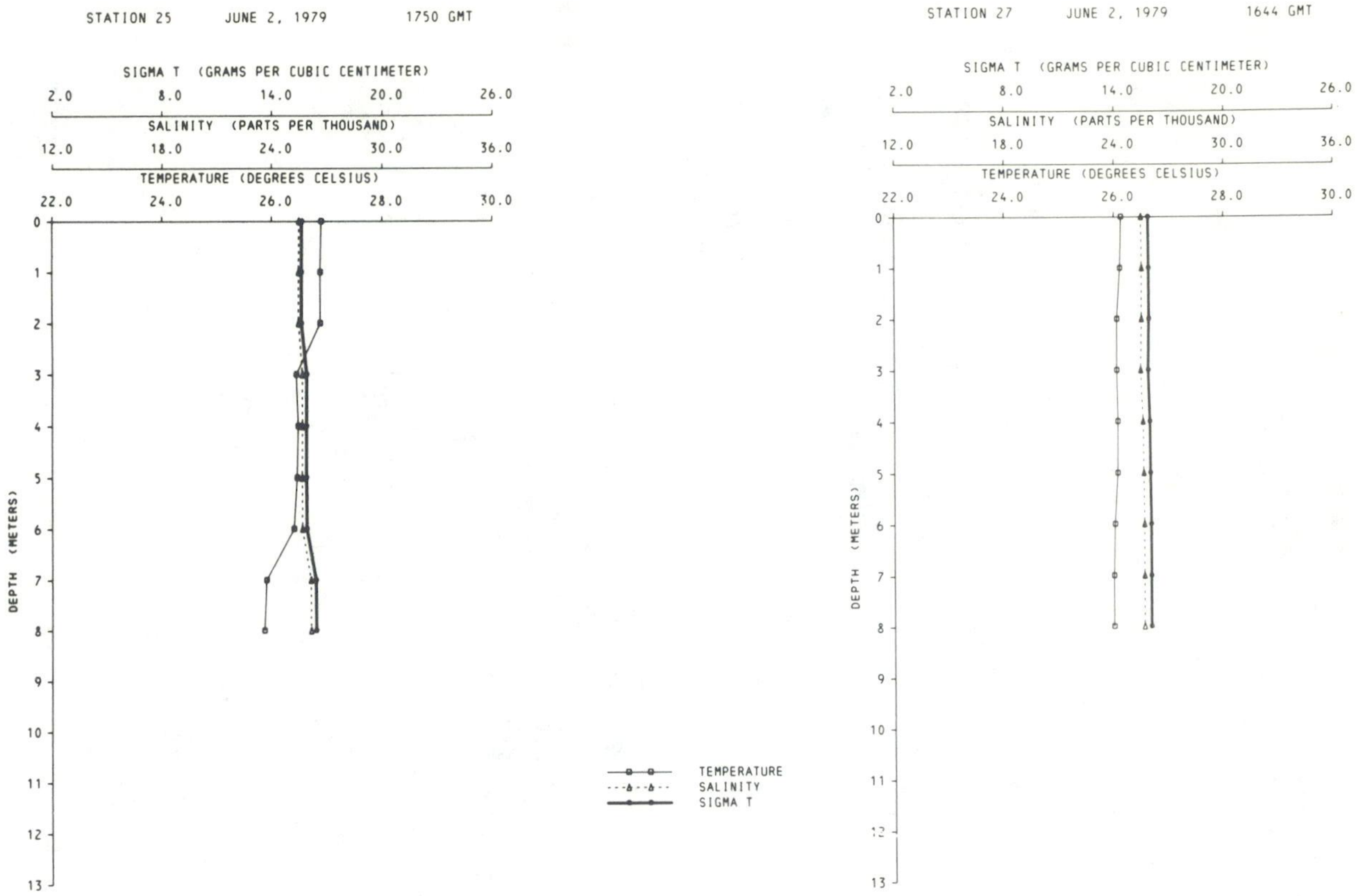

Figure F-18. Vertical profiles of temperature, salinity, and sigma-t for June 2, 1979, at stations 25 and 27.

APPENDIX G.

TIME SERIES PLOTS OF CURRENT SPEED AND DIRECTION FOR OBSERVATIONS 3 m ABOVE THE BOTTOM AT THE WEEKS ISLAND SITE.

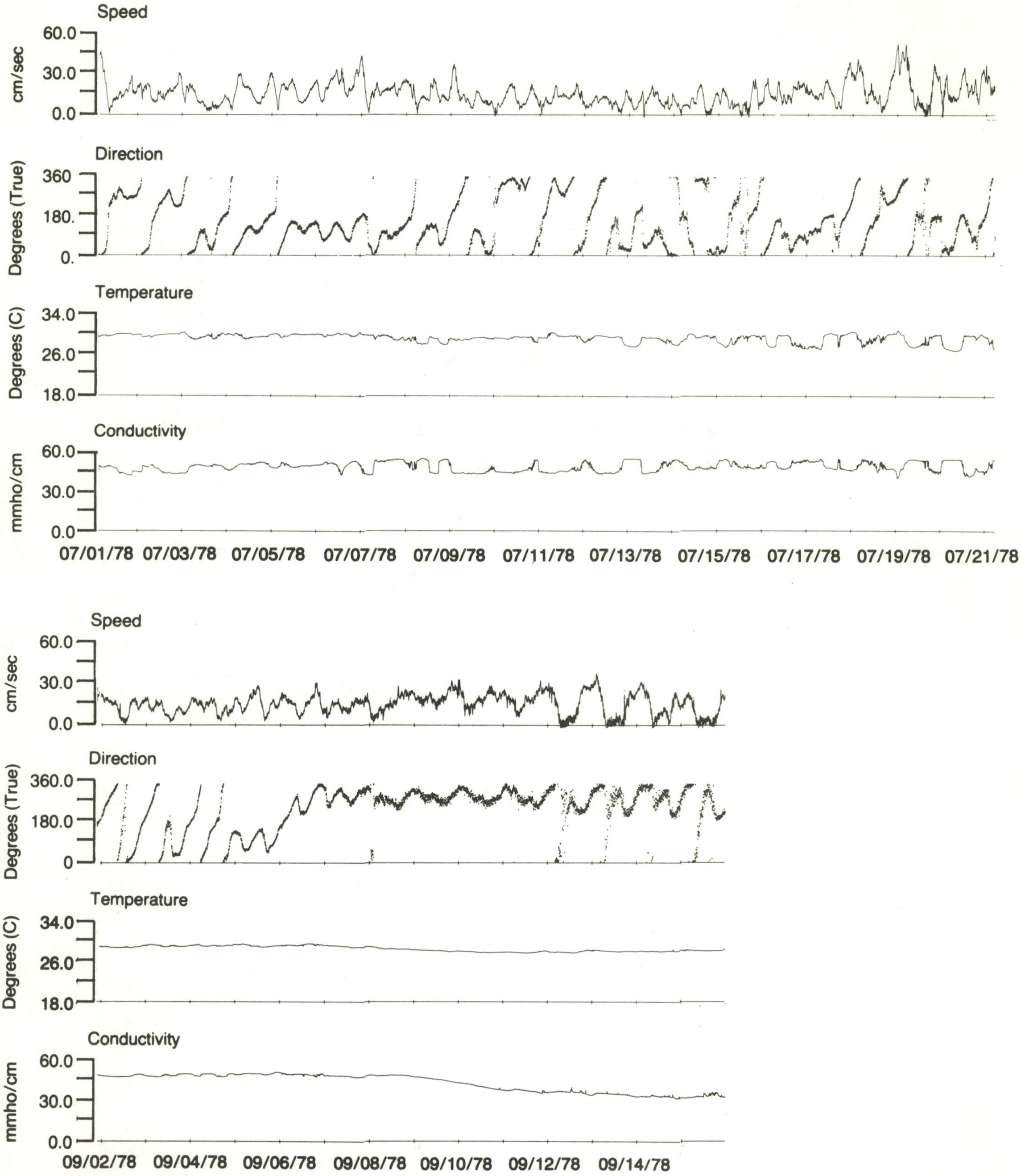

Figure G-1. Time series of current meter data at station 21, 3 m above bottom, for July 1-21, and September 9-15, 1978.

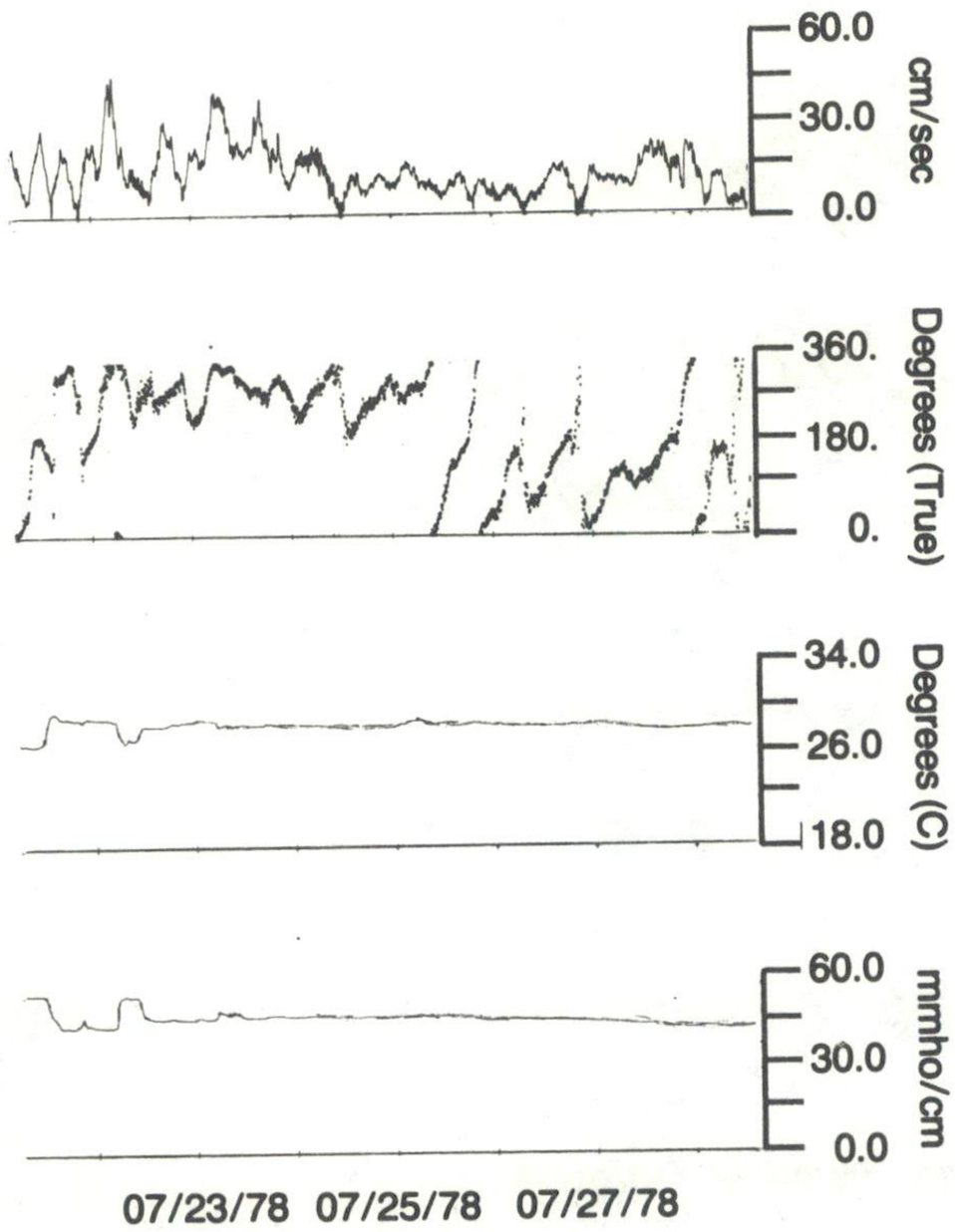

Figure G-1. Time series of current meter data at station 21, 3 m above bottom, for July 1-21, and September 9-15, 1978.

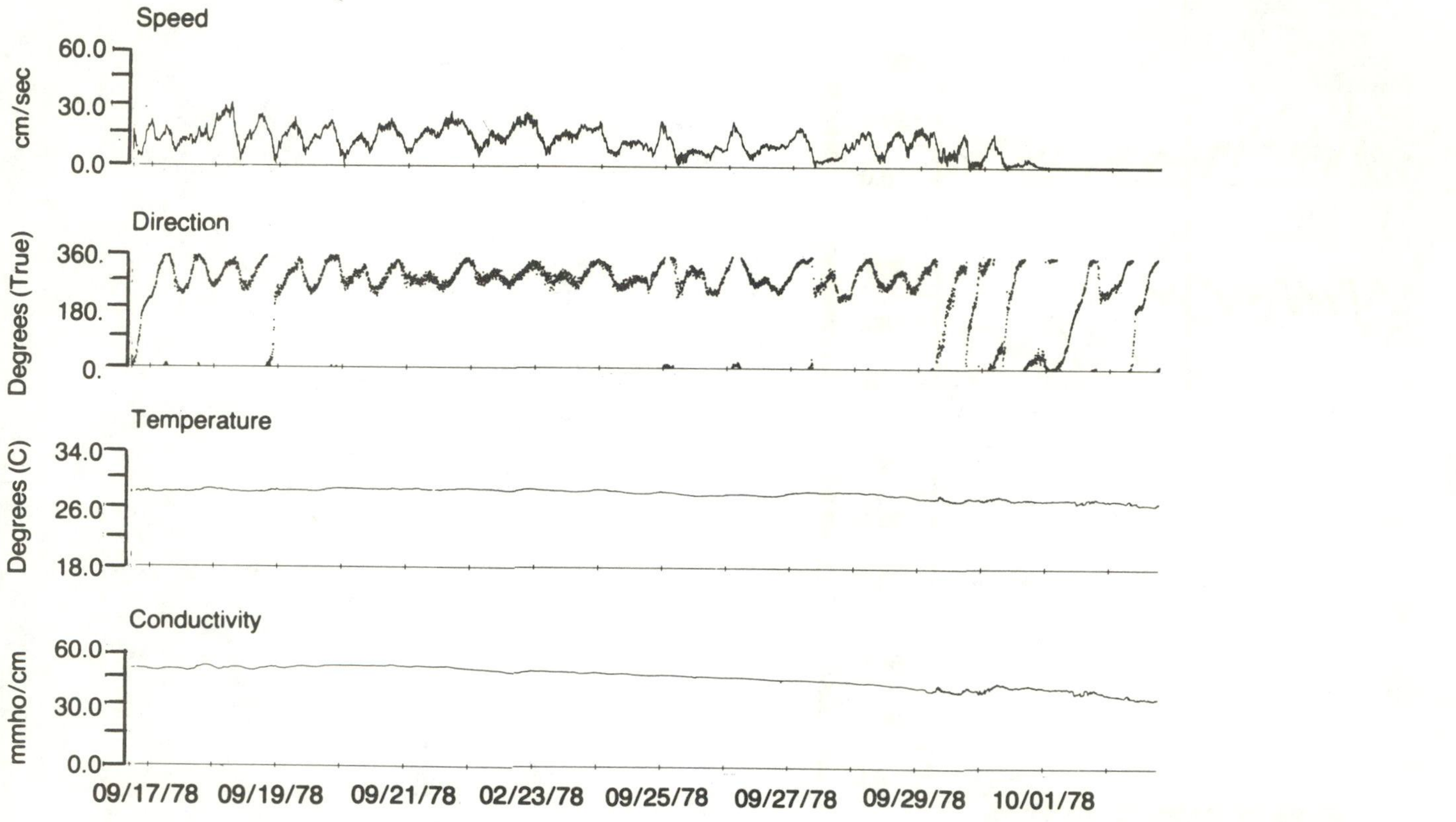

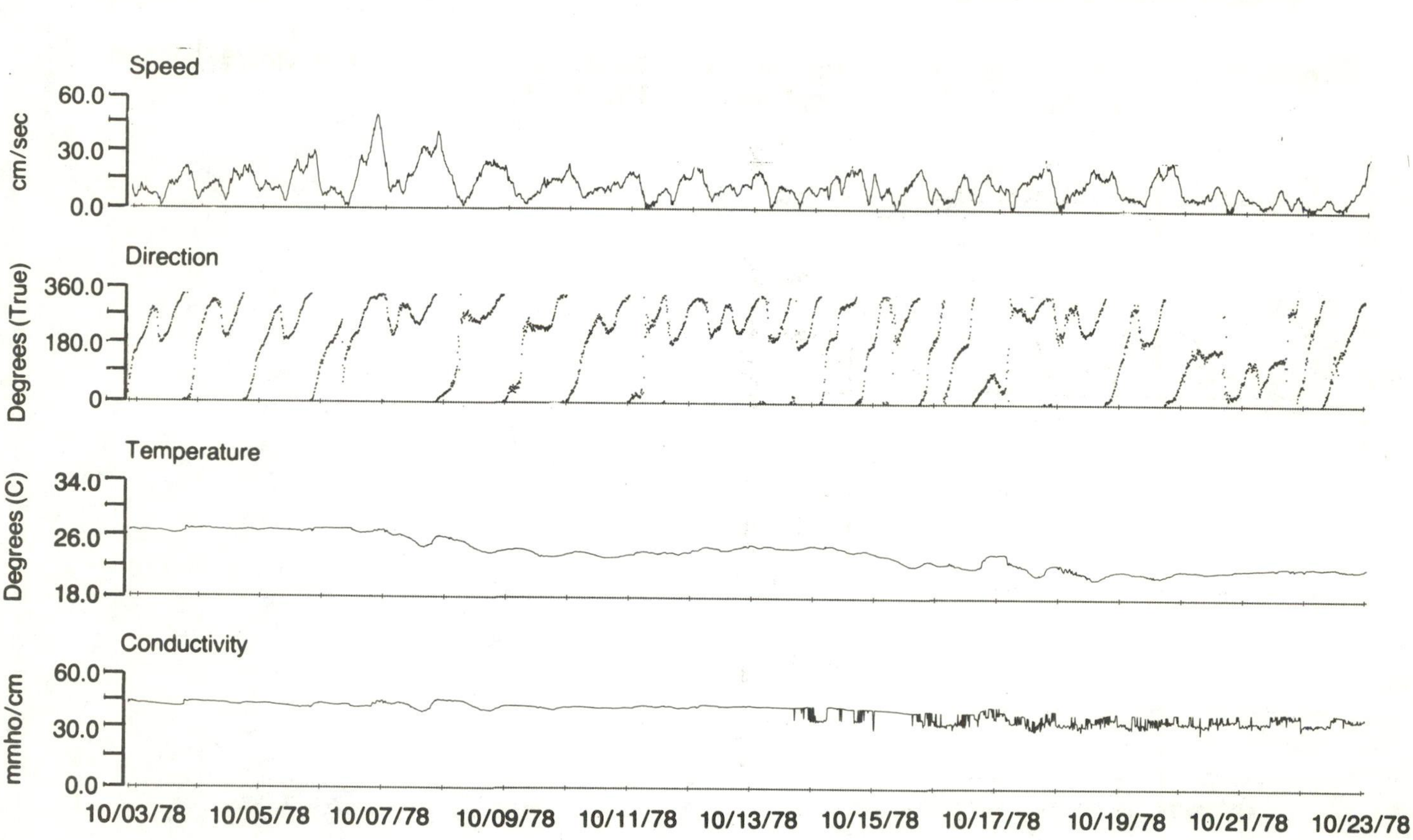

Figure G-2. Time series of current meter data at station 21, 3 m above bottom, for September 17 to October 2 and October 3-30, 1978.

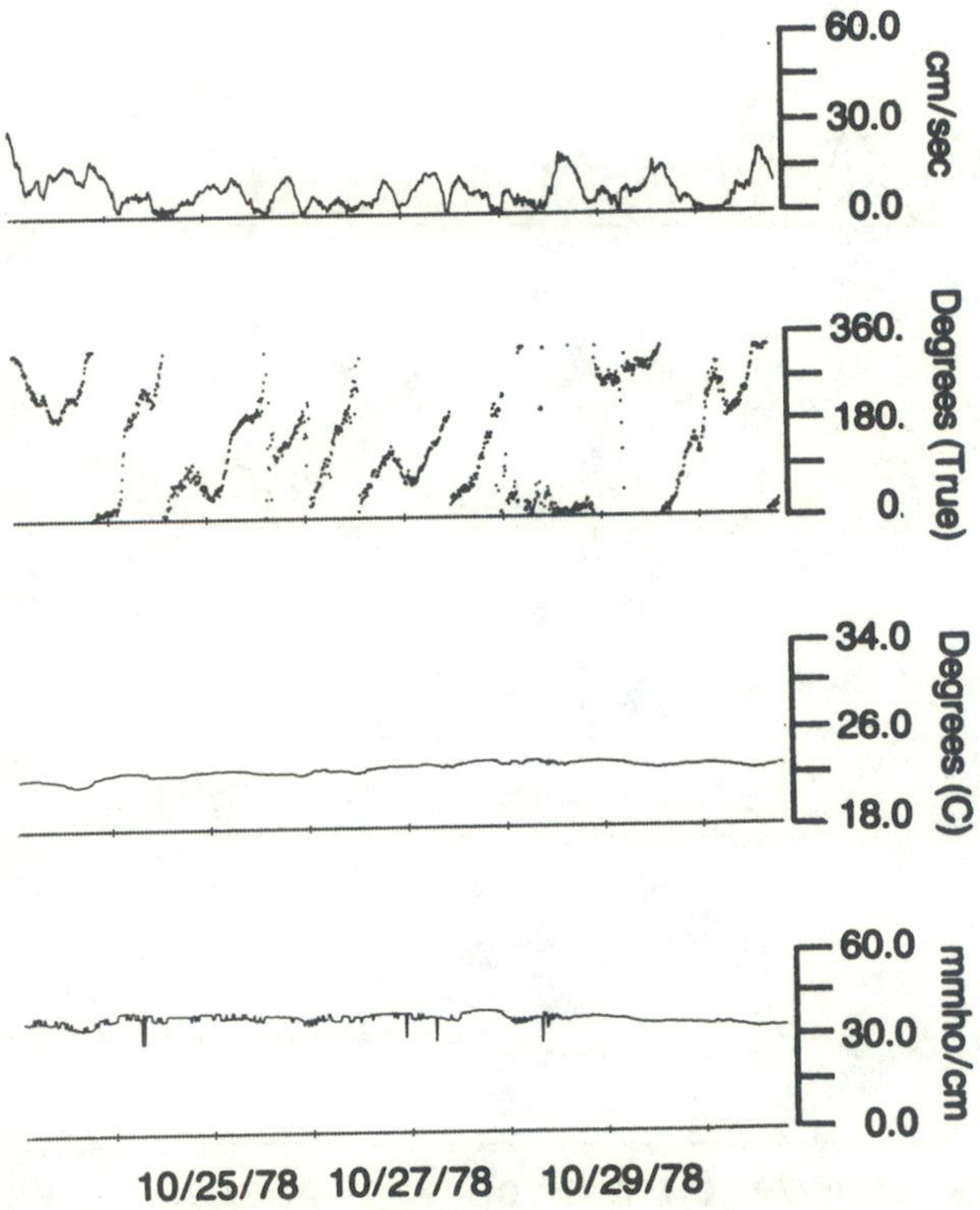

Figure G-2. Time series of current meter data at station 21, 3 m above bottom, for September 17 to October 2 and October 3-30, 1978.

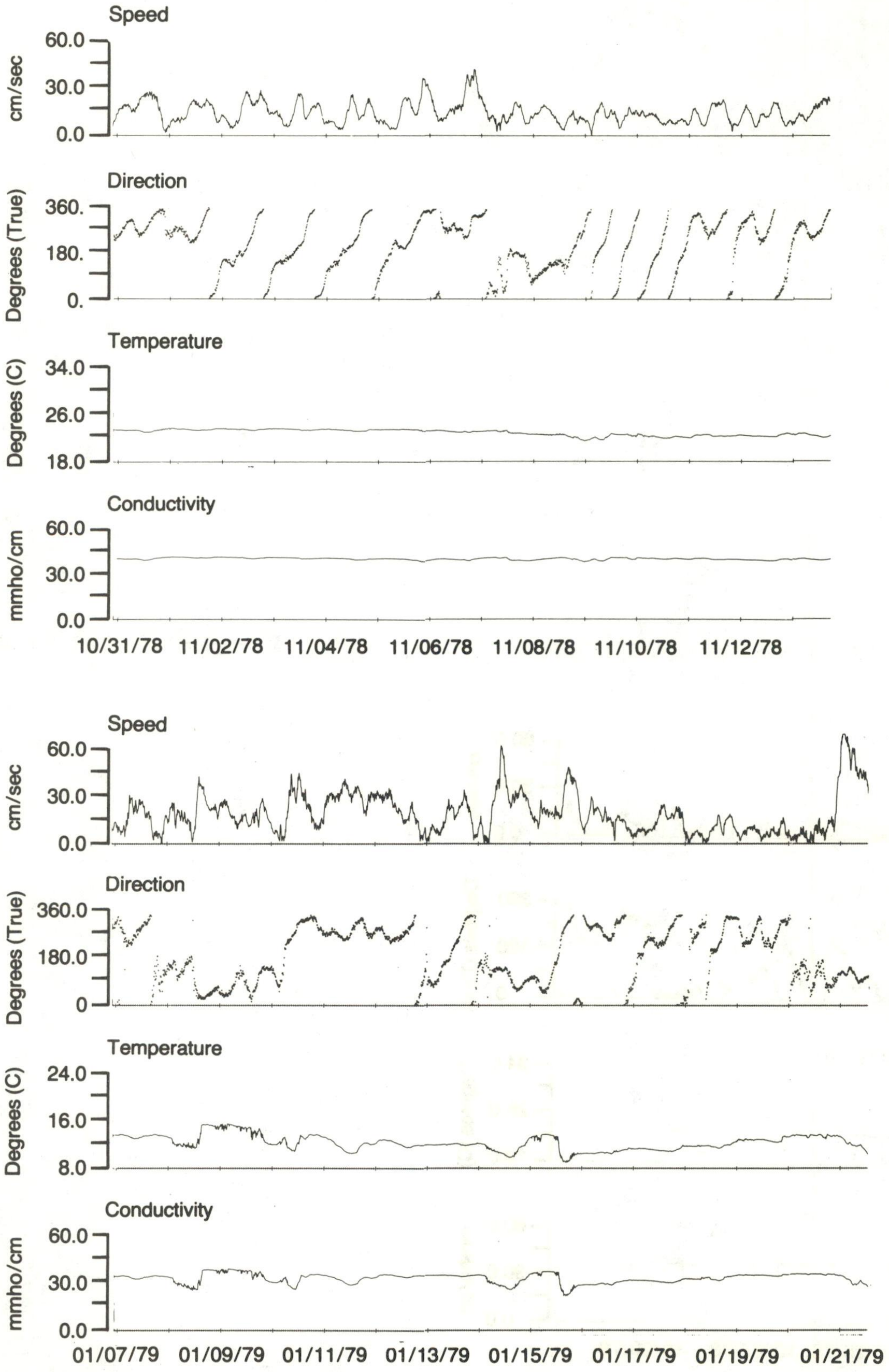

Figure G-3. Time series of current meter data at station 21, 3 m above bottom, for October 31 to November 13, 1978, and January 7-21, 1979.

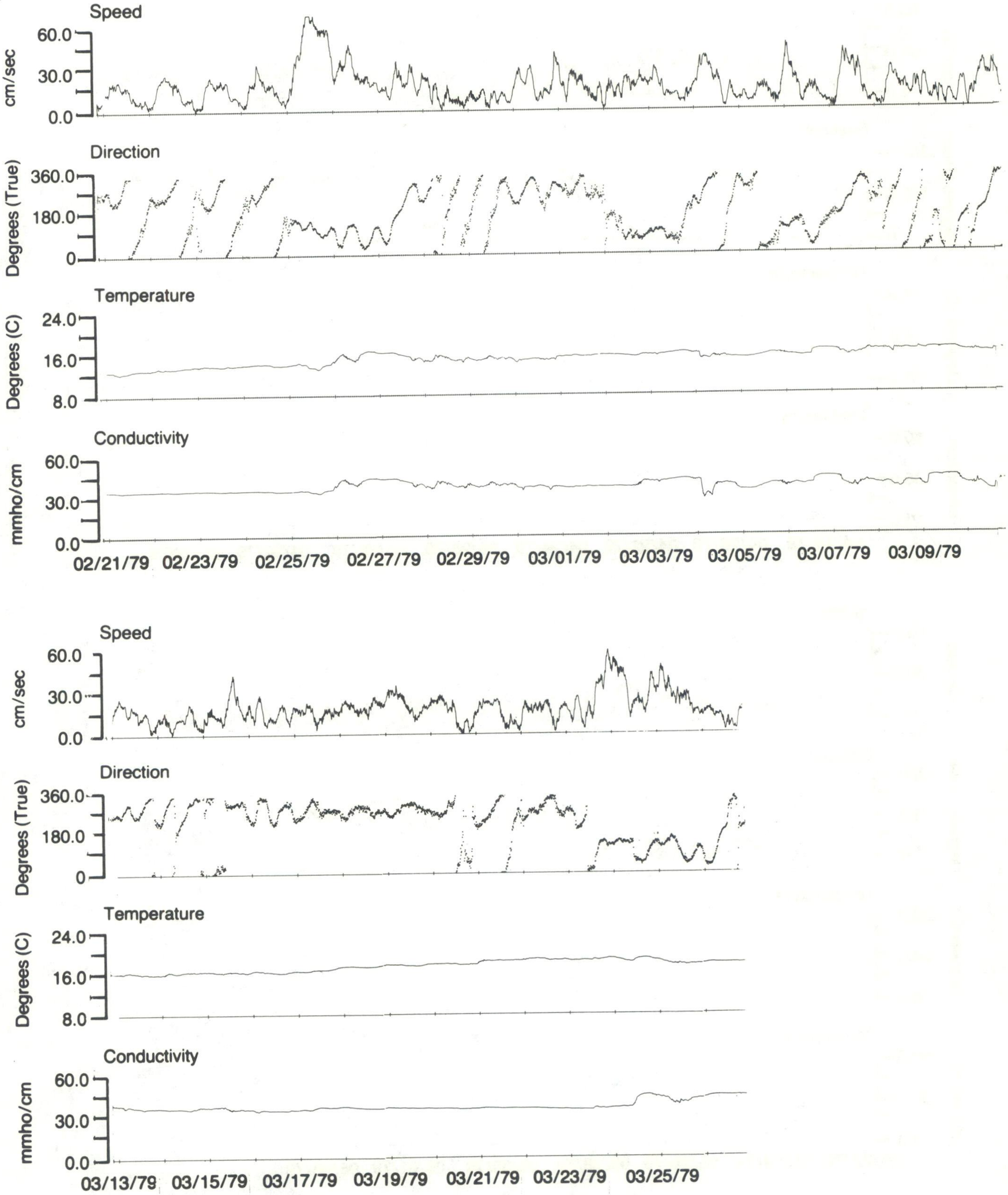

Figure G-4. Time series of current meter data at station 21, 3 m above bottom, for February 21 to March 10 and March 13-26, 1979.

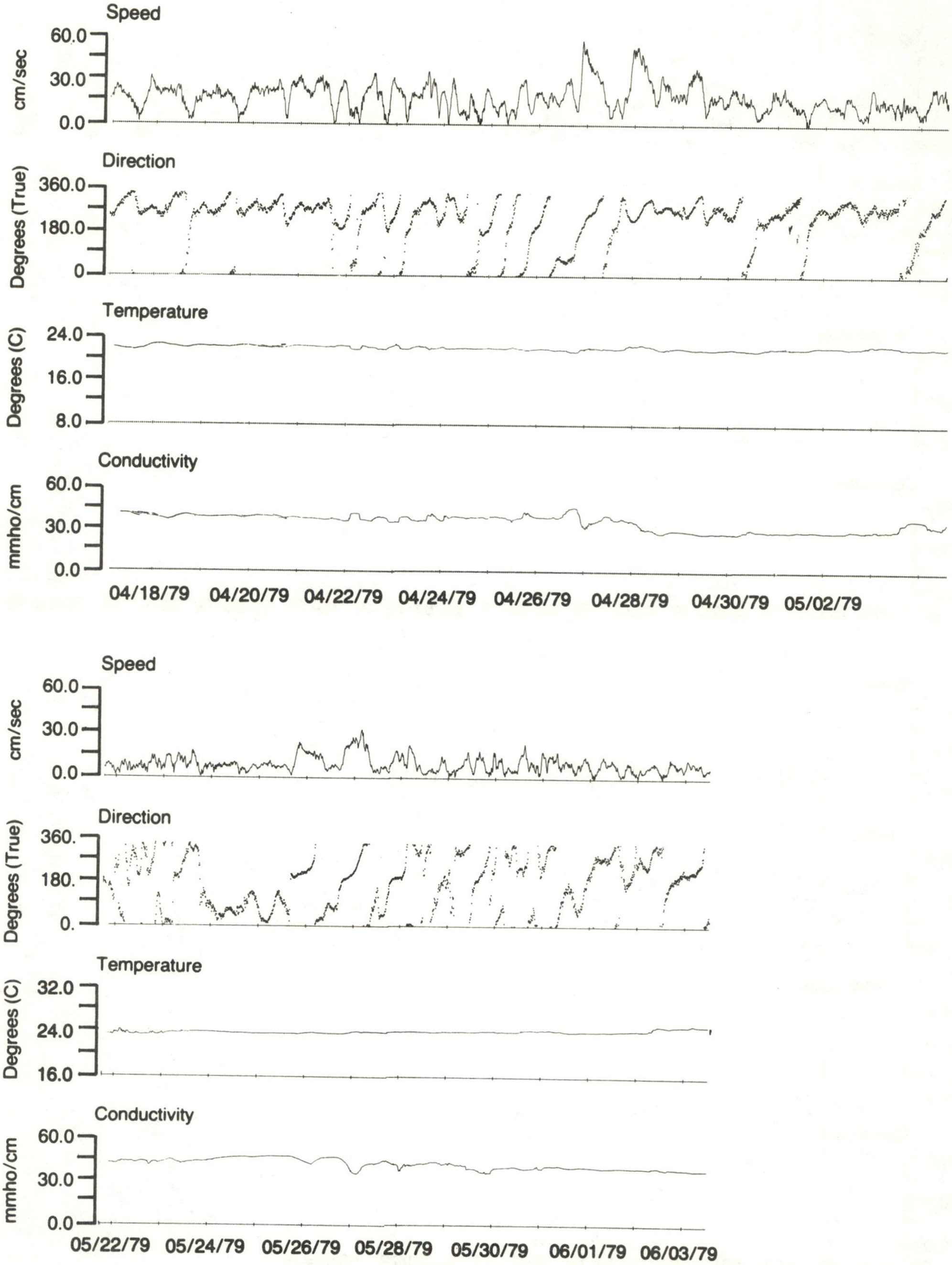

Figure G-5. Time series of current meter data at station 21, 3 m above bottom, for April 17 to May 2 and May 22 to June 1979.

APPENDIX H.

TRANSPORT AND CURRENT VECTOR DIAGRAMS FOR THE WEEKS ISLAND SITE.

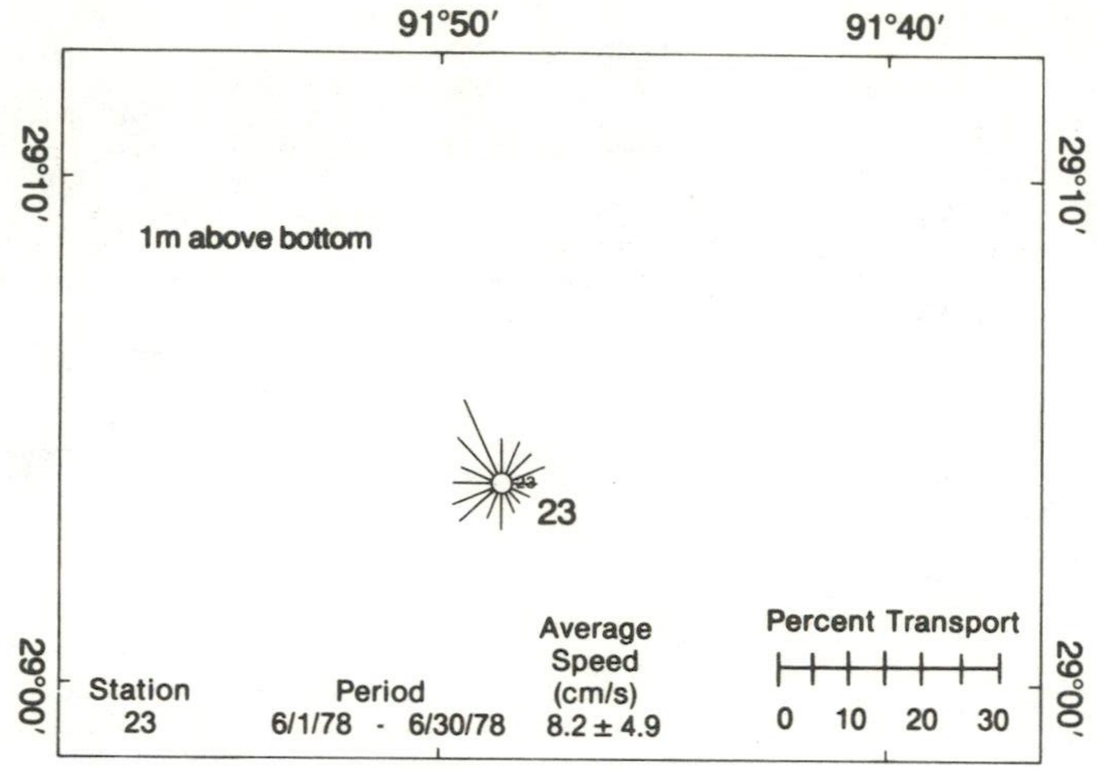

No 3-m level data obtained from June1, 1978 to June 30, 1978

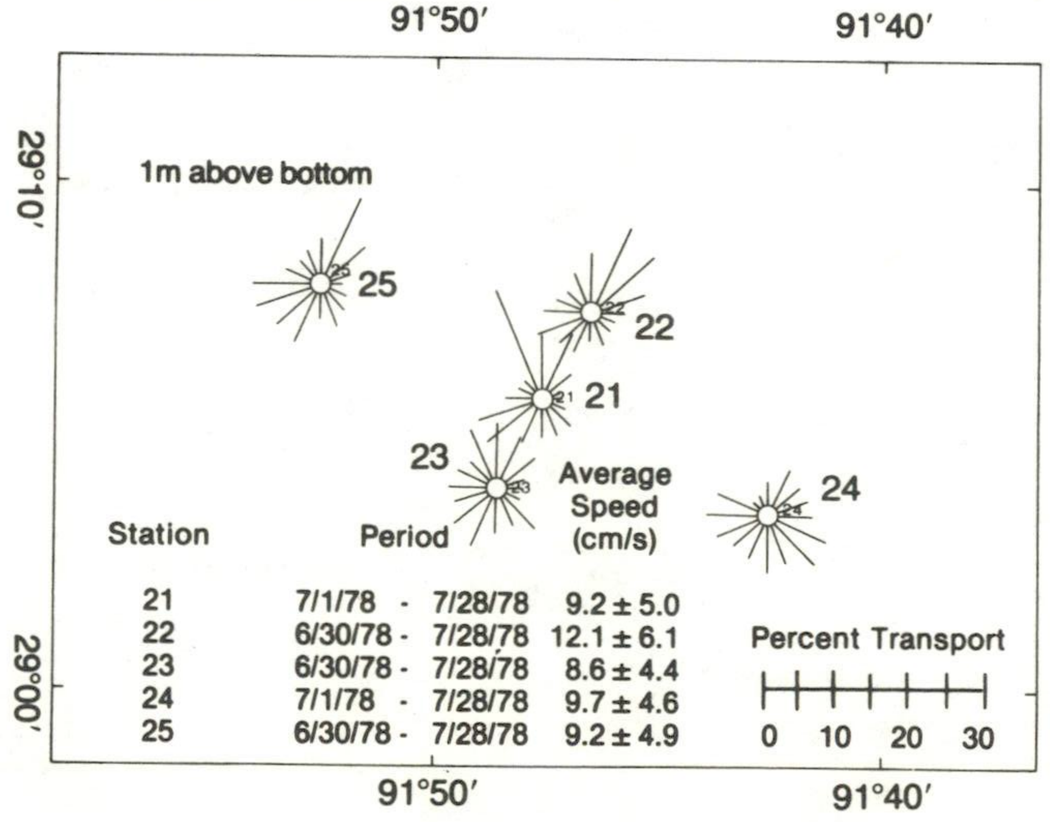

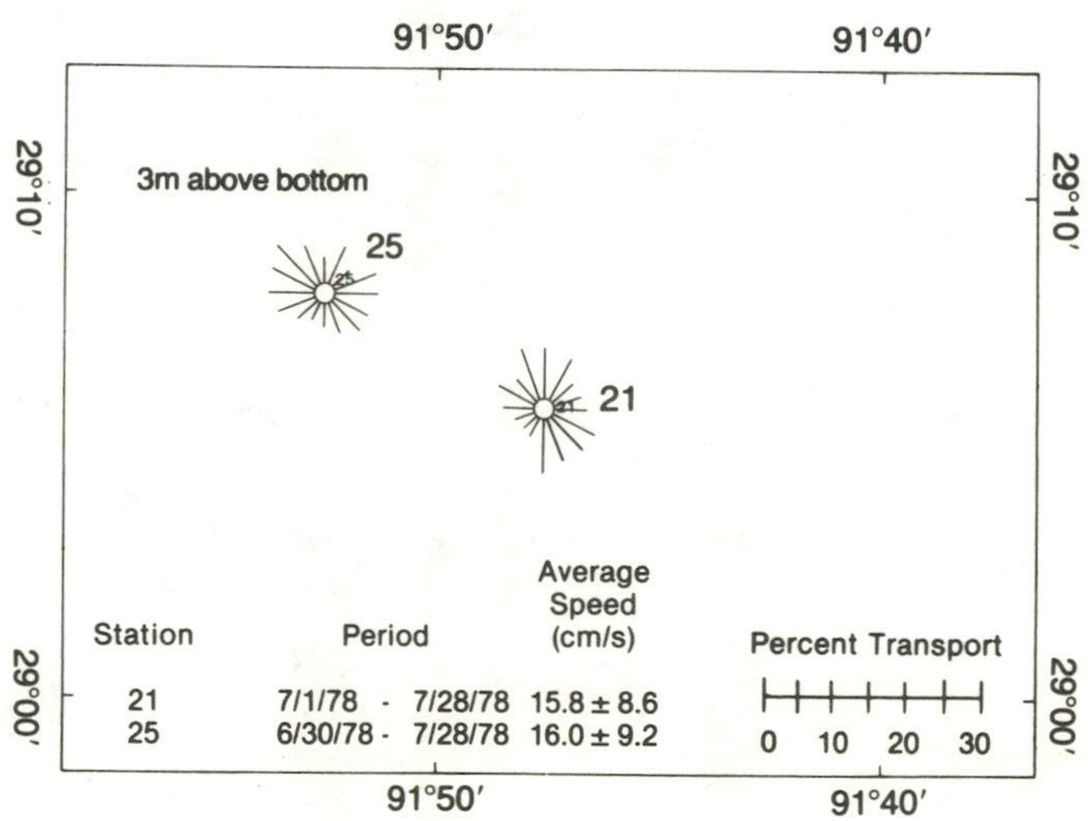

Figure H-1. Relative volume transports at Weeks Island site for June 1 to July 28, 1978.

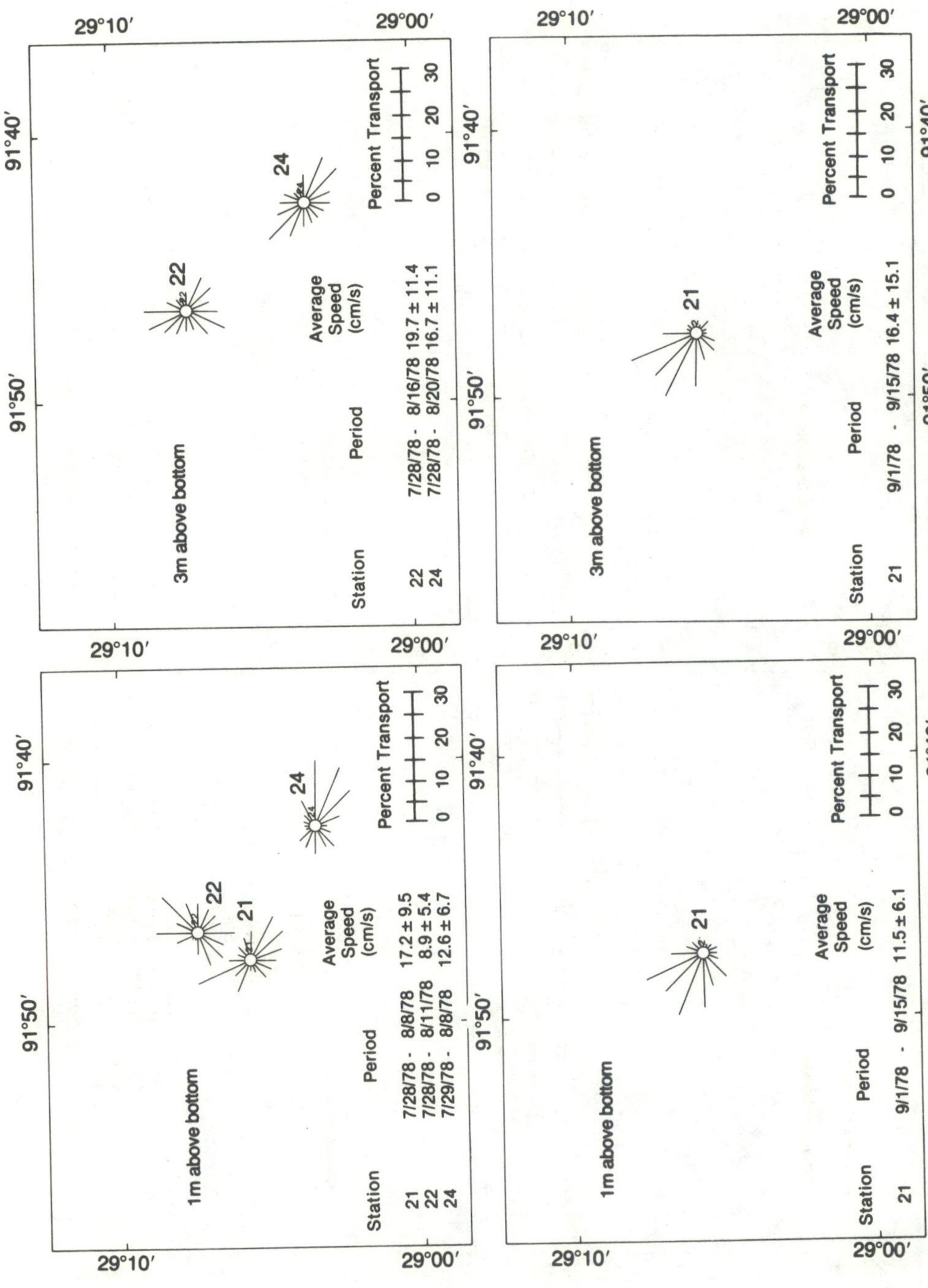

Figure H-2. Relative volume transports at Weeks Island site for July 28 to September 15, 1978.

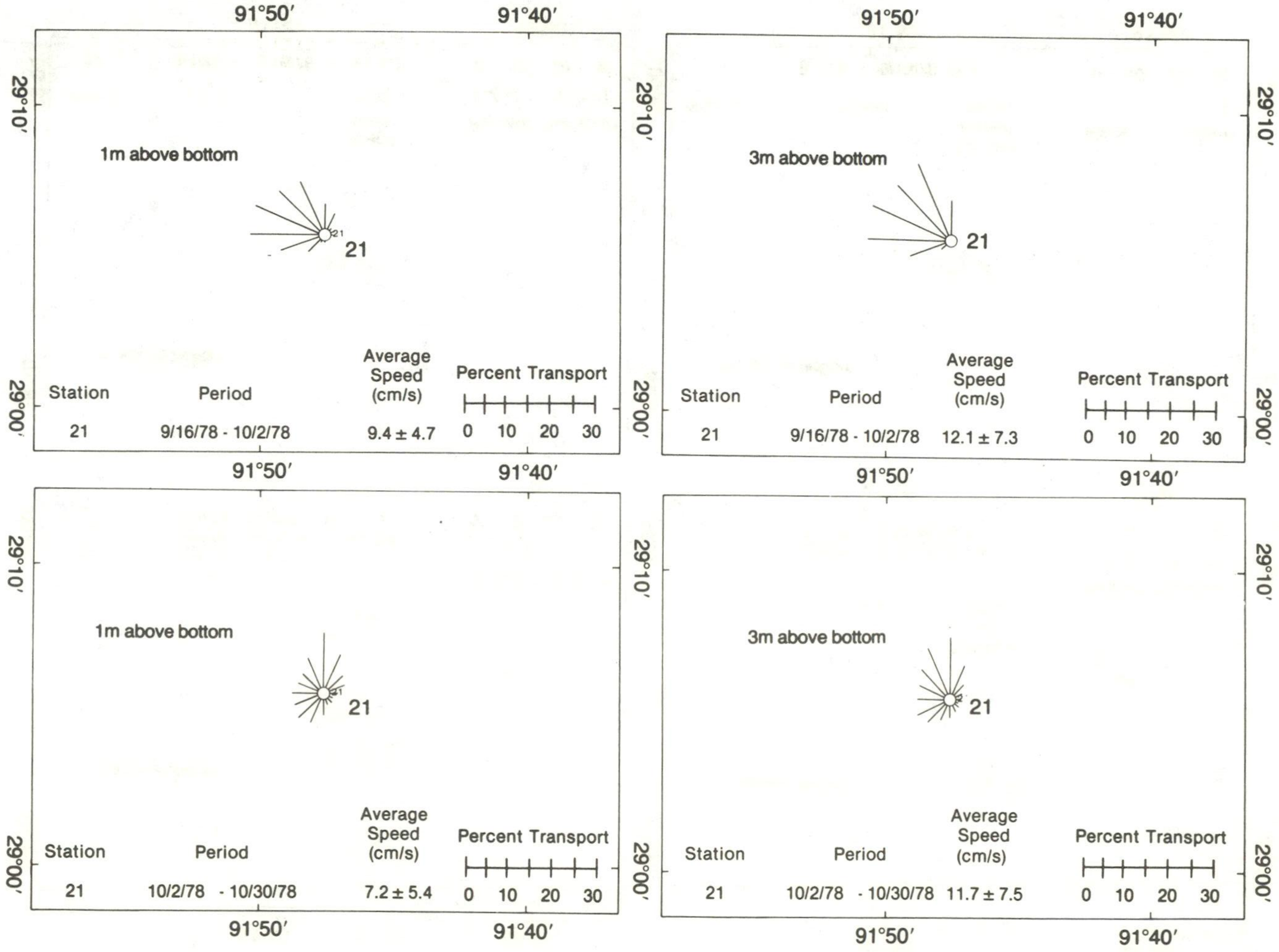

Figure H-3. Relative volume transports at Weeks Island site for September 16 to October 30, 1978.

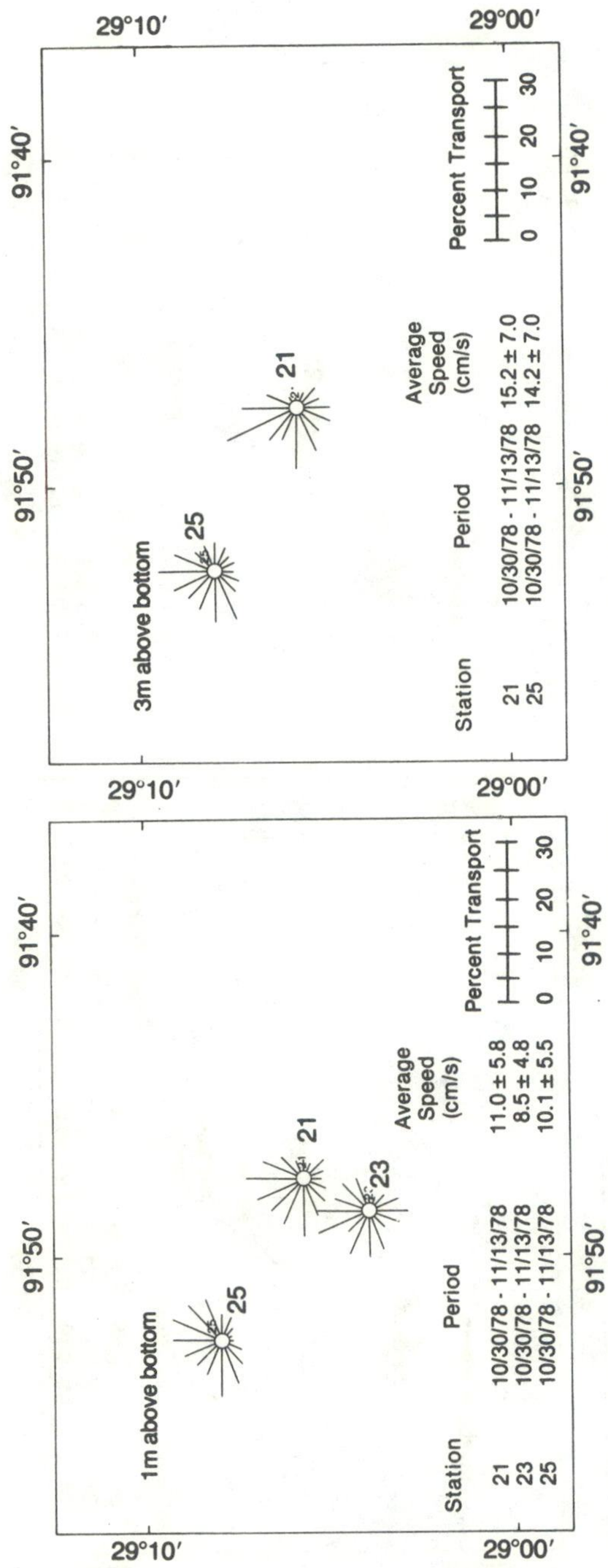

Figure H-4. Relative volume transports at Weeks Island site for October 30 to December 11, 1978.

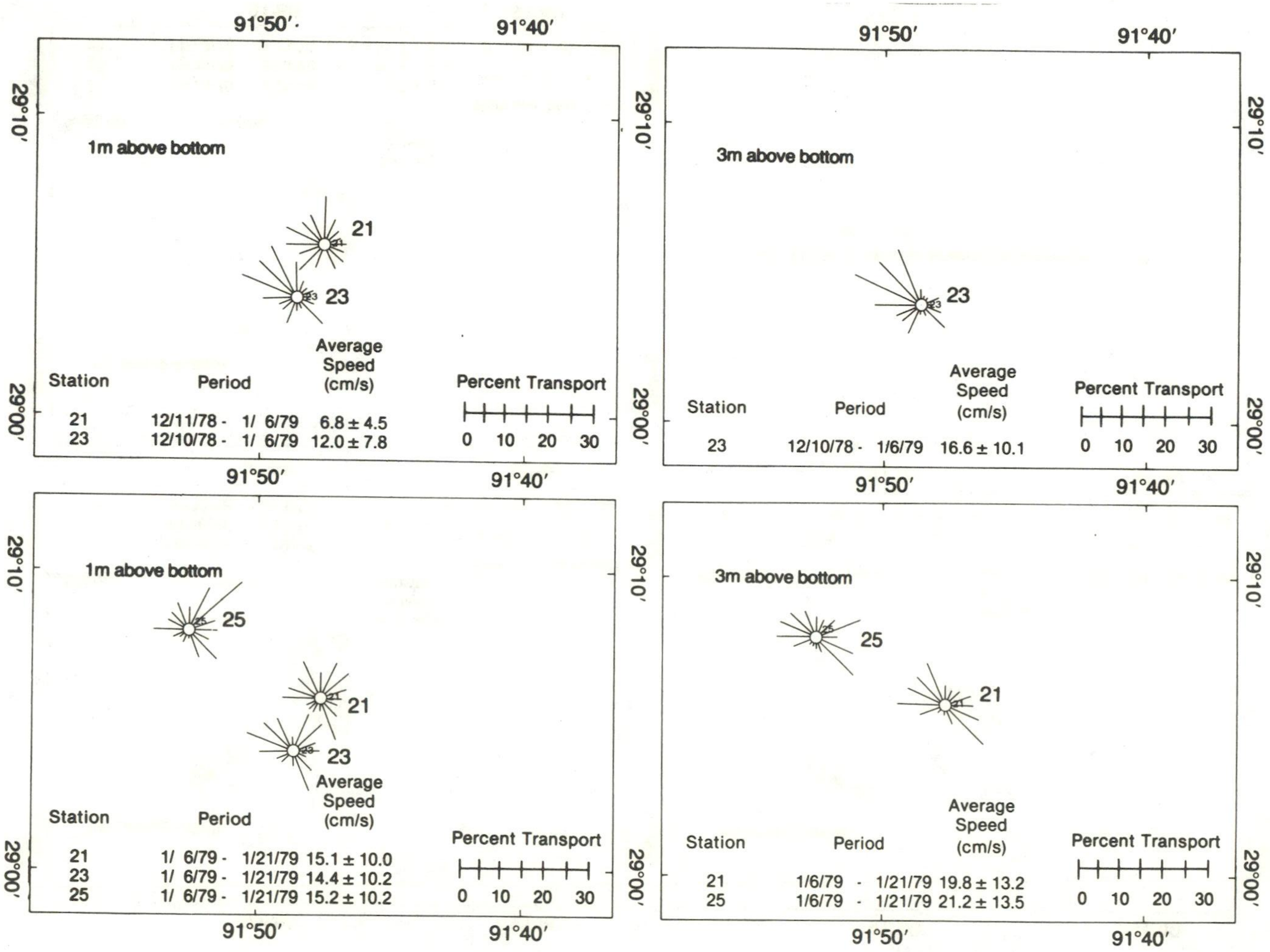

Figure H-5. Relative volume transports at Weeks Island site for December 10, 1978, to January 21, 1979.

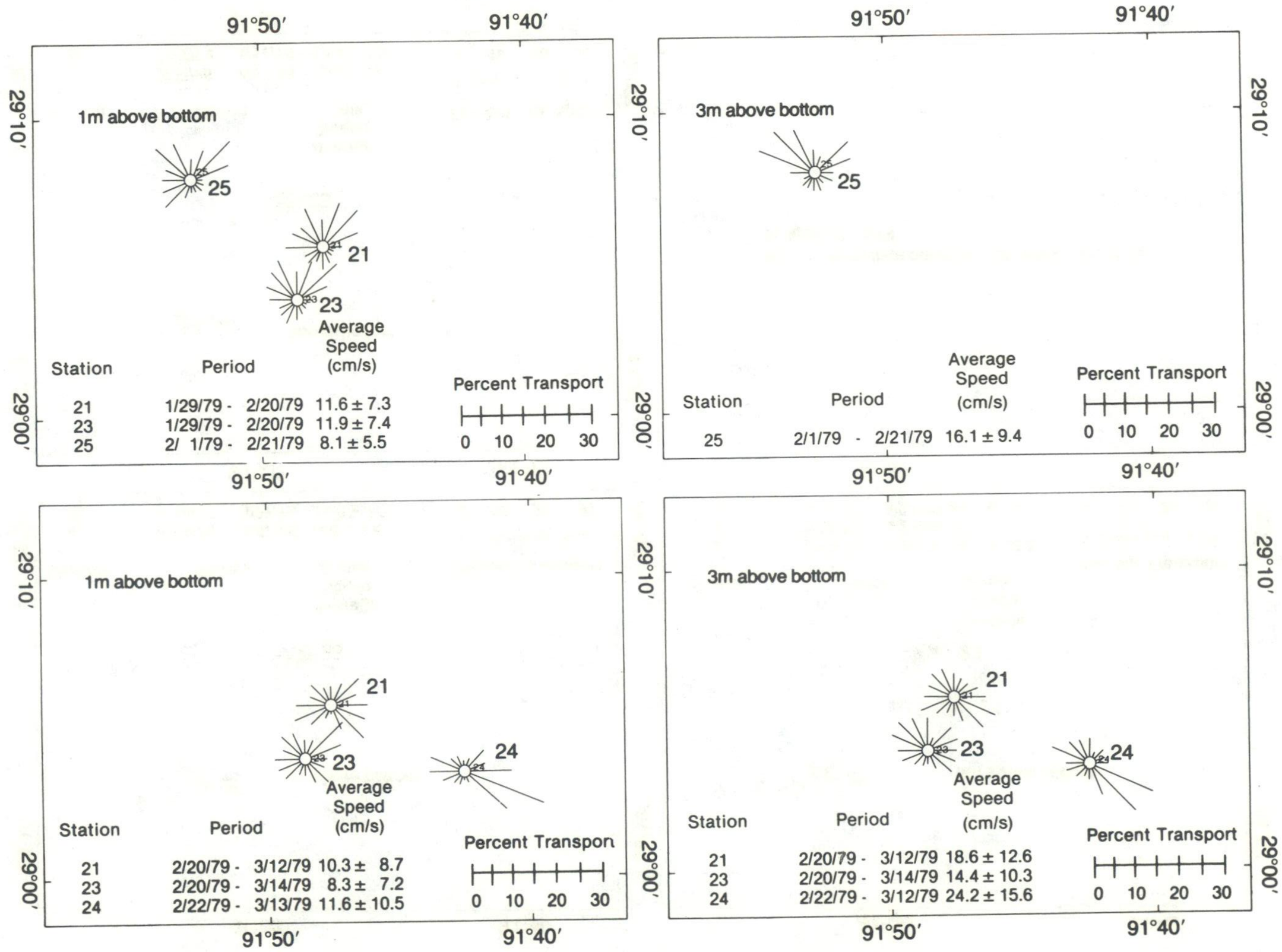

Figure H-6. Relative volume transports at Weeks Island site for January 29 to March 14, 1979.

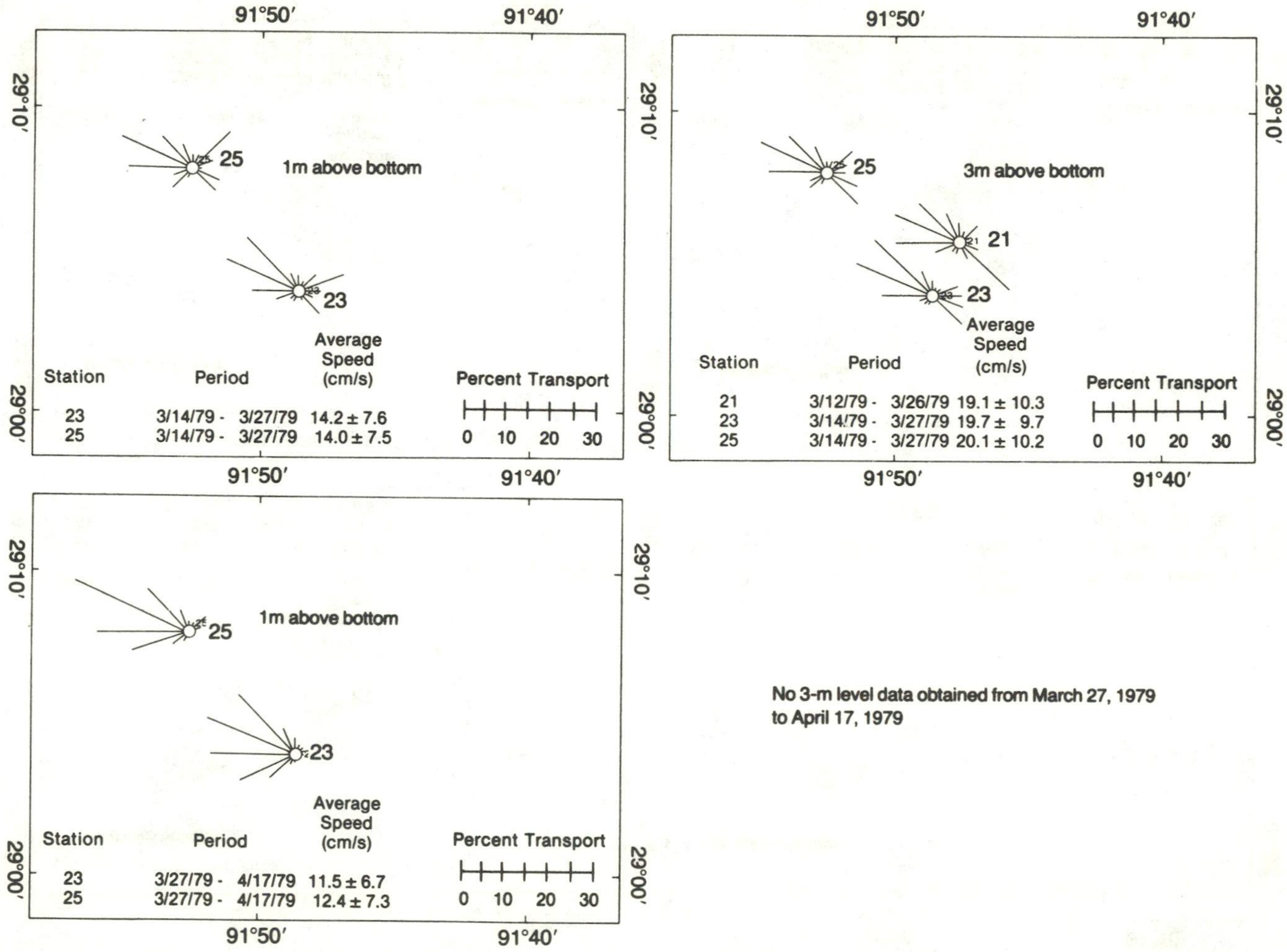

No 3-m level data obtained from March 27, 1979 to April 17, 1979

Figure H-7. Relative volume transports at Weeks Island site for March 12 to April 17, 1979.

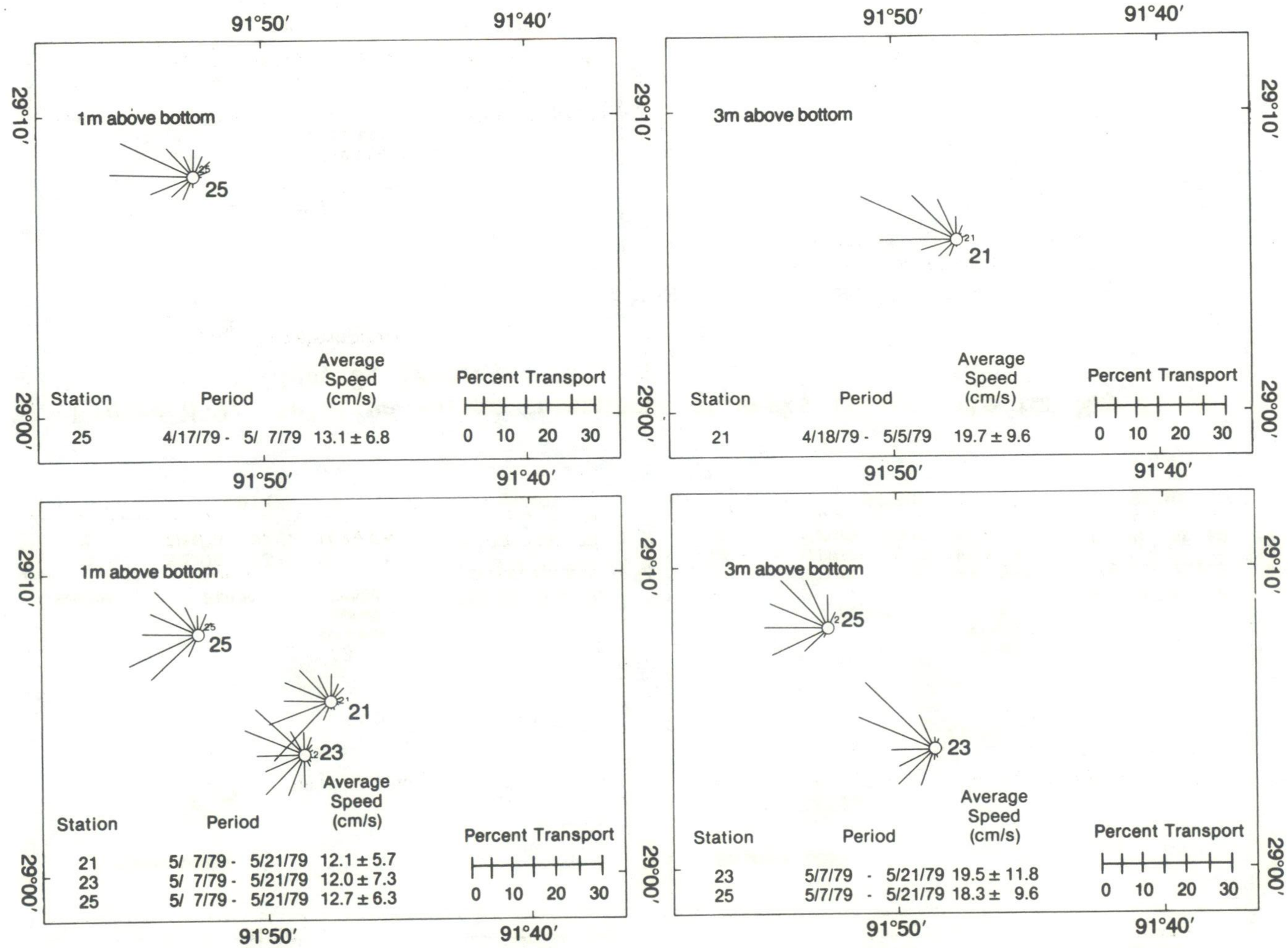

Figure H-8. Relative volume transports at Weeks Island site for April 17 to May 21, 1979.

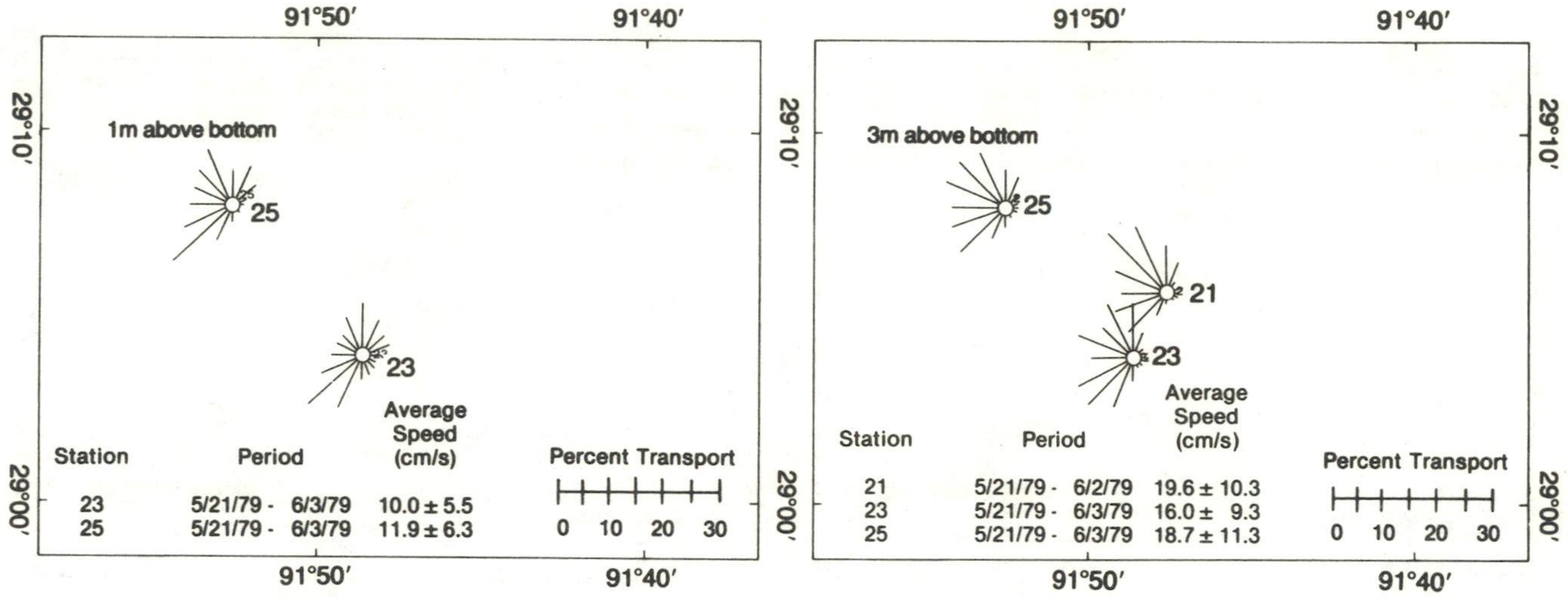

Figure H-9. Relative volume transports at Weeks Island site for May 21 to June 3, 1979.

APPENDIX I.

VERTICAL PROFILES OF TEMPERATURE, SALINITY, AND SIGMA-T AT THE TRACKLINE STATIONS.

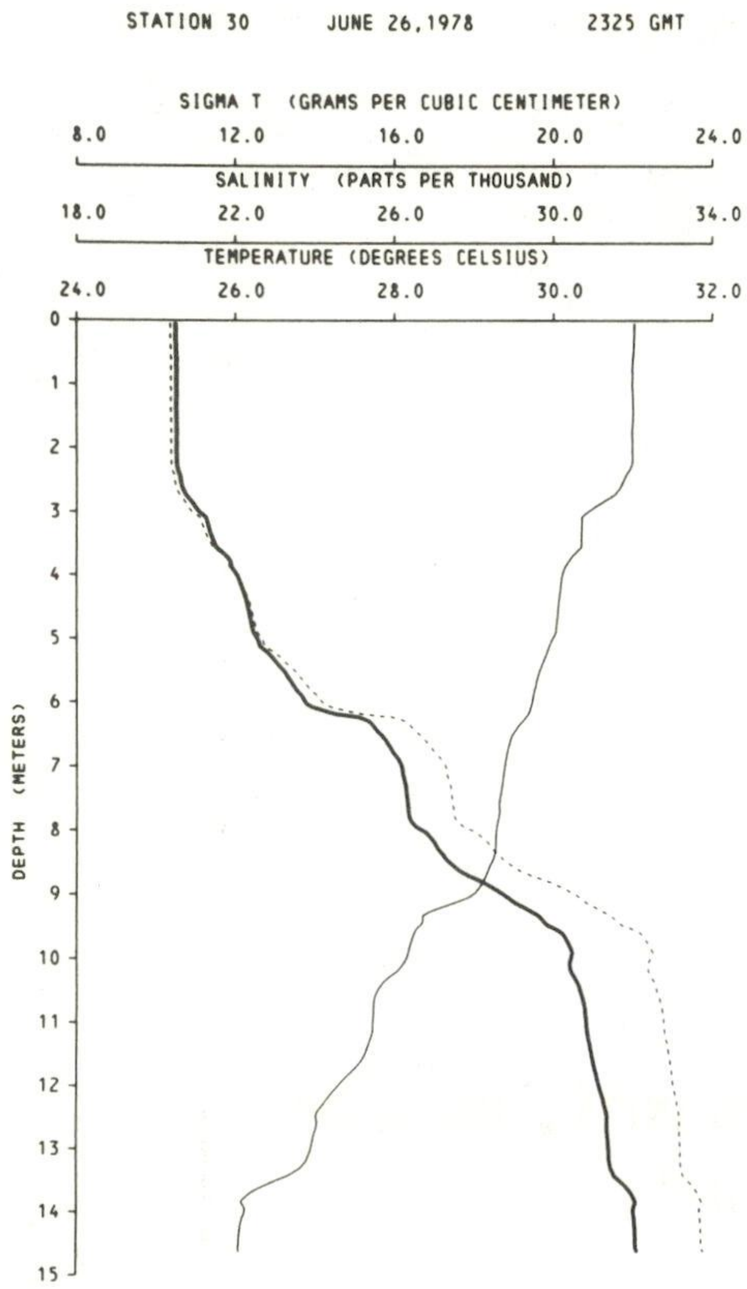

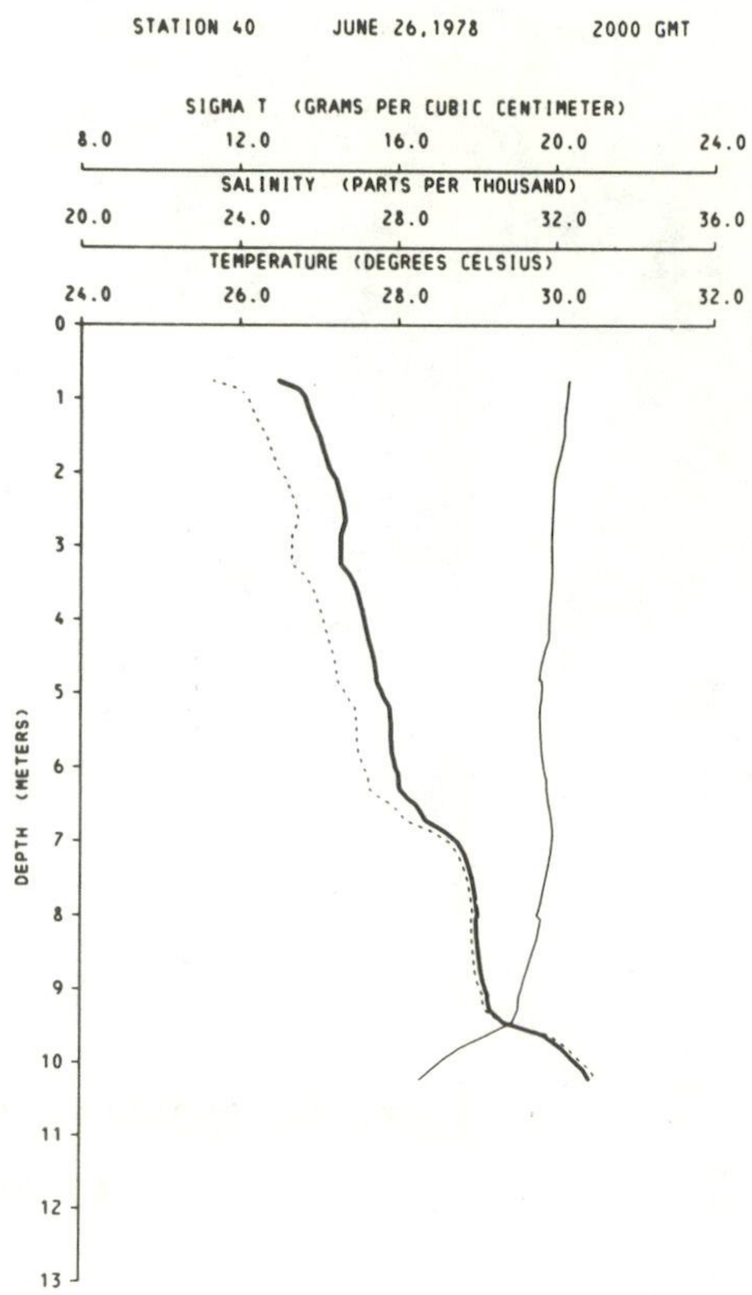

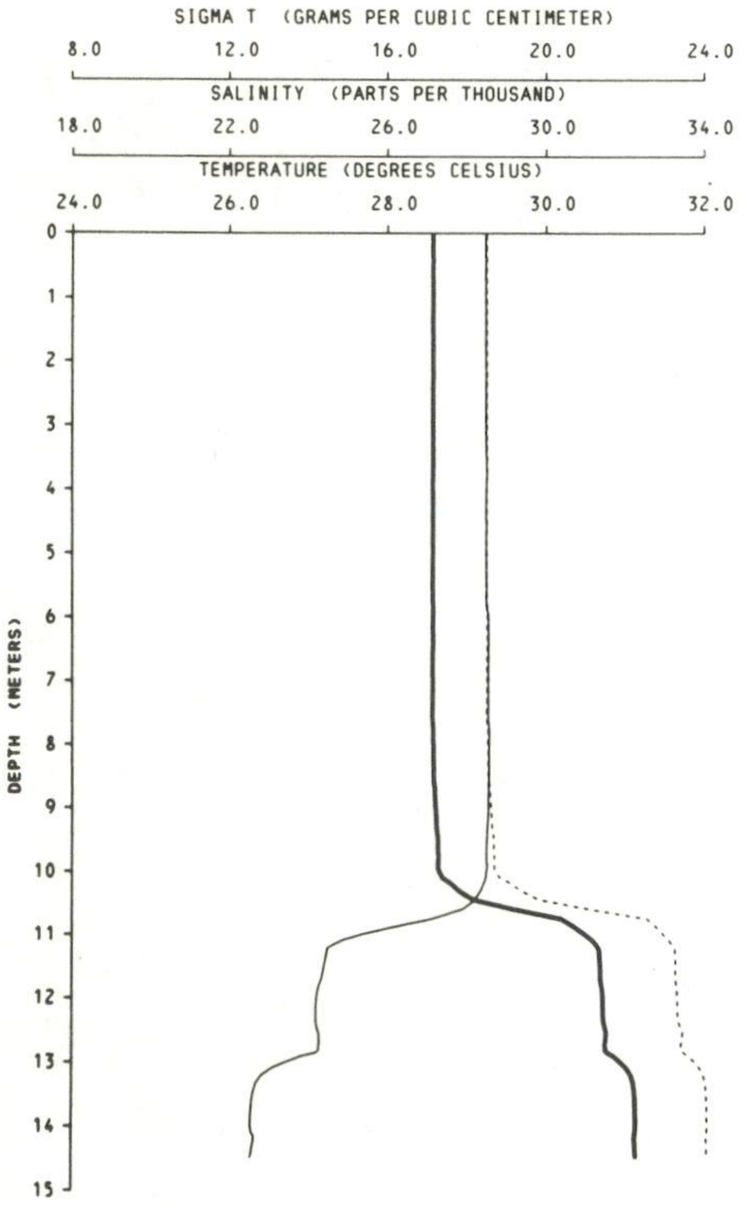

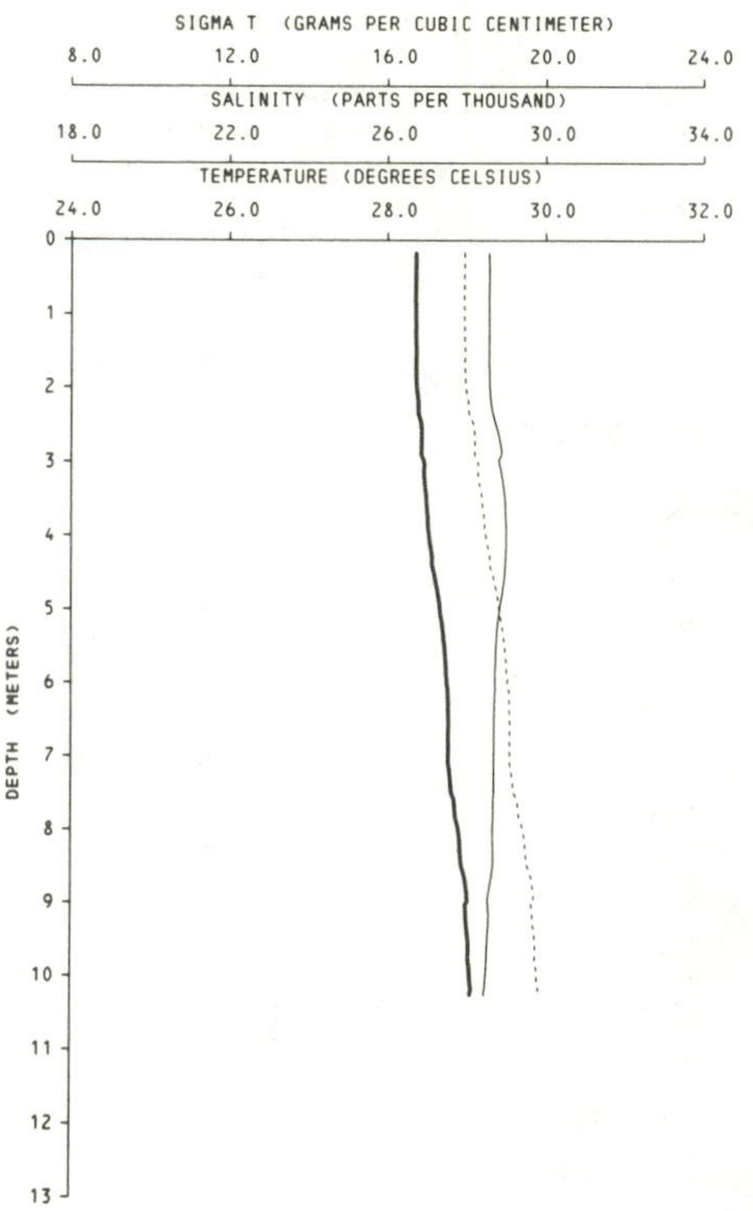

Figure I-1. Vertical profiles of temperature, salinity, and sigma-t for June 26 and July 27, 1978, at stations 30 and 40.

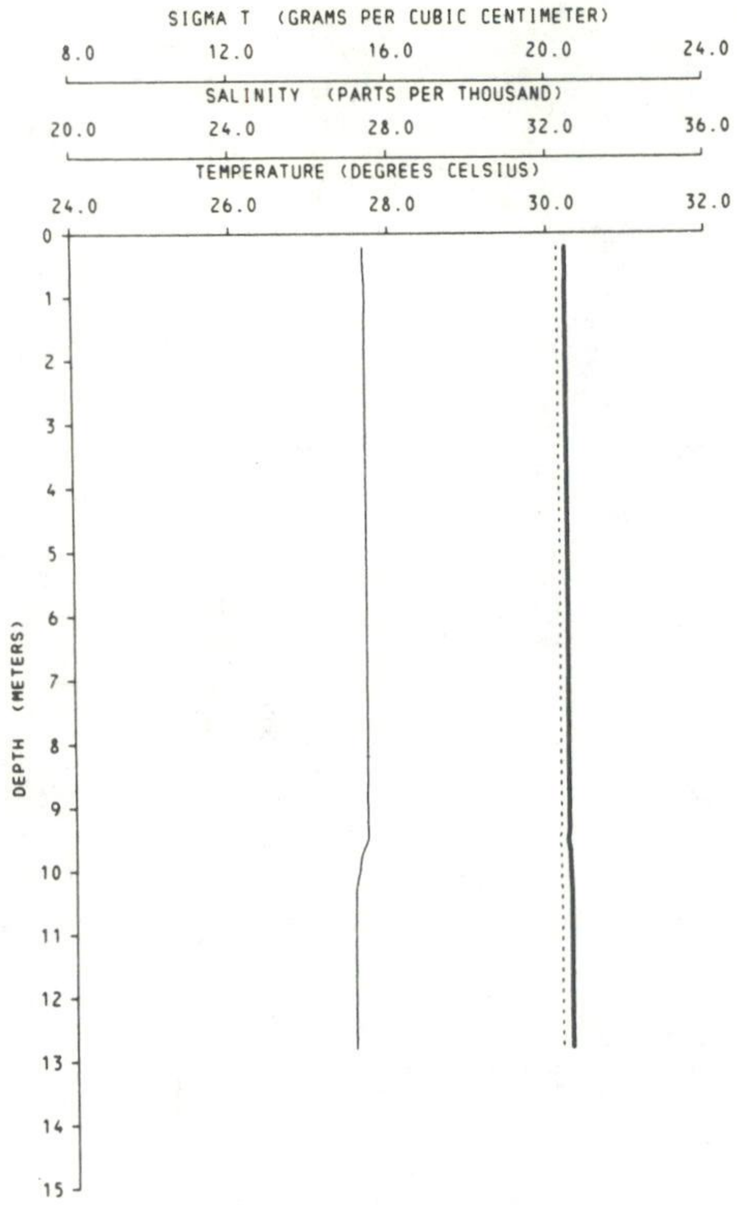

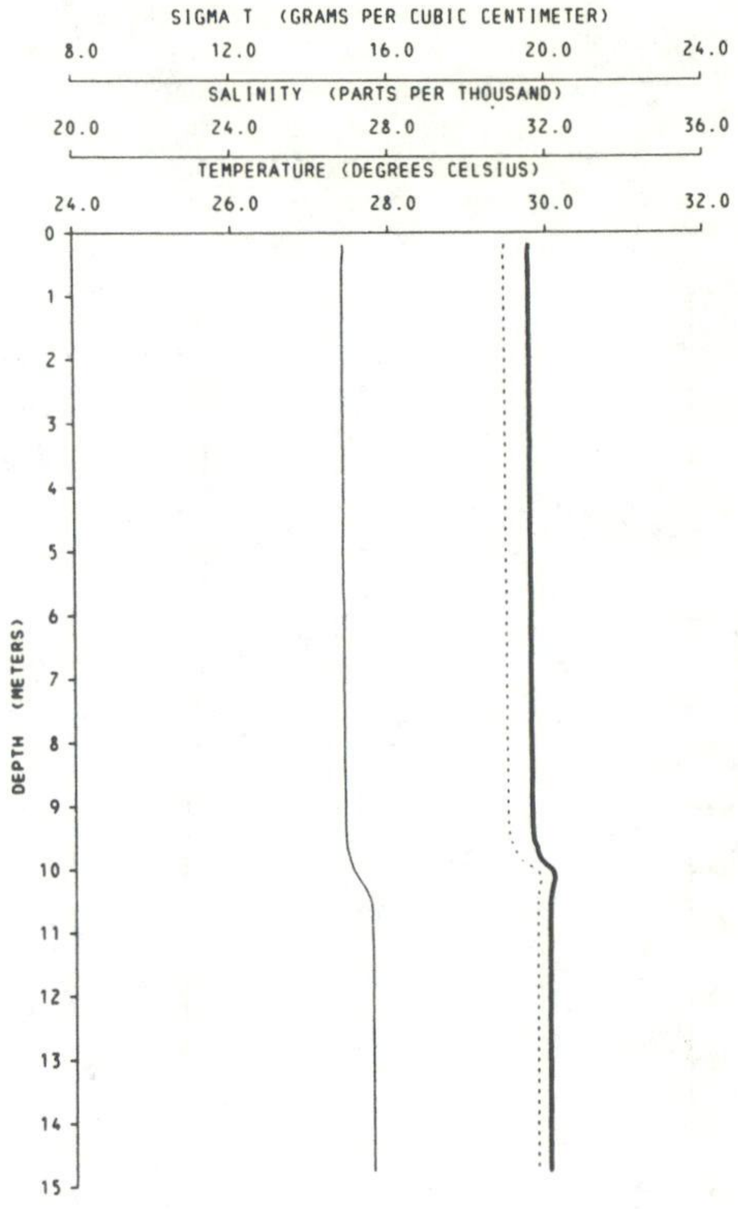

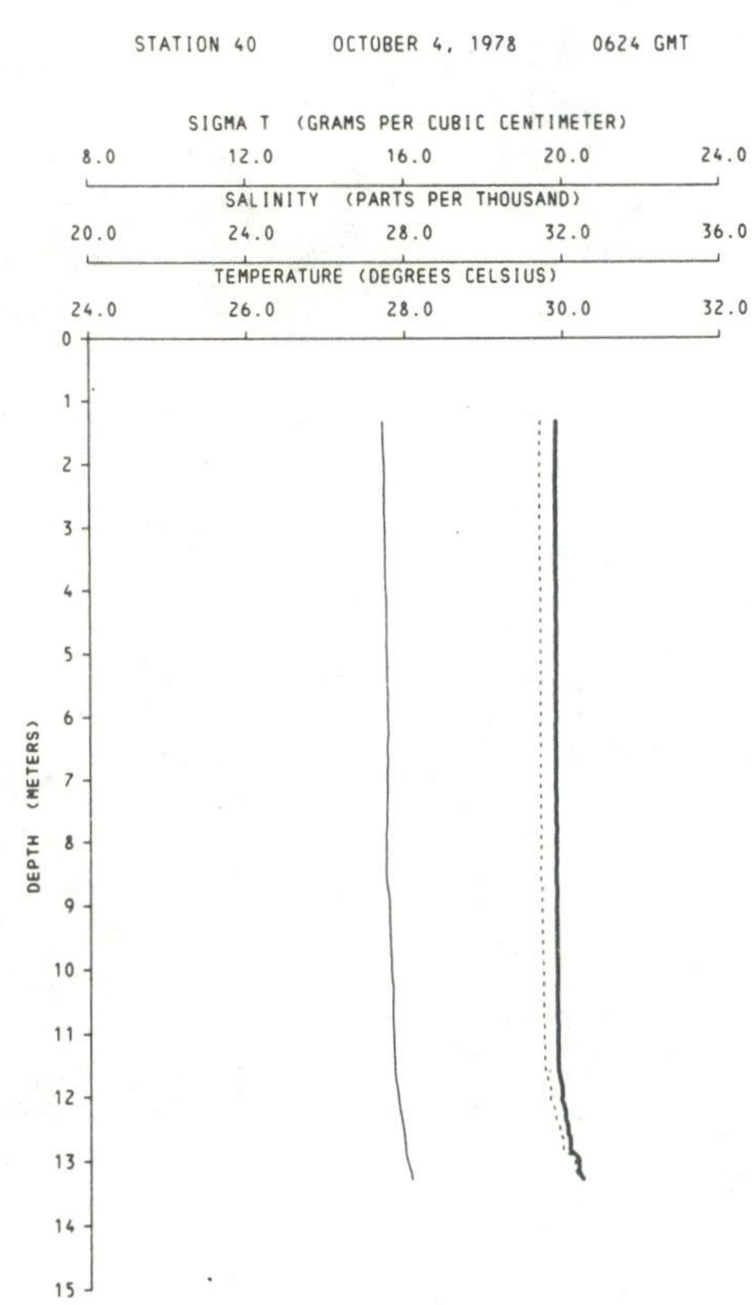

Figure I-2. Vertical profiles of temperature, salinity, and sigma-t for October 1978 at stations 20 through 40.

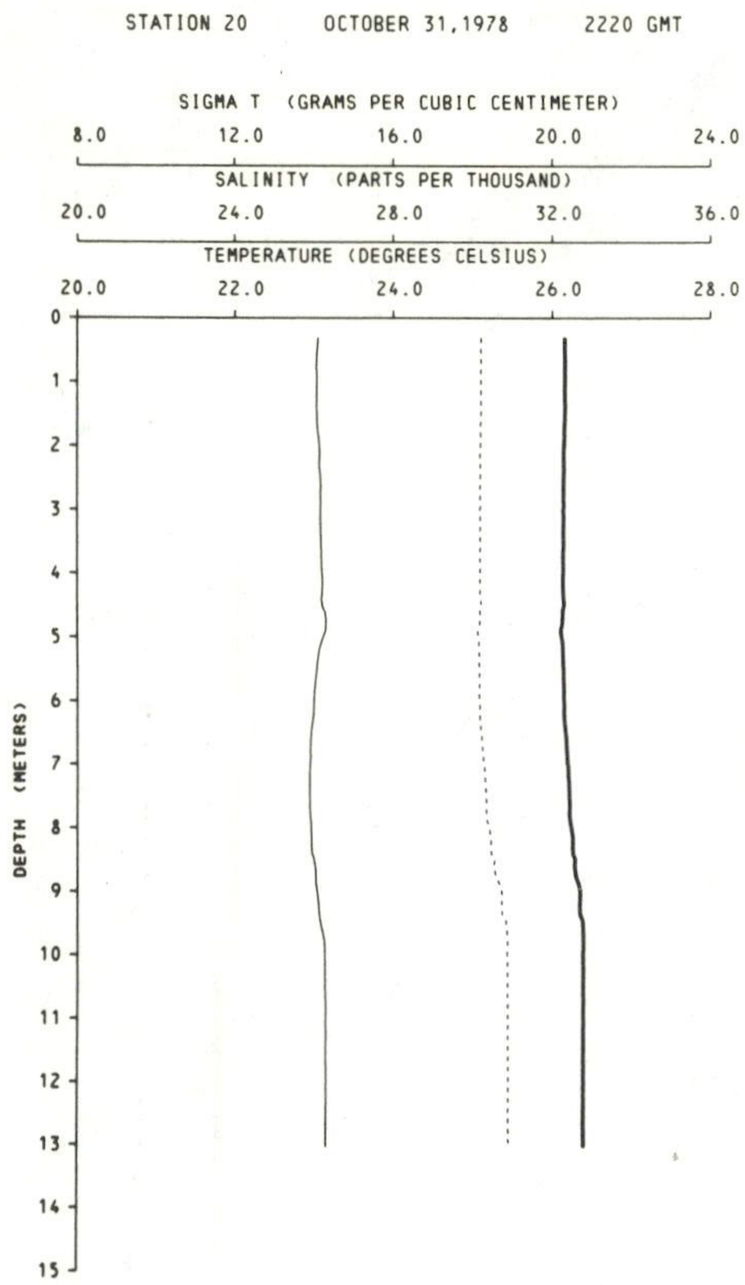

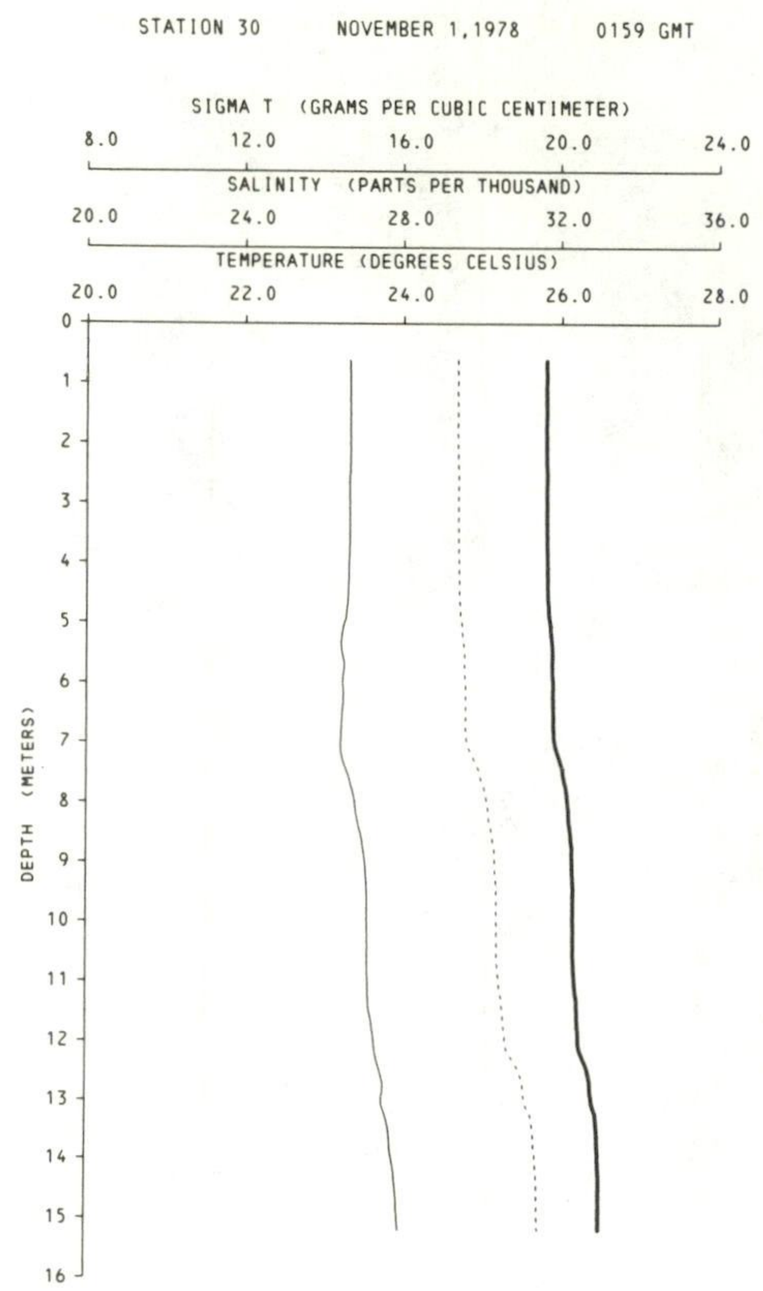

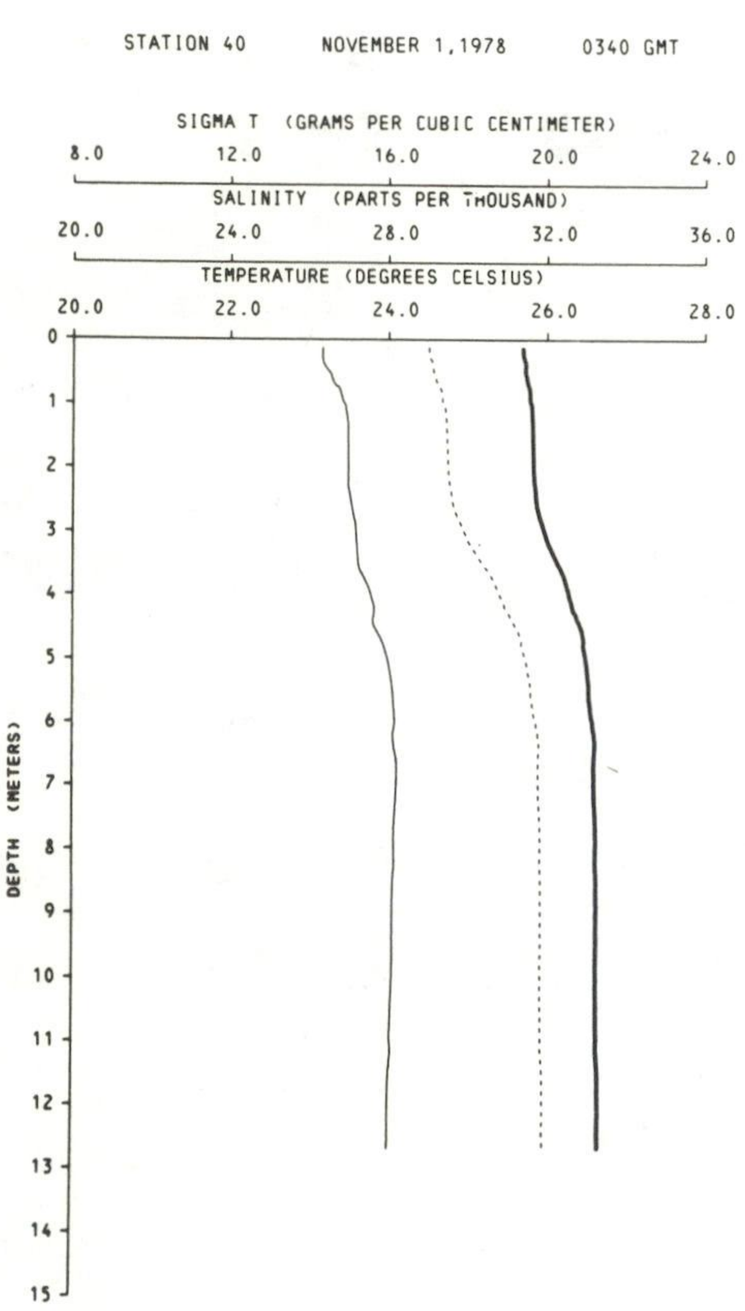

Figure I-3. Vertical profiles of temperature, salinity, and sigma-t for October 31 through November 1, 1978, at stations 20 through 30.

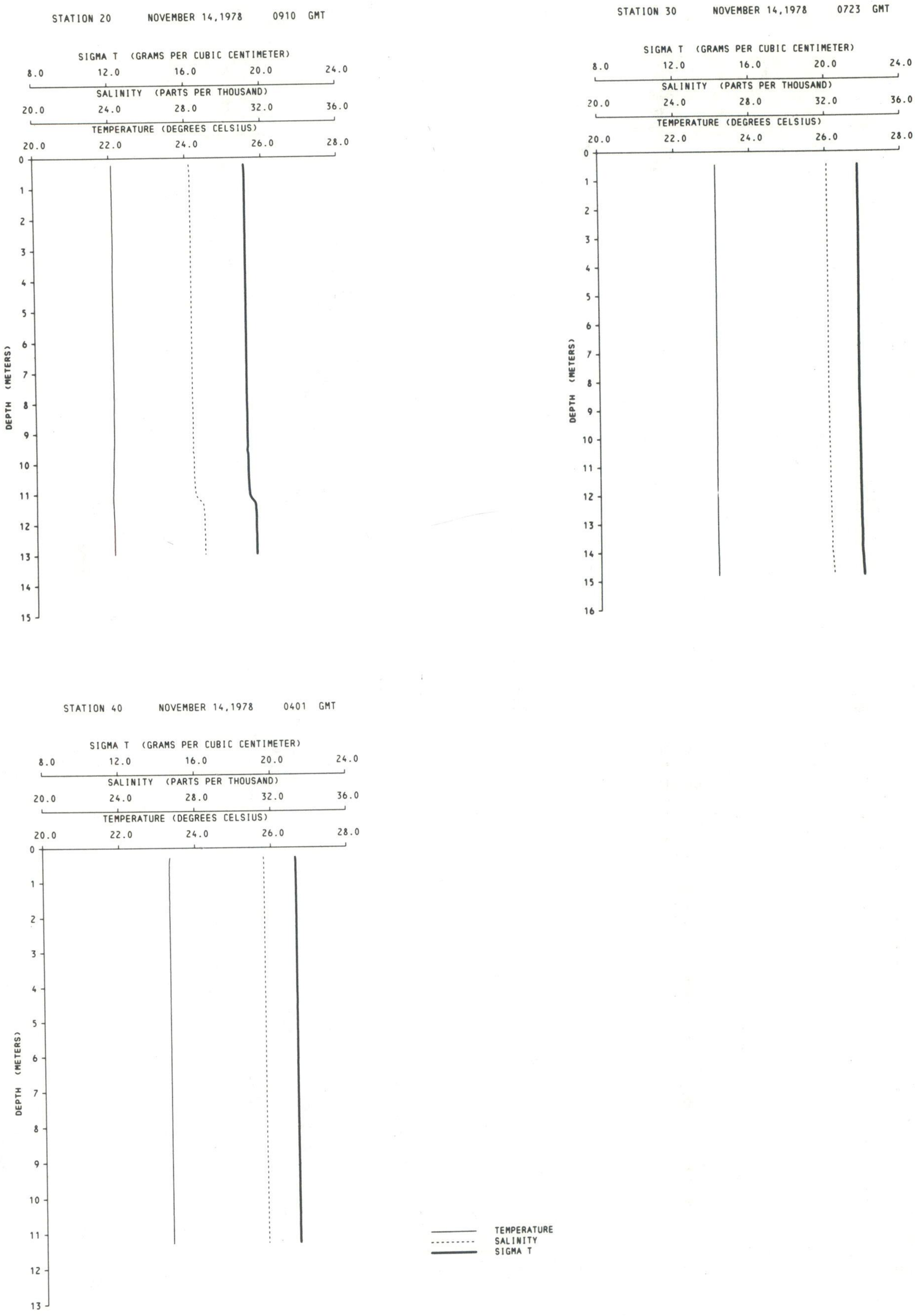

Figure I-4. Vertical profiles of temperature, salinity, and sigma-t for November 14, 1978, at stations 20 through 40.

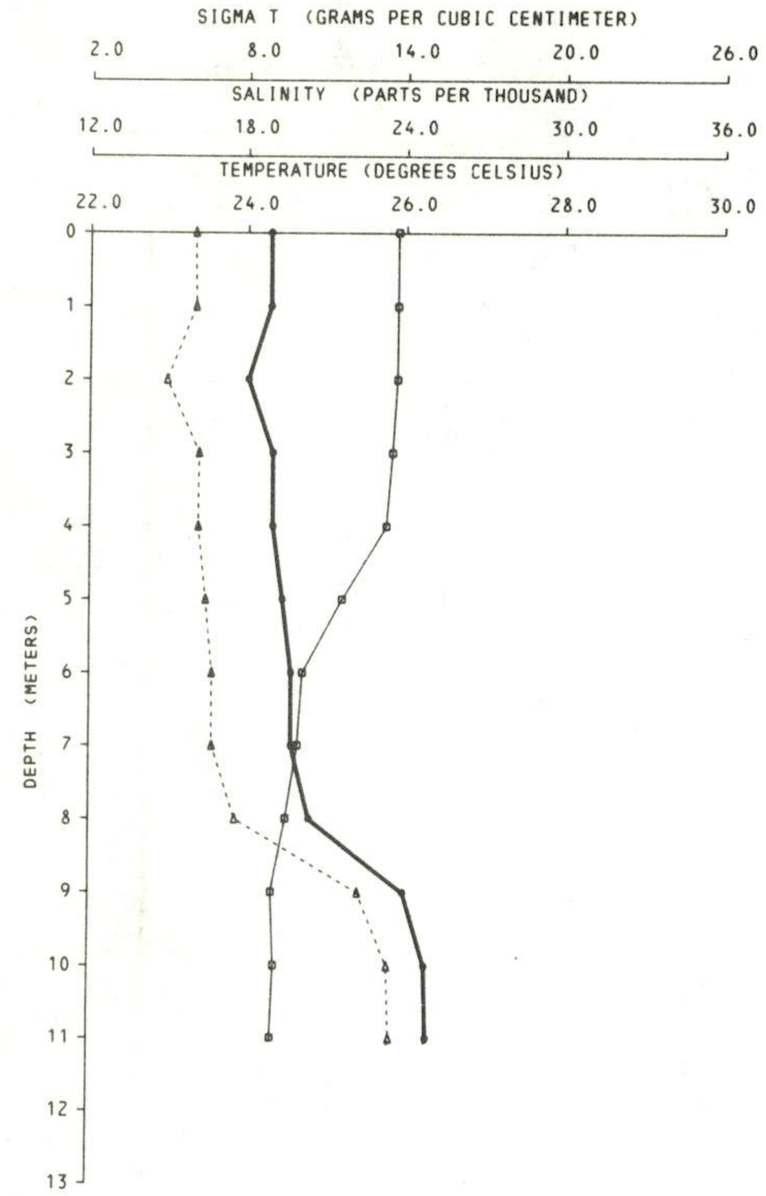

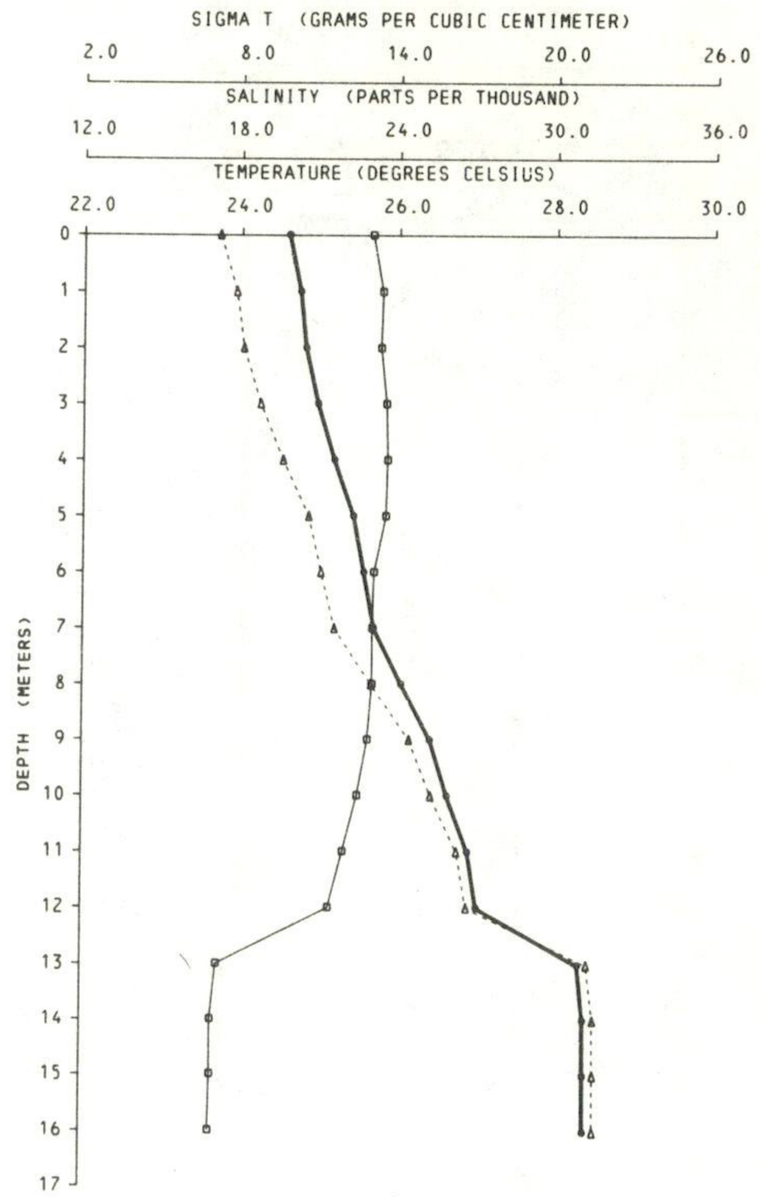

Figure I-5. Vertical profiles of temperature, salinity, and sigma-t for June 2, 1979, at stations 20 through 40.

☆U.S. GOVERNMENT PRINTING OFFICE: 1982-363-913/7281